

# 제86회 정기총회 식순

사회자 : 총무담당 실무이사 정 세 영

## 제 1 부

- 개 회
- 국민의례
- 개 회 사

회 장 이 영 백

## 제 2 부 : 제86회 정기총회

- 한국물리학회상 시상
  - 학술상
  - 논문상
  - 장려상
  - 젊은물리학자상
  - 우수여성대학원생상
  - 우수물리교사상
  - 백천물리학상
  - 봄비물리학상
  - 용봉상
  - 융문상
- 감사패 전달
- 2009년도 임시총회 회의록 인준
- 회무보고
- 감사보고
- 2009년도 사업 및 결산 승인
- 2010년도 사업계획 및 예산 보고
- 2010년도 사업계획 및 예산 승인
- 세칙개정
- 기 타
- 폐 회

총회 의장  
실무이사장  
감 사  
총회 의장  
실무이사장  
총회의장  
총회의장

## 제 3 부 : 평의원회

- 신임 편집위원 인준

# 한 국 물 리 학 회 회 보 차 례

응집물질, 응용, 통계, 반도체물리학분과 편

2009 한국물리학회 가을학술논문발표회 및 임시총회 전체 일정표 .....	i
구두발표 일정표 .....	ii
등록 및 발표장 안내 .....	viii
창원컨벤션센터 발표장 안내도 .....	ix
특별세션 안내 .....	x
구두발표논문 시간표 .....	1
포스터발표논문 시간표 .....	35
구두발표논문초록 .....	67
포스터발표논문 초록 .....	199
발표자 색인 .....	429

# 2009 한국물리학회 가을학술논문발표회 및 임시총회 전체 일정표

창원컨벤션센터, 2009.10.21(수)-23(금)

## 구두 발표

	301	302	601	602	603	604	605	606	607	컨벤션 I	컨벤션 II	컨벤션 III
	응용(E)/ 학회주관(A)	응집(D)/ 학회주관(A)	통계(F)/ 응용(E)	반도체(K)/ 응용(E)	광학(I)/ 핵(C)	교육(G)/ 핵(C)	플라스마(H)	천체(L)/ 원자분자(J)/ 응집(D)	입자(B)/ 핵(C)	학회주관세션(A) /Pioneering세션(P)/응집(D)		
[10.21] 09:00	등록시작											
11:15								[LT1]천체	[BG1]입자	[DT1]응집 STM		
13:30			[EG1] 응용		[CG1] 핵		[HG1] 플라스마	[LG1]천체	[BG2] 입자	[DG1]응집		
15:45			[EG2] 응용		[CG2] 핵		[HG2] 플라스마	[LG2]천체	[BG3] 입자	[DG2]응집	[A1]산학연 특별세션	[PC1] Pioneering세션
17:45			[A7] 신진교수 세션		핵분과총회	[A2]KPS-AKPA 특별세션 (17:00-18:15)		천체분과총회	입자분과총회			
[10.22] 09:00	[EG3]응용	[DF1]응집		[KG1]반도체				[LG3]천체	[BF1/CF1] 입자/원자핵	[PA1] Pioneering세션 (09:00-10:40)		
11:15	[EG4]응용	[DG3]응집	[FG1] 통계	[KF1]반도체	[IG1] 광학	[GG1] 물리교육	[HG3] 플라스마	[LG4]천체	[BF2/CF2] 입자/원자핵	[PA2] Pioneering세션 (11:00-12:30)	[A3]Open KIAS (11:00-13:00)	
13:30	[EG5]응용	[DG4]응집	[FG2] 통계	[KG2]반도체	[IG2] 광학	[GG2] 물리교육		[LG5]천체	[BG4]입자	[PA3] Pioneering세션 (14:00-15:40)	[PB1] Pioneering세션	[PC2] Pioneering세션
15:45	[EG6]응용	[DG5]응집	[FG3] 통계			물리교과 과정개편 공청회			[BG5]입자	[PA4] Pioneering세션 (16:00-17:30)	[PB2] Pioneering세션	[PC3] Pioneering세션
17:45			통계분과총회 (17:30-18:00)	[KT1]반도체 (17:00-18:00)				원자분자분과총회 (17:15-18:00)				
18:00										[A4] 대중강연 (18:00-20:00)	임시총회 (18:00-19:00)	평의원연찬회
[10.23] 09:00	[EG7]응용	[DG6]응집	[FG4] 통계	[KG3]반도체	[CG3] 핵	[CG4] 핵	[HG4] 플라스마	[JG1] 원자분자	[BG6]입자			
11:15	[EG8]응용	[DG7]응집		[KF2]반도체				[JG2] 원자분자		[DF2]응집 (10:30-12:30)	[PB3] Pioneering세션	[A5] ADD특별세션 (11:00-13:00)
13:30			[FG5] 통계		[CG5] 핵	[CG6] 핵		[DG8]응집		[DF3]응집		[A6] ADD특별세션

## 포스터 발표

세션	P1 [10.21(수)]14:00-16:00	P2 [10.22(목)]11:00-13:00	P3 [10.22(목)]15:00-17:00	P4 [10.23(금)]10:00-12:00	P5 [10.23(금)]13:00-15:00
분과명 [발표번호]	입자 [Bp-I-001~Bp-I-028]  응집 [Dp-I-001~Dp-I-058]  응용 [Ep-I-001~Ep-I-035]	응집 [Dp-II-059~Dp-II-126]  응용 [Ep-II-036~Ep-II-102]  반도체 [Kp-II-001~Kp-II-012]	물리교육 [Gp-III-001~Gp-III-015]  플라스마 [Hp-III-001~Hp-III-045, Hp-III-089]  광학 [Ip-III-001~Ip-III-55]  원자 및 분자 [Jp-III-001~Jp-III-014]  반도체 [Kp-III-013~Kp-III-045]  천체 [Lp-III-001~Lp-III-009]	핵물리 [Cp-IV-001~Cp-IV-045]  통계 [Fp-IV-001~Fp-IV-027]  플라스마 (10:30-12:00) [Hp-IV-046~Hp-IV-088]	응집 [Dp-V-127~Dp-V-223]  응용 [Ep-V-103~Ep-V-133]  반도체 [Kp-V-046~Kp-V-074]

구두발표 일정표

2009. 10. 21. 수

	301	302	601	602	603	604	605	606	607	컨벤션 I	컨벤션 II	컨벤션 III
11:15-11:30									B-01 서윤석	DT-01(초) 구자용		
11:30-11:45								LT-01(초) 박무인	B-02 박천수			
11:45-12:00									B-03 권오갑			
12:00-12:15								LT-02(초) 명연수	B-04 김경규			
12:15-12:30										DT-02(초) 김한철		
12:30-12:45								LT-03(초) 이형욱				
12:45-13:00												
13:00-13:15												
13:15-13:30												
13:30-13:45			E-01 LEE Jun Min		C-01(초) LEE Kang Seog		H-01 YUN G. S.	L-01(초) 김진영	B-05 이정훈	D-01 LEE Gun-Do		
13:45-14:00			E-02 김형준		C-02 강주환		H-02 황치옥		B-06 안효철	D-02 박재환		
14:00-14:15			E-03 LEE Hansung		C-03 송명근		H-03 이용인	L-02(초) 박달호	B-07 KIM Taekyung	D-03 강세준		
14:15-14:30			E-04 박대현		C-04 오근수		H-04 YOON Moohyun		B-08 김종욱	D-04 박수현		
14:30-14:45			E-05 손민수		C-05 조미희		H-05 HUR Min Sup	L-03(초) KIM Hongsu	B-09 신선영	D-05 YANG Seolun		
14:45-15:00			E-06 김성인						B-10 백종현	D-06 KIM Minkook		
15:00-15:15			E-07 이승현		C-07 WOO SUNG Park			L-04(초) 금용연	B-11 남시영	D-07 CHOI Jin-Ho		
15:15-15:30									B-12 김도훈	D-08 KIM Keun Su		
15:30-15:45												

# 2009. 10. 21. 수

	301	302	601	602	603	604	605	606	607	컨벤션 I	컨벤션 II	컨벤션 III
15:45-16:00			E-08 HAM Jinhee		C-08(초) RHO Mamque		H-06(초) KIM Kui Young	L-05(초) SUH In-Saeng	B-13(초) UOZUMI Satoru	D-09 정성철 D-10 SONG Sanghoon	A-01 이정환	PC-01(초) STANTON C. J.
16:00-16:15			E-09 KANG Jooheon		C-09(초) FUKUSHIMA Kenji		H-07(초) OH Y.K.	L-06(초) KIM Kyeong Ja	B-14(초) 이재승	D-11 SONG Inkyung D-12 SHIN Bong Gyu	A-02 민경남	PC-02(초) 이용탁
16:15-16:30			E-10 양형우		C-10(초) OZAKI Sho		H-08(초) NAM S. H.	L-07(초) 박 일홍	B-15(초) 이명재	D-13 장윤희 D-14 박찬현	A-03 이우영	PC-03 윤재호
16:30-16:45			E-11 최아정		C-11 유충열		H-09(초) 황용석	L-08(초) 김순옥	B-16 고병록 B-17 하현정	D-15 김동유 D-16 황영훈	A-04 이종태	PC-04 정덕영 PC-05 박수현
16:45-17:00			E-12 SHAHID Muhammad		C-12 YAKHSHEV U.							
17:00-17:15			E-13 안세정		C-13 KIM Kyung-il							
17:15-17:30			E-14 YUN Chan Ki			A-05 이기억						
17:30-17:45						A-06 김기현						
17:45-18:00			A-18 정창욱									
18:00-18:15			A-19 정중훈									
18:15-18:30			A-20 조성래									
			A-21 이정일									

# 2009. 10. 22. 목

	301	302	601	602	603	604	605	606	607	컨벤션 I	컨벤션 II	컨벤션 III
09:00-09:15	E-15 SUNDARAY B.	DF-01(초) JANG Jae Hyuck		K-01(초) KIM hyun-tak				L-09(초) 남지우	BF-01(초) CHOI Sookyung	PA-01(초) HONG Seung-Woo		
09:15-09:30	E-16 YOO Jai Seung											
09:30-09:45	E-17 LEE Seung-ho	DF-02(초) 노도영		K-02(초) KANG Bo Soo				L-10(초) LIM Heuljin	BF-02(초) OLSEN Stephen Lars	PA-02(초) SPROUSE Gene D.		
09:45-10:00	E-18 SONG Wooseok											
10:00-10:15	E-19 김명수	DF-03(초) 최은진		K-03(초) LI Tiefu				L-11(초) 이직	BF-03(초) KO Pyungwon	PA-03(초) YU Dai-Hyuk		
10:15-10:30	E-20 JANG Eunsoo											
10:30-10:45	E-21 정혜경	DF-04(초) 박용섭		K-04(초) 정규호				L-12(초) NA Sung-Ho	BF-04(초) 김현철	PA-04(초) HONG Byungsik		
10:45-11:00												

	301	302	601	602	603	604	605	606	607	컨벤션 I	컨벤션 II	컨벤션 III
11:00-11:15										PA-05(초) STEIGENBERGER Uschi	A-07 임지순	
11:15-11:30	E-22 CHO sanghee	D-17 최선명	F-01(초) GHIM Cheol-Min	KF-01(초) 노태원	I-01(초) 박주윤	G-01 박병윤	H-10 LIPING Zhu	L-13 KIM Kyungmin	BF-05(초) TANIDA Kiyoshi			
11:30-11:45	E-23 CHA Wonsuk	D-18 PARK Sunghun				G-02 최재형	H-11 HAN Hyunsun	L-14 조희석				
11:45-12:00	E-24 정보라	D-19 김규봉	F-02(초) 이덕선	KF-02(초) 백인규	I-02(초) 유태준		H-12 이동렬	PARK Dongho	BF-06(초) 안정근	PA-06(초) KADI Yacine	A-08 이후중	
12:00-12:15	E-25 홍영기	D-20 김지희				G-03 정용욱	H-13 KIM Hyunseok	L-16 OH Changheon		PA-07(초) 한인식		
12:15-12:30	E-26 BAEK Sujin	D-21 KIM Young Duck	F-03(초) 박주용	KF-03(초) HWANG Cheol Seong	I-03(초) 김인식	G-04 최승하	H-14 IHSAN Aamir	L-17 이혜영	BF-07(초) 윤용재			
12:30-12:45	E-27 KANG Sungjin	D-22 정재승			I-04(초) 추형규	G-05 노유정	H-15 KIM Min-Seok					
12:45-13:00	E-28 PARK Sora	D-23 CHOI In Sung	F-04(초) KIM Sungyun	KF-04(초) JEONG Doo Seok	I-05(초) 성재희	G-06 이용인						
13:00-13:15		D-24 CHOI Jaewu										
13:15-13:30												
13:30-13:45	E-29(초) 이상현	D-25 LEE Hyungjun	F-05 김민수	K-05(초) 임상범	I-06 LEE Soo-Young	G-07 이을수		L-18 KIM J.E.	B-18 KIM Seyong		PB-01(초) HUANG D. J.	PC-06(초) PARK Sangwook
13:45-14:00		D-26 KIM Min-Kook	F-06 KOH Dong-Wook		I-07 PHUNG Duy Khuong	G-08 윤정화		L-19 전진아	B-19 남수현			
14:00-14:15	E-30 김상환	D-27 김상민	F-07 JEON Chanil	K-06(초) 박래만	I-08 김수남	G-09 정민영		L-20 정수민	B-20 함승우	PA-08(초) NAKAMURA Takashi	PB-02(초) KOO Tae-Yeong	PC-07(초) 이정호
14:15-14:30	E-31 강보영	D-28 JANG Seunghun	F-08 JEONG Seong Min					L-21 나고운	B-21 LEE Jae Yong		PB-03(초) 허남정	
14:30-14:45	E-32 강보영	D-29 노현호	F-09 SHIN Jaehoh	K-07(초) LEE Hyo Jong	I-09 박영미	G-10 오광택		L-22 서정은	B-22 KIM Jihun	PA-09(초) KIM Wooyoung	PB-04(초) JEON Gun Sang	PC-08(초) 윤선진
14:45-15:00	E-33 정용우	D-30 장정원	F-10 KIM Bongsoo		I-10 김규환			L-23 정애라	B-23 허지행			
15:00-15:15	E-34 장정훈	D-31 JU chanjong	F-11 AHN Kang-Hun	K-08(초) THOMAS Kalarikad Jonah		G-11 이민경			B-24 BAE Kyu Jung	PA-10(초) CHEOUN Myung-Ki	PB-05 CHUN Sae Hwan	PC-09(초) 최 용우
15:15-15:30	E-35 변준석	D-32 이우람	F-12 BAEK Yongjoo							PA-11(초) KWON Young Kwan	PB-06 GO Ara	PC-10(초) YOON CHUL OH
15:30-15:45												

# 2009. 10. 22. 목

	301	302	601	602	603	604	605	606	607	컨벤션 I	컨벤션 II	컨벤션 III	
15:45-16:00	E-36 KIM JinBae	D-33 KIM GWANG-HEE	F-13 HWANG Sungmin						B-25 이주희		PB-07(초) TANAKA Hidekazu	PC-11(초) KIM Dongkyun	
16:00-16:15	E-37 PARK HONGWOO	D-34 HAN Jinhee	F-14 이규민						B-26 이상준	PA-12(초) SATOU Yoshiteru		PC-12(초) LEE Soonil	
16:15-16:30	E-38 이신범	D-35 정고은	F-15 최지혜						B-27 백광윤		PB-08(초) NOH Tae W.	PC-13(초) 김한기	
16:30-16:45	E-39 박민지	D-36 KIM T. H.	F-16 민병준						B-28 고재우	PA-13(초) MOON Changbum	PB-09(초) KIM Bog G.	PC-14 INAMDAR A. I.	
16:45-17:00	E-40 SHAKIR Imran	D-37 YANG Sang Mo	F-17 조원국						B-29 이효상	PA-14(초) 윤진희	PB-10(초) 박순용	PC-15 JEONG Ah Reum	
17:00-17:15	E-41 고향주	D-38 신영한	F-18 KIM Sang-Woo	KT-01(초) 임현식				원자 및 분자물리학 분과회 총회	B-30 김정현	PA-15(초) MOON Jun Young	PB-11 CHOI Woo Seok		
17:15-17:30	E-42 김지현	D-39 OH Young Jun	F-19 KIM Seongjin		B-31 LEE Soohyung								
17:30-17:45		D-40 KIM Jinwoong	통계물리학 분과회 총회						B-32 김정현		PB-12 KIM Tae-Suk		
17:45-18:00													
18:00-18:15										A-09 김항배			
18:15-18:30													
18:30-18:45													
18:45-19:00										A-10 이종필			
19:00-19:15													
19:15-19:30													
19:30-19:40													

2009. 10. 23. 금

	301	302	601	602	603	604	605	606	607	컨벤션 I	컨벤션 II	컨벤션 III
09:00-09:15	E-43 BYUN Kyung-Eun	D-41 YOON Sunghyun		K-09(초) HUH Chul	C-14(초) SAITO Take R.	C-21(초) TENREIRO Claudio	H-16 민선홍	J-01 문결	B-33 양병수			
09:15-09:30	E-44 SHAKIR Imran	D-42 LEE Chang Hoon	F-21 LEE Kwang-Sei				H-17 배효원	J-02 유예진	B-34 신승수			
09:30-09:45	E-45 이리미	D-43 JUNG Hyunok	F-22 조항현	K-10(초) CHOI Yang-Kyu	C-15(초) YASUI Shigehiro	C-22 RAHMAN Md. Shakilur	H-18 류진영	J-03 이현준	B-35 김성현			
09:45-10:00	E-46 HONG Seong Jong	D-44 TSOGBADRAKH N.	F-23 HA Meesoan		C-16 KIM Eunhee	C-23 문명환	H-19 김용희	J-04 장광훈	B-36 백승록			
10:00-10:15	E-47 이용재	D-45 CHO Sung Un	F-24 YANG Jae-Suk	K-11(초) NA Jong ho	C-17 황상훈	C-24 이주한	H-20 김선자	J-05 임신혁	B-37 CHOI Suyong			
10:15-10:30	E-48 유정선	D-46 YANG Chanuk	F-25 KWAK Wooseop	K-12 제구출	C-18 이종화	C-25 이민규		J-06 ZHUO Z. C.	B-38 공대정			
10:30-10:45	E-49 강봉근	D-47 YI Su Do	F-26 LEE Min-Ho	K-13 김상근	C-19 최봉혁	C-26 WANG Taofeng		J-07 BANG Jeongho	B-39 CHUNG J.	DF-05 LEE Sung-IK		
10:45-11:00		D-48 추성민	F-27 JOO Keehyoung	K-14 KANG HYON CHOL	C-20 김성준	C-27 TSHOO K.H.		J-08 LIM James		DF-06 KHIM Seunghyun		
11:00-11:15										DF-07 GHIM Jin Soo		
11:15-11:30	E-50 LEE Seungran	D-49 KIM Y.K		KF-05(초) CHOI W.K.				J-09 김경락		DF-08 MOON jisoo	PB-13(초) KIM Jun Sung	A-11 김광주
11:30-11:45	E-51 김고은	D-50 LEE SUN YOUNG						J-10 LEE Sangkyung		DF-09 MOON Chang-Youn	PB-14(초) CHOI Kwang-Yong	A-12 서민수
11:45-12:00	E-52 MARATHE S.	D-51 박창열		KF-06(초) 박철홍				J-11 이민호		DF-10 PARK Jewook	PB-15(초) 박두선	
12:00-12:15	E-53 임성일	D-52 박은성								DF-11 SONG Yoo-Jang		A-13 김성호
12:15-12:30	E-54 조덕용	D-53 KIM Chul		KF-07(초) 김상식						DF-12 LEE Nayoung	PB-16(초) KIM Ki-Seok	
12:30-12:45	E-55 임규옥	D-54 권용경									PB-17(초) NOH Han-Jin	A-14 강응철
12:45-13:00	E-56 이경재	D-55 송동준		KF-08(초) PARK Won Il							PB-18(초) CHUNG Jae-Ho	
13:00-13:15												

2009. 10. 23. 금

	301	302	601	602	603	604	605	606	607	컨벤션 I	컨벤션 II	컨벤션 III
13:15-13:30												
13:30-13:45			F-28 SON Seung-Woo		C-28(초) PARK Naewoong	C-35 박규준		D-56 이남기		DF-13 LEE Hyun-Sook		A-15 김연수
13:45-14:00			F-29 KIM Pan-Jun		C-36 NI Andrey	C-36 NI Andrey		D-57 LEE Sanghwa		DF-14 LEE Bumsung		
14:00-14:15			F-30 KIM Song-Ju		C-29(초) PARK Tae-Sun	C-37 조화연		D-58 LEE Jinwoo		DF-15 CHOI Ki-Young		A-16 SHIM Kyu-Min
14:15-14:30			F-31 윤창근		C-30 RYU Huiyoung	C-38 문봉선		D-59 BAE Sangsu		DF-16 CHOI Eun-Mi		
14:30-14:45			F-32 CHO Young Sul		C-31 류선영	C-39 박진용		D-60 KIM Sunghyun		DF-17 HONG J. B.		A-17 김대현
14:45-15:00			F-33 LEE Hyun Keun		C-32 SHIN JaeWon	C-40 YI JunGyu		D-61 JEON Yoonnam		DF-18(초) 황경식		
15:00-15:15			F-34 LIM Woochang		C-33 류상욱	C-41 이재기		D-62 CHA Seon Cheol				
15:15-15:35					C-34 이주환	C-42 안성환		D-63 LEE Eun-Cheol		DF-19 OH Hyungju		

## 등록 및 발표장 안내

### 1. 초록집 배부

발표논문의 초록집은 등록하신 분에게 배포합니다. 사전등록을 하신 경우 별도의 창구에서 초록집과 명찰을 수령하게 됩니다.

### 2. 등록비 및 회비

구 분		금 액	구 분		금 액
등록비	평의원·정회원	80,000원	구독료 (평의원·정회원)	1종류 구독	70,000원
	학생회원	50,000원		2종류 구독	110,000원
	비회원 일반	150,000원		3종류 구독	150,000원
	비회원 학생	70,000원	구독료 (학생회원)	1종류 구독	35,000원
회 비	평의원	70,000원		2종류 구독	55,000원
	정회원	40,000원		3종류 구독	75,000원
	학생회원	20,000원	입회비	신입회원	10,000원

### 3. 발표장

분과명	구두발표장	포스터발표장	학회 주관 행사
입자물리학분과	607호	포스터 (전시장)	임시총회(평의원회): 컨벤션 II 평의원 리셉션: 컨벤션 III 대중강연: 컨벤션 I 산학연 특별세션: 컨벤션 I 신진교수 세션: 601-602호 Pioneering 세션: 컨벤션 I, II, III KPS-AKPA: 604호 Open KIAS: 컨벤션 II ADD 특별세션: 컨벤션 III
원자핵물리학분과	603호, 604호, 607호		
응집물질물리학분과	302호, 606호, 컨벤션 I		
응용물리학분과	301호, 601-602호		
통계물리학분과	601호		
물리교육분과	604호		
플라스마물리학분과	605호		
광학 및 양자전자학분과	603호		
원자 및 분자물리학분과	606호		
반도체물리학분과	602호		
천체물리학분과	606호		

### 4. 포스터 발표

회원들이 시간적 여유를 가지고 포스터를 관람할 수 있도록 포스터는 지정된 포스터 세션 시작 30분 전에 미리 부착하여야 합니다. 또한, 포스터 세션 시작 후 1시간 동안은 공동저자 중 최소한 1명이 자리를 지키도록 의무화되어 있습니다. 그 시간 동안에는 자신의 포스터 앞에서 회원들의 질문에 답할 수 있도록 해주시기 바랍니다.

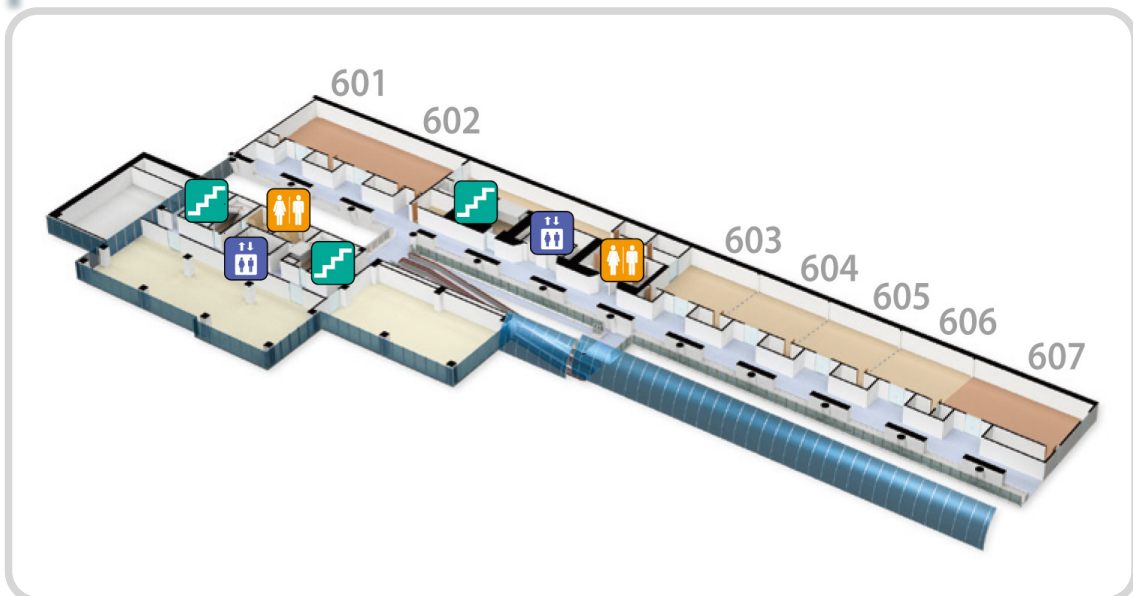
- 우수발표상 포스터부문에 후보로 선정되신 회원은 특히 자리를 지켜 주시기 바랍니다. 우수발표상에 선정이 되더라도 자리에 없는 경우 수상이 취소됩니다.
- 다음 발표자를 위하여 발표가 종료된 후 1시간 이내에 포스터를 수거하여 주실 것도 부탁드립니다.

### 5. 우수발표상 후보 논문은 초록집에 \*로 표시되어 있습니다.

# 3F



# 6F



## 특별세션 안내

### A1 산학연 특별세션: 산학연 협력 현황 및 활성화 방안

■ 일시: 10월 21일(수) 15:45 ■ 장소: 컨벤션 II ■ 좌장: 오차환 (한양대)

본 산학연 특별세션에서는 국내 대학 및 정부출연연구소에서 특별히 산학연 협력을 위하여 다양한 활동을 전개해오신 전문가들을 모시고 대학 및 정부출연연구소에서 산업체와의 상호협력을 위하여 진행해온 인력 네트워크 구성, 특허관리 및 기술이전 현황을 파악하고, 토론을 통해 향후 산·학·연의 상호 협력을 더욱 증대할 수 있는 방안을 모색하고자 한다.

[A-01] 한국기계연구원부설 재료연구소의 기업지원방향: 이정환(산업기술지원본부, 한국기계연구원)

[A-02] KIST 기술이전, 현황과 과제: 민경남(KIST 기술사업부)

[A-03] 지식기반시대의 산학협력 선진화 방안: 인력양성을 중심으로: 이우영(대학산업기술지원단, 연세대학교)

[A-04] 대학과 기업 간의 산학협력 모델: 이종태(한국대학기술이전협회(KAUTM), 동국대학교)

### A2 KPS-AKPA Session

■ Date: 17:00-18:15, Oct. 21(Wed.), 2009 ■ Place: CECO Room 604

Session Chair: Young Soon Kim (Professor of Myoung Ji University and Chairperson of Women Affairs, KPS)

Vice Chair: Ran Ju Jung (Professor of Kwang Woon University, Associate Secretary of KPS)

17:00-17:05	Opening Remark	Young Pak Lee (Professor of Hanyang Univ., President of KPS)
17:05-17:15	Welcoming Address	Sook-II Kwun (Professor Emeritus of Seoul National Univ., Former President of KPS, Former Minister of Science and Technology of Korea)
17:15-17:40	Shell Model And The Mass Asymmetry of Fission Fragments	Kiuck Lee (Professor emeritus of Marquette Univ., Former President of AKPA)
17:40-18:05	Science and Technology Infra-structure in Democratic People's Republic of Korea and Current Status of Nuclear Weapon Development Program	Kinney H. Kim (Professor of NC Central Univ., Former President of AKPA)
18:05-18:10	Closing Remark	Chairperson
18:10-18:15	Photosession	

### A7 신진교수세션

■ 일시: 10월 21일(수) 17:45 ■ 장소: 601-602호 ■ 진행: 홍석륜 총무담당 부실무이사 (세종대)

시간	내용 또는 강연제목	담당 또는 강연자
17:45~17:50	인사말	정세영(총무담당 실무이사, 부산대)
17:50~18:00	연구과제 일정 소개 및 연구팀 구성경험 소개	정창욱(한국외국어대 전자물리학과)
18:00~18:10	파이오니어링 심포지움 소개 및 soliciting of new proposals	정중훈(인하대 물리학과)
18:10~18:20	응집물리 관련분야 분과활동 소개	조성래(응집물리분과간사, 울산대 물리학과)
18:20~18:30	고에너지물리 관련분야 분과활동 소개	이정일(입자물리분과간사, 고려대 물리학과)

# 구두발표논문 시간표



[A1] 산학연 특별세션: 산학연 협력 현황 및 활성화 방안

장 소 : 컨벤션 II

10월 21일(수) 15:45 - 17:25

좌 장 : 오차환(한양대)

- A-01[15:45-16:10] 한국기계연구원부설 재료연구소의 기업지원방향: 이 정환(산업기술지원본부, 한국기계연구원부설 재료연구소)  
A-02[16:10-16:35] KIST 기술이전, 현황과 과제: 민 경남(KIST 기술사업부 성과확산실)  
A-03[16:35-17:00] 지식기반시대의 산학협력 선진화 방안: 인력양성을 중심으로: 이 우영(대학산업기술지원단)  
A-04[17:00-17:25] 대학과 기업 간의 산학협력 모델: 이 종태(한국대학기술이전협회)

[A2] KPS-AKPA 특별세션

장 소 : 604

10월 21일(수) 17:00 - 18:15

좌 장 : 김영순(명지대)

- [17:00-17:05] 인사말: 이 영백(물리학회 회장, 한양대)  
[17:05-17:15] 환영사: 권 숙일(전 과기부 장관, 전 물리학회 회장, 서울대)  
A-05[17:15-17:40] SHELL MODEL AND THE MASS ASYMMETRY OF FISSION FRAGMENTS: LEE Kiuck, LEE Linda(419 Bosworth Lane)  
A-06[17:40-18:05] Science and Technology Infra-structure in Democratic People's Republic of Koreaand Current Status of Nuclear Weapon Development Program: KIM Kinney H.(Professor of NC Central University, Former President of AKPA)

[A7] 신진교수 세션

장 소 : 601-602

10월 21일(수) 17:45 - 18:30

좌 장 : 홍석륜(세종대, 총무담당부실무이사)

- [17:45-17:50] 인사말: 정 세영(부산대, 총무담당 실무이사)  
A-18[17:50-18:00] 연구과제 일정 소개 및 연구팀 구성경험 소개: 정 창욱(한국외대 전자물리학과)  
A-19[18:00-18:10] 파이오니어링 심포지움 소개 및 soliciting of new proposals: 정 종훈(인하대 물리학과)  
A-20[18:10-18:20] 응집물리 관련분야 분과활동 소개: 조 성래(응집물리분과간사, 울산대 물리학과)  
A-21[18:20-18:30] 고에너지물리 관련분야 분과활동 소개: 이 정일(입자물리분과간사, 고려대 물리학과)

[A3] Open KIAS

장 소 : 302

10월 22일(목) 11:00 - 12:30

좌 장 : 김재완(고등과학원)

- A-07[11:00-11:45] 수소저장을 위한 수소 분자와 금속 간 상호작용의 규명: 임 지순(서울대)  
A-08[11:45-12:30] Phase-coherent Electrical Transport in Mesoscopic Dimensions: 이 후종(POSTECH)

[A4] 대중강연

장 소 : 컨벤션 I

10월 22일(목) 18:00 - 19:40

좌 장 : 김원정(창원대)

- A-09[18:00-18:50] 빅뱅이론과 LHC: 가장 작은 세계가 가장 큰 세계를 밝힌다.: 김 항배(한양대)  
A-10[18:50-19:40] 신의 입자를 찾아서: 이 종필(고등과학원)

[A5] 물리학과 국방과학 기술 I

장 소 : 컨벤션 III

10월 23일(금) 11:00 - 13:00

좌 장 : 송소영(국방과학연)

- A-11[11:00-11:30] 고압물리에서 다이아몬드 앤빌 셀의 응용 (Application of Diamond Anvil Cells on High-pressure Physics): 김 광주, 고 영호(국방과학연구소)  
A-12[11:30-12:00] 강유전체를 적용한 고밀도 전자방출 소스 연구 (Study on High Current Electron Emission Source Using Ferroelectric Materials): 서 민수(국방과학연구소)  
A-13[12:00-12:30] 플라즈마와 전자기력의 응용 연구 (Researches on the Application of Pulsed Plasma and Electromagnetic Forces): 김 성호, 김 진성, 양 경승, 이 병하(국방과학연구소)

A-14[12:30-13:00] 군사 분야 레이저 기술의 응용 현황과 개발 동향: 원격 정보탐지에서 미사일방어까지 (Applications and Trends of Laser Technology for Military Use: Remote Sensing to Missile Defense): 강 응철, 이 정환, 최 현진(국방과학연구소)

## [A6] 물리학과 국방과학 기술 II

장 소 : 컨벤션 III

10월 23일(금) 13:30 - 15:00

좌 장 : 송소영(국방과학연)

- A-15[13:30-14:00] 전자광학/열상센서 기술발전과 장비 소개(Introduction of Technical Development and Equipment for the ElectroOptic/InfraRed Sensor): 김 연수, 김 현숙, 김 창우(국방과학연구소)
- A-16[14:00-14:30] 현대 물리학에 의한 항법장치 기술의 발전 (The Development of Navigation Technologies by Modern Physics): SHIM Kyu-Min(국방과학연구소)
- A-17[14:30-15:00] 바다, 국방과학기술과 물리 (Physics in Maritime Defence Technology): 김 대연, 박 병욱, 전 재진, 김 영규(국방과학연구소)

**[PA1] Pioneering Symposium: 방사성 동위원소빔을 이용한 첨단 연구**

장 소 : 컨벤션 I

10월 22일(목) 09:00 – 10:40

좌 장 : 조동현(고려대)

PA-01(초)[09:00-09:20] Introduction to Heavy Ion Accelerator KoRIA: HONG Seung-Woo(성균관대)

PA-02(초)[09:20-10:00] Atomic Physics with Rare Isotope Beams: SPROUSE Gene D.(Stony Brook University (on leave) and Editor in Chief, American Physical Society)

PA-03(초)[10:00-10:20] 2-Stage MOT and Optical Lattice Trap of Yb atoms: YU Dai-Hyuk, PARK Chang Yong, LEE Won-Kyu, MOON Jongchul, KIM Eok Bong, LEE Sun Kyung(Korea Research Institute of Standards and Science)

PA-04(초)[10:20-10:40] Opportunity for Nuclear Symmetry Energy in Future Rare Isotope Accelerator in Korea: HONG Byungsik(Korea University)

**[PA2] Pioneering Symposium: 방사성 동위원소빔을 이용한 첨단 연구**

장 소 : 컨벤션 I

10월 22일(목) 11:00 – 12:30

좌 장 : 박제근(성균관대)

PA-05(초)[11:00-11:40] ISIS Facility – Past Achievements and Future Prospects: STEIGENBERGER Uschi(ISIS Facility, Rutherford Appleton Laboratory)

PA-06(초)[11:40-12:10] Science Opportunities in HIE-ISOLDE: KADI Yacine(Sungkyunkwan University &amp; CERN)

PA-07(초)[12:10-12:30] Explosive Nuclear Astrophysics using Radioactive Ion Beams: 한 인식(이화여대)

**[PA3] Pioneering Symposium: 방사성 동위원소빔을 이용한 첨단 연구**

장 소 : 컨벤션 I

10월 22일(목) 14:00 – 15:40

좌 장 : 김용균(한양대)

PA-08(초)[14:00-14:40] Exotic Nuclear Structures Probed by Breakup Reactions: NAKAMURA Takashi(Tokyo Institute of Technology)

PA-09(초)[14:40-15:00] Probing Nuclear Spin Structure with Radioactive Ion Beams and Polarized Targets: KIM Wooyoung(Department of Physics, Kyungpook National University)

PA-10(초)[15:00-15:20] Nucleosynthesis by the Radioactive Isotope Beam and Origin of Nuclear Abundance: CHEOUN Myung-Ki(Soongsil Univ.), KIM Kyungsik(Korea Aviation Univ.), HA Eunja, RYU Chungryeol(Soongsil Univ.)

PA-11(초)[15:20-15:40] Recent activities in nuclear astrophysics at CRIB: KWON Young Kwan, LEE Chun Sik(Department of Physics, Chung-Ang University), KUBONO Shigeru(Center for Nuclear Science (CNS), University of Tokyo)

**[PA4] Pioneering Symposium: 방사성 동위원소빔을 이용한 첨단 연구**

장 소 : 컨벤션 I

10월 22일(목) 16:00 – 17:30

좌 장 : 방형찬(서울대)

PA-12(초)[16:00-16:30] Invariant mass spectroscopy of  $^{19,17}\text{C}$  and  $^{14}\text{B}$  using proton inelastic and charge-exchange reactions: SATOU Yoshiteru(Seoul National University, Department of Physics and Astronomy)

PA-13(초)[16:30-16:50] Nuclear Structure Physics using Heavy-Ion Beams: MOON Changbum(Hoseo University, Department of Display Engineering)

PA-14(초)[16:50-17:10] Is there evidence of simple relationship between measured yrast energies in even-even nuclei?: 윤 진희, 김 두영, 차 동우(인하대)

PA-15(초)[17:10-17:30] Elastic scattering of  $^{26}\text{Si} + p$  using a radioactive ion beam of  $^{26}\text{Si}$ : MOON Jun Young, LEE Chun Sik, LEE Ju Hahn, YUN Chong Cheoul(Department of Physics, Chung-Ang Univ.), KIM Jong Chan, YOUN Min Young(Department of Physics, Seoul National Univ.), KUBONO Shigeru(CNS, Univ. of Tokyo), TERANISHI Takashi(Department of Physics, Kyushu Univ.)**[PB1] Pioneering Symposium: 복잡계 물질의 이머전트 현상**

장 소 : 컨벤션 II

10월 22일(목) 13:30 – 15:30

좌 장 : 박순용(중앙대)

PB-01(초)[13:30-14:00] Multiferroic Nanoregions and a Memory Effect in Cupric Oxide: HUANG D. J.(National Synchrotron Radiation Research Center, Taiwan)

PB-02(초)[14:00-14:20] Electric Polarization in Ferrimagnetic Cubic Spinel  $(\text{Co,Mn})_3\text{O}_4$ : KOO Tae-Yeong(POSTECH, Pohang Accelerator

Laboratory), KANG Sun-Hee, KIM Ill-Won(University of Ulsan, Department of Physics), YOON Hee-Jeong (POSTECH, Department of Physics)

- PB-03(초)[14:20-14:40] Antiferroelectricity underlies the magnetodielectric effect and the huge magnetostriction in rare-earth iron garnets: 허 남정, 송 기명, 박 영안, 이 경동, 윤 병길(인하대), 정 명화(서강대), 조 재훈(KBSI), 정 종훈(인하대)
- PB-04(초)[14:40-15:00] Magnetic-field-induced critical end point in multiferroics: JEON Gun Sang(Seoul National University), PARK Jin Hong(Sungkyunkwan University), KIM Jae Wook, KIM Kee Hoon(Seoul National University), HAN Jung Hoon(Sungkyunkwan University)
- PB-05[15:00-15:15] Realization of Giant Magnetoelectricity in Helimagnets: CHUN Sae Hwan, CHAI Yi Sheng, OH Yoon Seok, JAISWAL-NAGAR Deepshikha, HAAM So Young, KIM Ingyu, LEE Bumsung, NAM Dong Hak, KIM Kee Hoon(XMPL & FPRD, Department of Physics and Astronomy, Seoul National University), KO Kyung-Tae, PARK Jae-Hoon(Department of Physics & Division of Advanced Materials Science, POSTECH), CHUNG Jae-Ho(Department of Physics, Korea University)
- PB-06[15:15-15:30] The One-dimensional Hubbard Model in the Presence of Peierls Modulation: GO Ara, JEON Gun Sang (Department of Physics and Astronomy, Seoul National University)

## [PB2] Pioneering Symposium: 복잡계 물질의 이머전트 현상

장 소 : 컨벤션 II

10월 22일(목) 15:45 - 17:45

좌 장 : 정재호(고려대)

- PB-07(초)[15:45-16:15] Controlled Fabrication of Complex Oxide Epitaxial Artificial Nano-wire and Nano-dot Structures and Their Giant Properties: TANAKA Hidekazu(The Institute of Scientific and Industrial Research, Osaka University)
- PB-08(초)[16:15-16:35] Fundamental Thickness Limit of Itinerant Ferromagnetic SrRuO<sub>3</sub> Thin Films: Control of Stoner Magnetism?: NOH Tae W., CHANG Young Jun, KIM Choong H., PHARK S.-H., KIM Y.S., YU J.(Seoul National Univ.)
- PB-09(초)[16:35-16:55] Pulsed Laser Deposition of Perovskite Manganites and Titanates Heterostructures: KIM Bog G., KIM Bongju, KWON Daeyoung(Dept. of Physics, Pusan National University), KOZUKA Yusuke, HIKITA Yasuyuki, HWANG Harold Y.(Dept. of Advanced Materials Science, University of Tokyo)
- PB-10(초)[16:55-17:15] Microscopic evidence of strain-enhanced ferromagnetic state in LaCoO<sub>3</sub> films: PARK Soonyong(Department of Physics, Chung-Ang University, Rutgers Center for Emergent Materials & Department of Physics and Astronomy, Rutgers University, USA), FREELAND J. W.(Rutgers Center for Emergent Materials & Department of Physics and Astronomy, Rutgers University, USA), MA J. X., SHI J.(Advanced Photon Source, Argonne National Laboratory, USA), WU Weida(Rutgers Center for Emergent Materials & Department of Physics and Astronomy, Rutgers University, USA)
- PB-11[17:15-17:30] Strong Electron-Phonon Coupling as the Origin of Enhanced Thermoelectric Properties in Nb:SrTiO<sub>3</sub>/SrTiO<sub>3</sub> Superlattices: CHOI Woo Seok(ReCOE & FPRD, Dept. of Phys. and Astro., Seoul Nat'l Univ.), OHTA Hiromichi(Graduate School of Engr., Nagoya Univ., Japan and PRESTO, Japan Sci. and Tech. Agency, Japan), MOON Soon Jae(ReCOE & FPRD, Dept. of Phys. and Astro., Seoul Nat'l Univ.), LEE Yun Sang(Dept. of Phys., Soongsil Univ.), NOH Tae Won(ReCOE & FPRD, Dept. of Phys. and Astro., Seoul Nat'l Univ.)
- PB-12[17:30-17:45] Anomalous spin polarization in graphene under Rashba spin-orbit coupling: KIM Tae-Suk, HWANG Chanyong (KRISS)

## [PB3] Pioneering Symposium: 복잡계 물질의 이머전트 현상

장 소 : 컨벤션 II

10월 23일(금) 11:15 - 13:15

좌 장 : 허남정(인하대)

- PB-13(초)[11:15-11:35] Exploring the phase diagram of Fe-pnictides  $A\text{Fe}_2\text{As}_2$  ( $A = \text{Ca}, \text{Sr}, \text{Ba}, \text{and Eu}$ ): KI M Jun Sung(Department of Physics, Pohang University of Science and Technology), KIM Seunghyun(Department of Physics and Astronomy, Seoul National University), NA Sewoong, EOM Manjin(Department of Physics, Pohang University of Science and Technology), LAW Joseph, KREMER Reinhard(Max-Planck-Institut für Festkörperforschung, Germany), KIM Kee Hoon(Department of Physics and Astronomy, Seoul National University)
- PB-14(초)[11:35-11:55] Raman scattering measurements of the undoped and underdoped Fe-As superconductors: CHOI Kwang-Yong (Physics Department, Chung-Ang University)
- PB-15(초)[11:55-12:15] Origin and Consequence of Quantum Criticality in the Heavy Fermion Compound CeRhIn<sub>5</sub>: 박 두선(성균관대), THOMPSON Joe(Los Alamos National Laboratory)
- PB-16(초)[12:15-12:35] Beyond the spin-fluctuation mechanism in the strong coupling limit : Kondo induced multi-gap superconductivity

in the slave-fermion theory: KIM Ki-Seok(APCTP)

PB-17(초)[12:35-12:55] Anisotropic High Conductivity of Delafossite PdCoO<sub>2</sub> Investigated by ARPES and Polarization-dependent XAS: NOH Han-Jin, JEONG Jinwon, JEONG Jinhwan, SUNG Hojin, PARK Kyoung Ja, CHO En-Jin(Dep. of Physics, Chonnam National University), KIM Hyeong-Do, KIM Jae-Young(Pohang Accelerator Laboratory, POSTECH), KIM Sung Baek, KIM Kyoo, MIN B. I.(Dep. of Physics, POSTECH)

PB-18(초)[12:55-13:15] Orbital order and spin fluctuations in geometrically frustrated ferrimagnetic MnV<sub>2</sub>O<sub>4</sub> studied by neutron scattering: CHUNG Jae-Ho(Department of Physics, Korea University)

### [PC1] Pioneering Symposium: 광전압 물질과 디바이스 물리

장 소 : 컨벤션 III

10월 21일(수) 15:45 - 17:45

좌 장 : 김동욱(이화여대)

PC-01(초)[15:45-16:25] Semiconductor Optics: Applications to Photovoltaics and Solid State Lighting: STANTON C. J.(University of Florida, Department of Physics)

PC-02(초)[16:25-16:45] High-efficiency GaInP/LCM-GaInP/GaAs Triple-junction Solar Cells with Antireflective Subwavelength Structures: 이 용탁(광주과학기술원)

PC-03[16:45-17:05] CIGS Thin Film Solar Cells : Current Status and Key Issues: 윤 재호(한국에너지기술연구원)

PC-04[17:05-17:25] Chemical Solution Syntheses of Cu-In-Ga-Se Thin Films for Photovoltaic Cells: JUNG Duk-Young(Department of Chemistry, Institute of Basic Sciences and Sungkyunkwan Advanced Institute of NanoTechnology, Sungkyunkwan University)

PC-05[17:25-17:45] Characterizations of Polar- and Nonpolar-GaN Schottky Junctions by Conductive Atomic Force Microscopy: PHARK Soo-Hyon(Department of Physics and NREC, Ewha Womans University), KIM Hogyoung(College of Humanities and Sciences, Hanbat National University), SONG Keun Man, KANG Phil Geun, SHIN Heung Soo(Korea Advanced Nano Fab Center), KIM Haeri, KIM Dong-Wook(Department of Physics and NREC, Ewha Womans University)

### [PC2] Pioneering Symposium: 광전압 물질과 디바이스 물리

장 소 : 컨벤션 III

10월 22일(목) 13:30 - 15:30

좌 장 : 조준식(에너지기술연)

PC-06(초)[13:30-14:10] Third generation solar cells: all-silicon tandem solar cells: PARK Sangwook, CONIBEER Gavin, PEREZ-WURFL I., HUANG S.J., SONG D., CHO Eun-Chel, KÖNIG D., GENTLE A., HAO X.J., SO Y.H., GREEN Martin A.(University of New South Wales, ARC Photovoltaics Centre of Excellence)

PC-07(초)[14:10-14:30] Next-generation solarcells using Si and Si<sub>1-x</sub>Ge<sub>x</sub> nano- and microwire arrays: 이 정호(한양대)

PC-08(초)[14:30-14:50] ZnO-Based Transparent Conducting Oxide for Thin Film Solar Cells: 윤 선진, 김 준관, 임 정욱, 이 재민(한국전 자동차연구원)

PC-09(초)[14:50-15:10] Crystalline (bulk) and thin-film Si solar cells: 최 용우(LG 전자기술원)

PC-10(초)[15:10-15:30] Measurement Techniques and Instruments for Solar Cells: YOON CHUL OH(McScience Inc.)

### [PC3] Pioneering Symposium: 광전압 물질과 디바이스 물리

장 소 : 컨벤션 III

10월 22일(목) 15:45 - 17:20

좌 장 : 조재용(부산대)

PC-11(초)[15:45-16:05] Concentrator Solar Cells: KIM Dongkyun, KIM Dongho, CHANG Jieun, KIM Yungi(SAMSUNG Advanced Institute of Technology)

PC-12(초)[16:05-16:25] Organic Solar Cells on SWCNT Electrodes: LEE Soonil, YIM Jonghyuk(Division of Energy Systems Research, Ajou University)

PC-13(초)[16:25-16:45] Transparent conductive oxide technologies for organic photovoltaics: 김 한기(경희대 디스플레이재료공학과)

PC-14[16:45-17:05] Nanostructured Zinc Oxide Thin Films via Electrodeposition and their Photoelectrochemical Performance: INAMDAR A. I.(Shivaji University, Department of Physics), JUNG Kyooho, KIM Young sam, IM Hyunsik (Dongguk University, Department of Semiconductor Science), PATIL P. S.(Shivaji University, Department of Physics)

PC-15[17:05-17:20] Synthesis and characterization of Cu(In,Ga)Se<sub>2</sub> nanoparticles and thin-films: JEONG Ah Reum, KIM Gracia, JO William(Department of Physics, Ewha Womans University)

[BG1] General Session

장 소 : 607

10월 21일(수) 11:15 - 12:15

좌 장 : 임채호(서강대)

- B-01[11:15-11:30] Baryons and Mesons in Dense System: SEO Yunseok(CQUeST), SIN Sang-Jin(Hanyang University, Department of Physics), SHOCK Jonathan, ZOAKOS Dimitrios(IGFAE, Spain)
- B-02[11:30-11:45] Critical Phenomena of Holographic Superconductors: PARK Cheonsoo, HONG Deog Ki(Pusan National University)
- B-03[11:45-12:00] Extended Supersymmetry in ABJM Theory: 권 오갑, 오 필열(성균관대), 박 천수(부산대), 손 종수(성균관대)
- B-04[12:00-12:15] Compactification Of Horava-Lifshitz Theory: KIM Kyung Kiu(Institute for the Early Universe)

[BG2] General Session

장 소 : 607

10월 21일(수) 13:30 - 15:30

좌 장 : 현승준(연세대)

- B-05[13:30-13:45] Spinning membranes in  $AdS_4 \times Q^{1,1,1}$ : 이 정훈, 김 낙우(경희대)
- B-06[13:45-14:00] The Quark Mass Dependence of The Nucleon Mass in AdS/QCD: AHN Hyo Chul, HONG Deog-Ki(Pusan National University)
- B-07[14:00-14:15] Surplus Solid Angle: Toward Astrophysical Test of Horava-Lifshitz Gravity: KIM Sung-Soo(Universite Libre de Bruxelles and International Solvay Institutes), KIM Taekyung, KIM Yoonbai(Sungkyunkwan University)
- B-08[14:15-14:30] 3차원 Chern-Simons-Matter 이론의 중력 대응: 김 종욱(경희대)
- B-09[14:30-14:45] Walls in Supersymmetric Massive Nonlinear Sigma Model on Complex Quadric Surface: SHIN Sunyoung, ARAI Masato(양자시공간연구센터), LEE Sunggeun(경희대)
- B-10[14:45-15:00]\* The Effective Action Of The ABJM Model: 백 종현, 현 승준, 이 상현(연세대)
- B-11[15:00-15:15]\* Probing smearing effect by point-like graviton in plane-wave matrix model: NAM Siyoung, LEE Bum-Hoon(Sogang U. & CQUeST), SHIN Hyeonjoon(CQUeST)
- B-12[15:15-15:30]\* Pseudo Scalar Contributions To Light-by-light Correction Of Muon  $g-2$  In AdS/QCD: KIM Doyoun(Seoul National University), HONG Deog-Ki(Pusan National University)

[BG3] General Session

장 소 : 607

10월 21일(수) 15:45 - 17:45

좌 장 : 천병구(한양대)

- B-13(초)[15:45-16:15] R & D of next generation scintillation detector for future high energy experiments: UOZUMI Satoru, KIM DongHee, KIM Jieun, KAHN Adil, KONG Daejung, YANG Yuchul(Kyungpook National University, Physics Department), KAWAGOE Kiyotomo, JEANS Daniel(Kobe University, Department of Physics), TAKESHITA Tohru, NISHIYAMA Miho, SAKUMA Takayuki, KOTERA Katsushige(Shinshu University, Department of Physics), SUDO Yuji, IKUNO Toshinori(University of Tsukuba, Department of Physics), KAPLAN Alexander, FEEGE Nils(DESY)
- B-14(초)[16:15-16:45] Current Status of RENO Experiment: 이 재승, 강 보라, 김 수봉, 박 정식, 신 진욱, 최 선호(서울대), 김 성현, 김 병찬, 김 재률, 주 경광, 임 인택, 장 지승, 정 인식, 최 을임(전남대), 김 우영, 스테판난 사뮤엘, 서 준석, 오 영도, 김 안드레이(경북대), 박 인곤(경상대), 안 정근, 이 효상(부산대), 박 강순(서경대), 김 동현, 박 차원, 백 승록, 유 인태, 최 영일(성균관대), 강 윤구, 김 영덕, 마 경주, 전 은주(세종대), 김 현수(전북대), N. Danilov, YU Krylov, G. Novikova, E. Yanovich(INR/IPCE)
- B-15(초)[16:45-17:15] Results on the hadronic decays of tau lepton in the B-factory experiments: LEE MyeongJae, KIM Sunkee, OLSEN Stephen L., CHUNG Kwangzoo, RYU Soo(Seoul National University, Department of Physics and Astronomy)
- B-16[17:15-17:30] Search for CP Violation in the Decays  $D_{(s)}^+ \rightarrow Ks\pi^+$  and  $D_{(s)}^+ \rightarrow KsK^+$ : KO ByeongRok, WON Eunil(Korea University), (for the Belle Collaboration)
- B-17[17:30-17:45] Measurement Of The  $|V_{ub}|$  From The Exclusive Decay  $B^0 \rightarrow \pi^+ l^- \nu$  Branching Fraction Using Inclusive Loose Neutrino Reconstruction At Belle: HA Hyuncheong, WON Eunil(Korea University), BELLE Collaboration (KEK - High Energy Accelerator Research Organization)

---

**입자물리학회 총회****장 소 : 607****10월 21일(수) 17:45 - 18:30****B**

---

**[BF1]/[CF1] Focus Session (입자물리학회-원자핵물리학회 공동 세션)****장 소 : 607****10월 22일(목) 09:00 - 11:00****좌 장 : 권영준(연세대)**

BF-01(초)[09:00-09:30] Updated Results on Exotic Resonances: CHOI Sookyung(경상대)

BF-02(초)[09:30-10:00] Charmonium spectroscopy with new resonances: OLSEN Stephen Lars(Seoul National University)

BF-03(초)[10:00-10:30] X(3872): hadronic transitions and its isospin: KO Pyungwon, KIM Taewon(KIAS), YU Chaehyun(Korea University)

BF-04(초)[10:30-11:00] A recent status of exotic baryons:  $N^*(1680)$  and  $\Theta^+(1540)$ : 김 현철(인하대)

---

**[BF2]/[CF2] Focus Session (입자물리학회-원자핵물리학회 공동 세션)****장 소 : 607****10월 22일(목) 11:15 - 12:45****좌 장 : 최선호(서울대)**BF-05(초)[11:15-11:45] Plans of High Resolution Spectroscopic Searches for  $\Theta^+$  and  $\Theta$ -hypernuclei at J-PARC: TANIDA Kiyoshi(서울대)

BF-06(초)[11:45-12:15] Search for Exotic Baryons at SPring-8 and J-PARC: 안 정근(부산대)

BF-07(초)[12:15-12:45] Search for H-dibaryon resonance and study of Lambda-Lambda interaction: 윤 충재(C.J. Yoon)(Seoul National University, Department of Physics and Astronomy), KEK-PS E522 COLLABORATION, H. Akikawa, K. Aoki, Y. Fukao, H. Funahashi, M. Hyata, K. Imai, K. Miwa, H. Okada, N. Saito, H. D. Sato, K. Shoji, H. Takahashi, K. Taketani(Department of Physics, Kyoto University), J. Asai, M. Kurosawa(Department of Physics, Tokyo University of Science), M. Ieiri(IPNS, KEK), T. Hayakawa, T. Kishimoto, A. Sato, Y. Shimizu(Department of Physics, Osaka University), K. Yamamoto, T. Yoshida(Department of Physics, Osaka City University), T. Hibi, K. Nakazawa(Physics Department, Gifu University), J.K. Ahn, B.H. Choi, S.J. Kim(Department of Physics, Pusan National University), S.H. Kim, C.S. Yoon, J.S. Song, B.D. Park, I.G. Park(Department of Physics, Gyeongsang National University), K. Tanida(RIKEN), A. Ohnishi(Faculty of Science, Hokkaido University)

---

**[BG4] General Session****장 소 : 607****10월 22일(목) 13:30 - 15:15****좌 장 : 유채현(고려대)**

B-18[13:30-13:45] Baryon density effect in finite temperature two-color QCD: KIM Seyong(Sejong University, Department of Physics), HANDS Simon(Swansea University, Department of Physics), SKULLERUD Jon-Ivar(NUIM, Maynooth)

B-19[13:45-14:00]  $SU(4)_L \times U(1)_X$  models with little Higgs: 남 수현(KISTI), 금 용연(고려대), 이 강영(건국대)

B-20[14:00-14:15] Possibility of spontaneous CP violation in the BMSSM: 함 승우(고려대), 심 정아(성신여대), 오 선근(건국대)

B-21[14:15-14:30] Understanding general gauge mediation: LEE Jae Yong(KIAS)

B-22[14:30-14:45]\* Light Higgs Scenario In MSSM-like Theory And LEP Constraints: KIM Jihun, KIM Hyung Do, KIM Do-Youn, BAE Kyu Jung(Seoul National University, Department of Physics), DERMISEK Radovan(Indiana University, Department of Physics)

B-23[14:45-15:00]\* Minimal Supersymmetric Decaying Dark Matter model in PAMELA/Fermi-LAT era: 허 지행(서울대)

B-24[15:00-15:15]\* PAMELA/ATIC anomaly and decaying dark matter model: BAE Kyu Jung, KYAE Bumseok(Seoul National University, Department of Physics and Astronomy)

---

**[BG5] General Session****장 소 : 607****10월 22일(목) 15:45 - 17:45****좌 장 : 박환배(경북대)**

B-25[15:45-16:00]\* Study Of The Channeling Effect In The Nuclear Event Of The CsI(Tl) Crystal Scintillator: 이 주희, 고 은별, 김 선

기, S.L. Olsen, 김 승천, 명 성숙, 방 형찬, 이 상준, 이 재급, 정 광주, 최 정훈(서울대), 강 운구, 김 영덕, 이 정일(세종대), 김 홍주, 소 중호, 정 선우(경북대), 권 영준, 황 명진(연세대), 한 인식(이화여대), LI Jin, YUE Q., LI Y.J.(Tsinghua University, Department of Engineering Physics)

- B-26[16:00-16:15]\* Cryogenic Dual-channel Measurement for the Study of Neutrinoless Double Beta Decay in  $\text{CaMoO}_4$  Crystal: 이 상준(한국표준과학연구원), 김 선기, 명 성숙, 김 승천, 이 주희, 최 정훈(서울대), 김 용합, 이 민규, 이 경범, 김 일환, 이 화용, 장 용식(한국표준과학연구원), 김 홍주, 소 중호(경북대), 김 영덕, 강 운구, 이 정일(세종대)
- B-27[16:15-16:30]\* Development of the 500 MHz Flash ADC for the J-PARC E14 Kaon Rare Decay Experiment: 백 광윤(부산대), 김 상렬(NOTICE), 이 효상(한국기초과학지원연구원(KBSI)), 임 계엽(고에너지가속기연구기구(KEK)), 우 종관, 고 재우(제주대), 김 은주(전북대), 안 정근(부산대)
- B-28[16:30-16:45] Cosmic ray Response Characteristic of a hadron calorimeter in J-Parc E-14(K0to): 고 재우, 우 종관, 김 용주(제주대), 이 효상, 안 정근, 백 광윤(부산대), 임 계엽(KEK), 김 은주(전북대), 정 명신, 강 서곤, 김 유상(서울시립대)
- B-29[16:45-17:00] The Energy and Flux Measurement of GeV Neutron at the J-PARC KL Beam Line: 이 효상(한국기초과학지원연구원(KBSI)), 안 정근, 백 광윤(부산대), 임 계엽(고에너지가속기연구소(KEK)), 우 종관, 고 재우(제주대), 김 은주(전북대)
- B-30[17:00-17:15] search for  $B \rightarrow \phi \pi$  decays: 김 정현(SungKyunKwan Univ., (Present Institute: KISTI HEP Team))
- B-31[17:15-17:30] Study of  $D^+(s)$  Decay Properties at Belle: LEE Soohyung, WON Eunil, KO Byeongrok(Korea University), (for the Belle collaboration)
- B-32[17:30-17:45] The advanced data handling system with AMGA at the Belle II experiment: 김 정현, 조 기현(KISTI HEP team)

## [BG6] General Session

장 소 : 607

10월 23일(금) 09:00 - 10:45

좌 장 : 김동희(경북대)

- B-33[09:00-09:15]\* Solar Neutrino Measurements at Super-Kamiokande-III: 양 병수, 김 수봉(서울대), 최 영일(성균관대), 김 재률, 장 지승, 임 인택(전남대)
- B-34[09:15-09:30]\* CMS/LHC 실험을 위한 묶은 트리거 비저항검출기 운영 및 우주선 묶은 데이터 분석: 신 승수, 김 현철, 김 지현, 문 동호, 문 봉선, 박 성근, 심 광숙, 서 은성, 이 경세, 이 한범, 조 미희, 정 민수, 홍 병식(고려대)
- B-35[09:30-09:45] Status of RENO Detector Construction: 김 성현, 김 병찬, 김 재률, 임 인택, 장 지승, 정 인식, 주 경광, 최 올림(전남대), 김 우영, 사무엘 스테파난, 서 준석, 김 안드레이(경북대), 박 인곤(경상대), 박 명렬(동신대), 안 정근, 이 효상(부산대), 박 강순(서경대), 강 보라, 김 수봉, 박 정식, 신 진욱, 이 재승, 최 선호(서울대), 김 동현, 박 차원, 백 승록, 유 인태, 최 영일(성균관대), 강 운구, 김 영덕, 마 경주, 전 은주(세종대), 김 현수(전북대), N. Danilov, YU. Krylov, G. Novikova, E. Yanovich(INR/IPCE), 오 영도(경북대)
- B-36[09:45-10:00] Preparation for RENO DAQ System: 백 승록(성균관대), 김 우영, 사무엘 스테파난, 서 준석, 김 안드레이(경북대), 박 인곤(경상대), 박 명렬(동신대), 안 정근, 이 효상(부산대), 김 수봉(서울대), 박 강순(서경대), 박 정식, 이 재승, 최 선호(서울대), 권 은향, 김 동현, 박 차원, 유 인태, 최 영일(성균관대), 강 운구, 김 영덕, 마 경주, 전 은주(세종대), 김 선희, 김 성현, 김 병찬, 김 재률, 주 경광, 임 인택, 장 지승, 정 인식(전남대), 김 현수(전북대), 오 영도(경북대), N. Danilov, YU. Krylov, G. Novikova, E. Yanovich(INR/IPCE)
- B-37[10:00-10:15] Optimal Variable Construction using Symbolic Regression: CHOI Suyong(Sungkyunkwan University)
- B-38[10:15-10:30] Energy Containment Studies of CMS EM calorimetry: 공 대정(경북대/KISTI), 김 동희, 김 지은, 장 성현(경북대)
- B-39[10:30-10:45] Search for Randall-Sundrum Graviton Decaying to  $G^* \rightarrow ZZ \rightarrow \mu^+ \mu^- \mu^+ \mu^-$  at  $\sqrt{s} = 10$  TeV at CMS experiment: CHUNG J., PARK H.K., KIM G.N., SON D.C.(경북대)

[CG1] General Session: HIC

장 소 : 603

10월 21일(수) 13:30 - 15:25

좌 장 : 홍병식(고려대)

- C-01(초)[13:30-13:55] Hadronization of a Quark-Gluon Plasma via Recombination: LEE Kang Seog(전남대)
- C-02[13:55-14:10] FOrward CALorimeter for the PHENIX Experiment: 강 주환, 권 영일, 김 현주, 송 명근, 임 상훈(연세대), 심 광속, 홍 병식, 주 은아(고려대), 주 관식, 문 혜진(명지대), 한 인식, 박 일흥, 이 직, 이 혜영(이화여대), 김 은주(전북대)
- C-03[14:10-14:25] Silicon PAD Sensor For PHENIX FOCAL And Cosmic Muon Test: 송 명근, 강 주환, 권 영일, 김 현주, 임 상훈(연세대), 심 광속, 홍 병식, 주 은아(고려대), 주 관식, 문 혜진(명지대), 한 인식, 박 일흥, 이 직, 이 혜영(이화여대), 김 은주, 이 순례(전북대)
- C-04[14:25-14:40]\* STAR Asian Computing Center for Heavy Ion Analysis Computing Center at KISTI with PNU: 오 근수, 유 인권, 최 경언(부산대), 우 준, 이 상동, 김 현우, 이 식, 김 동균, 권 석면, 한 보영, 장 행진(한국과학기술정보연구원), LAURET Jerome, YU Dantong, PACKARD Jay(Brookhaven National Laboratory)
- C-05[14:40-14:55]\* Detector Readiness of RPC for Heavy Ion Collisions at CMS: 조 미희, 홍 병식, 김 현철, 문 동호, 김 지현, 이 한범, 이 경세, 박 성근, 심 광속(고려대)
- C-06[14:55-15:10] 발표 취소
- C-07[15:10-15:25]\* RAA of J/psi at midrapidity of RHIC: WOO SUNG Park(연세대)

[CG2] General Session: QCD

장 소 : 603

10월 21일(수) 15:45 - 17:45

좌 장 : 김영만(APCTP)

- C-08(초)[15:45-16:10] Nuclei and the Cosmos: RHO Mannque(Hanyang University and Saclay)
- C-09(초)[16:10-16:35] Topological P and CP violation in heavy ion collisions: FUKUSHIMA Kenji(Yukawa Institute for Theoretical Physics)
- C-10(초)[16:35-17:00] Regge approach in charged  $K^*$  photoproduction: OZAKI Sho(RCNP, Osaka University), NAGAIHIRO Hideko(Nara Women's University), HOSAKA Atsushi(RCNP, Osaka University)
- C-11[17:00-17:15] Neutron star under strong magnetic fields: 유 충열, 천 명기(숭실대)
- C-12[17:15-17:30] Hadrons in AdS/QCD in a unified approach: YAKHSHIEV Ulugbek, 김 현철(인하대), 김 영만(APCTP)
- C-13[17:30-17:45]\* Holographic Dual Model of Quantum Hadrodynamics: KIM Kyung-il(연세대), KIM Youngman(APCTP JRG Leader), LEE Suhong(연세대)

원자핵물리학과회 총회

장 소 : 603

10월 21일(수) 17:45 - 18:30

[CF1]/[BF1] Focus Session (입자물리학과회-원자핵물리학과회 공동 세션)

장 소 : 607

10월 22일(목) 09:00 - 11:00

좌 장 : 권영준(연세대)

- BF-01(초)[09:00-09:30] Updated Results on Exotic Resonances: CHOI Sookyung(경상대)
- BF-02(초)[09:30-10:00] 1 Charmonium spectroscopy with new resonances: OLSEN Stephen Lars(Seoul National University)
- BF-03(초)[10:00-10:30] X(3872): hadronic transitions and its isospin: KO Pyungwon, KIM Taewon(KIAS), YU Chaehyun(Korea University)
- BF-04(초)[10:30-11:00] A recent status of exotic baryons:  $N^*(1680)$  and  $\Theta^+(1540)$ : 김 현철(인하대)

[CF2]/[BF2] Focus Session (입자물리학과회-원자핵물리학과회 공동 세션)

장 소 : 607

10월 22일(목) 11:15 - 13:15

좌 장 : 최선호(서울대)

- BF-05(초)[11:15-11:45] Plans of High Resolution Spectroscopic Searches for  $^A\text{Th}$  and  $^A\text{Th}$ -hypernuclei at J-PARC: TANIDA Kiyoshi(서울대)
- BF-06(초)[11:45-12:15] Search for Exotic Baryons at SPring-8 and J-PARC: 안 정근(부산대)

BF-07(초)[12:15-12:45] Search for H-dibaryon resonance and study of Lambda-Lambda interaction: 윤 충재(C.J. Yoon)(Seoul National University, Department of Physics and Astronomy), KEK-PS E522 COLLABORATION, H. Aikawa, K. Aoki, Y. Fukao, H. Funahashi, M. Hyata, K. Imai, K. Miwa, H. Okada, N. Saito, H. D. Sato, K. Shoji, H. Takahashi, K. Taketani(Department of Physics, Kyoto University), J. Asai, M. Kurosawa(Department of Physics, Tokyo University of Science), M. Ieiri(IPNS, KEK), T. Hayakawa, T. Kishimoto, A. Sato, Y. Shimizu(Department of Physics, Osaka University), K. Yamamoto, T. Yoshida(Department of Physics, Osaka City University), T. Hibi, K. Nakazawa(Physics Department, Gifu University), J.K. Ahn, B.H. Choi, S.J. Kim(Department of Physics, Pusan National University), S.H. Kim, C.S. Yoon, J.S. Song, B.D. Park, I.G. Park(Department of Physics, Gyeongsang National University), K. Tanida(RIKEN), A. Ohnishi(Faculty of Science, Hokkaido University)

### [CG3] General Session: Hyper

장 소 : 603

10월 23일(금) 09:00 – 11:05

좌 장 : 박태선(성균관대)

- C-14(초)[09:00-09:25] Overview of the HypHI project at GSI: the hypernuclear spectroscopy with heavy ion collisions: SAITO Take R.(for the HypHI collaboration, GSI and Mainz University, Germany)
- C-15(초)[09:25-09:50] Exotic nuclei with open heavy mesons: YASUI Shigehiro(KEK)
- C-16[09:50-10:05] The HypHI Phase 0 experiment at GSI: KIM Eunhee(Seoul National University, Department of Physics and Astronomy, and GSI), HYPHI collaboration(GSI, Germany)
- C-17[10:05-10:20] Beam Asymmetries of  $K^*S^+$  Photoproduction from threshold to 3.0 GeV: 황 상훈, 안 정근(부산대), HICKS K(University, Department of Physics and Astronomy), NAKANO T(Osaka University, Research Center for Nuclear Physics), LEPS Collaboration(Spring-8)
- C-18[10:20-10:35]\*  $\pi^+$  Producing Process in  $^5_\Lambda\text{He}$  Hypernucleus and Effect of  $\Delta$ -Isobar: 이 종화, 박 태선, 홍 승우(성균관대)
- C-19[10:35-10:50] Search for  $\Xi$  hypernuclear Production in  $^{12}\text{C}(K, K^+)X$  Reactions: 최 봉혁, 김 성준, 안 정근(부산대), YOON C.J. (서울대), MIWA K.(Tohoku University, Department of Physics), IMAI K.(Kyoto University, Department of Physics), IEIRI M.(High Energy Accelerator Research Organization)
- C-20[10:50-11:05]\*  $\Xi$  Polarization from  $(K, K^+)$  Reaction on p and  $^{12}\text{C}$ : 김 성준, 최 봉혁, 안 정근(부산대 물리학과), 윤 충재(서울대 물리학과), MIWA K.(Tohoku University, Department of Physics), IMAI K.(Kyoto University, Department of Physics), IEIRI M.(High Energy Accelerator Research Organization)

### [CG4] General Session: LEN

장 소 : 604

10월 23일(금) 09:00 – 10:55

좌 장 : 천명기(숭실대)

- C-21(초)[09:00-09:25] Very low energy light ions resonant reactions: TENREIRO Claudio(Sungkyunkwan University & University of Talca)
- C-22[09:25-09:40] Studies of Multineutron Photonuclear Reactions on  $^{89}\text{Y}$ , and  $^{197}\text{Au}$  with Bremsstrahlung Beam: RAHMAN Md. Shakilur, KIM Kyung Sook, LEE Manwoo, KIM Guinyun(Department of Physics, Kyungpook National University), OH Youngdo, LEE Hee-Seock, CHO Moo-hyun, KO In Soo, NAMKUNG Won(Pohang Accelerator Laboratory, Pohang University of Science and Technology), CHO Y. S., LEE Y. O.(Nuclear Data Evaluation Laboratory, KAERI), RO Tae-Ik(Department of Physics, Dong-A University)
- C-23[09:40-09:55] Talys 코드를 이용한 Ni 동위원소에 대한 중성자 입사 핵반응의 전평형 연구: 문 명환, 이 영욱, 김 형일(Korea Atomic Energy Research Institute(KAERI))
- C-24[09:55-10:10] Monte Carlo Study on the Gamma-ray Absorption Rate of  $^{26}\text{Al}$  in a Stellar Plasma: 이 주한, 이 춘식(중앙대)
- C-25[10:10-10:25] The Q-value Energy Spectra for a Natural Uranium Sample Mixed with  $^{226}\text{Ra}$  Using a Low Temperature Detector: 이 민규, 이 상준, 장 용식, 김 일환, 이 화용, 이 경범, 김 용합(한국표준과학연구원)
- C-26[10:25-10:40] Experimental Determination of 550 keV-Neutron Capture Cross Sections and Gamma Spectrum on  $^{56}\text{Fe}$  and  $^{105}\text{Pd}$ : WANG Taofeng, LEE Manwoo, KIM Guinyun(Department of Physics, Kyungpook National University), OH Youngdo, NAMKUNG Won(Pohang Accelerator Laboratory, Pohang University of Science and Technology), RO Tae-Ik, KIM Gwon-jung, JUNG Hoon(Department of Physics, Dong-A University), IGASHIRA M., KATABUCHI T., KAMADA S.(Research Laboratory for Nuclear Reactors, Tokyo Institute of Technology)
- C-27[10:40-10:55]\* Measurement of the unbound excited states of  $^{24}\text{O}$ : TSHOO K.H., SATOU Y.(School of Physics, Seoul National University), NAKAMURA T.(Department of Physics, Tokyo Institute of Technology, Japan), AOI N.(RIKEN, Japan), BHANG H.C., CHOI S.H.(School of Physics, Seoul National University), DEGUCHI S.(Department of Physics, Tokyo Institute of Technology, Japan), DELAUNAY F., GIBELIN J.(LPC Caen, ENSICAEN, Université

de Caen, France), HONDA T.(Department of Physics, Rikkyo University, Japan), ISHIHARA M.(RIKEN, Japan), KAWADA Y., KONDO Y.(Department of Physics, Tokyo Institute of Technology, Japan), KOBAYASHI T. (Department of Physics, Tohoku University, Japan), KOBAYASHI N.(Department of Physics, Tokyo Institute of Technology, Japan), MARQUES F.M.(LPC Caen, ENSICAEN, Université de Caen, France), MATSUSHITA M.(Department of Physics, Rikkyo University, Japan), MIYASHITA Y.(Tokyo University of Science, Japan), MOTOBAYASHI T.(RIKEN, Japan), NAKAYAMA Y.(Department of Physics, Tokyo Institute of Technology, Japan), ORR N.A.(LPC Caen, ENSICAEN, Université de Caen, France), OTSU H., SAKURAI H.(RIKEN, Japan), SHIMOURA S.(Department of Physics, The University of Tokyo, Japan), SOHLER D.(Institute of Nuclear Physics (ATOMKI), Debrecen, Hungary), SUMIKAMA T.(Tokyo University of Science, Japan), TAKEUCHI S.(RIKEN, Japan), TANAKA K.N., TANAKA N.(Department of Physics, Tokyo Institute of Technology, Japan), TOGANO Y., YONEDA K.(RIKEN, Japan), YOSHINAGA K.(Tokyo University of Science, Japan), ZHENG T.(School of Physics and State Key Laboratory of Nuclear Physics & Technology, Peking University, China), LI Z.H.(RIKEN, Japan), CAO Z.X.(School of Physics and State Key Laboratory of Nuclear Physics & Technology, Peking University, China)

## [CG5] General Session: EFT

장 소 : 603

10월 23일(금) 13:30 - 15:35

좌 장 : 현창호(대구대)

- C-28(초)[13:30-13:55] Gauged linear sigma model and pion-pion scattering: PARK Naewoong(전남대), SCHECHTER Joseph(Syracuse Univ.)
- C-29(초)[13:55-14:20] Heavy-baryon chiral perturbation theory approach to thermal neutron capture on He-3: LAZAUSKAS Rimantas (Strasbourg, IReS), SONG Young-Ho(Duke U), PARK Tae-Sun(SKKU)
- C-30[14:20-14:35] Hadronic description for the  $\phi$ -photoproduction near the threshold: RYU Huiyoung(RCNP, Osaka University)
- C-31[14:35-14:50]\* Measurement of the  $\phi$ p scattering length from  $\phi$  photoproduction at threshold: 류 선영(RCNP Osaka/RIKEN IPA /부산대), 안 정근(부산대 물리학과), NAKANO Takashi(RCNP, Osaka), FOR the LEPS Collaboration(SPring-8)
- C-32[14:50-15:05]\* Parity-Violating Polarization In  $np \rightarrow d \gamma$  With A Pionless Effective Field Theory: SHIN JaeWon(Department of Physics, Sungkyunkwan University), ANDO Shung-ichi(Theoretical Physics Group, School of Physics and Astronomy, The University of Manchester), HYUN Chang-Ho(Department of Physics Education, Daegu University)
- C-33[15:05-15:20]\* Toroid or Dumbell?: 류 상욱, 민 동필(서울대), 박 병윤(충남대), VENTO Vicente(Departament de Fisica Teorica, Universidad de Valencia)
- C-34[15:20-15:35] Proton Computed Tomography Using Toroidal Coils: 이 주한(중앙대), 서 희(한양대), 정 인일, 권 영관, 윤 종철 (중앙대), 김 찬형(한양대), 최 영완, 이 춘식(중앙대)

## [CG6] General Session: Inst

장 소 : 604

10월 23일(금) 13:30 - 15:30

좌 장 : 유인권(성균관대)

- C-35[13:30-13:45] Ar Ion Beam Extraction of 2.45 GHz ECR Ion Source: 박 규준, 이 효상, 이 병섭(한국기초과학지원연구원), 박 진 용(부산대), 임 정환(한국기초과학지원연구원), 안 정근(부산대), 원 미숙, 배 종성(한국기초과학지원연구원)
- C-36[13:45-14:00] New properties of a scintillation counter equipped by fine mesh photomultipliers: NI Andrey(Kyungpook National University), 김 우영, KUZNETSOV Viacheslav, KIM Andrey, 장 주영, 도 호석(경북대), 양 태건, 김 유석, 이 민영 (한국원자력의학원)
- C-37[14:00-14:15]\* Performance of a 16-pixelated CdZnTe detector as an absorber of Compton camera: 조 화연, 이 주한, 문 준영, 정 효순, 이 춘식(중앙대 물리학과)
- C-38[14:15-14:30]\* Performance of a Beam Imaging array Detector for Proton Radiotherapies: 문 봉선, 홍 병식, 정 민수, 주 은아, 이 경세, 박 성근, 심 광숙(고려대)
- C-39[14:30-14:45]\* Design of 28 GHz ECR Ion Source with the Compact Linear Accelerator: 박 진용(부산대 한국기초과학지원연구원), 임 정환, 박 규준, 이 효상, 이 병섭, 원 미숙, 윤 장희(한국기초과학지원연구원), 안 정근(부산대 한국기초과학지원연구원)
- C-40[14:45-15:00]\* Research and Development of Ring Imaging Cherenkov Detector Prototype for CBM: YI JunGyu, JANG JungMin, LEE Hayoung, OH Kunsu, SON ChangWook, SONG Jihye, YOO In-Kwon(Pusan National University, Dep. of Physics)
- C-41[15:00-15:15]\* 포항 2.5 GeV 저장링의 제동복사 빔을 이용한 빔 진단 및 광생성 반응 실험: 이 재기, 황 상훈, 백 광윤, 박 진용,

이 효상, 안 정근(부산대)

C-42[15:15-15:30] Study on the Dosimetric Characteristic of Small Field Size Proton Beam Using Comparison with GEANT4 Monte Carlo Simulation: 안 성환, 신 정욱, 조 민국, 라 정은, 황 의중, 정 호진, 임 영경, 김 동욱, 윤 명근, 신 동호, 이 세병, 박 성용(국립암센터)

[DT1] Tutorial Session: STM 원리와 응용

장 소 : 컨벤션 I

10월 21일(수) 11:15 - 13:15

좌 장 : 여인환(연세대)

DT-01(초)[11:15-12:15] Scanning Tunneling Microscope의 원리와 표면화학에의 응용: 구 자용(한국표준과학연구원)

DT-02(초)[12:15-13:15] 제일원리계산을 이용한 STM 이미지 모사 기법과 표면 원자 구조 연구에의 응용: 김 한철(숙명여대)

[DG1] General Session: 표면/계면

장 소 : 컨벤션 I

10월 21일(수) 13:30 - 15:30

좌 장 : 황찬용(표준원)

D-01[13:30-13:45] Reconstruction and Evaporation at Graphene Nanoribbon Edges: LEE Gun-Do, YOON Euijoon, HWANG Nong-moon(Dept. of Materials Science and Engineering, Seoul National University), WANG Cai-Zhuang, HO Kai-Ming(Dept. of Physics, Iowa State University)

D-02[13:45-14:00] Effects of the Au intercalation into the graphene/Ni(111) surface: Density-functional theory calculations: 박 재환, 정 성철, 강 명호(Pohang Univetsity of Science and Technology, Department of Physics)

D-03[14:00-14:15]\* Tetra(4-carboxyphenyl)porphine을 이용한 그래핀 표면의 응용: 강 세준, 이 미지(포항공대), 신 현준, 김 기정, 김 봉수, 백 재윤(포항가속기연구소)

D-04[14:15-14:30] Surface Diffusion in Growth of Perovskite Oxides in a Nucleation Regime: 장 영준(서울대), 박 수현(이화여대), 노 태원(서울대)

D-05[14:30-14:45]\* Reduction Of Coulomb Interaction Energy And Charge Transfer Energy Of Ultrathin NiO Films On Ag(001): YANG Seolun, PARK HyunKook, KIM J. -S.(Sookmyung W. Univ., Physics), HWANG H. -N., HWANG C. -C., KIM H. -D.(Pohang Acceleration Laboratory)

D-06[14:45-15:00]\* One-dimensional Phase Separation on a vicinal Si(111) surface: KIM Minkook(BK21 Physics Research Division and CNNC, Sungkyunkwan University), OH Dong-Hwa(BK21 Physics Research Division, Sungkyunkwan University), BAIK Jaeyoon(CNNC, Sungkyunkwan University, Beamline Research Division, Pohang Accelerator Laboratory, POSTECH), JEON Cheolho(CNNC, Sungkyunkwan University), PARK Chong-Yun, AHN Joung Real(BK21 Physics Research Division and CNNC, Sungkyunkwan University)

D-07[15:00-15:15]\* Self-Assembly of One-Dimensional Molecular Wires on the Si(001) Surface: CHOI Jin-Ho, CHO Jun-Hyung(Hanyang University, Physics)

D-08[15:15-15:30]\* Nearly Massless Hole Carriers at Silicon Subsurface with a Monolayer Metal Film: KIM Keun Su, YEOM Han Woong(Institute of Physics and Applied Physics and Center for Atomic Wires and Layers, Yonsei University)

[DG2] General Session: 표면/계면

장 소 : 컨벤션 I

10월 21일(수) 15:45 - 17:45

좌 장 : 박용섭(경희대)

D-09[15:45-16:00] Van der Waals Interaction in the Adsorption of  $C_4H_4N_2$  on Si(100): DFT Calculations: JUNG Sung Chul, KANG Myung Ho(포스텍 물리학과)

D-10[16:00-16:15]\* Coherent x-ray scattering study of block copolymer films: SONG Sanghoon, CHA Wonsuk(Sogang University, Department of Physics & Interdisciplinary Program of Integrated Biotechnology), JIANG Zhang, NARAYANAN Suresh(Advanced Photon Source, Argonne National Laboratory), SINHA S. K.(University of California San Diego, Department of Physics), KIM Hyunjung(Sogang University, Department of Physics & Interdisciplinary Program of Integrated Biotechnology)

D-11[16:15-16:30]\* Indium-induced triple-period atomic wires on a vicinal Si(111) surface: In/Si(557): SONG Inkyung(BK21 Physics Research Division and CNNC, Sungkyunkwan University), OH Dong-Hwa(BK21 Physics Research Division, Sungkyunkwan University), NAM Jeong Ho(CNNC, Sungkyunkwan University), KIM Minkook(BK21 Physics Research Division and CNNC, Sungkyunkwan University), JEON Cheolho, PARK Chong-Yun, AHN Joung Real(CNNC, Sungkyunkwan University)

D-12[16:30-16:45]\* Room Temperature Growth Of Magic Atomic Wires On The Si(557) Surface: SHIN Bong Gyu, KIM Minkook, OH Dong-Hwa, PARK Jong-Yun, AHN Jong Real(BK21 Physics Research Division, Sungkyunkwan University)

D-13[16:45-17:00] First Principles Approach To Thermoelectric Material : Interaction Between Metal And  $Bi_2Te_3$  (001) Surface: CHANG Yun Hee, KONG Ki-jeong, CHANG Hyunju(Korea Research Institute of Chemical Technology)

- D-14[17:00-17:15] First-principles study of the native point defects in  $\text{CoSb}_3$ : 박 찬현, 김 용성(한국표준과학연구원)  
 D-15[17:15-17:30]\* Giant perpendicular magnetic anisotropy of an Ir monolayer on a  $\text{NiAl}(001)$  surface: 김동유, 양정화, 홍지상  
 (Department of Physics, Pukyong National University)  
 D-16[17:30-17:45] Ferrimagnetic ordering in  $(\text{Fe,Mn,Cr})_2\text{As}$  thin films induced by strain: 황 영훈, CHO Sunglae(울산대), CHOI Jeongyong(한국전자통신연구원), SHIN Yooleemi(울산대)

### [DF1] Focus Session: 계면분광학(Interface Spectroscopy)

장 소 : 302

10월 22일(목) 09:00 – 11:00

좌 장 : 한문섭(서울시립대)

- DF-01(초)[09:00-09:30] Electron energy-loss spectroscopy in semiconductor devices: JANG Jae Hyuck, KWON Ji Hwan, JEON Jong Myeong, KIM Miyong, PARK Tae Joo, HWANG Cheol Seong(서울대)  
 DF-02(초)[09:30-10:00] In-situ synchrotron x-ray scattering study on the surface and interface structures: NOH Do Young(광주과학기술원, 신소재공학과 & 나노바이오재료전자공학과), KIM Yongsam(School of Applied Engineering Physics, Cornell University), KIM Do Hyung(한국전력), CHO Inwha(광주과학기술원, 신소재공학과)  
 DF-03(초)[10:00-10:30] Infrared Spectroscopy of Interface Charge in  $\text{ZnO}$  Field-Effect Transistor: 최 은집, 김 주연, 정 성훈(서울시립대 물리학과), 김 기태, 이 기문, 임 성일(연세대)  
 DF-04(초)[10:30-11:00] 광전자 분광 및 관련 기술을 이용한 유기전자 소자의 계면 연구: 박 용섭(경희대)

### [DG3] General Session: 나노

장 소 : 302

10월 22일(목) 11:15 – 13:15

좌 장 : 이경수(부산대)

- D-17[11:15-11:30]\* Electronic Properties of Strained Graphene: 최 선명, 지 승훈(포항공대), 손 영우(Korea Institute for Advanced Study)  
 D-18[11:30-11:45]\* Berry Phase Effect in Bilayer Graphene Potential Step: PARK Sunghun, SIM H.-S.(KAIST 물리학과)  
 D-19[11:45-12:00]\* Electronic structure of Pt-graphenes complexes and H, O and CO absorption: 김 규봉, 지 승훈(포항공대 물리학과)  
 D-20[12:00-12:15] Dispersants Bond Dissociation at High Temperature in Polymerized Single walled Carbon Nanotubes revealed by Coherent Phonon Spectroscopy: 김 지희, 김 창섭, 이 기주, 이 철훈(충남대), 김 태환, 최 성민(한국과학기술원, 원자력 및 양자공학과)  
 D-21[12:15-12:30]\* Characterization of Anelastic effects in Metallic and Metallic-CNT Micromechanical Resonators: KIM Young Duck, CHO, Sung Wan, O ByeongGyun, LEE Joo Hyung, LEE Seung Ran, CHAR Kookrin, HONG Seunghun, PARK Yun Daniel(Department of Physics & Astronomy, Seoul National University)  
 D-22[12:30-12:45]\* Curvature-Enhanced Spin-Orbit Coupling in a Carbon Nanotube: 정 재승, 이 현우(포항공대)  
 D-23[12:45-13:00]\* Water-Assisted Growth of mm-long Thin Multiwalled Carbon Nanotubes with an Optimum Al Underlayer in Thermal CVD: CHOI In Sung, JEON Hong Jun, LEE Han Sung, LEE Naesung(세종대)  
 D-24[13:00-13:15] Carbon Nanotube Tunnel Sensor: CHOI Jaewu(경희대)

### [DG4] General Session: 나노

장 소 : 302

10월 22일(목) 13:30 – 15:30

좌 장 : 정명화(서강대)

- D-25[13:30-13:45] First-Principles Mobility Calculations in Doped Si/Ge Core-Shell Nanowires: LEE Hyungjun, CHOI Hyoung Joon(Department of Physics and IPAP, Yonsei University)  
 D-26[13:45-14:00] First-principles Study of Doped and Undoped Si/Ge Nanowire Superlattices: KIM Min-Kook, CHOI Hyoung Joon(Department of Physics and IPAP, Yonsei University)  
 D-27[14:00-14:15] The Effect of Energy Relaxation via Surface Levels on Quantum Yield in  $\text{CdSe}$  Quantum Dots: 김 상민(부산대), 홍 경수(한국기초과학지원연구원 부산센터), 양 호순(부산대)  
 D-28[14:15-14:30]\* Evolution of Photoluminescence of Plasma Power Modulated Silicon Nitride Films by Ionized  $\text{N}_2$  Gas Irradiation: JANG Seunghun, KIM Hyunseung, HAN Dongwoo, JEONG Kiyong, KO Changhun, HAN Moonsup(Department of Physics, University of Seoul)  
 D-29[14:30-14:45] Supercurrent Through Single Crystalline Gold Nanowires: 정 민경(KRISS), 노 현호(서울대), 도 용주(포항공대), 송 윤(KRISS), 최 만수(고려대), 정 연옥, 심 승보, 김 남(KRISS), 유 영동, 서 관용, 김 봉수(KAIST 화학과), 김 정구(서울대), 김 진희(KRISS)

- D-30[14:45-15:00] High-frequency single-crystalline Au nanowire as resonators: 김 진희, 장 정원, 정 민경, 심 승보, 노 현호(한국표준과학연구원), 김 봉수(한국과학기술원), 이 순걸(고려대)
- D-31[15:00-15:15]\* Investigation of transport mechanism of amorphous GST: JU chanjong, LU WENJIAN, CHAR Kookrin(서울대)
- D-32[15:15-15:30] Effects of Electron Interactions in Quantum Hall Antidots with Multiple Bound Modes: 이 우람, 심 흥선(KAIST, 물리학과)

## [DG5] General Session: 나노/기타

장 소 : 302

10월 22일(목) 15:45 – 17:45

좌 장 : 박철홍(부산대)

- D-33[15:45-16:00] Effect of the magnetic field sweep on Rabi spin oscillations in a molecular magnet: KIM GWANG-HEE(Dept. of Physics, Sejong Univ.)
- D-34[16:00-16:15]\* Effects of Boron Impurities on Transport Properties of Fe/MgO/Fe(100) Tunnel Junctions: HAN Jinhee, CHOI Hyoung Joon(Institute of Physics and Applied Physics, Yonsei University)
- D-35[16:15-16:30]\* 열 임피던스 측정을 통한  $Gd_2Zr_2O_7$  박막의 열전도도 분석 및 비교: 정 고은(부산대), 배 종성(한국기초과학연구소 부산센터), 양 호순(부산대)
- D-36[16:30-16:45]\* Visualization of Intriguing Polarization Switching Behaviors in Multiferroic  $BiFeO_3$  Thin Films: KIM T. H.(ReCOE & FPRD, Department of Physics and Astronomy, Seoul National University), BAEK S.-H.(Department of Materials Science and Engineering, University of Wisconsin, USA), YANG S. M., JANG S. Y.(ReCOE & FPRD, Department of Physics and Astronomy, Seoul National University), ORTIZ D.(Department of Materials Science and Engineering, University of Wisconsin, USA), SONG T. K.(School of Nano and Advanced Materials Engineering, Changwon National University), CHUNG J.-S.(Department of Physics and CAMDRC, Soongsil University), EOM C.-B.(Department of Materials Science and Engineering, University of Wisconsin, USA), NOH T. W.(ReCOE & FPRD, Department of Physics and Astronomy, Seoul National University), YOON J.-G.(Department of Physics, University of Suwon)
- D-37[16:45-17:00]\* Hysteresis Loops and Nonlinear ac Dynamics of Domain Walls in Epitaxial Ferroelectric Film: YANG Sang Mo, JO Ji Young, KIM Tae Heon(ReCOE & FPRD, Department of Physics and Astronomy, Seoul Nat'l Univ.), YOON Jong-Gul(Department of Physics, University of Suwon), SONG Tae Kwon(School of Nano and Advanced Materials Engineering, Changwon National University), LEE Ho Nyung(Materials Science and Technology Division, Oak Ridge Nat'l Lab., USA), PARK Seung-young, JO Young-Hun(Quantum Materials Research Team, Korea Basic Science Institute), NOH Tae Won(ReCOE & FPRD, Department of Physics and Astronomy, Seoul Nat'l Univ.)
- D-38[17:00-17:15] An Ab-initio Study on Ferroelectric Characteristics of  $ZnSnO_3$ : 신 영한(울산대), 손 종역, 이 근희, 조 문호(포항공대), 김 형준(연세대), 장 현명(포항공대)
- D-39[17:15-17:30]\* First-principles Study of the Electronic Structure of Lithium Silicides: OH Young Jun, RYU Byungki, CHANG Kee Joo(Department of Physics, KAIST)
- D-40[17:30-17:45] Ab initio studies of optical properties of TiN and ZrN : a procedure for color prediction of a given material: KIM Jinwoong, JHI Seung-Hoon(Physics Department, POSTECH)

## [DG6] General Session: 자성

장 소 : 302

10월 23일(금) 09:00 – 11:00

좌 장 : 유천열(인하대)

- D-41[09:00-09:15] Morphological investigation of mono-dispersed manganese ferrite nanoparticles by impedance measurements: YOON Sunghyun(Gunsan National University)
- D-42[09:15-09:30] Discotic Liquid Crystals with a Room-Temperature Ferromagnetism: LEE Chang Hoon(Chosun University, Department of Polymer Science & Engineering), KWON Young Wan, JIN Jung-Il(Korea University, Department of Chemistry), KOH Eui-Kwan(KBSI, Seoul Branch)
- D-43[09:30-09:45] Canted spin structure of checkerboard patterned  $Co_{0.6}Fe_{0.9}Mn_{1.5}O_4$  investigated by NMR and XAS: JUNG Hyunok, LEE Soonchil(KAIST, Physics), LEE H. J., KIM D. H., KANG J.-S.(Catholic University of Korea, Physics), ZHANG C. L., CHEONG S.-W.(Rutgers University, Physics)
- D-44[09:45-10:00] First-principles Study of the Ferromagnetism of Mn-doped ZnO Nanowires: TSOGBADRAKH Namsrai, CHOI Eun-Ae, LEE Woo-jin, CHANG Kee Joo(KAIST, Department of Physics)
- D-45[10:00-10:15] Magnetoresistance across a pinned domain wall in a GaMnAs nanowire: CHO Sung Un, CHOI Hyung Kook,

JANG Dong Hyun, YANG Chan Uk, PARK Yun Daniel(Department of Physics and Astronomy, Seoul National University), DASILVA Fabio C.S, OSMINER Teresa, PAPPAS David P.(National Institute of Standards and Technology, USA)

D-46[10:15-10:30]\* Two-state anomalous Hall effect response in GaMnAs micromechanical freestanding Hallbar structures: YANG Chanuk, CHOI Hyung Kook, O Byeonggyun, PARK Yun Daniel(Seoul National University, Department of Physics and Astronomy)

D-47[10:30-10:45] Skyrmions and Anomalous Hall Effect in a Dzyaloshinskii-Moriya Spiral Magnet: YI Su Do(Department of Physics, Sungkyunkwan University), ONODA Shigeki(Condensed Matter Theory Laboratory, RIKEN, Japan), NAGAOSA Naoto(Department of Applied Physics, The University of Tokyo, Japan), HAN Jung hoon(Department of Physics, Sungkyunkwan University)

D-48[10:45-11:00]\* 순수한 PbPdO<sub>2</sub> 박막에서의 ER & MR 효과: 추 성민, 이 규준, 박 성민, 박 광서, 이 성익, 정 명화(서강대), 조 영훈(한국기초과학지원연구원 나노물성팀)

## [DG7] General Session: 강상관계

장 소 : 302

10월 23일(금) 11:15 - 13:00

좌 장 : 김일원(울산대)

D-49[11:15-11:30] Cu doping effect on the electronic structure of NbSe<sub>2</sub> revealed by ARPES: KIM Y.K, KOH Y.Y, JUNG Y.S (Institute of Physics and Applied Physics, Yonsei University)

D-50[11:30-11:45] Ferroelectric Properties of Lead-free Na<sub>0.5</sub>K<sub>0.5</sub>NbO<sub>3</sub>-based Thin Films Derived from Chemical Solution Deposition Method: KIM ILL WON, LEE SUN YOUNG(Department of Physics, University of Ulsan), AHN CHANG WON, HWANG HAK IN(Convergence Components R&D Division, KETI), BAE SE HWAN(Department of Physics, Dong-A University)

D-51[11:45-12:00] 중성자 Pair Distribution Function 분석을 이용한 BaZr<sub>x</sub>Ti<sub>1-x</sub>O<sub>3</sub> 국소구조 연구: 박 창열, 안 재석, 박 성균, 정 일경(부산대)

D-52[12:00-12:15]\* Probing spin glass behavior in the strongly correlated electron system La<sub>2</sub>Cu<sub>1-x</sub>Li<sub>x</sub>O<sub>4</sub>: 박 은성, 박 두선(성균관대), SARRAO J.L., THOMPSON J.D.(Los Alamos National Laboratory)

D-53[12:15-12:30]\* Multiple Bosonic Mode Coupling In The Band Dispersion Of Sr<sub>2</sub>RuO<sub>4</sub>: KIM Chul, PARK Seung Ryong, LEEM C. S., SONG D. J., KIM Y. K., CHOI S. K., JUNG W. S., KOH Y. Y.(Institute of Physics and Applied Physics, Yonsei University), YOSHIDA Y.(Nanoelectronics Research Institute, National Institute of Advanced Industrial Science and Technology, Japan), KIM C.(Institute of Physics and Applied Physics, Yonsei University)

D-54[12:30-12:45]\* Nanoscale Supersolidity in <sup>4</sup>He Adsorbed on a C<sub>20</sub> Molecule: 권 용경, 신 현덕(건국대)

D-55[12:45-13:00]\* Electron and spin correlations in electron doped high T<sub>c</sub> superconductor Pr<sub>1-x</sub>LaCe<sub>x</sub>CuO<sub>4</sub>: 송 동준, 박 승룡, 최 성균, 김 철, 김 용관, 정 원식, 고 윤영(연세대), YOSHIDA Yoshiyuki, EISAKI Hiroshi(AIST), 김 창영(연세대)

## [DF2] Focus Session: FeAs-based Superconductors I

(한국물리학회-한국초천도학회 공동주관 I)

장 소 : 컨벤션 I

10월 23일(금) 10:30 - 12:30

좌 장 : 방윤규(전남대)

DF-05[10:30-10:45] Superconductivity of optimally doped single crystals of the BaFe<sub>1.8</sub>Co<sub>0.2</sub>As<sub>2</sub> superconductor: LEE Sung-ik(National Creative Research Initiative Center for Superconductivity, Department of Physics, Sogang University), CHOI Ki-Young(National Creative Research Initiative Center for Superconductivity, Department of Physics, Sogang University, Department of Physics, Seoul University), KIM Soo Hyun, CHOI Changho, JUNG Myung-Hwa(National Creative Research Initiative Center for Superconductivity, Department of Physics, Sogang University), WANG X. F., CHEN X. H.(Hefei National Laboratory for Physical Sciences at Microscale and Department of Physics, University of Science and Technology of China, China), NOH Jae Dong(Department of Physics, Seoul University)

DF-06[10:45-11:00] Nearly isotropic upper critical field in superconducting SrFe<sub>1.85</sub>Co<sub>0.15</sub>As<sub>2</sub> and FeSe<sub>0.4</sub>Te<sub>0.6</sub> single crystal: KHIM Seunghyun, KIM Jae Wook(FPRD, Department of Physics and Astronomy, Seoul National University), KIM Jun Sung(Department of Physics, Pohang University of Science and Technology), CHOI Eun Sang(National High Magnetic Field Laboratory, Florida State University, USA), BALAKIREV F. F.(National High Magnetic Field Laboratory, Los Alamos National Laboratory, USA), NOHARA Minoru(Department of Physics, Okayama University, Japan), LEE Suk Ho(Optical Engineering Research Institute, Mokpo National University), TAKAGI

- Hiddenori(Department of Advanced Materials, University of Tokyo, JST, TRIP, RIKEN, Japan), BANG Yunkyu (Department of Physics, Chonnam National University), KIM Kee Hoon(FPRD, Department of Physics and Astronomy, Seoul National University)
- DF-07[11:00-11:15] Single crystal growth and investigation of the new superconductor LiFeAs with  $T_c=18.3$  K: GHIM Jin Soo (Department of Physics, Sungkyunkwan University), JUNG MYUNG HWA(National Creative Research Initiative Center for Superconductivity, Department of Physics, Sogang University), KWON Young Seung(Department of Physics, Sungkyunkwan University)
- DF-08[11:15-11:30]\* Theoretical Study of Electronic Structures in Iron Pnictide Superconductors using the Coherent Potential Approximation: MOON Jisoo, CHOI Hyoung Joon(Department of Physics and IPAP, Yonsei University)
- DF-09[11:30-11:45] First-Principles Study On The Magnetic Properties of Iron Chalcogenide Superconductors: MOON Chang-Youn, CHOI Hyoung Joon(Department of Physics and IPAP, Yonsei University)
- DF-10[11:45-12:00]\* Direct observation of two-gap superconductivity in  $\text{SrFe}_{1.85}\text{Co}_{0.15}\text{As}_2$  single crystals by scanning tunneling microscopy and spectroscopy: PARK Jewook(Center for Strongly Correlated Materials Research, Department of Physics and Astronomy), KHIM Seunghyun, JEON Gun Sang(Department of Physics and Astronomy, Seoul National University), KIM Jun Sung(Department of Physics, Pohang University of Science and Technology), KIM Kee Hoon(Department of Physics and Astronomy, Seoul National University), CHAR Kookrin(Center for Strongly Correlated Materials Research, Department of Physics and Astronomy, Seoul National University)
- DF-11[12:00-12:15]\* Synthesis and Investigation of the New Superconductor  $\alpha\text{-FeSe}$  ( $T_c\sim 9.4\text{K}$ ): SONG Yoo-Jang(Department of Physics, Sungkyunkwan University), JUNG Myung Hwa(National Creative Research Initiative Center for Superconductivity, Department of Physics, Sogang University), RHYEE Jong-Soo(Materials Research Laboratory, Samsung Advanced Institute of Technology), KWON Young-Seung(Department of Physics, Sungkyunkwan University)
- DF-12[12:15-12:30] The interplay between superconductivity and magnetism in the sign reversed pairing model of the pnictides: LEE Nayoung, CHOI Han-Yong(Department of Physics, SungKyunKwan University)

## [DG8] General Session: 바이오/유기물

장 소 : 606

10월 23일(금) 13:30 – 15:30

좌 장 : 윤완수(표준연)

- D-56[13:30-13:45] Single-molecule Fluorescence Imaging in Living Cells: 이 남기(포항공대)
- D-57[13:45-14:00]\* Dynamic Bending and Cleavage of Single-DNA Molecules by Human Topoisomerase II $\alpha$ : LEE Sanghwa, HOHNG Sungchul(Seoul National University, Department of Physics and Astronomy)
- D-58[14:00-14:15]\* Multi-color FRET with Hundreds Single-molecules at a Time: LEE Jinwoo, HOHNG Sungchul(Department of Physics & Astronomy, Seoul National University)
- D-59[14:15-14:30]\* Conformational Dynamics between B- and Z-DNA probed via single-molecule FRET: BAE Sangsu(Seoul National University, Department of Physics and Astronomy), KIM Doyoun(Sungkyunkwan University School of Medicine, Department of Molecular Cell Biology), KIM Yang-Gyun(Sungkyunkwan University, Department of Chemistry), KIM KyeongKyu(Sungkyunkwan University, School of Medicine, Department of Molecular Cell Biology), HOHNG Sungchul(Seoul National University, Department of Physics and Astronomy)
- D-60[14:30-14:45]\* Single-molecule Detection of RecA Filament Dynamics: KIM Sunghyun(Sogang University, Department of Physics and Interdisciplinary Program of Integrated Biotechnology), JOO Chirlmin(School of Biological Sciences, Seoul National University), PARK Jeehae, RAGUNATHAN Kaushik(Howard Hughes Medical Institute, Department of Physics and Center for Biophysics and Computational Biology, University of Illinois at Urbana-Champaign), KIM Doseok(Sogang University, Department of Physics and Interdisciplinary Program of Integrated Biotechnology), HA Taekjip(Howard Hughes Medical Institute, Department of Physics and Center for Biophysics and Computational Biology, University of Illinois at Urbana-Champaign)
- D-61[14:45-15:00] Anion-dependant structural change of ionic liquids studied by infrared absorption spectroscopy: JEON Yoonnam, CHA Seoncheol, KIM Doseok(Sogang University, Department of Physics), KANG Minhyuck, MOON Bongjin (Sogang University, Department of Chemistry), MOON Hyerim, CHEONG Hyeonsik(Sogang University, Department of Physics), OUCHI Yukio(Nagoya University, Department of Chemistry)
- D-62[15:00-15:15]\* Effect of the Refractive Index of the Medium in Fluorescence Correlation Spectroscopy: CHA Seon Cheol, KIM Sung Hyun, KIM Doseok(Department of Physics, Sogang University)
- D-63[15:15-15:30] Covalent Interactions between PCBM and P3HT in Bulk Heterojunction Polymer Solar Cells: LEE Eun-Cheol, XIE Xiaoyin(College of Bio-Nano Technology, Kyungwon University)

## [DF3] Focus Session: FeAs-based Superconductors II

(한국물리학회-한국초천도학회 공동주관 II)

장 소 : 컨벤션 I

10월 23일(금) 13:30 - 15:30

좌 장 : 이후종(포항공대)

- DF-13[13:30-13:45] Effects of Two Gaps and Paramagnetic Pair Breaking on the Upper Critical Field of  $\text{SmFeAsO}_{0.85}$  and  $\text{SmFeAsO}_{0.8}\text{F}_{0.2}$  Single Crystals: LEE Hyun-Sook(Pohang University of Science and Technology, Department of Physics), BARTKOWIAK Marek(Forschungszentrum Dresden-Rossendorf, Hochfeld-Magnetlabor Dresden), PARK Jae-Hyun, LEE Jae-Yea(Pohang University of Science and Technology, Department of Physics), KIM Ju-Young, CHO B. K.(Gwangju Institute of Science and Technology, Materials Science and Engineering), JUNG Chang-Uk(Hankuk University of Foreign Studies, Department of Physics), KIM Jun Sung, LEE Hu-Jong(Pohang University of Science and Technology, Department of Physics)
- DF-14[13:45-14:00] Single Crystal Growth of Fe-chalcogenide  $\text{Fe}_{1+x}\text{Se}_{1-x}\text{Te}_x$  and their Physical Properties: LEE Bumsung, KHIM Seung Hyun, KIM Kee Hoon(Department of Physics and Astronomy, Seoul National University)
- DF-15[14:00-14:15] Vortex dynamic and gap symmetry for single crystals of the  $\text{BaFe}_{1.8}\text{Co}_{0.2}\text{As}_2$  superconductor: CHOI Ki-Young, LEE Sung-Ik, KIM Soo Hyun, CHOI Chanho, JUNG Myung-Hwa(Creative Research Initiative Center for Superconductivity, Department of Physics, Sogang University), NOH Jae Dong(Department of Physics, University of Seoul)
- DF-16[14:15-14:30] The Growth of High-quality c-axis Oriented Co-doped  $\text{SrFe}_2\text{As}_2$  Thin Films by Pulsed Laser Deposition with Excimer Laser: CHOI Eun-Mi, JUNG Soon-Gil, LEE Nam-Hoon, KWON Young-Seung, KANG Won Nam(BK21 Physics Division and Department of Physics, Sungkyunkwan University), KIM Dong Ho(Department of Physics, Yeungnam University), JUNG Myung-Hwa, LEE Sung-Ik(Department of Physics, Sogang University), SUN Liling(National Laboratory for Superconductivity, Institute of Physics, Chinese Academy of Sciences)
- DF-17[14:30-14:45]\* Superconducting properties of P-doped  $\text{BaFe}_2\text{As}_2$ : HONG J. B., JANG Y. R.(Department of Physics, Sungkyunkwan University), RHYEE J. S.(Material Research Laboratory, Samsung Advanced Institute of Technology), CHO J. H.(Nano Material Research Team, Korea Basic Science Institute), JUNG M. H.(Department of Physics, Sogang University), KWON Y. S.(Department of Physics, Sungkyunkwan University)
- DF-18(초)[14:45-15:15] 고온 초전도체의 분광학적 특성: 황 정식(부산대)
- DF-19[15:15-15:30]\* First-principles Study of Fermi Surface Topology in Underdoped High- $T_c$  Superconductors: OH Hyungju, CHOI Hyoung Joon(Department of Physics and IPAP, Yonsei University)

[EG1] General Session: Nanotubes and Nanowires

장 소 : 601-602

10월 21일(수) 13:30 - 15:15

좌 장 : 이우영(연세대)

- E-01[13:30-13:45]\* Hydrogen Sensing Mechanism of Pd Nanoparticle-grafted Single-walled Carbon Nanotubes with Dendrimers: LEE Jun Min(연세대), JU Seonghwa, JUNG Yeongri, KIM Sung-Jin(이화여대), LEE Wooyoung(연세대)
- E-02[13:45-14:00]\* Large-Scale Separation of Metallic and Semiconducting Single-Walled Carbon Nanotubes using Octadecylamine (ODA): 김 형준, 황 성식(Nanomaterial National Core Research Center, Yonsei University), 장 영욱(Department of Physics, Yonsei University), 오 제승(Nanomaterial National Core Research Center, Yonsei University), 유 경화(Nanomaterial National Core Research Center, Yonsei University; Department of Physics, Yonsei University)
- E-03[14:00-14:15]\* Stability of screen-printed carbon nanotube field emitters under residual gases: LEE Hansung, JANG Eunsoo, GOAK Jeungchoon, LEE Naesung(Faculty of Nanotechnology and Advanced Materials Engineering, Sejong University)
- E-04[14:15-14:30] Fabrication of Rigid and Low-Resistance Contacts for Carbon Nanotube Using Eutectic Alloy: JEON Dongryul, PARK Daehyun(Seoul National University)
- E-05[14:30-14:45] Plasmon-Induced Photoconductance In Mesoporous TiO<sub>2</sub> Nanofibers Loaded With Au Nanoparticles: 손 민수, 임 지은, 왕 강균, 오 승임, 김 용록, 유 경화(연세대)
- E-06[14:45-15:00] Reset Current Reduction in NiO Nanowires Array Using AAO Membrane: 김 성인, 장 영욱, 유 경화(연세대)
- E-07[15:00-15:15]\* Seebeck Coefficient of Individual Single-crystalline Bi Nanowires Grown by On-Film Formation of Nanowires: LEE Seung Hyun, HAM Jinhee, LEE Jun Min, LEE Wooyoung(Nanomaterial National Core Research Center and Department of Materials Science and Engineering, Yonsei University)

[EG2] General Session: Nanostructures and Materials

장 소 : 601-602

10월 21일(수) 15:45 - 17:30

좌 장 : 유경화(연세대)

- E-08[15:45-16:00]\* Semiconducting Bi Nanowires Showing Semimetal-to-semiconductor Transition Grown by On-Film Formation of Nanowires: HAM Jinhee, LEE Seunghyun, LEE Wooyoung(Department of Materials Science and Engineering, Yonsei University)
- E-09[16:00-16:15]\* Ultra-low Thermal Conductivity of Bi-Te Core/shell Nanowire: KANG Joohoon, ROH Jongwook, HAM Jinhee, LEE Seunghyun, LEE Wooyoung(Department of Materials Science and Engineering, Yonsei University)
- E-10[16:15-16:30]\* Building Lactate Biosensors via a Facile Layer-by-Layer Assembly: 양 형우, 김 동청(BK21 Physics Research Division, Department of Energy Science, Institute of Basic Science, SKKU Advanced Institute of Nanotechnology and Center for Nanotubes and Nanostructured Composites, Sungkyunkwan University), 유 상훈, 박 성호(Department of Chemistry, Department of Energy Science, Institute of Basic Science, SKKU Advanced Institute of Nanotechnology and Center for Nanotubes and Nanostructured Composites, Sungkyunkwan University), 강 대준(BK21 Physics Research Division, Department of Energy Science, Institute of Basic Science, SKKU Advanced Institute of Nanotechnology and Center for Nanotubes and Nanostructured Composites, Sungkyunkwan University)
- E-11[16:30-16:45] The Diminishing Magneto Resistance in High Electric Fields in Polyacetylene Nanofibers: 최 아경, 이 현정(서울대), KAISER Alan B.(Victoria University of Wellington, MacDiarmid Institute for Advanced Materials and Nanotechnology), 장 성호, 이 승현, 유 재승, 김 형섭, 남 영우, 박 승주, ALESHIN Andrey N.(서울대), 고 문주, AKAGI Kazuo (Department of Polymer Chemistry, Kyoto University), KANER Richard B.(University of California at Los Angeles, Department of Chemistry and Biochemistry), BROOKS James(Florida State University, National High Magnetic Field Laboratory), SVENSSON Johannes(Department of Physics, Göteborg University), BRAZOVSKII Serguei(Université Paris-Sud, LPTMS-CNRS), KIROVA Natasha(Université Paris-Sud, CNRS-UMR 8502), 박 영우(서울대)
- E-12[16:45-17:00] Facile Synthesis of Single Crystalline Vanadium Pentoxide Nanowires and their Photocatalytic Behavior: SHAHID Muhammad, SHAKIR Imran, RHEN Danielle(BK21 Physics Research Division, Department of Energy Science, Institute of Basic Science, SKKU Advanced Institute of Nanotechnology and Center for Nanotubes and Nanostructured Composites, Sungkyunkwan University), PATOLE Shashikant, 유 지범(School of Advanced Materials Science and Engineering, Sungkyunkwan University), 강 대준(BK21 Physics Research Division, Department of Energy Science, Institute of Basic Science, SKKU Advanced Institute of Nanotechnology and Center for Nanotubes and Nanostructured Composites, Sungkyunkwan University)
- E-13[17:00-17:15] Fluctuation-Induced Tunneling Conduction in Perchlorate Doped Tetrathiafulvalene-Diamide Nanofibers: 안 세정, 김 유경, 백 승재(서울대), ISIMOTO Shohei, IYODA Masahiko(Department of Chemistry, Graduate School of Science

and Engineering, Tokyo Metropolitan University), 홍 성주, 박 영우(서울대)

E-14[17:15-17:30]\* Flexible Transparent Conductive Films of Multiwall Carbon Nanotube/PEDOT-PSS: YUN Chan Ki, CHA Yun Mi, HA Byeongchul(The Department of Nano Science, Cheongju University)

---

### [EG3] General Session: Nanostructures and Materials

장 소 : 301

10월 22일(목) 09:00 – 10:45

좌 장 : 박영우(서울대)

- E-15[09:00-09:15] Electrical Properties of Electrospun Polyaniline- Polyethylene Oxide Nanofibrous Membranes Filled with Single-walled Carbon Nanotubes: SUNDARAY Bibekananda, 최 아정, 박 영우(서울대)
- E-16[09:15-09:30] Aharonov Bohm Effects in Graphene Nanorings: PARK Yung Woo, YOO Jai Seung, NAM Young Woo, CHU Seung Wan(Department of Physics and Astronomy, Seoul National University), SMET Jurgen H., SKAKALOVA Viera, ROTH Siegmar(Max-Planck-Institut für Festkörperforschung, Germany)
- E-17[09:30-09:45]\* Fabrication of Transparent Conductive Single-Walled Carbon Nanotube Films With Surfactant Dispersion and Chemical Modification: LEE Naesung, LEE Seungho, GOAK Jungchoon, KIM myoungsu(세종대)
- E-18[09:45-10:00] Size-homogeneous metal nanoparticles supported on multi-walled carbon nanotubes via MeV electron beam irradiation: SONG Wooseok, JEON Cheolho, KWON Young Taek, JUNG Dae Sung, CHOI Won Chel, PARK Chong-Yun(Sungkyunkwan University, Department of Physics, Center for Nanotubes and Nanostructured Composites (CNNC))
- E-19[10:00-10:15]\* Fabrication of Transparent Conductive Carbon Nanotube Films Having Low Sheet Resistance: 김 명수, 꺾 정춘, 이 승호(세종대), 한 종훈(전자부품연구원), 이 내성(세종대)
- E-20[10:15-10:30]\* Light Passing Through a Cathode Plate Fabricated by Using Transparent Single-Walled Carbon Nanotube Field Emitters: LEE Naesung, JANG Eunsoo, GOAK Jeungchoon, LEE Hansung, LEE Seungho(세종대)
- E-21[10:30-10:45] Enhanced Electric Double Layer Capacitance of Poly Sodium 4-Styrenesulfonate/Graphene Oxide Electrodes with High Cyclic Performance: JEONG Hae-Kyung, JIN Meihua, RA Eun Ju(Sungkyunkwan University, BK21 Physics, Department of Energy Science, Center for Nanotubes and Nanostructured Composites), SIM Kyu Yun(Samsung SDI, Energy Lab), AREPALLI Sivaram(Sungkyunkwan University, Department of Energy Science), LEE Young Hee (Sungkyunkwan University, BK21 Physics, Department of Energy Science, Center for Nanotubes and Nanostructured Composites)

---

### [EG4] General Session: Nanostructures and Materials

장 소 : 301

10월 22일(목) 11:15 – 13:00

좌 장 : 권영균(경희대)

- E-22[11:15-11:30] Imaging the anisotropic thermoelectric power of  $\text{Ti}_3\text{SiC}_2$  with nanometer resolution: CHO sanghee, LYEO H.-K., CHUNG T.(Korea Research Institute of Standards and Science), YOO H.-I.(Seoul National University, School of Materials Science and Engineering)
- E-23[11:30-11:45]\* Deformation Field Distribution of Zeolites Induced by Negative Thermal Expansion: CHA Wonsuk, SONG Sanghoon(Sogang University, Department of Physics and Interdisciplinary Program of Integrated Biotechnology), JEONG Nak Cheon, YOON Kyung Byung(Sogang University, Department of Chemistry and Interdisciplinary Program of Integrated Biotechnology), ROSS Harder(Argonne National Laboratory, Advanced Photon Source), ROBINSON Ian K.(University College London, Department of Physics and Astronomy), KIM Hyunjung(Sogang University, Department of Physics and Interdisciplinary Program of Integrated Biotechnology)
- E-24[11:45-12:00]\* Formation of Ti metal nano-dot arrays by an indentation method using atomic force microscopy: 정 보라, 조 월렬 (이화여대 물리학과)
- E-25[12:00-12:15] 전자빔 조사에 의한  $\pi$ -공액 고분자 나노 물질 특성 개질 연구: 홍 영기, 박 동혁, 구 민호(고려대), 김 대철, 김 정용 (인천대), 주 진수(고려대)
- E-26[12:15-12:30] A facile method to prepare regioregular poly(3-hexylthiophene) nanorod arrays using anodic aluminium oxide templates and capillary force: BAEK Sujin, PARK Jong Bae(Korea Basic Science Institute, Jeonju Center), LEE Soo-Hyoung(Chonbuk National University, School of Semiconductor and Chemical Engineering), YOUN Hyung-Joong, LEE Jouhahn(Korea Basic Science Institute)
- E-27[12:30-12:45]\* Theoretical Investigation on Structural and Mechanical Properties of Fe-based Alloys: KANG SungJin, KIM Miyoung(서울대), KWON Young Kyun(경희대)

E-28[12:45-13:00]\* Negative Curvature Effects on the Vibrational Spectra of Various Fullerene-like Structures: Density Functional Study: PARK Sora, AHN Jeung Sun(Department of Physics, Kyung Hee University), KWON Young-Kyun(Department of Physics and Research Institute for Basic Sciences, Kyung Hee University)

## [EG5] General Session: Photonics and Metamaterials

장 소 : 301

10월 22일(목) 13:30 - 15:30

좌 장 : 김철구(연세대)

- E-29(초)[13:30-14:00] Acoustic extraordinary transmission using Helmholtz resonator: 이 삼현(연세대 물리학과), 박 춘만(안양대 AEE 센터), 서 용문(명지대 물리학과), 김 철구(연세대 물리학과)
- E-30[14:00-14:15]\* 광자 결정 밴드에 레이저를 이용한 혼합 광결정의 밴드에지의 조절: 김 성환, 이 정국, 전 현수(서울대)
- E-31[14:15-14:30] Symmetry controlled resonance of anisotropic micro-sized planar metamaterial lattice in terahertz regime: 강 보영, 최 은영, 이 현희, 김 은선, 우 제훈, 김 정희, 우 정원(이화여대), 홍 태윤, 김 재훈(연세대)
- E-32[14:30-14:45] Chirality in metamaterials and its optical characteristics: 강 보영, 최 은영, 이 현희, 김 은선, 우 제훈, 김 정희, 우 정원(이화여대), 황 태종, 박 영준, 김 동호(영남대)
- E-33[14:45-15:00]\* 타원편광분석법을 이용한 AISb 유전함수 연구: 김 영동, 정 용우, 차 영훈, 김 승, 강 유진(경희대), 신 상훈, 송 진동(한국과학기술연구원 스핀소자연구센터)
- E-34[15:00-15:15]\* Active Feedback Cooling of a Quartz Tuning Fork with a Quality Factor Control: 장 정훈, 이 만희, 박 완, 제 원호(서울대)
- E-35[15:15-15:30]\* RCWA를 이용한 비대칭 나노구조의 연구: 변 준석, 김 태중, 한 승호, 공 태호, 윤 재진, 황 순용, 정 진모, 김 영동(경희대)

## [EG6] General Session: Devices and Applications

장 소 : 301

10월 22일(목) 15:45 - 17:30

좌 장 : 강대준(성균관대)

- E-36[15:45-16:00] Piezoresponse Force Microscopy of Ferroelectric Thin Films: KIM JinBae, CHOI MyungHoon, YOON KwanSeok, PARK Sang-il(Park Systems Corp.)
- E-37[16:00-16:15] Resistance switching mechanism of conducting STO: PARK HONGWOO, LEE SEUNGRAN, KIM MIYOUNG (Seoul National University, Department of Materials Science and Engineering), JUNG CHANGUK(Hankuk University of Foreign Studies, Department of Physics), YI Gyu-Chul(Seoul National University, Department of Physics and Astronomy)
- E-38[16:15-16:30]\* Transition from bipolar to unipolar resistance switching in a Pt/SrTiO<sub>x</sub>/Pt capacitor: 이 신범, 채 승철, 장 서형, 노 태원(서울대)
- E-39[16:30-16:45]\* Electrical and Optical transport of p-SWNT/n-ZnO Heterojunction Structure: 박 민지, 장 영욱, 강 봉근, 손 민수(연세대), 이 재상, 이 상렬(한국과학기술연구원 에너지재료연구센터), 유 경화(연세대)
- E-40[16:45-17:00]\* Semiconducting MoO<sub>3</sub> Nanorods for Highly Efficient UV/Visible Light Photocatalysis: SHAKIR Imran, SHAHID Muhammad, 강 대준(BK21 Physics Research Division, Department of Energy Science, Institute of Basic Science, SKKU Advanced Institute of Nanotechnology and Center for Nanotubes and Nanostructured Composites, Sungkyunkwan University)
- E-41[17:00-17:15] 조성변화에 따른 CuInSe<sub>2</sub> 박막물성과 태양전지의 성능: 고 항주(한국광기술원 광소자팀), 이 경훈(한국광기술원), 김 효진, 한 명수, 김 선훈(한국광기술원 광소자팀), 정 채환, 이 종호, 김 호성(한국생산기술연구원 광응용부품센터), 김 광복(금호전기(주) 태양광사업팀), 김 진혁(전남대)
- E-42[17:15-17:30] Enzymatic Biofuel Cells using Polypyrrole Nanowire Array: 김 지현, 김 성인, 유 경화(연세대)

## [EG7] General Session: Biophysics and Applications

장 소 : 301

10월 23일(금) 09:00 - 10:45

좌 장 : 홍승훈(서울대)

- E-43[09:00-09:15]\* Functionalization of Silicon Nanowires with Actomyosin Motor Protein for Bio-inspired Nanomechanical Applications: BYUN Kyung-Eun(Department of Physics and Astronomy, Seoul National University), HEO Kwang(Interdisciplinary Program in Nano-Science and Technology, Seoul National University), SHIM Sojung, CHOI Heon-Jin(Department of Materials Science and Engineering, Yonsei University), HONG Seunghun(Department of Physics and Astronomy,

Seoul National University)

- E-44[09:15-09:30]\* Amperometric Lactate Biosensor with High Sensitivity Using Immobilization of Lactate Oxidase onto Molybdenum Oxide Nanorods: SHAKIR Imran, 양 형우, SHAHID Muhammad(BK21 Physics Research Division, Department of Energy Science, Institute of Basic Science, SKKU Advanced Institute of Nanotechnology and Center for Nanotubes and Nanostructured Composites, Sungkyunkwan University), CHEREVKO S, 정 찬화(Department of Chemical Engineering, Sungkyunkwan University), 김 동청(청운대), 강 대준(BK21 Physics Research Division, Department of Energy Science, Institute of Basic Science, SKKU Advanced Institute of Nanotechnology and Center for Nanotubes and Nanostructured Composites, Sungkyunkwan University)
- E-45[09:30-09:45]\* Capacitance-Based Real Time Monitoring of Endocytosis: 이 리미, 김 평환, 최 정우, 김 규정, 김 경미, 박 윤정(연세대)
- E-46[09:45-10:00] Performances of Geiger-Mode Avalanche Photodiode PET Modules Transferring Scintillation Light via an Optical Fiber: HONG Seong Jong, KIM Chan Mi, CHO Sung Mook, WOO Heon(Eulji University, Department of Radiological Science), KWON Sun Il(Seoul National University, Department of Nuclear Medicine), RHEE June Tak(Konkuk University, Department of Physics), SONG In Chan(Seoul National University, Department of Radiology), LEE Jae Sung(Seoul National University, Department of Nuclear Medicine)
- E-47[10:00-10:15] 헌혈자 적합성 판별의 신뢰도 제고를 위한 혈액밀도 검사용 기준용액의 전국 혈액원과 KRISS의 상호비교: 이 용재, 장 경호, 정 호연(한국표준과학연구원)
- E-48[10:15-10:30] *In vivo* Imaging of Cancer Cells in the Primo-vascular System with Electroporation of Quantum Dots and Multispectral Imaging: 유 정선, 김 홍배(서울대 물리천문학부), 원 나연, 방 지원, 김 성지(포항공대 화학부), 안 세영, 소 광섭(서울대 물리천문학부)
- E-49[10:30-10:45]\* Anodized Aluminum Oxide-Based Capacitance Sensors for Direct Detection of DNA Hybridization: 강 봉근, 여 운진, 유 경화(연세대)

## [EG8] General Session: Surfaces, Interfaces, and Thin Films

장 소 : 301

10월 23일(금) 11:15 - 13:00

좌 장 : 김동욱(이화여대)

- E-50[11:15-11:30] Origin of oxygen migration in bipolar resistance switching of epitaxially grown NiO: LEE Seungran, KIM Hoonmin, CHAR Kookrin, BAK Junghoon, CHO Myoungae, PARK Yun Daniel(Seoul National University, Department of Physics and Astronomy), KIM Dongchirl, SEO Sunae, LI Xiangxu, PARK Gyeongsoo(Samsung Advanced Institute of Technology), JUNG Ranju(Kwangwoon University, Department of Electrophysics)
- E-51[11:30-11:45] 분무열분해법으로 성장된  $\text{Cd}_{1-x}\text{Zn}_x\text{S}$  박막의 구조와 광학적 특성: 서 동주, 김 고은, 이 소리, 박 정복, 김 지효, 김 나리, 오 상미(조선대), 김 진호(경상대)
- E-52[11:45-12:00]\* Surface profile measurement with *nanometer* scale resolution using oversampled coherent diffraction imaging in reflection geometry: 노 도영, MARATHE Shashidhara(광주과학기술원 신소재공학과), 김 상수(Argonne National Laboratory), 김 수남, 김 찬(광주과학기술원 신소재공학과), 강 현철(조선대)
- E-53[12:00-12:15]\* Spectral Response Analysis to Characterize the Channel/dielectric Interfacial Trap States for ZnO-based Thin-film Transistors: 임 성일, 이 기문(연세대), 오 민석(전자부품연구원), 박 찬호(연세대), 황 치선, 박 상희(한국전자통신연구원)
- E-54[12:15-12:30] X-선 광전자분광법과 흡수분광법을 이용한 비정질 ZnO 박막의 전자구조 연구: 조 덕용(성균관대), 김 정환, 나 광덕, 송 재원, 황 철성(서울대), 박 병규(포항공대)
- E-55[12:30-12:45] Structural phase Transition of Low-coverage Pentacene on  $\text{SiO}_2$  and Au surfaces: 임 규욱(포항공속기연구소), 이 경재(포항공대), 강 태희(포항공속기연구소), 정 석민(포항공대), 최 무영(서울대)
- E-56[12:45-13:00]\*  $\text{H}_2\text{O}$  Induced Structural Modification of Pentacene Crystal: 이 경재(포항공대), 임 규욱, 강 태희(포항공속기연구소), 정 석민(포항공대)

[FG1] General Session: 초청강연

장 소 : 601

10월 22일(목) 11:15 - 13:15

좌 장 : 정하웅(KAIST)

- F-01(초)[11:15-11:45] Control of Epigenetic Stability in Gene Expression: GHIM Cheol-Min(School of Nano-biotechnology & Chem Eng, Ulsan Nat'l Institute of Sci & Tech), ALMAAS Eivind(Dept of Biotechnology, Norwegian Univ. of Sci & Tech)
- F-02(초)[11:45-12:15] Networking metabolites, diseases, and drugs: 이 덕선(인하대)
- F-03(초)[12:15-12:45] 통계물리학 도구를 응용한 복잡계 네트워크 분석: 박 주용(서울대)
- F-04(초)[12:45-13:15] Entropy, self-organization and conditions of life: KIM Sungyun(Hoseo University)

[FG2] General Session

장 소 : 601

10월 22일(목) 13:30 - 15:30

좌 장 : 박형규(KIAS)

- F-05[13:30-13:45]\* 이차원 엑스웨이 모형에서의 정보전달 동역학: 최 무영, 김 민수, 정 다운, 권 현웅(서울대)
- F-06[13:45-14:00]\* Conformational Phases and Interaction of Polyelectrolytes: KOH Dong-Wook(Korea University, Department of Physics), YI Juyeon(Pusan National University, Department of Physics)
- F-07[14:00-14:15]\* Rotational Motion of Flow in Spirally Patterned Geometry: JEON Chanil, JEONG Hawoong(KAIST), JUNG YoungKyun(KISTI)
- F-08[14:15-14:30] A Mesoscopic Model of Transitions between B-DNA and Z-DNA: JEONG Seong Min, SUNG Wokyung(Department of Physics, POSTECH)
- F-09[14:30-14:45] Kramers problem for a polymer using path integral hyperdynamics: SHIN Jaeoh(Department of Physics, POSTECH), KHANDKAR Mahendra, ALA-NISSILA Tapio(Department of Applied Physics, Helsinki University of Technology), SUNG Wokyung(Department of Physics, POSTECH)
- F-10[14:45-15:00] Dynamics of Density Fluctuations for Interacting Brownian Particles: Field Theoretic Approach: KIM Bongsoo(창원대)
- F-11[15:00-15:15] An electromechanical hair cell: AHN Kang-Hun(Department of Physics, Chungnam National University)
- F-12[15:15-15:30] Correlation between price behavior and performance of different strategy evaluation schemes: BAEK Yongjoo, LEE Sang Hoon, JEONG Hawoong(KAIST 물리학과)

[FG3] General Session

장 소 : 601

10월 22일(목) 15:45 - 17:30

좌 장 : 국형태(경원대)

- F-13[15:45-16:00]\* Gaussian model and spectra dimensions of hierarchical scale-free networks: HWANG Sungmin(School of Physics and Center for Theoretical Physics, Seoul National University), LEE Deok-Sun(Inha University Natural Medical Sciences), KAHNG Byungnam, KIM Doochul(School of Physics and Center for Theoretical Physics, Seoul National University)
- F-14[16:00-16:15]\* Cascading Failure Dynamics on the World Trade Network: 이 규민, 양 재석(고려대), 김 건(서울대), 이 재성(서강대), 고 광일, 김 인묵(고려대)
- F-15[16:15-16:30]\* Human Disease Genes from Network Perspective: 최 지혜(고려대 물리학과), 노 한성, 최 인걸(고려대 생명공학부), 고 광일(고려대 물리학과)
- F-16[16:30-16:45]\* Noise Reduction In Genetic Oscillatory Systems: 민 병준, 고 광일, 김 인묵(고려대)
- F-17[16:45-17:00]\* Generalized Priority-Queue Network Dynamics: 조 원국, 민 병준, 고 광일, 김 인묵(고려대)
- F-18[17:00-17:15]\* Condensation in Zero Range Process with Pairwise Particle Interaction: KIM Sang-Woo, NOH Jae Dong(Department of Physics, University of Seoul)
- F-19[17:15-17:30]\* Length dependent charge conduction in DNA Duplex: KIM Seongjin(부산대), HWANG Sun-Yong(고려대), YI Juyeon(부산대)

통계물리학분과회 총회

장 소 : 601

10월 22일(목) 17:30 - 18:00

---

**[FG4] General Session****장 소 : 601****10월 23일(금) 09:00 - 11:00****좌 장 : 김상락(경기대)**

- F-20[09:00-09:15] 발표 취소
- F-21[09:15-09:30] Supercooled Liquid and Glass Transition in Aspirin: LEE Kwang-Sei(Inje University, Department of Nano Systems Engineering), KO Jae-Hyeon(Hallym University, Department of Physics), IKE Yuji, KOJIMA Seiji(University of Tsukuba, Institute of Materials Science)
- F-22[09:30-09:45] Metastable Patterns and Universality Classes in Directed Sandpile Models: 조 항현(고등과학원), 하 미순(한국과학기술원)
- F-23[09:45-10:00] Finite-size scaling in random  $K$ -satisfiability problems: HA Meesoon, LEE Sang Hoon, JEON Chanil, JEONG Hawoong(KAIST, Department of Physics)
- F-24[10:00-10:15] Phase transition and critical phenomena of generalized conserved lattice gas: YANG Jae-Suk, KIM In-mook(Korea University), KWAK Wooseop(Chosun University)
- F-25[10:15-10:30] Classification of stock markets according to their efficiency: YANG Jae-Suk(Korea University), CHOI Sooran, NAM Yeonghwan, KWAK Wooseop(Chosun University)
- F-26[10:30-10:45] Surface diffusion on an adatom or a void on an icosahedral cluster: LEE Min-Ho, KIM Do-Hyun, KIM Sangrak(Kyonggi Univ.), CHOI Je-Young(Youngdong Univ.)
- F-27[10:45-11:00] Prediction of protein structures with highly accurate backbone, side-chain, and hydrogen bond by using multiple layers of powerful global optimization: JOO Keehyoung(Korea Institute for Advanced Study, School of Computational Sciences), LEE Jinwoo(Kwangwoon University, Department of Mathematics), OH Mina(Korea Institute for Advanced Study, School of Computational Sciences), SHIN Seung-Woo(Soon Chun Hyang University, Genome Research Center for Allergy and Respiratory Diseases), KO Junsu, LEE Dongseon, PARK Hahnbeom, SEOK Chaok(Seoul National University, Department of Chemistry), LEE Sung Jong(Suwon University, Department of Physics), LEE Jooyoung(Korea Institute for Advanced Study, School of Computational Sciences)

---

**[FG5] General Session****장 소 : 601****10월 23일(금) 13:30 - 15:15****좌 장 : 강병남(서울대)**

- F-28[13:30-13:45] Polymer thin film growth model with vertically collimated flux: SON Seung-Woo, HA Meesoon, JEONG Hawoong(KAIST, Dept. Physics)
- F-29[13:45-14:00] Macroscopic Kinetic Effect of Cell-to-Cell Variation in Biochemical Reactions: KIM Pan-Jun, PRICE Nathan D.(Institute for Genomic Biology, University of Illinois at Urbana-Champaign)
- F-30[14:00-14:15] Biologically Inspired Computing Method for Two-armed Bandit Problem: KIM Song-Ju, AONO Masashi, HARA Masahiko(RIKEN, Advanced Science Institute)
- F-31[14:15-14:30] Criticality in Prisoner's Dilemma Game on Fractal Complex Networks: CHANG-KEUN Yun(Seoul National University, Department of Physics and Astronomy), NAOKI Masuda(The University of Tokyo, Graduate School of Information Science and Technology), BYUNGNAM Kahng(Seoul National University, Department of Physics and Astronomy)
- F-32[14:30-14:45] Underlying Dynamics of Explosive Percolation Transition: CHO Young Sul, KAHNG Byung Nam, KIM Doo Chul(서울대)
- F-33[14:45-15:00] Minimal Model for Traffic Flow: LEE Hyun Keun(Sungkyunkwan University), LEE Choongki(KIAS), KIM Beom Jun(Sungkyunkwan University)
- F-34[15:00-15:15] Stochastic Spiking Coherence in An Inhibitory Population of Subthreshold Neurons: LIM Woochang, KIM Sang-Yoon(강원대)

[GG1] General Session

장 소 : 604

10월 22일(목) 11:15 - 13:15

좌 장 : 박윤배(경북대)

- G-01[11:15-11:35] 지오데식 돔을 활용한 능동적인 벡터 학습 방안: 박 병윤, 이 호연(충남대)  
 G-02[11:35-11:55] 과학영재들의 협동적 문제 해결에서 아이디어 생성에 미치는 요인 분석: 최 재혁(전남대)  
 G-03[11:55-12:15] '입자-파동 이중성'에 관한 대학생의 개념 체계 조사: 정 용욱, 송 진웅(서울대)  
 G-04[12:15-12:35] ATmega128을 이용한 심전도 및 뇌파 측정기 제작 및 활용: 최 승하, 장 세중(한국교원대)  
 G-05[12:35-12:55] 과학교육에서 효과적 놀이 도입을 위한 놀이 분류 체계의 개발: 박 종호, 노 유정, 김 희진, 최 여진(진주교육대 과학교육과)  
 G-06[12:55-13:15] Demonstrations of the Action and Reaction Law and the Energy Conservation Law Using Fine Spherical Plastic Beads: KAGAWA K, TANAKA s, KOBAYASHI A(University of Fukui), 이 용인(전북대), KURINIAWAN KH, ISHII K, ISHII K, ISHII K(University of Fukui)

[GG2] General Session

장 소 : 604

10월 22일(목) 13:30 - 15:10

좌 장 : 최재혁(전남대)

- G-07[13:30-13:50]\* 장애학생에 대한 비장애학생의 태도 변화: 박 종호(진주교육대), 이 을수(부림초등학교)  
 G-08[13:50-14:10]\* 빛의 간섭과 회절과 관련된 개념 변화를 위한 탐구기반실험의 개발 및 적용: 윤 정화, 이 성묵(서울대)  
 G-09[14:10-14:30]\* ATmega8535를 이용한 음속측정 실험장치 개발: 정 민영, 박 명철, 장 세중(한국교원대 물리교육과)  
 G-10[14:30-14:50]\* 초등학교 영재 학생의 첨단 과학에 대한 인식 조사: 박 종호(진주교육대 과학교육과), 오 광택(용덕초등학교), 박 광훈(진주교육대 과학교육과)  
 G-11[14:50-15:10]\* 물리실험에서의 오차 및 불확실도 계산에 대한 학생들의 개념이해와 태도 분석: 이 민경, 이 성묵(서울대)

[HG1] General Session: New Technological Developments

장 소 : 605

10월 21일(수) 13:30 - 15:10

좌 장 : 정태훈(동아대)

- H-01[13:30-13:50] Development of Microwave Imaging Diagnostics for KSTAR: YUN G. S., LEE W., PARK H. K.(Department of Physics, POSTECH), DOMIER C. W., LIANG T., TOBIAS B., LUHMANN, JR. N. C.(Department of Electrical Engineering, University of California, Davis), MUNSAT T.(Center for Integrated Plasma Studies, University of Colorado, Boulder)
- H-02[13:50-14:10] Weak Landau Damping Instability Simulation using PIC: 황 치욱(국가수리과학연구소)
- H-03[14:10-14:30] Analysis of Organic Powder Samples Using Metal-Assisted Sub-Target Effect: 이 용인(전북대), KHUMAENI Ali, NIKI Hideaki, DEGUCHI Yoji, KURIHARA Kazuyoshi, KAGAWA Kiichiro(University of Fukui)
- H-04[14:30-14:50] Plan for Fourth Generation Radiation Source at Pohang Accelerator Laboratory: YOON Moohyun(POSTECH for the PAL FEL Task Force Team)
- H-05[14:50-15:10] Fine Structure of Injected Beam Charge in Laser Wakefield Acceleration in a Tapered Plasma Channel: HUR Min Sup, 신 동원(UNIST), 오 승용, 김 민석(APRI), 남 인혁(GIST), SUK Hyyong(APRI-GIST)

H

[HG2] General Session: Facility Reports

장 소 : 605

10월 21일(수) 15:45 - 17:45

좌 장 : 홍봉근(원자력연)

- H-06(초)[15:45-16:15] Status of the Proton Engineering Frontier Project: KIM Kui Young, CHOI Byung-Ho(Proton Engineering Frontier Project, Korea Atomic Energy Research Institute)
- H-07(초)[16:15-16:45] Status of the KSTAR operation and experiments: OH Y.K., KIM W. C., LEE J. H., KIM J. Y., YANG H.L., NA H. K., KWON M., LEE G. S.(National Fusion Research Institute)
- H-08(초)[16:45-17:15] PLS-II Status: NAM S. H., KIM K. R., KIM B. S., KIM D. E., PARK C. D., PARK S. J., KIM S. H., PARK S. S., HONG S. M., KIM J. Y., RAH S. Y., CHOI J. Y., KIM S. N., LEE H. S., KANG T. H., WIEDEMANN H., NAMKUNG W., REE M.(On Behalf of the PLS-II Project Team, PAL, POSTECH)
- H-09(초)[17:15-17:45] Design of Compact Spherical Tokamak Device at SNU: 황 용석, 성 충기(서울대)

[HG3] General Session: Fusion, New Concepts

장 소 : 605

10월 22일(목) 11:15 - 12:45

좌 장 : 권재민(핵융합연)

- H-10[11:15-11:30]\* Study of Impurity Distribution and Transport Coefficients Determination in ITER like Plasma: LIPING Zhu, WOOCHANG Lee, GUNSU Yun, HYEON Park(POSTECH, Department of Physics)
- H-11[11:30-11:45] Effect of Modification of Pressure Gradient on Low-n Ideal MHD Stability Limits in KSTAR Tokamak: HAN Hyunsun, NA Yong-Su, HONG Sang Hee(Department of Nuclear Engineering, Seoul National University), KWON Ohjin(Department of Physics, Daegu University)
- H-12[11:45-12:00] 입자궤도 추적을 통한 MHD 현상과 고에너지입자 수송현상의 상관관계연구: 이 동렬, 유 창모, 독고 경환(POSTECH)
- H-13[12:00-12:15] Modeling of Pedestal Build-up in Hybrid-modes at KSTAR: KIM Hyunseok, LEE Wonjae(Department of Energy System Engineering, Seoul National University), NA Yong-Su(Department of Nuclear Engineering, Seoul National University)
- H-14[12:15-12:30] Simulation of X-Ray Tube Based on a Microstructured X-Ray Target: IHSAN Aamir, HEO Sung Hwan, CHO Sung Oh(Dept. of Nuclear and Quantum Engineering, KAIST)
- H-15[12:30-12:45] Characteristics of a gas-filled capillary waveguide for laser-plasma acceleration: KIM Min-Seok, JANG Dogeun, JANG Donggyu, SUK Hyyong(Graduate Program of Photon Science and Technology, GIST)

[HG4] General Session

장 소 : 605

10월 23일(금) 09:00 - 10:15

좌 장 : 김경렬(포항가속기연)

- H-16[09:00-09:15]\* Efficient Focusing of High Power Microwave using COaxial Beam Rotating Antenna(COBRA) in Relativistic Backward Wave Oscillator (RBWO): 민 선홍, 정 희천, 박 건식(서울대), 안 지환, 이 상훈, 윤 영중(연세대), 김 준연, 최 준호, 소 준호(ADD)

- H-17[09:15-09:30]\* 전자빔에 의해 생성된 플라즈마에 관한 시뮬레이션 연구: 배 효원, 심 승보, 황 석원, 송 인철, 정 상영, 이 해준, 이 호준, 박 정후(부산대)
- H-18[09:30-09:45]\* 간섭계(Interferometer)를 이용한 빔사이즈 모니터링의 안정화 실험: 류 진영, 김 은산, 박 향규(경북대), 김 창범(포항가속기연구소)
- H-19[09:45-10:00] Spatiotemporal Behavior of Excited Xe atom density in the 1s5 metastable state according to He-Ne-Xe(20% ,25%, 30%) gas mixtures at alternating current plasma display panel(AC-PDP): 김 용희, 홍 영준, 최 은하(광운대)
- H-20[10:00-10:15] 상압 마이크로 플라즈마 jet을 이용한 세포 자연사 유도효과에 관한 연구: 김 선자, 박 혜선, 정 태훈, 배 세환(동아대)

[IG1] General Session

장 소 : 603

10월 22일(목) 11:15 - 13:20

좌 장 : 이종훈(영남대)

- I-01(초)[11:15-11:40] Generation of high-power sub-2-cycle laser pulses from a kHz Ti:Sapphire laser: 박 주윤(한국과학기술원 물리학과 /결맞는 X선 연구단)
- I-02(초)[11:40-12:05] 펄핑 빔과 입력빔 분포에 따른 페타와트급 증폭기 효율 계산: 유 태준, 성 재희, 이 성구, 이 창원, 이 종민, 정 태문, 이 종민(광주과학기술원, 고등광기술연구소 & 펄토과학기술연구센터)
- I-03(초)[12:05-12:30] 선편광된 Nd:YVO4-KTP 마이크로칩 레이저 개발: 김 인식(광주과학기술원, 광과학기술학제전공), 정 창수, 유 봉 안, 유 난이, 이 영락(광주과학기술원, 고등광기술연구소), 고 도경(광주과학기술원, 광과학기술학제전공, 고등광기술연구소)
- I-04(초)[12:30-12:55] Quantum Noise Squeezing of Solitonic Pulses in Optical Fibers: 주 형규, 이 은철(경원대)
- I-05(초)[12:55-13:20] 1-PW Femtosecond Laser at 0.1-Hz Repetition Rate: 성 재희, 이 성구, 유 태준, 정 태문, 이 창원, 이 종민, 진 율용, 이 종민(광주과학기술원, 고등광기술연구소 & 펄토과학기술연구센터)

[IG2] General Session

장 소 : 603

10월 22일(목) 13:30 - 15:10

좌 장 : 이종훈(영남대)

- I-06[13:30-13:50] Emission property of high-Q modes in deformed dielectric microcavities: LEE Soo-Young(Seoul National University), LEE Sang-Bum(Korea Research Institute of Standard and Science), KIM Sang Wook(Pusan National University), AN Kyungwon(Seoul National University)
- I-07[13:50-14:10] Effect of a linear thin film on the optical bistability of a nonlinear slab: PHUNG Duy Khuong, 김 기홍(아주대 에너지시스템학부), 임 한조(아주대 전자공학과)
- I-08[14:10-14:30]\* Diffractive Imaging using a Coherent Hard X-ray Source at Pohang Light Source: 노 도영, 김 수남, 김 찬, SHASHIDHARA Marathe, 이 수용(광주과학기술원 신소재공학과), 강 현철(조선대), 김 상수, SANDY Alec, SURESH Narayanan(Argonne National Laboratory)
- I-09[14:30-14:50]\* Broadband terahertz transparency of metamaterials using nanoantennas: 김 대식, 박 영미, 박 형렬, 김 현선, 경 지수, 서 민아, 정 영균, 안 광준(서울대), 안 영환(아주대), 박 규환(고려대)
- I-10[14:50-15:10]\* Phase-sensitive Near-field Scanning Optical Microscopy using Tungsten etched Tip: 김 대식, 김 규환, 김 현우, 안 재 성, 김 진은(서울대), 최 수봉, 박 두재(아주대), 안 광준(서울대)

[JG1] General Session

장 소 : 606

10월 23일(금) 09:00 - 11:00

좌 장 : 고광훈(원자력연)

- J-01[09:00-09:15]\* Measurement of trap parameters of a magneto-optical trap by the forced harmonic oscillation: 문 걸, 김 용희, 허 명선, 김 지현, 이 준현, 권 우진(서울대), 노 흥렬(전남대), 제 원호(서울대)
- J-02[09:15-09:30]\* Absorption Signal of Sub-Natural Width in the Hanle Configuration: 문 한섭, 유 예진(부산대), 노 흥렬(전남대)
- J-03[09:30-09:45]\* 파라핀이 코팅된 Rb 증기셀에서 EOM 을 통한 변조된 비선형 광자기 신호: 문 한섭, 이 현준, 유 예진, 배 인호(부산대)
- J-04[09:45-10:00]\* 전-정상 분산 공진기에서 무색수차  $\lambda/4$  파장판을 이용한 환경적으로 안정한 피코초 이터븀 광섬유 레이저 연구: 윤 태현, 장 광훈(고려대)
- J-05[10:00-10:15] Atomic Clock Based On Coherent Population Trapping: 임 신혁, 조 동현(고려대)
- J-06[10:15-10:30] Researches on EIT and Photonic Bandgap in Inhomogeneous Cs Atoms: ZHUO Z. C., SU X. M.(College of Physics, Jilin University), 김 중복(한국교원대)
- J-07[10:30-10:45]\* Statistical Quantum Optimization for Traveling Salesman Problem : Multi-stage Strategy: BANG Jeongho, LEE Jinhyoung(Department of Physics, Hanyang University)
- J-08[10:45-11:00] Nonclassicality as an entanglement monotone: LIM James, RYU Junghee(Department of Physics, Hanyang University), KIM Myung Shik(School of Mathematics and Physics, Queen's University), LEE Jinhyoung(Department of Physics, Hanyang University)

[JG2] General Session

장 소 : 606

10월 23일(금) 11:15 - 12:00

좌 장 : 조동현(고려대)

- J-09[11:15-11:30] Bell's Theorem in Weakly Coupled Electronic Mach-Zehnder Interferometers: 김 경락, 강 기천(전남대)
- J-10[11:30-11:45] Ultrafast Quantum Control for Optimal Nonlinear Absorption: LEE Sangkyung, LIM Jongseok, AHN Jaewook(KAIST)
- J-11[11:45-12:00] Ionization of an Atom in Ultrashort Elliptically-Polarized Laser Pulses: 이 민호, 최 낙렬, 변 창우(금오공대)

[KG1] General Session: 혼정 및 기타 반도체

장 소 : 602

10월 22일(목) 09:00 - 11:00

좌 장 : 김동욱(이화여대)

- K-01(초)[09:00-09:30] Mott Metal-Insulator Transition-Driven Memristive System and Electrical Oscillation in VO<sub>2</sub>: KIM hyun-tak, KIM Bong-jun(ETRI, MIT Device Lab.), LEE Yong Wook(ETRI, MIT Device Lab. & Pukyung Nat. Univ.), CHAE Byung-gyu(ETRI, MIT Device Lab.), DRISCOLL T., BASOV D.(UCSD)
- K-02(초)[09:30-10:00] 3D Unipolar Resistance Switching Memory Array Using NiO Storage Node and CuO/InZnO Diode: KANG Bo Soo(Hanyang University, Department of Applied Physics), KIM Ki Hwan(University of Delaware, Institute of Energy Conversion), LEE Myoung-Jae, BENAYAD 동욱, AHN Seung-Eon, LEE Chang Bum, KIM Chang Jung, PARK Youngsoo(Samsung Advanced Institute of Technology)
- K-03(초)[10:00-10:30] Making use of Suspended nano-Scale Devices: LI Tiefu(Institute of Microelectronics, Tsinghua University, China)
- K-04(초)[10:30-11:00] High band gap 산화물 반도체에서의 저항 변화 현상: 정 규호, 임 현식(동국대)

[KF1] Focus Session: ReRAM

장 소 : 602

10월 22일(목) 11:15 - 13:15

좌 장 : 김희상(숭실대)

- KF-01(초)[11:15-11:45] ReRAM의 기본 원리에 대한 물리학적 고찰: 노 태원, 채 승철, 장 서형, 이 신범, 이 재성, 강 병남(서울대 물리 천문학부)
- KF-02(초)[11:45-12:15] ReRAM의 응용분야와 상용화를 위한 전제조건: 백 인규(삼성전자)
- KF-03(초)[12:15-12:45] A correlation between the unipolar and bipolar resistance switching mechanisms in Pt/TiO<sub>2</sub>/Pt structure: KIM Kyung Min, CHOI ByungJoon, HAN Seungwu, HWANG Cheol Seong(Department of Materials Science and Engineering and Inter-university Semiconductor Research Center, Seoul National University)
- KF-04(초)[12:45-13:15] Abnormal bipolar-like resistance change behavior induced by symmetric electroforming in Pt/TiO<sub>2</sub>/Pt resistive switching cells: JEONG Doo Seok(Thin Film Materials Research Center, Korea Institute of Science and Technology), SCHROEDER Herbert, WASER Rainer(Institute of Solid State Research and JARA - Fundamentals of Future Information Technology, Research Center Jülich, Germany)

[KG2] General Session: III-V 화합물반도체

장 소 : 602

10월 22일(목) 13:30 - 15:30

좌 장 : 김진수(전북대)

- K-05(초)[13:30-14:00] 나노 분광기법을 이용한 단일 반도체 양자점의 광특성 연구: 임 상엽(Advanced Photonics Research Institute)
- K-06(초)[14:00-14:30] CIGS 태양전지 기술 동향: 박 래만, 정 용덕, 조 대형, 한 원석, 이 규석, 김 제하(한국전자통신연구원 차세대태 양광연구본부)
- K-07(초)[14:30-15:00] Formation of AlN Compounds on Al<sub>2</sub>O<sub>3</sub> Substrates During Nitridation: LEE Hyo Jong(Dong-A University, Materials Science and Engineering)
- K-08(초)[15:00-15:30] Bifurcation of a quasi-1D quantum wire at weak confinements: THOMAS Kalarikad Jonah(성균관대)

[KT1] Tutorial Session

장 소 : 602

10월 22일(목) 17:00 - 18:00

좌 장 : 김종수(영남대)

- KT-01(초)[17:00-18:00] Tunneling Spectroscopy in nano-scale Solid-State Devices: 임 현식(동국대)

[KG3] General Session: 원소, IV-IV, II-VI 화합물반도체

장 소 : 602

10월 23일(금) 09:00 - 11:00

좌 장 : 이상녕(해양대)

- K-09(초)[09:00-09:25] Recent Advances in Si Nanocrystal Light-Emitting Diodes: HUH Chul, KIM Kyung-Hyun, KO Hyun-Sung, KIM Bong-Kyu, KIM Wanjoong, HONG Jongcheol, SUNG Gun Yong(한국전자통신연구원 융합기술연구부)
- K-10(초)[09:25-09:50] High Speed Flash Memory by a Dopant-Segregated Schottky-Barrier MOSFET: CHOI Yang-Kyu(KAIST, EECS), JANG Moongyu(ETRI, Advanced I-MEMS Team), CHOI Sung-Jin(KAIST, EECS)
- K-11(초)[09:50-10:15] Complementary Use of Organic and Oxide Semiconductors: NA Jong ho, KITAMURA Masatoshi, ARAKAWA

- Yasuhiko(Institute for Nano Quantum Information Electronics (INQIE), University of Tokyo)
- K-12[10:15-10:30] THz response of dynamic Fano resonances in biased semiconductor superlattices: 제 구출(안양대)
- K-13[10:30-10:45]\* Simulation of Directed Self-Assembly for sub-10 nm Pattern Formation: Top-down and Bottom-up Approches: 김 상곤, 오 혜근, 정 영대, 안 일신, 권 영현(한양대)
- K-14[10:45-11:00]\* ZnO Nano-crystals Grown on a Profiled Sapphire(0001) Substrate with Au Nano-crystals: KANG HYON CHOL (Chosun University, Department of Advanced Materials Engineering)

---

## [KF2] Focus Session: ZnO 물성 및 응용

장 소 : 602

10월 23일(금) 11:15 - 13:15

좌 장 : 최경진(KIST)

- KF-05(초)[11:15-11:45] ZnO : Prospective oxide semiconductor: CHOI W.K.(Thin Film Materials Research Center, Korea Institute of Science and Technology)
- KF-06(초)[11:45-12:15] The microscopic properties and electronic structures of the ZnO-based amorphous oxides and O-vacancuy: 강 일준, 박 철홍(부산대 물리교육학과)
- KF-07(초)[12:15-12:45] ZnO nanomaterials를 이용한 flexible electronics: 김 상식(고려대)
- KF-08(초)[12:45-13:15] Surface polarity and morphology-controlled synthesis of one-dimensional ZnO nanostructures: PARK Won Il (Division of Materials Science and Engineering, Hanyang University)

[LT1] Tutorial Session: Tutorial on Horava Gravity and Progress Report of KGWG

장 소 : 606

10월 21일(수) 11:15 - 13:15

좌 장 : 이철훈(한양대)

LT-01(초)[11:15-12:00] The Horava Gravity: Introduction to Recent Developments: 박 무인(전북대)

LT-02(초)[12:00-12:45] Generalized Uncertainty Principle, Quantum Gravity and Horava-Lifshitz gravity: 명 연수(인제대)

LT-03(초)[12:45-13:15] Progress Report on the Gravitational Wave Research in Korea: 이 형목(서울대 물리천문학부), 강 공원(KISTI), 김 정리(Lund University, 스웨덴), 오 정근, 하 태영(NIMS)

[LG1] General Session: Gravitation

장 소 : 606

10월 21일(수) 13:30 - 15:30

좌 장 : 이형원(인제대)

L-01(초)[13:30-14:00] Fixing moduli with brane gas and flux in string cosmology: 김 진영(군산대, 물리학과)

L-02(초)[14:00-14:30] Generalization of Scaling Arguments for Gravitating Systems: 박 달호(상지대)

L-03(초)[14:30-15:00] Advent of GR via Induced Gravity theory followed by Chaotic Inflation: KIM Hongsu(한국천문연구원 국제천체 물리센터)

L-04(초)[15:00-15:30] Neutrino Oscillation in Magnetized Gamma-Ray Burst Fireball: KEUM Yong-Yeon(Korea University, Dept. of Physics)

[LG2] General Session: High Energy Astrophysics

장 소 : 606

10월 21일(수) 15:45 - 17:45

좌 장 : 박달호(상지대)

L-05(초)[15:45-16:15] Soft Gamma-ray Repeaters and Anomalous X-ray Pulsars in the Magnetar Model: SUH In-Saeng(University of Notre Dame, Center for Research Computing/Dept. of Physics), MATHEWS Grant J.(University of Notre Dame, Dept. of Physics), KONDRATYEV Vladimir(Taras Shevchenko National University, Nuclear Physics, Dept.)

L-06(초)[16:15-16:45] Gamma-ray production on the surface of the Moon using the MCNPX code system: KIM Kyeong Ja(한국지질자원 연구원), REEDY Robert C(Planetary Science Institute, USA), DRAKE Darrell(Tech Source, USA), HASEBE Nobuyuki(Waseda University, Research Institute of Science and Engineering, Japan)

L-07(초)[16:45-17:15] CREAM 고에너지 우주선 데이터 분석을 통한 에너지 스펙트럼의 새로운 결과: 박 일홍, 남 신우, 남 지우(이화 여대)

L-08(초)[17:15-17:45] The 1st Korea-Japan Experiments of the Real-time Transfer and Analysis for Very Large Scale Observational Data of Black Hole and Neutron Star Binaries and Stars: KIM Soon-Wook(Astronomy and Space Science Institute)

천체물리학과회 총회

장 소 : 606

10월 21일(수) 17:45 - 18:30

좌 장 : 김상표(군산대)

[LG3] General Session: Cosmic Rays

장 소 : 606

10월 22일(목) 09:00 - 11:00

좌 장 : 금용연(고려대)

L-09(초)[09:00-09:30] ANITA 실험을 통한 뉴트리노 탐색과 EAS 사건: 남 지우(이화여대)

L-10(초)[09:30-10:00] Fast Detection of the UV/Optical Photons from GRBs in Ultra Fast Flash Observatory: LIM Heuijin(Institute for the Early Universe (IEU), Ewha Womans University), SMOOT G. F., LINDER E. V.(Institute for the Early Universe (IEU), Ewha Womans University & Berkeley Center for Cosmological Physics (BCCP), University of California), GROSSAN B.(Berkeley Center for Cosmological Physics (BCCP), University of California), PARK I., JEONG J., KIM J. E., LEE H.Y.(Research Center of the MEMS Space Telescope, Ewha Womans University), LEE J., NAM J., NAM S.(Research Institute of Basic Science, Ewha Womans University), LEE C. H.(Physics Department, Pusan National University), PARK J.(School of Electronics and Electrical Engineering, Dankook University), YU H. J.(Department of Physics and Astronomy, Seoul National University.)

- L-11(초)[10:00-10:30] 극소형 MEMS 우주망원경 탑재체 개발 및 탑재: 이 직, 김 지은, 나 고운, 남 신우, 남 지우, 박 일홍, 서 정은, 이 혜영, 전 진아, 정 수민, 정 애라(이화여대), 박 재형(단국대), 이 창환(부산대), 박 용선, 유 형준, 김 민수, 김 용권, 유 병욱, 이 경진, 진 주영(서울대), GARIPOV Garik, KHRENOV Boris, KLIMOV Pavel(Moscow State University)
- L-12(초)[10:30-11:00] KASI new research of Earth Rotation - on going studies: NA Sung-Ho, CHO Jung-Ho, BAEK Jeongho, KWAK Younghee, YOO Sung-moon, SHIN Young-Hong, PARK Jong-Uk, PARK Pil-Ho(KASI)

## [LG4] General Session

장 소 : 606

10월 22일(목) 11:15 - 12:30

좌 장 : 김진영(군산대)

- L-13[11:15-11:30] Radial Dependence of Relative Abundances of Constituents in Compact Object: KIM Kyungmin, LEE Hyun Kyu(Hanyang University, Dept. of Physics)
- L-14[11:30-11:45]\* 블랙홀-중성자별 쌍성의 병합에 대한 해석적 연구: 조 희석, 이 창환(부산대)
- L-15[11:45-12:00] Numerical Simulations of General Relativistic Hydrodynamics in Spherical Symmetry: PARK Dongho(SNU, Department of Physics and Astronomy & KISTI)
- L-16[12:00-12:15] Instability of AdS Soliton Spacetime: OH Changheon(TechnovationPartners & Hanyang Univ.), KANG Gungwon (KISTI), LEE Chul H.(Hanyang Univ.)
- L-17[12:15-12:30]\* 실리콘 광증배소자 SIPM의 제작과 테스트: 이 혜영, 나 고운, 남 신우, 남 지우, 박 일홍, 이 직(이화여대)

## [LG5] General Session

장 소 : 606

10월 22일(목) 13:30 - 15:00

좌 장 : 이정재(대진대)

- L-18[13:30-13:45]\* Design of readout system in Ultra Fast Flash Observatory: KIM J.E., NA G.W, SUH J.E., LEE H.Y.(Research Center of the MEMS Space Telescope, Ewha Womans University), LEE Jik Lee(Research Institute of Basic Science, Ewha Womans University), PARK I., JEON J.A., JEONG S., JUNG A.R.(Research Center of the MEMS Space Telescope, Ewha Womans University), NAM S., NAM J.W.(Research Institute of Basic Science, Ewha Womans University), LIM H.(Institute for the Early Universe, Ewha Womans University), LINDER E. V., SMOOT G. F.(Institute for the Early Universe, Ewha Womans University, Berkeley Center for Cosmological Physics(BCCP), University of California, Berkeley), GROSSAN B.(Berkeley Center for Cosmological Physics(BCCP), University of California, Berkeley), LEE C.-H.(Physics Department, Pusan National University), PARK J.(School of Electronics and Electrical Engineering, Dankook University), YU H.J.(Department of Physics and Astronomy, Seoul National University), LEE C.-H.(Department of Physics, Pusan National University)
- L-19[13:45-14:00]\* 감마선 폭발관측을 위한 우주망원경의 반사경인 micromirror array의 디자인 및 제작: 전 진아, 서 정은, 박 일홍(이화여대), 박 재형(단국대), 김 민수(한국생산기술연구원)
- L-20[14:00-14:15]\* 감마선 폭발 관측을 위한 UFFO(Ultra Fast Flash Observatory) 우주 망원경의 시험모델의 광학 테스트: 정 수민, 남 신우, 남 지우, 박 일홍(이화여대), 박 재형(단국대), 이 직(이화여대), 이 창환(부산대), 임 희진, E. V. Linder, G.F. Smoot, B. Grossan(이화여대)
- L-21[14:15-14:30]\* 고충대기 극한 방전현상 관측을 위한 극소형 MEMS 우주망원경(MTEL: MEMS space Telescope for Extreme Lightning)의 제어시스템 및 통신 인터페이스: 나 고운, 김 지은, 박 일홍, 서 정은, 이 혜영, 전 진아, 정 수민, 정 애라, 남 신우, 남 지우, 이 직(이화여대), 박 재형(단국대), 이 창환(부산대), 박 용선, 유 형준, 김 민수, 김 용권, 유 병욱, 이 경진, 진 주영(서울대), GARIPOV Garik, KHRENOV Boris, KLIMOV Pavel(Moscow State University, The Department of Physics)
- L-22[14:30-14:45]\* 극한대기방전현상 관측을 위한 MTEL(MEMS Telescope for ExtremeLightning)의 최종 테스트: 서 정은, 김 지은, 나 고운, 박 일홍, 이 혜영, 전 진아, 정 수민, 정 애라(이화여대), 남 신우, 남 지우, 이 직(기초과학연구소), 박 용선, 유 형준(서울대), 박 재형(단국대), 김 용권, 유 병욱, 이 경진(서울대), 김 민수(한국생산기술연구원), GARIPOV G, KHRENOV B, KLIMOV P(Moscow State University, The Department of Physics)
- L-23[14:45-15:00]\* JEM-EUSO 실험의 트리거 논리회로 설계 및 작동: 정 애라, 남 신우, 박 일홍(이화여대)



# 포스터발표논문 시간표



10월 21일(수) 14:00 - 16:00

- Bp-I-001 MC study for SUSY with  $2e+\mu$  events at CMS: SONG Sanghyeon, KIM Zero, KIM Jae Yool(Department of Physics, Chonnam National University), CHOI Minkyoo, KANG Seo Kon(Department of Physics, University of Seoul), CHANG Sunghyun(Department of Physics, Kyungpook National University)
- Bp-I-002 Study on Gd Loaded Liquid Scintillator for RENO: 강 보라, 김 수봉, 박 정식, 신 진욱, 이 재승, 최 선희(서울대), 김 우영, 스테판 사뮤엘, 서 준석, 오 영도, 김 안드레이(경북대), 박 인곤(경상대), 안 정근, 이 효상(부산대), 박 강순(서경대), 김 동현, 박 차원, 백 승록, 유 인태, 최 영일(성균관대), 강 운구, 김 영덕, 마 경주, 전 은주(세종대), 김 병찬, 김 성현, 김 재를, 주 경광, 임 인택, 장 지승, 정 인석, 최 을임(전남대), 김 현수(전북대)
- Bp-I-003 3D Silicon Sensor의 전기적 특성의 Simulation 연구: 하 경호, 권 정택, 조 영권, 최 수용, 유 인태, 고 정환(성균관대)
- Bp-I-004 Update for the Background Estimations in  $W' \rightarrow \nu\mu$  Search at CMS: 김 지은, 장 성현, 김 동희(경북대), HOEPFNER Kerstin(RWTH Aachen), MALBERTI Martina(MIB Milano)
- Bp-I-005 Study of color coherence in LHC experiment: 박 상남, 강 서곤, 최 민규, 김 현용, 류 건모, 박 인규(서울시립대)
- Bp-I-006 Measurement of Optical Parameters in the RENO Liquid Scintillators: 박 정식, 강 보라, 김 수봉, 신 진욱, 이 재승, 최 선희(서울대), 김 우영, 스테판 사뮤엘, 서 준석, 오 영도, 김 안드레이(경북대), 박 인곤(경상대), 박 명렬(동신대), 안 정근, 이 효상(부산대), 박 강순(서경대), 김 동현, 박 차원, 백 승록, 유 인태, 최 영일(성균관대), 강 운구, 김 영덕, 마 경주, 전 은주(세종대), 김 병찬, 김 성현, 김 재를, 주 경광, 임 인택, 장 지승, 정 인석, 최 을임(전남대), 김 현수(전북대), N Danilov, YU Krylov, G Novikova, E Yanovich(INR/IPCE)
- Bp-I-007 Search for new physics in the  $\mu\mu^+e^+$ MET channel at CMS Detector at CERN: KIM Zero, SONG Sanghyeon, KIM Jae Yool(Department of Physics, Chonnam National University), KANG Seo Kon, CHOI Minkyoo(Department of Physics, University of Seoul), CHANG Sunghyun(Department of Physics, Kyungpook National University)
- Bp-I-008 Search for  $W' \rightarrow e\nu$  Decaying to an Electron-Neutrino Pair in  $PPbar$  Collision at  $\sqrt{s} = 1.96$  TeV: 김 지은, 양 유철, 김 동희, 오 영도, 서 준석, 장 성현, 칸 아딜, 우오즈미 사토르, 케몬 테루키(경북대, 물리및에너지학부), 김 수봉, 이 재승, 문 창성, 정 지은(서울대, 물리학부), 유 인태(성균관대, 물리학과), 주 경광(전남대, 물리학과), 김 현수(전북대, 물리학과), 전 은주(세종대, 물리학과), 조 기현, 공 대정, 조 일성(KISTI, 고에너지물리연구팀)
- Bp-I-009 Performance of the RENO Mockup Detector: 김 성현, 김 병찬, 김 재를, 주 경광, 임 인택, 장 지승, 정 인석, 최 을임(전남대), 김 우영, 사뮤엘 스테판, 서 준석, 오 영도, 김 안드레이(경북대), 박 인곤(경상대), 박 명렬(동신대), 안 정근, 이 효상(부산대), 박 강순(서경대), 강 보라, 김 수봉, 박 정식, 신 진욱, 이 재승, 최 선희(서울대), 김 동현, 박 차원, 백 승록, 유 인태, 최 영일(성균관대), 강 운구, 김 영덕, 마 경주, 전 은주(세종대), 김 현수(전북대), N. Danilov, YU Krylov, G. Novikova, E. Yanovich(INR/IPCE)
- Bp-I-010 Study of Lepton-Flavor-Violating Decays  $B^0 \rightarrow l^+ l^- \tau^+ \tau^-$  using untagged method from Belle: SOHN Youngsoo, KWON Youngjoon(Yonsei University, Institute of Physics and Applied Physics)
- Bp-I-011 Trigger performance for doubly charged Higgs analysis in CMS experiment: 서 현관, 최 수용, 조 영권, 유 인태, 박 차원, 최 영일(성균관대)
- Bp-I-012 실험-컴퓨팅-이론의 융합연구 패러다임 설계 및 구축: 조 기현, 김 정현, 공 대정, 남 수현, 조 일성(KISTI, 고에너지물리연구팀), 이 정일, 함 승우(고려대, 물리학과)
- Bp-I-013 A Search for purely leptonic decays  $B \rightarrow l \nu$  using the full reconstruction method: 조 일성(한국과학기술정보연구원), 권 영준(연세대 물리학과), 조 기현(한국과학기술정보연구원), 최 경산(연세대 물리학과)
- Bp-I-014 Gamma-ray Background Rate Hitting into a Spherical Detector in a Spherical Underground Laboratory: WOO Jong-Kwan, KO Je Wou(제주국립대)
- Bp-I-015 A study of Lepton-Number-Violating  $B$  decay at Belle: 선 옥수, 권 영준(연세대)
- Bp-I-016 OSG기반 입자물리 실험 지원을 위한 그리드 인프라 구축: 김 범균, BONNAUD Christophe, 권 석면, 박 형우, 유 진승, 윤 희준, 이 종숙, 장 행진, 조 금원, 한 보영, 장 행진(한국과학기술정보연구원)
- Bp-I-017 A study of  $B \rightarrow J/\psi \pi \pi X$  at CDF Run II: 공 대정, 조 일성, 조 기현(한국과학기술정보연구원), 김 동희, 김 지은, 양 유철, 장 성현(경북대), 김 수봉, 정 지은, 이 재승, 문 창성(서울대), 유 인태(성균관대), 주 경광(전남대), 김 현수(전북대), 전 은주(세종대), 오 영도(포항공대)
- Bp-I-018\* Low Energy Micro Gamma Source For A Large Liquid Xenon Detector: 이 화용(한국표준과학연구원), 김 영덕(세종대), 김 용합(한국표준과학연구원), 송 정훈(공주대), 이 경범, 이 민규(한국표준과학연구원)
- Bp-I-019\* Study of Detection of Thermal Neutron with RPC: RHEE J.T., JO Hyun Yong, JAMIL M., JHANG H.J.(Konkuk University), HONG S.J.(Eulji University), LEE S.J.(Seo Nam University), BAHK S.Y.(Won Kwang University), KIM Y.J.(Cheju National University)

- Bp-I-020\* Scintillator-based Electromagnetic Calorimeter R&D and Prototype: KHAN Adil, KIM DongHee, UOZUMI Satoru, KIM Jieun, KONG Daejung, YANG Yuchul(Kyungpook National University, Physics Department), KAWAGOE Kiyotomo, JEANS Daniel(Kobe University, Department of Physics), TAKESHITA Tohru, KOTERA Katsushige, NISHIYAMA Miho, TAKAYUKI Sakuma(Shinshu University, Department of Physics), SUDO Yuji, TOSHINORI Ikuno(University of Tsukuba, Department of Physics), KAPLAN Alex, FEEGE Nils(DESY)
- Bp-I-021\* Study of the  $\Xi_c^0$  decay asymmetry parameters in  $\Xi_c^0 \rightarrow \Xi^- \pi^+$  weak decay: KIM Sunghyun, UNNO Y., B.G Cheon(Hanyang Univ., Department of Physics)
- Bp-I-022\* CMSSW의 효율적인 개발을 위한 Integration Build: 류 건모, 박 인규, 강 서곤, 박 상남, 김 현용, 최 민규(서울시립대)
- Bp-I-023\* A study of purely leptonic decays  $B^+ \rightarrow l^+ \nu$  using untagged method: 최 경산, 권 영준(연세대), 조 일성(한국과학기술정보연구원), 경 성현(연세대)
- Bp-I-024\* Momentum Measurements of Secondary Particles Emitted from Electron Neutrino CC Interactions in DONuT Experiment: 김 지현, 박 병도, 윤 천실, 송 진섭(경상대)
- Bp-I-025\* Development of CMS RPC Performance Measurement Software and the Performance of CMS RPC Detector: JO Youngkwon, CHOI Suyong, LEE Sungeun, CHOI Youngil(Sungkyunkwan University)
- Bp-I-026\* Measurement of Refractive Index of Liquid Scintillator and Acrylic at RENO: 장 종호(전남대, 물리학과), 김 우영, 사뮤엘 스테판난, 서 준석, 오 영도, 김 안드레이(경북대, 물리학과), 박 인곤(경상대, 물리학과), 박 명렬(동신대, 물리학과), 안 정근, 이 효상(부산대, 물리학과), 박 강순(서경대, 물리학과), 강 보라, 김 수봉, 박 정식, 신 진욱, 이 재승, 최 선호(서울대, 물리학과), 김 동현, 박 차원, 백 승록, 유 인태, 최 영일(성균관대, 물리학과), 강 운구, 김 영덕, 마 경주, 전 은주(세종대, 물리학과), 김 병찬, 김 성현, 김 재률, 주 경광, 임 인택, 장 지승, 정 인석(전남대, 물리학과), 김 현수(전북대, 물리학과)
- Bp-I-027 Jet Analysis on CMSSW: KIM Hyunyong, PARK Inkyu, KANG Seokon, CHIO Minkyoo, RYU Geonmo, PARK Sangnam(University of Seoul, Department of Physics)
- Bp-I-028 Analysis of Cosmic Muon Events: NAM Soon-Kwon(Kangwon National Univ), 허 성구(강원대)

## ■SESSION P1■

## 응집물질물리학과회 포스터 발표

장 소 : 포스터 발표장

10월 21일(수) 14:00 - 16:00

- Dp-I-001 Ferroelectric and piezoelectric properties of (Na,K,Li)(Nb,Ta,Sb)O<sub>3</sub> ceramics fabricated by citric acid assisted sol-gel method: 김 일원, 김 주성, 이 해준(울산대), 안 창원, 황 학인, 조 남규(전자부품연구원, 융합부품연구부), 배 세환(동아대)
- Dp-I-002 Electromechanical Properties of BiAlO<sub>3</sub> Modified Bi<sub>0.5</sub>(Na<sub>0.78</sub>K<sub>0.22</sub>)<sub>0.5</sub>TiO<sub>3</sub> Piezoelectric Ceramics: 김 일원, 장 기봉, ULLAH Aman, HUSSAIN Ali, 이 재신(울산대), 안 창원, 조 남규, 황 학인(전자부품연구소, 융합부품연구부), 정 연학, 박 언철((주)삼전, 기술연구소)
- Dp-I-003 The Effect of Al<sub>2</sub>O<sub>3</sub> Ultra Thin Layer on the Bi<sub>0.5</sub>Na<sub>0.5</sub>TiO<sub>3</sub> Based Ferroelectric Thin Films: 김 일원, 원 성식(울산대), 안 창원, 조 남규, 황 학인(전자부품연구원, 융합부품연구부)
- Dp-I-004 High-Speed Optical Gating in VO<sub>2</sub>: 이 용욱(ETRI/부경대, 전기과), 김 봉준, 최 성열, 채 병규(ETRI), 서 기완(UST, 차세대소자공학과), 김 현택(ETRI)
- Dp-I-005 Lattice Dynamics in K<sub>2</sub>SnCl<sub>6</sub> Observed by NQR Near the Structural Phase Transition Temperatures: 김 영훈, 서 용문(명지대), 염 태호(청주대), 최 덕, 송 승기(명지대)
- Dp-I-006 Dielectric relaxtions of (1-x)K<sub>1-x</sub>Na<sub>x</sub>NbO<sub>3</sub>-BaTiO<sub>3</sub>(x) ferroelectric ceramics: 전 병익(한국과학영재학교 물리학과), LI Guojie, 김 셋별, 최 병춘, 문 병기, 정 중현(부경대)
- Dp-I-007 X-선 흡수 분광학을 이용한 Ni(S,Se)<sub>2</sub>의 도체 부도체 전이 연구: 박 경자, 정 진원, 노 한진(전남대), 김 재영, 김 형도(포항가속기연구소), 허 남정(인하대), 김 성백(포항공대)
- Dp-I-008 Diode And Photocurrent Effect In Ferroelectrics: 원 충재, 허 남정, 박 영안, 류 한열(인하대)
- Dp-I-009 Photoluminescence spectra in ZnO nanorods in various gas atmospheres: LEE D J, SEO Y K, LEE Y S(Department of Physics, Soongsil University), PARK J H(Electronics and Telecommunications Research Institute), YOON S H(Division of Nano Sciences and Department of Physics, Ewha Womans University), YEE K J(Department of Physics, Chungnam National University)
- Dp-I-010 발표 취소
- Dp-I-011 강상관 전자계의 내각준위 광전자분광 스펙트럼에 대한 동적 평균장 이론 계산: 김 형도(포항가속기연구소)
- Dp-I-012 Structure Analysis and Electrical Properties of VO<sub>2</sub> Thin Films Grown on Sapphire with Thickness Dependence: SEO Gi Wan(ETRI/University of Science and Technology), KIM Bong-Jun(ETRI), LEE Yong Wook(ETRI/Pukyong National University), CHOI Sungyul(ETRI), KIM Hyun-Tak(ETRI/University of Science and Technology)

- Dp-I-013 바나듐 첨가에 의한  $K_{0.5}Bi_{4.5}Ti_4O_{15}$  박막의 구조와 전기적 특성 변화: 김 상수, 김 진원, 도 달현, 최 은진, 김 가현, 김 태규(창원대)
- Dp-I-014 Investigation of La- and V-codoped  $Na_{0.5}Bi_{4.5}Ti_4O_{15}$  ferroelectric thin films: 김 상수, 도 달현, 김 진원, 최 은진, 김 가현, 김 태규(창원대)
- Dp-I-015 Superconductivity of Cu doped  $2H-NbSe_2$ : 고 윤영, 김 용관(연세대), 송 기명(인하대), 한 가람, 정 원식, 박 승룡, 임 춘식, 김 철, 최 성균, 송 동준, 경 원식, 최 환영(연세대), 허 남정(인하대), 김 창영(연세대)
- Dp-I-016 Investigation of V4+ ion-environment of  $GeO_2-B_2O_3-V_2O_5$  Polycrystalline Compounds: 김 영훈, 강 재필, 서 용문, 최 덕, 송 승기(명지대)
- Dp-I-017\* Photoemission and x-ray absorption study on metal-insulator transition in  $Ca_{1-x}Sr_xIrO_3$  ( $x=0, 0.5, 1$ ): USEONG Kim, S. Y. Jang, T. W. Noh, S.-J. Oh(서울대)
- Dp-I-018\* Thickness Dependence of Microstructure and Ferroelectric Properties in Lead-free  $(Na_{0.5}K_{0.5})(Nb_{0.995}Mn_{0.005})O_3$  thin films fabricated by chemical solution deposition: 김 일원, 석 해진, 이 선영, 이 해준(울산대), 안 창원, 조 남규, 황 학인(전자부품연구원, 융합부품연구부)
- Dp-I-019\* Thermally evaporated  $NiO_x$  thin films probed by Terahertz time-domain spectroscopy: HA Taewoo, LEE Kimoon, IM Seongil, KIM Jae Hoon(Department of Physics, Yonsei University)
- Dp-I-020\* Crystal Growth and Characterization of  $Sr_{n+1}Ir_nO_{3n+1}$  ( $n=1, 2$ ) and  $R_2Ir_2O_7$  ( $R=Pr, Eu$ ): JEON Byung-Gu, LEE Bumsung, KHM Seunghyun, KIM Kee Hoon(Department of Physics and Astronomy, Seoul National University)
- Dp-I-021\* Fermi Liquids Behavior In The Mixed-Valence  $YbInCu_4$ : WOO Bonghee(Department of Physics, Sungkyunkwan University, Suwon, Korea), V.A. Sidorov(Vereshchagin Institute for High Pressure Physics, Russia), J.L. Sarrao, J.D. Thompson(Los Alamos National Laboratory, USA), PARK Tuson(Department of Physics, Sungkyunkwan University)
- Dp-I-022\* Effects of spin-orbit interaction on electronic structures of 5d double perovskite  $A_2FeReO_6$  ( $A=Ba$  and  $Ca$ ): JEON Byung Chul, MOON Soon Jae, KIM Choong Hyun, CHOI Wook Seok(서울대), LEE Yoon Sang(숭실대), WON Choong Jae, JUNG Jong Hoon, HUR Nam Jung(인하대), YU Jae Joon, NOH Tae Won(서울대)
- Dp-I-023\* Self-Assembled Growth of Nanocomposites Consisting of  $TiO_2$  Nanopillars and  $Pb(Zr,Ti)O_3$  Thin Films: Effects of Ti-Excess-Amounts and Annealing Conditions: CHOI Yong Chan, YANG Sun A, CHO Sam Yeon, BU Sang Don(Chonbuk National University, Department of Physics)
- Dp-I-024\* Ferroelectric-like behavior of high dielectric constant perovskite-related oxide  $CaCu_3Ti_4O_{12}$ : KWON Hyosang, PARK Sungmin, PARK Doyoung, HWANG Jihwan, CHEONG Hyeonsik, PARK Gwangseo(Department of Physics, Sogang University)
- Dp-I-025\* Luminescence properties comparison of  $BaY_2ZnO_5:Eu^{3+}$  phosphors by high-energy ball milling and solid-state reaction: YANG Hyun Kyoung, MOON Byung Kee, CHOI Byung Chun, JEONG Jung Hyun(Department of Physics, Pukyong National University), KIM Jung Hwan(Department of Physics, Dongeui University)
- Dp-I-026\* Different Resistance Switching Behaviors of  $NiO$  Thin Films Deposited on Pt and  $SrRuO_3$  Electrodes: 최 진식, 김 진수, 황 인록, 홍 사환, 전 상호, 강 성웅, 박 배호(건국대), 김 동철, 이 명재, 서 순애(Samsung Advanced Institute of Technology)
- Dp-I-027\* Effects of Annealing Temperatures on Phase Formation of Sol-Gel Derived PMN-PT Thin Films: YANG Sun A, HAN Jin Kyu, BU Sang Don(Chonbuk National University, Department of Physics)
- Dp-I-028\*  $(1-x)BiScO_3-(x)PbTiO_3$  ( $x=0.64$ ) 강유전 박막의 결정구조 및 압전 특성 연구: JIN Yeryeong, KIM Bongju, KWON Daeyoung, WU youngsoo(부산대 물리학과), KIM Bog G(부산대)
- Dp-I-029\* Eu 함량별  $YVO_4:Eu^{3+}$ 와  $LaVO_4:Eu^{3+}$  형광체 분말의 형광특성 비교: 박 성욱, 문 병기, 최 병춘, 정 중현(부경대), 김 중환(동의대)
- Dp-I-030\* Synthesis of Ultra-Thin-Walled  $Pb(Zr_{0.52}Ti_{0.48})O_3$  Nanotubes with Different Outer Diameters of 50, 250, and 420 nm: CHOI Yong Chan, CHO Sam Yeon, BU Sang Don(Chonbuk National University, Department of Physics)
- Dp-I-031\* Superfluidity in Hydrogen-Deuterium Mixed Clusters: 심 수민, 권 용경(건국대)
- Dp-I-032\* Synthesis and luminescence properties of  $NaGd(WO_4)_2$  doped  $Sm^{3+}$  phosphor: CHEN Yeqing, JEONG Jung Hyun(Department of Physics, Pukyong National University)
- Dp-I-033\* Search for Experimental Evidence of Ferroelectric Quantum Criticality in  $SrTiO_3$  Through Thermal Expansion Study: JEON Byung-Gu, KIM Jae Wook, KIM Kee Hoon(Department of Physics and Astronomy, Seoul National University)
- Dp-I-034\* The ferroelectric properties of epitaxial  $PbZr_{0.3}Ti_{0.7}O_3$  thin films grown on the different thickness of  $SrRuO_3$  electrode: HWANG Jihwan, PARK Sungmin, KWON Hyosang(Department of Physics, Sogang University), GO Youngdong, CHUNG Jinseok(Department of Physics, Soongsil University), PARK Gwangseo(Department of Physics, Sogang University)
- Dp-I-035\* Effects of Etching Solutions on Dissolution Rate Behavior and Surface States of Alumina Nanowires Synthesized by Wet-Chemical Etching of Porous Alumina Membranes: HAN Jin Kyu, BU Sang Don(Chonbuk National University, Department of Physics)

- Dp-I-036\* 양성자 빔조사에 따른 산화물 박막의 구조적 전기적 특성 변화 연구: 박 배호, 황 인록, 김 진수, 최 진식, 변 익수, 전 상호, 홍 사환, 강 성웅(건국대)
- Dp-I-037 Nb-SrTiO<sub>3</sub>의 전기/구조적 특성 및 고체 연료전지 전극 응용: 김 맥, 송 철호, 이 상민, 김 영훈, 최 현우(부산대), 임 영훈(세명대), 양 용석(부산대)
- Dp-I-038 비정질 유전체 xLiTaO<sub>3</sub>-SiO<sub>2</sub> (x=2, 4, 8)의 온도에 따른 유전 특성 연구: 김 영훈, 김 맥, 송 철호, 최 현우, 양 용석(부산대)
- Dp-I-039 Ba<sub>0.77</sub>Ca<sub>0.23</sub>TiO<sub>3</sub> 단결정의 강유전상전이에 대한 분광학 연구: 김 태현, 고 재현(한림대), 김 성백(포항공대), KOJIMA Seiji (University of Tsukuba, Institute of Materials Science)
- Dp-I-040 P-T boundary between white tin and gray tin - First principles study: NA Sung-Ho(KASI), PARK Chul-Hong(Pusan National Univ.)
- Dp-I-041 Bi<sub>2</sub>O<sub>3</sub>-SiO<sub>2</sub>-B<sub>2</sub>O<sub>3</sub>계 비정질의 결정화 기구 및 전기전도 특성: 이 상민, 최 현우, 송 철호, 김 맥, 김 영훈, 양 용석(부산대)
- Dp-I-042 Conduction Ion and Conducting Pass Study using Electron Charge Density Distribution and Electrostatic Potential Analysis: KIM Su Jae, KIM Won-Kyung, LEE Seunghun, CHO Yong Chan, JEONG Se-Young(Department of Nano Fusion Technology, Pusan National University)
- Dp-I-043 Physical properties of ZnS-ZnO Thin Films Grown by Pulsed Laser Deposition: 정 준기, 도 달현, 김 진원, 김 상수, 송 태권, 배 동식, 김 명호, 김 원정(창원대)
- Dp-I-044 Fourier-Transform Infrared (FT-IR) Spectroscopic Ellipsometry of Pt Single Crystal: CHOI Kyujin, ROH Young Sup, KIM Jae Hoon(Department of Physics & Institute of Physics and Applied Physics)
- Dp-I-045 A study on thermal conductivity of Bi<sub>2</sub>Te<sub>3</sub>: KIM Ga Young, KIM Sang Hoon, PARK Sang Kook, LEE Sang Bong(경북대)
- Dp-I-046 Preparation and electrical properties of (1-x)Bi<sub>0.5</sub>Na<sub>0.5</sub>TiO<sub>3</sub>-LiNbO<sub>3</sub> lead-free piezoelectric ceramics: LEE H. S., CHUNG C. H.(Changwon National University, Physics), KIM J. S.(Pukyong National University, Physics), JANG K. W.(Changwon National University, Physics)
- Dp-I-047 <sup>87</sup>Rb Nuclear Magnetic Resonance Measurements of Ferroelectric RbKSO<sub>4</sub> Single Crystals: KANG Kihyeok, MEAN B. J., KIM Sung Hoon(Department of Physics, Konkuk University), LEE Jeffrey C.(Adlai E. Stevenson High School, U.S.A.), PARK Bae-Ho(Department of Physics, Konkuk University), LIM Ae Ran(Department of Science Education, Jeonju University)
- Dp-I-048 Characterization of ZnO nanofibers prepared by electrospinning method: KIM Jong Pil, PAK Eun Sick, BAE Jong-Seong (Surface Properties Research Team, Korea Basic Science Institute Busan Center), KIM Ju Hwan, SIM Jin Woo, HONG Kyung Woo, HWANG Jeong Hoon(Jang Young Sil Science High School)
- Dp-I-049 Thermal Analysis of the PLS II Crotch Absorber: HA Taekyun(Pohang Accelerator Laboratory), SHENG I. C.(NSRRC), PARK C. D.(Pohang Accelerator Laboratory)
- Dp-I-050 Structural and Electromagnetic Properties of Ti-substituted BiFeO<sub>3</sub> Ceramics: CHO J. H., CHOI B. C.(Department of Physics, Pukyong National University), YEO H. G., SUNG Y. S., KIM M. -H., SONG T. K.(School of Nano & Advanced Materials Engineering, Changwon National University), KIM S. S.(Department of Physics, Changwon National University)
- Dp-I-051 Thermomechanical and electrical properties of iron-manganese oxides for solid oxide fuel cell interconnect: CHOI Hyun Woo(Department of Physics, Pusan National University), UDDIN Md. Nizam(Department of Nanomaterials Engineering, RCDAMP, Pusan National University), YANG Yong Suk(Department of Nanomaterials Engineering, RCDAMP, Pusan National University)
- Dp-I-052 Crystal Structure Investigation on LiH<sub>2</sub>PO<sub>4</sub> by Neutron Diffraction at 100K: OH In-Hwan(Korean Atomic Energy Research Institute, Neutron Science Division), LEE Kwang-Sei(Inje University, Department of Nano System Engineering), MEVEN Martin(FRM II, Technische Universitaet, Germany), HEGGER Gernot(RWTH Aachen, Institut fuer Kristallographie), LEE Cheol Eui(Korea University, Department of Physics and Institute for Nano Science)
- Dp-I-053 Role of Symmetry in Thermal Transport Properties of Graphene Nanoribbons: OH Sang Soon, CHOI Choon-Gi, CHOI Sung-Yool(Convergence Components & Materials Research Lab, Electronics and Telecommunications Research Institute)
- Dp-I-054 Thermal and dielectric properties of mixed tellurium dioxide-lithium tetraborate glasses: OH S. J.(한국과학영재학교), CHOI H. W., SONG C. H., LEE S. M., YANG Y. S.(부산대)
- Dp-I-055 Design requirements for the PLS II Storage Ring Crotch Absorber: HA Taekyun(Pohang Accelerator Laboratory), SHENG I. C.(NSRRC), PARK C. D.(Pohang Accelerator Laboratory)
- Dp-I-056 Secondary electron generation in electron-beam-irradiated solids: LEE Cheol Eui, KIM Jin Soo, LEE Kyu Won(Korea University, Physics)
- Dp-I-057 비정질 유전체 2(Ba<sub>1-x</sub>Ca<sub>x</sub>TiO<sub>3</sub>)-SiO<sub>2</sub>의 몰 비율에 따른 열 및 유전 특성 변화: 고 재현, 송 철호, 김 영훈, 양 용석(부산대)
- Dp-I-058 Electrical and Thermal Properties of VO<sub>2</sub> Thin Film: CHOI Jeongyong, KIM Bong-Jun, KIM Hyun-Tak(Tera Electronics Research Team, Electronics and Telecommunications Research Institute), CHO Sunglae(Department of Physics, University of Ulsan)

10월 21일(수) 14:00 – 16:00

- Ep-I-001 Study of the Electron-Phonon Interactions and Vibrational Modes in Insulating Nanoparticles: 하 명규, 홍 경수, 정 의덕(한국기초과학지원연구원 부산센터), 양 호순(부산대)
- Ep-I-002 Fabrication of ordered arrays of double layer nanodots composed of two metals by physical vapor deposition: KIM kwang sub, JANG un jung, LEE chang young(동아대)
- Ep-I-003 Electrical Current Suppression of Pd-doped Vanadium Pentoxide Nanowire Network Due to Hydrogen Adsorption: 김 병훈, 오 순영, 정 후영, 유 한영, 윤 용주, 김 약연, 홍 원기(한국전자통신연구원), 이 정용(KAIST)
- Ep-I-004 Measurement of Carbon Soot Mass Distribution using High Resolution FT-ICR-Mass Spectrometer: 민 경철, 최 명철(한국기초과학지원연구원 질량분석 개발팀)
- Ep-I-005\* Diameter Effect on the Electrical Property of Single-walled Carbon Nanotubes Networks: JANG DONG KYU(School of Electrical Engineering, Korea University), HWANG DOO HEE(Department of Micro/Nano Systems, Korea University), KIM SUN KUG(School of Electrical Engineering, Korea University), LEE CHEOL JIN(School of Electrical Engineering and Department of Micro/Nano Systems, Korea University)
- Ep-I-006 Formation and Thermal Properties of Amorphous  $Ti_{40}Cu_{40}Ni_{10}Al_{10}$  Alloy Powder by Mechanical Alloying: 김 현구, 나 도선, 박 경화, 공 현식, 송 보미(조선대)
- Ep-I-007 Electrochemical Corrosion Behaviors of Amorphous  $Co_{69}Fe_{4.5}Ni_{1.5}Si_{10}B_{15}$  Alloy Produced by Quenching Method: 김 현구, 공 현식, 송 보미(조선대), 명 화남(전남대), 장 희진(조선대)
- Ep-I-008 Blinking Kinetics of Single CdSe/ZnS Nanocrystals Interpreted Using Different Temporal Resolutions: LEE SANG YUN(RIKEN, Flucto-Order Functions Asian Collaboration Team), HAYASHI TOMOHIRO(Tokyo Institute of Technology, Department of Electronic Chemistry), HARA MASAAHIKO(RIKEN, Flucto-Order Functions Asian Collaboration Team)
- Ep-I-009\* Raman Study of ETS-10 and Titanate Quantum Wires: LIM Hyunjin, CHEONG Hyeonsik, JEONG Nak Cheon, YOON Kyung Byung(서강대)
- Ep-I-010 MWCNT를 이용한 에탄올 가스센서의 제작: 장 경욱, 최 명규(경원대), 김 상걸(특허청), 김 태완(홍익대), 정 동희(송파공업고등), 안 준호(한국전력기술연구원)
- Ep-I-011\* Control of Giant Metal-Insulator Transition at Room Temperature on W Doped  $VO_2$  Thin Films: TAKAMI Hidefumi, KANKI, Teruo, CHA Nam-Goo, TANAKA Hidekazu(Osaka University)
- Ep-I-012\* Fabrication and Characterization of  $MoO_3$ ,  $H_xMoO_3$  Nanorods Metal-Insulator-Semiconductor (MIS) Capacitors: SHAKIR Imran, MUHAMMAD Shahid, 이 강우, 강 대준(BK21 Physics Research Division, Department of Energy Science, Institute of Basic Science, SKKU Advanced Institute of Nanotechnology and Center for Nanotubes and Nanostructured Composites, Sungkyunkwan University)
- Ep-I-013\* Chemical Solution Deposition Synthesis and Optical Properties of Single Crystalline Complex Metal Oxide  $BaCuV_2O_7$  Nanowires: SHAKIR Imran, SHAHID Muhammad, 강 대준(BK21 Physics Research Division, Department of Energy Science, Institute of Basic Science, SKKU Advanced Institute of Nanotechnology and Center for Nanotubes and Nanostructured Composites, Sungkyunkwan University)
- Ep-I-014\* Particle Size Regulation of Magnetic Nano-particles Synthesized by Aqueous Solution Method, and Their MR Contrast Properties: KANG Jongeun, KIM Youngnam, MOON Hyeyoung(Korea Basic Science Institute, MRI Team), HONG Kwan Soo(Korea Basic Science Institute, MRI Team; Chungnam National University, Graduate School of Analytical Science and Technology)
- Ep-I-015 수직자기이방성을 갖는 비정질 강자성체  $CoSiB/Pt$  다층박막의 자기적 특성 연구: 박 지선(숙명여대), 황 재연, 이 승백(한양대), 김 태완(세종대), 임 혜인(숙명여대)
- Ep-I-016 양성자 빔을 이용한 백금 나노 입자 사이즈 제어 연구: 정 명환, 나 세진, 김 계령(한국원자력연구원 양성자기반공학기술개발사업단), 채 근석, 민 명기((주)삼성 SDI)
- Ep-I-017\* Adsorption Properties of Hydrogen on  $Alq_3$  and its Derivatives: Ab Initio Study: KANG Seoung-Hun, KO Yoo Sun, PARK Sora, KWON Young-Kyun(Department of Physics and Research Institute for Basic Sciences, Kyung Hee University)
- Ep-I-018 Cathodoluminescence of Single ZnO nanorods: LEE Cheol Eui, LEE Su Chul, LEE Eunmo(Korea university)
- Ep-I-019 Synthesis of functionalized graphene sheets by thermal exfoliation in low temperature: JIN Meihua, JEONG Hae-Kyung (Sungkyunkwan University, BK21 Physics, Department of Energy Science, Center for Nanotubes and Nanostructured Composites), SO Kang Pyo(Sungkyunkwan University, BK21 Physics, Department of Energy Science, Center for Nanotubes and Nanostructured Composites, Sungkyunkwan Advanced Institute of Nanotechnology), KIM Tae-Hyung, LEE Young

Hee(Sungkyunkwan University, BK21 Physics, Department of Energy Science, Center for Nanotubes and Nanostructured Composites)

- Ep-I-020 Study on UV-Vis absorption spectra of fullerene (C<sub>60</sub>) clusters synthesized in toluene droplet by using ultrasonic nebulizer: YEO Seung Jun, CHO Dae Hee, PODE Ramchandra, AHN Jeung Sun(Kyung Hee univesity, Physics)
- Ep-I-021\* Multifunctional Nanoparticles for Combined Doxorubicin and Photothermal Treatments: 박 희열(연세 나노메디컬 협동과정), 양 재문, 이 재민, 함 승주, 최 인홍(연세대)
- Ep-I-022\* Electrical Field Dependence of Morphologies of Organic Light Emitting Devices: KO Changhyun, LEE Hyunwon (Department of Physics, Sogang University), YOO Insun, OH Hyoungyun(LG Display Co. Ltd), KIM Jinwoo(Department of Materials Science and Engineering, Gwangju Institute of Science and Technology), KIM Hyunjung(Department of Physics, Sogang University)
- Ep-I-023\* Cu<sub>2</sub>O 양자점 터널링 소자의 전기적 특성 연구: 박 상우, 서 주영, 김 재훈, 김 은규, 최 동주, 김 영호(한양대)
- Ep-I-024\* An Improved RF Circuit Model for Biosensors Based on Carbon Nanotube Coupled with Interdigital Capacitors: LEE Hee-Jo, YOOK Jong-Gwan(Department of Electrical and Electronic Engineering, Yonsei Univiersity)
- Ep-I-025 Synthesis of nanostructure arrays by using anodized aluminum oxide template: 김 일원, 박 정민, 이 선영(울산대), 안 창원 (전자부품연구원, 융합부품연구부), 배 종성(한국기초과학지원연구원, 부산센터), 김 영근, 박 우락, 윤 성욱, 정 종호, 배 해 경(울산과학고)
- Ep-I-026 Structural and Optical Properties of Proton-Implanted ZnO Nanorods: PARK changin, KIM B.-H.(Department of Physics and Institute of Fusion Science, Chonbuk National University), LEE Y.-B., KWAK C.-H., SEO S.-Y., KIM S.-H.(Department of Materials Science and Engineering, Pohang University of Science and Technology), PARK S.-H.(New Materials & Components Research Center, Research Institute of Industrial Science & Technology), HAN sangwook(Division of Science Education and Institute of Fusion Science, Chonbuk National University)
- Ep-I-027 Growth of Nitrogen-doped Carbon nanotube by Chemical Vapor Deposition: KONG So-Jeo(Kyungpook National University, Department of Physics), KIM Chang-Duk(Kyungpook National University, Faculty of Liberal Education), LEE Sung-Youp (Kyungpook National University, Department of Nano-science and Technology), SHIN Byong-Wook, KIM Sang-Hun, PARK Sun-Mi(Kyungpook National University, Department of Physics), SON Myeong-Rak(Kyungpook National University, Dept. of Physics), YI Jin-Neung(Kyungpook National University, Department of Physics), CHOO Na-Yun(Kyungpook National University, Dept. of Nano-science and Technology), LEE Eui-Wan, LEE Hyeong-Rag(Kyungpook National University, School of Physics and Energy Science)
- Ep-I-028 PEDOT:PSS를 이용한 탄소나노튜브 가스센서의 응용: 박 선미, 김 상훈, 이 성엽, 신 병욱, 공 소저, 손 명락, 이 진능, 추 나윤, 김 창득, 이 의완, 이 형락(경북대)
- Ep-I-029\* Gas Phase Synthesis of Cu, Cu<sub>2</sub>O and CuO Nanowires, Nanowalls and Porous Nanofibers and the Morphological Phase Diagram of Copper Oxide Nanostructures: RHEN Danielle, 강 대준(BK21 Physics Research Division, Department of Energy Science, Institute of Basic Science, SKKU Advanced Institute of Nanotechnology and Center for Nanotubes and Nanostructured Composites, Sungkyunkwan University)
- Ep-I-030\* P-type Si nanowire-based Devices for the Detection of Nerve Agent: KIM yeonju, LEE junmin, LEE seunghyun, LEE Wooyoung(Yonsei University, Department of Materials Science and Engineering)
- Ep-I-031 Three-Dimensional Architecture of Carbon Nanotube-Anchored Polymer Nanofiber Composite: TAEHYUNG Kim, ILHA Lee, YOUNGHEE Lee(BK21 Physics Division, Department of Energy Science, Sungkyunkwan Advanced Institute of Nanotechnology, and Center for Nanotubes and Nanostructured Composites, Sungkyunkwan University)
- Ep-I-032 Carbon nanotube field emitter for super miniature X-ray tube using brachytherapy radiation source: 허 성환, IHSAN Aamir, 여 동열, 조 성오(KAIST, 원자력 및 양자공학과)
- Ep-I-033\* Magnetic Properties of Patterned Co/Pd Multilayer Structures with Perpendicular Magnetic Anisotropy using Electron Beam Lithography: KIM Hyunsu, ROH Jong Wook(Department of Materials Science and Engineering, Yonsei University), KIM Sungman, CHUN Dong Won, JEUNG Won Yong(Korea Institute of Science and Technology (KIST)), LEE Wooyoung (Department of Materials Science and Engineering, Yonsei University)
- Ep-I-034 전자빔을 이용한 탄소 나노구조체 형성 장비 개발: 조 대희, 여 승준, PODE Ramchandre, 안 정선(경희대)
- Ep-I-035 Current Compensation circuit for QTF (Quartz Tuning Fork): AN Sang min, LEE Man hee, JAHNG Junhoon, JHE Won ho(Department of Physics and Astronomy, Seoul National University)

10월 22일(목) 11:00 - 13:00

- Dp-II-059 Terahertz conductivity of superconducting  $\text{La}_{1.84}\text{Sr}_{0.16}\text{CuO}_4$  thin film: HONG Taeyoon, KIM Jae Hoon(Department of Physics, Yonsei University), BOZOVIC Ivan(Department of Condensed Matter Physics and Materials Science, Brookhaven National Laboratory)
- Dp-II-060 Effect of Cu substitution on Superconductivity in  $(\text{Ru,Cu})\text{Sr}_2(\text{Eu,Ce})_2\text{Cu}_2\text{O}_z$  system: LEE Ho Keun(Kangwon National University, Physics Department)
- Dp-II-061 Effect of  $\text{Eu}^{+3}$  doping on the behavior of irreversibility lines in cuprate high- $T_c$  superconductor  $\text{Sm}_{1-x}\text{Eu}_x\text{Ba}_2\text{Cu}_3\text{O}_{7.4}$ : AHMAD dawood, PARK insuk, KIM G C, KIM Y C(부산대)
- Dp-II-062 HTC-Peltier Current Leads: KIM Sang Hoon, KIM Ga Young, PARK Sang Kook, LEE Sang Bong(경북대)
- Dp-II-063 Electrical Transport Properties Of  $\text{SmFeAsO}_{0.85}$  Single Crystals Along The C-axis: PARK Jae-Hyun, DOH Yong-Joo, LEE Hyun-Sook, LEE Jae-Yeap(Department of Physics, Pohang University of Science and Technology), KIM Ju-Young, CHO B. K.(Materials Science and Engineering, Gwangju Institute of Science and Technology), JUNG Chang-Uk(Department of Physics, Hankuk University of Foreign Studies), LEE Hu-Jong(Department of Physics, Pohang University of Science and Technology)
- Dp-II-064 PLD법에 의한 MgO 기판 위에 고온초전도 박막 증착용  $\text{CeO}_2$  완충층의 에피택시 성장: 장 세훈, 고 락길, 김 호섭, 하 홍수, 하 동우, 오 상수(한국전기연구원), 김 영철(부산대)
- Dp-II-065 A study on superconducting properties of YBCO Coated Conductors using Low-temperature Scanning Laser Microscopy: PARK Sang Kook, LEE Sang Bong, KIM Sang Hoon, KIM Ga Young, KIM Jong Man, RI Hyeong-Cheol(경북대)
- Dp-II-066 High-resolution angle-resolved photoemission spectroscopy studies on 2-dimensional graphite based system: 임 춘식, 경 원식, 박 승룡, 김 철, 송 동준, 최 성균, 김 용관, 정 원식, 고 윤영, 한 가람, 최 환영(연세대), 김 준성(포항공대), 이 한구, 김 형도(포항공속기연구소), 김 창영(연세대)
- Dp-II-067  $(\text{Ru,M})\text{A}_2(\text{Nd,R,Ce})_2\text{Cu}_2\text{O}_z$  계의 합성 및 초전도 특성: 문 종우, 이 상민, 이 호근(강원대)
- Dp-II-068 The magnetic phase diagram of  $(\text{Ca,Sr,Ba})\text{Fe}_2\text{As}_2$ : NA SEWOONG, EOM MANJIN(Department of Physics, POSTECH)
- Dp-II-069 Superconductivity of isovalent Ru substituted  $\text{BaFe}_{2-x}\text{Ru}_x\text{As}_2$ : EOM manjin, NA sewoong(Department of Physics, Pohang University of Science and Technology)
- Dp-II-070 Analysis of current distribution in YBCO thin film using Low Temperature Scanning Hall Probe Microscopy: LEE Sangbong, PARK Sangkook, KIM Sanghoon, KIM Kayoung(경북대)
- Dp-II-071 Attempt of  $\text{MgB}_2$  Powder Orientation in Magnetic Field: KANG Kihyeok, MEAN B. J., KIM Sung Hoon(Department of Physics, Konkuk University), LEE Jeffrey C.(Adlai E. Stevenson High School, U.S.A.), PARK Bae-Ho(Department of Physics, Konkuk University), CHO B. K.(Department of Materials Science and Engineering, GIST)
- Dp-II-072 Energy Level Quantization of a Collectively Pinned Josephson Vortex Chains in Naturally Stacked High- $T_c$  Josephson Junctions: 이 길호, 진 용덕, 이 후종(Department of Physics, Pohang University of Science and Technology)
- Dp-II-073 집속 이온빔 방법을 이용한  $\text{MgB}_2$  나노브릿지 dc SQUIDS 제작과 특성 연구: HONG Sung-Hak, LEE Soon-Gul(Korea University, Department of Display and Semiconductor Physics), SEONG Won Kyung, KANG Won Nam(Sungkyunkwan University, Physics Division and Department of Physics)
- Dp-II-074 Reactive co-evaporation 공정에 의한  $\text{SmBCO}$  박막형 초전도 선재의 자장 특성: 고 락길, 장 세훈(한국전기연구원), 송 규정(전북대), 하 홍수, 김 호섭, 하 동우, 오 상수(한국전기연구원), 김 영철(부산대)
- Dp-II-075 Phenomenological Theory of competing orders between Superconductivity and Magnetism with Magnetic Field: KIM Jinhee, BANG Yunkyu(Department of Physics, Chonnam National University)
- Dp-II-076\* Growth of  $(\text{Ba,K})\text{Fe}_2\text{As}_2$  Single Crystals by the In-flux Method and their Physical Properties: LEE Bumsung, KHIM Seung Hyun, KIM Kee Hoon(Department of Physics and Astronomy, Seoul National University)
- Dp-II-077\* 철계 초전도체인  $(\text{Ba, K})\text{Fe}_2\text{As}_2$ 의 단결정 성장과 기초 물성 분석: 장 유란, 홍 종범(성균관대), 정 명화(서강대), 강 원남, 권 용성(성균관대)
- Dp-II-078\* Reversible magnetization으로부터 FeAs 계열의 초전도체에서의 요동현상 연구: 최 창호, 김 수현, 최 기영, 정 명화, 이 성익(서강대)
- Dp-II-079\* 단결정 초전도체  $\text{BaFe}_{1.8}\text{Co}_{0.2}\text{As}_2$ 의 두 개의 S-파동 에너지 간격 대칭: 김 수현, 최 창호, 정 명화, 최 기영(서강대학원 물리학과), 노 재동(서울시립대), 이 성익(서강대학원 물리학과)
- Dp-II-080\* Pressure-induced superconductivity in the antiferromagnetic and orthorhombic phase of  $\text{CaFe}_2\text{As}_2$ : DEOKHEE Kim (Department of Physics, Sungkyunkwan University), HANOH Lee, E. D. BAUER, J. D. Thompson(Los Alamos National Laboratory, USA), TUSON Park(Department of Physics, Sungkyunkwan University)

- Dp-II-081\* ARPES and optical spectroscopy studies of  $Y_{1-x}Pr_xBa_2Cu_3O_7$ : 정 원식, 박 승룡, 임 춘식, 김 철, 최 성균, 송 동준, 김 용관, 고 윤영, 한 가람, 경 원식, 최 환영, 김 창영(연세대)
- Dp-II-082\* Strong field dependence of critical current density in  $a$ -axis-oriented  $MgB_2$  films: JUNG Soon-Gil, LEE Nam Hoon, CHO Kyu Hwan, SEONG Won Kyung, CHOI Eun-Mi, KANG Won Nam(성균관대), OH Sangjun(핵융합연구센터, 재료연구팀)
- Dp-II-083 초록 중복 삭제
- Dp-II-084  $Ba(Fe,Co)_2As_2$  thin films: MBE Growth and Superconducting Properties: 조 성래, DANG Dung Duc, 황 영훈, DUONG Van Thiet(울산대)
- Dp-II-085 외부자기장 인가에 따른  $LiFePO_4$  물질의 Mössbauer 분광 연구: 김 철성, 이 인규, 박 일진, 홍 중수, 이 찬혁(국민대), 원 봉연((주) ASK), 심 인보(국민대)
- Dp-II-086 Physical Characterization of  $BaTi_{1-x}Fe_xO_3$  compounds: NGUYEN Van Minh, PHAM Xuan Huu, DOAN Thi Thuy Phuong (Hanoi National University of Education, Center for Nano Science and Technology), YANG In-Sang(Ewha Womans University, Department of Physics)
- Dp-II-087 The microwave-assisted synthesis of  $Zn_{1-x}Co_xO$  nanopowders: LUC Huy Hoang, TRAN Dong Hai, NGUYEN Hoang Hai(Hanoi National University of Education, Department of Physics), CHEN Xiang Bai, NGUYEN Thi Minh Hien, YANG In-Sang(Ewha Womans University, Department of Physics)
- Dp-II-088 The gyration dependent magnetic interaction in an alkali superoxide  $KO_2$ : 김 범현, 김 민재, 민 병일(포항공대)
- Dp-II-089  $^{13}C$  NMR Study of  $CaC_6$  Single Crystals: KIM SungHoon, KANG Ki Hyeok, MEAN B. J., LEE Moohee(Department of Physics, Konkuk University), KIM Jun Sung(Department of Physics, POSTECH)
- Dp-II-090 The change of magnetic order and metallicity for doped perovskite system :  $SrMn_{1-x}Mo_xO_3$  ( $x=0, 1/16, 1/8, 1/4$ , and  $1/2$ ): KIM Bongjae, MIN B.I.(POSTECH, Physics), LEE Jieun(University of Michigan, Physics), KANG J.-S.(The Catholic University of Korea, Physics)
- Dp-II-091 Effect of strain on the magnetic properties of a hematite: a case study for  $BaTiO_3/a-Fe_2O_3$  nanoparticles: 구 용성, 윤 병길, 정 중훈(인하대)
- Dp-II-092 Investigation on  $CsMnCl_3 \cdot 2(H_2O)$  by Neutron Single Crystal Diffraction at Room Temperature: OH In-Hwan, KIM Je-Eun (Neutron Science Division, Korea Atomic Energy Research Institute), KOO Japil(Department of Physics, Pohang University of Science and Technology), PARK J.M.Sungil(Neutron Science Division, Korea Atomic Energy Research Institute), LEE cheol eui(Department of Physics, Korea University)
- Dp-II-093 Chirality-Controlled Domain Wall Depinning With Different Pad Geometry: LEE Bum-Woo, AHN Sung-Min, MOON Kyoung-Woong, CHOE Sug-Bong(Department of Physics, Seoul National University)
- Dp-II-094 Resonant Magnon Raman Scattering in Hexagonal  $HoMnO_3$  Films: YANG In-Sang, CHEN Xiang-Bai, NGUYEN Thi Minh Hien(Ewha Womans University, Department of Physics), LEE D., JANG S. Y., NOH T. W.(Seoul National University, Department of Physics)
- Dp-II-095 Magnetoresistance behavior of asymmetric  $Py/Nb/Py$  trilayers with different bridge direction respect to the magnetization easy axis: 황 태종, 박 영순, 김 동호(영남대)
- Dp-II-096 준안정 bcc Co의 안정화 및 자기변형: 이 선철, 윤 원석, 홍 순철(울산대)
- Dp-II-097 Analysis of current-voltage characteristics of  $GaAs/MgO/Fe$  junctions: SHIM Seong Hoon, CHANG Joonyeon, KIM Kyung-Ho, KIM Hyung-Jun, HAN Suk-Hee(Center for Spintronics Research, KIST), LEE Yun-Hi(National Research Laboratory for Nano Device Physics, Dept. of Physics, Korea Univ.)
- Dp-II-098  $TmFe_2O_4$ 의 물리적 현상 연구: 김 재영, 이 보화(한국외국어대)
- Dp-II-099  $NiFe/FeMn/CoFe$  3층 구조에서의 강자성공명의 linewidth에 관한 연구: 최 혁철(인하대), 김 기연(한국원자력연구소, 중성자과학연구부), 심 제호, 김 동현(충북대), 이 정수(한국원자력연구소, 중성자과학연구부), 유 천열(인하대)
- Dp-II-100 Electronic and Elastic Properties of  $(Fe,Mn)_3AlC$  Studied by Density Functional Theory Calculations: NOH Ji-Young, KIM Hanchul(Sookmyung Women's University, Department of Physics)
- Dp-II-101 자구벽이 있는 강자성 나노선의 열적 요동에 대하여 미세자기 동역학을 이용한 분석: 윤 정범, 유 천열(인하대), 조 영훈, 박 승영(한국기초과학지원연구원, 나노물성팀), 정 명화(서강대)
- Dp-II-102 The Magnetic Properties of Mn Ultrathin Films on  $Fe(001)$  Surface; First Principles Study: 양정화, 김동유, 홍지상(부경대)
- Dp-II-103 격자변형에 따른  $La_{0.7}Ba_{0.3}MnO_3$  박막의 전기적/자기적 성질: JUNG Dong-gyu, DHO Joonghoe, KI sanghoon(경북대)
- Dp-II-104 Spin-Orbital-Lattice Coupling in  $KO_2$  Superoxide: 김 민재, 김 범현, 최 홍철, 민 병일(Department of Physics, POSTECH)
- Dp-II-105 Electron Magnetic Resonance and Magnetic Susceptibility of  $CsMnCl_3 \cdot 2H_2O$  and  $CsMnCl_3$ : NA Sung-Ho(KASI), KIM Heung-Chul(Pusan National Univ.)
- Dp-II-106  $NiFe$ 와  $Cr_2(1-x)Fe_2xO_3(CFO; x = 0.1)$  이층박막에서의 교환바이어스와 보자력: KI sanghoon, DHO joonghoe, JUNG dong-gyu(경북대 물리학과)
- Dp-II-107 n-Si 위에 전기 증착한 Co film의 자기적 상호작용과 활성화부피: 김 상인(한국원자력연구원), 정 순영, 이 종덕, 김 현수(경

상대), 김 봉환(한국원자력연구원)

- Dp-II-108\*  $\text{La}_{0.7}\text{Sr}_{0.3}\text{MnO}_3/\text{STO}(001)$  강자성 박막의 두께에 따른 물성변화 연구: KIM bongju, KWON daeyoung(부산대), SONG jong hyun(충남대), HIKITA Yasuyuki(동경대), KIM Bog G.(부산대), HWANG Harold Y.(동경대)
- Dp-II-109\* NMR study on the memory effect of cobalt at low temperature: 윤 동영, 이 진원, 이 순철(한국과학기술원 물리학과)
- Dp-II-110\* 피스바우어 분광 분석을 통한 망간페라이트 나노입자의 양성자조사 연구: 김 철성, 홍 순천, 명 보라, 최 정훈, 이 용혜, 김 우철, 김 삼진(국민대)
- Dp-II-111\* 고온 전기 저항 측정 장치 개발: 박 준호, 심 하성, 최 성일, 박 제근(성균관대 물리학과)
- Dp-II-112\* Exchange Bias in  $\text{Cr}_2\text{O}_3/\text{Fe}_3\text{O}_4$  Core/shell Nanoparticles: 윤 병길, 정 종훈, 구 용성(인하대)
- Dp-II-113\* Magnetic impurity and Peierls-like transition in dodecylamine-intercalated vanadium oxides: KWEON Hyoecheon, LEE Kyu Won, LEE Cheol Eui(Department of Physics, Korea University)
- Dp-II-114\* F/AF 자성박막계에서 나타나는 SRT에 대한 Monte-Carlo Simulation 연구: 석 진호, 홍 상신, 권 희영, 원 창연(경희대)
- Dp-II-115\* Magnetic Properties of H. Pylori Ferritins Reconstituted under Two Different Magnetic Field Conditions: YOON S.-W.(Department of Physics, The Catholic University of Korea), SON K.(Department of Physics, Kookmin University), SUH B. J.(Department of Physics, The Catholic University of Korea), JANG Z. H.(Department of Physics, Kookmin University), CHO K. J.(Department of Life Sciences & Biotechnology, Korea University), KIM K. H.(Department of Biotechnology & Bioinformatics, Korea University)
- Dp-II-116\* Crystallographic and Magnetic Properties of Vanadium Doped and Substituted Ferrites: KWON Woo Hyun, LEE Seung Wha, LEE Jae-Gwang, CHAE Kwang Pyo(건국대)
- Dp-II-117\* Spontaneous antiferromagnetic interlayer exchange coupling in GaMnAs-based superlattices: SHIN Jinsik, LEE sangyup, LEE hakjoon, YOO Taehee, CHUNG Sunjae, LEE Sanghoon(Physics Department, Korea University), LIU X., FURDYNA J.K.(Department of Physics, University of Notre Dame, USA)
- Dp-II-118\* Measurement of Perpendicular Magnetic Anisotropy in Ultra Thin Films: Extraordinary Hall Effect Torque Measurement: CHO Cheong-Gu, MOON Kyoung-Woong, LEE Jae-Chul, CHOE Sug-Bong(Department of Physics, Seoul National University)
- Dp-II-119\* A Study on Sweeping Time Dependent Hysteresis in Trinuclear Manganese Complex,  $\text{Mn}_3\text{O}$ , using a Pulsed Magnet: PARK J.-N.(Department of Physics, Kookmin University), YOON S.-W.(Department of Physics, The Catholic University of Korea), JANG Z. H.(Department of Physics, Kookmin University), SUH B. J.(Department of Physics, The Catholic University of Korea), CHOI K.-Y.(Department of Physics, Chungang University), NOJIRI H.(Department of Physics, Dohoku University, JAPAN)
- Dp-II-120\* 자기 쌍극자 상호작용에 의한 자성 나노선 배열의 자기적 특성변화: 석 재권, 김 택수, 전 일근, 김 승호(연세대), 신 상원, 송 종한(한국과학기술연구원, 특성분석센터), 이 재용(연세대)
- Dp-II-121\* Ion mixing을 통한 NiFe 자성 나노 선 배열의 자기적 특성 변화: 전 일근, 김 승호, 석 재권, 이 재용(연세대), 신 상원, 송 종한(한국과학기술연구원 특성분석센터)
- Dp-II-122\* Detection of Spin-dependent Current in Metal by Using Spin Hall Effect Measurements: SUH Jooyoung, KIM Jae-Hoon, KIM Eun Kyu(Quantum-Function Spinics Laboratory & Department of Physics, Hanyang University)
- Dp-II-123\* 2차원 강자성체로 이루어진 계의 SRT(Spin Reorientation Transition)에서 나타나는 줄무늬영역 상의 성질: 권 희영, 석 진호, 홍 상신, 원 창연(경희대)
- Dp-II-124\* Magnetocrystalline anisotropy of  $\text{D}_{022}\text{-Mn}_3\text{Ga}$ : Density functional study: YUN Won Seok, CHA Gi-Beom, HONG Soon Cheol(Dept. of Physics, Univ. of Ulsan)
- Dp-II-125\* Triangular Plain  $\text{Ba}_3\text{NbFe}_3\text{Si}_2\text{O}_{14}$  Langasite의 피스바우어 분광연구: 김 철성, 김 진모, 현 성욱, 이 은중, 박 영욱(국민대), 김 성백(포항공대), 고 태준(국민대)
- Dp-II-126\* 납계 산화물질에서의 Co도핑에 의한 물성 변화: 이 규준, 추 성민(서강대), 윤 정범, 송 기명(인하대), Y. Saiga(Hiroshima University, ADSM), 유 천열, 허 남정(인하대), 이 성익(서강대), T. Takabatake(Hiroshima University, ADSM), 정 명화(서강대)

## ■SESSION P2■

## 응용물리학분과회 포스터 발표

장 소 : 포스터 발표장

10월 22일(목) 11:00 - 13:00

- Ep-II-036\* Interaction Of Cut-wire Pair And Continuous Wire Incombined Metamaterial: J. W. Park, N. T. Tung(q-Psi and Department of Physics, Hanyang University), W. H. Jang(Korea Communication Commission Radio Research Laboratory), V. D. Lam(Institute of Materials Science, Vietnamese Academy), Y. P. Lee(q-Psi and Department of Physics, Hanyang

University)

- Ep-II-037\* Microwave "Dark Body": A Proposed Mechanism For Perfect Absorber Based On Metamaterial: N. T. Tung, J. W. Park, S. J. Lee, Y. P. Lee(Quantum Photonic Science Research Center, Hanyang University), J. Y. Rhee(Department of Physics, Sungkyunkwan University), V. D. Lam(Institute of Materials Science, Vietnamese Academy of Science and Technology)
- Ep-II-038\* Photonic crystal single defect laser fabricated by a combination lithography and their mode characterization: AHN Sungmo, KIM Sihan, JEON Heonsu(Department of physics and astronomy, Seoul National University)
- Ep-II-039\* A Metamaterial Supporting Electromagnetically-induced Transparency: V. T. T. Thuy, N. T. Tung(Quantum Photonic Science Research Center and Department of Physics, Hanyang University), V. D. Lam(Institute of Materials Science, Vietnam Academy of Science and Technology), J. W. Park, Y. S. Lee(Quantum Photonic Science Research Center and Department of Physics, Hanyang University), W. H. Jang(Korea Communication Commission Radio Research Laboratory), Y. P. Lee(Quantum Photonic Science Research Center and Department of Physics, Hanyang University)
- Ep-II-040 다중양자우물의 Detuning 변화에 따른 O-band DFB-LD의 문턱전류 및 경사효율의 변화: 김 효진, 유 소영, 고 항주, 한 명수, 김 두근, 한 수욱, 김 선훈, 기 현철, 김 희중(한국광기술원, 광소자팀), 정 대철, 김 효정, 강 중구((주) 오이솔루션, 소자팀)
- Ep-II-041 레너드 효과(Lenard effect)로 발생된 음이온의 혈액순환 증진: 박 배식(수원대)
- Ep-II-042 정방 격자구조에 적용한 수정된 페나 모형 연구: 심 숙이(공주대), 김 기욱(우석대)
- Ep-II-043\* 갈륨이 도핑된 산화아연 투명전도막의 texturing에 관한 연구: 이 재민, 김 준관, 임 정욱, 윤 선진(과학기술연합대학원대)
- Ep-II-044 양전자 소멸 분광법에 의한 BaSrFBr:Eu의 결함 연구: 김 주홍, 이 종용(한남대), 김 재홍(원자력의학원 싸이클로트론연구실)
- Ep-II-045 Wave Propagation Characteristics Observed in a few types of 1-Dimensional Acoustic Metamaterials: 서 용문(명지대), 박 종진, 이 승환(연세대), 박 춘만(안양대), 이 삼현, 김 철구(연세대)
- Ep-II-046 The Simulations of Pressure Distributions in 1-dim Acoustic Metamaterials with Negative Bulk Modulus: 박 춘만(안양대), 김 철구, 이 승환, 박 종진, 배 찬미(연세대), 서 용문(명지대), 이 삼현(연세대)
- Ep-II-047 레이저 분광학으로 분석한 YVO<sub>4</sub>:Eu<sup>3+</sup> 박막의 Li 첨가 효과: 장 경혁, 김 은식, 시 랑, 전 병천, 교 학빈, 서 효진(부경대)
- Ep-II-048 Study of Simultaneous Thyroid Imaging and Uptake system: 박 진훈, 주 관식, 전 상준, 문 혜진, 김 은, 신 현철(명지대)
- Ep-II-049 ~ppb 수분표준가스 발생 기술: 최 병일, 우 상봉, 김 종철(한국표준과학연구원)
- Ep-II-050 ZrO<sub>2</sub> 비표면적 CRM 개발: 최 병일, 이 유진, 김 종철, 우 상봉(한국표준과학연구원)
- Ep-II-051 Luminescent properties of Eu<sup>3+</sup> Ions Doped in La<sub>2</sub>BaZnO<sub>5</sub> Phosphor: 시 랑, 장 경혁, 김 은식, 교 학빈, 전 병천, 서 효진(부경대)
- Ep-II-052 Luminescence and thermal stability of Eu<sup>2+</sup>-activated LiCaPO<sub>4</sub> phosphors for white light emitting diode: 교 학빈, 장 경혁, 김 은식, 시 랑, 전 병천, 서 효진(부경대)
- Ep-II-053 The luminescence properties of Eu<sup>3+</sup> doped AZr(PO<sub>4</sub>)<sub>2</sub>(A=Sr, Ba) phosphors for white light-emitting diodes: 전 병천, 장 경혁, 김 은식, 시 랑, 교 학빈, 서 효진(부경대)
- Ep-II-054 Optical absorption and fluorescence properties of Tm<sup>3+</sup>-doped K-Mg-Al phosphate glasses for laser applications: PRAVEENA Ravipati, 서 효진(부경대)
- Ep-II-055 Thermoluminescence of Ion Implanted Al<sub>2</sub>O<sub>3</sub>: KIM Taekyu(Jeonju National University of Education, Department of Science Education)
- Ep-II-056 Local Polymerization of Organic Monolayer Covalently Grafted on Silicon: LEE Joon Sung, CHI Young Shik(KRISS, Center for Nanoscience and Quantum Metrology), CHOI Insung S.(KAIST, Department of Chemistry and School of Molecular Science), YUN Wan Soo, KIM Jinhee(KRISS, Center for Nanoscience and Quantum Metrology)
- Ep-II-057\* Sonodynamic effects of 5-Aminolevulinic acid on solid tumors: SEO SEUNG-JUN(Biomedical Engineering, School of Medicine, Catholic University of Daegu), YU JAE-IN(Department of Physics, Yeungnam University), KIM KI-HONG(Department of Visual Optics, Kyungwoon University), KIM JONG-KI(Biomedical Engineering & Radiology, School of Medicine, Catholic University of Daegu)
- Ep-II-058 레너드 효과 (Lenard effect)로 초음파 가습공기청정기에서 발생한 음이온 발생 과정과 특성: 박 배식(수원대)
- Ep-II-059 Resistive Memory Switching Behaviors of Pt/NiO/SRO Memory Devices: LIU CHUNLI, 정 창욱(한국외국어대 전자물리학과), 박 홍우(서울대)
- Ep-II-060 LiFePO<sub>4</sub> Cathode Materials: Synthesis and Electrochemical Properties: 홍 경수, 하 명규, 정 의덕(한국기초과학지원연구원 부산센터), 양 호순(부산대)
- Ep-II-061 스핀 분포 조절이 가능한 이중 양자 디스크 구조의 제안: 김 남미, 김 희상(숭실대)
- Ep-II-062\* Titanium Substituted Bi<sub>1.5</sub>Zn<sub>1.0</sub>Nb<sub>1.5</sub>O<sub>7</sub> for High Density MIM Capacitor at Low Temperature: CHO Kwang-Hwan, KANG Min-Gyu, KANG Chong-Yun, YOON Seok-Jin(Korea Institute of Science and Technology, Thin Film Materials Research Center), LEE YoungPak(Hanyang University, q-Psi & Department of Physics)
- Ep-II-063 Luminescence Improvement of KNbO<sub>3</sub>:Eu<sup>3+</sup> Phosphors by Li<sup>+</sup> Doping: YI Soung Soo, R. Balakrishnaiah, KIM Dong

- Woo(Department of Electronic Materials Engineering, Silla University), KIM Sung Hoon(Department of Engineering in Energy and Applied Chemistry, Silla University), JANG Kiwan, LEE Ho Sueb(Department of Physics, Changwon National University), MOON Byung Kee, JEONG Jung Hyun(Department of Physics, Pukyong National University)
- Ep-II-064 쌍축성 네마틱 액정의 texture 관찰: 장 태석, 김 종현(충남대), 최 석원(경희대)
- Ep-II-065 Luminescent Properties Of  $\text{Er}^{3+}$ -Doped  $(\text{Y,Gd})\text{BO}_3$  Phosphors: R. Balakrishnaiah, YI Soung Soo, KIM Dong Woo (Department of Electronic Materials Engineering, Silla University), KIM Sung Hoon(Department of Engineering in Energy and Applied Chemistry, Silla University), JANG Kiwan, LEE Ho Sueb(Department of Physics, Changwon National University), JEONG Jung Hyun(Department of Physics, Pukyong National University)
- Ep-II-066 전기장에 따른 액정 방울 속 방향자의 변화 관찰: PARK Jin-Soon, KIM Jong-Hyun(충남대 물리학과), LEE Eun Seong, LEE Jae Yong, PARK Joo Hyun(한국표준과학연구원)
- Ep-II-067 Cooling Power of Field Emission from the n-Type Silicon Semiconductor: 정 문성, 금 관필, 구 자훈, 배 해경, 장 유진, 천 중필(울산대)
- Ep-II-068 The Enhanced Thermal Stability Of Low Dielectric Constant SiOC Film By Post Annealing In Ambient Forming Gas: 박 상한, 김 효진, 조 만호, 황 정남, 한 준희(연세대), 이 도형, 권 영수, 박 소연((주) ATTO), 김 무성(Air Products Korea)
- Ep-II-069 Field Enhancement Near the Contact between Dielectric and Metal: 정 문성, 구 자훈, 금 관필, 배 해경, 장 유진, 천 중필(울산대)
- Ep-II-070 이온조사에 의한 유기태양전지 회로의 P3HT/PCMB 레이어의 특성변화 연구: 박 성규, 이 용백, 이 석호, 주 진수(고려대)
- Ep-II-071\* I-V Properties of Albumin Adsorbed Porous Silicon: CHENG Horchhong, KIM Han-Jung, LEE Ki-Won, KIM Young-You (Department of Physics, Kongju National University)
- Ep-II-072 온도와 온도 변화량에 따른 블루페이즈 격자 구조와 크기의 변화 관찰: 이 호현, 김 종현(충남대), H. Kikuchi(Kyushu University, Department of Applied Chemistry)
- Ep-II-073 유기 태양전지에서의 solvent annealing 효과 및 광전기적 특성분석: 조 정민, 김 재령, 신 원석, 문 상진(한국화학연구원, 에너지소재연구센터)
- Ep-II-074 빛의 회절현상을 이용한 액체 속 음속도 측정: 박 세희, 김 인구, 이 재란, 김 석원(울산대)
- Ep-II-075\* Vanadium pentoxide nanowires as a functional material for Metal-Insulator-Semiconductor (MIS) Capacitor: SHAHID Muhammad, SHAKIR Imran, 이 강우, 강 대준(BK21 Physics Research Division, Department of Energy Science, Institute of Basic Science, SKKU Advanced Institute of Nanotechnology and Center for Nanotubes and Nanostructured Composites, Sungkyunkwan University)
- Ep-II-076 Study of the Novel Mass Production Method of  $^{64}\text{Cu}$  Radionuclide using  $^{64}\text{Ni}(p,n)^{64}\text{Cu}$  Nuclear Reaction with Energetic Protons: 전 권수, 박 현, 김 재홍(한국원자력의학원 방사선의학연구소)
- Ep-II-077 유기증기에 노출된 다공질규소 다층구조의 PL, 간섭색, 전도도의 변화 특성 연구: 서 동우, 이 기원, 김 영유, 김 한중, CHENG Horchhong(공주대)
- Ep-II-078\* Effect of Liq Thickness in Polymer Photovoltaic Cells Fabricated with P3HT:PCBM Blended Layer: SUNG Hyun-Su, KIM Jin-Man, LEE Su-Hwan, KIM Ji-Heon, LEE Gon-Sub, PARK Jea-Gun(Nano-SOI Process Laboratory, Hanyang University)
- Ep-II-079\* 대기 중 장시간 방치된 Pd-Pt/ $\text{WO}_3$  수소센서 박막의 반응성 연구: 진 정모, 정 현식(서강대)
- Ep-II-080 종이 기판 위에 top-emission type의 후막형 무기 electroluminescence 특성: 김 진영(성균관대), 유 세기(한국외국어대)
- Ep-II-081 Study on the charge transport characteristics of organic thin film transistor using near field scanning microwave microprobe: YOON Youngwoon, KIM Songhui, LEE Hanju, KIM Tae-dong, LEE Kiejin(Sogang Univ, Department of Physics)
- Ep-II-082 무냉매 전도냉각형 5 T 초전도자석: 김 동락, 김 재희, 최 연석, 양 형식(한국기초과학지원연구원)
- Ep-II-083\* Effect of Al Nanocrystals Surrounded by  $\text{Al}_2\text{O}_3$  in Nonvolatile Memory Characteristics for Polymer Memory-cells: PARK Jung-Yong, LEE Ho-Young(Department of Electrical & Computer Engineering, Hanyang University), KWON Kyoung-Cheol, KIM Chang-Hwan, LIM Jae-Sung, PARK Jea-Gun(National Program Center for Tera-bit-level Nonvolatile Memory Development, Hanyang University)
- Ep-II-084 Leakage Current Conduction Mechanism and Noise Properties of  $\text{ZrO}_2$  Thin Film: SEO Yohan, KIM Youngsang, JEON Hankyung, JEONG Heejun(한양대)
- Ep-II-085 OLED 소자에서 각 layer의 표면에 따른 특성연구: 김 태동, 윤 영운, 이 한주, 김 송희, 이 기진(서강대)
- Ep-II-086 Possible High-power Thin Film Varistor based on Metal-Insulator Transition: KIM Bong-Jun(ETRI), SEO Gi Wan(UST), CHOI Sungyoul, CHOI Jeongyong(ETRI), LEE Yong Wook(Pukyong National University), KIM Hyun-Tak(ETRI)
- Ep-II-087 Improving the Signal to Noise Ratio of MEG signal using lead superconductive hemispherical shield: YU Kwon Kyu, KIM Kiwoong, KWON Hyuckchan, KIM JinMok, LEE Yong Ho(KRISS)
- Ep-II-088 온도 변화에 따른  $\text{Ge}_2\text{Sb}_2\text{Te}_5$ 의 광학적 특성 연구: 서 윤경, 이 동재, 이 윤상(승실대 물리학과), 최 은집(서울시립대 물리학과), 이 택성(KIST)
- Ep-II-089 Electrical Characteristics of Aluminum Oxide Film Deposited by Electron Beam Evaporation for the Application of Thin-film

Transistors: IM Seongil, KO Gunwoo, LEE Kimoon, LEE Kwang H(Institute of Physics and Applied Physics, Yonsei University)

- Ep-II-090 RF 스퍼터링을 이용한 AZO 투명전도막 형성 및 특성 분석: 정 인승, 나 영혁(연세대), 최 명운((주) 야스), 정 광호(연세대)
- Ep-II-091 Hydrochlorosilole(HCS)을 기반으로 한 유기발광다이오드 (Organic Light-emitting diodes)의 임피던스 분석법을 이용한 최적화 구조연구: 박 영환, 신 용호, 이 수연, 김 용민(단국대)
- Ep-II-092 BiYIG박막의 테라헤르츠 특성 연구: 이 한주, 유 형근, 윤 영운, 김 태동, 김 송희, 이 기진(서강대)
- Ep-II-093 FOLED를 위한 Mg-Zn-F 봉지막 제작 및 특성 분석: 손 명락, 이 성엽, 신 병욱, 공 소저, 이 진능, 박 선미, 김 도억, 강 병호, 홍 석민, 추 나윤, 이 의완, 이 형락(경북대)
- Ep-II-094 Study of solvent effect for forming nanostructure of Organic solar cell: YI Jin Neung, SHIN Byong Wook(Kyungpook National University, Department of Physics), LEE Sung-Youp(Kyungpook National University, Department of Nano-science and Technology), PARK Sun Mi, SON Myeong Rak, KONG So Jeo(Kyungpook National University, Department of Physics), CHOO Na Yun(Kyungpook National University, Department of Nano-science and Technology), KIM Je Han(Kyungpook National University, Department of Physics), LEE Eui Wan, LEE Hyeong Rag(Kyungpook National University, School of Physics and Energy Science)
- Ep-II-095 박막태양전지 제조용 임의 방향 방출형 셀레늄 증발원 개발 및 Se/Glass 박막특성 분석: 김 은도, 정 예슬, 정 다운, 박 성동, 엄 기석((주) 알파플러스), 조 상진(경성대), 황 도원((주) 알파플러스)
- Ep-II-096 Plasma Dry Etching 방법에 의한 Wafer Backside Etch 특성 평가: 한 영기, 서 영수((주)소슬), 유 재하, 이 현범(하이닉스반도체), 서 상훈(KAIST), 황 옥중(나노종합팩)
- Ep-II-097\* High Temperature Thermoelectric Properties of  $\text{Ca}_3\text{Co}_4\text{O}_9$  Thin Film: KANG Min-Gyu, CHO Kwang-Hwan, KANG Chong-Yun(KIST, Thin Film Materials Research Center), KIM Sang-Sig(Korea University, School of Electrical Engineering), YOON Seok-Jin(KIST, Thin Film Materials Research Center)
- Ep-II-098 영상분석을 통한 초크랄스키 결정성장의 자동직경조절장치 개발: 이 정일(한국원자력연구원), 정 기수(경상대), 장 인수, 김 장렬(한국원자력연구원)
- Ep-II-099\* Local electrical properties of  $\text{CuIn}_{1-x}\text{Ga}_x\text{Se}_2$  thin films using conductive atomic force microscopy: SHIN R. H., JO W.(Department of Physics, Ewha Womans University), YUN Jae Ho, AHN Sejin(Korea Institute of Energy Research)
- Ep-II-100\* Photoluminescence properties of ZnO/Ag thin films prepared by rf-magnetron sputtering: 권 민지, 김 동욱, 신 혜영, 윤 석현(이화여대), 이 기주(충남대)
- Ep-II-101 고온고습 표준가스 발생 기술: 최 병일, 김 종철, 우 상봉(한국표준과학연구원)
- Ep-II-102 OLED 디스플레이 필름의 수분투과도 측정: 최 병일, 우 상봉, 김 종철(한국표준과학연구원)

## ■SESSION P2■

## 반도체물리학과회 포스터 발표

장 소 : 포스터 발표장

10월 22일(목) 11:00 - 13:00

- Kp-II-001 Resonant Tunneling Barriers in Quantum Dots-in-a-Well Photodetectors: BARVE Ajit V., SHAO J., SHARMA Y., R. Shenoi(University of New Mexico, Center for High Technology Materials), JUN OH Kim, SANG JUN Lee, SAM KYU Noh(Korea Research Institute of Standards and Science), SANJAY Krishna(University of New Mexico, Center for High Technology Materials)
- Kp-II-002 Effect of Pretreated Substrate on the Nucleation Characteristics of GaN Nanorods: 박 현규, 이 상화, 김 진교(경희대 물리학과)
- Kp-II-003 Photocurrent Spectroscopy of InAs/GaAs Quantum Dots Grown by MBE: 조 현준, 김 정화(영남대), 이 정열(현풍고), 김 종수, 배 인호(영남대)
- Kp-II-004 Contactless Electroreflectance Spectroscopy of  $\text{In}_{0.5}(\text{Ga}_{1-x}\text{Al}_x)_{0.5}\text{P}/\text{GaAs}$  Double Heterostructure: 김 정화, 조 현준, 김 종수, 배 인호(영남대)
- Kp-II-005 Growth and fabrication of high performance 365nm ultraviolet light-emitting diodes: 전 성란, 강 인기, 김 재범, 강 성구, 한 재광, 이 상헌, 김 종섭(한국광기술원, LED 융합기술팀), 손 성진(LG이노텍, Epi 개발 그룹)
- Kp-II-006 드레인 영역의 field plate 형성에 의한 누설전류 억제 효과에 관한 연구: 양 전욱, 홍 성기, 김 정진(전북대)
- Kp-II-007 Fabrication of Nonpolar a-plane (11-20) InGaN/GaN Light Emitting Diode: SEO Yong Gon(KETI Green Energy Research Center, Department of Physics, Yonsei University), BAIK Kwang Hyeon(KETI Green Energy Research Center), OH Kyungwhan(Department of Physics, Yonsei University), HWANG Sung-Min(KETI Green Energy Research Center)
- Kp-II-008\* Influence of Uniaxial Anisotropy on The Domain Pinning Fields in Ferromagnetic  $\text{Ga}_{1-x}\text{Mn}_x\text{As}$  Films: LEE Sangyeop, KIM Shinhee, KIM Yungjun, LEE Hakjoon, KHYM S., LEE Sanghoon(Physics Department, Korea University), LIU X.,

FURDYNA J. K.(Physics Department, University of Notre Dame, USA)

- Kp-II-009\* Mapping of magnetic anisotropy in strained ferromagnetic semiconductor GaMnAs films: KIM shinhee, SHIN jinsik, YOO taehee, KIM yungjun, KHYM S., LEE sanghoon(Physics Department, Korea University), LIU X., FURDYNA J.K. (Department of Physics, University of Notre Dame, USA)
- Kp-II-010\* InAs/GaSb 응력초격자의 계면층 분석 및 적외선검출소자의 특성 연구: 김 준오, 신 현욱, 최 정우(경희대), 이 상준, 김 창수, 노 삼규(한국표준과학연구원 나노소재측정센터)
- Kp-II-011\* Reciprocal Space Mapping in Grazing Incidence Geometry to Investigate Preferred Growth Directions of GaN Nanorods Non-catalytically Grown on Si Substrates: 이 상화, 손 유리, 김 진교(경희대 물리학과), 이 동렬(숭실대 물리학과), 이 현휘(포항공대, 방사광가속기연구소)
- Kp-II-012\* GaAs/AlGaAs 양자점에서 Franz-Keldysh oscillation 연구: 이 창호, 최 은미, 오 민우, 배 주희, 조 현준, 김 정화, 배 인호, 김 종수(영남대), 송 진동(한국과학기술연구원), 이 상준, 노 삼규(한국표준과학연구원), 김 진수(전북대), 임 재영(인제대), 강 훈수, 정 문석(광주과학기술원 고등광기술연구소)

10월 22일(목) 15:00 - 17:00

- Gp-III-001 바퀴에 작용하는 마찰력에 대한 중·고·대학생의 개념 이해 조사: 홍 성욱(대구대)
- Gp-III-002\* 11학년을 대상으로 한 과학적 근거 교육이 근거 판단에 미치는 효과: 김 정희, 윤 성현(한국교원대)
- Gp-III-003 교과서 도입부의 분석틀 구성 및 교사와 학생의 선호도조사- 10학년 '전기에너지' 소단원 중심으로 -: 김 진옥, 윤 성현(한국교원대)
- Gp-III-004\* 유체속 조화진동자의 역학적 특성: 이 상익, 박 준석, 손 영덕, 하 명훈, 임 도연, 전 운승, 지 혜림(경성대)
- Gp-III-005\* 비판적 탐구토론 중 예비교사들의 논증에 나타난 인지적 구조 및 증거의 유형 분석: 임 명선, 이 봉우(단국대), 김 희경(강원대)
- Gp-III-006\* 물리 문제 상황에 따른 남녀학생의 선택률과 정답률: 이 수아, 박 윤배(경북대)
- Gp-III-007 열 저장소에 있는 전선에서의 Ohm의 법칙: 추 민우, 김 인구, 김 석원(울산대)
- Gp-III-008 학부생을 위한 개선된 단색분광기 개발: 김 대환, 이 성묵(서울대)
- Gp-III-009 푸리에 분광기를 이용한 광원의 특성 학습: 강 영창, 신 광문, 이 성묵(서울대)
- Gp-III-010 시각장애 초등학생을 위한 '수평잡기' 영역의 실험관찰 교과서의 개발: 박 종호, 차 현수(진주교육대)
- Gp-III-011 Theoretical Calculation of the Thermal Conduction: KIM Taekyu(Jeonju National University of Education, Department of Science Education)
- Gp-III-012\* 안개상자를 이용한 라돈 기체의 반감기 측정: 박 병규, 강 준호, 박 찬영, 김 태경(한성과학고), 전 영석(서울교육대)
- Gp-III-013 전지의 연결방법에 대한 초등 교사와 초등 교과용도서에서의 설명 특성 분석: 박 상우(청주교육대), 한 용희(남이초등학교)
- Gp-III-014 초등학교 5학년 학생들의 그래프 작성 및 해석 능력과 논리적 사고력과 관계: 박 상우(청주교육대), 김 진선(용인신갈초등학교)
- Gp-III-015 중등 물리교과 1급 정교사 자격연수의 전공 심화학습에 대한 인식: 김 성원, 이 은정, 조 미영(이화여대)

10월 22일(목) 15:00 - 17:00

- Hp-III-001 A GUI Blanket Simulator, GUMBIS: LEE Young-Seok, YOON Seok-Heun, HAN Jung-Hoon, KIM Hyuck-Jong(National Fusion Research Institute)
- Hp-III-002\* Estimation of n=2 Resonant Field Configuration in KSTAR Tokamak: KIM Doohyun, HAN Hyunsun, KIM Ki Min, HONG Sang Hee(Seoul National University, Department of Nuclear Engineering)
- Hp-III-003 Quasilinear approach to neoclassical transport with ITG mode: 서 장훈, CHANG C.S.(KAIST)
- Hp-III-004\* Two-dimensional Numerical Simulation of Heat Flux Reduction on the Divertor Plate by Deuterium Puffing and Pumping in KSTAR: PARK JIn-Woo, HAN Hyunsun, KIM Hyunseok(Department of Energy System Engineering, Seoul National University), NA Yong-Su(Department of Nuclear Engineering, Seoul National University)
- Hp-III-005 MHD stability analysis for advanced tokamak target of the KSTAR device: YI Sumin(NFRI)
- Hp-III-006\* Effects of ECCD on NTM Suppression in Time-dependent Simulations Coupled with the Plasma Transport: KIM Kyungjin, PARK Y.S., KIM Hyunseok(Department of Energy System Engineering, Seoul National University), NA Yong-Su(Department of Nuclear Engineering, Seoul National University)
- Hp-III-007 One-dimensional Numerical Analysis on Transport Phenomena of Locally-heated Plasma in a Linear Divertor Simulator: LEE Wonjae, HAN Hyunsun, KIM Hyunseok(Department of Energy System Engineering, Seoul National University), HONG Sang Hee, NA Young-Su(Department of Nuclear Engineering, Seoul National University)
- Hp-III-008 Plasma Reconstruction of KSTAR 1st Plasma Equilibrium with EFIT Code: 유 광일, 이 덕교, 박 병호, 이 상곤, 박 준교, 서 성현, 한 상희(국가핵융합연구소), LAO L. L(GA, USA), KSTAR team(국가핵융합연구소)
- Hp-III-009 Electron cyclotron heating during ECRH-assisted plasma startup in a tokamak: 설 재춘, 박 병호, 김 성식, 김 진용(국가핵융합연구소), 나 용수(서울대)
- Hp-III-010 A Ultra-High Sensitivity Gridded Ionization Chamber For Neutron Monitoring: LEE Young-Seok(National Fusion Research Institute), KIM Gui-Nyun(Department of Physics, Kyungpook National University), YU.M. Gledenov(Frank Laboratory of Neutron Physics, Joint Institute for Nuclear Research, Russia)
- Hp-III-011 Improvement of the self compensating type analog integrators for the KSTAR tokamak: KA . E. M, LEE . S. G, BAK . J. G(National Fusion Research Institute), SON . D(Hannam University)

- Hp-III-012 Optics Design of KSTAR ECE Imaging System: LEE W., YUN G., PARK H. K.(Department of Physics, POSTECH), LIANG T., TOBIAS B., DOMIER C. W., LUHMANN, JR. N. C.(Department of Applied Science, UC Davis, USA)
- Hp-III-013 Current status of probe diagnostics for KSTAR: 박 준교, 이 상곤, 김 정엽, 위 한민(국가핵융합연구소)
- Hp-III-014 Halo current monitors for KSTAR: 박 준교, 이 상곤, 가 은미, 김 정엽(국가핵융합연구소)
- Hp-III-015 Design Study of the Magnetic Diagnostics in a Spherical Tokamak: KIM Jwa Soon, SUNG Choongki(Department of Energy System Engineering, Seoul National University), HWANG Yong-Seok, NA Yong-Su(Department of Nuclear Engineering, Seoul National University)
- Hp-III-016 Optical System Design For Charge Exchange Spectroscopy (CES) Of Korea Superconducting Tokamak Advanced Research (KSTAR): 오 승태, 고 원하, 이 종하(NFRI, DRT)
- Hp-III-017 KSTAR ECE 진단 시스템 Upgrade: 정 승호(한국원자력연구원), 이 규동(국가핵융합연구소)
- Hp-III-018 핵융합 중성자 진단용 스틸벤 검출기 제작 및 연구: 강 병휘, 김 용균, 이 승규, 이 철호(한양대)
- Hp-III-019\* 타겟 반사체를 이용한 마이크로파 영상 반사체의 데모 실험: 홍 인호, 남 윤범, 이 우창, 윤 건수, 박 현거(POSTECH 물리학과)
- Hp-III-020\* 극각 방향의 요동현상 측정을 위한 MIR 시스템 시뮬레이션: 남 윤범, 홍 인호, 이 우창, 윤 건수, 박 현거(POSTECH 물리학과)
- Hp-III-021 NBI heating for KSTAR tokamak: beam energy effects on the plasma: LAURENT Terzolo, 권 재민, 김 진용(국가핵융합연구소), 박 종구(한국원자력연구원)
- Hp-III-022 KSTAR 원형 플라즈마에서의 ICRF 가열 효율 예측과 TOMCAT 및 TORIC 코드의 비교분석: 왕 선정, 김 선호, 박 종구(한국원자력연구원)
- Hp-III-023 S-parameter 측정결과와 8-port 전송선 회로모델을 이용한 KSTAR ICRF 안테나 및 전송선의 전압 분포 계산: 김 선호, 왕 선정, 황 철규, 배 영덕, 윤 재성, 박 종구(한국원자력연구원)
- Hp-III-024 Conceptual Design Of The Spherical Tokamak and ECR Heating System Development: LEE Hyunyeong, KANG Jisung, SUNG Chungki, PARK Youngseok, HWANG Yongseok(Department of Nuclear Engineering, SNU)
- Hp-III-025 FPGA를 이용한 디지털 적분기 개발: 서 성현, 위 한민(국가핵융합연구소)
- Hp-III-026\* PIC simulation study for the nonlinear wave-wave interactions of Alfvén-ion-cyclotron waves: KAANG Helen, RYU Chang-Mo, MOK Chinook, RHA Kicheol(POSTECH, PHYSICS)
- Hp-III-027 Three-dimensional Particle in Cell Simulation of 2.45 GHz ECR Plasma Source with a Magnetron Magnetic Field Configuration: 장 현우, 김 성봉(포항공대), 유 석재(국가핵융합연구소), 유 창모(포항공대)
- Hp-III-028 Correlation Between Ion Does and Surface Resistivity of Polyimide with ECR Argon Ion Beam\*: 김 선영, 이 우창, 박 병재, 조 무현, 남궁 원(포항공대)
- Hp-III-029 Development of a 2.45 GHz ECR Plasma Source with a Race-track Magnetic Field Configuration for Generating Hyperthermal Neutral Beams: 김 성봉(포항공대), 구 동진, 김 대철, 유 석재(국가핵융합연구소), 조 무현, 남궁 원(포항공대)
- Hp-III-030\* Measurement of Electron Temperature and Density on DC Pulsed Plasma: 박 병재, 정 진현, 이 희재, 이 창호, 조 무현, 남궁 원(포항공대)
- Hp-III-031 Measurement of ultrasoft x-ray emission from a linear Electron Cyclotron Resonance Plasma source: 최 명철(한국기초과학지원연구원), 정 진일, 이 규동, 서 동철(국가핵융합연구소)
- Hp-III-032 음전성 SF<sub>6</sub> 플라즈마(Electronegative SF<sub>6</sub> Plasma)의 탐침 진단 연구: 조 헤민, 송 민아, 박 혜선, 이 헤란, 정 태훈(동아대)
- Hp-III-033 산소-아르곤 유도결합 플라즈마의 특성 연구: 이 헤란, 조 헤민, 정 태훈(동아대)
- Hp-III-034\* Capacitively Coupled Plasma에서 Radio Frequency 비보상 및 보상단일 탐침을 이용한 플라즈마 전자온도와 전자밀도 측정: 이 훈희, 정 규선(한양대)
- Hp-III-035\* Capacitively Coupled Plasma에서 방출탐침을 이용한 플라즈마 전위 특성 측정: 문 재원, 정 규선(한양대)
- Hp-III-036\* Radio Frequency 플라즈마에서의 Harmonic 특성분석: 정 재영, 정 규선(한양대)
- Hp-III-037 Effect of Hydrogenation on Electrical Properties of ZnO Films Deposited by a DC Arc Plasmatron: V. PENKOV Oleksiy, VADIM YU. PLAKSIN, SANG BEOM Joa, JI HUN Kim, HEON JU Lee(제주대)
- Hp-III-038\* RF Magnetron Sputtering 방법으로 증착한 AlN막의 전기적 및 구조적 특성: 박 정식, 류 성원, 김 상현, 박 용진, 박 승환(대구가톨릭대), 김 용모, 김 갑석(KI-Ximax), 김 화민(대구가톨릭대)
- Hp-III-039 RF-sputtering을 통한 ZnO 박막의 결정구조: 백 경철, 이 봉주(조선대), 김 태원(한국생산기술연구원 나노집적센터)
- Hp-III-040 TMOS/N<sub>2</sub>/Ar 혼합가스 방전의 PECVD Silicon Oxynitride Thin Films의 특성 연구: 송 민아, 조 헤민, 정 태훈(동아대)
- Hp-III-041\* 대향타겟식 스퍼터링법을 이용한 차세대 전자소자용 GZO 투명 전극의 특성분석: 김 미선, 배 강, 서 성보, 김 종재, 손 선영, 김 화민(대구가톨릭대)
- Hp-III-042\* Unbalanced Magnetron Sputtering법으로 제작된 ITO 박막의 특성: 지 승훈, 배 강, 윤 현오, 박 승환, 김 종재, 손 선영, 김 화민(대구가톨릭대)
- Hp-III-043\* A Micro Spark Gap Switch for a High Repetitive Pulser System: 남 종우(한국외대부속웅인외과), RAHAMAN Hasibur, 남

상훈(포항가속기연구소)

Hp-III-044 모세관 전극 대기압 마이크로 플라즈마 jet의 특성 연구: 박 혜선, 김 선자, 정 태훈, 배 세환(동아대)

Hp-III-045 Improvement of small thermal fuel reformers: V. YU. Plaksin, PENKOV. V. Oleksiy, J. H. Kim, S. B. Joa, H. J. Lee(제주대)

Hp-III-089 펄스 플라즈마에서 플라즈마 손실 속도의 변화와 이온 에너지 플럭스에 미치는 영향: 인 정환, 장 홍영, 나 병근(한국과학기술원, 물리학과)

## ■SESSION P3■

## 광학 및 양자전자학분과회 포스터 발표

장 소 : 포스터 발표장

10월 22일(목) 15:00 - 17:00

- Ip-III-001 Design of an Ultrabroadband Wave Plate for the Application to Sub-2-cycle Laser Pulses: 김 경승, 고 동혁, 남 창희(결맞는 X선 연구단 물리학과 한국과학기술원)
- Ip-III-002\* 민감도분석을 통한 폰카메라용 광학계 설계: 김 지현, 고 정휘, 김 세진, 김 기현, 김 진모, 윤 경환, 신 원진, 최 봉주, 윤 성로(국민대)
- Ip-III-003 Europium and terbium luminescence in YTaO<sub>4</sub>: NAZAROV Mihail(Department of Materials Science and Engineering, Gwangju Institute of Science and Technology), TSUKERBLAT Boris(Institute of Electronic Engineering and Industrial Technologies, Academy Sciences of Moldova), LEE SU WOONG(Graduate program of Photon Science and Technology, Gwangju Institute of Science and Technology), NOH Do Young(Department of Materials Science and Engineering, Gwangju Institute of Science and Technology)
- Ip-III-004\* Talbot effects of white x-ray propagation through a periodic structure and their applications in x-ray patterning: KIM Jae Myung, CHO In Hwa, LEE Su Yong, NOH DO YOUNG(Department of Materials Science and Engineering of Gwangju Institute of Science and Technology)
- Ip-III-005 회전 원판에 코팅된 중수소화 플라스틱을 표적으로 한 연속 중성자 발생 장치: 남 성모, 차 형기, 이 용주, 한 재민, 이 성만(한국원자력연구원 양자광학연구부)
- Ip-III-006\* X-ray/UV여기에 의한 YNbO<sub>4</sub>:Eu<sup>3+</sup> 발광 특성: 이 수웅(광과학기술학제전공, 광주과학기술원), 나자로프 미하일, 노 도영(신소재공학과, 광주과학기술원)
- Ip-III-007 New Optical properties of Be-doped GaAs thin films: CHOI SUNGYOUL, KIM BONG-JUN(Electronics and Telecommunications Research Institute), LEE YONG WOOK(School of Electrical and Control Engineering, Pukyong National University), CHOI JEONGYONG(Electronics and Telecommunications Research Institute), GI WAN Seo(School of advanced device technology, University of Science and Technology), HYUN-TAK Kim(Electronics and Telecommunications Research Institute)
- Ip-III-008\* Development of Multiplex CARS(Coherent anti-Stokes Raman Scattering) Microscopy: 이 장혁, 최 대식(광주과학기술원, 광과학기술학제학부), 오 명규, 엄 태중(광주과학기술원, 고등광기술연구소), 고 도경(광주과학기술원, 광과학기술학제학부, 고등광기술연구소)
- Ip-III-009 Photoluminescence Properties of Eu<sup>2+</sup>-doped NaSrPO<sub>4</sub> Phosphors for White-light-UVLEDs: JEONG Junho, SHIN Hyunjoon, YOON Jaeho, LEE Ho-Sueb, JANG Kiwan(창원대), YI Soung-soo(신라대), JEONG Jung-hyun(부경대)
- Ip-III-010\* Design of a fractal beam with optical vortices and the beam's dynamical behavior: 조 영권, 김 기홍(아주대 에너지시스템학부)
- Ip-III-011 Invariant imbedding method를 이용한 optical phase-conjugate wave의 반사율과 Goos-Hanchen shift의 계산: 함 홍우, 김 기홍(아주대 에너지시스템학부)
- Ip-III-012 Exact calculation of the probability density of the wave transmittance in one-dimensional random media: 이 광진, 김 기홍(아주대 에너지시스템학부)
- Ip-III-013 Transmission, reflection and localization of waves in an amplifying medium with nonlinear gain: NGUYEN Ba Phi, 김 기홍, ROTERMUND Fabian(아주대 에너지시스템학부), 임 한조(아주대 전자공학과)
- Ip-III-014 Butt-Coupling of Light into Surface Plasmon Waves in Metal-Dielectric-Metal Structures: PARK Jong-Moon, PARK Hae-Ryeong, LEE Myung-Hyun(Sungkyunkwan University, School of Information and Communication Engineering)
- Ip-III-015\* Relationship between surface relief grating and photoisomerization in an azobenzene polymer film: KIM Jung-Sung, HAN Cheolwoong, OH Cha-Hwan(Dept. of Physics, Hanyang Univ.)
- Ip-III-016\* Hard x-ray projection patterning using total external reflection from a Au grating: NOH Do Young, CHO In Hwa, LEE Su Yong, KIM Jae Myung, LEE Su Woong(광주과학기술원, 신소재공학과)
- Ip-III-017 전자빔 빔을 이용한 TiO<sub>2</sub>/SiO<sub>2</sub> 박막의 SiO<sub>2</sub> 두께에 따른 구조적, 광활성 특성: 이 우경, 편 민욱, 이 동열, 한 성홍(울산대)

- Ip-III-018 RF sputtering 법으로 제작한 Au 버퍼 이산화티탄 박막의 광활성 특성: 최 현욱, 이 우경, 편 민욱, 오 주희, 권 영상, 한 성홍, 김 의정(울산대), 지 성진, 심 창호((주)새한하이테크)
- Ip-III-019\* Tracking 공차를 줄여주는 집광형 태양전지용 광학계: 김 기현, 고 정휘, 김 세진, 김 지현, 김 진모, 윤 경환, 신 원진, 최 봉주, 윤 성로(국민대 물리학과), 김 영준(차바이오 & 디오스텍)
- Ip-III-020\* Nonlinear optical absorption of carbon nanotubes on the surface of D-shaped fibers with different evanescent field coupling: HAN young-geun, CHOO suho, KIM Hyun-Joo, KWON Oh-Jang(Hanyang University)
- Ip-III-021 지그재그 광학박막을 이용한 편광 광학소자의 광학적, 구조적 특성: 박 용준, SOBAHAN KMAbdus, 황보 창권(인하대)
- Ip-III-022 Beam Size Independence of Threshold in LiNbO<sub>3</sub> Optical Parametric Oscillator in the presence of Walkoff: RIM Min Ho (Department of Physics, Korea Advanced Institute of Science and Technology), CHO Gi Ho, RHEE Bum Ku(Department of Physics, Sogang University), YOON Choon Sup(Department of Physics, Korea Advanced Institute of Science and Technology)
- Ip-III-023 BSDF에 따른 LED Package 광특성 평가: 강 성구, 김 재범(한국광기술원), 안 치호, 정 창섭(전남대)
- Ip-III-024 LED 해상용 등면기의 성능개선을 위한 광학구조: 김 재범(한국광기술원), 정 창섭(전남대)
- Ip-III-025 투명전도성 산화물을 흡수체로 가지는 EUVL용 마스크 설계: 남 현정, 이 장훈, 황보 창권(인하대)
- Ip-III-026\* Theoretical calculation of optical trapping efficiency in intermediate regime: 오 차환, 김 현익, 전 형준(한양대)
- Ip-III-027\* Sagnac loop interferometer based on D-shaped polarization-maintaining fiber with evanescent field coupling: HAN Young-Geun, KWON Oh-Jang, SHIM Young-Bo, KIM Hyun-Joo(Hanyang Univ.)
- Ip-III-028\* Polarization-Maintaining Long-Period Fiber Gratings Based On Periodic Microbending: 한 영근, 김 현주, 권 오장(한양대), 이 상배(한국과학기술연구원, 지능시스템연구본부)
- Ip-III-029 Broadband Single-Polarization Single-Mode Operation in Highly Birefringent Photonic Crystal Fibers: 이 성구, 이 관일, 이 상배(한국과학기술연구원, 광기술연구실)
- Ip-III-030 눈안전 과장발진을 위한 OPO 레이저 발진 및 특성 분석: 윤 창준, 최 중규, 유 찬희, 유 재신, 나 준희, 신 수봉, 김 점수(삼성탈레스)
- Ip-III-031 펄스 전류로 구동된 다이오드 여기 수동형 Q-스위칭 레이저의 출력 특성 연구: 안 승인, 여 환섭, 최 윤호, 이 준엽, 이 준호, 송 우혁(경산과학고등), 이 강인, 이 종훈(영남대)
- Ip-III-032\* 거저벡터의 변환을 이용한 단일 광자-나노결정체 분자 계의 여기 특성 분석: 윤 재석, 남 석우, 홍 석경(고려대)
- Ip-III-033 액체 시료에서의 Faraday 회전: 한 예슬, 이 재란, 김 석원(울산대)
- Ip-III-034\* Generation of Femtosecond Laguerre Gaussian beam using LCoS spatial light modulator: 황 성인, 송 동훈(광주과학기술원 광과학기술학제전공), 강 훈수(광주과학기술원 고등광기술연구소), 고 도경(광주과학기술원 광과학기술학제전공, 고등광기술연구소)
- Ip-III-035\* Development of a Sub-10-fs Ti:sapphire Oscillator and a Real-time Mach-Zehnder Interferometric Autocorrelator: 송 동훈, 황 성인(광주과학기술원, 광과학기술학제전공), 유 태준, 성 재희(광주과학기술원, 고등광기술연구소), 고 도경(광주과학기술원, 광과학기술학제전공, 고등광기술연구소)
- Ip-III-036 Gain Saturation Effect on ASE Prepulse Profile in Ti:sapphire Laser: 이 성구, 유 태준, 성 재희, 진 유용, 이 창원, 정 태문, 이 종민(고등광기술연구소, 광주과학기술원)
- Ip-III-037 Shack-Hartmann Wavefront Sensor using Phase Retrieval for Measuring the Wavefront of the Ultrashort High-Power Laser: JEONG Tae Moon, KIM Chul Min, LEE Jongmin(GIST, Advanced Photonics Research Institute)
- Ip-III-038 KGW를 이용한 황색광 라만 레이저의 출력특성: 진 우진, 조 동기, 심 민정(단국대, 의학레이저), 김 태국(이오테크닉스), 한 은주(수원대, 물리학과), 김 영식(단국대, 의학레이저)
- Ip-III-039 A laser-produced fast neutron source operated up to 5 Hz: 이 성만, 박 상순, 정 영빈, 박 승규, 이 용우, 김 경남, 남 성모, 차 형기(한국원자력연구원, 양자광학연구부)
- Ip-III-040\* Lasing properties of the limaçon-shaped microcavity: YI Chang-Hwan(서강대)
- Ip-III-041 칼슘 분광을 위한 연속발진 자외선광의 발생: 고 광훈, 이 경현, 박 현민, 정 도영, 임 권, 김 택수, 한 재민, 차 용호(KAERI)
- Ip-III-042 Directional emission of a spiral-shaped microcavity with waveguide: 김 명운, 이 창환(서강대), 이 상훈(서남대), 김 철민(서강대)
- Ip-III-043 디지털 홀로그래프의 자동초점 조절 및 재생 알고리즘 연구: 한 성, 김 진태(조선대)
- Ip-III-044 장거리 광섬유 간섭계를 이용한 반사실 양자 암호 키 분배 실험: 조 석범, 노 태곤(한국전자통신연구원)
- Ip-III-045 포항가속기연구소 7B2 Bio-Image 빔라인: 최 효진, 김 효윤, 임 재홍, 황 정연(포항가속기연구소)
- Ip-III-046 공초점 형광 현미경 시스템 구성과 형광세포의 3차원 영상구현: 김 정민, 김 석원(울산대)
- Ip-III-047 Time variation of fluorescence lifetime in the enhanced cyan fluorescence protein: 이 순혁, 김 수용(한국과학기술원), 김 석원(울산대)
- Ip-III-048 Protein folding dynamics-A lifetime approach: 이 순혁, 김 수용(한국과학기술원), 김 석원(울산대)
- Ip-III-049 Confocal Microscopy를 이용한 분자의 Fluctuation 관찰: 이 재란, 김 정민, 박 세희, 김 석원(울산대, 물리과)

- Ip-III-050 초정밀 자동 차트 프로젝터(Auto-Chart Projector) 설계 및 제작: 이 상은, 조 재홍(한남대), 한 상준, 남 기준, 고 안수((주)포텍)
- Ip-III-051 조절을 고려한 단순화된 수정체 모델의 설계 및 분석: 강 은경, 황보 창권(인하대, 물리학과), 박 성찬(단국대, 물리학과)
- Ip-III-052 Fiber-optic common-path FD-OCT implementation for optical sensing and biomedical imaging: 마 혜준, 최 은서, 신 용진(조선대)
- Ip-III-053\* 단일 폴리머 나노선의 광특성 조작과 분광 이미징 연구: 김 도일, 김 대철, 김 정용(인천대), 홍 영기, 박 동혁, 주 진수(고려대)
- Ip-III-054\* Electric coupling resonance variation in THz metamaterials by liquid crystal: 우 제흔, 강 보영, 최 은영, 이 현희, 김 은선, 김 정희, 우 정원(Department of Physics, Quantum Metamaterials Research Center, Ewha Womans University), 홍 태윤, 김 재훈(Department of Physics, Yonsei University)
- Ip-III-055 Proton Radiography Using the 100 TW Femto-second Laser: 최 창일, 강 병휘, 강 상묵, 김 용균, 이 철호(한양대), 고 도경, 최 일우, 이 종민(광주과학기술원 고등광기술원)

### ■SESSION P3■

### 원자 및 분자물리학과회 포스터 발표

장 소 : 포스터 발표장

10월 22일(목) 15:00 - 17:00

- Jp-III-001 다각형 결맞음 상태의 비고전적 특성: 신 성국, 김 기식(인하대)
- Jp-III-002 이중핵 이원자 분자의 밀도 이전 검출을 위한 이온화 에너지: 김 진태(조선대)
- Jp-III-003 ATI and Momentum Distributions of Strong Field Ionization: 변 창우, 이 민호, 최 낙렬(금오공대)
- Jp-III-004 Structural and luminescent properties of  $Dy^{3+}$  doped  $Y_2O_3$  nanophosphors: JANG kiwan, RATNAM B.V., JAYASIMHADRI Mulla, LEE Ho Sueb(창원대), YI Soung-Soo(신라대), JEONG Jung-Hyun(부경대)
- Jp-III-005 Analytic solution of the saturated absorption spectrum for a two-level atomic medium with an open transition: 노 흥렬, 신 서로(전남대 물리학과)
- Jp-III-006\* 단일 광자 검출기를 이용한 광자계수 분포 측정: 문 한섭, 이 희정, 배 인호(부산대)
- Jp-III-007\* Measurement and calculation of absolute transmission spectra for  $85Rb$  atoms: 신 서로, 노 흥렬(전남대 물리학과)
- Jp-III-008\* Saturation of a Transition between two levels in a three level system: 정 지은, 조 동현(고려대)
- Jp-III-009\* 직접 전류 변조된 레이저를 이용한 Rb 셀에서의 CPT 신호: 김 호중, 문 한섭(부산대)
- Jp-III-010\* 냉각된  $85Rb$  원자 매질에서의 4광파 혼합: 김 정동, 이 경현, 유 훈, 김 중복(한국교원대), ZHUO Zhong Chang(Jilin University)
- Jp-III-011\* Optical cavity를 이용한 optoelectronic oscillator: 김 장면, 조 동현(고려대)
- Jp-III-012\* Ultracold Atoms in a time orbiting magnetic potential: LEE Wanhee, PARK Jina, YUM Dahyun, JHE Wonho(서울대)
- Jp-III-013\* Magneto optical trap of  $87Rb$  with an external atom chip: 유 훈, 김 정동, 김 중복(한국교원대)
- Jp-III-014\* Zeeman Slower for Loading  $7Li$  in a Magneto-Optical Trap: 김 휘동, 박 진신, 조 동현(고려대)

### ■SESSION P3■

### 반도체물리학과회 포스터 발표

장 소 : 포스터 발표장

10월 22일(목) 15:00 - 17:00

- Kp-III-013  $AgGaSe_2$ 와  $AgGaSe_2:Co^{2+}$  박막의 광유기 방전특성: 이 정주, 이 종덕, 박 창영, 김 동인, 김 진호(경상대)
- Kp-III-014 고온 동작 양자점 제작: 엄 영제, 정 윤철(부산대), 김 남(한국표준과학연구원)
- Kp-III-015 Investigation of Photoluminescence spectrum in  $CdGa_2Se_4$  layers: HONG Kwangjoon(Department of Physics, Chosun University)
- Kp-III-016 증착 온도에 따른  $In_2O_3$  박막의 특성 분석: 조 신호(신라대)
- Kp-III-017 4세대 이상 대면적 유기박막 증착을 위한 선형 증착원의 유동 해석: 최 범호(한국생산기술연구원 호남권기술지원본부 나노기술직접센터), 이 종호(한국생산기술연구원 호남권기술지원본부 광응용부품지원센터), 양 영수(전남대)
- Kp-III-018 Progress study for the large scale production of single-walled carbon nanotube field effect transistors: PARK Serin, KWAK Jun-Hyuk, JEON Eun-Kyoung, PARK Dong-Won, LO Young-Seop, SO Hye-Mi, LEE Jeong-O, CHANG Hyun-Ju(Korea Research Institute of Chemical Technology)
- Kp-III-019 Analysis of carrier dynamics in MOS structure with  $TiSi_2$  nanocrystals by using capacitance and current transient measurements: KIM Jin Soak, LEE Dong Uk, HAN Seung Jong, KIM Eun Kyu(Department of Physics and

Quantum-Function Spinics Laboratory, Hanyang University)

- Kp-III-020 Tungsten Dual-Poly Gate Technology for High Speed and Low Power Application in DRAM Devices: Y.S. KIM(Dep. of Physics, Univ. of Ulsan), M.G. SUNG(R&D Div., Hynix Semiconductor), K.Y. LIM(FEP Group, SEMATEC), J.C. KU, S.G. PARK(R&D Div., Hynix Semiconductor)
- Kp-III-021 Effect of Nb and Al doping on resistance switching properties of amorphous  $\text{TiO}_2$  for nonvolatile memory device: 나 희도, 김 종기, 손 현철(연세대)
- Kp-III-022 ArF 엑시머레이저를 사용한 가스센싱용 ZnO 박막의 제작 및 특성 측정: 오 철민, 배 가람, 나 용운, 정 태봉, 김 진영, 강 준희(인천대)
- Kp-III-023 루테튬계 염료를 이용한 태양전지의 제작과 특성 비교: 김 성준, 김 영호(과학기술연합대학원대(UST)), 노 삼규(한국표준과학연구원, 나노소재측정센터), 이 현용(명지대)
- Kp-III-024 Effect of heat-treatment for  $\text{ZnIn}_2\text{Se}_4$  layers: HONG Kwangjoon, KIM Haejeong(Department of Physics Chosun University)
- Kp-III-025 Optical absorption properties of the photoconductive  $\text{AgGaSe}_2$  layers grown by hot wall epitaxy: YOU Sangha, HONG Kwangjoon(Department of Physics, Chosun University)
- Kp-III-026 발표 취소
- Kp-III-027 진공증착법에 의해 제작된  $\text{AgInSe}_2$ 와  $\text{AgInSe}_2:\text{Co}^{2+}$  박막의 구조 및 광학적 특성: 이 정주, 이 종덕, 박 창영, 성 병훈, 김 건호(경상대)
- Kp-III-028 Effects of leveler in Growth of Cu film by Electroplating method: RHA Sa-Kyun, KANG Sung-Kyu(Department of Materials Engineering, Hanbat National University)
- Kp-III-029 Optical Characterization of  $\text{Cu}_2\text{ZnSnSe}_4$  grown by thermal co-evaporation: 박 도영, 정 현식(서강대), 정 성훈, 윤 재호, 안 세진, 궤 지혜, 윤 경훈(한국에너지기술연구원 태양전지연구단)
- Kp-III-030 Electrical properties and valence-band splitting energy from photocurrent response of photoconductive  $\text{CdGa}_2\text{Se}_4$  layers: LEE Sangyoul, HONG Kwangjoon(Department of Physics, Chosun University)
- Kp-III-031 유기 박막 연속 증착이 가능한 유기물 자동 공급 장치 및 박막 증착: 최 범호(한국생산기술연구원 호남권기술지원본부 나노기술집적센터), 이 종호(한국생산기술연구원 호남권기술지원본부 광응용부품지원센터), 유 하나, 임 용환(한국생산기술연구원 호남권기술지원본부 나노기술집적센터)
- Kp-III-032 Resistance Switching Behavior of W-doped poly-crystalline  $\text{NiO}_x$  with TiN and Pt Electrodes: 김 종기, 나 희도, 손 현철(연세대)
- Kp-III-033\* Carrier tunneling through barrier engineered tunnel layer in metal-silicide nano-floating gate memory: LEE Dong Uk, SEO Ki Bong, HAN Seung Jong, KIM Seon Pil, KIM Eun Kyu(Quantum-Function Spinics Laboratory and Department of Physics, Hanyang University), PARK Goon-Ho, CHO Won-Ju(Department of Electronic Materials Engineering, Kwangwoon University)
- Kp-III-034\* Nanoscopic characterization of electroforming of Pt/ $\text{TiO}_2$ /Pt planar junctions: 김 해리, 박 수현, 정 인구, 김 동욱(이화여대)
- Kp-III-035\*  $\text{WSi}_2$  Nanocrystal Memory with Crested Tunnel Barrier: SEO Ki Bong, LEE Dong Uk, KIM Seon Pil, KIM Eun Kyu (Hanyang University), YOU Hee Wook, CHO Won Ju(Kwangwoon University)
- Kp-III-036\* Chemical Mechanical Polishing Characteristics Of Phase Change Memory In Alkaline Slurry With Hydrogen Peroxide: KIM Chen-Lae, NA Sang-Bin, CUI Hao(Department of Electronics & Communication Engineering, Hanyang University), CHO Jong-Young(Department of Nanoscale Semiconductor Engineering, Hanyang University), PARK Jin-Hyung(Advanced Semiconductor Material & Device Development Center, Hanyang University), PAK Ungyu(Division of Advanced Materials Science Engineering, Hanyang University), PARK Jea-Gun(Department of Electronics & Communication Engineering, Hanyang University)
- Kp-III-037\* Properties of Copper Oxide Thin Films Prepared by Atomic Layer Deposition: LEE Byung Kook, KIM Seok Hwan, MIN Jae Ki, LEE Sun Sook, CHUNG Taek-Mo, KIM Chang Gyoung(Device Materials Research Center, Korea Research Institute of Chemical Technology), HWANG Jin Ha(Department of Material Science and Engineering, Hongik University, Seoul, Korea), AN Ki-Seok(Device Materials Research Center, Korea Research Institute of Chemical Technology)
- Kp-III-038\* 다층의 터널 절연막층을 이용한  $\text{TiSi}_2$  나노부유게이트 메모리소자의 전기적 특성 분석: 한 승중, 이 동욱, 김 선필, 김 은규 (한양대 물리학과), 오 준석, 조 원주(광운대 전자재료공학과)
- Kp-III-039\* Amorphous-to-Crystalline Phase Transformation of Thin-Film Rubrene: 임 성일, 염 한웅, 이 영국, 최 정민, 박 세웅(연세대)
- Kp-III-040\* Optical properties of metal oxide nano-particles embedded in the polyimide layer: KIM Soen Pil, LEE Dong Uk, KIM Eun Kyu(Quantum-Function Spinics Laboratory and Department of Physics, Hanyang University)
- Kp-III-041\* Degradation Pattern of  $\text{SnO}_2$  Nanowire Field Effect Transistors Analyzed by the Gate Dependent Mobility and Contact Resistance: NA Junhong, HUH Junghwan, KIM Gyu Tae(Korea University, School of Electrical Engineering), PARK Sung Chan, KIM Daell, HA Jeong Sook(Korea University, Department of Chemical and Biological Engineering)
- Kp-III-042\* 산소 유량비가  $\text{In}_2\text{O}_3$  박막의 특성에 미치는 영향: 궤 준호, 조 신희(신라대)

- Kp-III-043\* 실리콘과 유리 기판 위에 제작된 Ge-doped SbTe 박막의 유전함수 비교: 박 준우, 이 호선(경희대), 박 영욱, 정 병기(KIST)
- Kp-III-044\* Transmission electron microscopy investigation of tetragonal transformation in GeSbTe: 장 문형, 박 승중, 박 성진, 조 만호, 고 대홍, 손 현철(연세대)
- Kp-III-045\* 연 X-선 분광법을 이용한 a-GIZO 박막의 분광학적 특성 연구: 이 미지, 강 세준(포항공과대학, 물리학과), 백 재윤, 김 기정(포항가속기연구소), 정 재관, 이 재철, 이 재학(삼성전자 종합기술원), 신 현준(포항가속기연구소)

## ■SESSION P3■

## 천체물리학분과회 포스터 발표

장 소 : 포스터 발표장

10월 22일(목) 15:00 - 17:00

- Lp-III-001\* Study of UHECR Energy Reconstruction Method: SHIN B.K., CHO E.J., KIM J.H., KIM H.B., CHEON B.G.(Hanyang University, Department of Physics)
- Lp-III-002 Primary Energy Estimation of Cosmic Rays Measured by COREA Prototype System: 조 우람, 권 영준, 이 슬기(연세대), 임 선인, 양 종만, 남 신우(이화여대), 방 형찬(서울대), 천 병구(한양대), 홍 경희, 오 한슬, 손 근배, 이 정준, 김 주원, 황 채은, 정 지원, 김 인중, 이 승현(한성대학교), 정 유진(경기북대학교), 신 재익(연세대), 장 지현, 오 민지(이화여대), 조 일성(한국과학기술정보연구원)
- Lp-III-003 OMI 궤도에서 방사선 차폐 설딩이 OMI 센서에 미친 영향: 고 대호, 심 은섭, 용 상순, 연 정흠, 김 성희(한국항공우주연구원)
- Lp-III-004\* Study of the Correlation of Ultra-High Energy Cosmic Rays with Active Galactic Nuclei: KIM Hang Bae, CHEON ByungGu, KIM Jihyun, CHO Eunjung, SHIN Bokkyun(한양대)
- Lp-III-005 남쪽왕관자리 R CrA IRS 5b 원시성 자기권의 전파편광 관측: 최 민호(한국천문연구원), 이 정은(세종대)
- Lp-III-006 Geant4 Simulation for X-ray Detector coupled with Irregular Radiator: KIM Kyung Sook, LEE Manwoo, KIM Guinyun(Department of Physics, Kyungpook National University), COMMICHAU Volker, VON GUNTEN Hanspeter, LUSTERMAN W., ROESER Ulf, HERMANN P., VIETTEL Gert M.(ETH Zurich, Labor fuer Hochenergiephysik)
- Lp-III-007\* Status of Xe/YAP PMT calibration for Telescope Array cosmic ray experiment: CHO E.J., SHIN B.K., KIM J.H., CHEON B.G., KIM H.B.(Hanyang University, Department of Physics)
- Lp-III-008 Cyg X-3 during its Multiple Jet Ejections: KIM Soon-Wook(Korea Astronomy and Space Science Institute)
- Lp-III-009 Improved Results of Maser Activity in W75N: KIM Jeong-Sook(Korea Astronomy and Space Science Institute & Kyunghee University), KIM Soon-Wook(Korea Astronomy and Space Science Institute)

P3

포  
스  
터  
세  
션

10월 23일(금) 10:00 - 12:00

- Cp-IV-001 A Study of Exotic Nuclear Structure by the Deformed BCS and RPA: HA Eunja, CHEOUN Myung-Ki(Soongsil Univ.), KIM Kyungsik(Korea Aviation Univ.)
- Cp-IV-002\* Measurement of Elliptic flow at CMS: CHOI Minkyoo, PARK Inkyu, PARK Sangnam, KANG Seokon, KIM Hyunyoung, RYU Geonmo(서울시립대), 김 재호, 송 상현(전남대 물리학과)
- Cp-IV-003 Identification of Neutron Capture Resonance Energy of  $^{169}\text{Tm}$  by Using 46-MeV Electron Linear Accelerator, BGO Prompt Gamma Ray Spectrometer and TOF method: LEE Samyol(Department of Radiological Science, Nambu University)
- Cp-IV-004 The Production of micromodules for PHENIX FOCAL Beam Test: 김 현주, 강 주환, 권 영일, 임 상훈, 송 명근(연세대), 심 광숙, 홍 병식, 주 은아(고려대), 주 관식, 문 혜진(명지대), 한 인식, 박 일홍, 이 직, 이 혜영(이화여대), 김 은주, 이 순례(전북대)
- Cp-IV-005 Empirical formula applied to the lowest excitation energies of the unnatural parity states in even-even nuclei: KIM Dooyoung, YOON Jin-Hee, CHA Dongwoo(Department of Physics, Inha University)
- Cp-IV-006 Jet Energy Corrections of L2 and L3 at CMS(LHC) in Heavy Ion physics: 강 서곤, 박 인규, 박 상남, 최 민규, 김 현용, 류 건모(서울시립대), 김 재호, 송 상현(전남대), 장 성현(경북대)
- Cp-IV-007 Thermal quenching on the initial rise method in RTL quartz: HONG Duk-Geun(Department of Physics, Kangwon National University), KIM Ki-Bum(Cyclotron Research Institute, Kangwon National University)
- Cp-IV-008 Radiocarbon Dating of Korean Wooden Statues Using Wiggle Matching Method: 박 규준(한국기초과학지원연구원), 정 민선, 백 승이(서울대), 박 원규(충북대), 최 선일(문화재청 인천국제공항 문화재감정관실), 김 요정(충북대)
- Cp-IV-009\* Test Simulation For Low Energy Gamma Source Using Monte Carlo Method: SHIN JaeWon(Department of Physics, Sungkyunkwan University), LEE Chung-Il(Department of Biomedical Engineering, College of Medicine), HONG Seung-Woo(Department of Physics, Sungkyunkwan University), SUH Tae-Suk(Department of Biomedical Engineering, College of Medicine)
- Cp-IV-010 Monte Carlo Study : Changes In Dose Distributions Due To The Induced Magnetic Fields For The  $^{60}\text{Co}$  Therapy Unit: SHIN JaeWon(Department of Physics, Sungkyunkwan University), LEE Chung-Il(Department of Biomedical Engineering, College of Medicine), HONG Seung-Woo(Department of Physics, Sungkyunkwan University), SUH Tae-Suk(Department of Biomedical Engineering, College of Medicine)
- Cp-IV-011 Elastic Scattering of 120-MeV Alpha Particles by  $^{28}\text{Si}$ : KWON Young Kwan, LEE Chung Sik(Department of Physics, Chung-Ang University), KUBONO Shigeru(Center for Nuclear Study(CNS), University of Tokyo)
- Cp-IV-012 Effect of Coulomb distortion for Charged Neutrino-nucleus Scattering: KIM Kyungsik(한국항공대), CHEOUN MyungKi(송실대)
- Cp-IV-013 Proton Beam Energy Determination through a Range Measurement Device for Incident Charged Particles: PARK Yeun-Soo, YANG Tae-Keun, KIM Jae-Hong, HWANG Won-Taek, CHO Sung-Jin(Department of Radiation Physical Engineering Research, Korea Institute of Radiological and Medical Sciences)
- Cp-IV-014 Neutron Capture Cross-section Measurements of  $^{57}\text{Fe}$  In The Neutron Energy at 550 keV: JUNG HOON, KIM Gwon Jung, KANG Yeong-Rok, RO Tae-Ik(Dong-A University), KIM Guinyun, LEE Man Woo, WANG Taofeng(Kyungpook National University), LEE Jong Hwan(Donggeui University), IGASHIRA Masayuki, KATABUDNI Tatsuya(Tokyo Institute of Technology)
- Cp-IV-015 Neutron Capture Yield measurements of 155,156,157,158,160Gd: KANG YEONG-ROK, RO TAE-IK(Dong-A University), CHUNG WON-CHUNG(Hangyang University), KIM GUINYUN(Kyungpook National University), R.C Block, Y. Danon, D.P Barry(Rensselaer Polytechnic Institute)
- Cp-IV-016 Measurement of Neutron Capture Cross-Section of  $^{56}\text{Fe}$  in The Neutron Energy at 550 keV: KIM Gwon Jung, JUNG HOON, KANG Yeong-Rok, YOON Jung-Ran, RO Tae-Ik(Dong-A University), KIM Guinyun, LEE Man Woo, WANG Taofeng(Kyungpook National University), IGASHIRA Masayuki(Tokyo Institute of Technology)
- Cp-IV-017 액티나이드 핵종에 대한 중성자 입사 핵분열 단면적 평가: 김 형일, 이 영욱(한국원자력연구원)
- Cp-IV-018 Measurement of Activation Cross-sections for the  $^{nat}\text{Pd}(p,x)$  processes upto 40 MeV: KHANDAKER M.U., KIM K., KIM K.S., LEE M.W.(Department of Physics, Kyungpook National University), CHO Y.S., LEE Y.O.(Nuclear Data Evaluation Laboratory, Korea Atomic Energy Research Institute), KIM G.N.(Department of Physics, Kyungpook National University)
- Cp-IV-019 1 MeV 영역 중성자에 대한  $^{nat}\text{Bi}$ ,  $^{nat}\text{Ta}$ 의 (n,tot) 반응단면적 측정: 양 태진(한국원자력의학원, 방사선물리공학연구부), 이 삼열(남부대 방사선학과), 김 기동(한국지질자원연구원, 지질자원특성분석센터)
- Cp-IV-020 Threshold Anomaly for  $^6\text{Li}+^{90}\text{Zr}$  system: 소 윤영(강원대)
- Cp-IV-021 Measurement of (n,tot) Cross Section of Natural Cobalt and Niobium in the Neighborhoods of 1 MeV by Using 2.94 MeV

Proton Tandem Accelerator: LEE Samyol(Department of Radiological Science, Nambu University), YANG Tae-gun (Laboratory of Accelerator Application Development, Korea Institute of), KIM Gidong(Ion Beam Application Group, Korea Institute of Geoscience and Mineral)

- Cp-IV-022 Offline Data Analysis Of PHENIX FOCAL Beam Test At CERN: 임 상훈, 강 주환, 권 영일, 김 현주, 송 명근(연세대), 심 광숙, 홍 병식, 주 은아(고려대), 주 관식, 문 혜진(명지대), 한 인식, 박 일홍, 이 직, 이 혜영(이화여대), 김 은주, 이 순례(전북대)
- Cp-IV-023\* Chemical freeze-out from an expanding fireball: CHOI Suk, CHOI Jung Ok, LEE Kang Seog(Chonnam National University)
- Cp-IV-024 Activation cross-sections of alpha and deuteron induced nuclear reactions on iron upto 40 MeV: KIM Kwangsoo(Department of Physics, Kyungpook National University), KHANDAKER M.U.(Nuclear Data Evaluation Lab., Korea Atomic Energy Research Institute), KIM Kyung-Sook, LEE Manwoo(Department of Physics, Kyungpook National University), CHO Y-S., LEE Y-O.(Nuclear Data Evaluation Lab., Korea Atomic Energy Research Institute), KIM Guinyun(Department of Physics, Kyungpook National University)
- Cp-IV-025 PHITS code를 사용하여 증이온 빔 조사에 따른 표적의 residuals 계산 및 특성 평가: 양 성철, 김 귀년(경북대), 이 영옥, 이 철우(한국원자력연구원)
- Cp-IV-026 45 MeV 양성자 빔 조사와 이차적인 중성자에 의한 방사화 연구: 나 세진, 정 명환, 김 계령(한국원자력연구원), 양 태건(한국원자력의학원)
- Cp-IV-027 Measurement of Total Cross Section of Ho: 박 세환, 송 태영, 이 영옥(한국원자력연구원), 오 영도(경북대)
- Cp-IV-028 AMS를 이용한  $^{13}\text{C}(n,\gamma)^{14}\text{C}$  핵반응 단면적 측정: 박 중현, 김 기동, 홍 완(한국지질자원연구원)
- Cp-IV-029 1 MeV 근방의 중성자 에너지에 대한  $^{nat}\text{Fe}$ ,  $^{nat}\text{Ti}$ ,  $^{nat}\text{Cu}$ 의 중성자 전단면적 측정: 김 기동, 우 형주, 김 준곤, 최 한우, 홍 완, 박 중현, 음 철현(한국지질자원연구원), 이 영옥(한국원자력연구소)
- Cp-IV-030 QRPA 모델에 의한 중성미자-원자핵 반응단면적의 계산: CHEOUN Myung-Ki, 하 은자(Soongsil Univ.), 김 경식(한국항공대)
- Cp-IV-031 Gas Mixture Dependence of the Performance for the Multi-gap Timing Resistive Plate Chambers: 조 미희(고려대), 유 민상(한국원자력연구원), 홍 병식, 이 경세(고려대)
- Cp-IV-032\* Development of a Beam-imaging Detector for Proton Radiography: 주 은아, 홍 병식, 정 민수, 이 경세, 문 봉선, 박 성근, 심 광숙(고려대)
- Cp-IV-033 비행시간측정법을 이용한 하나로 냉중성자 유도관의 중성자 분포 측정: 문 명국, 이 승욱, 유 민상, 전 영규(한국원자력연구원)
- Cp-IV-034 CNU-GEM 검출기를 이용한 방사선 영상측정 장치의 개발과정: 안 봉재, 하 영자(창원대), 박 성태(University of Texas Arlington), 한 창희(창원대)
- Cp-IV-035 실리콘 광 센서의 제작 및 특성 평가: 가 동하, 김 현옥, 김 홍주, 박 환배, 배 재범, 소 증호, 황 용석, 현 효정(경북대)
- Cp-IV-036 중양자 빔 변형 시스템의 설계: 김 기동, 홍 완, 박 일용(한국지질자원연구원), 김 용균(한양대), 양 태건(한국원자력의학원), 이 삼열(남부대)
- Cp-IV-037 Performance of Silicon Pad Sensors from Beam Tests for PHENIX FORWARD Calorimeter: 이 순례, 김 은주(전북대), 심 광숙, 홍 병식, 주 은아(고려대), 주 관식, 문 혜진(명지대), 강 주환, 권 영일, 김 현주, 송 명근, 임 상훈(연세대), 한 인식, 박 일홍, 이 직, 이 혜영(이화여대)
- Cp-IV-038 DAQ System for Neutron Time-Of-Flight Experiment based on FADC: LEE MANWOO, KIM KYUNGSOOK, KIM GUINYUN(Department of Physics, Kyungpook National University), SKOY VADIM(Joint Institute for Nuclear Research, Russia), NAMKUNG WON(Department of Physics, Pohang University of Science and Technology), EUNCHAN KIM, WOORYOUNG JANG(Department of Physics, Kyungpook National University)
- Cp-IV-039\* Cryogenic Alpha Spectrometers for Extreme Energy Resolution: 김 일환(대전대), 김 용합(한국표준과학연구원), 송 인걸(대전대), 이 경범, 이 민규(한국표준과학연구원), 이 상준(서울대), 이 화용(한국표준과학연구원), 장 용식(경북대)
- Cp-IV-040\* The Development of the Bunch Length Detector (BLD): KIM Joon Yeon, KIM Do Gyun, BHANG Hyoung Chan(Seoul National University, Department of Physics & Astronomy), KIM Jong Won(National Cancer Center), YUN Chong Chul (Chung-Ang University)
- Cp-IV-041\* Development of Cryogenic Neutron Detectors: 장 용식(한국표준과학연구원, 경북대), 김 용합, 김 일환, 이 경범, 이 민규, 이 상준, 이 화용(한국표준과학연구원), 이 형철(경북대)
- Cp-IV-042 Buffer layer 전극을 이용한 CdZnTe 검출기의 성능에 대한 연구: 조 윤호, 박 세환, 이 재형, 하 장호(한국원자력연구원), 김 용균(한양대)
- Cp-IV-043\* 고압 세는 챔버 제작 및 선형성 평가: 이 철호, 강 병휘, 김 용균, 박 병현, 장 도윤(한양대), 김 한수, 박 세환(한국원자력연구원)
- Cp-IV-044 Neutron Production of Electron Accelerator-based Neutron Source: SONG Tae-Yung, PARK Se-Hwan, LEE Byung Cheol, LEE Young Ouk(Korea Atomic Energy Research Institute)

Cp-IV-045 Simulation Study for low energy RI beam from CRIB: YUN Chong Cheoul, LEE Chun Sik, MOON Jun Young, KWON Young Kwan(Department of Physics, Chung Ang University)

■SESSION P4■

통계물리학과회 포스터 발표

장 소 : 포스터 발표장

10월 23일(금) 10:00 - 12:00

- Fp-IV-001 일차원 양자계의 에너지 갭에 대한 연구: 박 태영, 이 용철, 이 지우, 최 영진(명지대)
- Fp-IV-002 Multiple fragmentation of critical continuum percolation clusters: LEE Changhan, LEE Sang Bub(Kyungpook National University, Department of Physics)
- Fp-IV-003 Influence of quenched disorder on the critical behavior of absorbing phase transitions in conserved lattice gas model: LEE Changhan, LEE Sang Bub(Kyungpook National University, Department of Physics)
- Fp-IV-004 Continuum Percolation Under Achlioptas Type Process: 윤 여광, 육 순형, 김 엽(경희대)
- Fp-IV-005 Random disposition with relaxation model on a fractal substrate: KIM DAE HO, KIM JIN MIN(숭실대)
- Fp-IV-006 Conserved-Mass Aggregation Model with Mass Repulsion: CHOI Woosik, KWON Sungchul, KIM Yup(경희대)
- Fp-IV-007\* Generalized restricted curvature model on fractal substrate: 장 원우, 김 진민(숭실대)
- Fp-IV-008\* 으뜸방정식을 통한 비스듬 분포의 떠오름: 최 무영, 고 세진, 권 현웅(서울대)
- Fp-IV-009 Symmetry Effects on Dynamics of Coupled Pitchfork Systems: 김 영태, 김 재석(아주대, 물리학과)
- Fp-IV-010 Phase synchronization in a diode laser pumped Nd:YAG laser coupled with a chaotic oscillator: LEE Dae-Sic, KIM Guang-Hoon, KANG Uk(KERI, SOI-KOREA Center), KIM Chil-Min(Sogang University, Department of Physics)
- Fp-IV-011 Surface Transformations of Hydrogen-Bonded Crystals at High Temperatures as Complex Phenomena and Topochemical Nature: LEE Kwang-Sei(Inje University, Department of Nano Systems Engineering)
- Fp-IV-012 Dynamical Behaviors of Rainfall Analyses in Korean Cities: 김 경식, 이 동인(부경대), 김 수용(한국과학기술원)
- Fp-IV-013 Random Walk을 이용한 Community 검색: 한 범희, 김 엽, 육 순형(경희대 물리학과)
- Fp-IV-014\* Wealth Dynamics in the World Trade Network: 차 문용, 이 덕선, 이 재우(인하대)
- Fp-IV-015 Modularity and Community Structure in Directed Networks: KIM Youngdo, SON Seung-Woo, JEONG Hawoong(물리학과, KAIST)
- Fp-IV-016\* Ising Model Study on Fractal and Non-Fractal Complex Networks: CHOI Chulho, KAHNG Byungnam, KIM Doochul(Department of Physics and Astronomy, Seoul National University)
- Fp-IV-017 Fractal Structure in Protein Interaction Network: KIM Purin, KAHNG Byoungnam, KIM Doochul(서울대)
- Fp-IV-018 Evolution of Real World Networks: LEE Deokjae(Seoul National University), GOH Kwang-il(Korea University), KAHNG Byungnam, KIM Doochul(Seoul National University)
- Fp-IV-019 Structure of Bipartite Ecological Networks: 맹 성은, 이 덕선, 이 재우(인하대)
- Fp-IV-020\* Tracing dynamic network of thalamocortical circuit with symbolic representation: SHIN Jeongkyu(Nonlinear and Complex System Lab., Pohang University of Science and Technology), HWANG Eunjin(Nonlinear and Complex System Lab., Pohang University of Science and Technology and Center for Neuroscience, Korea Institute of Science and Technology), CHOI Jee Hyun(Center for Neuroscience, Korea Institute of Science and Technology), KIM Seunghwan(Nonlinear and Complex System Lab., Pohang University of Science and Technology and Asia Pacific Center for Theoretical Physics)
- Fp-IV-021\* Giant Unilamellar Vesicles by Spin-Coating Electroformation and Electro-Osmotic Effect: 박 혁규, 김 성진(부산대)
- Fp-IV-022 진동하는 고체/액체 계면에서의 전기이중층과 계면에너지 연구: 문 종균, 박 혁규(부산대)
- Fp-IV-023 Thermal random circuit breaker network model : Effects of Joule heatings on the unipolar resistance switching: 이 재성, 채 승철, 이 신범, 장 서형(서울대), LIU Chunli(HUFS), 강 병남, 노 태원(서울대)
- Fp-IV-024 확산하는 자원 공급이 있는 2차원 평면에서 개체 증식: 홍 상신, 석 진호, 원 창연(경희대)
- Fp-IV-025\* Orientational Ordering of Quantum Quadrupolar Rotors: Path-integral Monte Carlo Study with Extrapolated High-order Propagators: 권 용경, 신 현덕, 박 성진(건국대)
- Fp-IV-026 Molecular dynamics study of atom-cluster or cluster-cluster collisions: KIM Do-Hyun(Kyonggi Univ.), LEE Min-ho(Kyonggi Univ.), KIM Sangrak(Kyonggi Univ.), CHOI Je-Young(Youngdong Univ.)
- Fp-IV-027 NMR Structure Determination by Conformational Space Annealing: LEE Jinhyuk(고등과학원, 계산과학부), LEE Jinwoo(광운대, 수학과), LEE Jooyoung(고등과학원, 계산과학부)

P4

포  
스  
터  
세  
션

10월 23일(금) 10:30 - 12:00

- Hp-IV-046 Bending magnetic field effect on ECI at KEKB LER: JIN Hyunchang, YOON Moohyun(POSTECH)
- Hp-IV-047 Effects of resistive wall impedance in the PLS-II: 이 수연, 황 지광, 김 혜진, 김 은산(경북대)
- Hp-IV-048 PEFP RCS에서의 빔 콜리메이션: 장 지호, 조 용섭, 권 혁중(PEFP/KAERI), 이 용영(BNL)
- Hp-IV-049 Undulator Tolerance Study for the 0.1nm PAL XFEL: LEE Jae yu, YOON Moohyun(POSTECH 물리학과)
- Hp-IV-050 PLS - II의 삽입장치의 영향과 동력학적 구경(dynamic aperture): 김 정기(포항공대), 신 승환(포항가속기연구소), 윤 무현(포항공대)
- Hp-IV-051 Lattice Design of the Linac and BTL for PLS2: 김 문경(포항공대 가속기연구소)
- Hp-IV-052 Nonlinear behavior of electron orbits in a two-frequency wiggler with self-generated fields: NAM Soon-Kwon(Department of Physics, Kangwon National University), KIM Ki-Bum(Cyclotron Research Institute, Kangwon National University)
- Hp-IV-053 Effects of Electron Beam Parameters in a Free Electron Laser Oscillator with a Short Undulator: NAM Soon-Kwon, JULIUS Nfor(Department of Physics, Kangwon National University), KIM Ki-Bum(Cyclotron Research Institute, Kangwon National University)
- Hp-IV-054 RCS의 육극 전자석에 의한 비선형 빔 동력학 연구: 장 시원(경북대)
- Hp-IV-055\* Formation of a Relativistic Electron Mirror by the Interaction of an Intense Laser Pulse with Two Nanofolios: NAM Inhyuk (GIST, Graduate Program of Photon Science and Technology), VICTOR V. Kulagin(Advanced Photonics Research Institute), SUK Hyyong(GIST, Graduate Program of Photon Science and Technology)
- Hp-IV-056 Status of the PLS Diagnostic Beamline: 김 창범, 김 승남, 김 명진, 김 희섭, 류 춘길, 박 종도, 이 채순, 이 해철, 홍 만수 (포항가속기연구소)
- Hp-IV-057 중간 에너지 양성자 빔이 두꺼운 C, Al, Fe 표적과 충돌하여 생성된 중성자 생성물의 계산(Yield Calculations of the Neutron Produced by Intermediate Energy Proton Beam with Thick C, Al, Fe Targets): 오 주희, 박 수열, 고 승국(울산대), 이 희석 (포항공대 포항가속기연구소)
- Hp-IV-058 PLS-II Lattice Design: 황 일문, 신 승환, 최 진혁, 김 문경, 김 창범, 박 성주, 김 경렬, 남 상훈(포항가속기연구소)
- Hp-IV-059 가속기 RF 제어시스템의 개선 및 PLS-II 성능향상을 위한 연구: 윤 종철, 박 홍집, 박 성주, 김 경렬(포항가속기연구소)
- Hp-IV-060 PAL HLS EPICS IOC 개발 및 Data Web Service: 김 재명, 최 효진, 이 은희, 김 지화, 강 홍식, 윤 종철, 이 진원, 박 성주(포항가속기연구소), 서 광원((주)SAE)
- Hp-IV-061 PLS Storage Ring Performance Improvement: 신 승환, 황 일문, 김 문경, 김 창범, 이 은희, 박 성주, 김 경렬, 남 상훈(포항가속기연구소, POSTECH)
- Hp-IV-062 포항가속기연구소에서의 Matlab Middle Layer: 이 은희, 신 승환, 이 진원, 김 재명, 박 성주, 김 경렬(포항가속기연구소)
- Hp-IV-063 INTENSE THz RADIATION GENERATION FROM A COMPACT ELECTRON LINAC: 강 홍식(포항가속기연구소)
- Hp-IV-064 램류어 탐침법을 이용한 2.45 GHz 전자 램돌이 공명 이온원의 플라스마 진단: 임 정환, 이 병섭, 박 진용, 박 규준, 이 효상, 김 종필, 원 미숙(한국기초과학지원연구원), 안 정근(부산대)
- Hp-IV-065 Beam Profile Measurement of the PEFP Proton Injector: 권 혁중, 김 한성, 김 대일, 장 지호, 조 용섭(한국원자력연구원)
- Hp-IV-066 Beam Induced Fluorescence monitor for proton beam profile measurement in KIRAMS-13: NAM Soon-Kwon, JULIUS Nfor (Department of Physics, Kangwon National University), KIM Ki-Bum(Cyclotron Research Institute, Kangwon National University)
- Hp-IV-067 Control of Spurious Harmonic Resonances in the PLS-II Storage Ring Vacuum Chamber: JOO Young-Do, PARK Sung-Ju, PARK Chong-Do, KIM Kyung-Ryul, NAM Sang-Hoon(Pohang Accelerator Laboratory, POSTECH)
- Hp-IV-068 PEFP 빔라인을 위한 고속단펄스(FCV)의 성능시험 연구: 이 화련, 박 범식, 홍 인석, 권 혁중, 조 용섭(한국원자력연구원)
- Hp-IV-069 PLS-II 전자총 진공이원화 제어시스템 설계 및 제작: 손 윤규, 황 일문, 박 용정, 김 승환, 박 성주, 김 경렬, 남 상훈(포항가속기연구소)
- Hp-IV-070 The Preliminary Design for LLRF System at PAL: 박 기현, 전 명환, 정 맹호, 손 영욱, 유 인하, 박 인수, 손 안, 강 홍식, 박 종도(포항가속기연구소)
- Hp-IV-071 Low Temperature Test of the PEFP Two-cell SRF Cavity: 김 한성, 권 혁중, 조 용섭(한국원자력연구원)
- Hp-IV-072 중이온 RFQ의 기초 설계 연구 중이온 RFQ의 기초 설계 연구: 조 용섭, 장 지호, 김 한성, 권 혁중(한국원자력연구원, 양성자기반공학기술개발사업단)
- Hp-IV-073 Spectroscopic Analysis of Helium or Hydrogen-filled Capillary Discharge Plasmas for Laser Wakefield Acceleration: OH Seong Yong(고등광기술연구소), KIM Min-Seok, NAM In Hyuk, THO Do Duy(광과학기술학제전공), SUK Hyyong(고등광기술연구소)
- Hp-IV-074 양성자가속기의 고주파 제어를 위한 IQ modulation 시스템 제작 및 시험: 설 경태, 권 혁중, 김 한성, 조 용섭(한국원자력

연구원)

- Hp-IV-075 Application of I/O Control Method based on Multitasking for the PEFP Vacuum Control System: SONG Young gi, AN Eun mi, LEE Hwa Ryun, HONG In seok, KWON Hyeok jung, CHO Yong sub(PEFP, KAERI)
- Hp-IV-076 PLS-II 열량에 대한 빔라인 냉각장치의 기본적 열해석: 길 계환, 최 재영(포항공대)
- Hp-IV-077 EPICS CA를 이용한 가속기 제어 신호 전송을 위한 데이터 포워딩 메커니즘의 구현: 안 은미, 송 영기, 조 용섭(한국원자력연구원 양성자기반공학기술개발사업단)
- Hp-IV-078 PLS-II 선형가속기 제어 시스템 개발: 김 지화, 김 재명, 김 성철, 윤 종철, 이 은희, 박 병률, 이 진원, 박 성주(포항가속기연구소)
- Hp-IV-079 PLS-II 전자석전원장치 시스템: 김 성철, 손 윤규, 박 종도, 김 경렬, 남 상훈(포항가속기연구소)
- Hp-IV-080 PLS-II 빔라인 프론트 엔드 layout: 김 승남, 김 명진, 김 희섭, 류 춘길, 이 채순, 서 인득(포항가속기연구소)
- Hp-IV-081 Temperature Control Test of the RCCS Pumping Skid for 20 MeV DTL: KIM Kyung Ryul, PARK Jun, KIM Hyung Gyun, KIM Hee Seob, YOON Chong Chul, KWON Sei Jin, SON Yoon Gyu(POSTECH, PAL), KWON Hyeok Jung, KIM Han Sung, CHO Yong Sub(KAERI, PEFP)
- Hp-IV-082 Beam Commissioning of L-band Intense Electron Accelerator for Irradiation Applications: 김 상훈, 양 해룡, 조 무현, 남궁 원(포항공대), 장 성덕(포항가속기연구소), 오 종석(국가핵융합연구소)
- Hp-IV-083 PLS-II 진공 챔버의 Eddy Current에 의한 Lorentz Force: 서 형석, 김 동연(POSTECH 포항가속기연구소)
- Hp-IV-084 Commissioning Status of C-band Standing-wave Accelerating Structure: 양 해룡, 김 상훈, 문 성익(포항공대), 김 승환, 박 용정, 박 성주(포항가속기연구소), 오 종석(국가핵융합연구소), 조 무현(포항공대), 남궁 원(포항가속기연구소)
- Hp-IV-085 발표 취소
- Hp-IV-086 Design of a High Pressure SF<sub>6</sub> Filled Spark Gap Switch for High Voltage Pulse Generator: RAHAMAN H., HEO H., PARK S.S., NAM S.H.(Pohang Accelerator Laboratory)
- Hp-IV-087\* Narrow band terahertz polarizer using the sub-wavelength rectangular hole array: 최 다혜, 박 건식(서울대)
- Hp-IV-088\* Terahertz Response Through Single Subwavelength Circular Hole: 권 오준, 최 다혜, 박 건식(서울대)

10월 23일(금) 13:00 - 15:00

- Dp-V-127 The Effects of Carbonaceous Impurity with Functional Group on the Oxidized SWCNTs: LEE Jung-Ah(KIST/고려대 물리학과), LEE Byung Chul, LEE Sang-Myung(KIST 나노바이오 연구센터), PAEK Kyeong-Kap(대진대 전자공학과), LEE Yun-Hi(고려대 물리학과), SHIN Hyun Joon(KIST 나노바이오 연구센터)
- Dp-V-128 Evaluating Adhesion of Carbon Nanotubes in Transparent Conducting Films: LEE Sang Won(BK21 Physics, Center for Nanotubes and Nanostructured Composites), YAN CUI(SKKU advanced Institute of Nanotechnology (SAINT)), CHO Young Woo(BK21 Physics, Center for Nanotubes and Nanostructured Composites), KIM Su Min(SKKU Advanced Institute of Nanotechnology (SAINT)), LEE Young Hee(BK21 Physics, Center for Nanotubes and Nanostructured Composites, SKKU Advanced Institute of Nanotechnology (SAINT), Sungkyunkwan University)
- Dp-V-129 Spin Stiffness Of Graphene And Zigzag Graphene Nanoribbon: MOON Kyungsun, RHIM Jun-Won(연세대)
- Dp-V-130 Synthesis of Large area Graphene by rapid-thermal low pressure CVD method: 이 종희, 김 윤중, 이 윤희(고려대)
- Dp-V-131 Vertically-aligned high quality ZnO nanorod growth on bufferlayers: KIM B.H., PARK C.I.(Department of Physics and Institute of Fusion Science, Chonbuk National University), KWAK C.H., SEO S.Y., KIM S.H.(Department of Materials Science and Engineering, Pohang University of Science and Technology), HAN S.W.(Division of Science Education, Institute of Fusion Science, and Institute of Science Education, Chonbuk National University)
- Dp-V-132 Transport properties of artificial bilayer graphene: KIM Youngwook(Department of Physics, Pohang University of Science and Technology), YUN Hyeol, LEE Jeong-Ah, JUNG Unseok, LEE Sangwook(Division of Quantum Phases & Devices, School of Physics, Konkuk University), KIM Dongchul, SEO Sunae(Samsung Advanced Institute of Technology), KIM Junsung(Department of Physics, Pohang University of Science and Technology)
- Dp-V-133 Sintering temperature effect and luminescence properties of  $\text{Eu}^{3+}:\text{Ca}_2\text{Gd}_3(\text{SiO}_4)_6\text{O}_2$  nanophosphors: GANJI Seeta RamaRaju, 정 홍채, 박 진영, 문 병기, 정 중현(부경대)
- Dp-V-134  $\text{WO}_3$ 에  $\text{CuO}$ 를 첨가한 후막 가스센서 특성: 신 덕진, 이 지영, 유 일, 이 돈규(동의대)
- Dp-V-135 Orientation-Dependent Structural Properties of  $\text{Zn}_{1-x}\text{Mg}_x\text{O}$  Nanorods Studied by Extended X-ray Absorption Fine Structure: EUN-SUK JEONG, CHANG-IN Park(Institute of Fusion Science, Institute of Science Education and Division of Science Education, Chonbuk National University), JINKYOUNG Yoo(National CRI Center for Semiconductor Nanorods, Department of Materials Science and Engineering, POSTECH), GYU-CHUL Yi(National CRI Center for Semiconductor Nanorods and Department of Physics, Seoul National University), SANG-WOOK Han(Institute of Fusion Science, Institute of Science Education and Division of Science Education, Chonbuk National University)
- Dp-V-136 마이크로웨이브 열처리에 의해 Ag-Cu 합금 박막 상에 형성된 탄소나노튜브 방출원의 전계 방출 특성: 권 영택, 이 승엽, 송 우석, 김 유석, 최 원철, 박 종윤(성균관대)
- Dp-V-137 Optical reflectometry for nanomechanical motion detection in suspended metal electromechanical resonator: 심 승보(한국표준과학연구원), 노 현호(서울대), 정 민경, 김 상균(한국표준과학연구원), 유 영동, 김 봉수(KAIST 화학과), 김 정구(서울대), 이 광철, 우 병철, 김 진희(한국표준과학연구원)
- Dp-V-138 그래핀 소자의 전자-포논 상호작용에 대한 전기장 효과: 김 윤중, 이 종희, 이 윤희(고려대)
- Dp-V-139 Crystal growth and luminescence properties of  $\text{Ce}^{3+}$  doped aluminum garnet nanocrystals: 정 홍채, 박 진영, GANJI Seeta RamaRaju, 문 병기, 정 중현(부경대)
- Dp-V-140 Luminescence properties of  $\text{Ce}^{3+}$  doped  $\text{Y}_3(\text{Sb}_x\text{Al}_{2-x})\text{Al}_3\text{O}_{12}$  and  $\text{Gd}_3(\text{Sb}_x\text{Ga}_{2-x})\text{Al}_3\text{O}_{12}$  yellow phosphors for WLED: 정 홍채, 박 진영, GANJI Seeta RamaRaju, 문 병기, 정 중현(부경대)
- Dp-V-141 Rf Coupling and Random Telegraphic Noise for SAW-Driven Single Electron Pump Device: SEO Minky(Pusan National University), KIM Nam, WOO Byung-chill, KIM Jinhee(KRISS), CHUNG Yunchul(Pusan National University)
- Dp-V-142 The T2-Weighted Magnetic Resonance Images by using Dextran- and Chitosan-Coated Ferrite Nanoparticle Contrast Agents: HONG Sungwook(Division of Science Education, Daegu University), CHANG Yongmin(Department of Diagnostic Radiology, College of Medicine, Kyungpook National University and Hospital), RHEE Ilsu(School of Physics and Energy Sciences, Kyungpook National University)
- Dp-V-143 Analysis of gallium oxide nuclei for  $\text{Ga}_2\text{O}_3$  nanowire grown by VS growth mechanism: 정 창희, 권 남오, 권 명희(인천대)
- Dp-V-144 Linear Prediction by Singular Value Decomposition on Coherent Lattice Vibrations in Small Diameter Single-Wall Carbon Nanotubes: 한 혜선, 한 현택(건국대, 신소재과학부 나노과학기술), 이 기주(충남대, 물리학과), 주 태하(포항공대, 화학과), J. Kono(Rice Univ.), 임 용식(건국대, 신소재과학부 나노과학기술)
- Dp-V-145 그래핀에서 일어나는 스핀 수송 특성: 엄 종화, 오 영만(세종대), 구 현철, 한 석희(한국과학기술연구원 스핀트로닉스연구단)
- Dp-V-146  $\text{CuO}$ 를 첨가한  $\text{SnO}_2$  후막가스 센서의 특성: 이 지영, 신 덕진, 이 돈규, 유 일(동의대)

- Dp-V-147 Effect of Hydrogen Plasma Treatment on a-IGZO Thin Film: KIM Won-Kyung(Dept. of Cogno Mechatronics, Pusan National University), LEE Seunghun(Dept. of Nano Fusion Technology, Pusan National University), KIM Taeyoung(Dept. of Nanomaterials Engineering, Pusan National University), JEONG Se-Young(Dept. of Nano Fusion Technology, Pusan National University)
- Dp-V-148 Oxygen plasma effects on the electrical properties of single-walled carbon nanotube bundles: 김 상훈, 김 호종(한국표준과학연구원), 이 형락(경북대), 송 정훈(공주대), 이 삼녕(한국해양대), 하 동한(한국표준과학연구원)
- Dp-V-149 Fabrication of turnstile pump using Ni nano-crystal as metallic island with Al as superconducting electrodes: 김 소라(한국표준과학연구원, 전략기술연구부), 김 범규(전북대), 김 진희, 우 병철, 김 남(한국표준과학연구원, 전략기술연구부)
- Dp-V-150 Inter-Wall Length Dependence of Double-Wall Carbon Nanotube Resonators: KANG JEONG WON(충주대)
- Dp-V-151\* Water-Assisted Synthesis of Vertically Aligned Carbon Nanotubes(VACNTs) with Sub-centimeter Height in Low Pressure Chemical Vapor Deposition(LPCVD): KIM sangyong, LEE soonil, KOH kenha(Division of Energy Systems Research, Ajou University)
- Dp-V-152\* 탄소 나노튜브를 이용한 단전자 펌프 소자 제작: 김 범규(전북대), 김 소라(한국표준과학연구원, 전략기술연구부), 김 주진(전북대), 김 남(한국표준과학연구원, 전략기술연구부)
- Dp-V-153\* Thermal Conductance Measurement of Metal-CNT Composites Using Micro-sized Suspended Structure: CHO Myung Rae, CHO Sung Un, PARK Yun Daniel(Department of Physics and Astronomy, Seoul National University)
- Dp-V-154\* Calcium-hydroxyl group complex for potential hydrogen storage media: A density functional theory study: CHA Moon-Hyun, NGUYEN Manh Cuong, LEE Yealee, BAE Jaehyun, IM Jino, PARK Changwon, KIM Youngkuk, CHOI Keunsu, KIM Gunn, IHM Jisoon(Department of Physics and Astronomy, Seoul National University)
- Dp-V-155\* C<sub>60</sub> 분자를 포함한 Polymethyl methacrylate 고분자 박막을 사용하여 제작한 비휘발성 메모리 소자: 윤 동열, 곽 진구, 정 재훈, 김 태환(한양대)
- Dp-V-156\* Spin-dependent transport on Graphene Nanoribbon with magnetic impurities: KIM kyung Yeon, CHOI Hyoung Joon(Department of Physics and IPAP, Yonsei University)
- Dp-V-157\* 단일벽 탄소나노튜브의 산 처리에 의한 특성 변화: 정 희성, 권 봉준, 권 향명, 임 종혁, 안 영환, 이 순일, 박 지용(아주대)
- Dp-V-158\* Alkali metal 흡착밀도에 따른 그래핀 특성변화: 진 경환, 최 선명, 지 승훈(포항공대 물리학과)
- Dp-V-159\* 라만 이미징 분광법을 통한 그래핀의 가장자리 형태 판별: 우 승우, 윤 두희, 문 혜림, 정 현식(서강대)
- Dp-V-160\* Study on Effect of Uniaxial Strain on Graphene by Raman Spectroscopy: YOON DUHEE, MOON HYERIM, WOO SEOUNGWOO(Department of Physics, Sogang University), SON YOUNG-WOO(Korea Institute for Advances Study), CHEONG HYEONSIK(Department of Physics, Sogang University)
- Dp-V-161\* SnO<sub>2</sub> 나노 입자를 포함한 Poly(methyl methacrylate)층을 사용하여 제작한 유기 쌍안정성 소자의 메모리 효과: 곽 진구, 윤 동열, 정 재훈, 이 대욱, 손 동익, 김 태환(한양대)
- Dp-V-162\* Dependence of Raman spectrum of graphene on excitation laser power: MOON Hyerim, YOON Duhee, WOO Seongwoo, CHEONG Hyeonsik(Department of Physics, Sogang University)
- Dp-V-163\* Synthesis, luminescence characteristics of Bi<sup>3+</sup> ions co-doped Gd<sub>2</sub>O<sub>3</sub>:Eu<sup>3+</sup> phosphors by solvothermal method: CHUNG Jong Won, JEONG Jung Hyun(Department of Physics, Pukyong National University), JANG Ki-wan, LEE Ho Sueb(Department of Physics, Changwon National University), YI Soung Soo(Department of Electronic Materials Engineering, Changwon National University)
- Dp-V-164\* Semi-metallic Kondo lattice observed in a single-crystalline Fe<sub>1-x</sub>Co<sub>x</sub>Si nanowire: 이 성훈(KAIST, KRISS), 인 준호(KAIST), 장 정원(KRISS), 서 관용(KAIST), 정 명화(Sogang University), 김 진희(KRISS), 김 봉수(KAIST)
- Dp-V-165\* Raman Mapping of Epitaxial Lateral Overgrown GaN: 송 지선, 김 진홍, 노 희석, 주 진우, 이 인환(전북대)
- Dp-V-166\* Electric-Field Effect and Transport Properties of Fe<sub>3</sub>O<sub>4</sub> Nanoparticle Compact: HER Eun Ju, BAE Yu Jeong, LEE Nyun Jong, AHN Jae Young(Department of Physics, Ewha Womans University), JANG Jung-tak, MOON Seung Ho, CHEON Jinwoo(Department of Chemistry, Yonsei University), KIM Tae Hee(Department of Physics, Ewha Womans University)
- Dp-V-167\* Manipulation of Graphene Using Nano Contact Transfer Technique: YUN Hoyeol, LEE Jeong-Ah, JUNG Unseok(Division of Quantum Phases & Devices, School of Physics, Konkuk University), KIM Dongchul, SEO Sunae(Samsung Advanced Institute of Technology), KIM Youngwook, KIM Junsung(Department of Physics, Pohang University of Science and Technology), KIM C, YOON S(Department of Physics, Ewha Womans University), KIM Hak-sung, LEE Jinkyung, LEE Sangwook(Division of Quantum Phases & Devices, School of Physics, Konkuk University)
- Dp-V-168\* 분산제 흡착에 따른 탄소나노튜브 네트워크 소자의 전기적 특성 변화 측정: 권 향명, 임 종혁, 정 희성, 권 봉준, 안 영환, 이 순일, 박 지용(아주대)
- Dp-V-169\* Raman scattering studies of SAM structure of 4-MPy molecules on ZnO nanorods: SHIN H.-Y.(Dept. of Physics and Dept. of Chemistry and Nano Science, Ewha Womans University), SHIM E. L.(Dept. of Physics, MyongJi University), CHOI Y. J.(Dept. of Physics and Dept. of Nano Science and Engineering, MyongJi University), PARK J. H.(Electronics and

Telecommunications Research Institute(ETRI)), YOON S.(Dept. of Physics and Dept. of Chemistry and Nano Science, Ewha Womans University)

- Dp-V-170\* 성장조건 변화에 따른 산화아연(ZnO) 나노선 소자의 특성 연구: 권 봉준, 정 희성, 권 향명, 안 영환, 이 순일, 박 지용(아주대)
- Dp-V-171\* 백색 유기발광소자의 색변환층으로 작동하는 적색 무기물 형광체의 구조적 및 광학적 성질: 정 환석, 안 성대, 추 동철, 김 태환(한양대), 박 정현, 권 명석(서울시립대)
- Dp-V-172\* Electrical characterization of SiC nano-crystals nonvolatile memory with various tunnel barrier: HAN Dong Seok, LEE Dong Uk, KIM Seon Pil, KIM Eun Kyu(Quantum-Function Spinics Laboratory and Department of Physics, Hanyang University), CHO Won-Ju(Department of Electronic Materials Engineering, Kwangwoon University)
- Dp-V-173\* Electrical property control of carbon nanotube conducting channel by metal over-layer deposition with different work functions: 이 아름, 김 효숙, 전 은경, 김 주진(전북대), 이 정오(한국화학연구원)
- Dp-V-174\* Study on Transport Properties of Silicon Nanowires: CHO Hwanwoong, LI Xianhong, BEAK Inbok, LEE Seongjae(Dept. of Physics, Hanyang University), YANG Jongheon, AHN Changgeun, PARK Chanwoo, SUNG Gunyong(Nano-Bio Electronic Devices Team, ETRI)
- Dp-V-175\* Facile Synthesis and Electrical Transport of Copper Vanadate Nanowires: SHAHID Muhammad, SHAKIR Imran, 장 아랑, 양 형우, 강 대준(BK21 Physics Research Division, Department of Energy Science, Institute of Basic Science, SKKU Advanced Institute of Nanotechnology and Center for Nanotubes and Nanostructured Composites, Sungkyunkwan University)
- Dp-V-176\* The Influence of Thermal Annealing on Volmer-Weber Type ZnO Nanorods via Photoluminescence and X-ray Photoelectron Spectroscopy: PARK Se-Jeong, HE Weizhen, HWANG Yoon-Hwae, KIM Hyung-Kook(부산대)
- Dp-V-177\* Thermodynamic temperature measurement from shot noise in a metal tunnel junction: 박 정환, REHMAN Mustaq(KRISS), 류 상완(전남대), 김 정구, 전 건상(서울대), 최 정숙, 송 윤, 정 연욱(KRISS)
- Dp-V-178\* The effect of carbon vacancies on the electrical properties of carbon nanotubes: LEE Alex Taekyung(Department of Physics, KAIST), KANG Yong-Ju(Samsung Elec. Co.), CHANG Kee Joo(Department of Physics, KAIST)
- Dp-V-179 발표 취소
- Dp-V-180 Piezoelectric properties in the  $(\text{Na}_{0.5}\text{K}_{0.47}\text{Li}_{0.03})(\text{Nb}_{0.8}\text{Ta}_{0.2})\text{O}_3$  ceramics prepared by a tape casting process: KANG Bo Ram, KIM Sin Woong, LEE Sung Chan, LEE Myang Hwan, SUNG Yeon Soo(School of Nano & Advanced Mat. Eng., Changwon Nat'l Univ.), CHO Jong Ho(Department of Physics, Pukyong Nat'l Univ.), KIM Myong-Ho, SONG Tae Kwon(School of Nano & Advanced Mat. Eng., Changwon Nat'l Univ.), KIM Sang Soo(Department of Physics, Changwon Nat'l Univ.), CHOI Byung Chun(Department of Physics, Pukyong Nat'l Univ.)
- Dp-V-181 Formation Of Fe Silicide Film On Si(111) 7×7 Surface: 김 효상, 신 선영, 엄 상훈, 성 시진, 정 진욱(POSTECH)
- Dp-V-182 Pulsed electro beam을 이용한 비정질 Si 박막의 결정화 연구: 고 락길, 장 세훈, 하 동우, 손 명환(한국전기연구원)
- Dp-V-183 Co/Au(001)에서의 자성과 궤도질서: 홍 순철, 김 태은, 윤 원석(울산대), 윤 석주(경상대)
- Dp-V-184 Ir(001) 위의 철 단층의 자성: 이 재일(인하대 물리학과), 김 동철(한라대)
- Dp-V-185 Growth and Electrical Characteristics of Carbon Films on ITO and Si Substrates: LEE Jong Duk, KIM Hyeon Soo, KIM Kun Ho, PARK Chang Young, LEE Jeoung Ju(Gyeongsang National University, Department of Physics)
- Dp-V-186 High-Temperature Phase Transformation in Ferroelastic  $(\text{NH}_4)_2\text{SO}_4$  and Topochemical Nature: LEE Kwang-Sei(Inje University, Department of Nano Systems Engineering), KIM Jae-Hyung(Inje University, School of Computer-Aided Science), OH In-Hwan(Korea Atomic Energy Research Institute, Neutron Science Division)
- Dp-V-187  $\text{Pt}_3\text{Fe}$  합금의 촉매적 특성 : 밀도 범함수 이론: 정 재훈, 권 오룡, 윤 원석, 홍 순철(울산대)
- Dp-V-188 Electronic Excitations at the Initial Stage of Graphitization of 6H-SiC(0001): 신 선영, 황 춘규, 엄 상훈, 김 효상, 성 시진, 이 팽로, 정 진욱(포항공대)
- Dp-V-189 Effects of  $\text{BaTiO}_3$  based-solid solutions with  $\text{SiO}_2$  and  $\text{Bi}_4\text{Ti}_3\text{O}_{12}$  on piezoelectric and dielectric properties: KIM Da Jeong, LEE Sung Chan, LEE Myang Hwan, KIM Myong-Ho, SUNG Yeon Soo, SONG Tae Kwon(School of Nano & Advanced Materials Engineering, Changwon National University), KIM Sang Soo(Department of Physics, Changwon National University), CHO Jong Ho, CHOI Byung Chun(Department of Physics, Pukyong National University)
- Dp-V-190 Optical properties of the  $\text{Sr}_2\text{SiO}_4:\text{Eu}^{2+}$  phosphor coated with  $\text{SiO}_2$  nano-particles: HAN Su Jin, LEE Sang Mok, SOHN Sang Ho(Kyungpook National University, Department of Physics)
- Dp-V-191 Error Analysis of Bistable Poisson States Using Periodic Measurements: LEE Jinwoo, LYO In-Whan(Dept. of Physics and IPAP, Yonsei University)
- Dp-V-192 각분해 광전자분광법을 이용한 준이차원  $\text{CeTe}_2$ 의 전자구조 연구: 김 대현, 이 현진, 이 선미, 이 민주, 강 정수(가톨릭대), 권 용성(성균관대), 이 한구, 김 형도(포항공속기연구소)
- Dp-V-193 Catalytic activity: Density-Functional Theory of  $\text{O}_2$  on Pt(111) surface: 권 오룡, 홍 순철(울산대)
- Dp-V-194 Molecular directionality change of rubbed polyimide(PI) films upon annealing condition: 김 기정(포항공속기연구소 빔라인

- 부), 곽 무선, 권 혁민, 이 상문, 이 철구(LG Display), 김 봉수(포항공속기연구소 빔라인부)
- Dp-V-195 Preparation and Photoluminescence Properties of Three-Dimensionally Ordered Macroporous  $\text{ZrO}_2: \text{Tb}^{3+}$  Films: QU Xuesong, YANG Hyun Kyoung, JEONG Jung Hyun(Department of Physics, Pukyong National University)
- Dp-V-196 Terahertz time-domain spectroscopy of Bi and  $\text{Bi}_2\text{Te}_3$  thin films: PARK Byung-cheol, KIM JaeHoon(Institute of Physics and Applied Physics, Yonsei University)
- Dp-V-197 Depolarization temperature and ferroelectric properties of BNT-BKT-BZ lead-free piezoelectric ceramics: PARK Jin Su, LEE Sung Chan, LEE Myang Hwan, SUNG Yeon Soo, KIM Myong-Ho, SONG Tae Kwon(School of Nano & Advanced Materials Engineering, Changwon National University), CHO Jong Ho, CHOI Byung Chun(Department of Physics, Pukyong National University)
- Dp-V-198 Pt(111) 표면 위에 증착된  $\text{NiO}/\text{Ni}_2\text{O}_3$  극초박막의 화학적 상태에 관한 연구: 한 동훈, 조 성국, 남 창우(한양대)
- Dp-V-199\* Order-disorder transition in Pt-Ni bimetallic nanocrystals: 서 옥균, 황 재성, 오 필건(광주과학기술원 신소재공학과), 강 현철(조선대), 노 도영(광주과학기술원 신소재공학과)
- Dp-V-200\* The electronic structure of oxygen-vacancy in  $\text{ZnO}/\text{HfO}_2$  interface structures: RYU Byungki, CHANG Kee Joo(Department of Physics, KAIST)
- Dp-V-201\* Ab Initio Study of Atomic Structure of Carbon Atoms Adsorbed on Cu(111) Surfaces: RYOU Junga, HONG Suklyun(Department of Physics and Institute of Fundamental Physics, Sejong University), HWANG Chanyong(Korea Research Institute of Standards and Science)
- Dp-V-202\* First-principles study of graphene on insulating substrates: CHOI Hyoung Joon, GOH Jung Suk(Department of Physics and IPAP, Yonsei University)
- Dp-V-203\* Optical Spectroscopic Investigation on the Electronic Structure of  $\text{LaVO}_3/\text{SrVO}_3$  Superlattices: JEONG Da Woon, CHOI Woo Seok(ReCOE, Department of Physics and Astronomy, Seoul National University), DAVID Adrian(Laboratoire CRISMAT, CNRS UMR 6508, ENSICAEN, France), LEE Yun Sang(Department of Physics, Soongsil University), PRELLIER Wilfrid(Laboratoire CRISMAT, CNRS UMR 6508, ENSICAEN, France), NOH Tae Won(ReCOE, Department of Physics and Astronomy, Seoul National University)
- Dp-V-204\* LOW LEAKAGE CURRENT AND ENHANCED FERROELECTRIC PROPERTIES OF Zn AND Mn CODOPED  $\text{BiFeO}_3$  THIN FILMS: LEE Myang Hwan, SONG Tae Kwon, LEE Sung Chan, KIM Myong Ho, SUNG Yeon Soo(School of Nano & Advanced Mat. Eng., Changwon Nat'l Univ.), CHO Jong Ho(Department of Physics, Changwon Nat'l Univ.), CHOI Byung Chun(Department of Physics, Pukyong Nat'l Univ.), KIM Sang Soo, DO Dal Hyun, KIM Won-Jeong(Research Institute of Basic Sciences, Changwon Nat'l Univ.)
- Dp-V-205\* Scanning Tunneling Microscopy of Methanol Adsorption on  $\text{NiAl}(110)$  and  $\text{Al}_2\text{O}_3/\text{NiAl}(110)$  Deposited by Pulsed Injection: CHOI Eunyeoung, LEE Younjoo, LYO In-Whan(Institute of Physics and Applied Physics(IPAP), Yonsei University)
- Dp-V-206\* Ab Initio Study on Structural and Electronic Properties of Interfaces between Metal and HAT-CN Molecule for OLED Applications: KIM Ji-Hoon, PARK Yongsup, KWON Young-Kyun(Department of Physics and Research Institute for Basic Sciences)
- Dp-V-207 발표 취소
- Dp-V-208\* Effect of Mg Cation Substitution on the Resistance Switching Behavior in Epitaxial  $\text{NiO}$  Films: KIM Hoonmin, LEE Seungran(Department of Physics and Astronomy and Center for Strongly Correlated Materials Research, Seoul National University), PARK Junghun(Samsung Electronics), CHO Myungrae, PARK Daniel Yun(Department of Physics and Astronomy, Seoul National University), CHAR Kookrin(Department of Physics and Astronomy and Center for Strongly Correlated Materials Research, Seoul National University)
- Dp-V-209\* Study of chromium doped  $\text{SrTiO}_3$  and  $\text{SrZrO}_3$  system: CHO Suyeon, PARK Wongoo, OH S.-J.(Department of Physics and Astronomy, Seoul National University)
- Dp-V-210\* Dehydrogenation of Graphane Using the Current Induced Cleaning Technique in UHV System: CHO Doohee, KIM Minseong, LYO In-Whan(Department of Physics, Yonsei Univ.)
- Dp-V-211 Charge distribution of O-H...O bonds in proton irradiated  $\text{KH}_2\text{PO}_4$  ferroelectrics: KIM Se-Hun(Faculty of Science Education, Jeju National University), HAN Doug Young(Nano-Bio Team, Korea Basic Science Institute), CHAE S. A.(Korea Basic Science Institute), HAN J. H., LEE Cheol Eui(Department of Physics and Institute for Nano Science, Korea University)
- Dp-V-212 Single-molecule fluorescence study of recombination protein-DNA interactions: 김 철희, 김 승현, 전 효은, 이 남기(포항공대 물리학과)
- Dp-V-213 Transport in Armchair Graphene Nanoribbons Modulated by Magnetic Barriers: MYOUNG Nojoon, IHM Gukhyung(Department of Physics, Chungnam National University)
- Dp-V-214 정공저지층과 전자저지층 역할을 하는 이중발광층을 사용한 청색 유기발광소자의 색순도 향상 메커니즘: 서 수열, 방 현성, 추 동철, 김 태환(한양대), 서 지현, 김 영관(홍익대)

- Dp-V-215\* The study of kinetics of membrane protein into lipid bilayer: LEE Hyunwon, SONG Sanghoon, CHA Wonsuk, CHOI Ahreum, JUNG Kwanghwan, KIM Hyunjung(서강대)
- Dp-V-216\* Single-molecule Fluorescence Study on the DNA Bending: 김 재열, 안 태기, 이 남기(포항공대, 물리학과)
- Dp-V-217\* Enhancement of frequency selectivity of sound sensor in water inspired auditory hair cell: KIM Hyery, SONG Taegeun, PARK Hee Chul, PARK Ikgon, KIM Hanna, PARK Ji Eun, AHN Kang-Hun(Department of Physics, Chungnam National University)
- Dp-V-218\* Temperature- and Concentration- dependence of Lipid Multilayer Formation by X-ray reflectivity: SHIN Kwangwoo, SONG Sanghoon, KIM Hyunjung(Sogang University, Department of Physics & Interdisciplinary Program of Integrated Biotechnology)
- Dp-V-219\* Proton-Irradiation effects on the resistance of highly-oriented pyrolytic graphite: LEE Cheol Eui(Korea University, Physics), KIM Jin Soo, LEE Kyu Won(Korea University, Physics)
- Dp-V-220\* Cesium Fluoride/C60 이중 전자주입층을 이용해 전자주입효율을 향상한 고효율 녹색유기발광소자: 양 지성, 추 동철, 김 태환(한양대), 진 유영, 서 지현, 김 영관(홍익대)
- Dp-V-221\* Ag 나노입자가 분산된 Polymethyl methacrylate 박막을 플로팅 게이트로 사용하는 비휘발성 메모리 소자의 전기적 성질: 김 원태, 박 진구, 윤 동열, 정 재훈, 김 태환(한양대)
- Dp-V-222\* 요오드 도핑에 의한 유기반도체 Tetramethyletetrathiafulvalene(TMTSF)의 광학적 특성 변화: 윤 미라, 이 인재(전북대)
- Dp-V-223\* Spectroscopic study of Proton-irradiated PCBM: LEE cheol eui, KIM hyojung, LEE Kyu Won(고려대)

## ■SESSION P5■

## 응용물리학과회 포스터 발표

장 소 : 포스터 발표장

10월 23일(금) 13:00 – 15:00

- Ep-V-103\* Giant Diamagnetic Properties of Half-metallic Thin Films: EOM T. W.(q-Psi and Department of Physics, Hanyang University), KIM K. W.(Department of Information Display, Sunmoon University), RHEE J. Y.(Department of Physics, Sungkyunkwan University), KUDRYAVTSEV Y. V., PROKHOROV V. G.(Institute for Metal Physics, National Academy of Sciences of Ukraine), LEE Y. P.(q-Psi and Department of Physics, Hanyang University)
- Ep-V-104\* Anomalous Magneto-transport Properties of Two-dimensional Ni/Co Anti-dot Arrays: KIM G. H., NAM W. C., SEO M. S., LEE S. J., LEE Y. P.(Quantum Potonic Science Research Center, Hanyang University), RHEE J. Y.(Quantum Potonic Department of Physics, Sungkyunkwan University), KIM K. W.(Department of Physics, Sunmoon University)
- Ep-V-105 Intrinsic Ferromagnetism Of Pure ZnO Film: D. F. Wang, V. T. T. Thuy, G. H. Kim, T. U. Um, Y. P. Lee(q-Psi and Department of Physics, Hanyang University)
- Ep-V-106 Er이 첨가된 tungsten-tellurite 유리의 upconversion 형광특성: 김 중환(동의대 물리학과), 최 혜영(부경대 물리학과), 노 현미, 양 진복, 박 경락(동의대 물리학과), 정 중현, 문 병기(부경대 물리학과)
- Ep-V-107 Transient Current Measurements of PEDOT:PSS and EG-PEDOT:PSS films: LEE Jung-Keun, HAMZA Ammar(Department of Physics, Chonbuk National University)
- Ep-V-108 용매에 녹는 Alq3유도체를 사용한 OLED소자의 발광특성: 김 형욱, 조 성윤, 이 순일, 고 근하(아주대)
- Ep-V-109\* 전도성 고분자 물질의 특성과 유기 태양전지의 효율에 미치는 영향: 조 성윤, 임 종혁, 김 형욱, 고 근하, 이 순일(아주대)
- Ep-V-110 분무열분해법으로 성장된 CdO:Cu 박막의 구조와 광학적 전기적 특성: 서 동주, 김 지효, 김 고은, 이 소리, 박 정복, 김 나리, 오 상미(조선대), 김 진호(경상대)
- Ep-V-111 Displacement Currents from a Capacitor Structure with Poly-4-vinylphenol (PVP) Dielectrics: HAMZA Ammar, LEE Jung-Keun(Department of Physics, Chonbuk National University)
- Ep-V-112 Soft-Baking 시간 변화에 따른 PMMA 박막의 물성 연구: 김 수인, 김 용석, 원 상연, 김 동년, 한 재현, 이 창우(국민대)
- Ep-V-113\* Non-Radiative Energy Transfer in Inorganic-Organic Heterostructures: LEE Cheol Eui, PARK Jun Kue, KIM Hyo Jung, LEE Kyu Won(고려대)
- Ep-V-114\* Co-sputtering 법으로 제작된 CuInSe<sub>2</sub> 박막형 태양전지의 후열처리 효과: 김 지환, 김 해진, 김 동영, 이 혜지, 손 선영, 김 화민(대구가톨릭대)
- Ep-V-115 나노 스케일 박막의 XRR 두께 측정 및 불확도 분석: 유 병윤, 박 재환, 빈 석민, 김 창수(한국표준과학연구원), 오 병성(충남대), 최 용대(목원대)
- Ep-V-116 IBSD 박막증착과 물성평가: 유 병윤, 박 재환, 빈 석민, 김 창수(한국표준과학연구원), 오 병성(충남대), 최 용대(목원대)
- Ep-V-117 Surface Analysis and Photoluminescent Properties of Lithium Incorporated Y<sub>2</sub>O<sub>3</sub>:Eu<sup>3+</sup> Thin Film Phosphor Grown on Si (100) Substrate using PLD method: 배 종성, 홍 태은, 김 종필(한국기초과학지원연구원, 부산센터), 박 성균(부산대), 정 중현(부경대)
- Ep-V-118 열-반사율법에 의한 고열전도도 박막의 열전도도 측정: 오 은지, 김 인구, 김 용수, 김 석원(울산대)

- Ep-V-119 Cr/Zn 이중 금속박막의 제조 및 접합 특성에 관한 연구: 강 상백, 김 송희, 채 영안, 윤 창선(군산대), 이 기진(서강대), 김 진태(한국표준과학연구원), 차 덕준(군산대)
- Ep-V-120\* Large scale patterning of ultra thin film graphite oxide on the Si/SiO<sub>2</sub> substrate by UV photolithography for four terminal measurements: LEE In-Yeal(School of Electrical and Electronic Engineering Sungkyunkwan University), KANNAN E S, KIM Gil-Ho(School of Information and Communication Engineering, Sungkyunkwan University)
- Ep-V-121\* L<sub>10</sub>-FePt 박막의 제작과 구조 및 자성 연구: 김 승호, 이 재용(연세대), 송 종한(한국과학기술연구원)
- Ep-V-122 마그네슘합금의 PEO 표면처리에 대한 특성 연구: 유 재인, 윤 재곤, 김 진희, 유 재용, 박 창훈, 윤 기열, 송 경호, 김 기홍((주)세미유 기업부설연구소), 김 기홍(경운대)
- Ep-V-123 X-ray Scattering Study on Moisture Induced Interfacial Degradation of Alq<sub>3</sub> on Silicon: LEE Young Joo, KO Changhyun (Department of Physics, Sogang University), YOO Insun, OH Hyoung-yun(LG Display Co., Ltd.), KIM Jinwoo, KIM Hyunjung(Department of Materials Science and Engineering, Gwangju Institute of Science and Technology)
- Ep-V-124 펄스 DC 마그네트론 스퍼터링 방법으로 증착시킨 indium-zinc-tin-oxide(IZTO) 박막의 투명전도 특성에 관한 연구: 김 용성, 손 동진, 남 은경, 정 동근(성균관대)
- Ep-V-125 Structure and optical properties of Ta<sub>2</sub>O<sub>5</sub> dielectric layer for thin film electroluminescence device: 최 상현, 이 상목, 문 희승(경북대), 이 상걸(기초과학지원연구원 대구센터), 손 상호(경북대)
- Ep-V-126 마그네슘합금의 PEO 표면처리에 대한 열처리 효과 연구: 유 재용, 김 덕희, 유 재인, 이 미경, 윤 재곤, 윤 기열, 송 경호((주)세미유 기업부설연구소), 김 기홍(경운대)
- Ep-V-127 마그네슘합금의 전처리 효과 연구: 박 창훈, 유 재인((주)세미유 기업부설연구소), 김 기홍(경운대)
- Ep-V-128 In situ GIWAXS Study of bulk heterojunction organic film for solar cell: SHIN Byong-Wook(Kyungpook National University, Department of Physics), KIM Jehan, KIM Kwang-Woo(Pohang Accelerator Laboratory), LEE Sung-Youp (Kyungpook National University, Department of Nano-Science and Technology), YI Jin-Neung, PARK Sun-Mi, SON Myeong-Rak, KONG So-Jeo(Kyungpook National University, Department of Physics), CHOO Na-Yun(Kyungpook National University, Department of Nano-Science and Technology), LEE Eui-Wan, LEE Hyeong-Rag(Kyungpook National University, Department of Physics)
- Ep-V-129 마그네슘합금의 인산염 표면처리에 따른 특성 연구: 김 진희, 유 재인, 윤 재곤((주)세미유 기업부설연구소)
- Ep-V-130 Investigation of BaY<sub>2</sub>O<sub>4</sub>: Eu<sup>3+</sup> Phosphors by Site-selective Laser-excitation Spectroscopy: 김 은식, 장 경혁, 시 랑, 교 학빈, 전 병천, 서 효진(부경대)
- Ep-V-131 Spectral and Structural Properties of Eu<sup>3+</sup> in Sol-gel-derived Nanocrystalline ZrO<sub>2</sub> by Site-selective Luminescence Spectroscopy: 제 재용, 시 랑, 김 은식, 교 학빈, 장 경혁(부경대), 노 경석(마산대학, 방사선과), 서 효진(부경대)
- Ep-V-132 고체의 전기 저항률 및 전도도 특성 연구: 서 주희, 임 선아, 이 현진(전남대학교)
- Ep-V-133 SEM을 이용한 기능성 직물의 물리적 나노 구조와 기능의 상관관계 연구: 김 기연, 이 나원, 이 서은(한국외국어대)

## ■SESSION P5■

## 반도체물리학과회 포스터 발표

장 소 : 포스터 발표장

10월 23일(금) 13:00 - 15:00

- Kp-V-046 Silicon-On Nothing 소자 구현을 위한 SiGe Selective Lateral Wet Etching에서 Strained SiGe Layer의 두께에 따른 선택비 및 Etch Rate Issue: 길 연호, 이 훈기, 김 택성, 심 규환(전북대)
- Kp-V-047 SiGe HBT 소자 시뮬레이션 및 특성 고찰: SHIN MI IM, CHOI SANG SIK, CHOI CHEOL JONG, SHIM KYU HWAN (전북대)
- Kp-V-048 Compton Suppression System에서 환경시료의 방사능 농도 측정: 장 은성, 김 연, 박 정남(부산대)
- Kp-V-049 Low Power Consumption of Cap-less Memory in Silicon-on-insulator n-Metal-Oxide-Semiconductor Field-effect Transistor: SHIN Mii-Hee, HIROFUMI Enomoto, KIM Tae-Hyun, KIM Seong-Je, SHIM Tae-Hun, PARK Jea-Gun(Advanced Semiconductor Materials & Devices Development Center, Hanyang University)
- Kp-V-050 Surface Morphological Characteristics of Ge Islands Grown by RT-CVD on Si(001) Substrates: JU Mi Yeon, LEE Sanghwa, KIM Chinkyo(Kyung Hee University, Dept. of Physics), YANG Heon-Deok, CHOI Chel-Jong, SHIM Kyu-Hwan(Chonbuk National University, School of Semiconductor and Chemical Engineering, Semiconductor Physics Research Center)
- Kp-V-051 Dependency of Retention Characteristics of Cap-less Memory Cell on Top Silicon Thickness of Silicon-on-insulator Substrate: LEE Ho-Kuen, PARK Jae-Kyu(Division of Electronics, Communications, and Computer Engineering, Hanyang University), CHOI Ki-Ryoung, KIM Seong-Je, SHIM Tae-Hun, PARK Jea-Gun(Advanced Semiconductor Materials & Devices Development Center, Hanyang University)
- Kp-V-052\* 이온빔 스퍼터링과 열처리에 의해 제작한 p형 실리콘 나노결정/n형 실리콘 웨이퍼 접합구조의 태양전지 특성 연구: 홍 승

- 회, 신 동희, 최 석호(경희대 국제캠퍼스 응용물리학과), 김 경중(한국표준과학연구원 나노소재측정센터)
- Kp-V-053\* Nonvolatile memory characteristics of Ge-nanodot floating-gate MOSFETs: 김 민철, 홍 승휘, 최 석호(경희대 국제캠퍼스 응용물리학과), 김 경중(한국표준과학연구원 나노소재측정센터)
- Kp-V-054\* Ge nanowires Heteroepitaxy on Ge layer deposited Si Substrates: 정 재훈, 김 유리, 윤 현식, 김 정혁, 송 만석, 김 용(동아대), GAO Qing, TAN H. Hoe, CHENNUPETI Jagadish(The Australian National University), CHEN Zhi Gang, ZOU Jin(The University of Queensland)
- Kp-V-055\* Effects of Anode in Cu Electroplating: SEO Jung-Hye, LEE Youn-Seoung(Department of Information Communication Engineering, Hanbat National University), RYU Young-Ho, HONG Kimin(Department of Physics, Chungnam National University), KANG SUNG-KYU, RHA Sa-Kyun(Department of Materials Engineering, Hanbat National University)
- Kp-V-056\* Reproducible resistive switching in Cu/a-Si/Si structures with micron-sized active device area: 차 동재, 이 성주, 강 보수(한양대), 박 수현(이화여대), 엄 한돈, 이 정호(한양대), 김 동욱(이화여대)
- Kp-V-057 Magneto-optical Properties of CdS:Mn Film Grown by HWE: LEE Jooyong, KIM Hyungmin, PARK Seungmin(University of Ulsan, Department of Physics)
- Kp-V-058 콜로이드 CdSe 양자점의 광학적 특성 및 광전소자로의 응용: 오 은순, 김 태수, 이 병우, 김 의태, KUMAR kiran(충남대)
- Kp-V-059 Spatially Resolved Optical Properties of Periodically Polarity Inverted ZnO Films Grown on (0001)  $\text{Al}_2\text{O}_3$  by Cr-compound Intermediate Layers: CHO Yong-Hoon, KWON Bong-Joon, KIM Je Hyung(KAIST, Department of Physics, Graduate School of Nanoscience & Technology (WCU), and KAIST Institute for the NanoCentury), PARK Jin-Sub, YAO Takafumi(Tohoku University, Institute for Materials Research)
- Kp-V-060 Properties on Optical Gain of CdZnO Quantum Wells: JEON H. C., LEE S. J.(Dongguk University), PARK S. H.(Catholic University of Daegu), KANG T. W.(Dongguk University)
- Kp-V-061 1,3-DMP, BAL 등의 thiol 화합물이 CdS 양자구슬의 물성에 미치는 영향: 하 성용, 유 동선, 김 일곤, 이 정두, 유 준원, 이 은성, 추 문식, 김 곤우(창원대)
- Kp-V-062 급속 열처리 온도가 Al 도핑된 ZnO 박막에 미치는 효과: 정 재용, 조 신호(신라대)
- Kp-V-063 열벽 적층 성장법으로 얻은  $\text{Cd}_{1-x}\text{Mn}_x\text{S}$  박막의 XPS 분석과 타원분광학적 특성: 김 대중(목원대), 박 재환, 오 병성(충남대), 이 종원(한밭대), 최 용대(목원대)
- Kp-V-064 Fabrication and electrical properties of wide-band-gap  $\text{Mg}_x\text{Zn}_{1-x}\text{O}$  ceramics: 김 셋별, LI GUO JIE, 최 병춘, 정 중현, 문 병기(부경대), 전 병익(한국과학영재학교)
- Kp-V-065 산소농도에 따른 ZnO 박막의 특성변화: 백 경철, 이 봉주, 정 진(조선대)
- Kp-V-066 유전영동기술을 이용한 나노갭 전극에서 CdSe 나노 입자의 제어 및 정렬: 김 옥원, 서 영교, KUMAR Sanjeev, 김 길호(성균관대)
- Kp-V-067 유전영동을 이용하여 나노갭 전극에서의 ZnO 나노 입자 제어 및 정렬: 양 은표, 서 영교, KUMAR sanjeev, 김 길호(성균관대)
- Kp-V-068 초음파를 이용한 ZnO nanorods의 성장과 광학적 특성 분석: 오 은순, 이 병우, 김 태수(충남대), 김 진태, 임 한나(한국표준과학연구원), 정 승호(경북대)
- Kp-V-069 Effects of Deposition Temperature on the Structural, Optical and Electrical Properties of ZnO Thin Films on Glass Substrate: 조 신호(신라대)
- Kp-V-070\* KOH 및 NaOH 알칼리성 촉매를 이용하여 화학적 수조 방법으로 성장시킨 ZnS 및  $\text{Zn}(\text{S}, \text{OH})$  박막의 특성 비교: 천 성현, 최 인환(중앙대)
- Kp-V-071\* Synthesis of ZnO nano-structures on  $\text{Au}/\text{SiN}_x/\text{Si}(001)$  substrate by radio-frequency magnetron sputtering: 선 정호, 강 현철(조선대)
- Kp-V-072\* CdS/CdSe 측면 헤테로 나노벨트 성장 및 광학적특성: 김 유리, 정 재훈, 윤 현식, 김 정혁, 송 만석, 배 세환, 김 용(동아대), GAO Qing, TAN H. Hoe, CHENNUPETI Jagadish(Australian National University), ZOU Jin, CHEN Zhigang(The University of Queensland)
- Kp-V-073\* Si 나노결정의 크기에 따른 Si 나노결정-ZnO 박막 상호간의 에너지 전이 특성 연구: 신 동희, 김 창오, 홍 승휘, 최 석호(경희대 국제캠퍼스 응용물리학과), 김 성(호주국립대학 전자재료공학과)
- Kp-V-074\* Enhanced Ultraviolet Emission from V Implanted ZnO Films: Correlation with Structural Properties: 김 창오, 신 동희, 오 형택, 최 석호(경희대), BELAY K., ELLIMAN R. G.(호주국립대학 전자재료공학과)

# 구두발표논문 초록



## A-01

## 한국기계연구원부설 재료연구소의 기업지원방향

이 정환

산업기술지원본부, 한국기계연구원부설 재료연구소, 경남, 창원, 641-010.

한국기계연구원부설 재료연구소는 소재분야의 산업원천기술 개발 및 성과확산, 시험평가 지원 등을 통해 국가 소재산업의 발전에 기여하는 것을 임무로 하는 국가 출연연구소로서, 1976년 창원에서 한국기계 금속시험연구소로 출범하였다. 1992년 한국기계연구원으로 개칭하면서 기계분야의 본원이 대전으로 이전하고, 재료분야의 창원본원이 2007년 재료연구소로 부설화되었다. 재료연구소는 주력산업 고도화 소재 및 미래시장 선점 소재에 대한 기술개발 이외에도 목적지향형 산업기술지원을 중점 과제로 추진하고 있으며 이를 위해 4본부 2부 조직체계상에 산업기술지원본부를 두고 있다. 산업기술지원본부는 재료특성 평가그룹, 안정성평가그룹, 표준계측그룹, 재료정보그룹 및 원자력공인검사단으로 이루어져 있으며 생산 현장 애로기술지원, 공인시험평가 및 표준계측 지원, 국가기간설비의 공인검사 및 안전성 평가, 보유기술 실용화사업 등을 수행하고 있다. 또한 중소기업의 근접지원을 위해 연간 2억원의 자체예산을 들여 별도의 운영체조직으로 애로기술 클리닉센터를 설립하여 생산기술 전문분야별로 경험이 풍부한 중견 연구원을 중심으로 기업의 기술적 애로사항을 해소하기위해 노력하고 있다. 이외에도 기술 후견인 제도를 통해 전문인력의 상시 전담지원체계를 구축/운영하고 있으며, 적극적인 기업의 현장애로기술 발굴 및 지원방안의 모색을 위해 소장을 비롯한 전문연구원이 정기적으로 기업을 방문하고 있으며 이러한 방문활동에는 중소기업청에서도 관심을 가지고 참여하고 있다. 또한 중소기업의 시험검사/교정 수수료 지원, 현장교정검사, Package형 시험검사 기술지원 및 convention 시설개방 등 기업활동과 관련된 인프라 지원뿐만 아니라 신기술 실용화 개발지원 및 지역기반 구축 등을 수행하고 있다. 이와 같이 재료연구소는 능동적으로 기업을 찾아가는 뒷바라지 서비스 문화정착을 통해 기업과의 실질적인 협력관계 강화 및 실질적인 기업지원을 위해 노력하고 있다.

## A-02

## KIST 기술이전, 현황과 과제

민 경남

KIST 기술사업부 성과확산실, 서울 성북구 하월곡동 39-1.

KIST에서는 수 년 전부터 산학협력단 또는 기술사업부 등을 조직하여 연구를 통하여 개발된 기술을 산업화로의 연계 및 기술이전을 촉진하기 위하여 다양한 활동을 전개해 오고 있다. 본 산학연 특별세션에서는 KIST의 특허관리 현황, KIST의 기술이전 현황 그리고, 기술이전을 위한 추진 과제 등 기술사업부에서의 다양한 산학협력관련 사업을 소개한다.

## A-03

## 지식기반시대의 산학협력 선진화 방안: 인력양성을 중심으로

이 우영

*대학산업기술지원단 서울시 강남구 역삼동 701-7, 연세대학교.*

최근 우리나라 과학기술계의 화두는 산학협력이다. 산학협력의 세 가지 축은 크게 인력양성, 기술이전, 정보교류로 나눌 수 있다. 특히 우리나라는 지식기반경제로 진입하면서 과학기술을 이끌어 나갈 핵심 인재를 양성하는데 국가적 역량을 기울이고 있다. 본 강연에서는 이공계 위기를 중심으로 이공계 인재에 대한 환경 변화를 분석하고 이를 기초로 이공계 교육 혁신에 대한 정책의 목표와 방향을 설정하기 위한 중요한 논거를 알아본다. 또한 산학협력의 중심에서 전국적인 기술·인력 네트워크를 구축하고 중소기업의 기술혁신을 선도하는 대학산업기술지원단의 다양한 산학협력관련 사업을 소개한다.

## A-04

## 대학과 기업 간의 산학협력 모델

이 종태

*한국대학기술이전협회 (KAUTM), 동국대학교 산학협력단 서울 중구 필동 2가.*

학문의 발전이 산업발전과 함께 상승작용을 일으키기 위해서 산학협력은 가장 중요한 활동이며 선진국으로 진입하기 위한 필수요소이다. 그러나 한국은 국력에 걸맞지 않게 산학협력이 걸음마 단계이며 크게 벌어져 있는 기업의 시각과 대학의 시각차를 좁히지 않는다면 앞으로도 개선될 여지가 없다. 이를 위해서는 정부의 역할이 무엇보다 중요하겠지만 올바른 방향성에 대해서는 대학이 깊은 통찰력을 가지고 방안을 제시해야 한다. 본 발표에서는 그간 논의되어 왔던 대학과 기업의 협력개념과 성공사례, 해결해야 할 난제를 중심으로 조기에 산학협력을 선진국 수준으로 끌어올리기 위한 방안을 토의하고자 한다.

**A-05****SHELL MODEL AND THE MASS ASYMMETRY OF FISSION FRAGMENTS**

LEE Kiuck, LEE Linda

*419 Bosworth Lane.*

The mass asymmetry\* of fission fragments was a puzzle for a long time, and some people suggested that it may be related to the shell structure, though no one showed the relationship between the two in the past. We would like to present it in a simple way. The solution is related to the determination of the location of the schision points. There are two schision points, one for the neutrons and another for the protons. It has been assumed that the neutrons break off simply at  $N = 82$ , a major shell. The neutrons are different due to the Coulomb force. The proton levels are generally higher than those of the neutrons. Hence, the last bound state level would be  $1g_{7/2}$  shell, or the total number of protons would be  $Z = 50 + 8$ . The total number of nucleons of the heavy fragment would be  $N = 82$ ,  $Z = 58$ , or in total,  $A_H = N + Z = (82 + 58) = 140$ . The schision points should be near  $N \approx 82$  and  $Z \approx 58$ , hence the fissioning nucleus breaks off into two fragments near  $N = 82$  and  $Z = 88$ . The mass number of the light fragment can be expressed:  $A_L = A_F + N - (A_H - nN)$ , where the number of free neutrons,  $n = 0, 1, 2$ , etc. More simply,  $A_L = A_F - A_H - (n-1)N$  and the mass ratio would be  $140/A_L$ . The examples of the mass ratio, with  $n = 2$  are shown in the following table:

Table

$A_F$	$A_H/A_L$	$A_H/A_L$
	Experimental	Theoretical
Pu <sup>239</sup>	140/100	140/98
U <sup>235</sup>	140/95	140/94
U <sup>233</sup>	140/95	140/92

We hope that the present method may be applied to the study of heavy and superheavy elements. \* A different version of this topic has been presented at the UKC 2009 conference by the same authors.

**A-06****Science and Technology Infra-structure in Democratic People's Republic of Korea and Current Status of Nuclear Weapon Development Program**

KIM Kinney H.

*Professor of NC Central University Former President of AKPA.*

## A-07

## 수소저장을 위한 수소 분자와 금속 간 상호작용의 규명

임 지순

서울대학교

화석연료에서 발생하는 이산화탄소가 지구온난화의 주된 원인으로 드러나면서 이산화탄소를 배출하지 않는 소위 녹색에너지에 대한 연구가 각 분야에서 활발히 이루어지고 있다. 수소를 자동차의 휘발유와 대체하여 연료로 사용할 경우, 수소를 안전하고 효율적으로 저장하기 위해 제안된 방법 중의 하나가 다공성물질 표면에 수소 분자를 흡착시키는 것이다. 상온에서 작동하기 위한 이상적인 흡착에너지는 0.3eV 인데 이것은 일반적인 공유결합, 이온결합, 혹은 금속결합 에너지보다 훨씬 약하고, van der Waals 상호작용보다는 훨씬 강하다. 이처럼 화학흡착과 물리흡착의 중간 크기의 흡착에너지를 얻기 위한 연구에서, 수소분자와 각종 금속원자 간의 상호작용도 규명하고 특히 전이금속에서 spin 상태가 수소 분자 흡착에너지에 미치는 영향을 밝힌다. 밀도 범함수 이론에 기초한 제일원리적 전자구조 계산을 통하여 전자의 이동, 전기 쌍극자의 생성 등을 분석하며 실제 물질 합성에서의 문제점도 논의한다.

## A-08

## Phase-coherent Electrical Transport in Mesoscopic Dimensions

이 후종

POSTECH.

The mesoscopic scale, ranging from nanometer to micrometer, is in between the microscopic and the classical macroscopic world. Both mesoscopic and microscopic systems are governed by the quantum mechanical principles. Mesoscopic physics addresses fundamental phenomena that occur when an object is miniaturized. It thus deals with the most fascinating phenomena occurring in condensed matter in mesoscopic length scales, such as ballistic transport, single electron tunneling, conductance and energy-level quantization, interference of carriers in normal and superconducting states, etc. Among these, the phase coherence and the consequent interference effect of carriers are the hallmark of the mesoscopic-scale phenomena. In the lecture I will focus on this phase-coherence effect revealed in the electrical transport properties for various mesoscopic systems, including metallic films, two-dimensional electron gas systems, nanowires, graphene, various systems hybridized with superconductors, etc. The subjects include weak localization, universal conductance fluctuations, Aharonov-Bohm and Al'tshuler-Aronov-Spivak oscillations, Andreev reflection vs specular reflection, superconducting proximity effect in diverse mesoscopic systems, etc.

**A-09****빅뱅이론과 LHC: 가장 작은 세계가 가장 큰 세계를 밝힌다.**

김 항배

*한양대학교.*

20세기 과학의 가장 큰 성과 중의 하나는 우리가 볼 수 있는 가장 작은 세계인 소립자의 세계와 가장 큰 세계인 우주에 대한 근사한 이론인 입자물리 표준 모형과 표준 우주론을 갖게 되었다는 것이다. 이 두 이론은 우리 세계의 궁극적 이론을 얻는 데 상호보완적인 역할을 한다. 현재 가장 작은 세계를 밝히기 위한 실험들과 가장 큰 세계를 밝히기 위한 실험들을 돌아보고, 소립자의 세계를 연구하는 LHC 실험이 어떻게 우주의 신비를 밝히는 데 필요한지 알아본다.

A

**A-10****신의 입자를 찾아서**

이 종필

*고등과학원.*

탈레스 이래 2600년에 걸친 수수께끼가 이제 막 풀리려고 한다. 세상은 과연 무엇으로 만들어졌을까? 지난 40년 간 인류가 써 내려간 모범답안에서 아직 공개되지 않은 마지막 답안지의 채점결과가 드디어 공개된다. 그 것은 바로 모든 소립자들에게 질량을 부여하는 신의 입자, 곧 힉스 입자에 관한 이야기이다. 아직까지 발견되지 않은 신의 입자는 과연 존재하는 것일까? 스티븐 호킹이 선뜻 100달러 내기를 걸었던 그 문제, 곧 '신의 입자'를 찾아나선 인류의 대장정을 소개한다.

## A-11

## 고압물리에서 다이아몬드 앤빌 셀의 응용 (Application of Diamond Anvil Cells on

## High-pressure Physics)

김 광주, 고 영호

국방과학연구소 (Agency for Defense Development).

최근 자온상태나 고온상태 또는 자기장이나 전기장을 이용하여 물성을 연구하는 실험실에서 고압기술을 응용하는 연구가 증가하고 있다. 이러한 현상은 제작이 수월하고 크기가 작으며 안전한 고압발생장치인 다이아몬드 앤빌 셀이 그 중심에 있다. 백만 기압 이상을 발생하는 고압 셀, 고온과 고압을 동시에 발생하는 셀, 그리고 개구각이 넓은 대칭 셀과 같은 다이아몬드 앤빌 셀을 제작하고 고압 X-선 회절실험에 적용하여 유용성을 검토하였다. 앤빌 셀에서 발생하는 압력은 루비 형광을 이용하여 계측하였고 온도는 열전대를 이용하여 측정하였다. 실험실 X-선 발생장치 및 포항 방사광 가속기를 이용하여 고압 X-선 회절실험을 수행하였으며, 시료는 PZT와 Fe합금, 그리고 몇 가지 금속 원소이며, 이 물질들에 대한 상온 및 고온 상태에서의 상태 방정식(EOS)과 고압 상변이를 측정한 결과를 소개한다.

## A-12

## 강유전체를 적용한 고밀도 전자방출 소스 연구 (Study on High Current Electron

## Emission Source Using Ferroelectric Materials)

서 민수

국방과학연구소 (Agency for Defense Development).

전통적으로 고체에서 전자방출은 열전자 방출, 장전자 방출, 광전자 방출, 2차전자 방출이 있다. 하지만 강유전체에 강하고 빠른 전기장 펄스를 인가할 경우 전통적인 방법과는 다른 새로운 형태의 전자방출 현상이 가능하다고 알려지면서 강유전체 적용 전자방출 연구가 활발하게 진행되고 있다. 강유전체 전자방출은 저압 및 상온에서 작동이 가능하고, 방출시간을 제어할 수 있으며, 낮은 가속전압에서도 고밀도의 전자가 방출 가능하므로 고비용의 열전자 및 장전자 방출 소스의 대용 방안으로 고려되고 있다. 음극 형태에 따라 약전자 및 강전자의 방출이 가능하며, 평판형 구조의 전자총으로서 전자현미경 등의 전자원 및 전계 방출 디스플레이 등의 응용이 기대되고, 마이크로파 발생 소스, X-ray 발생 소스, 개스 스파크갭 스위치, 그리고 대면적 개스 이온화 소스 등의 연구가 진행되고 있다. 본 발표에서는 강유전체 음극의 전자방출 원리 및 현재 개발 중인 강유전체 음극의 기초연구 결과들을 소개한다.

**Plasma and Electromagnetic Forces)**

김 성호, 김 진성, 양 경승, 이 병하

국방과학연구소 (Agency for Defense Development).

추진제를 이용한 현재의 화포는 연소에 의해 발생된 압력을 탄체 가속의 원동력으로 삼고 있는데 주어진 탄체에 대해 추진제의 양을 늘리더라도 기체 자신의 에너지 때문에 탄체의 속도가 더 이상 증가하지 않는 한계에 도달해 있다. 한편으로 오래 전부터 전기에너지를 이용한 탄체의 가속 기술에 대한 연구도 꾸준히 진행되어 왔다. 기존의 추진제보다 분자량이 작은 물질에 대규모의 전기에너지를 투입하여 전열(electrothermal) 플라즈마를 발생시키고 추진 압력을 얻는 전열포와 추진제 없이 오직 전자기력으로만 움직이는 전자기포가 대표적인 연구 분야이다. 순수한 전열포나 전자기포는 수십 MJ을 넘는 대규모의 펄스 전원 투입을 요구한다. 다소 작은 규모로는 화학적 방식에 의한 기존의 추진제 점화 대신 수만도, 수천기압의 플라즈마로 점화하는 기술을 들 수 있다. 이 기술은 정밀 점화, 연소 압력 제어, 안전성 강화 등의 장점을 가지고 있으며, 펄스 전원 개발, 플라즈마의 발생 및 추진제의 연소 등을 이론 및 실험적으로 연구하고 있다. 한편 에너지의 이용 추세로 볼 때 미래에는 순수한 전자기력으로 탄체를 가속하여 기존 화포가 가진 속도의 한계를 극복할 수 있는 레일건 연구가 미국, 중국 및 유럽에서 진행되고 있다. 이 연구는 레일-아마추어의 미끄럼 접촉 상태에 대해 전자기, 열, 구조 모두를 고려한 해석과 가속 실험을 통하여 현상에 대한 이해 및 소재의 한계적인 상황들을 극복하기 위한 방법들을 찾고 있다. 본 발표에서는 현재 연구 중인 플라즈마 점화기술과 더불어 펄스 전력의 활용이 가능한 전자기적 방호, 전자기력에 의한 가속 등의 응용 분야들을 기본 원리와 함께 소개할 것이다.

**까지 (Applications and Trends of Laser Technology for Military Use: Remote Sensing to Missile Defense)**

강 응철, 이 정환, 최 현진

국방과학연구소 (Agency for Defense Development).

레이저 발명 당시부터 군사적 응용 가능성을 검토할 만큼 오늘날 레이저 기술은 군사 분야에서 매우 다양하게 적용되는 중요한 기술 중의 하나이다. 이와 같은 군사적 응용은 고휘도성, 직진성, 가간섭성 등의 레이저광의 기본 특성 뿐만 아니라 초단 광펄스 발생 및 광속 이용 등의 고정밀도 특성 등 레이저가 갖는 고유한 성능 때문에 가능하게 되었다. 현재 레이저 기술은 펄스형 레이저를 이용하는 거리측정, 표적지시, 3차원 영상 획득 등의 원격 정보탐지 분야에서 가장 많이 적용되고 있으며 최근에는 산업용 고출력 레이저 가공 분야 뿐만 아니라 군사적 목적으로 연속발진형 고출력 레이저 기술의 개발이 진전됨에 따라 레이저광으로 직접 군사표적을 무력화시키기 위한 고에너지 레이저무기 개발이 진행 중에 있다. 가혹한 전장 환경 및 소형·경량화를 추구하는 현대무기의 특성에 대응하기 위해 현재 적용되는 레이저는 주로 고체 레이저이며 최근에는 민수 분야에서 응용이 점차 확대되고 있는 광섬유 레이저가 차세대 레이저로 많은 연구개발이 수행되고 있다. 본 고에서는 현재 군에서 사용 중이거나 개발 중인 레이저 기술에 대해 저에너지의 레이저 센서와 고에너지의 레이저 무기로 구분하여 각각에 대해 개발사례를 중심으로 기본 개념 및 주요 특성에 대해 설명하고 레이저 기술의 발전 방향에 대해 살펴본다.

## A-15

## 전자광학/열상센서 기술발전과 장비 소개 (Introduction of Technical Development and Equipment for the ElectroOptic/InfraRed Sensor)

김 연수, 김 현숙, 김 창우

국방과학연구소 (Agency for Defense Development).

전자광학/열상(ElectroOptic/InfraRed) 센서의 종류는 매우 다양하며 넓은 의미로는 빛 에너지를 전기신호로 변환하여 응용하는 모든 센서를 말한다. EO/IR 센서의 가장 큰 장점은 인간의 인식체계에 가장 익숙한 영상정보를 제공한다는 점이다. 그러나 EO/IR 센서는 근본적으로 대기를 투과하여 센서에 입사하는 빛을 받아 영상화하므로 주위 환경조건에 많은 제약을 받는 단점이 있다. 군사적인 면에서는 수동형 센서로서 적에게 노출될 위험이 상대적으로 매우 낮으므로 개인 병사의 휴대용 장비로부터 감시정찰 위성에 이르기까지 매우 광범위하게 응용되고 있다. EO/IR 센서는 감시정찰 분야의 핵심 센서로 다양한 탑재체에 적용되고 있으며, 성능 또한 꾸준한 발전을 지속하고 있다. 특히 반도체 및 검출기 기술의 눈부신 발달로 센서가 소형/경량화 되어 동일한 응용분야의 탑재체에 적용하더라도 관측 및 거리성능은 과거와는 비교가 안 될 정도로 향상되었다. 현재 이 분야의 발전추세는 핵심센서로서의 지속적인 성능향상 외에도 과거에는 사용하지 않던 파장대역까지 영역을 넓혀가고 있다. 예를 들면 근적외선 대역(SWIR; Short Wave Infra-Red)의 경우 2차원 배열의 InGaAs 검출기가 실용화되어 영상센서로서의 응용이 증가하고 있다. 또 다른 발전추세로는 파장 영역을 잘게 분해하여 영상화하는 초분광 센서를 들 수 있다. 이 경우 각 물체마다 특정 파장에서 다르게 흡수 또는 반사되는 특징을 영상화 할 수 있어 그 응용분야는 매우 다양하다. 이와 같이 센서의 파장영역을 넓혀 나가는 발전추세 외에도 서로 다른 파장의 센서 영상을 융합하여 주변의 전장 상황을 한눈에 빠르게 인식할 수 있도록 하는 기술도 발전추세에 있다. 본 발표에서는 전자광학/열상 센서의 기술발전과 감시정찰용 장비 및 개발 내용 일부를 소개하고자 한다.

## A-16

## 현대 물리학에 의한 항법장치 기술의 발전 (The Development of Navigation

## Technologies by Modern Physics)

SHIM Kyu-Min

국방과학연구소 (Agency for Defense Development).

In this paper we conceptually introduce the INS(Inertial Navigation System) technologies such as GINS(Gimbaled INS), SDINS(Strap Down INS), GPS(Global Positioning System), and DBRN(Data Base Reference Navigation). And, next, we introduce the gyroscope technologies which are one of the most important parts of the INS technologies. The first gyroscope had mechanically intricate structures for measuring the inertial momentum change. That technology produced the GINS which has gimbals for stabilizing the platform because of narrow measurement range of this mechanical gyroscope. By the development of the laser, several types of optical gyroscopes are developed with using the principles of interferometers. The measurement ranges of optical gyroscopes are generally so wide that those gyroscope technologies produce the SDINS in which gyroscopes are directly attached to the vehicle structures without gimbals. In these days those optical gyroscopes and the SDINS are widely applied and become more and more accurate and compact. And we also introduce the atom interferometer type gyroscopes for developing the precision INS which is widely studied by western research institutes with considering them as a next generational gyroscope.

김 대연, 박 병욱, 전 재진, 김 영규

국방과학연구소 (Agency for Defense Development).

바다는 우리와 세계를 연결해 주는 통로이자 민족의 생존과 번영에 없어서는 안 될 중요한 자산이다. 특히, 세계 10위권의 경제교역대국으로 발돋움하고 있는 우리나라의 경우 수출입 물동량의 대부분을 해상 수송에 의존하고 있으며, 선박 건조량이 세계 1위로서 바다는 '우리의 미래'와 직결된다고 해도 과언이 아니다. 또한, 바다는 석유, 수산자원, 에너지, 공간자원 등 무한한 자원의 보고로서 그 가치가 크면 클수록 협력의 가능성과 더불어 분쟁의 가능성도 커질 수밖에 없다. 즉, 중국, 일본 등 주변국가의 배타적 경제수역(EEZ)선포에 따라 해양영토 확장과 개발경쟁과 더불어 영유권 분쟁 등이 가속화 되고 있는 실정이다. 이렇듯 인접국간의 이해가 첨예하게 대립될 수밖에 없는 환경으로 적정한 해군력의 확보 유지는 필수적이다. 본 고에서는 수중/수상에서 일어나는 물리적인 현상들과 국방과학기술과의 관계를 소개하고 앞으로의 발전추세 및 전망에 대해 알아본다.

**PA-01(초)****Introduction to Heavy Ion Accelerator KoRIA**

HONG Seung-Woo

성균관대학교.

The Korean government announced a plan to construct a Heavy Ion Accelerator facility in Korea. Planning for the construction of a Heavy Ion Accelerator to produce rare isotope beams is underway. The construction of this facility will be one of few mega-projects for basic science research facility in Korea. This facility, tentatively referred to as KoRIA (Korea Rare Isotope Accelerator), will be used for multipurpose research, including nuclear science, atomic, material & energy sciences, and bio-medical sciences. The present status of the planning will be presented.

**PA-02(초)****Atomic Physics with Rare Isotope Beams**

SPROUSE Gene D.

*Stony Brook University (on leave) and Editor in Chief, American Physical Society.*

Rare Isotope beams provide atoms with unique properties. The classic example is francium, which is the heaviest simple atom, but has no stable isotopes. Precision measurements of parity violation in Fr can test the standard model in ways complementary to high energy physics experiments, and measurement of anapole moments can also probe new physics. The availability of intense rare isotope beams opens up a broad spectrum of physics that can be attacked with the precision methods of atomic, molecular and optical physics, and should be an important part of the research program of any rare isotope facility. There are pure atomic physics experiments such as studying the properties of Fr molecules. There are nuclear physics experiments such as measuring charge radii of a long chain of isotopes extending toward the r-process path, and there are fundamental symmetry measurements searching for nuclear electric dipole moments, where specific rare isotopes provide greatly enhanced sensitivity. However, there are surely other experiments, because when a new accelerator is built, not everything that can be done with it is generally known beforehand, and its existence will provide a motivation for new ideas.

**PA-03(초)****2-Stage MOT and Optical Lattice Trap of Yb atoms**

YU Dai-Hyuk, PARK Chang Yong, LEE Won-Kyu, MOON Jongchul, KIM Eok Bong, LEE Sun Kyung  
*Korea Research Institute of Standards and Science.*

We are developing an Yb optical lattice clock. About  $10^6$  Yb atoms were first trapped and cooled in a 2-stage magneto-optical trap (MOT). The temperature was measured to be 32 micro-Kelvin by time-of-flight method. The atoms then transferred to the optical lattice potential formed by the counter-propagating Ti:Sapphire laser with wavelength of 759 nm. Potential depth of the optical lattice was about 70 micro-Kelvin and 2000 atoms were trapped in the lattice. Further optimization is going on and will be presented at the conference. Possible applications of the atom and ion trap for the rare isotope beam (or radioactive ion beam) research will also be introduced.

P

**PA-04(초)****Opportunity for Nuclear Symmetry Energy in Future Rare Isotope Accelerator in**

**Korea**

HONG Byungsik

*Korea University.*

Presently, probing the nuclear symmetry energy above the saturation density is one of the prime interests in nuclear physics. It plays an important role in understanding heavy-ion reactions and various astrophysical processes. The nuclear symmetry energy is essential for various properties of neutron-rich nuclei, the particle production in heavy-ion collisions, and the neutron stars. Although the nuclear symmetry energy has been investigated actively in NSCL (National Superconducting Cyclotron Laboratory) in USA and GSI (Helmholtz Center for Heavy Ion Research) in Germany, the future radioactive ion beam facilities such as KoRIA (Korea Rare Isotope Accelerator) will play crucial role. The new rare isotope accelerators are expected provide an opportunity to investigate the isospin dependence of the nuclear equation of state with much larger lever arm for the neutron-to-proton ratio of the nuclear matter than any existing machines with unprecedented high intensity. In this presentation, we will overview the prospects of the nuclear symmetry energy study in KoRIA.

**PA-05(초)****ISIS Facility – Past Achievements and Future Prospects**

STEIGENBERGER Uschi

*ISIS Facility, Rutherford Appleton Laboratory.*

The ISIS Pulsed Neutron and Muon Facility is enabling world class science across a diverse range of science disciplines. Since 2008 ISIS operates a second target station, optimised for long wavelength neutron applications. We will describe the current status of the facility and the impact of the science programme in areas ranging from energy, environment, health and engineering. We will discuss the opportunities arising from the specific characteristics of the second target station and the future development potential of ISIS, also in the context of providing a next generation neutron source for European researchers.

**PA-06(초)****Science Opportunities in HIE-ISOLDE**

KADI Yacine

*Sungkyunkwan University & CERN.*

Radioactive nuclei from various sources have been used for condensed matter investigations for a long time. The earliest application of radiotracers was the investigation of diffusion processes [J. Groh and G. Hevesy, Ann. Phys. (Leipzig) 63 (1920) 85]. Nuclei are now being routinely used as probes of their environment in metals and semiconductors via various methods. More recently, these techniques have also been applied to the study of complex bio-molecules, surfaces, and interfaces. This spin-off from nuclear physics research has been increasing steadily in scope. With the routine availability of high-purity radioactive ion beams from isotope separators the possibilities for such investigations have been greatly expanded, permitting technologically ever more demanding experiments. In particular, the use of on-line isotope separation at the CERN/ISOLDE facility has demonstrated the great potential of nuclear probes for solid-state physics research: during the last 17 years approximately 25% of the beam time has been devoted to condensed matter applications. If a mid-term upgrade of the ISOLDE facility is planned, it is natural to expect that applications in materials science are going to constitute an important research field there too. The future user of ISOLDE would be able to utilize the higher beam energies, qualities, and intensities available.

**PA-07(초)****Explosive Nuclear Astrophysics using Radioactive Ion Beams**

한 인식

*이화여자대학교*

Nuclear reactions in explosive stellar sites such as X-ray bursts, nova, and supernova are not well understood. Experimental measurements of these nuclear reactions often involve radioactive ion beams and require careful preparation of detectors and reaction conditions. The most important factor in many nuclear astrophysics experiments is the quality of the beams, which include the intensity and energy resolution. Therefore, the new generation radioactive beam facilities such as KoRIA are expected to be crucial for the advances in determining explosive nuclear reactions. The prospect of nuclear astrophysics experiments in stellar explosions will be discussed.

P

**PA-08(초)****Exotic Nuclear Structures Probed by Breakup Reactions**

NAKAMURA Takashi

*Tokyo Institute of Technology*

One of the highlights in modern nuclear physics is exotic structure appearing in nuclei with large neutron excess. For instance, nuclear halo is formed for a very weakly-bound light nuclei near the neutron-drip line. We have developed a method to probe structures of halo nuclei by using breakup reactions. In this talk, I will focus on Coulomb breakup study on the Borromean three-body halo nucleus  $^{11}\text{Li}$ , and on halo candidates  $^{22}\text{C}$  and  $^{31}\text{Ne}$ . In the former case, we have observed a strong dipole transitions, (soft E1 excitation), which is indicative of di-neutron like structure in  $^{11}\text{Li}$ . The latter study was performed at the newly commissioned RIBF (RI Beam factory) at RIKEN, where the large Coulomb breakup cross sections have provided evidence for halo structures in these nuclei. We also discuss the project, called SAMURAI/NEBULA at RIBF.

**PA-09(초)****Probing Nuclear Spin Structure with Radioactive Ion Beams and Polarized****Targets**

KIM Wooyoung

*Department of Physics, Kyungpook National University.*

We propose to perform spin structure study of the unstable nuclei with proposed radioactive ion beams and polarized nuclear targets. A polarized proton target and a polarized  $^3\text{He}$  target for use in scattering experiments with radioactive isotope beams are discussed. Present status and future plan for spin physics in world's leading RIB facilities will be reviewed. A polarized  $^3\text{He}$  target has been developed using the optical pumping and spin exchange method. The results of performance test with constructed polarized  $^3\text{He}$  target will be presented.

**PA-10(초)****Nucleosynthesis by the Radioactive Isotope Beam and Origin of Nuclear****Abundance**CHEOUN Myung-Ki, KIM Kyungsik<sup>1</sup>, HA Eunja, RYU Chungryeol*Soongsil Univ.. <sup>1</sup>Korea Aviation Univ..*

Understanding of origin of matter in the universe is strongly related with the evolution of stars, in which most of nuclei are believed to be synthesized and emitted by various explosion mechanisms at their last stages. The nucleosynthesis is sensitive on the given conditions of the site, such as preceding matter, temperature, masses of stars. Usually it is characterized as slow, rapid, rapid proton, neutrino-process and so on. Since nuclear reactions relevant to the processes are presumed as thermally balanced, the nuclei unstable at the present time and their structure can play important roles in the nucleosynthesis. Radioactive isotope beam facility could produce the exotic unstable nuclei and investigate their key reactions on the ground, so that it could give invaluable microscopic information of the origin of matter complementary to the observational astronomical data. In this talk we present a few examples with results available from observational, experimental and theoretical data.

KWON Young Kwan, LEE Chun Sik, KUBONO Shigeru<sup>1</sup>

*Department of Physics, Chung-Ang University. <sup>1</sup>Center for Nuclear Science (CNS), University of Tokyo.*

Nuclear reactions in various stellar environments have been studied in order to understand the evolution of the universe. Especially, reactions involving unstable nuclei play an important role in many astrophysical sites. Radioactive ion (RI) beams provide a unique tool to investigate the structure of such unstable nuclei as well as the cross sections for many reactions of astrophysical relevance. Low-energy RI beams are essentially needed for investigating nuclear reactions in the hydrogen-burning process under the explosive stellar environments such as novae, X-ray bursts and supernovae. The low-energy in-flight RI beam separator CRIB is one of the most powerful low-energy RI beam facilities in the world, constructed by the Center for Nuclear Study (CNS) of the University of Tokyo. Over the past decade, we have made efforts in various nuclear astrophysical experiments under the Korea-Japan Joint Research Project. Details of CRIB and recent experimental results from our nuclear astrophysics collaboration will be presented. Possibilities of the CRIB facility in near future will be also briefly discussed.

SATOU Yoshiteru

*Seoul National University, Department of Physics and Astronomy.*

Nucleon-induced inelastic and charge-exchange reactions have been one of the major tools for nuclear structure study. A variety of transfers in spin, isospin, and momentum take place during the collision processes, populating various types of excited states. Theoretical treatments are well established to yield quantitatively reliable information, allowing a detailed study of the wave function via the transition amplitude. As part of a systematic investigation of exotic nuclear structure of nuclei far from stability using the nucleon induced reactions, we have measured the  $^{19,17}\text{C}(p,p')$  and  $^{14}\text{Be}(p,n)^{14}\text{B}$  reactions in inverse kinematics. Measurements were carried out at RIKEN by the invariant mass method. One new state in  $^{19}\text{C}$  and three new states in  $^{17}\text{C}$  were identified; for these as well as for the ground state of  $^{19}\text{C}$  spin-parity assignments were made [1]. In the invariant mass spectrum of  $^{14}\text{B}$ , a peak corresponding to the  $1^+$  state at 1.28 MeV was observed. By extrapolating the differential cross section to  $q=0$ ,  $B(\text{GT})_{(p,n)}$  value was deduced. The value was in good agreement with that from a  $\beta$ -decay study [2], showing a capability of using the (p,n) reaction in inverse kinematics on unstable nuclei as a practical probe of  $\beta$ -decay transition strengths of such nuclei. [1]Y.Satou et al., Phys. Lett. B600 (2008) 320.[2]N.Aoi et al., Phys. Rev. C66 (2002) 014301.

**PA-13(초)****Nuclear Structure Physics using Heavy-Ion Beams**

MOON Changbum

*Hoseo University, Department of Display Engineering.*

Current developments in nuclear structure at the limits are briefly reviewed. Studies of nuclear shapes, exotic excitations, and high-spin isomers by using heavy-ion accelerators are introduced mainly concentrating on medium mass nuclei just above proton magic number 50. Finally, I will talk some programs on nuclear structure physics at heavy-ion accelerator facilities in Europe (NuPECC).

**PA-14(초)****Is there evidence of simple relationship between measured yrast energies in even-even nuclei?**

윤 진희, 김 두영, 차 동우

*인하대학교 물리학과.*

We benefit sometimes by studying particular nuclear properties in terms of simple nuclear variables over the wide span of the chart of nuclides. One such example is the Weizsacker's mass formula which can reproduce the binding energy of the ground state of nuclei very accurately throughout the entire chart of nucleides. However, there have seldom appeared similar studies on observables concerning the excited states of nuclei. In this talk, we collect all the yrast energies which are measured up to now in even-even nuclei, and present them in such a way appropriate to check whether there exist any underlying simple relationship between them or not.

**PA-15(초)****Elastic scattering of  $^{26}\text{Si} + \text{p}$  using a radioactive ion beam of  $^{26}\text{Si}$** 

MOON Jun Young, LEE Chun Sik, LEE Ju Hahn, YUN Chong Cheoul, KIM Jong Chan<sup>1</sup>, YOUN Min Young<sup>1</sup>, KUBONO Shigeru<sup>2</sup>, TERANISHI Takashi<sup>3</sup>

*Department of Physics, Chung-Ang Univ.. <sup>1</sup>Department of Physics, Seoul national Univ.. <sup>2</sup>CNS, Univ. of Tokyo. <sup>3</sup>Department of Physics, Kyushu Univ..*

The resonant states in  $^{27}\text{P}$  within Gamow window have been investigated through the elastic scattering and the thick-target scan technique. We used a radioactive beam of  $^{26}\text{Si}$  which was extracted from CRIB facility and AVF cyclotron (CNS and RIKEN, Japan), whose energy and intensity are 3.745 (63) MeV/u on target and 1.762 kcps, respectively. With a thick polyethylene foil as a proton target which is enough thick to stop the incident beam, we could measure the proton excitation function up to  $E_{\text{c.m.}} = 3.6$  MeV above the proton capture threshold ( $Q_p = 0.859$  MeV), and analyze the observed peaks with R-matrix theory. As a result, we have suggested new resonance states at  $E_x = 3.053$  (23), 3.327 (25), 3.460 (28), 3.507 (29), and 3.831 (31) MeV and assigned spin-parities to them along with the proton widths. Taking advantage of mirror nucleus  $^{27}\text{Mg}$  and the measured spectroscopic information of nucleus  $^{27}\text{P}$ , we calculated the resonant reaction rate of  $^{26}\text{Si}(\text{p}, \gamma)^{27}\text{P}$  as a function of temperature, from which it has been found that the contribution of five newly found states becomes more significant at higher temperature  $T_9 > 2$ .

**PB-01(초)****Multiferroic Nanoregions and a Memory Effect in Cupric Oxide**

HUANG D. J.

*National Synchrotron Radiation Research Center, Hsinchu 30076, Taiwan.*

Transition-metal oxides exhibit various intriguing phenomena such as high-temperature superconductivity and colossal magnetoresistance. Recent extensive studies unveil another potential of transition-metal oxides as multiferroics in which magnetism and ferroelectricity coexist and are coupled. One well-known issue is the formation of local ferroelectric clusters embedded in a paraelectric matrix, known as 'polar nanoregions,' which govern exceptional dielectric properties of 'relaxors' – ferroelectrics in a special class with giant piezoelectric effects. In analogy to polar nanoregions in relaxors, 'multiferroic nanoregions' are expected to form in some multiferroics and to prescribe their magnetoelectric properties. In this talk, based on resonant soft x-ray magnetic scattering, we will present the observation of multiferroic nanoregions in cupric oxide CuO. There exists an anomalous memory effect for the direction of the electric polarization in the commensurate-incommensurate magnetic transition that coincides with the ferroelectric transition. Scattering results, incorporated with simulations of diffuse scattering, lead us to propose a scenario that preserved spin handedness in the multiferroic nanoregions is responsible for this memory effect in the magnetically-induced ferroelectric properties of CuO

**PB-02(초)****Electric Polarization in Ferrimagnetic Cubic Spinel (Co,Mn)<sub>3</sub>O<sub>4</sub>**

KOO Tae-Yeong, KANG Sun-Hee<sup>1</sup>, KIM Ill-Won<sup>1</sup>, YOON Hee-Jeong<sup>2</sup>

POSTECH, Pohang Accelerator Laboratory. <sup>1</sup>University of Ulsan, Department of Physics. <sup>2</sup>POSTECH, Department of Physics.

A new relaxor type ferroelectricity coexisting with ferrimagnetic long range order in the inverse oxide spinel Co<sub>3-x</sub>Mn<sub>x</sub>O<sub>4</sub> has been studied. Structural phase boundary was determined from the polycrystalline specimens at room temperature and mixed phase problem in tetragonal region is discussed with phase diagram. Several exotic phenomena such as electric polarization, possible non-collinear magnetic configuration and anomalous zero thermal expansion behavior below the magnetic transition temperature were investigated. Diffraction-spectroscopy techniques were also used to identify the local chemical and structural environments of both Co and Mn ions at two crystallographic sites of the spinel structure. It should be emphasized that the discrepancy between local and global symmetry seems to play a crucial role for the emergent ferroelectric phase in the magnetically and structurally isotropic cubic spinel system.

**PB-03(초)****Antiferroelectricity underlies the magnetodielectric effect and the huge****magnetostriction in rare-earth iron garnets**

허 남정, 송 기명, 박 영안, 이 경동, 윤 병길, 정 명화<sup>1</sup>, 조 재훈<sup>2</sup>, 정 종훈

인하대학교 물리학과. <sup>1</sup>서강대학교 물리학과. <sup>2</sup>KBSI.

Multiferroics, where ferroelectricity and magnetism coexist, have attracted a great deal of attention due to their spectacular coupling phenomena. Particularly, the discovery of ferroelectrics induced by peculiar magnetic structures brought about extensive theoretical and experimental studies. The key driving force for these magnetic ferroelectrics appears to lie in the inverse Dzyaloshinskii-Moriya (DM) interaction in magnets with long wavelength “non-collinear” spin structures. Here, we report experimental observations supporting the induction of antiferroelectricity in dysprosium iron garnet with a non-collinear spin structure in a single unit cell, seemingly through the similar DM interaction. We attribute the observed magnetoelectric/magnetodielectric effects and the huge magnetostriction to the magnetic field induced spin reorientation from non-collinear to collinear, which weakens the antiferroelectric distortion. Our result may suggest an alternative way of exploring new magnetoelectric materials and enrich the theoretical understanding of phenomena related with peculiar magnetic structures.

**PB-04(초)****Magnetic-field-induced critical end point in multiferroics**

JEON Gun Sang, PARK Jin Hong<sup>1</sup>, KIM Jae Wook, KIM Kee Hoon, HAN Jung Hoon<sup>1</sup>

*Seoul National University. <sup>1</sup>Sungkyunkwan University.*

Multiferroic systems have attracted much attention on the rich physics arising from the intimate coupling of magnetic and electric degrees of freedom. Interesting critical properties on the electric polarization which are induced by a strong magnetic field has been observed in a recent experiment. We propose a theoretical model based on the exchange-striction mechanism to describe the interplay of the spin and dipolar moments in the presence of a magnetic field. Our model essentially reproduces the behavior of the dielectric constants, magnetic susceptibility, and the polarization which have been observed in the experiment. The critical behavior observed near the polarization reversal point in the phase diagram is interpreted as arising from the proximity to the critical end point. This work was partially supported by the KRF (KRF-2007-314-C00075).

P

**PB-05****Realization of Giant Magnetoelectricity in Helimagnets**

CHUN Sae Hwan, CHAI Yi Sheng, OH Yoon Seok, JAISWAL-NAGAR Deepshikha, HAAM So Young, KIM Ingyu, LEE Bumsung, NAM Dong Hak, KIM Kee Hoon, KO Kyung-Tae<sup>1</sup>, PARK Jae-Hoon<sup>1</sup>, CHUNG Jae-Ho<sup>2</sup>  
*XMPL & FPRD, Department of Physics and Astronomy, Seoul National University, Seoul 151-747, Korea. <sup>1</sup>Department of Physics & Division of Advanced Materials Science, POSTECH, Pohang 790-784, Korea. <sup>2</sup>Department of Physics, Korea University, Seoul 136-713, Korea.*

Multiferroics, wherein magnetic and ferroelectric order parameters coexist and cross-couple to each other, evoke the potential for new devices, such as multi-bit memories, ultra-sensitive field sensors, and electrically tunable microwave filters. In order to pave the pathways for such technical exploitations, it is necessary to be able to control and optimize cross-coupled magnetoelectric (ME) phenomena. Herein, we report a novel chemical route to engineer the ME properties of multiferroic hexaferrites  $\text{Ba}_{0.5}\text{Sr}_{1.5}\text{Zn}_2(\text{Fe}_{1-x}\text{Al}_x)_{12}\text{O}_{22}$  with magnetically induced ferroelectricity. As the Al-concentration increases, the critical magnetic field for switching the electric polarization is systematically reduced from  $\sim 1$  T down to  $\sim 1$  mT, and the ME susceptibility is enhanced up to 470 times its value at 0 Al-concentration. The optimum ME properties are obtained at  $x = 0.08$ , which produces a giant ME susceptibility of  $2.0 \times 10^4$  ps/m and magnetodielectric effects as large as  $\sim 6\%$  at a magnetic field of 20 mT. We find that control of nontrivial orbital moment in the octahedral Fe sites through the Al-substitution is crucial for fine tuning of magnetic anisotropy and obtaining the conspicuously improved ME characteristics.

**PB-06****The One-dimensional Hubbard Model in the Presence of Peierls Modulation**

GO Ara, JEON Gun Sang

*Department of Physics and Astronomy, Seoul National University.*

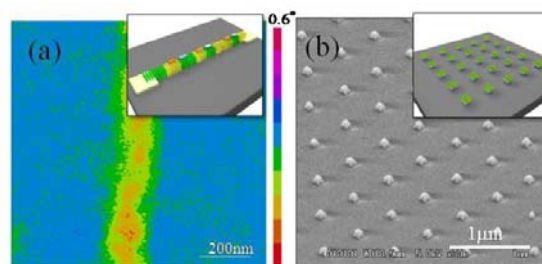
We investigate the one-dimensional half-filled Peierls Hubbard model at zero temperature. This model corresponds to the Hubbard model in the absence of the Peierls modulation and a series of independent dimers in the limit of perfect dimerization. We use the cellular dynamical mean-field theory employing the exact diagonalization technique as an impurity solver. The Peierls Hubbard model is known to be a band insulator in the noninteracting limit and evolved to a Mott insulator under increasing interaction strength. We calculate the double occupancy and the density of states to examine the effect of the Peierls modulation under local Coulomb interaction. The effects of Peierls modulation on the correlation energy is discussed in comparison with the Hubbard model. The results are also compared with those of the ionic Hubbard model. This work was supported by the KRF (KRF-2007-314-C00075).

**PB-07(초)****Controlled Fabrication of Complex Oxide Epitaxial Artificial Nano- wire and****Nano-dot Structures and Their Giant Properties**

TANAKA Hidekazu

*The Institute of Scientific and Industrial Research, Osaka University.*

The combination of scale reduction and the use of materials exhibiting important properties - such as complex functional oxides - is particularly promising. Unfortunately, controlling the size and position of nano-materials for fabricating nano-devices is still challenging. We report a strategy for fabricating artificial nano-wires (NW) and nano-dot (ND) of epitaxial ferromagnetic  $(\text{Fe,Mn})_3\text{O}_4$  (FMO) and  $(\text{Fe,Zn})_3\text{O}_4$  (FZO) [1] with tight control of length, width, position in combination of pulsed laser deposition and Atomic Force Microscope (AFM) or Nano-Imprint lithography. The wire widths of FMO artificial NW structures were systematically controlled down to 100nm by controlling AFM lithography current for Mo-mask [2]. Magnetic Force Microscope revealed that FMO-NW with 120nm showed single line of aligned ferromagnetic domains [3]. As further development, FMO nano-constriction structures within the NW-structures were constructed and their MR ratio was dramatically increased up to 150% at room temperature. We also report fabrication of  $(\text{Fe,Zn})_3\text{O}_4$  highly integrated ND structure by combination of nano-imprint lithography [4] and enhancement of their spin polarization. *References:* [1] Phys. Rev. B, 76 (2007) 205108, [2] Adv. Mater, 20 (2008) 909, [3] Nano Lett., 9 (2009) 1962, [4] Small, 4 (2008) 1661

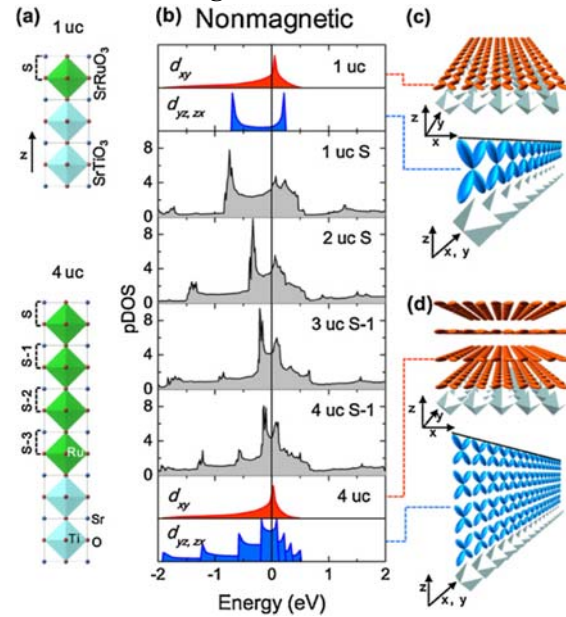


**PB-08(초)****Fundamental Thickness Limit of Itinerant Ferromagnetic SrRuO<sub>3</sub> Thin Films:****Control of Stoner Magnetism?**

NOH Tae W., CHANG Young Jun, KIM Choong H.,  
PHARK S.-H., KIM Y.S., YU J.

Seoul National Univ..

We report on a fundamental thickness limit of the itinerant ferromagnetic oxide SrRuO<sub>3</sub> that might arise from the orbital-selective quantum confinement effects. Experimentally, SrRuO<sub>3</sub> films remain metallic even for a thickness of 2 unit cells (uc), but the Curie temperature  $T_C$  starts to decrease at 4 uc and becomes zero at 2 uc. Using the Stoner model, we attributed the  $T_C$  decrease to a decrease in the density of states ( $N_o$ ). Namely, in the thin film geometry, the hybridized Ru  $d_{yz,zx}$  orbitals are terminated by top and bottom interfaces, resulting in quantum confinement and reduction of  $N_o$ .

**PB-09(초)****Pulsed Laser Deposition of Perovskite Manganites and Titanates****Heterostructures**

KIM Bog G., KIM Bongju, KWON Daeyoung, KOZUKA Yusuke<sup>1</sup>, HIKITA Yasuyuki<sup>1</sup>, HWANG Harold Y.<sup>1</sup>

Dept. of Physics, Pusan National University. <sup>1</sup>Dept. of Advanced Materials Science, University of Tokyo.

Recently there have been considerable interests in ultra thin film and heterostructure of perovskite manganites and titanates, not only because of its potential applications but also because of scientific importannces.<sup>1)-4)</sup> Pulsed laser deposition (PLD) method can be extensively used to produce atomic-scale multilayer of strongly correlated oxide materials, such as titanates, manganites, cuprates, and vanadates. By using RHEED monitoring, oxide materials can be deposited with layer-by-layer growth control and superlattice of different oxide materials can be produced. However, PLD process is highly non-equilibrium process and has many dependent control parameters, such as growth tempeprature, oxygen partial pressure, energy density of laser, and spot size of laser. In this talk, we would like to present our recent results on the process optimization of PLD of manganites and titanites and physical characterization of the grown films. 1) A. Ohtomo *et al.*: Nature 419, 378 (2002).2) A. Ohtomo and H. Y. Hwang, Nature 427, 423 (2004).3) N. Nakagawa *et al.*: Nat. Mater. 5, 204 (2006).4) H. Yamada *et al.*: Science 305, 646 (2004).

## PB-10(조)

Microscopic evidence of strain-enhanced ferromagnetic state in  $\text{LaCoO}_3$  films

PARK Soonyong, FREELAND J. W.<sup>1</sup>, MA J. X.<sup>2</sup>, SHI J.<sup>2</sup>, WU Weida<sup>1</sup>

*Department of Physics, Chung-Ang University, Seoul 156-756, Republic of Korea, Rutgers Center for Emergent Materials & Department of Physics and Astronomy, Rutgers University, 136 Frelinghuysen Road, Piscataway, NJ, 08854, USA. <sup>1</sup>Rutgers Center for Emergent Materials & Department of Physics and Astronomy, Rutgers University, 136 Frelinghuysen Road, Piscataway, NJ, 08854, USA. <sup>2</sup>Advanced Photon Source, Argonne National Laboratory, Argonne, IL, 60439, USA.*

Strain engineered thin film devices with tunable physical properties have significant impacts on both technology and material science. Recently, it has been reported that an intriguing ferromagnetic ground state emerge in biaxially strained  $\text{LaCoO}_3$  thin film imposed by underlying substrates, while  $\text{LaCoO}_3$  in its unstressed form has non-magnetic ground state. Yet these studies cannot exclude the possibility of strain enhanced chemical inhomogeneity. We studied strain-induced modification of magnetic properties in epitaxially grown  $\text{LaCoO}_3$  thin films on different substrates by variable temperature magnetic force microscopy (VT-MFM). Real space observation confirms the ferromagnetic ground state on a tensile-strained film grown on the  $\text{SrTiO}_3$  (001) substrate. Nanoscale magnetic clustering is, instead, observed on a low-strained film grown on the  $\text{LaAlO}_3$  (001) substrate, indicating that chemical inhomogeneity alone cannot induce the observed ferromagnetism on the tensile-strained film. Our results also demonstrate that VT-MFM in high magnetic field can be utilized as a very sensitive tool to detect the nanoscale defects of strain engineered ferromagnetic thin films.

## PB-11

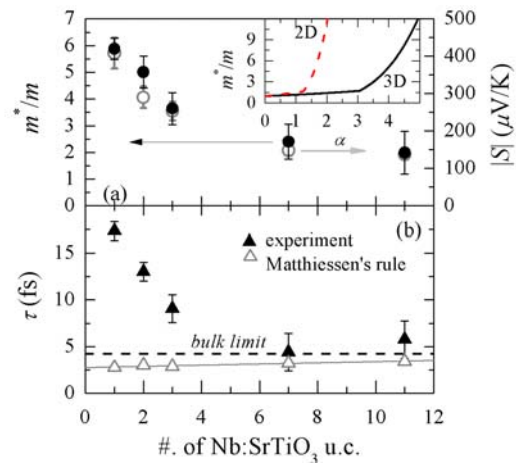
## Strong Electron-Phonon Coupling as the Origin of Enhanced Thermoelectric

Properties in  $\text{Nb:SrTiO}_3/\text{SrTiO}_3$  Superlattices

CHOI Woo Seok, OHTA Hiromichi<sup>1</sup>, MOON Soon Jae, LEE Yun Sang<sup>2</sup>, NOH Tae Won

*ReCOE & FPRD, Dept. of Phys. and Astro., Seoul Nat'l Univ., Seoul 151-747, Korea. <sup>1</sup>Graduate School of Engr., Nagoya Univ., Furo-cho, Chikusa, Nagoya 464-8603, Japan and PRESTO, Japan Sci. and Tech. Agency, Kawaguchi 332-0012, Japan. <sup>2</sup>Dept. of Phys., Soongsil Univ., Seoul 156-743, Korea.*

Recently, low dimensional oxide structures have been drawing much interest due the discovery of novel physical properties. In this contribution, we studied novel physical properties in superlattices using optical spectroscopy [1]. Due to the long penetration of light, optical spectroscopy is an excellent tool to investigate superlattices. In particular, we focus on the polaron dynamics in  $\text{Nb:SrTiO}_3/\text{SrTiO}_3$  superlattices, where a large enhancement of Seebeck coefficient has been reported [2]. With the decrease of the conducting  $\text{Nb:SrTiO}_3$  layer thickness down to 1 unit cell, we observed a dimensional crossover of polaron, where the effective mass and the relaxation time showed a threefold enhancement. The enhanced polaron effective mass was identified as an origin of the enhanced thermoelectricity in the superlattices, where it enhances the Seebeck coefficient without affecting the mobility of the system. Our results suggest that the strong electron-phonon coupling in low dimensional system could benefit the thermoelectric property. [1] W. S. Choi, *et al.*, arXiv:0906.5391v1 (2009). [2] H. Ohta, *et al.*, Nature materials 6, 129 (2007).



KIM Tae-Suk, HWANG Chanyong  
KRISS.

Electrons in graphene have attracted lots of research interests due to their chiral nature arising from two sublattices (pseudo spin). In this work, we study the spin structure of electrons close to the two Dirac points,  $K$  and  $K'$ , under the influence of the Rashba spin-orbit coupling. Since the graphene layer is formed on the SiC substrate or deposited on metallic substrates, the Rashba spin-orbit coupling can be generated from the structural asymmetry perpendicular to the graphene plane. Usually the Rashba interaction leads to the spin alignment in the plane, but the recent spin-polarized photoemission experiment suggests the possible alignment of spins normal to the plane close to the two Dirac points. We propose the asymmetry in two sublattices as a possible explanation of the anomalous spin structure in graphene and suggest that the Coulomb interaction between chiral electrons may be responsible for the broken symmetry in the pseudo spin degree of freedom.

KI M Jun Sung, KIM Seunghyun<sup>1</sup>, NA Sewoong, EOM Manjin, LAW Joseph<sup>2</sup>, KREMER Reinhard<sup>2</sup>, KIM Kee Hoon<sup>1</sup>

*Department of Physics, Pohang University of Science and Technology, Pohang, Korea. <sup>1</sup>Department of Physics and Astronomy, Seoul National University, Seoul, Korea. <sup>2</sup>Max-Planck-Institut für Festkörperforschung, Stuttgart, Germany.*

High- $T_c$  iron-pnictides,  $A\text{Fe}_2\text{As}_2$  ( $A = \text{Ca, Sr, Ba, and Eu}$ ) have a layered structure consisting of metallic FeAs planes intercalated by alkaline earths. Here we present recent investigations on single crystals of undoped and Fe-site doped  $A\text{Fe}_2\text{As}_2$ . The parent undoped compound has an antiferromagnetic spin-density-wave ground state, which can be suppressed by changing the alkaline earths at the A-sites or the substitution of Co/Mn/Ru at the Fe-sites. Superconducting state is induced by Co substitution or isovalent Ru- substitution, while no superconductivity is observed upon Mn substitution at the Fe sites. The magnetic and superconducting phase diagram will be presented and discussed in terms of the inter-band nesting effect and its possible influence on the high- $T_c$  superconductivity.

**PB-14(초)****Raman scattering measurements of the undoped and underdoped Fe-As****superconductors**

CHOI Kwang-Yong

*Physics Department, Chung-Ang University, Seoul, Korea.*

In this talk we discuss self-energy effects and electron-phonon coupling of the undoped SrFe<sub>2</sub>As<sub>2</sub> and superconducting Sr<sub>0.85</sub>K<sub>0.15</sub>Fe<sub>2</sub>As<sub>2</sub> ( $T_c=28$  K) and Ba<sub>0.72</sub>K<sub>0.28</sub>Fe<sub>2</sub>As<sub>2</sub> ( $T_c=32$ K) single crystals studied by Raman spectroscopy. The frequency and linewidth of the B<sub>1g</sub> mode at 210 cm<sup>-1</sup> shows an appreciable temperature dependence induced by a superconducting and spin density wave transition. We give estimation to the electron-phonon coupling related to this renormalization. In addition, we observe pronounced quasi-elastic Raman response for the undoped compound, suggesting persisting magnetic fluctuations to low temperatures. In the superconducting state, the renormalization of an electronic continuum is seen with threshold energy of 61 cm<sup>-1</sup>.

**PB-15(초)****Origin and Consequence of Quantum Criticality in the Heavy Fermion****Compound CeRhIn<sub>5</sub>**박 두선, THOMPSON Joe<sup>1</sup>*성균관대학교, 물리. <sup>1</sup>Los Alamos National Laboratory.*

In strongly correlated electronic systems, where strong Coulomb interactions are important, competing interactions are almost degenerate and multiple degrees of freedom such as spin, charge, and lattice interact non-linearly, leading to new complex phenomena that cannot be captured by conventional theory. At a quantum critical point, where a phase transition occurs at absolute zero temperature, it is no more possible to describe the emergent state by Landau-Fermi liquids, namely the material organizing principle. The breakdown of Fermi liquids requires a new paradigm to properly address the new quantum liquids. In this symposium, we present recent progress in our understanding of the origin and consequence of quantum fluctuations in rare earth-based 4f quantum critical compounds, especially the heavy fermion compound CeRhIn<sub>5</sub> [1-5]. When subjected to pressure, ground state of the prototypical antiferromagnet CeRhIn<sub>5</sub> continuously varies between antiferromagnetism, coexistence of magnetism and superconductivity, and superconductivity. At a hidden quantum critical point where magnetic transition is completely suppressed to zero temperature, electrical resistivity shows isotropic quantum scattering, indicating a local nature of the quantum fluctuations. Dichotomy of strong enhancement of the electronic scattering and highest superconducting  $T_c$  at this critical point evidences that the unconventional superconductivity observed in CeRhIn<sub>5</sub> is a consequence of the local quantum fluctuations. References: [1] Tuson Park *et al.*, "Hidden magnetism and quantum criticality in the heavy fermion superconductor CeRhIn<sub>5</sub>," *Nature* 440, 65 (2006). [2] Tuson Park *et al.*, "Electronic duality in strongly correlated matter" *Proc. Nat. Acad. Sci. (USA)* 105, 6825 (2008). [3] Tuson Park *et al.*, "Isotropic quantum scattering and unconventional superconductivity," *Nature* 456, 366 (2008). [4] Tuson Park *et al.*, "Probing the nodal gap in the pressure-induced heavy fermion superconductor CeRhIn<sub>5</sub>," *Phys. Rev. Lett.* 101, 177002 (2008). [5] Tuson Park and J. D. Thompson, "Magnetism and superconductivity in strongly correlated CeRhIn<sub>5</sub>," *New. J. Phys.* 11, 55062 (2009).

KIM Ki-Seok

APCTP.

We find new mechanism of superconductivity beyond the spin-fluctuation theory, the standard model for unconventional superconductivity in the weak coupling approach, where Kondo fluctuations result in multi-gap superconductivity around an antiferromagnetic quantum critical point of the slave-fermion theory. Fingerprints of the hybridization mechanism are two kinds of resonance modes in not only spin but also charge fluctuations, originating from  $d$ -wave pairing of conduction electrons and spinless holons, respectively, thus differentiated from the spin-fluctuation mechanism. We show that the ratio between each superconducting gap for conduction electrons  $\Delta_c$  and holons  $\Delta_f$  and the transition temperature  $T_c$  is  $\Delta_c / T_c \sim 9$  and  $2\Delta_f / T_c \sim \mathcal{O}(10^{-1})$ , remarkably consistent with  $\text{CeCoIn}_5$ .

## Polarization-dependent XAS

NOH Han-Jin, JEONG Jinwon, JEONG Jinhwan, PARK Kyoung Ja, CHO En-Jin, KIM Hyeong-Do<sup>1</sup>, KIM Jae-Young<sup>1</sup>, KIM Sung Baek<sup>2</sup>, KIM Kyoo<sup>2</sup>, MIN B. I.<sup>2</sup>

*Dep. of Physics, Chonnam National University. <sup>1</sup>Pohang Accelerator Laboratory, POSTECH. <sup>2</sup>Dep. of Physics, POSTECH.*

Delafossite  $\text{PdCoO}_2$  is an interesting oxide in that its in-plane electrical conductivity is higher than that of Pd metal, which is quite contrast to the general trend that metallic oxides have lower conductivity due to electron correlation effects. In order to understand the peculiar property, we investigated the electronic structure by using angle-resolved photoemission spectroscopy (ARPES), core level x-ray photoemission spectroscopy (XPS), and polarization-dependent x-ray absorption spectroscopy (XAS). The XAS spectra show the Co valence state and the orbital character of the conduction band of delafossite  $\text{PdCoO}_2$ . The XPS spectra reveal that the compound consist of correlated insulator layers and good metallic layers[1]. The ARPES spectra show that the bulk electronic structure is in a good agreement with the band calculation result by the LDA method. An explicit connection between the electronic structure and the anisotropic high conductivity has been established by ARPES [2,3]. By combining all the spectroscopic data, we provide a consistent picture on the origin of the good conductivity of the delafossite oxide. [1] H.-J. Noh et al., Phys. Rev. B 80, 073104 (2009). [2] H.-J. Noh et al., Phys. Rev. Lett. 102, 256404 (2009). [3] K. Kyoo et al., Phys. Rev. B 80, 035116 (2009).

**PB-18(초)****Orbital order and spin fluctuations in geometrically frustrated ferrimagnetic  $\text{MnV}_2\text{O}_4$  studied by neutron scattering**

CHUNG Jae-Ho

*Department of Physics, Korea University.*

Geometrical frustration is a phenomenon in which geometrical properties of the crystal lattice prevents simultaneous minimization of the interaction energies, resulting in highly degenerate ground states. One of the best known examples is observed from the family of  $\text{ACr}_2\text{X}_4$  ( $A = \text{Zn, Cd, Hg}$ ;  $X = \text{O, S, Se}$ ) spinels, where the strong geometrical frustration exists in the antiferromagnetic interactions between  $\text{Cr}^{3+}$  ( $3d^3$ ,  $S = 3/2$ ) ions located at the vertices of the corner-shared network of tetrahedra. In their disordered cubic phases, highly degenerate spin fluctuations are observed in the form of novel short-range spin clusters. The degeneracy is often overcome by different types of symmetry-lowering lattice distortions. When interactions beyond the nearest neighbors are turned on, complex magnetic order is often accompanied by interesting physical properties, such as relaxor ferroelectricity or colossal magnetoresistance. Recently, we have used neutron scattering and investigated the magnetic order and spin fluctuations in ferromagnetic  $\text{MnV}_2\text{O}_4$  spinel. The magnetism in this compound involves secondary antiferromagnetic interactions between  $\text{Mn}^{2+}$  ( $3d^5$ ,  $S = 5/2$ ) and  $\text{V}^{3+}$  ( $3d^2$ ,  $S = 1$ ). As a result, noncollinear magnetic order via multiple transitions is observed. In the ordered phase, the lattice becomes tetragonally distorted due to ordering of  $t_{2g}$  electron orbital. The spin wave dispersions observed by neutron spectroscopy reveal that the exchange interactions between  $\text{V}^{3+}$  ions are spatially anisotropic. The interactions are stronger within the tetragonal  $ab$  plane, reflecting the associated orbital order. In the disordered phase, a new kind of fluctuating spin clusters is observed by neutron scattering. Although the primary interaction is between  $\text{V}^{3+}$  spins, their geometrical frustration forces them to be superseded by the secondary interaction between  $\text{Mn}^{2+}$  and  $\text{V}^{3+}$  spins. As a result, medium-range spin clusters involving both spins emerge as the basic unit of the quasi-elastic spin fluctuations.

**PC-01(초)****Semiconductor Optics: Applications to Photovoltaics and Solid State Lighting**

STANTON C. J.

*University of Florida, Department of Physics.*

We provide an overview of the fundamental semiconductor physics relevant to Photovoltaics (solar cells) and Solid State Lighting (LEDs and lasers). Topics to be discussed include: 1) electronic structure, 2) excitonic and many-body effects, 3) diffusion and transport and 4) scattering and recombination mechanisms. We discuss how each of these affects the optical properties of semiconductors and limits device performance. We will show how optical properties can be enhanced or modified through the use of heterojunctions as well as nano-engineered structures (quantum wells, quantum dots and quantum wires) where quantum confinement effects are important. As an example, we show how quantum confinement can be utilized to create luminescence in porous Silicon. Finally, we show how semiconductors can be used to generate radiation below the visible portion of the spectrum, which is important for developing new THz sources.

**PC-02(초)****High-efficiency GaInP/LCM-GaInP/GaAs Triple-junction Solar Cells with****Antireflective Subwavelength Structures**

이 용탁

광주과학기술원.

Currently, state-of-the-art high efficiency III-V solar cells utilize a triple-junction design that includes a Ge bottom junction formed in the Ge substrate in conjunction with lattice-matched GaInP and GaAs top junctions. However, the Ge junction absorbs approximately two times more low energy photons (0.67 eV) than that of the GaInP (1.86 eV) and GaAs (1.39 eV) junctions, which leads to difficulty of the current matching together with growth instability. In this study, we propose a novel design that contains a lateral composition modulation (LCM) GaInP layers to improve the device performance and reliability. In addition, we propose and demonstrate the antireflective subwavelength structures to enhance the light absorption over a wide wavelength and angular range of incident light.

P

**PC-03****CIGS Thin Film Solar Cells : Current Status and Key Issues**

윤 재호

한국에너지기술연구원.

CIGS 박막 태양전지는 결정질 실리콘 태양전지에 비해 제조단가가 낮고 박막 태양전지중에서 가장 효율이 높아 현재 많은 연구가 진행되고 있으며 대면적 모듈의 상용화도 성공적으로 진행되고 있다. 미국의 NREL에서도 19.9% 효율의 보고 하고 있으며 본 연구팀에서도 18.8%의 최고 효율을 보고한 바 있다. 세계적으로 이러한 공정기술의 발전에도 불구하고 CIGS 재료 및 소자에 대한 체계적인 이해는 부족한 상황이다. Defect을 통한 도핑, 결정립계의 역할, Na 도핑효과, 광흡수층 밴드갭 효과, CdS 버퍼층의 역할 등이 그 대표적 이슈들이다. 본 발표에서는 CIGS 박막 태양전지의 개요 및 연구동향과 함께 최근 논의되고 있는 재료 및 소자에 대한 이슈들을 소개할 예정이다. 이를 통하여 CIGS 박막 태양전지에 대한 이해를 높일 수 있는 방법론을 모색해 보고자 한다.

## PC-04

## Chemical Solution Syntheses of Cu-In-Ga-Se Thin Films for Photovoltaic Cells

JUNG Duk-Young

Department of Chemistry, Institute of Basic Sciences and Sungkyunkwan Advanced Institute of NanoTechnology, Sungkyunkwan University, Suwon 440-746, Korea.

Nano powder of the I-III-VI compound semiconductor, Cu(InGa)Se<sub>2</sub> (CIGS), was synthesized by ultrasound irradiation under ambient pressure below 100°C and characterized by powder X-ray diffraction, scanning electron microscopy, absorption spectroscopy and energy-dispersive X-ray analyses. The samples have single phase chalcopyrite structure and the particle sizes less than 50 nm. Synthetic conditions were determined for the crystallized CIGS nanoparticle formation to prevent from Cu<sub>2</sub>Se, Cu<sub>2</sub>-xSe, and CuSe etc. The single phase CIGS nanoparticles were applied to paste coating of thin films photovoltaic cells. The electrochemical deposition of CIGS thin films will be also presented. In aqueous solutions, the different chemical compositions of CIGS thin films were obtained, depending on pH, concentration of starting materials and deposition potentials. The surface morphology of the prepared CIGS thin films was also influenced by applying ligands to the solutions during the electrochemical deposition.

## PC-05

## Characterizations of Polar- and Nonpolar-GaN Schottky Junctions by

## Conductive Atomic Force Microscopy

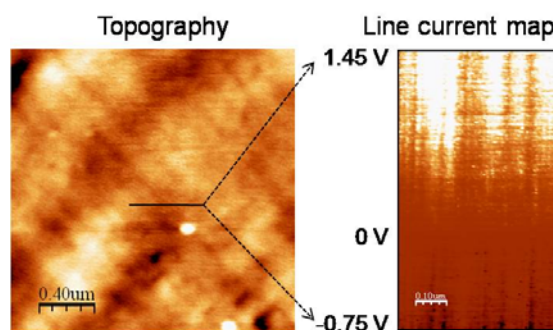
PHARK Soo-Hyon, KIM Hogyoung<sup>1</sup>, SONG Keun Man<sup>2</sup>, KANG Phil Geun<sup>2</sup>, SHIN Heung Soo<sup>2</sup>, KIM Haeri, KIM Dong-Wook

Department of Physics and NREC, Ewha Womans

University. <sup>1</sup>College of Humanities and Sciences, Hanbat

National University. <sup>2</sup>Korea Advanced Nano Fab Center.

We have characterized the local electrical properties of Pt/nonpolar a-GaN (np-GaN) and Pt/polar c-GaN (p-GaN) Schottky contacts. Topographic images and corresponding current maps were obtained simultaneously by conductive atomic force microscopy (C-AFM). Contrary to the p-GaN, np-GaN shows additional groove structures much bigger than the granular structures. I-V curves, obtained by C-AFM measurements, showed rectifying behaviors. This indicated that the Pt/GaN contacts formed Schottky junctions. Two dimensional current maps of both junctions revealed a correlation between the grain structures and the local conduction properties. In addition, the groove structures in np-GaN significantly affected the spatial distribution of the current flow. All these observations indicate that microstructural inhomogeneity played important roles in the GaN-based junction characteristics.



**PC-06(초)****Third generation solar cells: all-silicon tandem solar cells**

PARK Sangwook, CONIBEER Gavin, PEREZ-WURFL I., HUANG S.J., SONG D., CHO Eun-Chel, KÖNIG D., GENTLE A., HAO X.J., SO Y.H., GREEN Martin A.

*University of New South Wales, ARC Photovoltaics Centre of Excellence.*

Material costs will continually push photovoltaics to ever increasing efficiency to take advantage of the cost leverage thereby available. The tandem cells is one of good approaches for using a full solar spectrum and improving solar cell performance. By restricting the dimensions of silicon to less than Bohr radius of bulk crystalline silicon (~ 5 nm), quantum confinement cause its effective bandgap to increase. Therefore silicon quantum dot superlattice can be a good candidate for realizing all silicon tandem solar cells. This work seeks to engineer wide-bandgap silicon-based materials by using quantum-confinement in silicon quantum dots or quantum dots from other Group IV elements dispersed in a matrix of silicon carbide, nitride or oxide. The material properties of silicon (Si) quantum dot (QD) superlattices are experimentally investigated. Further, Si QDs heteroface devices and homojunction devices were fabricated to investigate carrier properties and conduction behaviour. Uniformly sized quantum dots dispersed in a silicon dioxide (SiO<sub>2</sub>) matrix with dopants (phosphorus and boron) were fabricated by precipitation from silicon rich oxide (SRO) deposited by RF co-sputtering. The Si QDs in SiO<sub>2</sub> matrix films were investigated by various optical and electrical characterisation techniques. The electrical and photovoltaic properties of the devices were characterized by illuminated and dark *I-V* measurements, *C-V* measurements and spectral response measurements. Temperature dependent dark *I-V* measurements suggest that the carrier transport in the devices is controlled by recombination in the space charge region. Current tunnelling through the QD layer was observed from the solar cells with dot spacing of 2 nm or less. Successful demonstration of Si QD photovoltaic devices is an encouraging step towards realisation of all-silicon tandem solar cells based on Si QD materials.

**PC-07(초)****Next-generation solar cells using Si and Si<sub>1-x</sub>Ge<sub>x</sub> nano- and microwire arrays**

이 정호

*한양대학교 재료화학공학부.*

Silicon wire-based solar cells are one of the attractive candidates for next-generation photovoltaic devices; however, Si has a relatively weak absorption in infrared region, alloying with Ge allows for the useful range of the solar spectrum spanning into a longer wavelength band due to a lower bandgap of Ge. Here, I present the vertical Si and Si<sub>1-x</sub>Ge<sub>x</sub> wires fabricated by metal-assisted electroless etching at a large wafer scale. Shallow junctions could be formed using plasma immersion ion implantation (PIII) and spin on doping (SOD) for making a radial p-n junction of wire-based solar cells. Scanning electron microscope (SEM) image of the Si and Si<sub>1-x</sub>Ge<sub>x</sub> wire arrays revealed the periodic, uniform arrays of a vertical wire which were patterned using a 300-nm-thick oxide mask with a hole size of 2 μm and 4 μm pitches. The diameter and a length of these wires are ~2 and ~20 μm, respectively.

**PC-08(초)****ZnO-Based Transparent Conducting Oxide for Thin Film Solar Cells**

윤 선진, 김 준관, 임 정욱, 이 재민

한국전자통신연구원.

최근 환경오염과 자원고갈에 대한 자각이 고조됨에 따라 대체 청정에너지에 대한 관심과 투자가 크게 증가하고 있으며, 청정에너지 중에서도 특히 태양전지에 대한 기술 개발 요구가 커지고 있다. 여러 종류의 태양전지 중 박막태양전지가 가진 많은 장점 때문에 기술개발이 집중적으로 이루어지고 있는데, 고효율 박막태양전지를 얻기 위한 핵심 기술 중 하나이며, 모든 박막태양전지에서 공통적으로 요구되는 기술이 바로 투명전극 기술이다. 투명전극으로 사용되는 투명전도성 산화막 (transparent conducting oxide, TCO)은 대표적으로 InSnO, SnO:F, ZnO:Al, ZnO:Ga, ZnO:B 등이 있는데, 본 논문에서는 여러 종류의 투명전극 소재에 대해 개괄적으로 특징을 살펴보고, 박막태양전지 종류 별로 유망한 투명전극 소재를 소개하고자 한다. 또한 저자 등이 Magnetron sputter deposition 기술을 이용하여 연구 개발하고 있는 ZnO 계 TCO의 특성과 공정 조건에 따른 특성변화를 보고하고, 전도성과 투명도에 영향을 미치는 박막 물성 등에 대해 논의한다. RF-Magnetron sputter deposition 공정으로 제조한 ZnO:Ga TCO 박막의 비저항은  $2 \times 10^{-4} \Omega \cdot \text{cm}$ , 가시광선 투과도는 92%였다. 아울러 박막태양전지의 효율향상에 크게 기여하는 것으로 알려져 있는 TCO texturing 공정에 관하여 소개하고자 한다.

**PC-09(초)****Crystalline (bulk) and thin-film Si solar cells**

최 용우

LG 전자기술원.

태양광 시장은 결정질 실리콘 태양전지가 주도하고 있고, 원재료 사용량을 크게 줄일 수 있는 박막 실리콘 태양전지는 제조원가를 낮출 수 있어 많은 연구가 이루어지고 있다. "Grid Parity"는 태양광 발전단가가 타 발전원의 발전단가와 같아지는 것으로, "Grid Parity"가 실현되면 태양광 발전시장은 보조금 없이도 경제성을 확보, 폭발적으로 성장할 것으로 기대하고 있다. 태양전지 제조시설에 대한 과잉투자와 전 세계적인 금융위기로 공급과잉이 초래되었고, 태양광 모듈의 가격은 크게 낮아졌다. 일부 지역에서는 이미 "Grid Parity"가 실현되었다.본 발표에서는 결정질 및 박막 실리콘 태양전지의 "Grid Parity" 달성을 위한 노력을 소개하고자 한다.

**PC-10(초)****Measurement Techniques and Instruments for Solar Cells**

YOON CHUL OH

*McScience Inc..*

Various techniques for measurements of photovoltaic efficiency and spectral response as well as methods for characteristic mapping and imaging of solar cell products will be introduced. International test standards for characterization of photovoltaic cells will be reviewed, and technical details relevant to optical components for light sourcing/detection and electronic components for power control and measurement, which constitute currently available standard test systems, will be discussed. Brand-new testing technologies for industrial application of solar cells also will be introduced.

P

**PC-11(초)****Concentrator Solar Cells**

KIM Dongkyun, KIM Dongho, CHANG Jieun, KIM Yungi

*SAMSUNG Advanced Institute of Technology, Gyeonggi-Do 443-742.*

In order to increase energy conversion efficiency and reduce the electricity generation cost at the same time, many different solar cell technologies are being extensively explored. As a solution, concentrator solar cells combine high efficiency solar cells with low cost concentrating optics. Many design parameters need to be optimized to get the most benefit out of concentrator solar cells: high or low concentration? III-V multijunction or Si? lens or mirror? 1-axis or 2-axis tracking? In this presentation, we will review the current status of concentrator solar cells and discuss technological as well as industrial challenges to reach grid parity with concentrator solar cells.

**PC-12(초)****Organic Solar Cells on SWCNT Electrodes**

LEE Soonil, YIM Jonghyuk

*Division of Energy Systems research, Ajou University.*

Some of the key issues related to next-generation solar cells are the fabrication of flexible and light devices, compatibility with solution processing, and very high energy conversion efficiency. Flexibility and light weight of solar cells are important because they can make solar cells omnipresent and more portable. One of the serious roadblock to the fabrication of flexible solar cells is the development of flexible electrodes. At least one electrode has to be transparent for solar cells, and ITO has been the most popular transparent conducting material. However, ITO is not flexible and can be easily cracked when deformed. Therefore, it is essential to find an alternative transparent conducting material. We have been working on new types of transparent electrodes that consist of network films of single-wall carbon nanotubes (SWCNTs). We are going to report how to make SWCNT transparent conducting films, and how to reduce their sheet resistance without losing their transparency in visible wavelength range. Because the SWCNT films can be made from a SWCNT-dispersion solution, it is possible to fabricate organic solar cells through a series of solution processes. We are going to present examples of bulk-heterojunction organic solar cells on SWCNT electrodes, and the correlation between the operation of solar cells and the characteristics of SWCNT electrodes.

**PC-13(초)****Transparent conductive oxide technologies for organic photovoltaics**

김 한기

*경희대학교, 디스플레이재료공학과.*

최근 유기태양전지가 가지는 여러가지 장점으로 인해 차세대 태양전지로서의 가능성이 날로 높아지고 있다. 특히 단순한 구조, 간단한 제작공정, 저가 제작 가능성 및 플렉시블 태양전지 응용성으로 인해 그 가능성이 높이 평가되고 있다. 이러한 유기태양전지를 구성하는 핵심 요소중 ITO로 대표되는 투명전극은 빛의 투과를 위한 높은 투과도와 형성된 홀 캐리어의 이동을 위해 낮은 저항을 필요로 하는 매우 중요한 요소이다. 특히 대면적의 유기태양전지를 구현하기 위해선 낮은 저항과 높은 투과도를 가지는 투명전극의 구현이 매우 중요하다. 최근 PEDOT:PSS 전극이나 CNT sheet를 이용한 전극이 유기태양전지용 전극으로 가능성이 높아지고 있으나 전극의 낮은 비저항을 고려할 때 아직까지 산화물 재료를 근간으로 하는 투명전도산화물(Transparent conducting oxide:TCO)을 배제할 수 없는 상황이다. 따라서 본 발표에서는 유기태양전지에 있어 투명전극의 역할 및 중요성을 설명하고 현재 까지 진행되어 온 여러가지 투명전극 기술을 소개한다. 특히 본 연구진에 의해 진행되어 온 다양한 DMD 구조의 투명전극과 저가의 In-free 투명전극의 특성을 소개하고 유기태양전지로서의 응용가능성을 논하고자 한다. 또한 Roll-to-Roll 스퍼터에 의해 제작된 플렉시블 투명 전극의 특성을 소개하고 기존의 ITO 전극을 대체하기 위한 가능성을 소개하고자 한다.

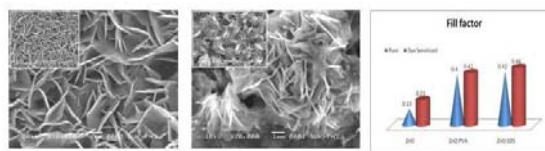
## PC-14

### Nanostructured Zinc Oxide Thin Films via Electrodeposition and their

#### Photoelectrochemical Performance

INAMDAR A. I., JUNG Kyooho<sup>1</sup>, KIM Young sam<sup>1</sup>, IM Hyunsik<sup>1</sup>, PATIL P. S.

Shivaji University, Department of Physics. <sup>1</sup>Dongguk University, Department of Semiconductor Science.



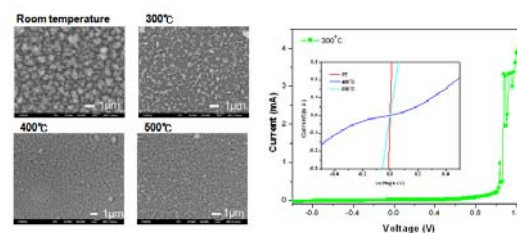
Dye-sensitized solar cells (DSSCs) based on porous thin film of wide band gap oxide semiconductor modified by dye molecules have received considerable attention as a cost effective alternative to conventional solar cells. ZnO is one of the potential semiconductor materials in DSSCs due to its stability against photo corrosion and photochemical properties similar to TiO<sub>2</sub>. It is well known that nanoporous film like TiO<sub>2</sub> reported by Grätzel and co-workers can lead to very high solar-to-electric energy conversion efficiency (above 10%). Therefore, the preparation of nanoporous ZnO film is a key to improve the performance of ZnO-based DSSCs. However, it still remains a big challenge to develop simple and reliable synthetic methods for hierarchical architectures with controlled morphology, orientation, and surface architectures, which strongly affect the properties of nanostructured materials. A plethora of physical and chemical methods have been used for the synthesis of ZnO nanostructures. Electrodeposition is of particular interest due to low cost, environmentally friendly, and room temperature growth. In the present investigation the main aim is to synthesize ZnO nanocrystalline thin films and to enhance photoelectrochemical performance of ZnO electrode. In this direction the attempts were made to deposit ZnO nanocrystalline thin films by varying various process parameters and by using novel approaches, as well. The structural, morphological, optical and photoelectrochemical properties of ZnO nanostructures have been studied.

## PC-15

### Synthesis and characterization of Cu(In,Ga)Se<sub>2</sub> nanoparticles and thin-films

JEONG Ah Reum, KIM Gracia, JO William  
Department of Physics, Ewha Womans University, Seoul, Korea.

The semiconductors in the quaternary system containing Cu, In, Ga, and Se have been considered as one of the candidate absorber materials for high efficiency solar cell. Using these materials, a solar conversion efficiency of 19.9% has recently been reported in Cu(In,Ga)Se<sub>2</sub> (CIGS) device [1]. Although studies for improving the performance of CIGS solar cell devices have been progressed, fundamental understanding of the CIGS materials is insufficient, especially in nano-scale dimension. CIGS nanoparticles and thin-films of a thin absorber layer for the CIGS based solar cells were synthesized by pulsed laser ablation and co-evaporation, respectively [2]. Typical size of the nanoparticles was ~10nm and they were treated under various temperatures to investigate characteristic change because temperature has been known one of the key points to decide properties as well as structure. Morphology, phase formation, chemical composition, and junction of these nanoparticles-derived films and thin-films have been characterized using field emission scanning electron microscopy (FE-SEM), X-ray diffraction (XRD), atomic force microscope (AFM), energy dispersive x-ray spectroscopy (EDS), micro-Raman spectroscopy, X-ray photoelectron spectroscopy (XPS), current-voltage measurements and so on. In this study, we investigate the physical properties of each sample and consider the potential application of solar cells. Study of CIGS nano-materials is worthy of understanding their properties and improving solar cell applications. [1] Ingrid Repins, Miguel A. Contreras, Brian Egaas, Clay DeHart, John Scharf, Craig L. Perkins, Bobby To, and Rommel Noufi, *Prog. Photovolt: Res. Appl.* 16, 235 (2008).[2] A. R. Jeong, H. R. Yoon, Y. J. Oh, T. Y. Kim, W. Jo, and M. Kim, *J. Nanosci. Nanotechnol.* 9, 901 (2009).



Left: SEM micrograph of CIGS nanoparticles obtained, Right: electrical properties of Ag / CIGS nanoparticles / ITO after different thermal treatment

**D-01****Reconstruction and Evaporation at Graphene Nanoribbon Edges**

LEE Gun-Do, YOON Euijoon, HWANG Nong-moon, WANG Cai-Zhuang<sup>1</sup>, HO Kai-Ming<sup>1</sup>

*Dept. of Materials Science and Engineering, Seoul National University. <sup>1</sup>Dept. of Physics, Iowa State University.*

Reconstruction and evaporation of carbon atoms at the edges of graphene nanoribbon are investigated by tight-binding molecular dynamics simulations and ab initio calculations. The simulations show that reconstruction through the formation of zigzag pentagon-heptagon pairs can take place quickly along the zigzag edge. Such reconstruction is energetically favorable and can help carbon atoms to evaporate from the edge easily. On the other hand, graphene nanoribbons with armchair edges are very stable. Only at very high temperature the armchair edge is found to change into zigzag edge structure which further accelerates the evaporation of carbon atoms and leads to formation of carbon linear chains between the patches of zigzag edge. Evaporation of carbon atoms in both zigzag and armchair edges is preceded by the formation of heptagon rings which service as a gateway for carbon atoms to escape. In the simulation for graphene nanoribbon junction of armchair-zigzag-armchair, carbon atoms are evaporated row-by-row from the outermost row of the zigzag edge while the armchair edge almost kept intact.

**D-02****Effects of the Au intercalation into the graphene/Ni(111) surface: Density-functional theory calculations**

박 재환, 정 성철, 강 명호

*Pohang university of Science and Technology, Department of physics.*

We use density functional theory calculations to investigate the atomic and electronic structure of the graphene/Au/Ni(111) surface. A recent ARPES study [1] reported that Au intercalation greatly changes the properties of a single-layer graphene grown on Ni(111) and the resulting surface electronic structure is almost identical to that of a free-standing graphene layer. Based on our total-energy calculations, we propose a structural model with a Au coverage of 0.75 ML and determine the equilibrium graphene/Au/Ni(111) structure. The resulting structure shows a surface band structure featuring well resolved carbon-derived states bearing the Dirac cone structure of an isolated graphene layer with the crossing point almost at the Fermi energy. This theory thus supports the experimental suggestion that the graphene on Au/Ni(111) represents a quasi-free-standing graphene layer. [참고문헌]1. A. Varykhalov, J. Sanchez-Barriga, A. M. Shikin, C. Biswas, E. Vescovo, A. Rybkin, D. Marchenko, and O. Rader, Phys. Rev. Lett. 101, 157601 (2008)

**D-03****Tetra(4-carboxyphenyl)porphine를 이용한 그래핀 표면의 응용**

강 세준, 이 미지, 신 현준<sup>1</sup>, 김 기정<sup>1</sup>, 김 봉수<sup>1</sup>, 백 재윤<sup>1</sup>

포항공과대학교, 물리학과. <sup>1</sup> 포항가속기연구소.

Tetra(4-carboxyphenyl)porphine(TCPP) 흡착으로부터 그래핀 표면의 기능화에 대한 연구를 방사광을 이용한 광전자 분광법으로 분석하였다. 최근 들어 그래핀을 이용한 소자개발에 있어서 그래핀의 우수한 전기적 특성을 저해하지 않으며 그 표면의 화학적 활성도를 개선하고자 하는 필요성이 대두되고 있다. 본 연구에서는 6H-SiC 표면 위에 수층으로 에피텍셀리 성장시킨 그래핀을 이용하였고, 분자 당 4개의 수산화 작용기를 가지고 있는 TCPP를 이용하여 그래핀 표면과 비공유성 결합을 유도하는데 성공하였다. 수산화기의 존재는 밸런스밴드, O1s, C1s core-level 스펙트럼으로부터 확인할 수 있었다. 또한 그래핀 표면 위에 TCPP의 흡착량을 증가시킴으로서 일함수 감소현상을 관찰할 수 있었으며 이는 음성전하가 TCPP 분자로부터 그래핀으로 흘러가는 n-type 도핑 현상을 간접적으로 보여줌을 의미한다. 나아가 수산화기 기능성을 이용한 초박막 증착의 대표적 방법인 원자적층법에 본 연구 결과를 적용했을 때 그래핀 표면 위에 초박막 유전층을 효과적으로 증착할 수 있음을 확인하였고, 격자구조물을 이용하여 초박막 유전층의 pattern이 가능함을 Scanning PhotoEmission Microscopy(SPEM)를 이용하여 확인하였다. 따라서 연구결과가 표면위에 박막 증착을 필요로 하는 다양한 응용분야에 새로운 대안의 방법이 될 수 있음을 제안한다.

D

**D-04****Surface Diffusion in Growth of Perovskite Oxides in a Nucleation Regime**

장 영준, 박 수현<sup>1</sup>, 노 태원

서울대학교 물리천문학부 산화물전자공학연구단. <sup>1</sup> 이화여자대학교 물리학과.

Thin film growth systems combined with scanning tunneling microscopy (STM) can provide a powerful way for the in-situ analysis on the surfaces/interfaces of transition metal oxide thin films down to the atomic level. STM combined with the classical nucleation theory was utilized to verify the nucleation and surface diffusion behaviors of perovskite oxides SrRuO<sub>3</sub> and SrTiO<sub>3</sub>, grown on TiO<sub>2</sub>-terminated SrTiO<sub>3</sub> (001) surface by pulsed laser deposition (PLD). We observed that the critical minimal size of SrTiO<sub>3</sub> is 16 unit cells (4 x 4) in typical growth conditions. The growth behavior of the first monolayers of both oxides look very similar each other, also were confirmed by the activation energies calculated from the island densities, while they showed different growth modes from the second layers. We attribute the diffusion behaviors for the first layers in both oxides to the same interface chemical configurations(SrO-TiO<sub>2</sub>) each other.

**D-05****Reduction Of Coulomb Interaction Energy And Charge Transfer Energy Of****Ultrathin NiO Films On Ag(001)**

YANG Seolun, PARK HyunKook, KIM J. -S., HWANG H. -N.<sup>1</sup>, HWANG C. -C.<sup>1</sup>, KIM H. -D.<sup>1</sup>

*Sookmyung W. Univ., Physics. <sup>1</sup>Pohang Acceleration Laboratory.*

NiO is a representative charge transfer insulator in which both the onsite Coulomb interaction on Ni cation and charge transfer between oxygen anion and Ni cation play significant role in the determination of its electronic structure. Since charge transfer energy  $\Delta$  and on-site Coulomb interaction energy  $U$  are sensitive to the environment of the NiO film, we have investigated the variation of  $\Delta$  and  $U$  upon reducing the thickness of the film down to 1 ML that is assumed to be a quasi-two dimensional system. We retrieve the information of both  $\Delta$  and  $U$  from the peak position and intensity of Ni 2p and Ni LMM Auger energy. [1] As the thickness of NiO films is decreased from 15.90 to 0.53 ML, monotonic decrease of both  $\Delta$  and  $U$  is observed. Such reduction is attributed to the image potential screening by Ag substrate and polarization energy of nickel oxide. [1] Altieri et al., Phys. Rev. B 59 R2517 (1999)

**D-06****One-dimensional Phase Separation on a vicinal Si(111) surface**

KIM Minkook, OH Dong-Hwa<sup>1</sup>, BAIK Jaeyoon<sup>2</sup>, JEON Cheolho<sup>3</sup>, PARK Chong-Yun, AHN Joung Rea<sup>1</sup>  
*BK21 Physics Research Division and Center for Nanotubes and Nanostructured Composites (CNNC),  
 Sungkyunkwan University, Suwon 440-746, Korea. <sup>1</sup>BK21 Physics Research Division, Sungkyunkwan  
 University, Suwon 440-746, Korea. <sup>2</sup>Center for Nanotubes and Nanostructured Composites (CNNC), Sungkyunkwan  
 University, Suwon 440-746, Korea, Beamline Research Division, Pohang Accelerator Laboratory, POSTECH,  
 Pohang 790-784, Korea. <sup>3</sup>Center for Nanotubes and Nanostructured Composites (CNNC), Sungkyunkwan  
 University, Suwon 440-746, Korea.*

We studied the one-dimensional (1D) phase separation of the  $5 \times 5$  and  $7 \times 7$  phases on vicinal Si(111) surfaces using scanning tunneling microscopy and first principle calculations. A small change of the crystallographic orientation of a Si(557) surface produced two types of (111) terraces with different widths ( $L$ ), and stabilized the  $5 \times 5$  phase and separated it from the  $7 \times 7$  phase, while only the  $7 \times 7$  phase is stable on the Si(557) surface. Interestingly, this makes a 1D (111) terrace prefer selectively only one of the  $5 \times 5$  and  $7 \times 7$  phases resulting in long-range orders along the step edge direction above 300nm. The widths of 1D  $5 \times 5$  and  $7 \times 7$  domains were  $L=12$  and  $L=9$ , which are close to that of the single unit cell of a  $5 \times 5$  phase and the half unit cell of a  $7 \times 7$  phase. However, the 1D  $5 \times 5$  and  $7 \times 7$  phases were arranged randomly across the step edge direction. This anisotropic coherent length of the  $5 \times 5$  and  $7 \times 7$  phases implies that the phase separation is strictly 1D. These phases were stable energetically by terminating their unit cell boundary at the step edges at room temperature, which is supported by first principle calculations. In this presentation, we will introduce the detailed STM images of 1D phase separation on vicinal Si(557) surfaces compared with a Si(557) surface and will describe the relative stability of the separated  $5 \times 5$  and  $7 \times 7$  phases on (111) terrace with a finite width ( $L$ ) using first principle calculations.

**D-07****Self-Assembly of One-Dimensional Molecular Wires on the Si(001) Surface**

CHOI Jin-Ho, CHO Jun-Hyung

*Hanyang university, Physics.*

One-dimensional (1D) molecular wire formed on semiconductor surfaces can be utilized as a nano-electronic circuit connecting two electronic devices. Thus, it is important to understand and control the formation of 1D molecular wires, thereby designing a nano-electronic circuit on the substrate. Using first-principles density-functional theory calculations, we have investigated the growth mechanism of various self-assembled 1D molecular wires on H-terminated Si(001) surface. Here we focus on two issues for the formation of 1D molecular wires on Si(001): (i) how to enhance the stability of 1D molecular wires formed parallel to the Si dimer rows [1] and (ii) growth mechanism for the formation of 1D molecular wires across the Si dimer rows [2]. [1] Jin-Ho Choi and Jun-Hyung Cho, Phys. Rev. Lett. 98, 246101(2007). [2] Jin-Ho Choi and Jun-Hyung Cho, Phys. Rev. Lett. 102, 166102 (2009).

D

**D-08****Nearly Massless Hole Carriers at Silicon Subsurface with a Monolayer Metal Film**

KIM Keun Su, YEOM Han Woong

*Institute of Physics and Applied Physics and Center for Atomic Wires and Layers, Yonsei University.*

Silicon is the prime host material for today's electronic device technology. However, it has recently been challenged by other materials like graphene and bismuth compounds whose conducting properties are characterized by extremely light (or massless) Dirac particles with linear energy-momentum relation. The carrier mobility in those materials is thus exceptionally high while that in silicon has been limited to be improved. Here we report using angle-resolved photoemission that the characteristic surface band structure in a lead overlayer on silicon substrates derives the hole states in subsurface Si inversion layers to have nearly linear dispersion with an extremely small effective mass. This can be accounted for by repulsive interaction between surface and subsurface Si bands as is well modeled by k-p perturbation theory with the Kane model. This mechanism, in principle, can be applied to any other semiconductors to improve their mobility and particularly offers a practical solution for imbalance between hole and electron mobility in III-V compound semiconductors.

**D-09****Van der Waals Interaction in the Adsorption of  $C_4H_4N_2$  on Si(100): DFT****Calculations**

JUNG Sung Chul, KANG Myung Ho

포스텍 물리학과.

In a recent density-functional theory (DFT) study for  $C_6H_6/Si(100)$ , Johnston et al. [1] reported that the van der Waals (vdW) interaction is important not only in weakly interacting systems but also in chemically bonding systems. They showed that, when including a correction using the vdW density functional (vdW-DF) developed by Dion et al. [2], the butterfly structure becomes more stable by 0.05 eV than the tight-bridge structure, the previously most stable in several DFT studies without vdW corrections. In the present study, we examine the effect of the vdW interaction on the adsorption of  $C_4H_4N_2$  on Si(100) by applying the vdW-DF correction of the Ref. [2]. We find that, while in the routine DFT calculations the end-on structure is more stable by 0.10 eV than the cross-row structure, in the vdW-DF calculations the cross-row structure becomes more stable by 0.11 eV than the end-on structure. This result provides another example that the vdW interaction can have a strong influence on the adsorption energetics of the covalent bonding systems. [1] K. Johnston, J. Kleis, B. I. Lundqvist, and R. M. Nieminen, Phys. Rev. B 77, 121404 (R) (2008). [2] M. Dion, H. Rydberg, E. Schroder, D. C. Langreth, and B. I. Lundqvist, Phys. Rev. Lett. 92, 246401 (2004).

**D-10****Coherent x-ray scattering study of block copolymer films**SONG Sanghoon, CHA Wonsuk, JIANG Zhang<sup>1</sup>, NARAYANAN Suresh<sup>1</sup>, SINHA S. K.<sup>2</sup>, KIM Hyunjung

Sogang University, Department of Physics & Interdisciplinary Program of Integrated Biotechnology. <sup>1</sup>Advanced Photon Source, Argonne National Laboratory. <sup>2</sup>University of California San Diego, Department of Physics.

We have studied the surface dynamics of poly(styrene)-b-poly(dimethylsiloxane) (PS-b-PDMS) block copolymer films by x-ray photon correlation spectroscopy (XPCS). In this case, PDMS forms micelle cores surrounded by PS shells. The surface tension of films by x-ray diffuse scattering showed an evidence of PDMS-rich layer near the surface. By x-ray reflectivity, we observed the segregation layer near the surface appeared with increasing temperature and obtained the roughness, thickness and electron density of each layer. The results of surface relaxation time as a function of in-plane wave vector transfer from XPCS were analyzed with the bilayer model based on the theory of hydrodynamics. Finally we obtained the viscosity of each layer as a function of temperature. This work was supported by National Research Foundation of Korea, Seoul Research and Business Development Program, and Sogang University Research Grant.

**D-11****Indium-induced triple-period atomic wires on a vicinal Si(111) surface: In/Si(557)**

SONG Inkyung, OH Dong-Hwa<sup>1</sup>, NAM Jeong Ho<sup>2</sup>, KIM Minkook, JEON Cheolho<sup>2</sup>, PARK Chong-Yun<sup>2</sup>, AHN Joung Real<sup>2</sup>

*BK21 Physics Research Division and Center for Nanotubes and Nanostructured Composites (CNNC), Sungkyunkwan University, Suwon 440-746, Korea. <sup>1</sup>BK21 Physics Research Division, Sungkyunkwan University, Suwon 440-746, Korea. <sup>2</sup>Center for Nanotubes and Nanostructured Composites (CNNC), Sungkyunkwan University, Suwon 440-746, Korea.*

An indium-induced one-dimensional (1D) surface reconstruction on a Si(557) surface was studied by the combined approach of scanning tunneling microscopy (STM) and first principles calculations. Low-energy electron diffraction revealed a (1×3) phase with a triple-period along the step edge direction, which was also confirmed by STM. The STM images showed that the 1D structure consists of two atomic chains. One is located on the terrace and consists of triple-period bright protrusions. The other shows a weak ×3 modulation at the step edge. Five atomic structure models based on the In adatom of a In/Si(111)-r3×r3 surface were considered to figure out the underlying structure of the STM images of the In/Si(557)-1×3 surface. Interestingly, a heterogeneous In–Si adatom chain model reproduced most of the features of STM images and was the most stable energetically at a wide range of In chemical potential.

**D-12****Room Temperature Growth Of Magic Atomic Wires On The Si(557) Surface**

SHIN Bong Gyu, KIM Minkook, OH Dong-Hwa, PARK Jong-Yun, AHN Jong Real

*BK21 Physics Research Division, Sungkyunkwan University, 300 Cheoncheon-dong, Jangan-gu, Suwon 440-746, Republic of Korea.*

We have investigated magic atomic wires on the Si(557) surface using first-principles calculations and scanning tunneling microscope (STM). The reconstructed Si(557) surface is composed of one (111) terrace and three (112) terraces in its single unit cell[1]. STM images showed that the indium-induced magic atomic wires form on the second and third (112) terraces at room temperature. The whole unit cell is too large to be calculated. For this reason, we considered only the (112) terraces. Structural models are thus based on the bulk terminated Si(112)-(1×1) surface [2]. For a reasonable approach, we testified various structural models based on the basic building blocks of the In/Si(111) surfaces; In/Si(111)-(7×7), -(4×1), and -(root3xroot3)R30degrees. We found the one-dimensional counterpart of the indium magic cluster on the Si(111)-(7×7) surface was the most stable structure. In the structural model, indium atoms preferred to replace Si adatoms. The simulated STM images of the structural model were matched with the observed line protrusion. [1] Himpsel *et al.* Applied Physics Letters 79, 1608 (2001), [2] Oh *et al.* Physical Review B 77, 155430 (2008)

**D-13****First Principles Approach To Thermoelectric Material : Interaction Between Metal And  $\text{Bi}_2\text{Te}_3$  (001) Surface**

CHANG Yun Hee, KONG Ki-jeong, CHANG Hyunju

*Korea Research Institute of Chemical Technology.*

Thermoelectric devices have attracted much attention because it can convert directly thermal energy to electric energy without producing any harmful substance. To improve the performance of thermoelectric devices, the increasing thermoelectric figure of merit (ZT) of bulk thermoelectric materials is a conventional method. Another method to improve the performance is using thin film nano-structured materials. Recently, the effect at the interface between a thermoelectric material and a metal electrode has a newly marked influence on the performance of thermoelectric devices. In this presentation, we have performed the density functional theory calculations to investigating the interaction between  $\text{Bi}_2\text{Te}_3$  surface and metal electrode. We considered the various adsorption sites of Cu, Ni and Co metal atoms on  $\text{Bi}_2\text{Te}_3(001)$  surface. We find explicit difference of their electronic structures with adsorption of Cu, Ni, and Co atoms. For the comparing the mobility of metal atoms in the  $\text{Bi}_2\text{Te}_3$ , we compared the diffusion barrier of metal atoms on the surface as well as through the bulk materials.

**D-14****First-principles study of the native point defects in  $\text{CoSb}_3$** 

박 찬현, 김 용성

*한국표준과학연구원.*

Binary skutterudite compound  $\text{CoSb}_3$  is currently used for high-temperature thermoelectric devices.  $\text{CoSb}_3$  is a narrow gap semiconductor, and typically shows p-type conductivity at high temperature above  $250^\circ\text{C}$ . At room temperature, on the other hand, the conductivity type depends on the stoichiometry; the Sb-rich  $\text{CoSb}_3$  has the p-type, while the Co-rich has the n-type conductivity. In order to understand the doping properties of  $\text{CoSb}_3$ , we investigated the native point defects in  $\text{CoSb}_3$  through the first-principles electronic structure calculations. In Co-rich  $\text{CoSb}_3$ , Co-interstitial is found to be the lowest in formation enthalpy, which is only about 0.8 eV, whereas the Sb-vacancy has a very high formation enthalpy of 2.7 eV. In Sb-rich  $\text{CoSb}_3$ , Co-vacancy is found to be more stable than Sb-interstitial with the formation enthalpy of about 1.5 eV. Both the Co-interstitial and Co-vacancy are found to be acceptor-like defects. By pairing of the Co-interstitials, the defect levels are found to be increased and the pair becomes donor-like. We propose that the Co-interstitial pairs can give the n-type conductivity in Co-rich  $\text{CoSb}_3$  at room temperature, and they can be decomposed into the acceptor-like isolated Co-interstitials at high temperature.

**D-15****Giant perpendicular magnetic anisotropy of an Ir monolayer on a NiAl(001)****surface**

KIM Dongyoo(김동유), YANG Jeonghwa(양정화), HONG Jisang(홍지상)

*Department of Physics, Pukyong National University.*

Using the state-of-the-art full potential linearized augmented plane-wave method, we have investigated the magnetic properties of Os and Ir monolayer(ML) film on NiAl(001) surface. It has been found that the one ML of Os and Ir film can have ferromagnetic ground state with magnetic moment of 0.35 and 0.64  $\mu_B$  on Ni terminated surface, whereas both films display no sign of magnetic state on Al terminated surface. In addition, the surface Ni atom has an induced magnetic moment of 0.26  $\mu_B$  in Ir/NiAl(001), while only 0.09  $\mu_B$  is observed in Os/NiAl(001). We attribute the existence of magnetism to the interaction between 5d of adlayer and 3d of surface Ni. Moreover, we have obtained that the Os/NiAl(001) and Ir/NiAl(001) films show a perpendicular magnetic anisotropy(PMA). Surprisingly, it appears that the Ir/NiAl(001) has a giant PMA energy of 7.18 meV.

D

**D-16****Ferrimagnetizing ordering in (Fe,Mn,Cr)<sub>2</sub>As thin films induced by strain**황 영훈, CHO Sunglae, CHOI Jeongyong<sup>1</sup>, SHIN Yooleemi*울산대학교, 물리학과. <sup>1</sup> 한국전자통신연구원.*

Epitaxial ferromagnetic(FM) or ferrimagnetic(FIM) thin films on semiconductor have recently attracted much interests for hybrid spintronic devices. Arsenide (As) of transition metals with formula  $M_2As$  ( $M = Mn, Fe, Cr$ ) usually crystallize in three different crystal structures such as hexagonal ( $P-62m$ ), tetragonal ( $P4/nmm$ ) or orthorhombic ( $Pnma$ ) structures. The most stable crystal structure of  $M_2As$  ( $M = Mn, Fe, Cr$ ) is tetragonal with the lattice constants  $a = 3.769 \text{ \AA}$  /  $c = 6.278 \text{ \AA}$ ,  $a = 3.627 \text{ \AA}$  /  $c = 5.973 \text{ \AA}$ , and  $a = 3.620 \text{ \AA}$  /  $c = 6.330 \text{ \AA}$ , which exhibited antiferromagnetic(AFM) ordering at 573, 325, and 393 K, respectively. We have successfully grown (Fe,Mn,Cr)<sub>2</sub>As thin film on semiconductors substrate by molecular beam epitaxy. The reflection high-energy electron diffraction (RHEED) and X-ray diffraction (XRD) studies indicate the rough film surface and  $c$ -axis orientation in tetragonal crystal structure. (Fe,Mn,Cr)<sub>2</sub>As thin film exhibited a ferrimagnetic ordering at room temperature, which is supported by the magnetization, magnetoresistances and anomalous Hall effect measurements.

**D-17****Electronic Properties of Strained Graphene**최 선명, 지 승훈, 손 영우<sup>1</sup>포항공과대학교, 물리학과. <sup>1</sup>Korea Institute for Advanced Study.

We studied the electronic properties of graphene under uniaxial strains with the use of first-principles pseudopotential method. It was found that the semi-metallic nature of graphene persists up to a strain of 30% except a tiny gap opening in a very narrow range of strains, while the energy spectra of strained graphene are altered significantly. We also studied the Fermi velocity and the work function of strained graphene. A strong anisotropy in the group velocities was observed. As the strain is increased, the group velocity at the Fermi energy perpendicular to the strain direction increases by as much as 25% while the one parallel to the strain decreases very fast to become zero. We showed that the generalized Weyl's equation is an appropriate model for strained graphene that incorporates all assessed properties that go beyond the simple tight-binding approximations. The work function in graphene is predicted to increase substantially as the strain increases and to exhibits a directional dependence on applied strains. Implications of calculated results to measurements are also discussed.

**D-18****Berry Phase Effect in Bilayer Graphene Potential Step**

PARK Sunghun, SIM H.-S.

KAIST 물리학과.

Bilayer graphene has attracted much attention due to a pseudospin degree of freedom of a charge carrier in low-energy limit, which represents the two sublattice sites in each layer. We theoretically study the phase of the reflection amplitude at a potential step with varying the incidence angle ' $\theta$ ' of a plane wave to the step. The reflection phase shows an abrupt jump of ' $\pi$ ' at  $\theta = \pi/4$  when the step height is much smaller than the kinetic energy of the wave. We found that the phase jump is attributed to the Berry phase associated with the pseudospin. This Berry-phase effect is robust against the band gap opening due to external gates generating step. We show that the phase jump can be detected in an interferometry setup in which collimated waves can be generated and tuned.

**D-19****Electronic structure of Pt-graphenes complexes and H, O and CO absorption**

김 규봉, 지 승훈

포항공대 물리학과.

Platinum is the key catalyst of fuel cells because of its unusually high catalytic properties. However, Pt-based catalysts are very costly and their performance degrades too quickly for practical use. Hence, creating more active surfaces and improving durability with less expensive methods are the central issues in fuel cell technology. Currently electrocatalysts make use of Pt cluster or Pt-alloy cluster, and Pt monolayer or Pt-alloy monolayer. Platinum on carbon (Pt/C) is one of the most common anode catalysts used in a PEM fuel cell. Here we study the electronic structures of Pt clusters on various graphene structures and corresponding adsorption properties of several important adsorbates such as H, O and CO. We observe the wide range of binding strengths of Pt clusters depending on the graphenes impurity conditions, and also the high correlation between Pt d-states near Fermi level and the adsorption strengths of such adsorbates. Our results will help to understand the active sites and improve performance of Pt/C based catalysts.

D

**D-20****Dispersants Bond Dissociation at High Temperature in Polymerized Single walled Carbon Nanotubes revealed by Coherent Phonon Spectroscopy**김 지희, 김 창섭, 이 기주, 이 철훈<sup>1</sup>, 김 태환<sup>2</sup>, 최 성민<sup>2</sup>충남대학교, 물리학과. <sup>1</sup>충남대학교 분석과학기술대학원, 분석과학기술과. <sup>2</sup>한국과학기술원, 원자력 및 양자공학과.

수용액 분산기술을 바탕으로 분산된 단일벽 탄소나노튜브 필름 물질에서 펄스초 티타늄 사파이어 레이저를 이용한 여기-탐침 실험을 실시하여, 온도변화에 따른 결맞은 G-mode 진동의 중심주파수 변화와 감쇄 시간 변화에 대해 분석해보았다. 여기 펄스로는 중심파장이 800 nm이고, 200 nm에 걸친 넓은 파장영역을 갖고 있는 약 12 fs의 펄스폭을 사용하여 진동주기가 21 fs인 결맞은 G-mode 진동신호의 측정이 가능케 하였다. 연구에 사용된 탄소나노튜브 시료는 계면활성제인 cetyltrimethylammounium 4-vinylbenzoate (CTVB)를 이용하여 분산시킨 후 중합반응 시켰다. 저온(4K)부터 고온(800K)까지 시료의 온도를 올렸다가 다시 내리면서 결맞은 G-mode 진동의 중심주파수를 살펴보고, 탄소나노튜브와 중합반응된 분산제의 접착에 연관된 임계온도 근처에서 보이는 중심주파수의 특이한 변화에 대해 분석, 논의하고자 한다.

**D-21****Characterization of Anelastic effects in Metallic and Metallic-CNT****Micromechanical Resonators**

KIM Young Duck, CHO , Sung Wan, O ByeongGyun, LEE Joo Hyung, LEE Seung Ran, CHAR Kookrin, HONG Seunghun, PARK Yun Daniel

*Department of Physics & Astronomy, Seoul National University, Seoul, 151-747, South Korea.*

Metallic thin-film based microelectromechanical and nanoelectromechanical systems (MEMS/NEMS) have unique advantages, with their high conductivity, reflectivity and bio-compatibility, for multifunctional device applications. However, metallic thin film has unfavorable mechanical properties, such as low Young's modulus, low yield strength, ductility, and plastic deformation, which all limit the performance and the dynamic ranges of mechanical devices, especially at micro- and nanoscales. Furthermore, as dimension of metallic film is reduced to nano scale, anelastic effect becomes significant [1]. At nanoscale, dislocation or grain boundary motion causes time dependency of internal stress. Thus, anelastic effect is important in stabilization and durability of nano-scaled devices. Incorporating superior mechanical properties of CNTs has been suggested as reinforcement component for nanoscale composites, since added CNTs enhance Young's modulus and yield strength of metallic thin film based nanocomposites structures as reported previously [2]. In addition to previous experiment, we report the incorporation-effect of CNTs stabilizing resonant response and suppressing anelasticity in metallic-thin nanomechanical resonators. Stabilization of resonant frequency is related with internal stress relaxation in material and structure. This stress relaxation is induced by long-cycle strain exciting the dislocation motion or grain boundary sliding. Additionally, we conducted time-dependent Creep experiment of metal and metal-CNT resonators with AFM. [1] S. Hyun et al., Appl. Phys. Lett. 87, 061902 (2005). [2] Y.D. Kim, J.H. Bak, , *et al.*, *Nature Materials* 7, 459 (2008).

**D-22****Curvature-Enhanced Spin-Orbit Coupling in a Carbon Nanotube**

정 재승, 이 현우

*포항공과대학교 물리학과.*

Structure of the spin-orbit coupling varies from material to material and thus finding the correct spin-orbit coupling structure is an important step towards advanced spintronic applications. We show theoretically that the curvature in a carbon nanotube generates two types of the spin-orbit coupling, one of which was not recognized before. In addition to the topological phase-related contribution of the spin-orbit coupling, which appears in the off-diagonal part of the effective Dirac Hamiltonian of carbon nanotubes, there is another contribution that appears in the diagonal part. The existence of the diagonal term can modify spin-orbit coupling effects qualitatively, an example of which is the electron-hole asymmetric spin splitting observed recently, and generate four qualitatively different behavior of energy level dependence on parallel magnetic field. It is demonstrated that the diagonal term applies to a curved graphene as well. This result should be valuable for spintronic applications of graphitic materials.

**D-23****Water-Assisted Growth of mm-long Thin Multiwalled Carbon Nanotubes with an Optimum Al Underlayer in Thermal CVD**

CHOI In Sung, JEON Hong Jun, LEE Han Sung, LEE Naesung

세종대학교 나노공학과.

Vertically aligned, mm-long multiwalled carbon nanotubes (CNTs) were synthesized by water-assisted thermal chemical vapor deposition (CVD). The 0.5-nm-thick Fe layer served as a catalyst, underneath which an Al layer was coated as a diffusion barrier on a Si wafer. The CNTs were grown while a little amount of water vapor was introduced. The growth, in particular, the length of CNTs, was in-depthly investigated by varying the deposition parameters such as a growth temperature, a period of growth time, gas flow rates, thickness of the Al underlayer. The optimum conditions for these parameters were as follows: pressure of 95 torr, growth temperature of 815 °C, growth for 30 min, 60 sccm Ar + 60 sccm H<sub>2</sub> + 20 sccm C<sub>2</sub>H<sub>2</sub>. Interestingly, the effect of the Al thickness was crucial, implying that Al was very good at producing the nm-size catalyst particles by preventing “Ostwald ripening”. The Al underlayer was varied over the range of 15~40 nm in thickness, producing the longest CNTs at 30 nm. The water vapor also had a great effect on the growth of CNTs. CNTs grew 5.03 mm long for 30 min with the water vapor added (7.2 sccm) while CNTs were 1.53 mm long without water vapor at the same condition. High-resolution transmission electron microscopy showed that the as-grown CNTs were of ~3 graphitic walls and ~ 6.6 nm in diameter.

D

**D-24****Carbon Nanotube Tunnel Sensor**

CHOI Jaewu

경희대학교, 정보디스플레이학과.

Carbon nanotube (CNT) tunnel sensors consisted of laterally grown CNTs from two isolated metal electrodes. The CNTs grown from each electrode weakly contact each other, with the charge transport between them based on tunneling. The signal modulation amplitude with exposure to the volatile organic liquid is higher than two orders in magnitude. The sensing mechanism is based on the capillary force between CNTs by the organic liquids.

**D-25****First-Principles Mobility Calculations in Doped Si/Ge Core-Shell Nanowires**

LEE Hyungjun, CHOI Hyoung Joon

*Department of Physics and IPAP, Yonsei University, Seoul 120-749, Korea.*

We have calculated mobilities in doped Si/Ge core-shell nanowires (NWs) using atomic-scale models of the structures and density functional theory. We have investigated the effects of point defects on electron (hole) mobilities in these structures by introducing phosphorus (boron) impurities. We describe their atomic and electronic structures using norm-conserving pseudopotentials with Kleinman-Bylander's nonlocal projectors and the local density approximation for the exchange-correlation potential. Mobilities of carriers are estimated from scattering properties of impurities which are obtained by using the scattering-state method for quantum conductance. We examine different atomic configurations and compare their electron and hole mobilities to find out optimal doping methods. This work was supported by the IT R&D program of MKE/KEIT [2008-F-023-01]. Computational resources have been provided by KISTI Supercomputing Center (KSC-2008-S02-0004).

**D-26****First-principles Study of Doped and Undoped Si/Ge Nanowire Superlattices**

KIM Min-Kook, CHOI Hyoung Joon

*Department of Physics and IPAP, Yonsei University.*

We investigate structural and electronic properties of doped and undoped H-passivated Si/Ge nanowire superlattices (NWSLs) oriented along [110] direction using an *ab-initio* pseudopotential density functional method with the local density approximation. The obtained electronic structures of fully relaxed NWSLs show flat bands in both conduction and valence bands due to confined electronic states present near the band edges. The confinement effects are studied in NWSLs with different lengths and diameters. We then introduce substitutional boron and phosphorus impurities into Si/Ge NWSLs and study effects of doping on the electronic properties of the NWSLs near the band edges. We discuss possibility of electronic and photonic applications of doped and undoped Si/Ge NWSLs. This work was supported by the IT R&D program of MKE/KEIT [2008-F-023-01]. Computational resources have been provided by KISTI Supercomputing Center (KSC-2008-S02-0004).

**D-27****The Effect of Energy Relaxation via Surface Levels on Quantum Yield in CdSe****Quantum Dots**

김 상민, 홍 경수<sup>1</sup>, 양 호순

부산대학교 물리학과, <sup>1</sup>한국 기초과학지원연구원 부산센터.

높은 광학적 이득, 크기에 따른 에너지 변화, 화학적 콜로이드 합성 방법을 이용한 균일한 크기 및 대량 합성 등에 의하여 CdSe 나노 결정의 경우 광학 재료로 많은 관심을 받고 있다. 그렇지만 나노 결정의 경우 표면적의 상태가 발광 process와 양자 이득 (Quantum Yield : QY)와 같은 나노 결정의 광학적 특성을 결정 하는데 중요한 역할을 하게 된다. 본 연구에서는 양자점의 표면 상태의 변화가 발광 process와 QY에 미치는 영향을 알아 보았다. 먼저 나노 결정의 표면적의 상태를 변화시키기 위해서 합성에 사용된 유기물들의 종류 (ODE, HDA)와 양을 변화시켜서 QY가 다른 여러 CdSe 나노 결정을 합성 하였으며 Time correlated single photon counter (TCSPC)를 이용하여 time resolved spectrum을 측정하여 decay process를 연구 하였다. CdSe 나노 결정의 time resolved spectrum의 경우 decay process가 double exponential 의 형태로 fit 되었고 각각 decay time 에 대응되는 amplitude 의 비 (ratio)와 QY의 관계를 통하여 결정 표면에 관련된 발광 process를 분석 하였다. 실험에 사용된 유기물 (ODE, HDA) 들이 결정 표면의 trap level과 직접적으로 관련이 있음을 확인 할 수 있었으며 trap level 에 갇힌 전자의 decay process가 결정의 QY를 결정하는데 중요한 역할을 하는 것을 알 수 있었다.

**D-28****Evolution of Photoluminescence of Plasma Power Modulated Silicon Nitride Films by Ionized N<sub>2</sub> Gas Irradiation**

JANG Seunghun, KIM Hyunseung, HAN Dongwoo, JEONG Kiyoun, KO Changhun, HAN Moonsup

Department of Physics, University of Seoul.

Visible light emission from silicon with nano-sized structures is important to achieve low cost application such as Si-based integrated optoelectronic device, Si-based light emitting diode. Hence, the various nanostructures have been studied intensively by many researchers and several origins were proposed to explain the luminescent phenomena. It has been suggested that dominant mechanism for light emission from the Si QDs in silicon nitride (SiN<sub>x</sub>) films is the quantum confinement effect (QCE). However, for the visible luminescence from Si QDs, the QCE doesn't seem to be the unique mechanism to explain the photoluminescence (PL). The effect of surface or interface states should be a considerable factor affecting the luminescence. In this work, we investigate the evolution of PL of plasma power modulated silicon nitride (PMSN) films by ionized N<sub>2</sub> Gas irradiation, and classify the luminescent origin through the analysis for the PL results in detail. We fabricated the silicon nitride films by using plasma-enhanced chemical-vapor deposition (PECVD). We could have controlled the peak position of PL in the visible range by adjusting the plasma power of reactant gas from 60 W to 100 W. Subsequently, samples were irradiated to the ionized N<sub>2</sub> Gas at room temperature (RT) using an AG5000 cold cathode ion gun made by VG Microtech. The exposing gas-pressure was typically maintained at 3.0x10<sup>-6</sup> torr. The irradiation time varied from 10 to 60 min at RT. As a result, the PL intensity is decreased for all samples as the irradiation time increase. Especially, the peak at 380 nm in sample 100W changes drastically in a short time irradiation. In order to investigate relation between the luminescence property and chemical states of the PMSN films, we measured core-level spectra of related elements using x-ray photoelectron spectroscopy (XPS). We also employed Raman scattering spectroscopy (RSS), Fourier transform infrared spectroscopy (FTIR) to interpret the luminescence mechanism for the PMSN films in detail.

**D-29****Supercurrent Through Single Crystalline Gold Nanowires**

정 민경, 노 현호<sup>1</sup>, 도 용주<sup>2</sup>, 송 운, 최 만수<sup>3</sup>, 정 연옥, 심 승보, 김 남, 유 영동<sup>4</sup>, 서 관용<sup>4</sup>, 김 봉수<sup>4</sup>, 김 정구<sup>1</sup>, 김 진희

KRISS. <sup>1</sup>서울대학교 물리천문학부. <sup>2</sup>포항공과대학교 물리학과. <sup>3</sup>고려대학교 물리학과. <sup>4</sup>KAIST 화학과.

We have investigated electron transport of Au nanowire proximity junction. The single crystalline gold nanowires of various diameter and length ( $D=70\sim300\text{nm}$ ,  $L=300\sim700\text{nm}$ ) were synthesized by chemical vapor deposition. We have fabricated two aluminum based superconducting electrodes that connect gold nanowires. The electric characteristics were measured in a  $^3\text{He}$  refrigerator with base temperature 260mK. Transport measurements on the superconductor – metal nanowire – superconductor proximity junction present high-order multiple Andreev reflections, indicating that the charge transport through the nanowire is highly coherent. AC Josephson effect in these Au/Al proximity junction reveals integer and fractional integer Shapiro steps. We will address on the origin of the fractional Shapiro steps which is not well understood yet.

**D-30****High-frequency single-crystalline Au nanowire as resonators**

김 진희, 장 정원<sup>1</sup>, 정 민경, 심 승보, 노 현호<sup>2</sup>, 김 봉수<sup>3</sup>, 이 순걸<sup>4</sup>

한국표준과학연구원. <sup>1</sup>한국표준과학연구원, 고려대학교. <sup>2</sup>한국표준과학연구원, 서울대학교. <sup>3</sup>한국과학기술원. <sup>4</sup>고려대학교.

Nano resonator has attracted a lot of attention recently due to its potential applications to a highly sensitive sensor. Its electrical, thermal and mechanical properties are investigated intensively. As a building block of a nano resonator, single-crystalline nanowire has many advantages and is considered as a good candidate to achieve a high resonance frequency and a high quality factor. We have fabricated single-crystalline (tension- and distortion-free) Au nanowire resonators and measured their high frequency resonance properties with magnetomotive detection scheme. We have fabricated and investigated various dimensions of resonators operating 32 ~ 118 MHz and realized the quality factor  $Q = 1800 \sim 12000$  at 4 K. Our work, with further study, will provide potential application of single-crystalline Au nanowire for the nano resonator with a high quality factor.

**D-31****Investigation of transport mechanism of amorphous GST**

JU chanjong, LU WENJIAN, CHAR Kookrin

서울대학교 물리학과.

Recently  $\text{Ge}_2\text{Sb}_2\text{Te}_2$  (GST) has attracted great attention due to its potential applications for phase change memory (PCM) devices. However, the electrical transport mechanism of GST has not been clearly elucidated and it still remains controversial. To understand the mechanism, we measured temperature dependence and length dependence of the GST resistances. For these purposes we deposited amorphous GST thin film junction by DC magnetron sputtering methods. According to the R-T characteristics, the resistance of GST did not obey the ohms law when the thickness of sample was increasing above the tens of nanometer. Our experimental results suggest that various transport mechanisms such as direct tunneling and resonant tunneling are involved in the resistance of amorphous GST in nanometer scale.

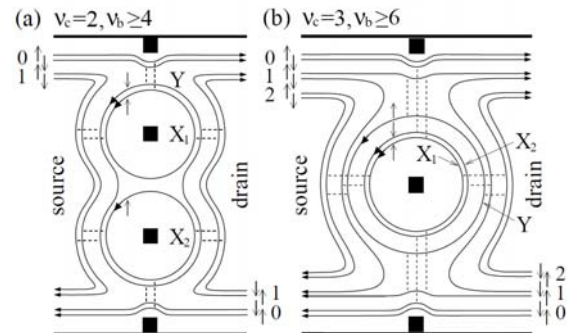
D

**D-32****Effects of Electron Interactions in Quantum Hall Antidots with Multiple Bound****Modes**

이 우람, 심 흥선

KAIST, 물리학과.

We theoretically study the effects of electron-electron interactions on Aharonov-Bohm resonances in antidot systems with multiple bound modes in the integer quantum Hall regime. The resonance signals are found to show the spectator behavior: The resonances of some modes disappear and instead are replaced by those of the other modes, due to inter-mode charge relaxation. This behavior can give a unified understanding on the unexplained features of previous experimental data, spectator behavior in an antidot molecule and resonance peaks in a single antidot with three modes.



**D-33****Effect of the magnetic field sweep on Rabi spin oscillations in a molecular magnet**

KIM GWANG-HEE

*Dept. of Physics, Sejong Univ..*

Single-molecule magnets have attracted much interest because they provide possibility to observe quantum effects at the macroscopic scale. Among these effects are step-wise magnetization curve caused by resonant spin tunneling, topological interference of tunneling trajectories, and crossover between classical and quantum superparamagnetism. Landau-Zener theory has been used to describe spin transitions that occur during the field sweep. It has been recognized that spin-phonon interactions play an important role in the dynamics of spins in molecular magnets. Possibility of Rabi oscillations of spins caused by the acoustic wave has been studied. In that work the initial state of every spin was assumed to be in the ground state before the sound wave arrived. However, it is meaningful to study how strongly Rabi spin oscillations is affected by the change of the initial state. In order to study such effects, we first saturated the sample. The field is then varied at a constant rate until a desired value of the field is reached. Maintaining this field value, we deliver to the sample the acoustic wave to see the acoustic Rabi oscillation. Employing the rotating wave approximation, we obtain the general form of the expectation value of the projection of the spin onto the anisotropy axis in the presence of the acoustic wave. We find that Rabi spin oscillations between spin states of molecular magnets can be strongly affected by changing the initial condition. In addition we present the probability to find the spin in the excited states. These features can be tested experimentally in nanomagnetic systems.

**D-34****Effects of Boron Impurities on Transport Properties of Fe/MgO/Fe(100) Tunnel Junctions****Junctions**

HAN Jinhee, CHOI Hyoung Joon

*Institute of Physics and Applied Physics, Yonsei University.*

We study effects of various boron impurities on transport properties of Fe/MgO/Fe(100) tunnel junctions using the scattering-state method for quantum conductance. We first generate atomic structures of MgO with boron impurities by minimizing the total energy, considering different oxidation states of the boron impurities such as BO, BO<sub>2</sub>, and B<sub>2</sub>O<sub>3</sub>. Then we calculate transport properties of Fe/MgO/Fe(100) tunnel junctions with the boron impurities in MgO layers. Our results show that the boron impurities in MgO enhance the tunneling through MgO layers regardless of parallel or anti-parallel configuration of iron magnetizations, decreasing the tunneling magnetoresistance ratio of the structures. This work was supported by National Research Foundation of Korea (Grant No. 2009-0081204), and KISTI Supercomputing Center (KSC-2008-S02-0004).

**D-35****열 임피던스 측정을 통한 Gd<sub>2</sub>Zr<sub>2</sub>O<sub>7</sub> 박막의 열전도도 분석 및 비교**

정 고은, 배 종성<sup>1</sup>, 양 호순

부산 장전동 부산대학교 자연과학대학 물리학과, <sup>1</sup>부산 장전동 한국 기초 과학 연구소 부산센터.

Pyrochlore 구조의 Gd<sub>2</sub>Zr<sub>2</sub>O<sub>7</sub>는 낮은 열전도성을 가지는 물질로서 열차단에 효과적인 물질로 주목 받고 있다. Pyrochlore 구조를 가지는 물질들이 낮은 열전도성을 나타내는 것은 Fluorite 구조에서 8a 위치의 산소 vacancy로 인하여 포논의 평균 자유거리가 줄어들기 때문이다. 지금까지 분말형태의 Gd<sub>2</sub>Zr<sub>2</sub>O<sub>7</sub> 연구가 이루어진 것과는 달리 본 연구는 PLD (Pulsed Laser Deposition) 방법을 이용 하여 YSZ 단결정 기판과 Al<sub>2</sub>O<sub>3</sub> 기판에 100~600nm 두께의 Gd<sub>2</sub>Zr<sub>2</sub>O<sub>7</sub>박막을 증착한 후 물리적 특성을 연구하였다. 증착된 Gd<sub>2</sub>Zr<sub>2</sub>O<sub>7</sub> 박막의 결정성, 표면 거칠기와 두께를 XRD, AFM, SEM을 이용하여 확인하였다. 열전도도 측정에 사용된 3ω 방법은 벌크 또는 박막의 열전도도에 널리 이용되고 있는 방법이다. Al<sub>2</sub>O<sub>3</sub> 기판의 경우 열 전도도가 Gd<sub>2</sub>Zr<sub>2</sub>O<sub>7</sub> 박막의 열전도도 보다 훨씬 높은 값을 가지므로 박막 내에서 온도가 선형적으로 변하기 때문에 일반적인 3ω 방법을 이용하여 열전도도 측정이 가능하다. 그렇지만 YSZ 기판의 경우 증착된 박막과 열전도도에서 큰 차이를 가지지 않는다고 알려져 있으므로 기존의 3ω 방법과는 조금 다른 박막의 열 임피던스 (thermal impedance)를 이용하여 박막의 열전도도를 측정하였다. 이는 높은 주파수의 열 발생원을 사용할 수 있는 장점 뿐만 아니라 다층 박막의 열 전도도를 분석하는데도 유용한 방법이다. 또한 여러 가지 두께의 박막의 측정 결과를 분석하여 박막과 기판 사이의 경계면이 미치는 영향도 확인하였다.

**D-36****Visualization of Intriguing Polarization Switching Behaviors in Multiferroic****BiFeO<sub>3</sub> Thin Films**

KIM T. H., BAEK S.-H.<sup>1</sup>, YANG S. M., JANG S. Y., ORTIZ D.<sup>1</sup>, SONG T. K.<sup>2</sup>, CHUNG J.-S.<sup>3</sup>, EOM C.-B.<sup>1</sup>, NOH T. W., YOON J.-G.<sup>4</sup>

ReCOE & FPRD, Department of Physics and Astronomy, Seoul National University, Seoul 151-747, Korea. <sup>1</sup>Department of Materials Science and Engineering, University of Wisconsin, Madison, WI 53706, USA. <sup>2</sup>School of Nano and Advanced Materials Engineering, Changwon National University, Changwon, Gyengnam 641-773, Korea. <sup>3</sup>Department of Physics and CAMDRC, Soongsil University, Seoul 156-743, Korea. <sup>4</sup>Department of Physics, University of Suwon, Kyunggi-do 445-743, Korea.

BiFeO<sub>3</sub> (BFO) is one of remarkable multiferroic materials. It has a very high ferroelectric Curie temperature ( $T_C$ ) of ~1,100 K and an antiferromagnetic Neel temperature ( $T_N$ ) of ~640 K. Its ferroelectric polarization is comparable to that of Pb(Zr,Ti)O<sub>3</sub>. Therefore, understandings on its polarization switching phenomena could be quite interesting scientifically as well as technologically. In this presentation, we will present our efforts to visualize intriguing polarization switching behaviors in vicinal BFO(001) and (111) thin films using our modified piezoelectric force microscopy configuration. In BFO(001) films, we found that ferroelectric domains grow along a particular direction, which is quite different from the isotropic domain growth observed in most other ferroelectric thin films. The directionality depends on the electrical polarity of applied switching pulse. We elucidated that such a directional domain growth should come from the strain gradient of BFO layer on terraces, which leads to a difference between the nucleation energy barriers at each unit cell. On the other hand, in BFO(111) films, we observed that domain growth pattern changes from a circular-like growth to a dendritic stripe growth with an increasing negative bias. Such a change in domain growth behavior might be originated from a competition between nucleation process and domain wall motion. Further experimental evidences will be discussed during the presentation.

**D-37****Hysteresis Loops and Nonlinear ac Dynamics of Domain Walls in Epitaxial****Ferroelectric Film**

YANG Sang Mo, JO Ji Young, KIM Tae Heon, YOON Jong-Gul<sup>1</sup>, SONG Tae Kwon<sup>2</sup>, LEE Ho Nyung<sup>3</sup>, PARK Seung-young<sup>4</sup>, JO Young-Hun<sup>4</sup>, NOH Tae Won

*ReCOE & FPRD, Department of Physics and Astronomy, Seoul Nat'l Univ., Seoul 151-747, Korea.* <sup>1</sup>*Department of Physics, University of Suwon, Suwon, Gyeonggi-do 445-743, Korea.* <sup>2</sup>*School of Nano and Advanced Materials Engineering, Changwon National University, Changwon, Gyeongnam 641-773, Korea.* <sup>3</sup>*Materials Science and Technology Division, Oak Ridge Nat'l Lab., Oak Ridge, Tennessee 37831, USA.* <sup>4</sup>*Quantum Materials Research Team, Korea Basic Science Institute, Daejeon 305-333, Korea.*

Ferroelectric (FE) materials have been one of the most intriguing matters for last decades, due to scientific interest as well as potential for applications. For this reason, there have been developed many experimental methods to determine properties of the FE materials, such as piezoresponse force microscopy [1]. The measurement of hysteresis loop is widely and easily used. However, there are little experimental efforts to deduce an intriguing domain wall dynamics from the hysteresis loops. Here, we report our recent studies on the nonlinear *ac* dynamics of domain walls in  $\text{PbZr}_{0.2}\text{Ti}_{0.8}\text{O}_3$  (PZT) thin films [2], by using polarization-electric field hysteresis loops. We found the dynamic phase crossover for domain wall motions played an important role in the shape of hysteresis. We built the dynamic phase diagram for domain wall dynamics in random media from frequency-dependent hysteresis loops measured at various temperatures. This work provides us new insight on the relation between microscopic switching dynamics of domains and macroscopic hysteresis loops in ferroic materials. [1] S. M. Yang *et al.*, Appl. Phys. Lett. 92, 252901 (2008); S. M. Yang *et al.*, J. Korean Phys. Soc. 55, 820 (2009) [2] H. N. Lee *et al.*, Phys. Rev. Lett. 98, 217602 (2007).

**D-38****An Ab-initio Study on Ferroelectric Characteristics of  $\text{ZnSnO}_3$** 

신 영한, 손 종억<sup>1</sup>, 이 근희<sup>1</sup>, 조 문호<sup>1</sup>, 김 형준<sup>2</sup>, 장 현명<sup>1</sup>

*울산대학교, 물리학과.* <sup>1</sup>*포항공과대학교, 신소재공학과.* <sup>2</sup>*연세대학교, 전기전자공학부.*

The origin of ferroelectricity in typical perovskite oxides is known as the  $d^0$ -ness of the *B*-site ion, which makes strong covalent bonds with neighbouring oxygen ions with an off-centered configuration. Another mechanism of ferroelectrics is the stereochemical activity of the *A*-site ion by the lone-pair electrons, which was reported in the case of the *A*-site Bi materials. However, it is also possible to make ferroelectrics with the combination of the different ionic size of *A*- and *B*-site ions. In this presentation, we will show the ferroelectric characteristics of the *A*-site Zn complex perovskite with the *B*-site ion of Sn with considerable polarizations observed in this material  $\text{ZnSnO}_3$ .

**D-39****First-principles Study of the Electronic Structure of Lithium Silicides**

OH Young Jun, RYU Byungki, CHANG Kee Joo

*Department of Physics, KAIST.*

Recently, lithium silicides have attracted much attention due to their higher charge storage capacity, compared with graphite which is widely used as an anode material in lithium-ion batteries. According to the phase diagram of Li-Si systems, various compositions can exist in crystalline lithium silicides. In this work, we investigate the electronic structure of  $\text{Li}_{13}\text{Si}_4$ , which is one of the crystalline phases, through first-principles calculations within the density-functional-theory framework. As the charge transfer occurs from Li to Si, the valence band states are mainly derived by the Si 3s and 3p orbitals. The electronic structure of  $\text{Li}_{13}\text{Si}_4$  is well described by a simple molecular orbital model.

**D****D-40****Ab initio studies of optical properties of TiN and ZrN : a procedure for color****prediction of a given material**

KIM Jinwoong, JHI Seung-Hoon

*Physics department, POSTECH.*

Transition metal (Ti, Zr) nitrides are preferred as coating materials because of their hardness and lustrous color. Their mechanical properties are well understood but the color properties still rely on empiricism. The color of a given material can be predicted from its dielectric function, which can be obtained by *ab initio* density functional calculation. Therefore we studied a full procedure for color prediction and practical applications for TiN and ZrN. We found that these metal nitrides have many interband transition states in low energy (0~2eV) range that produce free electron-like dielectric function. This may result in metallic color with ordinary free electrons in metals. Because these low energy transitions are sensitive to Fermi level, defects may affect significantly the color of the material. The effects of some defects will also be discussed in this presentation.

**D-41****Morphological investigation of mono-dispersed manganese ferrite nanoparticles by impedance measurements**

YOON Sunghyun

*Gunsan National University.*

Morphological study of mono-dispersed manganese ferrite nanoparticles, synthesized by the decomposition of metal-organic precursors was carried out using the impedance measurement method. Direct TEM image showed that nominal diameter of the particles was 15 nm with narrow distribution width. Frequency dependence of complex ac susceptibility was measured by means of the slit-toroid method. Subsequently, the real and the imaginary parts of the susceptibility,  $\chi'$  and  $\chi''$  were calculated following the method of Fannin. During the calculation, the single particle response  $\chi(w)$  was weight-averaged with proper particle size distribution (PSD) function. We proposed a new, intuitive and simple lognormal distribution function suitable for describing narrow distribution width, slightly modified from the Chantrell's distribution function. Instead of using the reduced radius  $y=r/r_0$ , a new parameter  $\theta$  was introduced to control the peak position.  $r_0$  is a scaling constant included for correct dimensionality. Average radius is defined as a first moment of the distribution function. In this study, we integrate the weighted-averaged  $\chi(w)$  numerically to find values of  $r_0$ ,  $\sigma$  and  $\theta$  which give the best fit to the measured result throughout the whole data range. Though it showed some discrepancy due to the occurrence of magnetic resonance in the high frequency region, the real and the imaginary parts of the susceptibility at room temperature were shown to be in fair agreement with a theoretical curve calculated for a particle size distribution with an averaged radius of 8.2 nm, and the distribution width 0.3 nm. As long as the distribution width is concerned, to good approximation, the magnetite ferrofluid synthesized in our laboratory can be considered to be highly mono-dispersed.

**D-42****Discotic Liquid Crystals with a Room-Temperature Ferromagnetism**LEE Chang Hoon, KWON Young Wan<sup>1</sup>, JIN Jung-Il<sup>1</sup>, KOH Eui-Kwan<sup>2</sup>*Chosun University, Department of Polymer Science & Engineering. <sup>1</sup>Korea University, Department of Chemistry. <sup>2</sup>KBSI, Seoul Branch.*

We successfully achieved room-temperature ferromagnetic compositions by intercalating 2,9(10),16(17),23(24)-Tetra(2-decyltetradecyloxy)-phthalocyanine, an organic semiconducting discotic liquid crystal, with low levels of iron(III) phthalocyanine. The compositions exhibit definite magnetic hysteresis loops in the magnetization(M)-magnetic field intensity(H) measurements. The detailed studies of their magnetic properties were conducted by the electron-magnetic resonance (EMR) spectroscopy and the superconducting quantum interference device (SQUID) magnetization measurements.

**D-43****Canted spin structure of checkerboard patterned  $\text{Co}_{0.6}\text{Fe}_{0.9}\text{Mn}_{1.5}\text{O}_4$  investigated****by NMR and XAS**JUNG Hyunok, LEE Soonchil, LEE H. J.<sup>1</sup>, KIM D. H.<sup>1</sup>, KANG J.-S.<sup>1</sup>, ZHANG C. L.<sup>2</sup>, CHEONG S.-W.<sup>2</sup>KAIST, Physics. <sup>1</sup>Catholic University of Korea, physics. <sup>2</sup>Rutgers University, physics.

급냉하여 만들어진 스핀넬 화합물  $\text{Co}_{0.6}\text{Fe}_{0.9}\text{Mn}_{1.5}\text{O}_4$ 는 열적 불림을 하면 스스로 나노 크기의 체크 보드 패턴을 형성하는 물질로 알려져 있다. 급냉한 (WQ) 시료와 열적 불림을 하여 체크 보드 패턴을 띄는 (CB) 시료의 원자가 상태와 스핀 구조의 변화를 관측하기 위해서 nuclear magnetic resonance (NMR)과 X ray absorption spectroscopy (XAS) 측정을 수행하였다. CB 시료에 대한 Co, Fe 그리고 Mn 2p XAS spectrum들의 측정하여 WQ 시료의 spectrum들과 비교하였다. 두 시료의 각 이온들에 대한 XAS spectrum의 line-shape이 거의 동일하다는 사실로부터 CB 시료에 존재하는 이온들의 종류가 WQ 시료와 다르지 않았음을 알 수 있었다. 외부 자기장을 가하지 않은 CB 시료의 NMR spectrum을 측정하여 WQ 시료의 NMR spectrum과 비교하였다. WQ 시료로부터 관측된 peak들과 유사한 주파수 영역에서 관측된 CB 시료의 peak들은 WQ 시료와 동일한 이온으로부터 얻어진 신호이고 따라서 각 이온들의 자기 모멘트의 크기가 변화하지 않았다는 것을 알 수 있었다. CB 시료의 총 자화가 WQ 시료와 비교하여 줄어든 현상을 설명하기 위해서 양이온 중 절반을 차지하는 Mn 이온에 대한 외부 자기장의 NMR 주파수 의존성을 측정하였다. WQ와 CB 시료의  $\text{Mn}^{2+}$  이온의 자기 모멘트는 외부 자기장 방향에 대해서 약  $112^\circ$ 와  $122^\circ$ 의 기울어짐 각을 가지고 이 기울어짐 각의 차이로 인한 총 자화의 차이는  $0.8\mu_B$ 임을 알 수 있었다. 외부 자기장에 대한  $\text{Mn}^{3+}$  이온의 NMR 주파수 이동은 모두 약 10.5 MHz/T이었고 따라서 WQ 시료와 CB 시료의  $\text{Mn}^{3+}$  이온의 자기모멘트는 거의 기울어져 있지 않음을 알았다.

**D-44****First-principles Study of the Ferromagnetism of Mn-doped ZnO Nanowires**

TSOGBADRAKH Namsrai, CHOI Eun-Ae, LEE Woo-jin, CHANG Kee Joo

KAIST, Department of Physics.

Among diluted magnetic semiconductors, Mn-doped ZnO nanowires have attracted much attention because of the potential applications to spintronic devices and possible Curie temperatures above room temperature in low-dimensional structures. Despite many theoretical attempts, the origin of ferromagnetism is still not clearly understood. Here we present the results of first-principles calculations for Mn-doped ZnO nanowires, which are based on the local-spin-density-functional approximation (LSDA). We also perform the LSDA+U calculations to examine the magnetic interactions between the Mn ions, where U represents the Coulomb repulsion on the localized orbitals of the magnetic ion. We find that the ferromagnetic state is energetically unfavorable in the absence of free carriers. On the other hand, the ferromagnetic state can be stabilized if the antibonding  $t^a$  state formed by two adjacent Mn ions is partially occupied by hole doping.

**D-45****Magnetoresistance across a pinned domain wall in a GaMnAs nanowire**

CHO Sung Un, CHOI Hyung Kook, JANG Dong Hyun, YANG Chan Uk, PARK Yun Daniel, DASILVA Fabio C.S.<sup>1</sup>, OSMINER Teresa<sup>1</sup>, PAPPAS David P.<sup>1</sup>

*Department of Physics and Astronomy, Seoul National University, Seoul 151-747, Korea. <sup>1</sup>Natinal Institute of Standards and Technology, Boulder CO 80305, USA.*

Magnetoresistance (MR) across pinned domain wall is studied in GaMnAs nanoconstrictions patterned by e-beam lithography and wet etching processes [1,2]. GaMnAs wires varied constriction size are realized in LT-MBE 100 nm Ga<sub>1-x</sub>Mn<sub>x</sub>As (x =0.05)/GaAs epilayers with  $T_C$  of  $\sim 90$  K. Four-point probe DC  $IV$  measurements- with applied fields up to 5 T parallel to the wire axis- are utilized to study the transport mechanism as well as the magnetic properties. As the constriction size decrease, positive MR jump are observed and enhanced. Bias dependence of the MR are characterized and observed to change with temperature. This result is consistent with spin-dependent transport across a domain wall [1,2,3,4]. Since width of domain wall pinned in constriction can decrease [5], as the width of constriction decrease, spin dependent scattering phenomena across thin domain wall are possible and can be enhanced by bias and temperature inducing kinetic energy gain of polarized spin passing pinned thin domain wall. The experiment is extended by fabrication of a nanowire structure containing a series of constrictions. Multi-state MR is realized across the structure. It can be explained that the MR depends the position of domain wall in the constrictions. [1] S.U. Cho *et al.*, Appl. Phys. Lett. 91, 122514 (2007). [2] S.U. Cho *et al.*, Appl. Phys. Lett. 95, 022517 (2009). [3] G. Vignale and M. E. Flatt, Phys. Rev. Lett. 89, 098302 (2002). [4] M. Deutsch, G. Vignale, and M. E. Flatte, J. Appl. Phys. 96, 7424 (2004). [5] D. Backes *et al.*, Appl. Phys. Lett. 91, 112502 (2007).

**D-46****Two-state anomalous Hall effect response in GaMnAs micromechanical freestanding Hallbar structures**

YANG Chanuk, CHOI Hyung Kook, O Byeonggyun, PARK Yun Daniel  
*Seoul National University, Department of Physics and Astronomy.*

The nonmagnetic manipulation of magnetic properties of diluted magnetic semiconductors (DMS) has recently drawn much attention, such as magnetization by electric field [1], and magnetic anisotropy by strain engineering [2-5]. Magnetic properties' dependence on strain in DMS stems from ferromagnetic exchange coupling between localized magnetic moments of Mn and itinerant carriers in valence band. Here, we present large differences in the anomalous Hall effect (AHE) in a suspended micro-Hallbars between their bistable mechanically buckled states. We prepared GaMnAs(100nm) / GaAs(35nm) / Al<sub>0.55</sub>Ga<sub>0.45</sub>As(1μm) / *p*-type GaAs(001) substrate by low temperature molecular beam epitaxy (LT-MBE). GaMnAs micromechanical freestanding Hallbar structure was fabricated by typical photo and e-beam lithography and selective wet etching. After fabrication, we found the micro-Hallbars to be either buckled up (deformed upward) or more likely buckled down (deformed downward). Between numerous magnetotransport measurements as well as from microscopy, only two distinct states of AHE have been observed, corresponding to two mechanically buckled states. We have observed large and discernable changes in AHE but small/unnoticeable changes in other properties such as magnetic field and temperature dependence of resistivity. We will discuss the results in view of the strong sensitivity of both effective field and spin-orbit coupling to the strain corresponding to the mechanical buckled states. [1] H. Ohno *et al.*, Nature 408, 944 (2000); Y.D. Park *et al.* Science 295, 651 (2002); Chiba *et al.*, Science 301, 943(2003)[2] T. Dietl *et al.* Phys. Rev. B 63, 195205 (2001); M. Abolfath *et al.*, PRB 63, 054418 (2001)[3] M. Glunk *et al.*, Phys. Rev. B 79,195206(2009)[4] J. Wenisch *et al.*, Phys. Rev. Lett. 99, 077201 (2007); J. Wunderlich, *et al.*, Phys. Rev. B 76, 054424 (2007)[5] A. W. Rushforth *et al.*, Phys Rev B 78, 085314 (2008)

**D-47****Skyrmions and Anomalous Hall Effect in a Dzyaloshinskii-Moriya Spiral Magnet**YI Su Do, ONODA Shigeki<sup>1</sup>, NAGAOSA Naoto<sup>2</sup>, HAN Jung hoon*Department of Physics, Sungkyunkwan University, Korea. <sup>1</sup>Condensed Matter Theory Laboratory, RIKEN,**Japan. <sup>2</sup>Department of Applied Physics, The University of Tokyo, Japan.*

Monte Carlo simulation study of a classical spin model with Dzyaloshinskii-Moriya interaction and the spin anisotropy under the magnetic field is presented. We found a rich phase diagram containing the multiple spinspace [or Skyrme crystal] phases of square, rectangular, and hexagonal symmetries in addition to the spiral spinspace. The Skyrme crystal states are stabilized by a spin anisotropy or a magnetic field. The Hall conductivity  $\sigma_{xy}$  is calculated within the sd model for each of the phases. Applying a magnetic field induces nonuniform chirality and the anomalous Hall conductivity simultaneously. The field dependence of  $\sigma_{xy}$  is shown to be a sensitive probe of the underlying magnetic structure. Relevance of the present results to several recent experiments on MnSi is discussed.

**D****D-48****순수한 PbPdO<sub>2</sub> 박막에서의 ER & MR 효과**추 성민, 이 규준, 박 성민, 박 광서, 이 성익, 정 명화, 조 영훈<sup>1</sup>*서강대학교 물리학과. <sup>1</sup>한국기초과학지원연구원 나노물성팀.*

최근 새로운 납계 산화물에서 colossal electroresistance (ER)과 giant magnetoresistance (MR)이 발견되었다. 이 물질은 스핀 틈 없는 반도체로써 특별한 밴드 구조를 가지고 있기에 이 두 현상을 잘 설명할 수 있을 것이다. 그래서 우리는 Co가 도핑된 기존의 산화물과 도핑이 되지 않은 순수한 산화물 사이의 차이점을 보기 위해 pulsed laser deposition 방법으로 제조한 박막을 사용하여 ER과 MR을 포함한 다양한 물성을 연구하였다. 순수한 PbPdO<sub>2</sub> 박막의 특성은 전반적으로 PbPdO<sub>2</sub> 벌크와 유사한 모습을 보였다. 온도에 따른 전기저항의 변화를 보면 고온에서 저온으로 떨어질 때 금속에서 절연체로의 상전이를 보이는데 이것은 벌크에서의 데이터와 약간의 이동을 보였다. 그리고 주목할 점은 순수한 PbPdO<sub>2</sub> 박막에서는 ER 효과가 발견되지 않았다는 점이다. 오히려 전기저항이 전류에 따라 변하지 않으며 전류와 전압 사이에 선형적인 모습을 보였다. 이것은 Co가 도핑된 산화물 박막의 결과와 상충된다. 전류의 방향에 수직으로 자기장을 인가하여 MR을 측정하였다. 저온에서의 MR 곡선이 음에서 양으로 변화하는 스위칭 자기장이 벌크와 유사하기는 하나, 약간 고자기장으로 이동한 결과를 보였다. 그리고 더욱이 자기장 방향에 따라 비대칭적인 MR 곡선을 보인 Co 도핑된 박막의 경우와는 달리, 순수한 산화물 박막의 경우는 매우 대칭적인 MR 곡선을 보여주었다. 이러한 결과로부터 우리는 PbPdO<sub>2</sub> 박막에서의 틈 없는 밴드구조가 Co 도핑에 의해 비대칭적인 스핀 틈 없는 밴드구조로의 변화를 추측할 수 있으며, 이는 다른 Co 도핑량에 따른 물성 연구를 통해서 체계적으로 연구될 수 있다.

**D-49****Cu doping effect on the electronic structure of NbSe<sub>2</sub> revealed by ARPES**

KIM Y.K, KOH Y.Y, JUNG Y.S

*Institute of Physics and Applied Physics, Yonsei University, Seoul 120-749, Korea.*

NbSe<sub>2</sub> is the one of the most studied transition metal dichalcogenide(TMD) materials. It has two phases : superconducting and charge density wave(CDW) phases. The superconductivity in NbSe<sub>2</sub> is known to be conventional and should be explained within the BCS theory. On the other hand, CDW mechanism in NbSe<sub>2</sub> cannot be explained by the conventional Fermi surface nesting scenario. Recently, it was discovered that barely occupied state plays an important role in forming CDW states. To find out the exact mechanism of the CDW in NbSe<sub>2</sub>, we try to change the electronic structure of NbSe<sub>2</sub> by Cu doping which gives additional electrons in the system. In this presentation, we present the electronic structure of the Cu doped NbSe<sub>2</sub> measured by angle resolved photoemission spectroscopy (ARPES). We observe the effect of doping on the Fermi surface topology. Fermi level increases and hole-pocket near the  $\Gamma$ -point becomes smaller. As Fermi surface topology changes, the nesting condition for CDW phase might be changed. To see the nesting condition more clearly, we performed auto-correlation calculation.

**D-50****Ferroelectric Properties of Lead-free Na<sub>0.5</sub>K<sub>0.5</sub>NbO<sub>3</sub>-based Thin Films Derived****from Chemical Solution Deposition Method**KIM ILL WON, LEE SUN YOUNG, AHN CHANG WON<sup>1</sup>, HWANG HAK IN<sup>1</sup>, BAE SE HWAN<sup>2</sup>*Department of Physics, University of Ulsan, Ulsan 680-749, South Korea. <sup>1</sup>Convergence Components R&D**Division, KETI, Seongnam 463-816, South Korea. <sup>2</sup>Department of Physics, Dong-A University, Busan 604-714, South Korea.*

Lead pollution from waste of industrial products has become a serious environmental problem, and the use of industrial products including lead compounds has been gradually restricted. Therefore, it is necessary to development lead-free materials with excellent piezoelectric properties for replacing the lead-based materials. Recently, in searching for environmentally friendly piezoelectric materials, (Na,K)NbO<sub>3</sub> (NKN)-based materials have attracted much interest. However, the NKN thin films typically have large leakage currents because the alkaline elements volatilize during sintering process, and it is always difficult to obtain well saturated polarization hysteresis loops. To improve the sinterability and ferroelectric properties, many researchers\* have studied extensively A-site excess, A and/or B site substitution, and polymer modification method for NKN-based thin films. From these points of view, we have deposited NKN-based thin films on the Pt/TiO<sub>2</sub>/SiO<sub>2</sub>/Si substrate by polymer modified chemical solution deposition (CSD) method and their crystallinity, dielectric, ferroelectric, and piezoelectric properties were studied in detail. \*C. W. Ahn, E. D. Jeong, S. Y. Lee, H. J. Lee, S. H. Kang, and I. W. Kim, Appl. Phys. Lett. 93, 212905 (2008).

**D-51****중성자 Pair Distribution Function 분석을 이용한  $\text{BaZr}_x\text{Ti}_{1-x}\text{O}_3$  국소구조 연구**

박 창열, 안 재석, 박 성균, 정 일경<sup>1</sup>

부산대학교 물리학과, <sup>1</sup>부산대학교 물리교육학과 및 유전체 물성연구소.

본 연구에서는  $\text{ABO}_3$  페로브스카이트 구조를 가진 비납계 강유전체  $\text{BaTi}_{1-x}\text{Zr}_x\text{O}_3$  의 국소 구조를 조성과 온도에 따라 분석했다. 이를 위해  $\text{BaTi}_{1-x}\text{Zr}_x\text{O}_3$  ( $x=0.2, 0.25, 0.3$ )을 합성 하였고 300K에서 50K까지 온도를 변화시키면서 중성자 회절 실험을 수행하였다. 측정된 중성자 회절 패턴을 실 공간으로 푸리에 변환하여 PDF 함수를 구하였고, 이로부터 Ti-O본드와 Zr-O본드 길이가 서로 확연히 다름을 확인 할 수 있었다. 보다 구체적인 국소구조 분석을 위해 Reverse Monte Carlo modelling을 수행하였다. 그 결과 Ti이온은  $\text{O}_6$  octaheron의 중심에서 많이 이동 하였으나 Zr 이온은 대체로  $\text{O}_6$  중심에 자리 잡고 있음을 확인 하였다.

D

**D-52****Probing spin glass behavior in the strongly correlated electron system  $\text{La}_2\text{Cu}_{1-x}\text{Li}_x\text{O}_4$** 

$\text{La}_2\text{Cu}_{1-x}\text{Li}_x\text{O}_4$

박 은성, 박 두선<sup>1</sup>, SARRAO J.L.<sup>2</sup>, THOMPSON J.D.<sup>2</sup>

성균관대학교 물리학과, <sup>1</sup>성균관대학교 물리학과, Los Alamos National Laboratory. <sup>2</sup>Los Alamos National Laboratory.

We have measured ac magnetic susceptibility on  $\text{La}_2\text{Cu}_{1-x}\text{Li}_x\text{O}_4$  at  $x=0.023$ , which revealed a spin-glass frequency-dependent behavior below a spin-glass freezing temperature ( $T_{SG}$ ). Depending on directions of ac driving magnetic field ( $H_{ac}$ ), the susceptibility shows a strong anisotropy. When  $H_{ac}$  is parallel to the  $\text{CuO}_2$  plane, it displays a normal frequency dependence with decreasing temperature. In contrast, anomalous frequency dependent behavior appears when  $H_{ac}$  is perpendicular to the  $\text{CuO}_2$  plane, where the anomaly is suppressed with large dc magnetic field. In order to properly understand the anisotropic behavior in the Li-doped cuprate, we have studied both in-phase and out-of-phase components of the ac magnetic susceptibility as a function of frequency at fixed temperatures.

**D-53****Multiple Bosonic Mode Coupling In The Band Dispersion Of  $\text{Sr}_2\text{RuO}_4$** 

KIM Chul, PARK Seung Ryong, LEEM C. S., SONG D. J., KIM Y. K., CHOI S. K., JUNG W. S., KOH Y. Y., YOSHIDA Y.<sup>1</sup>, KIM C.

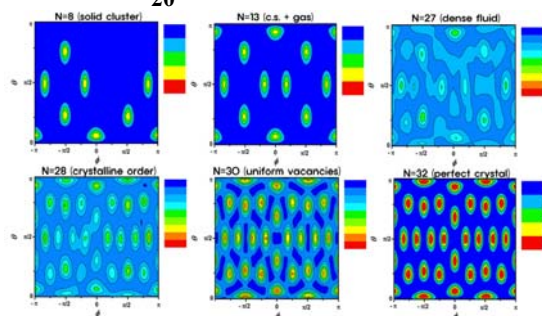
*Institute of Physics and Applied Physics, Yonsei University. <sup>1</sup>Nanoelectronics Research Institute, National Institute of Advanced Industrial Science and Technology, Japan.*

High resolution angle-resolved photoemission spectroscopy data along the high symmetry cuts reveal fine structures in the band dispersion of 4d transition metal oxide  $\text{Sr}_2\text{RuO}_4$ . Band renormalization or so-called "kink" at binding energies of 20meV, 40meV and 70meV were observed. Comparing the kinks with the phonon dispersion[1] and the magnetic excitations[2] from inelastic neutron scattering, we conclude that the origin of these kinks are due to electron phonon coupling. Reference [1] M. Braden, *et al.*, Physical Review B, 76, 014505 (2007) [2] M. Braden, *et al.*, Physical Review B, 66, 064522 (2002)

**D-54****Nanoscale Supersolidity in  $^4\text{He}$  Adsorbed on a  $\text{C}_{20}$  Molecule**

권 용경, 신 현덕  
건국대학교 물리학과

We have performed the path integral Monte Carlo calculations to study adsorption of  $^4\text{He}$  on a single  $\text{C}_{20}$  fullerene molecule. The sum of all interatomic pair potentials between a carbon and a  $^4\text{He}$  atom is employed for the  $^4\text{He}-\text{C}_{20}$  interaction to investigate helium corrugations on the fullerene surface. The radial density distribution shows a sharp peak located at a distance of  $\sim 4.9 \text{ \AA}$  from the center of  $\text{C}_{20}$ . It is found that this first peak is a solid layer consisting of 32  $^4\text{He}$  atoms, with twelve of them being localized on the top of the pentagon centers of the  $\text{C}_{20}$  surface and the other twenty atoms on the top of 20 carbon atoms. As more  $^4\text{He}$  atoms are added, we see the emergence of the second density peak which is almost completed for  $N \geq 150$  and represents a liquid layer. Detailed analysis of both energetics and angular density distributions reveals that the partially-filled first layer is in various quantum states as the number of helium atoms changes (see Fig. 1). It is observed that near completion of the first layer, mobile vacancies can be activated at low temperatures, which results in a finite superfluid fraction as well as a crystalline order. This is a manifestation of the vacancy-based supersolidity in a nanometer scale. Fig 1 : Angular density distributions of  $^4\text{He}$  on the surface of the  $\text{C}_{20}$  molecule as the number of  $^4\text{He}$  atoms( $N$ ) varies.



**D-55****Electron and spin correlations in electron doped high  $T_c$  superconductor  $\text{Pr}_{1-x}\text{LaCe}_x\text{CuO}_4$**  **$\text{Pr}_{1-x}\text{LaCe}_x\text{CuO}_4$** 

송 동준, 박 승룡, 최 성균, 김 철, 김 용관, 정 원식, 고 윤영, YOSHIDA Yoshiyuki<sup>1</sup>, EISAKI Hiroshi<sup>1</sup>, 김 창영  
연세대학교, 물리학과. <sup>1</sup>AIST.

Magnetic properties of electron doped high  $T_c$  superconductor (HTSC)  $\text{Pr}_{1-x}\text{LaCe}_x\text{CuO}_4$  (PLCCO) have been extensively studied by using neutron scattering experiments. The magnetic behavior is different from that of typical electron doped HTSCs such as  $\text{Nd}_{2-x}\text{Ce}_x\text{CuO}_4$ . Its static anti-ferromagnetic (AFM) ordering disappears at a lower Ce concentration than  $\text{Nd}_{2-x}\text{Ce}_x\text{CuO}_4$  but the spin fluctuations survives into the superconducting phase until it disappears together with superconductivity. It is therefore interesting to study in detail the magnetic states of PLCCO and investigate its effect on the superconductivity. As signatures of the magnetic state are reflected in the electronic structures, one may investigate the magnetic state by studying the electric properties by using angle resolved photoemission spectroscopy (ARPES). We performed ARPES studies on PLCCO( $x=0.09, 0.12, 0.15$ ) to investigate the doping dependent electronic structures. Different from other electron doped cuprates, no nodal gap, even for  $x=0.09$  doped samples, is observed. That is, the hole pocket near region survives for dopings as low as  $x=0.09$ . Yet, the pseudo gap (PG) is well defined for  $x=0.09$  and is gradually suppressed as the doping increases to  $x=0.15$ . This behavior can be explained by a weaker but distinct PG effect and reveals existence of electron spin correlations even in the over doping region. These are consistent with neutron scattering results.

**D****D-56****Single-molecule Fluorescence Imaging in Living Cells**

이 남기

포항공과대학교, 물리학과.

Recent advances in single-molecule fluorescence microscope techniques have allowed single-molecule sensitivity to probe various protein-DNA interactions, their structural changes, and fundamental cellular processes in a living cell. Here I introduce a novel single-molecule fluorescence microscope technique for in vivo single protein detection. To study transcription the process of DNA-directed RNA biosynthesis in living cells, I used localization-enhancement fluorescence detection technique. I used a fluorescently tagged T7 RNA polymerase in bacteria containing a T7 promoter integrated into the chromosome. Since there are no other endogenous T7 promoters in the E. coli genome, localized T7 polymerase molecules correspond to transcription at the engineered promoter. In this way, I demonstrated that it is possible to detect single RNA polymerase in living cells and directly measured promoter searching time, transcription initiation and elongation rates by T7 RNA polymerase. This work paves the way to observe individual protein machinery to reveal fundamental cellular processes in living cells.

**D-57****Dynamic Bending and Cleavage of Single-DNA Molecules by Human****Topoisomerase II $\alpha$** 

LEE Sanghwa, HOHNG Sungchul

*Seoul National University, Department of Physics and Astronomy.*

Double helical nature of DNA duplex imposes serious topological problems during DNA transactions. Human topoisomerase II $\alpha$  is a type IIA topoisomerase, which resolves this topological problems encountered during DNA replication and RNA transcription. Because of its high activity especially in fast duplicating cells, it has been a target of the most successful anticancer drugs such as etoposide and teniposide. Type IIA topoisomerases are believed to operate through the following mechanism. First, a DNA duplex, called G-segment, is bound to the central DNA cleavage-religation domain of the topoisomerase. Second, another DNA duplex, called T-segment, is trapped by N-gate domain of the topoisomerase. This clamping motion of N-gate is believed to be correlated with ATP binding to the N-gate. Third, G-segment is open, and T-segment is transported through the open DNA-gate. Finally, the G-segment is religated and T-segment is released through the open C-gate. Because only one gate among three gates (N-gate, DNA-gate, and C-gate) is open in the mechanism, it is called a “two-gate” model. Biochemical and structural studies for more than thirty years support the two-gate model, but many open questions are still remaining. For example, 1) how the cleavage site is selected, 2) what are the mechanistic steps of cleavage and religation, 3) what are the kinetic parameters of each elementary reaction are questions unanswered yet. To address those questions, we developed single-molecule FRET assays. We prepared a G-segment DNA with a specific cleavage site in the center. The DNA was labeled with a FRET pair for the observation of conformation dynamics during cleavage reaction. Interaction between immobilized G-segment DNA and human topoisomerase II $\alpha$  was monitored by using prism-type single-molecule FRET setup. As a result, we could observe elementary reaction steps of cleavage and relegation process in real time. We also studied the effect of etoposide on the operation of topoisomerase II $\alpha$ .

**D-58****Multi-color FRET with Hundreds Single-molecules at a Time**

LEE Jinwoo, HOHNG Sungchul

*Department of Physics & Astronomy, Seoul National University.*

Single-molecule FRET has contributed to solving many of fundamental problems in molecular biology. By using conventional two-color FRET, however, we could get only the inter-dye distance of a FRET pair, and, as a result, it was very hard to resolve complex dynamics of molecular complex, for example, a correlated motion of an enzyme and its substrate. To overcome this limitation, we previously developed a three-color FRET setup based on confocal microscopy, and successfully observed correlated motion of three helical arms of the Holliday junction. In this study, we extended the capability of single-molecule three-color FRET to the regime of total internal reflection microscopy. By adopting fast switching of two excitation lasers (532-nm and 633-nm) and synchronizing CCD filming with laser switching, we could observe the correlated motion of three helical arms of hundreds of the Holliday junction. We will also discuss the possibility of single-molecule 4-color FRET.

**D-59****Conformational Dynamics between B- and Z-DNA probed via single-molecule****FRET**

BAE Sangsu, KIM Doyoun<sup>1</sup>, KIM Yang-Gyun<sup>2</sup>, KIM KyeongKyul<sup>1</sup>, HOHNG Sungchul

*Seoul National University, Department of Physics and Astronomy.* <sup>1</sup>*Sungkyunkwan University School of medicine, Department of Molecular Cell Biology.* <sup>2</sup>*Sungkyunkwan University, Department of Chemistry.*

Since the first discovery of the left-handed DNA structure, Z-DNA, in 1979, its biological role has been under constant debate, partly because of the unclear understanding of the Z-DNA formation mechanism in the cell. Here, we report the first single-molecule FRET experiments on Z-DNA formation. A series of DNA duplexes containing varying CG repeats and different junction numbers were tagged with Cy3 (donor) and Cy5 (acceptor) for FRET measurements, and biotinylated at the end for surface immobilization. Prism-type single-molecule FRET setup was used to monitor the conformational dynamics of hundreds of single molecules simultaneously at varying salt concentrations and with or without Z-DNA inducing protein factors. The salt-induced B-to-Z transition occurred fast with transition time of  $\sim 10$  seconds at 5 M of NaClO<sub>4</sub>, and was reversible because B-form DNA was readily recovered when the salt concentration was reduced back. The transition due to the Z-DNA binding domain (hZ $\alpha_{\text{ADAR1}}$ ) from the human editing enzyme, double-stranded RNA adenosine deaminase, however, was relatively slow with  $\sim 10$  minutes of transition time. Contrary to the salt-induced cases, B-form DNA was not readily recovered after protein removal, which implies the tight binding between Z-DNA and hZ $\alpha_{\text{ADAR1}}$ . We determined the free energy change of protein-induced B-Z transition by measuring the equilibrium constant of duplex DNAs with varying CG repeats. The junction free energy was also determined by comparing duplex DNAs with one B-Z junction or two B-Z junctions. And we also elucidated that hZ $\alpha_{\text{ADAR1}}$  induced B-DNA to Z-DNA passively.

**D-60****Single-molecule Detection of RecA Filament Dynamics**

KIM Sunghyun, JOO Chirlmin<sup>1</sup>, PARK Jeehae<sup>2</sup>, RAGUNATHAN Kaushik<sup>2</sup>, KIM Doseok, HA Taekjip<sup>2</sup>

*Sogang University, Department of Physics and Interdisciplinary Program of Integrated Biotechnology.* <sup>1</sup>*School of Biological Sciences, Seoul National University.* <sup>2</sup>*Howard Hughes Medical Institute, Department of Physics and Center for Biophysics and Computational Biology, University of Illinois at Urbana-Champaign.*

RecA protein plays a key role in DNA repair mechanisms in cells. It forms a filament on the single-stranded (ss) DNA, which allows ssDNA to be stretched for homologous searching followed by recombination. Molecular detail of RecA filament formation and disassembly is not fully understood yet. Here, we use single-molecule fluorescence resonance energy transfer (FRET) method to dissect the monomer binding and dissociation processes. We investigate the influence of the DNA sequence and the solution pH to the binding and dissociation processes of RecA monomer. We characterize each step of ATP hydrolysis process by NTP cofactor exchange via microfluidics. Based on our observation we propose a model of RecA-ssDNA interaction coupled with ATP hydrolysis in a molecular level.

**D-61****Anion-dependant structural change of ionic liquids studied by infrared absorption****spectroscopy**

JEON Yoonnam, CHA Seoncheol, KIM Doseok, KANG Minhyuck<sup>1</sup>, MOON Bongjin<sup>1</sup>, MOON Hyerim, CHEONG Hyeonsik, OUCHI Yukio<sup>2</sup>

*Sogang University, Department of Physics.* <sup>1</sup>*Sogang University, Department of Chemistry.* <sup>2</sup>*Nagoya University, Department of Chemistry.*

By using Attenuated Total Reflection (ATR) infrared absorption and <sup>1</sup>H NMR spectroscopy, we investigated structural difference of ionic liquids (ILs) based on 1-butyl-3-methylimidazolium ([BMIM]<sup>+</sup>) cation and three different halide anions ([X]<sup>-</sup>, X = Cl, Br, and I). When heavy water was mixed with the [BMIM][X] ionic liquids, isotopic substitution of the proton attached to the most acidic carbon (C(2)) of the imidazolium ring was the fastest for [BMIM][Cl], and the slowest for [BMIM][Br]. Above trend does not correlate well with the ionic strength of the anions (Cl<sup>-</sup> > Br<sup>-</sup> > I<sup>-</sup>). This isotopic exchange of H-C(2) for D-C(2) helped to assign the CH<sub>x</sub> (x=1,2,3) vibration peaks in the region between 2800 cm<sup>-1</sup> and 3200 cm<sup>-1</sup>, and the changes of these peaks for different halide anions were also observed. The changes were mostly in the νCH vibration modes of the imidazolium ring, suggesting the relative position of the anion in the bulk liquid is different for these ionic liquids having different halide anions.

**D-62****Effect of the Refractive Index of the Medium in Fluorescence Correlation****Spectroscopy**

CHA Seon Cheol, KIM Sung Hyun, KIM Doseok

*Department of Physics, Sogang University.*

Fluorescence correlation spectroscopy (FCS) has been used to study molecular diffusion in liquid media as it measures resident time of a dye molecule in a small excitation volume in confocal microscopy. We measured the diffusion coefficient of dye molecules dissolved in sucrose aqueous solutions of various concentrations. The diffusion coefficient of the dye molecule dissolved in sucrose solution decreased as the viscosity of the solution increased. In addition, we found a systematic deviation from their literature values. We propose that the difference came mainly from the change of confocal volume with the change in the refractive index in sucrose solutions of different concentrations. To check for this possibility, several liquids having the same viscosity values but different refractive indices were chosen to dissolve dye molecules. The variance in the observed diffusion coefficients in solutions having the same viscosity value manifests that care needs to be taken in the common practice of using sucrose to change the viscosity in the FCS experiment.

**D-63****Covalent Interactions between PCBM and P3HT in Bulk Heterojunction Polymer****Solar Cells**

LEE Eun-Cheol, XIE Xiaoyin

*College of Bio-Nano Technology, Kyungwon University.*

We investigate atomic and electronic structures of the bulk heterojunction of poly-3-hexylthiophene (P3HT) and [6,6]-phenyl-C61 butyric (PCBM) through first-principles density-functional calculations. It is found that the open-circuit voltage can be increased by the chemical hybridization of P3HT and PCBM polymers, which possibly improve the power conversion efficiency of the solar cell. Although this chemical reaction is endothermic by 1.39 eV, the breaking of the chemical bond is suppressed by an energy barrier of 0.71 eV. We will discuss how these metastable chemical interactions can be used to design processes improving the efficiency of P3HT/PCBM composite solar cells.

D

**DF-01(초)****Electron energy-loss spectroscopy in semiconductor devices**

JANG Jae Hyuck, KWON Ji Hwan, JEON Jong Myeong, KIM Miyoung, PARK Tae Joo, HWANG Cheol Seong

*서울대학교, 재료공학부.*

Electron energy-loss spectra contain information on electronic structures and frequency dependent dielectric function. Local variation in composition and electronic structures at the interface of high-k materials are studied by high-resolution electron energy-loss spectroscopy in a scanning transmission electron microscope. While the interfacial reaction between substrates and high-k dielectrics often causes atomic diffusion, the interface between dielectrics and electrode may suffer from the Fermi-level pinning. The investigation of diffusion at the interface layer, leakage current paths of the dielectrics, and local phase identification of alloying structures will be presented.

**DF-02(초)****In-situ synchrotron x-ray scattering study on the surface and interface structures**

NOH Do Young, KIM Yongsam<sup>1</sup>, KIM Do Hyung<sup>2</sup>, CHO Inwha<sup>3</sup>

광주과학기술원, 신소재공학과 & 나노바이오재료전자공학과. <sup>1</sup>School of Applied Engineering Physics, Cornell University. <sup>2</sup>한국전력. <sup>3</sup>광주과학기술원, 신소재공학과.

Surface x-ray scattering techniques based on synchrotron x-rays provide a great opportunity to investigate surface and interface structures in non-destructive manner. In this paper, we present two examples of interface characterization using surface x-ray scattering. The first example is the structure of the metallic Si(001) surface above 900 K. Above 900 K, the ( 2, 1) integer-order surface peak decreases anomalously while the (3/2, 0) reconstruction order peak increases. These results together with the behavior of the crystal truncation rod profile exclude the structural models of the metallic Si (001) surface based on the enhanced Debye-Waller factor and the transition to the symmetrical dimer. The experimental results are explained by the enhanced dynamic step-edge fluctuations induced by the adatom attachments and detachments above 900 K. The second example is the chemical depth profile of the passive oxides grown on a stainless-steel surface was obtained quantitatively by *in situ* anomalous x-ray reflectivity. The passive film consists of a Cr oxide inner layer and a Fe/Cr oxide outer layer. The absence of Fe oxide underneath Cr oxide indicates that Cr oxide provides the passivity in stainless steel by inhibiting oxygen anion diffusion. The oxide grows by limited metallic cation transfer.

**DF-03(초)****Infrared Spectroscopy of Interface Charge in ZnO Field-Effect Transistor**

최 은집, 김 주연, 정 성훈, 김 기태<sup>1</sup>, 이 기문<sup>1</sup>, 임 성일<sup>1</sup>

서울시립대 물리학과. <sup>1</sup>연세대학교 물리학과.

In contrast with the surface and bulk analysis, it is difficult and challenging to probe interface of two- or multi-layer materials in electronic/optical devices using spectroscopic methods. In this work, we applied the infrared (IR) transmission spectroscopy to study ZnO based field-effect transistor (FET) where interface charge layer is induced by the source-gate voltage  $V_{GS}$  in ZnO / SiO<sub>2</sub> / p-Si structure. The carrier absorption spectrum in far-IR region 100 cm<sup>-1</sup>~700cm<sup>-1</sup> exhibits a non-Drude, incoherent conduction behavior at low gate-source voltages ( $V_{GS}$  <40 V), which evolves toward a standard Drude behavior as  $V_{GS}$  is increased. This IR change indicates that the interface carrier undergoes strong backscattering collisions at low  $V_{GS}$  in contrast with the isotropic scattering behavior in bulk ZnO. The electron scattering behavior of IGZO films—as deposited, thermal annealed, UV-irradiated, and H<sup>+</sup> irradiated—are measured and compared. Our work shows that infrared spectroscopy can provide invaluable information on the microscopic scattering mechanism of the interface charge in FET device.

**DF-04(초)****광전자 분광 및 관련 기술을 이용한 유기전자 소자의 계면 연구**

박 용섭

경희대학교 물리학과.

OLED (organic light-emitting diode), 혹은 OTFT (organic thin film transistor) 소자는 유기 반도체 물질 박막에 금속 전극을 붙여 전압을 가하면 유기물질에서 빛이 나오거나 트랜지스터 특성을 보이는 성질을 이용한 유기 전자 소자(organic electronic devices) 이다. 본 발표에서는 이러한 소자들의 성능에 중요한 영향을 미치는 금속과 유기물질, 또는 서로 다른 유기물 사이의 계면의 전자구조 변화와 에너지 준위의 정렬을 X-ray 및 UV 광전자 분광법 (X-ray & UV photoelectron spectroscopy)을 이용하여 연구한 내용을 살펴보고, 이를 통해서 소자의 성능향상에 어떻게 기여할 수 있는지 고찰한다.

D

**DF-05****Superconductivity of optimally doped single crystals of the  $\text{BaFe}_{1.8}\text{Co}_{0.2}\text{As}_2$  superconductor**

LEE Sung-IK, CHOI Ki-Young<sup>1</sup>, KIM Soo Hyun, CHOI Changho, JUNG Myung-Hwa, WANG X. F.<sup>2</sup>, CHEN X. H.<sup>2</sup>, NOH Jae Dong<sup>3</sup>

*National Creative Research Initiative Center for Superconductivity, Department of Physics, Sogang University, Seoul 121-742, Republic of Korea. <sup>1</sup>National Creative Research Initiative Center for Superconductivity, Department of Physics, Sogang University, Seoul 121-742, Republic of Korea, Department of Physics, Seoul University, Seoul 130-743, Republic of Korea. <sup>2</sup>Hefei National Laboratory for Physical Sciences at Microscale and Department of Physics, University of Science and Technology of China, Hefei, Anhui 230026, China. <sup>3</sup>Department of Physics, Seoul University, Seoul 130-743, Republic of Korea.*

To understand the superconductivity of iron-pnictide superconductors, we synthesized optimally doped single crystals of  $\text{BaFe}_{1.8}\text{Co}_{0.2}\text{As}_2$ , which had a critical temperature,  $T_c$ , of 23.6 K. We observed that the fluctuation magnetization and fluctuation conductivity follow the three dimensional scaling form in the critical fluctuation region above 0.5 Tesla which indicates that this material belongs to the three dimensional superconductors. The I-V characteristics in magnetic field followed the 3D scaling behavior and identified the existence of vortex glass phase. The full range of the temperature dependence of  $H_{c1}$  was explained by using a multi-gap structure, such as two s-wave gap symmetry. We estimated the magnitude of the two gap as  $\Delta_1(0) = 1.64$  0.2 meV for the small gap and  $\Delta_2(0) = 6.20$  meV for the large gap. The super-fluid density deviated from the Uemura relation.

**DF-06****Nearly isotropic upper critical field in superconducting  $\text{SrFe}_{1.85}\text{Co}_{0.15}\text{As}_2$  and  $\text{FeSe}_{0.4}\text{Te}_{0.6}$  single crystal**

KHIM Seunghyun, KIM Jae Wook, KIM Jun Sung<sup>1</sup>, CHOI Eun Sang<sup>2</sup>, BALAKIREV F. F.<sup>3</sup>, NOHARA Minoru<sup>4</sup>, LEE Suk Ho<sup>5</sup>, TAKAGI Hidenori<sup>6</sup>, BANG Yunkyu<sup>7</sup>, KIM Kee Hoon

*FPRD, Department of physics and astronomy, Seoul National University, Seoul 151-742, Republic of*

*Korea. <sup>1</sup>Department of Physics, Pohang University of Science and Technology, Pohang 790-784, Republic of*

*Korea. <sup>2</sup>National High Magnetic Field Laboratory, Florida State University, Tallahassee, Florida 32310,*

*USA. <sup>3</sup>National High Magnetic Field Laboratory, Los Alamos National Laboratory, Los Alamos, New Mexico*

*87545, USA. <sup>4</sup>Department of Physics, Okayama University, Okayama 700-8530, Japan. <sup>5</sup>Optical Engineering*

*Research Institute, Mokpo National University, Muam 534-729, Republic of Korea. <sup>6</sup>Department of Advanced*

*Materials, University of Tokyo, Kashiwa, Chiba 277-8561, JST, TRIP, Kashiwa, Chiba 277-8561, RIKEN (The*

*institute of Physical and Chemical Research), Wako, Saitama 351-0198. <sup>7</sup>Department of Physics, Chonnam*

*National University, Kwangju 500-757, Republic of Korea.*

The discovery of superconductivity in Fe-pnictide has triggered much of interests in recent years. In particular the upper critical field is one of key parameter to investigate underlying properties such as pairing strength and electronic structure. So far It has been observed in anisotropic behavior in  $\text{ReOFeAs}$  ( $\text{Re}$  = rare earth) and isotropic in  $\text{AFe}_2\text{As}_2$  ( $\text{A}$  = alkali metal) system. And two-band model with dirty limit provided a quite well understanding. In this report, we show the nearly isotropic upper critical field properties in superconducting  $\text{SrFe}_{1.85}\text{Co}_{0.15}\text{As}_2$  and  $\text{FeSe}_{0.4}\text{Te}_{0.6}$  single crystals. And we suggest the possibility on Pauli limiting behavior in Fe-based superconductors.

**DF-07****Single crystal growth and investigation of the new superconductor  $\text{LiFeAs}$  with  $T_C=18.3$  K**

GHIM Jin Soo, JUNG MYUNG HWA<sup>1</sup>, KWON Young Seung

*Department of Physics, Sungkyunkwan University, Suwon 440-746, Republic of Korea.. <sup>1</sup>National Creative*

*Research Initiative Center for Superconductivity, Department of Physics, Sogang University, Seoul, Korea..*

$\text{LaFeAsO}_{1-x}\text{F}_x$  철계 초전도체가 발견된 이래로 다양한 상을 가진 새로운 물질들이 합성되었다. 우리는 그 중 가장 합성하기 어렵다고 알려진 리튬 철계 초전도체  $\text{LiFeAs}$ 의 단결정 성장에 성공하였다. 출판된 다른 논문들의 보고에 의하면  $\text{LiFeAs}$ 는 SDW에 의한 초전도가 아닌 다른 자기적 상호작용에 의해 초전도가 야기된다고 추정되고 있다. 단결정 성장 방법은  $\text{FeAs}$ 의 전물질(precursor)을 만들고 리튬 와이어를 비율에 맞게 텅스텐 도가니에 넣어 밀봉한 후 브리지만 방법을 이용하여 전기로에서 성장시켰다. 비저항 측정 결과 다른 논문의 10배 큰 잔류저항비(RRR)를 얻었고, 일부 논문들에서 상압에서 저항이 0이 되지 않는 현상을 시료의 오염이나 밴드갭 사이에 불순물에 의해 야기하는 것으로 보고했지만, 우리 시료는 비저항이 0인  $T_c$ 가 18.3K로 타 논문의 18K보다도 약간 높다. 자화를 측정에서는 자성은 없는 것으로 나왔고  $T_c$ 는 18.6K 정도였다. 보고된 논문에 의하면  $\text{LiFeAs}$ 는 높은 임계자기장이 기대되므로 여러 조건들과 합성비를 변화시키면서 양질의 단결정을 만들고자 한다

**DF-08****Theoretical Study of Electronic Structures in Iron Pnictide Superconductors****using the Coherent Potential Approximation**

MOON Jisoo, CHOI Hyoung Joon

*Department of Physics and IPAP, Yonsei University.*

Iron pnictide superconductors have a magnetically ordered low-temperature phase and an apparently non-magnetic high-temperature phase. We study electronic structures in iron pnictide superconductors using the coherent potential approximation in order to consider fluctuations in the direction of Fe magnetic moments. At low temperature, partial fluctuations are considered, while, at high temperature, full fluctuations are considered. Electronic structures at low and high temperatures are compared with corresponding experimental measurements. This work was supported by the KRF (KRF-2007-314-C00075) and by the KOSEF Grant No. R01-2007-000-20922-0. Computational resources have been provided by KISTI Supercomputing Center (KSC-2008-S02-0004).

D

**DF-09****First-Principles Study On The Magnetic Properties of Iron Chalcogenide****Superconductors**

MOON Chang-Youn, CHOI Hyoung Joon

*Department of Physics and IPAP, Yonsei University.*

We have investigated the magnetic properties of iron chalcogenide superconductors using the first-principles pseudopotential method. FeTe is known to have a unique magnetic ordering pattern called 'double stripe' with  $(\pi, 0)$  ordering vector, in contrast to the well-known 'single stripe'  $(\pi, \pi)$  ordering of iron pnictide superconductors. We investigate in detail the origin of this double stripe ordering and compare with the single stripe ordering which is calculated to be the ground state phase for FeSe, and find that this different ordering patterns in fact can be understood by a general mechanism of magnetic interactions. Together with known experimental observations, our results propose a comprehensive view in the magnetism and the superconductivity in these materials. This work was supported by the KRF (KRF-2007-314-C00075) and by the KOSEF Grant No. R01-2007-000-20922-0. Computational resources have been provided by KISTI Supercomputing Center (KSC-2008-S02-0004).

**DF-10****Direct observation of two-gap superconductivity in  $\text{SrFe}_{1.85}\text{Co}_{0.15}\text{As}_2$  single****crystals by scanning tunneling microscopy and spectroscopy**

PARK Jewook, KHIM Seunghyun<sup>1</sup>, JEON Gun Sang<sup>1</sup>, KIM Jun Sung<sup>2</sup>, KIM Kee Hoon<sup>3</sup>, CHAR Kookrin  
*Center for Strongly Correlated Materials Research, Department of Physics and Astronomy, Seoul National University, Seoul 151-747, Republic of Korea.* <sup>1</sup>*Department of Physics and Astronomy, Seoul National University, Seoul 151-747, Republic of Korea.* <sup>2</sup>*Department of Physics, Pohang University of Science and Technology, Pohang 790-784, Republic of Korea.* <sup>3</sup>*Department of Physics and Astronomy, Seoul National University, Seoul 151-747, Republic of Korea.*

Scanning tunneling microscopy and spectroscopy (STM/S) studies on the recently discovered superconductor,  $\text{SrFe}_{1.85}\text{Co}_{0.15}\text{As}_2$  single crystal, and its parent material  $\text{SrFe}_2\text{As}_2$  reveal a 0.8 nm stripe pattern in the atomic resolution topographic images of both samples. In the conductance spectra taken along a line on the  $\text{SrFe}_{1.85}\text{Co}_{0.15}\text{As}_2$  surface robust superconducting gaps ( $2\Delta_{\text{large}} = 17.3$  meV) as well as additional small gap ( $2\Delta_{\text{small}} = 2.9$  meV) structures were simultaneously observed. To the best of our knowledge, these are the first observations of such two-gap structures in pnictides in STS/M studies.

**DF-11****Synthesis and Investigation of the New Superconductor  $\alpha\text{-FeSe}$  ( $T_c \sim 9.4\text{K}$ )**

SONG Yoo-Jang, JUNG Myung Hwa<sup>1</sup>, RHYEE Jong-Soo<sup>2</sup>, KWON Young-Seung  
*Department of Physics, Sungkyunkwan University, Suwon 440-746, Republic of Korea.* <sup>1</sup>*National Creative Research Initiative Center for Superconductivity, Department of Physics, Sogang University, Seoul, Korea.* <sup>2</sup>*Materials Research Laboratory, Samsung Advanced Institute of Technology, Yongin 446-712, Republic of Korea.*

We synthesized the tetragonal iron-chalcogenide superconductor FeSe by using a Bridgeman method. Electrical resistivity and magnetic moment measurements confirm a superconductivity with  $T_c$  at around 9.4K under an atmospheric pressure. The analysis of Electron Probe Micro Analyzer (EPMA) for our sample indicates that the stoichiometric ratio of Fe:Se is 1:1( $\pm 0.002$ ) within error limit. The ratio of room temperature-to-residual resistance (RRR) is  $\approx 9.3$ , and the upper critical field  $H_{c2}(0)$  is estimated to be  $\sim 43\text{T}$  at  $T_c$  onset. Based on the Bean model, We also report critical current density,  $J_c$ , which is estimated to be order of  $\sim 10^3$  A/cm<sup>2</sup> below  $T_c$  by using field-dependent magnetic moments, though this is smaller than  $\sim 10^5$  A/cm<sup>2</sup> of other iron-pnictide superconductors.

**DF-12****The interplay between superconductivity and magnetism in the sign reversed****pairing model of the pnictides**

LEE Nayoung, CHOI Han-Yong

*Department of Physics, SungKyunKwan University, Suwon 440-746, Korea.*

We studied the interplay between the superconductivity (SC) and antiferromagnetism (AF) as a function of the temperature,  $T$ , and doping,  $x$ , of the Fe based superconductors. By a combination of the Ginzburg-Landau expansion of the free energy around the multi-critical point up to the 4th order in the AF and SC order parameters and the self-consistent numerical calculations of the gap equation of the four band sign reversed pairing model, we construct the phase diagram in the  $T$ - $x$  plane for the pnictides. Based on these results we discuss the conditions for the phase separation and coexistence of the superconducting and antiferromagnetic states. These are compared with the various experimental observations for the pnictide superconductors like  $\text{Ba}(\text{Fe}_{1-x}\text{Co}_x)_2\text{As}_2$  and  $\text{Ba}_{1-x}\text{K}_x\text{Fe}_2\text{As}_2$ .

D

**DF-13****Effects of Two Gaps and Paramagnetic Pair Breaking on the Upper Critical Field of  $\text{SmFeAsO}_{0.85}$  and  $\text{SmFeAsO}_{0.8}\text{F}_{0.2}$  Single Crystals**LEE Hyun-Sook, BARTKOWIAK Marek<sup>1</sup>, PARK Jae-Hyun, LEE Jae-Yea, KIM Ju-Young<sup>2</sup>, CHO B. K.<sup>2</sup>, JUNG Chang-Uk<sup>3</sup>, KIM Jun Sung, LEE Hu-Jong

*Pohang University of Science and Technology, Department of Physics. <sup>1</sup>Forschungszentrum Dresden-Rossendorf, Hochfeld-Magnetlabor Dresden. <sup>2</sup>Gwangju Institute of Science and Technology, Materials Science and Engineering. <sup>3</sup>Hankuk University of Foreign Studies, Department of Physics.*

We investigated the temperature dependence of the upper critical field [ $H_{c2}(T)$ ] of fluorine-free  $\text{SmFeAsO}_{0.85}$  and fluorine-doped  $\text{SmFeAsO}_{0.8}\text{F}_{0.2}$  single crystals by measuring the resistive transition in low static magnetic fields and in pulsed fields up to 60 T. We compared the  $H_{c2}(T)$  data of our crystals with the conventional Werthamer-Helfand-Hohenberg (WHH) theory.  $H_{c2}^c(T)$ 's for both crystals are enhanced compared to the WHH prediction, while  $H_{c2}^{ab}(T)$ 's are suppressed below the WHH curve with a flattening behavior. We confirmed that the  $H_{c2}^c(T)$ 's well follow the two-gap dirty-limit prediction and the flattening of  $H_{c2}^{ab}(T)$  is governed mainly by the paramagnetic pair-breaking effect rather than the two-gap effect. This study shows that the upper critical field in Sm-based iron-pnictides is determined by the complex interplay of a two-band nature and the paramagnetic effect depending on the direction of magnetic field application with respect to the crystal axes. We believe this is the generic characteristics of different families of iron-pnictide compounds.

**DF-14****Single Crystal Growth of Fe-chalcogenide  $\text{Fe}_{1+\delta}\text{Se}_{1-x}\text{Te}_x$  and their Physical****Properties**

LEE Bumsung, KHIM Seung Hyun, KIM Kee Hoon

*Department of Physics and Astronomy, Seoul National University.*

We report single crystal growth and physical properties of Fe-chalcogenides  $\text{Fe}_{1+\delta}\text{Se}_{1-x}\text{Te}_x$ , in which superconductivity has been found recently, similar to the case of Fe-pnictides [1]. This system has the simplest structure among the Fe-chalcogenides and -pnictides, in which alternate stacking of Fe and Se layers along the  $c$ -axis forms the tetragonal structure. Moreover, a possibility of unconventional superconductivity with a pairing symmetry beyond  $s_{\pm}$  was suggested based on ARPES [2] and muon spin rotation studies [3]. To systematically study the superconducting properties of this system, we have thus grown a series of  $\text{Fe}_{1+\delta}\text{Se}_{1-x}\text{Te}_x$  single crystals by the self-flux method with control of excess Fe and Se ratio. Self-flux growth was successful only for  $x > \sim 0.5$ . According to our resistivity and magnetization studies,  $x=0.6$  and  $0.8$  samples showed superconductivity at  $T_C \approx 14$  K, while an  $x=1.0$  sample showed a signature of a spin-density-wave ordering around 65 K. In the magnetization data, however, a positive magnetic susceptibility was observed in the superconducting phase, which indicates presence of local magnetic moment or enhanced Pauli magnetism related to excessive Fe. Effects of enhanced magnetism driven by excess Fe, or deficient Se/Te, on physical properties such as upper critical fields and the paramagnetic susceptibility are further discussed [4]. [1] F.-C. Hsu, *et al.* PNAS 105, 14262-14264 (2008) [2] Y. Xia, *et al.* PRL 103, 037002 (2009) [3] R. Khasanov, *et al.* PRB 78, 220510 (2008) [4] K.W.-Lee, *et al.* PRB 78, 174502 (2008)

**DF-15****Vortex dynamic and gap symmetry for single crystals of the  $\text{BaFe}_{1.8}\text{Co}_{0.2}\text{As}_2$  superconductor** **$\text{BaFe}_{1.8}\text{Co}_{0.2}\text{As}_2$  superconductor**

CHOI Ki-Young, LEE Sung-Ik, KIM Soo Hyun, CHOI Chanho, JUNG Myung-Hwa, NOH Jae Dong<sup>1</sup>

*Creative Research Initiative Center for Superconductivity, Department of Physics, Sogang University. <sup>1</sup>Department of Physics, University of Seoul.*

To understand the superconductivity of iron-pnictide superconductors, we synthesized optimally doped single crystals of  $\text{BaFe}_{1.8}\text{Co}_{0.2}\text{As}_2$ , which had a critical temperature,  $T_c$ , of 23.6 K. We observed that the fluctuation magnetization and fluctuation conductivity follow the three dimensional scaling form in the critical fluctuation region above 0.5 Tesla which indicates that this material belongs to the three dimensional superconductors. The I-V characteristics in magnetic field followed the 3D scaling behavior and identified the existence of vortex glass phase. The full range of the temperature dependence of  $H_{c1}$  was explained by using a multi-gap structure, such as two s-wave gap symmetry. We estimated the magnitude of the two gap as  $\Delta_1(0) = 1.64 \pm 0.2$  meV for the small gap and  $\Delta_2(0) = 6.20 \pm 0.2$  meV for the large gap. The superfluid density deviated from the Uemura relation.

**DF-16****The Growth of High-quality *c*-axis Oriented Co-doped SrFe<sub>2</sub>As<sub>2</sub> Thin Films by****Pulsed Laser Deposition with Excimer Laser**

CHOI Eun-Mi, JUNG Soon-Gil, LEE Nam-Hoon, KWON Young-Seung, KANG Won Nam, KIM Dong Ho<sup>1</sup>, JUNG Myung-Hwa<sup>2</sup>, LEE Sung-Ik<sup>2</sup>, SUN Liling<sup>3</sup>

*Bk21 Physics Division and Department of Physics, Sungkyunkwan University. <sup>1</sup>Department of Physics, Yeungnam University. <sup>2</sup>Department of Physics, Sogang University. <sup>3</sup>National Laboratory for Superconductivity, Institute of Physics, Chinese Academy of Sciences.*

The recent discovery of classes of Fe-based layered superconductors has attracted much attention to basic superconducting mechanism and practical application because of remarkably high superconducting transition temperature ( $T_c$ ) and zero-temperature upper critical field ( $H_{c2}(0)$ ) despite of ferromagnetic material base. These properties make the prospect for superconducting electronics. However success in superconducting electronics has been limited because of difficulties of fabricating high quality thin film. Here we report the growth of high-quality *c*-axis oriented Co-doped SrFe<sub>2</sub>As<sub>2</sub> thin films with bulk superconductivity by a pulsed laser deposition (PLD) technique using 248-nm-wavelength KrF excimer laser and As-rich phase (about 30 %) target to prevent the deficiency of As in thin film. The thin film show higher superconducting transition temperature, low resistivity and smooth surface. We firstly reported magnetization versus temperature and field curve showing strong diamagnetism and transport critical current density ( $J_c$ ). These results supply necessary information for practical application of Fe-based superconductor.

**DF-17****Superconducting properties of P-doped BaFe<sub>2</sub>As<sub>2</sub>**

HONG J. B., JANG Y. R., RHYEE J. S.<sup>1</sup>, CHO J. H.<sup>2</sup>, JUNG M. H.<sup>3</sup>, KWON Y. S.

*Department of Physics, Sungkyunkwan university, Suwon 440-746, Republic of Korea. <sup>1</sup>Material Research Laboratory, Samsung Advanced Institute of Technology, Yongin 446-712, Republic of Korea. <sup>2</sup>Nano Material Research Team, Korea Basic Science Institute, Daejeon 305-333, Republic of Korea. <sup>3</sup>Department of Physics, Sogang University, Seoul 121-742, Republic of Korea.*

We have studied the superconducting properties of P-doped BaFe<sub>2</sub>As<sub>2</sub> single crystal via electrical resistivity, specific heat and magnetic susceptibility measurements. Single crystal of BaFe<sub>2</sub>(As, P)<sub>2</sub> was grown by using vapor transport and Bridgeman method. The electrical resistivity shows the superconducting transition with  $T_C^{onset} = 31$  K. The magnetic susceptibility also shows the diamagnetism at 31 K. Partial substitution of As with P generates chemical pressure to the system, suppresses the magnetism in its parent compound and induces the superconducting state. We will report the single crystal method and its physical properties of P-doped BaFe<sub>2</sub>As<sub>2</sub> in this KPS fall meeting.

**DF-18(초)****고온 초전도체의 분광학적 특성**

황 정식

부산대학교, 물리학과.

산화구리 고온 초전도체는 1986년 처음으로 발견된 이후 응집물리 물질 중에 가장 많이 연구된 물질 중의 하나이다. 분광학으로 이 물질의 광학적 특성을 연구하였다. 광학적 자체에너지 (optical self-energy)는 일반화된 드루드(extended Drude) 모델에서 정의된 양으로 각분해능 광전자 분광학 (angle-resolve photoemission spectroscopy)으로 측정될 수 있는 유사입자의 자체에너지(quasiparticle self-energy)와 대응되는 광학적 양이다. 이 광학적 자체에너지는 전자들 사이에 강한 상호작용이 있는 계(strongly correlated systems)내의 전자들 사이의 상호작용의 정보를 포함하고 있는 흥미있는 양이다. 고온 초전도체의 광학적 자체에너지가 이 물질내의 전자쌍을 형성하는 힘을 보여 줄 수 있을 것으로 기대된다. 본 발표에서는 Bi-계 고온 초전도체의 광학적 자체에너지를 분석하였다. 이 연구의 결과는 보존을 매개로 하는 초전도 매카니즘이 가능성있는 것임을 입증하며 또한 그 매개보존이 자기적 성질을 띌 수 있다는 것을 제시한다. 참고 자료: 1. J. Hwang, T. Timusk and G.D.Gu, *Nature* 427, 714-717 (2004). 2. J. Hwang, T. Timusk, E. Schachinger and J. P. Carbotte, *Physical Review B* 75, 144508/1-6 (2007). 3. J. Hwang, E. Schachinger, J. P. Carbotte, F. Gao, D. B. Tanner and T. Timusk, *Physical Review Letters* 100, 137005/1-4 (2008).

**DF-19****First-principles Study of Fermi Surface Topology in Underdoped High- $T_c$** **Superconductors**

OH Hyungju, CHOI Hyoung Joon

Department of Physics and IPAP, Yonsei University.

The exhibition of clear quantum oscillations in the magnetization (de Haas-van Alphen) and conductivity (Shubnikov-de Haas) were recently reported in ortho-II  $\text{YBa}_2\text{Cu}_3\text{O}_{6.5}$  and  $\text{YBa}_2\text{Cu}_4\text{O}_8$ , showing the existence of a closed Fermi surface in the normal state of the underdoped cuprates. In addition to quantum oscillations, negative values of Hall coefficients were reported in ortho-II  $\text{YBa}_2\text{Cu}_3\text{O}_{6.5}$ , implying existence of electron pockets on the Fermi surface. In the present work, we study the electronic structures of  $\text{YBa}_2\text{Cu}_3\text{O}_{6.5}$  and  $\text{YBa}_2\text{Cu}_4\text{O}_8$  using the LDA+U method in which on-site Coulomb repulsion  $U$  is added to the local density approximation (LDA). It is shown that with antiferromagnetic order in  $\text{CuO}_2$  planes, small-size hole pockets are formed near the so-called Fermi-arc positions, and these reproduce the low-frequency oscillations. Also a large electron pocket is formed in  $\text{YBa}_2\text{Cu}_3\text{O}_{6.5}$ , and it gives rise to the high-frequency oscillations and the negative Hall coefficient. Our study shows that magnetic fluctuations are important in the electronic structures in underdoped high- $T_c$  cuprates. This work was supported by the KRF (KRF-2007-314-C00075) and by the NRF of Korea (Grant No. 2009-0081204). Computational resources have been provided by KISTI Supercomputing Center (KSC-2008-S02-0004).

## DT-01(초)

### Scanning Tunneling Microscope의 원리와 표면화학에의 응용

구 자용

한국표준과학연구원.

1980년대 초까지도 개별원자의 위치나 거동을 관찰하는 것은 원리적으로 불가능하다고 생각되었다. 1980년대 초에 개발된 STM은 이러한 선입관을 깨고 도체나 반도체 표면의 형상을 원자수준의 분해능으로 관찰할 수 있는 능력을 보여주었다. 이후 AFM을 비롯하여 비슷한 원리로 작동하는 여러 종류의 Scanning Probe Microscope들이 개발되어 과학/공학의 넓은 분야에 많은 기여를 해왔다. STM의 작동원리는 의외로 매우 간단한데 여기서는 그 기본원리를 알아보고 최근 20여년에 걸쳐 발전해온 STM의 역사를 간단히 조망해본다. 그리고 반도체 재료인 실리콘의 표면에서 일어나는 몇 가지 간단한 화학반응에 STM을 적용하여 연구한 예를 소개한다.

D

## DT-02(초)

### 제일원리계산을 이용한 STM 이미지 모사 기법과 표면 원자 구조 연구에의 응용

김 한철

숙명여자대학교 물리학과.

제일원리계산은 고체 내부에 존재하는 전자들의 양자역학적인 해를 구하는 수치계산법으로서, 1970년대 말에 도입된 이후에 약 30여 년 간 응집물질계의 물성을 예측하는 데 매우 성공적으로 적용되어 왔다. 최근에는, 병렬 슈퍼컴퓨터의 성능 향상과 PC 연산능력의 눈부신 발달 그리고 PC 기반 클러스터 컴퓨터의 보급으로 인해, 약 1,000여개의 원자를 포함하는 물질계를 제일원리계산으로 다룰 수 있게 되었다. 나노과학기술의 발전은 물질에 대한 양자역학적인 이해를 제공하는 제일원리계산의 필요성을 더욱 증가시키고 있다. 한편, 나노과학의 많은 연구는 물질 표면의 원자 구조, 표면에서의 이종 원자 및 분자의 반응 (흡착, 확산, 분해, 혼입 등), 표면에 형성되는 나노구조들에 대한 이해를 필요로 한다. 깨끗한 물질 표면 및 이종 원소에 의해 변형된 표면에 대한 원자 수준의 미시적인 정보를 얻을 수 있는 가장 직접적인 실험 수단은 주사투과현미경 (Scanning tunneling microscope, STM)이며, 실제로 STM을 이용한 표면 원자 구조의 관측 및 표면에서의 원자 조작 등 놀라운 실험 결과들이 지속적으로 보고되고 있다. 이 발표에서는 제일원리계산법과 STM 이론 및 모사 기법들을 간략히 소개할 예정이다. 또한, 응용 사례로서 STM 실험과 제일원리계산의 성공적인 공동 연구 결과 몇 가지를 소개하려 한다.

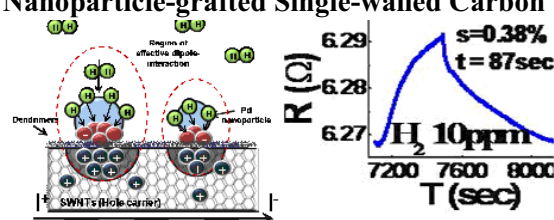
**E-01****Hydrogen Sensing Mechanism of Pd Nanoparticle-grafted Single-walled Carbon Nanotubes with Dendrimers**

LEE Jun Min, JU Seonghwa<sup>1</sup>, JUNG Yeongri<sup>1</sup>, KIM Sung-Jin<sup>1</sup>, LEE Wooyoung

연세대학교 신소재공학과, <sup>1</sup>이화여자대학교 화학과.

We successfully functionalized Pd nanoparticles (NPs) on the surfaces of single-walled carbon nanotubes (SWCNTs) by dendrimer-mediated synthesis using NH<sub>2</sub>-terminated

PAMAM dendrimers. The size of the Pd-NPs can be controlled by adjusting the pH, and the number of attached Pd-NPs on the SWCNTs can be increased because of the presence of dendrimers on the SWCNTs. Pd-NPs-grafted directly on SWCNTs (Sample I) displayed a high sensitivity (25%) to hydrogen gas but a very slow response time (324 s) and poor recovery. Pd-dendrimer-SWCNTs (Sample II) showed good recovery and a much faster response time (3 s) but lower sensitivity (8.6%) than Sample I, which we attributed to induced dipole moments in the dendrimers. Sample III (fabricated by heating Sample II) showed fast response time (7 s) and high sensitivity (25%) and satisfied Sievert's law, indicating that the pyrolysis of the dendrimers in Sample II plays a key role in improving sensitivity by reducing the distance between the surface of the SWCNTs and the functionalized Pd-NPs. Our fabrication method allows the production of highly sensitive hydrogen gas sensors that exhibit a broad dynamic detection range, fast response times, and an ultra-low detection limit of 10 ppm. We discuss the hydrogen gas sensing mechanism in Pd nanoparticle-grafted single-walled carbon nanotubes with dendrimers.

**E-02****Large-Scale Separation of Metallic and Semiconducting Single-Walled Carbon****Nanotubes using Octadecylamine (ODA)**

김 형준, 황 성식, 장 영욱<sup>1</sup>, 오 제승, 유 경화<sup>2</sup>

Nanomedical National Core Research Center, Yonsei University, Seoul 120-749, Korea. <sup>1</sup>Department of Physics, Yonsei University, Seoul 120-749, Korea. <sup>2</sup>Nanomedical National Core Research Center, Yonsei University, Seoul 120-749, Korea; Department of Physics, Yonsei University, Seoul 120-749, Korea.

Separation of semiconducting and metallic single-walled carbon nanotubes has been achieved for arc-discharged SWNTs. The bulk separation of semiconducting from metallic single-walled carbon nanotubes has been done by using octadecylamine (ODA). The selective interaction of amine groups to carboxyl functionalized semiconducting SWNTs, as opposed to metallic SWNTs, leads to the large-scale separation. Separated SWNTs were characterized by Raman, UV-VIS-NIR, and X-ray photoelectron spectroscopy and electrical transport measurements.

**E-03****Stability of screen-printed carbon nanotube field emitters under residual gases**

LEE Hansung, JANG Eunsoo, GOAK Jeungchoon, LEE Naesung

*Faculty of Nanotechnology and Advanced Materials Engineering, Sejong University.*

Carbon nanotubes (CNTs) are one of the most promising field emitter materials due to their excellent electrical conductivity and chemical and mechanical stability as well as their high aspect ratios. Although much effort has been made to commercialize CNT field emitter devices, several obstacles, in particular, emitter lifetime, still remain to be overcome. Among many factors affecting the lifetime of CNT emitters working in vacuum, residual gases inside a panel would be one of the most crucial causes, especially when the CNT emitters are made from the organic vehicle-based paste. The residual gases can cause a catastrophic damage to the vacuum microelectronic devices by electrical arcing or ion bombardment onto the cathode plate. This study analyzed the composition of residual gases inside a vacuum-sealed panel, which was composed of a CNT emitter cathode plate, a phosphor anode, and glass spacers, all kept in vacuum, revealing that CO, CO<sub>2</sub>, N<sub>2</sub>, CH<sub>4</sub>, H<sub>2</sub>, C<sub>2</sub>H<sub>6</sub>, and Ar existed inside the panel. The CNT emitter cathode was prepared in a diode structure by using the CNT paste, producing an array of dots with a diameter of 10 μm and a pitch of 300 μm over an active area of 2x2 cm. Prior to investigating the effect of each residual gas on the emission properties of CNTs, the sample was electrically conditioned in ozone of 5x10<sup>-4</sup> torr to improve the emission uniformity over an area by reducing the height difference between CNT emitters. The conditioning was continued until the electric field reached 9 V/μm by applying the pulse voltages with the duty ratio of 1/60 and the frequency of 500 Hz while keeping the constant emission current of 28 μA. The chamber was then evacuated and maintained at a high vacuum of ~10<sup>-8</sup> torr for 10 h while emitting 28 μA of electrons all the way long. Thereafter, each gas species was introduced to a vacuum chamber up to 5x10<sup>-5</sup> torr for 2 h while continuing electron emission, and then gas injection was terminated to keep a high vacuum of ~10<sup>-8</sup> torr for a 20 h. Here, we observed the variation of voltages under the electron emission of the constant current during these whole procedures from ozone electrical conditioning, through the injection of each residual gas, to maintaining a high vacuum.

**E-04****Fabrication of Rigid and Low-Resistance Contacts for Carbon Nanotube Using****Eutectic Alloy**

JEON Dongryul, PARK Daehyun

*Seoul National University.*

Au-Al eutectic alloy melts at 250 °C lower than their original melting points. Using a eutectic alloy electrode, we fabricated a rigid and low-resistance contact for carbon nanotube (CNT). After patterning the electrode which consisted of Au/Al binary thin film, CNT was laid on the electrode by AC dielectrophoresis or spin coating. The sample was then annealed at 250 °C for a few minutes in air. AFM images after annealing showed that MWNT was embedded into the Au-Al electrode as if it was originally made by a top contact process. The resulting contact was rigid enough to sustain ultrasonic agitation in dichlorobenzene for 90 sec and *I-V* measurement exhibited that the contact resistance was reduced by more than a factor of 4. We could fabricate a crossed CNT junction by performing standard semiconductor manufacturing process on CNT-deposited substrate to add another electrodes pair and dielectrophoresis. This work was supported by the Korea Science and Engineering Foundation through SNU-NCRC.

**E-05****Plasmon-Induced Photoconductance In Mesoporous TiO<sub>2</sub> Nanofibers Loaded****With Au Nanoparticles**

손 민수, 임 지은<sup>1</sup>, 왕 강균<sup>1</sup>, 오 승임<sup>1</sup>, 김 용록<sup>1</sup>, 유 경화

연세대학교 물리학과, 나노메디컬 국가핵심 연구센터. <sup>1</sup>연세대학교 화학과.

We have synthesized mesoporous TiO<sub>2</sub> nanofibers loaded with Au nanoparticles (MTNF-Au) and fabricated single nanofiber-based devices on SiO<sub>2</sub>/Si substrates. Upon illumination with visible light, the MTNF-Au device exhibited wavelength-dependent and reversible photoresponses, which were caused by the SPR absorption. In addition, we also investigated the temperature dependence of electronic transport properties for both the MTNF and MTNF-Au devices. These two devices differed in their temperature dependence at low temperatures. In particular, the single electron effects were demonstrated in the MTNF-Au device, suggesting that the variations in temperature difference were attributable to electronic tunneling among the Au nanoparticles embedded in the TiO<sub>2</sub>.

**E-06****Reset Current Reduction in NiO Nanowires Array Using AAO Membrane**

김 성인, 장 영욱, 유 경화<sup>1</sup>

연세대학교 물리학과. <sup>1</sup>연세대학교 물리학과, 나노메디컬 국가핵심 연구센터.

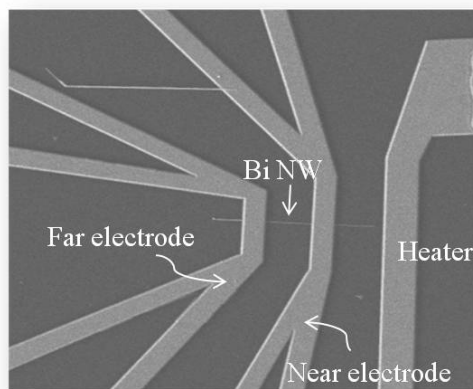
We have fabricated NiO nanowire-based resistive random access memory (ReRAM) devices by using anodized aluminum oxide (AAO) membranes formed on Si substrates and electrodeposition methods. NiO nanowire arrays exhibited clear resistive switching behaviors as in NiO films. For practical applications of ReRAM, however, the reduction of reset currents ( $I_{RESET}$ ) is necessary. Thus, we have investigated the dependence of  $I_{RESET}$  on the device size. Indeed, as the device size decreased,  $I_{RESET}$  was reduced, although the switching power given by  $I_{RESET} \times V_{RESET}$  was nearly independent of the device size.

**E-07****Seebeck Coefficient of Individual Single-crystalline Bi Nanowires Grown by On-Film Formation of Nanowires**

LEE Seung Hyun, HAM Jinhee, LEE Jun Min, LEE Wooyoung

*Nanomedical National Core Research Center and  
Department of Materials Science and Engineering, Yonsei  
University.*

Over the last decade, bismuth (Bi) nanowires have been of great importance in nanophysics to both theorists and experimentalists, as Bi is known to be a Group V semimetallic element that exhibits unusual transport properties due to its highly anisotropic Fermi surface. Moreover, single-crystalline Bi nanowires are expected to usher in new class of thermometric devices with high thermoelectric efficiency. In this work, we present the transport properties and thermoelectric power of individual single-crystalline Bi nanowires grown by on-film formation of nanowires (OFF-ON). The four-terminal devices based on individual Bi nanowires were successfully fabricated using a physical etching technique to remove an oxide layer. It was found that a Bi nanowire with  $d = 120$  nm exhibits an electron mobility of  $76,900 \text{ cm}^2/\text{Vs}$  and an extraordinary mean free path of  $1.35 \text{ nm}$  at  $300 \text{ K}$ , as measured by the electric field effects. We also measured the thermoelectric power of the Bi nanowire with  $d = 103 \text{ nm}$ , showing  $S$  of  $-70 \text{ } \mu\text{V/K}$ . This value is about three times of that in polycrystalline Bi nanowires. We discuss the enhanced thermopower of single-crystalline Bi nanowires for high-efficiency thermoelectric devices.

**E****E-08****Semiconducting Bi Nanowires Showing Semimetal-to-semiconductor Transition Grown by On-Film Formation of Nanowires**

HAM Jinhee, LEE Seunghyun, LEE Wooyoung

*Department of Materials Science and Engineering, Yonsei University.*

A novel stress-induced method to grow semiconducting Bi nanowires along with an analysis of their transport properties is presented. The growth method for Bi nanowires is termed the on-film formation of nanowires (OFF-ON), as based on the observation of the spontaneous growth of Bi nanowires from Bi thin films without the use of conventional templates, catalysts, or starting materials. OFF-ON is a stress-induced method for the growth of Bi nanowires that has received little attention in the nanotechnology community. A Bi thin film was initially deposited onto a thermally oxidized Si(100) substrate at a rate of  $32.7 \text{ } \text{\AA}/\text{s}$  using an ultrahigh vacuum (UHV) radio frequency (rf) sputtering system. Single crystalline Bi nanowires were found to grow on as-sputtered films after thermal annealing at  $260\text{-}270 \text{ } ^\circ\text{C}$ . This was facilitated by relaxation of stress between the film and the thermally oxidized Si substrate that originated from a mismatch of the thermal expansion. We found that the correlations between the thickness and mean grain size of the Bi films and the diameter of the Bi nanowires show the diameters of the Bi nanowires decrease in proportion to the thickness and grain size of the films. Our results demonstrate that the diameters of Bi nanowires depend on the mean grain sizes in the as-grown films, which are determined by the thickness of the films. It was clearly observed that a Bi nanowire grows at the grain of a Bi thin film, indicating that the Bi nanowire grew from the bottom of the wire, where it was attached to the film, fed by Bi via grain boundary diffusion from the supporting Bi thin film. The diameter of Bi nanowires grown by OFF-ON can be tuned by controlling the sputtering time and ambient temperature. In the present work, Bi nanowires with a diameter as small as  $30 \text{ nm}$  were obtained. A  $40\text{-nm}$ -thick Bi nanowire was found to exhibit semimetal-to-semiconductor transition.

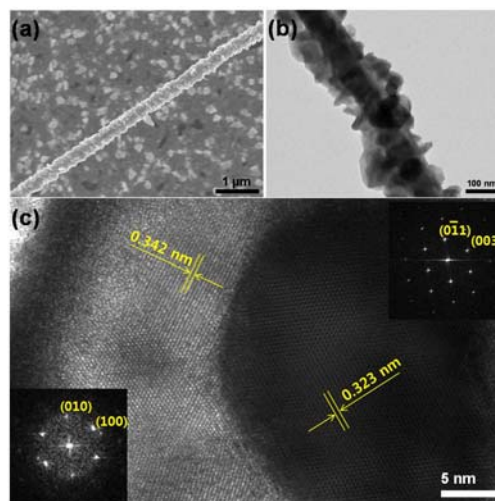
**E-09****Ultra-low Thermal Conductivity of Bi-Te Core/shell Nanowire**

KANG Jooheon, ROH Jongwook, HAM Jinhee, LEE

Seunghyun, LEE Wooyoung

*Department of Materials Science and Engineering, Yonsei University.*

The formation of various one-dimensional (1D) core-shell nanowire is of particular significance with respect to potential applications for high-efficiency thermoelectric devices. We report the thermal conductivity of Bi-Te core/shell nanowires grown by a novel growth method termed On-Film Formation of Nanowires (OFFON). A Bi thin film was initially deposited onto a thermally oxidized Si (100) substrate using an UHV sputtering system. Heating the thin film to 270 °C initiates thermal stress, which originates from a mismatch of the thermal expansion between the film and the substrate. Then Te was evaporated on the Bi nanowires. High-resolution TEM images were found to show a core/shell structure for which effective phonon scattering and quantum confinement effect are expected. First, we demonstrate that 1D heterostructure like Bi-Te core/shell nanowire can be grown successfully by OFFON method. We also measured the electrical transport properties of an individual Bi-Te core/shell nanowire. The electrical resistivity ( $\rho$ ) value which is dependent on the temperature obtained from a four-probe resistance measurement is about  $4 \times 10^{-6}$  (ohm-meter) at 300K. We also observed very low thermal conductivity of the Bi-Te core/shell nanowire, which can be attributable to increased interface of Bi-Te. We discuss the mechanism of reduced thermal conductivity in the Bi-Te core/shell nanowires in detail.

**E-10****Building Lactate Biosensors via a Facile Layer-by-Layer Assembly**양 형우, 김 동청, 유 상훈<sup>1</sup>, 박 성호<sup>1</sup>, 강 대준

*BK21 Physics Research Division, Department of Energy Science, Institute of Basic Science, SKKU Advanced Institute of Nanotechnology and Center for Nanotubes and Nanostructured Composites, Sungkyunkwan University, Suwon 440-746, Korea. <sup>1</sup>Department of Chemistry, Department of Energy Science, Institute of Basic Science, SKKU Advanced Institute of Nanotechnology and Center for Nanotubes and Nanostructured Composites, Sungkyunkwan University, Suwon 440-746, Korea.*

We have successfully fabricated lactate sensing bio-sensors. We found that the current value changes when detecting lactate. These lactate bio-sensors were fabricated by using chemisorption and layer-by-layer assembly technique, building a bio-architecture of b-HRP/avidin/b-LOD on well-dispersed three dimensional (3-D) gold nano structure that was prepared using electrochemical deposition on AAO. We found from the cyclicvoltametric measurement that the enzymes were catalytically active in the multilayer films, the functionalized films consisting of gold nanostructure act as excellent catalytic surfaces through the oxidation and the reduction process of lactate. This technique provides a facile synthetic route for constructing functional 3-D bio-architectures suitable for various viable biosensors.

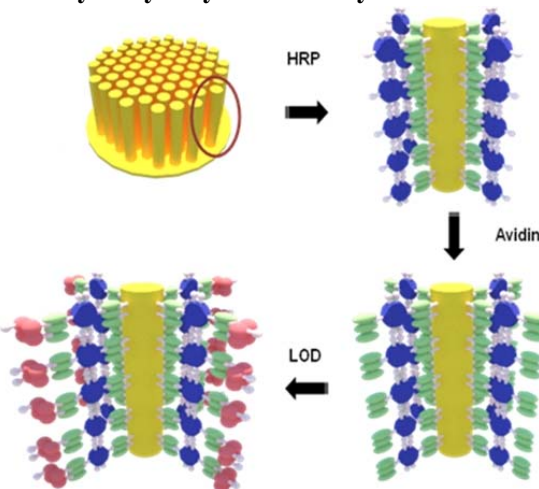


Fig. 1 | The layer-by-layer assembly process

**E-11****The Diminishing Magneto Resistance in High Electric Fields in Polyacetylene****Nanofibers**

최 아정, 이 현정, KAISER Alan B.<sup>1</sup>, 장 성호, 이 승현, 유 재승, 김 형섭, 남 영우, 박 승주, ALESHIN Andrey N.<sup>2</sup>, 고 문주<sup>3</sup>, AKAGI Kazuo<sup>3</sup>, KANER Richard B.<sup>4</sup>, BROOKS James<sup>5</sup>, SVENSSON Johannes<sup>6</sup>, BRAZOVSKII Serguei<sup>7</sup>, KIROVA Natasha<sup>8</sup>, 박 영우

서울대학교, 물리천문학부. <sup>1</sup>Victoria University of Wellington, MacDiarmid Institute for Advanced Materials and Nanotechnology. <sup>2</sup>서울대학교, 물리천문학부 & Russian Academy of Sciences, A. F. Ioffe Physical-Technical Institute. <sup>3</sup>Department of Polymer Chemistry, Kyoto University. <sup>4</sup>University of California at Los Angeles, Department of Chemistry and Biochemistry. <sup>5</sup>Florida State University, National High Magnetic Field Laboratory. <sup>6</sup>Department of Physics, Göteborg University. <sup>7</sup>Université Paris-Sud, LPTMS-CNRS. <sup>8</sup>Université Paris-Sud, CNRS-UMR 8502.

The high field magneto resistance (MR) for helical polycetylene(PA) nanofibers are measured up to H=30 tesla at low temperature. There is no orientation dependence in MR which indicates that the intrinsic spin response to the external magnetic field is observed. The positive MR diminish as the electric field increases, becoming zero at high electric field. It is understood as the doping induced spinless charged soliton pairs initially confined to a certain distance due to the interchain phase correlations, are deconfined in high electric field resulting in the diminishing MR(DMR). The results are compared with the MR of polyaniline nanofibers which shows no electric field dependence.

**E****E-12****Facile Synthesis of Single Crystalline Vanadium Pentoxide Nanowires and their****Photocatalytic Behavior**

SHAHID Muhammad, SHAKIR Imran, RHEN Danielle, PATOLE Shashikant<sup>1</sup>, 유 지범<sup>1</sup>, 강 대준

BK21 Physics Research Division, Department of Energy Science, Institute of Basic Science, SKKU Advanced Institute of Nanotechnology and Center for Nanotubes and Nanostructured Composites, Sungkyunkwan University, Suwon 440-746, Korea. <sup>1</sup>School of Advanced Materials Science and Engineering, Sungkyunkwan University, Suwon 440-746, Korea.

We have successfully grown high quality single crystalline V<sub>2</sub>O<sub>5</sub> nanowires without employing catalyst, surfactant or carrier gas by simple chemical solution deposition (CSD) method both on insulating Al<sub>2</sub>O<sub>3</sub> (0001) and conducting ITO coated glass substrates. A 50 nm-thick layer of vanadium oxide nanocrystals is formed by the decomposition of vanadium benzoylacetone complex at 250°C (Fig.1) to provide nucleation sites for the growth of nanowires. We showed that by simply controlling temperature and thickness of the coated film, high quality V<sub>2</sub>O<sub>5</sub> nanowires can be obtained easily (Fig.2). The photocatalytic activity of the synthesized nanowires under UV light was also evaluated by monitoring the degradation of toluidine blue O (TBO) solution. Our results indicate that the developed method in this work can be easily applied to obtain other high quality metal oxide nanowires.

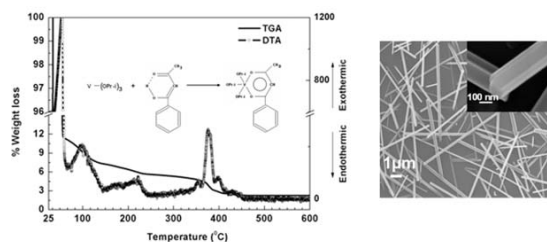
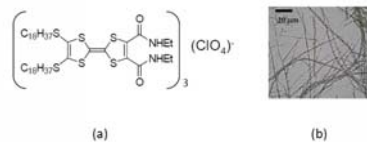


Figure.1. TGA of starting precursor. Inset reaction between starting precursor. Figure.2. SEM of nanowires.

**E-13****Fluctuation-Induced Tunneling Conduction in Perchlorate Doped****Tetrathiafulvalene-Diamide Nanofibers**안 세정, 김 유경, 백 승재, ISIMOTO Shohei<sup>1</sup>, IYODAMasahiko<sup>1</sup>, 홍 성주<sup>2</sup>, 박 영우<sup>2</sup>

서울대학교 나노과학기술협동과정. <sup>1</sup>Department of chemistry, Graduate School of Science and Engineering, Tokyo Metropolitan University. <sup>2</sup>서울대학교 물리천문학부.

Figure 1 (a) Structural formula (b) optical image of the ClO<sub>4</sub> doped TTF-diamide sample

TTF derivatives with a long alkyl chain are self-aggregated into a one-dimensional columnar structure in the solid state. Among the TTF derivatives, we investigated perchlorate (ClO<sub>4</sub><sup>-</sup>) doped 4,5-bis(octadecylthio)-4',5'-bis(ethylcarbamoyl)tetrathiafulvalene (TTF-diamide) (figure 1). We observed the helical structure of the sample by optical microscope through the dispersion in acetone with sonication and the XRD analysis showed a periodic lamellar pattern ( $d_{100} = 60.5 \text{ \AA}$ ). The temperature dependent conductance and current-voltage ( $I$ - $V$ ) characteristics of the sample were measured in the range  $70 \text{ K} < T < 300 \text{ K}$ . The conductance decreases as temperature decreases and the  $I$ - $V$  characteristics are nonlinear in the entire temperature range. The results are analyzed by the modified fluctuation-induced tunneling (FIT) conduction mechanism where the barrier height and width are affected by the electric field linearly.

**E-14****Flexible Transparent Conductive Films of Multiwall Carbon Nanotube/PEDOT-****PSS**

YUN Chan Ki, CHA Yun Mi, HA Byeongchul

The Department of Nano Science, Cheongju University.

A coating solution was prepared by the mixture of multiwall carbon nanotubes (MWCNTs) and Polyethylenedioxythiophene/poly-4-sulfonate (PEDOT-PSS). MWCNTs were evenly dispersed in the solution by a ultrasonication homognizer. The solution was coated on a PET film by a bar-coating method. The conductivity and transmittance of the MWCNT/PEDOT-PSS film are  $150 \text{ } \Omega/\text{sq}$  and 80%, respectively. Compared with Indium Tin Oxide (ITO), the prepared film is highly flexible, having a consistent conductivity with bending. The transparent conductive films of MWCNT/PEDOT-PSS can be utilized by flexible solar cells and displays.

**E-15****Electrical Properties of Electrospun Polyaniline- Polyethylene Oxide****Nanofibrous Membranes Filled with Single-walled Carbon Nanotubes**

SUNDARAY Bibekananda, 최 아정, 박 영우

서울대학교, 물리천문학부.

Highly conducting nanofibrous composite of well-oriented single-walled carbon nanotubes (SWNTs) in polyaniline and polyethylene oxide have been fabricated using electrospinning. The room temperature electrical conductivity show nearly four order enhancement with highest (11.89wt %) loading of SWNT, from their polymer blend counterpart. The temperature dependent conductivity measurement reveal the variable range hopping in addition to fluctuation assisted tunneling with polymer acting as barrier in bundle to bundle hopping model explain the conduction mechanism operative in these type of systems.

E

**E-16****Aharonov Bohm Effects in Graphene Nanorings**PARK Yung Woo, YOO Jai Seung<sup>1</sup>, NAM Young Woo<sup>1</sup>, CHU Seung Wan<sup>1</sup>, SMET Jurgen H.<sup>2</sup>, SKAKALOVA Viera<sup>2</sup>, ROTH Siegmund<sup>2</sup>

*Department of Physics and Astronomy, Seoul National University, Korea. <sup>1</sup>Department of Physics and Astronomy, Seoul National University, Korea. <sup>2</sup>Max-Planck-Institut für Festkörperforschung, Stuttgart, Germany.*

We observed Aharonov Bohm effects in graphene nanorings of 1 micro diameter and 125nm channel width, and analyzed it with phase coherence length estimated using the weak localization theory of graphene. Graphene nanorings were prepared in the geometry of ring by plasma etching for the flakes obtained by the micro exfoliation method, after patterned by electron beam lithography. And then Cr/Au were evaporated for electrodes. Optical images of pristine graphene flakes, Raman spectroscopy and quantum Hall effect at high magnetic field confirmed that the samples were graphene monolayer. The graphene nanorings were annealed at 400K for more than 4 hours and loaded into a dilution refrigerator which can reach to 20mK. The positive magnetoresistance measured at low magnetic field was analyzed with the weak localization theory of graphene estimating the phase coherence length to  $\sim 80$ nm. This short phase coherence length made the interference by Aharonov Bohm effect very poor. Considering the Fermi wave length of graphene, 15nm, at 80V for back gate voltage, we conclude that the graphene nanoring could show the Aharonov Bohm oscillation of 5 cycles. The experiment of this work has been performed at the Max Planck Institute, Stuttgart in Germany, supported by BK21 Frontier Physics Research Division, Seoul National University in South Korea and partially supported by Korea Sweden Carbon Based Nanostructure Research Center of GPP in Seoul National University, Korea.

**E-17****Fabrication of Transparent Conductive Single-Walled Carbon Nanotube Films With Surfactant Dispersion and Chemical Modification**

LEE Naesung, LEE Seungho, GOAK Jungchoon, KIM myoungsu

세종대학교, 나노공학과.

Single-walled carbon nanotubes (SWCNTs) belong to one of the promising candidates for the applications to flexible transparent conductive electrodes of touch panels, solar cells, and flat panel displays. Here, we systematically studied the optimum concentration of surfactants in aqueous solutions containing SWCNTs by using anionic, cationic, and neutral species in which mass conversion of dispersed SWCNTs was compared. Five surfactants were examined to disperse SWCNTs for comparison, which could disperse a high concentration of SWCNTs at an optimum concentration where the bundled SWCNT aggregates were minimized. It is noted that the capability of SDBS to suspend SWCNTs in an aqueous solution was much better than others. Then, a flexible transparent conductive SWCNT film was fabricated by using surfactant-SWCNT suspension by spraying it onto a poly(ethylene terephthalate) (PET) substrate. The electrical conductivity of the SWCNT film was improved by treating it in nitric acid ( $\text{HNO}_3$ ), because the nitric acid treatment removed the surfactants from the SWCNT network and minimized the contact resistance. This study will discuss chemical modification of CNTs to further lower the sheet resistance of the SWCNT films. TCFs were characterized by thermogravimetric analyzer (TGA), scanning electron microscopy (SEM), UV-Vis spectroscopy (optical transmittance), and four-point probe measurement (sheet resistance).

**E-18****Size-homogeneous metal nanoparticles supported on multi-walled carbon****nanotubes via MeV electron beam irradiation**SONG Wooseok, JEON Cheolho, KWON Young Taek, JUNG Dae Sung, CHOI Won Chel, PARK Chong-Yun  
*Sungkyunkwan University, Department of Physics, Center for Nanotubes and Nanostructured Composites (CNNC).*

The extraordinary properties of carbon nanotubes (CNTs) associated with one-dimensional structure make them into fascinating materials having a high potential in various application fields. Especially, CNT-supported metal nanoparticles are of great interest for applications of hydrogen storage, catalysts, CNT-based magnetic composites, low-resistance Ohmic contact CNT-based electronic devices. There are various approaches to obtain metal nanoparticles supported on CNTs, such as thermal evaporation, electrodeposition, and wet chemical route. Since the properties of the metal nanoparticles can be influenced by their size, it is a crucial issue to obtain the size-homogeneous metal nanoparticles. Herein, we demonstrate an ingenious method for anchoring the size-homogeneous Ni and Pt nanoparticles on multi-walled carbon nanotubes (MWNTs). Irradiation of MeV electron beam was employed to form the size-homogeneous Ni and Pt nanoparticles on CNTs. Measurement of transmission electron microscopy, electron energy loss spectroscopy, and energy dispersive X-ray spectroscopy clearly revealed that Ni and Pt nanoparticles with 5.16 nm (0.74 nm) and 1.63 nm (0.15 nm) in mean diameters (standard deviations) were formed on the MWNTs surface after MeV e-beam irradiation, respectively. A chemical transformation for the metal nanoparticles anchoring process was systematically investigated by X-ray photoelectron spectroscopy. From these results, we suggest that this method will provide a possible way for the formation of size-homogeneous metal nanoparticles on the MWNTs.

## Sheet Resistance

김 명수, 곽 정춘, 이 승호, 한 종훈<sup>1</sup>, 이 내성

세종대학교 나노신소재공학부, <sup>1</sup>전자부품연구원.

현재 ITO를 대체할 투명 전도성 재료로 탄소나노튜브(carbon nanotube, CNT) 필름에 대한 연구가 활발히 진행되고 있다. 특히 CNT 필름의 투과도에 따른 전기저항을 향상시키기 위해 많은 노력을 기울이고 있다. 본 연구에서는 sodium dodecylbenzene sulfonate(SDBS) 계면활성제로 분산시킨 단일벽 CNT (single-walled CNT) 수용액을 유리 기판 위에 spray시켜 CNT 필름을 제조한 후 투과도에 따른 면 저항(sheet resistance)의 변화를 관찰하였다. CNT 표면에 코팅되어 있는 계면 활성제를 제거하여 필름의 전기저항을 낮추기 위해 CNT 필름에 대해 질산(HNO<sub>3</sub>) 처리 및 플라즈마 처리를 수행하였다. CNT 필름의 형상과 광 투과도를 분석하기 위해 각각 SEM, UV-Vis spectroscopy를 이용하였고, 4-point probe로 면저항을 측정하였다. 본 연구에서는 CNT 표면에 잔류하고 있는 계면활성제를 제거하기 위한 수단으로 질산 처리 및 플라즈마 처리의 효과에 대해 논의한다.

LEE Naesung, JANG Eunsoo, GOAK Jeungchoon, LEE Hansung, LEE Seungho

세종대학교, 나노공학과.

Carbon nanotubes (CNTs) have been intensively studied, because of their outstanding properties such as superior electrical conductivity, chemical stability, and mechanical strength. In particular, CNTs are considered as an ideal field emitting material with the features allowing electron emission at low electric fields due to their unique geometry such as a large aspect ratio and a small tip radius of curvature. For these reasons, CNTs have been studied long to be applied to field emission devices including field emission displays, liquid crystal display (LCD) backlight units (BLU), and x-ray sources, etc. Among them, the CNT-BLU has been rapidly developed and has been expected close to commercialization. But several problems still remain to be overcome. Specially, heat generated on an anode plate should be dissipated because it can badly affect phosphor efficiency and BLU performance. In fact, heating of the anode plate is unavoidable in field emission because high-energy electrons always bombard the anode. Furthermore, in order to increase the luminous efficiency of phosphor, high voltages should be applied to the anode, which produces more heat. Thus, the heat issue becomes more serious in the CNT-BLUs as increasing anode voltages. In conventional CNT-BLUs, the anode plate is placed almost in contact with the TFT plate because light passes through the BLU anode plate, which makes heat dissipation structurally more difficult. The reason of such inefficient configuration is that light passing out of the BLU and heat generation occurs at the same plate. In this study, a light-passing plate is separated from heat-generating plate by turning the BLU upside down and instead making the cathode plate transparent. In our design, light, generated on the phosphor layer of the anode plate, passes through the transparent cathode plate. In the BLU application, the cathode plate passing light is placed close to the TFT plate, whereas the anode plate is located backward. Hence, the heat occurring on the anode plate can be easily removed in this configuration. The fabrication procedures of the transparent CNT cathodes are described below. A CNT aqueous solution was prepared by ultrasonically dispersing purified SWCNTs in deionized water with sodium dodecyl sulfate (SDS). Several milliliters or even a hundred of microliters of the well-dispersed CNT solution was deposited onto a porous alumina membrane through vacuum filtration. Thereafter, the alumina membrane was solvated with the 3 M NaOH solution, and the floating CNT film was easily transferred to an ITO glass substrate in an area of 1 cm diameter defined by using a film mask. The CNT film was subjected to an activation process with an adhesive roller, standing the CNTs up to serve as electron emitters. The light passing through the cathode plate was brighter than the one passing through the anode plate. A metal layer coated between the anode glass and the phosphor layer on the anode side reflected the light generated on the phosphor layer toward the cathode side, further enhancing the brightness of the light passing through the cathode plate. This study will discuss the morphologies and field emission characteristics of CNT emitters according to the fabrication parameters and the light brightness depending on the device structure.

**E-21****Enhanced Electric Double Layer Capacitance of Poly Sodium 4-****Styrenesulfonate/Graphene Oxide Electrodes with High Cyclic Performance**

JEONG Hae-Kyung, JIN Meihua, RA Eun Ju, SIM Kyu Yun<sup>1</sup>, AREPALLI Sivaram<sup>2</sup>, LEE Young Hee  
*Sungkyunkwan University, BK21 Physics, Department of Energy Science, Center for Nanotubes and Nanostructured Composites.* <sup>1</sup>*Samsung SDI, Energy Lab.* <sup>2</sup>*Sungkyunkwan University, Department of Energy Science.*

Nanocomposite of poly sodium 4-styrenesulfonate intercalated graphene oxide (PSS-GO) showed high performance of electric double layer capacitance (EDLC) compared to that of pristine graphene oxide. Specific capacitance of the composite reached to 190 F/g, and energy density was much improved up to 26.2 Wh/kg with momentum density of 91 W/kg. Cycle test of the cell showed that the specific capacitance decreased by 12 % after 14860 cycles, providing excellent cyclic stability. The high EDLC performance of PSS-GO could be explained by absorption and desorption measurement of electrolyte ions, and impedance spectroscopy, recommending it as a new potential material for energy storage devices.

**E-22****Imaging the anisotropic thermoelectric power of  $\text{Ti}_3\text{SiC}_2$  with nanometer****resolution**

CHO sanghee, LYE H.-K., CHUNG T., YOO H.-I.<sup>1</sup>

*Korea Research Institute of Standards and Science.* <sup>1</sup>*Seoul National University, School of Materials Science and Engineering.*

We report local measurement of the thermoelectric power of polycrystalline  $\text{Ti}_3\text{SiC}_2$  at the nanometer scale. The thermoelectric power of the material in the bulk-scale measurement is essentially zero ( $\sim 0 \mu\text{V/K}$ ) over a wide temperature range. By using a scanning thermoelectric microscopy based on ultra-high-vacuum atomic force microscopy, we explore the physical origin of the unique property from the microscopic length scale. New development of the microscopy method has enabled us to obtain two-dimensional maps of spatially resolved thermopower as well as topological maps simultaneously with nanometer resolution; we obtain the maps at the sample temperature between 240K and 390K. The local thermoelectric voltage measured on samples prepared from perpendicular faces of  $\text{Ti}_3\text{SiC}_2$  chunk displays unambiguously non-zero values across the length scale of tens  $\sim$  hundreds of nanometer; alternating signs are observed, and the magnitude of measured voltage increases with increasing temperature difference. This result can be described by the dependence of the thermopower on crystal axes; each crystal axis of the hexagonal structure contributes to different signs of the thermopower. Thus the measured thermopower is essentially a sum of thermopower with opposite polarity. The magnitude of either *p*- or *n*-type thermopower is on the order of tens of  $\mu\text{V/K}$  and exhibits a particular distribution.

**E-23****Deformation Field Distribution of Zeolites Induced by Negative Thermal****Expansion**

CHA Wonsuk, SONG Sanghoon, JEONG Nak Cheon<sup>1</sup>, YOON Kyung Byung<sup>1</sup>, ROSS Harder<sup>2</sup>, ROBINSON Ian K.<sup>3</sup>, KIM Hyunjung

*Sogang University, Department of Physics and Interdisciplinary Program of Integrated Biotechnology.* <sup>1</sup>*Sogang University, Department of Chemistry and Interdisciplinary Program of Integrated Biotechnology.* <sup>2</sup>*Argonne National Laboratory, Advanced Photon Source.* <sup>3</sup>*University College London, Department of Physics and Astronomy.*

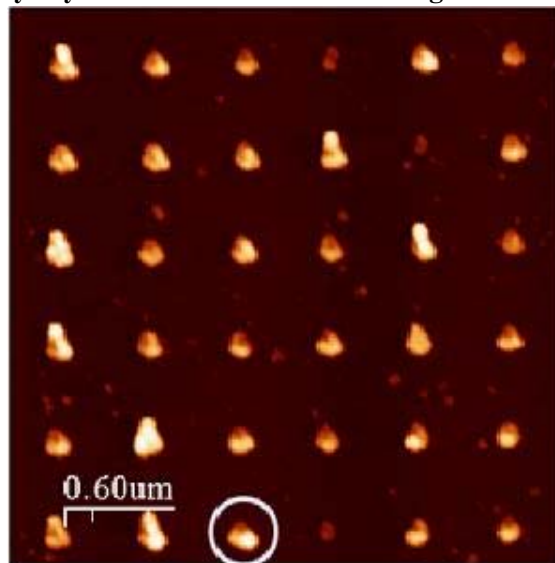
We measured the internal deformation fields of micrometer sized zeolite crystals by coherent x-ray diffraction (CXD). The samples were attached on the Si substrate by chemical bonding. Using phase retrieval method with combination of error reduction and hybrid input-output algorithms, the CXD patterns were inverted to the three-dimensional images and obtained internal deformation field distributions. The different thermal expansion behavior of Si substrate and zeolite crystals induce unique pattern of deformation field distribution. We also obtained negative thermal expansion coefficients of zeolite crystals along the CXD measurement and measured the absolute magnitude of lattice distortion as a function of the temperature. The deformation field distribution was changed with increasing temperature. This study was supported by National Research Foundation, Seoul Research and Business Development program and Sogang University Grant.

**E****E-24****Formation of Ti metal nano-dot arrays by an indentation method using atomic****force microscopy**

정 보라, 조 월령

*이화여자대학교, 물리학과.*

Ti metal nanodot arrays are fabricated by scanning probe microscopic indentation. A thin poly (methylmethacrylate) (PMMA) layer was spin-coated on Si substrates with thickness of 70 nm. By applying mechanical force to the PMMA layer using a cantilever, an indented array with nanometer-size pores was formed. Protuberances during the indentation process were observed to make surface rough and irregular. Without wet treatment of chemical materials, it was possible to get rid of the protrusions by control of indenting force of the cantilever. Using this treatment, we fabricated nanodots with a well-defined structure. Ti metal layers were coated on the patterned PMMA layers by a radio-frequency sputtering method and subsequently a lift-off process was conducted to obtain metal nanodot arrays. Topographic scanning shows that the fabricated metal dots have 200 nm of diameter and 500 nm of interdistance, which corresponds to a density of  $4 \times 10^8/\text{cm}^2$ . Current-voltage behaviors of Ti metal nanodots showed asymmetric characteristics while the I-V of Ti metal nanodots by e-beam lithography showed asymmetric Schottky characteristics.



**E-25****전자빔 조사에 의한  $\pi$ -공액 고분자 나노 물질 특성 개질 연구**

홍 영기, 박 동혁, 구 민호, 김 대철<sup>1</sup>, 김 정용<sup>1</sup>, 주 진수

고려대학교 물리학과 하이브리드 나노구조체 연구실, <sup>1</sup>인천대학교 물리학과 나노광전자연구실.

전자빔이 조사된  $\pi$ -공액 고분자 나노 물질은 물리적 구조 및 도핑 상태가 변화한다. 전자빔의 에너지나 선량 등 전자빔 처리 조건을 조절할 경우,  $\pi$ -공액 고분자 나노물질의 전기적, 광학적 물성을 정량적으로 제어할 수 있다. 본 연구에서는 전자빔 조사를 통해  $\pi$ -공액 고분자 나노물질을 전체적 또는 부분적으로 개질하여 물리적 특성 및 도핑 상태의 변화를 관찰하였고, 부분 개질된  $\pi$ -공액 고분자 나노 물질의 경우 나노 광전자소자로의 응용성을 조사하였다.  $\pi$ -공액 고분자 나노물질은 나노 기공을 가지는  $\text{Al}_2\text{O}_3$  다공성 템플레이트를 이용하여 전기화학 중합하였으며, 발광 고분자인 poly (3-methylthiophene) (P3MT)를 나노튜브의 형태로, 전도성 고분자인 polypyrrole (PPy)과 poly (3,4-ethylenedioxythiophene) (PEDOT)을 나노선의 형태로 각각 제작하였다. 전자빔 조사에 따른  $\pi$ -공액 고분자 나노물질의 구조적 물성 및 도핑 상태의 변화를 확인하기 위해 라만 (Raman) 및 자외선-가시광 (UV-Vis) 흡수 스펙트럼을 측정하였다. 레이저 공초점 현미경 (laser confocal microscope) 과 컬러 전하 결합 소자(color charge coupled device)를 이용한 P3MT 나노튜브 한 가닥의 광발광 (Photoluminescence) 실험을 통해 전자빔 조사에 따른  $\pi$ -공액 발광 고분자의 광학적 물성 변화를 분석하였다. 2-단자 접촉 방법을 이용하여 측정된 PPy 및 PEDOT 나노선의 전압-전류 특성을 통해 전자빔 조사에 따른  $\pi$ -공액 전도성 고분자의 전기적 물성 변화를 보고한다. 또한 초점이 맺힌 (focused) 전자빔을 이용하면 나노물질 한 가닥의 원하는 위치를 선택적으로 부분 개질할 수 있음을 관찰하였다.

**E-26****A facile method to prepare regioregular poly(3-hexylthiophene) nanorod arrays using anodic aluminium oxide templates and capillary force**

BAEK Sujin, PARK Jong Bae, LEE Soo-Hyoung<sup>1</sup>, YOUN Hyung-Joong<sup>2</sup>, LEE Jouhahn<sup>2</sup>

Korea Basic Science Institute, Jeonju Center. <sup>1</sup>Chonbuk National University, School of Semiconductor and Chemical Engineering. <sup>2</sup>Korea Basic Science Institute.

Regioregular poly(3-hexylthiophene) (RR-P3HT) nanorod arrays were prepared on the indium tin oxide (ITO) substrate by capillary force in a vacuum oven using a drop-coating of RR-P3HT and anodic aluminium oxide (AAO) templates. The AAO templates were prepared by two step anodizing process in an oxalic acid electrolyte. The templates had a highly ordered structure with a uniform pore diameter of ~55-80 nm and cell lengths of ~100-3930 nm. With suitable temperature and capillary force in the vacuum oven, the drop-coated RR-P3HT solution infiltrated the AAO templates. After removal of the AAO template, the RR-P3HT has a nanorod array form, with diameters of ~55 nm and heights of ~70 nm.

## Alloys

KANG SungJin, KIM Miyoung, KWON Young Kyun<sup>1</sup>서울대학교 재료공학부. <sup>1</sup>경희대학교 물리학과.

Iron-based alloys have been researched for better mechanical properties for a long period. Microstructures of iron-based alloys could vary the mechanical property dramatically by just injecting small amount of other elements. This phenomenon has been observed by experiments but not yet been investigated thoroughly to find the relation between their structures and the mechanical properties. We have performed density functional calculations combined with elastic theory to understand the structural and mechanical properties of iron-based alloys and their modifications as foreign elements such as Si/Al/Mn are added by 1 ~ 20 %. We have found a certain tendency between equilibrium structures and their bulk/shear modulus.

PARK Sora, AHN Jeung Sun, KWON Young-Kyun<sup>1</sup>

Department of Physics, Kyung Hee University, Seoul 130-701, Korea. <sup>1</sup>Department of Physics and Research Institute for Basic Sciences, Kyung Hee University, Seoul 130-701, Korea.

Using ab initio density functional theory, we investigate the electronic structures and vibrational spectra of various fullerene-like carbon-based materials, especially partly with negative curvature. After obtaining their equilibrium structures through the geometry relaxation, we study the effects of negative curvature on their electronic and vibrational properties. The IR intensities of their vibrational modes are computed and compared with the experimentally observed IR absorption data. From our comparison study, we suggest that some particular modes, which are not found in usual fullerene structures, would be attributed to negative curvature.

\* This work was supported by the Seoul Research and Business Development Program (Grant No. 10583) and by the Korea Science and Engineering Foundation (KOSEF) grant funded by the Korea government(MEST) (No. 2009-0074951)

**E-29(초)****Acoustic extraordinary transmission using Helmholtz resonator**

이 삼현, 박 춘만<sup>1</sup>, 서 용문<sup>2</sup>, 김 철구

연세대 물리학과, <sup>1</sup>안양대 AEE 센터, <sup>2</sup>명지대 물리학과.

We present experimental and theoretical results on a new type of acoustic extraordinary transmission. We achieved 40% intensity transmission through a thick solid wall perforated with subwavelength holes occupying only 3% area. The hole is a straight channel running through the wall thickness with a Helmholtz resonator connected in the middle. Transmission peak occurred at the resonance frequency of the Helmholtz resonators.

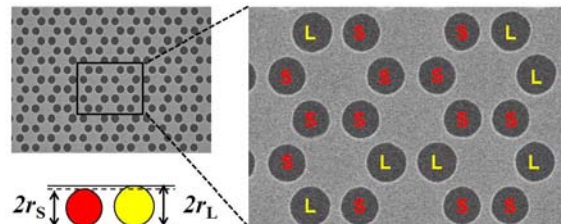
E

**E-30****광자 결정 밴드에지 레이저를 이용한 혼합 광결정의 밴드에지의 조절**

김 성환, 이 정국, 전 현수

서울대학교 물리천문학부.

본 연구 결과에서는 이차원 광자 결정 밴드에지 레이저를 이용하여 혼합 광결정의 개념을 실험적으로 보였다. 두 서로 다른 크기를 가지는 구멍을 각 격자 위치에 무작위적으로 배치함으로 광자 결정 레이저 구조를 제작하였으며 이러한 구조에서도 균일한 구조와 동일한 레이저 모드가 형성됨을 전산모사와 실험 결과를 통해 확인할 수 있었다. 이러한 실험 결과는 화합물 반도체에서의 중요한 개념인 밴드갭 엔지니어링의 개념이 광자 결정 구조에서도 성립함을 보여주는 실험적 결과라 할 수 있다.



**E-31****Symmetry controlled resonance of anisotropic micro-sized planar metamaterial lattice in terahertz regime**

강 보영, 최 은영, 이 현희, 김 은선, 우 제흔, 김 정희, 우 정원, 홍 태윤<sup>1</sup>, 김 재훈<sup>1</sup>

*이화여자대학교, 물리학과. <sup>1</sup>연세대학교, 물리학과.*

2-D arrays of double-splits-ring are prepared to examine the symmetry dependent resonances. The first planar metamaterial has the symmetric array of double-splits-ring and exhibits anisotropic resonance behavior with the resonance alternating between the low and high frequency dipole and quadrupole modes. By imbedding a symmetry breaking line in the first planar metamaterial, the second planar metamaterial is fabricated. Depending on the polarization direction of THz radiation, the resonance exhibits a coupling-dependent structure between the double-split-rings. The multipolar interactions between the meta-particle double-splits-ring is responsible for the anisotropic resonances.

**E****E-32****Chirality in metamaterials and its optical characteristics**

강 보영, 최 은영, 이 현희, 김 은선, 우 제흔, 김 정희, 우 정원, 황 태종<sup>1</sup>, 박 영순<sup>1</sup>, 김 동호<sup>1</sup>

*이화여자대학교, 물리학과. <sup>1</sup>영남 대학교, 물리학과.*

Chiral metamaterials are fabricated and its optical activity characteristics are investigated. Two gammadion structures possessing clockwise and counter-clockwise handedness are obtained by standard e-beam lithographic lift-off process in nano-scale patterns. Scanning electron microscope image showed that the gammadion arm width is on the order of 40nm and period is 250nm. In the transmission spectra, there exit two resonances, namely, plasmonic resonance and meta resonance. The meta resonance associated with the chirality exhibits optical activity property, which has handedness dependence.

## E-33

## 타원편광분석법을 이용한 AlSb 유전함수 연구

김 영동, 정 용우, 차 영훈, 김 승, 강 유진, 신 상훈<sup>1</sup>, 송 진동<sup>1</sup>

경희대학교 물리학과 및 나노광물성연구실, <sup>1</sup>한국과학기술연구원(KIST) 스핀소자연구센터.

본 연구에서는 적외선 광학소자 및 고속전자이동 트랜지스터 등에 폭넓게 이용되는 AlSb 화합물의 유전함수를 0.7 ~ 5.0 eV 의 에너지 영역에서 타원편광분석법을 이용하여 분석하였다. AlSb 는 산소와 급격히 반응하기 때문에, 대기 중에서 물질 고유의 광특성이 유지되기 어려울 뿐만 아니라, 박막 위에 생성되는 산화막 때문에 순수한 AlSb 의 유전함수 측정이 불가능하다. 본 연구에서는 물질의 유전함수에 미치는 산화 효과를 최소화하기 위하여 Molecular Beam Epitaxy로 성장한 1.5 mm 두께의 AlSb 박막을 초고진공 상태의 챔버 안에서 타원편광분석기를 이용하여 실시간으로 측정하였다. 본 연구에서 측정된 순수한 AlSb 의 유전함수에서는, 기존의 보고에 비하여  $E_1$  과  $E_2$  영역에서 두드러진 향상을 볼 수 있었고, 이를 통하여 산화막에 의한 유전함수 왜곡이 최소화 되었음을 확인하였다. 또한 이차미분을 이용한 전이점 (Critical Point) 분석결과 indirect bandgap 을 비롯한  $E_0, E_0 + \Delta_0, E_1, E_1 + \Delta_1, E_0', E_0' + \Delta_0', E_2, E_2 + \Delta_2$  밴드갭들을 측정할 수 있었으며, 이는 linear augmented Slater-type orbital (LASTO) method 를 이용한 AlSb Band-structure 계산결과로 설명될 수 있었다. AlSb 유전함수의 온도의존성 분석은 300 K ~ 800 K 사이의 온도에서 측정된 AlSb의 순수한 유전함수를 사용하였다. 상온(300 K)에서 측정된 AlSb 변수화모델을 기준으로 각 변수들의 온도 의존 궤적을 분석하였고 이를 통해 임의 온도에서의 AlSb의 유전함수를 유도할 수 있었다.

## E-34

## Active Feedback Cooling of a Quartz Tuning Fork with a Quality Factor Control.

장 (JAHNG) 정훈 (Junghoon), 이(LEE) 만희(Manhee), 박(BAK) 완(Wan), 제(JHE) 원호(Wonho)

서울대학교 물리학과.

We present general theoretical analysis and experimental realization of active quality factor control for the self-oscillating quartz tuning-fork (QTF). It is shown that the damping of QTF is controlled by using the active quality factor control which is to add a phase shifted signal, with respect to the QTF motion. By this technique, we cool down the fundamental mode of a 32kHz quartz tuning fork from room temperature to 18 kelvin in uncapped condition. This novel method prove simpler than related optical experiments, from which one can attain true ground state cooling of a micro mechanical oscillator in a cryogenic and vacuum systems.

**E-35****RCWA 를 이용한 비대칭 나노구조의 연구**

변 준석, 김 태중, 한 승호, 공 태호, 윤 재진, 황 순용, 정 진모<sup>1</sup>, 김 영동

경희대학교 물리학과 및 나노광물성연구실, <sup>1</sup>경희대학교 물리학과.

최근 critical dimension(CD)의 크기가 점점 작아지면서, 반도체 산업은 더욱 효율적으로 CD의 구조를 분석하는 기술을 필요로 하게 되었다. CD를 분석하는 방법들 중 광학적인 측정 방법은 비파괴적이며, 상대적으로 저렴한 비용, 높은 정밀도 등의 장점으로 크게 주목을 받고 있다. RCWA 계산 방법은 주기적인 구조에서의 전자기파의 회절을 묘사하는 방법으로 널리 이용되며, 빛을 이용하여 비파괴적인 측정을 하는 타원편광분석기와 결합하여 주기적인 CD의 분석을 하는 연구가 최근에 보고 되었다. 그러나 아직 비대칭적인 주기적인 구조의 분석은 연구된 바가 없다. 본 연구는 RCWA 계산 방법을 비대칭인 구조의 계산에 이용할 수 있음을 보이고자 하였다. 우리는 간단한 지수함수로 비대칭 효과를 표현하였고, 대칭인 RCWA 계산에 지수항을 곱함으로써 비대칭인 CD를 설명할 수 있었다. 비대칭 효과를 조사하기 위해서 간단한 대칭 주기적 구조 모델과 비대칭 모델을 RCWA 방법으로 계산하였다. 그 결과, 비대칭과 대칭인 경우에서의 타원분석변수  $\Psi$ 와  $\Delta$ 가 명백히 다른 점을 확인할 수 있었다. 이것은 비대칭 효과가 제작 과정 동안에 소자 구조의 결함을 관측하기 위해서 고려되어야 하며, 또한 타원편광분석기가 실시간으로 비파괴적인 CD 분석이 가능한 중요 장비로 주목될 수 있음을 보여준다.

E

**E-36****Piezoresponse Force Microscopy of Ferroelectric Thin Films**

KIM JinBae, CHOI MyungHoon, YOON KwanSeok, PARK Sang-il

Park Systems Corp..

The piezoresponse force microscopy (PFM) has been extensively studied for years not only because of the technological applicability but because of the fundamental physics. The PFM has been demonstrated as a powerful tool for investigating low-dimensional ferroelectrics for non-volatile memory devices and data storage applications. The PFM employs a conducting tip to probe the mechanical response of a surface to an applied bias. No special sample preparation is required for this method. Domain structures of the  $\text{Pb}(\text{Zr}_{0.35}\text{Ti}_{0.65})\text{O}_3$  sample was observed by a PFM system (Park Systems, XE-100) with TiPt coated Si cantilevers having a spring constant of 0.95 N/m.

**E-37****Resistance switching mechanism of conducting STO**

PARK HONGWOO, LEE SEUNGRAN, KIM MIYOUNG, JUNG CHANGUK<sup>1</sup>, YI Gyu-Chul<sup>2</sup>

*Seoul National University, Department of Materials Science and Engineering. <sup>1</sup>Hankuk University of Foreign Studies, Department of physics. <sup>2</sup>Seoul National University, Department of Physics and Astronomy.*

Conducting SrTiO<sub>3</sub> (STO) has attracted great attention because of its scientific interests and potential applications in non-volatile memory devices, i.e. resistance random access memory (ReRAM) device. Many efforts have been devoted to understand conduction mechanism of STO and associated resistance switching behavior. There are two main models for explaining resistance switching mechanism of STO: formation and rupture of conducting filaments in an insulating STO matrix and a change of Schottky barrier height and depletion width due to trap charges at an interface between STO and an electrode. Despite the extensive efforts, the switching mechanism of STO is still unclear and controversial. To investigate resistance switching mechanism of conducting STO, we used 0.5% Nb-doped STO. The I-V characteristics were studied by using Pt as the electrodes, which shows clear bipolar resistance switching with hysteretic I-V curves. To clarify the formation of the Schottky barrier and interfacial states, the I-V characteristics will be presented by different electrodes with various work functions. In addition, our efforts to study the conduction mechanism of STO with a high resolution transmission electron microscopy (HRTEM) will be discussed.

**E-38****Transition from bipolar to unipolar resistance switching in a Pt/SrTiO<sub>x</sub>/Pt capacitor**

**capacitor**

이 신범, 채 승철, 장 서형, 노 태원  
서울대학교 물리학과

The semiconductor industry has long searched for a next-generation nonvolatile memory device, which can retain its data even when the power is interrupted. A new concept called resistance random access memory (RRAM), in which its resistance can be repeatedly switched between a high and a low value by applying electric field, has recently attracted lots of scientific and technological interests. According to electric polarity dependence, RRAM can be classified into are two types: unipolar (URS) and bipolar resistance switching (BRS). For many binary oxides such as NiO and TiO<sub>2</sub>, current-voltage curves are symmetry about applied bias  $V$ , so called URS. On the other hand, for most perovskite oxides including SrTiO<sub>3</sub> and Pr<sub>0.7</sub>Ca<sub>0.3</sub>MnO<sub>3</sub>, they are highly asymmetry, so called BRS. Because of different mother materials and very diverse experimental findings, each resistance switching has been investigated separately with a great deal of confusion and many controversies. To explain these intriguing URS and BRS behaviors, numerous theoretical models have been proposed separately. However, most of these models leave unanswered questions. Furthermore, despite scientific and technical importance, underlying physics of URS and BRS seem to have no connections due to their respectively proposed mechanisms. Here, we show the observation on the coexistence of BRS and URS in a Pt/SrTiO<sub>x</sub>/Pt capacitor. Forming voltages of transition from BRS to URS were smaller than that of transition from pristine state to URS. While temperature dependence of each resistance state showed insulating behaviors, that of low resistance state in URS corresponded to a metallic behavior. The occurrence of BRS and URS in one sample demonstrates that these two phenomena should be closely related. Understanding on BRS and URS can provide us some insights how to tackle and use RRAM for next-generation nonvolatile memory devices.

**E-39****Electrical and Optical transport of p-SWNT/n-ZnO Heterojunction Structure**

박 민지, 장 영욱, 강 봉근, 손 민수, 이 재상<sup>1</sup>, 이 상렬<sup>1</sup>, 유 경화<sup>2</sup>

연세대학교 물리학과. <sup>1</sup>한국과학기술연구원 에너지재료연구센터. <sup>2</sup>연세대학교 물리학과 & 나노메디컬 국가핵심연구센터.

Recently, ZnO and carbon nanotubes have received considerable attention because of their unique properties and various potential applications. ZnO is a wide-bandgap oxide semiconductor with a direct energy gap of about 3.37 eV that is usually n-type. On the other hand, semiconducting single wall carbon nanotubes (SWNTs) exhibit p-type behaviors. Therefore, we fabricated p-SWNT/n-ZnO thin film heterojunction structures on SiO<sub>2</sub>/Si substrates and investigated their electrical and photoelectrical properties. The I-V curves of individual SWNT and ZnO film were found to linear, while the I-V curve measured across junctions exhibited diode rectifying behaviors. In addition, we have reported photoresponsive properties of these heterojunction structures under UV light.

E

**E-40****Semiconducting MoO<sub>3</sub> Nanorods for Highly Efficient UV/Visible Light****Photocatalysis**

SHAKIR Imran, SHAHID Muhammad, 강 대준

BK21 Physics Research Division, Department of Energy Science, Institute of Basic Science, SKKU Advanced Institute of Nanotechnology and Center for Nanotubes and Nanostructured Composites, Sungkyunkwan University, Suwon 440-746, Korea.

Ultraviolet and visible light ( $\lambda > 410\text{nm}$ ) driven MoO<sub>3</sub> and Cu doped MoO<sub>3</sub> nanorods photocatalysts were synthesized

and employed in the photocatalytic degradation of toluidine blue “O” (TBO) dye. The evaluation of photocatalytic activity showed that Cu doped MoO<sub>3</sub> nanorods exhibited higher photocatalytic activity than that of pure MoO<sub>3</sub> nanorods and a 99% of TBO was found to be degraded within 30 and 40 min for UV and Visible irradiation respectively (Fig.1). The increase in the photocatalytic activity by Cu doping is due to the increase in the surface active sites and the generation of more  $\cdot\text{OH}$  and  $\text{O}_2^-$  on the MoO<sub>3</sub> surface, which greatly improved the oxidation degradation rate of TBO.

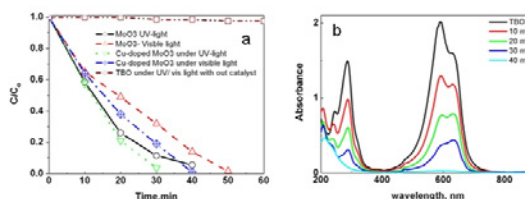


Figure 1. (a) Photocatalytic study of MoO<sub>3</sub> and Cu doped MoO<sub>3</sub> nanorods under UV and visible light irradiation (b) Degradation profile of TBO on Cu doped MoO<sub>3</sub> under Visible light irradiation.

## E-41

조성변화에 따른  $\text{CuInSe}_2$  박막물성과 태양전지의 성능

고 항주, 이 경훈<sup>1</sup>, 김 효진, 한 명수, 김 선훈, 정 채환<sup>2</sup>, 이 종호<sup>2</sup>, 김 호성<sup>2</sup>, 김 광복<sup>3</sup>, 김 진혁<sup>4</sup>

한국광기술원 광소자팀, <sup>1</sup>한국광기술원 광소자팀, 전남대학교 신소재공학부, <sup>2</sup>한국생산기술연구원 광응용부품센터, <sup>3</sup>금호전기(주) 태양광사업팀, <sup>4</sup>전남대학교.

최근 고유가와 화석연료 사용으로 인한 기후변화로 인해 청정에너지인 태양광발전에 대한 사회적 관심이 높아졌다. 특히,  $\text{CuInSe}_2$  계 박막 태양전지는 전력 생산에 적은 비용이 들어가는 태양전지의 유력한 후보로 인식되고 있다.  $\text{CuInSe}_2$  물질은 Si의 100배, GaAs 보다 10배 정도 높은 흡수계수를 갖고 있어 얇은 박막으로 높은 전력을 생산해 낼 수 있다고 여겨진다.  $\text{CuInSe}_2$ 가 높은 흡수율로 고효율을 내기 위해 우리는 고품질  $\text{CuInSe}_2$  박막 공정을 연구하고 있다. 본 논문은  $\text{CuInSe}_2$  박막 태양전지 제조에 있어서 Cu/In 조성비를 제어하여 양질의 흡수층을 얻고 소자성능을 향상시키는 공정을 발표한다. 우리는  $\text{CuInSe}_2$  박막 제조에 있어 Cu/In 조성비가 0.84 ~ 0.94로 변화시킴에 따라  $\text{CuInSe}_2$  박막 태양전지의 효율이 약 1% 변화하는 것을 알 수 있었다. 이러한 소자 성능변화는 흡수층의 품질과 밀접한 관계가 있는 것으로 사료된다.  $\text{CuInSe}_2$  박막 태양전지는 2mm 두께의 유리(Soda-lime glass) 위에 제조하였다. 소자의 구조는 Al/n-ZnO/CdS/ $\text{CuInSe}_2$ /Mo/Glass 이고 두께는 Al~1 $\mu\text{m}$ , n-ZnO~800nm, CdS~50nm,  $\text{CuInSe}_2$ ~2 $\mu\text{m}$ , Mo~900nm 이다. 소자 구조를 형성하는 모든 막은 스퍼터(sputter) 공정으로 제조되었고 스퍼터 챔버의 기준압력(base pressure)은  $\sim 10^{-6}$  Pa로 유지하였다. 흡수층인  $\text{CuInSe}_2$  막은 2단계로 제조하였는데 1단계에서는 300°C 이하에서 Cu, In, Se를 증착하고 2단계에서는 1단계의 박막을 Se 분위기에서 425°C로 15분간 열을 가한 후 기판을 식힌다. 제조된  $\text{CuInSe}_2$  박막은 Scanning electron microscopy, Energy dispersive x-ray spectroscopy, Atomic force microscopy, X-ray diffractometer, Hall effect measurement system으로 분석되었다. 태양전지의 유효면적은 0.54  $\text{cm}^2$ 이고, 광전 변환 효율측정은 AM1.5, 100  $\text{mW}/\text{cm}^2$  조건에서 실시하였다.

## E-42

## Enzymatic Biofuel Cells using Polypyrrole Nanowire Array

김 지현, 김 성인, 유 경화<sup>1</sup>

연세대학교 물리학과, <sup>1</sup>연세대학교 물리학과, 연세대학교 나노메디컬 국가핵심연구센터.

The one-compartment glucose/ $\text{O}_2$  biofuel cells were developed using polypyrrole (PPy) nanowires containing glucose oxidase (GOD) and 8-hydroxyquinoline-5-sulfonic acid hydrate (HQS) as an anode for the improvement of the power density. PPy-HQS-GOD nanowires were fabricated by electropolymerizing a mixture of pyrrole monomers, GOD, and HQS within the nanopores of AAO templates and then dissolving the AAO template. Compared with the film-type biofuel cells, the nanowire-type biofuel cells exhibited higher power density by two orders of magnitude at 37 °C and pH 7.4 because of the increase in surface area and enzyme loading. Additionally, we constructed the glucose/ $\text{O}_2$  biofuel cell covered with a fluidic channel. The fluidic biofuel cell showed comparable performances to the biofuel cell without the fluidic channel, demonstrating the feasibility of integrated biofuel cells within a fluidic cell.

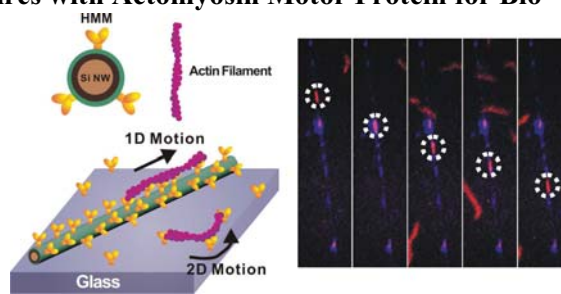
## E-43

### Functionalization of Silicon Nanowires with Actomyosin Motor Protein for Bio-inspired Nanomechanical Applications

BYUN Kyung-Eun, HEO Kwang<sup>1</sup>, SHIM Sojung<sup>2</sup>, CHOI Heon-Jin<sup>2</sup>, HONG Seunghun

Department of Physics and Astronomy, Seoul National University. <sup>1</sup>Interdisciplinary Program in Nano-Science and Technology, Seoul National University. <sup>2</sup>Department of Materials Science and Engineering, Yonsei University.

Biological motors such as actomyosin have been extensively studied as a component for highly-efficient hybrid nanomechanical systems. Herein, we report a method to functionalize silicon nanowires (Si-NWs) with heavy meromyosin (HMM) and to disperse them in aqueous solution. We successfully demonstrated the motility assay using the HMM-functionalized Si-NWs. Significantly, HMM-functionalized Si-NWs supported the linear motion of actin filaments over 100- $\mu$ m-long distance without any confining physical barrier. Detailed analysis revealed the *ballistic* nature of actomyosin motion on functionalized Si-NWs, which is qualitatively different from their *diffusive* motion on two-dimensional HMM-coated glass substrates. The HMM-functionalized Si-NW can be an ideal platform for one-dimensional motor protein assay study and a key component for various nanomechanical applications.



## E-44

### Amperometric Lactate Biosensor with High Sensitivity Using Immobilization of

#### Lactate Oxidase onto Molybdenum Oxide Nanorods

SHAKIR Imran, 양 형우, SHAHID Muhammad,

CHEREVKO S<sup>1</sup>, 정 찬화<sup>1</sup>, 김 동철<sup>2</sup>, 강 대준

BK21 Physics Research Division, Department of Energy Science, Institute of Basic Science, SKKU Advanced Institute of Nanotechnology and Center for Nanotubes and Nanostructured Composites, Sungkyunkwan University, Suwon 440-746, Korea. <sup>1</sup>Department of Chemical Engineering, Sungkyunkwan University, Suwon 440-746, Korea. <sup>2</sup>청운대학교, 충청남도 홍성, 350-701.

Large-scale orthorhombic single-crystalline Molybdenum oxide (MoO<sub>3</sub>) nanorods were synthesized through hydrothermal method and were explored for the construction of electrochemical biosensors. The electrochemical measurements revealed that the MoO<sub>3</sub> nanorods were immobilization matrix for lactate oxidase (LOx) with good enzymatic stability and bioactivity. Fourier-Transform Infrared Spectroscopy reveals that the lactate oxidase immobilized on the MoO<sub>3</sub> nanorods retains its native conformation. The MoO<sub>3</sub> nanorods offer the pathway for direct electron transfer between the electrode surface and the active redox centers of LOx. The biosensor at an applied potential of 0.8 V (vs. Ag/AgCl) in pH7.4 buffer showed a fast response (90% response time of 10 s) to lactate and a reproducible high sensitivity of 0.87  $\mu$ A/mM. The (Fig. 1).

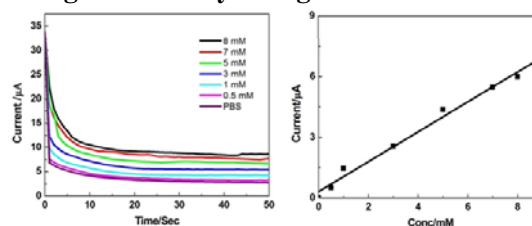


Figure 1: (A) Amperometric response to lactic acid of the Au-MoO<sub>3</sub>-LOx-Nafion electrode with concentration of, 0.5, 1, 3, 5, 7, 8 mM lactic acid into the 2 mM PBS solution every 50 s at the operating potential of 0.8 V versus Ag/AgCl. (B) calibration curve for the Au-MoO<sub>3</sub>-LOx-Nafion showing the oxidation current versus the lactate concentration.

**E-45****Capacitance-Based Real Time Monitoring of Endocytosis**

이 리미, 김 평환, 최 정우, 김 규정, 김 경미<sup>1</sup>, 박 윤정

연세대학교 나노메디컬 협동과정, <sup>1</sup>연세대학교 의과대학.

There exist three kinds of endocytosis; receptor mediated endocytosis, pinocytosis and phagocytosis. First, receptor-mediated endocytosis is essential for targeted gene/drug delivery to a specific cell type. Second, pinocytosis is the engulfing and digestion of dissolved substances and phagocytosis is the engulfing and digestion of microscopically visible particles. In this study, we developed a capacitance sensor to monitor and distinguish three kinds of endocytosis in real time. The capacitance sensor was able to detect a capacitance peak in different cell lines during the internalization of adenoviruses or antibodies via receptor-mediated endocytosis. In contrast, the capacitance declined without a capacitance peak when nanoparticles were taken up via non-specific pinocytosis. In case of phagocytosis, the capacitance shows a peak during the engulfing of bacterium, and then capacitance is abruptly increases due to the competition between engulfing the bacterium and bacteria dividing. Thus, our capacitance sensor represents a potential capacitance-based means of discrimination among receptor-mediated endocytosis, non-specific pinocytosis and phagocytosis. Moreover, we developed a capacitance sensor array to demonstrate capacitance-based high-throughput screening. We showed that the capacitance sensor array could rapidly identify antibodies or ligands with high specificity for target molecules. We propose that the capacitance sensor array will provide a valuable tool for high-throughput screening

**E-46****Performances of Geiger-Mode Avalanche Photodiode PET Modules Transferring Scintillation Light via an Optical Fiber**

HONG Seong Jong, KIM Chan Mi, CHO Sung Mook, WOO Heon, KWON Sun Il<sup>1</sup>, RHEE June Tak<sup>2</sup>, SONG In Chan<sup>3</sup>, LEE Jae Sung<sup>1</sup>

*Eulji University, Department of Radiological Science. <sup>1</sup>Seoul National University, Department of Nuclear Medicine. <sup>2</sup>Konkuk University, Department of Physics. <sup>3</sup>Seoul National University, Department of Radiology.*

A combined PET/MRI with simultaneous acquisition capability will play an important role for the studies of human brain. To take advantages of already existing MRIs in many hospitals and institutions, minimally modified PET/MRIs are highly desirable. In addition, current MRI trend is to utilize powerful body coils transmitting radio-frequency (RF) waves and local RF coils receiving signals. We propose a minimally modified brain-specific Geiger-mode avalanche photodiodes (G-APD) PET with optical fiber bundles which transfer scintillation lights from scintillation crystals to G-APDs. To investigate the feasibility of the G-APD PET with the optical fiber bundles, we studied the performances of G-APD/LGSO couplings with a single optical fiber. A GEANT4 Monte-Carlo simulation was used to study scintillation light transfer from scintillation crystals to G-APD. The Monte-Carlo simulation showed that light loss due to the bending of optical fiber with a diameter less than 2.0 mm is small for the fiber with a bending radius greater than 25 mm. Mechanical integrity against such as crack turned out to be far more important. Two Hamamatsu multi-photon photon counters (MPPC) were tested with double clad optical fibers of 1.5 mm and 2.0 mm diameter, and 25 mm and 50 mm bending radius. Two Hamamatsu MPPCs directly attached to LYSO crystals resulted in ~14% energy and ~1.3 ns coincidence time resolution, both full width half maximum (FWHM). With one of the MPPCs attached to an optical fiber of 1.5 mm diameter, 50 mm bending radius, and 300 mm length, energy and coincidence time resolutions were measured to be 27% and 2.2 ns, respectively. Initial results were encouraging for the combined G-APD PET using optical fiber.

**E-47****헌혈자 적합성 판별의 신뢰도 제고를 위한 혈액밀도 검사용 기준용액의 전국 혈액원과 KRISS의 상호비교**

이 용재, 장 경호, 정 호연

한국표준과학연구원

헌혈의 적합성 여부를 판별하기 위하여 헌혈자에 대한 혈액밀도를 검사한다. 혈액밀도는 기준용액인 황산구리수용액을 사용하여 비교검사된다. 헌혈을 하기 위하여 헌혈자의 혈액비중은 전혈헌혈은 비중 1.053, 성분헌혈은 1.052이상 되어야 한다. 본 연구는 전국 16개 혈액원에서 제조된 기준용액의 밀도정확도를 KRISS와 국내 최초로 상호비교를 통하여 혈액원의 제조 및 측정 그리고 검사능력을 제고하는데 있다. 본 연구를 통한 기준용액의 정확도는 0.0003 g/cm<sup>3</sup> 이하의 허용오차로서 설정되어야 함을 알 수 있었고 평가결과로서 KRISS와의 편차가 허용오차 이상인 기관은 7개 기관, 허용오차 이하인 기관은 9개 기관으로 평가되었다. 그러나 모든 기관의 측정불확도를 추정한 결과 0.001 g/cm<sup>3</sup>로서 허용오차범위를 벗어난 것으로 나타났다. 이로써 전 혈액원의 기준용액의 제조 및 밀도측정기술의 제고 및 혈액밀도측정의 표준화 필요성이 대두되었다.

E

**E-48*****In vivo* Imaging of Cancer Cells in the Primo-vascular System with Electroporation of Quantum Dots and Multispectral Imaging**유 정선, 김 홍배, 원 나연<sup>1</sup>, 방 지원<sup>1</sup>, 김 성지<sup>1</sup>, 안 세영, 소 광섭서울대 물리천문학부, <sup>1</sup>포항공대 화학부

Our knowledge of cancer metastasis is limited by our inability for long-term follow-up of this process *in vivo*. Fluorescence molecular imaging has the potential to image cancer cells with high contrast and sensitivity in living animals. For this purpose, intracellular delivery of near-infrared fluorescence quantum dots (QDs) by electroporation offers considerable advantages over organic fluorophores and other cell tagging methods. In this research, the dissemination and the growth of near-infrared quantum dot (NIR QD)-electroporated cancer cells in metastatic sites were investigated by using *in vivo* multispectral imaging techniques. We developed a multispectral imaging system that could eliminate two major parameters compromising *in vivo* fluorescence imaging performance, i.e., variations in the tissue optical properties and tissue autofluorescence. Development of these tools permits *in vivo* tracking of QD-labeled cancer cells that are disseminated via an independent fluid-conducting system has been called the primo-vascular system. The NIR QD-labeled cancer cells preferentially migrated through the primo-vascular system around the tumor and inside the abdominal cavity rather than through the lymphatic system. In addition, NIR QD-labeled cancer cells, which had been seeded intraperitoneally, specifically infiltrated the primo-vascular system in the omentum and the gonadal fat. This finding strongly suggests that the primo-vascular system may be an additional metastasis route, complementing the lymphatic and the hematogenous routes, that facilitates dissemination and colonization of cancer cells in secondary sites.

**E-49****Anodized Aluminum Oxide-Based Capacitance Sensors for Direct Detection of DNA Hybridization**

강 봉근, 여 운진, 유 경화  
연세대학교 물리학과

A capacitance sensor array based on an anodized aluminum oxide (AAO) nanoporous structure was fabricated by using the Au film deposited on the surface of the AAO membrane and Au nanowires infiltrated within the nanopores as the top and bottom electrodes, respectively. When the completely complementary target DNA molecule was added, the decrease in capacitance was found. However, the addition of the non-complementary DNA molecules including 1-base mismatch to the probe DNA caused no significant change in capacitance, demonstrating that DNA hybridization can be detected with single nucleotide polymorphism sensitivity. In addition, we investigated the dependence of the capacitance change on the target DNA concentration. For the concentration of 1 pM (pico Molar), the capacitance change of about 10% was observed.

**E-50****Origin of oxygen migration in bipolar resistance switching of epitaxially grown NiO**

LEE Seungran, KIM Hoonmin, CHAR Kookrin, BAK Junghoon, CHO Myoungrae, PARK Yun Daniel, KIM Dongchirl<sup>1</sup>, SEO Sunae<sup>1</sup>, LI Xiangxu<sup>1</sup>, PARK Gyeongsoo<sup>1</sup>, JUNG Ranju<sup>2</sup>

*Seoul National University, Department of Physics and Astronomy. <sup>1</sup>Samsung Advanced Institute of Technology. <sup>2</sup>Kwangwoon University, Department of Electrophysics.*

We investigated effects of crystalline properties of epitaxial NiO (epi-NiO) films on formation of interfacial metal oxide between top electrodes (TEs) and epi-NiO and associated resistance switching behavior. Crystalline quality of Epi-NiO grown on SrRuO<sub>3</sub> (SRO) at different temperatures were analyzed using X-ray diffraction spectra and transmission electron microscopy, indicating that epi-NiO grown at higher temperature shows high crystallinity. The I-V properties of epi-NiO were measured by using several top electrodes (TEs), and no resistance switching behavior was observed in epi-NiO with high crystallinity. From our previous observation that interfacial metal oxide formed at TE/epi-NiO interfaces play a key role in resistance switching behavior, we argued that the crystalline quality of epi-NiO is responsible for oxygen migration and formation of the interfacial oxide layer.

**E-51****분무열분해법으로 성장된  $\text{Cd}_{1-x}\text{Zn}_x\text{S}$  박막의 구조와 광학적 특성**

서 동주, 김 고은, 이 소리, 박 정복, 김 지효, 김 나리, 오 상미, 김 건호<sup>1</sup>

조선대학교. <sup>1</sup>경상대학교.

$\text{Cd}_{1-x}\text{Zn}_x\text{S}$  박막을 분무열분해법으로 유리기판 위에 성장시켰다.  $\text{Cd}_{1-x}\text{Zn}_x\text{S}$  박막을 성장시키기 위해 사용한 시약은 cadmium acetate, zinc acetate, thiourea이며, 이차증류수에 이들 시약을 녹여 0.02 mole 수용액을 만든 후 증류수를 혼합하여 분무용액을 만들어 사용하였다. 성장온도와 Zn 농도 변화에 따른  $\text{Cd}_{1-x}\text{Zn}_x\text{S}$  박막의 결정구조를 규명하기 위하여 X-선 회절분광기(XRD)를 이용하였으며,  $\text{Cd}_{1-x}\text{Zn}_x\text{S}$  박막의 표면과 미세구조는 주사전자현미경(SEM)을 이용하여 관찰하였다.  $\text{Cd}_{1-x}\text{Zn}_x\text{S}$  박막에 입사한 빛의 파장을 변화시키면서 광투과와 광흡수 스펙트럼을 측정하였고,  $\text{Cd}_{1-x}\text{Zn}_x\text{S}$  박막의 에너지 띠간격은 Zn의 농도가 증가함에 따라 증가하였다.

E

**E-52****Surface profile measurement with *nanometer* scale resolution using oversampled coherent diffraction imaging in reflection geometry**

노 도영, MARATHE Shashidhara, 김 상수<sup>1</sup>, 김 수남, 김 찬, 강 현철<sup>2</sup>

광주과학기술원 신소재공학과. <sup>1</sup>Argonne National Laboratory. <sup>2</sup>조선대학교.

We demonstrate a coherent diffraction imaging method which can be used to reconstruct surface images in reflection geometry. Using a He-Ne laser source we demonstrate that reflected scattered beam from a sample surface when collected using a converging lens at the back focal plane, can be used to retrieve phase information and surface image, without the prior knowledge of object or object support. With the help of a test sample we show that the phase map of the reconstructed object exit wave can be used to obtain quantitative information of surface depth profile with nanometer resolution. Pure amplitude object was also used to show the applicability of this method to real samples. We show the incident angle dependence on the reconstructed image and will discuss various aspects of the experimental parameters associated with the image reconstruction in reflection geometry. This method can be performed with a simple setup, and can be very useful in accessing the surface of the sample remotely for cases of in-situ experiments of growth on a substrate. We believe this should open up new application areas for coherent diffraction imaging research.

**E-53****Spectral Response Analysis to Characterize the Channel/dielectric Interfacial****Trap States for ZnO-based Thin-film Transistors**

임 성일, 이 기문, 오 민석<sup>1</sup>, 박 찬호, 황 치선<sup>2</sup>, 박 상희<sup>2</sup>

연세대학교 물리및응용물리사업단. <sup>1</sup> 전자부품연구원. <sup>2</sup> 한국전자통신연구원.

Oxide-based thin-film transistors (TFTs) have attracted much attention over the last several years because of their great potential toward display drivers and even future electronics integrated on glass. To understand and improve the electrical characteristics of such a device, it is essential to clarify the defect states especially on the channel/dielectric interface, but techniques to characterize that have been rarely reported yet. Now, the authors report on the novel method for characterization of interfacial trap states with transparent ZnO-based TFTs by spectral response analysis. When we measure the transfer characteristics of our ZnO-TFT in dark, we can observe the good electrical performance ( $m_{\text{sat}} \sim 4 \text{ cm}^2/\text{Vs}$ , on/off current ratio  $\sim 10^7$ , and  $V_{\text{th}} \sim 0 \text{ V}$ ) without any observable gate bias-induced hysteresis behavior. However, with an intense monochromatic illumination ( $> 10^{15} \text{ photons cm}^{-2} \text{ sec}^{-1}$ ) on the device, the  $V_{\text{th}}$  starts to shift negatively as the optical energy value (especially of  $\sim 1.31$ ,  $\sim 1.69$ , and  $\sim 1.95 \text{ eV}$ ) increase. This means that the electron occupied trap level should be released by an optical illumination which corresponds to the energy value from conduction ( $E_c$ ) to the trap level ( $E_t$ ), thus the  $V_{\text{th}}$  shift as large as the number of density of state (DOS). (Detailed mechanism and analysis will be shown in the meeting.) From these spectral response characteristics of ZnO-TFT, we can clarify and quantify simultaneously the origin of interfacial states on ZnO channel/ $\text{Al}_2\text{O}_3$  dielectric interface. As a result, we can conclude that this methodology of opto-electric spectral analysis is one of novel techniques to measure the channel/dielectric interface characteristics which can be adapted to most of field-effect device.

**E-54****X-선 광전자분광법과 흡수분광법을 이용한 비정질 ZnO 박막의 전자구조 연구**

조 덕용, 김 정환<sup>1</sup>, 나 광덕<sup>1</sup>, 송 재원<sup>1</sup>, 황 철성<sup>1</sup>, 박 병규<sup>2</sup>

성균관대학교, 물리학과. <sup>1</sup> 서울대학교, 재료공학부. <sup>2</sup> 포항공과대학교, 포항가속기연구소.

비정질 ZnO (2nm) 박막의 전자구조와 결정질 ZnO (50nm; wurtzite) 박막의 전자구조에 관하여, Zn L3-흡수 끝 흡수분광법과 광전자분광법을 이용하여 비교 연구하였다. 두 박막의 valence band 모양은 비슷한데 반해, conduction band는 그 모양이 다름이 관측되었다. 이를 이론적으로, 비정질 ZnO 내의 구조 무질서 (structural disorder)를 나타내는 가상의 변수를 도입하여 성공적으로 묘사할 수 있었다. 이는 불순물이나 산소공공 없이 단지 비정질 산화물 내의 구조 무질서만으로도 bandgap과 carrier 농도가 달라질 수 있음을 의미한다.

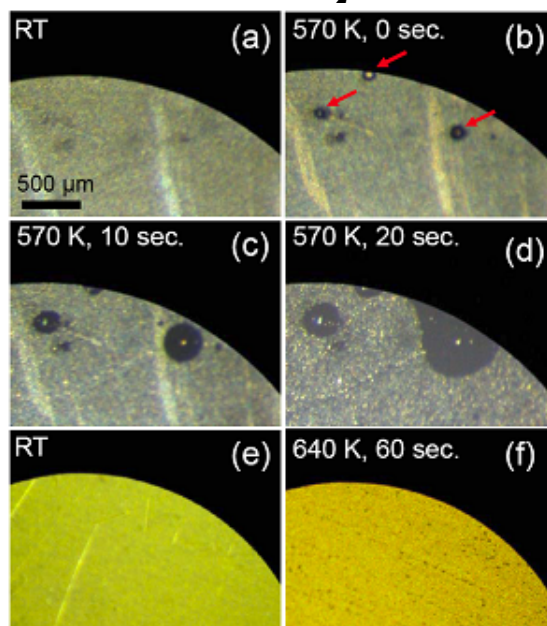
## E-55

### Structural phase Transition of Low-coverage Pentacene on SiO<sub>2</sub> and Au surfaces

임 규욱, 이 경재<sup>1</sup>, 강 태희, 정 석민<sup>1</sup>, 최 무영<sup>2</sup>

포항가속기연구소. <sup>1</sup>포항공과대학교, 물리학과. <sup>2</sup>서울대학교, 물리천문학부.

Thermodynamic behaviors of low-coverage pentacene molecules on both silicon oxide (SiO<sub>2</sub>) and gold (Au) surfaces have been observed via x-ray absorption spectroscopy. It reveals intriguing structural transitions with temperature: For the SiO<sub>2</sub> surface, monotonic decrease in the mean tilt angle of the pentacene layer is observed as the temperature is increased. For the Au surface, three different structural regimes are found, indicating double transitions. Such contrasting thermodynamic behaviors are explained in terms of a spin-1 Ising model, which includes three structural states: standing-up, lying-down, and desorbed.



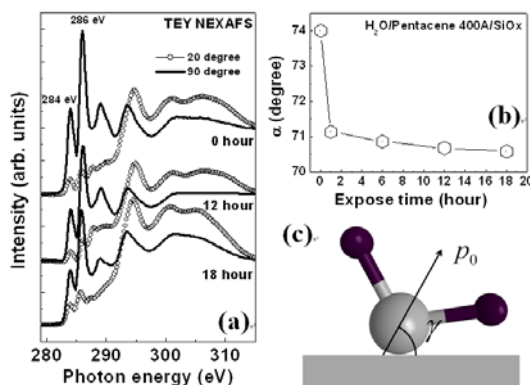
## E-56

### H<sub>2</sub>O Induced Structural Modification of Pentacene Crystal

이 경재, 임 규욱<sup>1</sup>, 강 태희<sup>1</sup>, 정 석민

포항공과대학교, 물리학과. <sup>1</sup>포항가속기연구소.

Water is one of the obstacles for prolonged life-time of organic based field-effect-transistors (OFETs). Here, we show how H<sub>2</sub>O molecules adsorb and affect pentacene crystal by using photoelectron spectroscopic methods. Diffusion into the crystal is accompanied with accumulation of H<sub>2</sub>O onto the crystal. Valence band, core level, and x-ray absorption spectra show that H<sub>2</sub>O molecules physisorb on the pentacene surface via oxygen, resulting in the increase of the hole-injection barrier. The diffused molecules results in the deteriorated crystallinity, and they reflect the weakening intermolecular interactions of pentacene crystal.



**F-01(초)****Control of Epigenetic Stability in Gene Expression**

GHIM Cheol-Min, ALMAAS Eivind<sup>1</sup>

*School of Nano-biotechnology & Chem Eng, Ulsan Nat'l Institute of Sci & Tech. <sup>1</sup>Dept of Biotechnology, Norwegian Univ of Sci & Tech.*

Stochastic fluctuation sets a fundamental limit to the fidelity of biochemical signaling in a cell. At the same time, it provides a means for diversifying phenotypic portfolio that potentially leads to enhanced survival of species under a changing environment. Here we propose a novel strategy for modulating this genetic 'noise' and identify the biochemical characteristics that determine the stability against the noise. A special emphasis is placed on the control of epigenetic switching from which we discuss the design principles for scalable synthetic-biological devices, accessible to experimentation or evolutionary selection.

F

**F-02(초)****Networking metabolites, diseases, and drugs**

이 덕선

*인하대학교 기초의과학부/물리학과.*

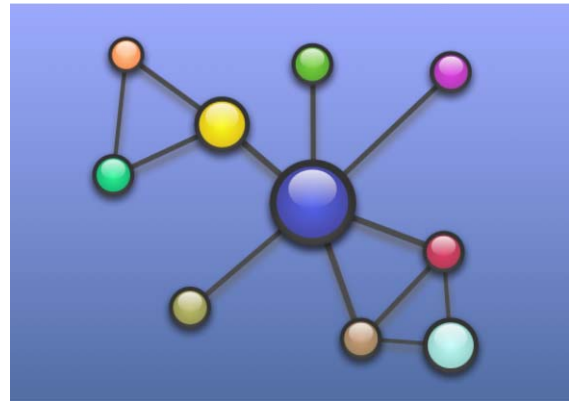
We show simple analyses of human and bacterial metabolic networks can guide drug discovery and disease diagnosis/prevention. Chemical reaction fluxes in cellular metabolism are strongly correlated while consuming and producing metabolites either simultaneously or sequentially. We first discuss evidence that diseases' comorbidity may be caused by such functional correlation of metabolic reactions. Next, we introduce an integrated drug discovery scheme for pathogenic bacteria, where a metabolic network analysis offers drug targets on the genome scale and computational chemistry provides drug candidates - small-molecule inhibitors of the targets.

**F-03(초)****통계물리학 도구를 응용한 복잡계 네트워크 분석**

박 주용

서울대학교 물리천문학부.

네트워크로 나타낼 수 있는 다양한 분야의 복잡계 데이터는 매우 빠른 속도로 축적되고 있으며, 이를 종합적으로 이해하고 분석하기 위하여 물리학을 위시한 여러 분야의 협력 필요성이 대두되고 있다. 여기에서는 전통적 통계물리학 이론에 기반한 사회 및 기술 네트워크 모형화 및 분석 방법을 살펴보고, 이동통신 사용자의 통화 기록으로부터 추출된 공간상 이동 행태의 분석법을 소개한다.



F

**F-04(초)****Entropy, self-organization and conditions of life**

KIM Sungyun

Hoseo University.

Entropy, self-organization and conditions of life are investigated. In information theory entropy is the ability to store information, and in this sense it is a subjective quantity. Using this concept self-organization can be defined according to the coarse-grained level of information. One of important aspects of life is self-replication. For self-replication, knowing self is necessary for a living being. A self-replicating program is compared as an example and it is pointed out that different levels of self-description is necessary for self-replication. Descriptions from self-organization are used for the different levels of self-description.

**F-05****이차원 엑스 와이 모형에서의 정보전달 동역학**최 무영, 김 민수, 정 다운<sup>1</sup>, 권 현웅서울대학교, 물리천문학부. <sup>1</sup>서울대학교, 화학부.

계와 주변 환경 사이의 정보 교환에 초점을 맞춘 정보전달 동역학(information transfer dynamics)을 이차원 엑스 와이 모형(two-dimensional XY model)에 적용하여 그 거동을 살펴본다. 먼저 엔트로피 추출 풀이법(entropic sampling algorithm)을 이용하여 이차원 엑스 와이 모형의 엔트로피를 수치적으로 얻는다. 그리고 낮은 에너지 영역과 높은 에너지 영역에 대한 근사를 하여 엔트로피의 해석적인 결과를 얻어 수치적인 결과와 비교한다. 엔트로피 추출 풀이법을 통해 올바른 엔트로피를 얻으면 이를 이용하여 엔트로피 추출 동역학(entropic sampling dynamics)을 수행한다. 엔트로피 추출 동역학은 정보전달 동역학의 되짚음이 가능한 정보교환을 하는 경우를 수치적으로 계산하는 방법이다. 엔트로피 추출 동역학을 이용하여 계의 에너지와 질서매개 변수의 시간 변화를 살펴본 후 시간에 대한 상관함수(correlation function)를 구한다. 이 상관함수의 거동을 기술하는 완화시간(relaxation time)을 얻은 후, 계의 크기에 따른 완화시간의 변화를 살펴본다. 이 변화를 이징모형(Ising model)의 경우와 비교하여 논의한다.

F

**F-06****Conformational Phases and Interaction of Polyelectrolytes**KOH Dong-Wook, YI Juyeon<sup>1</sup>Korea University, Department of Physics. <sup>1</sup>Pusan National University, Department of Physics.

We study conformational phases and interaction of flexible polyelectrolytes. Evaluating a scaling behavior of projection length with respect to the contour length of polyelectrolytes, we examine a crossover from the extended state to the coiled state, depending on system parameters such as ionic strength and Debye screening length. Intriguingly it is revealed that the competition between the net charge and the charge fluctuation determines the nature of the inter-polymer interaction, viz. attraction or repulsion. Also, we find that the interaction affects the conformation of polymers in such a way that the inter-polymer attraction stiffens polymers, explaining a polymer bundle aggregation often observed in experiments.

**F-07****Rotational Motion of Flow in Spirally Patterned Geometry**

JEON Chanil, JEONG Hawoong, JUNG YoungKyun<sup>1</sup>

*KAIST. <sup>1</sup>KISTI.*

We study the transport properties of the fluid flowing in a cylindrical geometry using molecular dynamics simulations. The surface is helically patterned with different wettability. We find that the rotational motion of the flow arises from the spiral geometry of the surface and the transverse and longitudinal motions depend on both the fluid density and helical wavelength. We also discuss the motion of the fluid is influenced by the width of the pattern. For small attractive bandwidth, it is observed that the fluid flow is much faster.

**F****F-08****A Mesoscopic Model of Transitions between B-DNA and Z-DNA**

JEONG Seong Min, SUNG Wokyung

*Department of physics POSTECH.*

It is known that the left-handed DNA, called Z-DNA, exists in specific situations of base sequences and ionic environments. Transition between right-handed BDNA, the regular form in cell, and the Z-DNA is critical in gene regulation. Within the mesoscopic model for double strand(ds) DNA recently developed[J-H. Jeon and W. Sung, manuscript in review], we incorporate an additional geometrical feature, i.e., tilting angle of base plane. This breaks symmetry of the energy profile, otherwise symmetric, with respect to helical angles, showing the energy minimum at the (positive) helical angle of the BDNA as well as meta-stability of the Z-DNA. It suggests that our model can explain some physical condition for Z-BNA and the B-Z transitions in an analytical manner.

**F-09****Kramers problem for a polymer using path integral hyperdynamics**SHIN Jaeh, KHANDKAR Mahendra<sup>1</sup>, ALA-NISSILA Tapio<sup>1</sup>, SUNG Wokyung*Department of Physics, POSTECH. <sup>1</sup>Department of Applied Physics, Helsinki University of Technology.*

We investigate the thermally activated crossing of flexible and semiflexible polymers over a metastable potential barrier using path integral hyperdynamics. We find, for a flexible polymer, a non-monotonic behavior of crossing rate with the polymer chain length ( $L$ ), due to the coil-stretch transition at a critical chain length ( $L_c$ ); For  $L$  less than a critical length  $L_c$ , a polymer crosses the barrier in coiled state and the crossing rate decreases with  $L$  increases, but for  $L > L_c$ , it crosses in a stretched state, with the barrier height effectively reduced and the rate increasing with  $L$  increase. We also find that as the chain stretching stiffness decreases or the bending stiffness increases, the polymers more effectively reduce the barrier heights and enhance the crossing rates. The polymers in barrier crossing manifest its unique features, conformation flexibility and cooperativity in response to external forces as a characteristic feature of soft matter dynamics.

F

**F-10****Dynamics of Density Fluctuations for Interacting Brownian Particles: Field****Theoretic Approach**

KIM Bongsoo

*창원대학교 물리학과.*

The time evolution of the density field of interacting Brownian particles is governed by a Langevin equation with multiplicative thermal noise, which is often called the Dean-Kawasaki (DK) equation. Due to its multiplicative nature, the DK equation poses a serious difficulty in constructing perturbation scheme consistent with the fluctuation-dissipation relationship (FDR): the naive loop-expansion was shown to be inconsistent with the FDR. This difficulty was elegantly resolved by Andreanov-Biroli-Lefevre (ABL) via discovery of time-reversal symmetry of the corresponding Martin-Siggia-Rose dynamic action. In this talk, I discuss the two types of perturbation theories in which the FDR is respected order by order. One method may be coined as the auxiliary field method, due originally to ABL. Here a new set of conjugate fields is introduced, and the standard loop-expansion scheme can be applied to the resulting dynamic action. The final one-loop equation for the density correlation function takes a similar but distinct form compared to that given by the mode coupling theory (MCT). Although not completely certain and is subject to numerical test, it is very likely that this one-loop equation becomes unstable in the long-time limit. This instability can be overcome via the irreducible memory function approach in which the one-loop result coincides with the MCT. The other method is a weak coupling (potential) expansion. Here the original dynamic action is separated into the noninteracting and interacting parts. The noninteracting part contains a thermal noise non-gaussian term. But this cubic nonlinearity can be treated nonperturbatively due to its form containing double hat-fields. Only the interaction part is perturbatively treated. Up to the second-order, the simultaneous equation for the correlation  $C$  and the MSR-response functions  $G$  (which is distinct from the physical response function  $R$ ) contain higher-loop (up to the three loop) contributions, in addition to the one-loop contributions which are the same as those given by the naive one-loop theory. Though the FDR between  $C$  and  $R$  is the standard linear relation, the FDR between  $C$  and  $G$  is nonlinear.

**F-11****An electromechanical hair cell**

AHN Kang-Hun

*Department of Physics, Chungnam National University, Daejeon 305-764, Republic of Korea.*

Hair cells in biological hearing organs transform mechanical stimuli into neuronal signals with great sensitivity and high frequency selectivity. By combining physiological principles of hair cells with electronic engineering, we have produced an analog electromechanical sensor with functional characteristics of hair cells. The sensitivity and frequency selectivity increases inversely proportional to the amplitude of input signal for periodic signal. The sensor detects pulse signals weaker than the noise strength. The electromechanical hair cell represents a step toward constructing artificial auditory systems which use realistic principles of hearing organs.

F

**F-12****Correlation between price behavior and performance of different strategy****evaluation schemes**

BAEK Yongjoo, LEE Sang Hoon, JEONG Hawoong

*KAIST 물리학과*

We observe the performances of three strategy evaluation schemes, which are the history-dependent wealth game, the trend-opposing minority game, and the trend-following majority game in a stock market where the price is exogenously determined. The price is either directly adopted from the real stock market indices or generated with the Markov chain of order at most 2. Each scheme's success is quantified by average wealth accumulated by the traders equipped with the scheme. The wealth game, as it learns from the history, generally shows good performance unless the market is highly unpredictable. The majority game is relatively successful in a trendy market dominated by long periods of sustained price increasing or decreasing. On the other hand, the minority game is suitable for a market with persistent zig-zag price patterns. These observations agree with our intuition and support the viability of the wealth game as a strategy evaluation scheme in typical markets.

**F-13****Gaussian model and spectra dimensions of hierarchical scale-free networks**

HWANG Sungmin, LEE Deok-Sun<sup>1</sup>, KAHNG Byungnam, KIM Doochul

*School of Physics and Center for Theoretical Physics, Seoul National University. <sup>1</sup>Inha University Natural Medical Sciences.*

Using the real space renormalization-group method, we calculate the spectral dimensions of hierarchical scale-free networks. The model contains the probability  $p$  of long-range edges. Tuning the parameter  $p$  from  $p=0$  to  $p=1$ , the model exhibits a crossover from large-world to small-world network. Using the Gaussian-model technique, we calculate the spectral dimension analytically. The obtained spectral dimension turns out to be insensitive to the parameter  $p$ . We also perform numerical simulations of random walks on the hierarchical network such as the probability to return to the origin on empirical networks to check our result.

**F-14****Cascading Failure Dynamics on the World Trade Network**

이 규민, 양 재석, 김 건<sup>1</sup>, 이 재성<sup>2</sup>, 고 광일, 김 인묵

*고려대학교, 물리학과. <sup>1</sup>서울대학교, 물리학과. <sup>2</sup>서강대학교, 수학과.*

We study a cascading failure model on top of a network of countries based on the trading data, the world trade network (WTN). We examine the avalanche dynamics of the model and the individual country's role in the cascading dynamics. We also consider similarity measure based on the country's responses to the cascading failure and use it for clustering countries in the world trade network.

**F-15****Human Disease Genes from Network Perspective**

최 지혜, 노 한성<sup>1</sup>, 최 인걸<sup>1</sup>, 고 광일

고려대 물리학과, <sup>1</sup>고려대 생명공학부.

We study the characteristics of human genes from the network perspective. Classifying the human genome into classes based on their disease-phenotypic context, we identify class-specific features, which can be interpreted in line with the selection-based argument. Disease module hypothesis is also tested for each class.

**F****F-16****Noise Reduction In Genetic Oscillatory Systems**

민 병준, 고 광일, 김 인묵

고려대학교 물리학과.

The negative feedback is known to form the core of the genetic oscillatory systems. Even though a negative feedback loop alone can produce sustained oscillations, oscillatory circuits in real biological system show more complex structures. Here, we study dynamics of the coupled genetic oscillatory systems using exact stochastic simulation to extract simple rules for noise reduction in the oscillatory activities.

**F-17****Generalized Priority-Queue Network Dynamics**

조 원국, 민 병준, 고 광일, 김 인욱

*고려대학교 물리학과.*

We study the generalized priority-queue network models by introducing additional interaction rule based on the team and hierarchy. It is numerically found that the waiting time distribution exhibits a power law for long waiting times in both cases, yet with different exponents depending on the team size and the position of queue nodes in the hierarchy, respectively. We also discuss the dynamics of the priority-queues on top of large-scale complex networks briefly.

**F-18****Condensation in Zero Range Process with Pairwise Particle Interaction**

KIM Sang-Woo, NOH Jae Dong

*Department of Physics, University of Seoul.*

We investigate the condensation phenomena in the zero range process with a pairwise particle interaction. In our model, every particle has its own partner, and there is a hardcore interaction between each pair. The interaction is very weak for a particle interacts with only a single one. Nevertheless, the pairwise repulsion changes the nature of the condensation drastically. We report our analytic and numerical results for the model.

**F-19****Length dependent charge conduction in DNA Duplex**KIM Seongjin, HWANG Sun-Yong<sup>1</sup>, YI Juyeon부산대학교, 물리학과. <sup>1</sup>고려대학교, 물리학과.

We examine the length dependence of charge conduction in DNA, with focus on the nature of long-range transfer essential for DNA damage and its repair. We find various decay types of charge transfer according to the charge carrier energy, for example, in the absence of environmental dissipation tunneling through the band gap in DNA exponentially decays with molecule length, while under strong dissipation, it decays linearly with the molecule length. Also found is a length independent decay near the band edge and inside the band. Interestingly, there exists a crossover distance  $N_c$  that determines the most efficient path between a direct path along one strand and a detour using the complementary strand, whose nontrivial consequence will be discussed with recent experimental results.

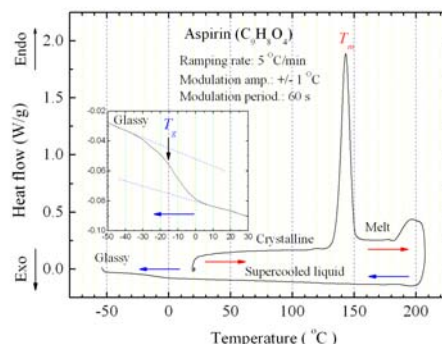
F

**F-21****Supercooled Liquid and Glass Transition in Aspirin**LEE Kwang-Sei, KO Jae-Hyeon<sup>1</sup>, IKE Yuji<sup>2</sup>, KOJIMA Seiji<sup>2</sup>

Inje University, Department of Nano Systems

Engineering. <sup>1</sup>Hallym University, Department ofPhysics. <sup>2</sup>University of Tsukuba, Institute of Materials Science.

The viscous and glassy states of matter are relevant in many different areas of technology but also in daily life. The advantage of the amorphous modification of some pharmaceuticals over their crystalline counterparts stems from practical aspects such as increased dissolubility and therapeutic activity. Many common drugs contain small molecules and therefore, as glass formers, they are also interesting on their own. In this work we report on the melting and freezing phenomena by the differential scanning calorimetry (DSC). This technique is applied to detect supercooled liquid and glass made from aspirin ( $C_9H_8O_4$ ) molecule. The traditional phenomenological asymmetry between melting and freezing is discussed by considering the liquid nucleation behavior during melting and the crystal nucleation behavior during freezing. The possible origin of formation of supercooled liquid and glass in aspirin is proposed.



**F-22****Metastable Patterns and Universality Classes in Directed Sandpile Models**조 항현, 하 미순<sup>1</sup>*고등과학원(KIAS). <sup>1</sup>한국과학기술원(KAIST).*

We discuss the universality class of directed sandpile models, in context of the interaction between spatially correlated metastable patterns (scars) and avalanche flow. The new scaling relations are conjectured and numerically confirmed for different toppling rules. In addition we investigate the relevance of the toppling bias in directed sanpile models and critical exponents in the upper critical dimension of directed sandpile models.

**F-23****Finite-size scaling in random  $\text{\$K\$}$ -satisfiability problems**

HA Meesoon, LEE Sang Hoon, JEON Chanil, JEONG Hawoong

*KAIST, Department of Physics.*

We propose a comprehensive view of threshold behaviors in random  $\text{\$K\$}$ -satisfiability ( $\text{\$K\$}$ -SAT) problems, in the context of the finite-size scaling (FSS) concept of nonequilibrium absorbing phase transitions using the average SAT (ASAT) algorithm. In particular, we focus on the value of the FSS exponent to characterize the SAT/UNSAT phase transition, which is still debatable. Moreover, we discuss the role of the noise (temperature-like) parameter in stochastic local heuristic search algorithms.

**F-24****Phase transition and critical phenomena of generalized conserved lattice gas**

YANG Jae-Suk, KIM In-mook, KWAK Wooseop<sup>1</sup>

*Korea University. <sup>1</sup>Chosun University.*

We study a generalized conserved lattice gas model (GCLG) in two dimensions by introducing an effective temperature  $T$  to the conserved lattice gas model (CLG), where the number of particles is conserved during the dynamic process. At  $T=\infty$ , GCLG model is identical to CLG model. GCLG model at  $T=0$ , it shows two transition behaviors; from localized active state to active state, and from localized active state to absorbing state. We also observed the critical behaviors of GCLG model between  $0 < T < \infty$ .

**F****F-25****Classification of stock markets according to their efficiency**

YANG Jae-Suk, CHOI Sooran<sup>1</sup>, NAM Yeonghwan<sup>1</sup>, KWAK Wooseop<sup>1</sup>

*Korea University. <sup>1</sup>Chosun University.*

We study the temporal evolutions of 10 stock markets. We observe that the probability function of the log-return has a fat tail but the tail index has been increasing continuously in recent years. We also find that the variance of the autocorrelation function and the scaling exponent of the standard deviation decrease, but the entropy density increases as time goes over time. We also measure the minimum entropy density method (MEDM) to detect the structure scale of a given time series. Then the temporal behavior of structure scale is obtained and analyzed in relation to the information delivery time and efficient market hypothesis.

**F-26****Surface diffusion on an adatom or a void on an icosahedral cluster**LEE Min-Ho, KIM Do-Hyun, KIM Sangrak, CHOI Je-Young<sup>1</sup>*Kyonggi Uni.. <sup>1</sup>Youngdong Uni..*

The diffusion of an adatom or a void on an icosahedral Lennard-Jones cluster consisting of 13 atoms was investigated via molecular dynamics simulations. We measured their diffusion constant at temperatures  $T=8.33\text{K} \sim 14.875\text{K}$  (for adatoms) and  $T=8.33\text{K} \sim 16.66\text{K}$  (for voids). The transition rate of an adatom or a void can be obtained by using the transition state theory within the harmonic approximation. The pre-exponential factor and the potential barrier about the transition that an adatom or a void moves into another nearby equilibrium point were compared with the simulation data. We also observed dimer diffusion in case of void.

**F-27****Prediction of protein structures with highly accurate backbone, side-chain, and hydrogen bond by using multiple layers of powerful global optimization**JOO Keehyoung, LEE Jinwoo<sup>1</sup>, OH Mina, SHIN Seung-Woo<sup>2</sup>, KO Junsu<sup>3</sup>, LEE Dongseon<sup>3</sup>, PARK Hahnbeom<sup>3</sup>, SEOK Chaok<sup>3</sup>, LEE Sung Jong<sup>4</sup>, LEE Jooyoung

*Korea Institute for Advanced Study, School of Computational Sciences. <sup>1</sup>Kwangwoon University, Department of Mathematics. <sup>2</sup>Soon Chun Hyang University, Genome Research Center for Allergy and Respiratory Diseases. <sup>3</sup>Seoul National University, Department of Chemistry. <sup>4</sup>Suwon University, Department of Physics.*

We have developed a procedure for protein structure prediction that generates highly accurate models in terms of backbone conformation, side-chain orientation, and hydrogen bonding formation. The powerful global optimization method called CSA (Conformational Space Annealing) was applied to the three stages of template-based modeling (TBM): multiple sequence alignment, all-atom model building, and side-chain re-modeling. A quality assessment method to select promising combinations of templates and the corresponding alignments was also developed. Loop modeling was applied to the regions with no aligned residues. With this procedure, we achieved the top performance in CASP8 (the 8th Critical Assessment of techniques for protein Structure Prediction) in terms of the combined accuracy of backbone and side-chain conformation and hydrogen bonding when compared with the other server models for TBM targets. More specifically, the average accuracies for backbone structures measured by GDT-TS and GDT-HA scores are 88.2 and 72.6 for high-accuracy TBM targets. The average percentages of correct prediction for side-chain orientation are 64.8 % and 45.2 % for  $\chi^1$  and  $\chi^{1+2}$ . The percentage of correctly formed hydrogen bonds is 69.41 % for the main chain and core side-chains and 65.21 % for the whole protein. Out of the 154 TBM target domains, our server and human prediction generated top models for 12 and 34 domains, and models within top five for 15 and 49 domains. Highly accurate models are shown to provide excellent binding site residue prediction.

**F-28****Polymer thin film growth model with vertically collimated flux**

SON Seung-Woo, HA Meesoon, JEONG Hawoong

*KAIST, Dept. Physics.*

In the recent work [J. Stat. Mech. P02031 (2009)], we proposed a simple model of the polymer thin film growth by vapor deposition and found that its structural properties exhibit anomalous kinetic roughening with multifractality in contrast to those of metal and semiconductor film growth. It is argued that such anomalies are attributed to the cosine flux of incidence for monomer deposition as well as the nonlocal shadowing effect of deposited monomers in process of polymerization. To support our argument, we consider vertically collimated flux in the same growth process, instead of cosine flux. Our extensive numerical results for the model with vertically collimated flux are discussed as the monomer diffusion coefficient increases, compared with the earlier results for the model with cosine flux in the context of the universality class for  $(1+1)$ -d kinetic roughening using dynamic scaling.

**F****F-29****Macroscopic Kinetic Effect of Cell-to-Cell Variation in Biochemical Reactions**

KIM Pan-Jun, PRICE Nathan D.

*Institute for Genomic Biology, University of Illinois at Urbana-Champaign.*

Genetically identical cells under the same environmental conditions can show strong variations in molecular content such as in protein copy numbers due to inherent stochastic events in individual cells. We here develop a theoretical framework to address how variations in enzyme abundance affect the collective kinetics of metabolic reactions observed with a population of cells. Kinetic parameters measured at the cell population level are shown to be systematically deviated from those of single cells, even within populations of homogeneous parameters. The Michaelis-Menten kinetics, besides, can be destroyed at such population level. Our findings elucidate the novel origin of discrepancy between in vivo and in vitro kinetics, and offer the potential utility of single-cell metabolomic analysis.

**F-30****Biologically Inspired Computing Method for Two-armed Bandit Problem**

KIM Song-Ju, AONO Masashi, HARA Masahiko

*RIKEN, Advanced Science Institute.*

Consider a number of slot machines. Each of the machines has an arm which gives a player a reward with a certain probability when pulled. The "multi-armed bandit problem" is to determine the optimal strategy for maximizing the total reward sum after a certain number of trials. To maximize the total reward sum, it is necessary to judge correctly and quickly which machine has the highest reward probability. Therefore, the player should explore many machines to gather much knowledge on which machine is the best, but should not fail to exploit the reward from the known best machine. These requirements are not easily met simultaneously, because there is a trade-off between the "exploration" and "exploitation." We consider that living organisms follow some efficient method to solve the problem. We propose a model, named as the "tug-of-war (TOW) model," based on the photoavoidance behavior of amoeba induced by light stimuli. We show that the TOW model exhibits good performance. The average accuracy rate of the TOW model is higher than that of well-known algorithms such as the modified epsilon-greedy algorithm and the modified softmax algorithm. Additionally, the TOW model is effective for solving relatively difficult problems in which the reward probabilities of the two machines are close. Finally, we show that the TOW model is good at adapting to a changing environment in which the reward probabilities are dynamically updated. The results are highly suggestive because, in order to survive in the unknown world, living organisms have to adapt to new environments as quickly as possible at the expense of a slight reduction in accuracy.

F

**F-31****Criticality in Prisoner's Dilemma Game on Fractal Complex Networks**CHANG-KEUN Yun, NAOKI Masuda<sup>1</sup>, BYUNGNAM Kahng*Seoul National University, Department of Physics and Astronomy. <sup>1</sup>The University of Tokyo, Graduate School of Information Science and Technology.*

Recently, evolutionary game dynamics, such as the Prisoner's Dilemma, have been investigated on complex networks. Despite the sensitivity of the results on the details of models, heterogeneous networks such as scale-free networks enhance cooperation in social dilemma games in many cases. Enhanced cooperation benefits from the abundant connection between hubs. However, such results cannot explain the diversity between cooperation and defection that is abundant in society. Here we report numerical results of the Prisoner's Dilemma game performed on fractal scale-free networks. While cooperator density is smaller in comparison with the one in the case of random scale-free networks, it is larger than in the case of random Erdos and Renyi network. More importantly, we find that diversity appears in the group size distribution of cooperation.

**F-32****Underlying Dynamics of Explosive Percolation Transition**

CHO Young Sul, KAHNG Byung Nam, KIM Doo Chul

서울대학교 물리학과.

Recently, it was discovered that the explosive percolation transition occurs in Erdos-Renyi model under Achlioptas process (AP). While abundance of such transitions in other systems has been investigated, a fundamental question, e.g., the origin of such explosive transitions is still in veil. Here, we investigate the dynamics of percolation evolution under the AP, finding that the cluster merging is a major process up to the percolation threshold. Based on this observation, we introduce a cluster merging model in which two clusters are randomly selected and merged. We show analytically that such a simple model generates a discontinuous percolation transition.

F

**F-33****Minimal Model for Traffic Flow**LEE Hyun Keun, LEE Choongki<sup>1</sup>, KIM Beom Jun*Sungkyunkwan University. <sup>1</sup>KIAS.*

We propose a microscopic traffic flow model that focuses on how the essential desire of driving, mobility and safety, should be quantified and modeled. It is indicated that the deceleration capability is the unique objective entity that can quantify the status of that desire, and this naturally provides the criterion to what the driver should do; apply the brake/gas pedal (if so how strong) or keep the current speed. The new model numerically generates three prototypical traffic phases which can be fitted to the empirical observation by additional modeling factor. We suggest a safety measure of traffic flow as an interpretation of the present model and finally discuss the implication of our findings from the perspective of automated driving in the future.

## Neurons

LIM Woochang, KIM Sang-Yoon<sup>1</sup>*강원대학교, 물리학과; 아주대학교, 물리학과. <sup>1</sup> 강원대학교, 물리학과.*

We study coherent population dynamics in an inhibitory ensemble of subthreshold neurons. Particularly, stochastic spiking coherence (i.e., collective coherence between noise-induced irregular neural spikings) is investigated. In a range of noise intensity  $D$ , “stripes” (indicating collective coherence) are found to be formed in the raster plot of spikings. However, these stripes are partially occupied, in contrast to the full occupation for the case of excitatory coupling. Each excitatory neuron fires spikes phase-locked to the global ensemble-averaged potential  $V_G$  at every cycle of  $V_G$ . On the other hand, inhibitory neurons exhibit intermittent spikings phase-locked to  $V_G$  at random multiples of the period of  $V_G$ . Due to this “random spike skipping,” partial occupation occurs. To characterize this collective coherence, we introduce a new type of spiking coherence measure  $M_s$ , based on the stripes in the raster plot. We note that the degree of spiking coherence depends on both the stripe density and the stripe smearing. Hence, the measure,  $M_s$ , is given by the product of the average fraction of firing neurons (representing the average density of stripes) and the average pacing degree of spikings (denoting the average smearing of stripes) per each stripe. In terms of  $M_s$ , we characterize the stochastic spiking coherence in coupled subthreshold neurons by varying  $D$ . Such spiking coherence measure  $M_s$  is found to reflect the degree of collective coherence seen in the raster plot well.

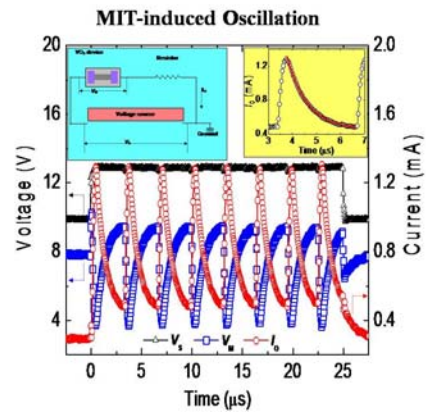
**K-01(초)****Mott Metal-Insulator Transition-Driven Memristive System and Electrical Oscillation in VO<sub>2</sub>**

KIM hyun-tak, KIM Bong-jun, LEE Yong Wook<sup>1</sup>, CHAE Byung-gyu, DRISCOLL T.<sup>2</sup>, BASOV D.<sup>2</sup>

ETRI, MIT Device Lab.. <sup>1</sup>ETRI, MIT Device Lab. & Pukyong Nat. Univ.. <sup>2</sup>UCSD.

One of the most important issues in contemporary solid-state physics has been to experimentally prove Mott's metal-insulator transition (MIT). Moreover, the Mott MIT has many practical applications. In particular, in order to reveal the mechanism of the Mott MIT, many physicists have paid attention to a representative paramagnetic insulator, VO<sub>2</sub> (4d<sup>1</sup>), with an abrupt resistance change near 68°C. The key issue is whether VO<sub>2</sub> is a Mott insulator, in which the abrupt

MIT is not caused by a structural phase transition (SPT), or a Peierls insulator undergoing the SPT near  $T_{\text{SPT}} > 68^\circ\text{C}$ . Here, for the MIT mechanism and application, we show both a shift of the resonance frequency with temperature for a metamaterial system with array of the split ring resonator (SRR) fabricated with VO<sub>2</sub>, and an electrical MIT oscillation shown in the attached figure. The metamaterial system can be used to tune a resonance frequency of a rf-device. The MIT oscillation possibly is generated from a temporal capacitor, which is comprised of both temporary dielectric components, arising from inhomogeneity in a VO<sub>2</sub> film, and metal phases acting like electrodes. This indicates that the electrical oscillation is a characteristic of the Mott MIT. (Ref: Metamaterial system: APL 93 (2008) 024101; Scienceexpress, 20 August 2009, (DOI: 10.1126/Science. 1176580); Electrical oscillation, APL 92 (2008) 162903).

**K-02(초)****3D Unipolar Resistance Switching Memory Array Using NiO Storage Node and CuO/InZnO Diode**

KANG Bo Soo, KIM Ki Hwan<sup>1</sup>, LEE Myoung-Jae<sup>2</sup>, BENAYAD 동욱<sup>2</sup>, AHN Seung-Eon<sup>2</sup>, LEE Chang Bum<sup>2</sup>, KIM Chang Jung<sup>2</sup>, PARK Youngsoo<sup>2</sup>

Hanyang University, Department of Applied Physics. <sup>1</sup>University of Delaware, Institute of Energy Conversion. <sup>2</sup>Samsung Advanced Institute of Technology.

Recently, there were a lot of studies on the application of unipolar resistance switching phenomena of metal oxide thin films such as NiO to memory devices. The memory density of this electrically-operated two-terminal device is maximized when it is made into 1D1R cross-point array with one diode and one resistance change element serially connected between the electrode lines. Since high temperature processes of the current silicon technology is prone to induce degradation of the underlying layers, low temperature process of non-Si semiconductors is favored. We have fabricated CuO/InZnO thin film diode with high current density and high on/off ratio using RF sputtering at room temperature. Degradation of Pt/InZnO Schottky diode and the control of the diode polarity using surface treatment are also discussed.

**K-03(초)****Making use of Suspended nano-Scale Devices**

LI Tiefu

*Institute of microelectronics, Tsinghua University, Beijing, China.*

We developed a novel technology, utilizing a combination of conventional angle evaporation technique and ashing of the underlying organic polymer, to fabricate suspended metallic nano-structures, such as single-electron transistors (SETs), nanomechanical resonators, and so on. They all show as good or even better quality as their non-suspended counterpart. Moreover, our method is compatible with the conventional fabrication process for nano-scale electronic circuits and thus offers a possibility of easily integrating the mechanical degree of freedom into superconducting charge and flux qubits as well as to coplanar waveguide resonators.

K

**K-04(초)****High band gap 산화물 반도체에서의 저항 변화 현상**

정 규호, 임 현식

*동국대학교 반도체 과학과.*

저항변화 현상은 크게 이성분계 (binary)와 페로브스카이트 (perovskite) 산화물에서 관찰되고 있으며, uni polar와 bi polar로 나뉘는 저항 변화 현상이 보고 되고 있다. 본 발표에서는 각각의 산화물에서의 저항 변화 특성을 확인하고 이에 따른 저항 변화 원리를 분석하는 과정을 소개하고자 한다. 변화된 각각의 저항 상태에서(초기 상태, 고저항 상태, 저 저항 상태) 온도 의존 특성을 통해 전기적 전송현상을 이해하고 구성 요소의 조성과 저항 변화 시 나타나는 박막특성의 변화를 FIB를 이용하여 microscopic 영역에서 관찰하였다. 또한 전극 의존성 연구를 통해 관찰 된 복합 저항 변화 특성을(uni polar와 bipolar 저항현상이 동시에 나타나는 현상) 페로브스카이트 물질인 Cr 0.2at% 도핑 된 SrZrO<sub>3</sub>에서 관찰하고 구조적 특성 분석을 통해 저항 변화 특성 원인을 분석하였다.

## K-05(초)

### 나노 분광기법을 이용한 단일 반도체 양자점의 광특성 연구

임 상엽

*Advanced Photonics Research Institute.*

인공원자라고까지 불리는 반도체 양자점은 크기를 조절함에 따라 전이 에너지를 변경할 수 있고, 원자와는 달리 공간상에 고정되어 있기 때문에 과학적으로나 기술적으로 매우 주목을 받는 구조이다. 그러나 반도체 양자점의 제조시 수 % 정도의 크기 차이가 생기고, 이에 따른 선폭 증가는 피할 수 없다. 따라서 단일 반도체 양자점의 광특성을 연구하고, 이를 응용할 필요성이 대두되었다. 단일 반도체 양자점의 광신호를 얻는 방법은 크게 두 가지로 구분할 수 있는데, 우선 기존 광학 현미경을 이용하기 위하여 양자점의 밀도를 낮추는 방법과, 나노 분광기법을 사용하여 고분해능으로 광신호를 얻는 방법이다. 마이크로 형광 혹은 공초점 주사 현미경은 저밀도 양자점에 적합하고, 근접장 광학 현미경이나 나노개구에 의한 분광은 고밀도 양자점에 적합하다. 본 연구에서는 다양한 나노 분광기법을 이용하여 측정된 단일 반도체 양자점의 광특성을 소개하고, 단일 반도체 양자점의 응용분야를 살펴보고자 한다.

K

## K-06(초)

### CIGS 태양전지 기술 동향

박 래만, 정 용덕, 조 대형, 한 원석, 이 규석, 김 제하

*한국전자통신연구원 차세대태양광연구본부.*

최근에 융합기술의 발전과 함께 환경오염 문제에 대한 대응이 심각하게 여겨지면서 태양전지 기술이 각광을 받고 있다. 본 발표에서는 2세대 태양전지로 여겨지는 박막태양전지 중에서도 앞으로 성장 가능성이 가장 큰 CIGS 태양전지 기술에 대해 살펴보고자 한다. CIGS 태양전지는 4원소의 복잡한 화합물이지만 동시증발법이라는 기술을 통하여 셀효율 19.5%의 놀라운 특성을 보고하고 있다. 그러나, 국내 태양전지 시장은 아직 시작단계이며, 더욱이 박막태양전지 분야는 미개척지라 해도 과언이 아니다. 본 발표에서는 CIGS 태양전지의 기술별 특징 및 각 기술들을 이용한 산업화 현황에 대해 자세히 알아보려고 한다.

**K-07(초)****Formation of AlN Compounds on Al<sub>2</sub>O<sub>3</sub> Substrates During Nitridation**

LEE, Hyo Jong

*Dong-A University, Materials Science and Engineering.*

Various semiconductor compounds have been grown on the sapphire substrate. Particularly, sapphire has been commercially used for the fabrication of GaN LED(light emitting diode). However, the initial growth of GaN on such sapphire substrate has not been well understood because the initial layer is too thin to investigate by conventional analysis tool. In this talk, we will survey our previous investigation of the nitrided layer through GIXRD(Grazing Incidence X-ray Diffraction) using synchrotron radiation source and HRTEM(High Resolution Transmission Electron Microscopy) techniques. We found out that there co-existed wurtzite AlN(w-AlN) and zincblend AlN(zb-AlN). In order to compare the formation enthalpies with each other, *ab-initio* calculation was performed on two phase AlNs. It was found out that while the w-AlN had lower formation enthalpy than the zb-AlN under free-strain state, the increasing rate of strain energy in the w-AlN is faster than the zb-AlN. Therefore, under the condition of 9.5% tensile strain, the formation enthalpy of the w-AlN is very similar with the zb-AlN. Considering the lattice mismatch of 14% between sapphire (0001) and AlN (0001) planes, it can be understood that the zb-AlN was formed together with the w-AlN by such lattice misfit strain.

K

**K-08(초)****Bifurcation of a quasi-1D quantum wire at weak confinements**

THOMAS Kalarikad Jonah

*성균관대학교 정보통신공학부 전자전기컴퓨터공학과.*

Electron-electron interactions are believed to be significant in one-dimension, and there has been a number of theoretical works on interacting 1D system from 1950s. In this talk I will discuss the recent experiments on quasi-one-dimensional electron systems defined in GaAs/AlGaAs hetero-structures. By strongly confining electrons to one dimension (1D), the transverse wave functions are spatially-quantised in accordance with the ‘particle in the box’ model. With little or no electron scattering, for example, in short quantum wires, transport is ballistic and the conductance accords well with the predictions of non-interacting theory, whereby each quantised level forms a sub-band contributing a conductance of  $2e^2/h$ , the factor of 2 arising from spin degeneracy. At weak confinement energies, when Coulomb repulsion is sufficiently strong to overcome the confinement potential, the electrons adjust their positions to minimise energy by forming a zigzag structure. Both quantum and classical calculations suggest that the zigzag will divide into two separate wires/rows as the electron density increases or confinement weakens further, leading to the formation of a lattice, initially of two and then of progressively more rows of electrons, until the system approaches a regular two-dimensional lattice. I shall present experimental results on the formation of double wires in a weakly confined quantum wire in the presence and absence of coupling between them [1,2]. 1. W. K. Hew, K. J. Thomas, M. Pepper, I. Farrer, D. Anderson, G. A. C. Jones and D. A. Ritchie, Incipient Formation of an Electron Lattice in a Weakly Confined Quantum Wire, *Phys. Rev. Lett.* 102, 056804 (2009). 2. L. W. Smith, W. K. Hew, K. J. Thomas, M. Pepper, I. Farrer, D. Anderson, G. A. C. Jones, D. A. Ritchie and, Row coupling in an interacting quasi-one-dimensional quantum wire investigated using transport measurements, *Phys. Rev. B.* 80, 041306(R) (2009).

**K-09(초)****Recent Advances in Si Nanocrystal Light-Emitting Diodes**

HUH Chul, KIM Kyung-Hyun, KO Hyun-Sung, KIM Bong-Kyu, KIM Wanjoong, HONG Jongcheol, SUNG Gun Yong

한국전자통신연구원 융합기술연구부문

An efficient Si-based light sources operating at room temperature has been intensively investigated to realize monolithic integrated circuits. Bulk silicon is, however, generally considered as highly inefficient light sources due to its indirect band gap. It was reported that if the size of Si nanocrystals (nc-Si) is smaller than the free exciton Bohr radius of bulk Si ( $\sim 4.6$  nm), the radiative emission efficiency could be much enhanced due to a quantum confinement effect.<sup>1</sup> Because of this, nc-Si has recently attracted a great interest due to their potential for applications in silicon-based optoelectronic devices. In order to enhance the efficiency of nc-Si light-emitting diodes (LEDs), the transparent doping layer, which has good electrical property and high transparency for the emitted light, and the optimized structure design of luminescent layer are indispensable. In our previous results,<sup>2-5</sup> by depositing of the amorphous SiC(N) films doped with a phosphorous on the nc-Si active layer, we obtained a p-n junction diode structure and observed that the electrons which stem from the SiC(N) doping layers could be effectively injected into the nc-Si and subsequently recombine radiatively. In this paper, we will present the recent advances in nc-Si LEDs. In particular, the effects of transparent SiCN doping layer and design of luminescent layer on the electrical and optical properties of nc-Si LEDs are reported and discussed. Acknowledgement This work was partly supported by Top Brand R&D program of KOCI [09ZC1410: Basic Research for the Ubiquitous Lifecare Module Development]. References 1. L. Pavesi and D. J. Lockwood, *Silicon Photonics: Silicon fundamentals for photonic applications*, p13, Heidelberg, Berlin, (2004). 2. K. S. Cho, N.-M. Park, T.-Y. Kim, K.-H. Kim, G. Y. Sung, and J. H. Shin, *Appl. Phys. Lett.*, 86, 071909 (2005). 3. C. Huh, N.-M. Park, J.-H. Shin, K.-H. Kim, T.-Y. Kim, K. S. Cho, and G. Y. Sung, *Appl. Phys. Lett.*, 88, 131913 (2006). 4. C. Huh, K.-H. Kim, J. Hong, H. Ko, W. Kim, and G. Y. Sung, *Electrochem. Solid-State Lett.*, 11, H189 (2008). 5. C. Huh, K.-H. Kim, J. Hong, H. Ko, W. Kim, and G. Y. Sung, *Electrochem. Solid-State Lett.*, 11, H296 (2008). \*E-mail: chuh@etri.re.kr

**K-10(초)****High Speed Flash Memory by a Dopant-Segregated Schottky-Barrier MOSFET**

CHOI Yang-Kyu, JANG Moongyu<sup>1</sup>, CHOI Sung-Jin

KAIST, EECS. <sup>1</sup>ETRI, Advanced I-MEMS team.

We demonstrate a new type of Flash memory cell based on the structure of dopant-segregated Schottky-barrier (DSSB) MOSFET, which has an ultra-thin pocket layer with high-dose dopants surrounding the interface between the metallic silicide material for source/drain (S/D) and the channel. The hot carriers intrinsically generated from the shallow DSSB S/D junctions can be utilized for the advancement of both the NAND and the NOR type Flash memory cell. With the aid of hot carriers that can be generated by elevated electric field at the DSSB S/D junctions stemming from the abrupt band bending, the probability to be trapped into a charge storage node of Flash memory, such as polysilicon layer in the floating gate memory device or the nitride layer in the SONOS memory device, is expected to be enhanced. Therefore, the DSSB MOSFET shows very fast programming time at low programming voltage, compared to conventional MOSFET based on p-n S/D junctions. Besides, the superior scalability resulting from the abrupt and shallow junctions, reduction of the 'characteristic screening length,  $\lambda$ ', is also achieved without the constraint of the parasitic resistance due to metallic silicided material. Furthermore, as the interest of the solid-state drive (SSD) as well as the mobile/portable device considerably increases in recent years, the embodiment of 3-D stackable Flash memory onto a structure of the DSSB thin-film transistor (TFT) based on polycrystalline silicon is also presented. In summary, the DSSB devices are a premier choice for future nano-electronics applications of the logic and Flash memory device since they do not only enable continuation of device scaling due to the improved electrostatics but also provide benefits for an alternative memory cell.

**K-11(초)****Complementary Use of Organic and Oxide Semiconductors**

NA Jong ho, KITAMURA Masatoshi, ARAKAWA Yasuhiko

*Institute for Nano Quantum Information Electronics (INQIE), University of Tokyo.*

Contrast to a p-type conductivity of most organic semiconductors, most oxide semiconductors have a n-type conductivity. The absent of each counterpart has limited their device applications such as complementary circuits and optoelectronic p-n junction devices. Here, we resolve the limitation by complementary use of p-type organic and n-type inorganic oxide semiconductors. Complementary inverters composed of pentacene and amorphous InGaZnO transistors exhibits good voltage transfer characteristics with a high gain of  $\sim 56$ . Complementary 5-stage ring oscillator with the inverters yields an output frequency of 200 Hz at 10 V, corresponding to a propagation delay of 1 ms. We also demonstrate a hybrid p-n junction light-emitting diode using *N,N'*-diphenyl-*N,N'*-bis(1-naphthyl)-1,1'-biphenyl-4,4'-diamine ( $\alpha$ -NPD) and sputtered ZnO. The hybrid junction shows a current rectifying characteristic similar with conventional p-n junction diodes and electroluminescence under forward bias. We found that the electroluminescence bands from the device agree well with the photoluminescence peaks from  $\alpha$ -NPD and ZnO, implying the radiative recombination of injected charges occurs in both components of the junction.

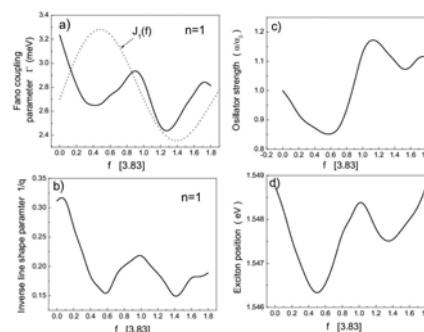
K

**K-12****THz response of dynamic Fano resonances in biased semiconductor superlattices**

제 구출

안양대학교, 교양학부, 물리학과.

We describe the dynamic Fano resonances due to the coupling the Wannier Stark ladders and dynamical Stark ladders with the continuum states of minibands using realistic three-dimensional model in biased GaAs/AlGaAs-semiconductor superlattices. We find that the dynamic Fano coupling strength is modulated by the strength of THz field via changing the localization properties of the excitons due to the band collapse phenomena and determined by the separated energy distance between two types of exciton resonances produced by the dc and THz fields. The strength increases, as the exciton resonance induced by the THz field approaches to the Wannier exciton state. The reverse is also true. Therefore, the dynamic Fano resonance can be controlled by the adjustment of excitonic energy distance induced by the band collapse phenomena.



**K-13****Simulation of Directed Self-Assembly for sub-10 nm Pattern Formation:Top-down and Bottom-up Approches**

김 상곤, 오 해근, 정 영대, 안 일신, 권 영현

*한양대학교 응용물리학과.*

극 자외선 (EUV:extrimely ultraviolet) 기술과 높은 굴절률을 갖는 액체를 이용한 immersion ArF 리소그래피 기술은 1,2 세대만 확장할 수 있어 10 nm 이하 패턴 형성에는 심각한 어려운 점이 있다. Self-assembly 은 차 세대 리소그래피 중의 하나이다. Self-assembly 공정은 여러가지나노 기술적 응용을 위해 쉽고 가격 경쟁력이 높은 공정이다. 그러나 아직 불확실한 공정 조건들과 대량 생산의 문제점들이 있다. 따라서 공정 시뮬레이션은 10 nm 패턴 형성을 위해 쉬운 공정, 낮은최소선폭 변화, 그리고 적은 defects 형성에 도움을 줄 수 있다. 본 연구에서는 graphoepitaxy 공정이 분자 크기로 모델화되고 시뮬레이션 하였다. Self-assembly 의 10 nm 패턴 형성에 대한 block polymer 성분들과 공정 조건들의 영향을 조사하였다.

K

**K-14****ZnO Nano-crystals Grown on a Profiled Sapphire(0001) Substrate with Au Nano-crystals**

KANG HYON CHOL

*Chosun University, Department of Advanced Materials Engineering.*

This paper reports the structural evolution of ZnO nano-crystals deposited on profiled Au/sapphire(0001) substrates by radio frequency sputtering. In contrast to the typical catalytic growth of ZnO nano-crystals with Au seeds, ZnO was initially formed as nano-discs on top of the Au nano-crystals, and their eventual shape became a replica of the cuboctahedral Au nano-crystals. The ZnO nano-discs transformed into hexagonal nano-pyramids through the intermediate morphology of sunflower typed ZnO nano-crystals. The ZnO nano-pyramids had a polar hexagonal (0001) basal plane and  $O^{2-}$  terminated facets. The ZnO nano-pyramids exhibited surface acceptor-bound exciton and donor-bound exciton emissions in the photoluminescence spectra.

**KF-01(초)****ReRAM의 기본 원리에 대한 물리학적 고찰**

노 태원, 채 승철, 장 서형, 이 신범, 이 재성, 강 병남

서울대 물리천문학부

최근 비휘발성 메모리에 대한 관심이 높아지고 있다. 특히 외부의 인가전압에 따른 두 전기저항 상태의 변환을 이용한 resistance random access memory (ReRAM)에 대한 연구가 활발히 진행되고 있다. 전기저항 변환은 외부 전압의 극성 변화에 따른 대칭성에 따라 단극성과 양극성으로 나눌 수 있다. 지금까지 단극성 및 양극성 전기저항 변환의 기본 원리에 대한 많은 모델이 제시되었으나, 아직까지도 이에 대한 우리의 이해는 매우 미흡한 실정이다. 이 발표에서는 단극성 전기저항 변환의 기본 원리를 설명하기 위하여, 우리가 새로이 제시한 random circuit breaker (RCB) network 모델을 설명하고자 한다 [1]. 특히 percolation 이론에 해당되는 이 모델은 시료 내의 전도성 필라멘트의 집단적인 움직임을 잘 기술함으로써, 단극성 ReRAM에서 일어날 수 있는 다양한 현상을 설명할 수 있다 [2,3]. 또한 RCB network 모델은 현재 단극성 ReRAM의 문제점으로 제시된 스위칭 전압의 변동 현상에 대한 해결 방안들을 찾는 데에 이용될 수 있다 [4]. 또한 우리는 단극성 전기저항 변환이 양극성 전기저항 변화와 어떠한 관계가 있는 지를 고찰하고자 한다. 이를 통하여 양극성 전기저항 변화에 대한 새로운 모델을 제시하고자 한다. 이러한 연구들은 ReRAM이라는 새로운 소자 개발에 기여함은 물론, 자연에서 널리 일어나는 전기저항 변환에 대한 우리의 이해를 새롭게 할 수 있을 것이다.[1] S. C. Chae, Adv. Mater. 20, 1154 (2008). [2] S. H. Chang, Phys. Rev. Lett. 102, 026801 (2009).[3] S. B. Lee, Appl. Phys. Lett. 93, 212105 (2008). [4] S. B. Lee, Appl. Phys. Lett. 94, 173504 (2009).

**KF-02(초)****ReRAM의 응용분야와 상용화를 위한 전제조건**

백 인규

삼성전자

지난 수 년간 반도체소자 기술이 급속히 미세화되고 그 기능이 융합화되면서 기존 소자가 가지는 한계를 극복할 수 있는 대안의 하나로 저항메모리소자(ReRAM)에 대한 관심이 고조되고 있다. ReRAM이 메모리소자로 사용되는 경우에 그 특성에 따라 다양한 종류의 메모리에 적용될 수 있으며, 최근에는 메모리소자 뿐만 아니라 스위치소자나 연산소자에 까지 그 응용분야를 넓혀가고 있다. 그러나 ReRAM을 상용화하기 위해서는 소자의 전기적 특성을 만족하더라도 신뢰성이나 재현성, 미세화 가능성, 제조 용이성 등의 조건들이 추가로 검증되어야 한다. 이를 검증하기 위해서는 저항변화를 일으키는 물질의 물리적 특성이나 동작 메커니즘에 대한 이해가 충분히 뒤따라야 하며, 이를 바탕으로 소자의 동작을 예측할 수 있는 모델의 정립이 필수적이다. 본 발표에서는 ReRAM의 다양한 응용분야와 반도체업계에서 진행되고 있는 연구동향을 소개하고 당면하고 있는 기술적인 문제점을 제시하여 ReRAM과 관련된 기초연구를 진행함에 있어서 도움이 되고자 한다.

in Pt/TiO<sub>2</sub>/Pt structure

KIM Kyung Min, CHOI ByungJoon, HAN Seungwu, HWANG Cheol Seong

*Department of Materials Science and Engineering and Inter-university Semiconductor Research Center, Seoul National University, Seoul 151-744, Korea.*

The resistance switching (RS) mechanism of the Pt/TiO<sub>2</sub>/Pt structure was examined. The concurrent presence of unipolar and bipolar RS and the correlation between them can be explained consistently through a microscopic model where the oxygen vacancies in the disconnected conducting channels play as electron traps in the reset state of unipolar RS and electronic bipolar RS. While the unipolar switching can be explained well by the formation and rupture of metallic filaments, the trap-free and trap-mediated space charge limited conduction (SCLC) governs the set and reset, respectively, states of the bipolar switching. This was understood from the fitting of the current – voltage characteristics at various temperatures. The bipolar switching layer was comprised of trap layer and trap-free layer which formed an asymmetric potential barrier. The asymmetric potential barrier induced the bias polarity-dependent bipolar electronic switching behaviour. The detailed parameters such as trap density and trap layer and trap-free layer thicknesses in the electronic bipolar switching were evaluated.

electroforming in Pt/TiO<sub>2</sub>/Pt resistive switching cellsJEONG Doo Seok, SCHROEDER Herbert<sup>1</sup>, WASER Rainer<sup>1</sup>*Thin Film Materials Research Center, Korea Institute of Science and Technology, Seoul 136-791, Republic of Korea. <sup>1</sup>Institute of Solid State Research and JARA – Fundamentals of Future Information Technology, Research Center Jülich, D-52425, Germany.*

Abnormal bipolar-like resistive changes are reported in TiO<sub>2</sub> thin films sandwiched between Pt top and bottom electrodes. The abnormal behavior is shown relying on the applied voltage range. That is, normal bipolar switching is also shown in the same sample with the optimized voltage range. In the abnormal mode, both set- and reset-like changes in resistance take place under the same polarity of the applied voltage. This abnormal behavior is considered to be due to symmetric electroforming which is assumed to activate electrochemical reactions involving oxygen vacancies at both Pt/TiO<sub>2</sub> interfaces. We analyze the abnormal behavior in terms of the interfacial resistive switching taking place on both interfaces nearly simultaneously.

CHOI W.K.

*Thin Film Materials Research Center, Korea Institute of Science and Technology, Cheongryang P.O Box 131,.*

Zinc oxide (ZnO) has been extensively studied due to its intense commercial potentiality for making short wavelength light emitting diodes (LED), diode lasers, and UV detector ever since it demonstrated the p-type conductivity. It has significant advantages over the III-V nitrides in terms of its abundant availability and large exciton binding energy of 60 meV at room temperature and tunable band gap from 3.3 eV to 4.5 eV through Cd and Mg doping or even larger than 5 eV by Be doping at Zn site. Due to high oscillation strength and optical gain, it would be very prominent in bright coherent emission and detection capability of near ultraviolet. The intrinsic defects related to oxygen vacancy and Zn interstitial, and H in undoped ZnO are reviewed. On the subject of doping, common n type dopants and reliable p-type ZnO processes, togetherwith LED structure and band gap engineering, are briefly summarized. In particular, successfully attained p-type ZnO using large-mismatched-size V-element dopants is surveyed in terms of the first principle calculations. In addition, since ZnO is also a very promising material for channel and electrode in transparent thin film transistor (TTFT) because it shows high transparency and conductivity using III element doping. In this paper, the status of ZnO-based transparent oxide transistor (TOS) in flat panel display and transparent conducting oxide (TCO) in photovoltaic solar cell and display will be briefly introduced.

**amorphous oxides and O-vacancy.**

강 일준, 박 철홍

*부산대 물리교육학과.*

Amorphous metal oxide complex semiconductor such as InGaZnO<sub>4</sub>, gallium tin zinc oxide, indium zinc tin oxide and zinc tin oxide are emerging as the base material of next generation thin-film transistor (TFT) for flat-panel displays and imagers and as transparent conducting oxide. Through first-principles calculations, we investigate the electronic structures of single crystal of InGaZnO<sub>4</sub> (sc-InGaZnO<sub>4</sub>), which has a complex structure consisting of InO<sub>2</sub> layers inter-stack with GaZnO<sub>2</sub> double-layers. Within GaZnO<sub>2</sub> layers, Zn and Ga atoms alternatively occupy the cation sites. We find that the conduction band of the sc-InGaZnO<sub>4</sub> is composed of the hybridization of In-s, Ga-s, Zn-s and O-p orbitals, while the valence bands are characterized dominantly by O-p orbitals. At the conduction band, the energy of bands by In-s are lower than that by Ga and Zn atoms, and the Ga-driven states are slightly lower than Zn-driven states and the band widths of Zn- and Ga-driven band are wider than that of In-driven band. In addition, the electronic structures and microscopic properties of the O-vacancies in transparent semiconductor oxide InGaZnO are investigated. The results are compared to those of vacancies in In<sub>2</sub>O<sub>3</sub>, Ga<sub>2</sub>O<sub>3</sub>, and ZnO. Electronic structure calculations indicate that the O-vacancy make deep-donor levels in binary oxides, while it becomes shallow donor-like in the quaternary InGaZnO. The O-vacancy induces tensile stress in all tested oxides. The total energy calculations indicate that the vacancy is energetically favored to be located between In-O and Ga-Zn-O layer in InGaZnO.

**KF-07(초)****ZnO nanomaterials를 이용한 flexible electronics**

김 상식

고려대학교 전기전자전파공학부

ZnO nanoparticles 와 nanowires를 이용한 다양한 flexible electronics의 특성에 대하여 설명한다. ZnO nanoparticles 와 nanowires는 solution process가 가능해서, plastic substrates 위에 ZnO nanoparticles/nanowires 기반의 FETs/TFTs 제작이 가능하다. 이들 FETs/TFTs를 좀 더 복잡한 구조로 제작하면, ZnO nanoparticles/nanowires 기반의 flexible memory 및 logic devices를 제작이 가능하다. 따라서, 본 세미나는 이들 FETs/TFTs/devices의 특성을 분석하여 ZnO nanomaterials가 갖는 다양한 성질을 이해하는데 중점을 둔다.

K

**KF-08(초)****Surface polarity and morphology-controlled synthesis of one-dimensional ZnO****nanostuctures**

PARK Won Il

Division of Materials Science and Engineering, Hanyang University, Seoul 133-791 (Korea).

ZnO nanocrystals exhibit several crystal surfaces with different atomic configurations and polarities, which have a major influence on the physical and chemical properties of materials. Control of the surface is therefore a crucial factor in designing nanomaterials for various applications. Here we introduce surface polarity and shape-controlled synthesis of 1D ZnO nanostuctures on the top of micro-faceted GaN hillocks by metal-organic vapor phase epitaxy (MOVPE). Decreasing the Zn/O feeding ratios enables ZnO nanostructures ranging from smooth-surfaced nanorod-nanowall networks with non-polar {} and {} planes as side faces to corrugated, stacked pyramid-structured nanorods terminated mainly with O-polar {} and () planes. We suggest that the morphologies of ZnO nanostructures are dominated by the path of mass transport of Zn adatoms from side facets of GaN hillocks to adjacent ZnO nanorods according to growth conditions. CL measurements reveal strong excitonic emission peaks with extremely low deep level emission for both type of the nanostructures, providing a significant opportunity to understand the surface polarity and shape-dependent luminescent properties of nanoscale materials. In addition, by introducing hexagonally close-packed colloidal monolayer template, ZnO nanotubes-nanorods hybrid hexagonal networks were successfully synthesized. Controlled synthesis of nanostructured materials with synthetically tuned structure, size, and morphology offer the significant technical advances towards the use of these materials in various fields of applications such as electronics and optoelectronics.

임 현식

동국대학교 반도체과학과.

공정 기술과 박막 성장의 비약적인 발전으로 인해 점차 소자의 크기가 나노 영역으로 작아졌으며 다양한 이종 접합 (heterostructures) 구조에서의 전기적 특성을 관측할 수 있게 되었고, 이에따른 새로운 물리적인 현상을 규명 및 증명할 수 있게 되었다. 이러한 나노 구조 이종 접합 소자에서의 전기적 특성을 결정하는 가장 중요한 메카니즘은 터널링 현상으로 고전 전자기학으로는 이해할 수 없는 순수한 양자 역학적인 현상이다. 본 튜토리얼 세션의 목적은 반도체, 자성체, 초전도체 및 이들의 혼성 (hybrid) 구조로 이루어진 나노 소자에서의 전기적인 특성을 터널링 관점에서 이해하고자 한다. 본 튜토리얼 세션의 수준은 학부 고급 물리학 과목을 이수한 대학생이면 쉽게 이해할 수 있게 정성적인 측면에서 터널링 현상을 고찰하고자 한다. 본 튜토리얼 세션의 진행은 다음과 같다.

1. 기초 터널링 현상 2. 공명 터널링 (Resonant tunneling) 3. Tunneling in SETs 4. 초전도체 소자에서의 Cooper pair tunneling 5. Tunneling in hybrid structures 6. Tunneling in Qubits

# 포스터발표논문 초록



**Dp-I-001****Ferroelectric and piezoelectric properties of (Na,K,Li)(Nb,Ta,Sb)O<sub>3</sub> ceramics****fabricated by citric acid assisted sol-gel method**

김 일원, 김 주성, 이 해준, 안 창원<sup>1</sup>, 황 학인<sup>1</sup>, 조 남규<sup>1</sup>, 배 세환<sup>2</sup>

울산대학교, 물리학과. <sup>1</sup>전자부품연구원, 융합부품연구부. <sup>2</sup>동아대학교, 물리학과.

The development of lead-free ferroelectric and piezoelectric materials has been required from the viewpoint of environmental preservation. So, there have many researchers devoted their research interest to non toxic lead free NKN system. However, the NKN system has the drawback of high leakage current density because of high hydrophile property of K<sup>+</sup> ion and is difficult to obtain high density piezoelectric ceramics. In this study, we have focused on the lead-free (Na<sub>0.44</sub>K<sub>0.52</sub>Li<sub>0.04</sub>)(Nb<sub>0.86</sub>Ta<sub>0.10</sub>Sb<sub>0.04</sub>)O<sub>3</sub> (LF4) ceramics[1] by preparing through a citric acid assisted sol-gel method, and compared the properties to LF4 ceramics fabricated by solid state reaction method. We have investigated ferroelectric and electric-field-induced behavior of the LF4 system. [1] Yasuyoshi Saito *et al.*, Nature 432, 84-87 (2004).

**Dp-I-002****Electromechanical Properties of BiAlO<sub>3</sub> Modified Bi<sub>0.5</sub>(Na<sub>0.78</sub>K<sub>0.22</sub>)<sub>0.5</sub>TiO<sub>3</sub>****Piezoelectric Ceramics**

김 일원, 장 기봉, ULLAH Aman, HUSSAIN Ali<sup>1</sup>, 이 재신<sup>1</sup>, 안 창원<sup>2</sup>, 조 남규<sup>2</sup>, 황 학인<sup>2</sup>, 정 연학<sup>3</sup>, 박 언철<sup>3</sup>

울산대학교, 물리학과. <sup>1</sup>울산대학교, 첨단소재공학부. <sup>2</sup>전자부품연구소, 융합부품연구부. <sup>3</sup>(주)삼전, 기술연구소.

Lead-free piezoelectric ceramics are important from the view point of environmental impact. As a lead-free piezoelectric ceramics, bismuth sodium titanate (BNT) and bismuth potassium titanate (BKT) have attracted attention due to its morphotropic phase boundary. So, We have synthesized (1-x)(Bi<sub>0.5</sub>(Na<sub>0.78</sub>K<sub>0.22</sub>)<sub>0.5</sub>TiO<sub>3</sub>)–xBiAlO<sub>3</sub> (abbreviated as BNKT22-BA, x = 0.00-0.100) by a conventional solid state reaction method. The effect of BA addition in the BNKT22 lattice was evaluated by X-ray diffraction (XRD), dielectric, ferroelectric and electric field induced strain behavior. The results of x-ray diffraction revealed that a pure perovskite phase was formed for x ≤ 0.045. The addition of BA decreased the static piezoelectric constant (*d*<sub>33</sub>), remnant polarization (*P*<sub>r</sub>), and coercive field (*E*<sub>c</sub>). The large electric field-induced strain (*S* = 0.35 %) and a dynamic piezoelectric coefficient (*d*<sub>33</sub><sup>\*</sup> = *S*<sub>max</sub>/*E*<sub>max</sub> = 592 pm/V) were obtained at x = 0.030. These results indicate that BNKT22-BA can be considered as a promising candidate material for lead-free electromechanical actuator applications.

**Dp-I-003****The Effect of  $\text{Al}_2\text{O}_3$  Ultra Thin Layer on the  $\text{Bi}_{0.5}\text{Na}_{0.5}\text{TiO}_3$  Based Ferroelectric****Thin Films**

김 일원, 원 성식, 안 창원<sup>1</sup>, 조 남규<sup>1</sup>, 황 학인<sup>1</sup>

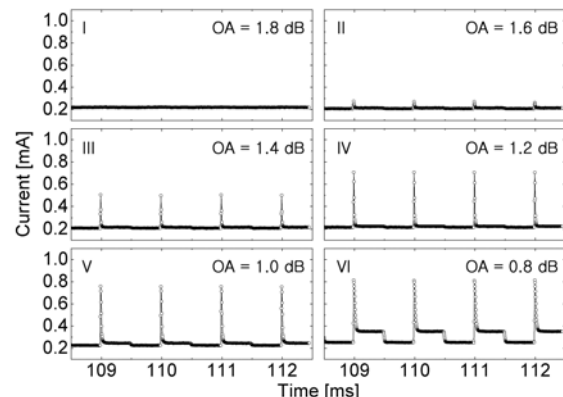
울산대학교, 물리학과. <sup>1</sup>전자부품연구원, 융합부품연구부.

Recently, lead free ferroelectric and piezoelectric materials has been a matter of great interest because of the environmental pollution coming from toxic lead based materials. The  $\text{Bi}_{0.5}\text{Na}_{0.5}\text{TiO}_3$  (BNT) based ceramics exhibited good ferroelectric and piezoelectric properties. So, we have deposited BNT based lead-free thin films on Pt (111)/ $\text{TiO}_2$ /SiO<sub>2</sub>/Si(100) substrates by chemical solution deposition. A 5 nm-ultra thin  $\text{Al}_2\text{O}_3$  top layer was deposited on the BNT based thin films by ALD technique.[1] The BNT-based thin films were annealed at 650, 700, 750, and 800°C in O<sub>2</sub> atmosphere. The x-ray diffraction (XRD) pattens of BNT based thin films show a perovskite structure. We have investigated the effects of  $\text{Al}_2\text{O}_3$  ultra thin layer on the BNT based thin films through the measurement of dielectric and ferroelectric properties. [1] An Quan Jiang, Hyun Ju Lee, Gun Hwan Kim, and Cheol Seong Hwang : Adv. Mater. 21, 2870 (2009)

**Dp-I-004****High-Speed Optical Gating in  $\text{VO}_2$** 

이 용욱, 김 봉준<sup>1</sup>, 최 성열<sup>1</sup>, 채 병규<sup>1</sup>, 서 기완<sup>2</sup>, 김 현탁<sup>1</sup>  
ETRI/부경대, 전기과. <sup>1</sup>ETRI. <sup>2</sup>UST, 차세대소자공학과.

A threshold voltage of a planar junction device based on  $\text{VO}_2$  thin film can be controlled by the intensity adjustment of the light directly illuminated onto the  $\text{VO}_2$  film, i.e., by the photo-assisted electrical gating (optical gating). With the optical gating scheme, the device structure can be simple because a gate oxide and electrode are not necessary. In the previous study, however, the switching speed of the optical gating could not be reduced to < 1 ms due to the limit of that of the optical switch. In this paper, we have demonstrated a high-speed optical gating in the  $\text{VO}_2$  junction devices by incorporating saturation-induced gain modulation of an erbium-doped fiber amplifier (EDFA). For the implementation of the high-speed optical gating, a transient gain of the EDFA was modulated by adjusting the chopping frequency of the input light down to 1 kHz, and gated signals whose temporal durations were reduced by > 50 times compared with those obtained in the previous scheme were successively generated.



## Transition Temperatures

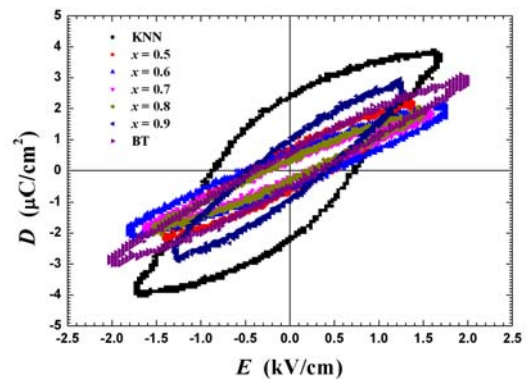
김 영훈, 서 용문, 염 태호<sup>1</sup>, 최 덕, 송 승기

명지대학교 자연대학 물리학과, <sup>1</sup>청주대학교 응용과학부.

Hexahalometallate, K<sub>2</sub>SnCl<sub>6</sub> shows a variety of lattice dynamics over the two structural phase transition temperatures. Among them, hindered rotation of SnCl<sub>6</sub> octahedra in the high temperature cubic phase seems to be responsible for the crystal instability that triggers the collective rotation of the SnCl<sub>6</sub> octahedra at the transition temperature and is frozen in below the transition temperature. We show that the characteristic NQR spectra corresponding to this molecular dynamics can be drastically exaggerated by the existence of the Ligand Defect Octahedra (LDO) through the change of their lattice potential and this offers details of lattice dynamics over the structural phase transitions.

전 병익, LI Guojie<sup>1</sup>, 김 셋별<sup>1</sup>, 최 병춘<sup>1</sup>, 문 병기<sup>1</sup>, 정 중현<sup>1</sup>  
한국과학영재학교, 물리학과, <sup>1</sup>부경대학교, 물리학과.

We studied the dielectric relaxations of ferroelectric composite between BaTiO<sub>3</sub> (BT) and K<sub>1-y</sub>Na<sub>y</sub>NbO<sub>3</sub> (KNN, y = 0.50). (1-x) KNN -(x)BT (KNN-BT, x = 0, 0.5 ~ 1.0) showed the ferroelectric behaviors displaying the perovskite (Pe) structures. It was considered that KNN-BT ceramics show a binary composite between KNN and BT. Although domain-engineered structures of BT based Pe structures became more important materials, KNN composition played a role of liquid phase sintering among the neighboring BT-based nano grains. We studied temperature shifts of the ferroelectric phase transition temperature  $T_C$  and the tetragonal to orthorhombic transition temperature  $T_{T-O}$  of the KNN-BT composite ceramics in terms of the dielectric properties in the low frequency range and the temperature range. The dielectric properties were examined using the complex dielectric constants and the complex electric modulus formalisms.



**Dp-I-007****X-선 흡수 분광학을 이용한 Ni(S,Se)<sub>2</sub>의 도체 부도체 전이 연구**

박 경자, 정 진원, 노 한진, 김 재영<sup>1</sup>, 김 형도<sup>1</sup>, 허 남정<sup>2</sup>, 김 성백<sup>3</sup>

전남대학교 물리학과. <sup>1</sup>포항가속기연구소. <sup>2</sup>인하대학교 물리학과. <sup>3</sup>포항공과대학교 물리학과.

Ni(S,Se)<sub>2</sub>의 도체 부도체 전이가 일어날 때 전자 구조의 변화를 XAS 실험을 통해 연구하였다. Ni 2p 내각 준위 전자 스펙트럼을 configuration interaction cluster model calculation 을 통해 분석하여 이 화합물의 전자 구조에 해당하는 물리적 변수를 얻을 수 있었다. Se의 조성 비율이 증가함에 따라 전하이동 에너지( $\Delta$ )는 감소하고, 혼성 상호작용 에너지( $V_{pd\sigma}$ )는 증가하였다. Ni(S,Se)<sub>2</sub>의 도체 부도체 전이는 전하이동 에너지( $\Delta$ )의 크기에 가장 민감하게 의존하는 것으로 나타났다. 분석 결과 얻어진 변수 값은 NiS<sub>2</sub>가 전하이동 에너지( $\Delta$ )에 의해 에너지 간격( $E_{gap}$ )이 결정되는 charge transfer insulator 임을 보여 준다. Se가 첨가 될수록 전하이동 에너지( $\Delta$ )가 작아지게 되어 에너지 간격( $E_{gap}$ )이 감소하고, 혼성 상호작용 에너지( $V_{pd\sigma}$ )는 커지므로 이 물질의 에너지밴드 폭(W)은 점점 증가하게 된다. U/W 값이 감소하면서 점점 이 시스템은 부도체에서 p전자와 d전자의 혼성화가 증가된 도체(p-d metal)로 전이가 된다. 이 연구는 학술진흥연구재단 (KRF-2008-314-C00086)의 지원을 받아 수행되었습니다.

**Dp-I-008****Diode And Photocurrent Effect In Ferroelectrics**

원 총재, 허 남정, 박 영안, 류 한열

인하대학교 물리학과.

The leakage current in ferroelectric is one of the major obstacles that need to be overcome. Recently, however, there have been studies on the relationship between electric transport properties and ferroelectric polarization, for example, the polarization dependent electric transport and significant photo-induced current in BiFeO<sub>3</sub>. However, the origin of such effect is largely unknown and it is not clear whether the diode effects can be observed generally in other lossy ferroelectrics or they are exceptional properties of BFO. Therefore further studies on other systems are required to understand the origin and characteristics of new effects in ferroelectrics. Here, we present the diode-like transport and the considerable photocurrent effect, both of which depend on the direction of the electric polarization in oxygen reduced ferroelectric single crystals. From the polarization dependent transport and the photon energy dependence of photocurrent effect, we proposed a plausible model for the diode effect in ferroelectrics. Our results in the carrier doped conventional ferroelectrics indicate that the diode effect can be observed in much wider class of ferroelectrics and may suggest an alternative way for the non-destructive of readout of polarization states in common ferroelectric memories.

**Dp-I-009****Photoluminescence spectra in ZnO nanorods in various gas atmospheres**LEE D J, SEO Y K, LEE Y S, PARK J H<sup>1</sup>, YOON S H<sup>2</sup>, YEE K J<sup>3</sup>

*Department of physics, Soongsil University. <sup>1</sup>Electronics and Telecommunications Research Institute. <sup>2</sup>Division of Nano Sciences and Department of physics, Ewha Womans University. <sup>3</sup>Department of Physics, Chungnam National University.*

ZnO based nanostructures have recently attracted much attention due to their potential applications in spintronic and ultraviolet (UV) to violet light-emitting and other optoelectronic device. We investigated the photoluminescence (PL) spectra of solution-based synthesized ZnO nanorods in various gas atmospheres such as N<sub>2</sub>, O<sub>2</sub>, and H<sub>2</sub>O. The ZnO nanorods were fabricated by using a simple sonochemical method. The typical feature in PL spectra is a strong and sharp peak near 375 nm (NBE peak) and a broad structure near 550 nm (deep level). In the N<sub>2</sub> atmosphere, the NBE peak is dramatically enhanced, but the deep level emission is significantly suppressed. These behaviors are reversed in the O<sub>2</sub> atmosphere. On the other hand, the intensities of both peaks are decreased in the H<sub>2</sub>O atmosphere. The results are compared with the transport, absorption, and Raman data obtained in the same conditions.

P1

포  
스  
터  
세  
션**Dp-I-011****강상관 전자계의 내각준위 광전자분광 스펙트럼에 대한 동적 평균장 이론 계산**

김 형도

포항가속기연구소.

강상관 전자계의 내각준위 광전자 분광 스펙트럼은 원자가 전자대를 기술할 것으로 여겨지는 Hubbard 모형 및 Anderson 모형의 매개변수들의 값을 어림잡을 수 있는 중요한 실험 방법이다. 다양한 위상구조를 보여주는 이들 스펙트럼을 해석하는 방법은 Mott 절연체인 경우에는 Anderson 불순물 모형을 풀거나, 금속인 경우에는 동적 평균장 이론을 이용해 Hubbard 모형의 해를 구하는 것이다. 이번 발표에는 전자 및 정공이 도핑된 시스템에서 내각준위 스펙트럼이 어떻게 변하는지를 보이고자 한다.

**Dp-I-012****Structure Analysis and Electrical Properties of VO<sub>2</sub> Thin Films Grown on****Sapphire with Thickness Dependence**SEO Gi Wan, KIM Bong-Jun<sup>1</sup>, LEE Yong Wook<sup>2</sup>, CHOI Sungyoul<sup>1</sup>, KIM Hyun-TakETRI/University of Science and Technology. <sup>1</sup>ETRI. <sup>2</sup>ETRI/Pukyong National University.

Vanadium dioxide was deposited on c-plane sapphire substrate by pulsed laser deposition technique with different thickness. Thickness dependence of metal-insulator transition (MIT) properties was studied on vanadium dioxide for revealing epitaxial growth mechanism and the relationship between the MIT and the crystal structure. In order to analysis structure, x-ray, scanning electron microscope (SEM) and resistance measurement were carried out. X-ray diffraction patterns show that b-axis of vanadium dioxide is normal to the surface of the substrate. This indicates that vanadium dioxide grows epitaxially on the sapphire substrate, even though the grain structure is observed on SEM images. Grain size and the resistance transition width near 68 °C increased with the thickness, and which were demonstrated that the thickness of vanadium dioxide thin films plays important role in their electrical characteristics. Especially, the film with the thickness of 240 nm has the transition width of  $9.3 \times 10^4$ .

**Dp-I-013****바나듐 첨가에 의한 K<sub>0.5</sub>Bi<sub>4.5</sub>Ti<sub>4</sub>O<sub>15</sub> 박막의 구조와 전기적 특성 변화**

김 상수, 김 진원, 도 달현, 최 은진, 김 가현, 김 태규

창원대학교 물리학과

$(\text{Bi}_2\text{O}_2)^{2+}(\text{A}_{m-1}\text{B}_m\text{O}_{3m+1})^{2-}$ 의 일반식을 갖는 비스무스 층 구조 형 강유전체 (bismuth layer-structured ferroelectrics : BLSFs) 중 하나인 K<sub>0.5</sub>Bi<sub>4.5</sub>Ti<sub>4</sub>O<sub>15</sub>는 A-site에 K<sup>+</sup>와 Bi<sup>3+</sup>, B-site에 Ti<sup>4+</sup>가 있으며 m=4 인 강유전체이다. K<sub>0.5</sub>Bi<sub>4.5</sub>Ti<sub>4</sub>O<sub>15</sub>는 SrBi<sub>2</sub>Ta<sub>2</sub>O<sub>9</sub> (m=2), Bi<sub>4</sub>Ti<sub>3</sub>O<sub>12</sub> (m=3) 에 비해서 큰 m(=4)을 가지므로 큰 잔류분극 값을 보일 것으로 예상되며 또한 상대적으로 높은 Curie 온도 ( $T_C \sim 655^\circ\text{C}$ )로 인해서 소자로써의 활용가능성이 기대되는 물질이다. 그러나 지금까지 이 물질에 대한 연구(특히, 박막)가 거의 이루어지지 않고 있는 실정이다. 본 연구에서는 화학용액 증착법으로 Pt(111)/Ti/SiO<sub>2</sub>/Si(100) 기판 위에 바나듐이 첨가된 K<sub>0.5</sub>Bi<sub>4.5</sub>Ti<sub>4</sub>O<sub>15</sub> (K<sub>0.5</sub>Bi<sub>4.5-x/3</sub>Ti<sub>4-x</sub>V<sub>x</sub>O<sub>15</sub> (KBTiV-x, x=0.00, 0.01, 0.03, 그리고 0.05)) 박막을 성장시켜 박막의 구조와 특성을 측정, 비교 분석하였다. 성장된 박막은 750°C의 산소 분위기에서 RTA 법으로 열처리하였으며 이 박막의 결정화 상태와 미세구조는 XRD, SEM 측정 결과로부터 알아보았다. 바나듐이 첨가된 박막의 전기적 특성은 순수한 K<sub>0.5</sub>Bi<sub>4.5</sub>Ti<sub>4</sub>O<sub>15</sub> (KBTiV-0.00) 박막보다 크게 향상되었는데 외부 전기장이 365 kV/cm일 때 NaBTiV-0.03 박막의 잔류분극( $2P_r$ )과 항전기장( $2E_c$ ) 값은 각각 75  $\mu\text{C}/\text{cm}^2$ , 217 kV/cm이었으며 외부 전기장이 100 kV/cm일 때 누설전류 밀도는  $5.01 \times 10^{-8} \text{ A}/\text{cm}^2$  이었다. 또한 1 MHz에서  $1.44 \times 10^9$  까지 큰 피로 현상을 보이지 않았다.

**Dp-I-014****Investigation of La- and V-codoped  $\text{Na}_{0.5}\text{Bi}_{4.5}\text{Ti}_4\text{O}_{15}$  ferroelectric thin films**

김 상수, 도 달현, 김 진원, 최 은진, 김 가현, 김 태규

창원대학교 물리학과

Ferroelectric La- and V-codoped  $\text{Na}_{0.5}\text{Bi}_{4.5}\text{Ti}_4\text{O}_{15}$  ( $\text{Na}_{0.5}\text{La}_{0.5}\text{Bi}_{3.99}\text{Ti}_{3.97}\text{V}_{0.03}\text{O}_{15}$ ) thin films were prepared on a Pt(111)/Ti/SiO<sub>2</sub>/Si substrate using a chemical solution deposition method. Structures of the film were investigated using x-ray diffraction and scanning electron microscopy. The film showed the same crystal structure but larger grains, compared to  $\text{Na}_{0.5}\text{Bi}_{4.5}\text{Ti}_4\text{O}_{15}$  thin films prepared by the same method. The codoped film exhibited better ferroelectric properties than the pure  $\text{Na}_{0.5}\text{Bi}_{4.5}\text{Ti}_4\text{O}_{15}$  thin film. Remnant polarization was larger and coercive electric field was smaller than the pure  $\text{Na}_{0.5}\text{Bi}_{4.5}\text{Ti}_4\text{O}_{15}$  thin film. Also lower leakage current density was observed. In addition, almost no polarization fatigue was observed up to  $1.44 \times 10^{10}$  switching cycles. These results indicate that codoping is one of the alternative ways to improve the ferroelectric properties of  $\text{Na}_{0.5}\text{Bi}_{4.5}\text{Ti}_4\text{O}_{15}$ .

P1

포  
스  
터  
세  
션**Dp-I-015****Superconductivity of Cu doped 2H-NbSe<sub>2</sub>**

고 윤영, 김 용관, 송 기명<sup>1</sup>, 한 가람, 정 원식, 박 승룡, 임 춘식, 김 철, 최 성균, 송 동준, 경 원식, 최 환영, 허 남정<sup>1</sup>, 김 창영

연세대학교 물리학과, <sup>1</sup>인하대학교 물리학과

2H-NbSe<sub>2</sub> is one of the layered transition-metal dichalcogenides that show charge-density-wave (CDW) order and superconductivity (SC) at low temperatures. The main focus of our research is, through Cu doping dependence studies, to investigate the issues on the competition between SC and CDW state. We report synthesis of the single crystals Cu doped NbSe<sub>2</sub>. Single crystals were grown by iodine vapor transport method using temperature gradient 3-zone furnace. The crystalline phases were determined by X-ray diffraction. Also we measured superconducting transition temperature of Cu doped NbSe<sub>2</sub> by PPMS.

**Dp-I-016****Investigation of V4+ion -environment of GeO<sub>2</sub>-B<sub>2</sub>O<sub>3</sub>-V<sub>2</sub>O<sub>5</sub> Polycrystalline****Compounds**

김 영훈, 강 재필, 서 용문, 최 덕, 송 승기

영지대학교 자연대학 물리학과.

Recently, we observed the EPR spectra of GeO<sub>2</sub>-B<sub>2</sub>O<sub>3</sub>-V<sub>2</sub>O<sub>5</sub> glasses and investigated the structure of V<sup>4+</sup>ions in the glass samples. In these glasses V<sup>4+</sup>ions exist as VO<sup>2+</sup>ions in octahedral coordination with a tetragonal symmetry[1]. In this work, EPR spectra in the polycrystalline compounds of GeO<sub>2</sub>-B<sub>2</sub>O<sub>3</sub>-V<sub>2</sub>O<sub>5</sub> system have been observed. Through this the spectral parameters,  $g_{\parallel}$ ,  $g_{\perp}$ ,  $\Delta g_{\parallel}$ ,  $\Delta g_{\perp}$ ,  $A_{\parallel}$ ,  $A_{\perp}$ ,  $A'_{\parallel}$ ,  $A'_{\perp}$ , P and K have been found. EPR spectra obtained at room temperature for these polycrystalline samples showed a well resolved hyperfine structure typical of isolated vanadium ions in a ligand field of C<sub>4v</sub> symmetry, being present as VO<sup>2+</sup>ions. These results are compared with those of GeO<sub>2</sub>-B<sub>2</sub>O<sub>3</sub>-V<sub>2</sub>O<sub>5</sub> glasses. [1]. Y.H.Kim et al, Bulletin of K.P.S., 26-4, 144 (2008).

**Dp-I-017****Photoemission and x-ray absorption study on metal-insulator transition in Ca<sub>1-x</sub>****Sr<sub>x</sub>IrO<sub>3</sub> (x=0, 0.5, 1)**

USEONG Kim, S. Y. Jang, T. W. Noh, S.-J. Oh

서울대학교 물리학과.

We studied metal-insulator transition (MIT) in Ca<sub>1-x</sub>Sr<sub>x</sub>IrO<sub>3</sub> (x=0, 0.5, 1) by using x-ray photoemission spectroscopy (XPS) and x-ray absorption spectroscopy (XAS). The resistivity of SrIrO<sub>3</sub> shows metallic behavior while that of CaIrO<sub>3</sub> shows insulating behavior. The Ca<sub>1-x</sub>Sr<sub>x</sub>IrO<sub>3</sub> becomes insulating as the x decreases. The results show no change in the core level XPS spectra suggesting that the MIT in Ca<sub>1-x</sub>Sr<sub>x</sub>IrO<sub>3</sub> cannot be explained by the bandwidth control in the 5d transition metal oxide.

**Dp-I-018****Thickness Dependence of Microstructure and Ferroelectric Properties in Lead-free  $(\text{Na}_{0.5}\text{K}_{0.5})(\text{Nb}_{0.995}\text{Mn}_{0.005})\text{O}_3$  thin films fabricated by chemical solution deposition**

김 일원, 석 해진, 이 선영, 이 해준, 안 창원<sup>1</sup>, 조 남규<sup>1</sup>, 황 학인<sup>1</sup>

울산대학교, 물리학과. <sup>1</sup> 전자부품연구원, 융합부품연구부.

Ferroelectric thin films have attracted considerable attentions for their potential applications in nonvolatile ferroelectric random access memories. In order to have a precise control on the device performance, the study of electrical properties dependence on the film thickness is extraordinarily important. The reduction of film thickness, which is usually associated with an internal strain change, has a great effect on ferroelectric behaviors. In this study, we have deposited  $(\text{Na}_{0.5}\text{K}_{0.5})(\text{Nb}_{0.995}\text{Mn}_{0.005})\text{O}_3$  thin films with thickness ranging from 200 to 500nm on Pt/TiO<sub>2</sub>/SiO<sub>2</sub>/Si substrate by chemical solution deposition and investigated the effects of film thickness by measuring on the surface morphology, crystal structure, electrical and ferroelectric properties.

P1

포  
스  
터  
세  
션**Dp-I-019****Thermally evaporated NiO<sub>x</sub> thin films probed by Terahertz time-domain spectroscopy**

HA Taewoo, LEE Kimoon, IM Seongil, KIM Jae Hoon

*Department of Physics Yonsei university.*

We have measured the terahertz transmittance of NiO<sub>x</sub> thin films grown on Si by thermal evaporation with different temperature at various annealing temperature. The frequency-dependent conductivities were determined without resorting to a Kramers-Kronig analysis. Large changes in these spectral functions occurred due to varying deposition rate and annealing temperature. We have demonstrated that the terahertz transmission and conductivity provide us with useful information on the insulating/metallic characteristics of thermally evaporated NiO<sub>x</sub> thin films and the relevant effects of annealing. A slow deposition rate leads to an insulating character while fast growth resulted in a metallic character, which can be converted to the insulator side through sufficient annealing.

**Dp-I-020****Crystal Growth and Characterization of  $\text{Sr}_{n+1}\text{Ir}_n\text{O}_{3n+1}$  ( $n=1, 2$ ) and  $\text{R}_2\text{Ir}_2\text{O}_7$** **(R=Pr, Eu)**

JEON Byung-Gu, LEE Bumsung, KHIM Seunghyun, KIM Kee Hoon

*Department of Physics and Astronomy, Seoul National University.*

Physics of iridates is getting increasing attention in recent years, owing to their exotic physical properties such as a  $J=1/2$  Mott insulating ground state in  $\text{Sr}_2\text{IrO}_4$  [1], driven by strong correlation/spin-orbit interaction of Ir 5d orbitals, and a metallic spin liquid state in  $\text{Pr}_2\text{Ir}_2\text{O}_7$ , linked to the Pr 4f local moments and Ir 5d conduction bands [2]. In order to fully understand those phenomena, growth of high-quality, large single crystals of a broad class of iridates are demanded. In this work, we report crystal growth and characterization of poly- and single-crystals of  $\text{R}_2\text{Ir}_2\text{O}_7$  (R=Pr, Eu), and single crystals of Ruddlesden-Popper series  $\text{Sr}_{n+1}\text{Ir}_n\text{O}_{3n+1}$  ( $n=1, 2$ ). Single crystals of  $\text{R}_2\text{Ir}_2\text{O}_7$  samples were successfully grown by KF-flux up to ~2 mm in a lateral length while those of  $\text{Sr}_{n+1}\text{Ir}_n\text{O}_{3n+1}$  were grown by self-flux up to 3 mm. Physical characteristics of these iridates including resistivity, Hall coefficients, and magnetization will be presented. [1] B. J. Kim *et al.*, Phys. Rev. Lett. 101, 076402 (2008) [2] S. Nakatsuji *et al.*, Phys. Rev. Lett. 96, 087204 (2006)

**Dp-I-021****Fermi Liquids Behavior In The Mixed-Valence  $\text{YbInCu}_4$** WOO Bonghee, V.A. Sidorov<sup>1</sup>, J.L. Sarrao<sup>2</sup>, J.D. Thompson<sup>2</sup>, PARK Tuson

*Department of Physics, Sungkyunkwan University, Suwon, Korea. <sup>1</sup>Vereshchagin Institute for High Pressure Physics, Troitsk, Russia. <sup>2</sup>Los Alamos National Laboratory, Los Alamos, New Mexico, USA.*

$\text{YbInCu}_4$  undergoes a first-order isostructural mixed valence transition at 42K and ambient pressure. Unlike normal metals where Kadowaki-Woods (KW) ratio is universal, the ratio of  $A/\gamma^2$  strongly deviates from the KW value of  $1 \times 10^{-5} \text{ mW cm mol}^{-2} \text{ K}^2 \text{ mJ}^{-2}$ , suggesting a breakdown of Fermi liquids. We have performed resistivity and specific heat measurements of  $\text{YbInCu}_4$  under pressure up to 27 kbar. At above 25 kbar where the mixed-valence transition temperature is completely suppressed, the normal value of KW ratio is recovered. The pressure dependence of the KW ratio suggests that the anomalous deviation could be ascribed to a change in f-orbital degeneracy and carrier density of  $\text{YbInCu}_4$ .

**A<sub>2</sub>FeReO<sub>6</sub> (A=Ba and Ca)**

JEON Byung Chul, MOON Soon Jae, KIM Choong Hyun, CHOI Wook Seok, LEE Yoon Sang<sup>1</sup>, WON Choong Jae<sup>2</sup>, JUNG Jong Hoon<sup>2</sup>, HUR Nam Jung<sup>2</sup>, YU Jae Joon, NOH Tae Won

서울대학교, 물리천문학과. <sup>1</sup> 숭실대학교, 물리천문학과. <sup>2</sup> 인하대학교, 물리천문학과.

Recently, the role of spin-orbit coupling (SOC) in 5d transition metal oxides (TMOs) attracted a lot of attention. In 5d TMOs, the energy scale of the SOC is larger than that of 3d or 4d TMOs and it can play an important role in determining the physical properties of 5d TMOs. We investigated the electronic structures of 5d double perovskite A<sub>2</sub>FeReO<sub>6</sub> (A=Ba and Ca) using optical spectroscopy, x-ray absorption spectroscopy, and first-principles calculations. We observed that the electronic ground state changes from metal to insulator when Ba ion was substituted with Ca ion which can be attributed to the bandwidth-controlled metal-insulator transition. The insulating ground state of Ca<sub>2</sub>FeReO<sub>6</sub> is unexpected since its 4d counterpart Ca<sub>2</sub>FeMoO<sub>6</sub> has metallic ground state. We found that the metal-insulator transition can be realized by the cooperation of the electron correlation and spin-orbit coupling. Our results demonstrate that the spin-orbit coupling can play a crucial role for the electronic structures of 5d transition metal oxides.

**(Zr,Ti)O<sub>3</sub> Thin Films: Effects of Ti-Excess-Amounts and Annealing Conditions**

CHOI Yong Chan, YANG Sun A, CHO Sam Yeon, BU Sang Don

Chonbuk National University, Department of Physics.

We report the self-assembled growth of the nanocomposites of 'TiO<sub>2</sub> nanopillars on Pb(Zr<sub>0.52</sub>Ti<sub>0.48</sub>)O<sub>3</sub> (PZT) thin films' using a modified sol-gel processing [1]. Both TiO<sub>2</sub> nanopillars and PZT thin films are simultaneously formed during the post-annealing process. The growth behaviors of TiO<sub>2</sub> nanopillars are controlled by adjusting Ti-excess-amounts of PZT solutions and post-annealing conditions. The self-assembled growth can be explained by five important factors, which can occur during the annealing process: a Ti ion diffusion to the surface, a phase separation of PZT and TiO<sub>2</sub>, a void formation on the film surface, a Ti oxidation, and a crystallite growth. [1] Y. C. Choi *et al.*, Nanotechnology, *in press*.

**Dp-I-024****Ferroelectric-like behavior of high dielectric constant perovskite-related oxide****CaCu<sub>3</sub>Ti<sub>4</sub>O<sub>12</sub>**

KWON Hyosang, PARK Sungmin, PARK Doyoung,  
HWANG Jihwan, CHEONG Hyeonsik, PARK Gwangseo  
*Department of Physics, Sogang university.*

Recently, a newly discovered ATiO<sub>3</sub>-type perovskite titanate CaCu<sub>3</sub>Ti<sub>4</sub>O<sub>12</sub>(CCTO) was extensively investigated due to its colossal dielectric constant ( $\epsilon \sim 10^4 - 10^5$ ) and weak temperature dependence in a wide temperature range from 100 to 600K, whose underlying mechanism is not still well understood. Dielectric constants greater than 1000 have traditionally been associated with intrinsic ferroelectric properties. However, no evidence for ferroelectricity and related phenomena like phase transition in CCTO has been found by means of either x-ray diffraction or Raman spectroscopy down to very low temperatures. In order to find their processing temperature dependent crystal structure and electrical characteristics, we prepared CCTO ceramic sintered at various temperatures. X-ray diffraction revealed that there are no secondary phases related to raw materials such as CaCO<sub>3</sub>, CuO and TiO<sub>2</sub>. From the Raman spectra, it is found that the pronounced Raman active modes of 445( $A_g$ ), 510( $A_g$ ) and 573 cm<sup>-1</sup>( $F_g$ ) which reply the rotation of TiO<sub>6</sub> octahedron are slightly shifted to higher frequency for doubly sintered CCTO ceramic. In addition, the ferroelectric-like hysteresis curve and weak butterfly  $C-V$  curve are observed for this ceramic. In this presentation, we will further discuss about the rotation of TiO<sub>6</sub> octahedron and their effect on ferroelectricity.

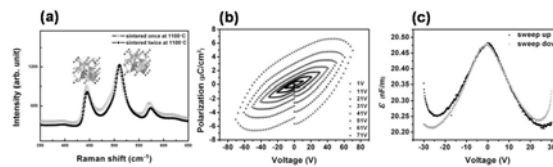


Fig1. (a) Raman spectra, (b)  $P-V$  curves at various applied voltage, (c)  $C-V$  curves

**Dp-I-025****Luminescence properties comparison of BaY<sub>2</sub>ZnO<sub>5</sub>:Eu<sup>3+</sup> phosphors by high-energy ball milling and solid-state reaction**

YANG Hyun Kyoung, MOON Byung Kee, CHOI Byung Chun, JEONG Jung Hyun, KIM Jung Hwan<sup>1</sup>  
*Department of Physics, Pukyong National University. <sup>1</sup>Department of Physics, Dongeui University.*

White light emitting diodes (LEDs) are candidates for new lighting systems in the future. The most dominant white LED uses a 450–470 nm blue emitting diode that excites a yellow-emitting yttrium aluminum garnet (YAG):Ce<sup>3+</sup> phosphor. However, the light color is not true because this systems lacks of a red emitting component. Current lighting technology employs UV-LED with triple-wavelength RGB phosphors to improve this problems. Recently, a lot of attention has been given to single-phased white light emitting phosphors, which have a large potential for white light LED applications. A proper host material doped with various concentrations of Eu<sup>3+</sup> phosphors can generate red emission from the <sup>5</sup>D<sub>0</sub> level and the blue and green emissions from higher <sup>5</sup>D levels, including <sup>5</sup>D<sub>1</sub>, <sup>5</sup>D<sub>2</sub>, and <sup>5</sup>D<sub>3</sub> of Eu<sup>3+</sup>, which could produce single-phased white light emitting phosphors. BaLn<sub>2</sub>ZnO<sub>5</sub> (Ln = Y, Gd, La) is a luminescence host with a stable crystal structure and high thermal stability. In this research, a facile synthetic route for the preparation of BaLn<sub>2</sub>ZnO<sub>5</sub>:Eu<sup>3+</sup> (Ln = Y, Gd, La) by high energy ball milling, the as-grown powders were found to be amorphous, which crystallized to the BaY<sub>2</sub>ZnO<sub>5</sub>:Eu<sup>3+</sup> by product after calcination at 1200 °C in air for 6 hours. The corresponding bulk BaY<sub>2</sub>ZnO<sub>5</sub>:Eu<sup>3+</sup> were synthesized by high temperature solid-state reaction. All the products were systematically characterized by powder X-ray diffraction (XRD), infrared spectroscopy (IR), field emission-scanning electron microscopy (FE-SEM), photoluminescence (PL) and photoluminescent excitation spectra (PLE). The luminescence mechanism and the size dependence of their fluorescence properties are also discussed.

## Different Resistance Switching Behaviors of NiO Thin Films Deposited on Pt and SrRuO<sub>3</sub> Electrodes

최 진식, 김 진수, 황 인록, 홍 사환, 전 상호, 강 성웅, 박 배호, 김 동철<sup>1</sup>, 이 명재<sup>1</sup>, 서 순애<sup>1</sup>

건국대학교, 물리학과. <sup>1</sup>Samsung Advanced Institute of Technology.

We have compared resistance switching of NiO films deposited on Pt and SrRuO<sub>3</sub> (SRO); uni-polar switching in Pt/NiO/Pt and bi-polar switching in Pt/NiO/SRO. Linear fitted current-voltage curves and capacitance-voltage results show that on- and off-states conductions in uni-polar switching are dominated by inductive Ohmic behavior and Poole-Frenkel effect, respectively. However, the conductions of on- and off-states in bi-polar switching follow capacitive Ohmic behavior and Schottky effect, respectively. Therefore, we infer that the mechanisms of the uni-polar and bi-polar switching behaviors in NiO films are related with changes in bulk-limited filamentary conduction and interfacial Schottky barrier, respectively.

## Effects of Annealing Temperatures on Phase Formation of Sol-Gel Derived PMN-PT Thin Films

YANG Sun A, HAN Jin Kyu, BU Sang Don

Chonbuk National University, Department of Physics.

Piezoelectric  $(1-x)\text{Pb}(\text{Mg}_{1/3}\text{Nb}_{2/3})\text{O}_3-x\text{TiO}_3$  (PMN-PT) thin films with the compositions near morphotropic phase boundary have attracted considerable attention because of their excellent dielectric, piezoelectric, and electromechanical properties, which make them useful in wide range of commercial applications. However, the formation of secondary pyrochlore phase with a low dielectric constant during the thermal treatment has limited the full use of this material. We report the synthesis of PMN-PT thin films and their phase formation dependence on annealing temperatures. The films were prepared by the sol-gel process with a spin-coating method on Pt/Si substrate. After the spin-coating process, they were annealed in the temperature range 550 to 750 °C for 30 min. in PbO atmosphere. The crystal structure of the PMN-PT thin films was characterized by X-ray diffraction (XRD) in the  $\theta$  -  $2\theta$  scan mode. The XRD profile indicates that the films have both of perovskite phase peaks of (110), (100), and (210) orientations and pyrochlore phase peaks of (222), (400), (440), and (622) orientations. The intensity of perovskite peaks are increased with increasing the annealing temperature to 750 °C. On the other hand, the intensity of pyrochlore peaks is decreased to 700 °C and then increased, which can be attributed to Pb loss caused by high temperature annealing processes. The crystal structure of the films is also analyzed by using transmission electron microscopy and their electrical properties are measured by using TF analyzer.

**Dp-I-028****(1-x)BiScO<sub>3</sub>-(x)PbTiO<sub>3</sub> (x=0.64) 강유전 박막의 결정구조 및 압전 특성 연구**JIN Yeryeong, KIM Bongju, KWON Daeyoung, WU youngsoo, KIM Bog G<sup>1</sup>부산대학교, 물리학과. <sup>1</sup> 부산대학교, 물리학과.

(1-x)BiScO<sub>3</sub>-(x)PbTiO<sub>3</sub> (x=0.64, BSPT) 강유전 박막을 성장시켜, 결정구조 및 압전 특성을 연구하였다. BSPT 박막은 off-axis magnetron sputtering 방법을 이용하여, Nb-doped SrTiO<sub>3</sub> (001) 기판 위에 증착 하였으며, High resolution x-ray diffraction (HRXRD)를 이용하여 결정구조 특성을 측정하였다. 이 결과에서, x-ray reflectivity (XRR) 실험으로 두께를 측정한 BSPT 박막은 각각 10nm, 30nm, 45nm, 60nm 의 두께를 가지며,  $\theta$ -2 $\theta$  scan 결과에서는 (001) 방향의 우선 배향성을 가지고 성장하였음을 확인하였다. 또한 Phi scan은 BSPT 박막이 STO기판 위에 4-fold symmetry로 가지런하게 올라갔음을 보이고 있으며, RSM측정을 통하여 두께가 30nm이하인 박막에서 fully strain 되어 성장 되었으나, 45nm이상에서는 strain relaxation을 확인하였다. Atomic force microscopy (AFM)의 Piezo-force microscopy (PFM) 방법을 이용하여, BSPT 박막의 polarization 반전, 전기이력특성에 따른 압전 특성을 조사하였다. 이를 바탕으로 BSPT thin film의 bias 전압에 따른 piezoelectric response의 변화 및 분극 반전 현상을 관찰하였다. 전기이력에 따른 압전특성 변화로부터, BSPT 박막의 piezoelectric response 및 effective piezoelectric constant d<sub>33</sub>(pm/v)를 측정하여, 두께가 10nm에 이르는 박막에서도 정량적인 압전특성 분석을 하였다. 이를 통해, 우리는 BSPT 박막의 높은 온도 안전성 및 뛰어난 압전 특성을 을 이용하여, 강유전 메모리 및 MEMS device, 전자회로의 기능소자 등으로 활용될 수 있는 가능성을 확인하였다.

**Dp-I-029****Eu 함량별 YVO<sub>4</sub>:Eu<sup>3+</sup>와 LaVO<sub>4</sub>:Eu<sup>3+</sup> 형광체 분말의 형광특성 비교**박 성욱, 문 병기, 최 병춘, 정 중현, 김 중환<sup>1</sup>부경대학교, 물리학과. <sup>1</sup> 동의대학교, 물리학과.

1996년 GaN 청색 LED가 상용화 된 이래 백색 LED에 이르기까지 많은 발전을 이루었으나 아직 질적 개선을 위한 과제는 산적해 있는 상태이다. 그 중 형광체에 관련하여 살펴보면, 최근 개발된 near-UV LED(약 370 ~ 420 nm)를 여기 광원으로 사용하여 적(Red), 녹(Green), 청(Blue)색 형광체와 조합할 경우 연색성(CRI)이 매우 뛰어난 백색 LED를 구현 할 수 있다. 본 연구에서는 현재 발광 소자의 주요 개발 분야인 자외선 여기 백색 LED 부문에서 가장 크게 요구되고 있는 새로운 고효율 적색 형광체 물질 합성에 초점을 맞추어, 자외선 영역대 에너지 흡수를 보이는 vanadate 계열 형광체인 YVO<sub>4</sub>:Eu<sup>3+</sup>, LaVO<sub>4</sub>:Eu<sup>3+</sup>를 Eu 함량을 변화시키며 합성, 조사해 보았다. 실험방법은 고상반응법(solid state reaction)을 이용하였으며, 시작물질로 순도 99.99% 이상의 Y<sub>2</sub>O<sub>3</sub>, La<sub>2</sub>O<sub>3</sub>, V<sub>2</sub>O<sub>5</sub>, Eu<sub>2</sub>O<sub>3</sub>를 사용하여 모든 시료를 화학양론(stoichiometry)으로 계산하였다. 계산된 시료의 양에 맞추어 칭량한 시료를 위성 불밀을 이용하여 회전수 350 rpm 하에서 10시간동안 분쇄, 혼합하였다. 각각의 시료를 전기로에 넣어 분당 2°C 간격으로 승온하였으며, 900 °C에서 5시간 동안 유지한 후 실온으로 하강시키는 과정을 통해 최종적으로 분말 형태의 형광체를 합성해내었다. YVO<sub>4</sub>:Eu<sup>3+</sup>와 LaVO<sub>4</sub>:Eu<sup>3+</sup> 형광체 분말을 각각 Eu<sup>3+</sup> 함량 0.01, 0.03, 0.05, 0.07, 0.09, 0.15, 0.20, 0.40, 0.60, 0.80, 1.0 mol의 비율로 총 22가지 샘플을 합성하였다. LaVO<sub>4</sub>:Eu<sup>3+</sup>의 형광효율 증가를 위해, Li<sup>+</sup> 이온을 증감제로 첨가하여 형광효율을 증대시키고자 하였고, XRD, SEM, PL 장비를 이용하여 각각의 결정구조, 입자모양 및 형광특성을 비교 분석하였다. Eu 함량 0.03 mol 이하일 경우 두 물질의 결정구조가 YVO<sub>4</sub>:Eu<sup>3+</sup>의 경우 tetragonal, LaVO<sub>4</sub>:Eu<sup>3+</sup>의 경우 monoclinic 구조를 갖는다. 특히 Eu 함량에 따라 결정구조의 변화를 보이게 되는데 이는 모체의 양이온과 활성제 양이온의 이온반경의 차이에 의한 것이다. 본 연구는 결정구조 변화에 따른 형광특성을 비교하는데 주안점을 두었다.

## Outer Diameters of 50, 250, and 420 nm

CHOI Yong Chan, CHO Sam Yeon, BU Sang Don

*Chonbuk National University, Department of Physics.*

In recent years, intensive research has been devoted on the synthesis and characterization of ferroelectric nanotubes, such as  $\text{Pb}(\text{Zr}_{0.52}\text{Ti}_{0.48})\text{O}_3$  nanotubes (PZT-NTs). However, the studies on the effects of sizes, such as diameter, wall thickness, and length of PZT-NTs, on their ferroelectric properties remain one of the main challenges. In this work, we report the ultra-thin-walled PZT-NTs with different outer diameters of 50, 250, and 420 nm fabricated using templates of porous anodic alumina (PAA). PZT-NTs with a diameter of ~50 nm were obtained using the PAA template with 50 nm pore diameter, anodized at a voltage of 40 V in 0.3 M oxalic acid. PZT-NTs with diameters of ~250 and ~420 nm were obtained from PAA templates with 250 and 420 nm pore diameters, fabricated at 194 V in 0.1 M phosphoric acid. They all have wall thickness of ~5 nm and lengths of 0.3–20  $\mu\text{m}$ . Field emission transmission electron microscopy shows that all PZT-NTs are polycrystalline and consist of mainly perovskites crystallites with sizes in the range of 3–7 nm.

심 수민, 권 용경

*건국대학교.*

Path-integral Monte Carlo calculations have been performed on para- $\text{H}_2$  clusters mixed with several ortho- $\text{D}_2$  molecules, to study their superfluid behavior at low temperatures. We consider the mixed clusters involving different numbers of  $\text{D}_2$  molecules, with the total number of particles  $N_{\text{tot}}$  ranging from 12 to 25.  $\text{D}_2$  molecules tend to be located near the center of the mixed cluster, but they do not necessarily fill the cluster from an inner shell to an outer shell. In the mixed clusters with  $N_{\text{tot}} \geq 23$  and  $\text{D}_2 \geq 2$ , one of  $\text{D}_2$  is found to be located in an outer shell and to interrupt exchange coupling among the neighboring  $\text{H}_2$  molecules, which results in significantly-suppressed superfluid fractions. As the number of additional  $\text{D}_2$  molecules increases, heavier  $\text{D}_2$  molecules push away more  $\text{H}_2$  molecules from the cluster center and occupy the inner shell region entirely. This trend is shown in a clear separation of  $\text{D}_2$  and  $\text{H}_2$  radial density distributions for the mixed clusters with  $N_{\text{D}} = 4$ , which is responsible for complete disruption of long exchange coupling among  $\text{H}_2$  molecules and the total quenching of  $\text{H}_2$  superfluidity. We find that the magic number stabilities of pristine  $\text{H}_2$  clusters, manifested by significant suppression of superfluidity at a specific size when compared to the neighboring sizes, hold true in the mixed clusters and are determined by the total number of particles. This leads us to conclude that the replacement of  $\text{H}_2$  with  $\text{D}_2$  molecules does not change the overall structure of the hydrogen clusters. We also compute local distributions of hydrogen superfluidity in the mixed clusters by using the local superfluid density estimator [1] based on the microscopic two-fluid model. It is found that local superfluidity of  $\text{H}_2$  is uniform except near  $\text{D}_2$  molecules, which provides a clear answer to a controversy about the local distribution of  $\text{H}_2$  superfluidity [2,3]. [1] Y. Kwon, F. Paesani, and K. B. Whaley, Phys. Rev. B 74, 174522 (2006). [2] S.A.Khairallah, M.B.Sevryuk, D.M.Ceperley, and J.P.Toennies, Phys. Rev. Lett. 98, 183401 (2007) [3] F. Mezzacappa and M. Boninsegni, Phys Rev. Lett. 100, 145301 (2008)

**Dp-I-032****Synthesis and luminescence properties of NaGd(WO<sub>4</sub>)<sub>2</sub> doped Sm<sup>3+</sup> phosphor**

CHEN Yeqing, JEONG Jung Hyun

*Department of Physics, Pukyong National University.*

White light-emitting diodes (LEDs) presented many advantages are receiving much attention to be the candidate for new lighting systems in the future. The most common used yttrium aluminum garnet (Ce<sup>3+</sup>:YAG) phosphor is dominating, however the lack of red emitting component cannot give rise to high quality true light. Studies are focusing on the UV-LED with triple-wavelength RGB phosphor to improve the problem recently. Tangstate phosphors, as a new host material, doped with Sm<sup>3+</sup> can generate red emission from <sup>4</sup>G<sub>5/2</sub> level to <sup>6</sup>H<sub>5/2</sub>, <sup>6</sup>H<sub>7/2</sub> and <sup>6</sup>H<sub>9/2</sub> respectively. Samarium(III) ions exhibit enhanced luminescence emission owing to excitation energy transfer from groups WO<sub>4</sub><sup>2-</sup> to Sm<sup>3+</sup> ions in the Sm:NaGd<sub>1-x</sub>(WO<sub>4</sub>)<sub>2</sub> salt. In this research, a common used solid state method of preparation of NaGd(WO<sub>4</sub>)<sub>2</sub> is reported. The as-grown powders were sintered at 700°C for 4 hours to form a crystalline of NaGd(WO<sub>4</sub>)<sub>2</sub>. All the products were systematically characterized by power X-ray diffraction(XRD), field emission-scanning electron microscopy(FE-SEM), photoluminescence(PL) and photoluminescence excitation spectra(PLE). The luminescence mechanism and the size dependence of their fluorescence properties are also discussed.

**Dp-I-033****Search for Experimental Evidence of Ferroelectric Quantum Criticality in SrTiO<sub>3</sub>****Through Thermal Expansion Study**

JEON Byung-Gu, KIM Jae Wook, KIM Kee Hoon

*Department of Physics and Astronomy, Seoul National University.*

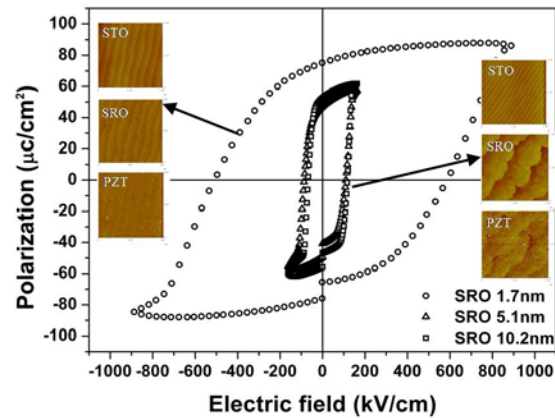
For about three decades of years, strontium titanate (SrTiO<sub>3</sub>) has been known as a quantum paraelectric [1], in which the continuous increase of dielectric constant ( $\epsilon$ ) is realized down to a proximate zero temperature without a long range ferroelectric ordering. Recently, quantum paraelectric behavior of SrTiO<sub>3</sub> was revisited with a viewpoint of quantum criticality [2]. Here, they adopted self-consistent phonon theory in the vicinity of quantum critical point of displacive ferroelectrics to predict temperature-dependence of dielectric susceptibility ( $\chi \equiv \epsilon - 1$ ) following a power-law form of  $\chi^{-1} \sim T^\gamma$  with  $\gamma=2$ . Indeed, this has been consistent with the experimental result over a temperature range below  $\sim 40$  K. In addition to  $\chi$ , quantum fluctuation is also expected to affect the lattice properties. Hence, we have investigated thermal expansion ( $\Delta L/L_0$ ) of a SrTiO<sub>3</sub> single crystal along [100] direction by using a home-made capacitance dilatometer. Power-law fitting was performed to estimate temperature dependence of  $\Delta L/L_0$  in a temperature window below  $\sim 120$  K. We found that a constant power-law exponent of about 3 exists in a temperature window of 10 to 40 K, in which the constant  $\gamma=2$  is also realized in  $\chi$ - $T$  experiment. This observation supports that the exponent measured is possibly related to the quantum critical behavior of thermal expansion. Above 40 K, the power-law exponent from  $\Delta L/L_0$  decreases to a lower value indicating a crossover from a quantum critical to a classical regime. We discuss a possible theoretical outcome expected in the thermal expansion of SrTiO<sub>3</sub>, based on existing theories that predicts dielectric properties near quantum critical point of ferroelectrics [2,3]. [1] K. A. Müller *et al.*, Phys. Rev. B 19, 3593 (1979). [2] S. Rowley *et al.*, arXiv:0903.1445 [cond-mat.str-el] [3] L. Pálková *et al.*, Phys. Rev. B 79, 075101 (2009).

**Dp-I-034****The ferroelectric properties of epitaxial  $\text{PbZr}_{0.3}\text{Ti}_{0.7}\text{O}_3$  thin films grown on the different thickness of  $\text{SrRuO}_3$  electrode**

HWANG Jihwan, PARK Sungmin, KWON Hyosang, GO Youngdong<sup>1</sup>, CHUNG Jinseok<sup>1</sup>, PARK Gwangseo

*Department of Physics, Sogang university. <sup>1</sup>Department of Physics, Soongsil university.*

We have investigated the ferroelectric properties of epitaxial  $\text{PbZr}_{0.3}\text{Ti}_{0.7}\text{O}_3$  (PZT) thin film depending on epitaxially strained  $\text{SrRuO}_3$  (SRO) film thickness. The leaky behavior of the hysteresis loop was observed 1.7nm thick SRO as well as its hysteresis curve was well saturated at 10V. On the other side, as SRO thickness exceeded over 5.1nm, the hysteresis curves were not only definitely saturated at 2V but also their polarization values were almost similar. In this presentation, we will discuss about the SRO thickness dependence of the coercive field and the polarization value for epitaxially grown PZT thin films.



P1

포  
스  
터  
세  
션**Dp-I-035****Effects of Etching Solutions on Dissolution Rate Behavior and Surface States of Alumina Nanowires Synthesized by Wet-Chemical Etching of Porous Alumina Membranes**

HAN Jin Kyu, BU Sang Don

*Chonbuk National University, Department of Physics.*

The alumina nanowires (ANWs) have recently received considerable attention since they may offer great potential for application including water purifications and fabrication of super-hydrophobic technology. The water purifications using highly electro-positive surface of the ANWs enables them to attract and retain electro-negatively charged ions or contaminants in water, such as pathogens and viruses. Various fabrication methods have been investigated to prepare the ANWs. The wet-chemical etching of porous anodic alumina membranes (PAMs), particularly, has become popular because of its simplicity, ease, and cost-effectiveness of its fabrication. The etching solutions such as  $\text{H}_3\text{PO}_4$  and  $\text{NaOH}$  solutions are mainly used for the synthesis of the ANWs. Here, we present effects of the etching solutions on the dissolution behavior and the surface structure of the ANWs. In  $\text{NaOH}$  solution, the dissolution of PAMs finishes within few minutes only, while, in  $\text{H}_3\text{PO}_4$  solution, the dissolution of those finishes within few hours. The dissolution behaviors of PAMs in both solutions are substantially different. The investigation of energy dispersive X-ray analysis and X-ray photoelectron spectroscopy spectra reveals that the composition and chemical state of ANWs are different depending on the etching solutions.

**Dp-I-036****양성자 빔조사에 따른 산화물 박막의 구조적 전기적 특성 변화 연구**

박 배호, 황 인록, 김 진수, 최 진식, 변 익수, 전 상호, 홍 사환, 강 성웅

건국대학교 물리학과

현재까지 차세대 비휘발성 메모리 중의 하나인 저항변화 메모리 (Resistive Random Access Memory)의 연구가 다양하게 진행되었으나 아직 명확하게 전도성 전이 특성의 메커니즘의 규명이 이루어지지 않았다. 전도성 전이 특성의 메커니즘을 분석하기 위한 다양한 방법중 양성자 빔조사를 이용하여 산화물 박막 내부의 결함을 인위적으로 제어하여 전도성 전이 특성의 변화를 관찰하고자 한다. 산화물 박막을 제작하여 다양한 조건의 양성자 빔을 조사한후 X-ray diffraction (XRD) 를 통하여 구조적인 변화를 측정하였으며, Scanning probe microscopy (SPM) 를 통하여 표면의 구조적인 변화를 관찰하였다. 또한 I-V 를 측정하여 결함 유도된 산화물 박막의 전도특성의 변화를 비교 분석하였다. 산화물 박막의 결함제어 방법을 양성자 조사를 이용하여 조절함으로 인하여 구조적, 전기적 변화의 분석으로 인하여 저항변화 메모리의 메커니즘을 규명하는데 도움이 될것으로 예상한다.

**Dp-I-037****Nb-SrTiO<sub>3</sub>의 전기/구조적 특성 및 고체 연료전지 전극 응용**김 맥, 송 철호, 이 상민, 김 영훈, 최 현우<sup>1</sup>, 임 영훈<sup>2</sup>, 양 용석<sup>3</sup>부산대학교, 나노융합기술학과. <sup>1</sup>부산대학교, 물리학과. <sup>2</sup>세명대학교, 교양과정부. <sup>3</sup>부산대학교, 나노정보소재공학과.

최근 차세대 에너지원으로 고체 연료전지가 많은 관심을 받고 있으며 해결해야 할 주요 과제는 높은 온도에서 구동 가능한 소재 개발, 부식 및 마모를 개선한 효율 증대, 넓은 온도 영역에서 좋은 전기전도 특성을 확보하는 것이다. 상온에서 매우 낮은 전기전도도를 나타내는 페로브스카이트 계열의 ABO<sub>3</sub> 물질은 고온에서 구조적으로 안정되고 결함이 쉽게 존재하여 열적, 전기적 전도 특성이 획기적으로 증대한다. 특히 첨가물 종류 및 함유량을 조절하면 이러한 전도 특성을 임의로 조절할 수 있는 효과가 있다. 본 연구에서는 페로브스카이트 계열의 SrTiO<sub>3</sub> 및 Nb-SrTiO<sub>3</sub>를 결정, 유리-세라믹으로 제조하고 이들의 온도에 따른 구조적, 전기적 특성을 연구하였다. SrTiO<sub>3</sub>는 고온에서 반도체에 버금갈 정도로 전기전도도가 높고, 공기 분위기에서 구조적으로 안정하다. 이 것은 곧 고체 연료전지의 전해질 물질로 좋은 특성을 나타내는 YSZ와 함께 접합부분에서의 전자 및 이온의 전도특성을 향상시키면 전극으로 활용할 좋은 응용 소재임을 나타낸다. 본 연구에서 전기전도 분석은 임피던스법, 온도에 따른 구조 분석은 ex-situ 법을 이용하였다.

**Dp-I-038****비정질 유전체  $x\text{LiTaO}_3\text{-SiO}_2$  ( $x=2, 4, 8$ )의 온도에 따른 유전 특성 연구**

김 영훈, 김 맥, 송 철호, 최 현우, 양 용석

부산대학교 나노과학기술학부 나노융합기술학과.

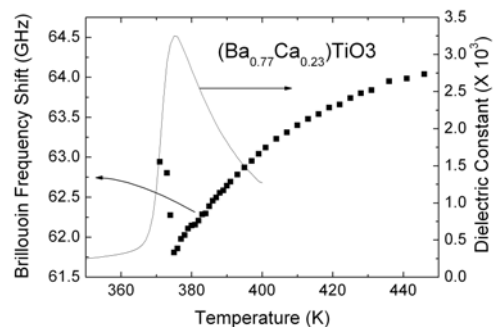
환경 문제의 대두로 인하여 비납계열의 강유전체 물질이 많은 관심을 받고 있다.  $\text{LiTaO}_3$  계는 비납계열의  $\text{ABO}_3$  형 강유전체로써 압전, 광학, 표면 탄성파 성질이 우수하여, 응용성에 대한 연구가 계속되고 있다.  $\text{LiTaO}_3$  단결정과 세라믹, 박막에 대한 전기적, 광학적, 구조적 특성에 대한 연구는 활발한 반면, 제조상의 어려움으로 비정질에 대한 연구는 미비하다. 그러나 나노 소재 및 소자 개발에 연관되어 비정질 및 비정질-세라믹 강유전체 연구가 많은 관심을 받기 시작하고 있다. 본 연구에서는 다결정  $\text{LiTaO}_3$ 에 비정질 형성제  $\text{SiO}_2$ 를 첨가하여  $x\text{LiTaO}_3\text{-SiO}_2$  ( $x=2, 4, 8$ ) 비정질을 제조하였다. 제조된 비정질  $x\text{LiTaO}_3\text{-SiO}_2$ 의 온도와 주파수에 따른 유전 특성을 Impedance/Gain phase analyzer를 사용하여 수행하였다. 지수법칙과 Cole-Cole 식을 사용하여 전기 완화 및 dc, ac 전도도를 구했으며 이온 강충 뛰기에 의해서 나타나는 전기 전도에 대한 활성화 에너지를 구하였다. 열처리 횟수에 따른 유전율 및 전기 전도도 변화를 구함으로써 산소 빈자리 효과를 확인하였다.

P1

포스터세션

**Dp-I-039** **$\text{Ba}_{0.77}\text{Ca}_{0.23}\text{TiO}_3$  단결정의 강유전상전이에 대한 분광학 연구**김 태현, 고 재현, 김 성백<sup>1</sup>, KOJIMA Seiji<sup>2</sup>한림대학교, 전자물리학과. <sup>1</sup>포항공과대학교, 물리학과. <sup>2</sup>University of Tsukuba, Institute of Materials Science.

$\text{Ba}_{0.77}\text{Ca}_{0.23}\text{TiO}_3$  단결정을 Optical Floating Zone방법을 이용하여 성장시킨 후 유전상수 측정, 브릴루앙 분광법, 라만 분광법을 이용하여 성장된 결정의 강유전상전이 특성을 광범위한 온도 영역에서 조사하였다. 유전상수 측정 결과 그림에서 확인할 수 있는 것처럼 약 375 K에서 강유전 상전이가 일어남을 확인하였으나 상유전상의 유전상수의 역수가 Curie-Weiss 법칙을 벗어남을 확인하였고, 이는 강유전체 릴랙서(relaxors)가 보여주는 특성과 비슷한 것으로서 Ba와 Ca의 무작위적 치환에 따른 무질서도에 의한 것으로 판단된다. 브릴루앙 산란법으로 구한 종음향모드의 브릴루앙 변이주파수는 500 K 이상의 고온에서는 일반적인 격자 비조화성에 의한 음의 기울기를 보이는데 반해 450 K 이하에서는 온도 저하에 따라 매우 현저한 무름(softening) 현상을 보였다. 아울러 상전이 온도 부근에서 중앙 피크(central peak)가 나타남도 확인하였다. 이러한 결과는 상유전상에서 강유전상전이 온도에 근접함에 따라 precursor polar clusters가 형성되어 국소적인 대칭성 파괴가 일어나고 이러한 polar clusters가 음파와 결합하여 음속도 (혹은 탄성계수)의 무름을 가져온 것으로 해석된다. 중앙 피크의 온도의존성을 조사한 결과  $\text{Ba}_{0.77}\text{Ca}_{0.23}\text{TiO}_3$  단결정은 질서-무질서형 상전이를 보이는 것으로 확인되었다.



**Dp-I-040****P-T boundary between white tin and gray tin - First principles study**NA Sung-Ho, PARK Chul-Hong<sup>1</sup>KASI. <sup>1</sup>Pusan National Univ.

Phonon dispersion relations of alpha- and beta- phases of tin are calculated by using the frozen phonon approximation, and then thermodynamic quantities such as entropy, helmholtz free energy, total pressure, and Gibbs free energy are calculated from the acquired phonon density of states. The calculated Gibbs free energy of the two different phases are used to identify the pressure and temperature of the structural phase transition.

**Dp-I-041****Bi<sub>2</sub>O<sub>3</sub>-SiO<sub>2</sub>-B<sub>2</sub>O<sub>3</sub>계 비정질의 결정화 기구 및 전기전도 특성**이 상민, 최 현우<sup>1</sup>, 송 철호, 김 맥, 김 영훈, 양 용석<sup>2</sup>부산대학교 나노융합기술학과. <sup>1</sup>부산대학교 물리학과. <sup>2</sup>부산대학교 나노정보소재공학과.

PbO-SiO<sub>2</sub>-B<sub>2</sub>O<sub>3</sub> 비정질 계는 적외선 차단, 비선형 광학, 광소자, 광섬유, 레이저, 광센서 등에 응용되며 제조가 용이하다. 한편 이 물질에 포함된 Pb는 환경 오염 원소이므로 다른 원소로 대체될 필요가 있다. Pb<sup>2+</sup>와 비슷한 전자배치 구조와 높은 분극성을 나타내는 Bi<sup>3+</sup> 이온을 포함하는 Bi<sub>2</sub>O<sub>3</sub>는 PbO를 대체할 수 있는 친환경적 물질이다. 최근 Bi<sub>2</sub>O<sub>3</sub>-SiO<sub>2</sub>-B<sub>2</sub>O<sub>3</sub> 계 비정질에 대한 광특성 연구가 활발하게 진행되고 있으나 열적 안정성, 결정화 과정, 전기 소자 응용 등에 대한 연구는 거의 이루어지지 않고 있다. 본 연구에서는 Bi<sub>2</sub>O<sub>3</sub>-SiO<sub>2</sub>-B<sub>2</sub>O<sub>3</sub> 계 비정질의 결정화 및 유전특성을 DSC, XRD, AFM, Impedance/gain-phase analyzer를 이용하여 수행 하였다. 결정화 과정에 대한 열분석 곡선은 승온을 변화에 무관하게 하나의 봉우리만이 나타나는 단일 결정 상전이를 보였으며 여러 온도에서 열처리한 시료의 XRD 분석을 통하여 이를 확인하였다. 결정화 과정 중의 핵 생성과 성장을 이용하여 결정화 기구를 규명하였다. 또한 온도와 주파수에 대한 유전을 변화를 통해 이온전도 기구를 분석하였다.

**Distribution and Electrostatic Potential Analysis**

KIM Su Jae, KIM Won-Kyung, LEE Seunghun, CHO Yong Chan, JEONG Se-Young

*Department of Nano Fusion Technology, Pusan National University.*

$\text{Li}_2\text{B}_4\text{O}_7$ (LBO) has been known as  $\text{Li}^+$  ion conduction material. The  $\text{Li}^+$  ion moves through c-axis channel and the ionic conductivity of c-axis is much higher than a, b- axis. But, it is not clear that why the  $\text{Li}^+$  ion acts as charge carrier and why the c-axis conductivity is so large. We study the electron charge density and electrostatic potential distribution of LBO system using MEM/Rietveld method and Ewald's technique. From the charge density distribution study, bonding nature of LBO system is investigated. We found that the Li atom exists without any bond and the ionic valence was nearly +1. The electrostatic potential distribution at the center of the all axis shows very big difference between c-axis channel and a, b-axis channel. All channels potential showed minus value but the depth and mean value at c-axis channel was quit small and it means the interaction between matrix and  $\text{Li}^+$  ion is small at c-axis channel. This is the reason of anisotropic conductivity. We found the reason of  $\text{Li}^+$  ionic conduction and anisotropic conductivity in LBO system using MEM/Rietveld method and Ewald's technique.

정 준기, 도 달현, 김 진원, 김 상수, 송 태권, 배 동식, 김 명호, 김 원정

*창원대학교.*

Wide band gap ZnS-ZnO thin films were grown on  $c\text{-Al}_2\text{O}_3$  by a pulsed laser deposition method using a pure ZnS target with a fixed substrate temperature of ranges of 400 ~ 700°C and a range of oxygen partial background pressures of  $5 \times 10^{-5} \sim 50$  Torr. It was found that the film growth were heavily depend on the deposition conditions, such as deposition temperatures and background oxygen pressures. With low oxygen deposition pressures, films were found to be mainly ZnS. However, with high oxygen pressures, the deposited thin films were found to be mainly ZnO. The formation of the ZnO films with high oxygen pressure could be attributed to the fast chemical reaction of O and S in the deposition chamber during deposition. Furthermore, energy band gap of the films changes from 3.7 to 3.3 eV with increasing oxygen pressure in the chamber. It was found that there is a good linear correlation between measured energy band gaps and S/Zn atomic ratio of the films as expected. Structural, chemical, optical, electrical, morphological and surface roughness has been investigated systematically by controlling deposition conditions, such as deposition temperature, oxygen pressure, and substrates. Details of the results will be discussed in the presentation.

**Dp-I-044****Fourier-Transform Infrared (FT-IR) Spectroscopic Ellipsometry of Pt Single****Crystal**

CHOI Kyujin, ROH Young Sup, KIM Jae Hoon

*Department of Physics & Institute of Physics and Applied Physics.*

Using the Fourier-transform infrared (FT-IR) spectroscopic ellipsometry, we measure the ellipsometric angles  $\psi$  and  $\Delta$  of single-crystal Pt in the mid-infrared spectral region from 0.1 to 0.8 eV. These values are related to the ratio of Fresnel reflection coefficient,  $R_p$  and  $R_s$  for  $p$  and  $s$ -polarized light. We calculate that the real and imaginary parts of the refractive index are directly without the need for a Kramers-Kronig analysis. We compare our results with transport measurements on Pt in the DC limit.

**Dp-I-045****A study on thermal conductivity of  $\text{Bi}_2\text{Te}_3$** 

KIM Ga Young, KIM Sang Hoon, PARK Sang Kook, LEE Sang Bong

*경북대학교 대학원 물리학과.*

Thermal conductivity is one of important properties of matter using Peltier element. We measured the thermal conductivity of commercialized semiconductor Peltier element, N-type and P-type based on  $\text{Bi}_2\text{Te}_3$ . First, we used long, thin cut Peltier element and give some heat at the top of sample, then measured the amount of heat, using the four-probe measure. We used thermocouple and measured the temperature difference of each pole of sample. This result of experiment will help for development of Peltier current lead.

## piezoelectric ceramics.

LEE H. S., CHUNG C. H., KIM J. S.<sup>1</sup>, JANG K. W.

*changwon national university, physics.* <sup>1</sup>*pukyong national university, physics.*

Lead-free piezoelectric ceramics  $(1-x)\text{Bi}_{0.5}\text{Na}_{0.5}\text{TiO}_3$ - $\text{LiNbO}_3$  by a conventional ceramic fabrication process. The starting raw materials mixed by ball-milling were calcined at 800°C for 2h. After the calcined powders underwent a second ball-milling for 24h, it was pressed into disk samples. The phase structure and surface morphology were confirmed by X-ray diffraction(XRD) and scan electromicroscopy (SEM), respectively.  $\text{Bi}_{0.5}\text{Na}_{0.5}\text{TiO}_3$  is a rhombohedral ferroelectric at room temperature.  $\text{LiNbO}_3$  is a trigonal ferroelectric at room temperature. Therefore, it is reasonable to anticipate that  $(1-x)\text{BNT-xLN}$  solid solution processes high piezoelectric properties due to the formation of MPB. In this study, the phase structure and electric properties of  $(1-x)\text{Bi}_{0.5}\text{Na}_{0.5}\text{TiO}_3$ - $\text{LiNbO}_3$  is investigated.

## Single Crystals

KANG Kihyeok, MEAN B. J., KIM Sung Hoon, LEE Jeffrey C.<sup>1</sup>, PARK Bae-Ho, LIM Ae Ran<sup>2</sup>

*Department of Physics, Konkuk University, Seoul, 143-701, Korea.* <sup>1</sup>*Adlai E. Stevenson High School, Lincolnshire IL 60069, U.S.A..* <sup>2</sup>*Department of Science Education, Jeonju University, Jeonju 560-759, Korea.*

<sup>87</sup>Rb Nuclear Magnetic Resonance (NMR) measurements have been performed on a single crystal of ferroelectric  $\text{RbKSO}_4$  at 4.8 and 8.0 T from room temperature down to 70 K. Two first-order phase transitions were reported to occur at 116 and 820 K. The crystal axes of  $\text{RbKSO}_4$  single crystal are well defined by XRD and NMR measurements. NMR spectrum, shift, linewidth, spin-lattice relaxation rate  $1/T_1$  and spin-spin relaxation rate  $1/T_2$  are measured as a function of temperature and rotation angle of the crystal axis to the magnetic field. The central peak of <sup>87</sup>Rb NMR spectrum at room temperature shows a different behavior for the three crystal axes. The satellite peaks are extremely broad compared with the central peak. The spin-lattice relaxation rate  $1/T_1$  significantly decreases as temperature goes down. The spin-spin relaxation rate  $1/T_2$  is almost same and independent of the temperature variation.

**Dp-I-048****Characterization of ZnO nanofibers prepared by electrospinning method**

KIM Jong Pil, PAK Eun Sick, BAE Jong-Seong, KIM Ju Hwan<sup>1</sup>, SIM Jin Woo<sup>1</sup>, HONG Kyung Woo<sup>1</sup>, HWANG Jeong Hoon<sup>1</sup>

*Surface Properties Research Team, Korea Basic Science Institute Busan Center, Busan 609-735, Korea. <sup>1</sup>Jang Young Sil Science High School, Busan, Korea 611-810, Korea.*

In recent years, much attention has been paid to the preparation and characterization of one-dimensional nanomaterials because of their great potential to test fundamental quantum mechanics concepts and to play a vital role in various applications such as photonics, nanoelectronics and data storage. In many of these applications, the sensitivity or efficiency is proportional to the surface area. Nanorods, nanowires, and nanofiber offer a larger surface area per unit mass compared to that of films or the bulk material. Nanorods or nanowires and nanofiber also offer the opportunity to study the physical properties of one-dimensional structures. ZnO has attracted much attention due to the strong commercial desire for blue and ultraviolet (UV) light emitters and detectors, transparent electrodes in solar cells, gas sensors, and piezoelectric transducers. It is well known that semiconductors with low dimensional size may have superior optical properties to bulk crystals owing to quantum confinement effects. These properties and potential applications have stimulated preparing and researching of well-controlled ZnO nanostructures. In this study, we report an electrospinning route for the synthesis of ZnO nanofibers. We described the phase formation, microstructure, chemical bonding state, and optical properties of ZnO nanofibers. The microstructure was analyzed by scanning electron microscope (SEM), Atomic force microscope (AFM) and transmission electron microscope (TEM). The chemical bonding states of film is measured by X-ray photoelectron spectroscopy (XPS). The transmission in the UV visible region and photoluminescence (PL) are reported here. Acknowledgment : This work was supported by grants-in aid for the Korea Foundation for the Advancement Science & Creativity and Science High School Research & Education Program(R2-2009-01-040).

**Dp-I-049****Thermal Analysis of the PLS II Crotch Absorber**

HA Taekyun, SHENG I. C.<sup>1</sup>, PARK C. D.

*Pohang Accelerator Laboratory. <sup>1</sup>NSRRC.*

The beam energy and design current of Pohang Light Source II (PLS II) will be 3 GeV and 400 mA respectively. With the design current, a total power of 7970 W is radiated by the circulating beam from a bending magnet. Only a small part of the synchrotron radiation from the bending magnet are extracted to the beamlines while the others are intercepted by the crotch absorbers. The PLS II storage ring crotch absorbers will be subjected to a very high photon loading power density of about 211 W/mm<sup>2</sup> at normal incidence. These absorbers which are made of copper alloy and water-cooled, should be designed to withstand the temperature and thermal stress induced by the high heat load. We designed a prototype of the crotch absorber to accommodate this heat load of PLS II and performed thermal analysis. The basic design and the detailed results are presented in this paper.

CHO J. H., CHOI B. C., YEO H. G.<sup>1</sup>, SUNG Y. S.<sup>1</sup>, KIM M. -H.<sup>1</sup>, SONG T. K.<sup>1</sup>, KIM S. S.<sup>2</sup>

*Department of Physics, Pukyong National University, Busan 608-737. <sup>1</sup>School of Nano & Advanced Materials Engineering, Changwon National University, Changwon, Gyeongnam 641-773. <sup>2</sup>Department of Physics, Changwon National University, Changwon, Gyeongnam 641-773.*

To improve the electrical properties in BiFeO<sub>3</sub> (BFO), the effects of ion doping have been studied. In this work, nonstoichiometric Bi(Fe<sub>1-x</sub>Ti<sub>x</sub>)O<sub>3</sub> ( $x = 0.0, 0.025, 0.05, 0.1, \text{ and } 0.2$ ) polycrystalline ceramics were prepared by the conventional solid state reaction method and their structural, dielectric, magnetic and ferroelectric properties have been investigated. The sintered ceramics have relative densities higher than 95% of theoretical values and decrease with Ti doping. From XRD experiments, phase transformation from rhombohedral to orthorhombic symmetry occurs at around  $x \sim 0.2$ . SEM images showed that Ti dopant initially significantly reduced the grain sizes and then saturates with the size of few  $\mu\text{m}$  above  $x = 0.025$  with porosities. The BiFeO<sub>3</sub> ceramic exhibited high dielectric permittivity. The dielectric anomaly in dielectric constant around Neel temperature shifted toward higher temperature with increasing Ti concentration. The values of loss tangent decrease as  $x$  increases at room temperature. Proper  $P$ - $E$  hysteresis loops of Bi(Fe<sub>1-x</sub>Ti<sub>x</sub>)O<sub>3</sub> samples were not observed due to low resistivity. Leakage currents were much decreased by about 5 orders of magnitude above  $x = 0.025$ . Similarly to the results of SEM images and dielectric constants, the leakage currents were also changed with Ti substitution.

CHOI Hyun Woo, UDDIN Md. Nizam<sup>1</sup>, YANG Yong Suk<sup>2</sup>

*Department of physics, Pusan National University. <sup>1</sup>Department of Nanomaterials Engineering, RCDAMP, Pusan National University. <sup>2</sup>Department of Nanomaterials Engineering, RCDAMP, Pusan National University.*

고유가, 자원의 유한성 및 환경오염 문제로 청정 에너지원의 개발이 요구되고 있으며 대체 에너지원 중 하나가 고체 산화물 연료전지(SOFC, Solid oxide fuel cell)이다. SOFC는 음극, 전해질, 양극, 연결재로 구성되고 고온에서 작동한다. 본 연구에서는 연결재로 사용이 가능한 Fe<sub>2</sub>O<sub>3</sub>-Mn<sub>2</sub>O<sub>3</sub>를 2:1, 1:2의 몰비율로 혼합하고 고온에서 열처리 하여 열기계/전기적 특성을 조사하였다. 열처리 시료에 대한 XRD 측정을 통하여 Fe<sub>2</sub>MnO<sub>4</sub>, FeMn<sub>2</sub>O<sub>4</sub>의 안정된 스피넬 상이 형성됨을 확인하였다. TEC(thermal expansion coefficients) 측정으로 온도 변화에 대한 열팽창계수가 각각  $1.09 \times 10^{-5}/^{\circ}\text{C}$ ,  $1.1 \times 10^{-5}/^{\circ}\text{C}$ 의 낮은 값으로 이는 강철의 열팽창계수와 매우 유사한 값을 가지는 것을 알 수 있었다. 또한, 고온에서 전지 구동 시 주위에 존재 가능한 공기, 질소, 유/무기물에 대한 화학적 안정성, 기공 형성, 그리고 이에 수반된 전기 특성을 조사 하였다.

**Dp-I-052****Crystal Structure Investigation on  $\text{LiH}_2\text{PO}_4$  by Neutron Diffraction at 100K**

OH In-Hwan, LEE Kwang-Sei<sup>1</sup>, MEVEN Martin<sup>2</sup>, HEGGER Gernot<sup>3</sup>, LEE Cheol Eui<sup>4</sup>

*Korean Atomic Energy Research Institute, Neutron Science Division. <sup>1</sup>Inje University, Department of Nano System Engineering. <sup>2</sup>FRM II, Technische Universitaet, Germany. <sup>3</sup>RWTH Aachen, Institut fuer Kristallographie. <sup>4</sup>Korea University, Department of Physics and Insitute for Nano Science.*

$\text{LiH}_2\text{PO}_4$  is known as a member of the famous  $\text{KH}_2\text{PO}_4$  (KDP) family, which shows remarkable ferroic properties due to the ordering of the H, D atoms in short O – (H,D) ... O hydrogen bonds. Generally, this family member has a phase transition caused by the hydrogen atom ordering. However, in LDP all hydrogen atoms are already ordered in all temperature ranges. Thus, no phase transition has been reported. In addition, the conductivity in LDP at room temperature shows a relatively higher value compared to related KDP family members such as ADP, KDP and CDP. It was believed that the small ionic radius and the mobility of Li atoms in this structure could be responsible for the high conductivity. But according to our former investigation by using neutron diffraction on LDP single crystal, Li atoms are very stable at room temperature. To investigate and confirm this unusual behavior of Li atoms, we carried out the single crystal investigation on LDP by neutron diffraction at 100 K on HeiDi at FRM II, Garching, Germany.

A large single crystal of about  $2 \times 1 \times 2 \text{ mm}^3$  was studied. LDP crystallizes in space group  $\text{Pna}2_1$  with  $a = 6.230(8)$ ,  $b = 7.623(3)$ ,  $c = 6.8752(5)$ ,  $Z = 4$ . In this study, the result at 100 K will be compared to the measurement at 300 K and discussed.

**Dp-I-053****Role of Symmetry in Thermal Transport Properties of Graphene Nanoribbons**

OH Sang Soon, CHOI Choon-Gi, CHOI Sung-Yool

*Convergence Components & Materials Research Lab, Electronics and Telecommunications Research Institute.*

Recently, the thermoelectric properties of nanostructure such as graphenes, silicon nanowires and single molecules have attracted much attention due to the experimental and theoretical importance of various scattering mechanisms in electrical transport properties and the potential applications in the field of energy devices. In this presentation, we calculate the thermopower (S) and the figure of merit (ZT) of zigzag graphene nanoribbons (ZGNR) with different widths ( $N=4,5,6,\dots$ ) using the density functional theory calculation and the non-equilibrium Green's function formalism. The thermal transport coefficients are calculated using the Landauer-Büttiker formalism. To investigate the role of geometrical symmetry of ZGNR in thermal transport properties, we changed bias voltages which create conductance gap for the symmetric ZGNR, i.e., when  $N$  is even. From the calculated thermopower and figure of merit, it is shown that the thermal transport properties of ZGNRs also dramatically change depending on the geometric symmetry under bias voltages.

## glasses

OH S. J., CHOI H. W.<sup>1</sup>, SONG C. H.<sup>2</sup>, LEE S. M.<sup>2</sup>, YANG Y. S.<sup>3</sup>*한국과학기술원. <sup>1</sup>부산대학교, 물리학과. <sup>2</sup>부산대학교, 나노융합기술학과. <sup>3</sup>부산대학교 나노정보소재공학과.*

Tellurite and borate glasses have been attracted attention because of their potential application as laser host, nonlinear optics, optical fiber amplification, optical guide. It has been known that those optical properties have close relationship with the bonding nature and dielectric phenomena of glasses. We fabricated the mixed glasses of tellurite and borate with different mole ratio, and measured thermal and dielectric properties by using differential scanning calorimetry and impedance gain analyzer. Jonscher's power law and impedance Cole-Cole model were adopted to analyze the dc and ac electrical response while changing temperature. As temperature and concentration change, systematic variations both in conductivity and thermal response were found. Analysing procedure by using those two models will be presented in detail.

HA Taekyun, SHENG I. C.<sup>1</sup>, PARK C. D.*Pohang Accelerator Laboratory. <sup>1</sup>NSRRC.*

The 3 GeV Pohang Light Source II (PLS II) storage ring crotch absorbers will be subjected to a very high photon loading power density. The absorbers should be designed to withstand the temperature and thermal stress induced by the high heat load. The mostly used design criterion is that the thermal stress in the absorber is lower than the elastic limit of the material. However this criterion is known to be too conservative for the synchrotron radiation thermal absorber. An appropriate design requirements for the PLS II crotch absorber is proposed in this paper.

**Dp-I-056****Secondary electron generation in electron-beam-irradiated solids**

LEE Cheol Eui, KIM Jin Soo, LEE Kyu Won

*Korea University, Physics.*

We have investigated the secondary electron generation in electron-beam-irradiated solids by means of Monte Carlo simulation. The slow secondary electron energy was found to be independent of the position and incidence energy of the electron beam, and the electron beam broadening in thin films by the secondary electrons was found to be at least 5-10 nm, setting limits to the nanolithographic resolution. This work was supported by the Seoul Research and Business Development Program, Grant No. 10583.

**Dp-I-057****비정질 유전체  $2(\text{Ba}_{1-x}\text{Ca}_x\text{TiO}_3)\text{-SiO}_2$ 의 몰 비율에 따른 열 및 유전 특성 변화**고 재현<sup>1</sup>, 송 철호<sup>1</sup>, 김 영훈<sup>1</sup>, 양 용석<sup>1</sup>*부산대학교 나노정보소재공학과. <sup>1</sup>부산대학교 나노융합기술학과.*

강유전체는 우수한 유전, 압전, 광학 성질을 가지고 있어 많은 전자 기기와 광학 소자의 응용되고 있다. 특히 그 중에서도  $\text{Ba}_{1-x}\text{Ca}_x\text{TiO}_3$ 는 메모리소자, 세라믹 축전기, tunable microwave 소자 등 많은 곳에서의 응용 가능성을 가지고 있어 단결정, 다결정, 박막 등의 형태로 연구가 진행되고 있다. 하지만  $\text{Ba}_{1-x}\text{Ca}_x\text{TiO}_3$ 의 비정질에 대한 연구는 거의 이루어지지 않고 있다. 그러나 비정질에 대한 연구는 나노 계를 이해하는 데 필수적일 뿐만 아니라 나노 크기를 제조하는 가장 좋은 방법 중의 하나가 비정질의 결정화를 이용하는 것이기 때문에 나노 소재 및 소자 개발에 있어서 매우 중요하다. 따라서 이번 실험에서는 유리 형성제인  $\text{SiO}_2$ 를 첨가하여 다양한 몰 비율의 비정질  $2(\text{Ba}_{1-x}\text{Ca}_x\text{TiO}_3)\text{-SiO}_2$  ( $x = 0, 0.1, 0.3, 0.5, 0.7, 0.9, 1$ )를 쌍 롤러 냉각법을 통해 제조하였다. 제조된 비정질  $2(\text{Ba}_{1-x}\text{Ca}_x\text{TiO}_3)\text{-SiO}_2$ 는 시차열분석기를 이용하여 몰 비율에 따른 열 특성 ( $T_g, T_c, \Delta T = T_c - T_g$ )을 분석하였고, 임피던스 분석기를 이용하여 주파수와 온도에 따른 유전 특성을 측정하였다. 분석 결과, 한 온도에서의 dc 전도도의 값과 보편법칙을 통해 구한 전기전도에 대한 활성화 에너지가 몰 비율에 따라 비선형적인 관계를 가졌다.

CHOI Jeongyong, KIM Bong-Jun, KIM Hyun-Tak, CHO Sunglae<sup>1</sup>

*Tera Electronics Research Team, Electronics and Telecommunications Research Institute. <sup>1</sup>Department of Physics, University of Ulsan.*

For the past many decades, Mott metal-insulator transition (MIT) has been widely studied for the mechanism of high-T<sub>C</sub> superconductivity and colossal magnetoresistance. Currently, MIT has been renewal of interest for switching devices, power transistors, and nonvolatile memory with the phenomena of current jump. VO<sub>2</sub>, which was a representative in MIT, has been investigated transport property such as electrical resistance and Hall carrier density on the peculiar states as function of temperature, using ordinary and anomalous Hall effect method. In the most of all, electrons was existed as majority carriers in VO<sub>2</sub>. But we have observed the change of the dominant carriers on the near boundary of critical point of MIT through Hall effect and thermopwer measurement. In this talk, we report electrical and thermal properties of VO<sub>2</sub> thin film, which was approximately 100 nm of thickness, on (1010) Al<sub>2</sub>O<sub>3</sub> substrate with sputtering system. Carrier density and type of VO<sub>2</sub> thin film was observed between the critical temperature using physical property measurement system (PPMS, Quantum Design). The temperature-dependent Hall effect and thermopower of VO<sub>2</sub> will be discuss in detail.

**Ep-I-001****Study of the Electron-Phonon Interactions and Vibrational Modes in Insulating****Nanoparticles**하 명규, 홍 경수, 정 의덕, 양 호준<sup>1</sup>한국기초과학지원연구원 부산센터, <sup>1</sup>부산대학교 물리학과.

We discussed the temperature and particle size dependence of linewidths and vibrational modes in nanoparticles. We calculated the size- and temperature-dependence of the electron-phonon interactions, assuming a two-phonon Raman scattering mechanism, which provides a good description of the obtained experimental results regarding the linewidth. We compared the results of optical dephasing measurements by using transient spectral hole burning with the results of calculations as a function of temperature of the samples for various particle sizes of  $\text{Eu}_2\text{O}_3$  nanoparticles. We assumed an electron-phonon interaction dominated by two-phonon Raman scattering and used the discrete low frequency normal modes of a homogeneous spherical nanocrystal in the calculation. Also we included the effect of the size restriction on the vibrational eigenstates and the electron-phonon interactions. The contribution to the linewidth of all the modes is summed using Fermi's golden rule. The best fit to the experiment occurs assuming that the bandwidth is proportional to  $\omega_{\text{in}}^2$  leading approximately to a linewidth proportional to  $T^3$  and  $d^{-2}$ . We calculated vibrational modes under stress-free boundary conditions in nanoparticles. The lowest lying transverse modes have large amplitude near the surface as the angular momentum increases. For the upper branches, we observed the surface modes as well as the inner modes in both transverse and longitudinal modes.

**Ep-I-002****Fabrication of ordered arrays of double layer nanodots composed of two metals****by physical vapor depositon**

KIM kwang sub, JANG un jung, LEE chang young

동아대학교 신소재 물리학과 초미세표면물리실험실.

나노 다공성 알루미늄 박막을 주형으로 이용하고, 단결정 Si의 [1, 0, 0]면을 기판으로 사용하여 물리적 기상 증착방법으로 이중층 구조의 금속 나노점 배열 구조를 제작하였다. 제작된 나노점들은 Al/Cu와 Ag/Cu의 이중층구조이다. Al, Ag, Cu의 융점들은 각각 660, 960과 1083 °C이다. 이렇게 융점이 서로 다른 금속들을 동시에 진공 가열하게 되면 융점이 낮은 순서대로 증발하여 기판 상에 증착될 것이기 때문에 이중층 구조의 나노점이 형성될 것이라는 점을 이용하였다. 제작된 이중층 구조의 금속 나노점들의 형태와 성분 분석은 SEM과 AFM, EDS, TEM으로 측정 분석하였다

**Ep-I-003****Electrical Current Suppression of Pd-doped Vanadium Pentoxide Nanowire Network Due to Hydrogen Adsorption**

김 병훈, 오 순영, 정 후영, 유 한영, 윤 용주, 김 약연, 홍 원기, 이 정용<sup>1</sup>

한국전자통신연구원. <sup>1</sup>KAIST.

Functionalization of the nanowires and nanotubes with metal is one of the methods to improve the performance of the nano-scaled devices such as gas sensors. Vanadium pentoxide nanowires (VON) have been reported as a gas-sensing material. Here, we report that the variation of current-voltage ( $I$ - $V$ ) characteristics of Pd-doped VON (Pd-VON) with various gases (He, Ne, Ar, N<sub>2</sub>, O<sub>2</sub>) including hydrogen gas. Especially, the current of Pd-VON is significantly suppressed by exposure to hydrogen gas.

P1

포  
스  
터  
세  
션

**Ep-I-004****Measurement of Carbon Soot Mass Distribution using High Resolution FT-ICR-Mass Spectrometer**

민 경철, 최 명철

한국기초과학지원연구원 질량분석 개발팀.

We have reserched mass distribution of carbon soot from buthane using FT ICR-Mass Spectrometer. Mass spectrum showed a principal carbon cluster pattern with a spacing of 24 mass unit(Da) in the range of 720-3000 m/z. Even numbered carbon cluster positive ions were founded and they showed distinct monoisotope mass which afford to compare theoretical mass to experimental mass of carbon aggregates. We expect that this study could attribute aquiring the exact mass number of interested materials.

**Ep-I-005****Diameter Effect on the Electrical Property of Single-walled Carbon Nanotubes****Networks**JANG DONG KYU, HWANG DOO HEE<sup>1</sup>, KIM SUN KUG, LEE CHEOL JIN<sup>2</sup>*School of Electrical Engineering, Korea University. <sup>1</sup>Department of Micro/Nano Systems, Korea**University. <sup>2</sup>School of Electrical Engineering and Department of Micro/Nano Systems, Korea University.*

Diameter control of single-walled carbon nanotubes (SWCNTs) produced by arc-discharge method is important for various applications. There have been many trials to realize diameter controlled growth of SWCNTs using arc-discharge but no successful result until now. We studied synthesis of diameter controlled SWCNTs using an arc-discharge method. Especially, we tried the diameter control of SWCNTs by using different kind of catalysts. The SWCNTs with a small diameter (a.v. diameter is 1.20nm) were synthesized at the condition of a mixture of Ni and Y catalyst in helium ambient. SWCNTs with more increased diameter (a.v. diameter is 1.53nm) were synthesized by using Fe catalyst in hydrogen ambient. And SWCNTs with a very large diameter (a.v. diameter is 2.01nm) were synthesized using a mixture of Fe catalyst and Bi promoter in hydrogen ambient. We fabricated CNT films using SWCNTs with different diameter from a filtration method. And then, we transferred each SWCNT films on the plastic substrate. Sequentially, we separated the SWCNT films on the substrate using nitric acid. Finally, we evaluated a sheet resistance of the SWCNT films. The sheet resistance of small diameter SWCNT film showed 5000~7000Ω/sq at 70~80% transmittance. And middle diameter SWCNT film showed 800~1000Ω/sq at 70~80% transmittance. The large diameter SWCNT film showed 200~400 Ω/sq at 70~80% transmittance. In this work, we found that the electrical property of SWCNT films is strongly dependent on the diameter of SWCNTs.

**Ep-I-006****Formation and Thermal Properties of Amorphous  $\text{Ti}_{40}\text{Cu}_{40}\text{Ni}_{10}\text{Al}_{10}$  Alloy Powder****by Mechanical Alloying**

김 현구, 나 도선, 박 경화, 공 현식, 송 보미

*조선대학교 물리교육과.*

The amorphization process and thermal properties of amorphous  $\text{Ti}_{40}\text{Cu}_{40}\text{Ni}_{10}\text{Al}_{10}$  powder during milling by mechanical alloying were examined by X-ray diffractometry(XRD), differential scanning calorimetry(DSC), and transmission electron microscopy(TEM). The chemical composition of the samples was examined by an EDX facility attached to the SEM. The as-milled powders showed a broad peak( $2\theta = 42.4^\circ$ ) with about crystalline size of about 4.5 nm in the XRD patterns. The entire milling process could be divided into three different stages, : agglomeration, disintegration, and homogenization. In the DSC experiment,  $T_p$  and  $T_x$  were 466.9°C and 444.3°C for HR=10 °C/min, respectively, and the values of  $T_p$  and  $T_x$  increased with heating rate for the as-milled powder. The activation energies of crystallization for the as-milled powder was 291.5 kJ/mol.

**Ep-I-007****Electrochemical Corrosion Behaviors of Amorphous  $\text{Co}_{69}\text{Fe}_{4.5}\text{Ni}_{1.5}\text{Si}_{10}\text{B}_{15}$  Alloy****Produced by Quenching Method**

김 현구, 공 현식, 송 보미, 명 화남<sup>1</sup>, 장 희진<sup>2</sup>

조선대학교 물리교육과. <sup>1</sup> 전남대학교 물리학과. <sup>2</sup> 조선대학교 금속재료공학과.

The corrosion behavior of amorphous  $\text{Co}_{69}\text{Fe}_{4.5}\text{Ni}_{1.5}\text{Si}_{10}\text{B}_{15}$  alloy ribbon was examined as functions of solution temperature, pH, and oxygenation time. The results of potentiodynamic polarization tests in  $\text{H}_2\text{SO}_4$  solution, NaCl solution, and HCl + NaOH solution at various pH showed that the corrosion resistance for alloy ribbons exponentially deteriorated with increasing temperature and decreasing pH for given conditions. Oxygenation of solution caused increase of corrosion potential and corrosion rate but the effects seemed to be saturated before 20 min of oxygenation

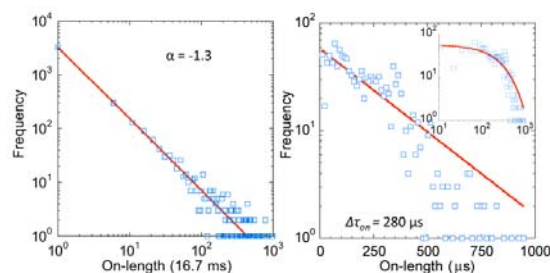
P1

포  
스  
터  
세  
션**Ep-I-008****Blinking Kinetics of Single CdSe/ZnS Nanocrystals Interpreted Using Different****Temporal Resolutions**

LEE SANG YUN, HAYASHI TOMOHIRO<sup>1</sup>, HARA MASAHICO

RIKEN, Flucto-Order Functions Asian Collaboration Team. <sup>1</sup>Tokyo Institute of Technology, Department of Electronic Chemistry.

Despite the predicted single exponential kinetics, fluorescence intermittency (blinking) of single semiconductor nanocrystals (NCs) have been subject to the universal power-law kinetics. Recently, we have reported that blinking of CdSe/ZnS NCs can be interpreted in terms of photon intervals at high temporal resolution of tens of microseconds by fast imaging on the NCs, which leads to single exponential kinetics. In this presentation, we employ tens of microseconds and tens of milliseconds to demonstrate that the blinking profiles can be described by short-term events, which contribute to the long-term “on” and “off” events as in the conventional interpretations. These results suggest that the temporal-resolution plays an important role in the interpretation of the blinking kinetics.



**Ep-I-009****Raman Study of ETS-10 and Titanate Quantum Wires**LIM Hyunjin, CHEONG Hyeonsik, JEONG Nak Cheon<sup>1</sup>, YOON Kyung Byung<sup>1</sup>서강대학교, 물리학과. <sup>1</sup>서강대학교, 화학과.

Nano-materials, especially quantum wires, have been studied extensively due to their interesting properties and the potential for applications to optoelectronic devices, high speed semiconductors, and so on. However, since nano-materials have extremely small sizes on the order of molecular dimensions, the charge transfer interaction between the environment and the quantum wire significantly affects the physical properties of the quantum wire. The electron injection into the quantum wires from their surroundings gives rise to changes in the vibrational frequency and the band-width. In this study, we changed the environment of titanate quantum wires in ETS-10 with ion (cation)-exchange and hydration. ETS-10 is a nanoporous titanate silicate that contains periodically positioned quantum wires (-Ti-O-Ti-O-) running along the two perpendicular directions in the crystal. We obtained Raman spectra as the cations are exchanged to K<sup>+</sup>, Na<sup>+</sup>, Ba<sup>+</sup>, Sr<sup>+</sup>, Ca<sup>+</sup>, Mg<sup>+</sup>, Pb<sup>+</sup>, Cd<sup>+</sup>, and Zn<sup>+</sup> in ETS-10 crystals. The longitudinal stretching vibrational frequency of the titanate quantum wires of pristine ETS-10 crystal is 724 cm<sup>-1</sup>, but the vibrational frequency shifted and the band-width changed as the cations were exchanged or the crystals were hydrated. In addition, we also observed the relationship between the electronegativity and the longitudinal vibration frequency and the band-width.

**Ep-I-010****MWCNT를 이용한 에탄올 가스센서의 제작**장 경욱, 최 명규, 김 상걸<sup>1</sup>, 김 태완<sup>2</sup>, 정 동화<sup>3</sup>, 안 준호<sup>4</sup>경원대학교 전기공학과. <sup>1</sup>특허청. <sup>2</sup>홍익대학교. <sup>3</sup>송파공업고등학교. <sup>4</sup>한국전력기술연구원.

본 연구에서는 화학적으로 안정된 MWCNT를 이용하여 에탄올 감응 가스센서를 만들고, 제작된 센서에 대해서 미세 구조적 측면, 전기 및 광학적 측면 그리고 분자 흡착 특성을 분석하여 그 특성을 파악 하고자 하였다. 가스센서는 에탄올 유기 용제를 이용하여 분산된 MWCNT 용액을 만들고, 이 분산 용액을 스프레이 방법으로 유리 기판위에 성막하여 제작하였다. 제작된 박막에 대해 SEM 분석을 통하여 미세구조 특성을 분석하였으며, 4프로브법으로 박막의 전기저항을 측정하였다. 제작된 박막을 가스센서로 활용하기 위해서 마스크를 이용하여 150마이크로미터의 전극간 거리를 갖도록 금전극을 박막 표면에 스퍼터링하여 증착 하였다. 제작된 가스센서는 20 마이크로리터의 에탄올을 주입한 정지계 가스 검출 시스템내에 장착하여 센서표면에 에탄올 분자의 흡착 정도에 따라서 박막의 저항율이 변화하는 특성을 이용하여 가스 검출 특성을 측정 하였다. 그림 1은 6 ppm 에탄올 가스 분위기에서 시간에 따른 센서의 감응 특성을 보이고 있다.

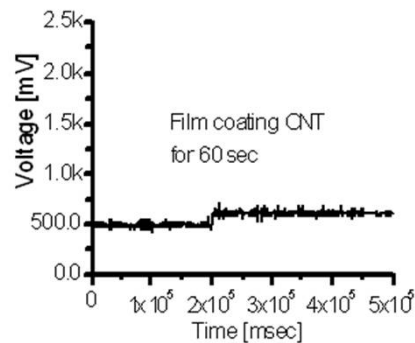


그림 1. 6 ppm 에탄올 가스 분위기에서 시간에 따른 센서의 감응특성

Fig. 1. The response properties of sensor in 6 ppm ethanol gas ambient

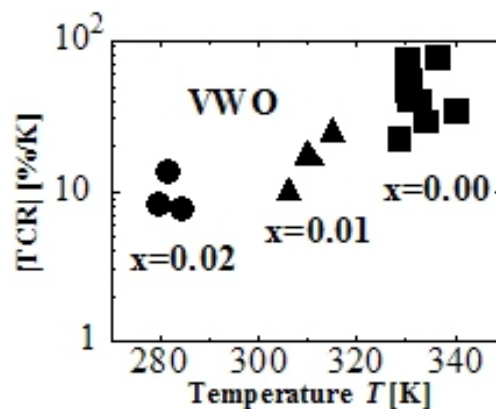
**Ep-I-011****Control of Giant Metal-Insulator Transition at Room Temperature on W Doped****VO<sub>2</sub> Thin Films**

TAKAMI Hidefumi, KANKI, Teruo, CHA Nam-Goo,

TANAKA Hidekazu

Osaka University.

The strongly correlated vanadium dioxide (VO<sub>2</sub>) which shows the giant metal-to-insulator transition is a good material for heat sensing devices, such as bolometer. Because it has a dynamic change of resistivity originated from the phase transition. Nevertheless, we need to control the phase transition to make it occur at room temperature because the phase transition temperature ( $T_p$ ) is 340[K] which is higher than room temperature. The practical oxygen deficient VO<sub>x</sub> thin films have the -2[%/K] TCR (temperature coefficient on resistivity defined as  $(1/\rho)(d\rho/dT)$ ) at around room temperature. This time, we fabricated tungsten doped VO<sub>2</sub> epitaxial thin films V<sub>1-x</sub>W<sub>x</sub>O<sub>2</sub> on Al<sub>2</sub>O<sub>3</sub> (0001) substrate to obtain the high TCR at room temperature. V<sub>1-x</sub>W<sub>x</sub>O<sub>2</sub> (x=0, 0.01, 0.02) thin films were fabricated by using Pulsed Laser deposition technique. It was confirmed that each thin film grew with (010) preferential orientation on Al<sub>2</sub>O<sub>3</sub> (0001) substrate by X-ray diffraction measurements. Fig. shows the dependence of TCR on transition temperature with various x samples. High TCR of -10% was achieved at room temperature in the x=0.01 sample. We discuss this control mechanism based on change of electronic structure with the doping ratio of W

**Ep-I-012****Fabrication and Characterization of MoO<sub>3</sub>, H<sub>x</sub>MoO<sub>3</sub> Nanorods Metal-****Insulator-Semiconductor (MIS) Capacitors**

SHAKIR Imran, MUHAMMAD Shahid, 이 강우, 강 대준

BK21 Physics Research Division, Department of Energy Science, Institute of Basic Science, SKKU Advanced Institute of Nanotechnology and Center for Nanotubes and Nanostructured Composites, Sungkyunkwan University, Suwon 440-746, Korea.

Metal-insulator-semiconductor (MIS) capacitors were fabricated with MoO<sub>3</sub> and H<sub>x</sub>MoO<sub>3</sub> nanorods on p-type SiO<sub>2</sub> substrates which have been synthesized by using simple hydrothermal method. The MIS capacitors configuration consists of 20 nm of insulating layer of ZrO<sub>2</sub> on the MoO<sub>3</sub> and H<sub>x</sub>MoO<sub>3</sub> nanorods which was deposited by using sputtering system. The electrical properties of this MIS diode were characterized by using capacitance-voltage (C-V) measurements, and the typical C-V hysteresis with voltage gap of about 2.5 V appeared at room temperature. The C-V measurements showed that the capacitance of the capacitor was increased from 1356pF to 3188pF with hydrogen doping in MoO<sub>3</sub> (Fig.1). These electrical properties imply that the use of MoO<sub>3</sub> nanorods can be used to make viable storage systems that provide both high energy density and high power density.

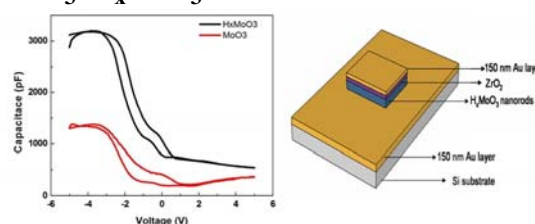


Figure 1. (a) Typical C-V characteristics of MIS devices with MoO<sub>3</sub> and H<sub>x</sub>MoO<sub>3</sub> nanorods measured at room temperature, (b) Details of the device structure.

**Ep-I-013****Chemical Solution Deposition Synthesis and Optical Properties of Single Crystalline Complex Metal Oxide  $\text{BaCuV}_2\text{O}_7$  Nanowires**

SHAKIR Imran, SHAHID Muhammad, 강 대준  
BK21 Physics Research Division, Department of Energy  
Science, Institute of Basic Science, SKKU Advanced Institute  
of Nanotechnology and Center for Nanotubes and  
Nanostructured Composites, Sungkyunkwan University,  
Suwon 440-746, Korea.

The synthesis of single crystalline complex metal oxides  $\text{BaCuV}_2\text{O}_7$  nanowires were attained by using surfactant free, economically favorable chemical solution deposition method.

A thin layer of  $\text{BaCuV}_2\text{O}_7$  nanocrystals is formed by the decomposition of complex metal oxide solution at  $150^\circ\text{C}$  to provide nucleation sites for the growth of nanowires. The synthesized nanowires were typically  $1\text{--}5\ \mu\text{m}$  long with diameters from 50 to 150 nm (Fig.1 (a)). It was found that by simply controlling the temperature and thickness of the coated film, we can easily obtain high quality  $\text{BaCuV}_2\text{O}_7$  nanowires. The optical band gap 3.6 eV of the nanowires was calculated from the optical transmission spectra. The temperature dependent resistances of  $\text{BaCuV}_2\text{O}_7$  nanowires agree with the exponential correlation, supporting that the conducting carriers are the quasi-free electrons (Fig.1 (b)). We believe that our methodology will provides a simple and convenient route for the synthesis of variety of complex metal oxides nanowires with controlled stoichiometry.

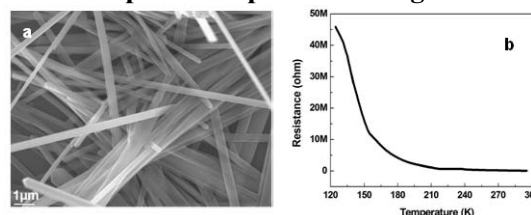


Fig. 1 (a) FE-SEM image of the  $\text{BaCuV}_2\text{O}_7$  nanowires, (b) Temperature dependence of resistance (R) of  $\text{BaCuV}_2\text{O}_7$  nanowires (below 300 K).

**Ep-I-014****Particle Size Regulation of Magnetic Nano-particles Synthesized by Aqueous Solution Method, and Their MR Contrast Properties**

KANG Jongeun, KIM Younghan, MOON Hyeyoung, HONG Kwan Soo<sup>1</sup>

Korea Basic Science Institute, MRI Team. <sup>1</sup>Korea Basic Science Institute, MRI Team; Chungnam National University, Graduate School of Analytical Science and Technology.

Magnetic nano-particle (MNP)-based MR (magnetic resonance) imaging contrast agent has been the subject of extensive research fields over the past decade. The iron-oxide particle size of this contrast agent varies widely, and influences their physicochemical and pharmacokinetic properties. There are well known two ways to synthesize magnetic MNPs, which are organo-metallic and aqueous solution co-precipitation methods. The former has an advantage in controlling particle size, and a disadvantage that the particle should be coated with hydrophilic compound to make it soluble in water. The MNPs made by the latter method are intrinsically water-soluble, but they have relatively wide particle size distribution. Size-controlled water-soluble MNPs may give us a lot of possibilities in MRI contrast agents, cell sorting and labeling applications. We synthesized  $\text{CoFe}_2\text{O}_4$  NPs by the aqueous solution co-precipitation method, then the MNPs were separated to four-sized groups by centrifugation depending on the spinning speed between 4,000 and 18,000 rpm. The crystal shapes and size distributions of the MNPs were measured and confirmed by TEM (transmission electron microscopy) and DLS (dynamic light scattering) measurements. The MNPs have inverse spinel structure which was confirmed by XRD (X-ray diffraction) measurement. The diameter distributions of the four groups were gaussian-like, and they were  $19\pm 4$ ,  $24\pm 5$ ,  $41\pm 8$ ,  $70\pm 15$  nm. Size-dependent MR contrast property ( $T_2$  relaxivity) was measured on 4.7 T MRI system, and the relaxivity was increased with the particle size in the range between 60 and  $300\ \text{mM}^{-1}\text{s}^{-1}$ . The saturation value of the  $T_2$  relaxivity with particle size was about  $320\ \text{mM}^{-1}\text{s}^{-1}$ . This size-regulation method may open wider applications with relatively homogeneous-sized MNPs made by aqueous solution co-precipitation method.

**Ep-I-015****수직자기이방성을 갖는 비정질 강자성체 CoSiB/Pt 다층박막의 자기적 특성 연구**박 지선, 황 재연<sup>1</sup>, 이 승백<sup>1</sup>, 김 태완<sup>2</sup>, 임 혜인숙명여자대학교 물리학과, <sup>1</sup>한양대학교 전자통신컴퓨터공학부, <sup>2</sup>세종대학교 신소재공학과

스핀전달토크 (Spin transfer torque, STT)를 고밀도 자기기록매체의 읽기헤드나 자기센서로 이용하기 위하여 수직자기이방성 (Perpendicular magnetic anisotropy, PMA)에 기반을 둔 자기터널접합 (Magnetic tunnel junctions, MTJs)이 고밀도 MRAM (magnetic random access memory)을 상용화할 수 있는 가능성 있는 후보로 널리 연구되고 있다 [1]. STT를 이용한 고밀도 MRAM의 가장 중요한 이슈는 큰 신호전압과 열적 안정성 (thermal stability) 확보이다 [2]. 이를 위해 다음과 같은 해결책이 연구되고 있다. 첫째는, 큰 신호전압을 위해 터널자기저항비 (Tunneling magnetoresistance, TMR)가 큰 MTJs 제작에 있어 각 층 사이의 평탄한 계면을 유지하기 위해 비정질의 강자성체 물질을 개발하는 것이다. 또한 높은 열적 안정성을 갖기 위해 높은 PMA 값을 갖는 새로운 물질 개발이 이루어지고 있다. 본 연구에서는 새로운 비정질 합금  $\text{Co}_{75}\text{Si}_{15}\text{B}_{10}$ 을 소개하고, 이 물질을 이용하여 큰 PMA를 갖는  $[\text{CoSiB } t_{\text{CoSiB}}/\text{Pt } t_{\text{Pt}}]_n$  다층박막의 구조 및 자기적 특성을 조사하였다. 6개의 타겟이 장착된 dc 스퍼터링 장치를 사용하여 (a) CoSiB 1000 단일박막과 (b) Si/SiO<sub>2</sub>/Pt 30/[CoSiB  $t_{\text{CoSiB}}/\text{Pt } t_{\text{Pt}}]_n/\text{Ta } 50$  (in Å) 다층박막을 제작하였다. 기본진공도는  $2 \times 10^{-7}$  Torr 이하, 공정압력은  $2 \times 10^{-3}$  Torr를 유지하였다. (a)는 비정질인 CoSiB의  $M_s$  값과 온도에 따른 결정 구조 변화를 알아보기 위해 증착 후  $5 \times 10^{-4}$  Torr 진공에서 자기장 300 Oe를 걸어주며 3시간 동안 다양한 온도에서 열처리를 진행하였다. (b)는 CoSiB과 Pt 두께와 반복 층수에 따른 PMA 의존성을 조사하기 위해 각 층의 두께를 달리하면서 여러 층을 갖는 다층 박막을 제작한 후 VSM과 XRD 측정을 통해 시편의 자기적 특성 및 결정구조를 조사하였다. Si/SiO<sub>2</sub> 기판 위에 제작한 1000 Å 두께의 비정질 강자성체 CoSiB 단일박막의 자기이력 특성 결과로 계산된 CoSiB의  $M_s$  값은 407 emu/cm<sup>3</sup>이었고, 열처리 후 XRD로 관찰해 본 결과, 350 °C까지 비정질 특성을 나타냄을 알 수 있었다.  $[\text{CoSiB } 3 \text{ Å}/\text{Pt } 14 \text{ Å}]_5$  구조에서 가장 높은 보자력( $H_c$ ) 224 Oe와  $2 \times 10^6$  erg/cm<sup>3</sup>의 높은 수직이방성 상수( $K_u$ )를 얻었다. 보자력은 CoSiB의 두께가 증가하면서 커지다가  $t_{\text{CoSiB}} = 3 \text{ Å}$ 일 때 최대값을 갖고 다시 감소하였다. 이에 반해, Pt 두께 ( $t_{\text{Pt}} = 10 \sim 16 \text{ Å}$ )나 반복횟수 ( $n = 1 \sim 20$ ) 변화는 보자력 변화에 큰 영향을 주지 않는 것으로 나타났다.

**Ep-I-016****양성자 빔을 이용한 백금 나노 입자 사이즈 제어 연구**정 명환, 나 세진, 김 계령, 채 근석<sup>1</sup>, 민 명기<sup>1</sup>한국원자력연구원 양성자기반공학기술개발사업단, <sup>1</sup>(주)삼성 SDI

백금 나노 입자는 벌크 상태의 물질에 비해서 독특한 전자기적, 광학적 특성을 가지며 촉매, 광촉매, 센서 등 광학적, 전자기적 장치등 많은 부분에 적용을 할 수 있으며 이러한 장점때문에 최근에 많은 연구가 진행되고 있다. 백금 나노 입자의 촉매 반응은 나노입자의 사이즈와 모양에 따라 크게 차이가 나기 때문에 백금 나노 입자의 사이즈와 모양을 조절하는 기술은 나노 입자 응용에 있어서 상당히 중요하다. 나노입자 제조는 주로 화학적, 광화학적 환원법 및 방사선 조사에 의한 환원에 의해서 제조가 이루어지고 있다. 백금 나노 입자 제조의 경우 국내에서 전자빔을 이용하여 백금 나노 입자를 제조하는 실험이 실시되었지만 사이즈와 모양을 조절할 수 있는 기술은 아직 확보되지 않은 상태이다. 본 연구에서는 양성자 빔을 백금 수용액에 조사하여 백금 나노 입자를 제조하고 나노 입자 사이즈와 모양을 제어할 수 있는 양성자 빔 조사 조건에 대해서 연구를 진행하였다.

**Ep-I-017****Adsorption Properties of Hydrogen on Alq3 and its Derivatives: Ab Initio Study**

KANG Seoung-Hun, KO Yoo Sun, PARK Sora, KWON Young-Kyun

*Department of Physics and Research Institute for Basic Sciences, Kyung Hee University.*

Hydrogen, which is clean and renewable energy carrier, is expected to replace fossil fuels in near future. However, hydrogen storage is a bottleneck to achieve this. For potential use as hydrogen storage, we investigate the adsorption properties of hydrogen molecules on Tris(8-hydroxyquinolino)aluminium(III) abbreviated Alq3 using density-functional formalism. Alq3 is known to form two stereoisomers, meridional and facial isomers as well as several polymorphs. We examine the stability and dynamical sorption-desorption process of H<sub>2</sub> molecules on various Alq3. We also investigate hydrogen adsorption on similar structures with transition metal atoms replacing Al in Alq3 for better hydrogen storage system.

**Ep-I-018****Cathodoluminescence of Single ZnO nanorods**

LEE Cheol Eui, LEE Su Chul, LEE Eunmo

*Korea university.*

Zinc oxide (ZnO) nanorods were synthesized via a hydrothermal process. The variation of ultraviolet (UV) and green emission of single ZnO nanorods was investigated by using post-annealing treatment at various temperatures. The morphology of single ZnO nanorods was observed using environment scanning electron microscopy (E-SEM) and the optical properties were studied by using cathodoluminescence (CL) in situ. As the post-annealing temperature increased, the UV peak (at 380 nm) was blueshifted while a visible peak (at 570 nm) was redshifted in the CL spectra. The side walls of the ZnO nanorods were irradiated for 300 s and 1200 s by using 5-kV and 18-nA e-beam irradiation, the CL spectra being recorded for every 300s. The UV peak intensity increased linearly while the visible peak did not change.

## temperature

JIN Meihua, JEONG Hae-Kyung, SO Kang Pyo<sup>1</sup>, KIM Tae-Hyung, LEE Young Hee

*Sungkyunkwan University, BK21 Physics, Department of Energy Science, Center for Nanotubes and Nanostructured Composites. <sup>1</sup>Sungkyunkwan University, BK21 Physics, Department of Energy Science, Center for Nanotubes and Nanostructured Composites, Sungkyunkwan Advanced Institute of Nanotechnology.*

Graphene has been much interest in experiment and theory because of the unique properties of it. Graphene sheets can be easily made from micro-mechanical exfoliation of highly ordered pyrolytic graphite (HOPG), chemical vapor deposition, and chemical & thermal exfoliation methods. Among the methods, the last method was investigated actively due to the mass production of graphene sheets. However, one drawback of the method is to use high temperature in a process of annealing which is more than 900 C. We recently developed new method in which expanded graphene sheets or functionalized graphene sheets were synthesized at the lower temperature than others. In our talk, we will show the synthesis method and characterization of the functionalized graphene sheets in detail.

## toluene droplet by using ultrasonic nebulizer.

YEO Seung Jun, CHO Dae Hee, PODE Ramchandra, AHN Jeung Sun

*Kyung Hee univesity, Physics.*

From the in-depth investigation of temperature dependence of the luminescence of C<sub>60</sub> in toluene, benzene and CS<sub>2</sub> solutions, we reported that the C<sub>60</sub> aggregates are formed during cooling at the freezing temperature of these solvents. Furthermore, the C<sub>60</sub> aggregates can be changed to stable structures by irradiating with UV pulse-laser (Nd:YAG laser, 355nm). As a consequence, we could obtain new-type of nanoscale C<sub>60</sub> clusters, which appear as round-shaped nanoscale particles in high resolution transmission electron-microscopy (HRTEM) images. However, the yield of the new-type C<sub>60</sub> clusters obtained by this mehod is too small. So we designed and developed a new system to obtain C<sub>60</sub> cluster of macroscopic quantity. In this system, C<sub>60</sub> solution was vaporized to droplet in vacuum by using ultrasonic nebulizer, resulting in formation of C<sub>60</sub> aggregates by evaporating solvent. The system was invented to produce new nanoscale carbon clusters by the irradiation of UV light upon C<sub>60</sub> aggregates in toluene droplet. So we can assume that some of these materials are the photo-polymerized C<sub>60</sub> clusters obtained by this system. In the presentation, the details of the system and the UV-Vis absorption spectra of the photo-polymerized C<sub>60</sub> clusters obtained by this system will be reported. This work was supported by the Seoul Research and Business Development Program (Grant No. 10583)).

### Ep-I-021

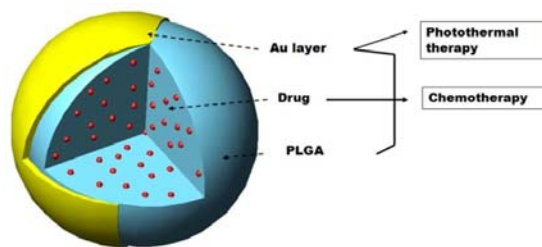
#### Multifunctional Nanoparticles for Combined Doxorubicin and Photothermal

##### Treatments

박 희열, 양 재문<sup>1</sup>, 이 재민<sup>2</sup>, 함 승주<sup>2</sup>, 최 인홍<sup>3</sup>

연세 나노메디컬 협동과정. <sup>1</sup>연세대학교 의과대학 진단 방사선과. <sup>2</sup>연세대학교 화공학과. <sup>3</sup>연세대학교 의과대학 미생물학과.

To facilitate combined doxorubicin and photothermal treatments, we developed doxorubicin-loaded poly(lactic-co-glycolic acid)-gold half-shell nanoparticles (DOX-loaded PLGA-Au H-S NPs) by depositing Au films on DOX-loaded PLGA NPs. As the PLGA NPs biodegraded, DOX was released, and heat was locally generated upon near-infrared (NIR) irradiation due to NIR resonance of DOX-loaded PLGA H-S NPs. Compared with chemotherapy or photothermal treatment alone, the combined treatment demonstrated a synergistic effect, resulting in higher therapeutic efficacy and shorter treatment times. Since our NPs selectively deliver both heat and drug to tumorigenic regions, they may improve the therapeutic effectiveness with minimal side effects.



P1

포스터  
세션

### Ep-I-022

#### Electrical Field Dependence of Morphologies of Organic Light Emitting Devices

KO Changhyun, LEE Hyunwon, YOO Insun<sup>1</sup>, OH Hyounghyun<sup>1</sup>, KIM Jinwoo<sup>2</sup>, KIM Hyunjung

Department of Physics, Sogang University. <sup>1</sup>LG Display Co., Ltd. <sup>2</sup>Department of Materials Science and Engineering, Gwangju Institute of Science and Technology.

We studied the structural degradation induced by electrical stress in the organic light emitting devices (OLEDs) by synchrotron X-ray scattering. The OLED has a multilayered structure of organic layers on indium tin oxide (ITO) coated glass. The constant current was applied between Al cathode and ITO anode of the OLEDs till the maximum luminescence of the electrically non-stressed OLED decreased to 80%, 60%, and 50%. We measured X-ray reflectivity and diffuse scattering of the OLED samples at room temperature at beamline 5C2 in Pohang Light Source. Certain degradation of the morphology of organic-organic interface was observed and the degradation was enhanced with increasing electrical stress. The detailed electrical stress induced interfacial morphology will be discussed.

**Ep-I-023****Cu<sub>2</sub>O 양자점 터널링 소자의 전기적 특성 연구**

박 상우, 서 주영, 김 재훈, 김 은규, 최 동주<sup>1</sup>, 김 영호<sup>1</sup>

한양대학교, 물리학과. <sup>1</sup>한양대학교, 신소재공학과.

화학적 반응법으로 형성시킨 Cu<sub>2</sub>O 나노입자를 이용하여 양자점 터널링 소자를 제작하고 이들의 전기적 특성에 대해 연구하였다. Cu<sub>2</sub>O 양자점 터널링 소자를 제작하기 위하여, 먼저 p형 Si 기판상부에 약 2~3nm의 SiO<sub>2</sub> 터널 절연막을 생성 후 5nm 두께의 Cu 박막을 thermal evaporator로 증착한 후 BPDA-PDA(biphenyl dianhydride - paraphenylene diamine) 폴리아믹 산을 스펀코팅 하였다. 다음, Cu 박막과 폴리아믹 산이 열적 화학반응을 하도록 실온에서 24시간 이온화 시킨 다음 135°C 30분 soft baking 후 350°C에서 2시간 동안 질소분위기에서 curing공정을 실시하였다. 이로써 형성된 Cu<sub>2</sub>O 나노입자의 크기는 금속박막의 두께와 반응 시간에 따라 조절할 수 있는데, 일반적으로 약 10 nm 정도의 크기를 갖는다. 마지막으로 photo-lithography와 Electron-beam lithography를 사용하여 100 nm 이하의 간극을 가지는 Ti-Au 전극을 형성하였다. 제작된 소자의 수직 또는 수평구조의 채널을 통한 전기적 특성을 C-V (capacitance-voltage)와 I-V (current-voltage) 측정을 통해 분석하였다.

**Ep-I-024****An Improved RF Circuit Model for Biosensors Based on Carbon Nanotube****Coupled with Interdigital Capacitors**

LEE Hee-Jo, YOON Jong-Gwan

Department of Electrical and Electronic Engineering, Yonsei University.

We present improved radio frequency (RF) circuit modeling of a biosensing element based on a single-walled carbon nanotube (SWNT)-combined interdigital capacitors at microwave frequencies. From the resulting circuit, the lumped element values for biomolecular binding are accurately obtained. It is thereby found that the completed RF circuit model shows excellent agreement with measured results. This implies that the electrical properties of a specific biomolecular binding system can be quantitatively analyzed if an optimal RF circuit model is constructed. Finally, we suggest that the suggested methodology can be used to analyze other biomolecular sensing methods.

**Ep-I-025****Synthesis of nanostructure arrays by using anodized aluminum oxide template**

김 일원, 박 정민, 이 선영, 안 창원<sup>1</sup>, 배 종성<sup>2</sup>, 김 영근<sup>3</sup>, 박 우락<sup>3</sup>, 윤 성욱<sup>3</sup>, 정 종호<sup>3</sup>, 배 해경<sup>3</sup>

울산대학교, 물리학과. <sup>1</sup>전자부품연구원, 융합부품연구부. <sup>2</sup>한국기초과학지원연구원, 부산센터. <sup>3</sup>울산과학기술대학교.

Nanostructure materials have great potential in microelectronics, optoelectronics, magnetic storage, and sensors because they display novel physical and chemical properties. In particular, ordered arrays of nano-particles, nano-wires, nano-tubes, and nano-dots have recently attracted much attention. Anodized aluminum oxide (AAO) membranes are one of the most common nano-templates for the preparation of nanostructure materials. In this study, we have prepared high ordered AAO membranes with a pore size of around 70 nm using by two-step anodization process. we have fabricated TiO<sub>2</sub> and ZnO nano-structure arrays (nano-tubes and nano-dots) by using sol-gel and PLD process with AAO membranes. and discuss the morphology of nano-structure arrays and their applications.

**Ep-I-026****Structural and Optical Properties of Proton-Implanted ZnO Nanorods**

PARK changin, KIM B.-H., LEE Y.-B.<sup>1</sup>, KWAK C.-H.<sup>1</sup>, SEO S.-Y.<sup>1</sup>, KIM S.-H.<sup>1</sup>, PARK S.-H.<sup>2</sup>, HAN sangwook<sup>3</sup>

Department of Physics and Institute of Fusion Science, Chonbuk National University, Jeonju 561-756,

Korea. <sup>1</sup>Department of Materials Science and Engineering, Pohang University of Science and Technology, Pohang

790-784, Korea. <sup>2</sup>New Materials & Components Research Center, Research Institute of Industrial Science &

Technology, Pohang 790-600, Korea. <sup>3</sup>Division of Science Education and Institute of Fusion Science, Chonbuk

National University, Jeonju 561-756, Korea.

We investigated the structural and the optical properties of H<sup>+</sup>-ion implanted ZnO nanorods. Vertically aligned ZnO nanorods were synthesized on Al<sub>2</sub>O<sub>3</sub> substrates by using catalyst-free metal organic chemical vapor deposition (MOCVD). H<sup>+</sup> ions with energies of 30 - 120 keV and beam flux of 1×10<sup>13</sup> - 1×10<sup>16</sup> cm<sup>-2</sup> were implanted on the ZnO nanorods. Field-emission scanning electron microscopy (FE-SEM) measurements revealed that the ZnO nanorods maintained good shapes after H<sup>+</sup> ions implanted. X-ray diffraction and Field-emission transmission tunneling microscopy (FE-TEM) measurements demonstrated that no detectable disorder was observed from the nanorods exposed to the ion beam, compared with untouched ZnO nanorods. Extended x-ray absorption fine structure analysis revealed a small but distinguishable amount of disorder in the ion-implanted nanorods, particularly, in the Zn-O bonds. From photoluminescence (PL) measurements, we found that the band gap peak intensity of PL was significantly reduced as proton beam energy increased. We also investigated the annealing effect of the ion-implanted nanorods. We will discuss the optical properties of the ion-implanted nanorods, considering the micro-structural changes and the annealing effect.

**Ep-I-027****Growth of Nitrogen-doped Carbon nanotube by Chemical Vapor Deposition**

KONG So-Jeo, KIM Chang-Duk<sup>1</sup>, LEE Sung-Youp<sup>2</sup>, SHIN Byong-Wook, KIM Sang-Hun, PARK Sun-Mi, SON Myeong-Rak<sup>3</sup>, YI Jin-Neung, CHOO Na-Yun<sup>4</sup>, LEE Eui-Wan<sup>5</sup>, LEE Hyeong-Rag<sup>5</sup>

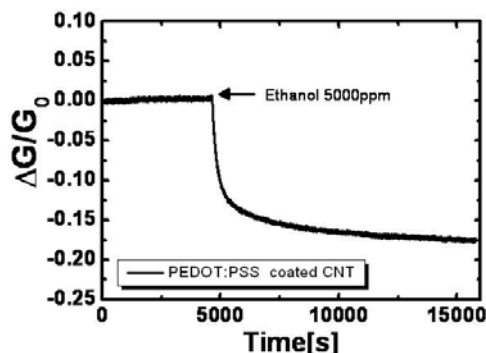
*Kyungpook National University, Department of Physics.* <sup>1</sup>*Kyungpook National University, Faculty of Liberal Education.* <sup>2</sup>*Kyungpook National University, Department of Nano-science and Technology.* <sup>3</sup>*Kyungpook National University, Dept. of physics.* <sup>4</sup>*Kyungpook National University, Dept. of Nano-science and Technology.* <sup>5</sup>*Kyungpook National University, School of Physics and Energy Science.*

Nitrogen-doped (N-doped) Carbon nanotubes (CNTs) have been prepared by Chemical Vapor Deposition (CVD). CVD is a normal technique to produce carbon materials. As doping accompanies with the recombination of carbon atoms into CNTs in the CVD process, N atoms can be substitutionally doped into the CNTs lattice, which is hard to realize by other synthetic methods. Doping of CNTs by boron and nitrogen renders them p-type and n-type, respectively. N-doped CNTs show n-type behavior regardless of tube chirality. The N-doped nanotubes show the G-band in the Raman spectrum at a lower frequency than the undoped ones. N doping introduces large amount of topological defects. Among all the doped CNTs, the N-doped CNTs are of special interest in both fundamental and application studies. We studied the growth of N-doped CNT with NH<sub>3</sub> gas ratio in CVD. By using Raman and XPS, we demonstrate the existence of the N-doped CNT.

**Ep-I-028****PEDOT:PSS를 이용한 탄소나노튜브 가스센서의 응용**

박 선미, 김 상훈, 이 성엽<sup>1</sup>, 신 병욱, 공 소저, 손 명락, 이 진능, 추 나윤<sup>1</sup>, 김 창득<sup>2</sup>, 이 의완, 이 형락  
*경북대학교 물리학과.* <sup>1</sup>*경북대학교 나노과학기술학과.* <sup>2</sup>*경북대학교 기초교육원.*

빗살형 전극형태(Interdigitated Electrode)의 기판위에 교류이중전기영동(AC dielectrophoresis)방법을 이용하여 탄소나노튜브를 배열한 소자를 제작하여 휘발성 유기화합물(VOC)의 한 물질인 에탄올에 대한 민감도를 측정해 보았다. 그 결과 탄소나노튜브와 에탄올과의 민감도 변화에는 반응이 없었다. 이러한 민감도를 향상시키기 위해 전도성 고분자 물질인 PEDOT:PSS를 이용하였다. 이때 탄소나노튜브 없이 PEDOT:PSS만을 코팅한 경우와 탄소나노튜브 위에 PEDOT:PSS를 코팅한 경우로 나누어 측정한 후 비교하였다. 그 결과 PEDOT:PSS를 코팅한 경우는 에탄올과의 민감도 변화가 0.5정도로 나타났으며, 탄소나노튜브 위에 PEDOT:PSS를 코팅한 경우는 0.2정도로 나타났다. 그러나 PEDOT:PSS를 코팅한 경우에는 오차가 매우 크게 나타나고 저항도 매우 커진 반면 탄소나노튜브 위에 PEDOT:PSS를 코팅한 경우에는 훨씬 안정적이고 오차도 많이 줄어든 결과를 보였다. 즉, 탄소나노튜브만으로는 에탄올과의 민감도 변화가 일어나지 않았으나 PEDOT:PSS와 함께 한 경우에는 민감도가 증가하였고, PEDOT:PSS과 에탄올과의 민감도 변화에 있어서 안정적인 결과가 나오도록 도와주는 역할을 한 것으로 추측된다.

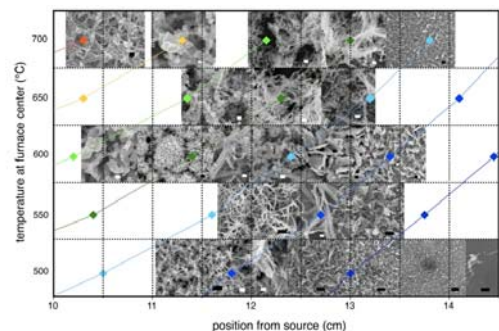


**Ep-I-029****Gas Phase Synthesis of Cu, Cu<sub>2</sub>O and CuO Nanowires, Nanowalls and Porous****Nanofibers and the Morphological Phase Diagram of Copper Oxide Nanostructures**

RHEN Danielle, 강 대준

*BK21 Physics Research Division, Department of Energy Science, Institute of Basic Science, SKKU Advanced Institute of Nanotechnology and Center for Nanotubes and Nanostructured Composites, Sungkyunkwan University, Suwon 440-746, Korea.*

Cu, CuO and Cu<sub>2</sub>O nanostructures were grown by vapor phase synthesis from a single commercially available carbon based precursor at different reaction temperatures and atmospheres at temperatures lower than that predicted by the Cu-O phase diagram. In addition to particles of all three phases, copper nanowires, Cu<sub>2</sub>O nanostructured walls and porous CuO nanofibers, nanoropes and nanowalls were reproducibly grown by taking advantage of the temperature gradient in the furnace for various reaction temperatures. Nanostructures were grown on various substrates including SiO<sub>2</sub> and ITO glass. We present a morphological phase diagram of CuO and we suggest the growth mechanism of the copper oxide nanostructures based on the initial phase of copper or copper oxide and subsequent oxygen diffusion as the synthesis time increases. We also explain our different results in the context of recent results of zinc oxide growth from acetate in a similar setup. Such an understanding is invaluable in the growth of transition metal oxide nanostructures from organometallic precursors and we predict other transition metal oxides could be grown from this method. The functionality of the porous CuO nanowires was investigated by catalytic oxidation of glucose in cyclic voltammetry and amperometry studies.

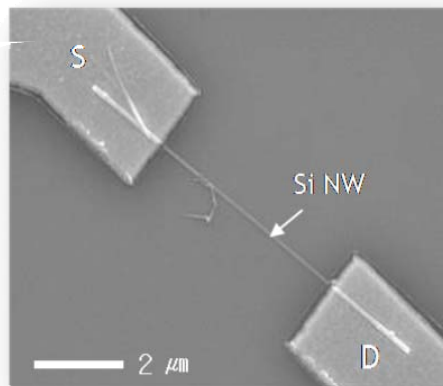


Morphological Phase Diagram of CuO nanostructures. Isothermic lines are 600°C for orange (upper left) and reducing in 50°C steps towards the dark blue (lower right).

**Ep-I-030****P-type Si nanowire-based Devices for the Detection of Nerve Agent**

KIM yeonju, LEE junmin, LEE seunghyun, LEE Wooyoung  
*Yonsei University, Department of Materials Science and Engineering.*

The gas sensors with fast-response time and high sensitivity for chemical warfare agents (CWAs) have been studied because CWAs can be fatal even at low concentration levels. For the purpose of protection from CWAs, it is essential to develop highly sensitive gas sensors for detection of a small amount of CWAs. However, the gas sensors using thin films or bulk materials have a problem of low sensitivity and grain boundary poisoning that limits the repeatability and long-term stability. In this work, we report highly sensitive Si nanowire-based gas sensors using Si-nanowire sensors, which enable the real-time electrical detection of DMMP, which is a stimulant of Sarin. A combination of photolithography and a lift-off process were utilized to fabricate a 50-nm-diameter single nanowire device. Rapid thermal annealing (RTA) was performed under vacuum conditions ( $< 10^{-6}$  Torr) at 300-600 °C for 3 min so as to make electric contacts between the Ti/Au electrodes. In order to demonstrate the real-time detection of DMMP, the fabricated Si-nanowire sensors were mounted in a sealed chamber. We present the possibility of implementing gas sensors for CWAs based on nanowires using the highly sensitive Si-nanowire sensors for the detection of vapor DMMP with various concentrations and ambient temperatures, respectively.



**Ep-I-031****Three-Dimensional Architecture of Carbon Nanotube-Anchored Polymer****Nanofiber Composite**

TAEHYUNG Kim, ILHA Lee, YOUNGHEE Lee

*BK21 Physics Division, Department of Energy Science, Sungkyunkwan Advanced Institute of Nanotechnology, and Center for Nanotubes and Nanostructured Composites, Sungkyunkwan University, Suwon, Kyunggi-do 440-746, Korea..*

Carbon nanotube (CNT)-anchored polymer nanofiber mats were designed by *in situ* spraying carbon nanotubes while simultaneously electrospinning polymer nanofibers. CNTs were intentionally located on the surface of polymer nanofibers by designing the hydrophobicity and hydrophilicity of CNT surfaces. The conductivity of the composite mat was significantly improved compared to the pristine nanofibers. By facilitating the CNT surface as well as nanofiber surface, the loading amount of Pt nanoparticles was increased twice with a uniform particle sizes of  $\sim 3$  nm, compared to the pristine nanofibers. High catalytic current ( $3400 \text{ mA/cm}^2/\text{mg Pt}$ ) and long term stability of the composite mat was attributed with the creation of the efficient formation of CNT bridges between nanofibers. This improves electron transport in the electrode and allow for the appropriate formation of mesopores in the carbon nanofiber mat.

P1

포  
스  
터  
세  
션**Ep-I-032****Carbon nanotube field emitter for super miniature X-ray tube using****brachytherapy radiation source**

허 성환, IHSAN Aamir, 여 동열, 조 성오

*KAIST, 원자력 및 양자공학과.*

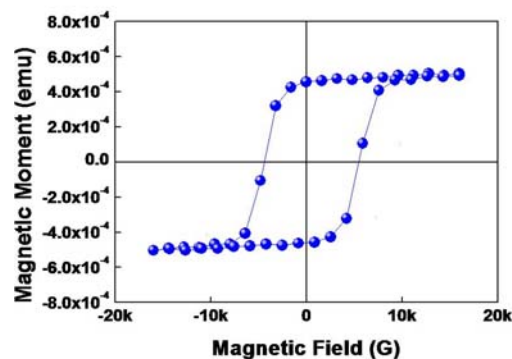
Carbon nanotube field emitter for super miniature X-ray tube has been developed. Carbon nanotube paste which mixed with multiwalled carbon nanotube, organic binder, and silver nanoparticle was coated on tungsten tip of 0.25 mm in diameter. The one end of the tungsten tip was mechanically polished for flatted shape, the coated carbon nanotube has been uniformly distributed. The coated tip was heated as two step,  $200^\circ\text{C}$  for burning out of organic binder and gradual change of  $300^\circ\text{C} \sim 500^\circ\text{C}$  for melting of silver nanoparticle. The melted silver nanoparticle might be a tight connecting layer between carbon nanotube and tungsten tip for a longer emission life time than several tens of hours. Field emission current of higher than  $100 \mu\text{A}$  at  $2.32 \text{ kV/mm}$  was continuously emitted over 3000 minutes with less than 5% fluctuation and was gradually decreased  $-0.01 \mu\text{A/min}$ .

## Ep-I-033

# Magnetic Properties of Patterned Co/Pd Multilayer Structures with Perpendicular Magnetic Anisotropy using Electron Beam Lithography

KIM Hyunsu, ROH Jong Wook, KIM Sungman<sup>1</sup>, CHUN Dong Won<sup>1</sup>, JEUNG Won Yong<sup>1</sup>, LEE Wooyoung  
*Department of Materials Science and Engineering, Yonsei University. <sup>1</sup>Korea Institute of Science and Technology (KIST).*

For the development of high-density magnetic recording media, the grain size of magnetic films should be reduced to increase recording data. However, as grain size smaller, thermal stability of magnetization in each bit drastically decreases so that ferromagnetic materials act as paramagnetic materials, referred to as superparamagnetism. One of the most promising methods is the use of patterned media to overcome this hurdle. It is well known that Co/Pd multilayer thin films exhibit high perpendicular magnetic anisotropy (PMA) and can be applied for patterned magnetic recording media. In the present work, Co/Pd multilayers were deposited on a glass substrate in an UHV dc/rf magnetron sputtering system. A vibrating sample magnetometer (VSM) was used to measure the magnetic properties of as-grown Co/Pd multilayer thin films, showing PMA and  $H_c = 4.9$  kOe. The coercivity of as-grown Co/Pd multilayer thin films was found to increase with the number of Co/Pd layer. In order to fabricate patterned structure of the Co/Pd multilayer, an ultra high-performance electron beam lithography system was utilized. Each dot of the fabricated patterned structures has a pitch of 100 nm and a diameter of 50 nm. We discuss the magnetic properties of lithographically patterned Co/Pd multilayer structures with respect to the size of the patterned dot.



## Ep-I-034

## 전자빔을 이용한 탄소 나노구조체 형성 장비 개발

조 대희, 여 승준, PODE Ramchandre, 안 정선  
*경희대학교 물리학과.*

플러렌( $C_{60}$ )은 이미 알려진 바와 같이 광, 압력, 전자빔, 도핑된 금속에 의해 쉽게 중합체를 형성하는 특성을 갖고 있으며 이는 독특한 분자구조에 기인한다. 이처럼 중합체를 용이하게 형성할 수 있다는 특성과 플러렌 분자 1개의 크기가 1 nm 이하인 점은 bottom-up process에 의해 나노 구조체를 형성할 수 있는 가능성이 충분한 재료임을 의미한다. 본 연구 그룹에서는 용액 중 플러렌 aggregation의 형성과 광중합 반응에 대해 연구한바 있으며, 타 연구 그룹에서는 전자빔을 박막 상태의 플러렌에 조사하여 중합체를 형성하는 것에 대한 연구도 보고되어 있다. 본 연구에서는 전자빔의 조사를 통해 플러렌의 중합체 형성 여부를 알아보는 것을 목적으로 하여, 승화되고 있는 플러렌에 전자빔을 조사하는 장비를 개발하였다. 전자빔을 조사하기 전의 진공도는  $10^{-7}$  torr 이며, 조사하는 동안의 진공도는  $1 \sim 4 \times 10^{-4}$  torr 를 유지 하였으며, 전자빔은 RF Power는 50 W 에서 300 W 까지, DC 전압은 100 V 에서 500 V 까지 조절이 가능한 전자빔을 사용하였다. 플러렌의 승화는 effusion cell을 이용하여 승화시켰으며, 형성된 물질의 특성을 평가하기 위해 기판에 증착하였다. 전자빔의 조사를 통해 형성된 물질의 특성을 알아보기 위하여, 증착된 박막의 UV 흡수 스펙트럼과 FT-IR 스펙트럼을 상온에서 측정하였다. 그 결과 승화 중에 전자빔이 조사되지 않은 플러렌 박막과 비교하였을 때 UV 흡수 스펙트럼의 형태가 변한 것과, FT-IR 스펙트럼에서는 플러렌의 4개의 진동모드( $526, 576, 1183$  과  $1429 \text{ cm}^{-1}$ )가 사라진 것을 확인할 수 있었다. 위의 결과에 대한 분석을 통하여 중합체 형성 가능성에 대해 본 연구 그룹과 타 연구 그룹의 결과와 비교하여 알아보려고 한다. \* 본 연구는 서울시 산학연 협력사업의 지원으로 수행되었음(과제번호 10583)

**Ep-I-035****Current Compensation circuit for QTF (Quartz Tuning Fork)**

AN Sang min, LEE Man hee, JAHNG Junghoon, JHE Won ho

*Department of Physics and Astronomy, Seoul National University.*

We demonstrated that QTF can be used accurate force sensor by compensate the stray capacitance's effect using current compensation circuit. The QTF is enough to measure the nano-scaled water's characteristics cause of its high Quarlity factor (nealy 4000, in ambient condition) and high spring constant. To measure accurate force, we have to choose the Simple Harmonic Oscillator. But the QTF's behavior can not show like SHO cause of stray capacitance of QTF. So we remove the stray capacitance effect by mixing up the 180 degree reversal phase signal. Used QTF's resonance frequency is 32,768Hz. As a result, we can have SHO force sensor using current compensated QTF.

**Dp-II-059****Terahertz conductivity of superconducting  $\text{La}_{1.84}\text{Sr}_{0.16}\text{CuO}_4$  thin film**HONG Taeyoon, KIM Jae Hoon, BOZOVIC Ivan<sup>1</sup>*Department of Physics, Yonsei University. <sup>1</sup>Department of Condensed Matter Physics and Materials Science, Brookhaven National Laboratory.*

The complex transmission coefficient of a superconducting  $\text{La}_{1.84}\text{Sr}_{0.16}\text{CuO}_4$  thin film (52nm) has been measured over the frequency range of 3 - 60 cm<sup>-1</sup> at temperatures from 4K to 300K using coherent time-domain terahertz spectroscopy. We observed a dramatic change in both the magnitude and phase of the terahertz transmission in the superconducting state caused by a rapid condensation of charge carriers. Both the real and imaginary parts of the complex conductivity are determined directly from the amplitude and phase of the transmitted electric field without a Kramers-Kronig analysis. The complex conductivity is well described as the sum of contributions from the condensate, quasiparticles, and order parameter fluctuations.

**Dp-II-060****Effect of Cu substitution on Superconductivity in  $(\text{Ru,Cu})\text{Sr}_2(\text{Eu,Ce})_2\text{Cu}_2\text{O}_z$** **system**

LEE Ho Keun

*Kangwon National University, Physics Department.*

The effect of Cu substitution on the structural and superconducting properties of the  $(\text{Ru}_{1-x}\text{Cu}_x)\text{Sr}_2(\text{Eu}_{1.34}\text{Ce}_{0.66})\text{Cu}_2\text{O}_z$  system with  $x = 0, 0.25$  and  $0.5$  prepared under ambient pressure have been investigated. The X-ray diffraction patterns indicated that the Ru ions are replaced by the Cu ions. It is found that the Cu substitution for Ru significantly reduces the ferromagnetic component, but results in a small change in diamagnetic onset transition temperature. In contrast to the  $\text{RuSr}_2(\text{Eu}_{1.34}\text{Ce}_{0.66})\text{Cu}_2\text{O}_z$ , bulk Meissner effect is observed in the field-cooled magnetization measurements of the Cu doped samples. The experimental results are discussed in connection with the spontaneous vortex phase interpretation.

**Dp-II-061****Effect of  $\text{Eu}^{+3}$  doping on the behavior of irreversibility lines in cuprate high- $T_c$** **superconductor  $\text{Sm}_{1-x}\text{Eu}_x\text{Ba}_2\text{Cu}_3\text{O}_{7-d}$ .**

AHMAD dawood, PARK insuk, KIM G C, KIM Y C

부산대학교 물리학과.

Irreversible properties of the cuprate high- $T_c$  superconductor  $\text{Sm}_{1-x}\text{Eu}_x\text{Ba}_2\text{Cu}_3\text{O}_{7-d}$  (where  $x=0.0, 0.3, 0.5, 0.7, 0.9$ ) are reported. Samples were synthesized by using the usual solid state reaction method and aligned under the high magnetic field of 6 T. Results showed that the transition temperature  $T_c$  was enhanced in the optimal doped samples ( $x=0.5-0.7$ ). It is found that the irreversibility line can be described by the power law dependence  $(1-T/T_c)^n$  in all series samples with  $n \gg 2$  with high value of irreversible fields in the optimal doped samples. No kink is observed in the series samples which are attributed to the development of superconducting gap and 2D-3D crossover in a vortex system.

**Dp-II-062****HTC-Peltier Current Leads**

KIM Sang Hoon, KIM Ga Young, PARK Sang Kook, LEE Sang Bong

경북대학교 일반대학원 물리학과.

For operating cryostat devices, we have developed experimental HTS-Peltier hybrid current leads. The HTS-Peltier hybrid current leads(HPCL) have been designed for 1000 A devices. As a result of our previous experiments, we had confirmed that 100A Peltier current leads's(PCL) normal metal section got cool to 237.6 K at room-temperature ( $\Delta T_{\text{max}}=63.6$  K). According to our calculation, Peltier elements can get cool to 221.5 K at room-temperature. So, for increasing  $\Delta T$ , we reducing electric resistance and improving thermal conductance, we have soldered Peltier elements and normal metal lead sections.

axis

PARK Jae-Hyun, DOH Yong-Joo, LEE Hyun-Sook, LEE Jae-Yeap, KIM Ju-Young<sup>1</sup>, CHO B. K.<sup>1</sup>, JUNG Chang-Uk<sup>2</sup>, LEE Hu-Jong

Department of Physics, Pohang University of Science and Technology. <sup>1</sup>Materials Science and Engineering, Gwangju Institute of Science and Technology. <sup>2</sup>Department of Physics, Hankuk University of Foreign Studies.

As a new class of Fe-based superconductors,  $\text{SmFeAsO}$  single crystal consists of a two-dimensional layered structure, which may suggest an existence of intrinsic Josephson coupling along the  $c$ -axis. We fabricated mesa-type structure of  $\text{SmFeAsO}_{0.85}$  single crystals with standard electron-beam lithography technique and characterized its electrical properties along the  $c$ -axis in a four-probe measurement configuration. The mesa structure has a lateral size of  $1 \times 4 \text{ mm}^2$  with a height of  $\sim 40 \text{ nm}$ . Resistance vs. temperature curve indicates the superconducting transition temperature  $T_c$  near 53 K. Below  $T_c$ , current-voltage ( $I$ - $V$ ) characteristic curves exhibit supercurrent without any voltage dissipation. The critical current density increases up to  $\sim 10^5 \text{ A/cm}^2$  at  $T=6.5 \text{ K}$ . Temperature dependence of the critical current ( $I_c$ ) is found to have the Ambegaokar-Baratoff dependence, though  $I$ - $V$  curve resembles the one of an overdamped Josephson junction in our experimental bias range. In in-plane magnetic field  $B$ ,  $I_c$  decreases in a monotonous way up to 6 T. The absence of Fraunhofer-like pattern is attributed to a very short Josephson penetration depth, caused by a high  $c$ -axis critical current density.

시 성장

장 세훈, 고 락길<sup>1</sup>, 김 호섭<sup>2</sup>, 하 홍수<sup>2</sup>, 하 동우<sup>2</sup>, 오 상수<sup>2</sup>, 김 영철<sup>3</sup>

한국전기연구원, 창원대학교 재료공학과. <sup>1</sup>한국전기연구원, 부산대학교 물리학과. <sup>2</sup>한국전기연구원. <sup>3</sup>부산대학교 물리학과.

최근 박막형 고온초전도 선재(Coated conductor; CC) 제조를 위한 금속 기판으로는 IBAD(Ion Beam Assist Deposition)법에 의해 MgO 물질이 (001) 방향으로 2축 결정화 배향된 IBAD-MgO 기판이 주로 이용되고 있다. 일반적으로 IBAD-MgO 기판 위에 결정성이 우수한 초전도 박막을 증착하기 위해서 Homo-epi MgO/LMO의 구조를 갖는 완충층을 증착하며, MOD와 같은 공정을 위해서는 화학적 안정성이 우수한  $\text{CeO}_2$  층이 추가적으로 증착된 완충층 기판을 사용하게 된다. 하지만 Homo-epi MgO/LMO/ $\text{CeO}_2$ 의 다층 구조를 갖는 완충층은 각 층마다 증착 공정이 추가되고 이는 CC의 생산 단가를 높이고, 생산 시간을 증가시키는 단점을 갖는다. 그러므로 MgO 물질 위에 바로  $\text{CeO}_2$ 를 (001) 방향으로 증착할 수 있다면 다층의 완충층 구조를 단순화시킬 수 있을 것이다. 그러나, MgO와  $\text{CeO}_2$  결정간에 약 28%의 큰 mismatch를 갖고 있어 이를 극복해야 한다. 본 연구에서는 PLD 장치를 이용하여 MgO(001) 위에  $\text{CeO}_2$ 가 (001) 방향으로 에피택시 성장할 수 있는 증착 조건을 찾기 위한 실험을 수행하였다. MgO (001) 단결정 기판 위에 PLD법의 증착 공정 변수인 기판 온도, 가스 분압, 가스 종류, 에너지 밀도 등을 변화시키며 그 영향을 분석했다. 증착된  $\text{CeO}_2$  층은 XRD를 이용하여 결정성 분석을 했으며, 표면과 단면 분석을 위해 AFM, SEM, TEM를 이용하였다. 그리고 제조된 MgO/ $\text{CeO}_2$  구조 위에 YBCO 초전도박막을 증착하여 그 성능을 평가하였다. 본 연구는 21세기프론티어 연구개발사업인 차세대초전도응용기술개발 사업단의 연구비 지원에 의해 수행되었습니다.

**Dp-II-065****A study on superconducting properties of YBCO Coated Conductors using Low-temperature Scanning Laser Microscopy**

PARK Sang Kook, LEE Sang Bong, KIM Sang Hoon, KIM Ga Young, KIM Jong Man, RI Hyeong-Cheol

경북대학교 대학원 물리학과.

We have analyzed the distribution of critical temperature ( $T_c$ ) and critical current density ( $J_c$ ) in YBCO coated conductor using LTSLM. For improving the temperature stability of the sample, we have modified the system into double-shielded cryostat. Then we can advance the stability of the sample temperature from  $\pm 10$  mK to  $\pm 2$  mK. For measuring the superconducting properties of YBCO coated conductors, we have prepared the sample of a narrow bridge type using wet etching process. We have observed a spatial nonuniformity of critical temperature and critical current density from the bolometric response, which is arisen from focused laser beam in the transition temperature region. And then we have displayed the data in a two-dimensional image.

**Dp-II-066****High-resolution angle-resolved photoemission spectroscopy studies on 2-dimensional graphite based system**임 춘식, 경 원식, 박 승룡, 김 철, 송 동준, 최 성균, 김 용관, 정 원식, 고 윤영, 한 가람, 최 환영, 김 준성<sup>1</sup>, 이 한구<sup>2</sup>, 김 형도<sup>2</sup>, 김 창영연세대학교, 물리 및 응용물리학과. <sup>1</sup> 포항공과대학교, 물리학과. <sup>2</sup> 포항가속기연구소.

Graphite intercalation compounds (GICs) have been studied for several decades by many researchers. Now more than 100 species of atoms or molecules can be intercalated into the graphite layers. Among those GICs, we conducted high-resolution angle-resolved photoemission spectroscopy (ARPES) on various alkali metal (such as Li, Ba, Sr, and Ca) intercalated compounds. We prepared samples by various intercalation methods such as vapor transport, Li alloy and electrochemical intercalation methods. ARPES spectra obtained from these materials show charge transferred feature and enhanced many-body interactions inconsistent with previous works. We also investigated the many-body interactions by extracting the electron self energy from ARPES data. In addition, by studying potassium dosed graphite surfaces in a similar way, we compared the many-body interactions in GICs and potassium dosed graphite surfaces. We believe that our comparative studies on various GICs and surface processed graphite will elucidate the mechanism of many-body interactions in 2-dimensional graphite and graphite-based systems.

**Dp-II-067****(Ru,M)A<sub>2</sub>(Nd,R,Ce)<sub>2</sub>Cu<sub>2</sub>O<sub>z</sub> 계의 합성 및 초전도 특성**

문 종우, 이 상민, 이 호근

강원대학교, 물리학과.

RuSr<sub>2</sub>(R,Ce)<sub>2</sub>Cu<sub>2</sub>O<sub>z</sub>(Ru-1222)계 강자성 초전도체를 보통의 상압 하에서 합성할 경우 희토류원소(R)가 주로 Sm, Eu 및 Gd 일 때 만 거의 단일상의 초전도체 합성이 가능하고 그 외 희토류 원소의 경우 단일상 형성이 어려운 것으로 알려져 있다. 그런데 이들 희토류 원소들은 모두 중성자 흡수계수가 매우 크기 때문에 중성자 회절실험을 통한 정밀한 구조분석 및 자기구조분석이 용이하지 않다. 이로 인해 이 계의 구조 및 자기적 구조 특성은 현재 잘 알려져 있지 않다. 그러므로 중성자 흡수계수가 적은 희토류 원소에 근거한 Ru-1222계 강자성 초전도체의 합성은 이 계의 특성 이해에 매우 중요하다. 특히 Nd의 경우 중성자 흡수계수가 적고 앞의 희토류 원소와 유사한 이온크기를 가지므로, 본 연구에서는 Nd에 근거한 Ru-1222계 초전도체 합성 및 특성 연구가 수행되었다. RuSr<sub>2</sub>(Nd,Ce)<sub>2</sub>Cu<sub>2</sub>O<sub>z</sub> 조성의 경우 시도된 모든 조성에서 예상대로 단일상이 형성되지 않았으며, 초전도 특성도 관측되지 않았다. 그리하여 (Ru,M)A<sub>2</sub>(Nd,R,Ce)<sub>2</sub>Cu<sub>2</sub>O<sub>z</sub> 조성 (M = Cu, Nb, A = Sr, Ba, R)의 합성 연구가 시도되었다. 그 결과 M을 치환한 특정조성에서 Nd에 근거한 (Ru,M)-1222 단일상이 합성될 수 있음을 관측했으며, 그 결과와 관련 초전도 특성에 대해 발표한다. 본 연구는 한국과학재단의 지원(2009-0075747)으로 수행되었다.

**Dp-II-068****The magnetic phase diagram of (Ca,Sr,Ba)Fe<sub>2</sub>As<sub>2</sub>**

NA SEWOONG, EOM MANJIN

Department of physic, POSTECH.

The parent compound of newly-discovered AFe<sub>2</sub>As<sub>2</sub> has an antiferromagnetic spin-density-wave(SDW) ground state, which can be suppressed by either carrier-doping or applying external pressure. We synthesized the chemical solution of (Ca,Sr,Ba)Fe<sub>2</sub>As<sub>2</sub> and investigated the magnetic transition using resistivity and magnetization measurements. The magnetic transition temperature is found to be sensitive to the change of alkaline earths, while the magnetic order is robust against the inhomogenities in the A-sites. The phase diagram of (Ca,Sr,Ba)Fe<sub>2</sub>As<sub>2</sub> is presented, and the effect of chemical pressure will be compared to that of physical pressure.

**Dp-II-069****Superconductivity of isovalent Ru substituted  $\text{BaFe}_{2-x}\text{Ru}_x\text{As}_2$** 

EOM manjin, NA sewoong

*Department of Physics, Pohang University of Science and Technology.*

We investigated the effect of substitution of isovalent Ru for Fe in  $\text{BaFe}_{2-x}\text{Ru}_x\text{As}_2$  using high-quality single crystals. The itinerant antiferromagnetic state in  $\text{BaFe}_2\text{As}_2$  is known to be suppressed by hole or electron doping, inducing high- $T_c$  superconductivity. Similarly substituting isovalent Ru for Fe weakens the AFM order and eventually induces the superconducting phase for relatively high doping level of  $x > 0.5$  as investigated by resistivity and magnetization measurements. The phase diagram and the superconducting properties of  $\text{Ba}(\text{Fe,Ru})_2\text{As}_2$  will be presented and compared with those of Co-doped  $\text{BaFe}_2\text{As}_2$  single crystals.

**Dp-II-070****Analysis of current distribution in YBCO thin film using Low Temperature****Scanning Hall Probe Microscopy**

LEE Sangbong, PARK Sangkook, KIM Sanghoon, KIM Kayoung

*경북대학교 물리학과.*

We studied the distribution of magnetic flux in YBCO film that we applied DC current. Shielded and trapped field were studied as a function of transport current. The results of Hall probe magnetic measurements were used in the inverse calculation to obtain the current distribution across the strips.

**Dp-II-071****Attempt of MgB<sub>2</sub> Powder Orientation in Magnetic Field**

KANG Kihyeok, MEAN B. J., KIM Sung Hoon, LEE Jeffrey C.<sup>1</sup>, PARK Bae-Ho, CHO B. K.<sup>2</sup>

*Department of Physics, Konkuk University, Seoul, 143-701, Korea.* <sup>1</sup>*Adlai E. Stevenson High School, Lincolnshire IL 60069, U.S.A..* <sup>2</sup>*Department of Materials Science and Engineering, GIST, Gwangju 500-712, Korea.*

The magnesium diboride MgB<sub>2</sub> has attracted a great deal of research interest after the discovery of superconductivity at  $T_c=39$  K. A number of measurements have been reported mainly for powder samples of MgB<sub>2</sub>. However, it is very difficult to make single crystals, in particular, of large size. The large size crystals of MgB<sub>2</sub> are essential for microscopic measurements such as NMR and neutron scattering experiments. These data are crucial for understanding of anisotropy of local electronic and magnetic structures. In this case magnetic orientation of MgB<sub>2</sub> powder grains is an alternative method. Therefore we have attempted magnetic alignment of MgB<sub>2</sub> powder grains in an epoxy resin under a strong magnetic field. Since we do not know of direction and magnitude of a magnetic anisotropy tensor, we devise difference alignment schemes assuming two cases; Case I for the easy along the c-axis and Case II for the easy axis perpendicular to the c-axis. For each case, we have built different devices. For example, for case II we have to apply rotation perpendicular to the magnetic field. Also, the device is designed to get rid of gravitational sedimentation by rotating the powder in an epoxy resin. For assessment of the c-axis alignment XRD measurements are utilized. However, the three XRD data for the unaligned powder, the Case I and the Case II are same and show no evidence of alignment. Possible reasons for the results will be discussed in detail.

**Dp-II-072****Energy Level Quantization of a Collectively Pinned Josephson Vortex Chains in Naturally Stacked High-Tc Josephson Junctions**

이 길호, 진 용덕, 이 후종

*Department of Physics, Pohang University of Science and Technology.*

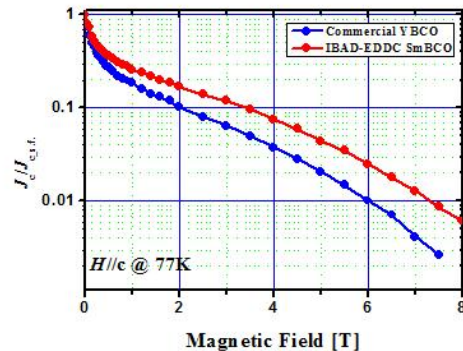
Atomically stacked natural Josephson junctions (IJJs) form in Bi<sub>2</sub>Sr<sub>2</sub>CaCu<sub>2</sub>O<sub>8+x</sub> single crystals, which consist of stacks of CuO<sub>2</sub> superconducting layers weakly coupled with each other. Josephson vortices are established in in-plane magnetic fields (~4.5 T) applied perpendicular to the long side of a stack. Josephson vortices are forced to move collectively along the junction by c-axis bias current, which results in multiple Josephson-vortex-flow branches (JVFBs) in current-voltage characteristics. Here, switching between JVFBs corresponds to depinning of Josephson vortex chains out of the collective pinning potential. In this study, the *switching current distribution* (SCD) of the last branch was measured with lowering temperature from 8 K to 0.3 K. Down to the crossover temperature,  $T_{cr} \sim 3.8$  K, SCD shows good agreement with a thermal activation (TA) process out of the microresistor-type pinning potential. Below a certain crossover temperature, however, the distribution width is almost insensitive to the temperature, which suggests a macroscopic quantum tunneling (MQT) of coupled Josephson vortices from a pinning potential. At the base temperature of 0.3 K we examined the *energy level quantization* (ELQ) in the pinning potential by applying microwave to the stack. In appropriate conditions of microwave frequency and power, double peaks in SCD are observed, where the primary and the resonance peak represent the ground and the first excited state, respectively. The resonance peak position ( $I_r$ ) well follows the microwave frequency ( $f$ ) dependence of a theoretical relation of  $f = f_0/n(1-(I_r/I_c))^{1/4}$ , where  $n$  is the number of photons involved,  $f_0$  is the small-oscillation frequency (~81 GHz), and  $I_c$  is the critical current in the absence of any fluctuations. The double peak feature of the SCD under microwave irradiation indicates the energy level quantization of collectively pinned Josephson vortices in the pinning potential.

HONG Sung-Hak, LEE Soon-Gul, SEONG Won Kyung<sup>1</sup>, KANG Won Nam<sup>1</sup>Korea University, Department of Display and Semiconductor Physics. <sup>1</sup>Sungkyunkwan University, Physics Division and Department of Physics.

집속이온빔(FIB) 방법을 이용하여  $\text{MgB}_2$  나노브릿지 dc SQUIDs를 제작하고 그 특성에 대해 연구하였다. SQUID 패턴에 사용된 Ga 이온빔의 에너지는 30kV이었으며 빔 전류는 1.5pA 내지 900pA였다. 최소 선폭이 100nm인 나노브릿지를 포함한 SQUID 루프는 홀 사이즈가  $3\ \mu\text{m} \times 3\ \mu\text{m}$  이고, 평균 선폭은  $2\ \mu\text{m}$  이었다. 본 연구에서는 Intergrain 나노브릿지와 Intragrain 나노브릿지 dc SQUIDs를 제작하였으며 그 특성을 비교하였다. Intergrain 나노브릿지 dc SQUID는 계단형 임계특성을 나타내었고, 전류-전압 곡선의 경우 조셉슨 효과가 우세하게 나타났다. 반면에 Intragrain 나노브릿지 dc SQUID는 임계 온도와 임계 전류 밀도가 박막의 특성과 크게 다르지 않았으며, 큰 과잉전류를 가지는 Flux-flow효과를 보였다. 하지만 Voltage modulation의 경우 두 종류 모두 우수한 특성을 보였으며 이를 통해 집속 이온빔 방법을 통한  $\text{MgB}_2$  나노브릿지 dc SQUIDs 제작에 대한 가능성을 확인할 수 있었다.

고 락길, 장 세훈<sup>1</sup>, 송 규정<sup>2</sup>, 하 홍수<sup>3</sup>, 김 호섭<sup>3</sup>, 하 동우<sup>3</sup>, 오 상수<sup>3</sup>, 김 영철<sup>4</sup>한국전기연구원, 부산대학교 물리학과. <sup>1</sup>한국전기연구원, 창원대학교 재료공학과. <sup>2</sup>전북대학교 물리교육학과. <sup>3</sup>한국전기연구원. <sup>4</sup>부산대학교 물리학과.

박막형 고온초전도 선재의 제조를 위해 사용되는 공정은 크게 2축 배향된 금속 기판을 제조하는 공정과 그 위에 고온초전도 박막을 증착하는 공정의 조합으로 나눌 수 있다. 금속 기판의 경우 IBAD, RABiTS, ISD가 있고, 초전도 박막 증착 공정의 주로 PLD, MOCVD, MOD, RCE (Reactive Co-evaporation) 등이 사용된다. 본 연구에서는 IBAD 금속 기판에 batch type RCE의 한 종류인 EDDC (Evaporation Drum in Dual Chamber) 방법을 사용하여 초전도 박막을 증착하는 IBAD-EDDC 공정으로 제조된 박막형 고온초전도 선재에 대한 자장 특성을 분석하였다. 증착된 초전도 물질은 희토류계의 고온초전도 물질인 SmBCO 초전도체로 기존 YBCO 고온초전도체에 비해 자장하에서의 임계온도와 임계전류밀도가 더 높은 장점이 있다. 외부 자장과 온도에 대한 박막형 초전도 선재의 통전 특성 평가를 위해 PPMS를 사용하였다. 높은  $I_c$ 를 갖는 박막형 초전도 선재에 laser striation 장치를 이용하여  $50\ \mu\text{m}$  이하의 선폭을 갖도록 마이크로 패턴링을 하여 측정하였다. 또한 상용화된 YBCO 선재와 자장 특성을 서로 비교하였다. 본 연구는 21세기프론티어 연구개발사업인 차세대초전도응용기술개발 사업단의 연구비 지원에 의해 수행되었습니다.



**Dp-II-075****Phenomenological Theory of competing orders between Superconductivity and Magnetism with Magnetic Field**

KIM Jinhee, BANG Yunkyu

*Department of Physics, Chonnam National University.*

The coexistence and competition of the superconductivity and magnetism in a material is studied by using Ginzburg-Landau theory. In particular, we study the effect of the external magnetic field on the reentrance of the magnetism. We compare our results with available experimental data of recent Fe pnictide superconductors.

P2

포  
스  
터  
세  
션**Dp-II-076****Growth of (Ba,K)Fe<sub>2</sub>As<sub>2</sub> Single Crystals by the In-flux Method and their Physical Properties**

LEE Bumsung, KHIM Seung Hyun, KIM Kee Hoon

*Department of Physics and Astronomy, Seoul National University.*

Since the discovery of new high temperature superconductivity in RFeAs ( $R$ = rare earth) in early 2008 [1], various structural forms of Fe-pnictides have been found, including the 1111, 122, and 11 systems. In particular, the so-called 122 system,  $A\text{Fe}_2\text{As}_2$  ( $A$ =Ca, Sr, Ba, Eu) with doping in  $A$  and Fe sites, has been heavily studied, possibly because the growth of large size single crystals with Sn- and self-flux methods were more easily achieved than in other systems. Although the Sn-flux method has been successful in obtaining large size ones over  $\sim 5$  mm in lateral dimension, there exist several problems in the Sn-flux grown crystals: (1) Superconducting transitions in (Ba,K)Fe<sub>2</sub>As<sub>2</sub> system has not reached an optimal value, as compared with the self-flux grown single-crystals. (2) Growth of BaFe<sub>2</sub>As<sub>2</sub> single crystals has been only successful with the self-flux method [2]. This indicates the Sn flux method might produce non-stoichiometric (Ba,K)Fe<sub>2</sub>As<sub>2</sub> [2]. On the other hand, the self-flux provided relatively small crystal sizes less than  $\sim 2$  mm. In this work, by use of In-flux, we report successful growth of a high quality BaFe<sub>2</sub>As<sub>2</sub> single crystal of a typical size  $\sim 5 \times 5 \times 0.2$  mm<sup>3</sup>, and on-going efforts to grow (Ba,K)Fe<sub>2</sub>As<sub>2</sub>. In contrast to the recent report in BaFe<sub>2</sub>As<sub>2</sub> crystals, grown by In-flux, that have shown a superconducting transition in resistivity at 20 K [3], we have not observed zero resistivity except a small decrease around 20 K. [1] Y. Kamihara, *et al.* J. Am. Chem. Soc. 130, 3296-3297 (2008) [2] N. Ni, *et al.* Phys. Rev. B 78, 014507 (2008) [3] J. S. Kim, *et al.* J. Phys.: Condens. Matter 21, 342201 (2009)

**Dp-II-077****철계 초전도체인 (Ba, K)Fe<sub>2</sub>As<sub>2</sub>의 단결정 성장과 기초 물성 분석**

장 유란, 홍 중범, 정 명화<sup>1</sup>, 강 원남, 권 용성

성균관대학교 물리학과, <sup>1</sup>서강대학교 물리학과.

최근 철과 비소를 기반으로 한 초전도체의 발견 이후, 전 세계적으로 많은 연구가 활발히 진행되고 있다. 이 철계 초전도체는 알칼리 금속 혹은 희토류 원소와 철, 그리고 비소가 결합하여 이루어진 형태를 띠고 있다. 이 철계 초전도체의 단결정 성장을 위해 많은 시도가 이루어지고 있지만, 비소가 매우 위험한 독성을 가진 중금속이고 증기압이 매우 크기 때문에 단결정 성장이 쉽지 않다. 또한 알칼리 금속의 경우 공기 중에서 쉽게 산화하고 또한 잘못 다루게 될 경우, 폭발의 위험성도 있어 역시 많은 어려움이 있다. 우리는 여러 번의 시도 끝에 철과 비소를 안전하게 다루는 방법을 찾았고, 알칼리 금속이나 희토류 금속을 안정적인 상태에서 다루어 양질의 단결정을 성장시켰다. 이번 가을 물리학회에서 우리는 단결정 성장방법들과 성장시킨 단결정들의 기초 물성을 발표 할 것이다.

**Dp-II-078****Reversible magnetization으로부터 FeAs계열의 초전도체에서의 요동현상 연구**

최 창호, 김 수현, 최 기영, 정 명화, 이 성익

서강대학교 물리학과.

우리는 초전도체 BaFe<sub>1.8</sub>Co<sub>0.2</sub>As<sub>2</sub> 단결정을 가지고 온도변화에 따른 자기모멘트를 측정하여 reversible 구간을 통한 요동현상을 관찰 하였다. 요동현상(fluctuation effect)은 높은 임계전이온도, 짧은 결맞음길이(coherence length), 비등방성, 그리고 차원이 낮은 물질에서 크게 나타난다. BaFe<sub>1.8</sub>Co<sub>0.2</sub>As<sub>2</sub>는 23.6K의 비교적 높은 임계전이온도를 가지며 층 구조를 띠어서 요동현상을 충분히 관찰할 수 있었다. 실험 시 외부 자기장은 0.5Tesla~7Tesla로 변화시켰으며 온도는 2K~37K까지 변화를 주어서 자기모멘트를 측정 하였다. Reversible 구간은 Zero Field Cooling(ZFC)과 Field Cooling(FC)이 같아지는 지점을 잡았으며 18K이상의 온도구간에서 요동현상을 가짐을 관찰할 수 있었다. 이러한 효과는 고온의 초전도체에 비해서는 작지만 FeAs계열의 초전도체의 물성을 관찰하기에는 충분하다. 마지막으로 임계전이온도 근처에서의 reversible구간을 사용하여 scaling을 한 결과 BaFe<sub>1.8</sub>Co<sub>0.2</sub>As<sub>2</sub>는 3차원의 scaling 형태를 볼 수 있었다. 이는 Co를 도핑한 BaFe<sub>2</sub>As<sub>2</sub> 초전도체는 비등방성이 작기 때문에 2차원에서보다 3차원에서 더 잘 맞는다고 볼 수 있다. 서로 다른 외부자기장과 임계전이온도를 변수로 갖는 온도-자기모멘트 곡선은 하나의 scaling 함수로 잘 나타나고 있음을 확인 할 수 있었다.

**Dp-II-079****단결정 초전도체  $\text{BaFe}_{1.8}\text{Co}_{0.2}\text{As}_2$  의 두 개의 S-파동 에너지 간격 대칭**

김 수현, 최 창호, 정 명화, 최 기영, 노 재동<sup>1</sup>, 이 성익

서강대학교 물리학과, <sup>1</sup>서울시립대학교 물리학과.

우리는 최적으로 도핑된  $\text{BaFe}_{1.8}\text{Co}_{0.2}\text{As}_2$ 를 자기 플럭스(self flux)로 만들어서 Fe-As 계열 초전도체의 에너지 간격 대칭을 연구해 보았다. 이 초전도에 자기장을 10 gauss 걸어 주었을 때, 전이온도는 23.6K가 나왔다. 에너지 간격 대칭을 알아보는 방법은 여러 가지 있지만 우리는 낮은 임계자기마당( $H_{c1}$ )을 통해서 그 값을 얻었다. 이 방법은 간단하면서도 샘플 표면에 관계 하지 않기 때문에 샘플 전체의 특성을 알아볼 수 있다.  $H_{c1}$ 은 자기장-자기모멘트 곡선을 통해 얻을 수 있고 마이스너 직선에서 벗어난 점을 택했다. 각 온도마다 낮은 임계자기마당을 나타내었을 때 3.5K 아래에서 포화된(saturation) 모습을 볼 수 있었다. 그리고 하나의 에너지 간격으로 설명이 안되고 두 개의 S-파동 에너지 간격으로 가정하였을 때 실험값과 잘 맞았다. 두 개의 에너지 간격 중 작은 값은  $\Delta_1(0)=1.64\pm0.2\text{meV}$ 이고 큰 값은  $\Delta_2(0)=6.2\pm0.2\text{meV}$ 를 얻었다. 그리고 평면 침투깊이( $\lambda_{ab}$ )는 169nm이고, 쿠퍼쌍 밀도는 우에무라(Uemura) 관계에서 벗어남을 보였다. 우에무라 관계는 양공이 도핑된 고온 초전도체의 쿠퍼쌍 밀도-전이온도간의 경향성을 나타낸 것이다. 우에무라 관계에서 우리 시료는 벗어났지만 무한대 층을 가진  $\text{SrLaCuO}$ 와 같은 선상에 있음을 알 수 있었다.

**Dp-II-080****Pressure-induced superconductivity in the antiferromagnetic and orthorhombic phase of  $\text{CaFe}_2\text{As}_2$** 

DEOKHEE Kim, HANOH Lee<sup>1</sup>, E. D. BAUER<sup>1</sup>, J. D. Thompson<sup>1</sup>, TUSON Park

Department of Physics, Sungkyunkwan University, Suwon 440-746, Korea. <sup>1</sup>Los Alamos National Laboratory, Los Alamos, New Mexico 87545, USA.

We study pressure-induced superconductivity and magnetism in  $\text{CaFe}_2\text{As}_2$ . This material is antiferromagnetic below 170 K at atmospheric pressure, but becomes superconducting with a slight amount of applied pressure. Preliminary reports suggest that magnetism and superconductivity may coexist over a broad range of pressure. In this presentation, we report an evidence for bulk superconductivity of  $\text{CaFe}_2\text{As}_2$  under pressure. With increasing pressure, a drop in ac magnetic susceptibility occurs at  $T_c$  due to Meissner effects, where the size of the drop is peaked at 5 kbar and is almost 50% of that of other bulk superconductors.

**Dp-II-081****ARPES and optical spectroscopy studies of Y1-x PrxBa2Cu3O7**

정 원식, 박 승룡, 임 춘식, 김 철, 최 성균, 송 동준, 김 용관, 고 윤영, 한 가람, 경 원식, 최 환영, 김 창영  
연세대학교 물리학과 첨단전자구조연구소.

Y1-x PrxBa2Cu3O7 system is one of the most studied high temperature superconductors. Substitution of Pr for Y in this system suppresses  $T_c$  and superconductivity disappears for  $x > 0.55$ . There are two different explanations about the suppression of  $T_c$  with increasing Pr content. First, it is assumed that Pr ion has the +4 valence state. This scenario is called the hole band filling. In another scenario, for which it is assumed that Pr is +3, it is proposed that the magnetic interaction due to localization of the charge carriers causes the suppression. The interaction is mediated by the hybridization between Pr 4f and O 2p bands and quenches the superconductivity. A peculiar aspect of this scenario is that there is z-direction distribution of charge carriers. We wish to grow Y1-x PrxBa2Cu3O7 ( $0 < x < 1$ ) single crystals in alumina and zirconia crucibles using a self-flux method. We investigate the bulk electronic structures by using ARPES and optical spectroscopy on these single crystals.

**Dp-II-082****Strong field dependence of critical current density in  $a$ -axis-oriented MgB<sub>2</sub> films**

JUNG Soon-Gil, LEE Nam Hoon, CHO Kyu Hwan, SEONG Won Kyung, CHOI Eun-Mi, KANG Won Nam, OH Sangjun<sup>1</sup>

성균관대학교, 물리학과. <sup>1</sup>핵융합연구센터, 재료연구팀.

We have fabricated MgB<sub>2</sub> films with the various oriented directions on the Al<sub>2</sub>O<sub>3</sub> (0001) substrates by using a hybrid physical-chemical vapor deposition (HPCVD) system. The oriented direction of MgB<sub>2</sub> films was controlled by changing concentration of B<sub>2</sub>H<sub>6</sub> gas and substrate temperature. The global growth direction was detected by using x-ray diffraction (XRD) and scanning electron microscopy (SEM). Then critical current density ( $J_c$ ) and the upper critical field ( $H_{c2}$ ) were measured by using a magnetic property measurement system (MPMS) and a physical property measurement system (PPMS), respectively. Critical current density of  $a$ -axis-oriented MgB<sub>2</sub> films showed much stronger field dependency over the wide magnetic field region than single crystalline MgB<sub>2</sub> thin film and MgB<sub>2</sub> thick film with columnar structure which known as very strong pinning center in MgB<sub>2</sub> superconductor. In addition, its  $H_{c2}(0)$ , ~ 25 T, was much higher than MgB<sub>2</sub> films with  $c$ -axis orientation. These results directly suggest that the intrinsic pinning by  $a$ -axis orientation is much stronger than any other pinning sites, such as point defect, grain boundary, and so on.

**Dp-II-084****Ba(Fe,Co)<sub>2</sub>As<sub>2</sub> thin films: MBE Growth and Superconducting Properties**

조 성래, DANG Dung Duc, 황 영훈, DUONG Van Thiet

울산대학교 물리학과.

최근 철계 고온 초전도체에 관한 연구가 활발하다. 철계 초전도체로서 LaFeOP는 초전도 전이온도가 4 K 낮은 값이라 주목을 받지 못하다가 다른원소, 즉 P를 As, Se, Te, S등으로 치환하거나 La를 Ba, Li, Sm등으로 치환하여 초전도 전이온도  $T_C$ 를 향상시키는 연구가 진행되고 있다. LaFeAsO의 La를 Sm으로 치환한 SmFeAsO의 경우 초전도 전이온도가 55 K로 보고되어 새로운 고온초전도체로 인식되고있다. 한편 BaFe<sub>2</sub>As<sub>2</sub>의 경우 초전도성을 가지지 않지만 압력의 변화에 따라서 초전도 전이온도가 35 K에서 나타난다고 보고되고 있다. 아울러, BaFe<sub>2</sub>As<sub>2</sub>의 Fe 위치에 Co, Ni를 치환시킨 경우 전이온도가 각각 약 20 K와 23 K에서 초전도체 현상이 일어남이 밝혀졌다. 그러나 현재까지 보고된 FeAs-기반 초전도체의 경우 대부분 자기-용제(Self flux) 방법에 의한 덩어리(bulk) 형태의 물질이며 박막 형태의 물질은 거의 보고가 되어 있지 않은 실정이다. 본 연구에서는 MBE 장치를 사용하여 FeAs-기반 BaFe<sub>2</sub>As<sub>2</sub>와 Ba(Fe,Co)<sub>2</sub>As<sub>2</sub>를 박막으로 성장시켜 초전도 현상에 대한 연구를 하였다. MBE 장치 내부의 Ba, Fe, As, Co 분출 셀을 이용하여 동시증발(co-evaporation)법과 적층 성장(layered growth)법으로 변화시켜가며 박막을 성장시켰으며, 10~20 K 온도 근처에서 초전도 전이가 발생함을 확인하였다.

**Dp-II-085****외부자기장 인가에 따른 LiFePO<sub>4</sub> 물질의 Mössbauer 분광 연구**김 철성, 이 인규, 박 일진, 홍 중수, 이 찬혁, 원 봉연<sup>1</sup>, 심 인보국민대학교, 물리학과. <sup>1</sup>(주) ASK.

리튬이차전지용 LiFePO<sub>4</sub> 물질을 고상반응법을 통하여 합성하였다. 이렇게 합성된 단일상의 LiFePO<sub>4</sub> 물질의 결정학적 특성을 X-선 회절(x-ray diffraction)실험을 통하여 연구하였다. 또한 외부자기장 인가 뢰스바우어 분광분석(External magnetic field Mössbauer spectroscopy)을 통하여 0 T 에서 4.8 T 까지 외부자기장이 LiFePO<sub>4</sub> 결정내 철 이온의 초미세자기구조에 미치는 영향을 연구하였다. 상온에서의 X-선 회절실험 결과, 제조된 시료는 Olivine-type의 Orthorhombic구조로 공간군이 *Pnma*인 단일상의 LiFePO<sub>4</sub>임을 확인하였다. 뢰스바우어 스펙트럼의 분석 결과, 자장을 가하지 않은 4.2 K에서의 초미세자기장과 전기사중극자 분열치는 각각 135 KOe, 2.84 mm/s 이고, 외부자기장이 증가함에 따라 증가하여 4.8 T 일때 140 KOe, 2.96 mm/s 까지 증가하였다. 또한, 이성질체 이동치는 인가자장에 관계없이 항상 1.24 mm/s 로 관측되어 철이온이 Fe<sup>2+</sup> 상태로 LiFePO<sub>4</sub> 결정내에 존재함을 확인할 수 있었다. 외부자기장 증가에 따른 뢰스바우어 스펙트럼 선폴이 증가는 반강자성 내에서 반평행하게 정렬된 스핀들이 외부자기장의 영향에 의한 Frustration 현상으로 생각된다.

NGUYEN Van Minh, PHAM Xuan Huu, DOAN Thi Thuy Phuong, YANG In-Sang<sup>1</sup>

*Hanoi National University of Education, Center for Nano Science and Technology. <sup>1</sup>Ewha Womans University, Department of Physics.*

Magnetoelectric compounds with the general formula  $\text{BaTi}_{1-x}\text{Fe}_x\text{O}_3$  ( $x=0.00-0.50$ ) have been synthesized by solid state reaction method. We investigated the effect of Fe on structural, Raman scattering, electrical and magnetic properties of  $\text{BaTi}_{1-x}\text{Fe}_x\text{O}_3$  compounds. The change in structure and some new peaks appear when the Fe content reaches to 0.20. The Raman spectra have been significantly changed at  $x = 0.20$ . As increasing of Fe content not only brings about the band gap become narrowed but also the magnetization increases. The impedance spectroscopy indicates the role of Fe in grain and grain boundary. The relation between the structural, optical and electromagnetic properties is also investigated in this report.

LUC Huy Hoang, TRAN Dong Hai, NGUYEN Hoang Hai, CHEN Xiang Bai<sup>1</sup>, NGUYEN Thi Minh Hien<sup>1</sup>, YANG In-Sang<sup>1</sup>

*Hanoi National University of Education, Department of Physics. <sup>1</sup>Ewha Womans University, Department of Physics.*

In this paper, a simple microwave-assisted chemical method has been successfully developed for synthesizing  $\text{Zn}_{1-x}\text{Co}_x\text{O}$  nanopowders. The nanopowders are characterized by X-ray diffraction (XRD), scanning electron microscopy (SEM), ultraviolet-visible absorption, micro-Raman spectroscopy, and vibrating sample magnetometry (VSM). We found, in the synthesis process, the surfactant Triethanolamine (TEA) plays an important role on the morphology of  $\text{Zn}_{1-x}\text{Co}_x\text{O}$  nanoparticles. The XRD study shows that for Co-doping up to 5%, no evidence of any other phases or impurities is observed, while for Co-doping of 7%, a second phase of  $\text{Co}_3\text{O}_4$  is clearly formed. The absorption spectra of  $\text{Zn}_{1-x}\text{Co}_x\text{O}$  ( $x=0-5\%$ ) nanopowders show several peaks at 660, 611 and 565 nm, indicating the presence of  $\text{Co}^{2+}$  ions in the tetrahedral sites. The Raman study shows that the full width at half-maximum (FWHM) of the  $\text{E}_2^{\text{low}}$  mode is increasing with increasing Co doping, which further indicates the incorporation of  $\text{Co}^{2+}$  ions into the ZnO host matrix. The magnetic measurement reveals that the  $\text{Zn}_{1-x}\text{Co}_x\text{O}$  ( $x=1\%-5\%$ ) nanopowders clearly exhibit room-temperature ferromagnetic behavior, and the ferromagnetism is increasing with the Co concentration.

**Dp-II-088****The gyration dependent magnetic interaction in an alkali superoxide  $\text{KO}_2$** 

김 범현, 김 민재, 민 병일  
포항공과대학교, 물리학과.

In alkali superoxide  $\text{KO}_2$ , partially filled  $p_g$  antibonding states of  $[\text{O}_2]^-$  anions induce the antiferromagnetic interactions. Near the magnetic transition temperature ( $T_N=7.1$  K), coherent rotation of magnetic  $[\text{O}_2]^-$  molecules, which is termed magnetogyration, is realized. Below  $T_N$ , the large gyration about  $20^\circ$  lifts the degeneracy of doubly degenerate  $p_g$  orbitals and causes the spin-orbit coupling to be quenched. Thus the magnetic interaction in the low symmetric  $\text{KO}_2$  phase is mainly influenced by the orbital occupation and electron hopping nature. In this study, we have set the effective spin-orbital model which describes the superexchange interactions of  $[\text{O}_2]^-$ - $[\text{O}_2]^-$  and  $[\text{O}_2]^-$ - $\text{K}^+$ - $[\text{O}_2]^-$  chains and investigated the magnetic interaction of low symmetric  $\text{KO}_2$ . According to gyration direction and orbital ordering pattern, we have calculated the exchange constants between two oxygen molecules and discussed the relation between the structural changes and the magnetic ground states.

P2

포  
스  
터  
세  
션**Dp-II-089** **$^{13}\text{C}$  NMR Study of  $\text{CaC}_6$  Single Crystals**

KIM SungHoon, KANG Ki Hyeok, MEAN B. J., LEE Moohee, KIM Jun Sung<sup>1</sup>

*Department of Physics, Konkuk University, Seoul, 143-701, Korea. <sup>1</sup>Department of Physics, POSTECH, Pohang, 790-784, Korea.*

$^{13}\text{C}$  NMR(Nuclear Magnetic Resonance) measurements have been performed to investigate the local electronic structure of a superconducting graphite intercalation compound  $\text{CaC}_6$  ( $T_c=11.4$  K). A large number of single crystals were packed and sealed in a quartz tube for naturally abundant  $^{13}\text{C}$  NMR. Spectrum, Knight shift, linewidth, spin-lattice relaxation time  $T_1$ , and the spin-spin relaxation time  $T_2$  were measured in the normal state as function of temperature down to 70 K at 4.8 T and 8.0 T.  $^{13}\text{C}$  NMR spectrum shows a narrow peak with a very small Knight shift. Knight shift and linewidth of the  $^{13}\text{C}$  NMR are almost temperature-independent around, respectively, 0.012% and 1.2 kHz. The spin-lattice relaxation rate  $1/T_1$  is proportional to temperature confirming a Korringa behavior as for nonmagnetic metals. The Korringa product is measured to be  $T_1 T = 210$  s·K. From this value, the Korringa ratio is deduced to be  $\xi=0.73$ , close to unity, which suggests that the independent-electron description works well for  $\text{CaC}_6$ , without complexity arising from correlation and many-body effects.

KIM Bongjae, MIN B.I., LEE Jieun<sup>1</sup>, KANG J.-S.<sup>2</sup>

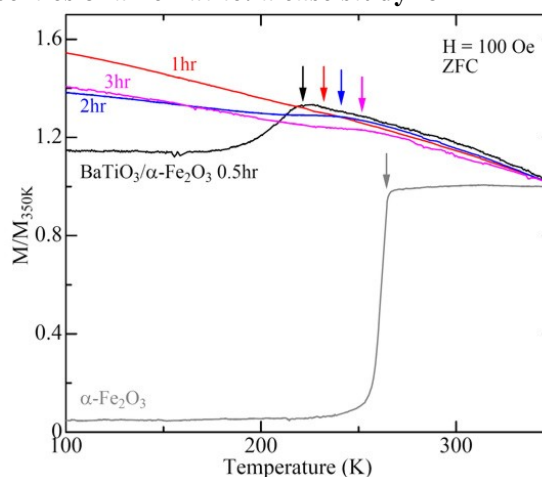
POSTECH, Physics. <sup>1</sup>University of Michigan, Physics. <sup>2</sup>The Catholic University of Korea, Physics.

$\text{CaMnO}_3$  and  $\text{SrMnO}_3$  are two well-known perovskite materials which have, in their ground state, a magnetic order of G-type antiferromagnetism with insulating nature. When Mo of high valence state ( $\text{Mo}^{6+}$ ) is introduced into B-site of  $\text{CaMnO}_3$ , some of Mn ions accept electrons and the ferromagnetic double-exchange interaction is activated. Likewise,  $\text{SrMnO}_3$  also has a similar behavior. For low doping case of Mo ion, the antiferromagnetic and ferromagnetic interactions compete and magnetic and transport properties are changed. In this presentation, we report the electronic structures and magnetic properties of  $\text{SrMn}_{1-x}\text{Mo}_x\text{O}_3$  based on the all-electron total energy band structure approach. We have also calculated the spectra of x-ray absorption spectroscopy (XAS), and compared them with the experimental spectra. Plus, we compare the calculational results of the  $\text{BaMn}_{1-x}\text{Mo}_x\text{O}_3$  system and discuss the issue of the antisite disorder of the B-site transition metal ions.

### $\text{BaTiO}_3/\alpha\text{-Fe}_2\text{O}_3$ nanoparticles

구 용성, 윤 병길, 정 중훈  
인하대학교, 물리학과.

Hematite ( $\alpha\text{-Fe}_2\text{O}_3$ ) is well known to show a drastic change of spin structure near 250 K, called Morin transition. The antiferromagnetic spins are canted from perpendicular to the c-axis above the transition, while the antiferromagnetic spins are parallel to the c-axis below the transition. In addition, the Morin transition is well-known to be very sensitive to defect and pressure. We have investigated the effect of strain on the Morin transition as well as the magnetic hysteresis of hematite by using specially designed  $\text{BaTiO}_3/\alpha\text{-Fe}_2\text{O}_3$  core/shell nanoparticles. With decrease of shell-thickness, the Morin transition temperature significantly decreases. And, the magnetic hysteresis loops are clearly seen below the Morin transition temperature of  $\text{BaTiO}_3/\alpha\text{-Fe}_2\text{O}_3$ . We have discussed the observed behaviors by using the critical thickness of strain and the formation of defect near the core/shell interfaces.



**Dp-II-092****Investigation on  $\text{CsMnCl}_3 \cdot 2(\text{H}_2\text{O})$  by Neutron Single Crystal Diffraction at Room****Temperature**

OH In-Hwan, KIM Je-Eun, KOO Japil<sup>1</sup>, PARK J.M.Sungil, LEE cheol eui<sup>2</sup>

Neutron Science Division, Korea Atomic Energy Research Institute. <sup>1</sup>Department of Physics, Pohang University of Science and Technology. <sup>2</sup>Department of Physics, Korea University.

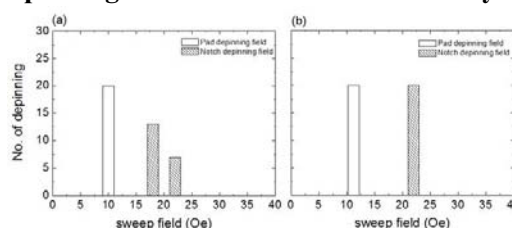
The crystal structure of the one-dimensional antiferromagnetic  $\text{CsMnCl}_3 \cdot 2(\text{H}_2\text{O})$  (caesium diaquatrichloromangante (II)) was investigated by single crystal neutron diffraction and the position of the hydrogen atoms was successfully localized for first time by neutron diffraction and the positions by X-ray diffraction are successfully verified. Whereas the anhydrate compound crystallizes in the rhombohedral space group and shows a higher antiferromagnetic phase transition temperature, the hydrate phase crystallizes in the orthorhombic space group and the Neel temperature is just 4.89K. The water molecules in this substance show a almost ideal geometry. Mn atoms are surrounded by two oxygen atoms and four chlorine atoms forming deformed octahedral and build the linear chains along the a-axis linked by Cl-bridge. The intermediate hydrogen bond  $\text{O} - \text{H}1 \dots \text{Cl}$  link Mn-octahedra resulting the stabilized the one-dimensional zig-zag chain along a-axis. Compared to the previous X-ray diffraction measurements where the parameters of hydrogen atoms are constrained or missing, no constraint was made on the hydrogen atoms. The obtained  $\text{H} - \text{O} - \text{H}$  angle in this compound was  $105.94^\circ$ , close to the ideal value of free water molecules.

**Dp-II-093****Chirality-Controlled Domain Wall Depinning With Different Pad Geometry**

LEE Bum-Woo, AHN Sung-Min, MOON Kyoung-Woong, CHOE Sug-Bong\*

Department of physics, Seoul National University.

There has been an intensive research interest in the behavior of domain walls (DWs) around notches of nanowires. When DWs are pinned at a notch, they experience depinning process which depends on the type and chirality of DW. So, the control of DW chirality becomes a hot issues in application of the the DWs mediated memory and logic devices. In this study, we investigate the way to control the chirality of the DWs by injecting them into ferromagnetic nanowires from artificially-designed pad geometry. We measure the depinning fields from the notches by detecting magneto-optical Kerr effect signal. In the case of type-A, for the nanowire conneted to the middle of the pad, two different depinning fields appear, which evidences the existence of two different chiralities in DWs. On the other hand, in the case of type-B for the nanowire conneted to lower part of pad, there is one depinning field resulting from the controlled chirality of DW



YANG In-Sang, CHEN Xiang-Bai, NGUYEN Thi Minh Hien, LEE D.<sup>1</sup>, JANG S. Y.<sup>1</sup>, NOH T. W.<sup>1</sup>

*Ewha Womans University, Department of Physics.* <sup>1</sup>*Seoul National University, Department of Physics.*

We present studies concerning resonant magnon Raman scattering in hexagonal HoMnO<sub>3</sub> thin film, which was grown on Pt(111)//Al<sub>2</sub>O<sub>3</sub> (0001) substrate by laser ablating deposition method. In the HoMnO<sub>3</sub> thin film, a broad peak at 760 cm<sup>-1</sup> is observed in the cross Raman scattering configuration, with linewidth several times wider than that of phonon and disappearing at the Neel temperature. Our previous studies indicate that it is originated from four-magnon scattering. In this study, we found, this broad peak can be strongly excited by the red lasers of 647 nm and 671 nm, while not detectable using 457 nm blue laser and 532 green laser. Our finding indicates that the four-magnon scattering at 760 cm<sup>-1</sup> in hexagonal HoMnO<sub>3</sub> is strongly dependent on the resonance condition, which may be related to the ~ 1.7 eV on-site Mn d-d optical transition in HoMnO<sub>3</sub>.

황 태종, 박 영순, 김 동호

*영남대학교, 물리학과.*

We study magnetoresistance behavior of the six bridges of Py/Nb/Py trilayer prepared on a single chip. Micro-Hall voltage to measure stray fields spreaded from the unpatterned trilayers shows that a significant amount of transverse component exists in the antiparallel domain (AD) state, which is originated in stray magnetic field from domain walls. The stray magnetic field could induce flux lines into the Nb layer and the motion of these flux lines is a primary factor of induction of reverse spin switch behavior in the AD state. Extraordinary transition was observed at one bridge with its bridge direction 72 ° away from the magnetization easy axis. It showed spin switch behavior similar to the magnetoresistance of a spin-valve structure with AF/F/S/F multilayers. In order to explain the extraordinary behavior, firstly, we consider that the flux pinning should be present in this particular sample to suppress the dissipation by flux motion. With different viewpoints, domain walls with transverse walls in head to head domain walls could be a factor in weak contribution to stray field or oblique orientation of easy axis relative to the bridge axis may suppress the wall formation.

**Dp-II-096****준안정 bcc Co의 안정화 및 자기변형**

이 선철, 윤 원석, 홍 순철

울산대학교.

자연적으로 hcp 구조가 안정한 Co를 GaAs, TiAl, FeAl, Ge 또는 Au 와 같은 기판 위에 에피탁셜하게 성장시키면 bcc 구조가 안정화 되는 것이 보고되었다. 3d 전이금속들은 그 구조에 따라 물성이 크게 좌우되는데 Fe 의 경우 가장 안정한 bcc 구조는 강자성이며 준안정한 fcc 에서는 다양한 자기구조를 갖는다. bcc Co 의 자기모멘트는 hcp, fcc 구조일 때의 자기모멘트( $1.58\sim 1.70 \mu_B$ )보다 더 큰 값( $1.70\sim 1.83 \mu_B$ )을 갖는 것으로 계산되었다. 평형 상태 체적의 bcc Co 는 정방 변형에 대해 안정하지 못하며 fcc 구조에 해당하는  $c/c_0$ 에서 더 안정되는 것으로 계산되었다. 격자 상수를 달리하면서 bcc Co 의 정방변형에 대한 안정성을 계산한 결과, 격자상수가  $2.87 \text{ \AA}$  이후에서 bcc 구조가 안정함을 보였다. 본 연구에서는 제일원리계산 방법을 이용하여 bcc Co의 안정화를 이론적으로 설명하고 자기변형계수에 대해 논의할 예정이다. 계산방법으로는 모든 전자를 고려하는 full-potential linearized augmented plane-wave (FLAPW)을 사용하였으며 교환 상관 포텐셜은 일반구배근사(general gradient approximation: GGA)로 표현하였다.

**Dp-II-097****Analysis of current-voltage characteristics of GaAs/MgO/Fe junctions**SHIM Seong Hoon, CHANG Joonyeon, KIM Kyung-Ho, KIM Hyung-Jun, HAN Suk-Hee, LEE Yun-Hi<sup>1</sup>Center for Spintronics Research, KIST. <sup>1</sup>National Research Laboratory for Nano Device Physics, Dept. of Physics, Korea Univ..

Effective spin injection from ferromagnetic metal into semiconductors is essential for the development of spintronics devices. Utilization of effective tunnel barrier helps to overcome the intrinsic conductance mismatch between metal and semiconductor, which is a major source of low electrical spin injection [1, 2]. The GaAs/MgO/Fe structure is a strong candidates for the spin injection/detection structure with spin filtering effect. This structure is quite attractive since it can be epitaxially prepared, and especially MgO/Fe structure forms a basic part of Fe (Co)/MgO/Fe(Co) magnetic tunnel junction (MTJ) structure with giant tunneling magnetoresistance (TMR). In this work, we report on the study of current-voltage (I-V) characteristics of the structure, which is important to understand the bias dependent spin filtering phenomena. [1] E. I. Rashba, Phys. Rev. B 62, R16267 (2000). [2] M G. Schmidt, D. Ferrand, L. W. Molenkamp, A. T. Filip, and B. J. van Wees, Phys. Rev. B 62, R4790 (2000).

김 재영, 이 보화

한국외국어대학교 물리학과.

TmFe<sub>2</sub>O<sub>4</sub>가 속해 있는 RFe<sub>2</sub>O<sub>4</sub> (R=Y, Ho, Er, Tm, Yb, Lu)는 같은 결정학적 Fe<sup>2+</sup>와 Fe<sup>3+</sup> 이온으로 인한 국소화된 Fe Moment 사이에서 강한 자기적 상호작용으로 인해 250 K 이하의 온도에서 magnetic ordering이 일어난다. 또한 R 이온의 따라 상이한 상전이 현상을 보이고 있다. R=Y, Er 의 경우 자기적 상전이와 구조적 상전이가 2단계로 일어나지만 R=Tm, Yb, Lu 인 시료에서는 이러한 상전이가 일어나지 않는다고 알려져 있다. 본 연구에서는 TmFe<sub>2</sub>O<sub>4</sub>의 다결정체 시료를 합성하고 자기적 상전이 현상과 전기적 특성을 살펴보았다. TmFe<sub>2</sub>O<sub>4</sub>의 자화율 측정 결과 250 K에서 반강자성 자기적 상전이가 일어났으며, 외부 자기장에 의한 잔류자기를 확인할 수 있는 열잔류자화 현상이 나타났다. 4단자 전기 저항 측정에 의한 결과 온도가 내려가며 비저항이 증가하는 부도체적인 특성을 보였다.

최 혁철, 김 기연<sup>1</sup>, 심 제호<sup>2</sup>, 김 동현<sup>2</sup>, 이 정수<sup>1</sup>, 유 천열인하대학교, 물리학과. <sup>1</sup>한국원자력연구소, 중성자과학연구부. <sup>2</sup>충북대학교, 물리학과.

교환 바이어스는 강자성 (F)과 반강자성 (AF) 사이의 계면에서의 교환 결합에 의한 현상으로 일방향이방성의 형성과 함께 자기이력곡선의 중심 이동과 보자력이 증가하는 등의 고유한 특성들을 보인다. 교환 바이어스 현상을 연구하기 위해 여러 가지 측정방법이 이용되고 있으며 그 중 강자성 공명 (FMR: Ferromagnetic Resonance) 측정을 통한 연구가 활발히 이루어지고 있다. 교환 바이어스가 존재하는 F/AF 계면에서, F층 두께의 함수로 교환 바이어스 자기장 H<sub>E</sub>의 감소와 함께 FMR linewidth가 증가하는 현상이 보고된 바 있다. 이 FMR linewidth 증가현상은 2-마그논 산란 과정(two-magnon scattering process)에 의한 추가적인 에너지의 풀림현상 때문으로 알려져 있고, 이때 추가적 산란의 원인은 불균일한 교환결합 에너지의 자화 용이축의 분포 때문이다 [1]. 본 연구에서는 강자성 공명 실험을 통하여 NiFe/FeMn/CoFe 3층 구조에서 FeMn 층의 두께를 변화시켜가며 H<sub>E</sub>와 FMR linewidth의 변화에 대해 연구하였다. 그 결과, 교환 바이어스가 생기는 AF의 임계 두께(~ 5 nm) 이상의 시료들에 대해서, AF 층의 두께 증가에 따라 H<sub>E</sub> 값이 증가함을 관측하였다. 그러나, AF 층의 두께에 따른 linewidth의 변화는 H<sub>E</sub>와는 다른 AF 층의 두께 의존성을 보였다. 이는 기존에 보고된 이층막 구조에서 관측된 결과[1, 2]와는 다른 것으로, 3층막 구조의 경우 기존의 이론으로 설명할 수 없는 추가적인 요인이 존재하는 것으로 추측된다. [1] S. M. Rezende, A. Azevedo, M. A. Lucena, and F. M. de Aguiar, Phys. Rev. B 63, 214418 (2001). [2] Shujuan Yuan, Baojuan Kang, Liming Yu, Shixun Cao, and Xinluo Zhao, J. Appl. Phys. 105, 063902 (2009).

## Dp-II-100

Electronic and Elastic Properties of  $(\text{Fe,Mn})_3\text{AlC}$  Studied by Density FunctionalTheory Calculations<sup>†</sup>

NOH Ji-Young, KIM Hanchul

Sookmyung Women's University, Department of Physics.

The aluminium-alloyed steel is light but has better ductility and strength, and further alloying with manganese can be used to change the crystal structure that determines the properties of steel. Thus Mn-Al-C steels have been extensively studied due to their technological applicability. We have studied structural, electronic, and elastic properties of  $(\text{Fe, Mn})_3\text{AlC}$  focusing on the change due to the varying contents of Mn. We employed the density functional theory (DFT) calculations in conjunction with the projected augmented wave (PAW) potentials and the generalized gradient approximation (GGA). In the perovskite-type structure ( $E2_1$ ) of  $(\text{Fe, Mn})_3\text{AlC}$ , iron (or manganese) atoms are located in the center of each face, aluminium atoms are on the corner of the cube, and the carbon atoms take the body-center site of the cube. We obtained the equilibrium crystal structure, and examined the change in formation energy for different concentrations of Mn. The electronic and magnetic properties were investigated by looking at charge density, spin density, and electronic density of states. Finally, we have calculated elastic coefficients, such as bulk modulus and shear moduli, of the alloys and compared them with the pure ferrite (ferromagnetic bcc-Fe) case. <sup>†</sup>This work has been supported by POSCO, Inc.

## Dp-II-101

## 자구벽이 있는 강자성 나노선의 열적 요동에 대하여 미세자기 동역학을 이용한

## 분석

윤 정범, 유 천열, 조 영훈<sup>1</sup>, 박 승영<sup>1</sup>, 정 명화<sup>2</sup>인하대학교, 물리학과. <sup>1</sup>한국기초과학지원연구원, 나노물성팀. <sup>2</sup>서강대학교, 물리학과.

강자성체에서 발생하는 열적 요동에 의한 자기 잡음은 강자성체의 자화율 및 공명 주파수와 관련된 정보를 제공하는 중요한 물성 측정 중 하나이다. 최근 활발히 연구되고 있는 강자성 나노선 구조에서의 열적 요동에 의해 생기는 자기 잡음에 대한 연구를 수행하기 위해, 열적 요동에 의한 무작위 자기장을 포함한 미세자기 동역학을 사용하였다[1]. 이 계산에서 강자성 나노선의 두께는 10 nm, 길이는 1  $\mu\text{m}$ 이며 폭은 50 nm에서 120 nm까지 10 nm 간격으로 변화시키며 계산을 수행하였고, 감쇠 변수는 0.01, 온도는 300 K, 포화 자화는  $8.6 \times 10^5 \text{ A/m}$ , 외부 자기장은 0 Oe를 이용하였다. 강자성 나노선 구조에서 길이 방향에 대하여 열적 요동에 의해서 발생하는 가로 방향의 자화 성분을 시간에 따라 기록한 후에 푸리에 변환을 거친 결과를 그림 1에 도식하였다. 나노선이 단일 자구인 경우와 중앙에 자벽이 존재하는 경우에 대해서 계산을 수행하여 비교 분석한 결과, 자벽이 존재하는 경우에 나노선 전체에서 발생하는 잡음 공명 주파수와 그것과 구분되는 또 다른 특성의 잡음 공명 주파수가 존재함을 발견하였다. 이는 자벽 내부에 존재하는 스핀들의 열적 요동 특성이 자구 내에 존재하는 스핀들과 다르기 때문이다. 본 연구를 기반으로 열적 요동에 의해 자벽에서 발생하는 자기 잡음을 측정하여 자벽 내부의 스핀에 대한 특성을 연구할 수 있을 것으로 기대된다. [1] J.L. Garcia-Palacios and F.J. Lazaro, Phys. Rev. B Vol.58, 14937

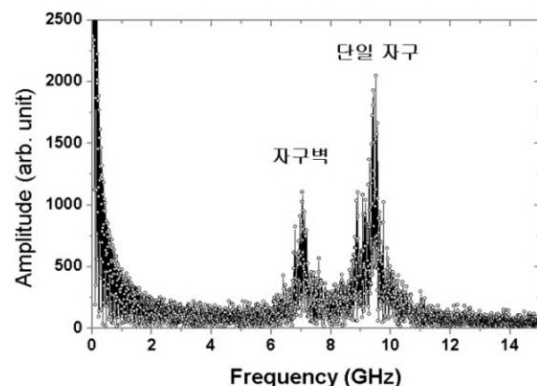


그림 1. 강자성 나노선의 열적 요동에 의한 자기 잡음. 강자성 나노선 구조에서 길이 방향에 대하여 열적 요동에 의해서 발생하는 가로 방향의 자화 성분을 시간에 따라 기록한 후에 푸리에 변환을 거친 결과를 그림 1에 도식하였다. 나노선이 단일 자구인 경우와 중앙에 자벽이 존재하는 경우에 대해서 계산을 수행하여 비교 분석한 결과, 자벽이 존재하는 경우에 나노선 전체에서 발생하는 잡음 공명 주파수와 그것과 구분되는 또 다른 특성의 잡음 공명 주파수가 존재함을 발견하였다. 이는 자벽 내부에 존재하는 스핀들의 열적 요동 특성이 자구 내에 존재하는 스핀들과 다르기 때문이다. 본 연구를 기반으로 열적 요동에 의해 자벽에서 발생하는 자기 잡음을 측정하여 자벽 내부의 스핀에 대한 특성을 연구할 수 있을 것으로 기대된다. [1] J.L. Garcia-Palacios and F.J. Lazaro, Phys. Rev. B Vol.58, 14937

## Principles Study

YANG Jeonghwa(양정화), KIM Dongyoo(김동유), HONG Jisang(홍지상)

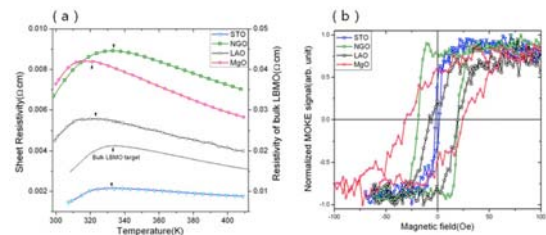
부경대학교, 물리학과.

Using the full potential linearized augmented plane wave (FLAPW) method, the magnetic properties of 2 monolayer(ML) Mn films on Fe(100) surface have been investigated. The main issue of this study is the magnetic properties depending on H adlayer and Ag spacer layer. To this aim, we have considered four different systems, such as Mn/Fe(001), Mn/Ag/Fe(001), H/Mn/Fe(001), and H/Mn/Ag/Fe(001). Here, we have assumed that the thickness of Mn and Ag is 2 ML, and H atom is placed on the hollow site above Mn layer with 1 ML thickness. We have found that Hydrogen adlayer strongly affect the magnetic state of the Mn thin films. However, Ag spacer layer has hardly effect on Mn thin films. The H added systems have antiferromagnetic(AFM) ground state. Nonetheless, the small energy difference between AFM state and FM state imply the possibility of FM ground state for H added systems. In addition, the calculated x-ray absorption spectroscopy (XAS) and x-ray magnetic circular dichroism (XMCD) will be presented. .

JUNG Dong-gyu, DHO Joonghoe, KI sanghoon

경북대학교 물리학과.

펄스레이저증착법(PLD)을 이용해서  $\text{LaAlO}_3$ (LAO),  $\text{NdGaO}_3$ (NGO), STO 및 MgO 기판 위에  $\text{La}_{0.7}\text{Ba}_{0.3}\text{MnO}_3$  (LBMO) 박막을 제작하고 구조적, 자기적 및 전기적 성질을 측정하여 LBMO 격자변형효과에 대해 연구하였다. 여기서, 우리는 LBMO의 물리적 특성에 격자변형효과 외에 다른 어떠한 요인에 의한 변화가 없도록 4가지 종류의 기판에 LBMO 박막을 동시에 증착하였다. 시료는 (100)LAO, (100)NGO, (100)STO, (100)MgO 기판을 한꺼번에 PLD 장치에 넣고 제작하였으며, 증착시 온도는 약 750°C, 산소 분압은 200mTorr였다. 박막의 두께는 증착시간을 통해서 조절하였고 약 50nm이다. 4가지 서로 다른 기판 위에 증착된 박막들은 동시에 증착되어 PLD 증착조건이 동일하여 관측된 LBMO 특성의 차이는 기판에 의한 영향이 결정적이다. XRD 데이터를 통해 LBMO 박막이 (100)STO, (100)NGO, (100)LAO, 그리고 (100)MgO 기판위에 에피택시 성장이 이루어졌음을 확인하였다. 온도에 따른 저항측정에서 저항 피크의 온도( $T_p$ )는 각각 STO에서 332 K, NGO에서 333 K, LAO에서 322 K, 그리고 MgO에서 320 K였다. 기판의 종류에 따른  $T_p$ 의 차이는 LBMO와 기판 사이의 격자 불일치에 의한 것으로 생각된다. 상온에서 자기장에 따른 자기광학효과 측정을 통하여 LBMO 박막의 보자력이 STO에서 1.7 Oe, NGO에서 19 Oe, LAO에서 14 Oe, 그리고 MgO에서 28 Oe임을 알 수 있었다.



**Dp-II-104****Spin-Orbital-Lattice Coupling in  $\text{KO}_2$  Superoxide**

김 민재, 김 범현, 최 홍철, 민 병일

*Department of Physics, POSTECH.*

In  $\text{KO}_2$  superoxide, the magnetic ordering from the incomplete pi level emerges concomitantly with a symmetry lowering such as gyration of anions. The simultaneous structural and magnetic phase transitions suggest the spin-orbital-lattice coupling in correlated  $2p$  electrons system. We have studied the interplay of the spin-orbital-lattice degrees of freedom in  $\text{KO}_2$  by employing the first-principles electronic structure theory. We used generalized gradient approximation (GGA) for the exchange correlation potential incorporating the Coulomb interaction  $U$  and the spin-orbit coupling (GGA+U+SO). For the high symmetry phase of  $\text{KO}_2$ , we have found that the band gap opens by the spin-orbit coupling which splits the degenerate pi anti-bonding level. For the low symmetry phase, we have found that the band gap opens by the strong Coulomb interaction and the crystal field effect from alkali cations. The simultaneous antiferro-spin and ferro-orbital orderings occur with the band gap opening.

**Dp-II-105****Electron Magnetic Resonance and Magnetic Susceptibility of  $\text{CsMnCl}_3 \cdot 2\text{H}_2\text{O}$  and  $\text{CsMnCl}_3$** NA Sung-Ho, KIM Heung-Chul<sup>1</sup>*KASI. <sup>1</sup>Pusan National Univ.*

For two compounds  $\text{CsMnCl}_3 \cdot 2\text{H}_2\text{O}$  and  $\text{CsMnCl}_3$ , the electron magnetic resonance (EMR) and other magnetic characteristics are analyzed. The exchange interaction strongly affects so that the EMR signal line-width is quite narrow. Double quantum transition and super-hyperfine interaction are clearly detected in the EMR signal. From the temperature dependence of the magnetic susceptibility curves, the exchange interaction constant  $J$ , Curie Weiss temperature, and Neel temperature of the each sample are identified.

**Dp-II-106****NiFe와 Cr<sub>2</sub>(1-x)Fe<sub>2</sub>xO<sub>3</sub>(CFO ; x = 0.1) 이층박막에서의 교환바이어스와 보자력**

KI sanghoon, DHO joonghoe, JUNG dong-gyu

경북대학교물리학과.

교환바이어스(exchange bias)현상은 자기이력곡선이 영점을 기준으로 한쪽 방향으로 이동하는 현상으로서 강자성체(FM)과 반강자성체(AF)의 접합계면에서의 교환상호작용에 의해 기인된다. 이 현상은 Meiklejohn과 Bean에 의해 CoO층으로 둘러싸인 Co 입자에서 처음으로 발견되었으며, 이후 FM/AF 다층박막에서 교환바이어스에 대한 많은 연구가 진행되어 왔다. 교환 바이어스를 연구함으로써 강자성 스핀과 반강자성의 스핀 사이의 교환상호작용을 이해할 수 있으며, 교환바이어스 현상은 자기정보 재생헤드 및 비휘발성 자기메모리 등 각종 스핀밸브소자 개발에 활용될 수 있다. 일반적으로 교환바이어스 시스템에서 발견되는 교환바이어스와 보자력의 증가 현상은 결정성장 방향에 따른 경계면 스핀구조, 산소분압과 같은 박막증착 조건에 따른 경계면 거침도, 측정온도 등의 변수에 따라 의존한다. 이번 연구에서는 FM/AF 구조에서의 교환바이어스 현상을 실험하였는데, AF층은 Cr<sub>2</sub>(1-x)Fe<sub>2</sub>xO<sub>3</sub>(CFO ; x = 0.1)를 펄스 레이저 증착법을 사용하여 Si 기판과 C-plane과 R-plane Al<sub>2</sub>O<sub>3</sub>기판 위에 성장 시키고 FM층으로 퍼멀로이(NiFe)를 RF 스퍼터링을 이용하여 CFO층 위에 두께 5nm로 증착 하였다. 원자힘 현미경(AFM)을 이용하여 CFO층의 표면 거침도를 측정하였고 X선 회절을 이용하여 박막의 결정구조를 조사하였다. 초전도양자간섭소자(SQUID) 자력계와 자기광학 Kerr효과를 이용하여 온도에 따른 NiFe/CFO 이층박막의 자기이력곡선을 측정하여 교환 바이어스 및 자기 보자력의 크기 변화를 분석하였다

**Dp-II-107****n-Si 위에 전기 증착한 Co film의 자기적 상호작용과 활성화부피**김 상인, 정 순영<sup>1</sup>, 이 종덕<sup>1</sup>, 김 현수<sup>1</sup>, 김 봉환한국원자력연구원. <sup>1</sup>경상대학교 물리학과.

n type의 Si(100)에 펄스전압을 달리하여 Cobalt film을 전기증착하였다. Co film은 Volmer-Weber 모드로 성장하였고 펄스전압이 증가하면 nucleus density도 증가하였다. 전압에 따른 Co film의 자기적 성질은 시료진동형자력계(VSM)로 상온에서 측정하였다. 직류탈자잔류곡선(DC demagnetization remanence curve)과 등온잔류곡선(Isothermal remanence curve)을 측정하여 ΔM을 구하여 입자간의 자기적 상호작용과 세기를 조사하였다. 그리고 자화감쇠의 시간의존성과 직류탈자잔류곡선 측정결과로부터 자기점성계수와 비가역자화율을 결정하여 활성화 부피를 구하였다. 이런 결과들에 의해 펄스전압이 자기적 상호작용과 활성화부피의 증감현상에 관여하는 것으로 해석되었다.

**Dp-II-108****La<sub>0.7</sub>Sr<sub>0.3</sub>MnO<sub>3</sub>/STO(001) 강자성 박막의 두께에 따른 물성변화 연구**

KIM bongju, KWON daeyoung, SONG jong hyun<sup>1</sup>, HIKITA Yasuyuki<sup>2</sup>, KIM Bog G., HWANG Harold Y.<sup>2</sup>

부산 대학교, 물리학과. <sup>1</sup>충남대학교, 물리학과. <sup>2</sup>동경대학교, 응용물리학과.

La<sub>0.7</sub>Sr<sub>0.3</sub>MnO<sub>3</sub> (LSMO) 강자성 박막을 pulsed laser deposition (PLD) 방법을 이용하여 bulk crystal의 물성에 매우 가까운 증착 조건에서, 박막의 두께에 따른 물성변화를 탐구하기 위하여, STO (001) 기판 위에 두께에 따라 성장 시켰다. HRXRD를 이용한 박막 구조 분석, 비저항 측정, 자화측정 등을 통하여 박막의 두께에 따른 종합적인 물성변화를 논의 하였으며, 그 결과를 종합하여 박막의 두께에 따른 상 그림을 구축하였다. 특히, 박막의 두께가 감소함에 따라 고온의 영역에서는 상자성/금속 상에서, 상자성/비금속 상으로 상전이 하며 저온에서는 강자성/금속 상에서 강자성/비금속 상으로 상전이 하는 특성을 보이고 있음을 확인하였다. 이것은 벌크 시료에서 electronic bandwidth를 변화시켰을 때 나타나는 현상과 매우 흡사한 유사성을 가지고 있다.

**Dp-II-109****NMR study on the memory effect of cobalt at low temperature**

윤 동영, 이 진원, 이 순철

한국과학기술원 물리학과.

코발트는 694 K 이상과 이하에서 각각 fcc와 hcp가 안정한 격자 구조 상태로 알려져 있다. 우리는 다결정 코발트를 870 K에서 공기 냉각을 하면, 상온에서 준안정상태인 fcc가 단일상으로 존재하는 것을 핵자기 공명(NMR)을 통해 관찰하였다. 이러한 코발트는 온도를 낮춤에 따라, fcc의 영역은 감소하고 적층결함 (stacking fault) 및 hcp의 영역이 증가하고, 상온으로 온도를 다시 올리면 fcc의 영역 또한 증가하는 기억효과를 가지는 것을 NMR로 관찰하였다.

**Dp-II-110****외스바우어 분광 분석을 통한 망간페라이트 나노입자의 양성자조사 연구**

김 철성, 홍 순천, 명 보라, 최 정훈, 이 용혜, 김 우철, 김 삼진

국민대학교, 물리학과.

본 연구에서는 Manganese(II) acetylacetonate, Iron(III) acetylacetonate를 초기 물질로 oleic acid와 oleylamine를 계면활성제로 사용하여 고온열분해법으로  $\text{MnFe}_2\text{O}_4$  시료를 합성하였다. 합성된 시료들은 각각 0, 5, 10  $\text{pC}/\mu\text{m}^2$ 의 양성자빔 조사실험을 수행하여 양성자빔 조사에 따른 자기적 특성의 변화를 알아보고자 하였다. 양성자빔 조사 전후에 X-선 회절기(XRD), 진동시료형 자화율 측정기(VSM), Mössbauer 분광 실험을 수행하여 시료의 결정학적 구조 및 자기적 성질에 대하여 연구하였다. X-선 회절도 분석 결과 결정구조는 inverse spinel 구조이고 공간그룹은  $Fd3m$ , 격자상수는  $8.345 \pm 0.005 \text{ \AA}$ 로 분석되었으며 scherrer식을 이용하여 입자크기를 구한결과, 10.8 nm임을 확인하였다. 진동시료형 자화율 측정기를 이용하여 1.5 T 외부자기장 하에서 실험한 결과, 자화율값은 53.3, 56.1, 58.0 emu/g으로 양성자빔 조사에 따라 증가하였으며, 보자력값은 거의 변화가 없음을 확인할 수 있었다. Mössbauer 스펙트럼을 상온에서 실험한 결과, 원 시료에서는 1-line 형태의 초상자성 현상을 보였으나, 양성자빔을 5  $\text{pC}/\mu\text{m}^2$  조사한 시료는 6-line 형태를 띄어 양성자빔 조사에 따라 강자성이 발현됨을 확인할 수 있었다.

**Dp-II-111****고온 전기 저항 측정 장치 개발**

박 준호, 심 하성, 최 성일, 박 제근

성균관대 물리학과.

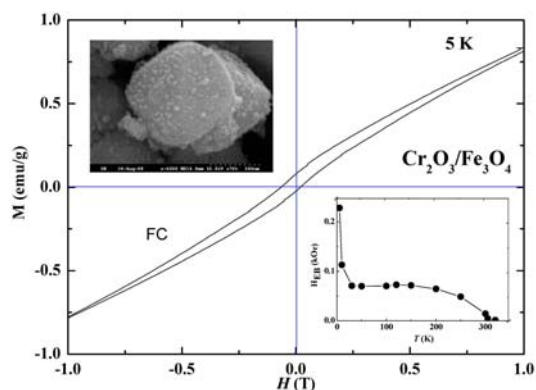
고온에서의 저항 측정은 상온 혹은 저온에서와 달리 신호선들을 샘플에 연결하기가 쉽지 않고 산화가 발생하여 측정이 용이하지 않다. spot welding 방법으로 시료에 신호선들을 연결하여 얻은 측정 값과, 범용으로 사용되는 Silver paste 및 Silver epoxy를 이용하여 신호선들을 연결하여 얻은 측정값을 비교·분석하여, Silver paste 및 Silver epoxy의 발화점 이후의 특성 변화가 저항 값에 어떻게 영향을 미치는지 확인하고자 하였다. 이를 토대로 실제 몇 가지 시료의 저항을 성공적으로 고온에서 측정하였다.

**Dp-II-112****Exchange Bias in  $\text{Cr}_2\text{O}_3/\text{Fe}_3\text{O}_4$  Core/shell Nanoparticles**

윤 병길, 정 종훈, 구 용성

인하대학교, 물리학과.

Core/shell nanoparticles, composed of antiferromagnetic  $\text{Cr}_2\text{O}_3$  core and ferrimagnetic  $\text{Fe}_3\text{O}_4$  shell, shows a robust shift of magnetic hysteresis loops when the nanoparticles were field-cooled from above Neel temperature ( $T_N \sim 308$  K). At 5 K (EB  $\sim 200$  Oe) and vertical ( $\Delta M \sim 0.030$  emu/g) shifts of hysteresis loops, and also reduction of both  $H_{EB}$  and  $\Delta M$  with cycling of applied field. The values of  $H_{EB}$  and  $\Delta M$  depend on the cooling field strength and slowly decrease and finally disappear near blocking temperature ( $T_B \sim T_N$ ). We discuss the observed results in conjunction with exchange interaction between antiferromagnetic and ferrimagnetic spins near core/shell interfaces.

**Dp-II-113****Magnetic impurity and Peierls-like transition in dodecylamine-intercalated****vanadium oxides**

KWEON Hyocheon, LEE Kyu Won, LEE Cheol Eui

Department of Physics, Korea University.

Mixed-valent dodecylamine-intercalated vanadium oxides of orthorhombic structure (OR) have been studied by means of magnetic susceptibility measurements as a function of temperature and magnetic field, which showed a Peierls-like transition at around  $T_p = 375$  K. Below  $T_p$ , one-dimensional antiferromagnetic spins and dimer spins were observed to coexist and the fraction of dimer spins rapidly increased with the applied magnetic field. Nonmagnetic  $\text{V}^{5+}$  ions act as nonmagnetic impurities giving rise to an impurity-induced antiferromagnetism, usually observed in (quasi) one-dimensional spin gap systems. High enough magnetic fields seem to remove the disturbance in the singlet ground state, leading to a field-driven transition from one-dimensional antiferromagnetism to spin dimerization.

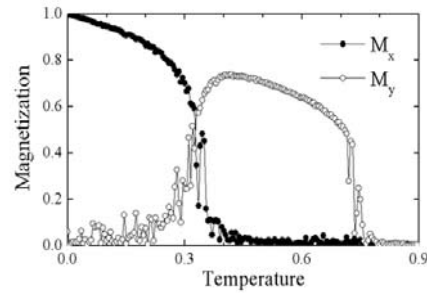
## Dp-II-114

### F/AF 자성박막계에서 나타나는 SRT에 대한 Monte-Carlo Simulation연구

석 진호, 홍 상신, 권 희영, 원 창연

경희대학교 물리학과

나노 스케일의 강자성박막과 반강자성박막이 서로 붙어 있는 자성 박막계에서 많은 실험적 연구가 수행되었고, 온도나 박막 두께의 변화에 따른 스핀의 급작스러운 천이 (Spin Reorientation Transition), 히스테리시스 곡선의 외부자기장에 대한 이동 (Exchange Bias) 등의 현상이 관찰되었다. 우리는 위의 자성 박막계를 시뮬레이션 방법을 통해 연구하였다. 자성 박막은 각각 가로와 세로가 원자 50개로 구성되어 있고 그 두께는 원자 1개 길이이고 전체 박막계의 살창구조가 bcc인 두 개의 겹쳐진 판을 도입하여 나타내었다. 모든 원자 스핀들 사이의 교환상호작용은 바로 옆(neighborhood)의 스핀들 사이의 작용만을 고려하고 나머지는 무시하였다. 그리고 각 박막이 모두 계면에 대해 평행한 (in-plane) 비등방성 (Crystalline Anisotropy) 을 가지고 있다고 가정하였고 스핀 배열의 온도에 따른 변화는 바른틀 앙상블 이론에 따르는 것으로 프로 그래밍하여 그 계를 시뮬레이션해 보았다. 두 박막의 비등방성 축이 모두 y축이고, 그 크기는 반강자성체가 조금 더 큰 경우에, 온도에 따른 스핀 배열을 살펴보면, 온도가 낮은 경우에 강자성체 박막과 반강자성체 박막의 스핀들이 서로 수직하게 결합(Perpendicular Coupling)되어 있다가, 온도가 높아지면서 서로 수평한 결합(Collinear Coupling)으로 스핀들의 천이가 발생함을 관찰하였다..



강자성박막에서 온도가 약 0.3 일 때, Perpendicular Coupling 으로부터 Collinear Coupling 으로의 Temperature-driven Spin Reorientation Transition 이 발생한다.

## Dp-II-115

### Magnetic Properties of H. Pylori Ferritins Reconstituted under Two Different

#### Magnetic Field Conditions

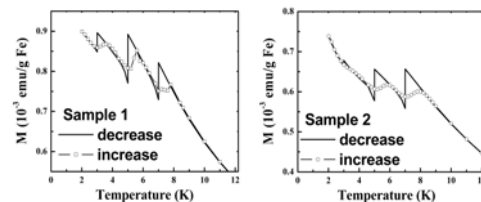
YOON S.-W., SON K.<sup>1</sup>, SUH B. J., JANG Z. H.<sup>1</sup>, CHO K. J.<sup>2</sup>, KIM K. H.<sup>3</sup>

Department of Physics, The Catholic University of Korea. <sup>1</sup>Department of Physics, Kookmin

University. <sup>2</sup>Department of Life Sciences & Biotechnology,

Korea University. <sup>3</sup>Department of Biotechnology & Bioinformatics, Korea University.

*Helicobacter pylori* ferritin were genetically engineered by being expressed from the plasmid. The apoferritins were then reconstituted with  $4160 \pm 30$  Fe ions/ferritin under two different conditions: one at normal environment (Sample 1) and the other under a high magnetic field,  $H = 9.4$  T (Sample 2) The magnetic properties of two variants were investigated using a SQUID magnetometer as functions of temperature and field. The blocking temperatures at  $H = 1,000$  Oe are  $T_B = 8$  K for both samples which is considerably smaller than those of a human ferritin and a horse spleen ferritin. From the hysteresis curves at  $T = 2$  K, we found that the saturation magnetization of Sample 2 is larger than that of Sample 1, whereas the coercive field is  $H_c = 700$  Oe for Sample 2, much smaller than  $H_c = 2,400$  Oe for Sample 1. By analyzing the field dependence of magnetization at various temperatures using a simple model including a Langevin function and a linear susceptibility term, we could extract successfully the Neel temperature and the temperature dependences of effective moment, saturation magnetization and linear susceptibility for both samples. Interestingly, we observed "memory effects" (see the figure) in both samples which was observed in magnetic nanoparticle system. The effect was confirmed from both the halted field-cooled (FC) measurement and the halted relaxation measurement. In addition, the relaxation of magnetization is observed to be considerably slower in Sample 2 than in Sample 1, suggesting that the magnetic field applied during iron intake affects the biomineralization process.



## Ferrites

KWON Woo Hyun, LEE Seung Wha, LEE Jae-Gwang, CHAE Kwang Pyo

건국대학교 전자정보전공.

The crystallographic and magnetic properties of the  $V_2O_5$  doped  $Ti_{0.2}Co_{1.2}Fe_{1.6}O_4$  and the  $Li_{0.5+x}Co_{0.2}Ti_{0.2}V_xFe_{2.1-2x}O_4$  ferrites were investigated by XRD, SEM, Mössbauer spectroscopy, and VSM. All of the samples showed a single spinel structure. For  $V_2O_5$  doped  $Ti_{0.2}Co_{1.2}Fe_{1.6}O_4$  ferrite, the average grain size showed a pronounced maximum about  $9.11\ \mu m$  at 2.6 wt.%  $V_2O_5$ . When  $x=0$ , in the  $x(V_2O_5)$  wt.% doped  $Ti_{0.2}Co_{1.2}Fe_{1.6}O_4$  the Mössbauer spectrum could be fitted with two Zeeman sextets, which is the typical spinel ferrite spectra with A and B sites. However for  $x>0.2$ , the Mössbauer spectrum could be fitted with two Zeeman sextets and one doublet. The magnetic behavior of the samples showed that an increase in the  $V_2O_5$  contents led to an increase in the saturation magnetization and the coercivity up to 2.2 wt.%, after which a subsequent decreased. The maximum of the saturation magnetization and the coercivity were 69.0 emu/g and 0.36 kOe, respectively. For  $Li_{0.5+x}Co_{0.2}Ti_{0.2}V_xFe_{2.1-2x}O_4$  ferrite, the lattice parameters were nearly constant as the substituted content increases. The average grain size of the samples increased with  $x$ . When  $x=0$ , the Mössbauer spectrum could be fitted with two Zeeman sextets. However for  $x\geq 0.05$ , the Mössbauer spectra could be fitted with two Zeeman sextets and one doublet. The magnetic behavior of the samples showed that an increase in the vanadium contents led to an increase in the saturation magnetization and then to some decreases, whereas the coercivity decreased. The maximum of the saturation magnetization was 44.58 emu/g at  $x=0.1$ , and the coercivity was 171 Oe at  $x=0$ .

## based superlattices

SHIN Jinsik, LEE sangyup, LEE hakjoon, YOO Taehee, CHUNG Sunjae, LEE Sanghoon, LIU X.<sup>1</sup>, FURDYNA J.K.<sup>1</sup>

Physics Department, Korea University, Seoul 136-701, Korea. <sup>1</sup>Department of Physics, University of Notre Dame, Notre Dame, IN 46556 USA.

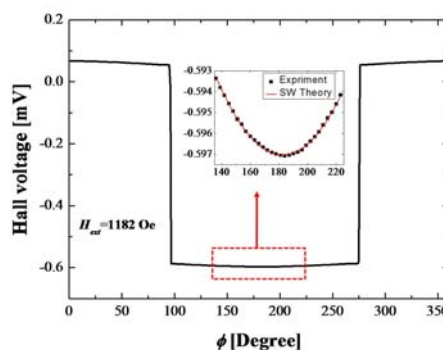
The antiferromagnetic (AFM) interlayer exchange coupling (IEC) leads to the giant magnetoresistance (GMR)[1] effect in the electrical transport, which has been the basic principle for the magnetic memory and sensor devices. Such observation of magnetization dependence of current flow in ferromagnetic systems opens a new field of "spintronics" in which both the charge and the spin degrees of freedom of the charge carriers are utilized for the new functionality. In the context of "spintronic", ferromagnetic semiconductor GaMnAs has received a great deal of attention, recently, due to the carrier mediated ferromagnetism, which allows one to manipulate the magnetic properties by controlling the carriers[2]. There has been serious effort to realize AFM IEC in GaMnAs based multilayer systems with a hope to take advantage of carrier tenability in this material. Though the oscillation between AFM and FM IEC has been theoretically expected depending on the carrier density and/or barrier properties [3][4], the only FM IEC is observed in most of the GaMnAs based multilayer structures. It took long time until recent report on the direct observation of AFM IEC by polarized neutron reflectivity (PNR) in the GaMnAs/GaAs:Be multilayer structures[5]. Here we present new evidences for the spontaneous AFM IEC in the GaMnAs/GaAs multilayer from magnetization and electrical transport measurements. Specially, the GRM-like effect is clearly observed in the magnetization reversal process revealing the details of spin-flip procedure of each magnetic layer. This electrically observed carrier dependent change of the IEC between AFM and FM in the GaMnAs/GaAs multilayer could provide an opportunity for magnetic information storage device controlled by electrical gate. [1] Viret, M. *et al.*, Phys. Rev. B. 53, 8463 (1996)[2] H. Ohno. *et al.*, Science. 281. 951(1998) [3] P. Sankowski *et al.*, Phys. Rev. B. 71, 201303(2005)[4] T. Jungwirth *et al.*, Phys. Rev. B. 59, 9818(1999)[5] J. -H. Chung *et al.*, Phys. Rev. Lett. 101, 237202 (2008)

**Extraordinary Hall Effect Torque Measurement**

CHO Cheong-Gu, MOON Kyoung-Woong, LEE Jae-Chul,  
CHOE Sug-Bong

*Department of Physics, Seoul National University.*

Ultrathin ferromagnetic films with perpendicular magnetic anisotropy (PMA) have been investigated for high density data storage applications. In particular, the measurement technique of the anisotropy field of PMA film has been actively researched to optimize the device performance in recent years. In this paper we present a method to measure the anisotropy field using extraordinary Hall effect measurement. In this technique, the extraordinary Hall voltage is measured with rotating the external magnetic field by small angle around the easy axis. We analyze data based on the Stoner-Wohlfarth (SW) theory. The experimental data shows a good accordance with the theoretical prediction as shown in Fig. 1. The dependence of the anisotropy field on the layer thickness and base substrate is discussed.

**Complex,  $\text{Mn}_3\text{O}$ , using a Pulsed Magnet**

PARK J.-N., YOON S.-W.<sup>1</sup>, JANG Z. H., SUH B. J.<sup>1</sup>, CHOI K.-Y.<sup>2</sup>, NOJIRI H.<sup>3</sup>

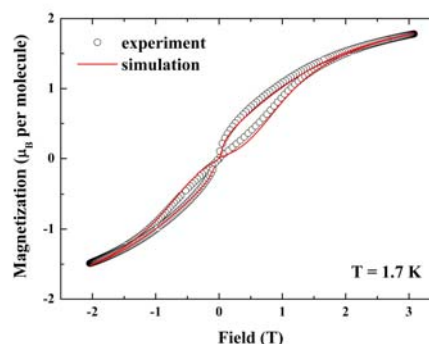
*Department of Physics, Kookmin University.* <sup>1</sup>*Department of*

*Physics, The Catholic University of Korea.* <sup>2</sup>*Department of*

*Physics, Chungang University.* <sup>3</sup>*Department of Physics,*

*Dohoku University, Sendai, JAPAN.*

We have investigated magnetic properties of a trinuclear oxo-centered manganese complex,  $\text{Mn}_3\text{O}$ . The  $\text{Mn}_3\text{O}$  complex is a isosceles-type single molecular magnet (SMM) consisting of one  $\text{Mn}^{2+}$  ( $S=5/2$ ) and two  $\text{Mn}^{3+}$  ( $S=2$ ) ions. Magnetization ( $M$ ) versus field ( $H$ ) at  $T = 2.0$  K and  $M$  versus temperature ( $T$ ) at  $H = 200$  Oe were measured using a SQUID magnetometer. The hysteresis curve and magnetization at high fields were measured using a pulsed magnet magnetometer. The analysis of equilibrium magnetization ( $M$  vs.  $H$ ,  $M$  vs.  $T$ ) using a Heisenberg spin Hamiltonian with single ion anisotropies reveals that the exchange interaction among Mn ions is antiferromagnetic and the exchange interaction constants are  $J_{12} = J_{13} = -13.2$  K between  $\text{Mn}^{2+}$  and  $\text{Mn}^{3+}$  ions,  $J_{23} = -4.0$  K between two  $\text{Mn}^{3+}$  ions, and anisotropy constants are  $D_1 = +1.0$  K for  $\text{Mn}^{2+}$  ion,  $D_2 = D_3 = +4.2$  K for  $\text{Mn}^{3+}$  ion, respectively. The stepwise jump at  $H = 0$  reflecting a Landau-Zener-Stückelberg (LZS) gap was observed by using a fast sweep pulsed magnet. A numerical simulation using a modified Bloch equation with the magnetic parameters obtained above shows that the LZS energy gap ( $\Delta E$ ) responsible for the magnetization step at  $H = 0$  is  $\Delta E \approx 5.5$  mK.



**Dp-II-120****자기 쌍극자 상호작용에 의한 자성 나노선 배열의 자기적 특성변화**

석 재권, 김 택수, 전 일근, 김 승호, 신 상원<sup>1</sup>, 송 종한<sup>1</sup>, 이 재용

연세대학교, 물리학과, <sup>1</sup>한국과학기술연구원, 특성분석센터.

나노선의 구조에 기반을 둔 실험들 대부분은 나노선 배열에 대한 연구이다. 자성 나노선 배열의 경우 나노선들 간의 자기 쌍극자 상호작용이 나노선의 특성에 중요한 영향을 준다. 최근 제안된 연구들은 자성 구역벽 운동에 기반을 둔 새로운 개념의 자성 저장매체와 자성 논리 소자이다. 이러한 연구들은 주변 나노선 간의 자기 쌍극자 상호작용을 고려하지 않은 것이다. 따라서 자기 쌍극자 상호작용에 의한 자성 나노선 배열의 자기적 특성변화는 꼭 필요한 연구이다. 자성 나노선 배열을 제작하기 위해 Laser Interference Lithography(LIL)를 이용해서 Photoresist(PR) 나노선 배열을 제작하였다. LIL은 substrate에 PR을 코팅한 후 두 개의 coherent laser beam을 입사 시키면 두 beam에 의해 생기는 standing wave에 의해 pattern을 제작하는 방식이다. 그 pattern의 주기(p)는 두 beam의 사이각이  $2\theta$ 라고 했을 때,  $p = \lambda / 2\sin\theta$ 로 나타낼 수 있다. 이 식으로부터 사이각  $2\theta$ 를 조절하면 패턴의 주기를 간단하게 조절할 수 있다. 또한, positive PR은 laser beam에 노출된 부분이 제거되는 특성이 있고, negative PR은 laser beam에 노출되지 않은 부분이 제거되는 특성이 있다. 이 두 가지 종류의 PR을 사용하여 나노선간의 간격이 나노선의 선포보다 짧은 것과 긴 것, 2가지 시료를 제작하였다. 제작한 PR 나노선 배열을 UHV chamber 내에서 E-beam evaporator를 사용하여 Ni80Fe20 박막을 증착한 후, PR 나노선을 제거하여 Ni80Fe20 나노선 배열을 제작하였다. 시료의 제작 상태는 SEM(scanning electron microscope)으로 확인하였다. 제작된 시료를 통해서 나노선간의 간격에 따라 자기 쌍극자 상호작용이 어떻게 달라지는지 알아볼 것이다. 자기적 특성은 MOKE(magneto-optic Kerr effect)장비로 측정하고, MFM(Magnetic force microscope) image를 얻어 자구벽 구조를 관찰할 것이다.

**Dp-II-121****Ion mixing을 통한 NiFe 자성 나노 선 배열의 자기적 특성 변화**

전 일근, 김 승호, 석 재권, 이 재용, 신 상원<sup>1</sup>, 송 종한<sup>1</sup>

연세대학교 물리학과, <sup>1</sup>한국과학기술연구원 특성분석센터.

자성의 특성 연구에 많이 이용되고 있는 NiFe 나노 선에 Ion mixing을 하여 자기적 특성 변화를 연구하였다. 자성 박막에 Ion mixing을 할 경우 박막의 자기이방성, 보자력(Coercive field), exchange anisotropy 등의 변화를 관찰할 수 있다. Ion mixing이 자성 나노 선에 주는 자기적인 특성 변화에 대한 영향을 알아보는 연구이다. 시료의 나노 선 제작은 Laser interference Lithography(LIL)를 이용하여 silicon기판위에 주기가 630nm인 PR(photoresist)배열을 제작하였다. 이 시료를 UHV chamber 안에서 E-beam evaporator를 사용해 buffer layer로 Cu를 증착하고 그 위에 NiFe를 증착한 후, PR 나노 선을 제거하여 NiFe 나노 선을 만들었다. 이 시료에 111keV Cu 이온의 dose를  $1 \times 10^{14}$ ,  $1 \times 10^{16}$ ,  $2 \times 10^{16}$  ions/cm<sup>2</sup> 으로 조절하면서 시료의 자성 나노 선 전체 부분에서 buffer layer층인 Cu와 NiFe층을 mixing 하였다. 이렇게 만들어진 시료의 상태는 SEM(scanning electron microscope)으로 확인하였고 자기적인 특성은 MOKE(magneto-Kerr effect)장비로 측정하였다. 시료를 Ion mixing을 하지 않은 것과 한 것을 MOKE로 측정하여 보았다. 그 시료의 보자력이 Ion mixing을 많이 하면 할수록 하지 않은 시료의 보자력보다 적게 나온다는 것을 MOKE로 확인 하였다. 이것은 이전에 연구 되었던 자성 박막에서 Ion mixing을 할 때 보자력이 늘어나던 것과는 다른 결과를 나타내었다. 추가적으로 Ion mixing을 할 때 시료에서 어떤 자기적인 성질이 변하고 표면에 어떤 영향을 주는지에 대해서 자세히 연구할 계획이다.

## Measurements

SUH Jooyoung, KIM Jae-Hoon, KIM Eun Kyu

*Quantum-Function Spinics Laboratory & Department of Physics, Hanyang University.*

Spintronics which is a new spin-electronic technology based on the spin degree of freedom as well as charge has been widely expected to execute a principle role in the future generation such as non-volatile memory, pick-up heads and magnetic sensors. First of all, it is important to realize spin-dependent currents in non magnetic materials. In general, spin-dependent current is affected by injection or detection efficiency, spin life time (spin diffusion length), and temperature. Nanoscale ferromagnet/metal spin Hall devices provide a simple model system which allows to study spin injection and accumulation phenomena. In this work, we fabricated spin Hall devices, consisting with cobalt (Co) and aluminum (Al), and measured series of anisotropy magnetoresistance and spin signal. We also measured the gate modulation experimentation by using electromagnetic field. This is an important issue to be addressed for measurement and evaluation of spin transport properties.

나는 줄무늬영역 상의 성질.

권 희영, 석 진호, 홍 상신, 원 창연

경희대학교 물리학과.

2차원 자성체에 대해, 원거리 자성 상호작용에 의해 여러 가지 상 들이 나타난다는 것과 그 상 들 사이의 SRT (Spin Reorientation Transition)에 대한 원리를 이해하기 위해 많은 연구가 있어왔다. 그중 우리의 연구는 줄무늬 상 일때, 면외 자화(out-of-plane magnetization)에서 면내 자화(in-plane magnetization)로의 SRT가 일어날 때 어떤 현상이 나타나는지에 초점을 맞췄다. 3차원 Heisenberg 모델을 바탕으로 한 계산과 Monte-Carlo 시뮬레이션을 이용한 컴퓨터 시뮬레이션과의 비교를 통해, 줄무늬 도메인의 SRT 영역에서 자기구역 벽의 두께가 줄무늬 두께와 같아지게 되고 정적 자화 파동 모양이 나타나게 된다는 것을 알 수 있었다. 즉 면외 자화가 정현파 형태로 존재하게 되고, SRT가 진행되면서 파장은 거의 변하지 않지만 파의 높이가 줄어들면서 면내 자화의 상으로 바뀌어 간다는 것을 알아 냈다. 이 SRT에서의 자화파동 형태의 성질은 몇가지 물리적 인자들에 의존하는데, 특히 동축 수직 비등방성값이 증가하면 파장도 증가하고, 자화구역벽의 두께도 줄무늬의 두께에 비해 줄어들면서 다시 원래의 줄무늬 상으로 돌아간다는 것을 볼수 있다.[Fig.1]

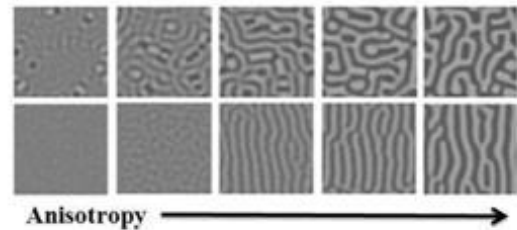


Fig.1. 비등방성에 따른 줄무늬영역의 변화  
위의 그림은 무작위 한 초기조건에서 Monte-Carlo 시뮬레이션의 결과이고, 아래 그림은 한 축으로 정렬시킨 초기조건으로부터의 결과이다.

**Dp-II-124****Magnetocrystalline anisotropy of  $D0_{22}$ - $Mn_3Ga$ : Density functional study**

YUN Won Seok, CHA Gi-Beom, HONG Soon Cheol

*Dept. of Physics, Univ. of Ulsan.*

Recently, research interest in perpendicular magnetic anisotropy (PMA) for applications in spin valves and magnetic tunnel junctions has been strongly raised. Because of PMA materials can overcome superparamagnetic limit so to retain the thermal stability of high-density magnetic recording media. The PMA materials with large spin polarization, low saturation magnetization, and high Curie temperature are further required. Among them,  $Mn_3Ga$  with  $D0_{22}$ -structure is a good candidate. Very recently, Wu *et al.* [1] reported that the  $Mn_{2.5}Ga$  film has a giant PMA ( $K_u^{eff} = 1.2 \times 10^7$  erg/cm<sup>3</sup>) and low saturation magnetization ( $M_s = 250$  emu/cm<sup>3</sup>). In this work, we focused on magnetocrystalline anisotropy (MCA) of  $D0_{22}$ - $Mn_3Ga$  by using all-electron full-potential linearized augmented plane-wave method within the generalized gradient approximation. In the  $D0_{22}$  structure, a pure Mn layer and a mixed Mn-Ga layer are repeated in turn along the z-coordinate. In result, there are two inequivalent positions of the Mn atomic types in  $D0_{22}$ . The magnetic ground state was calculated to be ferrimagnetic with respect to ferromagnetic by the energy difference of 144 meV/Mn. The calculated magnetic moment of Mn I (in the mixed Mn-Ga layer) and Mn II (in the pure Mn layer) are 2.86 and -2.32  $\mu_B$  for the bulk  $D0_{22}$ - $Mn_3Ga$ , respectively. We will discuss in more detail the MCA and magnetism at the bulk and the surface of  $D0_{22}$ - $Mn_3Ga$  with a single-particle energy spectra. [1] F. Wu, S *et al.*, Appl. Phys. Lett. 95, 122503 (2009).

**Dp-II-125****Triangular Plain  $Ba_3NbFe_3Si_2O_{14}$  Langasite 의 뢰스바우어 분광연구**김 철성, 김 진모, 현 성욱, 이 은중, 박 영욱, 김 성백<sup>1</sup>, 고 태준*국민대학교, 물리학과. <sup>1</sup> 포항공과대학교, 물리학과.*

본 연구에서는 Langasite 로 알려진  $Ba_3NbFe_3Si_2O_{14}$  의 결정학적 및 자기적 특성에 대하여 알아보하고자 하였다. 본 시료는 직접합성법을 사용하여 1180 °C 공기 중에서 24시간 열처리함으로써 합성하였다. X-선 회절 실험을 통하여  $Fe^{3+}$  이온이 Triangular plain 을 형성하는 공간그룹  $P321$  의 결정구조임을 판별할 수 있었다. 진동시료형 자화율 측정기(VSM)를 이용하여 1.5 T 의 외부자기장하에서 실험 결과, 상온에서 0.85 emu/g의 자화율값과 2331.3 Oe의 보자력값을 갖음을 확인할 수 있었다. 또한, 철 이온 주변의 초미세 상호작용을 알아보기 위하여 뢰스바우어 분광 실험을 수행하였다. 뢰스바우어 스펙트럼을 분석한 결과, 상온에서 하나의 사중극자 분열을 보이며 극저온 4.2 K에서 6-line 형태의 2-set 으로 나타남을 확인할 수 있었다. 이성질체 이동치값으로 철 이온은 3+의 이온가를 가지며,  $Fe^{3+}$  이온이 십면체의 자리를 제외한 팔면체 자리 (octahedral site)와 사면체 자리 (tetrahedral site)에 각각 위치하고 있음을 알 수 있었다.

이 규준, 추 성민, 윤 정범<sup>1</sup>, 송 기명<sup>1</sup>, Y. Saiga<sup>2</sup>, 유 천열<sup>1</sup>, 허 남정<sup>1</sup>, 이 성익, T. Takabatake<sup>2</sup>, 정 명화  
 서강대학교, 물리학과. <sup>1</sup>인하대학교, 물리학과. <sup>2</sup>Hiroshima University, ADSM.

스핀트로닉스 분야는 끊임없이 흥미로운 학문 분야로 2007년 giant magnetoresistance가 노벨 물리학상을 수상한 후, 더욱 많은 관심을 받게 되었다. 스핀트로닉스에 적합한 물질로는 틸 없는 자성 반도체가 적합하다. 이러한 틸 없는 자성 반도체로 납계 산화물질인  $\text{PbPdO}_2$ 와 Co가 도핑된  $\text{PbPdO}_2$ 에 관한 물성을 분석해보았다.  $\text{PbPdO}_2$ 와 Co가 도핑된  $\text{PbPdO}_2$ 는 저항의 온도 의존성 데이터로 미루어 보아 절연체에서 도체로의 상전이를 보이는 틸 없는 반도체인 것을 알 수 있다. Hall 측정 결과에 의해 전하 밀도 값 또한 틸 없는 반도체의 영역에 들어가 있다. 또한 자성 측정 결과, 자화율이 저온에서 상승하게 되고, 이것의 근원을 밝히기 위해 저온에서 자기장에 따른 자화를 측정 하였다. 그 결과 강자성의 특성을 보였는데, 이것을 자기 저항의 측정 결과와 함께 분석하여 보면 강한 스핀-궤도 결합에 의한 것으로 추측된다. 이 사실들로 미루어 보아  $\text{PbPdO}_2$ 와 Co가 도핑된  $\text{PbPdO}_2$ 는 저온 영역에서 커다란 스핀 분극을 가지고 스핀 자유 경로가 클 것으로 추정되는 스핀트로닉스에 적합한 물질로 제안한다.

**Ep-II-036****Interaction Of Cut-wire Pair And Continuous Wire Incombined Metamaterial**J. W. Park, N. T. Tung, W. H. Jang<sup>1</sup>, V. D. Lam<sup>2</sup>, Y. P. Lee*q-Psi and Department of Physics, Hanyang University.. <sup>1</sup>Korea Communication Commission Radio Research Laboratory. <sup>2</sup>Institute of Materials Science, Vietnamese Academy.*

The interaction between cut-wire pair and continuous wire in combined metamaterial structure, operating in the microwave-frequency regime, was investigated. When the electric component, normally the continuous wire is, incorporated with the magnetic one, the electric response of combined structure is not only due to that of the continuous wire, but also strongly affected by that of the magnetic component. This leads to a new effective plasma frequency, which is qualitatively determined as the sum of contributions from cut-wire pair and continuous wire, and is significantly lower than that of the continuous wire alone. Therefore, the design and the construction of combined structure should be carefully conducted, when a left-handed(LH) metamaterial is needed to operate, especially, at high frequencies. For that reason, the effects of the continuous-wire width as well as the position relative to the cut-wire pair on the electromagnetic (EM) response of combined structure were demonstrated. Both numerically and experimentally, we investigated the effect of width and position of the continuous wire relative to the cut-wire pair on the EM response of combined structure. It was found that these parameters play an important role in determining whether the LH behavior is obtained or not. In addition, we also studied the influence of lattice constants on the LH behavior of combined structure. Our results show that the LH behavior depends strongly on the lattice constant in the E direction. However, it remains unchanged according to the lattice constant in the H direction. A good coincidence between the measurements and the numerical simulations was accomplished. This study leads to the optimization of the appropriate characteristic parameters, even avoiding the trial-and-error fabrications.

P2

포스터세션

**Ep-II-037****Microwave “Dark Body”: A Proposed Mechanism For Perfect Absorber Based On Metamaterial**N. T. Tung, J. W. Park, S. J. Lee, Y. P. Lee, J. Y. Rhee<sup>1</sup>, V. D. Lam<sup>2</sup>*Quantum Photonic Science Research Center, Hanyang University. <sup>1</sup>Department of Physics, Sungkyunkwan University. <sup>2</sup>Institute of Materials Science, Vietnamese Academy of Science and Technology.*

The meaning of “dark body” is to merely maximize the absorption ( $A$ ) of materials. It is equivalent to minimize the transmission ( $T$ ) and to simultaneously reduce, through impedance matching, the reflectivity ( $R$ ) in  $A = 1 - T - R$ . As demonstrated [1], in the limit that impedance matching to free space is achieved (i.e.  $Z = Z_0$  resulting in zero reflectivity), the transmission comes to be  $T = \exp(-2n_2 dk) = \exp(-\alpha d)$ , where  $k$  is the free-space wave vector,  $d$  is the sample thickness,  $n_2$  is the imaginary part of the refractive index, and  $\alpha$  is the corresponding absorption coefficient. Thus, in the design of a near-unity resonant absorber,  $\epsilon(\omega)$  and  $m(\omega)$  must be optimized such that, at the desired central frequency,  $Z = Z_0$  together with  $n_2$  as large as possible. It is, however, extremely difficult to realize such conditions in natural materials. Recently, metamaterials, which permit us to tailor the electromagnetic responses of an effective medium, have been designed to be a microwave “dark body” [2]. In this report, we calculate and present in detail the electromagnetic responses of a perfect absorber based on metamaterial structure working at microwave frequency. A general mechanism is proposed to obtain an arbitrarily high absorption by independently controlling the electric and the magnetic resonators. It is shown to be possible to design and fabricate a very thin layer with near unity absorption by using simple techniques. We expect that it would have huge potential in providing a wide range of stealth science applications, more specially, in radar prevention technology.

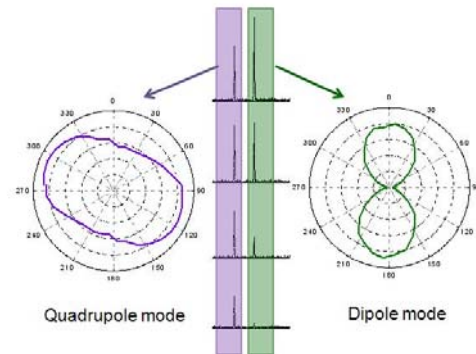
[1] J. D. Jackson, *Classical Electrodynamics*, 3rd ed. (Wiley, New York, 1999). [2] N. I. Landy, S. Sajuyigbe, J. J. Mock, D. R. Smith, and W. J. Padilla, *Phys. Rev. Lett.* 100, 207402 (2008).

**Ep-II-038****Photonic crystal single defect laser fabricated by a combination lithography and****their mode characterization**

AHN Sungmo, KIM Sihan, JEON Heonsu

*Department of physics and astronomy, Seoul National University.*

We successfully fabricated photonic crystal cavity lasers using laser holography combined with focused ion beam method. Two different cavity modes were observed in photoluminescence measurement. Through the finite difference time domain simulation, these two modes were expected to be the dipole and quadrupole mode respectively. Each mode was identified directly by measuring its polarization dependence. Strong linear polarization was measured from the dipole mode while the quadrupole mode did not show any specific polarization axis. We expect that this type of combination lithography will successfully substitute the electron beam lithography which suffers from its low throughput and high cost.

**Ep-II-039****A Metamaterial Supporting Electromagnetically-induced Transparency**

V. T. T. Thuy, N. T. Tung, V. D. Lam<sup>1</sup>, J. W. Park, Y. S. Lee, W. H. Jang<sup>2</sup>, Y. P. Lee

*Quantum Photonic Science Research Center and Department of Physics, Hanyang University. <sup>1</sup>Institute of Materials Science, Vietnam Academy of Science and Technology. <sup>2</sup>Korea Communication Commission Radio Research Laboratory.*

Electromagnetically-induced transparency (EIT) is the effect that gives rise to a narrow transparent window in the middle of absorption band due to the destructive quantum interference between different excitation pathways of the excited state. Interestingly, the EIT-like effects have been recently discovered in metamaterials composed of two weakly-coupled resonators: one of them plays the role of a “bright” component, and the other as a “dark” one [1, 2]. In this investigation, we employed the model proposed by Tassin *et al.* [2] to design and study the EIT behavior of a metamaterial consisting of cut wires (bright component) and split-ring resonators (dark component) operating at microwave frequencies. The results exhibit a narrow and high transparency peak (EIT effect) within the strongly dispersive region arising from the coupling between bright and dark components. Furthermore, the influence of coupling distance on the behavior of transmission window was systematically studied and the coupling mechanism between bright and dark components is thus elucidated. Reference[1.] S. Zhang, D. A. Genov, Y. Wang, M. Liu, and X. Zhang, “Plasmon-induced transparency in metamaterials,” *Phys. Rev. Lett.* 101, 047401 (2008).[2] P. Tassin, L. Zhang, T. Koschny, E. N. Economou, and C. M. Soukoulis, “Planar designs for electromagnetically induced transparency in metamaterials,” *Opt. Express* 17, 5595 (2009).

**Ep-II-040****다중양자우물의 Detuning 변화에 따른 O-band DFB-LD의 문턱전류 및 경사효율의 변화**

김 효진, 유 소영, 고 항주, 한 명수, 김 두근, 한 수옥, 김 선훈, 기 현철, 김 회종, 정 대철<sup>1</sup>, 김 효정<sup>1</sup>, 강 중구<sup>1</sup>

한국광기술원, 광소자팀. <sup>1</sup>(주) 오이솔루션, 소자팀.

최근 저밀도 파장분할 다중화 (CWDM, Coarse wavelength division multiplexing) 기술은 대도시 지역의 광 네트워크에 넓게 사용되고 있다. CWDM 방식에 있어서 가장 문제가 되고 있는 부분은 사용되는 광부품의 가격이 고가이므로 가입자망에 적용하기가 어렵다는 것이다. 또한, CWDM에 대한 수요는 좀 더 많은 정보의 유통을 위하여 1270 ~ 1610 nm의 18 channel을 요구하고 있다. 특히, 이 파장영역 중 O-band에 해당하는 1270 ~ 1350 nm 영역의 경우, 양자우물의 에너지 밴드 장벽이 높지 않아, 온도 특성을 개선하기가 쉽지 않다. 이를 해결하기 위한 방법으로, Grating의 두께, SCH(Separated confinement heterostructure) 도핑, 두께 조절 등 여러 가지 방법이 있으나, 본 연구에서는 다중양자우물 구조의 detuning 변화에 의한 문턱전류 및 경사효율에 대하여 조사하였다. 조사결과에 의하면, detuning 값이 positive일 경우 고온 특성에는 유리하나 저온 특성에는 불리하며, 반대로 negative로 클 경우 문턱전류나 경사밀도 특성에 불리한 결과를 얻었다. 최적소자의 경우, 문턱전류와 경사효율은 각각 8.0 mA, 0.331 W/A 이었다.

**Ep-II-041****레너드 효과(Lenard effect)로 발생된 음이온의 혈액순환 증진**

박 배식

수원대학교 물리학과.

레너드 효과(Lenard effect)로 발생되는 공기중의 폭포수 음이온은 그 발생과정의 특성으로 전기방식으로 발생되는 음이온과는 상당히 다른 특성을 보인다. 첫째, 전기방식 음이온의 발생에 수반되는 오존과 질소 산화물의 발생이 없다. 둘째, 음이온 발생기로 부터 훨씬 먼거리 까지 확산되어 상당히 높은 농도의 음이온 분포를 유지한다. 즉, 전기방식 음이온 발생기에서 발생된 음이온은 수명이 짧아 발생기 주변에서는 매우 높은 음이온 농도를 유지하나 2m 이상 떨어진 곳에서는 음이온이 거의 측정되지 않는다. 그러나 레너드 효과로 물에서 발생되는 음이온은 발생기로 부터 10m 이상 떨어진 거리에서도 상당히 높은 농도의 음이온 분포를 보인다. 따라서 레너드 효과로 발생된 음이온 공기는 호흡으로 혈액에 녹아들어 혈액을 약알카리화 하며, 혈액순환을 증진하는 효과를 보인다. 본연구에서는 건강한 대학생 5명을 대상으로 하여, 모세혈관을 통과하는 적혈구의 흐름을 관찰하여, 혈류속도가 현저히 증가함을 측정하였다.

심 숙이, 김 기옥<sup>1</sup>공주대학교 물리학과, <sup>1</sup>우석대학교 물리학과.

각 개체의 출산 가능 여부가 활성화 돌연변이 인자의 갯수에 의해 결정되는 수정된 페나 모형을 격자구조에 적용하여 집단의 진화를 연구하였다. 단순 사각형 정방 격자 공간을 고려하여 각 개체 위치의 최인접 격자에 빈자리가 없으면 후손을 출산하지 못하도록 하는 공간적 제약을 넣고 몽테 카를로 시뮬내기를 이용하여 총 개체수의 변화 및 나이에 따른 생존율을 계산하여 Verhulst 제약을 넣었을 경우의 계산 결과와 비교하여 정상상태에 이르렀을 때 Verhulst 제약이 과도하게 지배하게 되어 집단의 크기가 급격히 감소하는 현상을 개선할 수 있음을 보였다. 또한 각 변이 인자의 나이별 분포 확률 및 시간에 따른 공간적 분포의 변화를 계산하여 보았고 나이별 사망율을 계산하여 나이가 들수록 노화가 빠르게 진행되는 생물학적으로 자연스러운 현상을 재현함을 확인하였다.

이 재민, 김 준관, 임 정욱, 윤 선진

과학기술연합대학원대학교, 차세대소자공학과, 한국전자통신연구원, 차세대태양광연구본부.

태양전지의 상부 혹은 하부 전극으로는 저렴한 가격, 화학적 안정성을 비롯한 소재의 장점으로 인해 산화아연(ZnO) 기반의 투명전도성산화(TCO) 박막이 주로 사용되고 있다. 최근 표면 texture가 잘 발달한 ZnO계 TCO막의 texturing을 통한 태양전지의 효율 향상에 관해 활발한 연구가 이루어지고 있다. 본 연구에서는 ZnO 박막의 texturing에 흔히 사용되는 HCl 용액 대신, 태양광의 반사율을 더 크게 감소시킬 수 있는 ADN 용액을 개발하여 그 식각 특성과 효과를 연구하였다. 이번 연구에 사용한 TCO 박막은 ZnO:Ga으로서 rf-magnetron sputter 증착법을 이용하여 유리 기판 위에 증착하였다. 식각 전 박막의 두께와 비저항, 그리고 투과율은 각각 1000 nm,  $3.3 \times 10^{-4} \Omega \cdot \text{cm}$ , 87.8%이었다. ADN 용액 내의 혼합 비율이 박막의 선택적인 결정 입계의 식각에 미치는 영향을 관찰하기 위해 용액 혼합비를 변화시키며 texturing하였다. 박막의 특성 변화를 관찰하기 위해 texturing 전, 후의 비저항, 식각 두께, 투과율, 반사율, 그리고 평균 거칠기 값을 측정하였고, 그 결과를 HCl 용액을 사용하여 식각한 결과와 비교하였다. ADN 용액을 사용하여 texturing 할 때 HCl을 이용할 때보다 식각 속도가 다소 느리지만, 식각 후 비슷한 반사율을 보일 때 HCl이 약 3배 더 많은 박막 손실을 일으키는 것을 확인할 수 있었다. 동일한 정도의 반사율 감소를 얻기 위해 요구되는 비저항의 증가, 즉 박막 손실정도와 반사율을 비교하였을 때, HCl 용액을 사용할 때에 비해 ADN 용액을 사용하면 보다 선택적인 식각이 가능하고, 박막의 불필요한 손실을 줄여주어 보다 효과적으로 texturing이 진행되는 것을 알 수 있었다.

**Ep-II-044****양전자 소멸 분광법에 의한 BaSrFBr:Eu의 결함 연구**

김 주흥, 이 종용, 김 재홍<sup>1</sup>

한남대학교 물리학과, <sup>1</sup>원자력 의학원 싸이클로트론연구실.

본 연구에서는 양전자 소멸 측정 분석법을 통하여 BaSrFBr:Eu 형광물질의 결함 농도 분석을 시도하였다. 동시계수 방법과 Fast - Slow - Coincidence 시스템으로 구성된 양전자 소멸 분광법을 통하여 에너지의 변화에 따른 양성자 조사에 의한 시료 결함에 따른 동시 계수 도플러법과 양전자 수명의 변화를 측정 하였으며, SRIM 시뮬레이션을 통한 에너지에 따른 양성자 투과 깊이의 변화를 연구하였다

**Ep-II-045****Wave Propagation Characteristics Observed in a few types of 1-Dimensional****Acoustic Metamaterials**

서 용문, 박 종진<sup>1</sup>, 이 승환<sup>1</sup>, 박 춘만<sup>2</sup>, 이 삼현<sup>1</sup>, 김 철구<sup>1</sup>

명지대학교, 물리학과, <sup>1</sup>연세대학교, 물리학과, <sup>2</sup>안양대학교, AEE 센터.

In 1968 Veselago showed that the electromagnetic wave propagations inside the metamaterials had a number of exotic properties that can't be expected from the conventional theory such as the backwards propagation of the phase velocity and reverse Snell's law. Recently the study has been extended further to the region of acoustic waves providing many interesting application possibilities. We investigated the wave propagation in the single negative (SNG; one of the mass density and bulk modulus of the material is negative) as well as double negative (DNG; both of the mass density and bulk modulus are negative) 1-dimensional metamaterials as a function of the wave frequency. This reveals a variety of propagation characteristics; Diverging phase velocity on approaching the cutoff frequency, beyond which the wave becomes evanescent. Even negative phase velocity was observed below the lower cutoff frequency in the DNG metamaterial, where the wave travels towards its own source. The backwards propagation has been additionally confirmed by the observation of reverse Doppler effect inside the DNG metamaterial.

박 춘만, 김 철구<sup>1</sup>, 이 승환<sup>1</sup>, 박 종진<sup>1</sup>, 배 찬미<sup>1</sup>, 서 용문<sup>2</sup>, 이 삼현<sup>1</sup>

안양대학교, AEE center. <sup>1</sup>연세대학교, 물리학과. <sup>2</sup>명지대학교, 물리학과.

We had reported that the 1-dimensional acoustic tubes with regular array of Helmholtz resonators or side holes have negative bulk modulus in a certain frequency range. We simulate the pressure distributions in the negative B acoustic metamaterials in functions of time and position using FEM. Also, we obtain the acoustic wave propagation characteristics in these metamaterials. The calculating results agree well with experimental data.

장 경혁, 김 은식, 시 량, 전 병천, 교 학빈, 서 효진

부경대학교, 물리학과.

PLD로 Li 이온이 첨가된  $\text{YVO}_4:\text{Eu}^{3+}$  박막을 만들고 형광 특성을 시간 분해 레이저 여기 분광학으로 조사하였다. 사용된 레이저 파장은 Nd:YAG 266 nm, 355 nm 였으며 시료의 측정온도는 15 K 에서 실온까지 였다. 266 nm, 355 nm 레이저 여기에 의한 방출스펙트럼은  $^5\text{D}_3$ ,  $^5\text{D}_2$ ,  $^5\text{D}_1$ ,  $^5\text{D}_0$  준위에서  $^7\text{F}_j$  ( $j=0, 1, 2, \dots, 6$ ) 준위로 전이하는 형광을 관측할 수 있었다. 266 nm 여기 에너지는  $\text{VO}_4^{3-}$  흡수 밴드와 잘 일치 하여  $\text{Eu}^{3+}$  로의 에너지 전달을 통하여 강한 형광을 방출한다. 시간분해 형광 스펙트럼을 측정하여  $^5\text{D}_3$ ,  $^5\text{D}_2$ ,  $^5\text{D}_1$ ,  $^5\text{D}_0$  의 각각의 준위로부터  $^7\text{F}_j$  ( $j=0,1,2,\dots$ ) 준위로 방사 전이하는 형광스펙트럼을 분리할 수 있었다.  $\text{VO}_4^{3-}$  흡수 밴드 끝 단과 일치하는 355 nm 에너지는 온도가 증가할수록 포논의 도움으로 방출스펙트럼의 세기가 저온에서보다 실온에서 더 높은 사실을 확인하였다.  $\text{Eu}^{3+}$ 로 에너지가 전달되지 않고 직접 방출하는 매우 짧은 수명시간을 가진 호스트의  $\text{VO}_4^{3-}$  방출 밴드를 확인하였다. 방출 형광을 시간 분해 분광학의 방법으로 self-trapped exciton과  $\text{YVO}_4$  주격자의 near-band-edge로 분리할 수 있었다.  $\text{YVO}_4:\text{Eu}^{3+}$  에서 Li 이온이 첨가되면서 near-band-edge에서 상승이 감소되어 형광 강도의 증가가 발생한다.

**Ep-II-048****Study of Simultaneous Thyroid Imaging and Uptake system**

박 진훈, 주 관식, 전 상준, 문 혜진, 김 은, 신 현철

영지대학교, 물리학과.

The gamma camera and gamma counter combination system for a thyroid diagnosis are the diagnosis equipment which combines the existing equipment. Combining the development of diagnostic equipment to complement your existing skills of active gamma camera, a gamma counter to obtain the information at the same time the development of the equipment in preparation for opening the medical market, improve competitiveness and improving public health, the reliability of diagnostic information shall be secured can be expected. This report introduces the result which leads a simulation(Monte carlo simulation), discussing the research results for an actual equipment production.

**Ep-II-049****~ppb 수분표준가스 발생 기술**

최 병일, 우 상봉, 김 종철

한국표준과학연구원.

극미세 수분의 존재는 반도체 공정 같은 첨단산업에서는 제품의 품질에 크게 영향을 미치므로, 대부분의 첨단공정에서 미세 수분의 측정 및 조절을 하기 위한 다수의 장비가 설치되어 있다. 하지만 이런 장비들은 교정/검증이 제대로 안된 상태에서 사용되므로써 제품의 품질에 많은 오류를 주고 있다. 본 연구는 이러한 극정밀 수분측정 장치의 교정/검정을 위한 ~ppb 정도의 표준가스를 발생시킬 수 있는 극저상점습도표준가스 발생장치를 개발하였는데, 이의 발생영역은 10 nmole/mol ~ 130  $\mu$ mol/mol 이다. 이는 반도체 등 첨단산업의 기술개발에 크게 기여할 것으로 기대된다.

**Ep-II-050****ZrO<sub>2</sub> 비표면적 CRM 개발**

최 병일, 이 유진, 김 종철, 우 상봉

한국표준과학연구원

첨단기술의 발달은 많은 기능성 나노 소재들을 개발하게 되었고 이들에 대한 특성의 파악은 매우 중요한데, 특히 비표면적은 이런 기능성 소재의 특성평가에 있어 매우 중요한 지표가 되고 있다. 하지만 비표면적을 측정하는 상용장치와 측정방법들은 그 결과의 해석에 매우 제한적인 요소들이 많으며 이러한 측정방법 및 해석 방법에 따라 결과에서 많은 차이가 있어왔다. 본 연구는 상용 비표면적 측정장치의 신뢰성 검증을 위하여 2종의 ZrO<sub>2</sub> 비표면적 인증표준물질을 개발하였다. 이런 검증된 인증물질의 보급은 산업계에 신뢰성 있는 비표면적 측정결과를 줌으로서, 일관성 있는 공정운용에 의한 품질관리, 생산성 향상, 안정성 판단 및 신제품 개발 등에 기여할 것이다.

**Ep-II-051****Luminescent properties of Eu<sup>3+</sup> Ions Doped in La<sub>2</sub>BaZnO<sub>5</sub> Phosphor**

시 량, 장 경혁, 김 은식, 교 학빈, 전 병천, 서 효진

부경대학교, 물리학과

Eu<sup>3+</sup>-doped La<sub>2-x</sub>Eu<sub>x</sub>BaZnO<sub>5</sub> (x=0.05 %) phosphor was prepared by a solid state reaction method at high temperature. X-ray powder diffraction analysis confirmed the formation of single phase La<sub>2</sub>BaZnO<sub>5</sub>. Excitation spectrum in the UV region was performed from which we identify the charge transfer band of Eu-O in La<sub>2</sub>BaZnO<sub>5</sub>. Luminescence properties of La<sub>2</sub>BaZnO<sub>5</sub>:Eu<sup>3+</sup> are investigated by the site-selective laser-excitation and emission spectroscopy in the temperature region of 18 K – room temperature. Two different crystallographic sites for Eu<sup>3+</sup> are identified from the <sup>7</sup>F<sub>0</sub> → <sup>5</sup>D<sub>0</sub> excitation spectra obtained by monitoring the <sup>5</sup>D<sub>0</sub> → <sup>7</sup>F<sub>J</sub> (J=1,2,...6) emissions. The energy transfer between the two crystallographic Eu<sup>3+</sup> centers is investigated by the luminescence decays and temperature dependent <sup>5</sup>D<sub>0</sub> → <sup>7</sup>F<sub>J</sub> emissions of Eu<sup>3+</sup> at each site.

**Ep-II-052****Luminescence and thermal stability of  $\text{Eu}^{2+}$ -activated  $\text{LiCaPO}_4$  phosphors for****white light emitting diode**

교 학빈, 장 경혁, 김 은식, 시 량, 전 병천, 서 효진

부경대학교, 물리학과.

$\text{Eu}^{2+}$  doped  $\text{LiCaPO}_4$  was synthesized by a high-temperature solid-state reaction method in the reductive atmosphere and their photoluminescence properties are investigated. The excitation spectra show that  $\text{LiCaPO}_4:\text{Eu}^{2+}$  can be efficiently excited by the incident lights of 280-420 nm, which well match with the emission wavelength of near-UV LEDs. The phosphor showed bright blue luminescence with a peak wavelength centered at 470 nm. The temperature dependence of luminescence intensities is investigated and we show that the phosphor has an excellent thermal stability on temperature quenching effects. The emission wavelength shows a red-shift with increasing  $\text{Eu}^{2+}$  concentrations, and luminescence intensities are also investigated under different  $\text{Eu}^{2+}$  concentrations. The luminescence decay and the color coordinates are also discussed in order to further investigate the potential applications.

**Ep-II-053****The luminescence properties of  $\text{Eu}^{3+}$  doped  $\text{AZr}(\text{PO}_4)_2$  (A=Sr, Ba) phosphors for****white light-emitting diodes**

전 병천, 장 경혁, 김 은식, 시 량, 교 학빈, 서 효진

부경대학교, 물리학과.

$\text{Eu}^{3+}$  doped  $\text{AZr}(\text{PO}_4)_2$  (A=Sr, Ba) phosphors were synthesized by a high-temperature solid-state reaction method in the air atmosphere. X-ray powder diffraction analysis confirmed the formation of single phase  $\text{AZr}(\text{PO}_4)_2$  (A=Sr, Ba). The excitation spectra and near UV excited emission spectra are investigated. The luminescence of  $\text{AZr}(\text{PO}_4)_2:\text{Eu}^{3+}$  shows a broad emission band overlapped by the  $^5\text{D}_0 \rightarrow ^7\text{F}_0$  emission of  $\text{Eu}^{3+}$ . There is an energy transfer from the host to the  $\text{Eu}^{3+}$  ions. Under near UV excitation, the phosphor shows bright white luminescence that is due to the host and characteristic red luminescence from  $\text{Eu}^{3+}$  ions. The luminescence decay and the color coordinates of the phosphors are measured in order to further investigate the potential applications for white light-emitting diode phosphors pumped by near-UV chip.

**Ep-II-054****Optical absorption and fluorescence properties of  $\text{Tm}^{3+}$ -doped K-Mg-Al****phosphate glasses for laser applications**

PRAVEENA Ravipati, 서 효진

부경대학교, 물리학과.

Metaphosphate glasses doped with different concentrations of  $\text{Tm}^{3+}$  ions have been prepared and characterized through absorption, emission and decay measurements at room temperature. The peak positions in the absorption spectra were identified and analyzed using free-ion Hamiltonian model. Judd-Ofelt analysis has been carried out on the absorption spectrum of 1.0 mol %  $\text{Tm}^{3+}$ -doped phosphate glass. These intensity parameters have been used to predict the radiative properties for the fluorescent levels of the  $\text{Tm}^{3+}$  ion. The emission spectra in the UV-VIS region have been recorded with an excitation wavelength of 355 nm. The branching ratios and stimulated emission cross-sections show that the  $^1\text{D}_2 \rightarrow ^3\text{F}_4$  transition of  $\text{Tm}^{3+}$  ions has the potential for laser applications. The fluorescence decay curves for the  $^1\text{D}_2$  level of  $\text{Tm}^{3+}$  ions have been measured by monitoring the  $^1\text{D}_2 \rightarrow ^3\text{F}_4$  transition. The decay curves exhibit non-exponential nature for all concentrations and are analyzed under the framework of Inokuti-Hirayama model. The results obtained in this paper are compared with other reported  $\text{Tm}^{3+}$ -doped glasses.

**Ep-II-055****Thermoluminescence of Ion Implanted  $\text{Al}_2\text{O}_3$** 

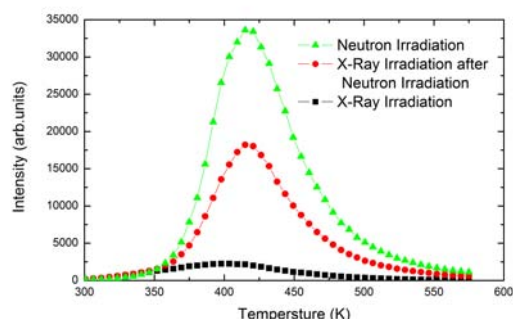
KIM Taekyu

Jeonju National University of Education, Department of Science Education.

Thermoluminescence(TL) were measured from ion implanted  $\text{Al}_2\text{O}_3$  induced by  $^{137}\text{Cs}$  gamma ray irradiation. The glow curves of  $\text{Na}^+$  implanted  $\text{Al}_2\text{O}_3$  shows two shoulders located at 407 K and 415 K and three TL peaks at 450 K, 510 K, and 570 K. The 450 K TL peak intensity of  $\text{Na}^+$  implanted  $\text{Al}_2\text{O}_3$  induced by  $^{137}\text{Cs}$  gamma ray is higher than that of  $\text{Al}_2\text{O}_3$  implanted only  $\text{Na}^+$  and that of  $\text{Al}_2\text{O}_3$  irradiated with only  $^{137}\text{Cs}$  gamma ray. The TL curve of  $\text{Al}_2\text{O}_3$  implanted with 6-

keV  $\text{Na}^+$  at various ion dose followed by gamma ray irradiation at a dose of 10 Gy were measured to investigate the relationship between the TL peak intensity and ion dose. The incident ion doses were varied from  $5 \times 10^{13} \text{ cm}^{-2}$  to  $5 \times 10^{15} \text{ cm}^{-2}$ . As the ion doses increase, the intensities of 450 K TL peaks increase due to the increase in the concentration of vacancies produced by ion implantation in  $\text{Al}_2\text{O}_3$ . This result shows that the TL intensity has a close relationship with the vacancies generated by ion implantation. The TL curves induced by gamma ray irradiation of  $\text{Al}_2\text{O}_3$  implanted with  $\text{Na}^+$  were measured for the various ion implantation energies. As the ion energy increases, the TL intensities of the 407 K and 415 K TL shoulders are reduced to be absorbed into the 450 K TL peak. These results show that the TL intensity is related with the ion dose, ion energy, and ion mass.

file name : spinel\_t



**Ep-II-056****Local Polymerization of Organic Monolayer Covalently Grafted on Silicon**

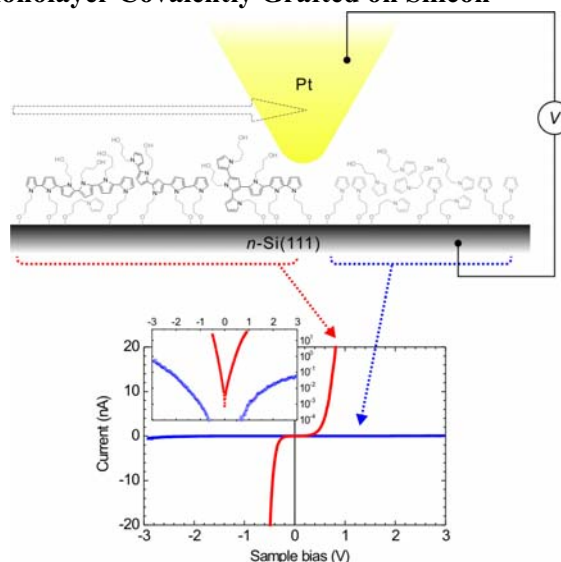
LEE Joon Sung, CHI Young Shik, CHOI Insung S.<sup>1</sup>, YUN

Wan Soo, KIM Jinhee

KRISS, Center for Nanoscience and Quantum

Metrology. <sup>1</sup>KAIST, Department of Chemistry and School of Molecular Science.

The concept of lateral extension of *pi*-conjugation within a covalently grafted molecular monolayer by a scanning probe-based method was tested. A molecular layer derived from *w*-(*N*-Pyrrolyl)propanol was formed on *n*-Si(111) surface. Application of sample biases greater than +4 V during conductive AFM scans under UHV resulted in changes of mechanical and electrical characteristics of the molecular layer: the tip-sample conductance was increased greatly, the friction was reduced significantly, and the surface potential of the scanned area was increased. The reduction in friction may be attributed to a decrease in available mechanical energy dissipation routes caused by increased molecular linking within the layer. The increased conductance strongly suggests enhanced conjugation among the pyrrolyl endgroups. Therefore, it was inferred that the biased AFM scans successfully induced local polymerization within the covalently grafted molecular layer.



P2

포스터세션

**Ep-II-057****Sonodynamic effects of 5-Aminolevulinic acid on solid tumors**

SEO SEUNG-JUN, YU JAE - IN<sup>1</sup>, KIM KI-HONG<sup>2</sup>, KIM JONG-KI<sup>3</sup>

Biomedical Engineering, School of Medicine, Catholic University of Daegu. <sup>1</sup>Department of Physics, Yeungnam

University. <sup>2</sup>Department of Visual Optics, Kyungwoon University. <sup>3</sup>Biomedical Engineering & Radiology, School of Medicine, Catholic University of Daegu.

The sonodynamic therapy(SDT) is a novel treatment modality, which produces local tissue necrosis with ultrasound following the prior administration of a photosensitizing agent. 5-Aminolevulinic acid(5-ALA) has recently been shown to be a promising SDT sensitizer. In order to elucidate the antitumor effects of SDT using 5-ALA on cancer, growth inhibition studies on tumor cell line, CT-26 cells in vitro and animals with an established CT-26 tumor in vivo were determined. CT-26 tumor cells were exposed to various concentrations of 5-ALA and SDT, with irradiation of 5~10 min at the frequency 1 MHz using an ultrasonic system. BALB/C mice with CT-26 tumor were injected with 5-ALA via different routes and treated with SDT in vivo. A growth suppression study was then used to evaluate the effects at various time points after SDT. The results showed that irradiation of CT-26 tumor cells in the presence of 5-ALA induced significant cell growth inhibition. Animals with established CT-26 Tumors exhibited significantly smaller tumor sizes over time when treated with 5-ALA and irradiation. SDT after the application of 5-ALA appears to be effective against CT-26 tumors both in vitro and in vivo.

**Ep-II-058****레너드 효과 (Lenard effect)로 초음파 가슴공기청정기에서 발생한 음이온 발생****과정과 특성**

박 배식

수원대학교 물리학과.

필립 레너드(Phillip A. Lenard)는 폭포수에서 음이온이 발생하는 현상인 레너드 효과(Lenard effect)를 1892년에 발표하였다. 최근에 와서 음이온에 의한 공기정화작용과 건강증진기능을 활용하려는 연구가 활성화되면서 레너드 효과의 응용연구가 주목을 받고 있다. 본 연구에서는 초음파 진동자를 이용한 물의 충밀리기 현상으로 다량의 음이온이 발생됨을 관찰하였다( 1.5m 거리에서 316,200개/CC). 또한 레너드 효과로 발생하는 음이온의 생성과정을 규명하여, 다른 물리적 과정으로 발생된 음이온과는 다른 2가지의 중요한 특성을 관찰하였다. 즉, 오존과 질소산화물의 발생이 없이 음이온만 생성되며, 발생장치로부터 10m 떨어진 지역까지 상당히 높은 음이온 농도를 보인다(10m 거리에서 5,000개/CC)..

**Ep-II-059****Resistive Memory Switching Behaviors of Pt/NiO/SRO Memory Devices**LIU CHUNLI, 정 창욱, 박 홍우<sup>1</sup>한국외국어대학교전자물리학과. <sup>1</sup> 서울대학교 재료공학과.

Resistance switching phenomena have recently regained intensive research efforts due to their potential for realizing high-density resistance random access memory (RRAM) devices. As one of the most promising candidates, NiO thin film memory devices have been reported to show both unipolar and bipolar switching, depending on the substrate used. In this study, we will study the resistance switching behaviors of NiO thin films grown on Pt/TiO<sub>2</sub>/SiO<sub>2</sub>/Si substrates and STO substrates using pulsed laser deposition. Based on the observed switching behavior, the switching mechanism dependence on the growth conditions and substrates will be discussed. We will also try to investigate the difference between the switching mechanisms of unipolar switching and bipolar switching.

**Ep-II-060****LiFePO<sub>4</sub> Cathode Materials: Synthesis and Electrochemical Properties**

홍 경수, 하 명규, 정 의덕, 양 호순<sup>1</sup>

한국기초과학지원연구원 부산센터, <sup>1</sup>부산대학교 물리학과.

We synthesized LiFePO<sub>4</sub> powders with different processes such as sol-gel and solid-state reaction methods. In this presentation, we describe the obtained results by adding aluminums in LiFePO<sub>4</sub>. The surface conditions of LiFePO<sub>4</sub> powder were modified by adding AlF<sub>3</sub> and Al<sub>2</sub>O<sub>3</sub> by using the sol-gel process to improve its electrochemical properties. The nano-sized AlF<sub>3</sub> and Al<sub>2</sub>O<sub>3</sub> partially covered the surface of LiFePO<sub>4</sub> powders, confirmed from an transmission electron microscope image. The state of coated Al materials was examined by using X-ray photoelectron spectrometer results. The nano-sized AlF<sub>3</sub> and Al<sub>2</sub>O<sub>3</sub>-coated LiFePO<sub>4</sub> powders showed no difference in the bulk structure compared with the pristine one. However, the AlF<sub>3</sub> and Al<sub>2</sub>O<sub>3</sub> coating on LiFePO<sub>4</sub> powder improved the overall electrochemical properties such as the cyclability and the rate capability compared with those of the pristine LiFePO<sub>4</sub>. Specially, the Al<sub>2</sub>O<sub>3</sub>-coated LiFePO<sub>4</sub> powder shows relatively high discharge capacity and good cycling stability. Its discharge capacity was 148 mAh/g at the 0.2 C rate and the capacity retention was about 93 % of its initial capacity after 50 cycles under 0.2 C rate. Such enhancements were attributed to the presence of the stable AlF<sub>3</sub> and Al<sub>2</sub>O<sub>3</sub> layer which acts as the interfacial stabilizer on the surface of LiFePO<sub>4</sub>.

P2

포스터  
세션

**Ep-II-061****스핀 분포 조절이 가능한 이중 양자 디스크 구조의 제안**

김 남미, 김 희상

충실대학교 물리학과.

강자성 디스크와 비자성반도체 디스크로 이루어진 이중 혼성 디스크 구조에서 자기장의 변화에 의하여 이중 디스크 구조내의 스핀 분포를 조절하는 양자구조를 제안한다. 외부 자기장을 변화시킬때 디스크의 크기 비대칭과 g-상수의 차이에 의하여 양 디스크 내의 에너지 준위의 변화가 생기므로 스핀의 분포가 달라지는 현상을 이용한다. 전하의 서브밴드별 확률밀도도 뿐만 아니라 스핀분극 변화도 함께 보여준다. 이 구조의 특성은 장래 스핀디바이스, 예를 들어 메모리디바이스로 응용 가능하다.

## Low Temperature

CHO Kwang-Hwan, KANG Min-Gyu, KANG Chong-Yun, YOON Seok-Jin, LEE YoungPak<sup>1</sup>

*Korea Institute of Science and Technology, Thin Film Materials Research Center. <sup>1</sup>Hanyang University, q-psi & department of physics.*

A high density metal-insulator-metal (MIM) capacitor at 300°C with a titanium substituted  $\text{Bi}_{1.5}\text{ZnNb}_{1.5}\text{O}_7$  (BZN) dielectric prepared by physical vapor deposition (PVD) is presented for the first time. A significant improvement was shown in both the capacitance density and temperature coefficient of capacitance of MIM capacitors. A 67-nm-thick  $(\text{Bi}_{1.5}\text{Zn}_{0.5})(\text{Zn}_{0.43}\text{Nb}_{1.37}\text{Ti}_{0.2}\text{O}_7)$  film exhibited a high capacitance density of 14.8 fF/cm<sup>2</sup> at 100 kHz. The leakage current density was low, approximately 2.92 nA/cm<sup>2</sup> at 1V. The quadratic voltage and temperature coefficient of capacitance were approximately 136 ppm/V<sup>2</sup> and 98 ppm/°C at 100 kHz, respectively. All of these make the Ti-substituted BZN capacitor to be very suitable for use in silicon RF and mixed signal IC application

YI Soung Soo, R. Balakrishnaiah, KIM Dong Woo, KIM Sung Hoon<sup>1</sup>, JANG Kiwan<sup>2</sup>, LEE Ho Sueb<sup>2</sup>, MOON Byung Kee<sup>3</sup>, JEONG Jung Hyun<sup>3</sup>

*Department of Electronic Materials Engineering, Silla University. <sup>1</sup>Department of Engineering in Energy and Applied Chemistry, Silla University. <sup>2</sup>Department of Physics, Changwon National University. <sup>3</sup>Department of Physics, Pukyong National University.*

Recently, potassium niobate ( $\text{KNbO}_3$ ) is recognized to be one of the best host matrices for Ln ions as it is a useful candidate for ferroelectric materials with excellent electro-optic and nonlinear optical coefficients.  $\text{Eu}^{3+}$  is one of the most interesting Ln ions due to its simple lower energy levels scheme as well as applications in the fields such as red emitting phosphor because of its intense, narrow, monochromatic and hypersensitive red emission around 610 nm as a result of  $^5\text{D}_0 \rightarrow ^7\text{F}_2$  transition.  $\text{Li}^+$  ion having small ionic radius is found to be one of the best modifier ions as it affects the luminescence properties of various phosphor materials to a better interesting extent. Therefore,  $\text{Li}^+$ -doped  $\text{KNbO}_3:\text{Eu}^{3+}$  phosphors have been prepared by solid state reaction method with 0.05, 0.10, 0.15 and 0.20 mol concentration of  $\text{Li}^+$  ions and 0.03 mol % of  $\text{Eu}^{3+}$  ions in the present work using high purity chemicals of  $\text{Li}_2\text{CO}_3$ ,  $\text{K}_2\text{CO}_3$ ,  $\text{Nb}_2\text{O}_5$  and  $\text{Eu}_2\text{O}_3$ . The synthesized materials were characterized by X-ray diffraction, scanning electron microscopy, excitation and emission measurements. The dependence of various optical and morphological properties of the prepared materials on  $\text{Li}^+$  ion concentration has been discussed and the results are compared with those reported in earlier literature.

**Ep-II-064****쌍축성 네마틱 액정의 texture 관찰**장 태석, 김 중현, 최 석원<sup>1</sup>충남대학교 물리학과, <sup>1</sup>경희대학교, 디스플레이재료 공학과.

일반적으로 네마틱 액정은 하나의 축 방향으로 정렬하는 성질을 갖는다. 그리고 그 축에 수직방향으로 균질한 성질을 나타낸다. 그렇지만 오래 전부터 이론적으로 쌍축성 네마틱 액정의 가능성이 논의되어 왔고 바나나 모양의 액정이 매우 높은 가능성을 가지고 있다고 알려져 있다. 여기서는 바나나 모양으로 생긴 특정한 네마틱 액정이 나타내는 texture의 관찰, 전기장에 의한 반응을 통해서 그 액정의 쌍축성의 가능성에 대하여 알아본다.

**Ep-II-065****Luminescent Properties Of Er<sup>3+</sup>-Doped (Y,Gd)BO<sub>3</sub> Phosphors**R. Balakrishnaiah, YI Soung Soo, KIM Dong Woo, KIM Sung Hoon<sup>1</sup>, JANG Kiwan<sup>2</sup>, LEE Ho Sueb<sup>2</sup>, JEONG Jung Hyun<sup>3</sup>

*Department of Electronic Materials Engineering, Silla University. <sup>1</sup>Department of Engineering in Energy and Applied Chemistry, Silla University. <sup>2</sup>Department of Physics, Changwon National University. <sup>3</sup>Department of Physics, Pukyong National University.*

Recently, Yttrium and lanthanide (Ln) orthoborate phosphors have attracted much attention due to their high stability, low synthesis temperature, high VUV absorption and exceptional optical damage threshold. Among Ln ions, Er<sup>3+</sup> is one of the most popular and efficient ions to obtain infrared eye-safe emission at 1.5 μm as a result of <sup>4</sup>I<sub>13/2</sub> → <sup>4</sup>I<sub>15/2</sub> transition of Er<sup>3+</sup> ions, which is useful for optical amplification at the third telecommunication window, in addition to the possible NIR to VIS upconversion emission. Also, it has strong absorption bands in the UV-VIS-NIR regions where efficient pumping sources are available. In our present work, Er<sup>3+</sup>-doped YBO<sub>3</sub> and (Y,Gd)BO<sub>3</sub> phosphors have been prepared by solid state reaction method with 3 mol % of Er<sup>3+</sup> and 0, 1, 3, 5 and 7 mol % of Gd<sup>3+</sup> ions using high purity chemicals of Y<sub>2</sub>O<sub>3</sub>, H<sub>3</sub>BO<sub>3</sub>, Gd<sub>2</sub>O<sub>3</sub> and Er<sub>2</sub>O<sub>3</sub>. The synthesized materials were characterized by X-ray diffraction (XRD), scanning electron microscopy (SEM), excitation, emission and lifetime measurements. The dependence of various optical, morphological and energy transfer properties of the prepared materials on the Ln ion concentration has been discussed and the results are compared with those reported in earlier literature.

**Ep-II-066****전기장에 따른 액정 방울 속 방향자의 변화 관찰**PARK Jin-Soon, KIM Jong-Hyun, LEE Eun Seong<sup>1</sup>, LEE Jae Yong<sup>1</sup>, PARK Joo Hyun<sup>1</sup>충남대 물리학과, <sup>1</sup>한국표준과학연구원.

일반적으로 네마틱 액정은 막대 모양의 분자가 서로 평행하게 배열하려는 성질을 갖는다. 이러한 네마틱 액정을 실리콘 오일 속에 액정 방울로 만든 다음 전기장을 인가하였다. 광학현미경을 이용하여 전기장의 크기 변화에 따른 액정 방울 속의 방향자의 변화를 관찰하였다. 또한 본 연구는 CARS (Coherent anti-Stokes Raman Stokes) 현미경을 이용하여 전기장의 변화에 따른 액정 방울의 변화를 3차원 이미지화함으로써 액정 방울내의 분자 배열을 관찰하려 한다.

**Ep-II-067****Cooling Power of Field Emission from the n-Type Silicon Semiconductor**

정 문성, 금 관필, 구 자훈, 배 해경, 장 유진, 천 중필

울산대학교 물리학과.

Field emission from metals yields heating at low temperatures and cooling at high temperatures. It is, however, found that field emission from the semiconductor cathode has been found to yield only cooling at all temperatures. The dual character of the metallic cathode changes to be one-way in semiconductor cathodes. By considering the outgoing and incoming electrons in the region of emission, we make the numerical calculation of the energy exchange per field electron. Even though the Joule heat is taken into account, the energy exchange is large enough for cooling. The cooling power needed for micro-electronic device is obtained for field emission from the highly n-doped Si semiconductor. This implies that there is a lot of feasibility for a new type of solid state cooler if an appropriate semiconductor is found.

**Ep-II-068****The Enhanced Thermal Stability Of Low Dielectric Constant SiOC Film By Post Annealing In Ambient Forming Gas**박 상한, 김 효진, 조 만호, 황 정남, 한 준희, 이 도형<sup>1</sup>, 권 영수<sup>1</sup>, 박 소연<sup>1</sup>, 김 무성<sup>2</sup>연세대학교 물리학과. <sup>1</sup>(주) ATTO. <sup>2</sup>Air Products Korea.

The low- $\kappa$  SiOC films was deposited by plasma-enhanced chemical vapor deposition (PECVD) and then treated with post annealing in ambient of forming gas (10% H<sub>2</sub>). We studied about electrical and chemical properties of low- $\kappa$  SiOC films by XPS, FT-IR and C-V measurement. In this study, we focused on post annealing effects by using forming gas on the SiOC films, particularly. The precursor of SiOC films has advantage feature which is OCH<sub>x</sub>CH<sub>y</sub> groups sustaining harder films than previously reported low- $\kappa$  materials, when it is applied to memory devices. The dielectric constant ( $\kappa$ -value) of the as-grown film was measured about 2.45 by MOS CV measurement at 100 kHz. In order to investigate the changes of properties in this film, we use a rapid thermal annealing (RTA) process in N<sub>2</sub> and forming gas ambient at temperature range between 400, 500 and 600 °C for 10 min. XPS and FT-IR are used to investigate the chemical structures of annealed films. Carbon groups are almost maintained until the temperature up to 500 °C, while the annealing under N<sub>2</sub> gas, the carbon groups are critically decreased and shows higher dielectric constant than the former, during the post annealing in forming gas. In case of the film treated by RTA at 600 °C, the carbon groups of the film were released and Si-O network enhanced for both ambient gas. In conclusion, hydrogen increase thermal stability of SiOC films by disturbing oxidation of silicon.

**Ep-II-069****Field Enhancement Near the Contact between Dielectric and Metal**

정 문성, 구 자훈, 금 관필, 배 해경, 장 유진, 천 중필

울산대학교 물리학과.

Dielectrics are considered to play only the role of reducing the electric field intensities. For a long time, however, strongly enhanced electric fields have often been observed in the vicinity of the contact between metal and dielectric. Thus we investigated the behavior of the electric field near a junction composed of metal, dielectric, and vacuum. By assuming that the junction is symmetric along one direction, we use a two-dimensional model to calculate the electric field near the junction as a function of configuration. For the triple junction of metal-vacuum-dielectric, the electric field is found to be enhanced and reduced according to the ratio of the angels subtended by dielectric and vacuum portions. The use of the same model also leads to the result that the quadruple junction of metal-vacuum-dielectric-vacuum yields a much larger field enhancement than the triple junction. It is noted that the total enhancement of the electric field at the junction is the product of the two enhancements due to dielectric and the shape of the metallic emission portion.

**Ep-II-070****이온조사에 의한 유기태양전지 회로의 P3HT/PCMB 레이어의 특성변화 연구**

박 성규, 이 용백, 이 석호, 주 진수

고려대학교, 물리학과.

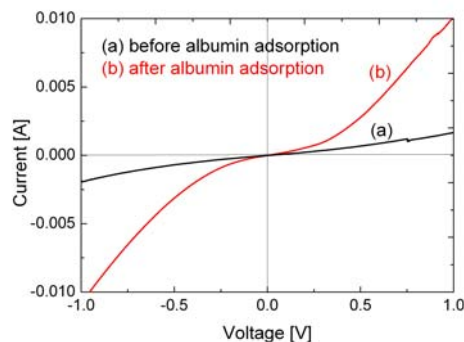
P3HT (poly(3-hexylthiophene)와 PCBM ([6,6]-phenyl C<sub>61</sub> butyric acid methyl ester)의 혼합체를 활성층으로 사용한 유기태양전지 회로를 제작하였다. 정공쪽은 ITO (indium tin oxide)와 PEDOT (3,4 ethylenedioxythiophene)을 전극으로, 전자쪽은 Al을 전극으로 사용하였다. 본 연구에서는 활성층과 ETL (electron transport layer) 사이의 계면의 특성을 개선하여 유기태양전지의 효율을 증대하고자 하였다. 활성층 고분자 계면에 이온빔을 조사하여 금속전극과의 접합특성을 개선하고 고분자 체인의 구조적인 변화를 적용하였다. 이온조사는 50 keV H<sup>+</sup> 이온을 1X10<sup>12</sup> ~ 1X10<sup>14</sup> ions/cm<sup>2</sup>의 이온밀도로 활성층에 조사하였다. 표면변화를 관측하기 위해 SEM과 AFM을 측정하였다. 구조적 변화를 측정하기 위해 UV/Vis, Raman 스펙트럼을 측정하였다. 또한 이온주입 전과 후의 PL 스펙트럼을 비교, 연구하였다.

**Ep-II-071****I-V Properties of Albumin Adsorbed Porous Silicon**

CHENG Horchhong, KIM Han-Jung, LEE Ki-Won, KIM Young-You

Department of physics, Kongju National university.

In this work, we explored the possibility of a biosensor based on porous silicon. We produced single layer porous silicon, multilayer porous silicon and microcavity porous silicon on a silicon substrate, and then investigated the *I-V* properties before and after Albumin adsorption. The result shows that there is a stronger intensity current for all samples as a present of Albumin. This sensitive response shows the effect of Albumin absorbed into the pore and the effect of Albumin on the carrier mobility. So, it is shown that porous silicon is possible to be applied in the field of electrical biosensor.



**Ep-II-072****온도와 온도 변화량에 따른 블루페이즈 격자 구조와 크기의 변화 관찰**이 호현, 김 종현, H. Kikuchi<sup>1</sup>충남대학교, 물리학과. <sup>1</sup>Kyushu University, Department of Applied Chemistry.

일반적으로 블루페이즈는 카이랄 네마틱 액정의 등방상에서 카이랄 네마틱 상으로의 상전이 과정에서 나타난다. 이러한 블루페이즈는 상전이 될 때의 조건에 따라 크기와 모양이 다른 도메인을 가지게 된다. 블루페이즈는 카이랄 네마틱 액정의 Chirality에 따라 격자구조와 격자상수가 다르게 나타나게 된다. 본 연구는 상전이하는 과정에서의 온도 변화율과 블루페이즈 도메인의 크기변화와 격자구조, 격자상수의 변화를 브래그법칙을 이용하여 설명할 것이다.

**Ep-II-073****유기 태양전지에서의 solvent annealing 효과 및 광전기적 특성분석**

조 정민, 김 재령, 신 원석, 문 상진

한국화학연구원, 에너지소재연구센터.

ITO가 코팅된 glass 기판 위에 hole transport layer로서 poly(3,4-ethylenedioxythiophene):poly(styrene sulfonate) (PEDOT:PSS (Baytron P, AI 4083))를 spin coating하고, active layer로는 도너 물질인 poly(3-hexylthiophene) (P3HT)와 억셉터 물질인 [6,6]-phenyl-C61-butyric acid methyl ester (PCBM) blend로서 spin coating을 하였다. 전극으로서 LiF/Al을 thermal 증착하여 유기 태양전지를 제작하였다. 일반적으로 P3HT:PCBM blend 유기태양전지는 열처리를 통해서 mobility와 conductivity 등의 증가로 fill factor(FF)와 current가 크게 증대된다. 우리는 모포로지 개선을 통한 광전변환효율(PCE(%)) 증가를 위해, solvent annealing 방법[1,2]을 이용하여 유기 태양전지를 제작하였다. 일반적인 방법으로 제작한 시료와 비교하여 current와 FF의 증가된 결과를 확인하였다. Solvent annealing을 통해 제작된  $V_{oc}$ ,  $J_{sc}$ , FF, 그리고 PCE(%)는 AM 1.5G 조건 하에서 각각 0.58V, 10.08mA/cm<sup>2</sup>, ~3.7%를 나타냈다. Solvent annealing 방법은 vapor 내에서 경과하는 시간과 용매가 휘발되면서 건조되는 시간이 결정성 형성에 중요한 요인으로 사료되었다. AFM, XRD, UV-visible, solar simulator, 그리고 IPCE를 이용하여 solvent annealing에 따른 광전기적특성을 조사하였다. Reference [1] Adv. Funct. Mater. 17, 1636 (2007), [2] Appl. Phys. Lett. 89, 063505 (2006).

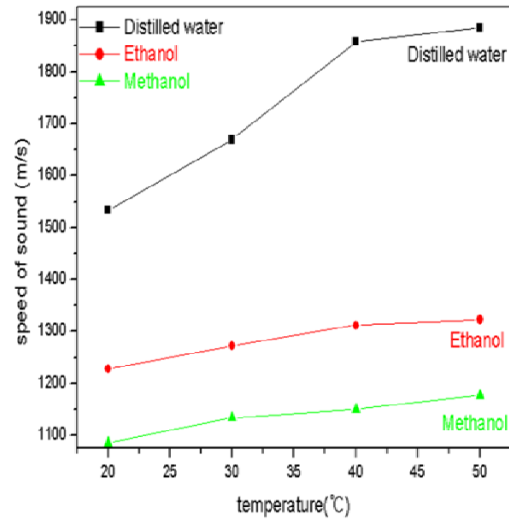
## Ep-II-074

### 빛의 회절현상을 이용한 액체 속 음속도 측정

박 세희, 김 인구, 이 재란, 김 석원

울산대학교 물리학과

빛의 회절 현상은 광학의 파동 영역에서 필수적인 내용으로서 고등학교와 대학교 과정에서 많은 실험을 통해 배우고 있다. 본 연구에서는 회절 현상과 간섭 현상을 이용하여, 밀도가 서로 다른 네가지 용액인 증류수, 에탄올, 메탄올, 글리세린 속에서의 음속도를 측정하였다. 관 내에 액체를 채운 후 관의 윗부분을 초음파 흡수용 고무막으로 막고, 다른 한쪽 면에 압전체를 부착하여 1.77 MHz의 교류전압을 인가시킴으로써 액체 내에 초음파가 진행하도록 하였다. 초음파에 의하여 액체 내부에 규칙적인 밀도 변화가 형성되어, He-Ne laser beam에 회절격자가 작용함으로써 관을 통과한 빛이 스크린에 간섭무늬를 형성하도록 하였다. 형성된 간섭무늬의 간격을 측정하여 액체를 통과하는 음속도를 구할 수 있었다. 또한 hot plat를 이용하여 액체의 온도를 20 °C, 30 °C, 40 °C, 50 °C 로 가열하여 온도에 따른 액체 매질 내에서의 음속도 변화를 관찰하였다. 연구 결과, 증류수에서는 초기 온도 (20 °C)에서 1534 m/s, 1670 m/s (30 °C), 1858 m/s (40 °C), 최종 온도 (50 °C)에서 1885 m/s 으로 다른 용액도 마찬가지로 온도에 따라 액체 속의 입자 운동이 더 활성화되어 음파속도가 증가함을 볼 수 있었다.



Figure—온도에 따른 액체 속의 음속도

마찬가지로 온도에 따라 액체 속의 입자 운동이

## Ep-II-075

### Vanadium pentoxide nanowires as a functional material for Metal-Insulator-

#### Semiconductor (MIS) Capacitor

SHAHID Muhammad, SHAKIR Imran, 이 강우, 강 대준  
BK21 Physics Research Division, Department of Energy Science, Institute of Basic Science, SKKU Advanced Institute of Nanotechnology and Center for Nanotubes and Nanostructured Composites, Sungkyunkwan University, Suwon 440-746, Korea.

Large scale orthorhombic  $V_2O_5$  nanowires with diameter 100–200 nm and length into the tens of micrometer have been synthesized by hydrothermal and calcination route (Fig.1). The synthesized nanowires were employed to fabricate Metal-insulator-semiconductor (MIS) capacitor. The fabrication of MIS capacitor was achieved by depositing 20 nm of insulating layer of  $ZrO_2$  on the  $V_2O_5$  nanowires. The top 150 nm Au gate was deposited by using e-beam evaporator system. The transport properties of capacitor were characterized by using capacitance-voltage (C-V) measurements at room temperature. The C-V measurements showed that the capacitance of the synthesized nanowires was 670 pF (Fig.2). The electrical properties suggest that we can use  $V_2O_5$  nanowires for memory and tunneling devices applications.

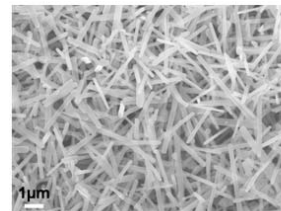


Figure.1.SEM of  $V_2O_5$  nanowires.

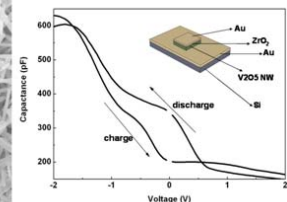


Figure.2. CV curve of the sample (inset device image)

## Ep-II-076

## Study of the Novel Mass Production Method of $^{64}\text{Cu}$ Radionuclide using $^{64}\text{Ni}$

### (p,n) $^{64}\text{Cu}$ Nuclear Reaction with Energetic Protons

전 권수, 박 현, 김 재홍

한국원자력의학원 방사선의학연구소.

Recently,  $^{64}\text{Cu}$  ( $T_{1/2}=12.7\text{h}$ ,  $\beta^-$  decay: 40%,  $\beta^+$  decay: 19%, E.C. decay: 41%) is considered as a useful radioisotope in the nuclear medicine due to its multiple decay modes and the intermediate half-life. Several nuclear reactions such as  $^{64}\text{Ni}(p,n)^{64}\text{Cu}$ ,  $^{68}\text{Zn}(p,n)^{64}\text{Cu}$  and  $^{64}\text{Ni}(d,2n)^{64}\text{Cu}$  have been employed for the production [1]. In this work, we have investigated the method on proton irradiation to the enriched  $^{64}\text{Ni}$  target for mass and routine production [2]. And a novel effective chemical process is developed for the separation of  $^{64}\text{Cu}$  from the irradiated  $^{64}\text{Ni}$  target, recycling of very expensive enriched material. The yield of  $^{64}\text{Cu}$  production is achieved as 8.9 mCi/mAh at EOB, which is in good agreement with one predicted by Szelecsenyi et al[3]. The radionuclidic purity is indicated as high as 99% and the recovery yield with anion/cation ion exchange resin is measured as higher than 98%. The new method could be applied to mass production of  $^{64}\text{Cu}$  radionuclide, which can be used as a cancer diagnostic and therapeutic agency in nuclear medicine. REFERENCES [1] V.S. Smith, Molecular Imaging with Copper-64, J. Inorg. Biochem., Vol.98, p.1874-1901, 2004. [2] IAEA Technical report Series No. 432. "Standardized High Current Solid Targets for Cyclotron Production of Diagnostic and Therapeutic Radionuclides" IAEA, Vienna, 2004. [3] F. Szelecsenyi, G. Blessing and S.M. Qaim, Excitation Functions of Proton Induced Nuclear Reactions on Enriched  $^{61}\text{Ni}$  and  $^{64}\text{Ni}$ : Possibility of Production of No-carrier-added  $^{61}\text{Cu}$  and  $^{64}\text{Cu}$  at a small Cyclotron, Appl. Radiat. Isot., Vol.44, p575-580, 1993.

P2

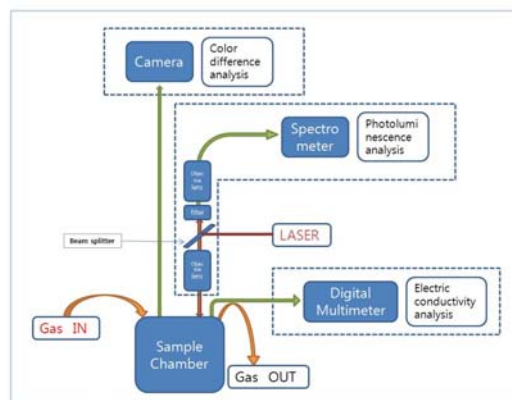
포스터세션

## Ep-II-077

## 유기증기에 노출된 다공질규소 다층구조의 PL, 간섭색, 전도도의 변화 특성 연구

서 동우, 이 기원, 김 영유, 김 한중, CHENG Horchhong  
공주대학교 물리학과.

고굴절률과 저굴절률 층이 주기적으로 구성된 다공질 규소 다층구조를 제작하고, 서로 다른 농도를 갖는 유기물 증기에 노출시켰다. 다공질규소의 기체 감응 특성에 대한 연구는 photoluminescence의 강도변화, 반사율의 변화, 전기전도도의 변화를 이용하고 있다. 기존의 연구는 이러한 감응변수들을 서로 독립적으로 측정하였기 때문에, 각 감응변수들 사이의 민감도와 감지시간을 절대적으로 비교하는 것이 힘들었다. 그러나 본 연구에서는 이제 가지 감응변수들을 동시에 측정함으로써 민감도와 감지시간에 대한 절대적인 비교가 가능하였다. 또한 본 연구에서는 간섭색의 변화를 기존의 반사율 스펙트럼 측정이 아닌 색상분석기술을 도입하고 색차분석을 시도함으로써 측정 장치를 간소화하고 보다 실용적인 측면을 강화하였다. 본 연구를 통해 주기수가 서로 다른 다공질규소 다층구조의 에탄올 기체 감응 특성을 체계적으로 연구할 수 있었고, 감응신호의 민감도와 감지시간에 대한 절대비교가 가능해짐으로서 다공질규소를 센서물질로서 응용하기 위한 기초자료가 얻어졌다.



**Ep-II-078****Effect of Liq Thickness in Polymer Photovoltaic Cells Fabricated with P3HT:PCBM Blended Layer**

SUNG Hyun-Su, KIM Jin-Man, LEE Su-Hwan, KIM Ji-Heon, LEE Gon-Sub, PARK Jea-Gun

Nano-SOI Process Laboratory, Hanyang University.

Organic photovoltaic (OPV) cell has advantages that low-cost fabrication, large-area devices, light-weight cells with flexibility, and material diversity. However, it has a problem of low power conversion efficiency (PCE). Many researchers are trying to solve this problem in a variety of ways. For example, Zhao et al. reported that PCE could be improved by electron injection layer (EIL, LiF). EIL reduces the amount of dipole formation between top electrode and [6,6]-phenyl-C<sub>61</sub> butyric acid methyl ester (PCBM). It also decreases recombination of electron-hole pairs. Consequently, this PV cell has dependent that the PCE sharply increased along with the thickness of the LiF layer up to ~1 nm and then suddenly decreased as the thickness of the LiF layer continued to increase. However, processing this material require a high temperature for thermal evaporation and precise control of the material thickness to usually less than ~1 nm. Therefore, we use 8-hydroxy quinolinato lithium (Liq) as a new EIL material and analyze characteristics of polymer PV cell. Generally, the Liq is an organic semiconductor material, and it has lower energy band-gap. In our presentation, a polymer PV cell consisting of ITO/PEDOT:PSS/P3HT:PCBM/BCP/Liq/Al was prepared. We fabricated with polymer PV cell on various Liq-thick. We optimized the Liq thickness at ~1 nm, open-circuit voltage ( $V_{oc}$ ) of 0.645 V, short-circuit current ( $J_{sc}$ ) of 14.67 mA/cm<sup>2</sup>, fill factor (FF) of 61.8 %, and PCE of 5.8 % are measured. In addition, we suggest that the electron injection mechanism of the Liq layer between the small molecular hole/exciton blocking layer (BCP) and metal electrode (Al) strongly influences the PCE of the polymer PV cell. \*This project was supported by “The National Research Program for Tera-bit-level Non-volatile Memory Development” sponsored by the Korean Ministry of Knowledge Economy

P2

포스터  
세션**Ep-II-079****대기 중 장시간 방치된 Pd-Pt/WO<sub>3</sub> 수소센서 박막의 반응성 연구.**

진 정모, 정 현식

서강대학교 물리학과.

차세대 대체 에너지로서 수소연료의 중요성이 커짐에 따라 활발한 연구가 진행되고 있다. 그러나 수소는 공기 중의 산소와 결합하여 자연발화하거나 폭발하는 특성이 있기 때문에 안전하게 사용하기 위해서는 수소누출을 검지하는 수소센서의 역할이 중요하다. WO<sub>3</sub> 박막은 전기채색 및 가스채색 특성때문에 많은 관심을 받고 있다. 이러한 특성을 이용하여 수소가스에 노출 시 박막의 광 투과도가 변화하는 반사식 수소 검지 광센서에 활용 할 수 있다. 이와같은 수소 안전센서에는 장기적인 안정성과 높은 검지 감도가 필수적으로 요구된다. 본 연구에서는 공기 중의 오염물질에 의해 수소센서 박막이 열화되어 내구성이 떨어지는 것을 방지하기 위해 기존에 연구되었던 Pd/WO<sub>3</sub>에 Pt를 합금하여 sputter로 증착한 Pd-Pt/WO<sub>3</sub> 박막을 제작하였다. 증착한 Pd-Pt/WO<sub>3</sub> 박막을 6개월간 대기 중에 방치시킨 후 광투과도 특성을 연구하였다. 센서박막을 6개월동안 1개월 간격으로 수소와 공기에 노출하여 박막의 광투과도 변화를 측정하였다. 그 결과, 박막 제작 직후 측정한 광투과도 변화보다 6개월 후 측정한 투과도 변화가 다소 작았지만 장기간 대기에 노출되어도 지속적인 광투과도 반응 보임을 확인하였다. 따라서 단일 Pd 촉매보다 Pd-Pt alloy 촉매가 공기 중의 오염물질에 의해 덜 열화되는 것을 확인하였고 박막이 장기간 대기에 노출되어도 수소에 반응하기 때문에 이를 활용하면 내구성이 향상된 수소센서로 활용이 가능함을 확인하였다.

**Ep-II-080****종이 기판 위에 top-emission type의 후막형 무기 electroluminescence 특성**김 진영, 유 세기<sup>1</sup>성균관대학교, 물리학과. <sup>1</sup> 한국외국어대학교, 전자물리학과.

Top-emission 구조의 후막형 무기 electroluminescence(EL) device를 신문지, 잡지, 스티커 종이 등 여러 종이 위에 제작 하였다. 후막형 무기 EL device를 형성하는 동안 물과 화학약품으로부터 종이를 보호하기 위해 spin-on-glass (SOG) buffer layer를 종이 기판 위에 코팅하였다. 종이 기판의 불투명한 특징으로 기존의 bottom-emission 구조가 아닌 top-emission 구조를 선택하였다. 이 종이 기판 위의 무기 EL device는 기존의 플라스틱 기판위의 무기 EL device와 동일한 좋은 휘도를 보였다. 포스터에서 이 buffer layer의 특성과 구조적인 차이에 대한 자세한 분석을 다룰 예정이다.

**Ep-II-081****Study on the charge transport characteristics of organic thin film transistor using near field scanning microwave microprobe**

YOON Youngwoon, KIM Songhui, LEE Hanju, KIM Tae-dong, LEE Kiejin

Sogang Univ, Department of Physics.

We have studied crystalline thin film fabrication by thermal evaporation. An amorphous rubrene thin film was initially obtained on a 200 nm thick SiO<sub>2</sub>/Si substrate at 40 °C. In situ long time post annealing at 80 °C transformed the amorphous phase into crystalline phase. Four heating conditions were investigated: (a) preheating (b) annealing (c) preheating and annealing (d) preheating, cooling (35 °C) and annealing, sequentially. We observed the changes of crystal structure of rubrene polycrystalline thin films at various in situ substrate temperature and processes by optical absorption spectra, x-ray diffraction, and near-field microwave microprobe (NFMM). The conductivity of rubrene polycrystalline thin films on SiO<sub>2</sub> substrates was studied by measuring the reflection coefficient S<sub>11</sub> and compared with microwave transmission line theory.

**Ep-II-082****무냉매 전도냉각형 5 T 초전도자석**

김 동락, 김 재휘, 최 연석, 양 형석

한국기초과학지원연구원

소형냉동기의 축열재로 사용되는 자성재료 기술의 발전으로 인하여 냉매를 사용하지 않고 ~3 K까지의 극저온을 실험실에서 간단히 얻을 수 있게 되었다. 극저온 냉각이 필요한 초전도자석을 소형냉동기를 이용하여 전도냉각형으로서 냉매를 사용하지 않고 고자기장을 얻을 수 있게 되어, 자기장 환경을 다양한 분야의 연구에 활용할 수 있게 되었다. 상온 직경 52 mm, 자기장 5 테슬라의 전도냉각초전도자석을 개발하고 성능시험한 결과를 발표하고자 한다.

**Ep-II-083****Effect of Al Nanocrystals Surrounded by  $\text{Al}_2\text{O}_3$  in Nonvolatile Memory****Characteristics for Polymer Memory-cells**

PARK Jung-Yong, LEE Ho-Young, KWON Kyoung-Cheol<sup>1</sup>, KIM Chang-Hwan<sup>1</sup>, LIM Jae-Sung<sup>1</sup>, PARK Jea-Gun<sup>1</sup>

*Department of Electrical & Computer Engineering, Hanyang University. <sup>1</sup>National Program Center for Tera-bit-level Nonvolatile Memory Development, Hanyang University.*

We studied the effect of Al nanocrystals on nonvolatile memory characteristics as memory margin, retention time and endurance cycles of program and erase for polymer memory-cells. The advantage of polymer memory-cells is the smallest memory-cell feature size of  $4F^2$ , fast access and store time, a simplicity of manufacturing process and high physical mechanical flexibility. The memory-cells have the architecture of a triple layer (polymer/metal nanocrystals/polymer) sandwiched between two metal electrodes. The polymer is PS (polystyrene) and the metal is Al. The polymer memory-cells need the metal nanocrystals to make nonvolatile memory characteristics. Therefore, after deposition of the Al layer on the bottom PS layer, we used the  $\text{O}_2$  plasma process to make Al nanocrystals surrounded by  $\text{Al}_2\text{O}_3$ . In case of a polymer memory-cell embedded with Al layer without  $\text{O}_2$  plasma process, we found they have no characteristics of memory. Otherwise, when embedded with Al nanocrystals surrounded by  $\text{Al}_2\text{O}_3$  by using  $\text{O}_2$  plasma process, they have characteristic of memory such as memory margin ( $I_{\text{on}}/I_{\text{off}}$ ) of  $0.13 \times 10^2$ , the retention time of more than  $-1 \times 10^5$  sec, and more than 100 endurance cycles of program and erase.

Acknowledgement\* This research was supported by "The National Research Program for Terabit Nonvolatile Memory Development" sponsored by the Korean Ministry of Knowledge Economy.

**Ep-II-084****Leakage Current Conduction Mechanism and Noise Properties of  $\text{ZrO}_2$  Thin Film**

SEO Yohan, KIM Youngsang, JEON Hankyung, JEONG Heejun

한양대학교 응용물리학과.

We studied the leakage current conduction mechanism and noise properties in metal-oxide-semiconductor (MOS) structure with atomic layer deposited  $\text{ZrO}_2$  gate dielectric. Under negative biasing, the leakage current in  $\text{ZrO}_2$  film is caused by the trap assisted tunneling in the low bias region, while the space charge limited conduction controls the leakage current flow in the high bias region. We observed that the Lorentzian-like noise power spectrum in the low bias region that is the result of the random telegraph signal (RTS) fluctuation based on the trap assisted tunneling process. The trap assisted tunneling process was verified by the voltage scaling of the normalized noise power at a low frequency. In the high bias region, a Lorentzian spectrum was degraded and the  $1/f$  noise became dominant which is due to the carrier number fluctuation. This work was supported by the Korea Science and Engineering Foundation (KOSEF) grant funded by the Korea government (MEST) (No. 2009-0075053).

P2

포  
스  
터  
세  
션

**Ep-II-085****OLED소자에서 각 layer의 표면에 따른 특성연구**

김 태동, 윤 영운, 이 한주, 김 송희, 이 기진

서강대학교 물리학과.

OLED소자의 multi layer구조에서 각 layer의 구조 또는 전기적 특성은 OLED소자의 효율을 결정짓는 중요한 요소 중 하나이다. 홀 주입 층으로 쓰이는 CuPc 박막의 phase에 따른 전기적 특성과 실제로 소자를 만들었을 때의 효율이 다른 것을 발견 하였는데 이는 layer표면의 거칠기 때문에 생긴 결과 임을 알 수 있었다. 그래서 CuPc뿐만이 아닌 홀수송층과 발광층 그리고 buffer layer등의 표면 거칠기에 따른 OLED소자의 전기적, 구조적 특성을 알아 보았다.

**Ep-II-086****Possible High-power Thin Film Varistor based on Metal-Insulator Transition**

KIM Bong-Jun, SEO Gi Wan<sup>1</sup>, CHOI Sungyoul, CHOI Jeongyong, LEE Yong Wook<sup>2</sup>, KIM Hyun-Tak  
ETRI. <sup>1</sup>UST. <sup>2</sup>Pukyong National University.

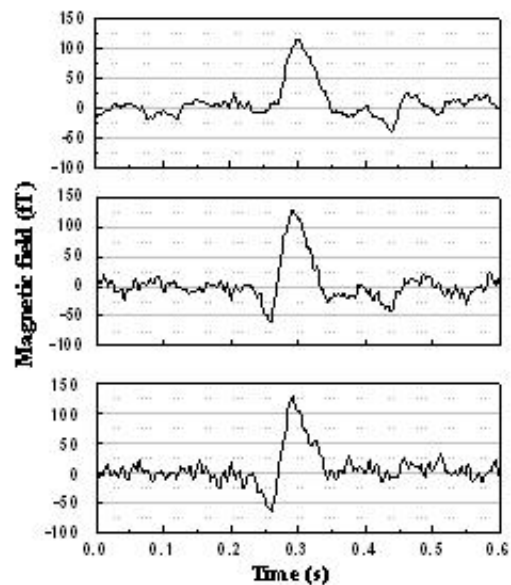
VO<sub>2</sub> thin film varistors for electronic applications are fabricated and tested here, and the metal-insulator transition (MIT) of the fabricated varistors is used to provide protection from abrupt current jumps. As a MIT material, VO<sub>2</sub> is deposited on a sapphire substrate. For the varistor application, a VO<sub>2</sub> thin film varistor is fabricated with a parallel stripe pattern, and the varistic property of the film is examined by electrostatic discharge experiments. The abrupt current jump in VO<sub>2</sub> thin film varistors can be compared with the gradual current increase of ZnO polycrystals with intergranular boundaries. The varistic coefficient of the thin film VO<sub>2</sub> varistor is estimated to be larger than 500. An overvoltage protection test is carried out by applying high electrostatic discharge voltages to VO<sub>2</sub> thin film varistors up to 3.3 kV. The maximum response voltage ( $V_m$ ) is less than 200V at 1600V. Response times of <20ns are sufficient to protect a device perfectly.

**Ep-II-087****Improving the Signal to Noise Ratio of MEG signal using lead superconductive hemispherical shield**

YU Kwon Kyu, KIM Kiwoong, KWON Hyuckchan, KIM JinMok, LEE Yong Ho  
KRISS.

To improve the signal to noise ratio (SNR) of MEG signal, we have fabricated a whole head magnetoencephalogram (MEG) system with Pb superconductive shield. We measured the shielding factor for the position of helmet shape Pb and for changing the distance from Pb surface. To make a uniform magnetic field, a 1.5 x 1.5 meter set of the helmholtz coils activated at several frequencies. The shielding factor of hemispherical shape Pb was from 28 to 55 dB and of Pb plate was about 20 dB. The shielding factor was rapidly reduced as increasing the distance from Pb surface. The white noise of Superconductive Quantum Interference Device(SQUID) with Pb superconductive shield was about 10 fT/Hz<sup>1/2</sup> at 1Hz, 7 fT/Hz<sup>1/2</sup> at 100 Hz. The white noise was more increased about two times than conventional SQUID system without Pb shielding. An auditory signal was measured by first order gradiometer and magnetometer with Pb superconductive shield and compared the SNR. The SQUID system with Pb shield had better performance at low frequency noise level.

( Fig 1. Comparison with auditory evoked signal measured by several MEG system.:(a) conventional MEG system, (b) MEG system with superconductive shield(open door), (c) MEG system with superconductive shield (close door).)



### Ep-II-088 온도 변화에 따른 $\text{Ge}_2\text{Sb}_2\text{Te}_5$ 의 광학적 특성 연구

서 윤경, 이 동재, 이 윤상, 최 은집<sup>1</sup>, 이 택성<sup>2</sup>

송실대학교, 물리학과. <sup>1</sup>서울시립대학교, 물리학과. <sup>2</sup>KIST.

차세대 광 기록매체로 주목 받고 있는  $\text{Ge}_2\text{Sb}_2\text{Te}_5$ (GST)는 대표적인 phase change material로, 열처리 조건에 따라 구조변화와 함께 부도체상과 도체상 간의 전이가 일어난다. Amorphous phase GST의 FCC structure는 대략 150°C 근처에서 이루어지고, 이 때 도체상으로의 전이가 일어난다. 대략 280°C 근처에서 도체상을 유지한 채 hexagonal 구조로 변화하며 630°C 부근에서 melting이 되는 것으로 알려져 있다. 우리는 각각 amorphous(a-GST)와 crystalline phase(c-GST)의 GST( $\text{SiO}_2$ (200nm)/Si) film을 상온에서 400°C까지 온도를 올려가며 온도 변화에 따른 광학 상수(n,k)를 측정하였다. 타원분광법(ellipsometry)을 사용하였고, 산화에 의한 영향을 줄이기 위해  $\text{N}_2$  분위기에서 실험하였다. a-GST sample로 실험했을 때, amorphous phase에서 crystalline(FCC) phase로 변하는 150°C 근처에서 광학상수의 큰 변화가 있었고, FCC 구조에서 hexagonal 구조로 변하는 280°C 근처에서는 별다른 변화가 보이지 않았다. 또한 c-GST sample에 상온에서 400°C까지 온도 변화를 주어도 광학 상수에는 별다른 변화가 나타나지 않았다. 이러한 온도에 따른 광학적 특성은 전자구조의 변화와 관련 지어 논의한다.

### Ep-II-089 Electrical Characteristics of Aluminum Oxide Film Deposited by Electron Beam Evaporation for the Application of Thin-film Transistors

IM Seongil, KO Gunwoo, LEE Kimoon, LEE Kwang H

*Institute of Physics and Applied Physics, Yonsei University.*

We report on the electrical properties of amorphous aluminum oxide ( $\text{AlOx}$ ) films fabricated by electron beam (e-beam) evaporation. The oxide films were deposited on indium-tin-oxide (ITO) glasses using electron-beam evaporation at room temperature under various deposition rate of 0.2, 2.5 and 10 Å/s with or without  $\text{O}_2$  ambient gas. The highest breakdown electric field ( $\sim 3$  MV/cm) was obtained from the samples deposited at the  $\text{O}_2$  ambient with deposition rate 10 Å/s. Our optimally-processed aluminum oxide films show the dielectric constant of  $\sim 8$  by capacitance-voltage measurements. We also fabricated ZnO and pentacene-based thin-film transistors (TFTs) with our e-beam processed  $\text{AlOx}$ , showing maximum field effect mobility of  $\sim 1$   $\text{cm}^2/\text{Vs}$ , operating at  $\pm 3$  V with an on/off current ratio of  $\sim 10^3$ . Our e-beam processed  $\text{AlOx}$  might be a potential candidate of dielectric materials for the application of TFTs.

**Ep-II-090****RF 스퍼터링을 이용한 AZO 투명전도막 형성 및 특성 분석**

정 인승, 나 영혁<sup>1</sup>, 최 명운<sup>2</sup>, 정 광호<sup>1</sup>

연세대학교 물리및응용물리, <sup>1</sup>연세대학교 물리학과, <sup>2</sup>(주) 야스.

투명전도막을 형성하기 위하여, RF magnetron sputtering 법을 이용하여 Glass 기판에 Al 첨가된 ZnO를 증착하였다. AZO는 밴드갭이 넓어, 투명도가 높고, 전도성이 좋아 태양광소자 및 발광소자의 전극으로 많이 활용되는 물질이다. 본 실험에서 일정한 기판-타겟 거리와 파워에서 기판의 온도를 상온에서 400도까지 변화를 주어 AZO(Al doped ZnO)를 1000Å 성장시켰고, 두께는 a-step으로 확인하였다., 4-point 측정법을 이용하여 박막의 전도성을 측정하여, 비저항(Resistivity)은 100Ωcm에서 7\*10<sup>-2</sup>Ωcm까지 관찰되었다. 가장 작은 비저항은 400도에서 7\*10<sup>-2</sup> Ωcm 이 관찰되었다.

**Ep-II-091****Hydrochlorosilole(HCS)을 기반으로 한 유기발광다이오드 (Organic Light-emitting diodes)의 임피던스 분석법을 이용한 최적화 구조연구**

박 영환, 신 용호, 이 수연, 김 용민

단국대학교 응용물리학과.

미세신호 AC 임피던스 분석법(Impedance Spectroscopy)은 DC 바이어스에 따른 전극의 편극 현상이 발생하지 않는 새로운 종류의 전극 물질에 대한 전기적 특성 분석에 적합한 방법으로 잘 알려져 있다. 또한, 임피던스 분석법을 통해 측정된 데이터를 이용하면 동질의 특성을 나타내는 전극과 물질들로 이루어진 시스템의 계면 및 bulk 특성에 필요한 이동도 (mobilities), 유전상수(dielectric constant) 등과 같은 변수들의 분석에도 이용할 수 있다. 최근 들어 임피던스 분석법은 유기발광다이오드의 수명, 특성감소 및 구조적 결함과 같은 현상분석에 이용되고 있다. AC frequency sweep 을 통하여 얻은 전도도(conductance)와 전기용량(capacitance) 을 이용하여 유기발광다이오드의 전하이동 주파수 의존성에 대한 측정할 수 있다. 본 연구에서는 Alq<sub>3</sub> 와 TPD 를 발광층(EML)과 정공수송층(HTL) 으로 이용하였으며, hydrochlorosilole (HCS)가 전자수송층(Electron transport layer ; ETL)물질로 이루어진 유기발광다이오드를 열기상증착 방법을 이용하여 제작하였다. 전자수송층(ETL)의 증착 두께가 전기전도도에 미치는 영향을 알아보기 위하여 증착두께를 5 nm 부터 25 nm 까지 변화시키며 AC frequency range 10 Hz ~ 10 MHz 에 대한 임피던스값을 측정한 결과 증착 두께 7 nm 일 때 contact resistance (R<sub>c</sub>)와 bulk resistance (R<sub>p</sub>) 값이 각각 2.96 Ω, 833.3 kΩ 으로 가장 낮은 값을 나타냈으며, 전도도 또한 가장 좋은 특성을 보이는 것으로 확인되었다.

**Ep-II-092****BiYIG박막의 테라헤르츠 특성 연구**

이 한주, 유 형근, 윤 영운, 김 태동, 김 송희, 이 기진  
서강대학교, 물리학과.

BiYIG 박막의 테라헤르츠 영역에서의 분광 특성을 연구하였다. BiYIG박막은 Metal Organic Decomposition방법으로 Glass 기판위에 제작되었으며 Bismuth 도핑농도에 따른 테라헤르츠 영역에서의 특성 변화를 분석하기 위하여 0, 0.5, 1.0, 1.5 의 도핑농도를 가진 박막을 제작하였다. XRD 분석을 통하여 박막의 결정성 및 결정구조를 분석하였으며 SEM 측정을 통하여 박막의 두께 및 grain의 구조를 분석하였다. 최종적으로 각 박막의 테라헤르츠 영역에서의 흡수도 및 분광학적 특성을 분석하였다.

**Ep-II-093****FOLED를 위한 Mg-Zn-F 봉지막 제작 및 특성 분석**

손 명락, 이 성엽<sup>1</sup>, 신 병욱, 공 소저, 이 진능, 박 선미, 김 도억<sup>2</sup>, 강 병호<sup>2</sup>, 홍 석민<sup>3</sup>, 추 나윤<sup>1</sup>, 이 의완<sup>4</sup>, 이 형락<sup>4</sup>

경북대학교, 물리학과. <sup>1</sup>경북대학교, 나노과학기술학과. <sup>2</sup>경북대학교, 전자전기컴퓨터학부. <sup>3</sup>경북대학교, 센서 및 디스플레이공학과. <sup>4</sup>경북대학교, 물리및에너지학부.

현재까지 알려진 실리콘 산화물이나 질산화물 봉지막의 경우 일반적으로 OLED에서 요구하는  $10^{-5}$  g/( $m^2 \cdot day$ ) 수분 투과도와 광투과도를 동시에 만족시키는 데에 많은 한계가 있다. 본 연구에서는 광학적 특성이 우수하면서, 수분 및 산소 투과도가 우수한 Mg-Zn-F 박막을 제작하기 위해  $MgF_2$ 와 Zn을 6:4, 5:5, 4:6, 3:7 비율로 타겟을 제작하였고, RF 스퍼터를 이용하여 PEN필름위에 증착시켰다. Mg-Zn-F 박막의 두께는 약 200nm이며 광투과도는 가시광 영역에서 약 85% 이상이었다. 4:6 비율의 타겟을 이용하여 증착한 박막의 Zn 비율이 가장 높았으며, 수분 투과도는  $1 \times 10^{-3}$  g/( $m^2 \cdot day$ ) 이하의 결과를 보였다. 제작된 박막은 SEM, XPS, EDS 등을 이용하여 물리적인 특성을 확인하였다. 그리고 폴리머 기판을 이용한 FOLED 소자를 제작하고 Mg-Zn-F 박막을 적용하여 특성 및 수명을 평가하였다.

**Ep-II-094****Study of solvent effect for forming nanostructure of Organic solar cell**

YI Jin Neung, SHIN Byong Wook, LEE Sung-Youp<sup>1</sup>, PARK Sun Mi, SON Myeong Rak, KONG So Jeo, CHOO Na Yun<sup>1</sup>, KIM Je Han, LEE Eui Wan<sup>2</sup>, LEE Hyeong Rag<sup>2</sup>

*Kyungpook National University, Department of Physics.* <sup>1</sup>*Kyungpook National University, Department of Nano-science and Technology.* <sup>2</sup>*Kyungpook National University, School of Physics and Energy Science.*

Study of solvent effect for forming nanostructure of organic solar cell In bulk heterojunction organic solar cell, regioregular poly(3-hexylthiophene-2,5-diyl)(P3HT) and fullerene derivative [6,6]-phenyl-C61-butyric acid methyl ester(PCBM) solution in chlorobenzene was coated on glass ITO/PEDOT:PSS(CLEVIOS PH 500) substrate. In active layer, the P3HT and PCBM respectively formed crystalline and cluster of nanosize through the thermal annealing process after aluminum deposition as cathode. To study the effect of solvent, the samples were put down in a vacuum chamber for different times without cathode and baked on hot plate at various temperature after aluminum deposition. From measuring Voc, Jsc, fill factor(FF) and power conversion efficiency(PCE) by using solar simulator, the electric property of samples was investigated. The nanostructure of samples was shown in image of scanning electron microscope(SEM) and atomic force microscope(AFM)

**Ep-II-095****박막태양전지 제조용 임의 방향 방출형 셀레늄 증발원 개발 및 Se/Glass 박막특****성 분석**

김 은도, 정 예슬, 정 다운, 박 성동, 엄 기석, 조 상진<sup>1</sup>, 황 도원

(주) 알파플러스. <sup>1</sup>경성대학교 물리학과.

단순한 제조공정과 대형화로 저가 생산의 장점을 가지고 있는 박막형 태양전지가 차세대 태양전지 기술로 각광받고 있다. 그중, CIGS 태양전지는 실험실적으로 만든 박막태양전지 중에서 가장 높은 효율을 기록하고 있어 최근 많은 연구가 진행되고 있다. 특히 진공증발원의 개발은 CIGS 태양전지의 제조와 효율향상에 핵심 요소라고 할 수 있다. 기존의 방식인 상향식 증착 방식은 상향으로 증발된 소스 물질이 중력의 영향을 받게 되므로 상부에 위치한 기관의 표면에 접촉하지 못하고 낙하하는 소스 물질이 생기게 되므로 소스 물질의 사용 효율이 낮다는 문제점이 있다. 또한, 마스크를 사용해야 하는 경우에는 마스크 처짐 현상이 있고, 기관을 고온으로 가열해야 하는 경우 대면적 기관과 같은 경우에는 휨 현상이 발생할 수 있어서 대면적 기관에 적용하기 어렵다는 단점이 있다. 본 논문에서는 CIGS 박막태양전지 제조에서 사용되는 셀레늄 증발원 또는 황 증발원의 증발소스 분자선 방향을 상향 또는 하향으로 조절할 수 있는 핵심부품을 개발 및 제작하였다. 또한 이를 이용하여 박막을 제조하고 박막에 관한 특성을 SEM, Reflectometer, EDAX를 이용하여 조사하였다.

## Ep-II-096

## Plasma Dry Etching 방법에 의한 Wafer Backside Etch 특성 평가

한 영기, 서 영수, 유 재하<sup>1</sup>, 이 현범<sup>1</sup>, 서 상훈<sup>2</sup>, 황 옥중<sup>3</sup>

(주)소솔, <sup>1</sup>하이닉스 반도체, <sup>2</sup>KAIST, <sup>3</sup>나노종합팩.

반도체 소자가 점점 소형화, 고집적화 됨에 따라 wafer backside에 대한 중요도도 점점 크게 부각되고 있다. 그것은 소자의 신뢰성에 영향을 주는 민감한 부분 중의 하나로 공정 중 발생하거나 wafer의 이송 중에 발생하는 particle, 또는 wafer backside에 증착되는 원치 않는 막에 의한 warpage 등이 소자업체의 생산성에 심각한 영향을 주기 때문이다. 본 연구는 자체 개발한 wafer backside plasma dry etcher 장비를 이용하여 wafer backside에 남아 있는 막 및 particle 제거에 대한 연구를 진행하였고, 그 결과를 바탕으로 반도체 소자의 수율에 미치는 영향을 평가하였다. 그림 1은 Wafer 후면에 증착되어 있는 혼합막을 over etching 한 후 Si 표면에 대한 영향을 분석한 결과이다. Etching을 진행한 혼합막의 구성은 Poly/SiO<sub>2</sub> 구조로 되어 있다. 그림에서 보듯이 혼합막에 대한 잔막은 확인 할 수 없었으며, plasma를 사용했음에도 불구하고 Si 표면에는 damage가 발생하지 않은 것을 확인할 수 있었다. 그림 2는 particle 제거 test를 진행한 결과이다. Wafer 표면에 남아 있던 particle은 급격히 감소하는 것을 확인할 수 있었다. 그림 3은 양산 중인 DRAM 소자에 wafer backside etching을 진행하고, 실제 수율에 미치는 영향을 평가한 결과이다. 그림에서 보듯이 wafer backside etching을 적용한 wafer에서 평균 수율이 약 2% 이상을 증가한 것을 확인할 수 있었다. 이러한 원인은 wafer backside에 남아 있던 particle을 제거함으로써 photo 공정에서의 beam align 개선 효과와 wafer warpage 개선에 따른 효과로 사료된다. 본 연구는 지식경제부 나노반도체장비 원천기술상용화사업 지원에 의해 수행되었습니다.

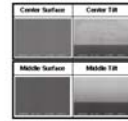


그림 1. Wafer Backside Over Etch Test 결과

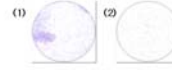


그림 2. Particle 제거 Test 결과  
(1)Before, (2)After

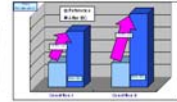


그림 3. DRAM 소자 적용 Test 결과

## Ep-II-097

High Temperature Thermoelectric Properties of Ca<sub>3</sub>Co<sub>4</sub>O<sub>9</sub> Thin Film

KANG Min-Gyu, CHO Kwang-Hwan, KANG Chong-Yun, KIM Sang-Sig<sup>1</sup>, YOON Seok-Jin

KIST, Thin Film Materials Research Center. <sup>1</sup>Korea University, School of Electrical Engineering.

Recently, layered cobaltates have emerged as promising thermoelectric materials due to their excellent thermoelectric properties. The Ca<sub>3</sub>Co<sub>4</sub>O<sub>9</sub> is among the best thermoelectric oxides, and thus has been extensively studied in single crystalline and bulk polycrystalline forms. Thermoelectric thin films can have a low resistivity and a high Seebeck coefficient intrinsic to their electronic band structures. At the same time, thin films are expected to have thermal conductivity lower than that of the single crystals due to strong phonon scatterings at both surfaces and film/substrate interfaces. However, thin films are difficult to analyze thermoelectric characteristics at high temperature due to unstable ohmic contact, maintaining thermal gradient and oxidation of measuring system. We prepared Ca<sub>3</sub>Co<sub>4</sub>O<sub>9</sub> thin films on Al<sub>2</sub>O<sub>3</sub> substrates by RF-magnetron sputtering at 50mtorr partial pressure and variable substrate temperature. As-deposited Ca<sub>3</sub>Co<sub>4</sub>O<sub>9</sub> films were annealed at 800 °C in order to improve crystallinity of films. To measure the thermoelectric properties, S-type thermocouples(Pt/Pt-Rh) contacted different two point and generated thermal gradient. The Seebeck coefficient was calculated using generated Seebeck voltage and thermal differential across a wide temperature range (R.T~1000K). The electrical resistivity was measured by Van der pauw method.

**Ep-II-098****영상분석을 통한 초크랄스키 결정성장의 자동직경조절장치 개발**이 정일, 정 기수<sup>1</sup>, 장 인수, 김 장렬한국원자력연구원, <sup>1</sup>경상대학교

고주파 가열 방법이 적용된 초크랄스키 단결정 성장시스템에서 단결정의 직경을 측정하고 제어하는 것은 성장된 단결정의 품질에 중요한 영향을 미치는 요소 중의 하나이다. 기존에 정밀한 전자저울을 사용하여 단결정이 성장된 무게를 분석한 후 결정의 직경을 제어하는 방법 등이 잘 알려져 있으나 무게만 측정하여 분석하는 방법으로는 성장되는 단결정 잉곳의 형태에 대한 정보 얻지 못하는 단점이 있다. 이에 영상처리 기법과 무게 제어 방식을 동시에 적용한 방법의 자동 직경 조절 장치를 개발하였다. 이 방법은 결정이 성장되는 동안 분해능이 높은 CCD카메라로 결정의 성장영역을 촬영하여 영상을 제어용 PC에 전송해주며 제어용 PC는 전송받은 영상을 분석하여 단결정 잉곳의 직경을 산출하고 성장되는 잉곳의 형태를 기록한다. 이와 동시에 전자저울이 성장된 단결정의 무게 변화를 측정하여 제어용 PC에 전송해주며 제어용 PC는 단결정의 무게변화를 분석하여 성장된 단결정 잉곳의 부피를 알아낸다. 영상에서 분석된 직경 값을 기본데이터로 하고 정밀 저울로 측정한 잉곳의 부피의 변화량을 보조데이터로 하여 성장되고 있는 잉곳의 지름과 부피변화를 분석해 제어용 PC가 RF 발전기의 전력을 제어하여 직경을 설정 값으로 유지하게 한다. 이 자동직경조절장치가 적용된 초크랄스키 단결정 성장장치는 20 kW의 출력을 가지는 RF generator, RF 코일의 직경은 128 mm로서 직경 30 mm 정도의 고온산화물 단결정 성장이 가능하다.

P2

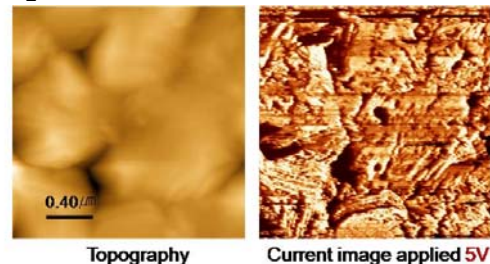
포스터  
세션**Ep-II-099****Local electrical properties of  $\text{CuIn}_{1-x}\text{Ga}_x\text{Se}_2$  thin films using conductive atomic****force microscopy**SHIN R. H., JO W., YUN Jae Ho<sup>1</sup>, AHN Sejin<sup>1</sup>

Department of Physics, Ewha Womans University, Seoul

120-750. <sup>1</sup>Korea Institute of Energy Research, Daejeon 305-

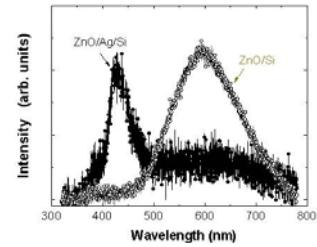
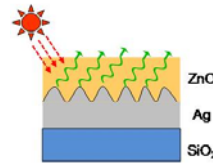
343.

Chalcopyrite  $\text{CuIn}_{1-x}\text{Ga}_x\text{Se}_2$  (CIGS) is currently used as an absorber layer for high-efficiency thin-film polycrystalline solar cells owing to high optical absorption coefficient of near  $10^5 \text{ cm}^{-1}$  in the visible region. The highest efficiency of solar cells with CIGS layers has surpassed 20%. In CIGS thin films, there is controversy about the role of recombination in grain boundary (GB) that the GB is either electrically active or inactive as a recombination center for photogenerated carriers. Thus, it is important to obtain nanoscale observation of electrical properties. The CIGS samples were deposited about 2  $\mu\text{m}$  on Mo coated glass substrates with different orientation. Triangular pyramid grains were obtained in the (112)-preferentially oriented CIGS film. Conductive atomic force microscopy (C-AFM) with Pt coated tip was used to observe surface conductivity in preferentially and randomly oriented CIGS thin films. In the C-AFM images, the two CIGS thin films showed different conduction in intra grain and GB. In randomly oriented film, rectifying junction between tip and sample was observed while a Schottky-like junction characteristic was measured in (112)-preferentially oriented film in local current-voltage characteristics.



**Ep-II-100****Photoluminescence properties of ZnO/Ag thin films prepared by rf-magnetron sputtering****sputtering**권 민지, 김 동욱, 신 혜영, 윤 석현, 이 기주<sup>1</sup>이화여자대학교, 물리학과. <sup>1</sup>충남대학교, 물리학과.

ZnO and Ag thin films were grown on silicon and glass substrates by RF-sputtering technique. The presence of the Ag layer significantly affected the photoluminescence (PL) spectra of the ZnO films: the bandgap emission, at around 400 nm, was enhanced and the defect-related emission, at around 600 nm, was suppressed. The PL spectra were also largely dependent on the Ag underlayer roughness, examined by atomic force microscopy. This suggested that the interface morphology could affect the electron-hole pair generation and recombination processes of the ZnO layers, as well as the surface-plasmon-mediated emission at the ZnO/Ag interface. Since ZnO/Ag thin films have been used as a vital part of photovoltaic systems through the back side reflector, our study may suggest a new way of efficient light trapping in silicon thin-film solar cells.



P2

포스터  
세션**Ep-II-101****고온고습 표준가스 발생 기술**

최 병일, 김 종철, 우 상봉

한국표준과학연구원.

최근 반도체산업 같은 첨단산업에서는 극저수분 습도표준가스에 대한 필요성의 대두와 더불어, 고온고습영역에서 습도표준가스에 대한 필요성은 첨단산업과 더불어 전통산업에서도 꾸준히 증대하고 있다. 이는 산업의 고도화 및 효율화에 따른 고온고습과 같은 극한 상황에서의 공정을 관리해야 할 분야가 많아 졌기 때문이다. 본 연구는 고온고습 영역에서의 습도표준가스를 발생시키기 위해 이온도이압력식 표준습도발생장치를 개발하였다. 이의 습도발생능력은 (-10 ~ +95) °C D.P. 이었고, 발생 표준가스의 불확도는 (0.05 ~ 0.15) °C D.P. 이었다.

최 병일, 우 상봉, 김 종철

한국표준과학연구원

힘이 가능한 OLED 디스플레이 필름은 차세대 디스플레이 기술로 인식되고 있다. 하지만 현재 OLED에 사용되는 재질들이 수증기에 매우 취약하므로, 필름의 수분투과도는 매우 중요한 요소이며, 더불어 매우 낮은 (10-3~10-6) [g/m<sup>2</sup> day] 영역에서의 수분투과도 측정기술은 OLED 산업 발전을 위해 꼭 필요한 기술이다. 본 연구는 이영역에서의 수분투과도 측정기술을 확립하고 저, 방사선 동위원소인 삼중수소를 이용한 측정장치를 구성하였는데, 이는 수분의 정량적인 측정이 가능하다. 측정 불확도는 수분투과도가 10-5 [g/m<sup>2</sup> day] 정도인 시료에 대해 대략  $1.88 \times 10^{-6}$  [g/m<sup>2</sup> day]를 주었다. 이는 앞으로 차세대 디스플레이 산업의 필름 봉지 기술개발에 기여할 것이다.

**Kp-II-001****Resonant Tunneling Barriers in Quantum Dots-in-a-Well Photodetectors**

BARVE Ajit V., SHAO J., SHARMA Y., R. Sheno, JUN OH Kim<sup>1</sup>, SANG JUN Lee<sup>1</sup>, SAM KYU Noh<sup>1</sup>, SANJAY Krishna

*University of New Mexico, Center for High Technology Materials. <sup>1</sup>Korea Research Institute of Standards and Science.*

Quantum-dots-in-a-well (DWELL) detectors, in which InAs QDs are placed in In<sub>0.15</sub>Ga<sub>0.85</sub>As-GaAs quantum well, combine advantages of quantum dot infrared photodetectors (QDIP) such as three-dimensional confinement for carriers, normal incidence response, lower dark current while offering additional advantages such as reproducible control over the response wavelength, optimum growth temperatures in the capping materials leading to superior optical quality of the quantum dots. We demonstrate the use of resonant tunneling filters in the barrier of DWELL detectors in order to suppress the dark current without reducing the photocurrent, to increase the signal to noise ratio. Two resonant tunneling DWELL detectors (RT-DWELL) are designed to extract the longwave and midwave component of spectral response, respectively. 2-3 orders of magnitude improvement in the dark current over the control sample, for a similar peak wavelength has been obtained as a result of resonant tunneling action. The specific detectivity has been improved by factor of 5, as a result of improved signal to noise ratio in the detectors. Spectral tuning by the use of resonant tunneling filters has also been demonstrated. Resonant tunneling barriers for the strain optimized DWELL detectors result in much superior detector performance, leading to higher operating temperatures.

P2

포스터  
세션**Kp-II-002****Effect of Pretreated Substrate on the Nucleation Characteristics of GaN****Nanorods**

박 현규, 이 상화, 김 진교

*경희대학교, 물리학과.*

GaN nanorods were grown on c-plane sapphire substrates with (0.3°-miscut toward M-plane (10-10) by hydride vapor phase epitaxy (HVPE) and the effect of Ga pretreatment on the nucleation characteristics of the GaN nanorods was investigated. Ga pretreatment significantly influenced on the density of GaN nanorods and in particular when the substrates were pretreated with Ga, the density of GaN nanorods notably decreased with increasing pretreatment duration. The density of GaN nanorods on Ga-pretreated sapphire substrates was also sensitively changed by varying V/III ratio, but this kind of behavior was not observed at all when the substrates were not Ga-pretreated.

**Kp-II-003****Photocurrent Spectroscopy of InAs/GaAs Quantum Dots Grown by MBE**조 현준, 김 정화, 이 정열<sup>1</sup>, 김 종수, 배 인호영남대학교 물리학과, <sup>1</sup>현풍고등학교

The properties of InAs/GaAs quantum dots grown by MBE were studied by photocurrent (PC) spectroscopy at low temperature. Two signals around 1.2 and 1.5 eV were related to quantum dots and GaAs epilayers, respectively. The results of PC spectra were presented differently with electrode connection direction. These results were caused by interaction between Schottky barrier and electric potential by amperemeter. The bias voltage dependences were investigated. Due to barrier effects, PC spectra were shown differently with direction of electric field. The temperature dependences were also investigated. With increasing temperature the current direction was changed from 120 K because of thermal effects.

**Kp-II-004****Contactless Electoreflectance Spectroscopy of  $\text{In}_{0.5}(\text{Ga}_{1-x}\text{Al}_x)_{0.5}\text{P}/\text{GaAs}$  Double****Heterostructure**

김 정화, 조 현준, 김 종수, 배 인호

영남대학교 물리학과

We have investigated the contactless electoreflectance(CER) properties of  $\text{In}_{0.5}(\text{Ga}_{1-x}\text{Al}_x)_{0.5}\text{P}/\text{GaAs}$  double heterostructure grown by metal-organic chemical vapour deposition(MOCVD). The CER measurements on the sample were studied as a function of temperature and dc bias voltage. Four signals observed at room temperature are related to the GaAs,  $\text{In}_{0.5}\text{Ga}_{0.5}\text{P}$ ,  $\text{In}_{0.5}(\text{Ga}_{0.73}\text{Al}_{0.27})_{0.5}\text{P}$  and  $\text{In}_{0.5}(\text{Ga}_{0.5}\text{Al}_{0.5})_{0.5}\text{P}$  transitions, respectively. From the temperature dependence of CER spectrum, the Varshni coefficients and broadening parameters were determined and discussed. In addition we have also studied the variation of the CER line shapes as a function of dc bias voltage. The behavior of the CER intensity for the reverse bias is larger than that of the forward bias.

**Kp-II-005****Growth and fabrication of high performance 365nm ultraviolet light -emitting****diodes**

전 성란, 강 인기, 김 재범, 강 성구, 한 재광, 이 상헌, 김 종섭, 손 성진<sup>1</sup>

*한국광기술원, LED 융합기술팀, <sup>1</sup>LG이노텍, Epi 개발 그룹.*

AlGaIn 물질에 의한 자외선 발광소자는 반도체조명, 수지경화, 바이오/의료 및 살균, 공기정화 등 다양한 분야에 사용된다. 이러한 분야에 응용하기 위해서는 고출력의 자외선(Ultraviolet: UV) LED가 필요하다. UV LED는 AlGaIn 박막 내의 많은 Al 조성비에 의한 결함준위 형성에 의해 고품위의 박막을 얻기가 어려워 고출력의 UV LED를 얻기가 힘들다. 더불어 UVLED 소자의 효율은 고품위 AlGaIn 박막 뿐만 아니라 패키지 재료 및 UV LED 용 봉지재 등에 의한 효율 문제도 대두되고 있다. 본 연구에서는 365nm 영역의 발광파장을 갖는 고출력 UV LED 제작을 위하여 먼저 사원계 AlGaInN 박막 성장조건을 최적화하여 결함밀도가 낮은 활성층을 성장함으로써 내부양자효율을 증가시켰다. InGaIn 박막에 Al 유량 변화에 따른 표면 특성 및 광학적 특성연구를 실시하였으며, GaN와 격자정합을 이룬 AlGaInN 박막 성장조건을 얻었다. 이와 함께 UV LED의 패키지 효율을 증가시키기 위하여 Si 봉지재의 특성에 따른 연구와 패키지 종류에 따른 광 추출 효율을 연구하였다. 사원계 AlGaInN/InGaIn MQWs를 이용하여 500x500mm<sup>2</sup> 크기의 UV LED 소자를 제작하고 Dome lens 패키지를 사용한 결과 100mA 인가 전류에서 10mW의 광출력을 얻었으며 주입전류를 500mA 증가할 때까지 출력 저하 없이 광출력이 증가함을 알 수 있었다.

**Kp-II-006****드레인 영역의 field plate 형성에 의한 누설전류 억제 효과에 관한 연구**

양 전욱, 홍 성기, 김 정진

*전북대학교 반도체과학기술학과.*

GaN HEMT는 AlGaIn/GaN 이종접합 구조에서 발생 하는 높은 전자 밀도 및 빠른 전자 이동도를 가지는 2차원전자가스층을 채널로 이용하는 소자이다. GaN HEMT 소자에서 게이트와 드레인 영역 표면상태의 문제는 전하 트랩이나 불순물 등에 기인한 누설전류 성분을 유발 할 수 있기 때문에 이러한 누설 전류 성분을 억제하는 공정이 필요하다. 본 연구는 드레인 영역에 field plate를 형성하여 AlGaIn/GaN HEMT 게이트와 드레인 영역 표면상태에 기인한 특성의 저하를 개선하도록 하였다. Field plate는 게이트와 드레인 사이의 표면에 증착된 SiN 위에 드레인 전극과 접촉하여 형성하였다. 제작된 트랜지스터의 임계전압과 트랜스컨덕턴스는 각각 -4V, 120mS/mm 내외의 값을 나타냈으며 드레인과 field plate에 인가된 바이어스는 표면의 트랩을 포획하여 특성의 변화를 억제하고 이차원전자층의 캐리어를 증가시켜 특성의 개선을 꾀하였다.

SEO Yong Gon, BAIK Kwang Hyeon<sup>1</sup>, OH Kyungwhan<sup>2</sup>, HWANG Sung-Min<sup>1</sup>

*KETI Green Energy Research Center, Department of Physics, Yonsei University. <sup>1</sup>KETI Green Energy Research Center. <sup>2</sup>Department of Physics, Yonsei University.*

Nonpolar GaN have attracted much attention due to their potential in eliminate undesirable electric field effects, thus leading to greater efficiency than conventional c-plane III- nitrides. As one of the promising candidates for nonpolar GaN devices, a-plane (11-20) GaN grown on r-plane (1-102) sapphire has been investigated.<sup>2-4</sup> However, it still suffers from a high density of threading dislocations (TDs) and stacking faults (SFs) due to the difficulty in finding optimum growth conditions for N-face and Ga-face in GaN. Bulk GaN substrates have been used to fabricate nonpolar/semipolar light emitting diodes (LEDs) to circumvent process difficulties for a-plane GaN growth on a r-plane sapphire. In this paper, we report on high crystalline a-plane (11-20) GaN epitaxial films directly grown on a r-plane (1-102) sapphire substrate and the electroluminescence properties of nonpolar a-plane InGaN/GaN LEDs subsequently regrown on an a-plane (11-20) GaN template.

**Ga<sub>1-x</sub>Mn<sub>x</sub>As Films**

LEE Sangyeop, KIM Shinhee, KIM Yungjun, LEE Hakjoon, KHYM .S, LEE Sanghoon, LIU .X<sup>1</sup>, FURDYNA .J. K<sup>1</sup>

*Physics Department, Korea University, Seoul, Korea. <sup>1</sup>Physics Department, University of Notre Dame, Notre Dame, IN 46556, USA.*

The domain pinning fields of ferromagnetic Ga<sub>1-x</sub>Mn<sub>x</sub>As films was investigated by using the planar Hall effect (PHE). A series of Ga<sub>1-x</sub>Mn<sub>x</sub>As layers were grown on (001) GaAs substrates with molecular beam epitaxy (MBE). The magnetic anisotropy, which determines magnetic easy axes, in the GaMnAs film contains both cubic and uniaxial anisotropies. Since the cubic anisotropy is dominant at low temperature in GaMnAs, the effect of uniaxial anisotropy is normally ignored in the calculation of domain pinning field. However, the uniaxial anisotropy becomes increasingly important as the carrier concentration or Mn composition in the GaMnAs film increases. In this study, we have focused on the Influence of uniaxial anisotropy on the domain pinning fields in ferromagnetic Ga<sub>1-x</sub>Mn<sub>x</sub>As films. The values of domain pinning fields were obtained from the angle dependence of the PHE. In the calculation, we have include uniaxial anisotropy by considering deviation angle of magnetic easy axes from the <100> direction given as  $\delta = 1/2 \sin^{-1}(K_u/K_c)$ , where  $K_c$  and  $K_u$  are cubic and uniaxial anisotropy constants. The results show a systematic increase (decrease) of domain pinning fields for crossing uniaxial hard (easy) direction as the deviation angle increases.

**Kp-II-009****Mapping of magnetic anisotropy in strained ferromagnetic semiconductor****GaMnAs films**

KIM shinhee, SHIN jinsik, YOO taehee, KIM yungjun, KHYM .S, LEE sanghoon, LIU .X<sup>1</sup>, FURDYNA .J.K<sup>1</sup>

Physics Department, Korea University, Seoul Korea. <sup>1</sup>Department of physics, University of Notre Dame, Notre Dame, IN 46556, USA.

The effect of strain on the magnetic anisotropy of GaMnAs films has been investigated by Hall effect measurements. To introduce different strain on the GaMnAs film, GaInAs buffer layer was grown on (001) GaAs substrate prior to deposit GaMnAs layer. The magnitude of the tensile strain, which cause out-of-plane magnetic easy axis, was controlled by adjusting In composition in the GaInAs buffer layer. Both in-plane and out-of-plane components of magnetic anisotropy was obtained from the angular dependence of the planar Hall resistance (PHR) and the anomalous Hall resistance (AHR), respectively [1]. The obtained anisotropy constants allow us to construct three-dimensional (3-D) magnetic free energy surface [2]. All sample shows 6 energy minima along the <100> crystallographic directions. However, the depth of the minima along [001] direction (i.e., out-of-plane) systematically increases as the value of tensile strain increases in GaMnAs film. The result, therefore, indicates that strain is a crucial parameter in determining the direction of magnetic easy axis either in-plane or out-of-plane in the GaMnAs films. [1] Hyunji Son, Sun-jae Chung, Sun-young Yea, Sanghoon Lee, X. Liu, and J. K. Furdyna, J. Appl. Phys. 103, 07F313 (2008)[2] X. Liu, W. L. Lim, L. V. Titova, M. Dobrowolska, J.K. Furdyna, M. Kutrowski, and T. Wojtowicz, J. Appl. Phys. 98, 063904(2005)

**Kp-II-010****InAs/GaSb 응력초격자의 계면층 분석 및 적외선검출소자의 특성 연구**

김 준오, 신 현욱, 최 정우, 이 상준<sup>1</sup>, 김 창수<sup>1</sup>, 노 삼규<sup>1</sup>

경희대학교 물리학과. <sup>1</sup>한국표준과학연구원 나노소재측정센터.

최근 부준위간 천이에 의한 제2형 응력초격자 (strained-layer superlattice, SLS)는 종파장과 장파장 영역에서 상온 동작 적외선 검출소자를 실현시킬 수 있는 구조로 그 관심이 증가하고 있다. 그러나 [InAs/GaSb]-SLS 계면에 존재하는 InSb-like 또는 GaAs-like 계면층은 SLIP 효율을 감소시키는 원인이 될 수 있다. 본 연구에서는, InAs/GaSb 두께를 [4/4]-ML에서 [21/8]-ML까지 변화시킨 50 주기 SLS 구조의 계면층을 분석하기 위하여 고분해능 X선회절 (x-ray diffraction, XRD)과 TEM을 이용하였다. 고분해능 XRD 결과 InAs 두께 증가에 따라 압축변형에서 인장변형으로 변화함을 보여주었고, XRD Simulation 결과 InAs/GaSb 계면에 약 1.4 ML의 InSb-like 계면층이 존재함을 확인하였다. XRD 역격자분포 (RSM)에서 SLS의 위성픽과 GaSb 기관픽이 동일한 X축 선상 관측되었는데, 이는 SLS와 GaSb 기관이 수평방향으로는 coherent하나 수직방향(성장방향)으로 응력을 받고 있음을 의미하는 것이다. XRD 결과와 비교하기 위하여 세 종류의 시료 [8/8], [15/8], [21/8]의 단면 TEM을 측정하였다. [8/8]-ML 시료의 경우 InAs/GaSb 계면에는 1-2 ML의 InSb-like 계면층이 존재함을 확인 하였으며, 이는 XRD 결과와도 잘 일치하는 것이다. InAs 두께 증가에 따른 계면층 변화를 분석을 위하여 [15/8], [21/8]-ML의 시료도 단면 TEM 사진을 통한 분석을 수행하고 있다. [8/8]-ML SLS의 천이 에너지는 약 300meV (4um) 로 보고되어 지고 있는데, InAs 두께 변화와 계면층 형성으로 인한 응력의 변화에 따른 천이 에너지 변화를 관찰하기 위하여 InSb detector [1-5um]를 이용한 Photoluminescence (PL) 측정과 Fourier-transformed infrared(FTIR) spectrometer 측정을 진행중이다. InAs/GaSb-SLS를 활성층으로 사용하는 150주기의 [8/8]-ML SLIP 시험소자를 제작하여 그 특성을 평가하였는데, 차단파장 (cutoff wavelength)과 최대 반응을 보이는 3.25 um에서 검출률 (detectivity)은 각각  $\lambda CO \sim 5 \mu m$ 와  $D^* \sim 109 \text{ cm.Hz}^{1/2}/W$  (13 K)이었다.

**Kp-II-011****Reciprocal Space Mapping in Grazing Incidence Geometry to Investigate Preferred Growth Directions of GaN Nanorods Non-catalytically Grown on Si Substrates**이 상화, 손 유리, 김 진교, 이 동렬<sup>1</sup>, 이 현휘<sup>2</sup>경희대학교, 물리학과. <sup>1</sup> 숭실대학교, 물리학과. <sup>2</sup> 포항공대, 방사광 가속기 연구소.

GaN nanorods were grown on Si(111) substrates by using hydride vapor phase epitaxy, and the crystallographic characteristics associated with their preferred growth directions were investigated by utilizing synchrotron x-ray reciprocal space mapping in a grazing incidence geometry and scanning electron microscopy. Crystallographic analysis reveals that the nanorods containing both wurtzite and zinc blende phase tend to have narrower distribution of the preferred growth directions than those containing only wurtzite phase. This tendency is partly attributed to the subtle interplay between polytypism and the preferred growth directions of GaN nanorods.

**Kp-II-012****GaAs/AlGaAs 양자점에서 Franz-Keldysh oscillation 연구**이 창호, 최 은미, 오 민우, 배 주희, 조 현준, 김 정화, 배 인호, 김 종수, 송 진동<sup>1</sup>, 이 상준<sup>2</sup>, 노 삼규<sup>2</sup>, 김 진수<sup>3</sup>, 임 재영<sup>4</sup>, 강 훈수<sup>5</sup>, 정 문석<sup>5</sup>영남대학교 물리학과. <sup>1</sup> 한국과학기술연구원. <sup>2</sup> 한국표준과학연구원. <sup>3</sup> 전북대학교 신소재공학부. <sup>4</sup> 인제대학교 나노공학부. <sup>5</sup> 광주과학기술원 고등광기술연구소.

본 연구에서는 GaAs/AlGaAs 양자점에 의한 표면전기장의 효과를 Photoreflectance (PR) 방법을 이용하여 관측하였다. 시료의 전기장에 의한 Franz-Keldysh oscillation (FKO)의 변화를 관측하여 GaAs/AlGaAs 양자점의 존재에 의한 시료의 전기장을 측정하였다. 또한 시료에 형성된 전기장의 세기를 계산하기 위해 PR 신호로부터 fast Fourier transformation (FFT)을 이용하였다. FFT로부터 주파수 영역에서 두개의 주기를 확인하였으며 이는 각각 heavy-hole (HH)과 light-hole (LH) 과 관련된 것으로 해석 하였다. 특히 온도의 존성 실험을 통하여 내부전기장의 변화를 관측 하였으며 양자구속효과와 관련성에 대하여 고찰 하였다. 이 결과는 InAs/GaAs 양자점에서의 기존 결과와 비교 분석하였다.

**Kp-III-013****AgGaSe<sub>2</sub>와 AgGaSe<sub>2</sub>:Co<sub>2+</sub> 박막의 광유기 방전특성**

이 정주, 이 종덕, 박 창영, 김 동인, 김 건호

경상대학교 물리학과

진공증착 법으로 ITO(indium tin oxide) 기판 위에 AgGaSe<sub>2</sub>와 AgGaSe<sub>2</sub>:Co<sub>2+</sub>박막을 성장시켜 그 구조와 광유기 방전특성(PIDC)을 조사하였다. X-선 회절분석에 의하여 구해진  $a=5.979 \text{ \AA}$ 와  $c=10.808 \text{ \AA}$ 를 가지는 황동광(chalcopyrite) 구조를 하고 있었으며, 그 성장 방향은 (112) 방향으로 선택 성장됨을 알 수 있었다. 광흡수 측정으로부터 300 K에서 에너지 띠 간격은 1.82 eV로 주어졌다. 또한 열린회로로 구성되어 있는 시료의 표면에 광 펄스를 주입하여 표면에서 형성된 전하들의 거동을 광유기 방전특성 방법을 이용하여 조사하였다. 초기전위  $V_0$ 로 형성된 시료의 양단을 주행하는 운반자 농도, 전류밀도 및 전기장 효과를 관찰하여 운반자의 주행시간과 이동도를 구하였다. 계산된 이동도의 값은  $6 \times 10^{-3} \text{ cm}^2/\text{Vs}$ 이고 운반자 농도는  $\sim 1024/\text{cm}^3$  이었다. 또한 다수 운반자는 양공(hole)이었다.

**Kp-III-014****고온 동작 양자점 제작**엄 영제, 정 윤철, 김 남<sup>1</sup>부산대학교 물리학과, <sup>1</sup>한국표준과학연구원

기존의 GaAs/AlGaAs 이종접합구조에 금속게이트를 증착하여 제작하는 평면형 양자소자의 경우 다양한 양자소자를 자유자제로 만들 수 있다는 장점에도 불구하고 1K이상의 온도에서는 양자현상을 관측하기 힘들기 때문에 실용성이 떨어진다. 평면형 양자소자의 경우 금속 게이트들이 웨이퍼 표면에 있는 반면, 이차원전자계는 웨이퍼 표면으로부터 약 100nm정도 밑에 존재하게 된다. 금속게이트를 이용하여 이차원전자계에 양자구조를 형성시키는 경우, 양자구조 내부의 에너지 간격이 너무 작기 때문이다. 본 연구에서는 mesa etching 방법을 이용, 내부의 에너지 간격이 일반적인 양자점보다 매우 큰 양자점을 제작하였으며 stability diagram 측정을 통해 양자점의 charging energy와 양자점 내부의 에너지 간격을 측정하였다. 기존의 양자점은 동작 온도가 수십 mK 이하이기 때문에 실용적으로 사용하기는 매우 어려웠으나 이번 실험을 통해 양자점의 동작 온도를 4.2K (액체 헬륨 환경) 까지 끌어올려 실용적으로 사용될 가능성을 보여 주었다.



**Kp-III-015****Investigation of Photoluminescence spectrum in  $\text{CdGa}_2\text{Se}_4$  layers**

HONG Kwangjoon

Department of Physics Chosun University.

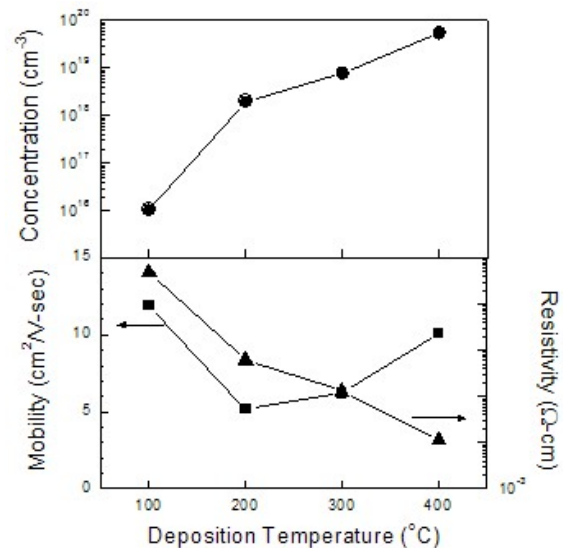
From typical PL spectrum of the  $\text{CdGa}_2\text{Se}_4$  layer measured at 10 K, the two peaks on the shoulder appear at 474.5 (2.6130 eV) and 475.6 nm (2.6069 eV) toward the shorter-wavelength region. These peaks are associated with the free exciton,  $E_x$ . Also, the 474.5- and 475.6-nm peaks represents the light-hole exciton,  $E_x^{\text{lh}}$ , and the heavy-hole exciton,  $E_x^{\text{hh}}$ , respectively. The splitting energy between the  $E_x^{\text{lh}}$  and the  $E_x^{\text{hh}}$  was 6.1 meV. This splitting is known to be caused by the strain due to the lattice mismatch between the substrate and epilayer in the heteroepilayer growth.

**Kp-III-016****증착 온도에 따른  $\text{In}_2\text{O}_3$  박막의 특성 분석**

조 신희

신라대학교 전자재료공학과.

$\text{In}_2\text{O}_3$ 는 상온에서 3.6 eV의 직접 전이 밴드갭 에너지를 갖는 n-type 반도체로서, 태양전지, 전계발광 디스플레이, 리튬이온전지, 바이오센서, 광전자 소자 영역에 응용될 수 있다. 본 연구에서는 박막 증착 변수로 증착 온도 (100°C, 200°C, 300°C, 400°C)를 선택하여 RF-마그네트론 스퍼터링 방법으로 유리 기판 위에  $\text{In}_2\text{O}_3$  박막을 성장시켰다. 전기적 특성 결과는 그림에서 보듯이, 100°C에서 증착한 박막의 경우에 전하 운반자의 농도는  $1.1 \times 10^{16} \text{ cm}^{-3}$ , 홀 이동도는  $12 \text{ cm}^2/\text{Vsec}$ , 비저항값은  $4.9 \times 10^1 \Omega\text{cm}$ 이었다. 증착 온도가 증가함에 따라 박막의 비저항값은 감소하였으나, 전하 운반자의 농도와 홀 이동도는 전반적으로 증가하는 경향을 보였다. 증착 온도의 변화에 따른 박막의 결정성, 광학적 특성, 밴드갭 에너지의 변화가 중점적으로 논의된다.



P3

포스터세션

**Kp-III-017****4세대 이상 대면적 유기박막 증착을 위한 선형 증착원의 유동 해석**최 범호, 이 종호<sup>1</sup>, 양 영수<sup>2</sup>한국생산기술연구원 호남권기술지원본부 나노기술집적센터. <sup>1</sup> 한국생산기술연구원 호남권기술지원본부 광응용부품지원센터. <sup>2</sup> 전남대학교 기계공학과.

본 연구에서는 4세대 이상 (730×920mm<sup>2</sup>) 대면적 기관 상에 균일하고 안정적인 유기 박막을 증착하기 위한 선형 증착원의 유동 해석을 수행하였다. 대면적 기관 상에 균일한 유기 박막을 증착하기 위해 선형 증착원의 핵심 부품인 노즐의 크기 및 직경, 그리고 노즐 사이의 간격을 수치 해석 프로그램인 Fluent를 이용하여 해석하였다. 선형 증착원에서 기화되어 챔버로 분출되는 유기물 기체의 속도 분포, 온도 균일도, 압력 분포 등을 계산함으로써 최적의 선형 증착원 설계에 적용하였다. 균일한 유기 박막을 얻기 위해서는 노즐의 간격을 일정하게 유지한 상태에서 중앙에서 가장 자리로 갈수록 노즐의 크기가 커져야 함을 확인할 수 있었다. 증착된 박막의 균일도는 5% 이내로서 수치 해석 결과와 거의 일치함을 확인 할 수 있었고, 수치 해석 결과가 실제 유기 증착기에 적용 가능함을 제시하는 결과이다.

**Kp-III-018****Progress study for the large scale production of single-walled carbon nanotube****field effect transistors**

PARK Serin, KWAK Jun-Hyuk, JEON Eun-Kyoung, PARK Dong-Won, LO Young-Seop, SO Hye-Mi, LEE Jeong-O, CHANG Hyun-Ju

*Korea Research Institute of Chemical Technology.*

Carbon nanotubes (CNTs) have been extensively studied for some years. Among various applications of CNTs, electronic sensors based on single-walled carbon nanotubes (SWNT) are particularly exiting, since SWNTs have an unusual sensibility for chemical and biological interactions at the surface because all carbon atoms are exposed to the surface. For electronic sensor applications of SWNT, one needs high performance semiconducting SWNTs to improve sensitivity. In our group, we demonstrated various chemical and biological sensors that were fabricated using SWNTs grown in an 1 inch furnace. However, for practical applications and mass production of SWNT-based sensors, it is essential to develop large scale growth process. Under the ultimate goal of large-scale, chirality controlled growth of SWNTs, we performed patterned SWNT growth on full 4 inch wafers. Liquid catalyst that contains Fe/Mo was spun over the PMMA-patterned substrate, and growth was carried out in a 6 inch furnace using CH<sub>4</sub> as a carbon feedstock. To obtain optimum growth conditions, we performed computational fluid dynamics (CFD) simulations as well. Using the optimized parameters from CFD, inlet port of the carbon feedstock was reconstructed, as well as the growth parameters. While SWNT yields before CFD optimization is 34 %, we got 96.4 % yield (1388/1440 Transistor in 4" wafer) after optimization. Details regarding growth; catalyst deposition, feedstock effect will be discussed in detail.

**Kp-III-019****Analysis of carrier dynamics in MOS structure with  $\text{TiSi}_2$  nanocrystals by using****capacitance and current transient measurements**

KIM Jin Soak, LEE Dong Uk, HAN Seung Jong, KIM Eun Kyu

*Department of Physics and Quantum-Function Spinics Laboratory, Hanyang University, Seoul 133-791, Korea.*

A nanocrystal system as carrier charging nodes is one of the most proper candidates for nonvolatile memory device. Thus, many research groups have developed a good memory device by using the nanocrystals. However, the exact mechanisms such as origins of carrier trapping site and carrier dynamics in the devices were not clearly revealed. In this study, the carrier dynamics in metal-oxide-semiconductor (MOS) structure with  $\text{TiSi}_2$  nanocrystals were investigated by using capacitance and current transient measurements. The  $\text{TiSi}_2$  nanocrystal MOS was fabricated on *p*-type Si (100) wafers. Several kinds of tunnel layers, such as  $\text{SiO}_2$ ,  $\text{SiO}_2/\text{Si}_3\text{N}_4$ , and  $\text{SiO}_2/\text{Si}_3\text{N}_4/\text{SiO}_2$  were fabricated on Si substrates. And then, the 5-nm thick  $\text{TiSi}_2$  layer and the 30-nm thick  $\text{SiO}_2$  control layer were deposited on the multi-stack tunnel layer by using magnetron sputtering. The single layered  $\text{TiSi}_2$  nanocrystals were created between the  $\text{SiO}_2$  control layer and tunnel layer after post-thermal annealing at 800 °C for 2 min. The aluminum gate electrode was evaporated by using thermal evaporator. The carrier charging and discharging were clearly observed by long time capacitance transient. Moreover, several kinds of defects in the *p*-Si substrates were also found.

**Kp-III-020****Tungsten Dual-Poly Gate Technology for High Speed and Low Power Application****in DRAM Devices**Y.S. KIM, M.G. SUNG<sup>1</sup>, K.Y. LIM<sup>2</sup>, J.C. KU<sup>1</sup>, S.G. PARK<sup>1</sup>*Dep. of Physics, Univ. of Ulsan. <sup>1</sup>R&D Div., Hynix Semiconductor. <sup>2</sup>FEP group, SEMATEC.*

In this report, we present different effects of WSix or Ti inserted gate as a diffusion barrier metal on various characteristics in tungsten dual poly gate for DRAM application. Each gate stack shows different behavior in terms of gate interfacial resistance, gate oxide reliability, and gate sheet resistance. The WSix/WN barrier shows higher gate  $R_c$  and worse gate oxide reliability characteristics, compared to those of the Ti/WN barrier. It is due to the B-N interaction at the interface during post annealing process. However, by applying gate electrode deposited by PVD methods, the Ti/WN barrier shows higher  $R_s$  than that of the WSix/WN, due to polycrystalline growth of the WN. Optimized gate stacks with CVD-W based Ti/WN barrier is evaluated, which is applicable for high speed application in DRAM devices.

**Kp-III-021****Effect of Nb and Al doping on resistance switching properties of amorphous TiO<sub>2</sub>****for nonvolatile memory device**

나 희도, 김 종기, 손 현철

연세대학교, 신소재 공학과.

In this work, we investigated the effect of Nb and Al doping on the resistance switching behavior of TiO<sub>2</sub> films. We expected that the Nb and Al-doping produced oxygen vacancies and metal vacancies respectively because Nb has high valence state and Al has low valence state compared to Ti in TiO<sub>2</sub>. Also, physical properties such as atomic density and chemical bonding states of TiO<sub>2</sub> were characterized in addition to the resistance switching characteristics. Even though Nb doping into TiO<sub>2</sub> produced the lower resistance value of high resistance states (HRS), Al doping into TiO<sub>2</sub> produced the higher resistance value of compared to the un-doped TiO<sub>2</sub> films with the larger memory window. Nb and Al doping improved the resistance switching endurance with the narrower distribution of R<sub>off</sub> states. Depth profiles of chemical composition and chemical bonding states in the deposited films were investigated by XPS. Nb and Al-doping into TiO<sub>2</sub> films produced higher and lower density of metallic Ti (Ti<sup>0</sup>) than that of undoped TiO<sub>2</sub> film, respectively. This work demonstrated that the resistive switching behavior of TiO<sub>2</sub> can be enhanced by doping TiO<sub>2</sub> with Nb and Al of different oxidation valence.

**Kp-III-022****ArF 엑시머레이저를 사용한 가스센싱용 ZnO 박막의 제작 및 특성 측정**

오 철민, 배 가람, 나 용운, 정 태봉, 김 진영, 강 준희

인천대학교.

ArF 엑시머 레이저를 사용한 Pulsed Laser Deposition 기법으로 SiC 기판 위에 ZnO 박막을 증착하여 가스 센싱용 반조체를 제작하였다. ZnO는 안정된 여기자와 3.37eV의 넓은 bandgap을 가지며 600°C의 높은 온도에서도 작동이 가능하다는 장점을 갖고 있다. SiC 기판은 C side에 백금 코팅을 하여 ZnO 박막의 증착 후 Schottky junction이 형성될 수 있도록 하였다. 박막의 균일성을 개선하기 위해 기판을 300rpm으로 회전시키며 박막을 증착하였으며 증착시 기판의 표면온도를 300°C로 유지하였다. 193nm의 파장을 가지는 ArF 레이저의 펄스는 5Hz 주기와 230mJ/pulse의 에너지를 갖도록 하였다. 제작된 박막은 XRD와 SEM을 이용하여 분석하였으며 제작된 ZnO 박막의 박막표면 granularity는 약 1500 grains/mm<sup>2</sup> 밀도로 나타났으며 박막의 두께는 100~150nm정도를 얻었다. 제작된 박막의 비저항은 약 .3 Ω·cm로 측정되었다. ZnO 박막의 성장방향은 기판의 표면구조에 따라 결정되므로 기판의 Si side에 박막을 증착하였으며, 레이저 파워와 타겟과 기판사이의 거리에 따라 박막 표면의 상태를 변화시킬 수 있었다. 가스센서로서의 특성파악을 위해 수소와 프로판 가스를 사용하고 가스농도와 박막의 표면 온도를 변화하여 I-V 특성을 조사/분석하였다.

**Kp-III-023****루테늄계 염료를 이용한 태양전지의 제작과 특성 비교**

김 성준, 김 영호, 노 삼규<sup>1</sup>, 이 현용<sup>2</sup>

과학기술연합대학원대학교(UST), 나노전자소자공학. <sup>1</sup>한국표준과학연구원, 나노소재측정센터. <sup>2</sup>영지대학교, 전기공학과.

염료감응 태양전지 (dye-sensitized solar cell, DSSC)는 기존의 Si 기반 태양전지보다 경제성과 활용성이 우수하여 최근 그 연구개발이 활발하게 진행되고 있다. 본 연구에서는 루테늄계 (ruthenium, Ru) 광감응염료를 사용하여 DSSC 시험소자를 제작하고, 탄소 (carbon)과 백금 (Pt)의 2종류 부전극 (counter-electrode)에 대한 특성을 비교하였다. 광전극은 다공질의  $\text{TiO}_2$  나노결정을 이용하였으며, 염료는 N719 (Ru 535-bis TBA)와 N3 (Ru 535)를 사용하였다. 부전극은 전해질을 환원할 수 있는 촉매제 역할을 하는 Pt이 주로 이용되고 있는데, 이것은 광전극으로부터 탈착된 염료분자가 백금표면에 흡착하여 산화-환원 쌍의 재생을 방해하는 단점을 가지고 있다. 그러므로 촉매특성이 우수한 Pt를 대체할 수 있는 새로운 부전극 물질로서 탄소가 후보물질로 논의되고 있다. 본 연구에는 Platisol (Solaronix)을 이용한 Pt과 활성탄소/카본블랙을 혼합하여 CMC로 접착하여 제작한 탄소를 부전극으로 사용한 DSSC cell을 시험 제작하여 그 특성과 광전변환 효율을 비교 분석하였다. 탄소전극을 사용한 cell의 광전변환효율은 1.2%로 Pt 전극의 2.1% 보다 낮은 값을 나타내었는데, 탄소전극 제조과정이 최적화되지 않아 전극의 전기저항이 높았기 때문으로 추정되어 전기적 특성 비교 분석을 수행하고 있다. 탄소전극이 실용소자에 적용되기 위해서는 활성탄소와 카본블랙의 혼합율 최적화를 통하여 전극 저항을 최소화시키는 연구가 선행되어야 할 것으로 사료된다.

**Kp-III-024****Effect of heat-treatment for  $\text{ZnIn}_2\text{Se}_4$  layers**

HONG Kwangjoon, KIM Haejeong

Department of Physics Chosun University.

Single crystalline  $\text{ZnIn}_2\text{Se}_4$  layers were grown on thoroughly etched semi-insulating GaAs(100) substrate at 400°C with hot wall epitaxy (HWE) system by evaporating  $\text{ZnIn}_2\text{Se}_4$  source at 630°C. After the as-grown  $\text{ZnIn}_2\text{Se}_4$  single crystalline thin films was annealed in Zn-, Se-, and In-atmospheres, the origin of point defects of  $\text{ZnIn}_2\text{Se}_4$  single crystalline thin films has been investigated by the photoluminescence(PL) at 10 K.

**Kp-III-025****Optical absorption properties of the photoconductive AgGaSe<sub>2</sub> layers grown by****hot wall epitaxy**

YOU Sangha, HONG Kwangjoon

*Department of Physics Chosun University.*

The photoconductive AgGaSe<sub>2</sub> (AGS) layers were grown by the hot wall epitaxy method. The AGS layer was confirmed to be the epitaxially grown layer along the <112> direction onto the GaAs (100) substrate. Silver gallium diselenide (AgGaSe<sub>2</sub>, AGS), which crystallizes to the chalcopyrite structure, has received considerable attention in recent years because of its high optical absorption. The band gap at each temperatures obtained by PC measurement is nearly equivalent to that measured by optical absorption. The band-gap variation as a function of temperature on AGS was well fitted by  $E_g(T) = 1.9501 - 8.37 \times 10^{-4}T^2/(T + 224)$ . The band-gap energy of AGS obtained at 293 K was determined to be 1.8111 eV through the PC experiment and optical absorption.

**Kp-III-027****진공증착법에 의해 제작된 AgInSe<sub>2</sub>와 AgInSe<sub>2</sub>:Co<sup>2+</sup> 박막의 구조 및 광학적 특****성**

이 정주, 이 종덕, 박 창영, 성 병훈, 김 건호

*경상대학교 물리학과.*

진공증착 법으로 ITO(indium tin oxide) 기판 위에 AgInSe<sub>2</sub>와 AgInSe<sub>2</sub>:Co<sup>2+</sup>박막을 성장시켜 그 구조와 광학적 특성을 조사하였다. X-선 회절 분석에 의하여 구해진  $a=6.102 \text{ \AA}$ 와  $c=11.69 \text{ \AA}$ 을 가지는 황동광(chalcopyrite) 구조를 하고 있었으며, 그 성장 방향은 (112) 방향으로 선택 성장됨을 알 수 있었다. 증착된 박막과 열처리한 박막에 대하여 실온에서 측정한 광학적인 에너지 띠 간격은 1.76 eV에서 1.91 eV까지 변화하였다. 또한 열린회로로 구성되어 있는 시료의 표면에 광 펄스를 주입하여 표면에서 형성된 전하들의 거동을 광유기 방전특성(PIDC) 방법을 이용하여 조사하였다. 초기전위  $V_0$ 로 형성된 시료의 양단을 주행하는 운반자 농도, 전류밀도 및 전기장 효과를 관찰하여 운반자의 주행시간과 이동도를 구하였다. 광유기 방전특성을 이용하여 분석한 결과 시료들의 운반자의 주행시간과 이동도는 각각  $8 \mu s \sim 40 \mu s$ 와  $7 \text{ cm}^2/\text{Vs} \sim 37 \text{ cm}^2/\text{Vs}$  이었다. 원자 힘 현미경실험으로 제곱평균 제곱근 거칠기와 입계크기를 조사하였으며, X-선 광전자 분광실험으로 원소들의 결합상태를 관찰하였다.

**Kp-III-028****Effects of leveler in Growth of Cu film by Electroplating method**

RHA Sa-Kyun, KANG Sung-Kyu

*Department of Materials Engineering, Hanbat National University.*

We researched the effect of a leveler on the growth of Cu thin film by electrochemical plating. Cu thin film were plated by electrochemical plating over Cu seed layer (Cu seed layer (20 nm) and Ti barrier (20 nm) were deposited onto an p-type Si (100) substrate by electron-beam evaporation). The electrolyte ( $\text{CuSO}_4 \cdot 5\text{H}_2\text{O}$ ,  $\text{H}_2\text{SO}_4$ , and HCl) and organic additives (Viaform Accelerator and Viaform Suppressor) were fixed. The addition-quantity of leveler was gradually changed from 0 mL/L to 3 mL/L. The surface Morphology and roughness were measured by FE-SEM and AFM. The film thickness was measured by  $\alpha$ -step. The presence of impurity in Cu thin film was estimated by XPS. The sheet resistance of Cu film was measured by four-point probe. The surface morphology of Cu thin film is rough (Leveler : 0 mL/L ), unless the leveler is added to Cu electroplating solution. However, the surface roughness of Cu film decreased abruptly by addition of leveller.

**Kp-III-029****Optical Characterization of  $\text{Cu}_2\text{ZnSnSe}_4$  grown by thermal co-evaporation**박 도영, 정 현식, 정 성훈<sup>1</sup>, 윤 재호<sup>1</sup>, 안 세진<sup>1</sup>, 곽 지혜<sup>1</sup>, 윤 경훈<sup>1</sup>*서강대학교 물리학과. <sup>1</sup>한국에너지기술연구원 태양전지연구단.*

$\text{CuInGaSe}_2$  (CIGS) is widely studied due to its promise as low-cost material for high-efficiency thin film solar cells. However, since indium and gallium are becoming scarce and expensive, high-efficiency and low cost solar cell absorber materials to replace CIGS such as quaternary  $\text{Cu}_2\text{ZnSnSe}_4$  (CZTSe) and  $\text{Cu}_2\text{ZnSnS}_4$  (CZTS) have been suggested. In previous years, the direct bandgap energy of CZTSe was suggested as being around 1.5eV, estimated from optical absorption data. However, recent theoretical analysis and photoluminescence measurements suggest it to be around 1.0eV. In this study, we investigated quaternary CZTSe by various optical spectroscopic techniques, including photoluminescence and contactless electroreflectance (CER). Since CER is a modulation technique, the critical points of a semiconductor is pronounced in CER spectra, which helps identify the bandgap energy. The photoluminescence spectra show a peak at around 1.0 eV, which is consistent with previous measurements. Photoluminescence results are compared with CER measurements.

P3

포  
스  
터  
세  
션

**Kp-III-030****Electrical properties and valence-band splitting energy from photocurrent response of photoconductive CdGa<sub>2</sub>Se<sub>4</sub> layers**

LEE Sangyoul, HONG Kwangjoon

*Department of Physics Chosun University.*

The photoconductive CdGa<sub>2</sub>Se<sub>4</sub> layer, which has the carrier density of  $8.27 \times 10^{17} \text{ cm}^{-3}$  and the Hall mobility of  $3.45 \times 10^2 \text{ cm}^2/\text{V s}$  at 293 K, was grown by using the HWE method. From the PC measurements, three peaks of A, B, and C were observed, indicating the intrinsic transitions from the valence-band states of  $\Gamma_6(\Gamma_7)(A)$ ,  $\Gamma_5(\Gamma_8)(B)$ , and  $\Gamma_6(\Gamma_7)(C)$  to the conduction band state of  $\Gamma_5(\Gamma_8)$ . The intensities of the PC spectra decreased with decreasing temperature. The valence-band splitting on CdGa<sub>2</sub>Se<sub>4</sub> was also observed using PC measurement. The  $\Delta_{\text{cr}}$  and  $\Delta_{\text{so}}$  were 0.1604 and 0.4179 eV at 10 K, respectively. By conducting the PC and absorption experiments, the band-gap energy on CdGa<sub>2</sub>Se<sub>4</sub> was extracted out.

**Kp-III-031****유기 박막 연속 증착이 가능한 유기물 자동 공급 장치 및 박막 증착**최 범호, 이 종호<sup>1</sup>, 유 하나, 임 용환

*한국생산기술연구원 호남권기술지원본부 나노기술집적센터. <sup>1</sup>한국생산기술연구원 호남권기술지원본부 광응용부품지원센터.*

최근 실리콘 반도체 이후를 대체할 수 있는 반도체 소자로서 유기반도체에 대한 많은 관심이 집중되고 있다. 유기반도체의 양산을 위해서는 공정 가능한 유기박막의 연속 증착 시간을 늘리는 기술이 가장 큰 화두로서 대두되었다. 이는 유기 반도체의 양산성 뿐 아니라 제조 단가를 낮출 수 있는 획기적인 기술이다. 본 연구에서는 288시간 이상 연속 증착이 가능한 유기물 자동 공급장치와 선형 증착원을 제작하여 특성을 평가하였다. 유기물 자동 공급장치는 진공 모터를 이용하여 교반시켜줌으로서 고체 분말 상태의 유기물의 뭉침 현상을 방지하였으며, 회전 수에 따른 유기물 자동 공급의 안정성 및 재현성을 평가하였다. 180RPM에서 자동 공급 재현성 3% 이내로서 가장 안정된 결과를 얻을 수 있었으며, 288시간 연속 동작 시간에서도 안정된 공급률을 얻을 수 있었다. 유기물 자동 공급 장치와 대면적용 선형 증착원을 이용한 유기 박막 증착 실험에서도 5% 이내의 균일한 박막 증착이 가능함을 확인 할 수 있었다. 본 연구에서 제작된 시스템은 유기박막트랜지스터, 유기발광다이오드 등의 유기 반도체 소자의 양산에 적용할 수 있을 것으로 본다.

**Kp-III-032****Resistance Switching Behavior of W-doped poly-crystalline NiO<sub>x</sub> with TiN and****Pt Electrodes**

김 종기, 나 희도, 손 현철

연세대학교, 신소재 공학과.

In this work, we investigated the effect of W doping on the resistance switching behavior of NiO<sub>x</sub> films. The W-doping is expected to produce cation-rich NiO<sub>x</sub> film because W has high valence state compared to Ni in NiO<sub>x</sub>. To measure resistance switching behavior, Pt/NiO<sub>x</sub>/Pt and TiN/NiO<sub>x</sub>/Pt MIM stacks were fabricated by reactive DC magnetron sputtering with various W doping contents in NiO<sub>x</sub>. Also, physical properties such as atomic density and chemical bonding states of NiO<sub>x</sub> were characterized in addition to the resistance switching characteristics. Increasing W doping into NiO<sub>x</sub> produced the higher resistance value of high resistance states (HRS) compared to the un-doped NiO<sub>x</sub> films with large memory window. Even though Pt/NiO<sub>x</sub> with W/Pt stacks showed a unipolar resistance switching behavior, TiN/NiO<sub>x</sub> with W/Pt stacks showed bipolar resistance switching. Depth profiles of chemical composition and chemical bonding states in the deposited films were investigated by XPS. W-doping into NiO<sub>x</sub> films produced higher density of metallic Ni (Ni<sup>0</sup>) than that of NiO<sub>x</sub> films deposited at the same conditions. This work demonstrated that the resistive switching behavior of NiO<sub>x</sub> can be enhanced by doping NiO<sub>x</sub> with W of different oxidation valence.

**Kp-III-033****Carrier tunneling through barrier engineered tunnel layer in metal-silicide nano-floating gate memory**LEE Dong Uk, SEO Ki Bong, HAN Seung Jong, KIM Seon Pil, KIM Eun Kyu, PARK Goon-Ho<sup>1</sup>, CHO Won-Ju<sup>1</sup>*Quantum-Function Spinics Laboratory and Department of Physics, Hanyang University. <sup>1</sup>Department of Electronic Materials Engineering, Kwangwoon University.*

The tunnel oxide thickness has a difficult problem to scale down for the improvement of endurance and charge retention properties of the non-volatile memory. Also, the nano-floating gate memory (NFGM) applications require the tunnel barrier to have relatively low applied voltage for long retention time and fast speed. The metal oxide semiconductor (MOS) structures with TiSi<sub>2</sub> and WSi<sub>2</sub> nanocrystals were fabricated on *p*-type and *n*<sup>+</sup>-type Si (100) wafers. The tunnel oxide layer of 4.5-nm-thickness was grown by thermal oxidation process at 1000 °C for 17 min. Also, the barrier engineered multi-stack tunnel layers of SiO<sub>2</sub>/Si<sub>3</sub>N<sub>4</sub>/SiO<sub>2</sub> (2nm/2nm/3nm), Si<sub>3</sub>N<sub>4</sub>/SiO<sub>2</sub>/Si<sub>3</sub>N<sub>4</sub>/ (2nm/3nm/3nm) and SiO<sub>2</sub>/Si<sub>3</sub>N<sub>4</sub> (2nm/3nm) were deposited on Si substrate. The electrical properties of devices were measured by using a HP-4156a semiconductor parameter analyzer, an Agilent 81104 A pulse pattern generator system and a liquid-nitrogen and helium cryostat (15 ~ 700 K). The metal-silicide nanocrystal memories with the multi-stacked tunnel layer were fabricated and their electrical properties were characterized as a function of temperature. It appeared that the dominant mechanism for carrier charging/discharging of the metal silicide nanocrystals in MOS structures with multi-stack tunnel layer is Fowler-Nordheim tunneling. We will discuss also the current and capacitance transient characteristics.

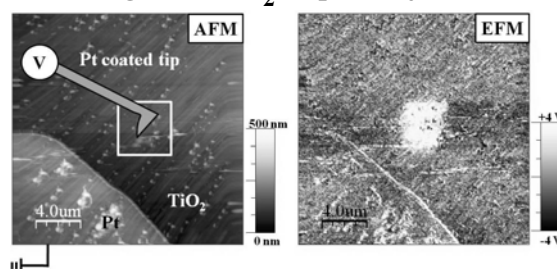
P3

포  
스  
터  
세  
션

**Kp-III-034****Nanoscopic characterization of electroforming of Pt/TiO<sub>2</sub>/Pt planar junctions**

김 해리, 박 수현, 정 인구, 김 동욱  
이화여자대학교, 물리학과.

Memristive behaviors of metal/oxide/metal structures have attracted great attention due to scientific interest and possible applications for non-volatile memory devices [Adv. Mater. 21, 2632 (2009)]. To investigate the detailed behaviors, we fabricated Pt/TiO<sub>2</sub>/Pt planar junctions with micron-sized gaps between electrodes. Symmetric transport properties were changed to asymmetric (rectifying) ones, after applying the voltage between Pt electrodes for several minutes ('electroforming'). Usually it is difficult to directly characterize the physical state at the interface, which is beneath the metal electrodes. Electrostatic force Microscopy (EFM) enables us to obtain charge distribution in local area and Pt-coated tips can be used as electrodes for the electroforming process. The EFM images showed that the charge modification was significantly affected by the bias voltage polarity. This result suggests that migration of ions, presumably oxygen vacancies, and resulting alteration of the junction properties should play key roles in the memristive behaviors of the Pt/TiO<sub>2</sub>/Pt junctions.

**Kp-III-035****WSi<sub>2</sub> Nanocrystal Memory with Crested Tunnel Barrier**

SEO Ki Bong, LEE Dong Uk, KIM Seon Pil, KIM Eun Kyu, YOU Hee Wook<sup>1</sup>, CHO Won Ju<sup>1</sup>

Hanyang University. <sup>1</sup>Kwangwoon University.

The trade-off between programming/erasing (P/E) speeds and charge retention characteristics is emerging problem of the nanocrystal memory devices with the conventional SiO<sub>2</sub> tunnel barrier. To overcome this problem, the crested tunnel barrier has been studied as a tunnel barrier of nonvolatile memory device. The crested barriers has a barrier height peaks in the middle of tunnel barrier. In crested barriers, the highest part of crested barrier (in the middle) is pulled down by the electric field very quickly. Therefore, the faster P/E speeds are achieved than single SiO<sub>2</sub> tunnel barrier. Moreover, the long retention time also can be achieved due to the thick physical thickness of crested tunnel barrier. In this study, we fabricated the WSi<sub>2</sub> nanocrystal memory with crested tunnel barrier. The crested tunnel barrier composed of Si<sub>3</sub>N<sub>4</sub>, SiO<sub>2</sub>, and Si<sub>3</sub>N<sub>4</sub> (NON) layer to achieve the fast P/E speed and long retention time, simultaneously. For the purpose of comparison, a control sample with the conventional SiO<sub>2</sub> tunnel barrier and the variable oxide thickness tunnel barrier composed of SiO<sub>2</sub>, Si<sub>3</sub>N<sub>4</sub>, and SiO<sub>2</sub> (ONO) layer were also prepared. Then, their electrical properties such as threshold voltage shift, P/E speeds, and retention time were evaluated. Through these electrical properties, the effects of crested tunnel barrier on the performance of WSi<sub>2</sub> nanocrystal memory devices were also discussed.

**Kp-III-036****Chemical Mechanical Polishing Characteristics Of Phase Change Memory In Alkaline Slurry With Hydrogen Peroxide**

KIM Chen-Lae, NA Sang-Bin, CUI Hao, CHO Jong-Young<sup>1</sup>, PARK Jin-Hyung<sup>2</sup>, PAIK Ungyu<sup>3</sup>, PARK Jea-Gun  
*Department of Electronics & Communication Engineering, Hanyang University.* <sup>1</sup>*Department of Nanoscale Semiconductor Engineering, Hanyang University.* <sup>2</sup>*Advanced Semiconductor Material & Device Development Center, Hanyang University.* <sup>3</sup>*Division of Advanced Materials Science Engineering, Hanyang University.*

The chemical mechanical polishing of crystalline phase change material  $\text{Ge}_2\text{Sb}_2\text{Te}_5$  (GST) was investigated in alkaline slurries with different alkaline agent with and without hydrogen peroxide addition. Comparing with other common alkaline agent, the polishing rate of the GST was highest in the TMAH based slurry, while that of the  $\text{SiO}_2$  remained at a relatively low level, resulting in a largest selectivity between the GST and  $\text{SiO}_2$ . To further increase the polishing rate of the GST, hydrogen peroxide was added in the TMAH and  $\text{NH}_4\text{OH}$  based slurry. It was found that the addition of hydrogen peroxide can considerably increases the polishing rate of the GST in the both slurry, while that of the  $\text{SiO}_2$  was not obviously changed. Thus, the high GST polishing rate and the high selectivity were obtained by the addition of hydrogen peroxide to the alkaline slurry. The surface characteristics of the GST in the TMAH and  $\text{NH}_4\text{OH}$  based slurries were totally different. Without hydrogen peroxide, the GST in the TMAH based slurry showed a more aggressive grain boundary etching effect. With hydrogen peroxide, however, more severe pit corrosion was found in the  $\text{NH}_4\text{OH}$  based slurry. The surface stoichiometric of the GST was analyzed by energy-dispersive x-ray microscopy after dipping in the slurries.

**Kp-III-037****Properties of Copper Oxide Thin Films Prepared by Atomic Layer Deposition**

LEE Byung Kook, KIM Seok Hwan, MIN Jae Ki, LEE Sun Sook, CHUNG Taek-Mo, KIM Chang Gyoun,  
 HWANG Jin Ha<sup>1</sup>, AN Ki-Seok

*Device Materials Research Center, Korea Research Institute of Chemical Technology.* <sup>1</sup>*Department of Material Science and Engineering, Hongik University, Seoul, Korea.*

Recently, p-type metal oxide semiconductors have been widely investigated for p-channel thin film transistors. Generally, copper oxide thin films, exiting  $\text{CuO}$  and  $\text{Cu}_2\text{O}$ , have p-type conductivity that they have possible application for p-channel layer of TFTs and p-n junction devices. Besides, theses materials have some advantages such as low production cost and non-toxic. In this study, copper oxide thin films are prepared using Cu (II) aminoalkoxide precursor  $\text{Cu}(\text{dmamb})_2$  [dmamb = 1 - dimethylamino - 2 - methyl - 2 - butanolate  $\text{OC}(\text{Me})(\text{Et})\text{CH}_2\text{NMe}_2$ ] with oxygen plasma, as oxygen sources by ALD and investigated for possibility of p-channel TFTs application as a p-type semiconductor. The self-limiting ALD process was estimated by thickness of the films measured as function of the  $\text{Cu}(\text{dmamb})_2$  pulse time and the number of ALD cycles. The properties of the films were performed by XPS, AES depth-profile and AFM. To investigate the optical and electrical properties, as-grown and annealed samples were measured by UV-vis and Hall measurements.

**Kp-III-038****다층의 터널 절연막층을 이용한  $\text{TiSi}_2$  나노부유게이트 메모리소자의 전기적 특성 분석**

한 승중, 이 동욱, 김 선필, 김 은규, 오 준석<sup>1</sup>, 조 원주<sup>1</sup>

한양대 물리학과, <sup>1</sup>광운대 전자재료공학과.

나노부유게이트 메모리소자 (NFGM: Nano-Floating Gate Memory)란 기존 플래시 메모리소자 구조와 상당히 유사하나 플래시 메모리소자의 플로팅 게이트를 나노사이즈(5-20 nm)의 실리콘, 금속, 금속 산화물, 금속 실리사이드 등으로 대체한 1개 트랜지스터의 구조를 가지는 메모리 소자를 일컫는다. 특히 저장전극으로 다수의 나노입자를 이용하면 소자의 크기를 줄일 수 있음으로써 소자의 초고집적화를 가능하게 할 수 있으며, 저 전력소모, 쓰기/지우기 동작특성이 낮은 동작전압에서도 빠르며, 장기간 데이터를 유지할 수 있는 비휘발성이 우수하다는 이점 때문에 현재 다양한 연구가 활발히 진행되고 있다. 그러나 이러한 장점에도 불구하고 나노 부유 게이트메모리 소자는 쓰기/지우기 동작특성과 retention 유지특성 사이에서의 trade-off 현상 등이 문제점으로 대두되고 있다. 따라서, 본 연구에서는 소자특성을 개선하기 위하여 기존의 나노부유게이트 메모리 소자에 다층구조의 터널 절연막 층을 도입하였으며 전하 저장소로써  $\text{TiSi}_2$  나노입자를 이용하는 소자구조를 제작하였다. 먼저, 소스와 드레인이 형성되어 있는 p형 Si 기판위에 다층의 터널 절연막층을 성장시킨 다음  $\text{TiSi}_2$  박막을 Ar 분위기에서 Sputter를 이용하여 5 nm 두께로 증착하였다. 그리고 30 nm 두께의  $\text{SiO}_2$ 를 추가적으로 증착한 후, rapid thermal annealing (RTA)법으로 800 °C의 온도로 2분 동안 질소 분위기에서 열처리하여  $\text{TiSi}_2$  나노입자를 제조하였다. 마지막으로 알루미늄 막을 증착한 후 포토리소그래피와 에칭 공정을 통하여 게이트 전극을 형성하였다. 제작된 소자의 전기적 특성은 HP-4156A semiconductor parameter analyzer를 이용하여 문턱전압 이하 영역의 전달특성 (VG-ID)과 출력특성 (VD-ID), 전압 인가에 따른 문턱전압의 이동, 메모리 속도 그리고 retention 특성 등을 측정하였다.

**Kp-III-039****Amorphous-to-Crystalline Phase Transformation of Thin-Film Rubrene**

임 성일, 염 한웅, 이 영국<sup>1</sup>, 최 정민, 박 세웅

연세대학교 물리 및 응용물리 사업단, <sup>1</sup>연세대학교 금속공학과.

We report on the amorphous-to-crystalline phase transformation of rubrene thin films. The crystallization of the organic thin films displays disc-like domains whose nucleation and growth follow phase transformation kinetics well-established for inorganic materials under a certain time and temperature condition. We understood that the crystallization of amorphous rubrene thin film shows site-saturated nucleation behavior while the crystalline growth involves both diffusion and interface-controlled kinetics. The activation energy of the transformation kinetics was about 0.78 eV on hexamethyldisilazane-functionalized  $\text{SiO}_2$  substrate as mostly consumed at the growth process. The crystallization kinetics changes with the film substrate; more hydrophobic substrate induces less number of crystalline nuclei while causing faster growth of those nuclei.

**Kp-III-040****Optical properties of metal oxide nano-particles embedded in the polyimide layer**

KIM Soen Pil, LEE Dong Uk, KIM Eun Kyu

*Quantum-Function Spinics Laboratory and Department of Physics, Hanyang University.*

We have fabricated metal-oxide nano-particles ( $\text{In}_2\text{O}_3$ ,  $\text{ZnO}$ ,  $\text{SnO}_2$ ,  $\text{CuO}$  and  $\text{Cu}_2\text{O}$ ) in polymeric matrix for optoelectronic and photovoltaic applications. Then, the polymer layer has also possibility for an application to flexible devices. The metal oxide nano-particles in a polyimide (PI) film were formed by a chemical reaction between the metal thin film and polyamic acid (PAA). The metal films with thickness of 2 ~ 10 nm were deposited on the Si substrates by thermal evaporator, and then the PAA layer with a thickness of 50 nm was spin coated on the deposited metal layer. The polyamic acid (PAA) precursor used in this study was prepared by dissolving biphenyltetracarboxylic dianhydride-phenylene diamine (BPDA-PDA) commercial PAA (PI2610D) in N-methyl-2-pyrrolidone (NMP). During the metal dissolving process, PAA and metal layer were maintained at room temperature for 24 ~ 48 hours. The PI precursor was treated at 135 °C for 30 min removing the solvent. Finally, the PAA/indium layers were cured at 300 °C ~ 500 °C for 1 ~ 2 hour in  $\text{N}_2$  atmosphere for creates the metal oxide nano-particles. The metal oxide nano-particle size and distribution could be controlled by the curing temperature and time. In this study, the optical properties of metal oxide nano-particles formed in the PI layer were characterized by UV-Vis absorption and optical responsivity measurements. We will discuss the relation between size and optical properties of metal oxide nano-particles in the polyimide layer.

**Kp-III-041****Degradation Pattern of  $\text{SnO}_2$  Nanowire Field Effect Transistors Analyzed by the****Gate Dependent Mobility and Contact Resistance**NA Junhong, HUH Junghwan, KIM Gyu Tae, PARK Sung Chan<sup>1</sup>, KIM DaeIl<sup>1</sup>, HA Jeong Sook<sup>1</sup>

*Korea University, School of Electrical Engineering. <sup>1</sup>Korea University, Department of Chemical and Biological Engineering.*

We have figured out the degradation pattern of  $\text{SnO}_2$  nanowire field effect transistors from  $R_s$  (serial resistance)- $\mu$  (mobility) patterns. The devices were configured with the unpassivated, the PMMA (poly methyl methacrylate) passivated, and the  $\text{Al}_2\text{O}_3$  passivated  $\text{SnO}_2$  nanowire field effect transistor on one single  $\text{SnO}_2$  nanowire to avoid the different sample issues. The time dependent  $R_s$ - $\mu$  traces rotated in a counter-clockwise direction for two months, indicating a sign of the degradation. This analytical method could be used as an index for evaluating the efficiency of passivation in nanowire electronic devices.

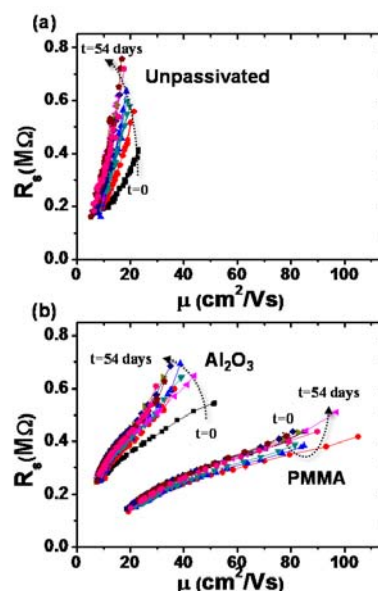


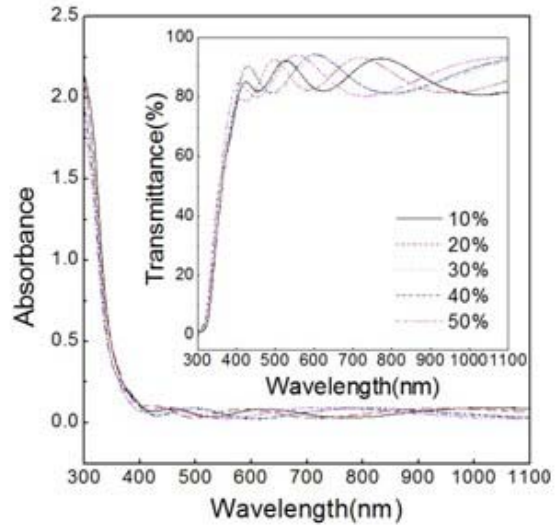
Figure 1.  $R_s$ - $\mu$  plots of (a) the unpassivated portion and (b) the passivated portions of a single  $\text{SnO}_2$  nanowire FET, clearly showing the effects of the passivation. The unpassivated part shows a wide range of the change in the serial resistance with time, a sign of the faster degradation of the serial resistance.

**Kp-III-042****산소 유량비가  $\text{In}_2\text{O}_3$  박막의 특성에 미치는 영향**

곽 준호, 조 신희

신라대학교 전자재료공학과

최근  $\text{In}_2\text{O}_3$  박막은 넓은 밴드갭 에너지를 갖기 때문에 청색/자외선 발광 다이오드와 태양 전지의 윈도우 층으로 구현하기 적합한 물질로 각광 받고 있다. 본 연구에서는 투과율과 전기 전도성을 향상시키기 위해서 라디오파 반응성 마그네트론 스퍼터링 방식으로  $\text{In}_2\text{O}_3$  박막을 유리 기판 위에 성장시켰다. 금속 인듐 (순도: 99.99%)을 스퍼터링 타겟으로 사용하였고, 산소를 반응성 가스로 공급하였다. 특히, 산소 유량비  $[(\text{O}_2/\text{Ar}+\text{O}_2)=10, 20, 30, 40, 50\%]$  변화에 따른  $\text{In}_2\text{O}_3$  박막의 전기, 구조, 광학 특성을 조사하였다. 삽입 그림은 파장 300~1100nm 영역에서 측정한 흡수율과 투과율을 파장의 함수로 표시한 것이다. 가시광 영역에서  $\text{In}_2\text{O}_3$  박막의 평균 투과율은 85% 이상이었고, 관측된 진동은 증착된 박막의 간섭 무늬로써 박막의 균일성을 보장한다. 이 결과를 바탕으로 하여 광학 밴드갭 에너지를 계산 하였는데, 산소 유량비가 증가함에 따라서 광학 밴드갭 에너지의 값은 증가하는 경향을 보였다.

**Kp-III-043****실리콘과 유리 기판 위에 제작된 Ge-doped SbTe 박막의 유전함수 비교**박 준우, 이 호선, 박 영욱<sup>1</sup>, 정 병기<sup>1</sup>경희대학교, 응용물리학과, <sup>1</sup>KIST.

RF 마그네트론 스퍼터링 방법을 이용하여 실리콘 기판과 유리 기판 위에 각각 제작된 Ge-doped SbTe 박막의 유전함수를 분광타원해석기를 이용하여 측정하였다. 100nm와 300nm 두께의 Ge-doped SbTe 박막을 3 가지 조성으로 제작하였다. 조성측정은 XRF를 이용했다. 기판 종류와 열불림 조건에 따른 광학적 특성의 변화를 논하였다. 유전함수가 비정질시료는 기판의 종류에 관계없이 거의 비슷하나, 결정화된 시료는 기판의 종류에 따라 큰 변화가 있음을 밝혔다. 특히 Sb 조성이 클 때는, Si 기판 위에 제작된 박막의 유전함수가 유리 기판 위에 제작된 것 보다 훨씬 더 크다. 측정된 유전함수로부터 광학흡수계수를 구하여 선허바깥늘림법을 이용하여 광학적 간격에너지를 측정했다. 비정질은 0.5 eV, 결정질은 0.2 eV 이었다. 광학적 간격에너지는 기판의 종류에 따라 큰 변화가 없으나, Si 조성이 가장 클 때는 상당한 차이가 있음을 보였다. 기판의 종류에 따른 유전함수의 변화는 박막 성장시의 핵형성(nucleation) 모드의 차이에 의한 것으로 생각된다.

**Kp-III-044****Transmission electron microscopy investigation of tetragonal transformation****in GeSbTe**

장 문형, 박 승종, 박 성진, 조 만호, 고 대홍<sup>1</sup>, 손 현철<sup>1</sup>

연세대학교 물리 및 응용물리 사업단, <sup>1</sup>연세대학교 세라믹공학과.

The amorphous  $\text{Ge}_2\text{Sb}_2\text{Te}_5$  (GST) films were deposited on silicon nitride membrane. To minimize contamination,  $\text{SiO}_2$  layer was sequentially deposited *in vacuo*. After the annealing treatment at 220 °C, some part of amorphous GST was transformed to face centered cubic (FCC) phase. In addition, another crystalline phase was confirmed at amorphous-FCC boundary. This phase was identified as a base centered tetragonal (BCT) structure. We found that volume of BCT is almost 5 % smaller than that of FCC. This indicates thermal expansion during the annealing treatment resulted in transformation from FCC to BCT at the amorphous-FCC boundary. We supposed that diffusionless martensite transformation is responsible for this FCC-to-BCT transformation which is triggered by thermal stress.

**Kp-III-045****연 X-선 분광법을 이용한 a-GIZO 박막의 분광학적 특성 연구**

이 미지, 강 세준, 백 재윤<sup>1</sup>, 김 기정<sup>1</sup>, 정 재관<sup>2</sup>, 이 재철<sup>2</sup>, 이 재학<sup>2</sup>, 신 현준<sup>1</sup>

포항공과대학, 물리학과. <sup>1</sup>포항가속기연구소. <sup>2</sup>삼성전자 종합기술원.

차세대 투명전극 TFT 대안 소재로 각광받고 있는  $\text{GaInZnO}$  물질은 비정질상태에서 높은 전하 운동성을 가지는 것으로 알려져 있다. 따라서 비정질의 우수한 전기적 물성을 유지할 수 있는 다양한 환경조건에 대한 연구가 활발히 진행되고 있으며 실제공정에서 그 연구결과에 대한 수요가 증가하고 있다. 본 연구는 고분해능의 방사광 연-X-선을 이용하여 각 원소 조성 및 온도 조건에 따른 화학적 상태변화, 그리고 대기 오염물질 제거를 위한 이온빔 식각과정에서의 표면 상태 변화에 대한 보다 정확한 물성정보를 제공하기 위하여 수행되었다.  $\text{Ga}_2\text{O}_3:\text{In}_2\text{O}_3:\text{ZnO}$ 의 비율이 각각 1:1:1, 2:2:1, 3:2:1 그리고 4:2:1인 시료를 준비하여 valence band maximum을 측정한 결과 Ga 원소의 조성비 증가에 따라 그 값이 증가함을 관찰하였다. 이로부터 Ga이 wide 밴드갭을 유도하는 물질로서 필요에 따라 알맞은 조건의 전기적 특성을 가지는 재료를 구현될 수 있음을 알 수 있었다. 반면 약 400도의 열처리로부터 상대적으로 In과 Zn의 양이 감소하여 물질의 상태가 변화하는 것을 관찰하였다. 또한 이온빔을 이용하여 식각 처리하는 경우, 상대적으로 Ga에 비하여 In, Zn의 양은 감소하고 산소 양은 증가하는 것을 관찰할 수 있었다. 이는 기존 문헌에 보고된 산소 감소에 따른 저항증가현상과 상이한 결과로 보다 다양한 방향으로의 분석 및 토의의 과제로 남아있다.

**Fp-IV-001****일차원 양자계의 에너지 갭에 대한 연구**

박 태영, 이 용철<sup>1</sup>, 이 지우<sup>1</sup>, 최 영진

명지대학교 물리학과, 나노공학과. <sup>1</sup>명지대학교 물리학과.

일차원 양자계 중에서 하드코어 보존 모형과 스핀이 없는 페르미온 모형의 에너지 갭에 대해 연구하였다. 이들 모형은 뛰어다니는 에너지와 가장 가까운 이웃에 있을 때 밀어내는 에너지가 있는 모형으로 가장 간단하게 양자상전이를 구현할 수 있는 모형이다. 란쑤스 방법으로 기저상태를 알아내었고, 갭을 구하기 위해 그로소의 란쑤스 방법으로 들뜬 상태와 에너지를 구하였다. 이를 통해 동적 임계 지수를 바로 측정할 수 있어서 향후에 보다 실질적인 모형에도 이용하고자 한다. 기저 상태의 양자 상태가 상전이 전후에 어떤 성질이 있는지 연구하였고, 보존과 페르미온의 양자 상태의 차이점에 대해서도 논의한다.

**Fp-IV-002****Multiple fragmentation of critical continuum percolation clusters**

LEE Changan, LEE Sang Bub

Kyungpook National University, Department of Physics.

The scaling properties of binary, ternary, and quaternary fragmentation of critical percolation clusters were studied via Monte Carlo simulations with respect to the continuum percolation models consisted of permeable disks and spheres. In continuum percolation models, inclusion disks and spheres are multiply connected to other particles and, therefore, clusters may be more easily fragmented by removing a single inclusion particle, thus, enabling one to study multiple fragmentation. The scaling exponents for binary fragmentation were found to be similar to the corresponding lattice values reported previously; i.e., the exponents  $\lambda$  and  $\Phi$  associated, respectively, with the power-law behaviors  $a_s \sim s^\lambda$  and  $b_{s',s} \sim s^{-\Phi} g(s'/s)$ , remained unchanged,  $a_s$  being the mean number of fragmenting particles and  $b_{s',s}$  being the probability of finding daughter clusters of size  $s'$  after fragmentation of a cluster of size  $s$ . This observation is consistent with the fact that the continuum percolation models belong to the same universality class as that of the lattice counterparts as long as the static properties are considered. In the ternary and quaternary fragmentation, the exponents were also found to be similar to those for the binary fragmentation, and the scaling relation of the first moment of daughter clusters  $\mu_s = \sum_{s'=1} s' c_{s',s} \sim s^{2+\lambda-\Phi} \sim s^\psi$  appeared to be held, where  $c_{s',s} = a_s b_{s',s}$ . In both two and three dimensions and in both binary and multiple fragmentation, the scaling relation  $\Phi = 2 - 1/v d_f$  and  $d_f$  being the correlation length exponent and the fractal dimension of critical percolation clusters, appeared to be valid.

**Fp-IV-003****Influence of quenched disorder on the critical behavior of absorbing phase****transitions in conserved lattice gas model**

LEE Changhan, LEE Sang Bub

*Kyungpook National University, Department of Physics.*

Motivated by the Harris criterion, nonequilibrium absorbing phase transitions of the conserved lattice gas (CLG) model from an active phase into an absorbing state was studied on lattices with quenched disorders, i.e., on infinite percolation clusters both in two and three dimensions. Harris criterion implies that, in a magnetic system, the pure fixed point is unstable if the specific heat exponent is positive. For the CLG model, the specific heat exponent is undefined but may be calculated by the hyperscaling relation  $\alpha = 2 - dv$ ,  $d$  and  $\nu$  being, respectively, the lattice dimensionality and the spatial correlation length exponent. In two dimensions, it will be positive if the exponent  $\nu$  obtained by Lübeck<sup>(1)</sup> is employed and will be negative if  $\nu$  obtained by Lee and Lee<sup>(2)</sup> is used, and, in three dimensions, it is found to be positive with the available value of  $\nu$ . Therefore, the impurity sites might yield nontrivial effects on the critical behaviors in three dimensions and, in two dimensions, the disorder might be irrelevant, implying that an influence of disorder might be different depending on the lattice dimensionality. By extensive numerical simulations, it was found that, for the fraction of disordered sites less than the critical fraction, the critical exponents were found to be similar to those on a regular lattice, both in two and three dimensions. When the fraction of disordered sites reached the critical fraction, the critical exponents were found to be different from those on a pure lattice in both dimensions. These results are contrasted to the critical behaviors of the contact process with quenched disorder, for which non-universal Griffith phase was observed when any amount of the disordered sites is introduced. (1) S. Lübeck and P. C. Heger, Phys. Rev. E, 68, 056102 (2003) (2) S. B. Lee and S.-G. Lee, Phys. Rev. E. 78, 040103(R) (2008)

**Fp-IV-004****Continuum Percolation Under Achlioptas Type Process**

윤 여광, 육 순형, 김 엽

*경희대학교 물리학과.*

Recent studies have shown that a cooperative Achlioptas type process, in which the probability to connect a link between different clusters depends on the masses of clusters, causes a first-order kinetic transition [1,2]. Here, using the Monte Carlo simulations we study of the effect of the Achlioptas type process on the continuum percolation transition of sticks. Since the stick percolation is closely related to various phenomena in nano-tube systems, some possible applications and other related physical phenomena are also discussed.[1] D. Achlioptas, R. M. D'Souza, and J. Spencer, Science 323, 1453 (2009)[2] R. M. Ziff, Phys. Rev. Lett. 103, 045701 (2009).

**Fp-IV-005****Random disposition with relaxation model on a fractal substrate**

KIM DAE HO, KIM JIN MIN

승실대학교.

Random deposition with relaxation (Family) model on Sierpinski gasket fractal substrate which have the fractal dimension  $d_f = 1.585$  is studied. The interface width  $W$  grows as  $t^\beta$  with  $\beta = 0.1581$ . For the saturated regime,  $W$  follows  $L^\alpha$  with  $\alpha = 0.3736$ . The dynamic exponent  $z = 2.345$  was obtained by the relation  $z = \alpha / \beta$ . The scaling relation  $2\alpha + d_f = z_{RW}$  was satisfied. The numerical simulation results on Sierpinski gasket is in a good agreement with the predictions of the fractional Langevin equation.

**Fp-IV-006****Conserved-Mass Aggregation Model with Mass Repulsion**

CHOI Woosik, KWON Sungchul, KIM Yup

경희대학교.

We investigate the condensation phenomena of conserved-mass aggregation model with mass repulsion. The model evolves via two dynamical rules, diffusion and chipping of masses. For diffusion with unit rate, mass of a site moves to the site with minimum mass among the nearest neighboring sites. The biased diffusion causes the repulsive interaction between masses. With rate  $\omega$ , unit mass is chipped from a site with mass  $m$  and hops to one of the nearest neighboring site with equal probability. Due to the repulsive interaction, we expect that the condensation of masses strongly depends on the spatial dimensions  $d$ . In one dimension we numerically confirm that condensation transition is normal mean-field type. In contrast, we numerically confirm that  $\rho_c$  diverges with the system size  $L$  and mass distribution  $P(m)$  decay as  $m^{-\tau}$  with  $\tau < 2$  on the random networks. We also study the condensation transition of this model on the scale-free networks with the degree exponent  $\gamma < 3$ .

**Fp-IV-007****Generalized restricted curvature model on fractal substrate**

장 원우, 김 진민

충실대학교 물리학과.

We study the surface structure of a generalized restricted curvature model(RC) on fractal substratesuch as Sierpinski gasket. The surface width  $W$  increase as  $t^{\eta}$  with time  $t$  and becomes saturated at  $L^{\alpha}$  with system size  $L$ . We find the roughness exponent  $\alpha \sim 1.55$ , the growth exponent  $\eta \sim 0.325$  and the dynamic exponent  $z \sim 4.77$ . It is known that the RC model on regular substrate is well described by the fourth order Mullin-Herring equation. However the results of the generalized RCmodel on fractal substrate are consistent with the analytical predictions of a fractional Langevinequation.

**Fp-IV-008****으뜸방정식을 통한 비스듬 분포의 떠오름**

최 무영, 고 세건, 권 현웅

서울대학교, 물리천문학부.

역함수분포나 로그틀맞춤분포, 와이불분포와 같은 비스듬 분포는 물리, 생물, 사회계에서 다양하게 나타나지만 통합적인 이해는 아직부족하다. 여기서는 계의 각 구성요소의 자라남이 현재 크기에 비례하는 모형을 기술하는 으뜸방정식을 통해서 비스듬 분포를 이해하려 하며, 특히 일반적인 계에서 구성요소의 수가 변화하는 경우를 다루었다. 으뜸방정식으로부터 계의 분포를 기술하는 편미분방정식을 얻어내고, 이를 만족하는 일반적인 풀이를 찾아내었는데, 이를 통해 해당하는 비스듬 분포를 모두 얻었다. 곧 일정한 크기의 요소가 만들어지는 경우에는 역함수 분포를 보이며, 로그틀맞춤분포나 와이불분포는 새로 생겨나는 요소의 분포가 원래의 분포와 같을 때 얻어짐을 알 수 있었다. 해석적으로 얻은 이러한 풀이는 수치시뮬을 통해 확인하였다.

**Fp-IV-009****Symmetry Effects on Dynamics of Coupled Pitchfork Systems**

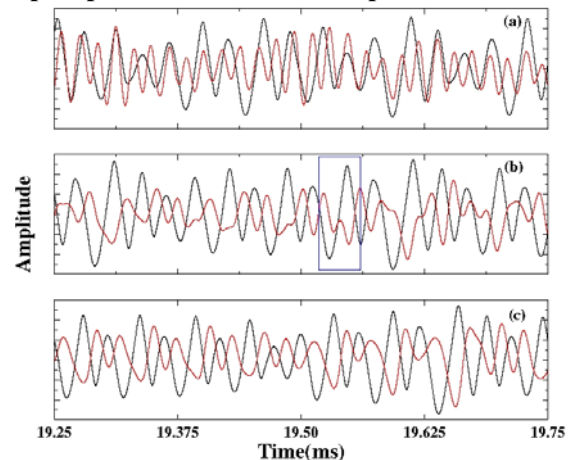
김 영태, 김 재석  
아주대, 물리학과

Detailed bifurcation analysis on coupled one-dimensional pitchfork systems is carried out using a numerical continuation method. Although the bifurcation of a uncoupled one-dimensional pitchfork system is simple, the bifurcations of the coupled system consisting of two one-dimensional pitchfork systems are quite complicated so it cannot be understood without numerical analysis. Depending on symmetry of couplings, we found that bifurcation structures are quite different but details of functional forms of the coupling give minor effects to the bifurcation structures.

**Fp-IV-010****Phase synchronization in a diode laser pumped Nd:YAG laser coupled with a****chaotic oscillator**

LEE Dae-Sic, KIM Guang-Hoon, KANG Uk, KIM Chil-Min<sup>1</sup>  
KERI, SOI-KOREA Center. <sup>1</sup>Sogang University, Department of Physics.

We have studied synchronous behaviors between diode laser pumped Nd:YAG laser and electronically implemented Rossler oscillator. When the Rossler oscillator is unidirectionally coupled to the Nd:YAG laser, the two chaotic systems develops from a non-synchronous state to a phase synchronization state with  $\pi$  phase shift through a  $2\pi$  phase jump state as the coupling strength increases. To verify that the  $\pi$  phase shift is not anti-phase synchronization but phase synchronization with  $\pi$  phase shift, we propose two kinds of similarity function. From the similarity functions, we confirm that the synchronous phenomenon is PS with  $\pi$  phase shift.

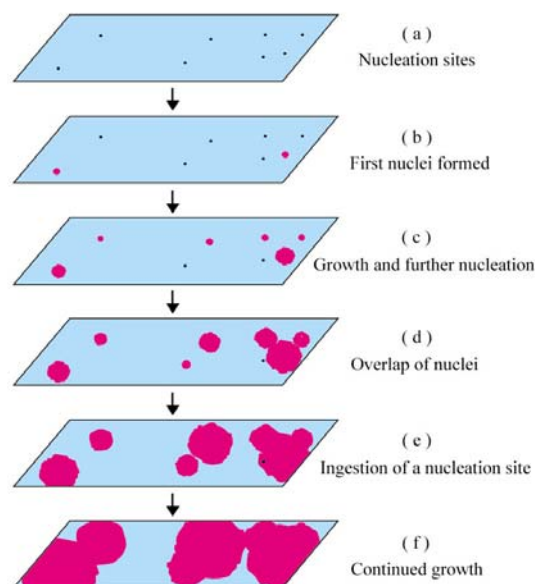


**Fp-IV-011****Surface Transformations of Hydrogen-Bonded Crystals at High Temperatures as****Complex Phenomena and Topochemical Nature**

LEE Kwang-Sei

*Inje University, Department of Nano Systems Engineering.*

Many hydrogen-bonded crystals undergo surface transformations at high temperatures. However, it is obscure whether the high-temperature phase transformations are structural phase transitions in the bulk, surface melting, or thermal decomposition (chemical reaction) at the surface. The crystal surfaces in  $\text{KH}_2\text{PO}_4$ ,  $\text{RbH}_2\text{PO}_4$ ,  $\text{CsH}_2\text{PO}_4$ ,  $\text{TiH}_2\text{PO}_4$ ,  $(\text{NH}_4)_2\text{SO}_4$ , and  $\text{LiH}_3(\text{SeO}_3)_2$  reveal drastic change near onset temperature ( $T_p$ ) and various kinds of patterns appear in the form of cracks, pores, sheaves, spherulites and so on. These results are discussed in terms of ‘nucleation-and-growth’ and ‘topochemical’ nature.

**Fp-IV-012****Dynamical Behaviors of Rainfall Analyses in Korean Cities**김 경식, 이 동인, 김 수용<sup>1</sup>부경대, <sup>1</sup>한국과학기술원.

We study the multifractal property of the rainfall in seven cities of Korea. We mainly estimate the generalized Hurst exponent, Renyi exponent, and singularity spectrum for tick data of the rainfall. In particular, we discuss the recent findings that suggest the scaling exponents characterizing the rainfall multifractality. After analyzing the multifractality of rainfalls, we compare the multifractal property of seven different cities and discuss the different behavior of each city.

**Fp-IV-013****Random Walk을 이용한 Community 검색**

한 범희, 김 업, 육 순형

*경희대 물리과.*

최근 사회계, 생체계 등에서 발견되어지는 community 또는 modular structure의 효율적인 검색 방법에 대한 다양한 연구가 진행되어 왔다. 본 연구에서는 (biased) random walk의 동역학적 특성을 이용하여 기존의 방법들 보다 효율적인 community 검색 방법에 대한 연구를 수행하였다. 인위적으로 만들어진 community를 가진 네트워크를 이용하여, random walker가 각 node를 처음 방문하는 시간의 spectrum을 측정하였다. 전산 시뮬네기를 이용하여 시간의 spectrum이 community구조가 있는 경우 각 community마다 뚜렷이 구분되는 현상을 발견하였다. 이를 이용하여 다양한 실제 네트워크에서의 community 검색에 응용을 하였다.

**Fp-IV-014****Wealth Dynamics in the World Trade Network**차 문용, 이 덕선<sup>1</sup>, 이 재우*인하대학교 물리학과. <sup>1</sup>인하대학교 기초의과학부, 인하대학교 물리학과.*

We investigate the statistics of the Gross Domestic Product(GDP) and international trades of countries to gain insight into the underlying wealth dynamics. Stochastic growth and partial exchange of each country's wealth are formulated in the Bouchaud-Mezard model (BM model). Its parameters and their broad distributions are obtained from the studied datasets and using these results, we simulate the disordered version of the BM model. The obtained results such as the wealth distribution are compared with the real data results and their implications are discussed.

**Fp-IV-015****Modularity and Community Structure in Directed Networks**

KIM Youngdo, SON Seung-Woo, JEONG Hawoong

*물리학과, KAIST.*

We propose a generalized modularity by introducing a new random-walk related quantity, LinkRank, for the directed networks. The LinkRank has some analogy with the time of random walker spent on a specific link while the PageRank is related with the time of random surfer spent on a web site. Our generalization is consistent with the undirected version of modularity. Thus the various methods of the modularity optimization developed for undirected networks can also be applied to the directed ones by optimizing the generalized modularity. We test the generalized modularity in several model networks and compare with the previous methods. Especially we discuss the null ensembles used in the generalized modularity and its mathematical meaning.

**Fp-IV-016****Ising Model Study on Fractal and Non-Fractal Complex Networks**

CHOI Chulho, KAHNG Byungnam, KIM Doochul

*Department of Physics and Astronomy, Seoul National University.*

We study the crossover behavior of the spin domains of the Ising model as the embedded structure changes from large-world to small-world networks by performing extensive numerical simulations on the hierarchical network. We reproduced the theoretical prediction of the critical temperature,  $T_c(p)$  successfully for various values of the fraction  $p$  of long-range edges. Moreover, the domain size distribution was obtained for various  $p$  and  $T$ , which follows a power-law at  $T_c(p)$ . We discuss how the characteristics of the spin domains change as a function of  $p$ .

**Fp-IV-017****Fractal Structure in Protein Interaction Network**

KIM Purin, KAHNG Byoungnam, KIM Doochul

*서울대학교.*

Fractal complex networks have been observed in diverse systems in the range from the world-wide web to biological networks. Recently, it has been shown that fractal networks can be obtained in the evolution of the coauthorship network. Such behavior can also be reproduced from the coauthorship network model. In the model, there are two control parameters governing short-range and long-range connections. Fractal networks are found near the percolation threshold in the parameter space. Here, we simulate a protein-protein interaction model introduced by Sole et al, and check if fractal structure can be found near the percolation threshold. Indeed, the number of boxes needed to cover the network obtained of the Sole model exhibits a heavy-tailed distribution, and its skeleton can be regarded as a critical branching tree with the mean branching ratio being one. Thus, we conclude that this model can be used to generate fractal complex networks.

**Fp-IV-018****Evolution of Real World Networks**LEE Deokjae, GOH Kwang-il<sup>1</sup>, KAHNG Byoungnam, KIM Doochul*Seoul National University. <sup>1</sup>Korea University.*

We inspect evolution of two kinds of real world networks; co-authorship networks of various scientific disciplines and word-collocation networks of infants. The data enable us to track their evolution from beginning to late steady state. The co-authorship networks evolve through an intermediate tree-like growing stage which is topologically distinct from late steady state stage. We find that the intermediate stage is originated from cluster aggregation process in the evolution. In contrast to the co-authorship networks, the evolution process of word-collocation networks do not have such tree-like intermediate stage nor cluster aggregation process and show typical characteristics of small-world networks from their beginning stage.

**Fp-IV-019****Structure of Bipartite Ecological Networks**

맹 성은, 이 덕선, 이 재우

인하대학교.

We analyze the structures of six plant-pollinator mutualistic networks, where plants and pollinators are connected by links weights representing the visiting frequency of pollinators to plants. It is found that the cumulative distribution functions of the plant's degree and strength are of stretched exponential form, and those of pollinators follow power-law form. Our analysis also shows that the link weights are unevenly distributed and the degrees of connected nodes exhibit negative correlations. We propose a simple model to construct bipartite networks having degree distributions of stretched exponential and power-law form. We discuss the biological implications of this model.

**Fp-IV-020****Tracing dynamic network of thalamocortical circuit with symbolic representation**SHIN Jeongkyu, HWANG Eunjin<sup>1</sup>, CHOI Jee Hyun<sup>2</sup>, KIM Seunghwan<sup>3</sup>

*Nonlinear and Complex System Lab., Pohang University of Science and Technology. <sup>1</sup>Nonlinear and Complex System Lab., Pohang University of Science and Technology and Center for neuroscience, Korea Institute of Science and Technology. <sup>2</sup>Center for neuroscience, Korea Institute of Science and Technology. <sup>3</sup>Nonlinear and Complex System Lab., Pohang University of Science and Technology and Asia Pacific Center for Theoretical Physics.*

We studied dynamics of thalamocortical connectivity during anesthetic-induced transition by constructing dynamic network of two cortical and two thalamic regions. Networks are constructed for every 10 seconds based on the cross-correlation of band-pass filtered EEG (electroencephalogram) signals in that analysis window. To understand dynamic signature of the system with a small number of nodes like this system, we used link durability (lifespan) and symbolic representation of connection. Link durability distribution showed the power-law behavior with universal slope ( $r \sim 3$ ) through every frequency bands. By tracing the network ensembles, we found that the origin of power-law distribution for each band was different from the others. With defining the states of network ensemble for analysis windows, symbolization and patternization of circuit states was also studied.

**Fp-IV-021****Giant Unilamellar Vesicles by Spin-Coating Electroformation and Electro-****Osmotic Effect**

박 혁규, 김 성진

부산대학교 물리학과.

Giant unilamellar vesicle (GUV) has been studied as a 'cell size' model system for biological studies. Until now, a number of methods for preparation of liposomes have been proposed. Many groups is using the electroformation instead of gentle hydration method is originally developed. The hydration force is not sufficient to separate the multilayer structures because of the surface/lipid bilayers and lipid bilayers/lipid bilayers interaction. But the electroformation process can separate them by increasing the repulsive electrostatic inter-membrane forces to overcome surface/lipid and lipid/lipid interaction such as van der Waals attraction. Particularly, electro-osmotic effect is the driving force for large separation because of electro-osmotically induced mechanical stresses. In this work, We used to yield the GUV between with the size 10  $\mu\text{m}$  and 100  $\mu\text{m}$  by using the spin coating method in conjunction with the electroformation technique.

**Fp-IV-022****진동하는 고체/액체 계면에서의 전기이중층과 계면에너지 연구**

문 종균, 박 혁규

부산대학교 물리학과.

고체와 액체가 만나는 계면은 특수한 물리적 성질을 갖는다. 특히 전해질 액체와 고체가 만나는 계면은 계면장력 외에도 특별한 전기적 성질을 갖는다. 만약 고체 표면이 어떠한 표면전하 밀도를 가지고 분포한다면 전기적 인력에 의해 액체 내부에 있는 반대이온이 고체/액체 계면에 존재하게 된다. 고체 표면 가까이 강하게 흡착된 양은 층을 stern층이라 하고 조금 더 떨어진 곳에서 전기적 인력에 의한 힘을 받지만 열적 힘에 의해 어느 정도 자유롭게 움직이는 과잉 반대 전하가 존재하는 층을 확산층이라 한다. 이 두층을 통합해서 전기 이중층이라 한다. 이 실험에서는 두 ITO 고체판 사이에 전해질 물방울을 두고 아래쪽 판을 일정한 진동수  $f$ 로 진동시켜 물방울과 고체 사이의 계면 면적을 변화 시켰을 때 교류 전압이 생성 되는 것을 관찰하였다. 이러한 결과를 바탕으로 진동하는 계면에서 전기 이중층의 물리적 특성과 함께 계면에너지가 미치는 영향에 대해 연구하였다.



**Fp-IV-023****Thermal random circuit breaker network model : Effects of Joule heatings on the unipolar resistance switching**이 재성, 채 승철, 이 신범, 장 서형, LIU Chunli<sup>1</sup>, 강 병남, 노 태원서울대학교, <sup>1</sup>HUFS.

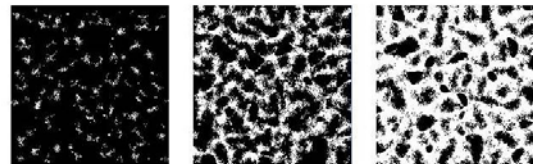
The unipolar resistance switching (RS) behaviors have received renewed interest due to the possibility of high density and nonvolatile memory application. The random circuit breaker (RCB) model can explain the long-standing material issue of how unipolar RS occurs. In this presentation, we first review the random circuit breaker (RCB) network model, which was proposed to simulate rupturing and forming of conducting filament by using reversible on and off switching depending only on electric bias applied to circuit breakers. And we present several simulation results of the RCB network model explaining characteristic current-voltage curves, distributions of switching voltages, and anomalous RS behaviors. Secondly, we introduce temperature dependent RCB model, in which off-switching is determined by circuit breaker temperature and heat is transferred by thermal contact, and also present related simulation results of the model explaining non-linearity observed in low resistance state, origin of unipolar RS type, voltage ramp rate dependence, and universality in Reset operation.

**Fp-IV-024****확산하는 자원 공급이 있는 2차원 평면에서 개체 증식**

홍 상신, 석 진호, 원 창연

경희대학교 물리학과.

증식과 생존을 위해서 지속적인 자원의 공급을 필요로 하는 개체에 관한 증식에 관해서 2차원에서 증식을 하게 되면 증식 형태에 따른 패턴과, 계의 개체수와 자원 량의 변화는 특별한 형태를 가지게 된다. 우리가 연구한 개체의 기본적인 성질은 개체의 증식은 일정 자원 이상에서 확률을 가지고 일정한 거리에서 하게 되고 생존에 대한 자원의 기본량을 충족시키지 못하면 소멸하게 된다. 자원의 기본적인 성질은 2차원에 평면에 균질하게 일정한 량이 매시간마다 공급되면 평면에 특성에 따라 자원이 많은 곳에서 적은 곳으로 분산을 한다. 이러한 성질은 가지는 개체와 자원의 2차원 평면을 우리는 Monte-Carlo 방법으로 시뮬레이션을 하였다. 일정한 량으로 지속적인 자원 공급이 있는 경우, 증식의 기본적인 형태는 초기의 개체를 중심으로 한 방사상이다. 그리고 점점 시간이 흐르게 되면 그 영역이 점점 커지다가 가운데가 비는 환 모양이 된다. 다음으로는 여러 환들이 서로 연결이 되어서 그물의 형태를 띠게 되고 가득 채워진 평면에 구멍들이 있는 형태가 되었다가 마지막으로 다 채워지게 된다. 그리고 자원 공급량 증가에 따른 평면 전체의 개체 수의 평균의 량은 일정 공급량 이상이 되면 초반에 아주 잠깐 급격하게 증가를 하게 되다가 그 후에는 포화가 될 때 까지 거의 선형으로 증가를 하게 된다. 하지만 개체 수의 시간 흐름에 따른 편차는 개체수가 증폭을 시작하여 포화가 되는 중간쯤에서 커지다가 포화가 되는 시점에서 다시 거의 0으로 수렴을 하게 된다. 자원 량의 평균은 개체가 증식을 하기 전까지 선형으로 증가를 하게 되며 초반에 잠깐 개체수가 급격하게 증가하는 시점에서 급격하게 감소를 하다가 다시 조금씩 증가를 하며 어느 정도가 지나면 개체 수가 포화가 될 때 까지 조금씩 감소를 한다. 하지만 자원 량의 전체적인 양은 크게 변하지 않는다. 자원 량의 편차는 개체 수의 편차와 비슷한 모양을 가진다.



자원의 량

자원의 공급량에 따른 패턴: 한 점이 각각의 개체를 나타낸다.

**Fp-IV-025****Orientational Ordering of Quantum Quadrupolar Rotors: Path-integral Monte****Carlo Study with Extrapolated High-order Propagators**

권 용경, 신 현덕, 박 성진

건국대학교 물리학과.

Due to competition between large rotational kinetic energy and highly-anisotropic intermolecular interaction, quantum solids of molecular hydrogen exhibit complex phase diagrams over a wide range of temperatures and pressures. A solid of asymmetric HD molecules whose nuclei are distinguishable, shows a peculiar reentrant behavior in the orientational order-disorder phase transition. Since most of the anisotropic interaction between the hydrogen molecules can be accounted for by the electric quadrupole-quadrupole interaction, we here consider a system of asymmetric quadrupolar rotors localized at face-centered cubic lattice sites. Using the path-integral Monte Carlo (PIMC) method which enables us to make a full quantum treatment of the rotational dynamics of the rotors, we find a reentrant shape as observed experimentally in solid HD. The PIMC result based on the primitive approximation, however, shows a significant quantitative discrepancy with the experimental value for the critical pressure, which is understood to be due to the time step error in the high-temperature propagator. For the improvement of our calculation, we here employ extrapolated high-order propagators recently proposed by Zillich *et al.* [1]. We make a systematic analysis of the accuracy and the efficiency of these new propagators in dealing with the rotational degrees of freedom of a many-body system. [1] R. E. Zillich, J. M. Mayrhofer, and S. A. Chin, a preprint in <http://arxiv.org/abs/0907.3495>

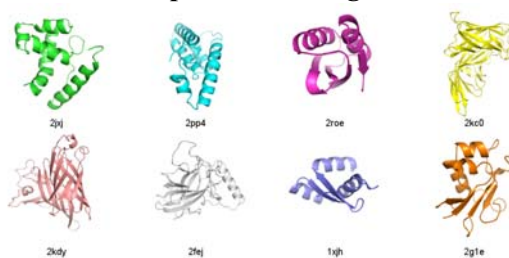
**Fp-IV-026****Molecular dynamics study of atom-cluster or cluster-cluster collisions**KIM Do-Hyun, LEE Min-ho<sup>1</sup>, KIM Sangrak, CHOI Je-Young<sup>2</sup>Kyonggi Uni.. <sup>1</sup>Kyonnggi Uni.. <sup>2</sup>Yongdong Uni..

We simulate atom-cluster and cluster-cluster collisions for icosahedral Ar cluster with different temperatures of the target cluster, impact parameters and impact velocities of the bullet. We draw phase diagrams of collisions about impact parameters and impact velocities. Furthermore, we measure energy differences between initial and final states of the bullet and ratios of broken pieces which are defined as size ratios of the largest cluster and the second largest cluster after collision.

LEE Jinhyuk, LEE Jinwoo<sup>1</sup>, LEE Jooyoung

고등과학원, 계산과학부, <sup>1</sup>광운대, 수학과.

We have carried out numerical experiments to investigate the applicability of global optimization method to the NMR structure determination. Since the number of NMR observables is relatively small in the early stage of NMR structure determination process and long range NOE observables are difficult to obtain, advanced sampling techniques are greatly in need to generate valid NMR structures from a small number of experimental restraints. By utilizing conformational space annealing method, we have determined solution NMR structures from NOE distance and backbone dihedral restraints. Several solution NMR structures are determined starting from fully randomized conformations. We have evaluated them by measuring the qualities of determined structures, such as structure convergence of ensemble, Ramachandran preferences, clash scores, and the total NOE violation. These qualities are compared to those from the corresponding PDB structures.



**Dp-V-127****The Effects of Carbonaceous Impurity with Functional Group on the Oxidized****SWCNTs**

LEE Jung-Ah, LEE Byung Chul<sup>1</sup>, LEE Sang-Myung<sup>1</sup>, PAEK Kyeong-Kap<sup>2</sup>, LEE Yun-Hi<sup>3</sup>, SHIN Hyun Joon<sup>1</sup>

KIST/고려대 물리학과. <sup>1</sup>KIST 나노바이오 연구센터. <sup>2</sup>대전대 전자공학과. <sup>3</sup>고려대 물리학과.

The properties of functionalized SWCNTs (f-SWCNTs) supernatant samples obtained through steps of acid oxidation-centrifugation-decantation were characterized by the spectroscopic tools. Fourier transform infrared spectroscopy provided the evidence for the chemical and structural variation generated on the f-SWCNTs within each supernatant sample. The ultraviolet-visible-near infrared absorption spectra of each sample were interpreted as the result of the depletion of valence band electrons resulting from the density difference of the carbonaceous impurity with functional groups on the f-SWCNTs. In Raman results, it was confirmed that the diameter of f-SWCNTs within each sample through the radial breathing mode was increased. In addition, the red-shift observed in the tangential mode indicates the attenuation of the electrical conductivity by the reduction of carbonaceous impurity.

**Dp-V-128****Evaluating Adhesion of Carbon Nanotubes in Transparent Conducting Films**

LEE Sang Won, YAN CUI<sup>1</sup>, CHO Young Woo, KIM Su Min<sup>1</sup>, LEE Young Hee<sup>2</sup>

BK21 Physics, Center for Nanotubes and Nanostructured Composites. <sup>1</sup>SKKU advanced Institute of Nanotechnology (SAINT). <sup>2</sup>BK21 Physics, Center for Nanotubes and Nanostructured Composites. SKKU advanced Institute of Nanotechnology (SAINT). Sungkyunkwan University, Suwon 440-746, Republic of Korea.

We propose a new method of evaluating the adhesion of carbon nanotube films on transparent substrates. Single wall carbon nanotubes (SWCNTs) dispersed with sodium dodecylbenzene sulfonate (NaDDBS) in water were sprayed onto polyethylene terephthalate (PET) and polyethylene naphthalate (PEN) substrates to form thin films. Scotch™ tape was then used to detach some loosely bound SWCNTs. An adhesion factor was defined using transmittance before and after detachment. The adhesion factor was strongly correlated to film thickness but not to sheet resistance. SWCNT adhesion to the substrate was strongly dependent on the surface roughness of the substrate due to mechanical interlocking effects.

**Dp-V-129****Spin Stiffness Of Graphene And Zigzag Graphene Nanoribbon**

MOON Kyungsun, RHIM Jun-Won

연세대학교 물리학과.

We theoretically study the spin stiffness of graphene and graphene nanoribbon based on the Hubbard-type Hamiltonian. Using the Hartree-Fock method with the inclusion of the adiabatic spin twist, we have obtained the effective energy functional and investigated the magnetic excitations of the 2D graphene and zigzag graphene nanoribbon (ZGNR). We have analyzed the spin stiffness of the system with varying temperature and the strength of on-site Coulomb repulsion. For ZGNR, we have also studied the effect of the lateral electric field on the spin stiffness. As the field increases, the spin stiffness decreases and reaches less than the half of the zero-field value. However, we remarkably notice that there exists a critical value of the electric field above which the stiffness starts to increase showing a cusp-like behavior. This critical point is found to coincide exactly with the metal-insulator transition point of ZGNR.

**Dp-V-130****Synthesis of Large area Graphene by rapid-thermal low pressure CVD method**

이 종희, 김 윤중, 이 윤희

고려대학교, 물리학과.

탄소원자의 2차원 배열로 이루어진 홀층 그래핀은 전자 이동도가 매우 높아 고속전자소자로서 많은 관심을 모으고 있을 뿐만 아니라 상온에서의 양자 홀 효과 및 Klein 터널링 등 실험적으로도 전례 없이 흥미롭고 다양한 결과들을 보여주고 있다. 현재 그래핀 소자 제작에는 기계적 추출법, 열화학 기상 증착법, 습식 화학적 방법 등 여러 방법이 보고되고 있다. 향후, 그래핀 물성이 좀더 다양하게 연구되고 응용되기 위해서는 보다 다양한 기판에 큰 면적으로 고순도의 그래핀 합성이 요구된다. 본 연구에서는 급속-저압-열화학 기상 증착법을 이용하여 그래핀의 직접 합성화되며 성장에 필수적인 촉매물질로서 가장 경제적인 금속 전자소재인 Cu를 도입하여 보았다. 합성된 그래핀 sheet는 화학적 후-처리를 거쳐 SiO<sub>2</sub>(300nm), glass, TEM grid 등의 다양한 기판에 배치하고 SEM, TEM 및 Raman 산란 실험을 통해 구조적 특성을 분석하였다.

**Dp-V-131****Vertically-aligned high quality ZnO nanorod growth on bufferlayers**

KIM B.H., PARK C.I., KWAK C.H.<sup>1</sup>, SEO S.Y.<sup>1</sup>, KIM S.H.<sup>1</sup>, HAN S.W.<sup>2</sup>

*Department of Physics and Institute of Fusion Science, Chonbuk National University, Jeonju 561-756, Korea. <sup>1</sup>Department of Materials Science and Engineering, Pohang University of Science and Technology, Pohang 790-784, Korea. <sup>2</sup>Division of Science Education, Institute of Fusion Science, and Institute of Science Education, Chonbuk National University, Jeonju 561-756, Korea.*

Vertically well-aligned ZnO nanorods were fabricated on ZnO homo-buffer layers and Ti bufferlayers using a catalyst-free metal-organic chemical vapor deposition. Field-emission transmission electron microscope (FE-TEM) measurements on the interface of the nanorod and substrate revealed that the ZnO nanorods grew with a one-step or a two-step mode, depending on the substrate conditions including surface roughness and lattice mismatch between the nanorods and substrates. Extended X-ray absorption fine structure measurements at Zn K edge clarified that the relaxation of the lattice mismatch in the *ab*-plane is a necessary condition for ZnO nanorod growth independent of the substrates.

**Dp-V-132****Transport properties of artificial bilayer graphene**

KIM Youngwook, YUN Hyeol<sup>1</sup>, LEE Jeong-Ah<sup>1</sup>, JUNG Unseok<sup>1</sup>, LEE Sangwook<sup>1</sup>, KIM Dongchul<sup>2</sup>, SEO Sunae<sup>2</sup>, KIM Junsung

*Department of physics, Pohang University of Science and Technology. <sup>1</sup>Division of Quantum Phases & Devices, School of Physics, Konkuk University.. <sup>2</sup>Samsung Advanced Institute of Technology.*

Using direct transfer method of monolayer graphenes sheet and their subsequent stacking, we fabricate artificially the bilayer graphene device. In contrast to the regular Bernal stacking of bilayer graphene, two layers of the artificial bilayer graphene are arbitrarily misoriented. Such a misorientation has been predicted to decouple the two graphene sheets. The coupling between the graphene layers is examined by the interlayer transport measurements. The possible realization of a double 2-dimensional-electron gas system with graphene will be discussed.

**Dp-V-133****Sintering temperature effect and luminescence properties of  $\text{Eu}^{3+}:\text{Ca}_2\text{Gd}_8(\text{SiO}_4)_6\text{O}_2$  nanophosphors** **$\text{Ca}_2\text{Gd}_8(\text{SiO}_4)_6\text{O}_2$  nanophosphors**

GANJI Seeta RamaRaju, 정 홍채, 박 진영, 문 병기, 정 중현

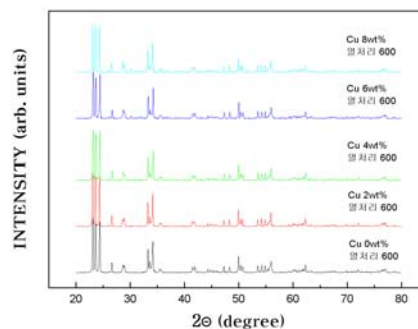
부경대학교, 물리학과.

In recent years, the solid state white-light emitting diodes (WLEDs) have more advantages than the traditional incandescent or fluorescent lamps, because several reports suggested that the WLEDs would reduce global electricity consumption by about 50% by taking advantage of the conversion from direct electricity to light rather than the processes in which light is the by-product of another conversion, as with traditional lamps. Basically, there are some approaches for WLED generation: 1. Blue LED with phosphor converters, 2. UV led with phosphor converters and 3. RGB LEDs (the mixture of three primary light colors to form white light). Among them the mix of three single primary color (Red, Green, Blue) LEDs is potential technique used to produce white light. RGB mixing is the most efficient way to produce white light, this approach offers excellent color rendering of white light. By changing the relative intensity of the different LEDs it is relatively easy to change the hue of this light source for different applications, and no quantum deficit arising from the Stokes shift loss. For this purpose, our contribution is to produce the efficient red light.

In this work, we report on the structural and luminescent properties of  $\text{Eu}^{3+}$  activated oxy apatite  $\text{Ca}_2\text{Gd}_8(\text{SiO}_4)_6\text{O}_2$  nanophosphors by means of solvothermal process. Spherically shaped particles in the nanometer ranges prepared by this method were evidenced by X-ray diffraction (XRD) and SEM analysis. Thermogravimetric/differential thermal analysis (TG/DTA) was used to investigate the phase transformations that occur during the preparation of these samples. Luminescent studies were carried out at different sintering temperatures by the measurement of their Photoluminescence (PL) and Photoluminescence excitation (PLE) along with lifetime curves. The PL spectra show an efficient red emission due to  ${}^5\text{D}_0 \rightarrow {}^7\text{F}_2$  hypersensitive transition at all sintering temperatures. The PLE spectra show strong charge transfer band (CTB) in the shorter wavelength region and f-f transitions in the longer wavelength region. The intensity of the CTB and f-f transitions are depends upon the sintering temperatures. Such luminescent powders are expected to find potential applications such as fluorescent lamps and optical display systems.

**Dp-V-134** **$\text{WO}_3$ 에  $\text{CuO}$ 를 첨가한 후막 가스센서 특성**신 덕진, 이 지영, 유 일, 이 돈규<sup>1</sup>동의대학교 물리학과(부산IT융합부품연구소). <sup>1</sup> 동의대학교 전기공학과(부산IT융합부품연구소).

가스 감지물질로  $\text{ZnO}$ ,  $\text{SnO}_2$ ,  $\text{TiO}_2$ ,  $\text{WO}_3$  등의 금속산화물 반도체 센서가 많이 연구되어왔고, 그 중  $\text{WO}_3$ 는 가연성 가스 및 유독가스에 대한 감도가 우수한 것으로 알려져 있다. 특히,  $\text{WO}_3$ 에  $\text{SnO}_2$ ,  $\text{ZnO}$ ,  $\text{TiO}_2$  등을 촉매로 첨가하여 여러가지 가스에 대한 감지특성을 향상시키는 연구도 활발히 진행되고 있다. 본 연구에서는  $\text{WO}_3$ 에  $\text{CuO}$ 를 촉매로 선택하여  $\text{CuO}$ 의 농도변화와 열처리 온도에 따른 감지물질의 미세구조 변화와 특성을 SEM, XRD 등으로 측정하였다.  $\text{CuO}$ 의 농도를 0~8wt%로 변화시켜  $\text{WO}_3$ 와 교반시킨 후, 8시간동안 오븐건조하여 얻어진  $\text{WO}_3\text{-CuO}$  분말을  $500^\circ\text{C} \sim 700^\circ\text{C}$ 에서 30분간 열처리 하여 각각의 감지물질을 제조하였고, 제조된 감지물질을 알루미늄 기판위에 스크린프린팅 법으로 도포하였다.



## Extended X-ray Absorption Fine Structure

EUN-SUK JEONG, CHANG-IN Park, JINKYOUNG Yoo<sup>1</sup>, GYU-CHUL Yi<sup>2</sup>, SANG-WOOK Han*Institute of Fusion Science, Institute of Science Education and Division of Science Education, Chonbuk National**University, Jeonju 561-756, Korea. <sup>1</sup>National CRI Center for Semiconductor Nanorods, Department of Materials**Science and Engineering, POTECH, Pohang 790-784, Republic of Korea. <sup>2</sup>National CRI Center for Semiconductor**Nanorods and Department of Physics, Seoul National University, Seoul 151-742, Korea.*

Orientation-dependent structural properties of the  $\text{Zn}_{1-x}\text{Mg}_x\text{O}$  nanorods with different Mg concentrations were investigated using polarized extended x-ray absorption fine structure (EXAFS) at Zn K edge. Vertically-aligned  $\text{Zn}_{1-x}\text{Mg}_x\text{O}$  nanorods were fabricated on Si substrate by a catalyst free metal-organic chemical vapor deposition (MOCVD). The polarized EXAFS revealed that the bonding length of Zn-O(1) pair in the c-axis was elongated while the bond lengths of Zn-O(2) pairs in the ab-plane was shrunken, compared with those of ZnO powder. EXAFS demonstrated that the bond lengths of Zn-O(1) and Zn-Zn(1) pairs decreased slightly with the Mg concentration while those of Zn-O(2) and Zn-Zn(2) pairs remained as constant. EXAFS revealed that only about 10 % of Mg was replaced for the zinc site in the sample number 7 which was expected to have over 30 % of Mg in the Zn site. These EXAFS results strongly suggested that Mg atoms were partially replaced for the Zn site and the left might placed on the boundary of the nanorod. We will discuss the detail structural properties of the nanorods, comparing with the physical properties of the nanorods in the presentation.

## 출원의 전계 방출 특성

권 영택, 이 승엽, 송 우석, 김 유석, 최 원철, 박 종윤

*성균관대학교, 물리학과.*

탄소나노튜브를 이용한 방출원의 제작방법들 중 spray method는 간단하고 대 면적 제작에 유리하며 ink-jet 기술과 호환성이 좋은 장점을 가지고 있지만 탄소나노튜브와 기판과의 adhesion 이 약한 단점이 있다. 이러한 단점을 보완하고자 In, Sn 등의 금속을 전극으로 사용한 연구 결과들[1]이 보고되었지만, 복사 가열 방법을 통한 후속 열처리 시 표면형상이 좋지 않고, 녹는점이 낮아 장시간의 전계 방출시 주열(Joule)열에 의해 변형이 되어 전계방출 특성을 악화시킬 수도 있을 것으로 생각된다. 본 연구에서는 녹는점이 높고 상대적으로 전기 전도성도 우수한 Ag-Cu 합금을 전극으로 이용하였으며 이 박막 위에 증착된 탄소나노튜브의 고착화를 위한 후속 열처리방법으로 마이크로웨이브를 사용하였다. 복사 가열 방법에 비해 마이크로웨이브를 이용한 방법은 기판을 보다 균일하게 열처리 할 수 있고 열처리 시간을 단축할 수 있으며, 또한 기판에 직접적으로 열을 가하지 않고 선택적인 부분을 열처리 할 수 있는 장점을 가지고 있다[2]. 이러한 장점을 이용하여 디스플레이분야로의 응용에 필수적인 유리 기판위에 효과적인 전계 방출 특성을 갖는 탄소나노튜브 방출원을 제작하였다. 마이크로웨이브 파워의 세기에 따른 Ag-Cu 합금 박막의 표면 형상(morphology)과 탄소나노튜브의 결정성 등의 변화를 주사전자현미경(Scanning Electron Microscope)과 라만 분광기(Raman spectroscopy)를 사용하여 측정하였으며, 그에 따른 전계 방출 특성의 변화를 연구하였다. 참고문헌[1] Seong Chu Lim, Ha Kyu Choi, Hee Jin Jeong, Young Il Song, Gil Yong Kim, Kyung Taek Jung, Young Hee Lee, Carbon, 44, 2809 (2006).[2] Chihyung Wang, Tsunghan Chen, Shihchin Chang, Syhyuh Cheng, and Tsungshune Chin, Adv. Funct. Mater. 17, 1979 (2007).

**Dp-V-137****Optical reflectometry for nanomechanical motion detection in suspended metal electromechanical resonator.**

심 승보, 노 현호<sup>1</sup>, 정 민경, 김 상균, 유 영동<sup>2</sup>, 김 봉수<sup>2</sup>, 김 정구<sup>1</sup>, 이 광철, 우 병철, 김 진희

한국표준과학연구원. <sup>1</sup>서울대학교 물리천문학부. <sup>2</sup>KAIST 화학과.

The sensitive detection of nanomechanical motion is fundamental for nanoelectromechanical systems(NEMS) application as well as fundamental academic research in NEMS. Here, we demonstrated the system for nanomechanical motion detection. Room temperature optical laser reflectometry were composed for detection of nanomechanical motion. In this technique, nanometer scale mechanical oscillators were driven by capacitive coupling force between oscillator and grounded bottom gate. Modulated optical signals were detected by high frequency photoreceiver by utilizing lock-in technique. The suspended mechanical oscillator were fabricated from single crystal Au nanoplates by standard top-down and bottom-up micromachining techniques. Mechanical structure were placed in vacuum space in order to reduce energy dissipation caused by air friction. Measured resonant frequency of 8 micrometer long Au nanoplate was 4.29 MHz with quality factor of 700. Au nanoplate oscillator showed strong nonlinear response at room temperature. Also we investigated the real-time motion of mechanical resonator which can possibly elucidate the nature of nonlinear dynamics in the nanometer scale mechanical oscillators.

**Dp-V-138****그래핀 소자의 전자-포논 상호작용에 대한 전기장 효과**

김 윤중, 이 종희, 이 윤희

고려대학교, 물리학과.

전자와 포논의 coupling 모드와 세기는 그래핀의 전자적 수송 물성에 중요한 영향을 미치는 것으로 알려져 있다. 그래핀에서 전자-포논의 coupling 특성을 연구하기 위하여 게이트 전극을 갖는 삼단자형의 그래핀 소자를 제작하고 수직 전기장을 인가하면서 라만산란 특성을 조사하였다. 그래핀 소자의 제작은 통상의 HOPG(Highly Oriented Pyrolytic Graphite)로 부터 기계적인 방법을 사용하여 추출하였으며 300nm 두께의 실리콘 산화막이 형성된 고전도성 실리콘 기판에 배치하였다. 전극은 전자빔 식각 공정을 이용하여서 정의하였으며 전극소재로서 Cr/Au 이중층을 형성하였다. 상온 대기압 상태에서 게이트 전압 크기의 가변에 따른 3-D 라만 mapping 실험을 통해 운반자 농도, 페르미 준위에 따른 FWHM 변화와 최대 주파수 위치를 분석하여 전자-포논 결합 세기를 추출하였으며 이론적 결과와 비교하여 보았다.

**Dp-V-139****Crystal growth and luminescence properties of  $\text{Ce}^{3+}$  doped aluminum garnet****nanocrystals**

정 홍채, 박 진영, GANJI Seeta RamaRaju, 문 병기, 정 중현  
 부경대학교, 물리학과.

The general chemical structural formula for an oxide garnet can be written as  $\text{C}_3\text{A}_2\text{D}_3\text{O}_{12}$ , with eight of these formula units per unit cell. The remarkable properties of garnet-type compounds have stimulated a great deal of interest. Among the garnet compounds, yttrium aluminum garnet ( $\text{Y}_3\text{Al}_5\text{O}_{12}$ , YAG) is commonly known as a host material in various solid-state lasers. Cerium doped YAG (YAG:Ce) is a comprehensively studied which is used as a yellow-emitting component. A combination of a blue light emitting diode (LED) and yellow phosphor is a widely adopted type for a white light production because of its low fabrication cost and high luminous efficiency compared to the white LED mixed with red, green, and blue LED. However, a yellow-emitting YAG:Ce based white LED inherently suffer from poor color rendering properties due to the red spectral deficiency. For general indoor lighting application, “warm” white light is recommended. So, we need to improve the red content in the yellow-emitting YAG:Ce. In this work, cerium-doped aluminum garnet crystals were grown by using rare earth acetylacetonate, gallium acetylacetonate, and aluminum alkoxide as starting material.  $\text{RE}_3\text{Al}_2\text{Al}_3\text{O}_{12}$ ,  $\text{RE}_3(\text{REAl})\text{Al}_3\text{O}_{12}$ , and  $\text{RE}_3\text{Ga}_2\text{Al}_3\text{O}_{12}$  (RE = Y, Tb, Gd, Sm, Eu) nanocrystals were synthesized by solvothermal method at 300 °C. The as-prepared crystals were characterized by X-ray diffraction (XRD), filed emission scanning electron microscopy (FESEM), transmission electron microscopy (TEM), UV-Vis absorption, and photoluminescence (PL) spectra.

**Dp-V-140****Luminescence properties of  $\text{Ce}^{3+}$  doped  $\text{Y}_3(\text{Sb}_x\text{Al}_{2-x})\text{Al}_3\text{O}_{12}$  and  $\text{Gd}_3(\text{Sb}_x\text{Ga}_{2-x})\text{Al}_3\text{O}_{12}$  yellow phosphors for WLED**

정 홍채, 박 진영, GANJI Seeta RamaRaju, 문 병기, 정 중현  
 부경대학교, 물리학과.

Yttrium aluminum garnet ( $\text{Y}_3\text{Al}_5\text{O}_{12}$ , YAG) is commonly known as a host material in various solid-state lasers. Cerium-doped yttrium aluminum garnet is used as a phosphor for white light emitting diodes, while garnet structure has a critical disadvantage of low CRI (color rendering index). For general indoor lighting application, “warm” white light is recommended. So, nowadays many researchers focused their research on the improvement of red content in the  $\text{Ce}^{3+}$  doped YAG phosphor. The general chemical structural formula of an oxide garnet can be written as  $\text{C}_3\text{A}_2\text{D}_3\text{O}_{12}$ , with eight of these formula units per unit cell. The  $\text{C}_3\text{A}_2\text{D}_3\text{O}_{12}$  garnet structure can be interconnected, where  $\text{A}^{3+}$  ions occupy the octahedral site and  $\text{D}^{3+}$  ions occupy the tetrahedral site and  $\text{C}^{3+}$  ions occupy the dodecahedral site in their oxygen environment. The emission and excitation for  $\text{Ce}^{3+}$  doped garnet phosphors change through compositional modifications for dodecahedral, octahedral, and tetrahedral site. In this work, Synthetic compounds of  $\text{Ce}^{3+}$  doped  $\text{Y}_3(\text{Sb}_x\text{Al}_{2-x})\text{Al}_3\text{O}_{12}$  and  $\text{Gd}_3(\text{Sb}_x\text{Ga}_{2-x})\text{Al}_3\text{O}_{12}$  phosphors with cubic garnet structure have been prepared by solvothermal reaction method. The as-prepared phosphors were characterized by X-ray diffraction, filed emission scanning electron microscopy (FESEM), and photoluminescence (PL). The chromaticity coordinates of as-prepared phosphors have been calculated with Commission International De l'Eclairage (CIE) diagrams and the spectral tuning of as-prepared phosphors yellow emission is investigated.

**Dp-V-141****Rf Coupling and Random Telegraphic Noise for SAW-Driven Single Electron****Pump Device**

SEO Minky, KIM Nam<sup>1</sup>, WOO Byung-chill<sup>1</sup>, KIM Jinhee<sup>1</sup>, CHUNG Yunchul

*Pusan National University. <sup>1</sup>KRISS.*

Random telegraphic noise (RTN) and rf coupling effects are the main obstacles to observe quantized current plateau generated by SAW-driven single electron pump device. In order to reduce the rf coupling effects, major part of the spit gate electrode was replaced by a high impedance Cr meandering line to prevent rf pick-up signal delivered to the spit gate section. We expect reduced rf pick-up by gate electrodes due to impedance mismatching. We also adopted bias cooling method in order to decrease RTN observed quite often in GaAs/AlGaAs two-dimensional electron system.

**Dp-V-142****The T2-Weighted Magnetic Resonance Images by using Dextran- and Chitosan-****Coated Ferrite Nanoparticle Contrast Agents**

HONG Sungwook, CHANG Yongmin<sup>1</sup>, RHEE Ilsu<sup>2</sup>

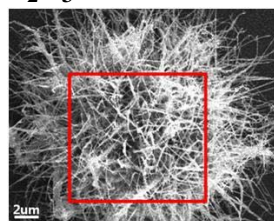
*Division of Science Education, Daegu University. <sup>1</sup>Department of Diagnostic Radiology, College of Medicine, Kyungpook National University and Hospital. <sup>2</sup>School of Physics and Energy Sciences, Kyungpook National University.*

Ferrite (Fe<sub>3</sub>O<sub>4</sub>) nanoparticles coated with dextran and chitosan, respectively, were synthesized for use as an MRI (magnetic resonance imaging) contrast agent. The mean diameter of the dextran- and chitosan-coated ferrite nanoparticles were about 36.63nm and 67.0nm, respectively. The hydrogen bond between polymers and the ferrite nanoparticles was checked by and FT-IR spectrometer. And their appearances were confirmed by high resolution TEM. The effects of the ferrite nanoparticles as a contrast agent were investigated by comparing MR image before and after the injection of coated ferrite nanoparticles as contrast agent into the liver of New Zealand white rabbit. We found that the average decrease values of the signal intensity due to dextran- and chitosan-coated contrast agent were 35.2% and 31.7%, respectively.

**Dp-V-143****Analysis of gallium oxide nuclei for  $\text{Ga}_2\text{O}_3$  nanowire grown by VS growth****mechanism**

정 창희, 권 남오, 권 명희  
인천대학교 물리학과.

$\text{Ga}_2\text{O}_3$  nanowires were synthesized on glass by thermal evaporation of gallium powder in the Ar atmosphere. Well crystallized white nanowires were grown on black oxide gallium macro/nanoscaled nuclei. High-resolution transmission electron microscopy (HRTEM), selected area electron diffraction (SAED) and X-ray diffraction (XRD) observations suggest that these synthesized nanowires have a single-crystalline structure with a diameter of few tens nanometer and length of microns by vapor-solid (VS) mechanism. We analysis oxide gallium cluster and discuss possible growth mechanism of  $\text{Ga}_2\text{O}_3$  nanowire.

**Dp-V-144****Linear Prediction by Singular Value Decomposition on Coherent Lattice****Vibrations in Small Diameter Single-Wall Carbon Nanotubes**

한 혜선, 한 현택, 이 기주<sup>1</sup>, 주 태하<sup>2</sup>, J. Kono<sup>3</sup>, 임 용식

건국대, 신소재과학부 나노과학기술. <sup>1</sup>충남대, 물리학과. <sup>2</sup>포항공대, 화학과. <sup>3</sup>Rice Univ..

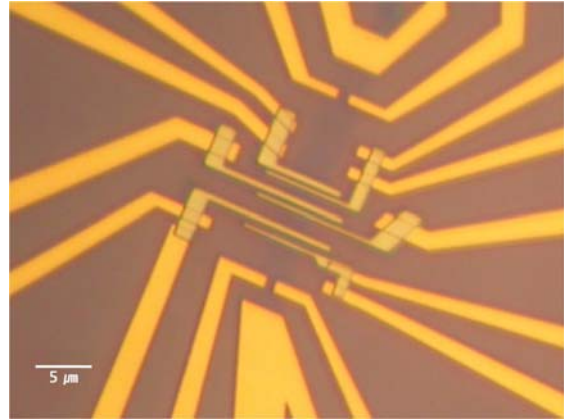
We report the generation and the detection of coherent lattice vibrations in micelle-suspended CoMoCAT single-walled carbon nanotubes (SWNTs) corresponding to the radial-breathing mode (RBM) using ultrashort laser pulses. We performed degenerate pump-probe measurements in a quartz cell using  $\sim 50$  fs pulses from a mode-locked Ti:Sapphire laser with a bandwidth of  $\sim 35$  nm and a tuning range from 710 nm to 840 nm in 5-nm step. In stark contrast to HiPco SWNTs, coherent lattice vibrations of CoMoCAT SWNTs show five and ten RBMs resonantly excited by the  $E_{11}$  optical transition as well as the  $E_{22}$  optical transition, respectively. We also performed a linear prediction based on singular value decomposition (LPSVD) to analysis active vibration modes. This method shows better results on relative comparison between the  $E_{11}$  and  $E_{22}$  transitions than for a fast Fourier-transform method. It shows that  $(n-m) \bmod 3 = +1$  nanotubes have less intensity than two times strength of  $(n-m) \bmod 3 = -1$  nanotubes due to specific narrow bandwidths for the  $E_{11}$  transitions, We will discuss on the relative vibration strength and each resonance bandwidths of all active modes, which is inaccessible with cw Raman scattering for chiral assignment of nanotubes.

**Dp-V-145****그래핀에서 일어나는 스핀 수송 특성**

엄 중화, 오 영만, 구 현철<sup>1</sup>, 한 석희<sup>1</sup>

세종대학교 물리학과, <sup>1</sup>한국과학기술연구원 스핀트로닉스 연구단.

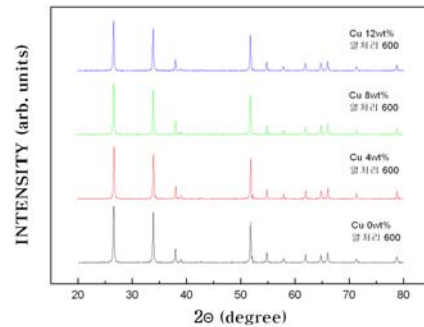
강자성(Co) 금속과 그래핀으로 이루어진 나노 크기의 spin valve 소자(Co/Graphene/Co)를 제작하고 그래핀에서의 스핀 축적에 관한 연구를 하였다. 아래 그림은 제작된 그래핀 스핀소자의 광학현미경 사진이며, 소자의 제작 공정은 다음과 같다. 원자 하나 두께의 탄소 단일 층인 그래핀을 얻기 위해 스카치 테이프를 이용하여 graphite로부터 기계적인 박리 작업을 통해 표면이 SiO<sub>2</sub> 산화 층으로 형성된 실리콘 기판 위에 그래핀을 추출해냈다. 그래핀을 중심으로 contact pad를 형성하기 위해 광 식각 공정을 거친 후 Cr/Au(50Å/250Å)박막을 thermal 및 e-beam evaporator을 이용하여 증착하였다. 다음으로 그래핀을 원하는 모양으로 만들기 위해 전자 빔 식각 공정을 한 후 Ar-milling을 하였다. Inner pad를 형성하기 위해 전자 빔 식각 공정을 거쳐 Cr/Au(35Å/500Å)박막을 증착 하였으며, 다시 한번 전자 빔 식각 공정을 통해 Co(800Å)를 증착 시켜 강자성 전극을 형성하였다. 두 강자성 전극의 보자력 차이를 주기 위해 강자성체(FM)의 폭을 각각 0.2μm, 0.4μm의 크기로 제작하였으며, 두 강자성체 전극 사이의 거리를 0.6μm에서 1.5μm정도로 여러 가지 소자를 제작하였다. 완성된 소자 구조에서는 local spin valve 효과, non-local spin valve 효과 등을 효과적으로 측정할 수 있었다.

**Dp-V-146****CuO를 첨가한 SnO<sub>2</sub> 후막가스 센서의 특성.**

이 지영, 신 덕진, 이 돈규<sup>1</sup>, 유 일

동의대학교 물리학과(부산IT융합부품연구소), <sup>1</sup>동의대학교 전기공학과(부산IT융합부품연구소).

CuO를 부착한 SnO<sub>2</sub> 감지물질은 출발 물질로 SnO<sub>2</sub>(Kojundo, 순도 99.9%, 입자 1μm), CuO(Dae jung)를 사용하였다. CuO의 농도를 0~12 wt% 변화시켜 증류수 200 ml에 녹인 후 교반된 SnO<sub>2</sub>에 첨가하여 5분간 교반 하였다. 그리고 NH<sub>4</sub>OH를 2~3방울 정도 떨어뜨린 후 10분 정도 교반하여 Cu가 부착된 SnO<sub>2</sub> 분말을 준비하였다. 만들어진 분말을 80℃에서 8시간 건조 후, 열처리 온도를 500, 600, 700℃까지 변화 시켜 SnO<sub>2</sub>:Cu 분말을 얻었다. SnO<sub>2</sub>:Cu가 스센서용 감지물질은 알루미나 기판에 스크린 프린터를 이용하여 후막으로 제조하였고, 열처리 온도에 따른 특성을 XRD, SEM등을 측정을 하였다.



**Dp-V-147****Effect of Hydrogen Plasma Treatment on a-IGZO Thin Film**

KIM Won-Kyung, LEE Seunghun<sup>1</sup>, KIM Taeyoung<sup>2</sup>, JEONG Se-Young<sup>1</sup>

*Dept. of Cogno Mechatronics, Pusan National University, Miryang, 627-706. <sup>1</sup>Dept. of Nano Fusion Technology, Pusan National University, Miryang, 627-706. <sup>2</sup>Dept. of Nanomaterials Engineering, Pusan National University, Miryang, 627-706.*

Since the superior semiconductor characteristics of amorphous InGaZnO (a-IGZO) were reported, intensive researches have been carried out to replace a-Si:H based devices[1]. Especially, the high electrical and optical properties of a-IGZO is considered to be suited for channel material of flexible transparent thin film transistors (TTFTs). However, the low carrier mobility has been an obstacle to realize a-IGZO based display devices. In order to enhance electrical properties of a-IGZO based devices, many researches have improved device structure, but the intrinsic low mobility is still remained as a difficult problem. In this work, we studied enhancement of the electrical properties at a-IGZO by using hydrogen doping which is well known for n-type shallow donor. Especially, it has been reported that hydrogen can enhance the carrier concentration and the mobility on ZnO. We investigated the change of structural, optical, and electronic characteristics of a-IGZO thin films depending on hydrogen injection by RF plasma treatment. In results, it was found that the strong hydrogen plasma process induced the crystallization of In in a-IGZO. In order to enhance the electrical properties without any secondary phase in a-IGZO, we developed the several hydrogen injection methods, which can enhance the mobility. [1] K. Nomura, H. Ohta, A. Takagi, T. Kamiya, M. Hirano, and H. Hosono, *Nature* 432, 488 (2004)

**Dp-V-148****Oxygen plasma effects on the electrical properties of single-walled carbon****nanotube bundles**

김 상훈, 김 호중, 이 형락<sup>1</sup>, 송 정훈<sup>2</sup>, 이 삼녕<sup>3</sup>, 하 동한

*한국표준과학연구원. <sup>1</sup>경북대학교. <sup>2</sup>공주대학교. <sup>3</sup>한국해양대학교.*

We aligned semiconducting SWCNTs between two electrodes with a gap of 8 micrometers using the AC dielectrophoresis method and investigated the effects of oxygen plasma treatment on the electrical properties of the device in the low bias-voltage regime. Raman spectroscopy verified that the plasma treatment increased the number of structural defects on the CNT surfaces, but the number of newly created defects was not enough to induce noticeable changes in the carrier concentration and tube-tube interactions. The resistance dependence on the plasma treatment time was well-fitted to an exponential equation, confirming the linear increase of the number of defects as a function of the plasma treatment time. We discussed the resistance behavior on the basis of the strong Anderson localization of electron states at structural defects. Moreover, we also showed that a small number of defects can remarkably enhance the sensitivity of the device to NH<sub>3</sub> molecules by forming strong bonds between the defects and NH<sub>3</sub> molecules that are mediated by oxygen species. We expect that the plasma treatment of SWCNTs will be a useful and non-contaminating tool to tune SWCNTs to have the necessary properties for the various potential applications.

**Dp-V-149****Fabrication of turnstile pump using Ni nano-crystal as metallic island with Al as superconducting electrodes.**김 소라, 김 범규<sup>1</sup>, 김 진희, 우 병철, 김 남한국표준과학연구원, 전라기술연구부, <sup>1</sup> 전북대학교, 물리학과.

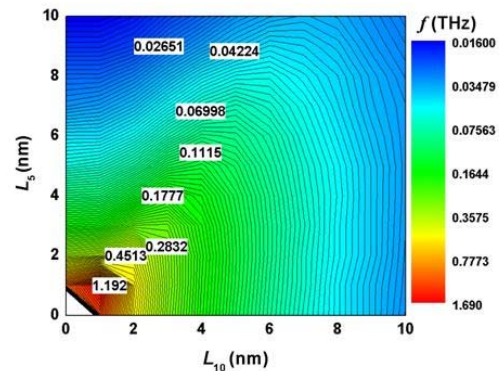
Novel type of NSN (normal metal-superconductor-normal metal) turnstile pump was reported by Pekola's group[1] to be one of promising electron pumps for the realization of the quantum metrology triangle. We wanted to apply this idea of the NSN turnstile pump to SFS (superconductor-ferromagnet-superconductor) type device where Ni nano-crystal of size of 100 ~ 300 nm diameter was used as ferromagnetic island and Al for electrodes. We expect to explore spin effects as well as improvement in speed of the device because of the reduced capacitance compared to Pekola's NSN pump. [1] Pekola, J. et al. Hybrid single-electron transistor as a source of quantized electric current. Nature Physics 4, 120 (2008).

**Dp-V-150****Inter-Wall Length Dependence of Double-Wall Carbon Nanotube Resonators**

KANG JEONG WON

충주대학교 컴퓨터공학과.

This presentation introduced the fundamental frequency change of a cantilevered DWCNT resonator with different inter-wall lengths. When the length of the inner or outer wall is controlled, various frequency devices can be realized by a single type of DWCNT with walls of equal length. For a DWCNT resonator with a short outer wall, the free edge of the short outer wall plays an important role in the vibration of the long inner wall. Therefore, all three boundaries, fixed, free, and semi-free conditions, are very important factors for understanding their operations. For a DWCNT resonator with a short inner wall, the short inner wall can be considered as a flexible core, thus, the fundamental frequency is influenced by its length.



**Dp-V-151****Water-Assisted Synthesis of Vertically Aligned Carbon Nanotubes(VACNTs) with Sub-centimeter Height in Low Pressure Chemical Vapor Deposition(LPCVD)**

KIM sangyong, LEE soonil, KOH kenha

*Division of Energy Systems Research, Ajou University.*

The effect of water-assistance in synthesis of VACNTs using a LPCVD method was studied. To compare with water-assisted synthesis, we investigated growth factors of VACNT film such as pressure, temperature and a supply rate of carbon feedstock without supply of water vapor. Water assisted synthesis was carried out by adding water vapor at the best growth condition without water. Supply of water vapor was precisely controlled using a variable leak valve and adjusting temperature of a water reservoir. As a result, VACNT films with 8 mm height were synthesized for two hours. The grown VA-CNT films were characterized by scanning electron microscopy (SEM), transmission electron microscopy (TEM), and Raman spectroscopy. In short, we investigated how water assistance affects important CNT-growth factors, such as life time of catalyst and growth rate of CNT films in a LPCVD process.

**Dp-V-152****탄소 나노튜브를 이용한 단전자 펌프 소자 제작**김 범규, 김 소라<sup>1</sup>, 김 주진, 김 남<sup>1</sup>*전북대학교, 물리학과, <sup>1</sup>한국표준과학연구원, 전략기술연구부*

탄소 나노튜브 트랜지스터(CNT)와 IDT (inter-digitized transducer)로 구성된 단일 전자펌프 소자를 제작하였다. IDT에 rf 신호를 인가하면 기판의 압전효과에 의해서 표면탄성파 (SAW, surface acoustic wave)가 발생되는데, SAW에 의해 형성된 주기적인 전기 포텐셜에 전자가 포획되어서 양자화된 전자 수송이 이루어진다. 따라서, 양자화된 전류의 크기는  $I = nef$  ( $n$ =포획된 전자의 갯수,  $e$ =전자의 전하량,  $f$ =SAW 주파수)라는 관계식을 보일 것으로 예상된다. 소자 기판으로는 압전효과가 우수한 켄트 기판 (42.75°, Y-cut quartz)이 사용되었다. 측정된 IDT의 공진 주파수  $f_0$ 는 약 2.1 GHz 이었고, 이는  $f_0 = l/v_s$  라는 관계식과 잘 일치한다. 여기서  $l = 1.5 \mu\text{m}$ ,  $v_s = 3200 \text{ ms}^{-1}$ . CNT 소자 제작에 사용된 기술은 일반적인 화학증착법(CVD)과 나노 리소그라피 기술이다.

**Dp-V-153****Thermal Conductance Measurement of Metal-CNT Composites Using Micro-sized Suspended Structure**

CHO Myung Rae, CHO Sung Un, PARK Yun Daniel

*Department of Physics and Astronomy, Seoul National University.*

Thermal properties of CNTs and their composite materials have been studied intensively, as CNTs are well known to possess excellent thermal transport properties [1-5]. Especially, thermal conductivity of CNTs is much larger than that of metals such as Ag, Au, Cu and Al. We expect that incorporating CNT network into metallic thin film would improve thermal conductivity of the resulting composites. Due to the significant difference in between thermal transport mechanism of metallic thin films and that of CNTs, temperature dependence of thermal conductivity would show considerable distinction between metal only sample and metal-CNT sample. Moreover, since metallic thin films have different wetting properties on CNT surface, the interaction between metallic thin films and CNTs can be investigated by comparing different enhancements in thermal conductance. Here, we present the fabrication and measurement for the investigation of the thermal conductance of Pd-CNT and Al-CNT nanocomposites. We have realized micron-size suspended structures, thermal links made of metal-only or metal-CNT composite and the two thermometers, by using e-beam lithography and selective etching. With careful DC steady-state measurement in closed cycle cryostat, we have observed remarkable enhancement of the thermal conductance by incorporating less than 1% (in volume) of CNT into metallic thin films. We will also present temperature dependence of thermal conductivity as a means to distinguish metallic thin-film contributions (electron) and CNT (phonon). [1] J.A. Eastman *et al.*, Appl. Phys. Lett. 78, 718 (2001)[2] S.U.S. Choi *et al.*, Appl. Phys. Lett. 79, 2252 (2001)[3] M.J. Biercuk *et al.*, Appl. Phys. Lett. 80, 2767 (2002)[4] R. Ramasubramaniam *et al.*, Appl. Phys. Lett. 80, 4647 (2003) [5] H.Q. Xia *et al.*, Appl. Phys. Lett. 94, 4967 (2003)

**Dp-V-154****Calcium-hydroxyl group complex for potential hydrogen storage media: A density functional theory study**

CHA Moon-Hyun, NGUYEN Manh Cuong, LEE Yealee, BAE Jaehyun, IM Jino, PARK Changwon, KIM Youngkuk, CHOI Keunsu, KIM Gunn, IHM Jisoon

*Department of Physics and Astronomy, Seoul National University.*

Using density functional theory electronic structure calculations, we investigate the calcium-hydroxyl group complex for potential applications to the hydrogen storage at near ambient temperature and pressure. The Ca atom is bound to the hydroxyl group with a binding energy comparable to the cohesive energy of bulk Ca, and we find that each Ca atom binds up to seven H<sub>2</sub> molecules in the molecular form. Binding of an unexpectedly large number of H<sub>2</sub> molecules is attributed to the fact that d orbitals of Ca positive ions are downshifted and partially occupied, thereby validating the empirical 18-electron rule as in the transition metal atoms. The binding energy turns out to be similar to 0.1 eV/H<sub>2</sub>, somewhat smaller than the requirement ( $\geq 0.2$  eV/H<sub>2</sub>) of the room-temperature application. We also show that an important bonding mechanism of H<sub>2</sub> molecules on Ca is the polarization, namely, the electric dipole moment of H<sub>2</sub> induced by the partially ionized Ca. Based on this result, the possibility of the organic material functionalized with hydroxyl groups for a hydrogen storage medium is discussed.

**Dp-V-155****C<sub>60</sub> 분자를 포함한 Polymethyl methacrylate 고분자 박막을 사용하여 제작한 비휘발성 메모리 소자**

윤 동열, 곽 진구, 정 재훈, 김 태환

한양대학교, 전자컴퓨터통신공학과.

C<sub>60</sub> 분자는 높은 전자 친화도에 의해 전자를 포획하는 능력이 우수하기 때문에 비휘발성 메모리 소자의 저장 매체로 응용하는 연구가 활발히 진행되고 있다. C<sub>60</sub> 분자를 절연성 고분자인 polymethyl methacrylate (PMMA) 박막에 분산시키고, 분산된 C<sub>60</sub> 분자를 저장 매체로 사용하는 유기 쌍안정성 소자에 전기적인 특성을 관찰하였다. 소자를 제작하기 위해 C<sub>60</sub> 분자를 용매인 톨루엔에 녹이고, PMMA를 용매인 테트라히드로푸란에 녹인 후, 초음파 교반기를 사용하여 두 물질이 용매에 고르게 섞어 C<sub>60</sub> 분자와 PMMA 용액을 제작하였다. 그 후 C<sub>60</sub> 분자와 PMMA가 녹아 있는 두 용액을 PMMA에 대한 C<sub>60</sub> 분자의 조성비가 5 wt%와 10 wt%의 비율로 혼합하였다. SiO<sub>2</sub> 기판위에 Al을 하부 전극으로서 열증착하고, 그 위에 C<sub>60</sub> 분자와 PMMA 혼합 용액을 스핀 코팅하고 열을 가해 용매를 제거하여 고분자 박막을 형성하였다. C<sub>60</sub> 분자가 분산되어 있는 PMMA 박막위에 Al을 상부 전극으로서 열증착하여 소자를 제작하였다. 전류-전압 특성 결과는 동일 전압에서 낮은 전도도 (OFF 상태)와 높은 전도도 (ON 상태)가 나타나는 전류 쌍안정성 특성을 보여주었다. 제작된 소자는 초기에 OFF 상태로 유지하다 2 V 이상의 전압이 인가되면 전도도가 갑자기 증가하여 ON 상태가 된다. ON 상태는 외부 전압이 차단해도 계속 유지되며, -3 V의 전압이 인가되면 다시 OFF 상태로 환원된다. C<sub>60</sub> 분자가 없이 PMMA 박막으로만 구성된 소자는 쌍안정성 특성이 나타나지 않았다. 따라서, 본 기억 소자의 전류 쌍안정성과 관련된 기억 특성은 PMMA 고분자 박막안에 포함된 C<sub>60</sub> 분자에 의한 것임을 알 수 있다. C<sub>60</sub> 분자 농도가 증가할수록 OFF 상태의 전압은 낮아지고, 그 결과 ON/OFF 전류 비율이 증가하였다. 이와 같은 결과는 PMMA 박막안에 분산된 C<sub>60</sub> 분자의 농도를 조절함으로써 차세대 비휘발성 메모리 소자의 기억용량을 조절할 수 있음을 보여준다. This work was supported by the Korea Science and Engineering Foundation(KOSEF) grant funded by the Korea government(MEST) (No. R0A-2007-000-20044-0).

**Dp-V-156****Spin-dependent transport on Graphene Nanoribbon with magnetic impurities**

KIM kyung Yeon, CHOI Hyoung Joon

Department of Physics and IPAP, Yonsei University.

We calculate the electronic transport properties of graphene nanoribbon (GNR) focusing on the effect of magnetic impurities by using first-principles calculations. In zigzag GNRs, the edge states play an important role since the electron density is localized mostly at the edges and these states can be either antiparallel or parallel. In zigzag GNRs, generation of net spin-polarized current is examined by breaking the symmetry of the magnetic moments with magnetic impurities, such as 3d transition metals (Mn, Fe, Co, and Ni). We use density functional theory within the local spin density approximation for the exchange-correlation energy, norm-conserving semicore pseudopotentials, and pseudo-atomic orbital basis set. The electrical transport properties of zigzag GNRs are calculated using the scattering-state method for quantum conductance. Effects of magnetic impurities on transport properties in armchair GNRs are also studied. This work was supported by the KRF (KRF-2007-314-C00075) and by NRF of Korea (Grant No. 2009-0081204). Computational resources have been provided by KISTI Supercomputing Center (KSC-2008-S02-0004).

**Dp-V-157****단일벽 탄소나노튜브의 산 처리에 의한 특성 변화**

정 희성, 권 봉준, 권 향명, 임 종혁, 안 영환, 이 순일, 박 지용

아주대학교 에너지 시스템학부 응용물리학 전공.

단일벽 탄소나노튜브(single-walled carbon nanotube, SWCNT)는 우수한 전기적, 기계적, 열적 특성으로 다양한 응용분야에서 연구되고 있는 1차원 나노물질이다. SWCNT는 응용 분야에 따라 다양한 화학적 처리를 통해 특성을 변화시킬 수 있는데, 산처리를 통한 단일벽 탄소나노튜브의 정제가 그 한 예다. 이러한 화학적 처리는 SWCNT의 벽에 흡착되거나 공유결합을 형성하여 SWCNT에 결함을 형성하거나 화학적인 도핑 효과로 나타나게 되어 그 전기적 특성에 큰 영향을 미칠 수 있는 것으로 알려져 있다. 본 연구에서는 화학 기상증착법으로 성장시킨 SWCNT에 전극을 형성시킨 소자를 제작한 후, 질산, 염산, 황산 등의 산에 담그거나 증기를 쏘여, 산처리 전후의 전도특성 변화를 I-V<sub>G</sub> 측정을 통해 조사하였다. 질산증기를 통한 처리이후에 대부분의 SWCNT네트워크소자는 on-state 전류가 향상되고, on-off비가 떨어지는 양상을 보여주었다. 이와 같은 거시적인 전기적 특성의 변화와 동시에 원자힘현미경 (AFM, Atomic Force Microscope)을 이용한 정전기힘현미경 (EFM, electrostatic force microscopy)와 주사게이트현미경 (SGM, scanning gate microscopy)법을 적용하여, 소자의 국소적인 전압분포의 변화와 게이트 특성의 변화를 측정하였다. 질산처리 후 SWCNT간의 접촉저항의 향상, 결함의 제거와 같은 소자 내부의 변화를 볼 수 있었다.

**Dp-V-158****Alkali metal 흡착밀도에 따른 그래핀 특성변화**

진 경환, 최 선명, 지 승훈

포항공대 물리학과.

큰 carrier mobility와 적은 impurity scattering 성질을 갖고 있는 그래핀은 electronic device응용을 위해 많은 연구가 진행중에 있다. 그 뿐만 아니라 촉매, 수소저장 물질로도 각광을 받고 있다. 이러한 연구에 있어서 금속과의 접합, 또는 금속원자의 흡착성질에 대한 연구는 매우 중요하다. 본 연구에서는 제일원리 계산을 통해 Alkali metal 흡착밀도 변화에 따른 그래핀의 특성변화를 조사하였다. Alkali금속 원자가 그래핀 표면에 흡착될 경우 그래핀의 hexagon 중앙(hollow site)에 위치하는 것이 가장 안정적이며 금속원자의 최외각 전자가 그래핀으로 옮겨가는 것을 확인하였다. 옮겨간 전자수는 그래핀의 Fermi level변화를 통해서 계산하였다. 또한 전송된 전자수는 금속원자의 흡착밀도와 밀접한 관련이 있었고, 이러한 현상은 '전송된 전자수에 따른 energy gain의 최대화'를 통해 설명하였다.

**Dp-V-159****라만 이미징 분광법을 통한 그래핀의 가장자리 형태 판별**

우 승우, 윤 두희, 문 혜림, 정 현식

서강대학교, 물리학과

그래핀은 이차원 구조를 가진 물질로서 전기 전도도와 기계적 유연성이 다른 물질에 비해 우수하여 차세대 나노 전자 및 디스플레이 소자 물질로 각광받고 있다. 이러한 그래핀이 층층이 쌓여있으면 3차원 구조의 흑연, 튜브 형태로 말려있으면 1차원 구조의 탄소나노튜브가 되고, 공모양으로 뭉쳐져 있으면 0차원 구조의 풀러린이 된다. 탄소원자들이 벌집 구조형태로 구성되어 있는 그래핀의 가장자리는 두가지 형태로 나뉘어지는데 그 형태에 따라서 암체어(*armchair*) 또는 지그재그(*zigzag*)라 부른다. 폭이 매우 좁은 형태의 그래핀 나노리본은 양자효과와 가장자리의 형태에 따라 전기적 특성이 달라지기 때문에 가장자리의 형태를 구분하는 연구는 매우 중요하다. 본 연구에 사용된 그래핀 시료는 천연 흑연으로부터 스카치 테이프를 이용하여 단 원자층의 그래핀을 벗겨 내어 300 nm의 실리콘 산화막이 덮여 있는 실리콘 기판 위에 제작되었다. 그래핀의 가장자리에서는 라만 D 밴드( $\sim 1345 \text{ cm}^{-1}$ )의 세기가 입사빔의 편광방향에 의존하는데, 그 정도가 가장자리 형태에 따라서 다르게 나타난다. 본 연구에서는 편광된 마이크로 라만 분광법을 이용하여 가장자리에서의 라만 D 밴드의 편광 의존성을 알아 보았다.

**Dp-V-160****Study on Effect of Uniaxial Strain on Graphene by Raman Spectroscopy**YOON DUHEE, MOON HYERIM, WOO SEOUNGWO, SON YOUNG-WOO<sup>1</sup>, CHEONG HYEONSIKDepartment of Physics, Sogang University. <sup>1</sup>Korea Institute for Advances Study.

Graphene has attracted immense interest from researchers in various disciplines because of its novel electronic properties, such as high carrier mobility and massless Dirac fermions. Various studies have shown the possibility of using graphene in electronics, spintronics, and display devices. Engineering of strain is sometimes useful in controlling the electronic or mechanical properties of materials. Recently, several experiments and theoretical calculations investigated the effect of strain on single layer graphene by bending graphene samples on flexible substrates. They proposed the possibility to control the properties of graphene by the strain. In this work, we investigate the uniaxial strain effect on single layer graphene by using Raman spectroscopy. We deposited graphene samples on acrylic substrates coated with SU-8 by micro-mechanical cleaving method. Raman spectra were obtained as a function of the uniaxial strain. The peak position and shape of *G* and *2D* bands vary significantly as the strain increases.

**Dp-V-161****SnO<sub>2</sub> 나노 입자를 포함한 Poly(methyl methacrylate)층을 사용하여 제작한 유기 쌍안정성 소자의 메모리 효과**

곽 진구, 윤 동열, 정 재훈, 이 대욱, 손 동익<sup>1</sup>, 김 태환

한양대학교 전자통신컴퓨터공학과, <sup>1</sup>한양대학교 정보디스플레이공학과

비휘발성 기억 소자 중에서 유기 쌍안정성 소자는 간단한 구조와 단순하고 저렴한 공정 과정에 의해 생산성이 높고 고집적이 용이하다는 장점으로 많은 연구가 진행되고 있다. 유기물/무기물 나노 복합체를 사용한 유기 쌍안정성 소자 제작에 대한 연구는 많이 진행되어 왔지만, SnO<sub>2</sub> 나노 입자를 포함한 고분자층을 사용하여 제작한 유기 쌍안정성 소자에 대한 연구는 거의 진행되지 않았다. SnO<sub>2</sub> 나노 입자를 포함한 Poly(methyl methacrylate)(PMMA)층을 사용하여 제작된 유기 쌍안정성 소자의 메모리 특성에 대한 관찰을 수행하였다. 기억 소자를 제작하기 위해 나노 입자의 원료가 되는 Tin 2-ethylhexanoate (95%) 2.4 mmol을 dibutyl ether (99.3%) 10 ml 에 용해시킨 다음, 용액을 화학적인 처리를 거쳐 용매 안에서 SnO<sub>2</sub> 나노 입자를 합성하였다. 용매로부터 추출된 SnO<sub>2</sub> 나노 입자 1 wt%와 100 mg의 PMMA 를 2ml 의 클로로벤젠에 용해시켜 고분자 용액을 제작하였다. 하부 전극이 되는 Indium Tin Oxide 기판 위에 고분자 용액을 스핀 코팅하고, 열을 가해 용매를 제거하여 SnO<sub>2</sub> 나노 입자가 분산되어 있는 PMMA 박막을 형성한다. 그 위에 Al 전극을 열증착하여 기억 소자를 완성하였다. 제작된 유기 쌍안정성 소자의 전류-전압 측정 결과에서는 소자의 기억 특성을 나타내는 전류의 히스테리시스 특성이 나타났다. SnO<sub>2</sub> 나노 입자가 있는 기억 소자에서는 동일 전압에서 낮은 전류가 흐르는 OFF 상태와 높은 전류가 흐르는 ON 상태가 뚜렷이 구별되었다. 그러나, SnO<sub>2</sub> 나노 입자가 없이 PMMA 박막으로 구성된 소자에서는 히스테리시스 특성이 나타나지 않는다. 따라서 PMMA층 안에 삽입된 SnO<sub>2</sub> 나노 입자가 유기 쌍안정성 소자의 메모리 효과에 큰 영향을 준 것을 알 수 있었다. 소자에 대한 전류-시간 측정 결과는 소자의 ON/OFF 비율이 시간에 따라 큰 감쇠현상이 없이 1000번 까지 지속적으로 유지됨을 알 수 있었다. This work was supported by the Korea Science and Engineering Foundation (KOSEF) grant funded by the Korea government (MEST) (No. R0A-2007-000-20044-0).

**Dp-V-162****Dependence of Raman spectrum of graphene on excitation laser power**

MOON Hyerim, YOON Duhee, WOO Seongwoo, CHEONG Hyeonsik

Department of Physics, Sogang University.

Graphene has a 2 dimensional hexagonal structure of carbon atoms. The thickness of monolayer graphene is about 0.34 nm. The number of graphene layers, the thermal conductivity of graphene, the influence of the substrate, and the doping effect have been investigated using Raman spectroscopy. Although Raman spectroscopy is widely used as a standard characterization tool, the excitation laser power varies for each experiment. Therefore, we measured the Raman spectrum of a single-layer graphene samples with various excitation laser power. The graphene samples were isolated from a graphite flake using micromechanical cleavage with adhesive tape. The 514.5 nm line of an Ar ion laser was used as the excitation source. The Raman G mode, corresponding to the Raman active E<sub>2g</sub> mode, was observed at ~1580 cm<sup>-1</sup>, and the 2D mode due to double resonance Raman scattering was observed at ~2680 cm<sup>-1</sup>. The frequencies of the G and 2D modes vary as functions of the excitation laser power, and the intensity ratio(2D/G) also varies as a function of the excitation laser power.

**Dp-V-163****Synthesis, luminescence characteristics of Bi<sup>3+</sup> ions co-doped Gd<sub>2</sub>O<sub>3</sub>:Eu<sup>3+</sup>****phosphors by solvothermal method**CHUNG Jong Won, JEONG Jung Hyun, JANG Ki-wan<sup>1</sup>, LEE Ho Sueb<sup>1</sup>, YI Soung Soo<sup>2</sup>*Department of Physics, Pukyong National University. <sup>1</sup>Department of Physics, Changwon National**University. <sup>2</sup>Department of Electronic Materials Engineering, Changwon National University.*

Nanoparticle materials have been the subject of increased scientific interest, both for fundamental research and for a wide area of application. This interest has arisen for various reasons. The large surface-to-volume ratio in nanoparticles can have a significant impact and influence on their physical properties compared to their bulk counterparts. The tendency for ever-smaller electronic devices opens the possibility for the use of nanoparticles. In addition, small particles are increasingly used in various medical applications, such as drug targeting, magnetic fluid hyperthermia, magnetic resonance imaging and others. In particular, Gadolinium oxide (Gd<sub>2</sub>O<sub>3</sub>) is an attractive host lattice for several lanthanide ions to produce efficient phosphors emitting a variety of colors. Eu<sup>3+</sup>-activated Gd<sub>2</sub>O<sub>3</sub> phosphors have been extensively studied for long time. Recently, Gd<sub>2</sub>O<sub>3</sub>:Eu<sup>3+</sup> phosphor has been considered as one of the better phosphor candidate for flat panel displays (FPDs) owing to its good color purity. The Bi<sup>3+</sup> ions have attracted much attention, because Bi<sup>3+</sup> ions play an important role as an activator or as a sensitizer in phosphors. It is well known that Bi<sup>3+</sup> ion is post transition metal ion with configuration of 6s<sup>2</sup>, which consists of a strong broad absorption due to <sup>1</sup>S<sub>0</sub>-<sup>3</sup>P<sub>0</sub> transition in UV region. From the literature, it is clear that the Bi<sup>3+</sup> ions have been studied as a host and also an activator, however, a very few reports have been found on the luminescent properties of Bi<sup>3+</sup> co-doped with Eu activator. The purpose of this study is to compare the luminescence properties of Bi<sup>3+</sup> ions co-doped Gd<sub>2</sub>O<sub>3</sub>:Eu<sup>3+</sup> nsophosphors which were synthesized at Bi<sup>3+</sup> ions concentration.

**Dp-V-164****Semi-metallic Kondo lattice observed in a single-crystalline Fe<sub>1-x</sub>Co<sub>x</sub>Si nanowire**이 성훈, 인 준호<sup>1</sup>, 장 정원<sup>2</sup>, 서 관용<sup>1</sup>, 정 명화<sup>3</sup>, 김 진희<sup>2</sup>, 김 봉수<sup>1</sup>*KAIST, KRISS. <sup>1</sup>KAIST. <sup>2</sup>KRISS. <sup>3</sup>Sogang University.*

A ternary formation of magnetic materials formed by doping has long been a subject of interests due to their peculiar electric and magnetic properties, in conjunction with the novel characteristics exhibited by parent materials. CoSi is known as diamagnet and FeSi is an archetypal material showing the Kondo effect, whereas Fe<sub>1-x</sub>Co<sub>x</sub>Si has shown unconventional ferromagnetic properties and not been interpreted by the Kondo model. We report unconventional magneto-transport properties of individual Fe<sub>1-x</sub>Co<sub>x</sub>Si nanowires through electric and magnetic measurements. By employing Kondo lattice model, we successfully explained temperature-dependent resistivity curve, and identified the Kondo temperature, the coherent Fermi-liquid temperature, and the Curie temperature. We also propose a semi-metallic two-carrier model to explain the positive magneto-resistance and its temperature dependence. The angle-dependent magneto-resistance shows a pronounced anisotropic behavior at low temperatures. The absence of hysteresis for the anisotropic magneto-resistance curve confirms the helical magnetic ordering below the Curie temperature. Relatively high MR ratio and AMR of the Fe<sub>1-x</sub>Co<sub>x</sub>Si nanowire suggest that it can be used for a high speed magnetic information storage, magnetic sensor, or spintronic devices.

**Dp-V-165****Raman Mapping of Epitaxial Lateral Overgrown GaN**

송 지선, 김 진흥, 노 희석, 주 진우<sup>1</sup>, 이 인환<sup>1</sup>

전북대학교, 물리학과. <sup>1</sup>전북대학교, 신소재공학부.

측면 방향으로 에피 성장된 GaN 박막의 공간 분해된 라만 산란 실험 결과를 보고한다. 성장된 시료는 본질적으로 비균질적인 결정구조를 지닌다. 이를 위해 공간 분해된 라만 산란 실험을 수행하여, 수직 방향으로 성장된 GaN 영역과 측면 방향으로 성장된 GaN 영역의 스펙트럼 차이를 비교하였다. 라만 산란 실험 결과  $569.5\text{ cm}^{-1}$  부근에서  $E_2(\text{high})$  포논 모드를 관측하였다.  $E_2(\text{high})$  포논 모드의 에너지, 선폭, 세기의 변화를 비교한 결과, 측면 방향으로 성장된 GaN 영역에서 얻은 라만 산란 반응이 수직 방향으로 성장된 GaN 영역에서 얻은 라만 산란 반응보다 포논 에너지가 더 크게 나타났다.  $E_2(\text{high})$  포논의 에너지 차이는 시료의 stress 분포가 비균질적임을 나타낸다. 포논 에너지 선폭은 측면 방향으로 성장된 영역에서 얻은 결과가 수직 방향으로 성장된 영역에서 얻은 결과보다 좁게 나타났다. 라만 산란 반응의 세기는 측면 방향으로 성장된 영역에서 얻은 결과가 그렇지 않은 영역에서 보다 강하게 나타났다. 이러한 포논 선폭과 세기의 차이는 측면 방향으로 성장된 GaN 영역의 결정성이 우수함을 나타낸다. 이 논문은 2009년 정부(교육과학기술부)의 재원으로 한국연구재단의 지원을 받아 수행된 연구임 (2009-0074315).

**Dp-V-166****Electric-Field Effect and Transport Properties of  $\text{Fe}_3\text{O}_4$  Nanoparticle Compact**

HER Eun Ju, BAE Yu Jeong, LEE Nyun Jong, AHN Jae Young, JANG Jung-tak<sup>1</sup>, MOON Seung Ho<sup>1</sup>, CHEON Jinwoo<sup>1</sup>, KIM Tae Hee

Department of Physics, Ewha Womans University, Seoul 120-750, Korea. <sup>1</sup>Department of Chemistry, Yonsei University, Seoul 120-749, Korea.

Recently, anomalous current-induced resistive switching behavior was reported in the magnetic oxide nanoparticle compacts.[1] Particularly for the magnetite ( $\text{Fe}_3\text{O}_4$ ) nanoparticles size below 10 nm, an abrupt and large resistance change (switching ratio of  $\sim 2000$  percent) appeared even at room temperature. However, the mechanism of this anomalous switching is not yet fully understood. Here, we focused on the transport property of 7 and 8 nm-sized nanoparticle assemblies in order to understand the origin of the room-temperature electrical switching behavior. The measurements of temperature-dependent resistance and current-voltage characteristics were carried out by the conventional dc four-probe method. For the transport measurement, the nanoparticle assemblies in the form of the compact pellets ( $1 \times 2 \times 8$  mm) were created by cold-pressing in a die under 160 Pa for 15 min. In order to avoid alteration of the surface properties of the nanoparticles, no heat-treatment step is used in the preparation of the pellets. Our experimental results show that the existence of the memory effect with glassy behavior. The structural analysis of nanoparticles was also performed by using high-resolution transmission electron microscope (HR-TEM). The HR-TEM images showed that highly monodispersed single crystalline magnetite nanoparticles were successfully prepared by using a nonhydrolytic chemical method. In this work, we have made an effort to understand our hysteretic switching characteristics in terms of time-dependent electric phenomena. This work is supported by Undergraduate Research Program for Science Program for Upbringing of Gifted Students funded by the Korea Foundation for the Advancement of Science and Creativity, Republic of Korea (2009-04-224). \* correspond author: taehee@ewha.ac.kr [1] Tae Hee Kim, et al., "Nanoparticle assemblies as Memristors", Nano Letter 9(6), 2229-2233 (2009)

**Dp-V-167****Manipulation of Graphene Using Nano Contact Transfer Technique**

YUN Hyeol, LEE Jeong-Ah, JUNG Unseok, KIM Dongchul<sup>1</sup>, SEO Sunae<sup>1</sup>, KIM Youngwook<sup>2</sup>, KIM Junsung<sup>2</sup>, KIM C<sup>3</sup>, YOON S<sup>3</sup>, KIM Hak-sung, LEE Jinkyung, LEE Sangwook

*Division of Quantum Phases & Devices, School of Physics, Konkuk University.. <sup>1</sup>Samsung Advanced Institute of Technology.. <sup>2</sup>Department of Physics, Pohang University of Science and Technology.. <sup>3</sup>Department of Physics, Ewha Womans University..*

In this presentation, we have fabricated suspended graphene and stacked bi-layer graphene using nano contact transfer printing technique. A single layer of graphene was exfoliated from graphite flakes on top of a SiO<sub>2</sub> substrate with pre-patterned coordinate markers. The nano contact transfer printing technique made it possible to deposit the single layer graphene flake with controlled manner. Suspended graphene and bi-layer graphene configuration were produced through depositing the graphene on top of the pre-patterned trench structure and on the pre-deposited graphene single layer respectively. The structures were investigated using micro Raman spectroscopy. In the case of the Raman spectra of the suspended graphene, we have noticed that there is no blue shift of peaks in the 2D and the G modes, which indicate no doping effect on the graphene. The 2D mode Raman spectra of bi-layer graphene stacked by transfer technique showed single Lorentzian shape, which is considered due to broken AB stacking of graphene layers.

**Dp-V-168****분산제 흡착에 따른 탄소나노튜브 네트워크 소자의 전기적 특성 변화 측정**

권 항명, 임 종혁, 정 희성, 권 봉준, 안 영환, 이 순일, 박 지용  
아주대학교 에너지시스템학부 응용물리학과

탄소나노튜브(CNT)는 우수한 기계적, 전기적, 열적 특성으로 인하여 응용성이 뛰어나 다양한 분야에서 활발히 연구가 진행 중에 있다. 하지만 CNT의 구조에 따라 그 특성이 금속성 혹은 반도체적 성질을 띄어 소자를 제작할 때 재연성 및 제어에 문제점이 발생하고 있다. 이를 극복하기 위하여 최근에는 대량생산한 CNT를 분산하여 박막 또는 네트워크 형태로 전자소자 또는 투명전극 등에 이용하는 연구가 활발하다. CNT 분산에는 다발화를 방지하기 위하여 다양한 극성 및 형태의 분산제가 사용되는데, 소자 제작 후 이러한 분산제가 소자의 전기적 특성에 영향을 미칠 가능성이 존재한다. 이는 분산제로 인한 CNT간의 접촉저항의 변화, CNT-금속전극의 접촉저항의 변화, 도핑효과등에 기인할 것으로 생각된다. 본 연구에서는 아크 방전방식으로 대량 성장시킨 단일벽 CNT를 DCE(1,2-Dichloroethane)에 분산하여 Si/SiO<sub>2</sub> 기판에 스퍼터링 방법으로 CNT 네트워크를 형성한 후 금속 전극을 증착하여 CNT 네트워크 소자를 제작하였다. 이와 같이 제작한 소자의 CNT를 여러가지 분산제를 이용하여 표면처리한 후 분산제의 흡착 및 제거에 따른 소자의 전기적 특성변화를 IV측정을 통해 조사하였다. 또한 원자힘현미경(AFM, Atomic Force Microscopy)을 응용한 정전기힘현미경(EFM, Electrostatic Force microscopy)과 주사게이트현미경 (SGM, Scanning Gate Microscope)법을 이용하여 소자내부의 전기적 특성변화양상을 동시에 관찰하였다. 이와 같은 측정을 통해 CNT네트워크 내부에서 접촉저항의 변화와 도핑양상을 확인할 수 있었다.

**Dp-V-169****Raman scattering studies of SAM structure of 4-MPy molecules on ZnO nanorods**

SHIN H.-Y., SHIM E. L.<sup>1</sup>, CHOI Y. J.<sup>2</sup>, PARK J. H.<sup>3</sup>, YOON S.

*Dept. of Physics and Dept. of Chemistry and Nano Science, Ewha Womans University, Seoul 120-750,*

*Korea. <sup>1</sup>Dept. of Physics, MyongJi University, Yongin, 449-728, Korea. <sup>2</sup>Dept. of Physics and Dept. of Nano*

*Science and Engineering, MyongJi University, Yongin, 449-728, Korea. <sup>3</sup>Electronics and Telecommunications Research Institute.(ETRI), Daejeon 305-700, Korea.*

We present the results of Raman scattering studies on 4-MPy SAM (self-assembled monolayer) molecules deposited on ZnO nanorods. It is shown by SEM and TEM that hydrothermally grown ZnO nanorods have a vertically well-aligned structure and each nanorod has typically a diameter of ~50 nm and length of ~1  $\mu$ m. An elemental analysis of ZnO nanorods by EDS is also studied. Raman scattering measurements were used to investigate optical phonon modes and structural properties of ZnO nanorods and used to research SAM structure of molecules by SERS or field enhancement. We used Raman scattering spectroscopy to study ZnO nanorods and observed enhancement of 4-MPy Raman signal.

**Dp-V-170****성장조건 변화에 따른 산화아연(ZnO) 나노선 소자의 특성 연구**

권 봉준, 정 희성, 권 향명, 안 영환, 이 순일, 박 지용

*아주대학교 에너지시스템학부 응용물리학 전공.*

3.3eV의 큰 밴드갭과 60mV의 높은 여기자에너지를 가지는 산화아연(ZnO) 나노선은 그 특성으로 인해 전자소자 및 광소자에 대한 연구가 활발하게 이루어지고 있다. 본 연구에서는 성장조건에 따른 산화아연(ZnO) 나노선의 전도특성 변화를 살펴보았다. 본 연구에서 사용한 산화아연(ZnO) 나노선은 화학기상증착법(thermal chemical vapor deposition)을 이용하여 성장시켰다. 기판의 차이, 촉매층의 두께와 산소분압을 조절하여 성장된 산화아연(ZnO) 나노선의 직경, 길이를 제어하였다. 이렇게 성장시킨 나노선을 기판에 전이한 후 전극을 형성하여 전도특성을 조사하였다. IV 전도특성의 조사와 더불어 음극선형광법(Cathodoluminescence), 원자힘현미경 (AFM)을 응용한 정전기힘현미경 (EFM)법을 동시에 적용하여 산화아연 (ZnO) 나노선의 특성을 비교하였다. 특히 성장조건에 따른 특성의 차이, 외부환경의 변화 (습도, 온도 등)에 따른 특성의 변화를 측정하여, 비교하였다. 성장조건에 따른 도핑정도의 변화와 트랜지스터 특성의 차이를 관찰하였다.

**Dp-V-171****백색 유기발광소자의 색변환층으로 작동하는 적색 무기물 형광체의 구조적 및 광학적 성질**정 환석, 안 성대, 추 동철, 김 태환, 박 정현<sup>1</sup>, 권 명석<sup>1</sup>한양대학교, 전자컴퓨터통신공학과, <sup>1</sup>서울시립대학교, 신소재공학과.

최근에 전색디스플레이의 배경조명 및 일반조명으로의 활용에 대한 가능성 때문에 다양한 종류의 무기물 형광체에 대한 연구가 관심을 갖게 되었다. 백색 유기발광소자는 일반적으로 적색, 청색 및 녹색의 삼원색을 혼합하여 제작하거나 청색 유기발광소자의 빛을 일부 변환하여 적색 또는 녹색을 발생하는 구조로 제작한다. 현재 사용되고 있는 삼원색 조합법은 구조가 복잡하여 제조단가가 상승하며 각각의 적색, 청색 및 녹색의 소자를 최적화하기 위한 복잡한 문제들이 있다. 색변환 방법은 최적화된 청색 유기발광소자에서 발광된 빛을 색변환 무기물 형광체 층에 의해 재흡수하여 재발광하는 과정에 의하여 빛이 발생되기 때문에 색변환 무기물 형광체 층을 사용한 백색 유기발광소자는 구조가 단순하며 무기물 형광체가 외부 노출에 안정하기 때문에 상대적으로 안정된 동작이 가능하다. 그러나 형광등 및 브라운관에 사용되던 무기물 형광체는 자외선 영역의 빛에 의해 여기되는 에너지 구조를 가지고 있어 가시발광영역의 유기발광소자에 그대로 적용하기 어려운 문제가 있다. 또한 기존에 일반적으로 제조하던 방법인 고상반응법에 의한 형광체입자의 크기는 마이크로 이상이며 그 형태도 불규칙한 단점이 있다. 본 연구에서는 졸겔방법으로 나노크기의 균일한 형태를 갖는 CaAl12O19:Mn 적색 무기물 형광체를 형성하였다. 주사전자현미경 측정 결과는 형성된 적색 무기물 형광체가 수백나노미터 크기의 균일한 크기의 입자로 형성되어 있음을 보여주고 있으며 X선 회절측정 결과는 JCPDS No.84-1613 의 결과와 정확히 일치하는 hexagonal 구조를 이루고 있음을 확인하였다. 450-470 nm 의 여기 광원을 이용한 형광 스펙트럼을 측정한 결과 640 nm, 653.6 nm, 663.6 nm 의 발광피크를 갖는 적색 발광특성을 나타내었다. 형광발광 피크들은 CaAl12O19 에 도핑된 Mn4+ 이온의 2E → 4A2 천이에 의한 피크들이다. 여기광원의 빛들은 CaAl12O19 에 흡수되어 엑시톤을 형성하고 형성된 엑시톤은 Mn4+ 이온으로 전이하여 발광하게 된다. 이 결과는 제작된 적색 무기물 형광체가 진청색 유기발광소자와 결합하여 백색 유기발광소자에 응용가능함을 보여준다. This work was supported by the Korea Science and Engineering Foundation (KOSEF) grant funded by the Korea government (MEST) (No. R0A-2007-000-20044-0).

**Dp-V-172****Electrical characterization of SiC nano-crystals nonvolatile memory with various tunnel barrier**HAN Dong Seok, LEE , Dong Uk, KIM Seon Pil, KIM Eun Kyu, CHO Won-Ju<sup>1</sup>Quantum-Function Spinics Laboratory and Department of Physics, Hanyang University. <sup>1</sup>Department of Electronic Materials Engineering, Kwangwoon University.

The roles of charge trap node, tunnel barrier, and gate oxide are very important factors to enhance an electrical performance of nano-floating gate memory (NFGM). We have selected SiC nano-crystal as charge trap node due to the large energy band gap and electron affinity in the ranges of 2.0-3.2 and 4.0-4.5 eV with different crystal structures. For these reasons, SiC has attracted much attention as a material for fabricating device. So, we especially used an ultra high vacuum (UHV) sputtering system to improve electrical properties of NFGM. This system has very high base-pressure with  $3 \times 10^{-10}$  torr. These nano-crystals were formed on *p*-type silicon wafers with (100) orientation with various tunnel barriers by using radio-frequency magnetron sputtering in argon ambient and post thermal annealing process of SiC film. The tunnel barriers used in this study composed of SiO<sub>2</sub> (O) type, Si<sub>3</sub>N<sub>4</sub>/SiO<sub>2</sub>/Si<sub>3</sub>N<sub>4</sub> (NON) type and, SiO<sub>2</sub>/Si<sub>3</sub>N<sub>4</sub>/SiO<sub>2</sub> (ONO) type. Then, the electrical properties of SiC nano-crystal NFGM with various tunnel barriers were characterized by capacitance-voltage (C-V) and current-voltage (I-V) measurements.

**Dp-V-173****Electrical property control of carbon nanotube conducting channel by metal over-layer deposition with different work functions**이 아름, 김 효숙, 전 은경, 김 주진, 이 정오<sup>1</sup>전북대학교 물리학과, <sup>1</sup>한국화학연구원.

We report the effect of metal overlayer, covering the central part of the nanotube conducting channel, on the electrical transport properties of carbon nanotube field-effect transistors (CNT-FETs). The CNT-FETs, consisting of a single-walled carbon nanotube (SWNT) between two metal electrodes (Cr/Au, Ti/Au, Pd) on top of SiO<sub>2</sub> layer, showed the typical *p*-type or ambipolar transport behavior before metal over-layer deposition. After metal deposition in the middle of carbon nanotube, however, their electrical properties have changed a great deal depending on the work function of over-layer metal. We ascribe such changes to the hole or electron doping through the Schottky barrier between CNT and over-layer in the metal-covered region, which leads to the local bending of the nanotube bands nearby the edges of the metal over-layer. This technique, metal over-layer deposition with different work function, could lead to a systematic control of electrical properties of CNT-FETs.

**Dp-V-174****Study on Transport Properties of Silicon Nanowires**CHO Hwanwoong, LI Xianhong, BEAK Inbok, LEE Seongjae, YANG Jongheon<sup>1</sup>, AHN Changgeun<sup>1</sup>, PARK Chanwoo<sup>1</sup>, SUNG Gunyong<sup>1</sup>Dept. of Physics, Hanyang University, Seongdong-gu, Seoul, Korea. <sup>1</sup>Nano-Bio Electronic Devices Team, ETRI, Yusong-gu, Daejeon, Korea.

Various p-type silicon nanostructures with fixed length 20  $\mu\text{m}$  and thickness 40 nm but with varying width in the range from  $\sim 100$  nm to 20  $\mu\text{m}$  were prepared by the silicon process technology and their intrinsic transport property was systematically studied. Based on their Id-Vg characteristic measurements, the hole mobility ( $\mu_h$ ) and concentration ( $n_h$ ) were extracted for all nanostructures. For the structures of small widths ( $w \leq 500$  nm, nanowire-type),  $n_h$  remains more or less constant at about  $2.4 \times 10^{17} \text{ cm}^{-3}$  as width narrows down from 500 to 96 nm, while  $\mu_h$  decreases steadily from 340 to 240  $\text{cm}^2\text{V}^{-1}\text{s}^{-1}$ . This behavior of mobility degradation with width narrowing is likely to originate from the enhanced surface scattering effect, but more detailed microscopic theory should be needed to explain this effect quantitatively.

**Dp-V-175****Facile Synthesis and Electrical Transport of Copper Vanadate Nanowires**

SHAHID Muhammad, SHAKIR Imran, 장 아람, 양 형우, 강대준

BK21 Physics Research Division, Department of Energy Science, Institute of Basic Science, SKKU Advanced Institute of Nanotechnology and Center for Nanotubes and Nanostructured Composites, Sungkyunkwan University, Suwon 440-746, Korea.

The growth of copper vanadate (CVO) nanowires was achieved by creating a thin layer of CVO nanoparticles on Si/SiO<sub>2</sub> from a spin coated film in ambient air. The structures and morphologies of the nanowires were characterized by x-ray diffraction, x-ray photoelectron spectroscopy, scanning electron microscopy, and high-resolution transmission electron microscopy. The growth process does not involve any metal catalyst, template, surfactant, or carrier gas. It was found that the formed nanoparticles served as seeds for the subsequent growth of CuV<sub>2</sub>O<sub>6</sub> nanowires by a simple thermal annealing. The grown nanowires have diameters in the range of 100 to 150 nm  $\pm$  10 nm and length 0.5 - 5  $\mu$ m (Fig.1). The temperature dependent resistances measurement (Fig. 2) of CuV<sub>2</sub>O<sub>6</sub> nanowires agree with the exponential correlation, supporting that the conducting carriers are the quasi-free electrons.

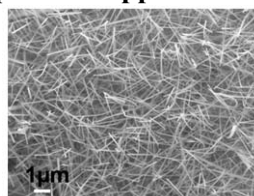


Figure 1. SEM image of CuV<sub>2</sub>O<sub>6</sub> nanowires.

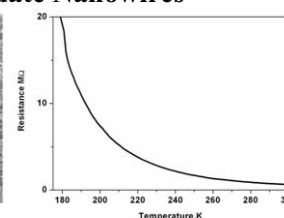


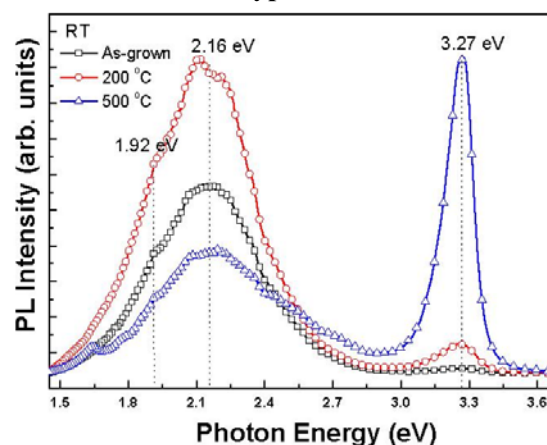
Figure 2. RT curve of CuV<sub>2</sub>O<sub>6</sub> nanowires<sup>1/2</sup>

**Dp-V-176****The Influence of Thermal Annealing on Volmer-Weber Type ZnO Nanorods via****Photoluminescence and X-ray Photoelectron Spectroscopy**

PARK Se-Jeong, HE Weizhen, HWANG Yoon-Hwae<sup>1</sup>, KIM Hyung-Kook<sup>1</sup>

부산대학교 나노융합기술학과. <sup>1</sup> 부산대학교 나노정보소재공학과.

We observed the change of photoluminescence of Volmer-Weber type ZnO nanorods prepared by hydrothermal method as the annealing temperature altered. At the stage of the as-grown, strong yellow emission was dominant because of hydroxyl groups on the surface of the nanorods. After the nanorods were annealed at high temperatures, UV emission was enhanced and the yellow emission was shrunk. To confirm the phenomena, X-ray photoelectron spectroscopy was conducted. It was found that there was another oxygen bound state related to hydroxyl group in the as-grown nanostructure.



**Dp-V-177****Thermodynamic temperature measurement from shot noise in a metal tunnel****junction**

박 정환, REHMAN Mustaq<sup>1</sup>, 류 상완<sup>2</sup>, 김 정구<sup>3</sup>, 전 건상<sup>3</sup>, 최 정숙<sup>4</sup>, 송 운<sup>4</sup>, 정 연욱<sup>4</sup>

KRISS, 서울대학교. <sup>1</sup>KRISS, 전남대학교. <sup>2</sup>전남대학교. <sup>3</sup>서울대학교. <sup>4</sup>KRISS.

We introduce our progress on noise thermometry based on the measurement of shot noise in a metal tunnel junction. We fabricated sub-micron scale tunnel junctions consisting of metal (Al)-insulator ( $\text{AlO}_x$ )-metal (Al) using electron-beam lithography and double-angle evaporation technique. We measured the bias-dependent shot noise in the frequency range of 600 - 800 MHz at temperatures from 4.2 K to 220 K. Cryogenic low noise HEMP amplifier technique was used to amplify the noise signal. From the shot noise trace, we could directly infer the temperature of the junction. This method can be used as a primary thermometry based on the thermodynamic temperature of the electrons in the junction electrodes. As an analysis on the source of errors, we considered the inelastic tunneling process to explain apparent higher inferred temperature in seemingly bad junctions. We suggest a model how the junction imperfection causes errors in determining the temperature.

**Dp-V-178****The effect of carbon vacancies on the electrical properties of carbon nanotubes**

LEE Alex Taekyung, KANG Yong-Ju<sup>1</sup>, CHANG Kee Joo

Department of physics, KAIST. <sup>1</sup>Samsung Elec. Co..

Carbon vacancies in nanotubes and graphene are of great importance because they significantly affect the structural and electronic properties of carbon systems. In this work, we study the effect of various vacancy defects on the electrical properties of carbon nanotubes. Using the matrix Green's function approach, we calculate conductances through carbon nanotubes in which vacancies are clustered and/or randomly distributed. For vacancy clusters,  $V_n$  ( $n \leq 4$ ), where  $n$  is the number of missing atoms, conductances are severely suppressed near the Fermi level for  $n = \text{even integer}$ , inducing the localization behavior. For  $n = \text{odd integer}$ , as conductances near the Fermi level are relatively higher due to the existence of the dangling bond state, the localization length becomes larger.

**Dp-V-180****Piezoelectric properties in the  $(\text{Na}_{0.5}\text{K}_{0.47}\text{Li}_{0.03})(\text{Nb}_{0.8}\text{Ta}_{0.2})\text{O}_3$  ceramics****prepared by a tape casting process**

KANG Bo Ram, KIM Sin Woong, LEE Sung Chan, LEE Myang Hwan, SUNG Yeon Soo, CHO Jong Ho<sup>1</sup>, KIM Myong-Ho, SONG Tae Kwon, KIM Sang Soo<sup>2</sup>, CHOI Byung Chun<sup>1</sup>

*School of Nano & Advanced Mat. Eng., Changwon Nat'l Univ.. <sup>1</sup>Department of Physics, Pukyong Nat'l*

*Univ.. <sup>2</sup>Department of Physics, Changwon Nat'l Univ..*

For more than a half century, piezoelectric ceramics have been based on the perovskite solid solution  $\text{Pb}(\text{Zr,Ti})\text{O}_3$ , commonly referred to PZT. However, the toxicity of lead oxide and its high vapor pressure during high temperature processing have led to a demand for lead-free piezoelectric ceramics. Much attention for lead-free piezoelectric ceramics has recently been paid to NKN based ceramics which have developed textured ceramics with piezoelectric properties comparable to those of unmodified PZT ceramics. NKN based ceramics is a very important piezoelectric material for its good ferroelectric properties and high Curie temperature. In this study,  $(\text{Na}_{0.5}\text{K}_{0.47}\text{Li}_{0.03})(\text{Nb}_{0.8}\text{Ta}_{0.2})\text{O}_3$  ceramics were prepared by a tape casting process using  $\text{LiNbO}_3$  as a seed material and measured microstructures and piezoelectric properties.

**Dp-V-181****Formation Of Fe Silicide Film On Si(111) 7x7 Surface**

김 효상, 신 선영, 엄 상훈, 성 시진, 정 진욱

POSTECH.

Metal deposition on Si surfaces has been extensively studied due to the wide application on silicon-based devices. Fe silicide thin film has been a typical example for such applications in microelectronics. Most FeSi phases including the CsCl-type phase have been known to be quite unstable and ill-defined both in their atomic structures and physical properties to hinder extensive industrial applications. Here we report that we have investigated the formation of Fe silicide by carefully controlling the dose of Fe atoms as well as annealing temperature of the sample. By utilizing low-energy-electron diffraction (LEED) and synchrotron radiation photoemission spectroscopy (SRPES), we find that a quite stable crystalline FeSi silicide film forms upon annealing the Fe-deposited Si(111) surface at room temperature.

**Dp-V-182****Pulsed electro beam을 이용한 비정질 Si 박막의 결정화 연구**

고 락길, 장 세훈<sup>1</sup>, 하 동우, 손 명환

한국전기연구원, <sup>1</sup>한국전기연구원, 창원대학교 재료공학과.

다결정 실리콘은 비정질 실리콘에 비해 높은 이동도를 가지므로 평판 디스플레이 소자 및 태양전지 등 다양한 전자 소자에 응용되고 있다. 이러한 다결정 실리콘 기판을 제조하는 방법으로는 고상결정화(SPC)법, 엑시머 레이저어닐링(ELA)법, 금속결정화(MIC)법, 금속유도결정화(MILC)법 및 순차적 측면 고상화(SLS)등 다양한 방법이 각각의 장단점을 가지고 제시되고 있다.본 연구에서는 새로운 비정질 Si의 결정화 방법으로 Pulsed Electro beam에 의한 저온 결정화 방법을 제시하며, 그 예비 시험으로 그 가능성을 제시하고자 한다. 본 연구에서는 PECVD로 증착된 비정질 Si 박막을 Pulsed Electro Beam을 이용하여 표면 처리하여 결정화 시켰으며, 이를 XED와 라만 분석을 통해 확인했으며, SEM, AFM을 이용하여 그 표면에 대한 분석을 하였다. 본 연구는 한국전기연구원의 중소기업기술지원사업의 연구비 지원에 의해 수행되었습니다.

**Dp-V-183****Co/Au(001)에서의 자성과 궤도질서**

홍 순철, 김 태은, 윤 원석, 윤 석주<sup>1</sup>

울산대학교 물리학과, <sup>1</sup>경상대학교 과학교육과.

일반적으로 궤도 질서는 궤도 구별이 명확한 부도체에서 나타나는 것으로 알려져 있으나, Co/Au(001)에 대한 제일원리계산에 의하면 금속에서도 궤도 질서가 관찰될 수 있음을 예측하였다. 실험에서 일어날 수 있는 상황을 고려하기 위해 Au/Co/Au와 Co/Co/Au 계에 대해서도 제일원리계산을 수행하여 Co/Au(001) 시스템과 비교해 보았다. 계산결과, Au/Co/Au와 Co/Co/Au 등의 계에서는 궤도 질서는 관측되지 않았다. 계산방법으로는 자성 연구에 가장 적합한 것으로 알려져 있는 FLAPW(Full-potential Linearized Augmented Plane Wave) 방법을 사용하였고, 교환 상관 포텐셜은 GGA(Generlized Gradient Approximation)를 사용하였다. Au(001) 기판 위에서 증착된 Co 단층은 기판의 결정구조와 조화롭게 성장하는 것으로 가정하였다. Co/Au(001)의 자기 이방성 에너지를 계산하여 단일 전자 에너지 스펙트럼, 스핀 질서, 궤도 질서, 자기이방성 사이의 상관관계에 대해 논의할 예정이다.

**Dp-V-184****Ir(001) 위의 철 단층의 자성**이 재일, 김 동철<sup>1</sup>인하대 물리학과, <sup>1</sup>한라대학교.

자연적 덩어리 상태에서 자성을 나타내지 않는 4d 나 5d 전이금속 위에 얹혀진 전이금속 단층의 자성에 대한 연구는 저차원 자성의 발현에 대한 본질적 문제와 연관 지어 흥미를 끌고 있다 [1]. 여기서는 Ir(001) 위에 얹혀진 철 단층의 자성을 제일원리 전자구조 계산방법 [2]을 통하여 이론적으로 탐구하였다. 비교를 위하여 Fe와 Ir이 규칙적으로 반반 섞인 윗층에 대하여도 계산하였다. 모두 Fe로 이루어진 단층의 경우 철 원자의 자기모멘트는 2.95 보어마그네톤으로 비교적 큰 값을 가졌으며, Fe와 Ir이 반반 섞인 윗층에서 Fe의 자기모멘트는 2.83 보어마그네톤이었다. 이러한 자성과 전자구조의 자세한 면은 계산된 상태밀도와 스핀밀도를 이용하여 논의한다. 각 윗층 원자의 평형위치를 구하기 위해 총에너지와 원자힘 계산을 하였다. 그 결과 Fe 윗층의 원자위치가 Fe와 Ir이 반반 섞인 윗층의 Fe 위치보다 Ir 밑층에 다소 가까웠다. [1] S. Bluegel, D. Drittler, R. Zeller, P. H. Dederichs, Appl. Phys. A49, 547 (1989). [2] E. Wimmer, H. Krakauer, M. Weinert, and A. J. Freeman, Phys. Rev. B, 24, 864 (1981), and references therein; M. Weinert, E. Wimmer, and A. J. Freeman, Phys. Rev. B, 26, 4571 (1982).

**Dp-V-185****Growth and Electrical Characteristics of Carbon Films on ITO and Si Substrates**

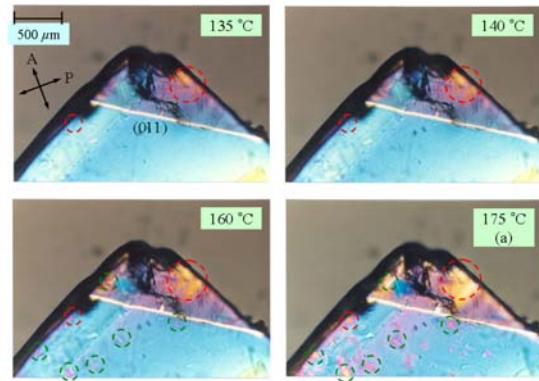
LEE Jong Duk, KIM Hyeon Soo, KIM Kun Ho, PARK Chang Young, LEE Jeoung Ju

Gyeongsang National University, Department of Physics.

Carbon films were grown on ITO (indium-tin oxide) and n-Si(100) substrates by using electrochemical deposition technique. Carbon films were deposited in various electrolyte solutions such as acetonitrile, acetone, methanol and ethanol. During the electrodeposition of carbon on ITO substrates the current densities increase abruptly and then decrease exponentially. In these cases, the current densities decreased more rapidly with increasing the deposition potential. In Si substrate, However, the deposition of carbon is prevented by the hydrogen generated on the Si surfaces. To remove hydrogen bubbles from the surface, the temperature of Si substrate was raised. As a result, the current density increased with increasing the potential but showed different behaviors compared with that of ITO substrates. The carbon films were characterized by Atomic force microscopy (AFM), Field emission scanning electron microscopy (FESEM), Raman spectroscopy and X-ray photoelectron spectroscopy (XPS). In all cases, two broad bands located at  $1350\text{ cm}^{-1}$  and  $1570\text{ cm}^{-1}$  were confirmed through Raman spectroscopy analysis and these peaks are indicative of presence of carbon. In addition, from FTIR spectroscopy, the characteristic peaks of carbon films were observed at  $\sim 2850\text{ cm}^{-1}$ ,  $\sim 2920\text{ cm}^{-1}$  and  $\sim 2955\text{ cm}^{-1}$  which correspond to the symmetric, anti-symmetric stretching vibrations of  $\text{sp}^3$  bonded  $\text{CH}_2$  group and the anti-symmetric stretching vibrations of  $\text{sp}^3$  bonded  $\text{CH}_3$  group, respectively. From X-ray diffraction (XRD) measurements we have found that single phase C8 films with cubic structure were preferentially grown on Si(100) substrates in all potential ranges. AFM and FESEM revealed that the surface morphology of carbon films depends strongly on the applied d.c. voltage but the grain sizes does not. From I-V measurement, it is found that carbon/n-Si heterojunction shows a typical rectifying characteristic like p-n junction when applied a positive voltage on carbon films.

**Dp-V-186****High-Temperature Phase Transformation in Ferroelastic  $(\text{NH}_4)_2\text{SO}_4$  and****Topochemical Nature**LEE Kwang-Sei, KIM Jae-Hyung<sup>1</sup>, OH In-Hwan<sup>2</sup>*Inje University, Department of Nano Systems**Engineering. <sup>1</sup>Inje University, School of Computer-Aided**Science. <sup>2</sup>Korea Atomic Energy Research Institute, Neutron Science Division.*

The electrical conductivity of ferroelastic ammonium sulfate  $(\text{NH}_4)_2\text{SO}_4$  revealed an anomaly at around 130 °C (= 403 K,  $T_p$ ) on heating with the large and irreversible thermal hysteresis through thermal cycle. The ferroelastic domain wall and surface morphology of  $(\text{NH}_4)_2\text{SO}_4$  were investigated by hot-stage polarizing microscopy. On heating structural phase transition from an orthorhombic ferroelastic phase to a hexagonal paraelastic phase was not identified at  $T_p$ . On heating above  $T_p$  the microscopic spots appeared at surface and grew, indicating that the high temperature anomaly at  $T_p$  is an indication of an onset of thermal decomposition controlled by the topochemical factors. The increase of electrical conductivity above  $T_p$  is attributed to proton migration.

**Dp-V-187** **$\text{Pt}_3\text{Fe}$  합금의 촉매적 특성 : 밀도 범함수 이론**정 재훈, 권 오룡, 윤 원석, 홍 순철  
*울산대학교.*

화석에너지의 높은 의존도로 인해 생겨난 온실효과 및 공기 오염들을 줄이기 위해 시작된 대체에너지 개발은 전세계에 걸쳐 다양하게 진행되고 있다. 그 중에서 연료 전지는 소형화 및 높은 효율로 인해 주목을 받고 있는 대표적인 대체에너지 중 하나이다. 그러나 연료전지의 음극과 양극 기판에 사용되는 Pt는 가격이 비싸며 매장량이 한정되어 있다. 비용과 공급량의 문제로 인해 Pt를 대체할 물질들이 연구 되어지고 있으며 연료 전지내 ORR(Oxygen Reaction Reduction)반응에서 Pt 표면의 촉매활동성은  $\text{OH}^-$  피독 현상으로 약화된다. 이 문제를 해결하기 위해 나온 물질이 Pt 이원합금이며 Pt 이원합금 표면에서 표면분리 현상이 관찰되고 표면분리는 피독 현상을 개선하는 것으로 알려져 있다.본 연구에서는 이러한  $\text{Pt}_3\text{Fe}$  합금 표면에서 촉매활동성을 낮추는  $\text{OH}^-$ 이온의 흡착에너지와 촉매로 이용되는  $\text{O}_2$ 의 흡착에너지를 계산하기 위해 제일 원리계산을 수행하였다. 본 연구에서는 PAW GGA 유사포텐셜을 이용한 VASP(Vienna Ab-initio Simulation Package)을 사용하였으며 면심입방구조(fcc)의 (111)면을 사용하였다.

**Dp-V-188****Electronic Excitations at the Initial Stage of Graphitization of 6H-SiC(0001)**

신 선영, 황 춘규, 엄 상훈, 김 효상, 성 시진, 이 팽로, 정 진욱  
포항공과대학교, 물리학과.

Epitaxial graphene layers grown on the SiC(0001) surface have been studied extensively to understand many unusual properties of massless Dirac fermions as well as to fabricate graphene-based electronic devices. However, it is still nontrivial to accurately identify in-situ under UHV condition the formation of a single-layer graphene (SLG). Here, we have investigated electronic excitations during the initial stage of graphitization of 6H-SiC(0001) surface using high-resolution electron energy loss spectroscopy (HREELS). From the  $(6\sqrt{3}\times 6\sqrt{3})R30^\circ$  reconstructed buffer layer, we find a characteristic loss feature with a loss energy at about 1.7eV, which is identified as an interband transition by studying the surface band structure determined from earlier photoemission results. We have also measured dispersion relations of the plasmon excitations observed from the SLG and the few-layer graphene (FLG), which appear to faithfully illustrate the evolution of the  $\pi$ -band with the increasing number of graphene layers as shown in earlier photoemission data. We thus suggest another efficient and accurate way of probing the presence of SLG during the growth period of graphene layers.

**Dp-V-189****Effects of BaTiO<sub>3</sub> based-solid solutions with SiO<sub>2</sub> and Bi<sub>4</sub>Ti<sub>3</sub>O<sub>12</sub> on piezoelectric****and dielectric properties**

KIM Da Jeong, LEE Sung Chan, LEE Myang Hwan, KIM Myong-Ho, SUNG Yeon Soo, SONG Tae Kwon, KIM Sang Soo<sup>1</sup>, CHO Jong Ho<sup>2</sup>, CHOI Byung Chun<sup>2</sup>

*School of Nano & Advanced Materials Engineering, Changwon National University. <sup>1</sup>Department of Physics, Changwon National University. <sup>2</sup>Department of Physics, Pukyong National University.*

PZT ceramics have a high piezoelectric, ferroelectric and electric properties so they have been applied in many fields, but they are currently facing global restrictions on use due to Pb toxicity. BaTiO<sub>3</sub> (BT) ceramics are one of the lead-free materials having a good ferroelectric property and its curie temperature (T<sub>c</sub>) is about 125 °C. Unfortunately BT is limited to applications because of low T<sub>c</sub>. In this study, piezoelectric and dielectric properties of BaTiO<sub>3</sub> based-solid solutions with SiO<sub>2</sub> and Bi<sub>4</sub>Ti<sub>3</sub>O<sub>12</sub> prepared by conventional solid state reaction process have been investigated. X-ray diffraction analysis revealed that no secondary phase appeared for all ceramics samples. The change of T<sub>c</sub> is little in BaTiO<sub>3</sub> based-solid solutions of SiO<sub>2</sub>.

**Dp-V-190****Optical properties of the  $\text{Sr}_2\text{SiO}_4:\text{Eu}^{2+}$  phosphor coated with  $\text{SiO}_2$  nano-particles**

HAN Su Jin, LEE Sang Mok, SOHN Sang Ho

*Kyungpook National University, Department of Physics.*

In this work, we investigated the effects of the  $\text{SiO}_2$  surface coating on the optical properties of the  $\text{Sr}_2\text{SiO}_4:\text{Eu}^{2+}$  phosphor which is used for white light source in the near-UV and blue LED chip. The  $\text{Sr}_2\text{SiO}_4:\text{Eu}^{2+}$  phosphor was synthesized by a solid state reaction method where  $\text{SrCO}_3$ ,  $\text{SiO}_2$  and  $\text{Eu}_2\text{O}_3$  were used as starting materials. A modified sol-gel method was used for the surface coating of the  $\text{Sr}_2\text{SiO}_4:\text{Eu}^{2+}$  phosphor with  $\text{SiO}_2$ . The comparison of the physical properties between the non coated and the  $\text{SiO}_2$  coated phosphor was done by using Scanning Electron Microscopy (SEM) and Photo luminance (PL) spectra. We can easily see that that the nano-sized  $\text{SiO}_2$  particles are coated well on the surface of the  $\text{Sr}_2\text{SiO}_4:\text{Eu}^{2+}$  phosphor in the SEM images. The PL spectra measured by using a near-UV region of wavelength of 370 nm reveal that the surface coating of phosphors with  $\text{SiO}_2$  nano-particles leads to the decrease in the intensity of the 555 nm peak. The decrease in the PL intensity may be attributed to the shielding of the transmitting near-UV through the surface  $\text{SiO}_2$  nano-particles.

**Dp-V-191****Error Analysis of Bistable Poisson States Using Periodic Measurements**

LEE Jinwoo, LYO In-Whan

*Dept. of Physics and IPAP, Yonsei University.*

Reversible molecular dynamics has been drawing scientific attention for a long time. Dynamical behavior of atoms and molecules is described by a characteristic energy barrier that determines residence time in thermodynamically accessible states. Such residence time of the states has been measured by using scanning tunneling microscopy at a single molecular level. These measurements are performed by detecting tunneling current or utilizing fast imaging methods at regular or irregular time intervals. We show that these methods have intrinsic errors; we performed numerical error analysis of the residence time of bistable Poisson states that was obtained via typical periodic measurement schemes such as analog-to-digital converters. Monte Carlo simulations show that the averaging method produces consistently more accurate result than conventional exponential fits. We will demonstrate these error factors by comparison with real experiment data obtained by detecting variation in tunneling current and atomic tracking method.

**Dp-V-192****각분해 광전자분광법을 이용한 준이차원 CeTe<sub>2</sub>의 전자구조 연구**

김 대현, 이 현진, 이 선미, 이 민주, 강 정수, 권 용성<sup>1</sup>, 이 한구<sup>2</sup>, 김 형도<sup>2</sup>

가톨릭대학교 물리학과. <sup>1</sup>성균관대학교 물리학과. <sup>2</sup>포항가속기연구소.

CeTe<sub>2</sub>에서 Te 원자들은 그 위치에 따라 두 종류가 있는데, 각각 Te 원자들이 이차원 사각형 모양을 이룬 Te(1) 평면층과 Ce와 Te 원자들이 주름 형태로 섞여 있는 Ce-Te(2) 이중층을 이루며, CeTe<sub>2</sub>는 Te(1) 평면층과 Ce-Te(2) 이중층이 번갈아 있는 준 이차원 구조를 가진다. CeTe<sub>2</sub>의 전기적, 자기적 성질들에서 매우 큰 이방성이 관찰되었으며, CeTe<sub>2</sub>는 전이온도가 매우 높은 (약 1000 K) 전하밀도파 (charge-density-wave system: CDW) 물질계로 알려져 있다. 물성에서 관찰된 큰 이방성은 CeTe<sub>2</sub>의 준 이차원 구조로 인한 것으로 생각되었고, CDW가 생기는 원인은 페르미 면의 nesting 때문으로 생각되었다. CeTe<sub>2</sub>의 전자 구조에 관하여 Ce 이온이 3가 상태이며, CDW 전이가 일어 나기 전에 Ce-Te(2) 이중층은 반도체 전자 구조를 가지고 있지만 Te(1) 평면층은 금속성 전자구조를 가지고 있어서 전하 운반자가 존재할 것으로 여겨지고 있다. 그러나 지금까지 보고된 CeTe<sub>2</sub>의 전자구조 실험결과들은 [1,2] 이러한 예측을 확실하게 입증하지 못하였다. 그러므로 CeTe<sub>2</sub>에서의 CDW 형성의 원인, CDW 에너지 갭의 크기, CDW 삼차원(lattice)의 대칭성, Te(1) 평면층의 전자 구조 등에 관하여 좀 더 정밀한 연구가 필요한 실정이다. 이 연구에서는 CeTe<sub>2</sub>를 대상으로 각분해 광전자 분광 (angle-resolved photoemission spectroscopy: ARPES) 실험을 수행하여, 페르미 준위 근처의 일정한 에너지 면들의 에너지 변화에 따른 형태 변화, 에너지 분포 곡선, 운동량 분포 곡선 등을 측정하였다. 이러한 ARPES 실험 결과를 분석하여 CeTe<sub>2</sub>의 띠 구조, 에너지 갭의 크기 및 대칭성, 페르미 준위 근처에서의 금속성 상태(states)의 존재 여부 등을 연구하였으며, CeTe<sub>2</sub>의 전자 구조가 CDW 형성에 미치는 역할을 이해하고자 하였다.[1] K. Y. Shin, et al., Phys. Rev. B 72, 085132 (2005).[2] J.-S. Kang, et al., Phys. Rev. B 74, 085115 (2006).

**Dp-V-193****Catalytic activity: Density-Functional Theory of O<sub>2</sub> on Pt(111) surface**

권 오룡, 홍 순철

울산대학교.

현재 우리는 화석연료의 한정적 매장량과 화석연료의 사용에 의한 대기오염문제로 대체연료에 대한 연구가 활발하게 진행되고 있다. 수소에너지가 대표적인 대체에너지 중 하나다. 수소에너지를 사용화하기까지는 수소저장, 수소발생 등 해결해야 할 여러 문제가 있다. 연료전지가 수소에너지를 운송 수단에 가장 적절하게 사용하는 방법 중 하나로 받아들여지고 있다. 운송 수단에 가장 많이 사용되는 PEM 연료전지의 음극과 양극 기판으로 Pt를 촉매로 사용하고 있다. 이 중 양극 Pt 촉매에서 일어나는 환원반응을 이해하기 위해 Pt 표면 위의 O<sub>2</sub>의 흡착 반응에 대하여 연구를 하였다. 본 연구에서는 Pt 촉매 표면의 촉매활동성에 대해 미시적으로 이해하기 위해 Pt 표면 위의 O<sub>2</sub>의 흡착 위치와 흡착에너지를 VASP(Vienna Ab-initio Simulation Package) 이용한 제일원리계산방법으로 계산하였다. 연구의 일관성을 유지하기 위해 총에너지 계산으로 덩치 구조를 우선 결정하였고, 계산된 덩치 격자 상수를 사용하여 Pt촉매 활동성이 가장 높다고 알려진 Pt(111) 표면 위의 흡착위치에 따른 O<sub>2</sub>의 흡착 특성과 전자구조를 총에너지와 상태밀도를 이용하여 논의하고자 한다.

**Dp-V-194****Molecular directionality change of rubbed polyimide(PI) films upon annealing****condition**

김 기정, 곽 무선<sup>1</sup>, 권 혁민<sup>1</sup>, 이 상문<sup>1</sup>, 이 철구<sup>1</sup>, 김 봉수

포항가속기연구소 빔라인부. <sup>1</sup>LG Display.

We measured the angle dependence near edge X-ray absorption fine structure (NEXAFS) spectra of PI films depending on the annealing condition at C K-edge. Two kinds of PI molecules, twisted nematic mode PI (PI-TN)s and in plane switching mode PI (PI-IPS) were introduced to understand the electrical property changes after annealing treatments. The intensity changes of C=C  $\pi$ -resonances implies that PI-IPS maintained good directional property after annealing but PI-TN lost directional property. In this presentation, we will analyze the origin of the thermal stability of PI-IPS and the thermal instability of PI-TN in conjunction with the molecular structure changes.

**Dp-V-195****Preparation and Photoluminescence Properties of Three-Dimensionally Ordered****Macroporous  $\text{ZrO}_2\text{: Tb}^{3+}$  Films**

QU Xuesong, YANG Hyun Kyoung, JEONG Jung Hyun

Department of Physics, Pukyong National University.

Three-dimensionally ordered macroporous (3DOM)  $\text{ZrO}_2\text{: Tb}^{3+}$  films were successfully fabricated using a polystyrene (PS) colloidal crystal template in combination with a sol-gel method. The structure, morphology, porosity, and optical properties of the materials were well characterized by X-ray diffraction (XRD), Field emission scanning electron micrograph (FESEM),  $\text{N}_2$  adsorption, and photoluminescence (PL) spectra. The results indicated that the closely packed material exhibited three-dimensional ordering of pores and strong green  $^5\text{D}_4\text{-}^7\text{F}_j$  ( $j = 3, 4, 5, 6$ ) transitions under charge transfer excitation. Strong PL and abundant porosity are of particular interest and enable this multifunctional material have potential in future.

**Dp-V-196****Terahertz time-domain spectroscopy of Bi and Bi<sub>2</sub>Te<sub>3</sub> thin films**

PARK Byung-cheol, KIM JaeHoon

*Institute of Physics and Applied Physics, Yonsei university.*

The complex transmission coefficients of Bi and Bi<sub>2</sub>Te<sub>3</sub> thin films (50nm) have been measured over the frequency range of 3-110 cm<sup>-1</sup> at room temperature via coherent time-domain terahertz spectroscopy. The films exhibited metal-like behavior, with a weak absorption feature at 70 cm<sup>-1</sup> in the case of Bi<sub>2</sub>Te<sub>3</sub>. We compare the observed characteristics by comparing their electronics structure and transport properties.

**Dp-V-197****Depolarization temperature and ferroelectric properties of BNT-BKT-BZ lead-free piezoelectric ceramics**

PARK Jin Su, LEE Sung Chan, LEE Myang Hwan, SUNG Yeon Soo, KIM Myong-Ho, SONG Tae Kwon, CHO Jong Ho<sup>1</sup>, CHOI Byung Chun<sup>1</sup>

*School of Nano & Advanced Materials Engineering, Changwon National University. <sup>1</sup>Department of Physics, Pukyong National University.*

Lead-free piezoelectric ceramics BNT-BKT-BZ piezoelectric ceramic have been studied. In the case of (Bi<sub>0.5</sub>Na<sub>0.5</sub>)TiO<sub>3</sub>-(Bi<sub>0.5</sub>K<sub>0.5</sub>)TiO<sub>3</sub>-BaTiO<sub>3</sub> (BNT-BKT-BT) ceramics,  $T_d$  (depolarization temperature) was reported to increase with substitution of BaTiO<sub>3</sub>. So in this work, the effects of Zr doping on the depolarization temperature and piezoelectric properties in BNT-BKT-BT ceramics have been studied. Ceramic samples prepared by the conventional solid state reaction method have been investigated their piezoelectric and dielectric properties in order to know the effect on  $T_d$  owing to Zr doping.

**Dp-V-198****Pt(111) 표면 위에 증착된 NiO/Ni<sub>2</sub>O<sub>3</sub> 극초박막의 화학적 상태에 관한 연구**

한 동훈, 조 성국, 남 창우

한양대학교 물리학과 서울 133-791.

Pt(111)면 위에 증착  $2.0 \times 10^{-6}$  Torr 산소 분압에서 동시 성장된 Ni 산화박막을 증착한 후 9단계의 후열처리 과정을 통해 각각의 온도마다 NiO, Ni<sub>2</sub>O<sub>3</sub>의 비율과 Ni 2p 및 O 1s 준위의 결합에너지 변화를 내각 준위 X선 광전자 분광법을 이용하여 관찰 하였다. 7.6 ML 산화박막에서는 과산화 영향으로 NiO, Ni<sub>2</sub>O<sub>3</sub> 두 개의 phase가 관찰되었고, 순차적인 후열처리에 따라 Ni<sub>2</sub>O<sub>3</sub>가 먼저 탈착되어 830 K에서 Ni<sub>2</sub>O<sub>3</sub>는 모두 탈착이 되고 NiO phase만 남아 있었다. 710 K이상의 온도에서는 Ni 원자들이 Pt 기판으로 섞여 들어감을 Ni 2p 준위의 스펙트럼 세기 변화와 속박에너지 변화로부터 알 수 있었다. 3 ML 산화박막에서는 NiO와 화학적 흡착된 상태만 관찰 되었다. 후열처리를 통해 순수 산소의 양이 점점 감소하였으며, 770 K이상의 온도에서는 NiO phase가 나타나지 않았다. 830 K 이상에서는 강하게 화학적 흡착되어 있던 산소원자들도 탈착 되었다.

**Dp-V-199****Order-disorder transition in Pt-Ni bimetallic nanocrystals**서 옥균, 황 재성, 오 필건, 강 현철<sup>1</sup>, 노 도영광주과학기술원 신소재공학과. <sup>1</sup> 조선대학교 신소재공학과.

The order-disorder transition in bimetallic alloys such as  $\beta$ -CuZn, Cu<sub>3</sub>Au, and CuAu have been investigated greatly by x-ray diffraction. After annealing the bimetallic alloys, the crystal structure changes as observed in the order-disorder transition of Cu<sub>3</sub>Au which changes from the face centered cubic to a simple cubic structure. Pt-Ni bimetallic alloy has been already reported to have the face centered cubic structure. However, in nanoscale Pt-Ni bimetallic alloy crystals the crystal structures changes to a simple cubic structure. In this experiment, we have studied the order-disorder transition in Pt-Ni bimetallic nanocrystals. Pt/Ni thin films were deposited on Al<sub>2</sub>O<sub>3</sub> (0001) substrates by e-beam evaporator and then Pt-Ni nano particles were formed by RTA at 1030°C in a vacuum environment. We measured the structure of Pt-Ni bimetallic alloy films and Pt-Ni nano particles as a function of the thickness ratio between Pt and Ni thin films using synchrotron x-ray diffraction.

RYU Byungki, CHANG Kee Joo

*Department of Physics, KAIST.*

Zn-based oxide semiconductors exhibit intrinsic n-type conductivity and have been used as an active channel in transparent thin-film transistors. Usually, device performance is very sensitive to the interface structure and the existence of defects. As compared to Si MOS devices, there have been a lack of studies on the interface structure between ZnO and gate oxide. In this work we generate interface models between ZnO and amorphous HfO<sub>2</sub> using first-principles molecular dynamics simulations. For two interface structures, in which HfO<sub>2</sub> is placed on ZnO (0001) and (000 $\bar{1}$ ) surfaces, we investigate the defect levels of O-vacancy ( $V_O$ ). The conduction band offset between ZnO and HfO<sub>2</sub> is estimated to be 2.14-2.39 eV, while the energy barrier for hole carriers is nearly zero. We find that the defect level and the formation energy of neutral  $V_O$  in ZnO are lower than those in oxide. Based on our calculations, we discuss the role of  $V_O$  in the threshold voltage instability in devices.

### Surfaces

RYOU Junga, HONG Suklyun, HWANG Chanyong<sup>1</sup>

*Department of Physics and Institute of Fundamental Physics, Sejong University, Seoul 143-747, Korea. <sup>1</sup>Korea Research Institute of Standards and Science, Daejeon 305-340, Korea.*

We have performed first-principles density functional theory calculations to study the atomic structure of carbon atoms adsorbed on Cu(111) surfaces. First, we investigate several adsorption sites of a single carbon atom on the Cu (111) surface or in its subsurface. The carbon atom located in the subsurface is found to be more stable in energy than on the (111) surface. Using the nudged elastic band method, we calculate the diffusion barrier of a carbon atom from the Cu(111) surface region to the subsurface of Cu(111). Also, we consider adsorption configurations of a carbon atom bound to a Cu adatom on the Cu(111) surface. Next, we investigate the formation of graphene-like structure when many carbon atoms are adsorbed on the Cu(111) surfaces. Such formation may be expected because the binding between carbon atoms is very strong. On the basis of these results, we discuss the graphene growth mechanism on the copper surface. Finally, theoretical results are compared with the available experiment.

**Dp-V-202****First-principles study of graphene on insulating substrates**

CHOI Hyoung Joon, GOH Jung Suk

*Department of Physics and IPAP, Yonsei University.*

We investigate graphene on insulating substrates using a first-principles density functional method. Potassium iodide (KI) and beryllium selenide (BeSe) are chosen among various binary insulators because of small lattice mismatch in supercell structures with graphene. The equilibrium distances and the total energies of possible atomic structures of graphene on (111) surfaces of binary insulators are analyzed. We study effects of binary insulating substrates on the electronic structures of graphene near the Dirac point. This work was supported by National Research Foundation of Korea (Grant No. 2009-0081204), and KISTI Supercomputing Center (KSC-2008-S02-0004).

**Dp-V-203****Optical Spectroscopic Investigation on the Electronic Structure of  $\text{LaVO}_3/\text{SrVO}_3$** **Superlattices**JEONG Da Woon, CHOI Woo Seok, DAVID Adrian<sup>1</sup>, LEE Yun Sang<sup>2</sup>, PRELLIER Wilfrid<sup>1</sup>, NOH Tae Won

*ReCOE, Department of Physics and Astronomy, Seoul National University, Seoul 151-747, Korea.. <sup>1</sup>Laboratoire CRISMAT, CNRS UMR 6508, ENSICAEN, 6 Blvd, Maréchal Juin, F-14050 Caen Cedex, France.. <sup>2</sup>Department of Physics, Soongsil University, Seoul 156-743, Korea..*

Discovery of high mobility 2-dimensional electron gas in  $\text{LaAlO}_3/\text{SrTiO}_3$  interface attracted a lot of interest in the oxide heterostructure. Oxide heterostructures frequently show novel physical properties, which could not have been observed in single-phase bulk materials. In particular, interfaces between different vanadium oxides have been extensively studied, where an intriguing physics has been observed due to the multi-valence nature of the vanadium ions. For examples, depending on the interface configuration of  $\text{LaVO}_3/\text{SrTiO}_3$  heterostructure, *p*-type  $\text{VO}_2/\text{SrO}/\text{TiO}_2$  interface shows insulating behavior, whereas *n*-type  $\text{VO}_2/\text{LaO}/\text{TiO}_2$  interface shows metallic behavior [1]. On the other hand, theoretical prediction for this phenomenon suggested orbital ordering of mixed valance state of vanadium ions in the 2-dimensionally confined geometry. [2] In this contribution, we investigated  $\text{LaVO}_3/\text{SrVO}_3$  superlattices by using optical spectroscopy.  $\text{LaVO}_3$  is a Mott insulator with  $\text{V}^{3+}$  ions ( $3d^2$ ) and  $\text{SrVO}_3$  is a metal with  $\text{V}^{4+}$  ( $3d^1$ ) ions. At the interface of the two oxide compounds, the different vanadium ion valence would be mixed to result in nominal valence state of  $\text{V}^{3.5+}$  ( $3d^{1.5}$ ). Using the variable angle spectroscopic ellipsometry, we derived in-plane and out-of-plane optical conductivity in the 0.72-5.6eV photon energy range. We could observe unusual sharp peak features in the out-of plane optical conductivity spectrum. We propose that this sharp feature comes from the 2-dimensional confinement of the vanadium orbital. [1] Y. Hotta, *et al.*, Phys. Rev. Lett 99, 236805 (2007)[2] G.Jackeli & G.Khaliullin, Phys. Rev. Lett 101, 216804 (2008)

**Dp-V-204****LOW LEAKAGE CURRENT AND ENHANCED FERROELECTRIC PROPERTIES OF Zn AND Mn CODOPED BiFeO<sub>3</sub> THIN FILMS**

LEE Myang Hwan, SONG Tae Kwon, LEE Sung Chan, KIM Myong Ho, SUNG Yeon Soo, CHO Jong Ho<sup>1</sup>, CHOI Byung Chun<sup>2</sup>, KIM Sang Soo<sup>3</sup>, DO Dal Hyun<sup>3</sup>, KIM Won -Jeong<sup>3</sup>

*School of Nano & Advanced Mat. Eng., Changwon Nat'l Univ., Gyeongnam.* <sup>1</sup>*Department of Physics, Changwon Nat'l Univ., Gyeongnam.* <sup>2</sup>*Department of Physics, Pukyong Nat'l Univ., Busan.* <sup>3</sup>*Research Institute of Basic Sciences, Changwon Nat'l Univ., Gyeongnam.*

To reduce leakage current and improve ferroelectric properties of multiferroic BiFeO<sub>3</sub> thin films, Zn and Mn co-doping effects were studied and compared with un-doped BiFeO<sub>3</sub> films. Bi(Fe<sub>0.96</sub>Zn<sub>0.01</sub>Mn<sub>0.03</sub>) thin films were deposited on Pt/Ti/SiO<sub>2</sub>/Si(100) substrates by a pulsed laser deposition. The substrate temperature changed from 500°C to 700°C and oxygen pressure ranged from 10 mTorr to 100 mTorr. The effects of Bi-excess in target were investigated because of the volatility of Bi during the deposition. Bulk Bi(Fe<sub>0.96</sub>Zn<sub>0.01</sub>Mn<sub>0.03</sub>)O<sub>3</sub> ceramics were also investigated for possible applications as piezoelectric ceramics.

**Dp-V-205****Scanning Tunneling Microscopy of Methanol Adsorption on NiAl(110) and Al<sub>2</sub>O<sub>3</sub>/NiAl(110) Deposited by Pulsed Injection**

CHOI Eunyeoung, LEE Younjoo, LYO In-Whan

*Institute of Physics and Applied Physics(IPAP), Yonsei university.*

Alcohol is a versatile polar solvent for molecules. As a preparation to deposit large molecules, we studied interaction of solvent molecules on metallic and oxide surface. In this work, we report on methanol adsorption on NiAl(110) and the thin oxide layer formed on NiAl(110) with scanning tunneling microscopy (STM). Methanol was deposited by using a pulse injection method suitable for deposition of thermally unstable molecules. The injection of liquid methanol onto the substrate in UHV was performed by using a high-speed solenoid valve with the back-pressure reduced down to 100 mb. This technique allowed precise control over the amount of dosing of molecules to less than 1 L. Methanol-induced features, attributed to methoxide, were found on bare NiAl(110) surface. When injected onto Al<sub>2</sub>O<sub>3</sub>/NiAl(110) surface, methanol etched away thin Al<sub>2</sub>O<sub>3</sub> layer, producing jagged step edges and short linear structures that is attributed to aggregates of methoxides.

### Ab Initio Study on Structural and Electronic Properties of Interfaces between Metal and HAT-CN Molecule for OLED Applications

KIM Ji-Hoon, PARK Yongsup, KWON Young-Kyun

*Department of Physics and Research Institute for Basic Sciences.*

Using *ab initio* density functional theory (DFT), we studied the electronic structures of interface between a metal surface and organic molecule, 1,4,5,8,9,11- hexaazatriphenylene-hexacarbonitrile (HAT-CN) which is known as an efficient hole injection layer for organic light emitting diodes (OLEDs) and a strong electron acceptor. We have investigated the geometrical and electronic properties of HAT-CN on different metal surfaces including Ca(111) and Cu(111). We found that the edge nitrogen atoms of HAT-CN have stronger interaction on metal surfaces than other atoms in the molecule. The resultant charge transfer between the HAT-CN molecule and the surface formed a dipole at the interface. We discuss the changes in electrostatic potential and work function of the surface due to these interactions in comparison with the experimental results.

### Effect of Mg Cation Substitution on the Resistance Switching Behavior in Epitaxial NiO Films

KIM Hoonmin, LEE Seungran, PARK Junghun<sup>1</sup>, CHO Myungrae<sup>2</sup>, PARK Daniel Yun<sup>2</sup>, CHAR Kookrin

*Department of Physics and Astronomy and Center for Strongly Correlated Materials Research, Seoul National University. <sup>1</sup>Samsung Electronics. <sup>2</sup>Department of Physics and Astronomy, Seoul National University.*

Bipolar resistance switching mechanism was investigated by substituting Mg cation at epitaxial NiO films (epi-NiO). We altered the interface between NiO and top electrode (TE) by 5-nm-thick 10 % substitution of Mg and 1-nm-thick MgO<sub>x</sub> interlayer by pulsed laser deposition method. Surface morphology and crystallinity were confirmed by XRD data and AFM images indicating that samples were grown to epitaxially. The number of cells which showed the bipolar resistance switching was lowered in case of 10 % substituted Mg on top surface in epi-NiO and no resistive switching was observed when MgO<sub>x</sub> thin layer was inserted between NiO and TE. Our experimental results suggest that oxygen ions migration from the defects in epi-NiO on top surface may play a critical role in the bipolar resistance switching of epi-NiO. The resistance transition may be suppressed due to the presence of Mg cations whose free energy of oxidation is much lower than that of Ni.

**Dp-V-209****Study of chromium doped SrTiO<sub>3</sub> and SrZrO<sub>3</sub> system**

CHO Suyeon, PARK Wongoo, OH S.-J.

*Department of Physics and Astronomy, Seoul National University, Seoul 151-747, Korea.*

Transition-metal doped insulators have shown many interesting phenomena in the field of condensed matter physics for several decades, for examples, colossal magneto-resistance (CMR), solid oxide fuel cells (SOFCs), diluted magnetic semiconductor (DMS), transparent conducting oxide (TCO), and non-volatile memory (Resistive random access memory, RRAM). We synthesized Cr doped SrTiO<sub>3</sub>, and SrZrO<sub>3</sub> as a form of the singlecrystal, the polycrystal and the thin film, They were measured their physical properties by X-ray diffraction (XRD), electron spin resonance (ESR), and Superconducting Quantum Interference Devices(SQUID). Their electronic structures were analyzed by *in-situ* UPS and XPS controlling the growth parameters. We studied the changes of the electrochemical properties caused by chromium ions in the system. We found that their electric/magnetic properties would depend on their growth conditions especially the sort of gas environment and substituted Cr ions could behave in different ways.

**Dp-V-210****Dehydrogenation of Graphane Using the Current Induced Cleaning Technique in****UHV System**

CHO Doohee, KIM Minseong, LYO In-Whan

*Department of Physics, Yonsei Univ..*

We report on the reversible hydrogenation of mono- and multi-layers of exfoliated graphene by using a high flux hydrogen atomizer and thermal desorption in a UHV system. Our atomizer allows the adsorption of hydrogen onto graphene without any damage, and the absorbed hydrogen atoms transformed metallic graphene into insulating graphane. Before and after hydrogenation, the joule-heated temperature-dependent resistance was obtained by two-probe measurements. Resistivity of graphene and graphane in high- and low- current regime will be compared..

**Dp-V-211****Charge distribution of O-H...O bonds in proton irradiated  $\text{KH}_2\text{PO}_4$  ferroelectrics**

KIM Se-Hun, HAN Doug Young<sup>1</sup>, CHAE S. A.<sup>2</sup>, HAN J. H.<sup>3</sup>, LEE Cheol Eui<sup>3</sup>

*Faculty of Science Education, Jeju National University, Jeju 690-756, Korea. <sup>1</sup>Nano-Bio Team, Korea Basic Science Institute, Seoul 136-713, Korea. <sup>2</sup>Korea Basic Science Institute, Daegu 702-701, Korea. <sup>3</sup>Department of Physics and Institute for Nano Science, Korea University, Seoul 136-713, Korea.*

The mechanism of charge distribution has been probed by measuring the  $^1\text{H}$  chemical shift on a proton-irradiated  $\text{KH}_2\text{PO}_4$  (KDP) single crystal. For the high resolution  $^1\text{H}$  chemical shift measurement, CRAMPS (Combined Rotation And Multiple Pulses) technique is utilized. The proton irradiation caused the increase in  $^1\text{H}$  chemical shift. It can be interpreted as the electronic charge transfer from the proton to oxygen atom, accompanied with the proton displacement along the hydrogen bond. The calculated Morse potentials are introduced by an evidence of electronic instabilities related to the proton displacive features.

**Dp-V-212****Single-molecule fluorescence study of recombination protein-DNA interactions**

김 철희, 김 승현, 전 효은, 이 남기

*포항공대 물리학과.*

DNA recombination is a fundamental process for the DNA repair in cells. In a prokaryote, DNA recombination occurs in two pathways: "RecBCD" and "RecFOR". Although "RecBCD" pathway has been studied well, "RecFOR" pathway is still poorly understood due to its complexity. "RecFOR" pathway consists of RecF, RecO, and RecR proteins, where RecR, forming a ring-shaped tetramer, plays a major role in their functions. The binding mode between RecR and DNA and the location of RecR on DNA are still unknown. In this work, we have prepared fluorescently labeled RecR and DNA and investigated the physical interactions of RecR and DNA using the technique of single-molecule Alternating-Laser Excitation Fluorescence Resonance Energy Transfer.

MYOUNG Nojoon, IHM Gukhyung

Department of Physics, Chungnam National University.

We studied one-dimensional transport in armchair nanoribbons modulated by a magnetic barrier structure to overcome the confinement problem of Dirac fermions. The inhomogeneous magnetic field distribution can be created by the use of ferromagnetic gates and plays the exact role of tunneling barrier experienced by Dirac fermions. In this study, conductance in our system is obtained as a function of incident energy. The results show stepwise increases superimposed upon the characteristic oscillations of order of height  $4e^2/h$ .

### 정공저지층과 전자저지층 역할을 하는 이중발광층을 사용한 청색 유기발광소자의 색순도 향상 메카니즘

서 수열, 방 현성<sup>1</sup>, 추 동철<sup>2</sup>, 김 태환<sup>1</sup>, 서 지현<sup>3</sup>, 김 영관<sup>3</sup>

한양대학교, 정보디스플레이공학과. <sup>1</sup>한양대학교, 전자컴퓨터통신공학과. <sup>2</sup>한양대학교, 디스플레이공학연구소. <sup>3</sup>홍익대학교, 정보디스플레이공학과.

청색 유기발광소자는 적색과 녹색 유기발광소자들에 비해 상대적으로 발광효율이 낮고 색 순도가 떨어지며 수명이 짧기 때문에 적색, 녹색 및 청색 유기발광소자를 사용하여 전색 발광소자를 구현하는데 문제점을 가지고 있다. 이런 문제점들을 해결하기 위하여 청색 발광재료의 개발, 다층 이중구조 및 형광 또는 인광 도펀트의 도핑에 대한 연구와 더불어 진청색 고효율 청색 유기발광소자에 대한 연구가 진행되어 왔다. 본 연구에서는 발광효율을 높이고 색 순도를 증가하기 위해 4,4'-Bis(2,2'-diphenyl-ethen-1-yl)biphenyl (DPVBi) 와 4,4'-Bis(carbazol-9-yl)biphenyl (CBP)로 구성된 이중 발광층 구조를 갖는 청색 유기발광소자를 제작하여 전기적 성질과 광학적 성질을 조사하였다. DPVBi/CBP 이중발광층을 가진 청색 유기발광소자에서 CBP의 highest occupied molecular orbital 에너지준위가 매우 크기 때문에 발광층에서 전자수송층으로 빠져나가는 정공을 막는 정공 장벽층의 역할을 하게 된다. DPVBi는 CBP보다 작은 lowest unoccupied molecular orbital을 갖기 때문에 CBP의 전자에 대한 주입장벽을 크게하여 발광층에 머무르는 전자의 양을 증가하였다. 이로 인하여 발광층내에는 단일발광층에 비해 더 많은 전자 및 정공이 존재하여 전자-정공의 재결합 확률을 높였으며 재결합하는 영역을 발광층 중앙으로 이동시켜 발광영역의 넓어짐을 방지하였다. 단일 발광층으로 구성된 청색유기발광소자에 비해 이중발광층으로 구성된 청색유기발광소자의 효율이 높음으로 이중 발광층에서 많은 엑시톤을 형성 된다는 것을 나타내고 있다. 이와 같은 결과는 DPVBi와 CBP로 구성된 이중 발광층을 사용하여 색순도가 증가된 고효율 청색유기발광소자를 제작할 수 있음을 보여준다. This work was supported by the Korea Science and Engineering Foundation (KOSEF) grant funded by the Korea government (MEST) (No. R0A-2007-000-20044-0).

**Dp-V-215****The study of kinetics of membrane protein into lipid bilayer**

LEE Hyunwon, SONG Sanghoon, CHA Wonsuk, CHOI Ahreum<sup>1</sup>, JUNG Kwanghwan<sup>1</sup>, KIM Hyunjung

서강대학교 물리학과 & 바이오융합기술협동과정, <sup>1</sup>서강대학교 생명과학과.

Lipid와 membrane protein의 layer 형성 및 구조에 관한 연구는 세포의 기능과 구성 요소 간 상호작용 메커니즘을 이해하는 데에 매우 중요하며, protein, DNA, 항체 또는 세포 등을 감지물질로 고밀도 집적화하는 나노 바이오칩 및 소자 기술 개발에 필수적이다. 본 연구에서는 수용액 속에서 자기조립방법으로 형성된 lipid의 적층 구조에 소포 형태를 이루고 있는 membrane protein의 크기를 조절하여 넣은 후, X-ray reflectivity를 이용하여 상호 작용 및 형성과정을 in-situ로 측정하였다. 본 실험은 포항가속기의 5A beamline에서 수행되었으며, 수용액을 통과하는 X-ray의 흡수를 최소화하기 위하여 20KeV의 X-ray를 이용하였다. 수용액 상태에서 자기조립방법을 통해 이중층으로 형성된 lipid에 단일막의 소포 형태를 이루고 있는 rhodopsin을 넣었을 때 tail 부분의 electron density가 증가하는 변화가 보이는 반면 그보다 큰 형태의 rhodopsin을 넣었을 때와 lipid를 첨가한 경우에는 아무런 변화가 보이지 않았다. 이를 통해 단일막의 소포 형태를 이루고 있는 rhodopsin의 침투 메커니즘을 설명하였다. This work was supported by National Research Foundation of Korea, Seoul Research and Business Development program, and Sogang University Research Grant.

**Dp-V-216****Single-molecule Fluorescence Study on the DNA Bending**

김 재열, 안 태기, 이 남기

포항공대, 물리학과.

Recently, mechanical properties of short dsDNA have become a subject of special interest due to the observation of the unexpected improvement of DNA flexibility. Several studies have suggested local melting of double-helix facilitates spontaneous bending, which increases the flexibility of short DNA. However, the study of the effects of DNA bending on its melting is relatively rare. In this work, we investigated bending induced melting (or hybridization) by single-molecule fluorescence technique (ALEX-FRET). We construct bent DNA using circular single-stranded DNA and complimenting it partially. We have observed the reduction of hybridization ratio, when we used bent DNA. Interestingly, the bent DNA had two discrete conformations depending on the salt concentrations.

**Dp-V-217****Enhancement of frequency selectivity of sound sensor in water inspired auditory****hair cell**

KIM Hyery, SONG Taegeun, PARK Hee Chul, PARK Ikgon, KIM Hanna, PARK Ji Eun, AHN Kang-Hun

*Department of Physics, Chungnam National University.*

Sound detection in water with high sensitivity has attracted great attention due to its possible application to advanced hydrophone for submarine detection, etc. Hair cell in the ear provides an ingenious design of hydrophone. Hair cells transform sound signals into neuronal signals with great sensitivity and large dynamic range where adaptation process is known to play important roles. Following the idea proposed in Ref. [1], we fabricated the sound sensor in water where adaptation process is implemented. The sensor is in cantilever type with typical length of 1cm. While the quality factor  $Q$  of the sensor without adaptation process in the air was about 70, the  $Q$  factor decreases as about 10 when the sensor is immersed in water. When we turn on the adaptation process, the frequency selectivity of the sensor in the water increases so that the  $Q$  factor increases by an order of magnitude. We show that the frequency selectivity and sensitivity of the sound sensor in water are dramatically enhanced due to the adaptation process we implemented.

**Dp-V-218****Temperature- and Concentration- dependence of Lipid Multilayer Formation by****X-ray reflectivity**

SHIN Kwangwoo, SONG Sanghoon, KIM Hyunjung

*Sogang University, Department of Physics & Interdisciplinary Program of Integrated Biotechnology.*

We measured the multilayers of lipid membranes by X-ray reflectivity. The understanding of the formation of lipids multilayer is important to develop biochips and biosensors. 1,2-Dioleoyl-sn-Glycero-3-Phosphocholine(DOPC) is dissolved in chloroform and spun cast on Si wafer. In order to minimize the solvent effect, we annealed the sample at room temperature in  $10^{-5}$  torr for 24hours. We observed the multilayer formation depending on the DOPC concentration. The selection rules for higher order diffraction peaks were calculated by form factors of stacking of head and tail parts of the lipids. We also observed the decrease of the thickness of lipid layers with increasing temperature but the slope changes near  $45^{\circ}\text{C}$ . Similar behavior has been observed with the sample annealed  $80^{\circ}\text{C}$  higher than the boiling temperature of chloroform for 24hours. When the sample is cooled down to room temperature, lipid multilayer recovers to its original length. This study was supported by National Research Foundation, Seoul Research and Business Development program and Sogang University Grant.

**Dp-V-219****Proton-Irradiation effects on the resistance of highly-oriented pyrolytic graphite**LEE Cheol Eui, KIM Jin Soo<sup>1</sup>, LEE Kyu Won<sup>1</sup>Korea University, Physics. <sup>1</sup>Korea university, Physics.

We have investigated the proton-irradiation effects on highly-oriented pyrolytic graphite (HOPG) by measuring the surface, bulk and c-axis resistance with a standard four-probe method. The HOPG samples were irradiated with 2.25-MeV proton beam to doses of  $10^{15}$  to  $10^{17}$  ions/cm<sup>2</sup> at room temperature and the current-voltage characteristics were measured. The surface resistance increased with increasing irradiation dose, presumably due to surface defects induced by the irradiation. The bulk and c-axis resistance decreased with increasing irradiation dose, presumably due to surplus charge carriers by the irradiation. This work was supported by the Seoul Research and Business Development Program, Grant No. 10583.

**Dp-V-220****Cesium Fluoride/C60 이중 전자주입층을 이용해 전자주입효율을 향상한 고효율 녹색유기발광소자**양 지성, 추 동철<sup>1</sup>, 김 태환<sup>1</sup>, 진 유영<sup>2</sup>, 서 지현<sup>2</sup>, 김 영관<sup>2</sup>한양대학교 정보디스플레이공학과. <sup>1</sup>한양대학교 전자통신컴퓨터공학과. <sup>2</sup>홍익대학교 정보디스플레이공학과.

유기발광소자의 발광층 내에서 전자와 정공의 효율적인 재결합은 발광효율에 중요한 영향을주기 때문에 발광층에서 재결합 확률을 높이는 구조에 대한 다양한 연구가 소자의 응용에 매우 큰 영향을 주고 있다. 그러나 대부분의 전도성 유기물내에서 전자의 이동도가 정공의 이동도보다 작기 때문에 전자와 재결합을 하지 못한 정공은 누설전류로써 소비되고 발광 효율이 낮아진다. 본 연구에서는 전자주입효율을 향상하기 위하여 강한 전자 받게 역할을 하는 플러렌(C60)의 장점을 이용한 이중 전자 주입층을 제작하고 녹색 유기발광소자에 적용하여 발광효율의 변화를 관찰하였다. 유기발광소자에서 전자의 이동도를 향상하여 발광층내로 주입되는 전자의 주입량을 증가시킴으로써 엑시톤 형성 확률을 증가하기 위하여 전자주입층 내에 플러렌을 첨가하였다. CsF(Cesium flouride)으로만 이루어진 단층 전자 주입층으로 구성된 유기발광 소자는 8-hydroquinolatolithium으로만 이루어진 단층 전자 주입층으로 구성된 유기발광 소자 보다 훨씬 높은 고효율을 보여주나 CsF와 플러렌으로 구성된 이중 전자 주입층을 구성된 유기 발광 소자보다 훨씬 낮은 효율을 보여주었다. 플러렌은 주변 분자들과 결합을 잘 형성하는 구조로 유기물 또는 금속내에 첨가시 전자의 주입을 방해하는 트랩으로 작용하기 때문에 플러렌 단층 전자 주입층은 매우 낮은 전류만이 측정되었다. 플러렌의 높은 전자전도성을 유지하며 금속과의 결합형성을 막기 위하여 매우 얇은 CsF 층을 알루미늄 금속과 플러렌 사이에 형성함으로써 알루미늄 금속과의 직접 접촉을 막았으며, 기존의 단층 전자주입층 및 플러렌단일층 으로 구성된 전자주입층을 사용한 유기발광소자와 발광특성을 비교하였을 때 CsF와 플러렌으로 구성된 이중 전자주입층을 가진 유기발광소자의 발광효율 향상이 나타남을 관찰하였다. This work was supported by the Korea Science and Engineering Foundation (KOSEF) grant funded by the Korea government (MEST) (No. R0A-2007-000-20044-0).

**Dp-V-221****Ag 나노입자가 분산된 Polymethyl methacrylate 박막을 플로팅 게이트로 사용하는 비휘발성 메모리 소자의 전기적 성질**

김 원태, 곽 진구, 윤 동열, 정 재훈, 김 태환

한양대학교 전자컴퓨터통신공학과.

유기물에 금속 나노 입자를 분산시켜 만들어진 유기물/무기물 복합 재료를 사용하여 제작된 비휘발성 메모리 소자의 전기적 특성에 관한 연구가 많이 진행되고 있다. Ag 나노입자가 포함된 고분자층을 플로팅 게이트로 사용하는 비휘발성 메모리에 관한 연구는 간단한 방법으로 고집적 비휘발성 메모리 제작에 대단히 유용하다. 본 연구에서는 Ag 나노입자를 절연성 고분자인 polymethyl methacrylate (PMMA) 층에 분산시켜 제작한 플로팅 게이트를 사용한 비휘발성 메모리 소자의 전기적 특성과 메모리 효과를 관찰하였다. 소자 제작에 사용된 Ag 나노입자는 화학 환원법을 사용하여 합성되었다. 소자를 제작하기 위해 제작된 Ag 나노 입자 분산되어 있는 PMMA 용액을 p-Si (100) 기판위에 스펀코팅을 하여 박막으로 형성한 후, 열을 가해 용매를 증발시켜 Ag 나노 입자가 분산되어 있는 PMMA 박막을 형성하였다. 형성된 PMMA 박막은 터널링 절연막 및 게이트 절연막의 역할을 하며, PMMA 안에 분산된 Ag 나노 입자는 플로팅 게이트의 역할을 하게 된다. PMMA 고분자 박막위에 Al을 열증착하여 게이트 전극을 형성하였다. 제작된 소자의 용량-전압 (C-V) 측정 결과에서는 금속-절연체-반도체 구조에서의 C-V 특성과 플로팅 게이트 내에서의 전하 포획에 의한 평탄 전압 이동 ( $\Delta V_{FB}$ )을 보여주었다. 고분자 박막층에 Ag 나노입자가 없을 경우에는  $\Delta V_{FB}$ 가 매우 작기 때문에 PMMA 자체에서의 전하 포획능력은 없음을 알 수 있다. Ag 나노입자의 농도가 0.1 wt%인 소자의 C-V 곡선에서  $\Delta V_{FB}$ 가 0.8 V로 나타났으며, Ag 나노 입자가 0.5 wt%의 농도로 포함된 기억소자는  $\Delta V_{FB}$ 가 2.3 V로 관찰되었다. PMMA 층의 Ag 나노입자의 농도가 증가함에 따라  $\Delta V_{FB}$ 가 증가 하였다. 따라서 PMMA 층의 Ag 나노입자의 농도를 조절하여 최적화된 저장 능력을 가진 비휘발성 메모리 소자를 제작할 수 있음을 알 수 있다. This work was supported by the Korea Science and Engineering Foundation (KOSEF) grant funded by the Korea government (MEST) (No. R0A-2007-000-20044-0).

**Dp-V-222****요오드 도핑에 의한 유기반도체 Tetramethyletraselenafulvalene(TMTSF)의 광학적 특성 변화**

윤 미라, 이 인재

전북대학교 물리학과.

Tetramethyletraselenafulvalene (TMTSF)는 저 차원 유기 초전도 금속 물질인  $(TMTSF)_2X$ 의 ( $X=ClO_4$ ,  $PF_6$ ,  $AsF_6$  등) 주축(backbone)물질로 잘 알려져 있으며,  $(TMTSF)_2X$ 에서 전자공여체의 역할을 한다. 아르곤(Ar)을 이송가스로 사용한 기상증착(PVD) 방법을 이용하여 음이온 X가 결합되어 있는, 반도체 특성을 가진 정질의 TMTSF 단결정을 성장시켰다. 단결정 TMTSF에 요오드를 확산도핑하기 위하여 TMTSF 단결정이 들어있는 상온의 반응조를 고상의 요오드가 들어있는 소스관에 연결하였다. 요오드 소스관의 온도를 243K로 조절하여 요오드의 증기압을 1 mtorr로 유지 함으로서 적절한 도핑속도를 유지하였다. 요오드( $I_2$ )로 도핑된 TMTSF 유기 반도체 결정의 광학적 특성을 알아보기 위하여 광 흡수분광실험(Absorption), 발광실험(Photoluminescence), X선 광전자 분광실험(X-ray photoelectron spectroscopy), 자외선 광전자 분광실험(Ultraviolet photoelectron spectroscopy)을 수행하였다.

We report proton-irradiation effects in [6,6]-phenyl-C61-butyric acid methyl ester (PCBM) thin-films, studied by using Fourier-transform infrared (FT-IR) spectroscopy. PCBM is an electron acceptor material and is often used in plastic solar cells. The PCBM thin films, spin-coated on glass, were irradiated with proton-beams of an energy range from 0.5 to 2 MeV and fluence from  $1 \times 10^{13}$  to  $1 \times 10^{16}$  ions/cm<sup>2</sup>. Sharp IR absorptions were observed at the frequencies of 650, 1430 and 1750 cm<sup>-1</sup>, corresponding to butyric acid methyl ester, fullerene and carbonyl group, respectively. Among them, the peak at 650 cm<sup>-1</sup> showed the largest change, indicating that the proton irradiation mostly attacked butyric acid methyl ester. (This work was supported by the Seoul Research and Business Development Program, Grant No. 10583)

**Ep-V-103****Giant Diamagnetic Properties of Half-metallic Thin Films**

EOM T. W., KIM K. W.<sup>1</sup>, RHEE J. Y.<sup>2</sup>, KUDRYAVTSEV Y. V.<sup>3</sup>, PROKHOROV V. G.<sup>3</sup>, LEE Y. P.

*q-Psi and Department of Physics, Hanyang University. <sup>1</sup>Department of Information Display, Sunmoon*

*University. <sup>2</sup>Department of Physics, Sungkyunkwan University. <sup>3</sup>Institute for Metal Physics, National Academy of Sciences of Ukraine.*

Peculiar magnetic properties of half-metallic  $\text{Co}_2\text{CrAl}$  and  $\text{La}_{0.8}\text{Ce}_{0.2}\text{MnO}_3$  thin films are investigated and the origin of a giant diamagnetism (GD) observed at low temperatures is analyzed in connection with the peculiar electronic structures of the materials.  $\text{Co}_2\text{CrAl}$  full Heusler-alloys thin film was prepared by flash evaporation of crushed alloy powders of 80 – 100  $\mu\text{m}$  in diameter onto a glass substrate. The thickness of  $\text{Co}_2\text{CrAl}$  film was about 135 nm.  $\text{La}_{0.8}\text{Ce}_{0.2}\text{MnO}_3$  thin film was prepared by cross-beam laser-ablation technique on a  $\text{LaAlO}_3$  substrate. The thickness of  $\text{La}_{0.8}\text{Ce}_{0.2}\text{MnO}_3$  film was about 300 nm. The magnetic properties were investigated in a temperature range of  $5 \leq T \leq 350$  K using a superconducting quantum interference device magnetometer for the samples cooled in field-cooled and zero-field-cooled (ZFC) modes. The ZFC magnetization exhibits a GD at low temperatures and the magnetization direction is flipped abruptly at a certain temperature ( $T_z$ ) upon heating.  $T_z$  is decreased as the strength of measuring field increases. We attribute this GD to the interplay between Landau diamagnetism and peculiar electronic structures which are closely related to the half-metallicity of both materials.

**Ep-V-104****Anomalous Magneto-transport Properties of Two-dimensional Ni/Co Anti-dot****Arrays**

KIM G. H., NAM W. C., SEO M. S., LEE S. J., LEE Y. P., RHEE J. Y.<sup>1</sup>, KIM K. W.<sup>2</sup>

*Quantum Potonic Science Research Center, Hanyang University, Seoul, 133-791, Korea. <sup>1</sup>Quantum Potonic*

*Department of Physics, Sungkyunkwan University, Suwon 440-746, Korea. <sup>2</sup>Department of Physics, Sunmoon University, Asan 336-708, Korea.*

Magnetic nanostructures have attracted intense research interest for decades. Keeping pace with the progress of nanoscience and nanotechnology, novel fabrication techniques have been developed for their realization in various forms to study the magnetic properties in anticipation of wide applications. We fabricated two-dimensional Ni/Co bi layer anti-dot arrays using the CMOS process. Two different structures of square- and hexagonal-lattice with a periodicity ranging from 600 to 1600 nm were prepared and their microstructures were examined by scanning electron microscopy and atomic force microscopy. In addition, the magneto-transport properties were measured systematically by using a Physical Property Measurement System in which an in-plane external field was applied. In this work, we report the anomalous behavior of longitudinal and transverse magnetoresistance of Ni/Co bi layer anti-dot arrays observed near room temperature, and discuss the possible origin.

**Ep-V-105****Intrinsic Ferromagnetism Of Pure ZnO Film**

D. F. Wang, V. T. T. Thuy, G. H. Kim, T. U. Um, Y. P. Lee

*q-Psi and Department of Physics, Hanyang University.*

Since the first discovery of ferromagnetism of pure  $\text{HfO}_2$  by Coey and his coworkers [1], there have been extensive efforts to study the magnetism of the conventional nonmagnetic oxide system. However, the ferromagnetism found in those systems by direct magnetization measurements is questionable, and its origin has been doubted to be from impurities [2]. In this work, by using the electrical characterization as well as the magnetization measurement, it is demonstrated that the ferromagnetism in pure ZnO is intrinsic, not from impurities. ZnO film was deposited on a silicon wafer by magnetron sputtering and it was characterized by x-ray diffraction, and by employing a superconducting quantum interference device magnetometer (SQUID), and a physical property measurement system (PPMS). The magnetic property measurements using SQUID show that the ZnO film is ferromagnetic at room temperature. The electrical measurement with PPMS shows that the ZnO film has a positive magnetoresistance as large as 30%, which provides the key information on the coupling between itinerant electrons and localized magnetic moments. Therefore, any contribution from unintentional contamination can be excluded, which confirms the ferromagnetism of ZnO film to be intrinsic. [1] M. Venkatesan, S. B. Fitzgerald, and J. M. D. Coey, *Nature*, 430, 630 (2004).[2] D. W. Abraham, M. M. Frank, and S. Guha, *Appl. Phys. Lett.*, 87, 252502 (2005).

**Ep-V-106****Er이 첨가된 tungsten-tellurite 유리의 upconversion 형광특성**김 중환, 최 혜영<sup>1</sup>, 노 현미, 양 진복, 박 경락, 정 중현<sup>1</sup>, 문 병기<sup>1</sup>*동의대 물리학과. <sup>1</sup>부경대 물리학과.*

Tungsten함량을 달리한 tungsten-tellurite유리에 1mole%의  $\text{Er}^{3+}$ 이온을 첨가한 유리를 합성하고 upconversion 형광의 특성을 조사하였다.  $\text{Er}^{3+}$  이온의  $4\text{I}_{15/2} \rightarrow 4\text{I}_{11/2}$  준위에너지에 해당되는 975nm의 광원으로 여기하여 녹색과 적색의 upconversion 형광을 측정하였다. Tungsten의 함량이 커짐에 따라 전체적인 upconversion 형광의 세기는 점차 감소하였다. Tellurite 유리에 비해 tungsten-tellurite 유리는 최대 광포논 에너지가 높아 비방사전이율이 증가하게 된다. Tungsten의 함량이 커지면  $4\text{I}_{11/2}$ 에서  $4\text{I}_{13/2}$  준위로의 비방사 전이율이 증가하고 중간준위인  $4\text{I}_{11/2}$  준위의 수명이 짧아져서  $4\text{I}_{15/2} \rightarrow 4\text{I}_{11/2} \rightarrow 2\text{H}_{11/2}$ ,  $4\text{S}_{3/2}$  전이에 의한 녹색의 upconversion 형광의 효율은 떨어진다. 적색형광의 경우  $4\text{I}_{13/2}$  준위의 밀도가 커지면  $4\text{I}_{13/2} \rightarrow 4\text{F}_9/2$ 의 여기준위 흡수는 증가하게 되나  $4\text{I}_{11/2}$  준위의 밀도가 줄어들므로  $4\text{I}_{11/2} + 4\text{I}_{13/2} \rightarrow 4\text{I}_{15/2} + 4\text{F}_9/2$ 의 에너지 전달 효율은 줄어들게 된다. 측정결과 텅스텐의 함량이 증가할수록 녹색형광과 함께 적색형광의 세기도 줄어들어 적색형광이 여기준위 흡수보다는  $4\text{I}_{11/2}$ 와  $4\text{I}_{13/2}$  준위가 관계된 에너지 전달과정에 의한 것임을 확인할 수 있었다. 이상의 결과는 5ns, 10Hz의 BBO-OPO를 여기광으로 하여 측정한 upconversion 형광의 시간적 거동에서도 확인할 수 있었다.

**Ep-V-107****Transient Current Measurements of PEDOT:PSS and EG-PEDOT:PSS films**

LEE Jung-Keun, HAMZA Ammar

*Department of Physics, Chonbuk National University.*

Time-dependent currents in poly(3,4-ethylenedioxythiophene):poly(styrene sulfonate) (PEDOT:PSS) and EG-PEDOT:PSS films were investigated. The  $I$  vs.  $V^2$  plot showed three different stages clearly: Ohmic, space-charge-limited, and thermally degrading stages. The EG-PEDOT:PSS showed an improvement in high voltage breakdown compared to PEDOT:PSS. From the space-charge limited current peak, we obtained the hole mobility,  $\mu_h = 2 \times 10^{-5} \text{ cm}^2/\text{Vs}$  for PEDOT:PSS, and  $\mu_h = 1 \times 10^{-2} \text{ cm}^2/\text{Vs}$  for EG-PEDOT:PSS. From the thermally-degrading current peak, we obtained electron mobility,  $\mu_n = 1 \times 10^{-7} \text{ cm}^2 \text{ V}^{-1} \text{ s}^{-1}$  for PEDOT:PSS, and  $\mu_n = 1 \times 10^{-4} \text{ cm}^2 \text{ V}^{-1} \text{ s}^{-1}$  for EG-PEDOT:PSS.  $V_{\text{offset}}$  was 10 V for PEDOT:PSS, while  $V_{\text{offset}}$  was 1 V for EG-PEDOT:PSS.

**Ep-V-108****용매에 녹는 Alq<sub>3</sub>유도체를 사용한 OLED소자의 발광특성**

김 형욱, 조 성윤, 이 순일, 고 근하

*아주대학교, 에너지시스템학부.*

Alq<sub>3</sub>는 높은 발광효율과 전자 전도성으로 OLED소자에서 녹색 발광물질 및 발광 호스트 물질 그리고 전자 수송층등으로 사용된다. 하지만 Alq<sub>3</sub>는 유기용매에 잘 녹지 않아 진공증착을 이용하여 박막을 형성하여야 되므로 OLED소자 제작 시 대형화를 하기 힘들다는 단점을 가지고 있다. 이러한 점을 개선하기 위하여 Alq<sub>3</sub>를 기반으로한 저분자, 고분자 유도체를 만들고 그 유도체의 특성을 분석하는 연구들이 활발하게 진행 중이다. 이번 실험에서는 본교 유기화학팀이 합성한 mono-5-d-8-Alq<sub>3</sub>를 사용하여 OLED소자를 제작하였다. OLED소자를 제작시 전공 수송물질로 사용되는 NPB를 합성한 Alq<sub>3</sub>를 녹인 용매인 톨루엔이 녹여 NPB와 Alq<sub>3</sub> 톨루엔에 녹인 후 섞어 스프인코팅으로 발광층을 만들고 발광특성 및 전류특성을 측정하였다. 그 결과 질량비 1:1로 섞은 용액으로 발광층 60nm를 만든 OLED소자가 9.5V에서 30cd/m<sup>2</sup>의 휘도와 400mA/cm<sup>2</sup>의 전류특성을 가지는 것을 확인하였다. NPB와 합성한 Alq<sub>3</sub>의 질량비를 바꾸어서 발광층을 형성한 후 전류특성을 측정한 결과 이 물질을 사용하여 만든 OLED는 전공에 의해서 전류특성이 좌우되는 것을 확인할 수 있었고 더 높은 발광효율을 얻기 위하여 TiO<sub>2</sub>층을 전자 수송층으로 사용하여 전자의 공급을 조절하거나, 낮은 온도에서 톨루엔에 녹지 않는 poly-TPD를 클로로 벤젠(chlorobenzene)에 녹여 전공수송층을 따로 형성하여 전공의 공급을 조절하여 각각의 경우에서 발광효율과 전류특성을 확인하였다.

**Ep-V-109****전도성 고분자 물질의 특성과 유기 태양전지의 효율에 끼치는 영향**

조 성윤, 임 종혁, 김 형욱, 고 근하, 이 순일

아주대학교 에너지시스템학부 응용물리전공

벌크이종접합 고분자 유기 태양전지는 대개 ITO 투명 전극과 광활성 유기층 사이에 PEDOT:PSS 층을 사용하여 만든다. 소자를 제작할 때 PEDOT:PSS 층을 넣을 경우 ITO 투명 전극에 비해 다소 큰 일함수를 가지므로 양극의 선택이 용이하고, 광활성 유기층과 음극 사이를 매끄럽게 해주는 등의 긍정적인 효과를 나타낸다. 또한 소자의 높은 효율을 위해 PEDOT:PSS 층의 전기적 특성은 매우 중요하다. 따라서 PEDOT:PSS 층의 전도성과 소자 효율과의 상관관계를 연구하였다. 그 후 두께, 표면 상태와 소자의 효율과의 관계를 조사하였다. PEDOT:PSS 층으로는 CLEVIOS 사의 P VP AI4083과 CLEVIOS P를 사용하여 그 결과를 비교하였다. 그 결과, P VP AI4083을 사용한 경우 소자 효율은 2.33%를 보였으며, CLEVIOS P를 사용한 소자의 효율은 2.80%의 효율을 보였다. 한 달 후 다시 측정해본 소자의 효율은 P VP AI4083를 사용한 경우 2.33%에서 2.21%로, CLEVIOS P 사용한 경우 2.80%에서 2.53%의 결과를 보인 바, P VP AI4083을 사용한 소자가 비교적 안정적인 소자 특성을 가짐을 확인했다. 추가로 실시한 ITO를 대체한 CNT 투명 전극을 사용한 실험에서도 비슷한 소자 특성을 보였다.

**Ep-V-110****분무열분해법으로 성장된 CdO:Cu 박막의 구조와 광학적 전기적 특성**

서 동주, 김 지효, 김 고은, 이 소리, 박 정복, 김 나리, 오 상미, 김 건호<sup>1</sup>

조선대학교, <sup>1</sup>경상대학교

CdO: Cu 박막을 분무열분해법으로 유리기판 위에 성장시켰다. CdO: Cu 박막을 성장시키기 위해 사용한 시약은 cadmium acetate, copper chloride이며, 이차증류수에 이들 시약을 녹여 0.02 mole 수용액을 만든 후 증류수를 혼합하여 분무용액을 만들어 사용하였다. 성장온도와 Cu 농도 변화에 따른 CdO: Cu 박막의 결정구조를 규명하기 위하여 X-선 회절분광기(XRD)를 이용하였으며, CdO: Cu 박막의 표면과 미세구조는 주사전자현미경(SEM)을 이용하여 관찰하였다. CdO: Cu 박막에 입사한 빛의 파장을 변화시키면서 광투과와 광흡수 스펙트럼을 측정하여 광학적인 특성과 에너지 간격을 구하였다. 시료에 대한 Hall의 효과를 van der Pauw법으로 실온에서 측정하여 비저항, 운반자 농도 등의 전기적 특성을 규명하였다.

## (PVP) Dielectrics

HAMZA Ammar, LEE Jung-Keun

Department of Physics, Chonbuk National University.

Time-dependent current measurements of a capacitor structure with poly-4-vinylphenol (PVP) dielectrics are reported. The time-dependent currents were mainly composed of transient polarization current plus steady leakage current. The decay of polarization current revealed the time dependence  $\exp[-(t/\tau)^\beta]$ , where  $\tau$  is the relaxation time constant and  $\beta$  is the dispersion parameter. For thin dielectric layers, the relaxation was characterized by a single relevant relaxation time ( $\tau = \sim 2$  sec). However, above a certain thickness ( $\sim 10 \mu\text{m}$ ), the degree of dispersion increased with the increasing thickness, yielding additive longer relaxation time constants. Finally, the relaxation curve became a nearly straight in the log-log plot, following the  $t^{-1}$  dependence. Meanwhile, plasma-treated samples showed a slow relaxation curve ( $\tau = \sim 80$  sec) supposedly due to trappings induced by plasma-treatment.

김 수인, 김 용석, 원 상연, 김 동년, 한 재현, 이 창우

국민대학교 나노전자물리학과.

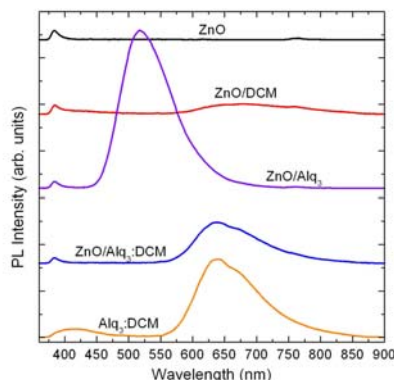
반도체 산업의 발달로 인하여 반도체 소자의 집적도는 비약적인 발전을 계속 진행 하고 있다. 이러한 반도체 소자의 집적도 향상을 위해서는 더 작은 선폭까지 구현 가능한 패턴의 미세화가 이루어져야 한다. 현재 대안으로 제시되고 있는 PMMA(Polymethylmethacrylate)를 이용한 패턴은 기존 PR(photoresist)를 이용한 패턴보다 더 미세화된 패턴을 제공하게 될 것이다. 그러나 더 미세화된 패턴은 일정한 외력에 의하여 더 쉽게 붕괴될 것으로 예상되고, 실제로 패턴 형성 후 세정 공정에서 패턴이 붕괴되는 현상이 발생하고 있다. 따라서 PMMA 박막의 물성 특성에 대한 연구를 통하여 패턴 붕괴력에 대한 연구가 절실히 필요하다. 이 논문에서는 PMMA(950K C4) 박막을 형성한 후 180도에서 soft-baking 시간을 5분에서 60분까지 변화시켜 제작한 후 박막의 특성을 나노인덴터를 이용하여 측정하였다. 그 결과 baking 시간 변화에 따라서 PMMA 박막의 경도(hardness)와 탄성계수(Elastic modulus)의 변화가 나타나는 것을 확인하였다. 또한 PMMA 박막의 경도의 탄성계수는 박막의 깊이에 따라서도 큰 차이를 나타내는 것을 확인하였다. 본 연구에서 사용된 나노인덴터는 Hysitron사의 Triboindenter를 사용하여 시료의 경도와 탄성계수를 측정하였다.

**Ep-V-113****Non-Radiative Energy Transfer in Inorganic-Organic Heterostructures**

LEE Cheol Eui, PARK Jun Kue, KIM Hyo Jung, LEE Kyu Won

고려대학교

We report on the temperature-dependent behaviors of non-radiative energy transfer in heterostructures where ZnO nanorods act as a donor (D) and a fluorescent dye, 4-(dicyanomethylene)-2-methyl-6-(4-dimethylaminostyryl)-4H-pyran (DCM), together with a phosphorescent sensitizer, tris (8-hydroxyquinoline) aluminum ( $\text{Alq}_3$ ), act as an acceptor (A). In particular, emission from the heterostructures of  $\text{ZnO}/\text{Alq}_3\text{:DCM}$ , was investigated upon controlling the A concentration in the temperature range of 30 - 300K.

**Ep-V-114****Co-sputtering 법으로 제작된  $\text{CuInSe}_2$  박막형 태양전지의 후열처리 효과**

김 지환, 김 해진, 김 동영, 이 혜지, 손 선영, 김 화민

대구가톨릭대학교 전자공학과

$\text{CuInSe}_2$  (CIS) 화합물 반도체를 광흡수층으로 하는 박막형 태양전지는 고유가 및 환경문제와 더불어 기존의 실리콘 태양전지에 비해 효율은 낮은 반면에 저비용으로 제작이 가능하며, 반영구적인 수명, 다양한 기판을 활용할 수 있다는 장점들로 인해 최근 CIS 박막형 태양전지의 상용화에 대한 연구가 활발하게 진행 중이다. 일반적으로  $\text{Al}/\text{MgF}_2/\text{ZnO}/\text{CdS}/\text{CIS}/\text{Mo}/\text{Glass}$  구조를 갖는 박막형 태양전지는 co-evaporation과 sputtering+selenization, electrodeposition 등의 까다로운 제조공정을 거치고 있다. 또한, 수  $\mu\text{m}$ 의 두께를 갖는 다원화 화합물로 구성된 CIS 층의 경우 박막 성장시 온도조건이 결정립의 크기와 결정구조, 화학양론적인 조성비를 변화시켜 소자의 효율에 영향을 끼친다. 따라서 본 실험에서는 기존의 증발법에 비해 상대적으로 낮은 온도에서 제작이 가능하고, 간단한 공정단계를 가지면서, 균일한 박막 두께를 가지며, 대면적화가 가능한 co-sputtering법을 이용하여 CIS 박막을 제조하였으며,  $150^\circ\text{C}$ - $550^\circ\text{C}$ 의 다양한 열처리 조건에 따른 박막의 전기적, 광학적, 그리고 구조적인 특성분석들을 통해 태양전지의 효율향상에 대한 메커니즘을 규명하고자 한다. 본 연구는 경북그린에너지 인력양성사업의 지원에 의한 것입니다.

**Ep-V-115****나노 스케일 박막의 XRR 두께 측정 및 불확도 분석**유 병윤, 박 재환, 빈 석민<sup>1</sup>, 김 창수<sup>1</sup>, 오 병성<sup>2</sup>, 최 용대<sup>3</sup>*한국표준과학연구원, 충남대학교 물리학과. <sup>1</sup>한국표준과학연구원. <sup>2</sup>충남대학교 물리학과. <sup>3</sup>목원대학교 기술마케팅학과.*

반도체 소자용 나노 스케일의 초박막에 대하여 높은 신뢰성의 정확한 두께를 측정하고자 많은 노력이 이루어지고 있다. 특히 수나노(nm) 이하의 얇은 두께의 고유전율(high-k) 산화막 두께의 정확한 측정이 많은 관심사가 되고 있다. XRR(X-ray reflectometry)은 수나노에서 수백나노 박막의 두께를 측정하기에 적절하고 사용된 장비(goniometer)의 각도와 X-선의 파장에 의하여 두께가 결정됨으로 XPS, Ellipsometry 등의 다른 두께 측정방법과는 달리 길이에의 소급성(traceability)이 유지될 가능성이 매우 높다. 따라서 XRR에 의한 결과는 두께 표준으로 응용할 수가 있으므로 측정 결과의 신뢰성을 향상시키기 위하여 많은 연구가 이루어지고 있다. 본 연구에서는 XRR의 두께 표준을 위한 소급성 확보를 위하여 사용 장비의 각도를 optical encoder를 이용하여 교정(calibration)하고 불확도를 살펴보았다. 또한 Si 기판 위에 성장시킨 5 nm 급 HfO<sub>2</sub> 고유전율 박막의 두께를 측정하고 측정 불확도(uncertainty)를 산출하였다. 본 연구에서는 고니오 교정에서 나타나는 교정 불확도와 XRR 측정에서의 불확도를 고찰하고 XRR을 이용하여 최종 결정된 나노 스케일 박막의 두께 및 측정 불확도(measurement uncertainty)에 관하여 논의하였다.

**Ep-V-116****IBSD 박막증착과 물성평가**유 병윤, 박 재환, 빈 석민<sup>1</sup>, 김 창수<sup>1</sup>, 오 병성<sup>2</sup>, 최 용대<sup>3</sup>*한국표준과학연구원, 충남대학교 물리학과. <sup>1</sup>한국표준과학연구원. <sup>2</sup>충남대학교 물리학과. <sup>3</sup>목원대학교 기술마케팅학과.*

본 연구에서는 박막을 증착시키기 위하여 Ion Beam Sputter 증착법을 이용하였다. IBS 증착법을 이용한 박막은 메탈박막과 산화물박막으로 증착시켰으며, 산화물박막을 증착할때 Ar ion이 Target과 충돌 시 주위에 Charge build-up이 생겨 Ion beam에 큰 영향을 미침으로써 증착이 원활히 안되는 현상을 최소화하기 위하여 Neutralizer를 사용하였다. Neutralizer를 사용하여 실리콘, 유리 기판위에 산화물인 Ta<sub>2</sub>O<sub>5</sub>, Cr<sub>2</sub>O<sub>3</sub>등의 물질을 증착하였다. 산화물박막은 박막이 증착되면서 부족한 산소를 채워주기 위하여 Chamber를 O<sub>2</sub>분위기속에서 증착을 시켰다. Metal 물질인 W 등은 Neutralizer 사용없이 단일 박막으로 증착시켰다. 산화물박막인 경우 Neutralizer를 사용함으로써 증착시 생기던 charge build-up의 문제를 해결하고 원활한 증착을 보였다. 증착된 박막의 두께, 거칠기, 밀도, 상분석등을 평가하기위해 XRD(X-ray Diffractometer)와 XRR(X-ray Reflectometer)을 이용하여 살펴보았고, TEM(Transmission Electron Microscope)으로 두께 측정을 하여 XRR로 얻은 데이터와, 비교, 분석하였다. 또한 XPS를 이용하여 증착된 박막의 정량분석을 통하여 원하는 물질이 박막으로 증착되는 것을 살펴보았다. Ar gas와 O<sub>2</sub> gas의 양, Substrate 온도, rotation의 속도등 증착조건을 다르게 하여 여러 종류의 박막을 만들어 각각의 특성의 차이를 알아봄으로써 양질의 박막을 얻기 위한 최적 조건을 확인하였다.

**Ep-V-117****Surface Analysis and Photoluminescent Properties of Lithium Incorporated** **$\text{Y}_2\text{O}_3:\text{Eu}^{3+}$  Thin Film Phosphor Grown on Si (100) Substrate using PLD method**배 종성, 홍 태은, 김 종필, 박 성균<sup>1</sup>, 정 중현<sup>2</sup>한국기초과학지원연구원, 부산센터. <sup>1</sup>부산대학교, 물리학과. <sup>2</sup>부경대학교, 물리학과.

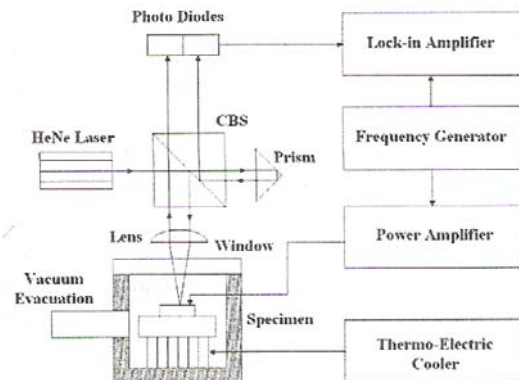
The influence of lithium doping on the crystallization, the surface morphology, chemical states and the luminescent properties of pulsed laser ablated  $\text{Y}_2\text{O}_3:\text{Eu}^{3+}$  thin film phosphors grown on Si (100) substrate were investigated. The structural, surface morphology characteristics and chemical states of the phosphors were analyzed by using X-ray diffraction (XRD), scanning electron microscope (SEM), X-ray photoelectron spectroscopy (XPS) and secondary ion mass spectroscopy (SIMS), respectively. The crystallinity, the surface morphology, and the photoluminescence (PL) of phosphors depended highly on the Li-doping and deposition condition, in particular, a deposition temperature and oxygen pressure. The relationship between the crystalline and morphological structures and the luminescent properties was studied, and  $\text{Li}^+$ -doping was found to effectively not only the enhanced crystallinity but also the luminescent brightness of  $\text{Y}_2\text{O}_3:\text{Eu}^{3+}$  thin film phosphors. In particular, the incorporation of  $\text{Li}^+$  ion into the  $\text{Y}_2\text{O}_3$  lattice could induce remarkable increase in the PL intensity. The enhanced photoluminescence brightness with Li doping may result not only from the improved crystallinity leading to higher oscillating strengths for the optical transitions, but also the enhanced the surface area due to the larger grain sizes.

**Ep-V-118****열-반사율법에 의한 고열전도도 박막의 열전도도 측정**

오 은지, 김 인구, 김 용수, 김 석원

울산대학교 물리학과.

전자회로의 집적도가 증가함에 따라 단위 면적당 발생하는 열도 급속히 증가하므로 열의 효과적인 방출을 위하여 넓은 band gap, 우수한 열안정성 그리고 낮은 누설 전류의 특징을 가지고 있는 high-k (고열전도도) 유전체 물질이 선행 연구되고 있다. 본 연구에서는 high-k 물질로 알려진  $\text{Al}_2\text{O}_3$ ,  $\text{TiO}_2$ ,  $\text{HfO}_2$  박막을 Si, Si/SiO<sub>2</sub>, GaAs 기판 위에 50 nm의 두께로 입히고 주기적인 교류 온도변화( $\omega$ )에 따른 박막 표면의 반사율 변화( $2\omega$ )를 이용한 열반사율법(thermo reflectance method)을 이용하여 열전도도를 측정하였다. 광원으로 632.8 nm의 He-Ne 레이저를 사용하였고, 광원으로부터 나온 빛은 beam splitter로 나누어져 시료를 거치지 않은 입사광과 vacuum chamber 내부에 장착된 시료에서 반사된 광을 실리콘 광 검출기와 lock-in amp로 측정하였다.



**Ep-V-119****Cr/Zn 이중 금속박막의 제조 및 접합 특성에 관한 연구**

강 상백, 김 송희, 채 영안, 윤 창선, 이 기진<sup>1</sup>, 김 진태<sup>2</sup>, 차 덕준

군산대학교, <sup>1</sup>서강대학교, <sup>2</sup>한국표준과학연구원.

금속과 금속의 접합, 금속과 비금속의 접합은 매우 다양하고 활용도도 크다. Cr/Zn의 접합의 경우 Zn 단일의 박막에 비해 Cr의 접합으로 인해 양질의 접합 효과를 얻을 수 있다. 특히 유리나 ITO를 기판으로 한 Cr/Zn의 접합은 II-VI 화합물 반도체의 전극용으로 ohmic contact에 중요한 부분을 차지한다. 본 연구에서는 thermal vacuum evaporation 기술에 의해 glass, ITO, SiO<sub>2</sub>/Si 을 기판으로 하여 ~10<sup>-6</sup> Torr 이내에서 Cr을 증착하고, Cr을 (-) 극, Zn을 (+) 극으로 한 전기도금 방법으로 Zn을 적층한다. Cr의 증착 시 기판의 온도를 상온, 100°C, 200°C, 300°C로 하고 Zn과의 접합 특성을 비교한다. 제조된 Cr/Zn에 대한 분석은 X-ray diffraction(XRD) 및 field emission scanning electron microscopy(FE-SEM)와 atomic force microscopy(AFM) 이 용하여 구조 및 표면 상태를 측정하여 접합 특성을 분석 하였다.

**Ep-V-120****Large scale patterning of ultra thin film graphite oxide on the Si/SiO<sub>2</sub> substrate**

**by UV photolithography for four terminal measurements**

LEE In-Yeal, KANNAN E S<sup>1</sup>, KIM Gil-Ho<sup>1</sup>

School of electrical and electronic engineering Sungkyunkwan university, <sup>1</sup>School of Information and Communication

Engineering, Sungkyunkwan Univeristy.

Recently thin film graphite oxide (GO) has been a subject of intense scientific investigation as it can be used as a starting material for the synthesis of graphene [1]. For the practical realization of GO based micro electronic devices, it is necessary to explore the possibility of fabricating large scale graphite oxide pattern using UV photolithography so that it can be successfully integrated with the current silicon processing technology. There are several challenges towards achieving this goal. In this present work, we present a detailed account of the various parameters that are necessary for the successful fabrication of ultra thin film GO pattern on a Si/SiO<sub>2</sub> substrate. We found that the thickness and thermal annealing time of GO is very critical for the successful fabrication. GO flakes thicker than 40 nm did not survive the lithographic procedures whereas the flakes with thickness less than 40 nm and annealed at 100 degrees for 10 secs after drying in convection oven for 40 mts remained intact. One such successfully patterned GO film is shown in Fig. 1. The bright regions in Fig. 1 are the thermally evaporated Ni/Au (20/200 nm) layers on GO which are used as contacts for the electrical measurements. Our work can find application in making top gated graphene field effect transistor with GO as an oxide layer.



**Ep-V-121****L1<sub>0</sub>-FePt 박막의 제작과 구조 및 자성 연구**김 승호, 이 재용, 송 중한<sup>1</sup>연세대학교, 물리학과, <sup>1</sup>한국과학기술연구원.

자기정보저장기술을 이용한 정보기록장치의 기록밀도를 향상하기 위해서는 자성재료의 크기를 줄여야한다. 이를 줄이다보면 상온에서 자화방향이 불안정해지는 초상자성효과가 나타나게 되어 기록장치로서의 역할을 못한다. 이를 극복하기 위해서 최근에 관심을 갖게 된 자성재료가 L1<sub>0</sub>-FePt 합금이다. 이것은 결정 자기이방성에 의해서 수직자화를 나타내고, 높은 자기이방성과 포화자화값, 그리고 내식성도 크기 때문에 차세대 기록매체로 각광 받고 있다. 이러한 FePt를 박막으로 제작하여 구조적 성질과 자기적 특성을 알아 보려한다. Sample은 Co-sputtering 방법을 이용해서 L1<sub>0</sub>-FePt 박막을 제작했다. Fe와 Pt의 조성비는 RBS (Rutherford back scattering) 장비를 이용해서 측정결과 약 50:50으로 확인하였다. 자기적 특성은 MOKE (magneto-optic Kerr effect) 장비를 이용해서 측정했다. 그 결과 in-plane 방향으로 자화곤란축 형태의 자기 이력곡선을 얻었고, out-of-plane 방향으로 약 2T의 자기장을 가해주었지만 saturation이 되지 않은 minor loop 형태의 자기이력곡선을 얻었다. 이로부터 이 sample이 수직자기이방성을 가지며, 굉장히 큰 포화자화를 갖는다는 것을 확인 할 수 있었다. 현재 다양한 조건하에서 시료를 제작하고 있으며, 그들의 제작 조건에 따른 구조 및 자기적 특성을 발표할 예정이다.

**Ep-V-122****마그네슘합금의 PEO 표면처리에 대한 특성 연구**유 재인, 윤 재곤, 김 진희, 유 재용, 박 창훈, 윤 기열, 송 경호, 김 기홍, 김 기홍<sup>1</sup>(주)세미유 기업부설연구소, <sup>1</sup>경운대학교 안경광학과.

표면처리 기술은 재료의 표면을 물리적, 화학적 또는 전기 화학적으로 처리하여 소재 및 부품의 내구성, 기능성을 개선 또는 창출시킬 뿐 아니라, 미관을 향상시켜 상품의 부가 가치를 제고시키는 기술로서, 일반적으로 물질의 Bulk 특성과는 다른 특성이 부여된다. 이러한 표면처리 방법에는 크게 습식과 건식 표면처리 두가지 방법이 있으며, 습식에는 화학처리, 양극산화(아노다이징), 전기도금, 무전해도금, 도장/전착도금이 있으며, 건식기술에는 증착식, 화학증착식, 플라즈마증착식이 있다. 습식 표면처리 기술은 제품을 생산하는 공정 중 주로 최종 마감공정으로 이용되며, 공해 유발성, 기술의 다양성 및 폐쇄성, 전문성의 특성이 있으므로 수주에 의한 다품종 소량 생산의 주종을 이루고 있다. 또한, 타 산업에 비해 설비 투자비가 적고, 작은 규모로 공장이 운영될 수 있기 때문에 업체들이 난립하여 수주 과정에서 과당경쟁의 현상이 나타나고 있고, 기술 개발보다는 가격 경쟁에 치중하여 자체적인 기술혁신 능력이 결여되어 기술 발전이 더욱 정체되고 있다. 그러나 습식 표면처리 기술은 일반 장식용의 악세사리에서부터, 현재 각국의 주요 수출산업인 자동차, 반도체, 전자산업분야는 물론, 향후 미래 주도 산업으로 주목되는 항공 우주산업에 이르기까지 주요·핵심부품에 광범위하게 응용되는 분야로서, 기술의 혁신이 크게 필요한 분야이다. 건식 표면처리 기술은 진공하에서 증착 또는 플라즈마 처리를 통해서 소재에 내식성, 내마모성, 윤활성 및 장식성을 부여하는 기술로 제품의 성능향상과 더불어 부가가치를 제고시킬 수 있는 공정으로 최근 활발히 개발·응용되고 있다. 특히 최근 습식표면처리 공정에서 문제시되고 있는 폐수공해문제 등을 진공공정으로 완전히 해결할 수 있을 뿐만 아니라 새로운 기능성 피막을 창출할 수 있어서 새로운 첨단 기술분야로 각광받고 있다. 이러한 건식 표면처리 기술은 공구·금형·자동차부품, 전기·전자 부품 및 기타 산업 분야의 내마모성 및 내식성 향상을 위한 기술로 널리 활용되고 있으며, 각종 장신구의 고부가가치 장식용 코팅에도 상당히 적용되고 있다. 건식 표면처리 기술은 습식 표면처리 및 열처리 기술을 통해서는 얻을 수 없는 새로운 기능의 경질피막, 내식피막, 윤활피막코팅 및 플라즈마 표면이 얻어진다. 따라서 본 연구에서는 PEO 표면처리에 대한 특성을 알아보고자 한다.

**Ep-V-123****X-ray Scattering Study on Moisture Induced Interfacial Degradation of Alq<sub>3</sub> on****Silicon**

LEE Young Joo, KO Changhyun, YOO Insun<sup>1</sup>, OH Hyoung-yun<sup>1</sup>, KIM Jinwoo<sup>2</sup>, KIM Hyunjung<sup>2</sup>

Department of Physics, Sogang University. <sup>1</sup>LG Display Co., Ltd.. <sup>2</sup>Department of Materials Science and Engineering, Gwangju Institute of Science and Technology.

We studied moisture induced degradation of tris-(8-hydroxyquinoline) aluminum (Alq<sub>3</sub>) on silicon substrate by X-ray scattering. Alq<sub>3</sub> is a green light emitting organic material for an organic light emitting device. Alq<sub>3</sub> was grown on silicon wafers by thermal evaporation. The samples were exposed for 1-7 days to moisture where the relative humidity was controlled to 40% or 90% at room temperature. After exposure, the samples were shielded from moisture by encapsulation boxes and then kept for aging for 1-13 days. A moisture permeation layer was observed near the surface in short period of exposure. Another moisture permeation layer was found near the interface of Alq<sub>3</sub> and silicon oxide on the silicon substrate with longer exposure. The thicknesses of the permeation layers were increased with increasing the exposure time and aging time. Along the degradation process of Alq<sub>3</sub>, transient variations of the roughness correlations were observed at the interfaces.

**Ep-V-124****펄스 DC 마그네트론 스퍼터링 방법으로 증착시킨 indium-zinc-tin-oxide(IZTO)****박막의 투명전도 특성에 관한 연구**

김 용성, 손 동진<sup>1</sup>, 남 은경<sup>1</sup>, 정 동근<sup>1</sup>

성균관대학교 신소재공학과. <sup>1</sup>성균관대학교 물리학과.

평판디스플레이 산업의 성장에 따른 ITO 타겟의 수요가 급증하고 있는 것에 반해 고가의 인듐자원은 그 매장량이 매우 적어 고갈 위기에 처해 있다. 따라서 인듐을 절감하는 투명전극 연구가 활발히 진행되어 오고 있다. 본 연구에서는 IZTO(In<sub>2</sub>O<sub>3</sub>:ZnO:SnO<sub>2</sub>=90:10:10 wt.%)의 In량을 절감한 조성의 타겟을 제조하였다. 그리고 유리기판 위에 IZTO 박막을 펄스 DC 마그네트론 스퍼터링을 이용하여 기판의 온도를 변화시키며 증착하였다. 기판 온도의 변화는 플렉시블 디스플레이 소자에 응용이 가능한 RT~200°C 범위에서 제어하였으며, 증착한 박막은 전기적, 광학적 및 구조적 특성 등을 조사하였다. 유리기판 위에 성장된 IZTO 박막은 기판의 온도가 증가함에 따라 전기적 특성이 향상되었지만 200°C 이상에서 급격히 열화되는 것을 알 수 있었다. 기판 온도 150°C에서 비저항은 3.87×10<sup>-4</sup>[Ω.cm]로 가장 낮게 나타났고, 이동도는 42.11[cm<sup>2</sup>/Vs], 캐리어 농도는 3.82×10<sup>20</sup>[cm<sup>-3</sup>]를 나타내어 가장 우수한 전기적 특성을 보였다. 박막의 투과율을 측정한 결과 평균 85% (400nm~800nm)이상의 우수한 광학적 특성을 보였다. 따라서, IZTO 박막은 인듐 절감효과와 150°C 미만의 공정온도 확보로 플렉시블 디스플레이에 적용이 가능한 투명전극 물질로 가능성을 보여주었다.

**Ep-V-125****Structure and optical properties of Ta<sub>2</sub>O<sub>5</sub> dielectric layer for thin film****electroluminescence device**

최 상현, 이 상목, 문 희송, 이 상걸<sup>1</sup>, 손 상호

경북대학교 물리학과, <sup>1</sup>기초과학지원연구원 대구센터.

TFELD (Thin film electroluminescence device) 에서 유전층으로 사용될 수 있는 거의 완벽에 가까운 성질을 지니고 있는 물질 중에 하나가 Ta<sub>2</sub>O<sub>5</sub> 입니다. TFELD 에서 샌드위치 구조의 유전층에 요구되어지는 중요한 물성중의 하나가 광학적 성질입니다. 본 연구는 Ta<sub>2</sub>O<sub>5</sub> 박막의 구조적, 광학적 성질을 연구하였습니다. 또한 구조적 특성을 파악하기 위해 SEM 및 AFM 을 측정하였으며, 광학적 특성을 알아보기 위해 투과율 측정 하였습니다.

**Ep-V-126****마그네슘합금의 PEO 표면처리에 대한 열처리 효과 연구**

유 재용, 김 덕희, 유 재인, 이 미경, 윤 재근, 윤 기열, 송 경호, 김 기홍<sup>1</sup>

(주)세미유 기업부설연구소, <sup>1</sup>경운대학교 안경광학과.

최근 자동차 및 항공기, 전기, 전자, 통신 및 컴퓨터 산업의 급격한 발달과 함께 사용부품의 경박, 탄소화가 일반적인 추세이다. 이에 따라 해당 부품의 크기와 무게가 현저하게 감소하면서 휴대용 산업기기뿐만 아니라 전자제품의 내외장 부품 및 자동차, 항공기 등의 부품분야에서 경량 및 고강도 소재의 사용이 불가피한 실정이다. 마그네슘은 보편적으로 사용하고 있는 대표적인 경량 금속인 알루미늄에 비해 약 35% 정도 가벼워서 기계 부품의 내·외장 구조재로서 주목받고 있는 금속소재이다. 이에 따라, 종전에 주 경량재료인 플라스틱 및 알루미늄으로 사용되던 부품들이 점차 마그네슘 소재로 변경되어 적용되고 있는 추세에 있다. 전자제품분야의 경우, 마그네슘합금의 경량화 및 전자파차폐효과로 휴대폰 및 통신기기 등 전자제품 케이스 위주의 부품에 많이 적용되고 있다. 본 연구에서는 마그네슘합금의 PEO 표면처리 후에 열처리에 대한 특성을 연구하고자 한다.

**Ep-V-127****마그네슘합금의 전처리 효과 연구**박 창훈, 유 재인, 김 기홍<sup>1</sup>(주)세미유 기업부설연구소, <sup>1</sup>경운대학교 안경광학과.

마그네슘은 실용화시 성능 향상을 위하여 제2, 제3의 원소를 첨가시킨다. 합금으로 만들어진 경우 강도, 내열성, 내크리프성이 개선된다. 아연을 첨가한 AZ계열 합금의 경우를 보면, 아연 첨가량에 따라 강도, 주조성, 가공성, 내식성, 용접성 등이 개선된다. 특히 Ce이나 Nd 등의 희토류원소를 첨가하면 200-250℃에서 강도가 높고, 내크리프 특성이 우수한 내열용 합금이 된다. 마그네슘합금이 노트북 컴퓨터, 휴대폰 케이스로 사용이 증가하는 배경에는 가공법의 큰 진전이 있었기 때문이다. 마그네슘합금은 상온에서 압연가공이 어려워 온도를 올려서 가공해 주어야 한다. 압출가공은 알루미늄합금과 열간변형저항이 비슷하여 알루미늄에 준한 가공이 가능하다. 다이캐스팅은 니어 넷 셰이프(near net shape)의 방법으로 양산하는 것이 유리하며, 반응용 가공법의 하나인 텍소몰딩(thixo molding)이 실용화되었고, 표면처리는 탄소강판이나 알루미늄 합금 다이캐스팅 제품과 동등한 수준까지 진보되어 있다. 본 연구에서는 마그네슘합금의 전처리 효과에 대한 특성을 연구하고자 한다.

**Ep-V-128****In situ GIWAXS Study of bulk heterojunction organic film for solar cell**SHIN Byong-Wook, KIM Jehan<sup>1</sup>, KIM Kwang-Woo<sup>1</sup>, LEE Sung-Youp<sup>2</sup>, YI Jin-Neung, PARK Sun-Mi, SON Myeong-Rak, KONG So-Jeo, CHOO Na-Yun<sup>2</sup>, LEE Eui-Wan, LEE Hyeon-Rag*Kyungpook National University, Department of Physics. <sup>1</sup>Pohang Accelerator Laboratory. <sup>2</sup>Kyungpook National University, Department of Nano-Science and Technology.*

Bulk Heterojunction polymer solar cells have been reported utilizing poly(3-hexylthiophene)(P3HT), as donor and / [6,6]-phenyl-C61-butyric acid methylester(PCBM) as acceptors. The improved power conversion efficiency of these devices results from the use of thermal annealing and solvent annealing processes, which enhance the film morphology relative to that of the as-cast film. The performance of these heterojunction solar cells depends critically on the morphology of their active layers. In this study, by grazing incidence wide angle x-ray scattering(GIWAXS) experiments, we have investigated the morphology of P3HT/PCBM with varying temperature. Utilizing this approach, we could therefore elucidate the relationship between the relative length scales of the PCBM clusters and P3HT crystallites and the device performance.

**Ep-V-129****마그네슘합금의 인산염 표면처리에 따른 특성 연구**

김 진희, 유 재인, 윤 재곤

(주)세미유 기업부설연구소

마그네슘합금 소재의 경우 표면처리기술은 크게 습식과 건식으로 구분된다. 습-건식 표면처리기술은 일반적으로 명명되지 않는 신청업체의 고유의 방법이다. 습식에는 화학처리, 양극산화(아노다이징), 전기도금, 무전해도금, 도장/전착도장이 있으며, 건식기술에는 증착식, 화학증착식, 플라즈마증착식이 있다. 습식 표면처리 기술은 제품을 생산하는 공정 중 주로 최종 마감공정으로 이용되며, 공해 유발성, 기술의 다양성 및 폐쇄성, 전문성의 특성이 있으므로 수주에 의한 다품종 소량 생산의 주종을 이루고 있다. 또한, 타 산업에 비해 설비 투자비가 적고, 작은 규모로 공장이 운영될 수 있기 때문에 업체들이 난립하여 수주 과정에서 과당경쟁의 현상이 나타나고 있고, 기술 개발보다는 가격 경쟁에 치중하여 자체적인 기술혁신 능력이 결여되어 기술 발전이 더욱 정체되고 있다. 그러나 습식 표면처리 기술은 일반 장식용의 악세사리에서부터, 현재 각국의 주요 수출산업인 자동차, 반도체, 전자산업분야는 물론, 향후 미래 주도 산업으로 주목되는 항공 우주산업에 이르기까지 주요·핵심부품에 광범위하게 응용되는 분야로서, 기술의 혁신이 크게 필요한 분야이다. 본 연구에서는 습식방법인 인산염 표면처리에 대한 마그네슘합금 표면 특성을 연구하고자 한다.

**Ep-V-130****Investigation of  $\text{BaY}_2\text{O}_4:\text{Eu}^{3+}$  Phosphors by Site-selective Laser-excitation****Spectroscopy**

김 은식, 장 경혁, 시 람, 교 학빈, 전 병천, 서 효진

부경대학교, 물리학과

$\text{Eu}^{3+}$ -doped  $\text{BaY}_2\text{O}_4$  phosphates were synthesized by the sol-gel method. X-ray powder diffraction analysis confirmed the formation of single phase  $\text{BaY}_2\text{O}_4$ . Luminescence properties of  $\text{BaY}_2\text{O}_4:\text{Eu}^{3+}$  are investigated by site-selective laser-excitation spectroscopy in the temperature region of 15 K – room temperature. Luminescence excitation spectra show the charge transfer band of Eu-O at 260 nm and the emission spectra exhibit a red performance at the region of 607-620 nm due to the  $^5\text{D}_0 \rightarrow ^7\text{F}_2$  transition of  $\text{Eu}^{3+}$ . Three different crystallographic sites corresponding to two  $\text{Y}^{3+}$  sites ( $\text{Y}^{3+}(1)$  and  $\text{Y}^{3+}(2)$ ) and  $\text{Ba}^{2+}$  site are identified for  $\text{Eu}^{3+}$  ions from the  $^7\text{F}_0 \rightarrow ^5\text{D}_0$  excitation spectra of the  $^5\text{D}_0 \rightarrow ^7\text{F}_J$  ( $J=1,2,\dots,6$ ) emission. Crystal field splitting of the  $^7\text{F}_1$  and  $^7\text{F}_2$  levels leads to classify corresponding three sites for  $\text{Eu}^{3+}$  in  $\text{BaY}_2\text{O}_4$  lattice. Luminescence decays and temperature dependent  $^5\text{D}_0$  emissions of  $\text{Eu}^{3+}$  at each site show an energy transfer between  $\text{Eu}^{3+}$  ions at  $\text{Y}^{3+}(1)$  and  $\text{Y}^{3+}(2)$  sites. The results are discussed in comparison with those of nanocrystalline and microcrystalline  $\text{SrY}_2\text{O}_4:\text{Eu}^{3+}$ .

**Ep-V-131****Spectral and Structural Properties of  $\text{Eu}^{3+}$  in Sol-gel-derived Nanocrystalline** **$\text{ZrO}_2$  by Site-selective Luminescence Spectroscopy**

제 재용, 시 량, 김 은식, 교 학빈, 장 경혁, 노 경석<sup>1</sup>, 서 효진

부경대학교, 물리학과, <sup>1</sup>마산대학, 방사선과.

$\text{Eu}^{3+}$ -doped  $\text{ZrO}_2$  phosphors were synthesized by the sol-gel method. X-ray diffraction and transmission electron microscopy (TEM) measurements identify the nanoparticles of  $\text{ZrO}_2$  phosphors. The phase transformation between monoclinic and tetragonal phases is observed. The luminescence properties of t- $\text{ZrO}_2$  and m- $\text{ZrO}_2$  are investigated by the site-selective excitation and emission spectroscopy and luminescence decay under a pulsed, tunable, narrowband dye laser at different temperatures. Non-site-selective excitation spectrum in the UV region and UV-excited emission spectrum were also performed. The results show that the isolated  $\text{Eu}^{3+}$  occupied one site in t- $\text{ZrO}_2$  and two sites in m- $\text{ZrO}_2$ . The shape of emission spectrum in m- $\text{ZrO}_2$  is nearly the same except for the line shift of the  $^5\text{D}_0$ - $^7\text{F}_2$  transition in several nanometers. The emission spectrum of t- $\text{ZrO}_2$  is very broad and its shape is quite different with that of m- $\text{ZrO}_2$ . The luminescence decay of the  $^5\text{D}_0$ - $^7\text{F}_2$  transition in m- $\text{ZrO}_2$  is single exponential, while it is non-exponential in t- $\text{ZrO}_2$ . The crystallography of isolated  $\text{Eu}^{3+}$  sites in t- $\text{ZrO}_2$  and m- $\text{ZrO}_2$  were discussed, among which energy transfers and charge compensation mechanism were illuminated.

**Ep-V-132****고체의 전기 저항률 및 전도도 특성 연구**

서 주희, 임 선아, 이 현진

전남과학고등학교, 전남 나주시 금천면 오강리 185-6번지.

전자는 원자핵으로부터 인력을 받고 있어 대부분 원자핵 주위를 돌며 속박되어 있다. 그러나 유전자는 특정한 원자에 속박되어 있지 않고 원자 사이를 자유롭게 돌아다닐 수 있다. 자유전자가 많아 전하를 잘 이동시켜 전기를 잘 통하는 물체에는 철, 구리, 은, 알루미늄 등이 있다. 이와 같은 것들을 도체라 한다. 도체와는 다르게 자유전자가 적어 전하를 잘 이동시키지 못하여 전기를 잘 통하지 못하는 물체에는 종이, 나무, 유리, 고무 등이 있다. 이를 부도체 또는 절연체라고 한다. 상황에 따라 도체와 부도체가 될 수 있는 반도체는 도체와 부도체 사이의 중간성질을 띠는 물질로 실리콘(Si), 게르마늄(Ge) 등이 대표적이다. 우리는 이번 실험을 통해 1) 도체와 반도체에서의 온도에 따른 전기저항률의 변화 2) 반도체의 광 전기전도도 특성 탐구 3) 다른 비정질 실리콘 시료에 대한 암 전기전도도와 광 전기전도도의 측정 비교에 관한 연구를 수행하였다. 본 실험에서는 금속저항 시료로 백금, 반도체 저항 시료로 비정질 실리콘을 사용하였으며, 실험 장치는 Electrometer(Keithley 619), Voltage Source(Keithley), Multimeter(Keithley) 그리고 온도 조절이 가능한 진동 Dewar 장치로 구성되어있다. 비정질 실리콘시료에 대해 측정한 암 전기전도도와 광 전기전도도를 역 온도함수로서 측정하려고 한다. 반도체에서는 온도의 산술적 증가에 따라 저항률은 기하급수적으로 감소한다. 그러므로 전도도는  $\sigma = \sigma_0 \cdot \exp(-\Delta E/kT)$ 로 표현할 수 있다. 이 식을 이용해 암전기전도도를 log함수로 표현할 수 있고, 직선의 기울기로부터  $\Delta E$ 값을 계산 하였다.

김 기연, 이 나원, 이 서은

한국외국어대학교 부속 용인외국어고등학교 경기도 용인시 처인구 모현면 산 232.

우리 생활의 다양한 방면에서 도움을 주고 있는 기능성 섬유는 물리적 구조와 이에 따른 기능에 대해 알아보기 위하여 각 섬유를 시편으로 만들어 주사전자현미경으로 관찰해보았다. 주사전자현미경은 전자들이 시편과 부딪힘으로써 생성된 2차 전자의 신호를 이미지 신호로 변환시켜 관찰하는 것이다. 만약 비전도성 시편을 금속박막코팅 없이 관찰하려 할 경우 charge-up 현상이 일어나게 된다. 이를 방지하기 위하여 플라즈마와 이온화 현상을 이용한 백금박막코팅기를 이용해 비전도체인 섬유의 시편을 코팅하였다. 백금박막을 입힌 시편을 주사전자현미경으로 관찰한 결과 기능의 비밀을 담고 있는 다양한 구조를 관찰할 수 있었다. 보다 효율적인 관찰을 위하여 중점적으로 관찰할 부분에 따라 두 부류로 나누었다. 첫째 부류는 그 직물을 구성하고 있는 원사의 단면을 관찰하였으며 둘째 부류는 직물의 표면적 구조 자체를 관찰하였다. 첫째 부류에 속하는 기능성 직물로는 속건성 섬유인 쿨맥스, 아쿠아에프, 에어로쿨, 쿨에버, 쿨론, Pyrocle 등이 있다. 쿨맥스와 아쿠아에프, 에어로쿨, 쿨에버, 쿨론은 공통적으로 원사의 단면을 조절하는 특수한 기술을 이용하여 기존의 둥근 원사에서 벗어나 만들어진 다양한 모양의 실로 직조되어 있다. 속건성 섬유들은 원사 자체의 표면적을 넓혀 모세관 효과를 촉진시키기 때문에 피부로부터 분비되는 수분을 빠르고 효율적으로 흡수하여 옷 밖으로 배출할 수 있도록 이루어져 있었다. 이는 상승된 체온을 낮추는 역할을 하여 스포츠선수들이 체온유지에 소모하는 에너지의 양을 절약해 보다 나은 기량을 발휘할 수 있게 도와준다. 특히 Pyrocle은 원사 내부에 구멍을 뚫어 공기를 채움으로써 부피에 비해 대단히 가벼울 뿐만 아니라 섬유에 비해 공기가 더 열전도율이 낮기 때문에 추운 날씨에 외부로 빼앗기는 열의 양을 줄일 수 있다. 두 번째 부류는 섬유가 직조되어있는 구조 자체에서 기능이 기인하는 고어텍스, 에픽, 극세사 등이 있다. 고어텍스는 등산복 제조에 쓰이고 있는 대표적인 방수섬유인데, 안쪽에 붙어있는 고어텍스 멤브레인이 바깥의 수분을 막아내는 동시에 뚫려있는 미세한 구멍들이 피부의 수분을 함께 배출하기 때문에 땀을 많이 흘리는 야외활동을 할 때 입기 적합하다. 백스텍사의 에픽 소재는 원사 하나하나가 방수 소재로 코팅되어 있는 encapsulation 기능을 차용하여 치밀하게 직조되어 있기 때문에 방수 효과가 뛰어나다. 일상생활에서도 많이 쓰이고 있는 극세사의 경우, 매우 가는 원사로 촘촘하게 짜인 구조를 갖고 있기 때문에 진드기의 번식을 막는데 효과적이며 따라서 천식, 아토피 환자들을 위한 침구 류로 사용하기 적합하다. SEM을 이용하여 각 직물의 미세구조를 관찰한 결과 같은 폴리에스테르로 만들어진 섬유들도 원사의 단면과 짜인 구조에 따라 다른 기능을 만들어낸다는 것을 알 수 있었다. 예를 들어, 원사의 단면을 조절한 아쿠아에프, 에어로쿨 등의 섬유들은 모세관 현상을 극대화 시키기 위해 부피 대비 표면적을 넓히는 방법으로 흡수속건성을 띤다는 것을 알 수 있었다. 또한 구조에 의해 기능이 결정되는 고어텍스, 에픽 등의 직물의 경우 섬유에 뚫려있는 구멍의 크기 혹은 원사 사이의 간격을 조절함으로써 방수, 방풍과 같은 기능을 보인다는 것을 관찰할 수 있었다.

**Kp-V-046****Silicon-On Nothing 소자 구현을 위한 SiGe Selective Lateral Wet Etching에서 Strained SiGe Layer 의 두께에 따른 선택비 및 Etch Rate Issue**길 연호, 이 훈기, 김 택성<sup>1</sup>, 심 규환<sup>2</sup>*전북대학교, 반도체 화학 공학부. <sup>1</sup>전북대학교, 반도체 물성 연구소. <sup>2</sup>전북대학교, 반도체과학기술학과.*

Si를 기반으로 한 소자는 현재까지 수많은 기술 발전과 집적도 향상을 통하여 뛰어난 성능을 기반으로 발전 되어 왔다. MOSFET 소자에 대하여 SOI(Silicon-On Insulator) 기술 이후 Channel 의 Leakage Current 개선을 위하여 SON(Silicon-On Nothing) 기술이 대두 되었다. 이를 위하여 SiGe Layer를 선택적으로 Lateral Etching 하기 위하여 BPA (HF : H<sub>2</sub>O<sub>2</sub> : CH<sub>3</sub>COOH = 1 : 2 : 3) Solution 을 이용해 SiGe의 두께에 따른 Etch Rate를 연구하였다. Si<sub>80</sub>Ge<sub>20</sub> Layer를 40nm의 Si Layer 사이에 10nm, 40nm, 60nm 로 적층한 후 ICP/RIE(F)를 이용한 Dry Etching 이후 Wet etching을 진행하였다. 충분히 Aging 되어 Saturation 된 Solution의 경우 Si<sub>80</sub>Ge<sub>20</sub>와 Si Layer의 선택비는 20:1정도로 관측되었다. 또한 이를 통하여 충분히 Relaxation 되지 않은 얇은 두께의 Strained Si<sub>80</sub>Ge<sub>20</sub> Layer의 경우 Etch window 크기가 작음에도 불구하고 Etch Rate가 큰 결과를 확인할 수 있었다.

**Kp-V-047****SiGe HBT 소자 시뮬레이션 및 특성 고찰**

SHIN MI IM, CHOI SANG SIK, CHOI CHEOL JONG, SHIM KYU HWAN

*전북대학교 반도체공학과.*

본 논문에서는 SiGe의 물리적인 특성과 SiGe을 이용한 HBT의 동작 특성을 알아보며 Base width와 Base concentration에 따른 transconductance를 비교하였다. 이를 통해 BJT에 비해 SiGe을 이용한 HBT의 소자 특성이 우수함을 알아보고, HBT 공정에 앞서 효율적인 실험이 가능하도록 시뮬레이션 특성을 분석하였다.

**Kp-V-048****Compton Suppression System에서 환경시료의 방사능 농도 측정**장 은성, 김 연<sup>1</sup>, 박 정남<sup>1</sup>부산대학교 핵물리방사선기술연구소, <sup>1</sup> 부산대학교 핵물리 방사선기술연구소.

표충토양 시료의 감마동위원소 분석은 발전소 부지주변 10개지점과 비교지점(울산)에서 시료를 채취한 후, 각 지점에서 채취한 시료를 비이커에 담아 감마핵종 분석기로 측정하였다. 단일 감마선 핵종들로 이루어진 표준선원과 더불어 방사능 제어 작업을 위한 환경 모니터링에 사용되는 환경시료인 표충토양을 측정하였다. 원통형의 40mL 측정용기의 표준선원을 이용하여 CSS 검출기를 교정하였다. '04 ~ '09년까지의 교정소스를 측정하였고, 환경시료인 표충토양은 시료측정량을 20g ~ 100g까지 변화를 주면서 측정하였다. 그리고 백그라운드.교정소스.표충토양을 측정시간에 변화를 주면서 측정하였다. 실험에 사용한 검출기는 Canberra 사의 CSS 검출기이다. 상대효율 60%의 컴프턴 억제 감마선 검출기 시스템(Compton Suppressed Gamma Detection System, CSS)의 Ge결정의 지름이 67mm이며, 60Co의 1332.5keV 감마선에 대한 에너지 분해능은 2.2keV이다. 그리고 컴프턴 효과 억제를 위하여 Ge 검출기 둘레에 원통형 NaI 결정과 광전증배관 4개가 설치되어 있다. 표충토양에 대한 감마동위원소 분석결과 인공방사선핵종인 137Cs이 측정되었으며, 비교지점에서는 최소검출가능농도 미만의 분석결과를 보였다. 일반지역에서 검출되고 있는 수준으로써 발전소 가동으로 인한 영향은 아닌 것으로 판단된다. 그러므로 본 연구결과를 통해 얻은 백그라운드 및 측정시간의 적절한 배분에 의한 MDA계산의 측정결과를 원자력 이용시설 주변 방사선 환경조사에 활용될 수 있다. 중심단어: CSS 검출기, 방사능농도, 환경시료, 혼합표준선원

**Kp-V-049****Low Power Consumption of Cap-less Memory in Silicon-on-insulator n-Metal-****Oxide-Semiconductor Field-effect Transistor**

SHIN Mii-Hee, HIROFUMI Enomoto, KIM Tae-Hyun, KIM Seong-Je, SHIM Tae-Hun, PARK Jea-Gun

*Advanced Semiconductor Materials & Devices Development Center, Hanyang University.*

In current dynamic random-access memory (DRAM) structure of 8F<sup>2</sup>, the scalability beyond 32 nm technology for realizing low power, high speed, and large capacitance is facing a physical limitation because of leaning effect between adjacent storage-capacitors. For this reason, Cap-less memory has been proposed as one of ways to overcome scalability issue because of its structure of 4F<sup>2</sup>, i.e., floating body cell is used accumulated holes as storage charges on the buried oxide (BOX) instead of storage capacitor. However, to realize Cap-less memory, there are technical issues to be resolved such as high power consumption and small memory margin. In this study, to improve this problem, we investigated the BOX thickness effect on the operation voltage. We fabricated Cap-less memory cells with two different BOX thicknesses; 26.2 nm for thin BOX and 141.9 nm for thick BOX. The gate oxide thickness for both cells was 8.4 nm and top silicon thicknesses of silicon-on-insulator (SOI) substrate were 21.6, 25.3, 34.5, 46.9, 66.9, and 84.1 nm, respectively. At a 2 V gate bias, the substrate bias was applied 0 to -10 V for thin BOX SOI cell and 0 to -20 V for thick BOX SOI cell. It was observed that the memory margin of thin BOX Cap-less memory cell was saturated at a -6 V substrate bias. Particularly, the memory margin of the 34.5 nm top silicon and thin BOX Cap-less memory cell was 47  $\mu$ A at the substrate bias of -6 V. Otherwise, the memory margin of ~47  $\mu$ A was observed at 46.9 nm top silicon and thick BOX Cap-less memory cell by applying the substrate bias of -12 V. In conclusion, we demonstrated the same memory margin of thin BOX as thick BOX Cap-less memory at lower substrate bias and suggested that thin (~26.2 nm) BOX is more preferable than thick (141.9 nm) BOX for realizing Cap-less memory cell in low-power consumption.\*This work was financially supported by the Acceleration Research Program of the KOSEF and MEST.

## (001) Substrates

JU Mi Yeon, LEE Sanghwa, KIM Chinkyo, YANG Heon-Deok<sup>1</sup>, CHOI Chel-Jong<sup>1</sup>, SHIM Kyu-Hwan<sup>1</sup>

*Kyung Hee University, Dept. of Physics. <sup>1</sup>Chonbuk National University, School of Semiconductor and Chemical Engineering, Semiconductor Physics Research Center.*

Heteroepitaxial growth of Ge on Si substrate has been intensively studied during past a few decades not only due to its relevant applicability to modern Si-based microelectronics, but also as an ideal model system for the study of strained semiconductor heteroepitaxy. One of the most important issues in the heteroepitaxial growth of Ge on Si is to fully understand the strain relaxation mechanism manifested in various ways such as the formation of three dimensional islands, the shape transition of islands, the formation of trenches. The various strain relaxation mechanisms activated under different conditions is due to subtle interplay between surface energy and strain relaxation energy. Thus, it is of great importance to investigate the relevant dominance between surface energy and strain relaxation energy of the system under different conditions. In this work, the morphological characteristics of Ge islands grown on Si(001) substrates are investigated by utilizing SEM, AFM. The substrate temperature was found to be one of the most influential parameters in determining surface morphology. More discussion will be given in detail. This work was supported by IT R&D program of the Ministry of Knowledge Economy, Korea.

## Thickness of Silicon-on-insulator Substrate

LEE Ho-Kuen, PARK Jae-Kyu, CHOI Ki-Ryoung<sup>1</sup>, KIM Seong-Je<sup>1</sup>, SHIM Tae-Hun<sup>1</sup>, PARK Jea-Gun<sup>1</sup>

*Division of Electronics, Communications, and Computer Engineering, Hanyang University. <sup>1</sup>Advanced Semiconductor Materials & Devices Development Center, Hanyang University.*

To realize the high-density and high speed dynamic random-access memory (DRAM), the scale down is necessary. However, DRAM cell consisting of 1 transistor and 1 capacitor has some difficulties to scale down such as leaning effect caused by the instability of the capacitor with the height more than 2  $\mu\text{m}$ . To overcome this problem, Cap-less memory cell has been considered as a promising device to replace the conventional one. Cap-less memory cell has no capacitor and stores charge in the body. In our paper, we investigated the characteristics of the retention time for the silicon-on-insulator Cap-less memory cells with the different top silicon thickness of 15.5, 23.7, 36.7, 46.9, 53.2, and 72.3 nm, respectively. The thickness of the gate oxide and the buried oxide was 8 nm and 142 nm, respectively. It was observed that for the thickness less than 23.7 nm, few recombination occurred and the read after write '0' ( $D0$ ) was unexpectedly degraded due to the increase in excess holes. On the other hand, for the thicker than 46.9nm, the source current abruptly decreased with the hole concentration in the read after write '1' ( $D1$ ) and the degradation of the  $D1$  current was shown dominantly. For the case of the thickness of 36.7 nm, both  $D0$  and  $D1$  states were maintained longer comparing with the other samples. Especially, the  $D0$  was maintained 8 times longer than the others. Consequently, the devices with the thickness of 36.7 nm showed the longest retention time of 145 msec. Finally, we confirmed that the retention time for the top silicon thickness of 36.7 nm was the optimum for the reasonable retention time of Cap-less memory cell.\*This work was financially supported by the Acceleration Research Program of the KOSEF and MEST.

**Kp-V-052****이온빔 스퍼터링과 열처리에 의해 제작한 p형 실리콘 나노결정/n형 실리콘 웨이퍼 접합구조의 태양전지 특성 연구**홍 승휘, 신 동희, 최 석호, 김 경중<sup>1</sup>경희대 국제캠퍼스 응용물리학과, <sup>1</sup>한국표준과학연구원 나노소재측정센터.

실리콘 나노결정은 반도체 양자점 물질 중에서 대표적인 것으로 지금까지는 발광소자나 비휘발성 메모리 분야에 많은 연구가 진행되어 왔다. 최근에는 양자구속효과에 의한 에너지의 증가로 실리콘 나노결정이 가시광선 영역의 빛흡수에 유리하다는 점에 착안해 태양전지 분야에 응용이 시도되고 있다. 본 연구에서는 B이 도핑된 실리콘 나노결정을 이용한 태양전지 제작을 위해 이온빔 스퍼터링과 열처리로 p형 실리콘 나노결정/n형 실리콘 웨이퍼 접합구조를 형성하였다. 가장 안정적이고 균일한 특성을 보이는 (SiO<sub>x</sub>/SiO<sub>2</sub>) 다층구조를 10주기에서 50주기까지 변화시켜서 증착하고 열처리하여 실리콘 나노결정층을 성장하였다. P형으로 도핑된 실리콘 나노결정은 질화붕소 (boron nitride)와 실리콘을 동시에 스퍼터링하여 얻을 수 있었으며 B의 도핑 여부는 이차이온질량 분석기(SIMS)를 통해 확인하였다. SiO<sub>x</sub> 제작을 위한 과잉실리콘 양과 시료의 성장 속도는 광전자 분광기 (XPS)를 이용해 결정하고 조절하였으며 실리콘 나노결정의 존재는 투과전자현미경과 광루미네선스 측정으로 이전의 연구결과와 비교해 확인하였다. 태양전지 구조를 위한 전면과 후면의 Al 전극은 열기상증착기를 이용해 증착하였으며 웨도우 마스크를 통해 일정한 패턴을 형성하였다. 실험결과, 실리콘 나노결정에 도핑된 B의 농도, 실리콘 나노결정 층의 두께, 박막의 총두께 등의 변화에 따라 각기 다른 태양전지 특성과 변환 효율을 나타내었으며 가장 높은 변환 효율을 기록한 시료의 경우 약 28mA/cm<sup>2</sup>의 전류 밀도와 7.2%의 효율을 보였다.

**Kp-V-053****Nonvolatile memory characteristics of Ge-nanodot floating-gate MOSFETs**김 민철, 홍 승휘, 최 석호, 김 경중<sup>1</sup>경희대 국제캠퍼스 응용물리학과, <sup>1</sup>한국표준과학연구원 나노소재측정센터.

One-to-three period multilayers (MLs) of Ge nanodots (NDs) have been self-assembled by alternate ion-beam-sputtering deposition of 5-monolayer Ge between SiO<sub>2</sub> layers at room temperature without post annealing. [1, 2] Using the structures of 4 nm SiO<sub>2</sub>/Ge-nanodot MLs (middle oxide: 2 nm) /15 nm SiO<sub>2</sub>, nonvolatile-memory MOSFET devices were fabricated based on the 0.6-μm CMOS standard processes. During programming, electrons are stored into Ge NDs through the tunnel oxide layer from Si substrate by direct tunnelling based on Fowler-Nordheim scheme. Program/erase (P/E) speeds, retention time, and endurance were measured with varying period of the MLs. The P/E memory window and P/E speeds increased from 1.1 V to 1.72 V and from 10 ms/200 ms to 500 ms/100 ms at +18 V/-15 V with increasing the period from 1 to 3, respectively. The programmed threshold voltages ( $V_{th}$ 's) in the endurance characteristics were almost constant within about 0.05 V up to  $\sim 10^4$  P/E cycles for the two- and three- period devices. In contrast, the erased  $V_{th}$ 's of all devices showed a drift-up, but the drift-up was decelerated in larger-period devices. The charge loss rate was also reduced for larger-period devices. [1] S. H. Hong, M. C. Kim, P. S. Jeong, S.-H. Choi, Y.-S. Kim, and K. J. Kim, Appl. Phys. Lett. 92, 093124 (2008). [2] S. H. Hong, M. C. Kim, P. S. Jeong, S.-H. Choi, and K. J. Kim, Nanotechnology 19, 305203 (2008).

**Kp-V-054****Ge nanowires Heteroepitaxy on Ge layer deposited Si Substrates**

정 재훈, 김 유리, 윤 현식, 김 정혁, 송 만석, 김 용, GAO Qing<sup>1</sup>, TAN H. Hoe<sup>1</sup>, CHENNUPETI Jagadish<sup>1</sup>, CHEN Zhi Gang<sup>2</sup>, ZOU Jin<sup>2</sup>

동아대학교 물리학과. <sup>1</sup>The Australian National University. <sup>2</sup>The University of Queensland.

Ge 나노선은 높은 전하이동도로 인하여 미래의 나노전자소자에서 아주 중요한 역할을 하리라 기대된다. 특히 Si 기판위에 epitaxy 로 성장되는 Ge 나노선은 소자 응용성이 크게 기대가 되는 체계이다. Si 의 산화특성 때문에 Ge 나노선을 epitaxy 로 성장시키는 것은 특히 어려운 기술이다. 이전의 보고에서는 초고진공 상태에서 촉매금속을 증착하는 등 복잡한 방법을 사용하였다. 그러나 본 연구에서는 이러한 기술적 어려움을 근원적으로 극복할 수 있는 새로운 기술을 시도하였다. Lamp Heated CVD(Chemical Vapor Deposition)에 의해 Si(111) 기판에 450-550 도의 낮은 온도에서 얇은 Ge 완충층 (buffer layer)을 증착한 후 그 위에 heteroepitaxy 한 Ge nanowires(NWs)를 성장하였다. Ge NWs는 VLS(Vapor-Liquid-Solid) 메커니즘을 통해 성장되었으며, 촉매로는 50nm Au colloid 용액을, source gas로는 diluted GeH<sub>4</sub>를 사용하였다. Ge 층을 증착한 기판 위에 Au 입자들을 정전기적으로 고정시키기 위해 poly-L-lysine 용액에 기판을 1분간 담근 후, Au colloid 용액을 살포하였다. Au 와 Ge의 공융점 온도 근방인 섭씨 320 - 380도 사이 온도에서 30 Torr 압력에 20분-60분 성장하여 FE-SEM(Field ion Scanning Microscope)을 이용하여 Ge NWs의 이미지를 관찰하였다. Ge 완충층이 비정질 혹은 다결정질 임에도 불구하고 Ge 나노선은 <111> 방향, 수직으로 성장되었다. 완충층의 두께에 따른 Ge 나노선의 성장방향에 대하여 보고하고 이 특이현상의 물리적인 이유에 대하여 논의할 예정이다. This work was supported by Korean Reserch Foundation Grant Funded by the Korean Government (MOEHRD) (KRF-2007-313-C00222)

**Kp-V-055****Effects of Anode in Cu Electroplating**

SEO Jung-Hye, LEE Youn-Seoung, RYU Young-Ho<sup>1</sup>, HONG Kimin<sup>1</sup>, KANG SUNG-KYU<sup>2</sup>, RHA Sa-Kyun<sup>2</sup>

Department of Information Communication Engineering, Hanbat National University. <sup>1</sup>Department of Physics, Chungnam National University. <sup>2</sup>Department of Materials Engineering, Hanbat National University.

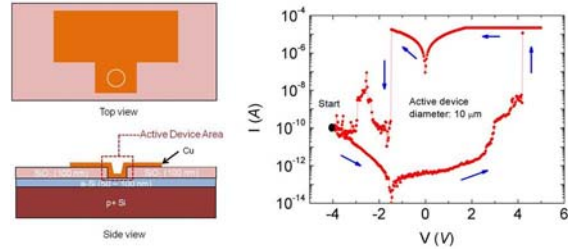
Electroplating (ECP) is among the popular methods used for Cu deposition in semiconductor fabrication processes. By a reaction between the Cu<sup>2+</sup> ions and the cathode surface, Cu film forms on the surface of the cathode. Cu<sup>2+</sup> ion current passes through both the cathode and the anode. Therefore, the role of anode is very important. In this work, the substrate used as cathode was Cu (20 nm) / Ti (20 nm) / p-type Si (100). Cu seed layer was deposited by electron-beam evaporation. We used two different anodes during plating. One is Cu anode doped with phosphorus, P, and the other is Pt anode. Generally, P prevents adverse competing reactions at the anode. When CuP is used as anode, Cu<sup>2+</sup> goes into the solution at the anode and then a constant concentration of Cu<sup>2+</sup> ions is maintained in the electrolytic solution. We investigated the characteristic of Cu films electroplated according to anodes. The microstructure of electroplated Cu films was measured by FE-SEM. The chemical states of Cu films were investigated with XPS. The electrical property was measured with a 4-point probe.

**Kp-V-056****Reproducible resistive switching in Cu/a-Si/Si structures with micron-sized****active device area**

차 동재, 이 성주<sup>1</sup>, 강 보수<sup>1</sup>, 박 수현<sup>2</sup>, 엄 한돈<sup>3</sup>, 이 정호<sup>3</sup>,  
김 동욱<sup>4</sup>

한양대학교, 응용물리학과. <sup>1</sup>한양대학교 응용물리학과.  
<sup>2</sup>이화여자대학교 물리학과. <sup>3</sup>한양대학교 재료화학  
공학부. <sup>4</sup>이화여자대학교, 물리학과.

We prepared amorphous silicon (a-Si) based memory device structures and investigated their resistive switching (RS) behaviors. Copper (Cu) layers and highly doped silicon substrates were used as top and bottom electrodes, respectively. The Cu/a-Si/Si structures, with active device diameter ranging from 2 to 50 micron, exhibited bipolar RS. Systematic and careful characterizations showed that compliance current and device area were important parameters, enabling repetitive RS behaviors. ON/OFF resistance ratio was as large as  $10^7$ , and the resistance switching could be repeated over 100 times. The Cu/a-Si/Si structures have advantages over other material systems, since all the constituent materials and processing techniques are compatible with mass-production-level fabrication technology.

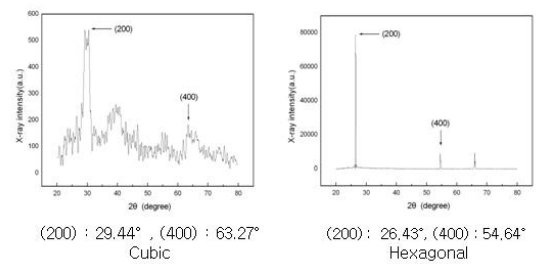
**Kp-V-057****Magneto-optical Properties of CdS:Mn Film Grown by HWE**

LEE Jooyong, KIM Hyungmin, PARK Seungmin  
University of Ulsan, Department of Physics.

CdS:Mn epilayers have been grown on GaAs(100) substrate by using Hot-wall epitaxy technique. Structural and magneto-optical properties of the CdS:Mn epilayers have been investigated by X-ray diffraction, PL and Faraday rotation. The structure of the CdS:Mn was phase-transited from hexagonal to cubic structure with increasing substrate temperature. From the XRD spectra, the [200] reflection peak of hexagonal CdS was observed at  $2\theta = 26.43^\circ$  and at  $54.64^\circ$  for [400] reflection, and the [200] and [400] reflection peaks of the cubic CdS were observed at  $2\theta = 29.44^\circ$  and at  $63.27^\circ$ , respectively.

PL spectra for the cubic CdS:Mn at 25K showed that the exciton emission peak ( $I_{be}$ ) and DAP emission peak appeared at 2.507eV and 2.448eV, respectively. Accordingly, the LO phonon energy was estimated 36.5meV. The absorption experiment at 25K showed that the band gap energy of the cubic CdS:Mn was 2.509eV, and the absorption edge shifted to lower energy with increasing temperature. Furthermore, we will present Faraday Rotation of the CdS:Mn.

CdS 박막의 XRD스펙트럼



**Kp-V-058****콜로이드 CdSe 양자점의 광학적 특성 및 광전소자로의 응용**오 은순, 김 태수, 이 병우, 김 의태<sup>1</sup>, KUMAR kiran<sup>1</sup>충남대학교 물리학과, <sup>1</sup>충남대학교 나노정보시스템공학과.

콜로이드 반도체 나노구조는 광전소자나 임상의학 분야에서 주목을 받고 있다. 콜로이드 양자점은 열분해 방법으로 trioctylphosphine oxide (TOPO) 리간드 양자점을 합성하였고 화학적 방법으로 TOPO리간드가 mercaptopropionic acid (MPA) 리간드로 치환된 양자점을 합성하였다. 콜로이드 양자점은 photoluminescence (PL) 와 시분해 PL측정을 통해 양자점의 리간드에 따른 광학적 특성을 관찰하였다. TOPO 리간드 양자점의 경우는 220 K 이상에서 PL의 세기와 수명이 증가하는 현상이 발견 되었는데 이는 TOPO 양자점 표면의 상변화에 의한 것으로 생각된다. MPA 리간드 양자점의 경우 PL의 세기와 수명은 온도에 따른 변화는 거의 없고 PL peak은 TOPO 리간드 양자점의 경우보다 장파장에서 관찰 되었다. 염료감응태양전지의 염료 대신 콜로이드 양자점을 사용 할 수 있는데 리간드의 종류나 전처리 여부에 따른 광전소자의 효율을 연구하였다.

**Kp-V-059****Spatially Resolved Optical Properties of Periodically Polarity Inverted ZnO****Films Grown on (0001) Al<sub>2</sub>O<sub>3</sub> by Cr-compound Intermediate Layers**CHO Yong-Hoon, KWON Bong-Joon, KIM Je Hyung, PARK Jin-Sub<sup>1</sup>, YAO Takafumi<sup>1</sup>

KAIST, Department of Physics, Graduate School of Nanoscience & Technology (WCU), and KAIST Institute for the NanoCentury. <sup>1</sup>Tohoku University, Institute for Materials Research.

ZnO is a wide-gap semiconductor studied for many decades, which has many benefits for ultraviolet optoelectric devices because it has direct wide band gap of 3.37 eV and a large exciton binding energy (~ 60 meV) at room temperature.

Study on the surface polarity of ZnO is promoted by many researchers in a point of view of crystalline quality, electrical property, p-type doping, surface morphology, and optical property. We investigated on the spatially resolved optical properties of periodically polarity inverted (PPI)ZnO films grown on (0001) Al<sub>2</sub>O<sub>3</sub> by Cr-compound intermediate layers, using micro-photoluminescence ( $\mu$ -PL) equipment. Figure 1. shows a schematic of the PPIZnO structure. At first, 20-nm-thick LT ZnO was grown on a Zn exposed CrN buffer layer. Second, stripe patterns were formed by wet etching using the conventional photoresistpatterned mask with 10- $\mu$ m-width stripes. The etching was selectively performed for LT ZnO on the CrN buffer layer. Next, O-plasma exposure was carried out to form the Cr<sub>2</sub>O<sub>3</sub> layer on the opened CrN buffer layer. Finally, the ZnO film was grown, resulting in the growth of ZnO on the LT ZnO/CrN and on the Cr<sub>2</sub>O<sub>3</sub> regions at the same time. We measured  $\mu$ -PL spectra of the A, B, C regions.

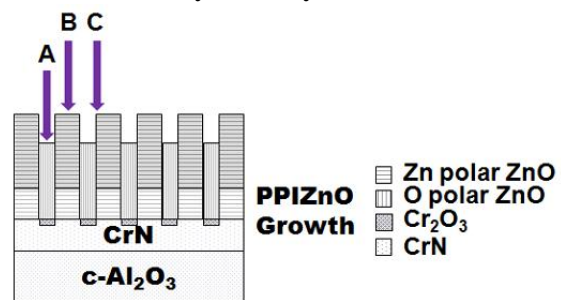


Fig.1. Schematic of the PPIZnO structure

**Kp-V-060****Properties on Optical Gain of CdZnO Quantum Wells**JEON H. C., LEE S. J., PARK S. H.<sup>1</sup>, KANG T. W.Dongguk University. <sup>1</sup>Catholic University of Daegu.

The wide band-gap wurtzite (WZ) semiconductors have attracted much attention due to their potential applications for optoelectronic devices in blue and ultraviolet (UV) regions. Recently, ZnO and related oxides have been proposed as the new wide band-gap semiconductors for short wavelength optoelectronic device applications. ZnO-based quantum well (QW) structures have several advantages compared to GaN-based QW structures. In addition, a (Zn,Cd)O mixed crystal has been proposed as a new well material to expand the wavelength tunability by virtue of its narrower band gap. With the current progress in the CdZnO material, fundamental properties of the CdZnO/MgZnO QW structures become very important for device applications. In this research, we investigate electronic and optical properties of CdZnO/MgZnO QW structures with spontaneous polarization and piezoelectric polarization. The many-body optical gain in CdZnO/MgZnO QW structures with spontaneous polarization and piezoelectric polarization are investigated by using many-body effects. As the Cd composition increases, the sign change of the internal field is observed. The CdZnO/MgZnO QW structure with high Cd composition is found to have smaller optical gain because the strain-induced piezoelectric polarization and the spontaneous polarization in the well increase with the inclusion of Cd. These results demonstrate that high performance laser diode operation can be realized in CdZnO/MgZnO QW structures.

**Kp-V-061****1,3-DMP, BAL 등의 thiol 화합물이 CdS 양자구슬의 물성에 미치는 영향**하 성용, 유 동선, 김 일곤, 이 정두, 유 준원<sup>1</sup>, 이 은성<sup>1</sup>, 추 문식<sup>1</sup>, 김 곤우<sup>1</sup>창원대학교 물리학과. <sup>1</sup>창원대학교 화학과.

전구물질로서 cadmium chloride, sodium sulfide 를 사용하고 첨가물질로서 1,3-DMP, BAL 등의 thiol 화합물을 사용한 수용성 합성법으로 콜로이드 상의 CdS 양자구슬을 합성하였으며 thiol 화합물인 1,3-DMP, BAL 등의 첨가물질이 양자구슬의 특성에 미치는 영향을 조사하였다. 1,3-DMP, BAL의 첨가는 생성된 양자구슬의 반경에 영향을 미쳤는데 이로 인해 이들의 농도가 증가할수록 양자구슬의 흡수단은 단파장으로 이동하였다. 이때 양자구슬 반경은 이들을 첨가하지 않은 경우의 ~5nm에서 ~2.6nm로 그 크기가 감소하였으며, 발광스펙트럼의 peak 위치 역시 이들 thiol 화합물의 농도가 증가할수록 단파장 쪽으로 이동하는 것을 확인하였다.

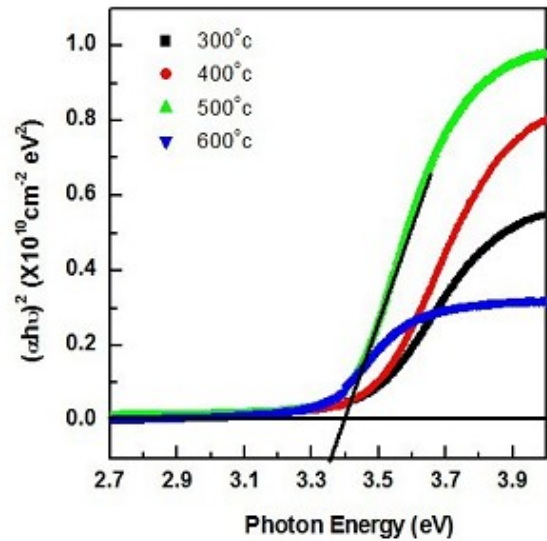
## Kp-V-062

### 급속 열처리 온도가 Al 도핑된 ZnO 박막에 미치는 효과

정 재용, 조 신희

신라대학교 전자재료공학과

최근 광전자산업 분야가 급속히 발전함에 따라 투과율과 전기전도도가 높은 투명 전도막에 대한 수요가 상당하다. 본 연구에서는 라디오파 마크네트론 스퍼터링 방법을 사용하여 증착 온도 300°C에서 유리 기판 위에 Al 도핑된 ZnO(AZO) 박막을 형성한 후에, 서로 다른 온도에서 급속 열처리를 수행하여 AZO 박막의 구조, 광학, 전기적 특성 변화를 조사하였다. AZO 박막은 로타리 펌프와 터보 펌프를 사용하여 초기 진공도  $5 \times 10^{-6}$  torr 까지 배기시킨 다음에, 56 sccm의 Ar 가스를 투입하여 압력  $3.5 \times 10^{-2}$  torr에서 70W의 rf 파워를 공급하여 성장시켰다. 급속 열처리는 질소 가스 분위기에서 1분 동안 온도 300-600 °C에서 수행하였다. 증착된 시편의 광학 투과율은 UV-VIS Spectrophotometer(Simazu, UV2410PC)를 사용하여 파장 영역 340-1100 nm에서 측정하였으며, 가시광 영역에서 평균 투과율은 90% 이상이였다. 광학 밴드갭 에너지는 Tauc의 모델을 사용하여 계산하였으며, 그 값은 열처리 온도에 상당한 의존성을 보였다 [그림 참조].



## Kp-V-063

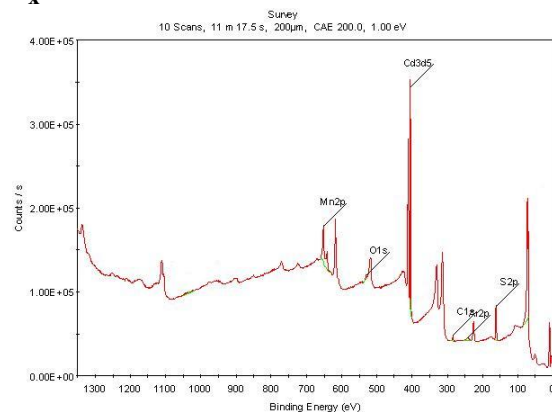
### 열벽 적층 성장법으로 얻은 $Cd_{1-x}Mn_xS$ 박막의 XPS 분석과 타원분광학적 특성

김 대중, 박 재한<sup>1</sup>, 오 병성<sup>1</sup>, 이 종원<sup>2</sup>, 최 용대<sup>3</sup>

목원대학교, 테크노과학연구소. <sup>1</sup>충남대학교, 물리학과. <sup>2</sup>한밭대학교, 신소재공학부. <sup>3</sup>목원대학교, 기술마케팅학과.

고품질의  $Cd_{1-x}Mn_xS$  박막들은 소스 온도에 변화를 주어 두께를 조절하였으며, 열벽 적층 성장법을 이용하여 GaAs (111) 기판위에 성장시켰다. 성장된 CdS 박막들은 X-선 회절 패턴을 분석한 결과 육방정 구조(hexagonal structure)를 갖는 것으로 확인되었고, 결정성을 알아보기 위하여 HRXRD를 측정하였다. 박막의 표면 상태와 성분비를 알아보기 위하여 SEM/EDX를 이용하였다. 또한 박막들의 표면과 계면층 사이의 성분비와 화학적 구성을 알아보기 위하여 x-ray photoelectron spectroscopy (XPS)

분석을 수행하였다. 성장된 박막들의 광학적 특성을 알아보기 위하여 분광학적 엘립소메트리를 사용하여 실온에서 2.0-8.5 eV 사이 포톤에너지 범위에서 측정하였다. 측정된 데이터들로부터 유사 유전함수 스펙트럼  $\langle \epsilon(E) \rangle = \langle \epsilon_1(E) \rangle + i \langle \epsilon_2(E) \rangle$ 에 나타난  $E_0$ ,  $E_{1A}$ ,  $E_{1B}$ ,  $E_2$ ,  $E_0'$ 와 같은 임계점 구조를 관측하였다. 박막의 복소 유전함수와 밀접한 관계를 가지고 있는 굴절지수  $n(E)$ , 소광계수  $k(E)$ , 반사계수  $R(E)$  그리고 흡수계수  $\alpha(E)$ 와 같은 광학적 특성 등을 조사하였다. (본 연구는 2009년도 정부의 재원으로 과학재단의 지원을 받아 수행된 연구임; 2009-0074688)



**Kp-V-064****Fabrication and electrical properties of wide-band-gap  $\text{Mg}_x\text{Zn}_{1-x}\text{O}$  ceramics**

김 셋별, LI GUO JIE, 최 병춘, 정 중현, 문 병기, 전 병억<sup>1</sup>

부경대학교 물리학과, <sup>1</sup> 한국 과학 영재학교.

Zinc oxide( $\text{ZnO}$ ) and related semiconductor crystals have recently attracted increasing interest toward application to UV light emitters, deep UV sensor, transparent thin film transistors, multifunctional integrated circuits, and so on.  $\text{MgO}$  is the prototype of an ionic compound semiconductor which is quite well investigated. Recently it has attracted much attention because it can be alloyed with  $\text{ZnO}$  to tune the band gap of  $\text{ZnO}$  from 3.4 up to 7.8 eV depending on the alloy concentration  $x$  of Mg content in  $\text{Zn}_{1-x}\text{Mg}_x\text{O}$ . Once p-type conducting  $\text{ZnO}$  is available, band-gap engineered electro-optical device based on this material will have a wide variety of application. We made  $\text{Zn}_{1-x}\text{Mg}_x\text{O}$  ( $x=0, 0.03, 0.05, 0.1, 0.2$ ) ceramics and investigated electrical properties, band gap energy. In this study, as increasing Mg concentration, the grain size, lattice constant decreased. Also, band gap energy increased linearly as Mg concentration.

**Kp-V-065****산소농도에 따른  $\text{ZnO}$  박막의 특성변화**

백 경철, 이 봉주, 정 진

조선대학교 물리학과.

$\text{ZnO}$ (Zinc oxide)로 만들어진 소자는 밴드 갭이 넓고( $\sim 3.37[\text{eV}]$ ) 전기전도성과 광학적 투과도가 우수하다. 지금까지 투명 전도막으로 널리 사용된 재료는 ITO로써 광학적 특성과 전기적 성질이 우수하지만 IN의 생산단가가 높고 플라즈마에 노출되는 경우 특성이 변화되는 문제점이 있었다. 하지만  $\text{ZnO}$ 는 적외선과 가시광 영역에서 높은 투과성과 전기전도성을 나타내며 플라즈마에 대한 내구성이 우수하고, 낮은 온도에서 공정이 가능하며 원료의 가격이 비교적 저렴한 장점을 가지고 있어서 ITO를 대체할 물질로 연구되고 있다. 본 실험실에서는 RF-sputtering법을 이용하여 산소농도에 따른  $\text{ZnO}$ 박막의 특성을 알아보았다.

**Kp-V-066****유전영동기술을 이용한 나노갭 전극에서 CdSe 나노 입자의 제어 및 정렬**김 옥원, 서 영교<sup>1</sup>, KUMAR Sanjeev, 김 길호성균관대학교, 전자전기공학과. <sup>1</sup>성균관대학교, 나노과학기술원.

반도체성 나노물질은 독특한 기계적, 화학적, 전기적 및 광학적 특성으로 인해 기초 연구분야 뿐만 아니라 여러 응용분야에 있어 많은 주목을 받고 있다. 그러나 이러한 나노반도체의 소자 응용에 대한 연구를 위해서는 선행적으로 나노물질의 제어 기술과 그리고 물질의 전기적 회로 형성 기술을 확립해야 한다. 그의 일환으로 본 연구에서는 유전영동 기술을 이용하여 나노갭 전극에서 CdSe (7nm) 나노입자의 제어와 정렬에 대해 연구하였다. 카드뮴과 셀레나이드의 화합물인 CdSe는 II-VI족 반도체 물질로써 1.74eV의 밴드갭, n-type 반도체 특성 등 독특한 전기적 광학적 특성을 가지고 있다. 특히 CdSe 나노구조체는 고효율 solar cell, 레이저 다이오드와 센서 응용 등 광범위 분야에서 연구가 수행되어 왔다. 유전영동 기술은 외부에서 인가된 non-uniform 전기장에 의한 입자의 분극현상을 이용하여 마이크로 또는 나노 물질을 제어하는 기술이다. 그러나 유전영동을 이용하여 반도체성 나노 입자 제어 기술에 대한 연구는 아직까지 미미한 편이다. 본 연구에서는 유전영동을 이용한 CdSe 나노입자의 정렬을 위해 우선 SiO<sub>2</sub>/Si 기판에 e-beam lithography와 lift-off기술을 이용하여 20~110nm의 금 나노 전극을 형성하였다. 유전영동 기술은 인가전압 (Vpp), 시간 (t) 그리고 주파수 (f) 세 가지 중요한 파라미터를 가지며, 안정적인 입자의 정렬을 위해서는 이 세 가지 파라미터의 조건을 최적화해야 한다. 본 실험에서는 두 파라미터를 고정한 후 한 파라미터의 조건을 변화시키면서 파라미터들의 최적 조건에 대해 연구하였다. 유전영동 실험 후 정렬된 CdSe 나노입자는 scanning electron microscopy (SEM) 을 이용하여 확인할 수 있었다. 나노갭 전극 사이에 정렬된 CdSe 나노입자들의 전류-전압 특성 연구를 통해 반도체 입자에 의한 전기적 연결을 확인할 수 있으며, 나아가 이러한 결과는 반도체 나노 입자를 기반으로 하는 전자소자의 응용가능성을 보여줄 것으로 기대 된다.

**Kp-V-067****유전영동을 이용하여 나노갭 전극에서의 ZnO 나노 입자 제어 및 정렬**양 은표, 서 영교<sup>1</sup>, KUMAR sanjeev, 김 길호성균관대학교, 전자전기공학과. <sup>1</sup>성균관대학교, 나노과학기술원.

유전영동을 이용하여 나노갭 전극에서의 ZnO 나노 입자 제어 및 정렬 양 은표, 서 영교, Sanjeev Kumar, 김 길호 성균관대학교 정보통신공학부 반도체 나노 소자 연구실 II-VI족 화합물 반도체 Zinc oxide(ZnO)는 전자 및 광학소자 응용 분야에서 많은 주목을 받고 있으며, 특히 나노구조의 ZnO는 자외선 레이저, 자외선 센서, 태양전지 그리고 가스센서 등 여러 분야에서 그 응용성 가능성이 보여 지고 있다. 그리고 앞으로 ZnO 나노구조의 특성 연구와 그를 이용한 소자 형성에 대한 기술 확립이 더욱 중요해 질 것이다. 그러나 나노 구조 안에 ZnO 나노입자의 제어 및 정렬 기술은 여전히 어려운 문제로 남아있다. 유전영동은 non-uniform한 전기장을 인가했을 때 입자의 유전분극 현상을 이용하여 나노구조를 제어하는 기술로서 gold nano-colloid, DNA, carbon nanotube 등 다양한 물질의 나노입자를 제어 및 정렬 하는데 효과적으로 사용된 기술이다. 하지만, ZnO를 포함하여 반도체 나노입자의 제어는 아직 많은 연구가 필요한 일이다. 본 연구에서는, 60~110 nm 의 ZnO 나노입자를 미리 제작된 금 나노갭 전극(20~110nm)위에 유전영동 기술을 이용하여 정렬하였다. 금 나노 전극은 e-beam lithography를 이용하여 Si/SiO<sub>2</sub> 기판위에서 형성 되었다. 본 논문에서는 ZnO 나노입자의 정렬을 위해 peak-to-peak voltage, 주파수, 시간 그리고 나노갭 사이즈 등 다양한 DEP 파라미터를 최적화 하였다. 정렬된 나노입자는 Scanning electron microscopy(SEM)을 이용하여 확인하였다. 본 연구로부터 제작된 ZnO 나노입자 기반 소자는 전자 및 광학 소자로서 응용 가능성을 보일 것이다.

**Kp-V-068****초음파를 이용한 ZnO nanorods 의 성장과 광학적 특성 분석**

오 은순, 이 병우, 김 태수, 김 진태<sup>1</sup>, 임 한나<sup>1</sup>, 정 승호<sup>2</sup>

충남대학교 물리학과, <sup>1</sup>한국표준과학연구원, <sup>2</sup>경북대학교 화학공학과.

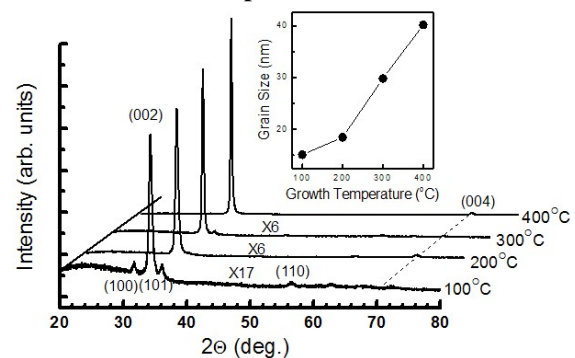
초음파의 화학적 효과를 이용하여 나노 구조 물질을 제조하는 방법은 저렴하고 간단한 방법으로 최근 관심을 불러일으키는 연구 주제이다. 본 연구에서는 초음파 화학법을 이용하여 용액 상태에서 ZnO 나노 선을 성장하였다. Precursor로는 Zn nitrate 와 Zn chloride를 사용하였다. Scanning Electron Microscope (SEM) 이미지를 통해 ZnO 가 나노 선 형태로 성장되었음을 확인할 수 있었다. Photoluminescence (PL) 분석에서는 precursor로 Zn nitrate를 사용했을 경우가 Zn chloride를 사용했을 경우에 비해서 PL 반치폭이 더 작게 나타났고 donor bound exciton (3.36 eV)이 더 뚜렷하게 나타났다. 또한 precursor로 Zn chloride 를 사용했을 경우가 Zn nitrate를 사용했을 경우에 비해 더 높은 에너지에서 PL peak 이 관찰되었다.

**Kp-V-069****Effects of Deposition Temperature on the Structural, Optical and Electrical****Properties of ZnO Thin Films on Glass Substrate**

조 신호

신라대학교 전자재료공학과.

The effects of deposition temperature on the optical and electrical properties of ZnO thin films on glass substrate are investigated. The ZnO films are deposited by radio-frequency magnetron sputtering at deposition temperatures from 100 °C to 400 °C. The crystalline orientation of the ZnO (002) plane is not changed but the full width at half maximum gets smaller as the deposition temperature increases. The intensity of the ZnO (002) peak for the film grown at 400 °C is the most intense and its FWHM is measured to be 0.23°. The dependence of electron concentration, mobility, and resistivity on deposition temperature exhibits that the ZnO films have higher electron concentration at higher temperatures, thus giving the low resistivity. From the spectra of optical absorbance measured at room temperature, the values of the optical transmittance and bandgap energy are determined. The transmittance for the ZnO film grown at 100 °C is found to be 92% at 700 nm.



**Kp-V-070****KOH 및 NaOH 알칼리성 촉매를 이용하여 화학적 수조 방법으로 성장시킨 ZnS 및 Zn(S, OH) 박막의 특성 비교**

천 성현, 최 인환

중앙대학교 물리학과.

태양전지 제작에 있어서 II-VI족 반도체는 Buffer Window 층으로 사용되어져 왔다. 가장 많이 사용되었던 것은 CdS인데, 카드뮴 및 카드뮴 화합물은 독성이 강하고, 환경오염을 유발하는 바, 이를 대체하기 위한 연구가 많이 이루어지고 있다. 그 중 많이 연구되고 있는 물질은 ZnS, ZnSe 등이 있다. 특히 ZnS는 에너지 띠 간격이 가장 큰 물질 중의 하나로 CdS를 대체하기 위한 많은 장점을 가지고 있다. 여기서는 추가 선택한 촉매인 KOH 및 NaOH를 이용하여 수조에서 화학적 수조 증착 방법으로 슬라이드 글라스 및 용융 수정판(Fused quartz plate)에 ZnS 및 Zn(S, OH) 박막을 성장하였다. 증착에 사용된 수용액의 경우 촉매로 알칼리성 시약을 사용한 경우 pH가 12.8 ~ 13.1 정도의 강한 알칼리성을 갖는 것으로 측정되었으며, 추가 촉매를 배제한 경우에는 11.2 ~ 11.5 정도로 관찰되었다. 증착된 박막을 UV-Visible Spectrometer를 이용하여 Absorption 및 Transmittance를 측정하였고, FT-IR(Fourier Transform Infra Red) Spectrometer를 이용하여 적외선 영역에서의 Transmittance와 반사를 이용한 Transmittance를 관찰, 박막의 분자 결합 구조를 분석하였다. 그리고 SEM을 이용하여 촉매에 따른, 시간에 따른 박막의 표면을 관찰하였다. 동시에 Energy Dispersive X-ray Microanalysis(EDAX)를 이용한 스펙트럼을 분석, 각 원소당 에너지 분포를 관찰하고, PL 측정을 통하여 박막의 광 특성도 분석하였다. UV-Visible Spectrometer를 이용한 측정에서 증착된 ZnS 박막이 UV영역의 흡수 스펙트럼을 가진다는 것을 확인할 수 있었고, Alkali catalyst인 NaOH 및 KOH의 양에 비례하여 흡수율이 증가하였다. FT-IR Spectrometer를 이용한 측정에서는 파수의 범위를  $4000\text{cm}^{-1}$  ~  $400\text{cm}^{-1}$ 로 하였고, Transmittance를 관찰한 결과, O-H<sup>-</sup> 결합 및 S-H<sup>-</sup> 결합구조를 확인하였고, 반사를 이용한 Transmittance를 관찰한 결과로는 동일 파수에서의 S-H<sup>-</sup> 결합구조 및 다른 파수에서의 O-H<sup>-</sup> 결합을 확인하였다. XRD 측정에서는 박막의 일부를 300°C에서 열처리한 것을 측정하였다. 측정 결과, 증착된 박막은 우르츠광(Wurtzite) 구조를 가지는 ZnS 박막임을 알 수 있었다. 그 외에 ZnO 및 Zn(OH)<sub>2</sub>의 peak도 관측되었다. 이에 따라서 최종 증착된 박막은 Zn(S, OH) 구조가 됨을 확인하였다.

**Kp-V-071****Synthesis of ZnO nano-structures on Au/SiN<sub>x</sub>/Si(001) substrate by radio-frequency magnetron sputtering**

선 정호, 강 현철

조선대학교, 신소재공학과.

지난 10여년 동안 ZnO 박막에 대한 연구가 활발히 진행되고 있다. 이는 ZnO 박막의 우수한 광학적 특성 때문이다. ZnO 관련 대표적인 광학소자로서 ultraviolet(UV) light emitting diode(LED)가 연구되고 있는데, 대부분 sapphire(0001) 기판위에 ZnO 박막을 증착하여 제조된다. 또한 저차원 ZnO 나노구조체를 제조하여 새로운 기능과 성능을 가진 다양한 소자들이 발표되고 있는데, 이는 대부분 self-assembly 방법을 이용하거나 귀금속 catalysts를 이용한 증착 기술로 제조된다. 귀금속 catalysts를 이용한 증착기술은 통상적으로 vapor-liquid-solid (VLS) 증착 mechanism을 이용하여 설명할 수 있는데, 고온에서 Au, Sn 등의 seeds 물질인 금속 nano-crystals이 표면녹음현상으로 용융되어 ZnO vapor와 함께 액체 상태로 존재하다가 기판위에 고체 상태로 성장한다. 따라서 VLS 성장방법으로 제조된 ZnO 나노막대 형태의 가장 큰 특징은 금속 catalysts가 나노막대 끝에 접합되어 있는 것이다. 하지만, 본 연구진의 지난 연구결과에 의하면, radio frequency (RF) magnetron sputtering 방법으로 제조된 ZnO 나노구조체의 제조과정에 있어서는, 금속 nano-crystals이 catalysts로서 역할보다는 표면 형상을 요철로 만드는 역할이 더 월등하다. 본 연구에서는 대면적 ZnO 나노구조체의 제조목적을 위한 선행 연구로서 SiN<sub>x</sub>/Si(001) 박막에 증착한 Au 박막을 열처리하여 생성된 Au seeds위에 RF magnetron sputtering 방법으로 제조한 ZnO 나노구조체의 구조적, 광학적 특성을 보고한다. E-beam evaporation방법으로 증착한 Au 박막을 Au seeds로 전이시키는 열처리온도 변화에 따른 ZnO 나노구조체의 구조적 특성의 변화를 관찰하였다.

**Kp-V-072****CdS/CdSe 측면 헤테로 나노벨트 성장 및 광학적특성**

김 유리, 정 재훈, 윤 현식, 김 정혁, 송 만석, 배 세환, 김 용, GAO Qing<sup>1</sup>, TAN H. Hoe<sup>1</sup>, CHENNUPETI Jagadish<sup>1</sup>, ZOU Jin<sup>2</sup>, CHEN Zhigang<sup>2</sup>

동아대학교 물리학과. <sup>1</sup>Australian National University. <sup>2</sup>The University of Queensland.

반도체 nanostructure의 다양한 특성은 전자공학과 광학적 소자로서의 적용가능성에 있어서 주목 받고 있다. 본 실험은 간단한 장치인 single-zone quartz tube furnace를 이용하여 Physical Vapor Transport에 의해 행하였다. 세척된 Si 기판위에 0.1% poly-L-lysine 에 1 분간 담가 표면에 polyelectrolyte 층을 형성시켰다. 이 polyelectrolyte 층은 양으로 대전되어 음으로 대전된 금 입자를 고정하는 역할을 한다. 다음 10nm 크기,  $5.7 \times 10^{12}$  particles/ml를 농도의 금 나노입자가 함유된 콜로이드 용액을 50%로 희석하여 표면에 분사한 다음 탈이온수로 세척하였다. 전기로의 중앙에 놓인 quartz boat 에 CdSe(200mg)를 놓고 하류에 준비된 기판을 놓았다. 10% H<sub>2</sub> 가 포함된 N<sub>2</sub> 가스를 200sccm을 흘렸고 원료가 놓인 지역의 온도를 900도로 2시간 동안 성장하였다. 이때 열전대를 이용하여 측정한 결과 소스와 기판의 온도 차이는 200도 정도였다. 같은 방법으로 CdS(200mg)로 2차 성장하여 CdSe나노박판에 후속으로 CdS 나노박판을 측면으로 성장하는 새로운 측면 나노박판 헤테로구조인 CdS/CdSe 나노벨트를 성장시키고 micro-PL을 관찰하였다. We acknowledge support by the Korean Science and Engineering Foundation (KOSEF) through Grant No. F01-2007-000-10087-0.

**Kp-V-073****Si 나노결정의 크기에 따른 Si 나노결정-ZnO 박막 상호간의 에너지 전이 특성****연구**

신 동희, 김 창오, 홍 승휘, 최 석호, 김 성<sup>1</sup>

경희대 국제캠퍼스 응용물리학과. <sup>1</sup>호주국립대학 전자재료공학과.

이온빔 스퍼터링 증착법을 이용하여 실리콘 (100)기판 위에 300 nm 두께의 SiO<sub>x</sub> 박막을 증착한 후 1100 °C에서 20 분간 질소분위기에서 급속 열처리 하였다. SiO<sub>x</sub> 박막의 x 값은 1.0부터 1.8까지 변화시켰으며 x 값은 X선 광전자분광기 (XPS)를 사용하여 결정하고 조절하였다. RF 스퍼터링 증착법을 이용하여 Si 나노결정막 박막 위에 100 nm 두께의 ZnO 박막을 증착하여 Si 나노결정/ZnO 복합구조 박막을 형성하고 900 °C에서 3 분간 산소분위기에서 급속 열처리를 하였다. 고분해능 투과전자현미경 분석 결과, SiO<sub>2</sub> 박막 안에서 Si 나노결정의 크기는 x값이 1.0부터 1.8까지 증가함에 따라 약 7에서 2 nm로 감소하였다. 488 nm (~2.55 eV)의 레이저 빛으로 여기할 경우 광루미네선스 (photoluminescence, PL)는 나노결정 단일층이나 복합구조 모두 동일한 위치에서 PL peak를 보이며, x값이 1.0~1.8로 증가함에 따라 PL peak는 1.42에서 1.68 eV로 청색전이한다. 그러나 모든 x값에 대하여 복합구조의 PL 세기는 Si 나노결정 단일층에 비해 약 1/2정도로 감소한다. 325 nm (3.83 eV)로 여기할 경우 Si 나노결정 단일층은 488 nm에 의해 여기할 경우와 마찬가지로 PL 스펙트럼이 거의 유사하게 관찰된다. 그러나 복합구조의 경우, Si 나노결정의 PL 밴드와 함께 ~3.3 eV 근처에서 ZnO 밴드띠끝 (near band edge, NBE)과 관련된 새로운 PL 밴드가 나타난다. x가 1.0에서 1.8로 증가함에 따라 ~3.3 eV의 NBE PL 세기는 감소지만 Si 나노결정 PL 밴드의 세기는 급격히 증가한다. 또한 x값 증가에 따라 Si 나노결정 PL 밴드는 1.55~1.66 eV로 청색전이하는 등, Si 나노결정 단일층의 PL 스펙트럼의 변화와 크게 다르다. 이는 325 nm에 의하여 여기된 ZnO 박막의 전자-정공 쌍들에 의해 Si 나노결정의 방사결합이 영향을 받았음을 의미한다. 본 연구에서는 이러한 결과와 더불어 복합구조의 온도 및 여기파위에 따른 PL 의존성 및 ZnO와 Si 나노결정 PL 밴드 들의 시분해 PL 감쇠시간의 변화를 관찰하여 Si 나노결정-ZnO 박막 상호간의 에너지 전이의 메커니즘을 규명하고자 한다.

## Structural Properties

김 창오, 신 동희, 오 형택, 최 석호, BELAY K.<sup>1</sup>, ELLIMAN R. G.<sup>1</sup>

경희대학교 응용물리학과 및 자연과학종합연구원. <sup>1</sup>호주국립대학 전자재료공학과.

Enhanced ultraviolet photoluminescence (PL) has been found in V implanted ZnO films (ZnO:V) and its correlation with structural properties of the ZnO:V films have been investigated by x-ray diffraction (XRD) and x-ray photoelectron microscopy (XPS). 100-nm-thick ZnO films were implanted with 100 keV V ions to doses ( $n_V$ ) of  $1.0 \times 10^{15}$ ,  $2.5 \times 10^{15}$ ,  $5 \times 10^{15}$ , and  $1.0 \times 10^{16} \text{ cm}^{-2}$  at room temperature and subsequently annealed at 300 ~ 900 °C for 20 min in an oxygen ambient. Near-band-edge (NBE) PL emission from ZnO:V films was observed at ~ 380 nm, irrespective of  $n_V$  and annealing temperature ( $T_A$ ). The PL intensity increased gradually with increasing  $n_V$  from 0 to  $2.5 \times 10^{15} \text{ cm}^{-2}$ , but at  $n_V \geq 5 \times 10^{15} \text{ cm}^{-2}$ , it decreased. As  $T_A$  increases from 300 to 900°C, the NBE PL intensity increased, and when  $T_A = 900^\circ\text{C}$ , it was almost 6 times enhanced for a sample with  $n_V = 2.5 \times 10^{15} \text{ cm}^{-2}$ , compared to that of the un-implanted ZnO film. The XRD patterns showed a dominant peak at ~ 34° for the ZnO:V films annealed at 900°C, which was attributed to the ZnO (002) plane. The XRD intensity increased steeply with increasing  $n_V$  up to  $2.5 \times 10^{15} \text{ cm}^{-2}$ , but  $n_V > 2.5 \times 10^{15} \text{ cm}^{-2}$ , it decreased, consistent with the  $n_V$ -dependent variation of the NBE PL intensity. At  $n_V > 2.5 \times 10^{15} \text{ cm}^{-2}$ , the XRD peaks not only from ZnO (002) phase but also from V clusters or V oxide phases were identified, whilst only the ZnO (002) XRD peak was observed at  $n_V \leq 2.5 \times 10^{15} \text{ cm}^{-2}$ , indicating that the solid solubility limit of V in ZnO film is below  $2.5 \times 10^{15} \text{ cm}^{-2}$ . The XPS intensities of V 2p states increase gradually with increasing  $n_V$  from 0 to  $2.5 \times 10^{15} \text{ cm}^{-2}$ , but when  $n_V > 2.5 \times 10^{15} \text{ cm}^{-2}$ , they decreased. This could explain why PL behaviors are changeable with respect to  $n_V = 2.5 \times 10^{15} \text{ cm}^{-2}$ . Possible physical mechanisms are discussed to explain the experimental results.

발표자 색인



가

가 동하	Cp-IV-035	고 대호	Lp-III-003	권 영준	B-25, Bp-I-015
가 은미	Hp-III-014	고 대홍	Kp-III-044	권 영준	Bp-I-013
강 궁원	LT-03(초)	고 도경	lp-III-055	권 영택	Dp-V-136
강 기천	J-09	고 도경	lp-III-034	권 영현	K-13
강 대준	Dp-V-175, E-10, E-12, E-40, E-44, Ep-I-012, Ep-I-013, Ep-I-029, Ep-II-075	고 도경	I-03(초), lp-III-035	권 오갑	B-03
강 명호	D-02	고 동혁	lp-III-008	권 오룡	Dp-V-187, Dp-V-193
강 병남	KF-01(초)	고 락길	lp-III-001	권 오장	lp-III-028
강 병남	Fp-IV-023	고 락길	Dp-V-182	권 오준	Hp-IV-088
강 병호	Ep-II-093	고 문주	Dp-II-064, Dp-II-074	권 용경	Dp-I-031
강 병휘	Cp-IV-043, Hp-III-018, lp-III-055	고 세건	E-11	권 용경	D-54, Fp-IV-025
강 보라	Bp-I-026	고 승국	Fp-IV-008	권 용성	Dp-II-077, Dp-V-192
강 보라	B-14(초), Bp-I-002, Bp-I-006, Bp-I-009	고 안수	Hp-IV-057	권 우진	J-01
강 보라	B-35	고 영호	lp-III-050	권 은향	B-36
강 보수	Kp-V-056	고 원하	A-11	권 재민	Hp-III-021
강 보영	E-31, E-32	고 윤영	Hp-III-016	권 정택	Bp-I-003
강 보영	lp-III-054	고 윤영	Dp-I-015	권 향명	Dp-V-157
강 봉근	E-39, E-49	고 윤영	Dp-II-081	권 향명	Dp-V-170
강 상목	lp-III-055	고 윤영	Dp-II-066	권 향명	Dp-V-168
강 상백	Ep-V-119	고 윤영	D-55	권 혁민	Dp-V-194
강 서곤	Bp-I-022	고 은별	B-25	권 혁중	Hp-IV-065, Hp-IV-068, Hp-IV-071, Hp-IV-074
강 서곤	B-28, Cp-IV-006	고 재우	B-27, B-28	권 혁중	Hp-IV-072
강 서곤	Bp-I-005	고 재우	B-29	권 혁중	Hp-IV-048
강 성구	lp-III-023	고 재현	Dp-I-057	권 현웅	F-05, Fp-IV-008
강 성구	Kp-II-005	고 재현	Dp-I-039	권 희영	Dp-II-114, Dp-II-123
강 성웅	Dp-I-036	고 정환	Bp-I-003	금 관필	Ep-II-067, Ep-II-069
강 성웅	Dp-I-026	고 정휘	lp-III-019	금 용연	B-19
강 세준	Kp-III-045	고 정휘	lp-III-002	기 현철	Ep-II-040
강 세준	D-03	고 태준	Dp-II-125	길 계환	Hp-IV-076
강 영창	Gp-III-009	고 항주	E-41	길 연호	Kp-V-046
강 윤구	Bp-I-026	공 대정	Ep-II-040	김 가현	Dp-I-013, Dp-I-014
강 윤구	B-14(초), B-26, B-36, Bp-I-002, Bp-I-006, Bp-I-009	공 대정	B-38	김 갑석	Hp-III-038
강 윤구	B-25, B-35	공 대정	Bp-I-017	김 건	F-14
강 원남	Dp-II-077	공 소저	Bp-I-008, Bp-I-012	김 건호	E-51, Ep-V-110
강 유진	E-33	공 소저	Ep-I-028	김 건호	Kp-III-013, Kp-III-027
강 은경	lp-III-051	공 태호	Ep-I-093	김 경남	lp-III-039
강 응철	A-14	공 현식	E-35	김 경락	J-09
강 인기	Kp-II-005	곽 명철	Ep-I-006, Ep-I-007	김 경렬	Hp-IV-058, Hp-IV-059, Hp-IV-062, Hp-IV-069, Hp-IV-079
강 일준	KF-06(초)	곽 무선	G-09	김 경렬	Hp-IV-061
강 재필	Dp-I-016	곽 정춘	Dp-V-194	김 경미	E-45
강 정수	Dp-V-192	곽 종구	E-19	김 경승	lp-III-001
강 주환	C-02, Cp-IV-022, Cp-IV-037	곽 준호	Hp-III-021, Hp-III-022, Hp-III-023	김 경식	Fp-IV-012
강 주환	C-03, Cp-IV-004	곽 지혜	Hp-III-042	김 경식	Cp-IV-030
강 준호	Gp-III-012	곽 진구	Kp-III-029	김 경중	Kp-V-052, Kp-V-053
강 준희	Kp-III-022	곽 진구	Dp-V-155	김 계령	Cp-IV-026
강 중구	Ep-II-040	곽 진구	Dp-V-221	김 계령	Ep-I-016
강 태희	E-55, E-56	교 학빈	Dp-V-161	김 고은	E-51, Ep-V-110
강 현철	E-52	구 동진	Ep-II-047, Ep-II-051, Ep-II-052, Ep-II-053, Ep-V-130, Ep-V-131	김 곤우	Kp-V-061
강 현철	Dp-V-199, I-08	구 민호	Hp-III-029	김 광복	E-41
강 훈수	Kp-V-071	구 용성	E-25	김 광주	A-11
강 흥식	lp-III-034, Kp-II-012	구 자용	Dp-II-091, Dp-II-112	김 귀년	Cp-IV-025
경 성현	Bp-I-023	구 자훈	DT-01(초)	김 규봉	D-19
경 원식	Dp-I-015	구 현철	Ep-II-067, Ep-II-069	김 규정	E-45
경 원식	Dp-II-081	권 남오	Dp-V-145	김 규환	I-10
경 원식	Dp-II-066	권 명석	Dp-V-143	김 기동	Cp-IV-028, Cp-IV-029, Cp-IV-036
경 지수	I-09	권 명희	Dp-V-171	김 기동	Cp-IV-019
고 광일	F-15	권 민지	Dp-V-143	김 기식	Jp-III-001
고 광일	F-16, F-17	권 봉준	Ep-II-100	김 기연	Ep-V-133
고 광일	F-14	권 봉준	Dp-V-157	김 기연	Dp-II-099
고 광훈	lp-III-041	권 석면	Dp-V-170	김 기욱	Ep-II-042
고 근하	Ep-V-109	권 석면	Dp-V-168	김 기청	D-03, Kp-III-045
고 근하	Ep-V-108	권 영광	C-04	김 기정	Dp-V-194
		권 영상	Bp-I-016	김 기태	DF-03(초)
		권 영수	C-34	김 기현	lp-III-019
		권 영수	lp-III-018	김 기현	lp-III-002
		권 영일	Ep-II-068	김 기홍	Ep-V-122
		권 영일	C-02, Cp-IV-022, Cp-IV-037	김 기홍	Ep-V-122, Ep-V-126, Ep-V-127
		권 영일	C-03, Cp-IV-004		
		권 영준	Bp-I-023, Lp-III-002		

김 기홍 I-07, Ip-III-010, Ip-III-011,  
 Ip-III-012, Ip-III-013  
 김 길호 Kp-V-066, Kp-V-067  
 김 나리 E-51, Ep-V-110  
 김 낙우 B-05  
 김 남 Kp-III-014  
 김 남 Dp-V-149, Dp-V-152  
 김 남 D-29  
 김 남미 Ep-II-061  
 김 대식 I-09, I-10  
 김 대연 A-17  
 김 대일 Hp-IV-065  
 김 대중 Kp-V-063  
 김 대철 Hp-III-029  
 김 대철 Ip-III-053  
 김 대철 E-25  
 김 대현 Dp-V-192  
 김 대환 Gp-III-008  
 김 덕희 Ep-V-126  
 김 도억 Ep-II-093  
 김 도일 Ip-III-053  
 김 동균 C-04  
 김 동년 Ep-V-112  
 김 동락 Ep-II-082  
 김 동언 Hp-IV-083  
 김 동영 Ep-V-114  
 김 동욱 C-42  
 김 동욱 Ep-II-100, Kp-III-034,  
 Kp-V-056  
 김 동유 Dp-II-102  
 김 동유 D-15  
 김 동인 Kp-III-013  
 김 동철 Dp-V-184  
 김 동철 Dp-I-026  
 김 동철 E-44  
 김 동철 E-10  
 김 동현 Bp-I-026  
 김 동현 B-14(초), B-36, Bp-I-002,  
 Bp-I-006, Bp-I-009  
 김 동현 B-35  
 김 동현 Dp-II-099  
 김 동호 E-32  
 김 동호 Dp-II-095  
 김 동희 Bp-I-008  
 김 동희 Bp-I-017  
 김 동희 Bp-I-004  
 김 동희 B-38  
 김 두근 Ep-II-040  
 김 두영 PA-14(초)  
 김 맥 Dp-I-038  
 김 맥 Dp-I-041  
 김 맥 Dp-I-037  
 김 명수 E-19  
 김 명운 Ip-III-042  
 김 명진 Hp-IV-056, Hp-IV-080  
 김 명호 Dp-I-043  
 김 무성 Ep-II-068  
 김 문경 Hp-IV-058  
 김 문경 Hp-IV-061  
 김 문경 Hp-IV-051  
 김 미선 Hp-III-041  
 김 민석 H-05  
 김 민수 F-05  
 김 민수 L-11(초), L-21  
 김 민수 L-22  
 김 민수 L-19  
 김 민재 Dp-II-088  
 김 민재 Dp-II-104  
 김 민철 Kp-V-053  
 김 범규 Dp-V-149, Dp-V-152

김 범현 Dp-II-088  
 김 범현 Dp-II-104  
 김 법균 Bp-I-016  
 김 병찬 Bp-I-026  
 김 병찬 B-14(초), B-36, Bp-I-002,  
 Bp-I-006, Bp-I-009  
 김 병찬 B-35  
 김 병환 Ep-I-003  
 김 봉수 D-03  
 김 봉수 Dp-V-194  
 김 봉수 D-30  
 김 봉수 Dp-V-164  
 김 봉수 D-29, Dp-V-137  
 김 봉수 Dp-I-004  
 김 봉환 Dp-II-107  
 김 삼진 Dp-II-110  
 김 상걸 Ep-I-010  
 김 상근 K-13  
 김 상근 Dp-V-137  
 김 상렬 B-27  
 김 상민 D-27  
 김 상수 Dp-I-043  
 김 상수 Dp-I-013, Dp-I-014  
 김 상수 E-52, I-08  
 김 상식 KF-07(초)  
 김 상인 Dp-II-107  
 김 상현 Hp-III-038  
 김 상훈 Ep-I-028  
 김 상훈 Hp-IV-084  
 김 상훈 Hp-IV-082  
 김 상훈 Dp-V-148  
 김 셋별 Kp-V-064  
 김 셋별 Dp-I-006  
 김 석원 Ip-III-049  
 김 석원 Ep-II-074, Ep-V-118,  
 Gp-III-007, Ip-III-033,  
 Ip-III-047, Ip-III-048  
 김 석원 Ip-III-046  
 김 선기 B-26  
 김 선기 B-25  
 김 선영 Hp-III-028  
 김 선자 H-20  
 김 선자 Hp-III-044  
 김 선필 Kp-III-038  
 김 선호 Hp-III-022, Hp-III-023  
 김 선훈 E-41  
 김 선훈 Ep-II-040  
 김 선희 B-36  
 김 성 Kp-V-073  
 김 성백 Dp-I-007  
 김 성백 Dp-I-039, Dp-II-125  
 김 성봉 Hp-III-029  
 김 성봉 Hp-III-027  
 김 성식 Hp-III-009  
 김 성원 Gp-III-015  
 김 성인 E-06, E-42  
 김 성준 Kp-III-023  
 김 성준 C-19  
 김 성준 C-20  
 김 성지 E-48  
 김 성진 Fp-IV-021  
 김 성철 Hp-IV-078  
 김 성철 Hp-IV-079  
 김 성현 Bp-I-026  
 김 성현 B-14(초), B-36, Bp-I-002,  
 Bp-I-006, Bp-I-009  
 김 성현 B-35  
 김 성호 A-13  
 김 성환 E-30  
 김 성희 Lp-III-003

김 세진 Ip-III-019  
 김 세진 Ip-III-002  
 김 소라 Dp-V-149, Dp-V-152  
 김 송희 Ep-V-119  
 김 송희 Ep-II-085  
 김 송희 Ep-II-092  
 김 수남 E-52, I-08  
 김 수봉 Bp-I-026  
 김 수봉 Bp-I-008  
 김 수봉 B-14(초), B-36, Bp-I-002,  
 Bp-I-006, Bp-I-009, Bp-I-017  
 김 수봉 B-33  
 김 수봉 B-35  
 김 수용 Fp-IV-012, Ip-III-047, Ip-III-048  
 김 수인 Ep-V-112  
 김 수현 Dp-II-078  
 김 수현 Dp-II-079  
 김 승 E-33  
 김 승남 Hp-IV-056, Hp-IV-080  
 김 승천 B-26  
 김 승천 B-25  
 김 승현 Dp-V-212  
 김 승호 Dp-II-121  
 김 승호 Dp-II-120, Ep-V-121  
 김 승환 Hp-IV-069, Hp-IV-084  
 김 안드레이 Bp-I-026  
 김 안드레이 B-14(초), B-36, Bp-I-002,  
 Bp-I-006, Bp-I-009  
 김 안드레이 B-35  
 김 약연 Ep-I-003  
 김 연 Kp-V-048  
 김 연수 A-15  
 김 엽 Fp-IV-013  
 김 엽 Fp-IV-004  
 김 엽관 Dp-V-220  
 김 엽관 Dp-V-214  
 김 영규 A-17  
 김 영근 Ep-I-025  
 김 영덕 Bp-I-026  
 김 영덕 B-14(초), B-26, B-36,  
 Bp-I-002, Bp-I-006, Bp-I-009,  
 Bp-I-018  
 김 영덕 B-25, B-35  
 김 영동 E-33, E-35  
 김 영만 C-12  
 김 영식 Ip-III-038  
 김 영유 Ep-II-077  
 김 영준 Ip-III-019  
 김 영철 Dp-II-064, Dp-II-074  
 김 영태 Fp-IV-009  
 김 영호 Kp-III-023  
 김 영호 Ep-I-023  
 김 영훈 Dp-I-005, Dp-I-016  
 김 영훈 Dp-I-038  
 김 영훈 Dp-I-041, Dp-I-057  
 김 영훈 Dp-I-037  
 김 요정 Cp-IV-008  
 김 용 Kp-V-054, Kp-V-072  
 김 용관 Dp-I-015  
 김 용관 Dp-II-081  
 김 용관 Dp-II-066  
 김 용관 D-55  
 김 용권 L-22  
 김 용권 L-11(초), L-21  
 김 용균 Cp-IV-036  
 김 용균 Cp-IV-042, Cp-IV-043,  
 Hp-III-018, Ip-III-055  
 김 용록 E-05  
 김 용모 Hp-III-038  
 김 용민 Ep-II-091

김 용석 Ep-V-112  
 김 용성 Ep-V-124  
 김 용성 D-14  
 김 용수 Ep-V-118  
 김 용주 B-28  
 김 용함 B-26, Bp-I-018, C-25, Cp-IV-039, Cp-IV-041  
 김 용희 H-19  
 김 용희 J-01  
 김 우영 Bp-I-026  
 김 우영 B-14(초), B-36, Bp-I-002, Bp-I-006, Bp-I-009, C-36  
 김 우영 B-35  
 김 우철 Dp-II-110  
 김 옥원 Kp-V-066  
 김 원정 Dp-I-043  
 김 원태 Dp-V-221  
 김 유경 E-13  
 김 유리 Kp-V-054, Kp-V-072  
 김 유상 B-28  
 김 유석 Dp-V-136  
 김 유석 C-36  
 김 윤중 Dp-V-130, Dp-V-138  
 김 은 Ep-II-048  
 김 은규 Kp-III-038  
 김 은규 Ep-I-023  
 김 은도 Ep-II-095  
 김 은산 H-18  
 김 은산 Hp-IV-047  
 김 은선 E-31, E-32  
 김 은선 Ip-III-054  
 김 은식 Ep-II-047, Ep-II-051, Ep-II-052, Ep-II-053, Ep-V-130, Ep-V-131  
 김 은주 Cp-IV-037  
 김 은주 C-02  
 김 은주 Cp-IV-022  
 김 은주 B-27, B-28  
 김 은주 C-03, Cp-IV-004  
 김 은주 B-29  
 김 의정 Ip-III-018  
 김 의태 Kp-V-058  
 김 인구 Ep-II-074, Ep-V-118, Gp-III-007  
 김 인목 F-16, F-17  
 김 인목 F-14  
 김 인식 I-03(초)  
 김 인중 Lp-III-002  
 김 일곤 Kp-V-061  
 김 일원 Dp-I-001, Dp-I-002, Dp-I-003, Dp-I-018, Ep-I-025  
 김 일환 Cp-IV-039  
 김 일환 B-26, C-25, Cp-IV-041  
 김 장렬 Ep-II-098  
 김 장면 Jp-III-011  
 김 재령 Ep-II-073  
 김 재률 Bp-I-026  
 김 재률 B-14(초), B-36, Bp-I-002, Bp-I-006, Bp-I-009  
 김 재률 B-33, B-35  
 김 재명 Hp-IV-078  
 김 재명 Hp-IV-060, Hp-IV-062  
 김 재범 Ip-III-023, Ip-III-024  
 김 재범 Kp-II-005  
 김 재석 Fp-IV-009  
 김 재열 Dp-V-216  
 김 재영 Dp-I-007  
 김 재영 Dp-II-098  
 김 재호 Cp-IV-006  
 김 재호 Cp-IV-002  
 김 재홍 Ep-II-044

김 재홍 Ep-II-076  
 김 재훈 E-31  
 김 재훈 Ep-I-023  
 김 재훈 Ip-III-054  
 김 재휘 Ep-II-082  
 김 점수 Ip-III-030  
 김 정구 Dp-V-177  
 김 청구 D-29, Dp-V-137  
 김 정기 Hp-IV-050  
 김 정동 Jp-III-010, Jp-III-013  
 김 정리 LT-03(초)  
 김 정민 Ip-III-049  
 김 청민 Ip-III-046  
 김 정엽 Hp-III-013, Hp-III-014  
 김 정용 Ip-III-053  
 김 정용 E-25  
 김 정진 Kp-II-006  
 김 정혁 Kp-V-054, Kp-V-072  
 김 정현 B-32  
 김 정현 Bp-I-012  
 김 정현 B-30  
 김 정화 Kp-II-003, Kp-II-004, Kp-II-012  
 김 정환 E-54  
 김 정희 E-31, E-32  
 김 정희 Gp-III-002  
 김 정희 Ip-III-054  
 김 제하 K-06(초)  
 김 종기 Kp-III-021, Kp-III-032  
 김 종섭 Kp-II-005  
 김 종수 Kp-II-003, Kp-II-004, Kp-II-012  
 김 종욱 B-08  
 김 종재 Hp-III-042  
 김 종재 Hp-III-041  
 김 종철 Ep-II-049, Ep-II-050, Ep-II-101, Ep-II-102  
 김 종필 Hp-IV-064  
 김 종필 Ep-V-117  
 김 종현 Ep-II-064  
 김 종현 Ep-II-072  
 김 주성 Dp-I-001  
 김 주연 DF-03(초)  
 김 주원 Lp-III-002  
 김 주진 Dp-V-173  
 김 주진 Dp-V-152  
 김 주홍 Ep-II-044  
 김 준곤 Cp-IV-029  
 김 준관 Ep-II-043  
 김 준관 PC-08(초)  
 김 준성 Dp-II-066  
 김 준연 H-16  
 김 준오 Kp-II-010  
 김 중복 Jp-III-010, Jp-III-013  
 김 중복 J-06  
 김 중환 Ep-V-106  
 김 중환 Dp-I-029  
 김 지은 Bp-I-008  
 김 지은 Bp-I-017  
 김 지은 Bp-I-004  
 김 지은 B-38  
 김 지은 L-22  
 김 지은 L-11(초), L-21  
 김 지현 E-42  
 김 지현 Bp-I-024  
 김 지현 B-34, C-05  
 김 지현 Ip-III-019  
 김 지현 Ip-III-002  
 김 지현 J-01  
 김 지화 Hp-IV-078  
 김 지화 Hp-IV-060  
 김 지환 Ep-V-114

김 지효 E-51, Ep-V-110  
 김 지희 D-20  
 김 진교 Kp-II-002, Kp-II-011  
 김 진모 Ip-III-019  
 김 진모 Ip-III-002  
 김 진모 Dp-II-125  
 김 진민 Fp-IV-007  
 김 진선 Gp-III-014  
 김 진성 A-13  
 김 진수 Dp-I-036  
 김 진수 Dp-I-026  
 김 진수 Kp-II-012  
 김 진영 L-01(초)  
 김 진영 Ep-II-080  
 김 진영 Kp-III-022  
 김 진옥 Gp-III-003  
 김 진용 Hp-III-009, Hp-III-021  
 김 진원 Dp-I-043  
 김 진원 Dp-I-013, Dp-I-014  
 김 진은 I-10  
 김 진태 Ip-III-043, Jp-III-002  
 김 진태 Ep-V-119, Kp-V-068  
 김 진혁 E-41  
 김 진홍 Dp-V-165  
 김 진희 Ep-V-122, Ep-V-129  
 김 진희 D-30, Dp-V-137  
 김 진희 Dp-V-149  
 김 진희 D-29, Dp-V-164  
 김 찬 E-52, I-08  
 김 찬 C-34  
 김 찬형 Ep-I-028  
 김 창범 H-18, Hp-IV-056, Hp-IV-058  
 김 창범 Hp-IV-061  
 김 창섭 D-20  
 김 창수 Ep-V-115, Ep-V-116  
 김 창수 Kp-II-010  
 김 창영 Dp-I-015  
 김 창영 Dp-II-081  
 김 창영 Dp-II-066  
 김 창영 D-55  
 김 창오 Kp-V-073  
 김 창오 Kp-V-074  
 김 창우 A-15  
 김 철 Dp-I-015  
 김 철 Dp-II-081  
 김 철 Dp-II-066  
 김 철 D-55  
 김 철구 E-29(초)  
 김 철구 Ep-II-045, Ep-II-046  
 김 철성 Dp-II-085, Dp-II-110, Dp-II-125  
 김 철희 Dp-V-212  
 김 철민 Ip-III-042  
 김 태경 Gp-III-012  
 김 태국 Ip-III-038  
 김 태규 Dp-I-013, Dp-I-014  
 김 태동 Ep-II-085  
 김 태동 Ep-II-092  
 김 태수 Kp-V-058, Kp-V-068  
 김 태완 Ep-I-015  
 김 태완 Ep-I-010  
 김 태원 Hp-III-039  
 김 태은 Dp-V-183  
 김 태충 E-35  
 김 태현 Dp-I-039  
 김 태환 D-20  
 김 태환 Dp-V-155  
 김 태환 Dp-V-221  
 김 태환 Dp-V-161, Dp-V-220  
 김 태환 Dp-V-171, Dp-V-214  
 김 택성 Kp-V-046

김택수 Dp-II-120  
 김택수 Ip-III-041  
 김평환 E-45  
 김한기 PC-13(초)  
 김한성 Hp-IV-065, Hp-IV-071, Hp-IV-074  
 김한성 Hp-IV-072  
 김한수 Cp-IV-043  
 김한중 Ep-II-077  
 김한철 DT-02(초)  
 김항배 A-09  
 김해리 Kp-III-034  
 김해진 Ep-V-114  
 김현주 C-02, Cp-IV-022, Cp-IV-037  
 김현주 C-03, Cp-IV-004  
 김현구 Ep-I-006, Ep-I-007  
 김현선 I-09  
 김현수 Dp-II-107  
 김현수 Bp-I-008, Bp-I-026  
 김현수 B-14(초), B-36, Bp-I-002, Bp-I-006, Bp-I-009, Bp-I-017  
 김현수 B-35  
 김현숙 A-15  
 김현옥 Cp-IV-035  
 김현용 Bp-I-022  
 김현용 Cp-IV-006  
 김현용 Bp-I-005  
 김현우 I-10  
 김현우 C-04  
 김현익 Ip-III-026  
 김현주 Ip-III-028  
 김현철 B-34, C-05  
 김현철 BF-04(초)  
 김현철 C-12  
 김현탁 Dp-I-004  
 김형도 Dp-I-007, Dp-I-011, Dp-II-066, Dp-V-192  
 김형섭 E-11  
 김형욱 Ep-V-109  
 김형욱 Ep-V-108  
 김형일 Cp-IV-017  
 김형일 C-23  
 김형준 D-38  
 김형준 E-02  
 김해진 Hp-IV-047  
 김호섭 Dp-II-064, Dp-II-074  
 김호성 E-41  
 김호중 Dp-V-148  
 김호중 Jp-III-009  
 김홍배 E-48  
 김홍주 B-26  
 김홍주 B-25, Cp-IV-035  
 김화민 Ep-V-114, Hp-III-038, Hp-III-042  
 김화민 Hp-III-041  
 김회중 Ep-II-040  
 김효상 Dp-V-188  
 김효상 Dp-V-181  
 김효숙 Dp-V-173  
 김효윤 Ip-III-045  
 김효정 Ep-II-040  
 김효진 Ep-II-068  
 김효진 E-41  
 김효진 Ep-II-040  
 김휘동 Jp-III-014  
 김희경 Gp-III-005  
 김희상 Ep-II-061  
 김희섭 Hp-IV-056, Hp-IV-080  
 김희진 G-05

## 나

나고운 L-17  
 나고운 L-22  
 나고운 L-11(초), L-21  
 나광덕 E-54  
 나도선 Ep-I-006  
 나병근 Hp-III-089  
 나세진 Cp-IV-026  
 나세진 Ep-I-016  
 나영혁 Ep-II-090  
 나용수 Hp-III-009  
 나용운 Kp-III-022  
 나준희 Ip-III-030  
 나희도 Kp-III-021, Kp-III-032  
 나자로프 미하일 Ip-III-006  
 남기준 Ip-III-050  
 남상훈 Hp-III-043, Hp-IV-058, Hp-IV-069, Hp-IV-079  
 남상훈 Hp-IV-061  
 남석우 Ip-III-032  
 남성모 Ip-III-005  
 남성모 Ip-III-039  
 남수현 B-19  
 남수현 Bp-I-012  
 남신우 L-22  
 남신우 L-17  
 남신우 L-23, Lp-III-002  
 남신우 L-07(초), L-11(초), L-20, L-21  
 남신우 E-11  
 남영우 Hp-III-019, Hp-III-020  
 남윤범 Ep-V-124  
 남은경 H-05  
 남인혁 Hp-III-043  
 남종우 L-22  
 남지우 L-17  
 남지우 L-07(초), L-11(초), L-20, L-21  
 남지우 L-09(초)  
 남창우 Dp-V-198  
 남창희 Ip-III-001  
 남현정 Ip-III-025  
 남궁원 Hp-IV-084  
 남궁원 Hp-III-029  
 남궁원 Hp-IV-082  
 남궁원 Hp-III-028, Hp-III-030  
 노경석 Ep-V-131  
 노도영 Dp-V-199, E-52, I-08  
 노도영 Ip-III-006  
 노삼규 Kp-II-012  
 노삼규 Kp-II-010  
 노삼규 Kp-III-023  
 노유정 G-05  
 노재동 Dp-II-079  
 노태곤 Ip-III-044  
 노태원 KF-01(초)  
 노태원 Fp-IV-023  
 노태원 D-04  
 노태원 E-38  
 노한성 F-15  
 노한진 Dp-I-007  
 노현미 Ep-V-106  
 노현호 D-29, Dp-V-137  
 노현호 D-30  
 노홍렬 J-01  
 노홍렬 J-02  
 노홍렬 Jp-III-005, Jp-III-007  
 노희석 Dp-V-165

## 다

달현 Dp-I-043  
 달현 Dp-I-013, Dp-I-014  
 도용주 D-29  
 도호석 C-36  
 독고경환 H-12

## 라

라정은 C-42  
 류건모 Bp-I-022  
 류건모 Cp-IV-006  
 류건모 Bp-I-005  
 류상완 Dp-V-177  
 류상욱 C-33  
 류선영 C-31  
 류성원 Hp-III-038  
 류진영 H-18  
 류춘길 Hp-IV-056, Hp-IV-080  
 류한열 Dp-I-008

## 마

마경주 Bp-I-026  
 마경주 B-14(초), B-36, Bp-I-002, Bp-I-006, Bp-I-009  
 마경주 B-35  
 마혜준 Ip-III-052  
 맹성은 Fp-IV-019  
 명보라 Dp-II-110  
 명성숙 B-26  
 명성숙 B-25  
 명연수 LT-02(초)  
 명화남 Ep-I-007  
 문걸 J-01  
 문동호 B-34, C-05  
 문명국 Cp-IV-033  
 문명환 C-23  
 문병기 Ep-V-106  
 문병기 Kp-V-064  
 문병기 Dp-I-006, Dp-I-029, Dp-V-133, Dp-V-139, Dp-V-140  
 문봉선 B-34, C-38, Cp-IV-032  
 문상진 Ep-II-073  
 문성익 Hp-IV-084  
 문재원 Hp-III-035  
 문종균 Fp-IV-022  
 문종우 Dp-II-067  
 문준영 C-37  
 문창성 Bp-I-008  
 문창성 Bp-I-017  
 문한섭 Jp-III-006  
 문한섭 J-02, J-03, Jp-III-009  
 문혜림 Dp-V-159  
 문혜진 C-02, Cp-IV-022, Cp-IV-037  
 문혜진 C-03, Cp-IV-004, Ep-II-048  
 문희송 Ep-V-125  
 민경남 A-02  
 민경철 Ep-I-004  
 민동필 C-33  
 민명기 Ep-I-016  
 민병일 Dp-II-088  
 민병일 Dp-II-104  
 민병준 F-16, F-17  
 민선홍 H-16

바

박 강순	Bp-I-026	박 세웅	Kp-III-039	박 정환	Dp-V-177
박 강순	B-14(초), B-36, Bp-I-002, Bp-I-006, Bp-I-009	박 세환	Cp-IV-027, Cp-IV-042, Cp-IV-043	박 정후	H-17
박 강순	B-35	박 세희	Ip-III-049	박 제근	Dp-II-111
박 건식	H-16, Hp-IV-087, Hp-IV-088	박 세희	Ep-II-074	박 종도	Hp-IV-056, Hp-IV-070, Hp-IV-079
박 경락	Ep-V-106	박 소연	Ep-II-068	박 종윤	Dp-V-136
박 경자	Dp-I-007	박 수열	Hp-IV-057	박 종진	Ep-II-045, Ep-II-046
박 경화	Ep-I-006	박 수현	D-04, Kp-V-056	박 종호	G-07, Gp-III-010
박 광서	D-48	박 수현	Kp-III-034	박 종호	G-05, G-10
박 광훈	G-10	박 승규	Ip-III-039	박 주용	F-03(초)
박 규준	C-35, C-39, Cp-IV-008, Hp-IV-064	박 승룡	Dp-I-015	박 주윤	I-01(초)
박 규환	I-09	박 승룡	Dp-II-081	박 준교	Hp-III-008, Hp-III-013, Hp-III-014
박 기현	Hp-IV-070	박 승룡	Dp-II-066	박 준석	Gp-III-004
박 달호	L-02(초)	박 승영	D-55	박 준우	Kp-III-043
박 도영	Kp-III-029	박 승중	Dp-II-101	박 준호	Dp-II-111
박 동혁	Ip-III-053	박 승주	Kp-III-044	박 중현	Cp-IV-028, Cp-IV-029
박 동혁	E-25	박 승환	E-11	박 지선	Ep-I-015
박 두선	D-52	박 언철	Hp-III-038, Hp-III-042	박 지용	Dp-V-157
박 두선	PB-15(초)	박 영미	Dp-I-002	박 지용	Dp-V-170
박 두재	I-10	박 영순	I-09	박 지용	Dp-V-168
박 래만	K-06(초)	박 영순	E-32	박 진신	Jp-III-014
박 명렬	Bp-I-026	박 영순	Dp-II-095	박 진영	Dp-V-133, Dp-V-139, Dp-V-140
박 명렬	B-36, Bp-I-006, Bp-I-009	박 영안	Dp-I-008, PB-03(초)	박 진용	C-35, C-41
박 명렬	B-35	박 영옥	Dp-II-125	박 진용	C-39
박 무인	LT-01(초)	박 영우	E-13	박 진용	Hp-IV-064
박 민지	E-39	박 영우	E-11, E-15	박 진홍	Ep-II-048
박 배식	Ep-II-041, Ep-II-058	박 영옥	Kp-III-043	박 차원	Bp-I-026
박 배호	Dp-I-036	박 영화	Ep-II-091	박 차원	B-14(초), B-36, Bp-I-002, Bp-I-006, Bp-I-009
박 배호	Dp-I-026	박 용선	L-22	박 차원	Bp-I-011
박 범식	Hp-IV-068	박 용선	L-11(초), L-21	박 차원	B-35
박 병규	E-54	박 용섭	DF-04(초)	박 찬영	Gp-III-012
박 병규	Gp-III-012	박 용정	Hp-IV-069, Hp-IV-084	박 찬현	D-14
박 병도	Bp-I-024	박 용준	Ip-III-021	박 찬호	E-53
박 병률	Hp-IV-078	박 용진	Hp-III-038	박 창열	D-51
박 병욱	A-17	박 우락	Ep-I-025	박 창영	Kp-III-013, Kp-III-027
박 병윤	C-33, G-01	박 원규	Cp-IV-008	박 창훈	Ep-V-122, Ep-V-127
박 병재	Hp-III-028, Hp-III-030	박 윤배	Gp-III-006	박 천수	B-03
박 병현	Cp-IV-043	박 윤경	E-45	박 철홍	KF-06(초)
박 병호	Hp-III-008, Hp-III-009	박 은성	D-52	박 춘만	E-29(초)
박 상남	Bp-I-022	박 인곤	Bp-I-026	박 춘만	Ep-II-045
박 상남	Cp-IV-006	박 인곤	B-14(초), B-36, Bp-I-002, Bp-I-006, Bp-I-009	박 춘만	Ep-II-046
박 상남	Bp-I-005	박 인규	B-35	박 태선	C-18
박 상순	Ip-III-039	박 인규	Bp-I-022	박 태영	Fp-IV-001
박 상우	Gp-III-013, Gp-III-014	박 인수	Cp-IV-006	박 향규	H-18
박 상우	Ep-I-023	박 일용	Bp-I-005	박 혁규	Fp-IV-021
박 상한	Ep-II-068	박 일용	Hp-IV-070	박 혁규	Fp-IV-022
박 상희	E-53	박 일진	Cp-IV-036	박 현	Ep-II-076
박 선미	Ep-I-028	박 일홍	Dp-II-085	박 현거	Hp-III-019, Hp-III-020
박 선미	Ep-II-093	박 일홍	L-17	박 현규	Kp-II-002
박 성규	Ep-II-070	박 일홍	C-02, Cp-IV-022, Cp-IV-037, L-22, L-23	박 현민	Ip-III-041
박 성균	D-51	박 일홍	C-03, Cp-IV-004, L-19	박 형렬	I-09
박 성균	Ep-V-117	박 일홍	L-20	박 형우	Bp-I-016
박 성근	B-34, C-05, C-38, Cp-IV-032	박 일홍	L-07(초), L-11(초), L-21	박 혜선	Hp-III-032
박 성동	Ep-II-095	박 재형	L-22	박 혜선	H-20
박 성민	D-48	박 재형	L-19	박 혜선	Hp-III-044
박 성용	C-42	박 재형	L-11(초), L-20, L-21	박 홍우	Ep-II-059
박 성욱	Dp-I-029	박 재환	Kp-V-063	박 홍집	Hp-IV-059
박 성주	Hp-IV-078	박 재환	Ep-V-115, Ep-V-116	박 환배	Cp-IV-035
박 성주	Hp-IV-058, Hp-IV-059, Hp-IV-060, Hp-IV-062, Hp-IV-069, Hp-IV-084	박 정남	D-02	박 회열	Ep-I-021
박 성주	Hp-IV-061	박 정민	Kp-V-048	박 완	E-34
박 성진	Ep-I-025	박 정민	Ep-I-025	방 지원	E-48
박 성진	Kp-III-044	박 정복	E-51, Ep-V-110	방 현성	Dp-V-214
박 성찬	Ip-III-051	박 정식	Hp-III-038	방 형찬	Lp-III-002
박 성태	Cp-IV-034	박 정식	Bp-I-026	방 형찬	B-25
박 성호	E-10	박 정식	B-14(초), B-36, Bp-I-002, Bp-I-006, Bp-I-009	배 가람	Kp-III-022
		박 정식	B-35	배 강	Hp-III-042
		박 정현	Dp-V-171	배 강	Hp-III-041

배 동식 Dp-I-043  
 배 세환 Kp-V-072  
 배 세환 H-20  
 배 세환 Dp-I-001, Hp-III-044  
 배 영덕 Hp-III-023  
 배 인호 Jp-III-006  
 배 인호 J-03  
 배 인호 Kp-II-003, Kp-II-004, Kp-II-012  
 배 재범 Cp-IV-035  
 배 종성 D-35  
 배 종성 C-35  
 배 종성 Ep-I-025  
 배 종성 Ep-V-117  
 배 주희 Kp-II-012  
 배 찬미 Ep-II-046  
 배 해경 Ep-I-025  
 배 해경 Ep-II-067, Ep-II-069  
 배 효원 H-17  
 백 경찰 Hp-III-039, Kp-V-065  
 백 광운 B-27, B-28, C-41  
 백 광운 B-29  
 백 승록 Bp-I-026  
 백 승록 B-14(초), B-36, Bp-I-002, Bp-I-006, Bp-I-009  
 백 승록 B-35  
 백 승이 Cp-IV-008  
 백 승재 E-13  
 백 인규 KF-02(초)  
 백 재운 D-03, Kp-III-045  
 백 종현 B-10  
 변 익수 Dp-I-036  
 변 준석 E-35  
 변 창우 J-11, Jp-III-003  
 빈 석민 Ep-V-115, Ep-V-116

## 사

사무엘 스테파난 B-35  
 사무엘 스테파난 Bp-I-026  
 사무엘 스테파난 B-36, Bp-I-009  
 서 관용 Dp-V-164  
 서 관용 D-29  
 서 광원 Hp-IV-060  
 서 기완 Dp-I-004  
 서 동우 Ep-II-077  
 서 동주 E-51, Ep-V-110  
 서 동철 Hp-III-031  
 서 민수 A-12  
 서 민아 I-09  
 서 상훈 Ep-II-096  
 서 성보 Hp-III-041  
 서 성현 Hp-III-025  
 서 성현 Hp-III-008  
 서 수열 Dp-V-214  
 서 순애 Dp-I-026  
 서 영교 Kp-V-066, Kp-V-067  
 서 영수 Ep-II-096  
 서 옥균 Dp-V-199  
 서 용문 E-29(초)  
 서 용문 Dp-I-005, Dp-I-016  
 서 용문 Ep-II-045, Ep-II-046  
 서 윤경 Ep-II-088  
 서 은성 B-34  
 서 인득 Hp-IV-080  
 서 장훈 Hp-III-003  
 서 정은 L-22  
 서 정은 L-19  
 서 정은 L-11(초), L-21  
 서 주영 Ep-I-023  
 서 주희 Ep-V-132

서 준석 Bp-I-008  
 서 준석 Bp-I-026  
 서 준석 B-14(초), B-36, Bp-I-002, Bp-I-006, Bp-I-009  
 서 준석 B-35  
 서 지현 Dp-V-220  
 서 지현 Dp-V-214  
 서 현관 Bp-I-011  
 서 형석 Hp-IV-083  
 서 효진 Ep-II-047, Ep-II-051, Ep-II-052, Ep-II-053, Ep-II-054, Ep-V-130, Ep-V-131  
 서 회 C-34  
 석 재권 Dp-II-121  
 석 재권 Dp-II-120  
 석 진호 Dp-II-114, Dp-II-123, Fp-IV-024  
 석 해진 Dp-I-018  
 선 옥수 Bp-I-015  
 선 정호 Kp-V-071  
 설 경태 Hp-IV-074  
 설 재춘 Hp-III-009  
 성 병훈 Kp-III-027  
 성 시진 Dp-V-188  
 성 시진 Dp-V-181  
 성 재회 Ip-III-036  
 성 재회 Ip-III-035  
 성 재회 I-02(초), I-05(초)  
 성 충기 H-09(초)  
 소 광섭 E-48  
 소 윤영 Cp-IV-020  
 소 준호 H-16  
 소 중호 B-26  
 소 중호 B-25, Cp-IV-035  
 손 근배 Lp-III-002  
 손 동익 Dp-V-161  
 손 동진 Ep-V-124  
 손 명락 Ep-I-028  
 손 명락 Ep-II-093  
 손 명환 Dp-V-182  
 손 민수 E-39  
 손 민수 E-05  
 손 상호 Ep-V-125  
 손 선영 Ep-V-114, Hp-III-042  
 손 선영 Hp-III-041  
 손 성진 Kp-II-005  
 손 안 Hp-IV-070  
 손 영덕 Gp-III-004  
 손 영우 D-17  
 손 영욱 Hp-IV-070  
 손 유리 Kp-II-011  
 손 윤규 Hp-IV-069, Hp-IV-079  
 손 종수 B-03  
 손 종역 D-38  
 손 현철 Kp-III-044  
 손 현철 Kp-III-021, Kp-III-032  
 송 경호 Ep-V-122, Ep-V-126  
 송 규정 Dp-II-074  
 송 기명 Dp-I-015, PB-03(초)  
 송 기명 Dp-II-126  
 송 동준 Dp-I-015  
 송 동준 Dp-II-081  
 송 동준 Dp-II-066  
 송 동준 D-55  
 송 동훈 Ip-III-034  
 송 동훈 Ip-III-035  
 송 만석 Kp-V-054, Kp-V-072  
 송 명근 C-02, Cp-IV-022, Cp-IV-037  
 송 명근 C-03, Cp-IV-004  
 송 민아 Hp-III-032  
 송 민아 Hp-III-040

송 보미 Ep-I-006, Ep-I-007  
 송 상현 Cp-IV-006  
 송 상현 Cp-IV-002  
 송 승기 Dp-I-005, Dp-I-016  
 송 영기 Hp-IV-077  
 송 우석 Dp-V-136  
 송 우혁 Ip-III-031  
 송 운 D-29, Dp-V-177  
 송 인걸 Cp-IV-039  
 송 인철 H-17  
 송 재원 E-54  
 송 정훈 Bp-I-018, Dp-V-148  
 송 종한 Ep-V-121  
 송 종한 Dp-II-121  
 송 종한 Dp-II-120  
 송 지선 Dp-V-165  
 송 진동 Kp-II-012  
 송 진동 E-33  
 송 진섭 Bp-I-024  
 송 진웅 G-03  
 송 철호 Dp-I-038  
 송 철호 Dp-I-041, Dp-I-057  
 송 철호 Dp-I-037  
 송 태권 Dp-I-043  
 송 태영 Cp-IV-027  
 스테파난 사무엘 B-14(초), Bp-I-002, Bp-I-006  
 시 량 Ep-II-047, Ep-II-051, Ep-II-052, Ep-II-053, Ep-V-130, Ep-V-131  
 신 광문 Gp-III-009  
 신 덕진 Dp-V-134, Dp-V-146  
 신 동원 H-05  
 신 동호 C-42  
 신 동희 Kp-V-052, Kp-V-073  
 신 동희 Kp-V-074  
 신 병욱 Ep-I-028  
 신 병욱 Ep-II-093  
 신 상원 Dp-II-121  
 신 상원 Dp-II-120  
 신 상훈 E-33  
 신 서로 Jp-III-005, Jp-III-007  
 신 선영 Dp-V-188  
 신 선영 Dp-V-181  
 신 성국 Jp-III-001  
 신 수봉 Ip-III-030  
 신 승수 B-34  
 신 승환 Hp-IV-050, Hp-IV-058, Hp-IV-062  
 신 승환 Hp-IV-061  
 신 영한 D-38  
 신 용진 Ip-III-052  
 신 용호 Ep-II-091  
 신 원석 Ep-II-073  
 신 원진 Ip-III-019  
 신 원진 Ip-III-002  
 신 재익 Lp-III-002  
 신 정욱 C-42  
 신 진욱 Bp-I-026  
 신 진욱 B-14(초), Bp-I-002, Bp-I-006, Bp-I-009  
 신 진욱 B-35  
 신 현덕 D-54, Fp-IV-025  
 신 현욱 Kp-II-010  
 신 현준 D-03, Kp-III-045  
 신 현철 Ep-II-048  
 신 혜영 Ep-II-100  
 심 광숙 B-34, C-05, C-38, Cp-IV-032  
 심 광숙 C-02, Cp-IV-022, Cp-IV-037  
 심 광숙 C-03, Cp-IV-004  
 심 규환 Kp-V-046

심 민정 lp-III-038  
 심 성아 B-20  
 심 수민 Dp-I-031  
 심 숙이 Ep-II-042  
 심 승보 H-17  
 심 승보 D-30, Dp-V-137  
 심 승보 D-29  
 심 은섭 Lp-III-003  
 심 인보 Dp-II-085  
 심 제호 Dp-II-099  
 심 창호 lp-III-018  
 심 하성 Dp-II-111  
 심 홍선 D-32

## 아

안 광준 I-09, I-10  
 안 봉재 Cp-IV-034  
 안 성대 Dp-V-171  
 안 성환 C-42  
 안 세영 E-48  
 안 세정 E-13  
 안 세진 Kp-III-029  
 안 승인 lp-III-031  
 안 영환 Dp-V-157  
 안 영환 Dp-V-170  
 안 영환 Dp-V-168  
 안 영환 I-09  
 안 은미 Hp-IV-077  
 안 일신 K-13  
 안 재석 D-51  
 안 재성 I-10  
 안 정근 C-31  
 안 정근 Bp-I-026  
 안 정근 B-14(초), B-36, Bp-I-002,  
 Bp-I-006, Bp-I-009  
 안 정근 B-27, B-28, C-35, C-41,  
 Hp-IV-064  
 안 정근 B-29, B-35, BF-06(초), C-17,  
 C-19  
 안 정근 C-20  
 안 정근 C-39  
 안 정선 Ep-I-034  
 안 준호 Ep-I-010  
 안 지환 H-16  
 안 창원 Dp-I-002  
 안 창원 Dp-I-001, Dp-I-003, Dp-I-018  
 안 창원 Ep-I-025  
 안 치호 lp-III-023  
 안 태기 Dp-V-216  
 양 경승 A-13  
 양 병수 B-33  
 양 성철 Cp-IV-025  
 양 영수 Kp-III-017  
 양 용석 Dp-I-038  
 양 용석 Dp-I-057  
 양 용석 Dp-I-041  
 양 용석 Dp-I-037  
 양 유철 Bp-I-008  
 양 유철 Bp-I-017  
 양 은표 Kp-V-067  
 양 재문 Ep-I-021  
 양 재석 F-14  
 양 건욱 Kp-II-006  
 양 정화 Dp-II-102  
 양 정화 D-15  
 양 종만 Lp-III-002  
 양 지성 Dp-V-220  
 양 진복 Ep-V-106  
 양 태건 C-36

양 태건 Cp-IV-026, Cp-IV-036  
 양 태건 Cp-IV-019  
 양 해룡 Hp-IV-084  
 양 해룡 Hp-IV-082  
 양 형석 Ep-II-082  
 양 형우 Dp-V-175, E-10, E-44  
 양 호순 D-35  
 양 호순 D-27, Ep-I-001, Ep-II-060  
 엄 기석 Ep-II-095  
 엄 상훈 Dp-V-188  
 엄 상훈 Dp-V-181  
 엄 영제 Kp-III-014  
 엄 종화 Dp-V-145  
 엄 태중 lp-III-008  
 엄 한돈 Kp-V-056  
 여 동열 Ep-I-032  
 여 승준 Ep-I-034  
 여 운진 E-49  
 여 환섭 lp-III-031  
 연 정흠 Lp-III-003  
 엄 태호 Dp-I-005  
 엄 한웅 Kp-III-039  
 오 광택 G-10  
 오 근수 C-04  
 오 명규 lp-III-008  
 오 민석 E-53  
 오 민우 Kp-II-012  
 오 민지 Lp-III-002  
 오 병성 Ep-V-115, Ep-V-116  
 오 병성 Kp-V-063  
 오 상미 E-51, Ep-V-110  
 오 상수 Dp-II-064, Dp-II-074  
 오 선근 B-20  
 오 순영 Ep-I-003  
 오 승용 H-05  
 오 승임 E-05  
 오 승태 Hp-III-016  
 오 영도 Bp-I-008  
 오 영도 Bp-I-026  
 오 영도 B-14(초), B-36, Bp-I-002,  
 Bp-I-006, Bp-I-009, Cp-IV-027  
 오 영도 B-35  
 오 영도 Bp-I-017  
 오 영만 Dp-V-145  
 오 은순 Kp-V-058, Kp-V-068  
 오 은지 Ep-V-118  
 오 정근 LT-03(초)  
 오 계승 E-02  
 오 종석 Hp-IV-082, Hp-IV-084  
 오 주희 Hp-IV-057  
 오 주희 lp-III-018  
 오 준석 Kp-III-038  
 오 차환 lp-III-026  
 오 철민 Kp-III-022  
 오 필건 Dp-V-199  
 오 필열 B-03  
 오 한슬 Lp-III-002  
 오 형택 Kp-V-074  
 오 혜근 K-13  
 왕 강균 E-05  
 왕 선정 Hp-III-022, Hp-III-023  
 용 상순 Lp-III-003  
 우 병철 Dp-V-137  
 우 병철 Dp-V-149  
 우 상봉 Ep-II-049, Ep-II-050, Ep-II-101,  
 Ep-II-102  
 우 승우 Dp-V-159  
 우 정원 E-31, E-32  
 우 정원 lp-III-054  
 우 제훈 E-31, E-32

우 제훈 lp-III-054  
 우 종관 B-27, B-28  
 우 종관 B-29  
 우 준 C-04  
 우 형주 Cp-IV-029  
 우오즈미 사토르 Bp-I-008  
 원 나연 E-48  
 원 미숙 C-35, C-39, Hp-IV-064  
 원 봉연 Dp-II-085  
 원 상연 Ep-V-112  
 원 성식 Dp-I-003  
 원 창연 Dp-II-114, Dp-II-123, Fp-IV-024  
 원 종재 Dp-I-008  
 위 한민 Hp-III-025  
 위 한민 Hp-III-013  
 유 경화 E-49  
 유 경화 E-39  
 유 경화 E-06  
 유 경화 E-05  
 유 경화 E-42  
 유 경화 E-02  
 유 광일 Hp-III-008  
 유 난이 I-03(초)  
 유 동선 Kp-V-061  
 유 민상 Cp-IV-031, Cp-IV-033  
 유 병욱 L-22  
 유 병욱 L-11(초), L-21  
 유 병윤 Ep-V-115, Ep-V-116  
 유 봉안 I-03(초)  
 유 상훈 E-10  
 유 석재 Hp-III-027, Hp-III-029  
 유 세기 Ep-II-080  
 유 소영 Ep-II-040  
 유 영동 D-29, Dp-V-137  
 유 예진 J-02, J-03  
 유 인권 C-04  
 유 인태 Bp-I-008, Bp-I-026  
 유 인태 B-14(초), B-36, Bp-I-002,  
 Bp-I-006, Bp-I-009, Bp-I-017  
 유 인태 Bp-I-003, Bp-I-011  
 유 인태 B-35  
 유 인하 Hp-IV-070  
 유 일 Dp-V-134, Dp-V-146  
 유 재승 E-11  
 유 재신 lp-III-030  
 유 재용 Ep-V-122, Ep-V-126  
 유 재인 Ep-V-122, Ep-V-126,  
 Ep-V-127, Ep-V-129  
 유 재하 Ep-II-096  
 유 정선 E-48  
 유 준원 Kp-V-061  
 유 지범 E-12  
 유 진승 Bp-I-016  
 유 찬희 lp-III-030  
 유 창모 Hp-III-027  
 유 창모 H-12  
 유 천열 Dp-II-099, Dp-II-101, Dp-II-126  
 유 총열 C-11  
 유 태준 lp-III-036  
 유 태준 lp-III-035  
 유 태준 I-02(초), I-05(초)  
 유 하나 Kp-III-031  
 유 한영 Ep-I-003  
 유 형근 Ep-II-092  
 유 형준 L-22  
 유 형준 L-11(초), L-21  
 유 훈 Jp-III-010, Jp-III-013  
 육 순형 Fp-IV-013  
 육 순형 Fp-IV-004  
 윤 건수 Hp-III-019, Hp-III-020

경환 Ip-III-019  
 경환 Ip-III-002  
 경훈 Kp-III-029  
 기열 Ep-V-122, Ep-V-126  
 동열 Dp-V-155  
 동열 Dp-V-221  
 동열 Dp-V-161  
 동영 Dp-II-109  
 두희 Dp-V-159  
 명근 C-42  
 무현 Hp-IV-050  
 미라 Dp-V-222  
 병길 PB-03(초)  
 병길 Dp-II-091, Dp-II-112  
 석주 Dp-V-183  
 석현 Ep-II-100  
 선진 Ep-II-043  
 선진 PC-08(초)  
 성로 Ip-III-019  
 성로 Ip-III-002  
 성욱 Ep-I-025  
 성현 Gp-III-002, Gp-III-003  
 여광 Fp-IV-004  
 영운 Ep-II-085  
 영운 Ep-II-092  
 영중 H-16  
 용주 Ep-I-003  
 원석 Dp-II-096, Dp-V-187  
 원석 Dp-V-183  
 장희 C-39  
 재근 Ep-V-122, Ep-V-126, Ep-V-129  
 재석 Ip-III-032  
 재성 Hp-III-023  
 재진 E-35  
 재호 PC-03  
 재호 Kp-III-029  
 정범 Dp-II-101, Dp-II-126  
 경화 G-08  
 중철 C-34  
 중철 Hp-IV-078  
 중철 Hp-IV-059, Hp-IV-060  
 진희 PA-14(초)  
 창선 Ep-V-119  
 창준 Ip-III-030  
 천실 Bp-I-024  
 총재 C-20  
 총재 BF-07(초)  
 태현 J-04  
 현식 Kp-V-054, Kp-V-072  
 현오 Hp-III-042  
 회준 Bp-I-016  
 철현 Cp-IV-029  
 강영 B-19  
 강우 Ep-I-012, Ep-II-075  
 강인 Ip-III-031  
 경건 L-22  
 경건 L-11(초), L-21  
 경동 PB-03(초)  
 경범 B-26, Bp-I-018, C-25, Cp-IV-039, Cp-IV-041  
 경세 B-34, C-05, C-38, Cp-IV-031, Cp-IV-032  
 경재 E-55, E-56  
 경현 Jp-III-010  
 경현 Ip-III-041  
 경훈 E-41  
 관일 Ip-III-029  
 광진 Ip-III-012  
 광철 Dp-V-137  
 규동 Hp-III-017, Hp-III-031

이 규민 F-14  
 이 규석 K-06(초)  
 이 규준 D-48  
 이 규준 Dp-II-126  
 이 근희 D-38  
 이 기문 E-53  
 이 기문 DF-03(초)  
 이 기원 Ep-II-077  
 이 기주 Dp-V-144  
 이 기주 D-20, Ep-II-100  
 이 기진 Ep-V-119  
 이 기진 Ep-II-085  
 이 기진 Ep-II-092  
 이 길호 Dp-II-072  
 이 나원 Ep-V-133  
 이 남기 D-56  
 이 남기 Dp-V-212  
 이 남기 Dp-V-216  
 이 내성 E-19  
 이 대욱 Dp-V-161  
 이 덕교 Hp-III-008  
 이 덕선 Fp-IV-019  
 이 덕선 Fp-IV-014  
 이 덕선 F-02(초)  
 이 도형 Ep-II-068  
 이 돈규 Dp-V-134, Dp-V-146  
 이 동렬 Kp-II-011  
 이 동열 H-12  
 이 동열 Ip-III-017  
 이 동욱 Kp-III-038  
 이 동인 Fp-IV-012  
 이 동재 Ep-II-088  
 이 리미 E-45  
 이 명재 Dp-I-026  
 이 미경 Ep-V-126  
 이 미지 Kp-III-045  
 이 미지 D-03  
 이 민경 G-11  
 이 민규 B-26, Bp-I-018, C-25, Cp-IV-039, Cp-IV-041  
 이 민영 C-36  
 이 민주 Dp-V-192  
 이 민호 J-11, Jp-III-003  
 이 병섭 C-35, C-39, Hp-IV-064  
 이 병우 Kp-V-058, Kp-V-068  
 이 병하 A-13  
 이 보화 Dp-II-098  
 이 봉우 Gp-III-005  
 이 봉주 Hp-III-039, Kp-V-065  
 이 삼녕 Dp-V-148  
 이 삼열 Cp-IV-036  
 이 삼열 Cp-IV-019  
 이 삼현 E-29(초)  
 이 삼현 Ep-II-045, Ep-II-046  
 이 상걸 Ep-V-125  
 이 상근 Hp-III-008, Hp-III-013, Hp-III-014  
 이 상동 C-04  
 이 상렬 E-39  
 이 상목 Ep-V-125  
 이 상문 Dp-V-194  
 이 상민 Dp-II-067  
 이 상민 Dp-I-041  
 이 상민 Dp-I-037  
 이 상배 Ip-III-029  
 이 상배 Ip-III-028  
 이 상은 Ip-III-050  
 이 상익 Gp-III-004  
 이 상준 Cp-IV-039  
 이 상준 B-25

이 상준 C-25, Cp-IV-041, Kp-II-012  
 이 상준 Kp-II-010  
 이 상준 B-26  
 이 상현 B-10  
 이 상현 Kp-II-005  
 이 상화 Kp-II-002, Kp-II-011  
 이 상훈 Ip-III-042  
 이 상훈 H-16  
 이 서은 Ep-V-133  
 이 석호 Ep-II-070  
 이 선미 Dp-V-192  
 이 선영 Dp-I-018, Ep-I-025  
 이 선철 Dp-II-096  
 이 성구 Ip-III-036  
 이 성구 I-02(초), I-05(초)  
 이 성구 Ip-III-029  
 이 성만 Ip-III-005  
 이 성만 Ip-III-039  
 이 성목 G-08  
 이 성목 Gp-III-009  
 이 성목 Gp-III-008  
 이 성목 G-11  
 이 성엽 Ep-I-028  
 이 성엽 Ep-II-093  
 이 성익 D-48, Dp-II-078  
 이 성익 Dp-II-126  
 이 성익 Dp-II-079  
 이 성주 Kp-V-056  
 이 성훈 Dp-V-164  
 이 세병 C-42  
 이 소리 E-51, Ep-V-110  
 이 수아 Gp-III-006  
 이 수연 Hp-IV-047  
 이 수연 Ep-II-091  
 이 수용 I-08  
 이 수웅 Ip-III-006  
 이 순걸 D-30  
 이 순례 Cp-IV-037  
 이 순례 Cp-IV-022  
 이 순례 C-03, Cp-IV-004  
 이 순일 Dp-V-157  
 이 순일 Ep-V-109  
 이 순일 Dp-V-170  
 이 순일 Dp-V-168  
 이 순일 Ep-V-108  
 이 순철 Dp-II-109  
 이 순혁 Ip-III-047, Ip-III-048  
 이 슬기 Lp-III-002  
 이 승규 Hp-III-018  
 이 승백 Ep-I-015  
 이 승엽 Dp-V-136  
 이 승욱 Cp-IV-033  
 이 승현 E-11  
 이 승현 Lp-III-002  
 이 승호 E-19  
 이 승환 Ep-II-045, Ep-II-046  
 이 식 C-04  
 이 신범 KF-01(초)  
 이 신범 Fp-IV-023  
 이 신범 E-38  
 이 아름 Dp-V-173  
 이 영국 Kp-III-039  
 이 영락 I-03(초)  
 이 영욱 Cp-IV-029  
 이 영욱 Cp-IV-017, Cp-IV-025, Cp-IV-027  
 이 영욱 C-23  
 이 용백 Ep-II-070  
 이 용영 Hp-IV-048  
 이 용우 Ip-III-039

이 용욱 Dp-I-004  
이 용인 G-06, H-03  
이 용재 E-47  
이 용주 Ip-III-005  
이 용철 Fp-IV-001  
이 용택 PC-02(초)  
이 용혜 Dp-II-110  
이 우경 Ip-III-017, Ip-III-018  
이 우람 D-32  
이 우영 A-03  
이 우창 Hp-III-028  
이 우창 Hp-III-019, Hp-III-020  
이 유진 Ep-II-050  
이 윤상 Ep-II-088  
이 윤희 Dp-V-130, Dp-V-138  
이 은성 Kp-V-061  
이 은정 Gp-III-015  
이 은중 Dp-II-125  
이 은철 I-04(초)  
이 은희 Hp-IV-078  
이 은희 Hp-IV-060, Hp-IV-062  
이 은희 Hp-IV-061  
이 을수 G-07  
이 의완 Ep-I-028  
이 의완 Ep-II-093  
이 인규 Dp-II-085  
이 인재 Dp-V-222  
이 인환 Dp-V-165  
이 장혁 Ip-III-008  
이 장훈 Ip-III-025  
이 재금 B-25  
이 재기 C-41  
이 재란 Ip-III-049  
이 재란 Ep-II-074, Ip-III-033  
이 재민 Ep-II-043  
이 재민 Ep-I-021  
이 재민 PC-08(초)  
이 재상 E-39  
이 재성 F-14  
이 재성 KF-01(초)  
이 재성 Fp-IV-023  
이 재승 Bp-I-026  
이 재승 Bp-I-008  
이 재승 B-14(초), B-36, Bp-I-002, Bp-I-006, Bp-I-009, Bp-I-017  
이 재승 B-35  
이 재신 Dp-I-002  
이 재용 Dp-II-121  
이 재용 Dp-II-120, Ep-V-121  
이 재우 Fp-IV-019  
이 재우 Fp-IV-014  
이 재일 Dp-V-184  
이 재철 Kp-III-045  
이 재학 Kp-III-045  
이 재형 Cp-IV-042  
이 정국 E-30  
이 정두 Kp-V-061  
이 정수 Dp-II-099  
이 정열 Kp-II-003  
이 정오 Dp-V-173  
이 정용 Ep-I-003  
이 정은 Lp-III-005  
이 정일 Bp-I-012  
이 정일 B-26  
이 정일 B-25  
이 정일 A-21  
이 정일 Ep-II-098  
이 정주 Kp-III-013, Kp-III-027  
이 정준 Lp-III-002  
이 정호 Kp-V-056, PC-07(초)

이 정환 A-14  
이 정환 A-01  
이 정훈 B-05  
이 종덕 Dp-II-107, Kp-III-013, Kp-III-027  
이 종민 Ip-III-036  
이 종민 Ip-III-055  
이 종민 I-02(초), I-02(초), I-05(초), I-05(초)  
이 종숙 Bp-I-016  
이 종용 Ep-II-044  
이 종원 Kp-V-063  
이 종태 A-04  
이 종필 A-10  
이 종하 Hp-III-016  
이 종호 E-41  
이 종호 Kp-III-017, Kp-III-031  
이 종화 C-18  
이 종훈 Ip-III-031  
이 종희 Dp-V-130, Dp-V-138  
이 주한 C-24, C-34  
이 주한 C-37  
이 주희 B-26  
이 주희 B-25  
이 준엽 Ip-III-031  
이 준현 J-01  
이 준호 Ip-III-031  
이 지영 Dp-V-134, Dp-V-146  
이 지우 Fp-IV-001  
이 직 L-22  
이 직 L-17  
이 직 C-02, Cp-IV-022, Cp-IV-037  
이 직 L-11(초), L-20, L-21  
이 직 C-03, Cp-IV-004  
이 진능 Ep-I-028  
이 진능 Ep-II-093  
이 진원 Hp-IV-078  
이 진원 Hp-IV-060, Hp-IV-062  
이 진원 Dp-II-109  
이 찬형 Dp-II-085  
이 창우 Ep-V-112  
이 창원 Ip-III-036  
이 창원 I-02(초), I-05(초)  
이 창호 Kp-II-012  
이 창호 Hp-III-030  
이 창환 L-14  
이 창환 L-11(초), L-20, L-21  
이 창환 Ip-III-042  
이 채순 Hp-IV-056, Hp-IV-080  
이 철구 Dp-V-194  
이 철우 Cp-IV-025  
이 철호 Cp-IV-043, Hp-III-018, Ip-III-055  
이 철훈 D-20  
이 춘식 C-24, C-34  
이 춘식 C-37  
이 택성 Ep-II-088  
이 팽로 Dp-V-188  
이 한구 Dp-II-066, Dp-V-192  
이 한범 B-34, C-05  
이 한주 Ep-II-085  
이 한주 Ep-II-092  
이 해준 H-17  
이 해준 Dp-I-001, Dp-I-018  
이 해철 Hp-IV-056  
이 현용 Kp-III-023  
이 현범 Ep-II-096  
이 현우 D-22  
이 현정 E-11  
이 현준 J-03

이 현진 Dp-V-192  
이 현진 Ep-V-132  
이 현휘 Kp-II-011  
이 현희 E-31, E-32  
이 현희 Ip-III-054  
이 형락 Dp-V-148  
이 형락 Ep-I-028  
이 형락 Ep-II-093  
이 형목 LT-03(초)  
이 형철 Cp-IV-041  
이 해란 Hp-III-032, Hp-III-033  
이 해영 L-17  
이 해영 C-02, Cp-IV-022, Cp-IV-037, L-22  
이 해영 C-03, Cp-IV-004  
이 해영 L-11(초), L-21  
이 해지 Ep-V-114  
이 호근 Dp-II-067  
이 호선 Kp-III-043  
이 호연 G-01  
이 호준 H-17  
이 호현 Ep-II-072  
이 화련 Hp-IV-068  
이 화용 B-26, C-25, Cp-IV-039, Cp-IV-041  
이 화용 Bp-I-018  
이 효상 Bp-I-026  
이 효상 B-14(초), B-36, Bp-I-002, Bp-I-006, Bp-I-009  
이 효상 B-28, C-41  
이 효상 B-35  
이 효상 C-35, C-39, Hp-IV-064  
이 효상 B-27, B-29  
이 후종 Dp-II-072  
이 후종 A-08  
이 훈기 Kp-V-046  
이 훈희 Hp-III-034  
이 희석 Hp-IV-057  
이 희재 Hp-III-030  
이 희정 Jp-III-006  
이 만희 E-34  
인 정환 Hp-III-089  
인 준호 Dp-V-164  
임 계엽 B-27  
임 계엽 B-29  
임 계엽 B-28  
임 권 Ip-III-041  
임 규욱 E-55, E-56  
임 도연 Gp-III-004  
임 명선 Gp-III-005  
임 상엽 K-05(초)  
임 상훈 C-02, Cp-IV-022, Cp-IV-037  
임 상훈 C-03, Cp-IV-004  
임 선아 Ep-V-132  
임 선인 Lp-III-002  
임 성일 Kp-III-039  
임 성일 E-53  
임 성일 DF-03(초)  
임 신혁 J-05  
임 영경 C-42  
임 영훈 Dp-I-037  
임 용식 Dp-V-144  
임 용환 Kp-III-031  
임 인택 Bp-I-026  
임 인택 B-14(초), B-36, Bp-I-002, Bp-I-006, Bp-I-009  
임 인택 B-33  
임 인택 B-35  
임 재영 Kp-II-012  
임 재홍 Ip-III-045

임 정욱 Ep-II-043  
 임 정욱 PC-08(초)  
 임 정환 C-35, C-39, Hp-IV-064  
 임 종혁 Dp-V-157  
 임 종혁 Ep-V-109  
 임 종혁 Dp-V-168  
 임 지순 A-07  
 임 지은 E-05  
 임 춘식 Dp-I-015  
 임 춘식 Dp-II-081  
 임 춘식 Dp-II-066  
 임 한나 Kp-V-068  
 임 한조 I-07, Ip-III-013  
 임 현식 K-04(초)  
 임 현식 KT-01(초)  
 임 해인 Ep-I-015  
 임 희진 L-20

## 자

장 경욱 Ep-I-010  
 장 경혁 Ep-II-047, Ep-II-051, Ep-II-052, Ep-II-053, Ep-V-130, Ep-V-131  
 장 경호 E-47  
 장 광훈 J-04  
 장 기봉 Dp-I-002  
 장 도윤 Cp-IV-043  
 장 문형 Kp-III-044  
 장 서형 KF-01(초)  
 장 서형 Fp-IV-023  
 장 서형 E-38  
 장 성덕 Hp-IV-082  
 장 성현 Bp-I-008  
 장 성현 Bp-I-017  
 장 성현 Cp-IV-006  
 장 성현 Bp-I-004  
 장 성현 B-38  
 장 성호 E-11  
 장 세종 G-04  
 장 세종 G-09  
 장 세훈 Dp-II-064, Dp-II-074, Dp-V-182  
 장 시원 Hp-IV-054  
 장 아람 Dp-V-175  
 장 영욱 E-06, E-39  
 장 영욱 E-02  
 장 영준 D-04  
 장 용식 Cp-IV-039  
 장 용식 B-26, C-25  
 장 용식 Cp-IV-041  
 장 원우 Fp-IV-007  
 장 유란 Dp-II-077  
 장 유진 Ep-II-067, Ep-II-069  
 장 은성 Kp-V-048  
 장 인수 Ep-II-098  
 장 정원 D-30  
 장 정원 Dp-V-164  
 장 종호 Bp-I-026  
 장 주영 C-36  
 장 지승 Bp-I-026  
 장 지승 B-14(초), B-36, Bp-I-002, Bp-I-006, Bp-I-009  
 장 지승 B-33, B-35  
 장 지현 Lp-III-002  
 장 지호 Hp-IV-065  
 장 지호 Hp-IV-072  
 장 지호 Hp-IV-048  
 장 태석 Ep-II-064  
 장 행진 C-04  
 장 행진 Bp-I-016, Bp-I-016

장 현명 D-38  
 장 현우 Hp-III-027  
 장 홍영 Hp-III-089  
 장 희진 Ep-I-007  
 장 정훈 E-34  
 전 건상 Dp-V-177  
 전 권수 Ep-II-076  
 전 명환 Hp-IV-070  
 전 병익 Kp-V-064  
 전 병익 Dp-I-006  
 전 병천 Ep-II-047, Ep-II-051, Ep-II-052, Ep-II-053, Ep-V-130  
 전 상준 Ep-II-048  
 전 상호 Dp-I-036  
 전 상호 Dp-I-026  
 전 성란 Kp-II-005  
 전 영규 Cp-IV-033  
 전 영석 Gp-III-012  
 전 우진 Ip-III-038  
 전 운승 Gp-III-004  
 전 은경 Dp-V-173  
 전 은주 Bp-I-008, Bp-I-026  
 전 은주 B-14(초), B-36, Bp-I-002, Bp-I-006, Bp-I-009, Bp-I-017  
 전 은주 B-35  
 전 일근 Dp-II-121  
 전 일근 Dp-II-120  
 전 재진 A-17  
 전 진아 L-22  
 전 진아 L-19  
 전 진아 L-11(초), L-21  
 전 현수 E-30  
 전 형준 Ip-III-026  
 전 호은 Dp-V-212  
 정 고은 D-35  
 정 광주 B-25  
 정 광호 Ep-II-090  
 정 규선 Hp-III-034, Hp-III-035, Hp-III-036  
 정 규호 K-04(초)  
 정 기수 Ep-II-098  
 정 다운 Ep-II-095  
 정 다운 F-05  
 정 대철 Ep-II-040  
 정 도영 Ip-III-041  
 정 동근 Ep-V-124  
 정 동회 Ep-I-010  
 정 맹호 Hp-IV-070  
 정 명신 B-28  
 정 명화 D-48, Dp-II-077, Dp-II-078, PB-03(초)  
 정 명화 Dp-II-101, Dp-II-126  
 정 명화 Dp-II-079  
 정 명화 Dp-V-164  
 정 명환 Cp-IV-026  
 정 명환 Ep-I-016  
 정 문석 Kp-II-012  
 정 문성 Ep-II-067, Ep-II-069  
 정 민경 D-30, Dp-V-137  
 정 민경 D-29  
 정 민선 Cp-IV-008  
 정 민수 B-34, C-38, Cp-IV-032  
 정 민영 G-09  
 정 병기 Kp-III-043  
 정 보라 E-24  
 정 상영 H-17  
 정 석민 E-55, E-56  
 정 선우 B-25  
 정 성철 D-02  
 정 성훈 DF-03(초)

정 성훈 Kp-III-029  
 정 수민 L-22  
 정 수민 L-20  
 정 수민 L-11(초), L-21  
 정 순영 Dp-II-107  
 정 승호 Kp-V-068  
 정 승호 Hp-III-017  
 정 애라 L-22, L-23  
 정 애라 L-11(초), L-21  
 정 연옥 D-29, Dp-V-177  
 정 연학 Dp-I-002  
 정 영균 I-09  
 정 영대 K-13  
 정 영빈 Ip-III-039  
 정 예술 Ep-II-095  
 정 용덕 K-06(초)  
 정 용우 E-33  
 정 용욱 G-03  
 정 원식 Dp-I-015  
 정 원식 Dp-II-081  
 정 원식 Dp-II-066  
 정 원식 D-55  
 정 유진 Lp-III-002  
 정 윤철 Kp-III-014  
 정 의덕 Ep-I-001, Ep-II-060  
 정 인구 Kp-III-034  
 정 인석 Bp-I-026  
 정 인석 B-14(초), B-36, Bp-I-002, Bp-I-006, Bp-I-009  
 정 인석 B-35  
 정 인승 Ep-II-090  
 정 인일 C-34  
 정 일경 D-51  
 정 재관 Kp-III-045  
 정 재승 D-22  
 정 재영 Hp-III-036  
 정 재용 Kp-V-062  
 정 재훈 Kp-V-054, Kp-V-072  
 정 재훈 Dp-V-187  
 정 재훈 Dp-V-155  
 정 재훈 Dp-V-221  
 정 재훈 Dp-V-161  
 정 종호 Ep-I-025  
 정 종훈 A-19  
 정 종훈 PB-03(초)  
 정 종훈 Dp-II-091, Dp-II-112  
 정 준기 Dp-I-043  
 정 중현 Ep-V-106  
 정 중현 Kp-V-064  
 정 중현 Dp-I-006, Dp-I-029, Dp-V-133, Dp-V-139, Dp-V-140, Ep-V-117  
 정 지원 Lp-III-002  
 정 지은 Jp-III-008  
 정 지은 Bp-I-008  
 정 지은 Bp-I-017  
 정 진 Kp-V-065  
 정 진모 E-35  
 정 진욱 Dp-V-188  
 정 진욱 Dp-V-181  
 정 진원 Dp-I-007  
 정 진일 Hp-III-031  
 정 진현 Hp-III-030  
 정 찬화 E-44  
 정 창섭 Ip-III-023, Ip-III-024  
 정 창수 I-03(초)  
 정 창욱 Ep-II-059  
 정 창욱 A-18  
 정 창희 Dp-V-143  
 정 채환 E-41

정 태문 lp-III-036  
정 태문 I-02(초), I-05(초)  
정 태봉 Kp-III-022  
정 태훈 Hp-III-032, Hp-III-033  
정 태훈 H-20  
정 태훈 Hp-III-040, Hp-III-044  
정 현식 Ep-II-079, Kp-III-029  
정 현식 Dp-V-159  
정 호연 E-47  
정 호진 C-42  
정 흥채 Dp-V-133, Dp-V-139, Dp-V-140  
정 환석 Dp-V-171  
정 화천 H-16  
정 효순 C-37  
정 후영 Ep-I-003  
정 회성 Dp-V-157  
정 회성 Dp-V-170  
정 회성 Dp-V-168  
제 구출 K-12  
제 원호 J-01  
제 채용 Ep-V-131  
제 원호 E-34  
제 금원 Bp-I-016  
조 기현 Bp-I-013, Bp-I-017  
조 기현 B-32  
조 기현 Bp-I-008, Bp-I-012  
조 남규 Dp-I-002  
조 남규 Dp-I-001, Dp-I-003, Dp-I-018  
조 대형 K-06(초)  
조 대회 Ep-I-034  
조 덕용 E-54  
조 동기 lp-III-038  
조 동현 J-05, Jp-III-008, Jp-III-011, Jp-III-014  
조 만호 Kp-III-044  
조 만호 Ep-II-068  
조 무현 Hp-III-029, Hp-IV-084  
조 무현 Hp-IV-082  
조 무현 Hp-III-028, Hp-III-030  
조 문호 D-38  
조 미영 Gp-III-015  
조 미희 B-34, C-05, Cp-IV-031  
조 민국 C-42  
조 상진 Ep-II-095  
조 석범 lp-III-044  
조 성국 Dp-V-198  
조 성래 Dp-II-084  
조 성래 A-20  
조 성오 Ep-I-032  
조 성운 Ep-V-109  
조 성운 Ep-V-108  
조 신호 Kp-III-016, Kp-III-042, Kp-V-062, Kp-V-069  
조 영권 Bp-I-003, Bp-I-011  
조 영권 lp-III-010  
조 영훈 D-48  
조 영훈 Dp-II-101  
조 융섭 Hp-IV-065, Hp-IV-068, Hp-IV-071, Hp-IV-074  
조 융섭 Hp-IV-077  
조 융섭 Hp-IV-072  
조 융섭 Hp-IV-048  
조 우람 lp-III-002  
조 원국 F-17  
조 원주 Kp-III-038  
조 월령 E-24  
조 윤호 Cp-IV-042  
조 일성 Bp-I-013, Bp-I-017, Bp-I-023, lp-III-002

조 일성 Bp-I-008, Bp-I-012  
조 재훈 PB-03(초)  
조 재훈 lp-III-050  
조 정민 Ep-II-073  
조 항현 F-22  
조 현준 Kp-II-003, Kp-II-004, Kp-II-012  
조 해민 Hp-III-032, Hp-III-033  
조 해민 Hp-III-040  
조 화연 C-37  
조 희석 L-14  
주 경광 Bp-I-008, Bp-I-026  
주 경광 B-14(초), B-36, Bp-I-002, Bp-I-006, Bp-I-009, Bp-I-017  
주 경광 B-35  
주 관식 C-02, Cp-IV-022, Cp-IV-037  
주 관식 C-03, Cp-IV-004, Ep-II-048  
주 은아 C-38, Cp-IV-032  
주 은아 C-02, Cp-IV-022, Cp-IV-037  
주 은아 C-03, Cp-IV-004  
주 진수 lp-III-053  
주 진수 E-25  
주 진수 Ep-II-070  
주 진수 Dp-V-165  
주 태하 Dp-V-144  
주 형규 I-04(초)  
지 성진 lp-III-018  
지 승훈 Hp-III-042  
지 승훈 D-17  
지 승훈 D-19, Dp-V-158  
지 해림 Gp-III-004  
진 경환 Dp-V-158  
진 용덕 Dp-II-072  
진 유영 Dp-V-220  
진 유용 lp-III-036  
진 유용 I-05(초)  
진 정보 Ep-II-079  
진 주영 L-11(초), L-21

## 차

차 덕준 Ep-V-119  
차 동우 PA-14(초)  
차 동재 Kp-V-056  
차 문용 Fp-IV-014  
차 영훈 E-33  
차 옹호 lp-III-041  
차 현수 Gp-III-010  
차 형기 lp-III-005  
차 형기 lp-III-039  
채 근석 Ep-I-016  
채 병규 Dp-I-004  
채 승철 KF-01(초)  
채 승철 Fp-IV-023  
채 승철 E-38  
채 영안 Ep-V-119  
천 명기 C-11  
천 병구 lp-III-002  
천 성현 Kp-V-070  
천 중필 Ep-II-067, Ep-II-069  
최 경산 Bp-I-023  
최 경산 Bp-I-013  
최 경언 C-04  
최 기영 Dp-II-078  
최 기영 Dp-II-079  
최 낙월 J-11, Jp-III-003  
최 다혜 Hp-IV-087, Hp-IV-088  
최 대식 lp-III-008  
최 덕 Dp-I-005, Dp-I-016  
최 동주 Ep-I-023  
최 만수 D-29

최 명규 Ep-I-010  
최 명운 Ep-II-090  
최 명철 Hp-III-031  
최 명철 Ep-I-004  
최 무영 E-55, F-05, Fp-IV-008  
최 민규 Bp-I-022  
최 민규 Cp-IV-006  
최 민규 Bp-I-005  
최 민호 lp-III-005  
최 범호 Kp-III-017, Kp-III-031  
최 병일 Ep-II-049, Ep-II-050, Ep-II-101, Ep-II-102  
최 병춘 Kp-V-064  
최 병춘 Dp-I-006, Dp-I-029  
최 봉주 lp-III-019  
최 봉주 lp-III-002  
최 봉혁 C-19  
최 봉혁 C-20  
최 상현 Ep-V-125  
최 석원 Ep-II-064  
최 석호 Kp-V-052, Kp-V-053, Kp-V-073  
최 석호 Kp-V-074  
최 선명 D-17  
최 선명 Dp-V-158  
최 선일 Cp-IV-008  
최 선호 Bp-I-026  
최 선호 B-14(초), B-36, Bp-I-002, Bp-I-006, Bp-I-009  
최 선호 B-35  
최 성균 Dp-I-015  
최 성균 Dp-II-081  
최 성균 Dp-II-066  
최 성균 D-55  
최 성민 D-20  
최 성열 Dp-I-004  
최 성일 Dp-II-111  
최 수봉 I-10  
최 수용 Bp-I-003, Bp-I-011  
최 승하 G-04  
최 아정 E-11, E-15  
최 여진 G-05  
최 연석 Ep-II-082  
최 영완 C-34  
최 영일 Bp-I-026  
최 영일 B-14(초), B-36, Bp-I-002, Bp-I-006, Bp-I-009  
최 영일 Bp-I-011  
최 영일 B-33, B-35  
최 영진 Fp-IV-001  
최 용대 Ep-V-115, Ep-V-116  
최 용대 Kp-V-063  
최 용우 PC-09(초)  
최 원철 Dp-V-136  
최 윤호 lp-III-031  
최 은미 Kp-II-012  
최 은서 lp-III-052  
최 은영 E-31, E-32  
최 은영 lp-III-054  
최 은진 Dp-I-013, Dp-I-014  
최 은집 DF-03(초)  
최 은집 Ep-II-088  
최 은하 H-19  
최 을림 B-35  
최 을림 B-14(초), Bp-I-002, Bp-I-006, Bp-I-009  
최 인걸 F-15  
최 인홍 Ep-I-021  
최 인환 Kp-V-070  
최 일우 lp-III-055

최 재영 Hp-IV-076  
 최 재혁 G-02  
 최 정민 Kp-III-039  
 최 정숙 Dp-V-177  
 최 경우 Kp-II-010  
 최 정우 E-45  
 최 정훈 Dp-II-110  
 최 정훈 B-26  
 최 정훈 B-25  
 최 준호 H-16  
 최 중규 Ip-III-030  
 최 지혜 F-15  
 최 진식 Dp-I-036  
 최 진식 Dp-I-026  
 최 진혁 Hp-IV-058  
 최 창일 Ip-III-055  
 최 창호 Dp-II-078  
 최 창호 Dp-II-079  
 최 한우 Cp-IV-029  
 최 혁철 Dp-II-099  
 최 현우 Dp-I-038  
 최 현우 Dp-I-041  
 최 현우 Dp-I-037  
 최 현욱 Ip-III-018  
 최 현진 A-14  
 최 혜영 Ep-V-106  
 최 홍철 Dp-II-104  
 최 환영 Dp-I-015  
 최 환영 Dp-II-081  
 최 환영 Dp-II-066  
 최 효진 Hp-IV-060, Ip-III-045  
 추 나운 Ep-I-028  
 추 나운 Ep-II-093  
 추 동철 Dp-V-220  
 추 동철 Dp-V-214  
 추 동철 Dp-V-171  
 추 문식 Kp-V-061  
 추 민우 Gp-III-007  
 추 성민 D-48  
 추 성민 Dp-II-126

## 카,파

칸 아딜 Bp-I-008  
 케몬 테루키 Bp-I-008  
 편 민욱 Ip-III-017, Ip-III-018

## 하

하 경호 Bp-I-003  
 하 동우 Dp-II-064, Dp-II-074,  
 Dp-V-182  
 하 동한 Dp-V-148  
 하 명규 Ep-I-001, Ep-II-060  
 하 명훈 Gp-III-004  
 하 미순 F-22  
 하 성용 Kp-V-061  
 하 영자 Cp-IV-034  
 하 은자 Cp-IV-030  
 하 장호 Cp-IV-042  
 하 태영 LT-03(초)  
 하 홍수 Dp-II-064, Dp-II-074  
 한 가람 Dp-I-015  
 한 가람 Dp-II-081  
 한 가람 Dp-II-066  
 한 동훈 Dp-V-198  
 한 명수 E-41  
 한 명수 Ep-II-040  
 한 범희 Fp-IV-013

한 보영 C-04  
 한 보영 Bp-I-016  
 한 상준 Ip-III-050  
 한 상희 Hp-III-008  
 한 석희 Dp-V-145  
 한 성 Ip-III-043  
 한 성홍 Ip-III-017, Ip-III-018  
 한 수옥 Ep-II-040  
 한 승중 Kp-III-038  
 한 승호 E-35  
 한 영근 Ip-III-028  
 한 영기 Ep-II-096  
 한 예술 Ip-III-033  
 한 용희 Gp-III-013  
 한 원석 K-06(초)  
 한 은주 Ip-III-038  
 한 인식 PA-07(초)  
 한 인식 C-02, Cp-IV-022, Cp-IV-037  
 한 인식 B-25, C-03, Cp-IV-004  
 한 재광 Kp-II-005  
 한 재민 Ip-III-005  
 한 재민 Ip-III-041  
 한 재현 Ep-V-112  
 한 종훈 E-19  
 한 준희 Ep-II-068  
 한 창희 Cp-IV-034  
 한 현택 Dp-V-144  
 한 혜선 Dp-V-144  
 함 승우 Bp-I-012  
 함 승우 B-20  
 함 승주 Ep-I-021  
 함 홍우 Ip-III-011  
 허 남정 Dp-I-007, Dp-I-008, Dp-I-015,  
 PB-03(초)

허 남정 Dp-II-126  
 허 명선 J-01  
 허 성구 Bp-I-028  
 허 성환 Ep-I-032  
 허 지행 B-23  
 현 성욱 Dp-II-125  
 현 승준 B-10  
 현 효정 Cp-IV-035  
 홍 경수 D-27  
 홍 경수 Ep-I-001, Ep-II-060  
 홍 경희 Lp-III-002  
 홍 만수 Hp-IV-056  
 홍 병식 B-34, C-05, C-38, Cp-IV-031,  
 Cp-IV-032

홍 병식 C-02, Cp-IV-022, Cp-IV-037  
 홍 병식 C-03, Cp-IV-004  
 홍 사환 Dp-I-036  
 홍 사환 Dp-I-026  
 홍 상신 Dp-II-114, Dp-II-123, Fp-IV-024  
 홍 석경 Ip-III-032  
 홍 석민 Ep-II-093  
 홍 성기 Kp-II-006  
 홍 성욱 Gp-III-001  
 홍 성주 E-13  
 홍 순천 Dp-II-110  
 홍 순철 Dp-II-096, Dp-V-187,  
 Dp-V-193  
 홍 순철 Dp-V-183  
 홍 승우 C-18  
 홍 승휘 Kp-V-052, Kp-V-053,  
 Kp-V-073  
 홍 영기 Ip-III-053  
 홍 영기 E-25  
 홍 영준 H-19  
 홍 완 Cp-IV-028, Cp-IV-029,  
 Cp-IV-036

홍 원기 Ep-I-003  
 홍 인석 Hp-IV-068  
 홍 인호 Hp-III-019, Hp-III-020  
 홍 종범 Dp-II-077  
 홍 종수 Dp-II-085  
 홍 지상 Dp-II-102  
 홍 지상 D-15  
 홍 태운 E-31  
 홍 태운 Ip-III-054  
 홍 태은 Ep-V-117  
 황 도원 Ep-II-095  
 황 명진 B-25  
 황 상훈 C-41  
 황 상훈 C-17  
 황 석원 H-17  
 황 성식 E-02  
 황 성인 Ip-III-034  
 황 성인 Ip-III-035  
 황 순용 E-35  
 황 영훈 Dp-II-084  
 황 영훈 D-16  
 황 용석 Cp-IV-035  
 황 용석 H-09(초)  
 황 옥중 Ep-II-096  
 황 의중 C-42  
 황 인록 Dp-I-036  
 황 인록 Dp-I-026  
 황 일문 Hp-IV-058, Hp-IV-069  
 황 일문 Hp-IV-061  
 황 재성 Dp-V-199  
 황 재연 Ep-I-015  
 황 정남 Ep-II-068  
 황 정식 DF-18(초)  
 황 정연 Ip-III-045  
 황 지광 Hp-IV-047  
 황 채은 Lp-III-002  
 황 철규 Hp-III-023  
 황 철성 E-54  
 황 춘규 Dp-V-188  
 황 치선 E-53  
 황 치욱 H-02  
 황 태종 E-32  
 황 태종 Dp-II-095  
 황 학인 Dp-I-002  
 황 학인 Dp-I-001, Dp-I-003, Dp-I-018  
 황보 창권 Ip-III-051  
 황보 창권 Ip-III-021, Ip-III-025

## A-Z

A. Ohnishi BF-07(초)  
 A. Sato BF-07(초)  
 AHMAD dawood Dp-II-061  
 AHN CHANG WON D-50  
 AHN Changgeun Dp-V-174  
 AHN Hyo Chul B-06  
 AHN Jae Young Dp-V-166  
 AHN Jaewook J-10  
 AHN Jeung Sun E-28  
 AHN Jeung Sun Ep-I-020  
 AHN Jong Real D-12  
 AHN Joung Real D-06  
 AHN Joung Real D-11  
 AHN Kang-Hun Dp-V-217  
 AHN Kang-Hun F-11  
 AHN Sejin Ep-II-099  
 AHN Seung-Eon K-02(초)  
 AHN Sung-Min Dp-II-093  
 AHN Sungmo Ep-II-038  
 AKAGI Kazuo E-11

ALA-NISSILA Tapio	F-09	CHAE S. A.	Dp-V-211	CHO Jong-Young	Kp-III-036
ALESHIN Andrey N.	E-11	CHAI Yi Sheng	PB-05	CHO Jung-Ho	L-12(초)
ALMAAS Eivind	F-01(초)	CHANG .C.S.	Hp-III-003	CHO Jun-Hyung	D-07
AN Eun mi	Hp-IV-075	CHANG Hyunju	D-13	CHO K. J.	Dp-II-115
AN Ki-Seok	Kp-III-037	CHANG Hyun-Ju	Kp-III-018	CHO Kwang-Hwan	Ep-II-097
AN Kyungwon	I-06	CHANG Jieun	PC-11(초)	CHO Kwang-Hwan	Ep-II-062
AN Sang min	Ep-I-035	CHANG Joonyeon	Dp-II-097	CHO Kyu Hwan	Dp-II-082
ANDO Shung-ichi	C-32	CHANG Kee Joo	D-39	CHO Moo-hyun	C-22
AOI N.	C-27	CHANG Kee Joo	Dp-V-178	CHO Myoungrae	E-50
AONO Masashi	F-30	CHANG Kee Joo	Dp-V-200	CHO Myung Rae	Dp-V-153
ARAI Masato	B-09	CHANG Kee Joo	D-44	CHO Myoungrae	Dp-V-208
ARAKAWA Yasuhiko	K-11(초)	CHANG Sunghyun	Bp-I-001, Bp-I-007	CHO Sam Yeon	Dp-I-023, Dp-I-030
AREPALLI Sivaram	E-21	CHANG Yongmin	Dp-V-142	CHO sanghee	E-22
B. Grossan	L-20	CHANG Young Jun	PB-08(초)	CHO Sung Mook	E-46
B.D. Park	BF-07(초)	CHANG Yun Hee	D-13	CHO Sung Oh	H-14
B.G Cheon	Bp-I-021	CHANG-IN Park	Dp-V-135	CHO Sung Un	Dp-V-153
B.H. Choi	BF-07(초)	CHANG-KEUN Yun	F-31	CHO Sung Un	D-45
BAE Jaehyun	Dp-V-154	CHAR Kookrin	D-31	CHO Sung Wan	D-21
BAE Jong-Seong	Dp-I-048	CHAR Kookrin	DF-10	CHO Sung-Jin	Cp-IV-013
BAE Kyu Jung	B-22	CHAR Kookrin	D-21	CHO Sunglae	D-16
BAE Kyu Jung	B-24	CHAR Kookrin	Dp-V-208	CHO Sunglae	Dp-I-058
BAE Sangsu	D-59	CHAR Kookrin	E-50	CHO Suyeon	Dp-V-209
BAE SE HWAN	D-50	CHEN X. H.	DF-05	CHO Won Ju	Kp-III-035
BAE Yu Jeong	Dp-V-166	CHEN Xiang Bai	Dp-II-087	CHO Won-Ju	Dp-V-172, Kp-III-033
BAEK Jeongho	L-12(초)	CHEN Xiang-Bai	Dp-II-094	CHO Y. S.	C-22
BAEK S.-H.	D-36	CHEN Yeqing	Dp-I-032	CHO Y.S.	Cp-IV-018
BAEK Sujin	E-26	CHEN Zhi Gang	Kp-V-054	CHO Yong Chan	Dp-I-042
BAEK Yongjoo	F-12	CHEN Zhigang	Kp-V-072	CHO Yong Sub	Hp-IV-081
BAHK S.Y.	Bp-I-019	CHENG Horchhong	Ep-II-077	CHO Yong sub	Hp-IV-075
BAIK Jaeyoon	D-06	CHENG Horchhong	Ep-II-071	CHO Yong-Hoon	Kp-V-059
BAIK Kwang Hyeon	Kp-II-007	CHENNUPETI Jagadish	Kp-V-072	CHO Young Sul	F-32
BAK . J. G	Hp-III-011	CHENNUPETI Jagadish	Kp-V-054	CHO Young Woo	Dp-V-128
BAK Junghoon	E-50	CHEON B.G	Lp-III-007	CHO Y-S.	Cp-IV-024
BAK Wan	E-34	CHEON B.G.	Lp-III-001	CHOE Sug-Bong	Dp-II-118
BALAKIREV F. F.	DF-06	CHEON ByungGu	Lp-III-004	CHOE Sug-Bong	Dp-II-093
BANG Jeongho	J-07	CHEON Jinwoo	Dp-V-166	CHOI Ahreum	Dp-V-215
BANG Yunkyu	Dp-II-075	CHEONG Hyeonsik	Ep-I-009	CHOI B. C.	Dp-I-050
BANG Yunkyu	DF-06	CHEONG Hyeonsik	Dp-I-024	CHOI Byung Chun	Dp-V-180
BARTKOWIAK Marek	DF-13	CHEONG HYEONSIK	Dp-V-160	CHOI Byung Chun	Dp-V-204
BARVE Ajit V.	Kp-II-001	CHEONG Hyeonsik	Dp-V-162	CHOI Byung Chun	Dp-I-025, Dp-V-189
BASOV D.	K-01(초)	CHEONG Hyeonsik	D-61	CHOI Byung Chun	Dp-V-197
BEAK Inbok	Dp-V-174	CHEONG S.-W.	D-43	CHOI Byung-Ho	H-06(초)
BELAY K.	Kp-V-074	CHEOUN MyungKi	Cp-IV-012	CHOI ByungJoon	KF-03(초)
BELLE Collaboration	B-17	CHEOUN Myung-Ki	Cp-IV-001, Cp-IV-030, PA-10(초)	CHOI Changho	DF-05
BENAYAD 동욱	K-02(초)	CHEREVKO S	E-44	CHOI Chanho	DF-15
BHANG H.C.	C-27	CHI Young Shik	Ep-II-056	CHOI Chel-Jong	Kp-V-050
BHANG Hyoung Chan	Cp-IV-040	CHIO Minkyoo	Bp-I-027	CHOI CHEOL JONG	Kp-V-047
BONNAUD Christophe	Bp-I-016	CHO B. K.	Dp-II-071	CHOI Choon-Gi	Dp-I-053
BOZOVIC Ivan	Dp-II-059	CHO B. K.	DF-13	CHOI Chulho	Fp-IV-016
BRAZOVSKI Serguei	E-11	CHO B. K.	Dp-II-063	CHOI Eun Sang	DF-06
BROOKS James	E-11	CHO B. K.	Dp-II-118	CHOI Eun-Ae	D-44
BU Sang Don	Dp-I-023, Dp-I-027, Dp-I-030, Dp-I-035	CHO Cheong-Gu	Ep-I-020	CHOI Eun-Mi	Dp-II-082
BYUN Kyung-Eun	E-43	CHO Dae Hee	Dp-V-210	CHOI Eun-Mi	DF-16
BYUNGNAM Kahng	F-31	CHO Doohee	Lp-III-007	CHOI Eunyoeung	Dp-V-205
C.J. Yoon	BF-07(초)	CHO E.J.	Lp-III-001	CHOI H. W.	Dp-I-054
C.S. Yoon	BF-07(초)	CHO En-Jin	PB-17(초)	CHOI Han-Yong	DF-12
CAO Z.X.	C-27	CHO Eun-Chel	PC-06(초)	CHOI Heon-Jin	E-43
CHA Dongwoo	Cp-IV-005	CHO Eunjung	Lp-III-004	CHOI Hyoung Joon	D-26, DF-08, DF-09, DF-19, Dp-V-156, Dp-V-202
CHA Gi-Beom	Dp-II-124	CHO Gi Ho	Ep-V-174	CHOI Hyoung Joon	D-25
CHA Moon-Hyun	Dp-V-154	CHO Hwanwoong	Ep-III-016	CHOI Hyoung Joon	D-34
CHA Nam-Goo	Ep-I-011	CHO In Hwa	Ep-III-004	CHOI Hyun Woo	Dp-I-051
CHA Seon Cheol	D-62	CHO In Hwa	DF-02(초)	CHOI Hyung Kook	D-45
CHA Seoncheol	D-61	CHO Inwha	Dp-I-050	CHOI Hyung Kook	D-46
CHA Wonsuk	Dp-V-215	CHO J. H.	DF-17	CHOI In Sung	D-23
CHA Wonsuk	D-10	CHO Jong Ho	Dp-V-204	CHOI Insung S.	Ep-II-056
CHA Wonsuk	E-23	CHO Jong Ho	Dp-V-180	CHOI J. Y.	H-08(초)
CHA Yun Mi	E-14	CHO Jong Ho	Dp-V-189	CHOI Jaewu	D-24
CHAE Byung-gyu	K-01(초)	CHO Jong Ho	Dp-V-197	CHOI Jee Hyun	Fp-IV-020
CHAE Kwang Pyo	Dp-II-116	CHO Jong Ho			

CHOI Jeongyong	D-16	DERMISEK Radovan	B-22	HA Hyuncheong	B-17
CHOI JEONGYONG	Ip-III-007	DHO Joonghoe	Dp-II-103	HA Jeong Sook	Kp-III-041
CHOI Jeongyong	Ep-II-086	DHO Joonghoe	Dp-II-106	HA Meesoon	F-23
CHOI Jeongyong	Dp-I-058	DO Dal Hyun	Dp-V-204	HA Meesoon	F-28
CHOI Je-Young	F-26, Fp-IV-026	DOAN Thi Thuy Phuong	Dp-II-086	HA Taekjip	D-60
CHOI Jin-Ho	D-07	DOH Yong-Joo	Dp-II-063	HA Taekyun	Dp-I-049, Dp-I-055
CHOI Jung Ok	Cp-IV-023	DOMIER C. W.	Hp-III-012	HA Taewoo	Dp-I-019
CHOI K.-Y.	Dp-II-119	DOMIER C. W.	H-01	HAAM So Young	PB-05
CHOI Keunsu	Dp-V-154	DRAKE Darrell	L-06(초)	HAM Jinhee	E-08, E-09
CHOI Ki-Ryoung	Kp-V-051	DRISCOLL T.	K-01(초)	HAM Jinhee	E-07
CHOI Ki-Young	DF-15	DUONG Van Thiet	Dp-II-084	HAMZA Ammar	Ep-V-107, Ep-V-111
CHOI Ki-Young	DF-05	E Yanovich	Bp-I-006	HAN Cheolwoong	Ip-III-015
CHOI Kwang-Yong	PB-14(초)	E. Yanovich	B-14(초), B-35, B-36,	HAN Dong Seok	Dp-V-172
CHOI Kyujin	Dp-I-044		Bp-I-009	HAN Dongwoo	D-28
CHOI Minkyoo	Cp-IV-002	E. D. BAUER	Dp-II-080	HAN Doug Young	Dp-V-211
CHOI Minkyoo	Bp-I-001, Bp-I-007	E. V. Linder	L-20	HAN Hyunsun	Hp-III-004, Hp-III-007
CHOI MyungHoon	E-36	EISAKI Hiroshi	D-55	HAN Hyunsun	H-11
CHOI S. K.	D-53	ELLIMAN R. G.	Kp-V-074	HAN Hyunsun	Hp-III-002
CHOI S.H.	C-27	EOM C.-B.	D-36	HAN J. H.	Dp-V-211
CHOI SANG SIK	Kp-V-047	EOM MANJIN	Dp-II-068	HAN Jin Kyu	Dp-I-027, Dp-I-035
CHOI Sookkyung	BF-01(초)	EOM manjin	Dp-II-069	HAN Jinhee	D-34
CHOI Sooran	F-25	EOM Manjin	PB-13(초)	HAN Jung hoon	D-47
CHOI Suk	Cp-IV-023	EOM T. W.	Ep-V-103	HAN Jung Hoon	PB-04(초)
CHOI Sung-Jin	K-10(초)	EUNCHAN KIM	Cp-IV-038	HAN Jung-Hoon	Hp-III-001
CHOI Sung-Yool	Dp-I-053	EUN-SUK JEONG	Dp-V-135	HAN Moon-sup	D-28
CHOI SUNGYOUL	Ip-III-007	FEEGE Nils	B-13(초), Bp-I-020	HAN S.W.	Dp-V-131
CHOI Sungyool	Dp-I-012, Ep-II-086	FOR the LEPS Collaboration	C-31	HAN sangwook	Ep-I-026
CHOI Suyong	B-37, Bp-I-025	FREELAND J. W.	PB-10(초)	HAN Seung Jong	Kp-III-019
CHOI W.K.	KF-05(초)	FUKUSHIMA Kenji	C-09(초)	HAN Seung Jong	Kp-III-033
CHOI Won Chel	E-18	FURDYNA J. K	Kp-II-008	HAN Seungwu	KF-03(초)
CHOI Woo Seok	PB-11	FURDYNA J.K	Kp-II-009	HAN Su Jin	Dp-V-190
CHOI Woo Seok	Dp-V-203	FURDYNA J.K.	Dp-II-117	HAN Suk-Hee	Dp-II-097
CHOI Wook Seok	Dp-I-022	G Novikova	Bp-I-006	HAN Young-Geun	Ip-III-027
CHOI Woosik	Fp-IV-006	G. Novikova	B-14(초), B-35, B-36,	HAN young-geun	Ip-III-020
CHOI Y. J.	Dp-V-169		Bp-I-009	HANDS Simon	B-18
CHOI Yang-Kyu	K-10(초)	G. H. Kim	Ep-V-105	HANOH Lee	Dp-II-080
CHOI Yong Chan	Dp-I-023, Dp-I-030	G.F. Smoot	L-20	HAO X.J.	PC-06(초)
CHOI Youngil	Bp-I-025	GANJI Seeta RamaRaju	Dp-V-133, Dp-V-139, Dp-V-140	HARA Masahiko	F-30
CHOO Na Yun	Ep-II-094	GAO Qing	Dp-V-072	HARA MASAHIKO	Ep-I-008
CHOO Na-Yun	Ep-V-128	GAO Qing	Kp-V-054	HASEBE Nobuyuki	L-06(초)
CHOO Na-Yun	Ep-I-027	GARIPOV G	L-22	HAYASHI TOMOHIRO	Ep-I-008
CHOO suho	Ip-III-020	GARIPOV Garik	L-11(초)	HE Weizhen	Dp-V-176
CHU Seung Wan	E-16	GARIPOV Garik	L-21	HEGER Gernot	Dp-I-052
CHUN Dong Won	Ep-I-033	GENTLE A.	PC-06(초)	HEO H.	Hp-IV-086
CHUN Sae Hwan	PB-05	GHIM Cheol-Min	F-01(초)	HEO Kwang	E-43
CHUNG C. H.	Dp-I-046	GHIM Jin Soo	DF-07	HEO Sung Hwan	H-14
CHUNG J.	B-39	GI WAN Seo	Ip-III-007	HEON JU Lee	Hp-III-037
CHUNG J.-S.	D-36	GIBELIN J.	C-27	HER Eun Ju	Dp-V-166
CHUNG Jae-Ho	PB-18(초)	GO Ara	PB-06	HERMANN P.	Lp-III-006
CHUNG Jae-Ho	PB-05	GO Youngdong	Dp-I-034	HICKS K	C-17
CHUNG Jinseok	Dp-I-034	GOAK Jeungchoon	E-20	HIKITA Yasuyuki	Dp-II-108
CHUNG Jong Won	Dp-V-163	GOAK Jeungchoon	E-03	HIKITA Yasuyuki	PB-09(초)
CHUNG Kwangzoo	B-15(초)	GOAK Jungchoon	E-17	HIROFUMI Enomoto	Kp-V-049
CHUNG Sunjae	Dp-II-117	GOH Jung Suk	Dp-V-202	HO Kai-Ming	D-001
CHUNG T.	E-22	GOH Kwang-il	Fp-IV-018	HOEPFNER Kerstin	Bp-I-004
CHUNG Taek-Mo	Kp-III-037	GREEN Martin A.	PC-06(초)	HOHNG Sungchul	D-58
CHUNG WON-CHUNG	Cp-IV-015	GROSSAN B.	L-10(초)	HOHNG Sungchul	D-57
CHUNG Yunchul	Dp-V-141	GROSSAN B.	L-18	HOHNG Sungchul	D-59
COMMICHAU Volker	Lp-III-006	GUNSU Yun	H-10	HONDA T.	C-27
CONIBER Gavin	PC-06(초)	GYU-CHUL Yi	Dp-V-135	HONG Byungsik	PA-04(초)
CUI Hao	Kp-III-036	H. Akikawa	BF-07(초)	HONG Deog Ki	B-02
D. F. Wang	Ep-V-105	H. Funahashi	BF-07(초)	HONG Deog-Ki	B-06, B-12
D.P Barry	Cp-IV-015	H. Kikuchi	Ep-II-072	HONG Duk-Geun	Cp-IV-007
DANG Dung Duc	Dp-II-084	H. Okada	BF-07(초)	HONG In seek	Hp-IV-075
DASILVA Fabio C.S	D-45	H. Takahashi	BF-07(초)	HONG J. B.	DF-17
DAVID Adrian	Dp-V-203	H. D. Sato	BF-07(초)	HONG Jisang	Dp-II-102
DEGUCHI S.	C-27	H. J. Lee	Hp-III-045	HONG Jisang	D-15
DEGUCHI Yoji	H-03	HA Byeongchul	E-14	HONG Jongcheol	K-09(초)
DELAUNAY F.	C-27	HA Eunja	Cp-IV-001, PA-10(초)	HONG Kimin	Kp-V-055
DEOKHEE Kim	Dp-II-080			HONG Kwan Soo	Ep-I-014

HONG Kwangjoon	Kp-III-015,	IMAI .K	C-19	JEONG Hawoong	F-07
	Kp-III-024, Kp-III-025,	IMAI K.	C-20	JEONG Hawoong	F-12
	Kp-III-030	INAMDAR A. I.	PC-14	JEONG Hawoong	F-23
HONG Kyung Woo	Dp-I-048	ISHIHARA M.	C-27	JEONG Hawoong	F-28
HONG S. M.	H-08(초)	ISHII K	G-06, G-06, G-06	JEONG Heejun	Ep-II-084
HONG S.J.	Bp-I-019	ISIMOTO Shohei	E-13	JEONG J.	L-10(초)
HONG Sang Hee	H-11, Hp-III-007	IYODA Masahiko	E-13	JEONG Jinhwan	PB-17(초)
HONG Sang Hee	Hp-III-002	J. Asai	BF-07(초)	JEONG Jinwon	PB-17(초)
HONG Seong Jong	E-46	J. Kono	Dp-V-144	JEONG Jung Hyun	Dp-I-025, Dp-I-032,
HONG Seunghun	D-21	J. D. Thompson	Dp-II-080		Dp-V-163, Dp-V-195,
HONG Seunghun	E-43	J. H. Kim	Hp-III-045		Ep-II-063, Ep-II-065
HONG Seung-Woo	PA-01(초)	J. W. Park	Ep-II-036	JEONG Jung-hyun	Ip-III-009
HONG Seung-Woo	Cp-IV-009,	J. W. Park	Ep-II-039	JEONG Jung-Hyun	Jp-III-004
	Cp-IV-010	J. W. Park	Ep-II-037	JEONG Junho	Ip-III-009
HONG Soon Cheol	Dp-II-124	J. Y. Rhee	Ep-II-037	JEONG Kiyoun	D-28
HONG Suklyun	Dp-V-201	J.C. KU	Kp-III-020	JEONG Nak Cheon	Ep-I-009
HONG Sung-Hak	Dp-II-073	J.D. Thompson	Dp-I-021	JEONG Nak Cheon	E-23
HONG Sungwook	Dp-V-142	J.K. Ahn	BF-07(초)	JEONG S.	L-18
HONG Taeyoon	Dp-II-059	J.L. Sarrao	Dp-I-021	JEONG Seong Min	F-08
HOSAKA Atsushi	C-10(초)	J.S. Song	BF-07(초)	JEONG Se-Young	Dp-I-042
HUANG D. J.	PB-01(초)	JAHNG Junghoon	Ep-I-035	JEONG Se-Young	Dp-V-147
HUANG S.J.	PC-06(초)	JAISWAL-NAGAR Deepshikha	PB-05	JEONG Tae Moon	Ip-III-037
HUH Chul	K-09(초)	JAMIL M.	Bp-I-019	JEUNG Won Yong	Ep-I-033
HUH Junghwan	Kp-III-041	JANG Dogeun	H-15	JHANG H.J.	Bp-I-019
HUR Min Sup	H-05	JANG Dong Hyun	D-45	JAHNG Junghoon	E-34
HUR Nam Jung	Dp-I-022	JANG DONG KYU	Ep-I-005	JHE Won ho	Ep-I-035
HUSSAIN Ali	Dp-I-002	JANG Donggyu	H-15	JHE Wonho	E-34
HWANG C. -C.	D-05	JANG Eunsoo	E-20	JHE Wonho	Jp-III-012
HWANG Chanyong	Dp-V-201	JANG Eunsoo	E-03	JHI Seung-Hoon	D-40
HWANG Chanyong	PB-12	JANG Jae Hyuck	DF-01(초)	JI HUN Kim	Hp-III-037
HWANG Cheol Seong	DF-01(초)	JANG JungMin	C-40	JIANG Zhang	D-10
HWANG Cheol Seong	KF-03(초)	JANG Jung-tak	Dp-V-166	JIN Hyunchang	Hp-IV-046
HWANG DOO HEE	Ep-I-005	JANG K. W.	Dp-I-046	JIN Jung-Il	D-42
HWANG Eunjin	Fp-IV-020	JANG Kiwan	Ip-III-009	JIN Meihua	E-21, Ep-I-019
HWANG H. -N.	D-05	JANG kiwan	Jp-III-004	JIN Yeryeong	Dp-I-028
HWANG HAK IN	D-50	JANG Kiwan	Ep-II-063, Ep-II-065	JINKYOUNG Yoo	Dp-V-135
HWANG Harold Y.	Dp-II-108	JANG Ki-wan	Dp-V-163	JO Hyun Yong	Bp-I-019
HWANG Harold Y.	PB-09(초)	JANG Moongyu	K-10(초)	JO Ji Young	D-37
HWANG Jeong Hoon	Dp-I-048	JANG S. Y.	D-36	JO W.	Ep-II-099
HWANG Jihwan	Dp-I-024, Dp-I-034	JANG S. Y.	Dp-II-094	JO William	PC-15
HWANG Jin Ha	Kp-III-037	JANG Seunghun	D-28	JO Young-Hun	D-37
HWANG Nong-moon	D-01	JANG un jung	Ep-I-002	JO Youngkwon	Bp-I-025
HWANG Sungmin	F-13	JANG Y. R.	DF-17	JOO Chirlmin	D-60
HWANG Sung-Min	Kp-II-007	JANG Z. H.	Dp-II-115, Dp-II-119	JOO Keehyoung	F-27
HWANG Sun-Yong	F-19	JAYASIMHADRI Mulla	Jp-III-004	JOO Young-Do	Hp-IV-067
HWANG Won-Taek	Cp-IV-013	JEANS Daniel	B-13(초), Bp-I-020	JU chanjong	D-31
HWANG Yongseok	Hp-III-024	JEON Byung Chul	Dp-I-022	JU Mi Yeon	Kp-V-050
HWANG Yong-Seok	Hp-III-015	JEON Byung-Gu	Dp-I-020, Dp-I-033	JU Seonghwa	E-01
HWANG Yoon-Hwae	Dp-V-176	JEON Chanil	F-07	JULIUS Nfor	Hp-IV-053, Hp-IV-066
HYEON Park	H-10	JEON Chanil	F-23	JUN OH Kim	Kp-II-001
HYPHI collaboration	C-16	JEON Cheolho	D-11	JUNG A.R.	L-18
HYUN Chang-Ho	C-32	JEON Cheolho	D-06	JUNG CHANGUK	E-37
HYUN-TAK Kim	Ip-III-007	JEON Cheolho	E-18	JUNG Chang-Uk	Dp-II-063
I.G. Park	BF-07(초)	JEON Dongryul	E-04	JUNG Chang-Uk	DF-13
IEIRI .M	C-19	JEON Eun-Kyoung	Kp-III-018	JUNG Dae Sung	E-18
IEIRI M.	C-20	JEON Gun Sang	PB-06	JUNG Dong-gyu	Dp-II-103
IGASHIRA M.	C-26	JEON Gun Sang	DF-10	JUNG dong-gyu	Dp-II-106
IGASHIRA Masayuki	Cp-IV-014,	JEON Gun Sang	PB-04(초)	JUNG Duk-Young	PC-04
	Cp-IV-016	JEON H. C.	Kp-V-060	JUNG Hoon	C-26
IHM Gukhyung	Dp-V-213	JEON Hankyung	Ep-II-084	JUNG HOON	Cp-IV-014, Cp-IV-016
IHM Jisoon	Dp-V-154	JEON Heonsu	Ep-II-038	JUNG Hyunok	D-43
IHSAN Aamir	H-14	JEON Hong Jun	D-23	JUNG Jong Hoon	Dp-I-022
IHSAN Aamir	Ep-I-032	JEON J.A.	L-18	JUNG Kwanghwan	Dp-V-215
IKE Yuji	F-21	JEON Jong Myeong	DF-01(초)	JUNG Kyooho	PC-14
IKUNO Toshinori	B-13(초)	JEON Yoonnam	D-61	JUNG M. H.	DF-17
ILHA Lee	Ep-I-031	JEONG Ah Reum	PC-15	JUNG Myung Hwa	DF-11
IM Hyunsik	PC-14	JEONG Da Woon	Dp-V-203	JUNG MYUNG HWA	DF-07
IM Jino	Dp-V-154	JEONG Doo Seok	KF-04(초)	JUNG Myung-Hwa	DF-15
IM Seongil	Dp-I-019	JEONG Hae-Kyung	E-21, Ep-I-019	JUNG Myung-Hwa	DF-16
IM Seongil	Ep-II-089	JEONG Hawoong	Fp-IV-015	JUNG Myung-Hwa	DF-05

JUNG Ranju	E-50	KANHG Byungnam	Fp-IV-018	KIM Dong Ho	DF-16
JUNG Soon-Gil	Dp-II-082	KANKI, Teruo	Ep-I-011	KIM Dong Woo	Ep-II-063, Ep-II-065
JUNG Soon-Gil	DF-16	KANNAN E S	Ep-V-120	KIM Dongchirl	E-50
JUNG Sung Chul	D-09	KAPLAN Alex	Bp-I-020	KIM Dongchul	Dp-V-132
JUNG Unseok	Dp-V-167	KAPLAN Alexander	B-13(초)	KIM Dongchul	Dp-V-167
JUNG Unseok	Dp-V-132	KATABUCHI T.	C-26	KIM DongHee	B-13(초), Bp-I-020
JUNG W. S.	D-53	KATABUDNI Tatsuya	Cp-IV-014	KIM Dongho	PC-11(초)
JUNG Y.S	D-49	KAWADA Y.	C-27	KIM Dongkyun	PC-11(초)
JUNG Yeongri	E-01	KAWAGOE Kiyotomo	B-13(초),	KIM Dong-Wook	PC-05
JUNG YoungKyun	F-07		Bp-I-020	KIM Dongyoo	Dp-II-102
KÖNIG D.	PC-06(초)	KEK-PS E522 COLLABORATION		KIM Dongyoo	D-15
K. Aoki	BF-07(초)		BF-07(초)	KIM Doo Chul	F-32
K. Imai	BF-07(초)	KEUM Yong-Yeon	L-04(초)	KIM Doochul	Fp-IV-017
K. Miwa	BF-07(초)	KHAN Adil	Bp-I-020	KIM Doochul	Fp-IV-016
K. Nakazawa	BF-07(초)	KHANDAKER M.U.	Cp-IV-018	KIM Doochul	F-13
K. Shoji	BF-07(초)	KHANDAKER M.U.	Cp-IV-024	KIM Doochul	Fp-IV-018
K. Taketani	BF-07(초)	KHANDAKAR Mahendra	F-09	KIM Doohyun	Hp-III-002
K. Tanida	BF-07(초)	KHIM Seung Hyun	DF-14, Dp-II-076	KIM Dooyoung	Cp-IV-005
K. Yamamoto	BF-07(초)	KHIM Seunghyun	Dp-I-020	KIM Doseok	D-62
K.Y. LIM	Kp-III-020	KHIM Seunghyun	DF-10	KIM Doseok	D-61
KA E. M.	Hp-III-011	KHIM Seunghyun	DF-06	KIM Doseok	D-60
KAANG Helen	Hp-III-026	KHRENOV B	L-22	KIM Doyoun	B-12
KADI Yacine	PA-06(초)	KHRENOV Boris	L-11(초)	KIM Doyoun	D-59
KAGAWA K	G-06	KHRENOV Boris	L-21	KIM Do-Youn	B-22
KAGAWA Kiichiro	H-03	KHUMAENI Ali	H-03	KIM Eok Bong	PA-03(초)
KAHN Adil	B-13(초)	KHYM .S	Kp-II-009	KIM Eun Kyu	Kp-III-019
KAHNG Byoungnam	Fp-IV-017	KHYM .S	Kp-II-008	KIM Eun Kyu	Kp-III-035
KAHNG Byung Nam	F-32	KI sanghoon	Dp-II-103	KIM Eun Kyu	Dp-II-122
KAHNG Byungnam	Fp-IV-016	KI sanghoon	Dp-II-106	KIM Eun Kyu	Dp-V-172, Kp-III-033,
KAHNG Byungnam	F-13	KI M Jun Sung	PB-13(초)		Kp-III-040
KAISER Alan B.	E-11	KIM Andrey	C-36	KIM Eunhee	C-16
KAMADA S.	C-26	KIM B. S.	H-08(초)	KIM G C	Dp-II-061
KANER Richard B.	E-11	KIM B.H.	Dp-V-131	KIM G. H.	Ep-V-104
KANG Bo Ram	Dp-V-180	KIM B.-H.	Ep-I-026	KIM G.N.	B-39
KANG Bo Soo	K-02(초)	KIM Beom Jun	F-33	KIM G.N.	Cp-IV-018
KANG Chong-Yun	Ep-II-097	KIM Bog G	Dp-I-028	KIM Ga Young	Dp-I-045, Dp-II-065
KANG Chong-Yun	Ep-II-062	KIM Bog G.	Dp-II-108	KIM Ga Young	Dp-II-062
KANG Gungwon	L-16	KIM Bog G.	PB-09(초)	KIM Gidong	Cp-IV-021
KANG HYON CHOL	K-14	KIM Bongjae	Dp-II-090	KIM Gil-Ho	Ep-V-120
KANG J.-S.	D-43	KIM bongju	Dp-II-108	KIM Gracia	PC-15
KANG J.-S.	Dp-II-090	KIM Bongju	Dp-I-028	KIM Guang-Hoon	Fp-IV-010
KANG JEONG WON	Dp-V-150	KIM Bongju	PB-09(초)	KIM Guinyun	C-22, C-26, Cp-IV-024
KANG Jisung	Hp-III-024	KIM BONG-JUN	Ip-III-007	KIM GUINYUN	Cp-IV-038
KANG Jongeun	Ep-I-014	KIM Bong-Jun	Ep-II-086	KIM Guinyun	Lp-III-006
KANG Joohoon	E-09	KIM Bong-jun	K-01(초)	KIM Guinyun	Cp-IV-014
KANG Ki Hyeok	Dp-II-089	KIM Bong-Jun	Dp-I-058	KIM GUINYUN	Cp-IV-015
KANG Kihyeok	Dp-I-047, Dp-II-071	KIM Bong-Kyu	K-09(초)	KIM Guinyun	Cp-IV-016
KANG Min-Gyu	Ep-II-097	KIM Bongsoo	F-10	KIM Gui-Nyun	Hp-III-010
KANG Min-Gyu	Ep-II-062	KIM C	Dp-V-167	KIM Gunn	Dp-V-154
KANG Minhyuck	D-61	KIM C.	D-53	KIM GWANG-HEE	D-33
KANG Myung Ho	D-09	KIM Chan Mi	E-46	KIM Gwon Jung	Cp-IV-014, Cp-IV-016
KANG Phil Geun	PC-05	KIM Chang Gyoung	Kp-III-037	KIM Gwon-jung	C-26
KANG Seo Kon	Bp-I-001, Bp-I-007	KIM Chang Jung	K-02(초)	KIM Gyu Tae	Kp-III-041
KANG Seokon	Cp-IV-002	KIM Chang-Duk	Ep-I-027	KIM H. -D.	D-05
KANG Seokon	Bp-I-002	KIM Chang-Hwan	Ep-II-083	KIM H.B	Lp-III-007
KANG Seoung-Hun	Ep-I-017	KIM Chen-Lae	Kp-III-036	KIM H.B.	Lp-III-001
KANG SungJin	E-27	KIM Chil-Min	Fp-IV-010	KIM Haejeong	Kp-III-024
KANG Sung-Kyu	Kp-III-028	KIM Chinkyo	Kp-V-050	KIM Haeri	PC-05
KANG SUNG-KYU	Kp-V-055	KIM Choong H.	PB-08(초)	KIM Hak-sung	Dp-V-167
KANG Sun-Hee	PB-02(초)	KIM Choong Hyun	Dp-I-022	KIM Han Sung	Hp-IV-081
KANG T. H.	H-08(초)	KIM Chul	D-53	KIM Hanchul	Dp-II-100
KANG T. W.	Kp-V-060	KIM Chul Min	Ip-III-037	KIM Hang Bae	Lp-III-004
KANG Uk	Fp-IV-010	KIM D. E.	H-08(초)	KIM Han-Jung	Ep-II-071
KANG Won Nam	Dp-II-082	KIM D. H.	D-43	KIM Hanna	Dp-V-217
KANG Won Nam	DF-16	KIM Da Jeong	Dp-V-189	KIM Hee Seob	Hp-IV-081
KANG Won Nam	Dp-II-073	KIM DAE HO	Fp-IV-005	KIM Heung-Chul	Dp-II-105
KANG Yeong-Rok	Cp-IV-014	KIM Daell	Kp-III-041	KIM Hogyoung	PC-05
KANG YEONG-ROK	Cp-IV-015	KIM Do Gyun	Cp-IV-040	KIM Hongsu	L-03(초)
KANG Yeong-Rok	Cp-IV-016	KIM Do Hyung	DF-02(초)	KIM Hoonmin	Dp-V-208
KANG Yong-Ju	Dp-V-178	KIM Do-Hyun	F-26, Fp-IV-026	KIM Hoonmin	E-50

KIM Hyeon Soo	Dp-V-185	KIM Jinhee	Dp-II-075	KIM KYUNGSOOK	Cp-IV-038
KIM Hyeong-Do	PB-17(초)	KIM Jinhee	Dp-V-141	KIM Kyung-Sook	Cp-IV-024
KIM Hyery	Dp-V-217	KIM Jinhee	Ep-II-056	KIM M. -H.	Dp-I-050
KIM Hyo Jung	Ep-V-113	KIM Jin-Man	Ep-II-078	KIM Minkook	D-11
KIM hyojung	Dp-V-223	KIM JinMok	Ep-II-087	KIM Minkook	D-06
KIM Hyuck-Jong	Hp-III-001	KIM Jinwoo	Ep-I-022	KIM Minkook	D-12
KIM Hyung Do	B-22	KIM Jinwoo	Ep-V-123	KIM Min-Kook	D-26
KIM Hyung Gyun	Hp-IV-081	KIM Jinwoong	D-40	KIM Min-Seok	Hp-IV-073
KIM Hyung-Jun	Dp-II-097	KIM Jong Chan	PA-15(초)	KIM Min-Seok	H-15
KIM Hyung-Kook	Dp-V-176	KIM Jong Man	Dp-II-065	KIM Minseong	Dp-V-210
KIM Hyungmin	Kp-V-057	KIM Jong Pil	Dp-I-048	KIM Miyoung	E-27
KIM Hyun-Joo	lp-III-027	KIM Jong Won	Cp-IV-040	KIM Miyoung	DF-01(초)
KIM Hyun-Joo	lp-III-020	KIM Jong-Hyun	Ep-II-066	KIM MIYOUNG	E-37
KIM Hyunjung	Dp-V-215	KIM JONG-KI	Ep-II-057	KIM Myong Ho	Dp-V-204
KIM Hyunjung	Ep-V-123	KIM Joon Yeon	Cp-IV-040	KIM Myong-Ho	Dp-V-180
KIM Hyunjung	Ep-I-022	KIM Ju Hwan	Dp-I-048	KIM Myong-Ho	Dp-V-189, Dp-V-197
KIM Hyunjung	D-10, Dp-V-218	KIM Jun Sung	DF-06, DF-10	KIM myoungsu	E-17
KIM Hyunjung	E-23	KIM Jun Sung	Dp-II-089	KIM Myung Shik	J-08
KIM Hyunseok	H-13, Hp-III-004,	KIM Jun Sung	DF-13	KIM Nam	Dp-V-141
	Hp-III-007	KIM Jung Hwan	Dp-I-025	KIM Pan-Jun	F-29
	Hp-III-006	KIM Jung-Sung	lp-III-015	KIM Purin	Fp-IV-017
KIM Hyunseok	D-28	KIM Junsung	Dp-V-167	KIM S. H.	H-08(초)
KIM Hyunseung	Ep-I-033	KIM Junsung	Dp-V-132	KIM S. N.	H-08(초)
KIM Hyunsu	Ep-II-086	KIM Ju-Young	DF-13	KIM S. S.	Dp-I-050
KIM Hyun-Tak	K-01(초)	KIM Ju-Young	Dp-II-063	KIM S.H.	Dp-V-131
KIM hyun-tak	Dp-I-012	KIM Jwa Soon	Hp-III-015	KIM S.-H.	Ep-I-026
KIM Hyun-Tak	Dp-I-058	KIM K.	Cp-IV-018	KIM Sang Hoon	Dp-I-045, Dp-II-065
KIM Hyunyong	Bp-I-027	KIM K. H.	Dp-II-115	KIM Sang Hoon	Dp-II-062
KIM Hyunyong	Cp-IV-002	KIM K. R.	H-08(초)	KIM Sang Soo	Dp-V-180
KIM ILL WON	D-50	KIM K. W.	Ep-V-103	KIM Sang Soo	Dp-V-189
KIM Ill-Won	PB-02(초)	KIM K. W.	Ep-V-104	KIM Sang Soo	Dp-V-204
KIM Ingyu	PB-05	KIM K.S.	Cp-IV-018	KIM Sang Wook	I-06
KIM In-mook	F-24	KIM Kayoung	Dp-II-070	KIM Sanghoon	Dp-II-070
KIM J. E.	L-10(초)	KIM Kee Hoon	DF-14, Dp-I-020,	KIM Sang-Hun	Ep-I-027
KIM J. S.	Dp-I-046		Dp-I-033, Dp-II-076	KIM Sangrak	F-26, Fp-IV-026
KIM J. -S.	D-05	KIM Kee Hoon	DF-10	KIM Sang-Sig	Ep-II-097
KIM J. Y.	H-07(초)	KIM Kee Hoon	PB-13(초)	KIM Sang-Woo	F-18
KIM J. Y.	H-08(초)	KIM Kee Hoon	DF-06	KIM sangyong	Dp-V-151
KIM J.E.	L-18	KIM Kee Hoon	PB-04(초)	KIM Sang-Yoon	F-34
KIM J.H	Lp-III-007	KIM Kee Hoon	PB-05	KIM Se-Hun	Dp-V-211
KIM J.H.	Lp-III-001	KIM Keun Su	D-08	KIM Seok Hwan	Kp-III-037
KIM Jae Hoon	Dp-I-044	KIM Ki Hwan	K-02(초)	KIM Seon Pil	Kp-III-035
KIM Jae Hoon	Dp-I-019	KIM Ki Min	Hp-III-002	KIM Seon Pil	Dp-V-172, Kp-III-033
KIM Jae Hoon	Dp-II-059	KIM Ki-Bum	Cp-IV-007, Hp-IV-052,	KIM Seong-Je	Kp-V-049, Kp-V-051
KIM Jae Myung	lp-III-016		Hp-IV-053, Hp-IV-066	KIM Seongjin	F-19
KIM Jae Myung	lp-III-004	KIM KI-HONG	Ep-II-057	KIM Seunghwan	Fp-IV-020
KIM Jae Wook	Dp-I-033	KIM Kinney H.	A-06	KIM Seunghyun	PB-13(초)
KIM Jae Wook	DF-06	KIM Ki-Seok	PB-16(초)	KIM Seyong	B-18
KIM Jae Wook	PB-04(초)	KIM Kiwoong	Ep-II-087	KIM shinhee	Kp-II-009
KIM Jae Yool	Bp-I-001, Bp-I-007	KIM Kui Young	H-06(초)	KIM Shinhee	Kp-II-008
KIM Jae-Hong	Cp-IV-013	KIM Kun Ho	Dp-V-185	KIM Sihan	Ep-II-038
KIM JaeHoon	Dp-V-196	KIM kwang sub	Ep-I-002	KIM Sin Woong	Dp-V-180
KIM Jae-Hoon	Dp-II-122	KIM Kwangsoo	Cp-IV-024	KIM Soen Pil	Kp-III-040
KIM Jae-Hyung	Dp-V-186	KIM Kwang-Woo	Ep-V-128	KIM Songhui	Ep-II-081
KIM Jae-Young	PB-17(초)	KIM Kyeong Ja	L-06(초)	KIM Song-Ju	F-30
KIM Je Han	Ep-II-094	KIM KyeongKyu	D-59	KIM Soo Hyun	DF-15
KIM Je Hyung	Kp-V-059	KIM Kyoo	PB-17(초)	KIM Soo Hyun	DF-05
KIM Je-Eun	Dp-II-092	KIM Kyung Kiu	B-04	KIM Soon-Wook	L-08(초)
KIM Jehan	Ep-V-128	KIM Kyung Min	KF-03(초)	KIM Soon-Wook	Lp-III-008, Lp-III-009
KIM Jeong-Sook	Lp-III-009	KIM Kyung Ryul	Hp-IV-081	KIM Su Jae	Dp-I-042
KIM Jieun	B-13(초), Bp-I-020	KIM Kyung Sook	C-22, Lp-III-006	KIM Su Min	Dp-V-128
KIM Ji-Heon	Ep-II-078	KIM kyung Yeon	Dp-V-156	KIM SUN KUG	Ep-I-005
KIM Ji-Hoon	Dp-V-206	KIM Kyung-Ho	Dp-II-097	KIM Sung Baek	PB-17(초)
KIM Jihun	B-22	KIM Kyung-Hyun	K-09(초)	KIM Sung Hoon	Ep-II-063
KIM Jihyun	Lp-III-004	KIM Kyung-il	C-13	KIM Sung Hoon	Ep-II-065
KIM JIN MIN	Fp-IV-005	KIM Kyungjin	Hp-III-006	KIM Sung Hoon	Dp-I-047, Dp-II-071
KIM Jin Soak	Kp-III-019	KIM Kyungmin	L-13	KIM Sung Hyun	D-62
KIM Jin Soo	Dp-I-056	KIM Kyung-Ryul	Hp-IV-067	KIM SungHoon	Dp-II-089
KIM Jin Soo	Dp-V-219	KIM Kyungsik	Cp-IV-012	KIM Sunghyun	Bp-I-021
KIM JinBae	E-36	KIM Kyungsik	Cp-IV-001, PA-10(초)	KIM Sunghyun	D-60

KIM Sung-Jin	E-01	KOH Y. Y.	D-53	LEE Bum-Hoon	B-11
KIM Sungman	Ep-I-033	KOH Y.Y	D-49	LEE Bumsung	DF-14, Dp-I-020,
KIM Sung-Soo	B-07	KOJIMA Seiji	Dp-I-039, F-21		Dp-II-076
KIM Sungyun	F-04(초)	KONDO Y.	C-27	LEE Bumsung	PB-05
KIM Sunkee	B-15(초)	KONDRATYEV Vladimir	L-05(초)	LEE Bum-Woo	Dp-II-093
KIM T. H.	D-36	KONG Daejung	B-13(초), Bp-I-020	LEE Byung Cheol	Cp-IV-044
KIM Tae Hee	Dp-V-166	KONG Ki-jeong	D-13	LEE Byung Chul	Dp-V-127
KIM Tae Heon	D-37	KONG So Jeo	Ep-II-094	LEE Byung Kook	Kp-III-037
KIM Tae-dong	Ep-II-081	KONG So-Jeo	Ep-I-027, Ep-V-128	LEE C. H.	L-10(초)
KIM Tae-Hyun	Kp-V-049	KOO Japil	Dp-II-092	LEE C.-H.	L-18
KIM Tae-Hyung	Ep-I-019	KOO Tae-Yeong	PB-02(초)	LEE C.-H.	L-18
KIM Taekyu	Ep-II-055, Gp-III-011	KOTERA Katsushige	B-13(초), Bp-I-020	LEE Chang Bum	K-02(초)
KIM Taekyung	B-07	KOZUKA Yusuke	PB-09(초)	LEE Chang Hoon	D-42
KIM Tae-Suk	PB-12	KREMER Reinhard	PB-13(초)	LEE chang young	Ep-I-002
KIM Taewon	BF-03(초)	KSTAR team	Hp-III-008	LEE Changhan	Fp-IV-002, Fp-IV-003
KIM Taeyoung	Dp-V-147	KUBONO Shigeru	PA-11(초)	LEE cheol eui	Dp-V-223
KIM W. C.	H-07(초)	KUBONO Shigeru	Cp-IV-011	LEE Cheol Eui	Ep-V-113
KIM Wanjoong	K-09(초)	KUBONO Shigeru	PA-15(초)	LEE Cheol Eui	Dp-V-211
KIM Won -Jeong	Dp-V-204	KUDRYAVTSEV Y. V.	Ep-V-103	LEE cheol eui	Dp-II-092
KIM Won-Kyung	Dp-I-042	KUMAR kiran	Kp-V-058	LEE Cheol Eui	Dp-II-113
KIM Won-Kyung	Dp-V-147	KUMAR Sanjeev	Kp-V-066	LEE Cheol Eui	Ep-I-018
KIM Wooyoung	PA-09(초)	KUMAR sanjeev	Kp-V-067	LEE Cheol Eui	Dp-I-052
KIM Y C	Dp-II-061	KURIHARA Kazuyoshi	H-03	LEE Cheol Eui	Dp-I-056, Dp-V-219
KIM Y. K.	D-53	KURINIAWAN KH	G-06	LEE CHEOL JIN	Ep-I-005
KIM Y.J.	Bp-I-019	KUZNETSOV Viacheslav	C-36	LEE Choongki	F-33
KIM Y.K	D-49	KWAK C.H.	Dp-V-131	LEE Chul H.	L-16
KIM Y.S.	PB-08(초)	KWAK C.-H.	Ep-I-026	LEE Chun Sik	Cp-IV-045
KIM Yang-Gyun	D-59	KWAK Jun-Hyuk	Kp-III-018	LEE Chun Sik	PA-15(초)
KIM yeonju	Ep-I-030	KWAK Wooseop	F-24, F-25	LEE Chun Sik	PA-11(초)
KIM Yongsam	DF-02(초)	KWAK Younghee	L-12(초)	LEE Chung Sik	Cp-IV-011
KIM Yoonbai	B-07	KWEON Hyocheon	Dp-II-113	LEE Chung-II	Cp-IV-009, Cp-IV-010
KIM Young Duck	D-21	KWON Bong-Joon	Kp-V-059	LEE D J	Dp-I-009
KIM Young sam	PC-14	KWON daeyoung	Dp-II-108	LEE D.	Dp-II-094
KIM Youngdo	Fp-IV-015	KWON Daeyoung	Dp-I-028	LEE Dae-Sic	Fp-IV-010
KIM Youngkuk	Dp-V-154	KWON Daeyoung	PB-09(초)	LEE Deokjae	Fp-IV-018
KIM Youngman	C-13	KWON Hyeok Jung	Hp-IV-081	LEE Deok-Sun	F-13
KIM Youngnam	Ep-I-014	KWON Hyeok jung	Hp-IV-075	LEE Dong Uk	Dp-V-172
KIM Youngsang	Ep-II-084	KWON Hyosang	Dp-I-024, Dp-I-034	LEE Dong Uk	Kp-III-019
KIM Youngwook	Dp-V-167	KWON Hyuckchan	Ep-II-087	LEE Dong Uk	Kp-III-035
KIM Youngwook	Dp-V-132	KWON Ji Hwan	DF-01(초)	LEE Dong Uk	Kp-III-033, Kp-III-040
KIM Young-You	Ep-II-071	KWON Kyoung-Cheol	Ep-II-083	LEE Dongseon	F-27
KIM Yungi	PC-11(초)	KWON M.	H-07(초)	LEE Eui Wan	Ep-II-094
KIM yungjun	Kp-II-009	KWON Oh-Jang	Ip-III-027	LEE Eui-Wan	Ep-V-128
KIM Yungjun	Kp-II-008	KWON Oh-Jang	Ip-III-020	LEE Eui-Wan	Ep-I-027
KIM Yup	Fp-IV-006	KWON Ohjin	H-11	LEE Eun Seong	Ep-II-066
KIM Zero	Bp-I-001, Bp-I-007	KWON Sei Jin	Hp-IV-081	LEE Eun-Cheol	D-63
KIROVA Natasha	E-11	KWON Sun Il	E-46	LEE Eunmo	Ep-I-018
KITAMURA Masatoshi	K-11(초)	KWON Sungchul	Fp-IV-006	LEE G. S.	H-07(초)
KLIMOV P	L-22	KWON Woo Hyun	Dp-II-116	LEE Gon-Sub	Ep-II-078
KLIMOV Pavel	L-11(초)	KWON Y. S.	DF-17	LEE Gun-Do	D-01
KLIMOV Pavel	L-21	KWON Young Kwan	Cp-IV-045	LEE H. J.	D-43
KO ByeongRok	B-16	KWON Young Kwan	Cp-IV-011, PA-11(초)	LEE H. S.	Dp-I-046
KO Byeongrok	B-31			LEE H. S.	H-08(초)
KO Changhun	D-28	KWON Young Kyun	E-27	LEE H.Y.	L-10(초), L-18
KO Changhyun	Ep-I-022, Ep-V-123	KWON Young Seung	DF-07	LEE hakjoon	Dp-II-117
KO Gunwoo	Ep-II-089	KWON Young Taek	E-18	LEE Hakjoon	Kp-II-008
KO Hyun-Sung	K-09(초)	KWON Young Wan	D-42	LEE Han Sung	D-23
KO In Soo	C-22	KWON Youngjoon	Bp-I-010	LEE Hanju	Ep-II-081
KO Jae-Hyeon	F-21	KWON Young-Kyun	Dp-V-206	LEE Hansung	E-20
KO Je Wou	Bp-I-014	KWON Young-Kyun	Ep-I-017	LEE Hansung	E-03
KO Junsu	F-27	KWON Young-Kyun	E-28	LEE Hayoung	C-40
KO Kyung-Tae	PB-05	KWON Young-Seung	DF-16	LEE Hee-Jo	Ep-I-024
KO Pyungwon	BF-03(초)	KWON Young-Seung	DF-11	LEE Hee-Seock	C-22
KO Yoo Sun	Ep-I-017	KYAE Bumseok	B-24	LEE Ho Keun	Dp-II-060
KOBAYASH T.	C-27	LAO L. L	Hp-III-008	LEE Ho Nyung	D-37
KOBAYASHI A	G-06	LAURENT Terzolo	Hp-III-021	LEE Ho Sueb	Jp-III-004
KOBAYASHI N.	C-27	LAURET Jerome	C-04	LEE Ho Sueb	Dp-V-163, Ep-II-063,
KOH Dong-Wook	F-06	LAW Joseph	PB-13(초)		Ep-II-065
KOH Eui-Kwan	D-42	LAZAUSKAS Rimantas	C-29(초)	LEE Ho-Kuen	Kp-V-051
KOH kenha	Dp-V-151	LEE Alex Taekyung	Dp-V-178	LEE Ho-Sueb	Ip-III-009

LEE Ho-Young	Ep-II-083	LEE Kyu Won	Dp-V-219	LEE soonil	Dp-V-151
LEE Hu-Jong	Dp-II-063	LEE Linda	A-05	LEE Soonil	PC-12(초)
LEE Hu-Jong	DF-13	LEE M.W.	Cp-IV-018	LEE Soo-Young	I-06
LEE Hwa Ryun	Hp-IV-075	LEE Man hee	Ep-I-035	LEE Su Chul	Ep-I-018
LEE Hyeong Rag	Ep-II-094	LEE Manhee	E-34	LEE Su Woong	Ip-III-016
LEE Hyeong-Rag	Ep-V-128	LEE Man Woo	Cp-IV-014, Cp-IV-016	LEE SU WOONG	Ip-III-003
LEE Hyeong-Rag	Ep-I-027	LEE Manwoo	C-22, C-26, Cp-IV-024	LEE Su Yong	Ip-III-016
LEE Hyun Keun	F-33	LEE MANWOO	Cp-IV-038	LEE Su Yong	Ip-III-004
LEE Hyun Kyu	L-13	LEE Manwoo	Lp-III-006	LEE Suhoung	C-13
LEE Hyungjun	D-25	LEE Min-Ho	F-26	LEE Su-Hwan	Ep-II-078
LEE Hyun-Sook	Dp-II-063	LEE Min-ho	Fp-IV-026	LEE Suk Ho	DF-06
LEE Hyun-Sook	DF-13	LEE Moohee	Dp-II-089	LEE Sun Kyung	PA-03(초)
LEE Hyunwon	Dp-V-215	LEE Myang Hwan	Dp-V-180	LEE Sun Sook	Kp-III-037
LEE Hyunwon	Ep-I-022	LEE Myang Hwan	Dp-V-204	LEE SUN YOUNG	D-50
LEE Hyunyeong	Hp-III-024	LEE Myang Hwan	Dp-V-189, Dp-V-197	LEE Sung Chan	Dp-V-180
LEE In-Yeal	Ep-V-120	LEE MyeongJae	B-15(초)	LEE Sung Chan	Dp-V-204
LEE J.	L-10(초)	LEE Myoung-Jae	K-02(초)	LEE Sung Chan	Dp-V-189, Dp-V-197
LEE J. H.	H-07(초)	LEE Myung-Hyun	Ip-III-014	LEE Sung Jong	F-27
LEE Jae Sung	E-46	LEE Naesung	D-23	LEE Sungeun	Bp-I-025
LEE Jae Yong	Ep-II-066	LEE Naesung	E-17, E-20	LEE Sunggeun	B-09
LEE Jae Yong	B-21	LEE Naesung	E-03	LEE Sung-Ik	DF-15
LEE Jae yu	Hp-IV-049	LEE Nam Hoon	Dp-II-082	LEE Sung-Ik	DF-16
LEE Jae-Chul	Dp-II-118	LEE Nam-Hoon	DF-16	LEE Sung-IK	DF-05
LEE Jae-Gwang	Dp-II-116	LEE Nayoung	DF-12	LEE Sung-Youp	Ep-I-027, Ep-II-094
LEE Jae-Yea	DF-13	LEE Nyun Jong	Dp-V-166	LEE Sung-Youp	Ep-V-128
LEE Jae-Yeap	Dp-II-063	LEE S. G.	Hp-III-011	LEE W.	H-01
LEE Jeffrey C.	Dp-II-071	LEE S. J.	Kp-V-060	LEE W.	Hp-III-012
LEE Jeong-Ah	Dp-V-167	LEE S. J.	Ep-V-104	LEE Wanhee	Jp-III-012
LEE Jeong-Ah	Dp-V-132	LEE S. M.	Dp-I-054	LEE Wonjae	H-13, Hp-III-007
LEE Jeong-O	Kp-III-018	LEE S.J.	Bp-I-019	LEE Won-Kyu	PA-03(초)
LEE Jeoung Ju	Dp-V-185	LEE Samyol	Cp-IV-003, Cp-IV-021	LEE Woo-jin	D-44
LEE Jieun	Dp-II-090	LEE Sang Bong	Dp-I-045	LEE Wooyoung	E-01
LEE Jik Lee	L-18	LEE Sang Bong	Dp-II-065	LEE Wooyoung	E-08, E-09, Ep-I-033
LEE Jinhyoung	J-08	LEE Sang Bong	Dp-II-062	LEE Wooyoung	E-07
LEE Jinhyoung	J-07	LEE Sang Bub	Fp-IV-002, Fp-IV-003	LEE Wooyoung	Ep-I-030
LEE Jinhyuk	Fp-IV-027	LEE Sang Hoon	F-12	LEE Y S	Dp-I-009
LEE Jinkyung	Dp-V-167	LEE Sang Hoon	F-23	LEE Y. O.	C-22
LEE Jinwoo	Fp-IV-027	LEE Sang Mok	Dp-V-190	LEE Y. P.	Ep-V-103
LEE Jinwoo	D-58	LEE Sang Won	Dp-V-128	LEE Y. P.	Ep-V-104
LEE Jinwoo	Dp-V-191	LEE SANG YUN	Ep-I-008	LEE Y.-B.	Ep-I-026
LEE Jinwoo	F-27	LEE Sangbong	Dp-II-070	LEE Y.O.	Cp-IV-018
LEE Jong Duk	Dp-V-185	LEE Sang-Bum	I-06	LEE Yealee	Dp-V-154
LEE Jong Hwan	Cp-IV-014	LEE Sanghoon	Dp-II-117	LEE Y-O.	Cp-IV-024
LEE Jongmin	Ip-III-037	LEE sanghoon	Kp-II-009	LEE Yong Ho	Ep-II-087
LEE Joo Hyung	D-21	LEE Sanghoon	Kp-II-008	LEE Yong Wook	K-01(초)
LEE Joon Sung	Ep-II-056	LEE Sanghwa	Kp-V-050	LEE Yong Wook	Dp-I-012
LEE Jooyong	Kp-V-057	LEE Sanghwa	D-57	LEE Yong Wook	Ep-II-086
LEE Jooyoung	Fp-IV-027	LEE Sangkyung	J-10	LEE YONG WOOK	Ip-III-007
LEE Jooyoung	F-27	LEE Sang-Myung	Dp-V-127	LEE Yoon Sang	Dp-I-022
LEE Jouhahn	E-26	LEE Sangwook	Dp-V-167	LEE Young Hee	Dp-V-128
LEE Ju Hahn	PA-15(초)	LEE Sangwook	Dp-V-132	LEE Young Hee	E-21, Ep-I-019
LEE Jun Min	E-01	LEE Sangyeop	Kp-II-008	LEE Young Joo	Ep-V-123
LEE Jun Min	E-07	LEE Sangyoul	Kp-III-030	LEE Young Ouk	Cp-IV-044
LEE Jung-Ah	Dp-V-127	LEE sangyup	Dp-II-117	LEE YoungPak	Ep-II-062
LEE Jung-Keun	Ep-V-107, Ep-V-111	LEE Seongjae	Dp-V-174	LEE Young-Seok	Hp-III-001, Hp-III-010
LEE junmin	Ep-I-030	LEE Seung Hyun	E-07	LEE Younjoo	Dp-V-205
LEE Kang Seog	C-01(초)	LEE Seung Ran	D-21	LEE Youn-Seoung	Kp-V-055
LEE Kang Seog	Cp-IV-023	LEE Seung Wha	Dp-II-116	LEE Yun Sang	Dp-V-203
LEE Kiejin	Ep-II-081	LEE Seungho	E-17, E-20	LEE Yun Sang	PB-11
LEE Kimoon	Dp-I-019	LEE Seunghun	Dp-I-042	LEE Yun-Hi	Dp-V-127
LEE Kimoon	Ep-II-089	LEE Seunghun	Dp-V-147	LEE Yun-Hi	Dp-II-097
LEE Kiuck	A-05	LEE Seunghyun	E-08, E-09	LEE, Hyo Jong	K-07(초)
LEE Ki-Won	Ep-II-071	LEE seunghyun	Ep-I-030	LEEM C. S.	D-53
LEE Kwang H	Ep-II-089	LEE Seungran	Dp-V-208	LEPS Collaboration	C-17
LEE Kwang-Sei	Dp-I-052	LEE SEUNGRAN	E-37	LI GUO JIE	Kp-V-064
LEE Kwang-Sei	Dp-V-186, F-21, Fp-IV-011	LEE Seungran	E-50	LI Guojie	Dp-I-006
LEE Kyu Won	Dp-V-223, Ep-V-113	LEE Soo-Hyoung	E-26	LI Jin	B-25
LEE Kyu Won	Dp-II-113	LEE Soohyung	B-31	LI Tiefu	K-03(초)
LEE Kyu Won	Dp-I-056	LEE Soonchil	D-43	LI Xiangxu	E-50
		LEE Soon-Gul	Dp-II-073	LI Xianhong	Dp-V-174

LI Y.J.	B-25	MUNSAT T	H-01	NOH T. W.	D-36
LI Z.H.	C-27	MYOUNG Nojoon	Dp-V-213	NOH T. W.	Dp-II-094
LIANG T	H-01	N Danilov	Bp-I-006	NOH Tae W.	PB-08(초)
LIANG T.	Hp-III-012	N. Danilov	B-14(초), B-35, B-36,	NOH Tae Won	Dp-I-022
LIM Ae Ran	Dp-I-047		Bp-I-009	NOH Tae Won	D-37
LIM H.	L-18	N. Saito	BF-07(초)	NOH Tae Won	PB-11
LIM Heuijin	L-10(초)	N. T. Tung	Ep-II-036	NOH Tae Won	Dp-V-203
LIM Hyunjin	Ep-I-009	N. T. Tung	Ep-II-039	NOHARA Minoru	DF-06
LIM Jae-Sung	Ep-II-083	N. T. Tung	Ep-II-037	NOJIRI H.	Dp-II-119
LIM James	J-08	NA G.W	L-18	O ByeongGyun	D-21
LIM Jongseok	J-10	NA H. K.	H-07(초)	O Byeonggyun	D-46
LIM Woochang	F-34	NA Jong ho	K-11(초)	OH Cha-Hwan	lp-III-015
LINDER E. V.	L-10(초)	NA Junhong	Kp-III-041	OH Changheon	L-16
LINDER E. V.	L-18	NA Sang-Bin	Kp-III-036	OH Dong-Hwa	D-12
LIPING Zhu	H-10	NA SEWOONG	Dp-II-068	OH Dong-Hwa	D-11
LIU CHUNLI	Ep-II-059	NA sewoong	Dp-II-069	OH Dong-Hwa	D-06
LIU Chunli	Fp-IV-023	NA Sewoong	PB-13(초)	OH Hyoungyun	Ep-I-022
LIU X.	Dp-II-117	NA Sung-Ho	Dp-I-040, Dp-II-105,	OH Hyoung-yun	Ep-V-123
LIU X.	Kp-II-009		L-12(초)	OH Hyungju	DF-19
LIU X.	Kp-II-008	NA Yong-Su	H-11, H-13, Hp-III-004,	OH In-Hwan	Dp-V-186
LO Young-Seop	Kp-III-018		Hp-III-015	OH In-Hwan	Dp-I-052
LU WENJIAN	D-31	NA Yong-Su	Hp-III-006	OH In-Hwan	Dp-II-092
LUC Huy Hoang	Dp-II-087	NA Young-Su	Hp-III-007	OH Kunsu	C-40
LUHMANN, JR. N. C.	Hp-III-012	NAGAIHIRO Hideko	C-10(초)	OH Kyungwhan	Kp-II-007
LUHMANN, JR. N. C.	H-01	NAGAOSA Naoto	D-47	OH Mina	F-27
LUSTERMAN W.	Lp-III-006	NAKAMURA T.	C-27	OH S. J.	Dp-I-054
LYEO H.-K.	E-22	NAKAMURA Takashi	PA-08(초)	OH S.-J.	Dp-V-209
LYO In-Whan	Dp-V-210	NAKANO T	C-17	OH Sang Soon	Dp-I-053
LYO In-Whan	Dp-V-191	NAKANO Takashi	C-31	OH Sangjun	Dp-II-082
LYO In-Whan	Dp-V-205	NAKAYAMA Y.	C-27	OH Seong Yong	Hp-IV-073
M. Hyata	BF-07(초)	NAM Dong Hak	PB-05	OH Y.K.	H-07(초)
M. leiri	BF-07(초)	NAM In Hyuk	Hp-IV-073	OH Yoon Seok	PB-05
M. Kurosawa	BF-07(초)	NAM Inhyuk	Hp-IV-055	OH Young Jun	D-39
M.G. SUNG	Kp-III-020	NAM J.	L-10(초)	OH Youngdo	C-22, C-26
MA J. X.	PB-10(초)	NAM J.W.	L-18	OHTA Hiromichi	PB-11
MALBERTI Martina	Bp-I-004	NAM Jeong Ho	D-11	OLSEN Stephen L.	B-15(초)
MARATHE Shashidhara	E-52	NAM S.	L-10(초), L-18	OLSEN Stephen Lars	BF-02(초)
MARQUES F.M.	C-27	NAM S. H.	H-08(초)	ONODA Shigeki	D-47
MATHEWS Grant J.	L-05(초)	NAM S.H.	Hp-IV-086	ORR N.A.	C-27
MATSUSHITA M.	C-27	NAM Sang-Hoon	Hp-IV-067	ORTIZ D.	D-36
MEAN B. J.	Dp-I-047, Dp-II-071,	NAM Siyoung	B-11	OSMINER Teresa	D-45
	Dp-II-089	NAM Soon-Kwon	Hp-IV-052,	OTSU H.	C-27
MEVEN Martin	Dp-I-052		Hp-IV-053, Hp-IV-066	OUCHI Yukio	D-61
MIN B. I.	PB-17(초)	NAM Soon-Kwon	Bp-I-028	OZAKI Sho	C-10(초)
MIN B.I.	Dp-II-090	NAM W. C.	Ep-V-104	PACKARD Jay	C-04
MIN Jae Ki	Kp-III-037	NAM Yeonghwan	F-25	PAEK Kyeong-Kap	Dp-V-127
MIWA .K	C-19	NAM Young Woo	E-16	PAIK Ungyu	Kp-III-036
MIWA K.	C-20	NAMKUNG W.	H-08(초)	PAK Eun Sick	Dp-I-048
MIYASHITA Y.	C-27	NAMKUNG WON	Cp-IV-038	PAPPAS David P.	D-45
MOK Chinook	Hp-III-026	NAMKUNG Won	C-22, C-26	PARK Bae-Ho	Dp-I-047, Dp-II-071
MOON Bongjin	D-61	NAOKI Masuda	F-31	PARK Byung-cheol	Dp-V-196
MOON Byung Kee	Dp-I-025, Ep-II-063	NARAYANAN Suresh	D-10	PARK C. D.	H-08(초)
MOON Changbum	PA-13(초)	NAZAROV Mihail	lp-III-003	PARK C. D.	Dp-I-049, Dp-I-055
MOON Chang-Youn	DF-09	NGUYEN Ba Phi	lp-III-013	PARK C.I.	Dp-V-131
MOON HYERIM	Dp-V-160	NGUYEN Hoang Hai	Dp-II-087	PARK Chang Yong	PA-03(초)
MOON Hyerim	Dp-V-162	NGUYEN Manh Cuong	Dp-V-154	PARK Chang Young	Dp-V-185
MOON Hyerim	D-61	NGUYEN Thi Minh Hien	Dp-II-087,	PARK changin	Ep-I-026
MOON Hyeyoung	Ep-I-014		Dp-II-094	PARK Changwon	Dp-V-154
MOON Jisoo	DF-08	NGUYEN Van Minh	Dp-II-086	PARK Chanwoo	Dp-V-174
MOON Jongchul	PA-03(초)	NI Andrey	C-36	PARK Cheonsoo	B-02
MOON Jun Young	Cp-IV-045	NIKI Hideaki	H-03	PARK Chong-Do	Hp-IV-067
MOON Jun Young	PA-15(초)	NISHIYAMA Miho	B-13(초), Bp-I-020	PARK Chong-Yun	D-06
MOON Kyoung-Woong	Dp-II-093	NOH Do Young	lp-III-016	PARK Chong-Yun	D-11
MOON Kyoung-Woong	Dp-II-118	NOH Do Young	DF-02(초)	PARK Chong-Yun	E-18
MOON Kyungsun	Dp-V-129	NOH DO YOUNG	lp-III-004	PARK Chul-Hong	Dp-I-040
MOON Seung Ho	Dp-V-166	NOH Do Young	lp-III-003	PARK Daehyun	E-04
MOON Soon Jae	Dp-I-022	NOH Han-Jin	PB-17(초)	PARK Daniel Yun	Dp-V-208
MOON Soon Jae	PB-11	NOH Jae Dong	DF-05	PARK Dongho	L-15
MOTOBAYASHI T.	C-27	NOH Jae Dong	DF-15, F-18	PARK Dong-Won	Kp-III-018
MUHAMMAD Shahid	Ep-I-012	NOH Ji-Young	Dp-II-100	PARK Doyoung	Dp-I-024

PARK Goon-Ho	Kp-III-033	PARK Sora	E-28	ROBINSON Ian K.	E-23
PARK Gwangseo	Dp-I-024, Dp-I-034	PARK Sun Mi	Ep-II-094	ROESER Ulf	Lp-III-006
PARK Gyeongsoo	E-50	PARK Sung Chan	Kp-III-041	ROH Jong Wook	Ep-I-033
PARK H. K.	H-01, Hp-III-012	PARK Sunghun	D-18	ROH Jongwook	E-09
PARK H.K.	B-39	PARK Sung-Ju	Hp-IV-067	ROH Young Sup	Dp-I-044
PARK Hae-Ryeong	Ip-III-014	PARK Sungmin	Dp-I-024, Dp-I-034	ROSS Harder	E-23
PARK Hahnbeom	F-27	PARK Sun-Mi	Ep-I-027, Ep-V-128	ROTERMUND Fabian	Ip-III-013
PARK Hee Chul	Dp-V-217	PARK Tae Joo	DF-01(초)	ROTH Siegmur	E-16
PARK HONGWOO	E-37	PARK Tae-Sun	C-29(초)	RYOU Junga	Dp-V-201
PARK HyunKook	D-05	PARK Tuson	Dp-I-021	RYU Byungki	D-39, Dp-V-200
PARK I.	L-10(초), L-18	PARK Won Il	KF-08(초)	RYU Chang-Mo	Hp-III-026
PARK Ikgon	Dp-V-217	PARK Wongoo	Dp-V-209	RYU Chungryeol	PA-10(초)
PARK Inkyu	Cp-IV-002	PARK Y.S.	Hp-III-006	RYU Geonmo	Cp-IV-002
PARK Inkyu	Bp-I-027	PARK Yeun-Soo	Cp-IV-013	RYU Geonmo	Bp-I-027
PARK insuk	Dp-II-061	PARK Yongsup	Dp-V-206	RYU Huiyoung	C-30
PARK J H	Dp-I-009	PARK Youngseok	Hp-III-024	RYU Junghee	J-08
PARK J.	L-10(초), L-18	PARK Youngsoo	K-02(초)	RYU Soo	B-15(초)
PARK J. H.	Dp-V-169	PARK Yun Daniel	D-21	RYU Young-Ho	Kp-V-055
PARK J.M.Sungil	Dp-II-092	PARK Yun Daniel	Dp-V-153	S. B. Joa	Hp-III-045
PARK J.-N.	Dp-II-119	PARK Yun Daniel	D-45	S. J. Lee	Ep-II-037
PARK Jae-Hoon	PB-05	PARK Yun Daniel	E-50	S. Y. Jang	Dp-I-017
PARK Jae-Hyun	Dp-II-063	PARK Yun Daniel	D-46	S.G. PARK	Kp-III-020
PARK Jae-Hyun	DF-13	PARK Yung Woo	E-16	S.H. Kim	BF-07(초)
PARK Jae-Kyu	Kp-V-051	PATIL P. S.	PC-14	S.J. Kim	BF-07(초)
PARK Jea-Gun	Kp-V-049, Kp-V-051	PATOLE Shashikant	E-12	S.-J. Oh	Dp-I-017
PARK Jea-Gun	Kp-III-036	PENKOV. V. Oleksiy	Hp-III-045	S.L. Olsen	B-25
PARK Jea-Gun	Ep-II-078	PEREZ-WURFL I.	PC-06(초)	SAITO Take R.	C-14(초)
PARK Jea-Gun	Ep-II-083	PHAM Xuan Huu	Dp-II-086	SAKUMA Takayuki	B-13(초)
PARK Jeehae	D-60	PHARK S.-H.	PB-08(초)	SAKURAI H.	C-27
PARK Jewook	DF-10	PHARK Soo-Hyon	PC-05	SAM KYU Noh	Kp-II-001
PARK Ji Eun	Dp-V-217	PHUNG Duy Khuong	I-07	SANDY Alec	I-08
PARK Jin Hong	PB-04(초)	PODE Ramchandra	Ep-I-020	SANG BEOM Joa	Hp-III-037
PARK Jin Su	Dp-V-197	PODE Ramchandre	Ep-I-034	SANG JUN Lee	Kp-II-001
PARK Jina	Jp-III-012	PRAVEENA Ravipati	Ep-II-054	SANG-WOOK Han	Dp-V-135
PARK Jin-Hyung	Kp-III-036	PRELLIER Wilfrid	Dp-V-203	SANJAY Krishna	Kp-II-001
PARK Jin-Soon	Ep-II-066	PRICE Nathan D.	F-29	SARRAO J.L.	D-52
PARK Jin-Sub	Kp-V-059	PROKHOROV V. G.	Ep-V-103	SATOU Y.	C-27
PARK JIn-Woo	Hp-III-004	QU Xuesong	Dp-V-195	SATOU Yoshiteru	PA-12(초)
PARK Jong Bae	E-26	R. Balakrishnaiah	Ep-II-063, Ep-II-065	SCHECHECHTER Joseph	C-28(초)
PARK Jong-Moon	Ip-III-014	R. Shenoi	Kp-II-001	SCHROEDER Herbert	KF-04(초)
PARK Jong-Uk	L-12(초)	R.C Block	Cp-IV-015	SEO Gi Wan	Dp-I-012
PARK Jong-Yun	D-12	RA Eun Ju	E-21	SEO Gi Wan	Ep-II-086
PARK Joo Hyun	Ep-II-066	RAGUNATHAN Kaushik	D-60	SEO Jung-Hye	Kp-V-055
PARK Jun	Hp-IV-081	RAH S. Y.	H-08(초)	SEO Ki Bong	Kp-III-035
PARK Jun Kue	Ep-V-113	RAHAMAN H.	Hp-IV-086	SEO Ki Bong	Kp-III-033
PARK Junghun	Dp-V-208	RAHAMAN Hasibur	Hp-III-043	SEO M. S.	Ep-V-104
PARK Jung-Yong	Ep-II-083	RAHMAN Md. Shakilur	C-22	SEO Minky	Dp-V-141
PARK Kyoung Ja	PB-17(초)	RATNAM B.V.	Jp-III-004	SEO S.Y.	Dp-V-131
PARK Naewoong	C-28(초)	REE M.	H-08(초)	SEO S.-Y.	Ep-I-026
PARK Pil-Ho	L-12(초)	REEDY Robert C	L-06(초)	SEO SEUNG-JUN	Ep-II-057
PARK S. H.	Kp-V-060	REHMAN Mustaq	Dp-V-177	SEO Sunae	Dp-V-132, E-50
PARK S. J.	H-08(초)	RHA Kicheol	Hp-III-026	SEO Sunae	Dp-V-167
PARK S. S.	H-08(초)	RHA Sa-Kyun	Kp-III-028, Kp-V-055	SEO Y K	Dp-I-009
PARK S.-H.	Ep-I-026	RHEE Bum Ku	Ip-III-022	SEO Yohan	Ep-II-084
PARK S.S.	Hp-IV-086	RHEE Ilsu	Dp-V-142	SEO Yong Gon	Kp-II-007
PARK Sang Kook	Dp-I-045, Dp-II-065	RHEE J. Y.	Ep-V-103	SEO Yunseok	B-01
PARK Sang Kook	Dp-II-062	RHEE J. Y.	Ep-V-104	SEOK Chaok	F-27
PARK Sang-il	E-36	RHEE J.T.	Bp-I-019	SEONG Won Kyung	Dp-II-082
PARK Sangkook	Dp-II-070	RHEE June Tak	E-46	SEONG Won Kyung	Dp-II-073
PARK Sangnam	Cp-IV-002	RHEN Danielle	E-12, Ep-I-029	SHAHID Muhammad	Dp-V-175,
PARK Sangnam	Bp-I-027	RHIM Jun-Won	Dp-V-129		E-12, E-40, E-44,
PARK Sangwook	PC-06(초)	RHO Mannque	C-08(초)		Ep-I-013, Ep-II-075
PARK Se-Hwan	Cp-IV-044	RHYEE J. S.	DF-17	SHAKIR Imran	Dp-V-175, E-12, E-40,
PARK Se-Jeong	Dp-V-176	RHYEE Jong-Soo	DF-11		E-44, Ep-I-012,
PARK Serin	Kp-III-018	RI Hyeong-Cheol	Dp-II-065		Ep-I-013, Ep-II-075
PARK Seung Ryong	D-53	RIM Min Ho	Ip-III-022	SHAO J.	Kp-II-001
PARK Seungmin	Kp-V-057	RO Tae-Ik	C-22, C-26	SHARMA Y.	Kp-II-001
PARK Seung-young	D-37	RO Tae-Ik	Cp-IV-014	SHASHIDHARA Marathe	I-08
PARK Soonyong	PB-10(초)	RO TAE-IK	Cp-IV-015	SHENG I. C.	Dp-I-049, Dp-I-055
PARK Sora	Ep-I-017	RO Tae-Ik	Cp-IV-016	SHI J.	PB-10(초)

SHIM E. L.	Dp-V-169	SONG jong hyun	Dp-II-108	TENREIRO Claudio	C-21(초)
SHIM KYU HWAN	Kp-V-047	SONG Keun Man	PC-05	TERANISHI Takashi	PA-15(초)
SHIM Kyu-Hwan	Kp-V-050	SONG Sanghoon	Dp-V-215	THO Do Duy	Hp-IV-073
SHIM Kyu-Min	A-16	SONG Sanghoon	D-10, Dp-V-218	THOMAS Kalarikad Jonah	K-08(초)
SHIM Seong Hoon	Dp-II-097	SONG Sanghoon	E-23	THOMPSON J.D.	D-52
SHIM Sojung	E-43	SONG Sanghyeon	Bp-I-001, Bp-I-007	THOMPSON Joe	PB-15(초)
SHIM Tae-Hun	Kp-V-049, Kp-V-051	SONG T. K.	Dp-I-050	TOBIAS B	H-01
SHIM Young-Bo	Ip-III-027	SONG T. K.	D-36	TOBIAS B.	Hp-III-012
SHIMOURA S.	C-27	SONG Tae Kwon	Dp-V-180	TOGANO Y.	C-27
SHIN B.K	Lp-III-007	SONG Tae Kwon	Dp-V-204	TOSHINORI Ikuno	Bp-I-020
SHIN B.K.	Lp-III-001	SONG Tae Kwon	Dp-V-189, Dp-V-197	TRAN Dong Hai	Dp-II-087
SHIN Bokkyun	Lp-III-004	SONG Tae Kwon	D-37	TSHOO K.H.	C-27
SHIN Bong Gyu	D-12	SONG Taegeun	Dp-V-217	TSOGBADRAKH Namsrai	D-44
SHIN Byong Wook	Ep-II-094	SONG Tae-Yung	Cp-IV-044	TSUKERBLAT Boris	Ip-III-003
SHIN Byong-Wook	Ep-I-027, Ep-V-128	SONG Wooseok	E-18	TUSON Park	Dp-II-080
SHIN H.-Y.	Dp-V-169	SONG Yoo-Jang	DF-11	UDDIN Md. Nizam	Dp-I-051
SHIN Heung Soo	PC-05	SONG Young gi	Hp-IV-075	ULLAH Aman	Dp-I-002
SHIN Hyeonjoon	B-11	SONG Young-Ho	C-29(초)	UNNO Y.	Bp-I-021
SHIN Hyun Joon	Dp-V-127	SPROUSE Gene D.	PA-02(초)	UOZUMI Satoru	B-13(초), Bp-I-020
SHIN Hyunjoon	Ip-III-009	STANTON C. J.	PC-01(초)	USEONG Kim	Dp-I-017
SHIN Jaeoh	F-09	STEIGENBERGER Uschi	PA-05(초)	V. D. Lam	Ep-II-039
SHIN JaeWon	C-32	SU X. M.	J-06	V. D. Lam	Ep-II-036
SHIN JaeWon	Cp-IV-009, Cp-IV-010	SUDO Yuji	B-13(초), Bp-I-020	V. D. Lam	Ep-II-037
SHIN Jeongkyu	Fp-IV-020	SUH B. J.	Dp-II-115, Dp-II-119	V. PENKOV Oleksiy	Hp-III-037
SHIN Jinsik	Dp-II-117	SUH In-Saeng	L-05(초)	V. T. T. Thuy	Ep-V-105
SHIN jinsik	Kp-II-009	SUH J.E.	L-18	V. T. T. Thuy	Ep-II-039
SHIN Kwangwoo	Dp-V-218	SUH Jooyoung	Dp-II-122	V. YU. Plaksin	Hp-III-045
SHIN MI IM	Kp-V-047	SUH Tae-Suk	Cp-IV-009, Cp-IV-010	V.A. Sidorov	Dp-I-021
SHIN Mii-Hee	Kp-V-049	SUK Hyyong	Hp-IV-073	VADIM YU. PLAKSIN	Hp-III-037
SHIN R. H.	Ep-II-099	SUK Hyyong	H-05	VENTO Vicente	C-33
SHIN Seung-Woo	F-27	SUK Hyyong	Hp-IV-055	VICTOR V. Kulagin	Hp-IV-055
SHIN Sunyoung	B-09	SUK Hyyong	H-15	VIERTEL Gert M.	Lp-III-006
SHIN Yooleemi	D-16	SUMIKAMA T.	C-27	VON GUNTEN Hanspeter	Lp-III-006
SHIN Young-Hong	L-12(초)	SUN Liling	DF-16	W. H. Jang	Ep-II-036, Ep-II-039
SHOCK Jonathan	B-01	SUNDARAY Bibekananda	E-15	WANG Cai-Zhuang	D-01
SIM H.-S.	D-18	SUNG Choongki	Hp-III-015	WANG Taofeng	C-26
SIM Jin Woo	Dp-I-048	SUNG Chungki	Hp-III-024	WANG Taofeng	Cp-IV-014, Cp-IV-016
SIM Kyu Yun	E-21	SUNG Gun Yong	K-09(초)	WANG X. F.	DF-05
SIN Sang-Jin	B-01	SUNG Gunyong	Dp-V-174	WASER Rainer	KF-04(초)
SINHA S. K.	D-10	SUNG Hojin	PB-17(초)	WIEDEMANN H.	H-08(초)
SKAKALOVA Viera	E-16	SUNG Hyun-Su	Ep-II-078	WON Choong Jae	Dp-I-022
SKOY VADIM	Cp-IV-038	SUNG Wokyung	F-08	WON Eunil	B-16, B-17, B-31
SKULLERUD Jon-Ivar	B-18	SUNG Wokyung	F-09	WOO Bonghee	Dp-I-021
SMET Jurgen H.	E-16	SUNG Y. S.	Dp-I-050	WOO Byung-chill	Dp-V-141
SMOOT G. F.	L-10(초)	SUNG Yeon Soo	Dp-V-180	WOO Heon	E-46
SMOOT G. F.	L-18	SUNG Yeon Soo	Dp-V-204	WOO Jong-Kwan	Bp-I-014
SO Hye-Mi	Kp-III-018	SUNG Yeon Soo	Dp-V-189, Dp-V-197	WOO Seongwoo	Dp-V-162
SO Kang Pyo	Ep-I-019	SURESH Narayanan	I-08	WOO SEOUNGWOO	Dp-V-160
SO Y.H.	PC-06(초)	SVENSSON Johannes	E-11	WOO SUNG Park	C-07
SOBAHAN KMABdus	Ip-III-021	T. Hayakawa	BF-07(초)	WOOCHANG Lee	H-10
SOHLER D.	C-27	T. Hibi	BF-07(초)	WOORYOUNG JANG	Cp-IV-038
SOHN Sang Ho	Dp-V-190	T. Kishimoto	BF-07(초)	WU Weida	PB-10(초)
SOHN Youngsoo	Bp-I-010	T. Takabatake	Dp-II-126	WU youngsoo	Dp-I-028
SON . D	Hp-III-011	T. Yoshida	BF-07(초)	XIE Xiaoyin	D-63
SON ChangWook	C-40	T. U. Um	Ep-V-105	Y. Danon	Cp-IV-015
SON D.C.	B-39	T. W. Noh	Dp-I-017	Y. Fukao	BF-07(초)
SON K.	Dp-II-115	TAEHYUNG Kim	Ep-I-031	Y. Saiga	Dp-II-126
SON Myeong Rak	Ep-II-094	TAKAGI Hidenori	DF-06	Y. Shimizu	BF-07(초)
SON Myeong-Rak	Ep-V-128	TAKAMI Hidefumi	Ep-I-011	Y. P. Lee	Ep-V-105
SON Myeong-Rak	Ep-I-027	TAKAYUKI Sakuma	Bp-I-020	Y. P. Lee	Ep-II-036
SON Seung-Woo	Fp-IV-015	TAKESHITA Tohru	B-13(초), Bp-I-020	Y. P. Lee	Ep-II-039
SON Seung-Woo	F-28	TAKEUCHI S.	C-27	Y. P. Lee	Ep-II-037
SON Yoon Gyu	Hp-IV-081	TAN H. Hoe	Kp-V-072	Y. S. Lee	Ep-II-039
SON YOUNG-WOO	Dp-V-160	TAN H. Hoe	Kp-V-054	Y.S. KIM	Kp-III-020
SONG C. H.	Dp-I-054	TANAKA Hidekazu	Ep-I-011	YAKHSHIEV Ulugbek	C-12
SONG D.	PC-06(초)	TANAKA Hidekazu	PB-07(초)	YAN CUI	Dp-V-128
SONG D. J.	D-53	TANAKA K.N.	C-27	YANG Chan Uk	D-45
SONG In Chan	E-46	TANAKA N.	C-27	YANG Chanuk	D-46
SONG Inkyung	D-11	TANAKA s	G-06	YANG H.I.L.	H-07(초)
SONG Jihye	C-40	TANIDA Kiyoshi	BF-05(초)	YANG Heon-Deok	Kp-V-050

YANG Hyun Kyoung	Dp-I-025, Dp-V-195	YOO In-Kwon	C-40	YOU Hee Wook	Kp-III-035
YANG In-Sang	Dp-II-086, Dp-II-087, Dp-II-094	YOO Insun	Ep-I-022	YOU Sangha	Kp-III-025
YANG Jae-Suk	F-24, F-25	YOO Insun	Ep-V-123	YOUN Hyung-Joong	E-26
YANG Jeonghwa	Dp-II-102	YOO Jai Seung	E-16	YOUN Min Young	PA-15(초)
YANG Jeonghwa	D-15	YOO Sung-moon	L-12(초)	YOUNGHEE Lee	Ep-I-031
YANG Jongheon	Dp-V-174	YOO Taehee	Dp-II-117	YU Chaehyun	BF-03(초)
YANG S. M.	D-36	YOO taehee	Kp-II-009	YU Dai-Hyuk	PA-03(초)
YANG Sang Mo	D-37	YOOK Jong-Gwan	Ep-I-024	YU Dantong	C-04
YANG Seolun	D-05	YOON C.J.	C-19	YU H. J.	L-10(초)
YANG Sun A	Dp-I-023, Dp-I-027	YOON Chong Chul	Hp-IV-081	YU H.J.	L-18
YANG Tae-gun	Cp-IV-021	YOON Choon Sup	Ip-III-022	YU J.	PB-08(초)
YANG Tae-Keun	Cp-IV-013	YOON CHUL OH	PC-10(초)	YU JAE - IN	Ep-II-057
YANG Y. S.	Dp-I-054	YOON DUHEE	Dp-V-160	YU Jae Joon	Dp-I-022
YANG Yong Suk	Dp-I-051	YOON Duhee	Dp-V-162	YU Krylov	B-14(초), B-36, Bp-I-006,
YANG Yuchul	B-13(초), Bp-I-020	YOON Euijoon	D-01		Bp-I-009
YAO Takafumi	Kp-V-059	YOON Hee-Jeong	PB-02(초)	YU Kwon Kyu	Ep-II-087
YASUI Shigehiro	C-15(초)	YOON J.-G.	D-36	YU. Krylov	B-35
YEE K J	Dp-I-009	YOON Jaeho	Ip-III-009	YU.M. Gledenov	Hp-III-010
YEO H. G.	Dp-I-050	YOON Jin-Hee	Cp-IV-005	YUE Q.	B-25
YEO Seung Jun	Ep-I-020	YOON Jong-Gul	D-37	YUM Dahyun	Jp-III-012
YEOM Han Woong	D-08	YOON Jung-Ran	Cp-IV-016	YUN Chan Ki	E-14
YI Chang-Hwan	Ip-III-040	YOON KwanSeok	E-36	YUN Chong Cheoul	Cp-IV-045
YI Gyu-Chul	E-37	YOON Kyung Byung	Ep-I-009	YUN Chong Cheoul	PA-15(초)
YI Jin Neung	Ep-II-094	YOON Kyung Byung	E-23	YUN Chong Chul	Cp-IV-040
YI Jin-Neung	Ep-I-027, Ep-V-128	YOON Moohyun	Hp-IV-046	YUN G.	Hp-III-012
YI JunGyu	C-40	YOON Moohyun	Hp-IV-049	YUN G. S.	H-01
YI Juyeon	F-19	YOON S	H-04	YUN Hoyeol	Dp-V-167
YI Juyeon	F-06	YOON S H	Dp-V-167	YUN Hoyeol	Dp-V-132
YI Soung Soo	Dp-V-163	YOON S.	Dp-I-009	YUN Jae Ho	Ep-II-099
YI Soung Soo	Ep-II-063, Ep-II-065	YOON S.-W.	Dp-V-169	YUN Wan Soo	Ep-II-056
YI Soung-Soo	Jp-III-004	YOON Seok-Heun	Dp-II-115, Dp-II-119	YUN Won Seok	Dp-II-124
YI Soung-soo	Ip-III-009	YOON Seok-Jin	Hp-III-001	ZHANG C. L.	D-43
YI Su Do	D-47	YOON Seok-Jin	Ep-II-097	ZHENG T.	C-27
YI Sumin	Hp-III-005	YOON Seok-Jin	Ep-II-062	ZHUO Z. C.	J-06
YIM Jonghyuk	PC-12(초)	YOON Sunghyun	D-41	ZHUO Zhong Chang	Jp-III-010
YONEDA K.	C-27	YOON Youngwoon	Ep-II-081	ZOAKOS Dimitrios	B-01
YOO H.-I.	E-22	YOSHIDA Y.	D-53	ZOU Jin	Kp-V-054
		YOSHIDA Yoshiyuki	D-55	ZOU Jin	Kp-V-072
		YOSHINAGA K.	C-27		

## 한국물리학회 조직명단

### 이사회

회 장 / 이영백  
부회장 / 권재술 김영순 노태원 박상일 박영아 이주열 이철의 정문성  
정창섭 조무현 황보창권 강태원(특별부회장)  
이 사 / 김건호 김도성 김영태 김정구 김재욱 김형국 남기봉 노삼규  
민동필 박승한 박종윤 배세환 손동철 오석근 오세정 우정주  
이경수 이공주복 이용희 이인원 임채호 최치규 한창희  
감 사 / 고인수 김철성

### 실무이사회

실무이사장 / 이철의  
총무담당실무이사 / 정세영  
재무담당실무이사 / 이보하  
새물리편집담당실무이사 / 정옥희  
JKPS편집담당실무이사 / 김항배  
홍보잡지편집담당실무이사 / 윤태현  
CAP편집담당실무이사 / 오경환  
물리교육담당실무이사 / 오원근  
학술담당실무이사 / 조월령  
섭외담당실무이사 / 김동호  
사업담당실무이사 / 김주진 임혜인 박인규 김중복 김기원  
총무부실무이사 / 홍석륜  
재무부실무이사 / 박지용  
새물리편집부실무이사 / 고재현  
JKPS편집부실무이사 / 홍승훈, 이윤상  
홍보잡지편집부실무이사 / 강지훈  
CAP편집부실무이사 / 문봉진  
물리교육부실무이사 / 김재우  
학술부실무이사 / 정종훈  
섭외부실무이사 / 정창욱  
사업부실무이사 / 한영근 정난주 이창환 이봉우 윤영귀

### 편집위원회

#### 홍보잡지편집위원회

자 문 위 원 / 이충희 최병두 황정남 김재욱  
위 원 장 / 조무현  
실 무 이 사 / 윤태현  
부실무이사 / 강지훈  
위 원 / 김문덕 김용민 김윤기 김윤배 김은규 김현철 송태권 신현준  
안기석 안상현 양동석 엄종화 육순형 이인호 정재호 정진석

#### 새물리 편집위원회

위 원 장 / 황보창권  
실 무 이 사 / 정옥희  
부실무이사 / 고재현  
위 원 / 김종락 김재완 박일우 박정만 송중현 유준희 이동한 이윤상  
이해준 이희정 조재홍 천병구 최재혁 E.J. Button

#### JKPS 편집위원회

위 원 장 / 이주열  
실 무 이 사 / 김항배  
부실무이사 / 홍승훈, 이윤상  
위 원 / 고도경 광종구 김주진 박혁규 서민아 윤의준 이근섭 장문규  
조병기 조용훈 조인용 천명기 천승현 최수용 한재원 홍지상  
황윤희 E.J. Button C.J. Wolfe

### 편집위원회

#### CAP 편집위원회

위 원 장 / 노태원  
실 무 이 사 / 오경환  
부실무이사 / 문봉진  
위 원 / 김길호 김동환 김용록 김은경 김현구 박병우 박병천 우한영  
정명화 정일경 정재준 조성래 최원호

### 포상위원회

위 원 장 / 최덕인  
부위원장 / 박종윤  
간 사 / 정세영  
위 원 / 김동희 남창희 박혁규 유경화 윤의준 이성익 이철의

#### 성봉물리학상위원회

위 원 장 / 민석기  
간 사 / 이철의  
위 원 / 송희성 송용진 조성호 최덕인 황정남

#### 백천물리학상위원회

위 원 장 / 민현수  
위 원 / 남순건 홍덕기

#### 봄비물리학상위원회

위 원 장 / 이종민  
위 원 / 고재귀 심광숙 염태호 유인석 윤종걸

### 제위원회

#### 물리교육위원회

위 원 장 / 권재술  
소위원장 / [기획정책소위원회] 한성홍 [교과/내용소위원회] 박종원  
간 사 / 오원근  
위 원 / 김성원 김중복 전동렬 최홍수 [기획정책소위원회] 김영동 김진승  
나오철 박완규 윤성현 이재봉 정병호 정진수 지찬수  
[교과/내용소위원회] 김영민 김재성 박병윤 임성민 조향숙  
한문섭 홍경희

#### 재정위원회

위 원 장 / 박상일  
부위원장 / 이충훈 황철주  
간 사 / 김주진  
위 원 / 남재국 박재근 신응수 오중훈 윤의준 채진석

#### APCTP 한국위원회

위 원 장 / 이범훈  
부위원장 / 박규환  
간 사 / 정세영  
위 원 / 고병원 김상표 김승환 남순건 민병일 방윤규 이철의 최무영  
홍덕기

#### 대외협력위원회

위 원 장 / 박영아  
소위원장 / [국제교류소위원회] 권면 [홍보전략소위원회] 신용진  
[IUPAP소위원회] 이현규 [AAPPS소위원회] 김승환  
간 사 / [국제교류소위원회] 정현식(총괄간사) [홍보전략소위원회] 김동호  
[IUPAP소위원회] 이공원 [AAPPS소위원회] 김상표  
위 원 / 이철의 [국제교류소위원회] 김귀년 남순건 박배호 박재훈 박혁규  
염한웅 윤의준 이우영 차국린 [홍보전략소위원회] 강양구 김상연  
박방주 이근영 이보화 이은정 정동근 정재승 조호진 한상준  
홍승우 [IUPAP소위원회] 남궁원(교문) 국양 남창희 신성철  
이승주 이후중 [AAPPS 소위원회] 남궁원 박영아

## 제위원회

### 물리올림피아드위원회

위 원 장 / 김성원  
부위원장 / 전동렬  
자문위원 / 유인석 이성묵  
간 사 / 정세영  
위 원 / 김경대 김도석 박배호 양우철 양인상 엄종화 윤용성 이철의  
최홍수 현승준

### 여성위원회

위 원 장 / 김영순  
부위원장 / 서은경 김혜림  
간 사 / 임혜인  
위 원 / 권경훈 김현정 양호순 윤진희 이철의 정난주 정옥희 천승현

### 자격심의위원회

위 원 장 / 정세영  
간 사 / 홍석륜  
위 원 / 김일원 김재성 박병주 이진형 임애란

### 윤리위원회

위 원 장 / 이해웅  
간 사 / 정세영  
위 원 / 강원 김동언 김재완 노태원 이주열 이철의 조동현 최상경  
황보창권

### 용어심의위원회

위 원 장 / 이재일  
자문위원 / 조성호 박대운 송희성 이준규  
간 사 / 유건호  
위 원 / 김창대 김항배 여인환 오원근 이공주복 이순철 이철의 장영록  
정옥희 정홍 천병구 홍지상

## 특별위원회

### 자문특별위원회

위 원 장 / 권숙일  
간 사 / 이철의  
위 원 / 김정구 김채욱 민석기 박동수 송희성 안세희 윤세원 이충희  
정석중 정중현 최덕인 황정남

### 기획정책특별위원회

위 원 장 / 최은하  
부위원장 / 한문섭 김윤배  
위 원 / 김영동 김철기 김태근 남철주 박배호 성맹제 윤성현 이보화  
이윤상 이철의 정세영

### 노벨상특별위원회

위 원 장 / 남창희  
부위원장 / 김수봉  
자문위원 / 조장희 박영우 장기주  
간 사 / 염한웅  
위 원 / 김은성 신상진 이규철 이영욱 황덕수

### 남북협력특별위원회

위 원 장 / 유성초  
간 사 / 박경완  
위 원 / 이성재 차덕준 이주열 김도석 황보창권 연구황

### 산학연특별위원회

위 원 장 / 이호성  
간 사 / 오차환 한일기  
위 원 / 고도경 김현탁 오병두 정재인 진윤식

## 특별위원회

### 지역활성화특별위원회

위 원 장 / 김우영  
부위원장 / 서동주 정중현  
위 원 / 원혜경 유인권 정진수 조재홍 주경광 차덕준 홍순철

## 분과회

입 자 물 리 학 분 과 회 위원장 / 김선기  
원 자 핵 물 리 학 분 과 회 위원장 / 박병운  
응 집 물 질 물 리 학 분 과 회 위원장 / 이재일  
응 용 물 리 학 분 과 회 위원장 / 우정원  
통 계 물 리 학 분 과 회 위원장 / 국형태  
물 리 교 육 분 과 회 위원장 / 최홍수  
플 라 스 마 물 리 학 분 과 회 위원장 / 권 면  
광학 및 양자전자학분과회 위원장 / 김진승  
원자 및 분자물리학분과회 위원장 / 조동현  
반 도 체 물 리 학 분 과 회 위원장 / 노삼규  
천 체 물 리 학 분 과 회 위원장 / 김상표

## 지부

대구·경북지부 지부장 / 김도성  
대전·충남지부 지부장 / 이윤희  
부산·울산·경남지부 지부장 / 정문성  
광주·전남지부 지부장 / 정창섭  
강 원 지 부 지부장 / 남기봉  
전 북 지 부 지부장 / 김상표  
충 북 지 부 지부장 / 오석근

## 한국물리학회 회보 제27권 제4호

인 쇄	2009년 10월 14일
발 행	2009년 10월 21일
발행인	이 영 백 사단법인 한국물리학회
발행처	서울특별시 강남구 역삼동 635-4 Tel. 02-556-4737 (대표전화) Fax. 02-554-1643 homepage: <a href="http://www.kps.or.kr">http://www.kps.or.kr</a> e-mail: <a href="mailto:office@kps.or.kr">office@kps.or.kr</a>
인쇄인	경희정보인쇄(주) 서울특별시 동대문구 회기동 105-33 Tel. 02-2263-7534 Fax. 031-904-1639